Funktionale Organische Salze mit Chalkogenolat-, Carboxylat- und Azolat-Anionen:

Auf der Suche nach neuen Elektrolytmaterialien
für Energie-Speicherung und -Konversion

Kumulative Dissertation

zur Erlangung des Doktorgrades der Naturwissenschaften
(Dr. rer. nat.)

dem Fachbereich Chemie
der Philipps-Universität Marburg
vorgelegt von

Lars Hendrik Finger
(M. Sc. Chemie)
aus Dortmund

Marburg 2016

Die vorliegende Arbeit wurde in der Zeit von April 2012 bis Januar 2016 unter Leitung von Herrn Prof. Dr. Jörg Sundermeyer am Fachbereich Chemie der Philipps-Universität Marburg angefertigt.

Vom Fachbereich Chemie der Philipps-Universität Marburg (Hochschulkennziffer: 1180) als Dissertation angenommen am: 02.02.2016

Erstgutachter: Prof. Dr. Jörg Sundermeyer

Zweitgutachterin: Prof. Dr. Stefanie Dehnen

Tag der mündlichen Prüfung: 09.03.2016

Meiner Familie gewidmet

Wissenschaftlicher Werdegang

04/2012 – Heute	**Doktorand**
	Philipps-Universität Marburg, FB Chemie, AG Prof. Sundermeyer
	Promotionsprogramm: DFG Graduiertenkolleg 1782,
	Funktionalisierung von Halbleitern
10/2011 – 11/2011	**Wissenschaftlicher Mitarbeiter**
	Philipps-Universität Marburg, FB Chemie, AG Prof. Sundermeyer
10/2009 – 09/2011	**Studiengang M.Sc. Chemie**
	Philipps-Universität Marburg, abgeschlossen am 30.09.2011
03/2011 – 09/2011	Masterarbeit
	”Koordinationschemie des 5,5'-Bistetrazols”
09/2009 – 12/2009	Erasmussemester
	Heriot-Watt University Edinburgh
10/2006 – 09/2009	**Studiengang B.Sc. Chemie**
	Philipps-Universität Marburg, abgeschlossen am 22.09.2009
04/2011 – 06/2011	Bachelorarbeit
	”Neue Hydroaminierungskatalysatoren auf Basis von Constrained-Geometry-CpPN-Zirkonium-Komplexen”
08/2005 – 04/2006	**Zivildienst**
	Archäologisches Landesamt Schleswig Holstein
08/1996 – 06/2005	**Gymnasium**
	Domschule Schleswig, Abitur am 10.06.2005

Publikationsliste

Artikel in Fachzeitschriften:

M. J. Leitl, T. Gneuß, T. Niehaus, L. H. Finger, J. Sundermeyer, H. Yersin; „Cu(I) Based Emitters with Tripodal Ligands for the Blue Showing Phosphorescence and Thermally Activated Delayed Fluorescence“, *in preparation*.

J. F. Kögel, D. Margetić, X. Xie, L. H. Finger, J. Sundermeyer; „Phosphorus Bisylide Proton Sponges – A New Class of Superbases with Two Interacting Carbon Atoms as Basicity Centers“, *in preparation*.

M. Jost, L. H. Finger, J. Sundermeyer, C. von Hänisch; „Synthesis of new Ionic Liquids Containing the Phosphaethynolate (PCO^-) Anion“, *in preparation*.

G. Thiele, C. Donsbach, H. Borkowski, L. H. Finger, J. Sundermeyer, S. Dehnen; „Mercurates from a Revised Ionothermal Synthesis Route: The Pseudo-Flux Approach“, *in preparation*.

L. H. Finger, P. Hofmann, J. Sundermeyer; „Synthesis of 1,3-Dialkylimidazole-2-chalcogenones from NHC-CO_2 Adducts“, *in preparation*.

L. H. Finger, F. G. Schröder, J. Sundermeyer; „New Borate Anions with Bistetrazolato^{2-} and Pyrazinediolato^{2-} Ligands“, *in preparation*.

L. H. Finger, J. Guschlbauer, K. Harms, J. Sundermeyer; „N-Heterocyclic Olefin – Carbon Dioxide and Sulfur Dioxide Adducts: Structures and Interesting Reactivity Patterns“, *in preparation*.

L. H. Finger, J. Sundermeyer; „Halide Free Synthesis of Hydrochalcogenide Ionic Liquids of the Type [Cation][HE] (E = S, Se, Te)“, *Chem. Eur. J.* ***2016,*** DOI: 10.1002/chem.201504577, *in press.*

L. H. Finger, J. Sundermeyer; „μ-Rhodizonato-1κO,1:2κO',2κO''-tetra(triphenylphosphine)-disilver(I): A Molecular Complex with the $[C_6O_6]^{2-}$ Ligand Template“, *Z. Anorg. Allg. Chem.* **2015**, 2565−2569.

T. Gneuß, M. J. Leitl, L. H. Finger, H. Yersin, J. Sundermeyer; „A New Class of Deep-Blue Emitting Cu(I) Compounds – Effects of Counter Ions on the Emission Behavior“, *Dalton Trans.* **2015**, *44*, 20045−20055.

L. H. Finger, F. Wohde, E. I. Grigoryev, A.-K. Hansmann, R. Berger, B. Roling, J. Sundermeyer; „Access to pure and highly volatile hydrochalcogenide ionic liquids“, *Chem. Commun.* **2015**, *51*, 16169−16172.

L. H. Finger, B. Scheibe, J. Sundermeyer; „Synthesis of Organic Trimethylsilyl-chalcogenolate Salts Cat[TMS-E] (E = S, Se, Te): the Methylcarbonate Anion as Desilylating Agent“, *Inorg. Chem.* **2015**, *54*, 9568−9575.

T. Gneuß, M. J. Leitl, L. H. Finger, N. Rau, H. Yersin, J. Sundermeyer; „A New Class of Luminescent Cu(I) Complexes with Tripodal Ligands – TADF Emitters for the Yellow to Red Color Range“, *Dalton Trans.* **2015**, *44*, 8506–8520.

J. F. Kögel, L. H. Finger, N. Frank, J. Sundermeyer; „The New NH-Acid $HN(C_6F_5)(C(CF_3)_3)$ and its Crystalline and Volatile Alkaline and Earth Alkaline Metal Salts“, *Inorg. Chem.* **2014**, *53*, 3839–3846.

L. H. Finger, F. G. Schröder, J. Sundermeyer; „Synthesis and Characterisation of 5,5'-Bistetrazolate Salts with Alkali Metal, Ammonium and Imidazolium Cations“, *Z. Anorg. Allg. Chem.* **2013**, *639*, 1140–1152.

B. Oelkers, L. H. Finger, J. Sundermeyer; „Dichlorido(dimethylsulfoxide-κS)(η^6-mesitylene)ruthenium(II)“, *Acta Crystallogr. E* **2011**, *67*, m319.

C. Lichtenberg, M. Elfferding, L. Finger, J. Sundermeyer; „Investigation of Novel and Reinvestigation of Known Cyclopentadienylphosphanes: News on [1,5]Sigmatropic Rearrangements“, *J. Organomet. Chem*. **2010**, *695*, 2000–2006.

Tagungsbeiträge (Auswahl):

Vortrag: L. H. Finger, J. Sundermeyer; „Ionic Liquids with Chalcogenide Anions and their Application for the Synthesis of Amorphous MoS_2,“ GRK 1782 ”Funktionalisierung von Halbleitern”, Seminar 2015, Hofheim, 07.10. bis 09.10.2015.

Poster: L. H. Finger, J. Sundermeyer; „Hydro-, Silyl- and Poly-Chalcogenide Ionic Liquids - Synthesis, Characterisation and Application“, GDCh Wissenschaftsforum Chemie, Dresden, 30.08. bis 02.09.2015.

Poster: L. H. Finger, B. Scheibe, J. Sundermeyer; „Low Temperature Synthesis of MoS_2 from Tetrathiomolybdate and Sulfide Ionic Liquids“, Materialforschungstag Mittelhessen, Marburg, 09.07.2015.

Vortrag: L. H. Finger, J. Sundermeyer; „Halogen Free Synthesis of Hydrochalcogenide Based Ionic Liquids“, 25. EuCheM Conference on Molten Salts and Ionic Liquids, Tallinn (Estland), 06.07 bis 11.07.2014.

Poster: L. H. Finger, S. Ullrich, J. Sundermeyer; „Cobalt Complexes with Bipyridine and Imidazolylpyridine Ligands“, GRK 1782 ”Funktionalisierung von Halbleitern”, Seminar 2013, Hofheim, 19.08. bis 22.08.2013.

Poster: L. H. Finger, F. G. Schröder, J. Sundermeyer; „Transition Metal Complexes of 5,5'-Bistetrazole“, 2nd EuCheMS Inorganic Chemistry Conference, Jerusalem (Israel), 07.07. bis 11.07.2013.

Poster: L. H. Finger, F. G. Schröder, J. Sundermeyer; „Coordination Behaviour of 5,5'-Bistetrazole towards Transition Metals“, 9. Koordinationschemietreffen, Bayreuth, 24.02. bis 26.02.2013.

Patentanmeldung:

L. H. Finger, J. Sundermeyer (Philipps-Universität Marburg); „Ionic Liquids with a Chalcogenide Anion“, EP2876081, **2015**.

Danksagung

Herrn Prof. Dr. Jörg Sundermeyer danke ich herzlich für die Möglichkeit in seiner Arbeitsgruppe zu promovieren, die gewährten Freiheiten bei der Bearbeitung der Themengebiete und die stete Unterstützung und Diskussionsbereitschaft.

Frau Prof. Dr. Stefanie Dehnen danke ich für die bereitwillige Übernahme des Zweitgutachtens und den Herren Prof. Dr. Bernhard Roling und Prof. Dr. Andreas Seubert, dass Sie sich als Prüfer zur Verfügung gestellt haben.

Dem Fonds der Chemischen Industrie und dem DFG Graduiertenkolleg 1782 danke ich für die finanzielle Unterstützung.

Mein besonderer Dank gilt den Serviceabteilungen für Röntgenstrukturanalyse, NMR-Spektroskopie und Massenspektrometrie und Elementanalytik für ihre verlässliche und zügige Arbeit. Speziell Heike Mallinger und Martina Gerlach, Radostan Riedel und Michael Marsch sowie Cornelia Mischke und Gert Häde danke ich sehr für die bevorzugte Bearbeitung besonders luftempfindlicher Proben. Dr. Klaus Harms, Dr. Xiulan Xie und Dr. Uwe Linne danke ich für die Diskussionsbereitschaft und tiefergehende Erläuterungen bei speziellen Fragestellungen.

Benedikt Huber und Marcel Drüschler danke ich herzlich für ihre umfassende Hilfe bei jeglichen elektrochemischen Schwierigkeiten.

Bei den Kooperationspartnern Günther Thiele, Maximilian Jost, Evgeny Grigoryev, Anna-Katharina Hansmann, Fabian Wohde und Carsten Donsbach sowie den jeweiligen Arbeitsgruppenleitern Frau Prof. Dr. Dehnen, Herrn Prof. Dr. von Hänisch, Herrn Prof. Dr. Berger und Herrn Prof. Dr. Roling bedanke ich mich für die fruchtbare Zusammenarbeit.

Den aktuellen und ehemaligen Mitgliedern des Arbeitskreises Sundermeyer danke ich herzlich für die angenehme Arbeitsatmosphäre, ihre Diskussions- und Hilfsbereitschaft, die gemeinsame Freizeitgestaltung und vor allem das gewissenhafte Korrekturlesen. Besonders Irene Barth und Lisa Hamel danke ich für ihre gewissenhafte Arbeit.

Ein besonderer Dank gebührt außerdem den Studierenden, die ich im Rahmen ihrer Bachelorarbeiten und Forschungspraktika betreuen durfte und die mich so bei meiner Doktorarbeit tatkräftig unterstützt haben.

Meiner langjährigen Mitbewohnerin und guten Freundin Janet danke ich für die entspannte Atmosphäre zu Hause und ihre unerschöpfliche Hilfsbereitschaft.

Mein abschließender Dank geht an meine Eltern für ihren unerschütterlichen Glauben an mich und ihre immerwährende Unterstützung; und an Svenja, für Alles.

Inhaltsverzeichnis

1 Einleitung

1.1 Energie-Speicherung und -Konversion

1.1.1 Der Lithium-Ionen-Akkumulator

Lithium-Ionen-Akkumulatoren gehören zu den wichtigsten und bekanntesten Energiespeichersystemen, die aktuell verfügbar sind. Sie stellen die Basis für den gesamten Markt der portablen elektronischen Kleingeräte dar und finden mittlerweile auch vermehrt Anwendung in größeren technischen Systemen wie Elektroautos, Robotern oder Batterie-speicherkraftwerken. Die typischste Form des Lithiumakkus besteht aus einer Graphitanode, in die im geladenen Zustand Lithiumatome interkaliert sind, einem Elektrolyten auf Basis eines organischen Lösungsmittels, häufig organische Carbonate und Polyether, mit Leitsalzen wie $LiPF_6$ und einer Metalloxidkathode (Abb. 1.1).*

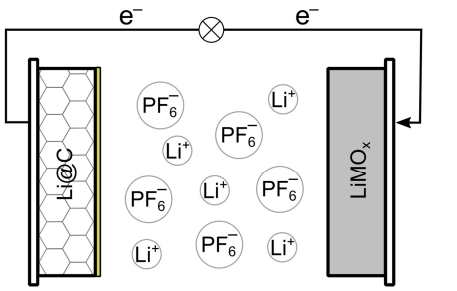

Abbildung 1.1. *Schematische Darstellung eines Lithium-Ionen-Akkumulators.*

Während des Entladevorganges geben die interkalierten Lithiumatome ein Elektron an den Stromkreis ab und wandern als Lithiumkationen zur Kathode, wo sie in das durch Elektronenaufnahme reduzierte Metalloxid eingelagert werden. Während des Ladevorganges wird eine Spannung in entgegengesetzter Richtung angelegt, wodurch die Lithiumkationen aus dem Metalloxid herausdiffundieren, in die Graphitelektrode zurück wandern und dort mit Elektronen zu neutralen Lithiumatomen rekombinieren.[1] Während die aktuellen Lithiumakkus für die meisten Anwendungen noch ausreichen, ist absehbar, dass neue Technologien erhöhte Ansprüche in Bezug auf Energiedichte, Spannung, Kapazität, Lebensdauer und auch Sicherheit der Batterien haben werden. Jede einzelne Komponente besitzt signifikanten Einfluss auf diese Kenngrößen und wird daher theoretisch[2] wie praktisch[3] intensiv weiter erforscht. Als alternative Anodenmaterialien werden aktuell vor allem Kompositmaterialien aus Kohlenstoff und Metalloxiden und -sulfiden untersucht.[4] Im

* Die Benennung als Anode und Kathode bezieht sich auf den Entladevorgang.

Bereich der Kathoden finden besonders Übergangsmetallphosphate und -silikate Beachtung.[5] Das Elektrolytsystem ist die variabelste Komponente der Zellen. Schon bei den Flüssigelektrolyten muss zwischen organischen Lösungsmitteln, Ionischen Flüssigkeiten und wässrigen Systemen unterschieden werden. Außerdem werden Gel- und Polymerelektrolyte sowie anorganische Festkörperelektrolyte untersucht.[6] Durch optimales Abstimmen der Bauweise mit den Elektrolyten und Anoden- und Kathodentypen lassen sich die spezifischen Eigenschaften der Zellen steuern. Es wird davon ausgegangen, dass dadurch die einzelnen Typen auf spezielle Anwendungen zugeschnitten werden können und sich mehrere Varianten in ihren eigenen Bereichen etablieren werden. So erlauben Gelelektrolyte besonders flexible Bauweisen und reine Feststoffzellen miniaturisierte Formate, während Flüssigelektrolyte aktuell die höchsten Energiedichten erreichen. Diese hohen Energiedichten bedingen in Kombination mit den flüchtigen und entflammbaren organischen Lösungsmitteln jedoch auch die höchsten Sicherheitsrisiken.[7] Für die Sicherheit während des Ladeprozesses ist vor allem die Ausbildung einer stabilen Schutzschicht auf der Anode wesentlich. Der Ladeprozess läuft an der Graphitelektrode bei einer Spannung von ca. 0.05 V gegen Li/Li^+ ab und liegt damit außerhalb des elektrochemischen Stabilitätsfensters typischer Elektrolytlösungen. Während der ersten Ladezyklen resultiert eine partielle Zersetzung des Elektrolytsystems und die Bildung einer *Solid Electrolyte Interface* (SEI, Abb. 1.2, links).

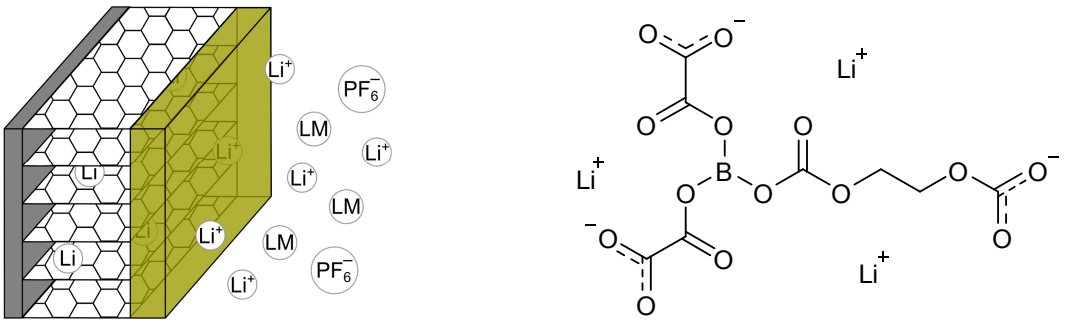

Abbildung 1.2. *Schematische Darstellung einer SEI auf der Graphitanode eines Lithiumakkus (links, LM = z. B. Propylencarbonat)[8] und vermutlicher Aufbau einer SEI bei Einsatz von LiBOB als Additiv (rechts).[8-9]*

Diese Schicht muss eine sehr gute Lithiumionenleitfähigkeit aufweisen, aber für Lösungsmittel- und andere Leitsalzmoleküle undurchlässig sein. Die Ausbildung einer stabilen SEI kann durch Additive im Elektrolyten positiv beeinflusst werden. Eines dieser Additive, das sich durch sehr gute Eigenschaften auszeichnet, ist Lithium-bis(oxalato)borat (LiBOB).[10] Es verringert die thermodynamisch vorgezeichnete Zersetzung des Lösungsmittels durch Lithium bzw. Elektronen und führt zur Bildung von carbonatreichen SEIs, die stabile Borsäureester enthalten (Abb. 1.2, rechts).[11] Weitere vielversprechende

Additive sind z. B. Vinylencarbonat, Tris(pentafluorphenyl)boran und Toluoldiisocyanat.[6] Kürzlich wurde ein Patent veröffentlicht, dass auch für 2,3-Dioxo-5,6-pyrazindicarbonitril sehr positive Eigenschaften nachweist.[12] Im Rahmen der eigenen Masterarbeit wurde versucht Alternativen zu LiBOB auf Basis von 5,5'-Bistetrazol zu synthetisieren.[13] Es bestand die Fragestellung ob die Bioisosterie der funktionellen Gruppen Carboxylat und Tetrazolat[14] auf Oxalsäure und 5,5'-Bistetrazol übertragen werden kann und ob sich analoge Koordinationsverbindungen mit potentiell ähnlichen Eigenschaften herstellen lassen (siehe auch Kap. 1.3.2, Seite 15).

1.1.2 Der Lithium-Schwefel-Akkumulator

Die spezifische Energie von aktuellen Lithiumakkus liegt im Bereich von 150 bis 200 $Wh \cdot kg^{-1}$. Beim Einsatz in Elektroautos bedeutet dies, dass die rein elektrisch erreichbare Reichweite der Fahrzeuge in der Regel noch sehr weit hinter der von Fahrzeugen mit Verbrennungsmotoren zurück liegt. Um in etwa konkurrenzfähige Reichweiten zu realisieren wird eine spezifische Energie von mindestens 500 $Wh \cdot kg^{-1}$ gefordert.[15] Um dies zu erreichen, werden aktuell alternative Akkumulatortypen entwickelt. Darunter sticht der Lithium-Schwefel-Akkumulator (LiS-Akku) mit einer theoretischen spezifischen Energie von ca. 2600 $Wh \cdot kg^{-1}$ und einer theoretischen maximalen Kapazität von 1672 $mAh \cdot g^{-1}$ hervor. Darin wird das Metalloxid der Kathode eines Standard-Lithiumakkus gegen Schwefel ersetzt und elementares Lithium findet Einsatz als Anode. Durch eine lithiumionenleitfähige Elektrolytlösung stehen die Elektroden in Kontakt (Abb. 1.3).

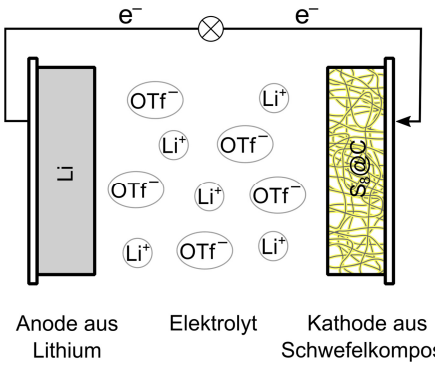

Abbildung 1.3. *Schematische Darstellung eines Lithium-Schwefel-Akkumulators; OTf = Triflat.*

Während des Entladevorganges wandern Lithiumkationen durch den Elektrolyten zur Kathode und reagieren mit dem Schwefel und den Elektronen aus dem Stromkreis im Idealfall zu Lithiumsulfid. Die sehr hohen theoretischen Leistungsmerkmale beruhen auf der Annahme, dass diese in Schema 1.1 gezeigte Reaktion vollständig abläuft, während nur das Eigengewicht von Lithium und Schwefel berücksichtigt werden.[16]

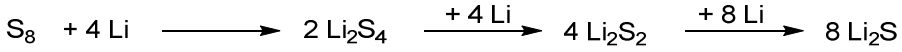

Schema 1.1. *Vereinfachter Ablauf der Reaktion an der schwefelhaltigen Kathode während der Entladung eines Lithium-Schwefel-Akkumulators; neben den gezeigten sind zahlreiche weitere Polysulfidintermediate denkbar.*[15a]

Diese vollständige Umsetzung ist in der Praxis jedoch so gut wie unmöglich, da elementarer Schwefel Lithiumionen und elektrischen Strom nur schlecht leitet.[17] Während mit Prototypen bereits tatsächliche Werte von 500 $Wh \cdot kg^{-1}$ bzw. 800 $mAh \cdot g^{-1}$ demonstriert werden konnten, müssen für eine verlässliche Markteinführung noch mehrere Schwierigkeiten überwunden werden. Die höchste spezifische Energie wäre mit Elektroden aus reinem Lithium und reinem Schwefel erreichbar. Neben der schlechten Leitfähigkeit von Schwefel ist dies auch wegen der mit der Konversion zu Li_2S verbundenen Volumenzunahme um ca. 80% nicht durchführbar.[18] Die mechanische Belastung führte in kurzer Zeit zur Zerstörung der Kathode. Aktuell werden vor allem poröse Komposite aus Kohlenstoff und Schwefel untersucht, die sowohl die Volumenzunahme tolerieren, als auch wegen der Diffusion der Lithiumionen weit in das Elektrodenmaterial hinein eine vollständigere Reaktion erlauben und schließlich durch den Kohlenstoffanteil eine erhöhte Leitfähigkeit aufweisen.[19] Die untersuchten Kathodenmaterialien sind jedoch im Regelfall nicht selbsttragend und müssen mit polymerbasierten Bindemitteln kombiniert werden, wodurch die Energiedichte weiter reduziert wird. Die Lithiumanode führt zu deutlichen Sicherheitsrisiken, da diese mit der Elektrolytlösung reagieren kann. Die Ausbildung fester Schutzschichten (SEIs) ist eine mögliche Abhilfe. Jedoch führen gerade diese Schichten während des Ladevorganges zur vermehrten Bildung von Lithiumdendriten, die bis zur Kathode wachsen und so zum Kurzschluss führen können.[20] Des Weiteren stellen sich die intermediären Reduktionsprodukte des Schwefels als problematisch heraus. Während sowohl elementarer Schwefel als auch Lithiumsulfid in typischen Elektrolytlösungen eine sehr geringe Löslichkeit zeigen, sind die intermediären Polysulfidanionen gut löslich. Es resultiert ein Shuttle-Prozess, in dem langkettige Polysulfide zur Anode wandern, dort reduziert werden, als kurzkettige Polysulfide zurück zu Kathode wandern und nach Oxidation den Prozess erneut starten. Dies führt zu einer kontinuierlichen Selbstentladung, welche die Coulomb-Effizienz deutlich verringert.[21] Diese Nebenreaktion hat außerdem die irreversible Abscheidung von Li_2S an der Anode zur Folge und führt so zu einem sehr schnellen Kapazitätsverlust des LiS-Akkus.[22] Der Prozess kann durch die Verwendung von hochkonzentrierten Lithiumlösungen und Ionischen Flüssigkeiten als Elektrolyt verringert werden, was sich durch eine verringerte Dendritenbildung zusätzlich positiv auswirkt. Unter der erhöhten Viskosität derartiger

Elektrolytsysteme und der verringerten Leitfähigkeit leidet jedoch die Leistung der Batterie.[23]

1.1.3 Die Farbstoffsolarzelle

Neben der effektiven Speicherung ist die Umwandlung von nachhaltiger Rohenergie wie Wind, Sonnenlicht und Wasserkraft in vor allem elektrische Energie der Kernaspekt einer dringend weiter zu forcierenden Energiewende. 2014 wurden in Deutschland $161.4 \cdot 10^9$ KWh elektrische Energie aus nachhaltigen Energiequellen erzeugt; 21.8% entfallen auf Photovoltaikanlagen. Über Biomasse und Windenergie werden aktuell zwar noch deutlich größere Anteile erzeugt (30.5% bzw. 35.5%), allerdings weist die Photovoltaik jährlich den prozentual größten Zuwachs auf.[24] Um diesen Markt weiter entsprechend ausbauen zu können, werden auch alternative Solarzellensysteme benötigt, die flexiblere Anwendungsmöglichkeiten als die starren und auf direktes Sonnenlicht angewiesenen Siliziumsolarzellen erlauben. Die von MICHAEL GRÄTZEL entwickelte Farbstoffsensibilisierte Solarzelle (DSSC, *Dye Sensitized Solar Cell*) ist eine besonders intensiv erforschte Alternative (Abb. 1.4).[25]

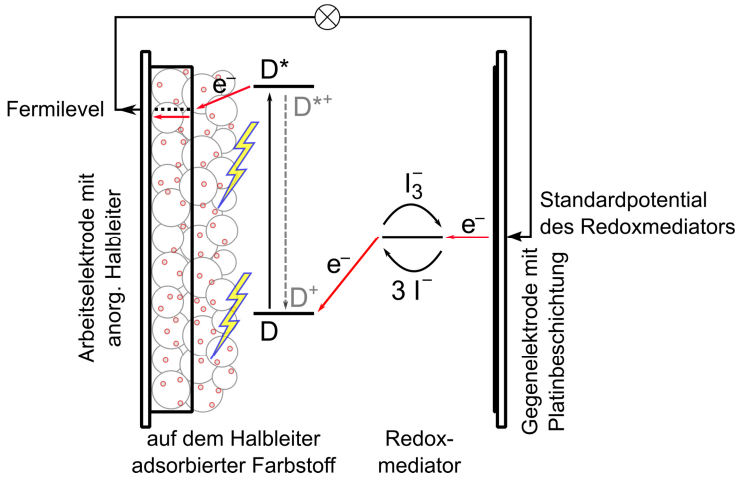

Abbildung 1.4. *Schematische Darstellung einer Farbstoffsolarzelle (DSSC); D: Farbstoff; rote Pfeile symbolisieren den Elektronenfluss innerhalb der Solarzelle.*[25a, 26]

Bei diesem System wird ein auf einem anorganischen Halbleiter adsorbierter Farbstoff (D) durch Licht angeregt (D*) und kann aus dem angeregten Zustand ein Elektron an das Leitungsband des farblosen, nicht Licht-absorbierenden Halbleiters (ZnO, TiO_2) und weiter an die Arbeitselektrode abgeben. An der Gegenelektrode wird ein Redoxmediator (z. B. I^-/I_3^-) reduziert, der anschließend zur Arbeitselektrode diffundiert und dort seinerseits den nach der Elektronenabgabe oxidierten Farbstoff (D^+) regeneriert. DSSCs zeichnen sich vor allem dadurch aus, dass sie auch unter diffusem Licht arbeiten können und auf flexiblen

Trägermaterialien beidseitig transparent hergestellt werden können. So wird ihr Anwendungspotential momentan vor allem in kleinflächigen Innenraumanwendungen und bei portablen Systemen gesehen.[25a, 27] Bezüglich ihres Wirkungsgrades stehen sie jedoch noch deutlich hinter den auf kristallinem Silizium basierenden Photovoltaikelementen zurück. Der Wirkungsgrad einer Solarzelle η ist das Verhältnis aus der jeweils pro Fläche generierten elektrischen Leistung (P_{max}^{A}) und eingestrahlten Sonnenenergie (P_{in}^{A}).

$$\eta = \frac{P_{max}^{A}}{P_{in}^{A}}$$

Die elektrische Leistung ist definiert als das Produkt aus Stromstärke und Spannung. Dabei dürfen nicht die jeweiligen Maximalwerte Kurzschlussstromstärke (I_{SC}) und Leerlaufspannung (V_{OC}) verwendet werden, sondern die Kombination, die nach der Stromspannungskennlinie (Abb. 1.5) die maximale Leistung ermöglicht.

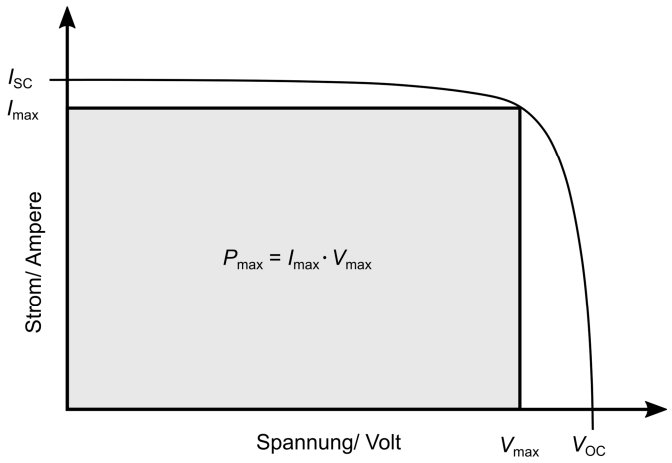

Abbildung 1.5. *Schematische Darstellung der Stromspannungskennlinie einer Solarzelle mit der maximal erreichbaren Leistung P_{max} (grau hinterlegt).*[17]

Da die Stromspannungskennlinie von den gegenwärtigen Betriebsbedingungen der Solarzelle abhängig ist, muss dieser Optimalwert kontinuierlich neu berechnet werden. Das erfolgt im Regelfall automatisch durch den angeschlossenen Wechselrichter.[28] In Abhängigkeit vom Typ erreichen auf Silizium basierte Solarzellen Wirkungsgrade zwischen 10% (amorphes Si) und 26% (monokristallin). Die besten Farbstoffsolarzellen erreichen unter standardisierten Testbedingungen kaum mehr als 12%.[18, 29] Bisher nicht unabhängig bestätigte Rekordwerte liegen bei über 14%.[30] Der geringere Wirkungsgrad von Farbstoffsolarzellen beruht unter anderem auf der kompetitiven Lichtabsorption durch den typischen Iodid-Triiodid Redoxmediator. Die Effizienz der Lichtabsorption durch den Farbstoff und der folgenden Elektronentransferprozesse bis in die Elektrode bestimmen maßgeblich den erreichbaren

Kurzschlussstrom (I_{SC}). Auch die Leerlaufspannung (V_{OC}) ist direkt mit dem Redoxmediator verknüpft; diese entspricht der Potentialdifferenz zwischen dem Standardpotential des Redoxmediators und dem Fermi-Niveau des Halbleiters (Abb. 1.4). Vor diesem Hintergrund werden auch bei DSSCs alternative Elektrolyt- und Redoxsysteme sehr intensiv weiterentwickelt.[18] Das ursprüngliche System aus einem flüssigen organischen Lösungsmittel ist nach wie vor am weitesten vertreten und liefert bisher die höchste Effizienz. Als Alternativen zum Iodid-Triiodid-Redoxpaar werden vor allem Cobaltkomplexe mit Bipyridinliganden untersucht.[31] Diese erlauben eine Anpassung des Standardpotentials über die Liganden, zeigen nur geringe Lichtabsorption und sind nicht korrosiv. Sie weisen aufgrund ihrer höheren Molmasse jedoch auch geringere Diffusionsgeschwindigkeiten und eine erhöhte Rekombination des oxidierten Mediators mit Elektronen aus dem Halbleiter auf. Neben weiteren Übergangsmetallkomplexen wurden auch andere Halogene und Pseudohalogene sowie Sulfid-Disulfid-Paare untersucht.[32] Im Bereich der IL-Flüssigelektrolytsysteme treten durch die erhöhte Viskosität und verringerte Ionenmobilität zusätzliche Schwierigkeiten auf. Die Anwendung reiner redoxaktiver ILs bietet in diesem Zusammenhang zusätzliche Möglichkeiten, da die Elektronenwanderung durch den Elektrolyten nicht nur über Diffusion stattfinden muss, sondern auch ein Grotthuß-ähnlicher Mechanismus möglich ist.[32] Dies ist zum Beispiel auch bei selenocyanat-[33] und ferrocenbasierten ILs denkbar.[34] Außerdem wurden Polysulfid-ILs erfolgreich als Elektrolyt und Redoxmediator in DSSCs mit organischen[35] und Ruthenium-Farbstoffen[36] sowie Quantenpunktsolarzellen auf Basis von CdS[37] und CdSe[36b, 38] Quantenpunkten getestet. Ähnlich wie bei Lithiumakkus finden sich auch im Bereich der Farbstoffsolarzellen zahlreiche Bestrebungen die Flüssigelektrolytsysteme durch gelartige, polymere oder feste Elektrolytsysteme zu ersetzen.[32]

1.2 Ionische Flüssigkeiten

1.2.1 Grundlagen und Anwendungspotential

Eine ausschließlich aus Ionen aufgebaute Substanz mit einem Schmelzpunkt unterhalb von 100 °C wird gemeinhin als ionische Flüssigkeit (IL, *Ionic Liquid*) bezeichnet. Diese Begrenzung geht vermutlich bis auf PAUL WALDEN, den Entdecker des ersten bereits bei Raumtemperatur flüssigen Salzes − Ethylammonium-nitrat − zurück.[39] Dieser formulierte als Vorgabe für die eigenen Untersuchungen und vermutlich ohne eine das Jahrhundert überdauernde Definition schaffen zu wollen: „Gewählt wurden *wasserfreie* Salze, welche bei

relativ *niedrigen Temperaturen*, etwa bis zu 100 °C schmelzen."[39] Bereits einige Jahre zuvor untersuchte CARL SCHALL Alkylchinolinium-triiodide mit Schmelzpunkten zwischen 30 und 95 °C bezüglich ihrer elektrischen Leitfähigkeit.[40] Über lange Zeit blieb dieser elektrochemische Fokus bei ILs bestehen, während meist etwas höher schmelzende rein anorganische Salzschmelzen schon intensiv als Reaktionsmedien untersucht wurden.[41] Erst Mitte der 1980er Jahre wurden in Pionierarbeiten auch ILs mit organischem Kation als Reaktionsmedium intensiver untersucht.[42] Mit der Synthese der ersten Tetrafluoroborat und Hexafluorophosphat ILs begann ein zunehmend rasanter Fortschritt in der Entwicklung neuer ILs und der Erforschung neuer Anwendungsmöglichkeiten.[43] Die unabhängige Variabilität von Kation und Anion erlaubt nahezu unendliche Kombinationsmöglichkeiten, und die spezifische Anpassung der IL an ein vorgesehenes Aufgabenprofil. Reichen diese nicht mehr aus, lassen sich durch Mischung von ILs die Eigenschaften weiter variieren.[44] Heutzutage sind ILs aus kaum einem Forschungsgebiet wieder wegzudenken. Sie finden Anwendung als Reaktionsmedium − sowohl als primäres Lösungsmittel als auch als quasi-heterogene Phase im SILP Verfahren (*Supported Ionic Liquid Phase*). Bei diesem ist ein Katalysator in der IL Phase immobilisiert und kann dadurch nach der Reaktion zurückgewonnen werden.[45] Weiter werden ILs z. B. als Basis für Elektrolytlösungen in Farbstoffsolarzellen[46] und Batteriesystemen[47] untersucht, als Adsorber für verschiedene Gase[48] und als Extraktionsmedium um Cellulose umweltfreundlich aus Pflanzenrohmasse zu gewinnen.[49] Die strukturelle Variabilität und die damit verbundenen vielfältigen Anwendungsmöglichkeiten haben zur Prägung des Begriffes *Task Specific Ionic Liquids* geführt.[50]

1.2.2 Synthese und Eigenschaften

Unter zahlreichen Synthesemethoden für ILs sticht die Alkylierung eines organischen Nukleophils (Nu, z. B.: Alkylimidazol, zyklisches oder azyklisches Trialkylamin, Trialkylphosphin, Pentaalkylguanidin, Pyridin, Dialkylsulfid) durch ein geeignetes Alkylierungsreagenz (RX, z. B.: Alkylhalogenid, Dialkylsulfat, Alkylsulfonat, Alkyltriflat, Dimethylcarbonat) als ein Standardverfahren heraus (Schema 1.2). Aus den gewonnen Salzen lassen sich in Salzmetathesereaktionen oder an polymeren Ionenaustauschern zahlreiche weitere ILs generieren.

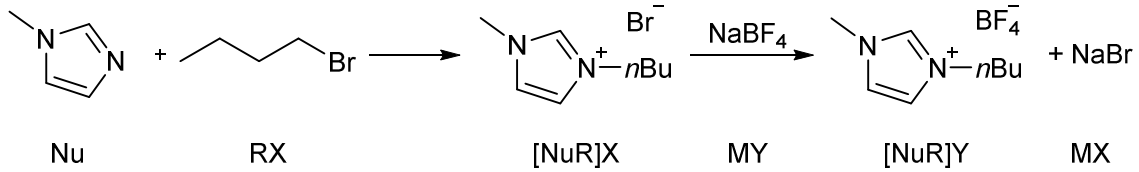

***Schema 1.2**. Klassische IL-Synthese am Beispiel der Alkylierung von Imidazol mit Butylbromid und anschließender Salzmetathese mit Natrium-tetrafluoroborat.*

Die Unterklasse der protischen ILs wird durch einen Protonenübertrag von der ursprünglichen Brønsted Säure HA auf eine Brønsted Base B gebildet. Im Unterschied zur vorangegangenen Alkylierungsreaktion stehen hier Edukt- und Produktseite miteinander im Gleichgewicht, welches vom Unterschied der Säurekonstanten von HA und der konjugierten Säure der ursprünglichen Base (HB^+) abhängig ist (Schema 1.3).

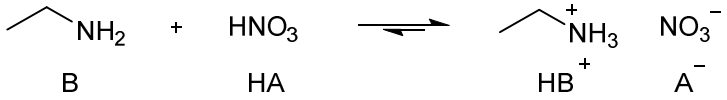

***Schema 1.3.** Synthese einer protischen IL am historischen Beispiel Ethylammonium-nitrat.[39]*

Die Vorteile von ILs gegenüber klassischen Lösungsmitteln liegen in ihrer höheren Temperaturstabilität, die einen breiteren Arbeitsbereich zulässt, ihrer häufig erhöhten chemischen und elektrochemischen Beständigkeit, ihrer häufig geringeren Toxizität und ihrem besonders geringen Dampfdruck. Speziell letzterer ist eine für viele Anwendungen essentielle Eigenschaft. Während lange Zeit davon ausgegangen wurde, dass ILs vor Erreichen des Zersetzungspunktes keinen messbaren Dampfdruck aufweisen und nicht flüchtig sind, ist seit etwa zehn Jahren bekannt, dass zahlreiche ILs tatsächlich unzersetzt destilliert werden können.[51] Nur unwesentlich früher wurde entdeckt, dass in der Unterklasse der protischen ILs Flüchtigkeit und elektrische Leitfähigkeit mit der Differenz der Säurekonstanten von HA und HB^+ korrelieren.[52] Dabei zeigt sich typischerweise das Phänomen, dass aprotische ILs als einzelne Ionenpaare (SIP, *Single Ion Pair*),[53] protische

ILs aber als separierte, ursprüngliche Säure und Base verdampfen.[54] Da diese neutralen Vorläufer im Regelfall geringere Verdampfungstemperaturen aufweisen als die gebildeten Salze, zeigen protische ILs meist eine höhere Flüchtigkeit als aprotische. Die klassische Unterscheidung von protischen und aprotischen ILs ist bezüglich der Abgrenzung des Verdampfungsverhaltens jedoch nicht hinreichend. So fallen zum Beispiel ILs aus Imidazoliumkationen und Anionen, welche die konjugierte Base einer schwachen Säure darstellen, dadurch auf, dass sehr wohl ein Gleichgewicht zwischen dem Imidazoliumkation (HB^+) und einem N-heterozyklischen Carben (B) beobachtet werden kann.[55] Ebenso existieren Ionenpaare, die zwar durch eine Säure-Base-Reaktion entstehen, bei denen aber aufgrund extremer Unterschiede der Säurekonstanten die Rückreaktion vernachlässigbar ist und die als SIPs verdampfen.[56]

1.2.3 Ionische Flüssigkeiten mit Methylcarbonat-Anionen

Die Alkylierung von organischen Nukleophilen mit Alkylhalogeniden und eine anschließende Salzmetathese bilden zwar einen verlässlichen und variablen Zugang zu ILs, dieser birgt aber den Nachteil, dass die Endprodukte sehr schwierig abzutrennende Metall- und Halogenidverunreinigungen enthalten. Diese sind besonders für elektrochemische Anwendungen und bei der Verwendung als Lösungsmittel für Katalysatoren unerwünscht.[57] Alkylierungsmittel wie Dialkylsulfate, Alkylsulfonate und -triflate ermöglichen halogenidfreie Synthesen, weisen jedoch eine hohe Toxizität auf und sind in Salzmetathesereaktionen weniger universell einsetzbar. Die mit Abstand beste Alternative findet sich in der Methylierung mit Dimethylcarbonat. Das Reagenz ist ungiftig, da es unter physiologischen Bedingungen nicht methylierend wirkt, chemisch stabil und einfach zu handhaben. Nachteilig ist die geringere Variabilität bezüglich des Substitutionsmusters des Kations, da längere Alkylgruppen in dieser S_N2-artigen Reaktion aus Dialkylcarbonaten in der Regel nicht selektiv übertragen werden können. Die resultierenden Methylcarbonatsalze lassen sich mit beinahe beliebigen Brønsted Säuren zu weiteren ILs umsetzen. Besonders vorteilhaft ist, dass die Methylcarbonatanionen nach der Protonierung spontan in Methanol und Kohlenstoffdioxid zerfallen. Dies erleichtert nicht nur die Aufreinigung, da ausschließlich flüchtige Nebenprodukte entstehen, sondern erlaubt auch die Umsetzung mit schwachen Säuren, da das Säure-Base-Gleichgewicht durch den irreversiblen Zerfall eines Produktes verlässlich verschoben wird (Schema 1.4).

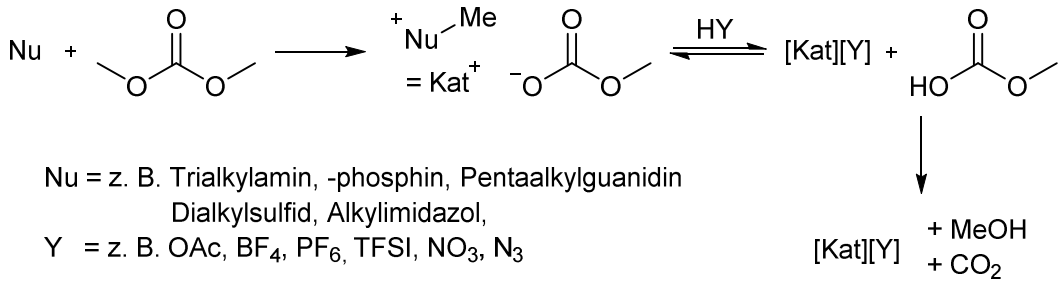

***Schema 1.4**. Die Methylcarbonatroute zur Darstellung von Ionischen Flüssigkeiten.*

Die erste Beschreibung dieser Methylcarbonatroute geht auf ein Patent von 1953 zurück. Darin wurde Triethylamin in Methanol mit Dimethylcarbonat methyliert und beschrieben, dass das entstehende Salz mit Säuren unter Freisetzung von CO_2 reagiert.[58] Diese Technologie wurde in zahlreichen weiteren Patentschriften und Fachartikeln aufgegriffen und weiter entwickelt.[59] Eine Besonderheit dieses Verfahrens ergibt sich bei der Verwendung von 1-Alkylimidazolen als Nukleophil (Schema 1.5).

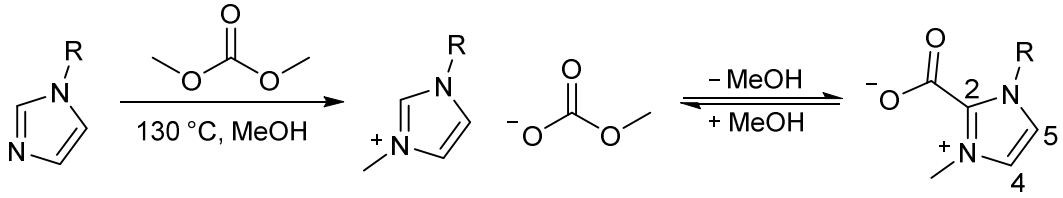

***Schema 1.5.** Methylierung eines 1-Alkylimidazols mit Dimethylcarbonat und Gleichgewicht mit dem entsprechenden 1-Alkyl-3-methylimidazolium-2-carboxylat.*

In diesem Fall ist das entstehende Imidazoliumkation ausreichend azide, um das Methylcarbonatanion zu protonieren; Endprodukt dieser Nebenreaktion sind unerwünschte Imidazoliumcarboxylate. Zahlreiche Publikationen widmen sich der Entstehung dieser Klasse von Zwitterionen, die Ergebnisse sind jedoch diskrepant. Verschiedenste Reaktionsbedingungen führen sowohl zum Methylcarbonat als auch zum 2- oder 4-Carboxylat. Ein Trend, welche Verbindung unter welchen Bedingungen bevorzugt ist, lässt sich kaum ausmachen. Ausschließlich das Auftreten des primär gebildeten Methylcarbonats scheint mit der Verwendung von Methanol als Lösungsmittel assoziiert. Die Literaturvorschriften zu 1-Alkyl-3-methyl-imidazolium-carboxylaten wurden mit den wichtigsten Reaktionsparametern in Tabelle 1.1 zusammengestellt.

Tabelle 1.1. *Zusammenstellung von Literaturberichten über die Darstellung von 1-Alkyl-3-methyl-imidazolium-carboxylaten. Darstellungsmethoden aus dem freien Carben wurden nicht berücksichtigt.*

R-1	CO_2-Pos.[a]	T/ °C	t/ h	LM (/%)[b]	Aufarbeitung / Bemerkung	Ref.
Bu/ Et	2	25	48−72	[BMIm] oder [EMIm][OAc]	Einleitung von CO_2 in z. B. 1-Ethyl-3-methylimizolium-acetat	[60]
Me	2	90	30	ohne	Filtration, Waschen mit CH_2Cl_2, Aceton, Et_2O	[61]
Me	2	95	48	ohne	Filtration, Waschen mit Et_2O	[62]
Me	4	120	30	ohne	Filtration, Waschen mit CH_2Cl_2, Aceton, Et_2O	[61]
Me	2	120	50	ohne	Filtration, nur 5% Ausbeute	[63]
Me	4	120	7	ohne	Filtration, Umkristallisation aus EtOH, 19% Ausbeute	[63]
Me	2	120	24	MeOH (k. A.) oder ohne	k. A.	[64]
Me	OMe : 2 (2:1)[c]	120	24	MeOH (15)	Einengen im Vakuum	[59g]
Me	4	140	20	ohne	Umkristallisation aus 1:1 MeOH/EtOH	[65]
Me	2	140	7	MeOH (57)	Einengen im Vakuum, Waschen mit Et_2O, >500 eq Dimethylcarbonat	[66]
Bu	OMe : 2 (4:1)[c]	150	3−12	MeOH (37)	Reaktionsmischung analysiert	[59j]
Me	2	200	0.3	MeOH (61)	Durchflussreaktor mit Al_2O_3 Katalysator, Reaktionsmischung analysiert	[67]

a) Position gemäß der Strukturformel in Schema 1.5, b) Anteil des Lösungsmittels an der Reaktionsmischung in Gewichts-%, c) Mischung aus Methylcarbonatanion (OMe) und C2-Carboxylat im Verhältnis (2:1 bzw. 4:1).

1.2.4 Ionische Flüssigkeiten mit Chalkogenid-Anionen

Vor allem Schwefel ist zwar ein prominenter Bestandteil zahlreicher ILs besitzt aber äußerst selten eine reaktive Position. Sowohl als Teil des Kations in zum Beispiel Sulfonium oder Thiouronium ILs, als auch in Anionen wie (Alkyl)Sulfaten, Sulfonaten und Sulfonimiden tritt Schwefel nur als Koordinationszentrum auf. Die Eigenschaften der Verbindungen werden primär von den Substituenten gesteuert. Die diesbezüglich lange Zeit einzige Ausnahme stellte das Thiocyanatanion dar. Einzelne Vertreter der Reihe der Tetralkylammonium-hydrogensulfide sind zwar schon seit den 1960er Jahren bekannt, wurden jedoch primär als wässrige oder alkoholische Lösung gehandhabt und nie im Detail charakterisiert.[68] Tatsächliche ILs mit sehr nukleophilen Hydrogensulfidanionen wurden 2011 zum ersten Mal beschrieben.[38, 69] Ausgehend von *N*-Butyl-*N*-methylpyrrolidinium-chlorid ([BMPyr]Cl) und Natriumsulfid-nonahydrat wurde [BMPyr][HS] nach aufwendiger Reinigung als gelbliches Öl isoliert (Schema 1.6). Die Substanz wurde zur Auflösung von Schwefel verwendet und das resultierende Polysulfid als Redoxmediator in Quantenpunkt Solarzellen getestet.[36b]

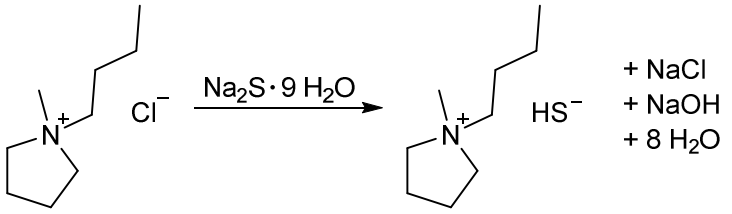

Schema 1.6. *Synthese von [BMPyr][HS] nach* JOVANOVSKI *et al.*[38]

Nur kurze Zeit später berichtete eine zweite Forschergruppe über ähnliche Versuche mit Tetramethylammonium- und 1,2-Dimethyl-3-propylimidazolium-Kationen.[35-36] Die Autoren geben an, Salze mit Sulfid-dianionen isoliert zu haben, was vor dem Hintergrund der wässrigen Reaktionsbedingungen, der sehr hohen Basizität des Sulfid-Dianions und der Instabilität von Imidazoliumkationen gegenüber nukleophilem Angriff jedoch zweifelhaft scheint. Des Weiteren beschrieben die Wissenschaftler ein Bis(tetramethylammonium)-pentasulfid in Form von farblosen Kristallen erhalten zu haben.[36a] Diese Beobachtung steht im Widerspruch zu zahlreichen anderen Publikationen, in denen jegliche Polysulfide mit einer Kettenlänge von mehr als zwei Schwefelatomen deutlich gelb bis hin zu rot gefärbt sind.[70] Trotz zweifelhafter Zusammensetzung wurden die synthetisierten Polysulfide als Redoxmediatoren für in diesem Fall Farbstoffsolarzellen erfolgreich getestet. Dies unterstreicht das bisher kaum ausgeschöpfte wissenschaftliche und wirtschaftliche Potential dieser Verbindungsklasse. In mehreren weiteren Fällen wurden Polysulfidsalze mit organischen Kationen als unerwartete Nebenprodukte isoliert und primär kristallographisch untersucht.[71] Gezielte Synthesen für organische Polysulfidsalze gehen von wässrigen Bedingungen aus und finden sich z. B. für Tetraphenylphosphonium und Tetraphenylarsoniumkationen[72] oder Tetrabutylammoniumkationen.[73] ILs mit Hydrogenselenid- oder Hydrogentelluridionen wurden bisher kaum beschrieben. Bereits Anfang der 1990er Jahre wurden Tetramethyl- und Tetrabutylammoniumsalze von HSe^- und HTe^- durch die Umsetzung von Tetrahydridoboraten mit den elementaren Chalkogenen synthetisiert und umfassend charakterisiert.[74] Daneben existieren aber ausschließlich Berichte über Polychalkogenidanionen mit organischen oder Komplexkationen.[75]

1.3 5,5'-Bistetrazol

1.3.1 Verbindungen und Derivate des 5,5'-Bistetrazols

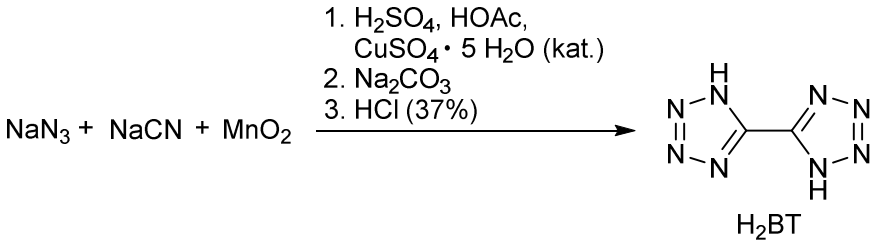

Schema 1.7. *Synthese von 5,5'-Bistetrazol nach* FRIEDERICH.[76]

5,5'-Bistetrazol (H_2BT) wurde bereits 1913 beschrieben fand aber bis in die 1990er Jahre kaum tiefergehende Beachtung.[8, 77] Im Verlauf des Jahrhunderts wurden jedoch sein energetisches Potential erkannt und patentiert (1922/24),[78] eine verlässliche Synthese entwickelt und optimiert (1956 und 1986, Schema 1.7),[76, 79] das Säure-Base-Verhalten (1981)[80] und auch die ^{13}C und ^{15}N NMR Spektren untersucht (1986),[79] sowie schließlich erste Übergangsmetallkomplexe und alkylsubstituierte Derivate hergestellt und die Kristallstruktur von H_2BT aufgeklärt (1995/96).[81] Erst seit den 1990er Jahren finden sich vermehrt Veröffentlichungen mit dieser Verbindung, die jedoch zum größten Teil Patentanmeldungen zu Explosiv- und Zündstoffen darstellen. Auf diese Patentanmeldungen soll an dieser Stelle nicht weiter eingegangen werden. Auch bei den Veröffentlichungen zu 5,5'-Bistetrazol in Fachzeitschriften wird die Forschung im Bereich der hochenergetischen Substanzen fokussiert. So untersuchten CHAVEZ *et al*. das thermische Zersetzungsverhalten von 5,5'-Bistetrazol und diverser BT-Salze mit z. B. Ammonium-, Hydrazinium- und Metallkationen auf der Suche nach wenig Rauch produzierender Pyrotechnik.[82] Die Gruppe um SHREEVE untersuchte unter anderem auf dem BT-Anion basierende Ionische Flüssigkeiten mit dem Ziel energiereiche Substanzen mit hoher Dichte zu generieren, die aber gleichzeitig eine für die gefahrlose Handhabung ausreichende kinetische Stabilität besitzen.[83] KLAPÖTKE und Mitarbeiter suchen stattdessen nach besonders effektiven Explosivstoffen. Im Zuge dessen wurden einerseits zahlreiche BT-Salze untersucht,[84] andererseits aber auch das Bistetrazol-Grundgerüst mit Hydroxyl-, Amino- und Nitraminogruppen derivatisiert.[85] H_2BT und seine Verbindungen wurden außerdem in theoretischen Studien bezüglich Ihres Zersetzungsverhaltens untersucht.[86] Im Gegensatz dazu wurde das Koordinationsverhalten von H_2BT bisher nur mit untergeordneter Relevanz betrachtet. Die ersten Übergangsmetallkomplexe wurden nicht strukturell charakterisiert,[81a] weshalb die ersten detaillierten Informationen über das Koordinationsverhalten aus einer Reihe von Salzen mit

Seltenerdmetallkationen gewonnen werden konnten.[87] In der Folgezeit wurden fernerhin ein Kupfersalz[88] und die Reihe der Erdalkalimetallsalze röntgenkristallographisch untersucht.[84a] Es finden sich chelatisierende, monodentate und gemischte Koordinationsweisen (Abb. 1.6). Zusätzlich ist das BT-Anion in Wasserstoffbrückenbindungen involviert.

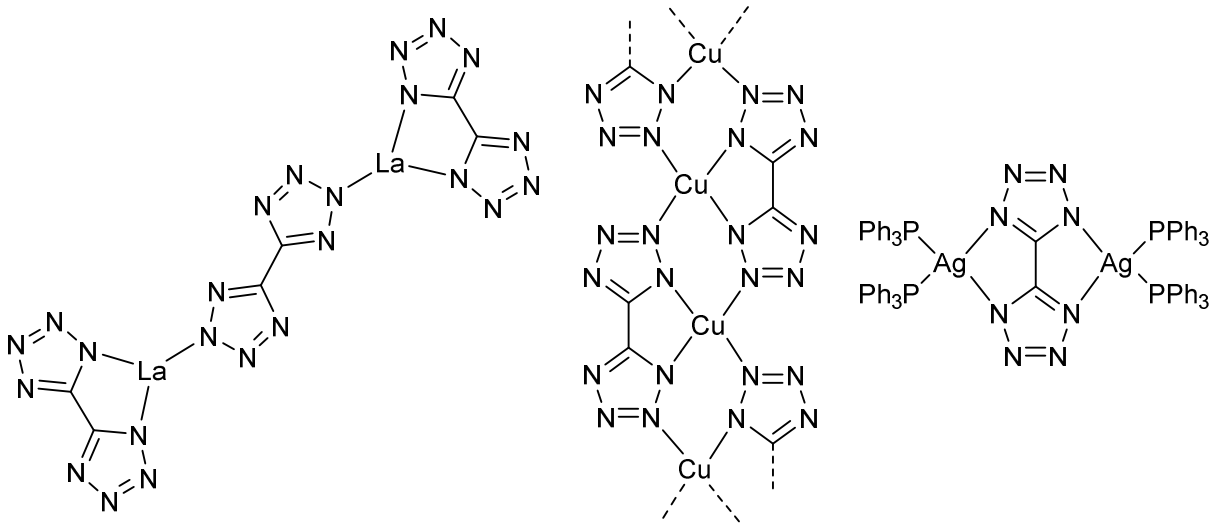

Abbildung 1.6. *Beispiele für röntgenkristallographisch charakterisierte Koordinationsverbindungen des 5,5'-Bistetrazol mit Lanthan,[87a] Kupfer[88] und Silber.[8] Während die ersten beiden Strukturen hydratisiert vorliegen (Aqua-Liganden sind nicht abgebildet), stellt der Silberkomplex eine molekulare wasserfreie Verbindung dar.*

Im Rahmen der eigenen Masterarbeit konnten mehrere Alkalimetallsalze und außerdem die ersten molekularen Übergangsmetall-BT-Komplexe strukturell charakterisiert werden.[8] Eine weitere Untersuchung des Koordinationsverhaltens von 5,5'-Bistetrazol scheint auch vor dem Hintergrund der Bioisosterie von Carboxylat- und Tetrazolatgruppen sehr interessant.

1.3.2 Das Konzept der Bioisosterie am Beispiel von Tetrazolat und Carboxylat

Das Bioisosteriekonzept beschreibt die biologisch-chemisch ähnliche Wirkung von zwei Resten. Konkret werden ähnliche sterische und elektronische Eigenschaften, ähnliche Hydro- bzw. Lipophilie, ähnliche chemische Reaktiviät und ähnliche Einflüsse auf den Molekülrest als Kriterien für Bioisosterie genannt.[8, 89] Dieses Konzept ist neben der ganzheitlichen quantitativen Struktur-Wirkungs-Beziehung (QSAR) ein wichtiges Instrument bei der Variierung und Optimierung von Wirkstoffen; dies zeichnet sich auch in der Einrichtung einer eigenen BIOSTER-Datenbank ab.[90]

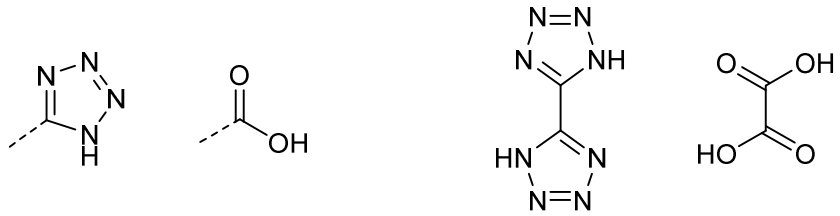

Abbildung 1.7. *Tetrazol und Carbonsäuregruppen werden als Bioisostere häufig gegeneinander ausgetauscht, um medizinische Wirkstoffe ähnlichen Wirkungsmusters zu gewinnen. Eine entsprechende grundsätzliche Ähnlichkeit findet sich auch zwischen 5,5'-Bistetrazol und Oxalsäure.*

Ein besonders prominenter und häufig erfolgreich angewandter bioisosterer Austausch ist der einer Carboxylatgruppe gegen eine Tetrazolatgruppe (Abb. 1.7).[14] Diese beiden Substituenten weisen eine sehr ähnliche Azidität, und Planarität auf; bei Elektronendelokalisation, H-Brücken Donor- und Akzeptorfähigkeit sowie Lipophilie gibt es aufgrund des Größenunterschiedes etwas stärkere Abweichungen.[91] Zusätzlich weist der Tetrazolatring eine höhere metabolische Stabilität als eine Carboxylatgruppe auf.[92]

Eine entsprechend hohe grundsätzliche Ähnlichkeit findet sich auch zwischen Oxalsäure und 5,5'-Bistetrazol. Z. B. wirken beide als zweiprotonige ungefähr gleich starke Säuren (Oxalsäure: pKs_1: 1.23, pkS_2 4.19, Bistetrazol: pKs_1: 1.41, pkS_2 4.25).[80] Aufgrund eingeschränkter Substitutionsmöglichkeiten, ist diese potentielle Bioisosterie jedoch im Bereich organischer Moleküle von geringer Bedeutung und wurde noch nicht untersucht. Im Rahmen der eigenen Masterarbeit wurden jedoch zu bekannten Koordinationsverbindungen der Oxalsäure analoge BT-Komplexe synthetisiert.[8] Ob diese eine ähnliche biologische Wirkung aufweisen, wurde noch nicht untersucht.

2 Aufgabenstellung

Ionische Flüssigkeiten und organische Salze mit Chalkogenidanionen waren bisher nur mit zweifelhafter Reinheit oder in aufwendigen Verfahren zugänglich. Auf dieser Ausgangslage basierend bestand das primäre Ziel der vorliegenden Arbeit in der Ausarbeitung eines verlässlichen und möglichst breit anwendbaren synthetischen Zuganges zu Chalkogenid-ILs (Schema 2.1). Im Hinblick auf potentielle elektrochemische Anwendungen, galt es besonders Halogenid- und Metallverunreinigungen so weit wie möglich zu vermeiden. Potentiell geeignete Ausgangsverbindungen sind Methylcarbonatsalze, die mit den Brønsted-sauren Chalkogenwasserstoffen H_2S, H_2Se und H_2Te reagieren sollten.

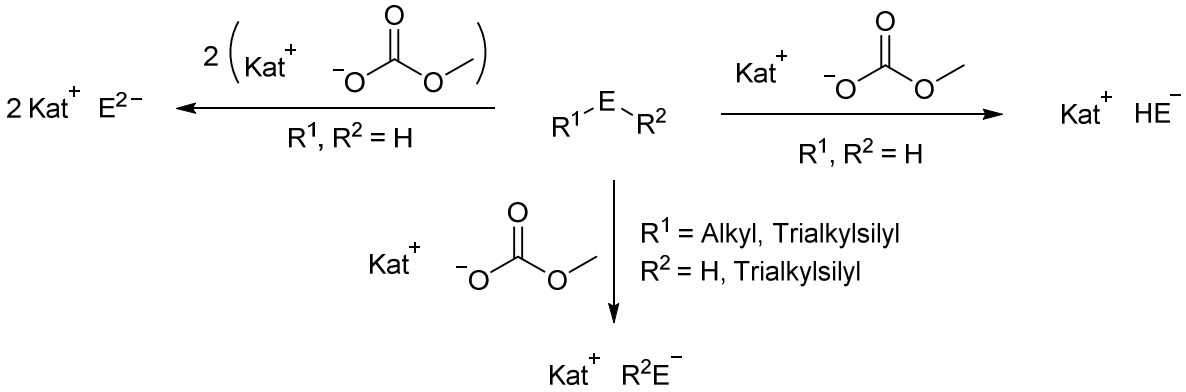

Schema 2.1. *Geplante Synthese von Chalkogenidbasierten Ionischen Flüssigkeiten; E = S, Se, Te.*

Neben der Synthese und Aufreinigung, sollte auch die umfassende Charakterisierung der neuen Substanzen im Vordergrund stehen, da bisher nur wenige Referenzdaten verfügbar sind. Besonders die Anion-Kation-Wechselwirkung sollte anhand von Kristallstrukturen und darauf aufbauend in theoretischen Rechnungen (Kooperation mit der Arbeitsgruppe Prof. Dr. BERGER) ergründet werden. Auch das Schmelz- und Zersetzungsverhalten sollte im Detail untersucht werden.

Vor dem Hintergrund der zukunftsträchtigen Verwendung von Polysulfidsalzen mit organischem Kation als Redoxsystem in Farbstoff- und Quantenpunkt-sensibilisierten Solarzellen, aber bisher teilweise fragwürdigen Berichten zu deren Synthese, sollte das Reaktionsverhalten von Sulfid-ILs mit elementarem Schwefel untersucht werden (Schema 2.2). Für den potentiellen Einsatz in Solarzellen sind besonders das elektrochemische Verhalten und die Absorptionseigenschaften im UV-Vis-Bereich relevant.

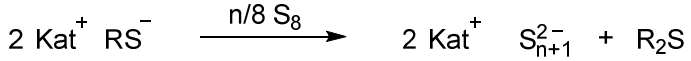

Schema 2.2. *Geplante Synthese von Polysulfid ILs (R = H, Me_3Si).*

Methylcarbonatsalze mit organischen Kationen sind eine wertvolle Ausgangssubstanz für zahlreiche Ionische Flüssigkeiten. Im Fall von Imidazoliumkationen gibt es jedoch mehrere abweichende und teilweise widersprüchliche Berichte zur Bildung von Imidazolium-Carboxylat-Zwitterionen. Da eine genaue Kenntnis der Ausgangssubstanzen essentiell für die Synthese reiner Verbindungen ist, sollten weiterführende Versuche zu den Entstehungsbedingungen der Carboxylate ein zweiter Schwerpunkt der vorliegenden Arbeit sein. So sollte auch untersucht werden, ob der Einsatz von in der besonders aziden C2-Position durch eine Methylgruppe geschützten Imidazoliumkationen diese Nebenreaktion wirksam einschränkt. Analog zur Bildung von 1,3-Dialkylimidazolium-2-carboxylaten über ein N-heterozyklisches Carben (NHC), ist hier die intermediäre Bildung eines N-heterozyklischen Olefins (NHO) oder eines atypischen NHCs denkbar (Schema 2.3).

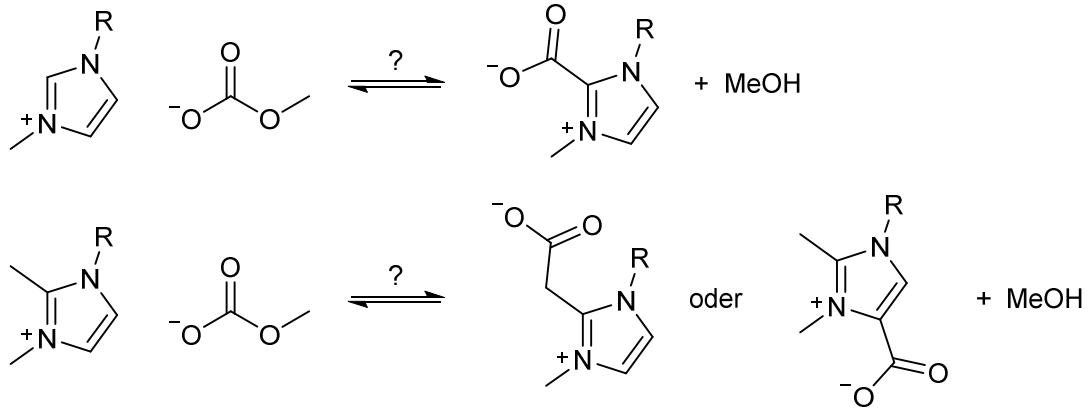

Schema 2.3. *Zu untersuchende Bildung von Imidazoliumcarboxylat-Zwitterionen aus Imidazolium-Methylcarbonat-Salzen; R = Alkyl.*

Um Nebenprodukte, die durch diese potentiellen Verunreinigungen der Ausgangssubstanzen entstehen, identifizieren und abtrennen zu können, sollten die Carboxylate auf ihre Reaktivität gegenüber verschiedenen Schwefeledukten und elementaren Chalkogenen untersucht werden (Schema 2.4).

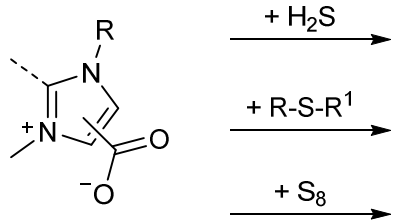

Schema 2.4. *Imidazoliumcarboxylate sollten auf ihre Reaktivität, besonders gegenüber Schwefelreagenzien untersucht werden; R, R^1 = H, Alkyl, Trialkylsilyl.*

Im dritten Teil sollten Arbeiten zur Gewinnung ionischer Batterieadditive und potentieller *Solid Electrolyte Interface* (SEI) Bildner aus der eigenen Masterarbeit fortgeführt und ausgeweitet werden. Zunächst bestand die Aufgabe, die bereits begonnene Reihe der Alkalimetall-Bistetrazolsalze zu vervollständigen um das Koordinationsverhalten des BT-Anions im Verhältnis zur Kationengröße analysieren zu können. Zusätzlich sollte versucht werden, Bistetrazolsalze mit nicht koordinierenden Kationen herzustellen, um Vergleichswerte für ein unkoordiniertes Anion zu erhalten (Schema 2.5).

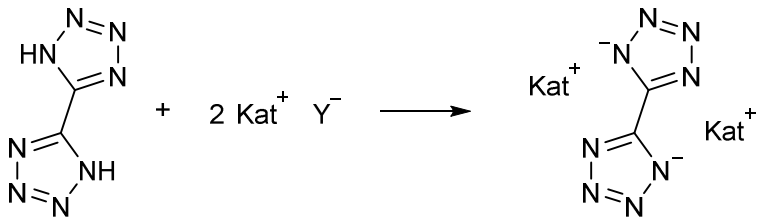

Schema 2.5. *Geplante Synthese von Bistetrazolatsalzen; Kat = Na, Rb, Imidazolium; Y = HO, HCO_3, OCO_2Me.,*

Ebenso in direkter Fortführung der Arbeiten aus der Masterarbeit – beruhend auf der potentiellen Bioisosterie zwischen Oxalsäure und 5,5'-Bistetrazol − wurden abschließende Versuche zu den ursprünglich angestrebten Bistetrazolat-Bor-Verbindungen geplant (Abb. 2.1). Nach Möglichkeit sollten die im Rahmen der Masterarbeit beobachteten Produktfragmente isoliert und näher analysiert werden.

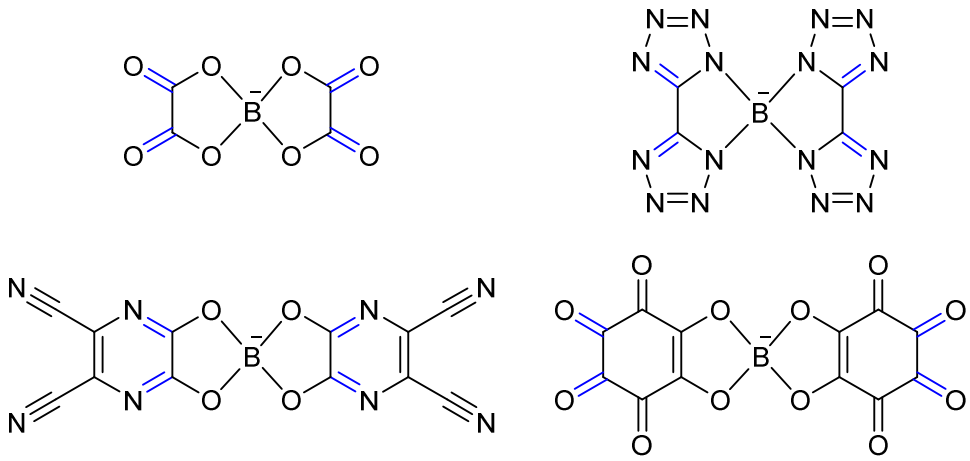

Abbildung 2.1. *Das prominente Bis(oxalato)boratanion und die angestrebten neue Boratanionen als Bestandteile neuer ILs oder als Additive für Lithium-Elektrolyt-Lösungen; rechts oben: Di(bistetrazolato)borat, links unten: Bis(pyrazin-5,6-dicarbonitril-2,3-diolato)borat, rechts unten: Bis(rhodizonato)borat.*

Als letzter Teilaspekt waren sondierende Versuche, zur Synthese von Pyrazindiolato- und Rhodizonato-boratanionen geplant (Abb. 2.1). Diese Liganden wurden gewählt, da sie erweiterte Strukturvarianten der Oxalsäure darstellen. Das 2,3-Dioxo-pyrazin-5,6-dicarbonitril stellt ein zyklisches Oxalsäurediamid und eine elektronenarme Catechol-Variante dar. Rhodizonsäure ist wie die Oxalsäure ein Vertreter aus der Reihe der Oxokohlenstoffsäuren. Die Lithiumsalze der entsprechenden Borate könnten Alternativen zu dem prominenten Elektrolytadditiv Lithium-bis(oxalato)borat (LiBOB) für Lithium-Ionen-Akkumulatoren sein, während Salze mit organischen Kationen Klassen neuer Ionischer Flüssigkeiten begründen sollen.

3 Kumulativer Teil

3.1 Zugang zu reinen und sehr flüchtigen Hydrogenchalkogenid Ionischen Flüssigkeiten

Chem. Commun. **2015**, **51**, 16169−16172

Access to pure and highly volatile hydrochalcogenide ionic liquids

Lars H. Finger, Fabian Wohde, Evgeny I. Grigoryev, Anna-Katharina Hansmann, Robert Berger, Bernhard Roling, Jörg Sundermeyer

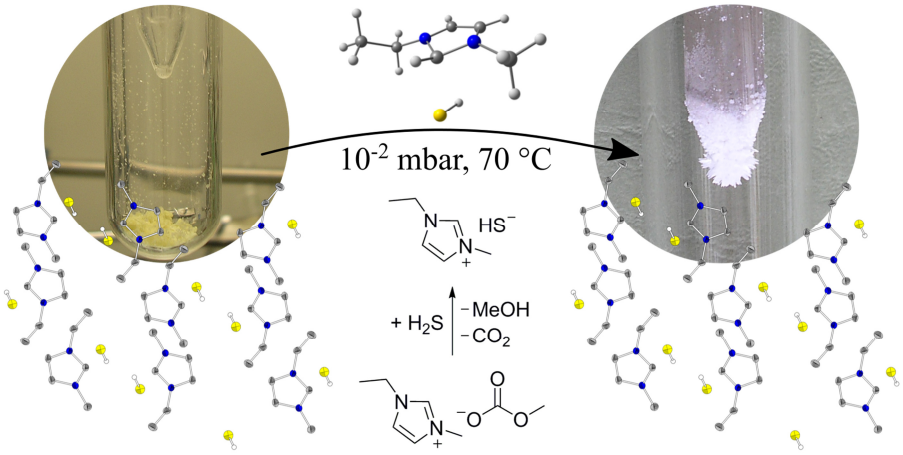

Ausgehend von den entsprechenden Methylcarbonatsalzen wurden Hydrogensulfid und Hydrogenselenidsalze mit Imidazolium- und Pyrrolidiniumkationen synthetisiert. Die angewandte Synthesestrategie zeichnet sich dadurch aus, dass die einfach zugänglichen Methylcarbonatvorläufer mit den aziden Reagenzien Schwefel- und Selenwasserstoff unter irreversiblem Zerfall zu Methanol und Kohlenstoffdioxid reagieren während die Zielverbindung die einzige geringflüchtige Komponente darstellt. Das hier vorgestellte Verfahren ist literaturbekannten Alternativen hinsichtlich der Reinheit der Produkte und des zeitlichen und materiellen Aufwandes deutlich überlegen. So war es zum Beispiel möglich *n*-Butyl-methylpyrrolidinium-hydrogensulfid, das zuvor als gelbes Öl beschrieben wurde, als farblosen Feststoff mit einem Schmelz und Zersetzungspunkt von 153 °C zu isolieren und dessen Struktur mittels Röntgenstrukturanalyse zu bestimmen. Bei weiterführenden Versuchen zu den Eigenschaften der Substanzen stellte sich heraus, dass die Imidazolium-hydrogensulfide und -selenide eine für aprotische ILs äußerst ungewöhnlich hohe Flüchtigkeit

aufweisen, die ihre Sublimation bei $1 \cdot 10^{-2}$ mbar und Temperaturen unterhalb von 100 °C ermöglicht. Als Aufreinigungsmethode angewendet, erlaubt die Sublimation der Substanzen die Präparation von hochreinen Proben. Im weiteren Verlauf wurden in Kooperation mit FABIAN WOHDE (Arbeitsgruppe Prof. Dr. ROLING) die Verdampfungsenthalpien der Substanzen mittels isothermer TGA-Experimente bestimmt. Es zeigte sich, dass die Verdampfungsenthalpien in der Größenordnung bekannter flüchtiger ILs liegen, dass aber die Dampfdrücke bei einer gegebenen Temperatur deutlich höher sind als die anderer ILs. In Kooperation mit EVGENY GRIGORYEV und ANNA-KATHARINA HANSMANN (Arbeitsgruppe Prof. Dr. BERGER) wurden mittels DFT-Rechnungen die stabilsten Ionenpaare, das Bindungsverhältnis zwischen Anion und Kation, experimentell gefundene und weitere mögliche Zerfallswege und die Sublimationsenthalpien berechnet. Die Resultate weisen darauf hin, dass die flüchtige Gasphasenspezies ein Kontaktionenpaar ist und die Flüchtigkeit nicht auf intermediär gebildete Neutralverbindungen zurückgeht. Die berechneten Sublimationsenthalphien zeigen eine sehr gute Übereinstimmung mit den experimentell bestimmten Werten.

Erklärung der Eigenleistung

Der größte Teil der synthetischen und analytischen Arbeiten wurden von mir persönlich im Rahmen meiner Doktorarbeit durchgeführt. Die Synthese von 1-Ethyl-2,3-dimethylimidazolium-hydrogensulfid erfolgte durch PHILIPP HOFMANN im Rahmen eines Forschungspraktikums unter meiner Anleitung. Die Aufnahme einzelner NMR-Spektren, der Massenspektren, die Durchführung der Elementaranalysen und die Kristalldatensammlung erfolgten durch die Serviceabteilungen des Fachbereiches Chemie. Die Vorbereitung und Durchführung der TGA-Experimente geschah gemeinsam mit FABIAN WOHDE, der die anschließende Auswertung vollständig übernahm. Alle quantenchemischen Berechnungen wurden von EVGENY GRIGORYEV und ANNA-KATHARINA HANSMANN durchgeführt. Das Manuskript wurde von mir verfasst, die dazugehörige *Supporting Informationen* wurde mit Ausnahme des von FABIAN WOHDE formulierten Abschnittes zu den TGA-Experimenten ebenfalls von mir erstellt. Für die Abschnitte zu den quantenchemischen Rechnungen diente ein Forschungsbericht von ANNA-KATHARINA HANSMANN als Vorlage. Alle Autoren beteiligten sich mit detaillierten Korrekturen an der Fertigstellung des Manuskriptes. Die wissenschaftliche Fragestellung und der jeweilige Projektfortschritt wurden mit den Betreuern Prof. Dr. JÖRG SUNDERMEYER, Prof. Dr. BERNHARD ROLING und Prof. Dr. ROBERT BERGER intensiv diskutiert.

3.2 Halogenidfreie Synthese von Hydrogenchalkogenid Ionischen Flüssigkeiten des Typs [Kation][HE] (E = S, Se, Te)

Chem. Eur. J. **2016**, DOI: 10.1002/chem.201504577, *in press*

Halide Free Synthesis of Hydrochalcogenide Ionic Liquids of the Type [Cation][HE] (E = S, Se, Te)

Lars H. Finger, Jörg Sundermeyer

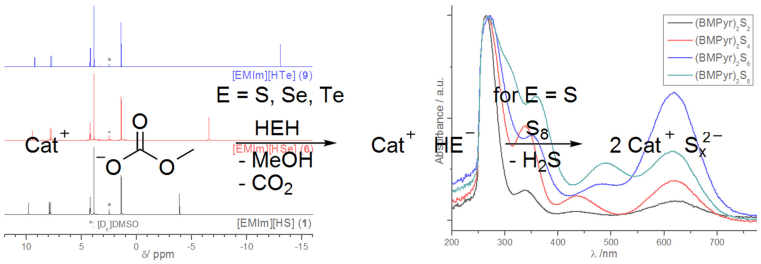

Die bereits im Manuskript von Abschnitt 3.1 vorgestellte Synthesestrategie zu Herstellung von Hydrogenchalkogenid-ILs wurde nun auch auf Hydrogentelluridanionen erweitert und mit einer größeren Reihe verschiedener Kationen realisiert. Die elf präsentierten Hydrogenchalkogenidsalze wurden vollständig charakterisiert und Trends vor allem innerhalb der homologen Reihe herausgearbeitet. Besonders charakteristisch sind die jeweiligen Wellenzahlen der H−E Streckschwingung im IR-Spektrum (ν(H−S) = 2561 cm^{-1}, ν(H−Se) = 2286 cm^{-1}, ν(H−Te) = 1988 cm^{-1}) und die chemische Verschiebung des Protons des HE^- Anions im ^{1}H NMR-Spektrum ($\delta_H(HS^-)$ = −3.9 ppm, $\delta_H(HSe^-)$ = −6.6 ppm, $\delta_H(HTe^-)$ = −13.0 ppm). Die Kristallstrukturen von Imidazolium-hydrogenchalkogeniden zeichnen sich durch ein Netzwerk von Wasserstoffbrückenbindungen aus. Im zweiten Teil des Manuskriptes wurden durch die Umsetzung von Hydrogensulfidsalzen mit verschiedenen Mengen Schwefel Polysulfidsalze ($[Cat]_2S_n$) mit unterschiedlichen mittleren Polysulfidkettenlängen (n = 2, 4, 6, 8) synthetisiert. Es zeigte sich, dass diese Reaktionen erst bei höherem Schwefelüberschuss vollständig ablaufen und andernfalls ein deutlicher Anteil Hydrogensulfidanionen zurückbleibt. Die Polysulfidsalze wurden mittels UV-Vis-Spektroskopie, Cyclovoltammetrie und kombinierter UV-Vis-Chronoamperometrie untersucht. Die vorherige Beobachtung bezüglich der Hydrogensulfidreste in kurzkettigen Polysulfidsalzen (n = 2, 4) bestätigte sich in den Cyclovoltammogrammen. Erst bei höheren Kettenlängen (n = 6, 8) zeigte sich ein reversibles Redoxverhalten, während vor allem beim angestrebten Disulfidsalz das Voltammogramm

dem des Hydrogensulfidsalzes weitestgehend entsprach. Durch spektroelektrochemische Experimente am Hexasulfidsalz, die vor allem Konzentrationsänderungen des Trisulfid-Radikalanions deutlich zeigten, und durch den Vergleich mit den UV-Vis-Spektren der Reihe der Polysulfidsalze konnten die elektrochemischen Prozesse einzelnen Redoxreaktionen zugeordnet werden.

Erklärung der Eigenleistung

Die präparativen und analytischen Arbeiten wurde weitestgehend von mir persönlich im Rahmen meiner Dissertation durchgeführt. Die Synthese von 1-Ethyl-2,3-dimethylimidazolium-hydrogensulfid erfolgte durch PHILIPP HOFMANN im Rahmen eines Forschungspraktikums unter meiner Anleitung. Erste Versuche zur Umsetzung von Schwefelwasserstoff mit 1-Ethyl-3-methylimidazolium-methylcarbonat erfolgten durch DEJAN PREMUŽIĆ im Rahmen eines Forschungspraktikums. Die Aufnahme einzelner NMR-Spektren, der Massenspektren, die Durchführung der Elementaranalysen und die Kristalldatensammlung erfolgten durch die Serviceabteilungen des Fachbereiches Chemie. Dr. GÜNTHER THIELE führte einzelne Langzeit ^{125}Te NMR-Messungen durch. Das Manuskript und die *Supporting Information* wurden von mir verfasst. Mit meinem Betreuer Prof. Dr. JÖRG SUNDERMEYER wurden die wissenschaftliche Fragestellung und die Ergebnisse intensiv diskutiert.

3.3 Synthese organischer Trimethylsilylchalkogenolatsalze Cat[TMS−E] (E = S, Se, Te): Das Methylcarbonatanion als Desilylierungsreagenz

Inorg. Chem. **2015**, *54*, 9568−9575

Synthesis of Organic (Trimethylsilyl)chalcogenolate Salts Cat[TMS-E] (E = S, Se, Te): the Methylcarbonate Anion as a Desilylating Agent

Lars H. Finger, Benjamin Scheibe, Jörg Sundermeyer

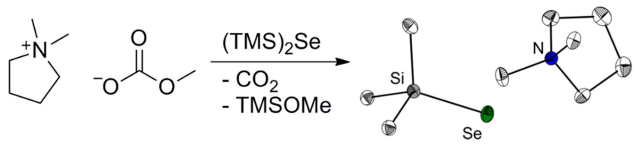

Die Umsetzung von Methylcarbonatsalzen mit Bis(trimethylsilyl)chalkogeniden unter strikt aprotischen Bedingungen liefert die Klasse der Trimethylsilylchalkogenolate mit organischen Kationen. Diese Synthesestrategie ist auf alle höheren Chalkogene (S, Se, Te) und eine Vielzahl von Kationen anwendbar. Die einzige bereits bekannte Substanz, Tetramethylammonium-trimethylsilylthiolat, wurde zuvor ausgehend von Tetramethylammonium-fluorid hergestellt. Die Verwendung von Methylcarbonatanionen als Desilylierungsreagenz ist im Vergleich mit dem Einsatz von Fluoridanionen wegen der geringeren Toxizität, selektiveren Reaktivität und der einfacheren Synthese der Startmaterialien deutlich zu bevorzugen. Die prinzipielle Möglichkeit, Methylcarbonatanionen zur Desilylierung zu verwenden wurde im Rahmen dieser Publikation erstmalig beschrieben und außerdem erfolgreich auf Trimethylsilylcyanid und -azid übertragen. Die acht neuen Trimethylsilylchalkogenolatsalze wurden umfassend analysiert und charakterisiert. Darunter sind die ersten strukturell charakterisierten unkoordinierten Trimethylsilylchalkogenolate. Es zeigte sich, dass alle ammoniumbasierten Salze nur unter Zersetzung schmelzen, aber z. B. mit einem Tri-*n*-butyl-methylphosphonium-kation auch bereits bei Raumtemperatur flüssige ILs zugänglich sind. Die Trimethylsilylthiolate erwiesen sich als sehr gute Ausgangsstoffe zur Synthese von Hexasulfidsalzen mit organischen Kationen. Die röntgenkristallographische Charakterisierung des Polyselenidsalzes Bis-(*n*-butyl-methylpyrrolidinium)-triselenid und des Polytelluridsalzes Tetrakis-(dimethylpyrrolidinium)-dodecatellurid, die als Zerfallsprodukte der Silylchalkogenolate

entstanden, lässt erwarten, dass dieses Verfahren auch auf die höheren Homologen anwendbar sein wird.

Erklärung der Eigenleistung

Der präparativen und analytischen Arbeiten wurden größtenteils von mir persönlich im Rahmen meiner Dissertation durchgeführt. Tri-*n*-butyl-methylphosphonium-trimethylsilylthiolat wurde erstmals von BENJAMIN SCHEIBE im Rahmen seiner von mir betreuten Bachelorarbeit synthetisiert.[93] Außerdem erfolgte die Synthese der Substanz, aus der Einkristalle von Bis-(*n*-butyl-methylpyrrolidinium)-triselenid gewonnen wurden, durch BENJAMIN SCHEIBE im Rahmen eines Forschungspraktikums unter meiner Anleitung. JANNICK GUSCHLBAUER synthetisierte und analysierte im Rahmen eines Forschungspraktikums unter meiner Anleitung Dimethylpyrrolidinium-trimethylsilylselenolat. Die Aufnahme einzelner NMR-Spektren, die Durchführung der Elementaranalysen und die Kristalldatensammlung erfolgten durch die Serviceabteilungen des Fachbereiches Chemie. Das Manuskript und die *Supporting Information* wurden von mir verfasst. Mein Betreuer Prof. Dr. JÖRG SUNDERMEYER begleitete die Arbeiten als Ideengeber und Diskussionspartner.

3.4 Kohlenstoffdioxid- und Schwefeldioxid-Addukte von N-heterozyklischen Olefinen: Strukturen und interessante Reaktivitätsmuster

in preparation

N-Heterocyclic Olefin – Carbon Dioxide and Sulfur Dioxide Adducts: Structures and Interesting Reactivity Patterns

Lars H. Finger, Jannick Guschlbauer, Klaus Harms, Jörg Sundermeyer

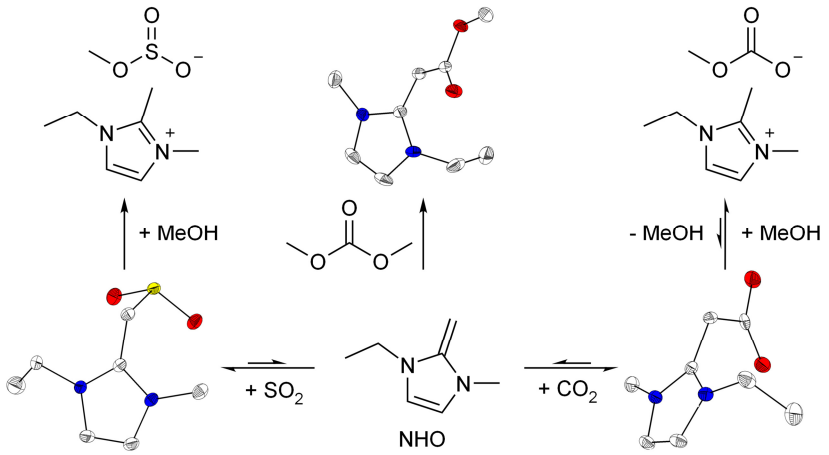

Die Bildung von CO_2 Addukten von N-heterozyklischen Carbenen und Olefinen (NHC-CO_2 bzw. NHO-CO_2 Addukte) aus den jeweiligen Imidazolium-methylcarbonatsalzen wurde detailliert untersucht. Es wurde gezeigt, dass sich bereits bei Raumtemperatur ein Gleichgewicht zwischen dem Methylcarbonatsalz und dem Imidazolium-Carboxylat-Zwitterion einstellt. In Folge wurde das Reaktionsverhalten des NHO-CO_2 Adduktes näher untersucht. Während mit schwachen Säuren die angestrebten Imidazoliumsalze entstehen, bilden sich mit starken Säuren protonierte CO_2 Addukte als Zwischenprodukte, die erst beim Erhitzen CO_2 abspalten und in die Imidazoliumsalze übergehen. Dies kann auf die Nukleophilie der jeweiligen konjugierten Base zurückgeführt werden. Starke Säuren, die wenig nukleophile Basen liefern, führen erst bei erhöhten Temperaturen zu einer Decarboxylierung des protonierten NHO-CO_2 Adduktes. Schwache Säuren mit nukleophilen Basen erlauben die Decarboxylierung bereits bei Raumtemperatur. Des Weiteren konnte im Rahmen der Carboxylierung der CH-Säure Acetonitril zu einem Cyanoacetatanion die erste C-C Bindungsknüpfung ausgehend von einem NHO-CO_2 Addukt beobachtet werden. Die Umsetzung des NHO-CO_2 Adduktes mit Dimethylcarbonat lieferte ein durch eine Methoxycarbonylgruppe stabilisiertes NHO, das ausgehend vom freien NHO und Dimethylcarbonat in höchster Selektivität zugänglich ist. Ausblickhaft wurde die Synthese

und Charakterisierung des ersten NHO-SO_2 Adduktes sowie dessen Umsetzung mit Methanol zu einem Imidazolium-Methylsulfitsalz vorgestellt. Konkurrenzexperimente zeigten, dass das NHO-SO_2 Addukt auch noch bei 50 °C stabil gegenüber CO_2 ist, das NHO-CO_2 Addukt jedoch bei Raumtemperatur mit SO_2 zum entsprechenden SO_2-Addukt reagiert.

Erklärung der Eigenleistung

Das Manuskript beruht größtenteils auf Experimenten, die ich im Rahmen meiner Dissertation selbst durchgeführt habe. Die erste Isolierung und Charakterisierung des NHO-CO_2 Adduktes sowie die Synthese von 1-Ethyl-2,3-dimethylimidazolium-*tert*-butylthiolat erfolgte durch BENAJMIN SCHEIBE im Rahmen eines Forschungspraktikums unter meiner Anleitung. Jeweils im Rahmen eines von mir betreuten Forschungspraktikums synthetisierte PHILIPP HOFMANN erstmals 1-Ethyl-2,3-dimethylimidazolium-trimethylsilylthiolat und REFIKA FIDAN erstmals das NHO-CO_2 Addukt 1-Ethyl-3-dimethylimidazolium-2-methylcarboxylat im präparativen Maßstab. Unter analogen Voraussetzungen synthetisierte JANNICK GUSCHLBAUER das NHO-SO_2 Addukt. Im Rahmen seiner Masterarbeit führte JANNICK GUSCHLBAUER die Konkurrenzexperimente zur relativen Stabilität der NHO-CO_2 und NHO-SO_2 Addukte durch. Die Aufnahme einzelner NMR-Spektren, der Massenspektren, die Durchführung der Elementaranalysen und die Kristalldatensammlung erfolgten durch die Serviceabteilungen des Fachbereiches Chemie. Die Lösung der Kristallstruktur von Bis(1-ethyl-2,3-dimethylimidazolium)-cyanomalonat erfolgte durch Dr. KLAUS HARMS. Das Manuskript und die *Supporting Information* wurden vollständig von mir verfasst. Mit meinem Betreuer Prof. Dr. JÖRG SUNDERMEYER wurden die wissenschaftliche Fragestellung und die Ergebnisse intensiv diskutiert.

3.5 Synthese von 1,3-Dialkylimidazol-2-chalkogenonen aus NHC-CO_2 Addukten

in preparation

Synthesis of 1,3-Dialkylimidazole-2-chalcogenones from NHC-CO_2 Adducts

Lars H. Finger, Philipp E. Hofmann, Jörg Sundermeyer

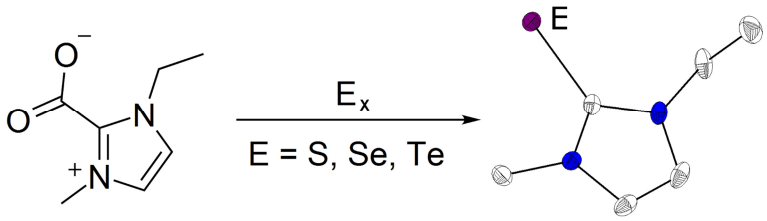

Das NHC-CO_2 Addukt 1-Ethyl-3-methylimidazolium-2-carboxylat wurde als Ausgangssubstanz für die Synthese von 1-Ethyl-3-methylimidazol-2-chalkogenonen verwendet. Die präsentierte Synthese zeichnet sich durch einen geringen Material- und Zeitaufwand und eine hohe Reinheit der Rohprodukte aus. Des Weiteren ist sie im Kontrast zu mehreren literaturbekannten Verfahren auf alle schwereren Chalkogene (E = S, Se, Te) anwendbar. Mit der Sublimation der Imidazol-2-chalkogenone wurde eine Aufreinigungsmethode entwickelt, die ebenso für die gesamte homologe Reihe praktikabel ist und die Herstellung hochreiner Proben erlaubt. Die Umsetzung des NHC-CO_2 Adduktes mit Bis(trimethylsilyl)sulfid lieferte durch einen formalen Sauerstoff-Schwefelaustausch das entsprechende NHC-COS Addukt.

Erklärung der Eigenleistung

Das Manuskript beruht zum größten Teil auf präparativen und analytischen Arbeiten, die von mir persönlich im Rahmen meiner Dissertation durchgeführt wurden. Die Synthese und Charakterisierung des NHC-COS Adduktes erfolgte durch PHILIPP HOFMANN im Rahmen eines Forschungspraktikums unter meiner Anleitung. Die Aufnahme einzelner NMR-Spektren, der Massenspektren, die Durchführung der Elementaranalysen und die Kristalldatensammlung erfolgten durch die Serviceabteilungen des Fachbereiches Chemie. Das Manuskript und die *Supporting Information* wurden vollständig von mir verfasst. Mein Betreuer Prof. Dr. JÖRG SUNDERMEYER wirkte mit umfassenden Diskussionen und zusätzlichen Anregungen an der Konzeption des Manuskriptes mit.

3.6 Synthese und Charakterisierung von 5,5'-Bistetrazolatsalzen mit Alkalimetall-, Ammonium- und Imidazolium-Kationen

Z. Anorg. Allg. Chem. **2013**, *639*, 1140–1152

Synthesis and Characterisation of 5,5'-Bistetrazolate Salts with Alkali Metal, Ammonium and Imidazolium Cations

Lars H. Finger, Fabian G. Schröder, Jörg Sundermeyer

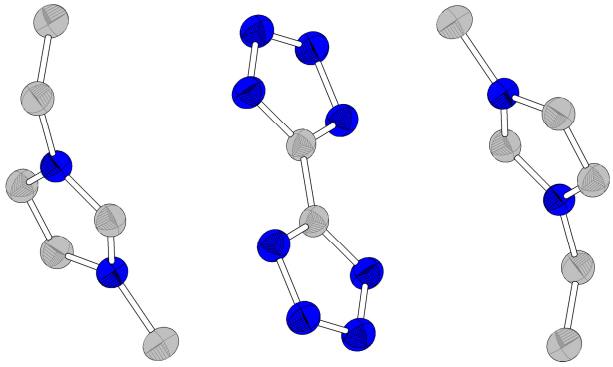

Auf Arbeiten aus der eigenen Masterarbeit aufbauend wurde eine Reihe von Bistetrazolatsalzen mit Alkalimetall-, Ammonium- und Imidazolium-Kationen synthetisiert und röntgenkristallographisch charakterisiert. Die Alkalimetallsalze sind ausgehend von den entsprechenden Hydroxiden oder Carbonaten unter wässrigen Bedingungen zugänglich. Das Ammonium-hydrogenbistetrazolat wurde ähnlich einer Komproportionierung aus der freien Säure Bistetrazol und Diammonium-bistetrazolat hergestellt. Zur Synthese der Imidazoliumsalze wurden ein Salzaustausch zwischen Bariumbistetrazolat und 1-Ethyl-3-methylimidazolium-hydrogensulfat sowie die Umsetzung des freien Bistetrazols mit zwei Äquivalenten 1-Ethyl-3-methylimidazolium-methylcarbonat herangezogen. Zusätzlich wurden neue Kristall-modifikationen der literaturbekannten Salze Bariumbistetrazolat und Diammonium-bistetrazolat vorgestellt. Der systematische Vergleich der präsentierten Strukturen und der weiteren strukturell charakterisierten Bistetrazolatsalze offenbart einen deutlichen Trend zwischen den Ionenradien der Metallatome und dem jeweiligen Koordinationsmodus. Es wurde postuliert, dass aufgrund der Rigidität des Bistetrazolatdianions nur ausreichend große Metallkationen chelatartig koordiniert werden können. Beim Vergleich der IR-Spektren der wasserfreien Alkalimetallsalze zeichnete sich ein deutlicher Effekt der Kationengröße auf die Ringdeformationsschwingungen des Bistetrazolats ab. Die Zersetzungstemperaturen der Alkalimetallsalze liegen größtenteils oberhalb von 400 °C und steigen mit sinkender Ordnungszahl des Metallkations; dies entspricht den Beobachtungen der verwandten Reihe der Erdalkalimetallsalze. Es konnte kein signifikanter Unterschied im Zersetzungsverhalten

von Ammonium-hydrogenbistetrazolat und Diammonium-bistetrazolat festgestellt werden. Bis(1-ethyl-3-methylimidazolium)-bistetrazolat stellt mit einem Schmelzpunkt von 93 °C das erste ohne Zersetzung schmelzbare Bistetrazolsalz und die erste Bistetrazol-IL dar.

Erklärung der Eigenleistung

Die erstmalige Synthese und teilweise Charakterisierung der Lithium-, Kalium-, Cäsium- und Bariumsalze erfolgte im Rahmen der eigenen Masterarbeit.[8] Die Kristallstrukturen dieser vier Verbindungen wurden von Dr. FABIAN SCHRÖDER gelöst und verfeinert. Die vollständige Charakterisierung dieser Salze und der größte Teil aller weiteren synthetischen und analytischen Arbeiten erfolgten durch mich im Rahmen meiner Dissertation. Die Aufnahme einzelner NMR-Spektren, der Massenspektren, die Durchführung der Elementaranalysen und die Kristalldatensammlung erfolgten durch die Serviceabteilungen des Fachbereiches Chemie. Das Manuskript und die *Supporting Information* wurden vollständig von mir verfasst. Mein Betreuer Prof. Dr. JÖRG SUNDERMEYER wirkte als Ideengeber und Diskussionspartner entscheidend an diesem Forschungsprojekt mit.

3.7 Neue Boratanionen mit Bistetrazolato^{2-} und Pyrazindiolato^{2-} Liganden

in preparation

New Borate Anions with Bistetrazolato^{2-} and Pyrazinediolato^{2-} Ligands

Lars H. Finger, Fabian G. Schröder, Jörg Sundermeyer

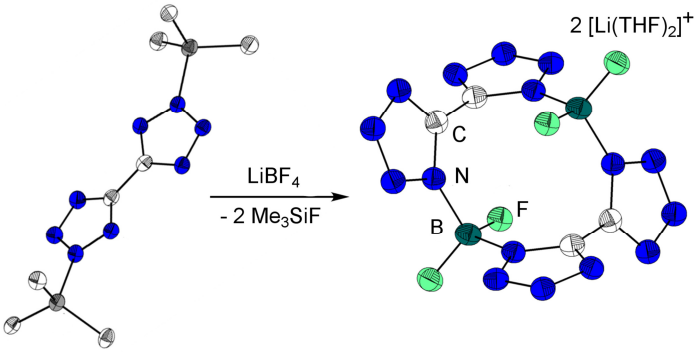

Das Vorhaben galt der Gewinnung von elektrochemisch zersetzlichen ionischen Additiven für Lithiumelektrolytsysteme, die die Ausbildung einer SEI-Schicht fördern sollten. In Fortführung von Arbeiten aus der eigenen Masterarbeit wurde die Reaktion zwischen 2,2'-Bis(trimethylsilyl)-5,5'-bistetrazolat (TMS_2BT) und Lithiumtetrafluoroborat untersucht. Im Zuge dessen wurden zwei Bistetrazolatoborate röntgenkristallographisch charakterisiert. Es bestätigte sich die bereits zuvor geäußerte

Vermutung, dass ein Boratom einen zu geringen Ionenradius aufweist, um von 5,5'-Bistetrazol chelatartig koordiniert zu werden. Stattdessen bildet sich eine dimere Verbindung, die einen ungewöhnlichen $C_4N_4B_2$-Decazyklus aufweist. Die Verbindung konnte NMR und massenspektrometrisch charakterisiert werden, die Isolierung präparativer Gramm-Mengen gelang nicht. Durch Umsetzung von 5,6-Dioxo-2,3-pyrazindicarbonitril mit organischen Tetrafluoroboratsalzen wurden zwei Salze mit dem neuen Bis(pyrazindiolato)-boratanion hergestellt.

Erklärung der Eigenleistung

Die Synthese und Charakterisierung von TMS_2BT, sowie erste Vorversuche zur Umsetzung dieser Substanz mit Lithiumtetrafluoroborat erfolgten bereits im Rahmen meiner Masterarbeit.[8] Dr. FABIAN SCHRÖDER löste und verfeinerte die Kristallstruktur von TMS_2BT. Die weiteren präparativen und analytischen Arbeiten wurde von mir persönlich im Rahmen meiner Dissertation durchgeführt. Die Aufnahme einzelner NMR-Spektren, die Durchführung der Elementaranalysen und die Kristalldatensammlung erfolgten durch die Serviceabteilungen des Fachbereiches Chemie. Das Manuskript und die *Supporting Information* wurden vollständig von mir verfasst. Mein Betreuer Prof. Dr. JÖRG SUNDERMEYER wirkte als Ideengeber und Diskussionspartner entscheidend an diesem Forschungsprojekt mit.

3.8 μ-Rhodizonato-1κO,1:2κO',2κO''-tetra(triphenylphosphin)-disilber(I): Ein molekularer Komplex mit $[C_6O_6]^{2-}$ Ligandmotiv

Z. Anorg. Allg. Chem. **2015**, *641*, 2565–2569

μ-Rhodizonato-1κO,1:2κO',2κO''-tetra(triphenylphosphine)disilver(I): A Molecular Complex with the $[C_6O_6]^{2-}$ Ligand Template

Lars H. Finger, Jörg Sundermeyer

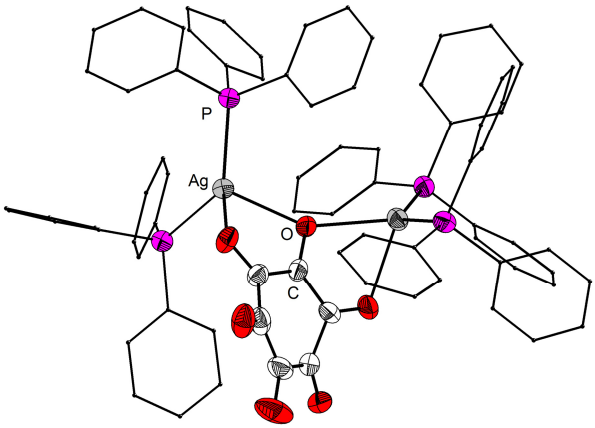

Das Projekt sollte die bislang wenig erforschte Chemie des redoxaktiven Rhodizonatliganden $[C_6O_6]^{2-}$ beleuchten. Im Rahmen von Versuchen Ausgangsverbindungen für Salzmetathese-Reaktionen mit dem Rhodizonat-Dianion zu generieren konnte ein dinuklearer Silberkomplex mit vier Triphenylphosphin- und einem Rhodizonat-Liganden synthetisiert werden. Als Vorläufer dienten das Bariumsalz der Rhodizonsäure und der Triphenylphosphinkomplex des Silbersulfats. In einer Zweiphasenreaktion unter Ausfällung von Bariumsulfat entsteht die Titelverbindung in guter Reinheit als leuchtend rotes Pulver. Die Kristallstruktur wurde anhand von Einkristallen aufgeklärt und zeigt eine für Rhodizonat bisher unbekannte Koordinationweise mit drei benachbarten Sauerstoffatomen an zwei Metallatome. Das mittlere Sauerstoffatom fungiert als direkter Brückenligand zwischen den Silberatomen.

Erklärung der Eigenleistung

Der gesamte präparative, sowie der größte Teil der analytischen Arbeiten wurde von mir persönlich im Rahmen meiner Dissertation durchgeführt. Die Aufnahme einzelner NMR-Spektren, die Durchführung der Elementaranalysen und die Kristalldatensammlung erfolgten durch die Serviceabteilungen des Fachbereiches Chemie. Dr. KLAUS HARMS lieferte wertvolle Hinweise zur Integrationsstrategie des nicht-meroedrischen Zwillings und Dr. XIULAN XIE half bei der Interpretation von Kopplungsphänomenen bei Tieftemperatur ^{31}P NMR-

Messungen. Das Manuskript und die *Supporting Information* wurden von mir verfasst. Mit meinem Betreuer Prof. Dr. JÖRG SUNDERMEYER wurden die Ergebnisse intensiv diskutiert.

3.9 Mitwirkung an weiteren Manuskripten

Bei der Veröffentlichung von Julius F. Kögel, Lars H. Finger, Nicholas Frank und Jörg Sundermeyer mit dem Titel „The New NH-Acid $HN(C_6F_5)(C(CF_3)_3)$ and its Crystalline and Volatile Alkaline and Earth Alkaline Metal Salts“ (*Inorg. Chem.* **2014**, *53*, 3839–3846) habe ich die Valenzbindungsanalysen durchgeführt und Julius Kögel bei der Lösung und Verfeinerung der Kristallstrukturen unterstützt.

Bei der Veröffentlichung von Timo Gneuß, Markus J. Leitl, Lars H. Finger, Nicholas Rau, Hartmut Yersin und Jörg Sundermeyer mit dem Titel „A New Class of Luminescent Cu(I) Complexes with Tripodal Ligands – TADF Emitters for the Yellow to Red Color Range“ (*Dalton Trans.* **2015**, *44*, 8506–8520) oblag mir die Lösung und Verfeinerung der zehn eingeflossen Kristallstrukturen.

Ebenso habe ich bei der Veröffentlichung von Timo Gneuß, Markus J. Leitl, Lars H. Finger, Hartmut Yersin und Jörg Sundermeyer mit dem Titel „A New Class of Deep-Blue Emitting Cu(I) Compounds – Effects of Counter Ions on the Emission Behavior“ (*Dalton Trans.* **2015**, *44*, 20045−20055) die Lösung und Verfeinerung der drei eingeflossenen Kristallstrukturen übernommen.

Am Manuskript von Günther Thiele, Carsten Donsbach, Hendrik Borkowski, Lars H. Finger, Jörg Sundermeyer und Stefanie Dehnen mit dem Arbeitstitel „Mercurates from a Revised Ionothermal Synthesis Route: The *Pseudo*-Flux Approach“ (*in preparation*) habe ich mit der Synthese der Ausgangssubstanz 1-Ethyl-3-methylimidazolium-hydrogensulfid und der in weiteren Versuchen verwendeten Salze 1-Ethyl-3-methylimidazolium-hydrogenselenid und *n*-Butyl-methylpyrrolidinium-hydrogensulfid mitgewirkt.

Die Salze Tri-*n*-butyl-methylphosphonium-methylcarbonat, *n*-Butyl-methylpyrrolidinium-methylcarbonat, *N*,*N*-Dimethylpyrrolidinium-methylcarbonat, Tetramethylammonium-methylcarbonat, Hexamethylguanidiniummethylcarbonat und 1-Ethyl-2,3-dimethyl-imidazolium-methylcarbonat wurden im Rahmen meiner Dissertation von mir persönlich oder unter meiner Anleitung in Forschungspraktika synthetisiert. Diese Verbindungen bilden die Grundlage für die experimentellen Arbeiten zum Manuskript von Maximilian Jost, Lars H.

Finger, Jörg Sundermeyer und Carsten von Hänisch mit dem Arbeitstitel „Synthesis of New Ionic Liquids Containing the Phosphaethynolate (PCO^-) Anion“, (*in preparation*). An diesem Forschungsprojekt habe ich mich außerdem im Rahmen von gemeinsamen durchgeführten Autoklavenreaktionen beteiligt und Maximilian Jost bei der Konzeption der Experimente sowie der Lösung und Verfeinerung der Kristallstrukturen unterstützt.

Bei dem Manuskript von Julius F. Kögel, Davor Margetić, Xiulan Xie, Lars H. Finger und Jörg Sundermeyer mit dem Arbeitstitel „Phosphorus Bisylide Proton Sponges – A New Class of Superbases with Two Interacting Carbon Atoms as Basicity Centers“ (*in preparation*) habe ich Julius Kögel bei der Lösung und Verfeinerung der Kristallstrukturen unterstützt und diese Arbeiten für einige Strukturen vollständig übernommen.

Bei dem Manuskript von Markus J. Leitl, Timo Gneuß, Thomas Niehaus, Lars H. Finger, Jörg Sundermeyer und Hartmut Yersin mit dem Arbeitstitel „Cu(I) Based Emitters with Tripodal Ligands for the Blue Showing Phosphorescence and Thermally Activated Delayed Fluorescence“ (*in preparation*) habe ich die Lösung und Verfeinerung der Kristallstrukturen übernommen.

4 Zusammenfassung

4.1 Ionische Flüssigkeiten auf Basis von Chalkogenidanionen

In der Umsetzung von Methylcarbonatvorläufern mit den Chalkogenwasserstoffen H_2S, H_2Se und H_2Te wurde ein halogenid-, metall- und wasserfreier Zugang zu Ionischen Flüssigkeiten und organischen Salzen mit Hydrogenchalkogenidanionen entwickelt. Dabei konnten die nur bedingt stabilen Gase H_2Se und H_2Te *in situ* aus dem jeweiligen Bis(trimethylsilyl)chalkogenid und Methanol erzeugt werden. Ebenso wie H_2S werden diese Brønsted-sauren Verbindungen durch das Methylcarbonatanion deprotoniert. Der irreversible Zerfall der intermediär gebildeten Methylkohlensäure zu Methanol und CO_2, erlaubt die quantitative Umsetzung durch Verschiebung des Gleichgewichts und erleichtert die Aufreinigung, da ausschließlich flüchtige Nebenprodukte gebildet werden (Schema 4.1).

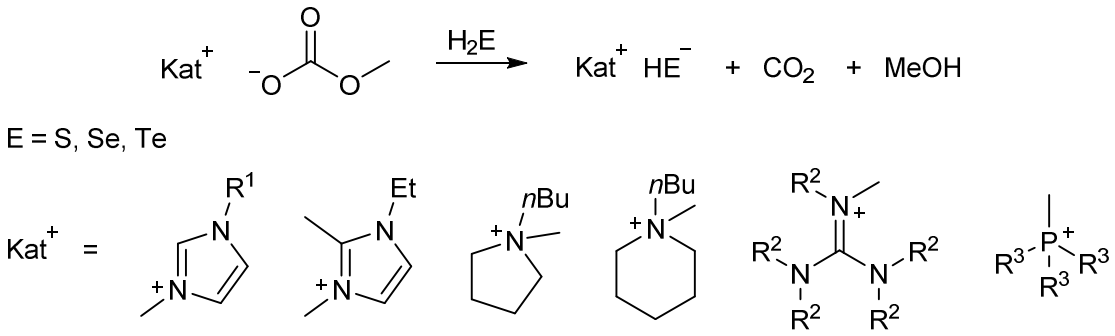

Schema 4.1. *Synthese von organischen Salzen mit Hydrogenchalkogenidanionen; R^1 = Ethyl, n-Butyl, R^2 = Methyl, n-Butyl,[93] R^3 = iso-Propyl, n-Butyl.*

Mit der Verwendung des Methylcarbonatanions als unter aprotischen Bedingungen desilylierendes Nukleophil konnte außerdem eine einfache Synthese zu Silyl- und Alkylchalkogenolatsalzen entwickelt werden (Schema 4.2). Sie stellen eine aktivierte Form der prominenten Chalkogenid-Quellen $(Me_3Si)_2E$ dar.

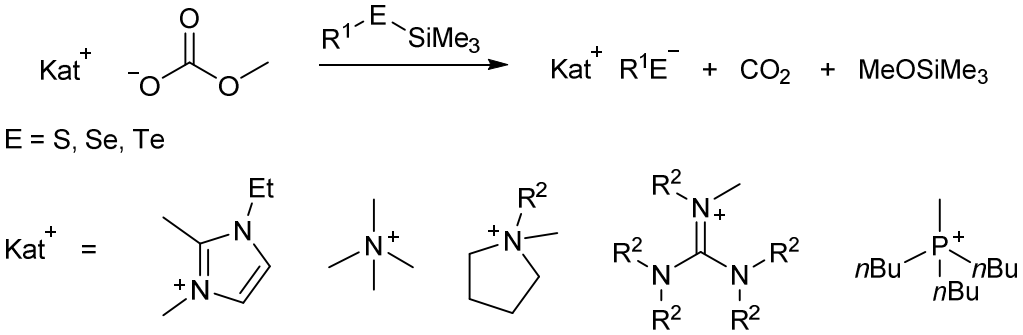

Schema 4.2. *Synthese von organischen Salzen mit Trimethylsilyl- und Alkyl-Chalkogenolatanionen; R^1 = Me_3Si, tert-Butyl, R^2 = Methyl, n-Butyl.*

Mit diesen Verfahren konnte ein komfortabler und universeller Zugang zur Klasse der organischen Salze mit Chalkogenidanionen geschaffen werden, der die Darstellung in hoher Reinheit ermöglicht. Im Rahmen der vorliegenden Arbeit wurde diese neue Gruppe hochreiner Substanzen umfassend charakterisiert und so eine Referenzbasis für organische Salze mit unkoordinierten Hydrogenchalkogenid- und Trimethylsilyl-chalkogenolatanionen geschaffen.

Bei der Untersuchung des thermischen Verhaltens zeigte sich, dass z. B.: Imidazolium-hydrogensulfide und -selenide reversibel und teilweise unter 100 °C schmelzen, während sich Pyrrolidiniumsalze nur unter Zersetzung verflüssigen. Durch Wahl großer Kationen mit ausreichend vielen Freiheitsgraden wie Methyl-tri-*n*-butylphosphonium sind auch Raumtemperatur ILs zugänglich. Die thermische Zersetzung verläuft häufig über eine S_N2-artige Dealkylierung des Kations

Zahlreiche Salze konnten zusätzlich anhand von Einkristallen röntgenographisch untersucht werden. Vor allem in den Kristallstrukturen der Imidazolium-hydrogenchalkogenide offenbarte sich ein ausgeprägtes Wasserstoffbrückennetzwerk (Abb. 4.1).

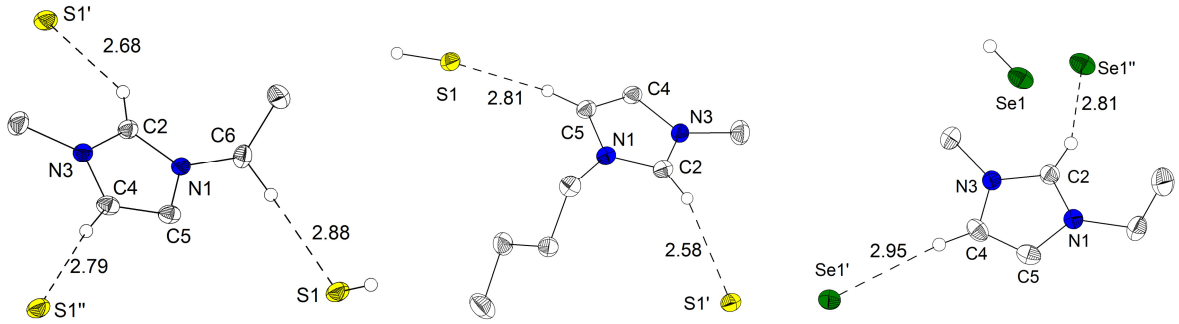

Abbildung 4.1. *Exemplarische Molekülstrukturen von 1-Ethyl-3-methylimidazolium-hydrogensulfid (links), 1-Butyl-3-methylimidazolium-hydrogensulfid (Mitte) und 1-Ethyl-3-methylimidazolium-hydrogenselenid (rechts); C-H···S Wasserstoffbrückenbindungen in Å, symmetrieäquivalente Atompositionen sind mit Indizes gekennzeichnet; H-Atome wurden der Übersichtlichkeit wegen nicht abgebildet.*

Bei Imidazolium-hydrogensulfiden und -seleniden wurde eine außergewöhnliche Flüchtigkeit festgestellt. Diese erlaubt die Sublimation der Salze bei 10^{-2} mbar und Temperaturen unter 100 °C und dadurch auch die Präparation hochreiner Proben. In Kooperation mit FABIAN WOHDE (AG ROLING) wurden mittels isothermer TGA-Experimente die Verdampfungsenthalpien bestimmt, während EVGENY GRIGORYEV und ANNA-KATHARINA HANSMANN (AG BERGER) die Anion-Kation-Wechselwirkung, die Zerfallswege der Salze und die Sublimationsenthalpien auf Basis von DFT-Rechnungen untersuchten. Im Vergleich mit anderen flüchtigen ILs zeigt sich ein deutlich höherer Dampfdruck bei einer gegeben

Temperatur, jedoch kein großer Unterschied bezüglich der Verdampfungsenthalpie (Abb. 4.2).

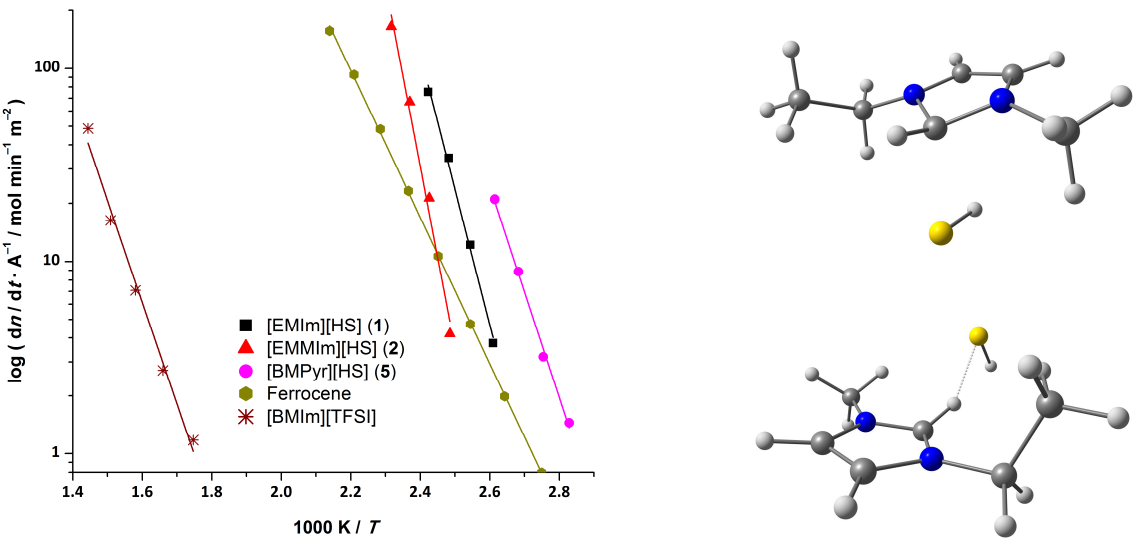

Abbildung 4.2. *Vergleich der Arrhenius-Plots der molaren Verlustrate pro Einheitsfläche für [BMIm][TFSI], Ferrocen und drei ausgewählte Hydrogensulfidsalze (links), sowie nach DFT-Rechnungen stabile Ionenpaare von 1-Ethyl-3-methylimidazolium-hydrogensulfid in der Gasphase (rechts).*

Ausgehend von *n*-Butyl-methylpyrrolidinium-hydrogensulfid und verschiedenen Mengen Schwefel wurden Salze mit Polysulfidanionen unterschiedlicher Kettenlänge synthetisiert. Es stellte sich heraus, dass die formale Reaktion aus Schema 4.3 nicht für beliebige Schwefelmengen durchführbar ist. Bei ein bis drei Äquivalenten Schwefel wurden hohe Restanteile von ca. 40% bzw. 10% des Hydrogensulfidanions beobachtet; die Reaktion läuft nicht vollständig ab. Im Fall von fünf und sieben Äquivalenten Schwefel bildeten sich reine Polysulfidsalze mit mittleren Kettenlängen von sechs und acht Schwefelatomen. Erst bei mehr als neun Äquivalenten Schwefel wurden ungelöste Schwefelrückstände in der Reaktionsmischung beobachtet.

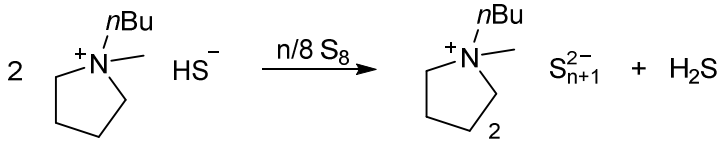

Schema 4.3. *Darstellung von n-Butyl-methylpyrrolidinium-polysulfiden, n = 1, 3, 5, 7; für n = 1 und 3 bleiben deutliche Reste des Hydrogensulfid-Ausgangsmaterials bestehen.*

Ausgehend von Trimethylsilyl- und *tert*-Butylthiolatsalzen bildet sich in THF mit hoher Selektivität das jeweilige Hexasulfidsalz. Die isolierten Salze wurden mittels UV-Vis-Spektroskopie und Cyclovoltammetrie auf ihr Absorptions- und Redoxverhalten untersucht. Erst bei Polysulfidkettenlängen von im Mittel sechs oder acht Atomen zeigt sich ein quasi-

reversibles Redoxverhalten. Im Fall von (n+1) = 2 oder 4 überwiegt das irreversible Redoxverhalten der Hydrogensulfidanionen. Durch spektroelektrochemische (UV-Vis-Chronoamperometrie) Experimente konnten den im Cyclovoltammogramm beobachteten Redoxprozessen einzelne Reaktionen zugeordnet werden. Diese Untersuchungen, die hier erstmals an reinen Polysulfidsalzen durchgeführt werden konnten, liefern die Grundlage um die potentiellen Redoxmediatoren für Farbstoff- oder Quantenpunkt-sensibilisierte Solarzellen näher zu erforschen. Auch für Lithium-Schwefel-Akkumulatoren ergeben sich durch die Möglichkeit, die isolierten Polysulfid-Shuttle-Komponenten zu betrachten, neue Perspektiven.

Die chalkogenidbasierten ILs und organischen Salze sind außerdem als unkoordinierte, hochreaktive Chalkogenidreagenzien interessant. Mögliche Anwendungsgebiete sind neben organischen Reaktionen zur Einführung von Chalkogenidfunktionalitäten die Darstellung von Chalkogenidometallaten sowie Metallchalkogenidclustern und Halbleitermaterialien. Anwendungspotential ergibt sich z. B. im Bereich der Abscheidung von Halbleiterdünnfilmen für Dünnschichttransistoren oder der Synthese von Quantenpunkten. BENJAMIN SCHEIBE synthetisierte im Rahmen seiner von mir betreuten Bachelorarbeit MoS_2 aus Phosphonium-hydrogensulfiden und -trimethylsilylthiolaten.[93] Das MoS_2 fiel in annähernd sphärischen Partikeln an und wies organische Verunreinigungen auf, die auf die IL-Kationen zurückgeführt werden konnten (Abb. 4.3, links). Diese Arbeiten werden zurzeit mit Fokus auf der Herstellung von MoS_2-Dünnfilmen und der Übertragung auf weitere Metalle weitergeführt.

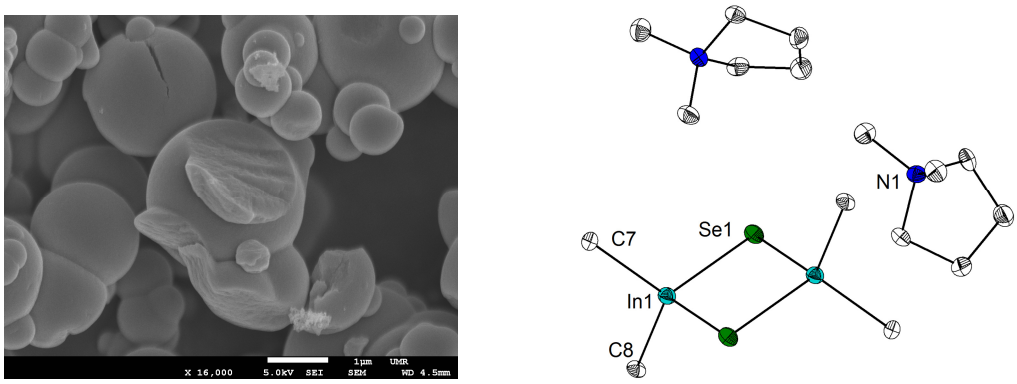

Abbildung 4.3. *Sphärische MoS_2-Partikel aus der Reaktion von Tri-n-butyl-methylphosphonium-hydrogensulfid mit $[MoCl_4(CH_3CN)_2]$ (links)[93] und Molekülstruktur des ersten Dimethylindiumselenolat-dianions (rechts); H-Atome wurden der Übersichtlichkeit wegen nicht abgebildet.*

Die Umsetzung von Trimethylaluminium, -gallium und -indium mit Onium-hydrogenchalkogeniden und -trimethylsilylchalkogenolaten lieferte einerseits monoanionische Addukte aus dem Chalkogenid und der Trielverbindung, andererseits aber auch das erste

Dimethylindiumselenolat-dianion (Abb. 4.3, rechts). Diese neue Substanzklasse wird gegenwärtig, auch hinsichtlich ihres Potentials als Vorläufer zu CIGS-Materialien zu fungieren, näher untersucht.

4.2 Imidazolium-Methylcarbonate und Imidazolium-Carboxylat-Zwitterionen

Während in mehreren vorangegangenen Publikationen die Bildung von Imidazolium-2-carboxylaten (formal CO_2 Addukte von N-heterocyclischen Carbenen (NHC-CO_2)) auf zu hohe Reaktionstemperaturen zurückgeführt wurde, konnte im Rahmen dieser Arbeit gezeigt werden, dass ihre Entstehung ausschließlich auf die Entfernung von Methanol aus dem Gleichgewicht von Methylcarbonatanion und Carboxylat-Zwitterion zurückzuführen ist (Schema 4.4, oben). Das Entfernen von Methanol bewirkt nicht nur die direkte Verschiebung des Gleichgewichts durch das Unterbinden der Rückreaktion, sondern führt auch zu einer Erhöhung der Basizität des Methylcarbonatanions durch die verringerte Solvatation.

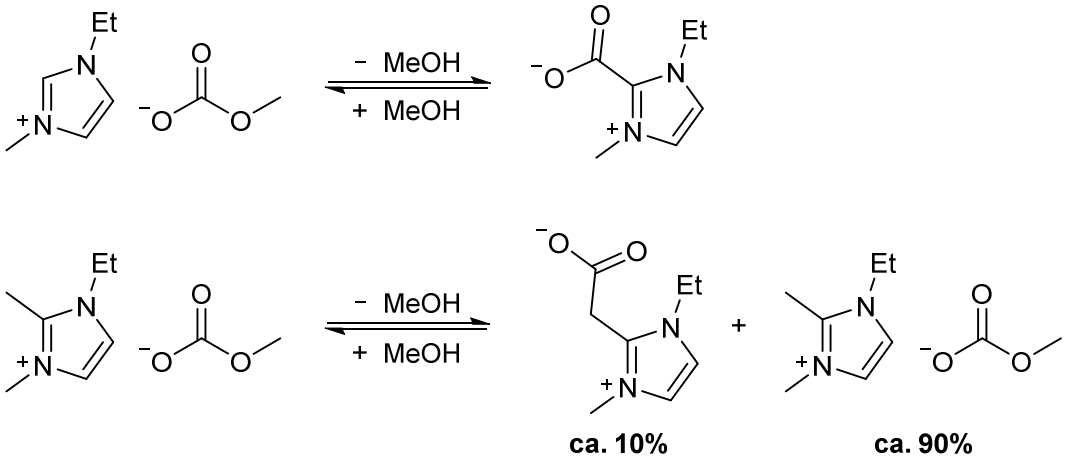

Schema 4.4. *Gleichgewicht von Imidazolium-Methylcarbonat-Salzen und Imidazolium-Carboxylat-Zwitterionen bei Raumtemperatur; die jeweilige Rückreaktion bedarf im Regelfall eines Nukleophils.*

Ein analoges Phänomen wurde auch bei Verwendung eines 1-Ethyl-2,3-dimethylimidazoliumkations beobachtet. Während im vorangegangenen Fall die Umsetzung weitgehend vollständig abläuft, entsteht in diesem Fall nur zu 5 bis 10% ein 1-Ethyl-3-methylimidazolium-2-methylencarboxylat als Verunreinigung des Methylcarbonatsalzes (Schema 4.4, unten).

Dieses CO_2-Addukt eines N-heterozyklischen Olefins (NHO-CO_2) wurde daraufhin bezüglich seiner Reaktivität gegenüber Brønsted-Säuren untersucht, um zu ergründen ob diese Verunreinigung die Folgesynthese von ILs beeinträchtigen kann. Es zeigte sich eine von der

Säurestärke des Reaktionspartners abhängige Reaktivität. Die schwache Säure Ammoniumhexafluorophosphat, die bei der Reaktion das Nukleophil Ammoniak freisetzt, führt zur Bildung des gewünschten Imidazoliumsalzes. Starke Säuren hingegen, die wenig basische und vor allem wenig nukleophile Anionen erzeugen, führen nur zur Protonierung des Carboxylates. Bei Raumtemperatur tritt keine Decarboxylierung ein. Erst bei erhöhter Temperatur oder bei Zugabe substöchiometrischer Mengens eines Nukleophils wie 4-Dimethylaminopyridin als Katalysator wird das Imidazoliumsalz gebildet (Schema 4.5).

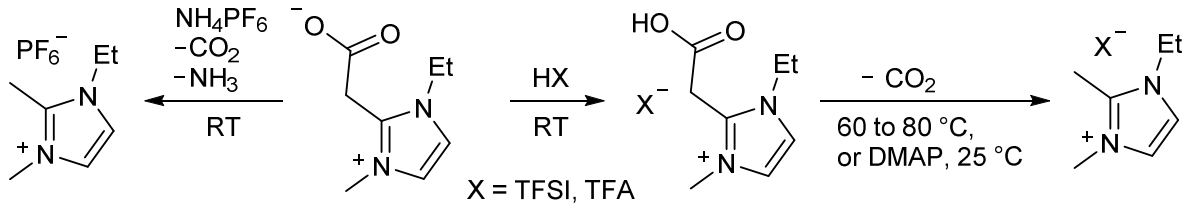

Schema 4.5. *Reaktionsverhalten von 1-Ethyl-3-methylimidazolium-2-methylencarboxylat mit starken und schwachen Brønsted-Säuren.*

Mit dem 2-Methylencarboxylat konnte außerdem die erste C-C Bindungsknüpfung ausgehend von einem NHO-CO_2 Addukt realisiert werden. Mit Acetonitril als CH-azider Verbindung reagiert das Carboxylat unter Übertragung der CO_2-Gruppe auf das zuvor deprotonierte Acetonitrilmolekül und Bildung von Cyanoacetat- und Cyanomalonatanionen (Schema 4.6). Dabei steht das als Folgeprodukt gebildete Cyanomalonatanion mit dem NHO-CO_2 Addukt und dem Cyanoacetatsalz im Gleichgewicht.

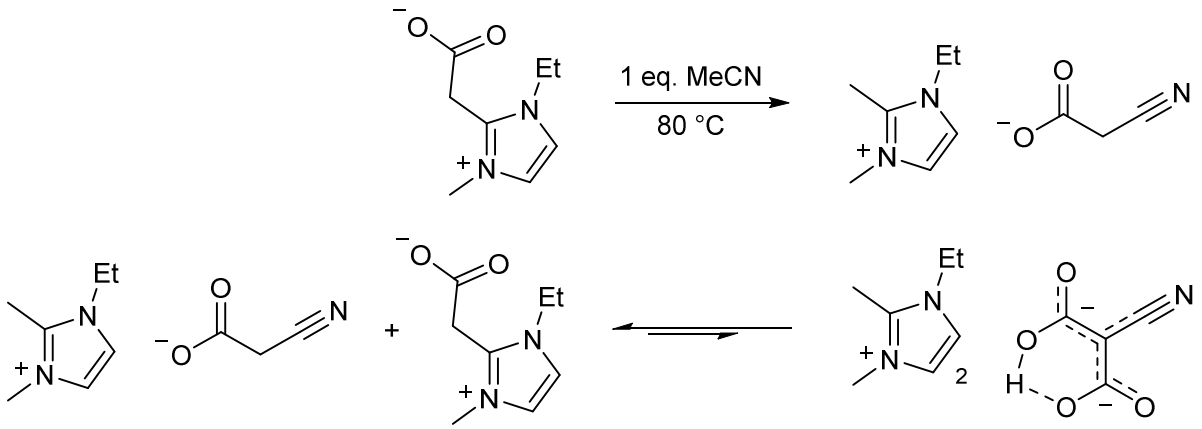

Schema 4.6. *Carboxylierung von Acetonitril mit 1-Ethyl-3-methylimidazolium-2-methylencarboxylat; die erste C-C Knüpfungsreaktion ausgehend von einem NHO-CO_2 Addukt.*

Ferner konnte das erste NHO-SO_2 Addukt synthetisiert werden, welches in der Reaktion mit Methanol einen neuen Zugang zu Methylsulfitsalzen ermöglicht (Schema 4.7).

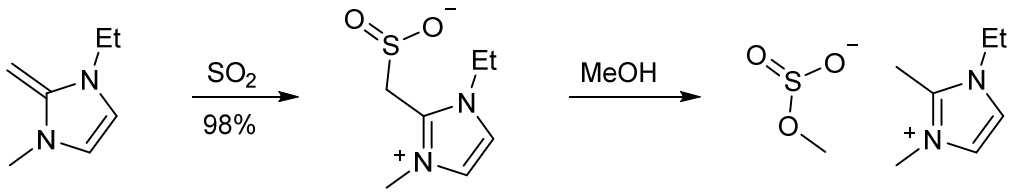

Schema 4.7. *Bildung des ersten NHO-SO_2-Adduktes und Reaktion mit Methanol zu 1-Ethyl-2,3-dimethylimidazolium-methylsulfit.*

Die Umsetzung des NHO-CO_2 Adduktes mit den im Rahmen der IL-Synthesen verwendeten schwefelhaltigen Reagenzien führte ausschließlich zu unselektiven Reaktionen. Das CO_2-Addukt des entsprechenden N-heterozyklischen Carbens hingegen, ging sowohl mit elementarem Schwefel als auch mit Bis(trimethylsilyl)sulfid eine sehr selektive Reaktion ein. So eröffnete sich zum einen ein neuer Zugang zu NHC-COS Addukten, die zuvor nur in aufwendigen und wenig ökonomischen Verfahren zugänglich waren (Schema 4.8). Zum anderen führte die Reaktion mit Schwefel zum 1-Ethyl-3-methylimidazol-2-thion und konnte erfolgreich auf die höheren Homologen Selen und Tellur übertragen werden. Im Vergleich mit herkömmlichen Synthesemethoden für Imidazol-2-chalkogenone zeichnet sich dieses Verfahren durch eine schnelle, sehr selektive und quantitative Reaktion aus. Es zeigte sich ferner, dass die Imidazol-2-chalkogenone im Feinvakuum sublimierbar sind und so hochreine Proben präpariert werden können.

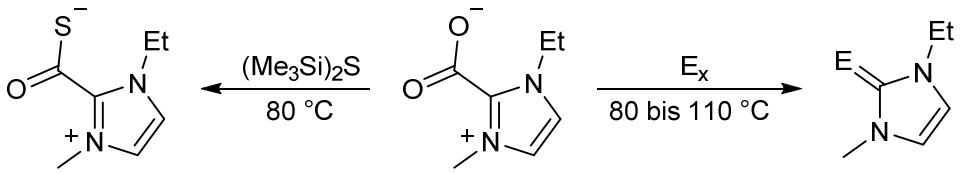

Schema 4.8. *Synthese eines NHC-COS Adduktes aus dem entsprechenden CO_2 Addukt und Zugang aus diesem zu Imidazol-2-chalkogenonen (E = S, Se, Te).*

4.3 Koordinationsverbindungen von 5,5'-Bistetrazolat, Pyrazindiolat und Rhodizonat

Auf der Suche nach neuen *Solid Electrolyte Interface* (SEI) bildenden Additiven für Lithiumakkus wurde in einer frühen Phase dieser Arbeit die Synthese neuer Boratanionen mit Bezug zum namhaften Bis(oxalato)boratanion angestrebt. 5,5'-Bistetrazol und Oxalsäure sind potentiell bioisostere Verbindungen. Zunächst konnte mit Na_2BT und Rb_2BT die Reihe der Alkalimetall-Bistetrazolate vervollständigt werden und der Koordinationsmodus des $C_2N_8^{2-}$-Liganden – chelatartig oder verbrückend − in Abhängigkeit von der Kationengröße innerhalb

dieser homologen Reihe analysiert werden. Auch unter Einschluss aller anderen bekannten Röntgenkristallstrukturen von Bistetrazolatverbindungen zeigte sich, dass eine chelatisierende Koordination im Regelfall erst bei ausreichend großem Ionenradius des Metallatoms auftritt.

Außerdem konnte mit Bis(1-ethyl-3-methylimidazolium)-bistetrazolat das erste reversibel schmelzende Bistetrazolatsalz synthetisiert und strukturell charakterisiert werden. Anion-Kation-Wechselwirkungen treten nur im Rahmen von C-H···N Wasserstoffbrückenbindungen auf. Im weiteren Verlauf wurden weitere Vertreter dieser Klasse mit 1-*n*-Butyl-3-methylimidazolium, Tri-*n*-butyl-methylphosphonium und Tri-*iso*-propyl-methylphosphonium als Kationen hergestellt und ihre Kristallstruktur aufgeklärt. Abbildung 4.4 zeigt repräsentative Molekülstrukturen. YODITA ASFAHA gelang im Rahmen ihrer von mir betreuten Bachelorarbeit die Synthese und Charakterisierung der ersten Cobalt-Bistetrazol-Komplexe.[94]

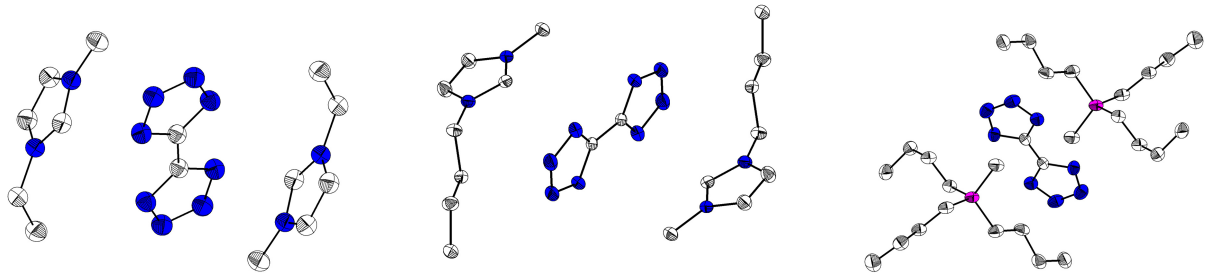

Abbildung 4.4. *Molekülstrukturen von Bis(1-ethyl-3-methylimidazolium)- (links), Bis(1-n-butyl-3-methylimidazolium)- (Mitte) und Bis(tri-n-butyl-methylphosphonium)-bistetrazolat (rechts); H-Atome wurden der Übersichtlichkeit wegen nicht abgebildet.*

Das bereits im Rahmen der Masterarbeit massenspektrometrisch beobachtete Bistetrazolatoborat-Fragment $(BT)BF_2^-$ konnte nun durch eine Kristallstruktur eindeutig nachgewiesen werden (Abb. 4.5).

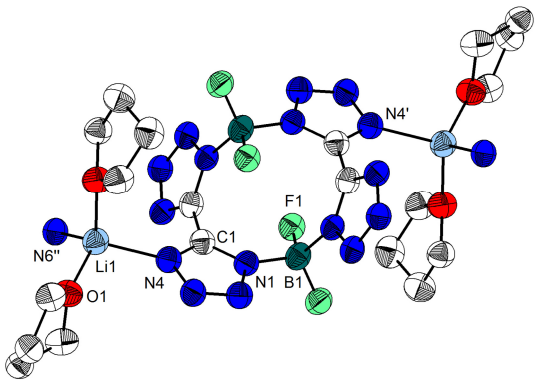

Abbildung 4.5. *Dimeres Strukturmotiv in Lithium-bistetrazolato-difluoroborat; die Lithiumatome sind zusätzlich durch zwei THF-Moleküle koordiniert; symmetrieäquivalente Atompositionen sind mit Indizes gekennzeichnet; H-Atome wurden der Übersichtlichkeit wegen nicht abgebildet.*

Es bestätigte sich die Vermutung, dass auch das Boratom zu klein ist um chelatartig koordiniert zu werden. Statt einer dem Bis(oxalato)borat ähnlichen mononuklearen Struktur zeigte sich ein dimeres Motiv, in dem zwei Bistetrazolatanionen über zwei BF_2-Brücken verknüpft sind.

Ausgehend von 2,3-Dioxo-pyrazin-5,6-dicarbonitril konnten zwei Salze mit einem neuen Bis(pyrazindiolato)boratanion hergestellt werden (Schema 4.9). Dieses stellt eine potentielle Alternative zum Bis(oxalato)boratanion als SEI-bildendes Additiv für Lithium-Ionen-Akkumulatoren dar.

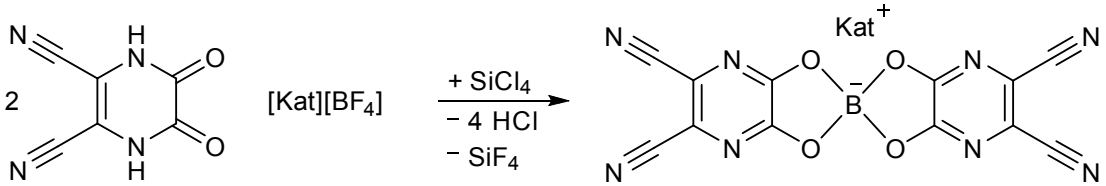

Schema 4.9. *Synthese von Bis(pyrazin-5,6-dicarbonitril-2,3-diolato)boratsalzen mit organischen Kationen (Kat = 1-Ethyl-3-methylimidazolium oder Dimethylpyrrolidinium).*

Die Synthese entsprechender Bis(rhodizonato)borate gelang aufgrund der Tendenz des Rhodizonatanions, unlösliche Koordinationspolymere zu bilden, nicht. Im Verlauf der Versuche konnte jedoch ein Silber-Rhodizonatkomplex mit Triphenylphosphinliganden, welche die molekulare Struktur ausreichend stabilisieren, isoliert und charakterisiert werden. Seine Kristallstruktur ist die insgesamt vierte eines Rhodizonatokomplexes und zeigt eine bisher unbekannte Koordinationsweise des $C_6O_6^{2-}$-Anions über drei benachbarte Sauerstoffatome. In allen bisher bekannten Strukturen erfolgt die Koordination mit vier Sauerstoffatomen, wobei keines der Sauerstoffatome eine verbrückende Position einnimmt (Abb. 4.6).

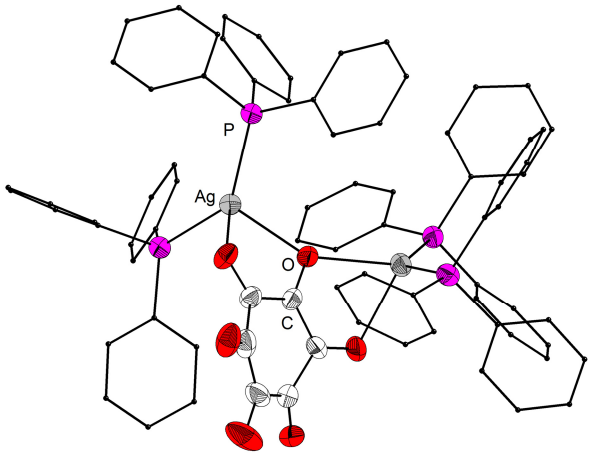

Abbildung 4.6. *Molekülstruktur des Silber-Rhodizonatokomplexes; der Übersichtlichkeit wegen wurden die C-Atome der Phenylringe mit minimalem Atomradius und ohne H-Atome abgebildet.*

5 Summary

5.1 Chalcogenide Anion Based Ionic Liquids

A metal, halide and water free access to Ionic Liquids (ILs) and organic salts with hydrochalcogenide anions, starting from methylcarbonate salts and hydrogen chalcogenides H_2S, H_2Se and H_2Te, was developed. Due to their limited stability H_2Se and H_2Te were generated *in situ* from the corresponding bis(trimethylsilyl)chalcogenide and methanol. These Brønsted acidic gases are deprotonated by the methylcarbonate anion analogously to H_2S. The irreversible decay of the intermediately formed methyl carbonic acid to methanol and CO_2 allows for the quantitative transformation by equilibrium shift. The purification is facilitated as only volatile side products are formed (Scheme 5.1).

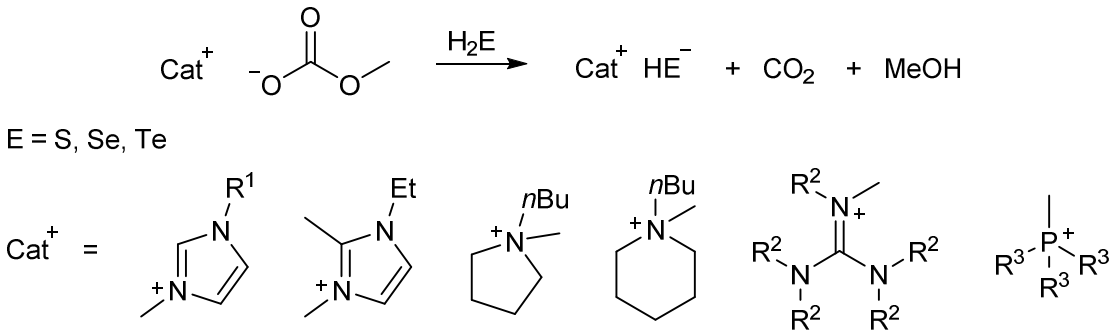

Scheme 5.1. *Synthesis of organic salts with hydrochalcogenide anions; R^1 = ethyl, n-butyl, R^2 = methyl, n-butyl,[93] R^3 = iso-propyl, n-butyl.*

Furthermore, a facile synthesis of trimethylsilyl- and alkylchalcogenolate salts was developed, which employs methylcarbonate anions under strictly aprotic conditions as desilylating nucleophiles (Scheme 5.2). These chalcogenolate anions represent an activated form of the prominent chalcogenide sources $(Me_3Si)_2E$.

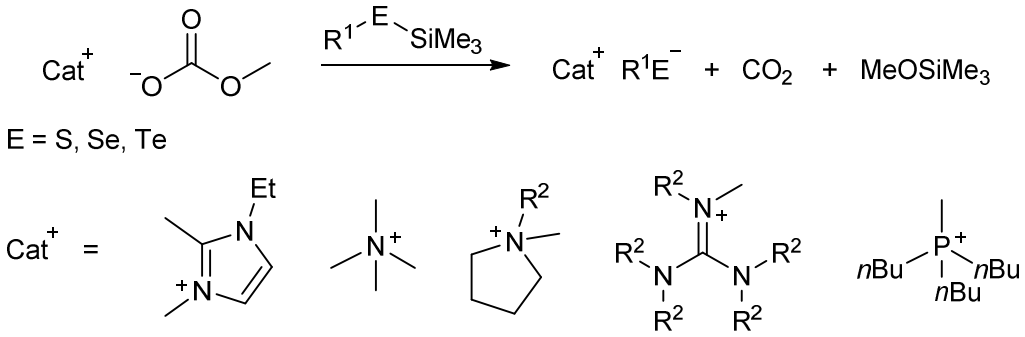

Scheme 5.2. *Synthesis of organic salts with trimethylsilyl- and alkylchalcogenolate anions; R^1 = Me_3Si, tert-butyl, R^2 = methyl, n-butyl.*

These procedures open a convenient and universal access to the class of organic salts with chalcogenide anions and allow their preparation in high purity. Within the course of this work this new series of pure substances was characterized extensively, whereby a reference basis for such organic salts with uncoordinated hydrochalcogenide and trimethylsilylchalcogenolate anions was built.

During the investigation of their thermal characteristics it was found that e. g. imidazolium hydrosulfides and -selenides melt reversibly − in part below 100 °C − while pyrrolidinium based salts decompose upon melting. By choosing large cations with sufficient degrees of freedom, such as methyl-tri-*n*-butylphosphonium, also room temperature ILs are accessible. The thermal decomposition typically occurs *via* S_N2 type dealkylation of the cation.

Additionally, numerous salts were investigated by single crystal X-ray crystallography. Especially the crystal structures of imidazolium hydrochalcogenides show a pronounced hydrogen bonding network (Figure 5.1).

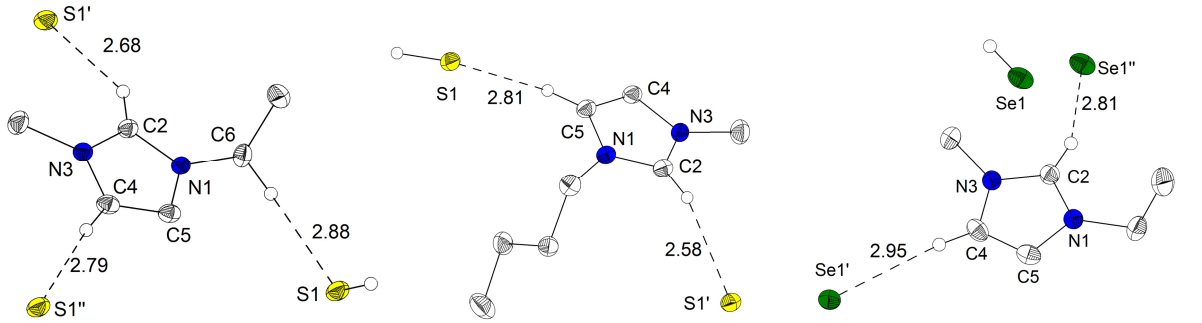

Figure 5.1. *Exemplary molecular structures of 1-ethyl-3-methylimidazolium-hydrosulfide (left), 1-butyl-3-methylimidazolium-hydrosulfide (center) and 1-ethyl-3-methylimidazolium-hydroselenide (right); C-H···S H bond distances in Å; symmetry equivalent atomic positions are marked by indices; H atoms were omitted for clarity.*

For imidazolium hydrosulfides and hydroselenides an astonishing volatility was observed, which allowed sublimation of these salts at 10^{-2} mbar and temperatures below 100 °C. Thereby, samples of highest purity were accessible. Vaporization enthalpies were determined in cooperation with FABIAN WOHDE (AG ROLING) *via* isothermal TGA experiments. EVGENY GRIGORYEV and ANNA-KATHARINA HANSMANN (AG BERGER) investigated anion cation interactions, decomposition pathways and the sublimation enthalpies in DFT calculations. In comparison with other volatile ILs a significantly increased vapor pressure is observed at a given temperature while there is no large difference concerning the vaporization enthalpy (Figure 5.2).

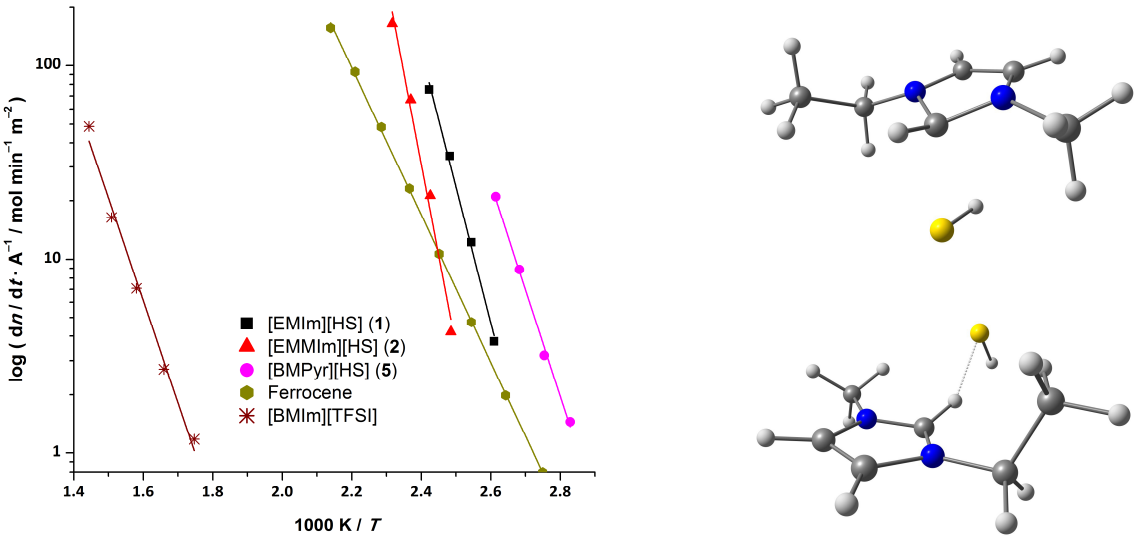

Figure 5.2. *Comparison of Arrhenius plots of the molar loss rate per unit area for [BMIm][TFSI], ferrocene and three selected hydrosulfide salts (left) and according to DFT calculations stable single ion pairs of 1-ethyl-3-methylimidazolium-hydrosulfide in the gas phase (right).*

Starting from *n*-butyl-methylpyrrolidinium-hydrosulfide and selected amounts of sulfur, organic salts with polysulfide anions of varying chain length were synthesized. It was found that the formal reaction of Scheme 4.3 is not realizable for arbitrary amounts of sulfur. In case of one and three equivalents of sulfur large residual hydrosulfide ion contents of 40% and 10%, respectively, were observed. The reaction cannot be forced to completion. In case of five and seven equivalents of added sulfur pure polysulfide salts with intermediate chain lengths of six and eight sulfur atoms are formed. Only when nine equivalents of sulfur are exceeded, undissolved sulfur remains in the reaction mixture.

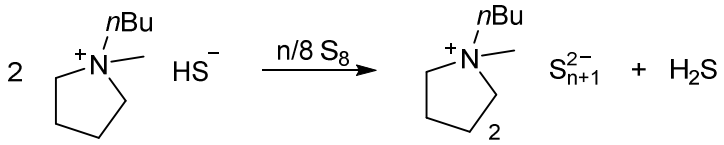

Scheme 5.3. *Preparation of n-butyl-methylpyrrolidinium-polysulfides, n = 1, 3, 5, 7; in case of n = 1 and 3 large amounts of the hydrosulfide anion reside.*

Starting from organic salts with trimethylsilylthiolate and *tert*-butylthiolate anions and sulfur, the corresponding hexasulfide salt is formed in THF with high selectivity. The polysulfide salts were investigated by UV-Vis spectroscopy and cyclic voltammetry concerning their absorption and redox behavior. Only with intermediate polysulfide chain lengths of six or eight atoms a quasi-reversible redox behavior is observed. In case of (n+1) = 2 or 4 the irreversible redox behavior of the hydrosulfide anions dominates. The redox processes, which were observed in the cyclic voltammograms, were assigned to specific reactions *via* spectroelectrochemical (UV-Vis-chronoamperometry) experiments. These investigations,

which were performed with pure organic polysulfide salts for the first time, form a foundation to further explore these potential redox mediators for dye and quantum dot sensitized solar cells. Furthermore, new perspectives arise for lithium sulfur secondary batteries from the possibility to examine the isolated polysulfide shuttle components.

In addition, the chalcogenide based ILs and organic salts are noteworthy in view of their potential to function as uncoordinated and highly reactive chalcogenide reagents. Potential applications are − besides organic reactions to introduce chalcogenide functionalities − the preparation of chalcogenido metalates as well as metal chalcogenide clusters and semiconductor materials. E. g. the thin layer deposition of semiconductors for thin-film transistors (TFTs) and the synthesis of quantum dots are highly topical areas. In the course of his bachelor thesis under my supervision BENJAMIN SCHEIBE synthesized MoS_2 from phosphonium hydrosulfides and trimethylsilylthiolates.[93] MoS_2 was formed in almost spherical particles but still contained organic impurities, which could be traced back to the former IL cations (Figure 5.3, left). These experiments are currently continued with a focus on preparation of MoS_2 thin films and transfer to other metals.

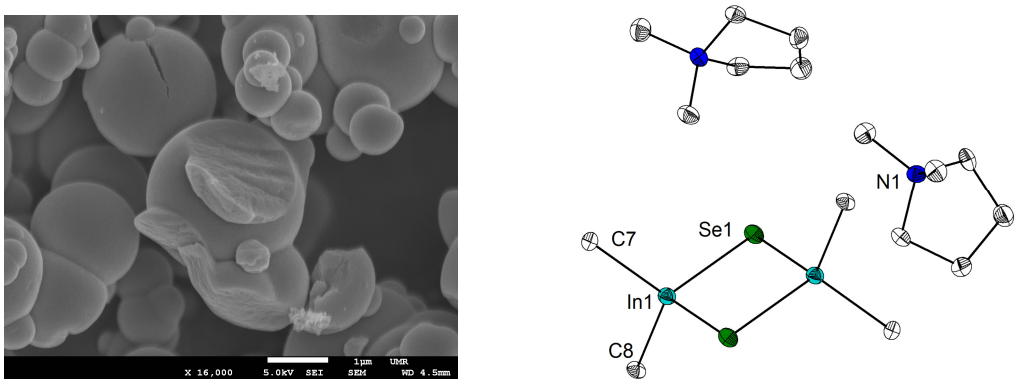

Figure 5.3. *Spherical MoS_2 particles from the reaction of tri-n-butyl-methylphosphonium hydrosulfide with $[MoCl_4(CH_3CN)_2]$ (left)[93] and molecular structure of the first (dimethylindium)selenolate dianion (right); H atoms were omitted for clarity.*

The reaction of trimethyl aluminum, gallium and indium with onium hydrochalcogenides and onium trimethylsilylchalcogenolates led on the one hand to monoanionic adducts of the particular chalcogenide and group 13 compound. On the other hand also the first (dimethylindium)selenolate dianion was synthesized (Figure 5.3, right). This new class of compounds is currently investigated in more detail, also concerning its potential to act as precursor for CIGS materials.

5.2 Imidazolium Methylcarbonates und Imidazolium-carboxylate Zwitterions

Several preceding publications attribute the formation of imidazolium-2-carboxylates (formally N-heterocyclic carbene (NHC) CO_2 adducts) to elevated reaction temperatures. In contrast, it could be shown in the course of this work that their formation is exclusively dependent on the removal of methanol from the equilibrium of methylcarbonate anions and carboxylate zwitterions (Scheme 4.4, top). The progressive removal of methanol not only directly shifts the equilibrium by preventing the back reaction but also leads to increased basicity of the methylcarbonate anion due to weaker solvation.

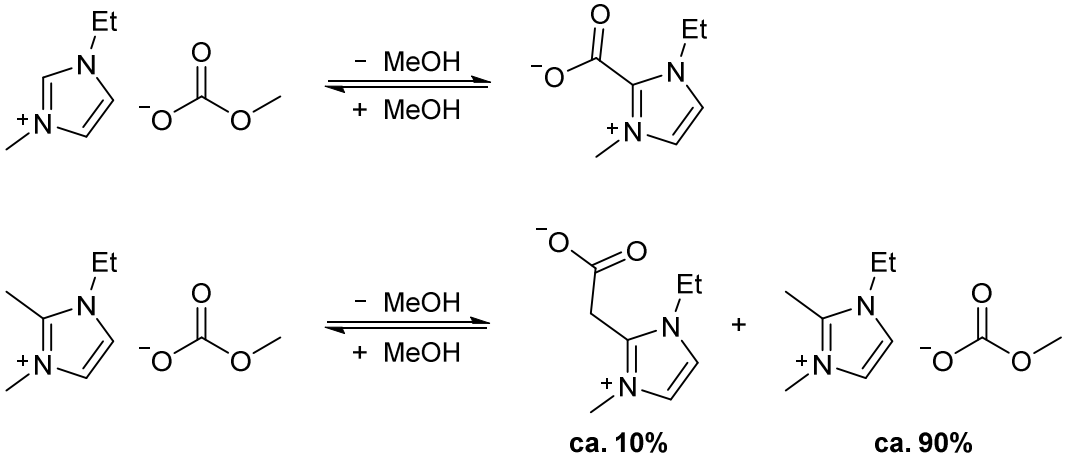

Scheme 5.4. *Equilibrium of imidazolium methylcarbonate salts and imidazolium carboxylate zwitterions at room temperature; the corresponding back reaction typically demands the presence of an appropriate nucleophile.*

An analogous phenomenon was observed with a 1-ethyl-2,3-dimethylimidazolium cation. While in the previous case the conversion is near to quantitative, this example yields only 5 to 10% of 1-ethyl-3-methylimidazolium-2-methylencarboxylate as a side product of the original methylcarbonate salt (Scheme 5.4, bottom).

Consequently, this CO_2 adduct of an N-heterocyclic olefin (NHO-CO_2) was investigated regarding its reactivity towards Brønsted acids. The question to be answered was if these impurities will complicate follow up syntheses of Ionic Liquids. The reactivity of the NHO-CO_2 adduct was shown to depend on the acidity of the particular reaction partner. The weak acid ammonium hexafluorophosphate, which releases nucleophilic ammonia upon deprotonation, led to the formation of the anticipated imidazolium salt. In contrast, strong acids, which form weakly basic and, in particular, weakly nucleophilic anions, only lead to the protonation of the carboxylate moiety. At room temperature no decarboxylation is observed. However, at elevated temperatures or upon addition of sub-stoichiometric amounts

of a nucleophilic catalyst such as 4-dimethylaminopyridine, the imidazolium salt is formed (Scheme 5.5).

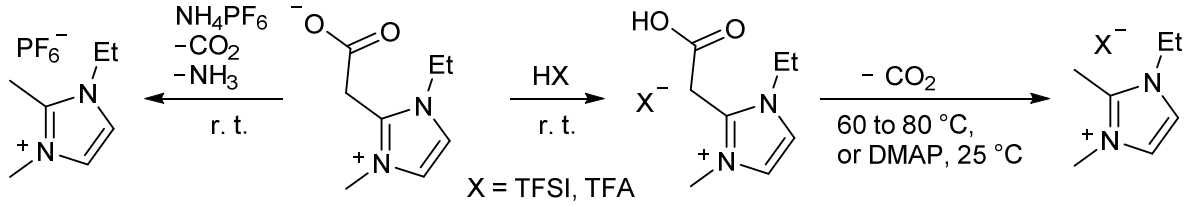

Scheme 5.5. *Reaction behavior of 1-ethyl-3-methylimidazolium-2-methylencarboxylate towards weak and strong Brønsted acids.*

Furthermore, the first C-C bond forming carboxylation starting from a NHO-CO_2 adduct was demonstrated. The NHO-CO_2 adduct reacts with CH acidic acetonitrile under CO_2 transfer to a previously deprotonated acetonitrile moiety forming cyanoacetate and cyanomalonate anions (Scheme 5.6). The cyanomalonate anion, which is formed as a follow up product, is in equilibrium with the NHO-CO_2 adduct and the cyanoacetate salt.

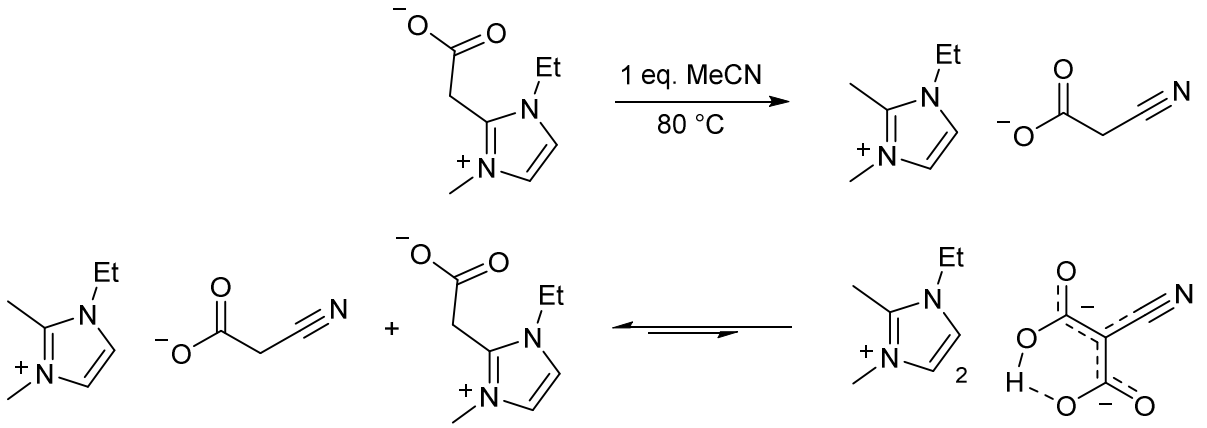

Scheme 5.6. *Carboxylation of acetonitrile by 1-ethyl-3-methylimidazolium-2-methylencarboxylate; the first C-C bond forming reaction starting from a NHO-CO_2 adduct.*

In addition, the first NHO-SO_2 adduct was synthesized. This allows a new access to imidazolium methylsulfite salts via methanolysis (Scheme 5.7).

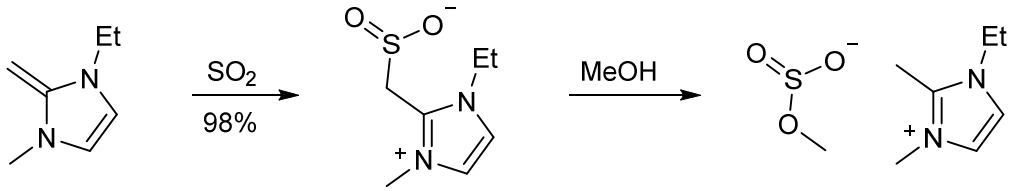

Scheme 5.7. *Formation of the first NHO-SO_2 adduct and reaction with methanol to form 1-ethyl-2,3-dimethylimidazolium-methylsulfite.*

Reacting the NHO-CO_2 adduct with the sulfur containing reagents used for the sulfide and thiolate based ILs did not lead to any selective transformations. The NHC-CO_2 adduct, in contrast, engaged in highly selective reactions with sulfur as well as bis(trimethylsilyl)sulfide. The latter opened an alternative access to NHC-COS adducts, which previously were only accessible in complicated and little economic procedures (Scheme 5.8). The reaction with sulfur allowed the synthesis of 1-ethyl-3-methylimidazole-2-thione and was successfully transferred to the higher homologs selenium and tellurium. In comparison with traditional syntheses this procedure stands out due to a quick, very selective and quantitative reaction. Furthermore, it was shown that the prepared imidazole-2-chalcogenones can be sublimed in medium vacuum to prepare samples of highest purity.

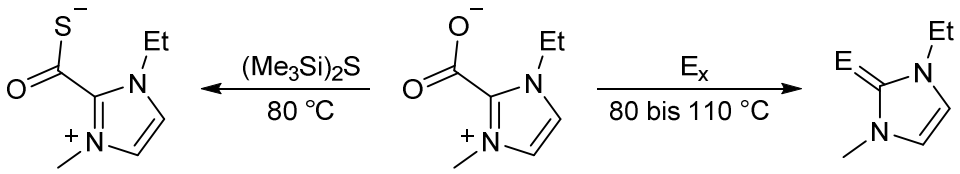

Scheme 5.8. *Synthesis of a NHC-COS adduct from the corresponding CO_2 adduct and access from the latter to imidazole-2-chalcogenones (E = S, Se, Te).*

5.3 Coordination Compounds of 5,5'-Bistetrazolate, Pyrazinediolate and Rhodizonate

On search for new solid electrolyte interface (SEI) forming additives for lithium ion secondary batteries a series of new borate anions related to the prominent bis(oxalato)borate anion was targeted at the early stages of this thesis. 5,5'-Bistetrazole and oxalic acid are potentially bioisosteric compounds. Firstly, the series of alkali metal 5,5'-bistetrazolate salts investigated during the master thesis was completed with the salts Na_2BT and Rb_2BT. This allowed correlating the coordination behavior of the $C_2N_8^{2-}$ ligand – chelate or bridging − with the cation diameter within this homologous series. This approach was extended to all known X-ray crystal structures of bistetrazolate coordination compounds and made it evident that a chelating coordination mode occurs typically only at metal cations of sufficiently large diameter.

Furthermore the organic salt bis(1-ethyl-3-methyl)imidazolium-bistetrazolate, which constitutes the first reversibly melting bistetrazolate salt, was synthesized and structurally characterized. Anion cation interactions occur only in form of C-H···N hydrogen bonds. Subsequently, further examples of this class of compounds, e. g. based on 1-*n*-butyl-3-methylimidazolium, tri-*n*-butyl-methylphosphonium and tri-*iso*-propyl-methylphosphonium

cations, were synthesized and their single crystal structures elucidated. Figure 5.4 shows representative molecular structures. YODITA ASFAHA synthesized and characterized the first cobalt bistetrazolate complexes in the course of her bachelor thesis under my supervision.[94]

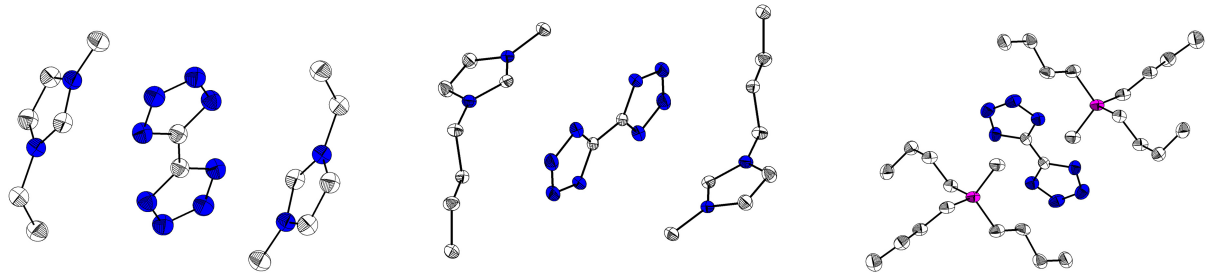

Figure 5.4. *Molecular structures of bis(1-ethyl-3-methylimidazolium)- (left), bis(1-n-butyl-3-methylimidazolium)- (center) and bis(tri-n-butyl-methylphosphonium)-bistetrazolate (right); H atoms were omitted for clarity.*

The bistetrazolato-borate fragment $(BT)BF_2^-$, which was observed by mass spectrometry already during the authors master thesis, was now irrefutably verified in the form of a single crystal X-ray structure. The assumption that the boron atom is too small to be coordinated in a chelating fashion was certified. Instead of a mononuclear structure, similar to the bis(oxalato)borate anion, a ten-membered heterocycle, formally a dimeric structural motive, where two bistetrazolate anions are bridged by two BF_2 moieties, is observed (Figure 5.5).

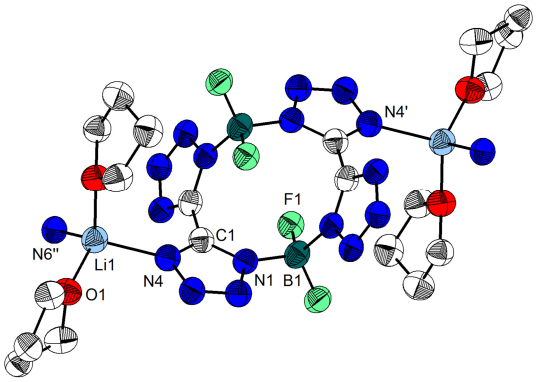

Figure 5.5. *The dimeric structure in lithium-bistetrazolato-difluoroborat; the lithium atoms are additionally coordinated by two THF molecules; symmetry equivalent atomic positions are marked by indices; H atoms were omitted for clarity.*

Starting from 2,3-dioxo-pyrazine-5,6-dicarbonitrile two salts with a new bis(pyrazinediolato)borate anion were synthesized (Scheme 5.9). This forms a potential alternative for the bis(oxalato)borate anion as SEI forming additive for lithium ion secondary batteries.

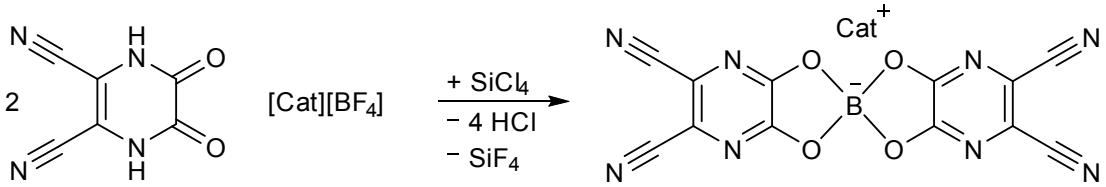

Scheme 5.9. *Synthesis of bis(pyrazine-5,6-dicarbonitrile-2,3-diolato)borate salts with organic cations (Cat = 1-ethyl-3-methylimidazolium or dimethylpyrrolidinium).*

The synthesis of similar bis(rhodizonato)borates was not possible due to the tendency of the rhodizonate anion ($C_6O_6^{2-}$) to form insoluble coordination polymers. However, in the course of this work, a silver rhodizonato complex with triphenyl phosphine ligands, which sufficiently stabilize the monomeric structure, could be isolated and structurally characterized. Its crystal structure is the overall fourth of a rhodizonato complex and shows a so far unknown coordination behavior. The $C_6O_6^{2-}$ anion coordinates two silver atoms via three neighboring oxygen atoms. In all literature known structures, the coordination occurs via four oxygen atoms of which none is in a bridging position (Figure 5.6).

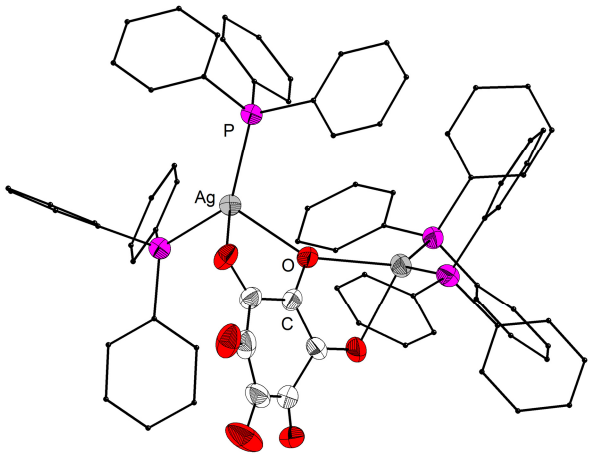

Figure 5.6. *Molecular structure of the silver rhodizonato complex; the C atoms of the phenyl rings are depicted with minimized atomic radius and H atoms are omitted for clarity.*

6 Volltexte der diskutierten Manuskripte

Die acht Manuskripte sind analog zur Reihenfolge im Abschnitt Kumulativer Teil angefügt. Die vier bereits online erschienenen Publikationen sind in ihrer Originalform dargestellt. Publikation 2 wurde von der Zeitschrift Chemistry - A European Journal zur Veröffentlichung akzeptiert, ist jedoch noch nicht online erschienen. Im Anhang befindet sich die nach Begutachtung der Referees erneut eingereichte Version des Manuskripts im Templat der Zeitschrift. In allen Fällen wurde die Erlaubnis des Verlages zur elektronischen und gedruckten Veröffentlichung eingeholt. Bei den Manuskripten 1 bis 3 wurde außerdem der Teil des elektronischen Supplements angefügt, der die experimentellen Grundlagen und weiterführende Diskussionen enthält. Die Abbildungen der IR, NMR, und MS-Spektren wurden hier nicht reproduziert. Die Manuskripte 4, 5 und 7 sind noch nicht zur Veröffentlichung eingereicht.

1) „Access to pure and highly volatile hydrochalcogenide ionic liquids“ Reproduced from „Lars H. Finger, Fabian Wohde, Evgeny I. Grigoryev, Anna-Katharina Hansmann, Robert Berger, Bernhard Roling, Jörg Sundermeyer *Chem. Commun.* 2015, 51, 16169−16172“ with permission from the Royal Society of Chemistry.

2) „Halide Free Synthesis of Hydrochalcogenide Ionic Liquids of the Type [Cation][HE] (E = S, Se, Te)” Lars H. Finger, Jörg Sundermeyer, *Chem. Eur. J.* **2016***,* DOI: 10.1002/chem.201504577*, in press.* Copyright © (2016) Wiley-VCH Verlag GmbH & Co. KGaA. Reproduced with permission.

3) „Synthesis of Organic (Trimethylsilyl)chalcogenolate Salts Cat[TMS-E] (E = S, Se, Te): the Methylcarbonate Anion as a Desilylating Agent“ Reprinted with permission from „Lars H. Finger, Benjamin Scheibe, Jörg Sundermeyer, *Inorg. Chem.* 2015, *54*, 9568−9575“ Copyright © (2015) American Chemical Society.

4) „N-Heterocyclic Olefin – Carbon Dioxide and Sulfur Dioxide Adducts: Structures and Interesting Reactivity Patterns“ Lars H. Finger, Jannick Guschlbauer, Klaus Harms, Jörg Sundermeyer, *in preparation*.

5) „Synthesis of 1,3-Dialkylimidazole-2-chalcogenones from NHC-CO_2 Adducts“ Lars H. Finger Philipp Hofmann, Jörg Sundermeyer, *in preparation*.

6) „Synthesis and Characterisation of 5,5'-Bistetrazolate Salts with Alkali Metal, Ammonium and Imidazolium Cations“ Reproduced from „Lars H. Finger, Fabian G. Schröder, Jörg Sundermeyer, *Z. Anorg. Allg. Chem*. 2013, *639*, 1140–1152“ Copyright © 2013, John Wiley and Sons. License Number: 3787011431565.

7) „New Borate Anions with Bistetrazolato^{2-} and Pyrazinediolato^{2-} Ligands“, Lars H. Finger, Fabian G. Schröder, Jörg Sundermeyer, *in preparation*

8) „μ-Rhodizonato-1κO,1:2κO',2κO''-tetra(triphenylphosphine)disilver(I): A Molecular Complex with the $[C_6O_6]^{2-}$ Ligand Template“ Reproduced from „Lars H. Finger, Jörg Sundermeyer, *Z. Anorg. Allg. Chem.* 2015, *641*, 2565–2569“ Copyright © 2015, John Wiley and Sons. License Number: 3787011296758.

6.1 Zugang zu reinen und sehr flüchtigen Hydrogenchalkogenid Ionischen Flüssigkeiten

Chem. Commun. **2015**, **51**, 16169−16172

Access to pure and highly volatile hydrochalcogenide ionic liquids

Lars H. Finger, Fabian Wohde, Evgeny I. Grigoryev, Anna-Katharina Hansmann, Robert Berger, Bernhard Roling, Jörg Sundermeyer

Volume 51 | Number 90 | 21 November 2015 | Pages 16149–16276

ChemComm

Chemical Communications

www.rsc.org/chemcomm

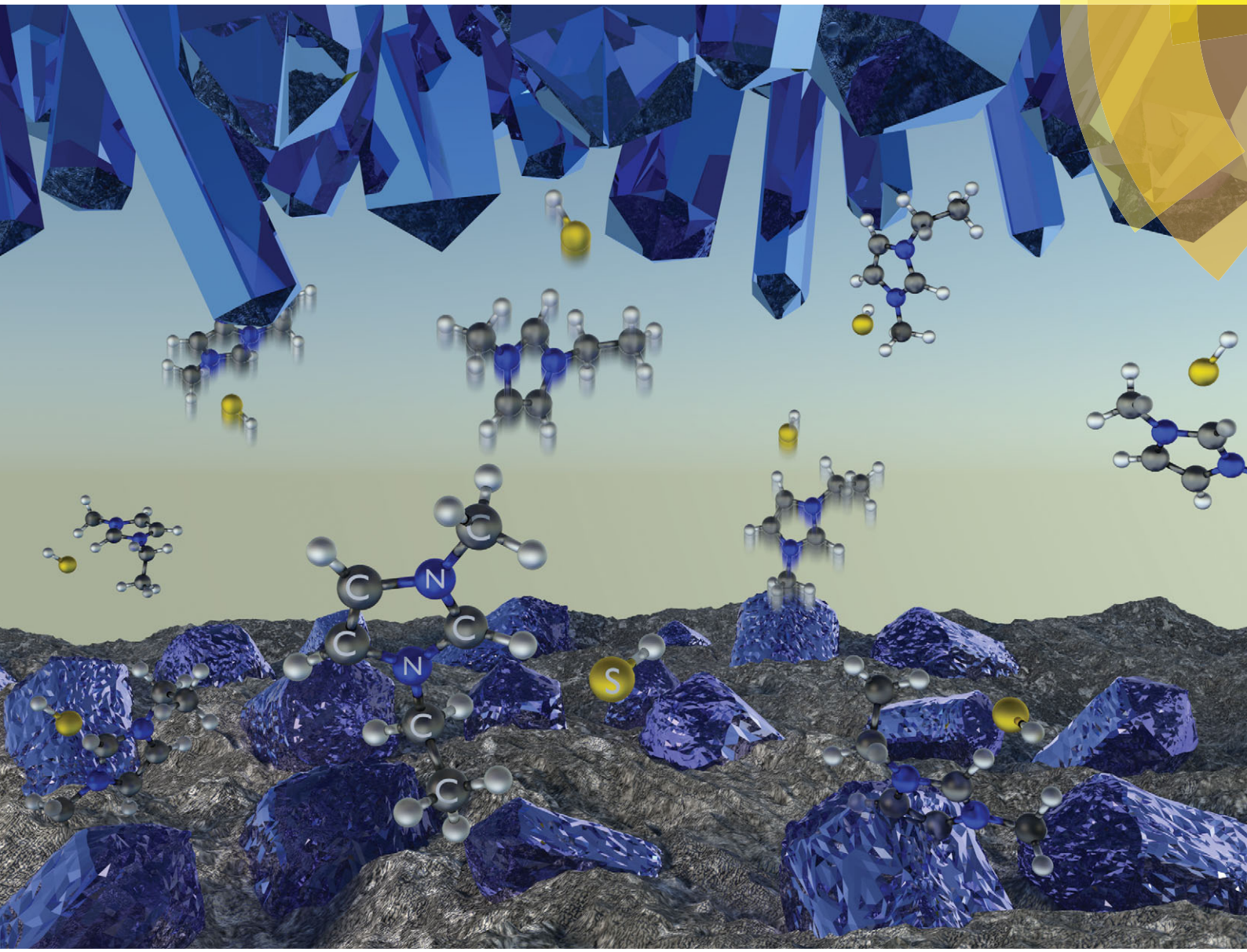

ISSN 1359-7345

ROYAL SOCIETY OF CHEMISTRY

COMMUNICATION

J. Sundermeyer *et al.*

Access to pure and highly volatile hydrochalcogenide ionic liquids

ChemComm

COMMUNICATION

View Article Online
View Journal | View Issue

Cite this: *Chem. Commun.*, 2015, **51**, 16169

Received 24th July 2015,
Accepted 3rd September 2015

DOI: 10.1039/c5cc06224a

www.rsc.org/chemcomm

Access to pure and highly volatile hydrochalcogenide ionic liquids†‡

L. H. Finger, F. Wohde, E. I. Grigoryev, A.-K. Hansmann, R. Berger, B. Roling and J. Sundermeyer*

The reaction of methylcarbonate ionic liquids with H_2S or H_2Se offers a highly selective synthesis of analytically pure, well-defined and soluble hydrosulphide and hydroselenide organic salts of general interest. Among them, imidazolium hydrochalcogenides show an astonishingly high volatility for cation-aprotic ILs, which allows their quantitative sublimation below 100 °C/10^{-2} mbar and actually results in ionic single crystal growth from the gas phase. Vaporisation and decomposition characteristics were investigated by isothermal TGA measurements and DFT calculations.

Tetraalkyl ammonium hydrosulphides, despite being known since the 1960s, were never characterised in detail.[1] They are important building blocks in the synthesis of chalcogenide metal complexes[2] and clusters.[3] More recently, the synthesis of imidazolium and pyrrolidinium hydrosulphides was published.[4] The assumed ionic liquids (ILs) were used as starting materials for organic polysulphide salts, which were investigated as redox mediators in dye or quantum dot sensitised solar cells. A close inspection of the experimental sections in these published articles unveils a considerable lack of analytical data of these ILs. The previous synthetic procedures start from water and halide containing reagents and the crude preparation was typically not accompanied by thorough purification.[4] These conditions are far from ideal, to say the least – especially in view of the targeted electrochemical applications. This class of compounds is also relevant to lithium sulphur batteries, where they occur as a soluble, capacity-limiting shuttle system[5] and to the fabrication of chalcogenide semiconductor materials.[6] Also, the general redox and dissolution behaviour of sulphur and related elements in ILs is of continuing general interest.[7] In view of the high relevance of these substances, we set out to develop an access to high purity hydrosulphide ILs. It was aspired to exclude water, halides and metals and to establish reliable purification allowing the detailed characterisation of all substances. This could be accomplished by the proton induced decarboxylation of methylcarbonate anions[8] employing H_2S as the acidic reagent (Scheme 1). The elegant reaction is easily expanded to the hydroselenide salts and a range of different cations. It is characterised by yielding only volatile, easily separated by-products and comprising no equilibria due to the irreversible decay of the methylcarbonate anion to methanol and carbon dioxide.

Recrystallisation proved to be an effective purification method. Also [BMPyr][HS] (**5**), which was formerly described as a yellow oil,[4a] could be isolated in a crystalline form (Fig. 1).[9] Upon attempting to reproduce the synthesis of bisimidazolium sulphides from the corresponding hydrosulphides under vacuum conditions,[4b] we noticed an unforeseen volatility of the ILs **1** and **3**. Subsequently, we were able to implement sublimation at 10^{-3} mbar and temperatures significantly below 100 °C as an elaborate, high end purification method. Increasing the pressure to 1 mbar still yields pure [EMIm][HS] by sublimation, but the mass transfer rate is significantly decreased. Application of higher temperatures leads to partial thermolysis of the ILs, with 1-alkylimidazole and

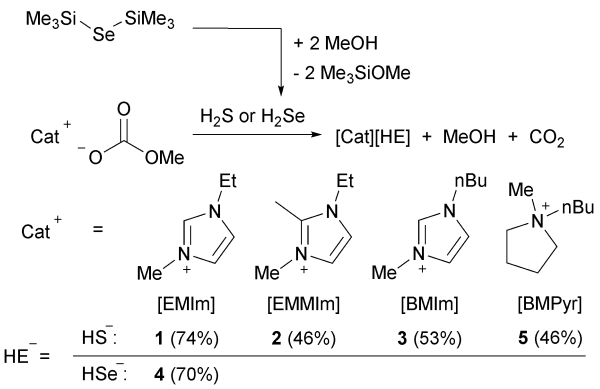

Scheme 1 Synthesis of imidazolium and pyrrolidinium hydrochalcogenides, yields after recrystallisation in parentheses.

Fachbereich Chemie and Materials Science Center, Philipps-Universität, Hans-Meerwein-Str. 4, 35043 Marburg, Germany. E-mail: JSU@staff.uni-marburg.de

† Dedicated to Professor Bernd Harbrecht on the occasion of his 65th birthday.

‡ Electronic supplementary information (ESI) available: Experimental procedures, analytical data, additional information regarding sublimation, isothermal TGA and DFT calculations. CCDC 1414150 and 1414154. For ESI and crystallographic data in CIF or other electronic format see DOI: 10.1039/c5cc06224a

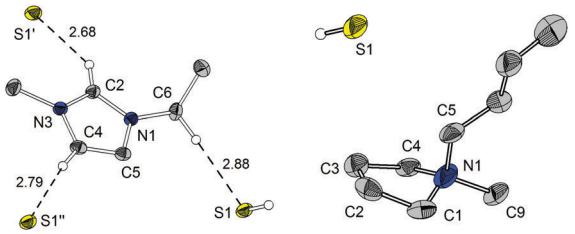

Fig. 1 Molecular structure of [EMIm][HS] (**1**, left) and [BMPyr][HS] (**5**, right), H-bond distances in Å, only H-atoms on sulphur and those participating in H-bonds are shown (symm. op. **1**: I: $x + 1/2, -y + 3/2, z - 1/2$; II: $-x + 1, -y + 1, -z + 1$).

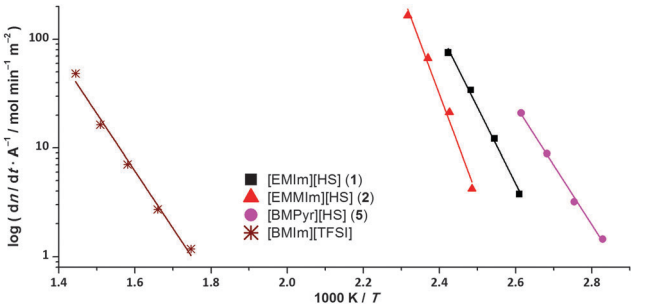

Fig. 2 Arrhenius plots of the molar loss rates per unit area for compounds **1**, **2** and **5** in comparison with [BMIm][TFSI].

dialkylimidazole-2-thione as the main decomposition products. In the case of [EMIm][HS] (**1**), even single crystals suitable for the X-ray structure determination could be obtained by sublimation (Fig. 1).[10] The structure is characterised by hydrogen bonds between the C2 proton and the hydrosulphide anion. Weaker C–H···S contacts are formed from C4, and the aliphatic CH_2 group of C6 (for a H-bond table and graphics of the crystal packing please refer to the ESI‡).

While aprotic ILs have long been understood to exhibit negligible vapour pressure, the last decade has shown that not only do aprotic ILs have a measurable vapour pressure but can also in fact be distilled in a vacuum at elevated temperatures.[11] Nevertheless, the very high degree of volatility observed here is, to the best of our knowledge, unprecedented for aprotic ILs. Typical conditions for the vaporisation of aprotic ILs either make use of UHV chambers with a nominal pressure of 1×10^{-7} mbar with temperatures still ranging mostly above 100 °C or employ highly elevated temperatures.[12] Detailed studies of the vapour phase have proven that under distillation conditions neutral contact ion pairs are the dominant species.[13] In the case of protic ILs, volatility can be ascribed to the acid base equilibrium in the substance being directly correlated with the difference in pK_a values of the cation and the anion's conjugate acid. Here the parent acid and base form the volatile species, while the vapour pressure depends on the acid–base equilibrium.[14] However, the differentiation between protic and aprotic ILs is not as straightforward as it was assumed for some time. Recent investigations have proven that, on the one hand, several protic ILs distil as neutral ion pairs, if the respective pK_a difference is very large.[15] On the other hand, if the IL anion is sufficiently basic, *e.g.* acetate, some 1,3-dialkylimidazolium salts distil as the formal parent acid and base, *e.g.* acetic acid and the 1,3-dialkyl-NHC.[16] The volatile components still form a strongly hydrogen bonded complex though.

These discrepancies motivated us to investigate the phenomenon in more detail. In contrast to **1** and **3**, [BMPyr][HS] (**5**) does not vaporise undecomposed. In this case, decomposition occurs in the form of a ring opening S_N2-type attack. We were able to extend the series of volatile hydrosulphide salts to the C2-methylated [EMMIm][HS] (**2**), though. This proves that the unusual volatility cannot be solely based upon strong hydrogen bonds from the apical proton. Also, the heavier homologue [EMIm][HSe] (**4**) shows a comparable volatility. Subsequently, we conducted isothermal thermo-gravimetric analysis (TGA) experiments to investigate the vaporisation enthalpies and to relate our substances to literature known values.[17] Fig. 2 shows the temperature dependence of the molar loss rates per unit area of compounds **1**, **2** and **5** in comparison with [BMIm][TFSI]; Table 1 lists the values for ΔH_{vap}, at the average measurement temperature (T_{av}) and extrapolated to 298 K. The values determined for ferrocene and [BMIm][TFSI] are included for comparison.

Table 1 Melting temperatures T_m, vaporisation enthalpies ΔH_{vap}, at the average measurement temperature T_{av} and corrected to 298 K and calculated ΔH_{sub} (all ΔH in kJ mol^{-1})

Comp.	T_m/K	T_{av}/K	ΔH_{vap} (T_{av})	ΔH_{vap} (298)	ΔH_{sub} (calc.)
1	366	398	134	144	154
2	401	417	180	192	174
3	328	388	148	157	163
4	375	397	134	144	157
5[a]	427	368	105	112	—
[BMIm][TFSI]		632	101	135	—
FcH		423	72[b]	84	—

[a] Decomposes completely upon melting and sublimation. [b] Sublimation as ($T_m > T_{av}$).

The vaporisation enthalpies of the hydrochalcogenide salts span a very broad range. [EMMIm][HS] shows the highest value of 192 kJ mol^{-1} while [BMPyr][HS] exhibits the lowest ΔH_{vap}, at only 112 kJ mol^{-1}. While the determined vaporisation enthalpies of the hydrochalcogenide salt are mostly higher than that of [BMIm][TFSI], the temperature at which the compounds exhibit a significant mass loss rate is strikingly low. In contrast to [BMIm][TFSI], which has to be exposed to an average temperature of 632 K, the imidazolium hydrochalcogenides showed comparable volatility at average temperatures below 417 K. This difference of more than 200 K is in accordance with the very high volatility under sublimation conditions *in vacuo*. Note that, whereas under vacuum conditions a true sublimation occurs, in the TGA experiments at ambient pressure the elevated temperatures cause a vaporisation from the molten phase. The surprisingly low sublimation enthalpy of [BMPyr][HS] has to be attributed to the decomposition, although T_{av} lies significantly below T_m. As the small sample volume and the instability of the hydrochalcogenide salts under ambient conditions prevented an examination of the remainder in the TGA crucibles, we conducted vaporisation experiments for salts **1** and **5** at 1 bar and 100 °C under inert conditions. Here the condensate of [BMPyr][HS] consists only of decomposition products as well. In the case of

[EMIm][HS], a mixture of 61% IL and 39% decomposition products was observed. For both compounds, the residual substance showed only a minor degree of thermolysis, which confirms that the decomposition products are significantly more volatile than the IL. Thus, the determined vaporisation enthalpies do not represent the pure compound's inherent value, as also for the imidazolium salts, a partial decomposition has to also be anticipated. To determine the vaporisation enthalpies of these salts experimentally, studies in a vacuum using the Langmuir or Knudsen evaporation method are mandatory. We calculated the cohesive energies of the imidazolium ILs **1** to **4** within the density functional theory (DFT, please refer to the ESI‡ for details) in order to estimate the ΔH_{vap} values (Table 1). The results are in reasonable agreement with the TGA experiments and, with the exception of the value for salt **2**, are slightly larger by about 10 kJ mol^{-1}.

In view of the recent observation that imidazolium ILs with sufficiently basic anions act as pseudo-protic ILs during vaporisation[16] and the unusual volatility of the present imidazolium hydrochalcogenides, we applied the DFT as well as EI mass spectrometry to identify the gas phase species. As has to be expected, the EI mass spectra do not show any single ion pairs (SIPs). Instead, the respective carbene, its fragments and hydrogen sulphide as the conjugate acid are observed. This agrees well with the results of Hollóczki *et al.*, who observed the same phenomenon with imidazolium acetate ILs.[16] Also, the respective dialkylimidazole-2-chalcogenone, which was identified as a thermal decomposition product, could be found in the EI mass spectra. DFT calculations concerning the most stable single ion pairs of [EMIm][HS] in the gas phase were conducted on the BP86/def2-TZVP level. An ion pair, where the HS anion is positioned above the plane of the imidazolium cation, was found to be the most stable configuration (Fig. 3). This structure is not solely based on electrostatic interaction but can partially be attributed to a weak π-type orbital interaction between the HOMO of the anion and the LUMO of the cation. Similar interactions were already observed for imidazolium ILs with several anions.[18] Ion pairs, in which the cation forms a hydrogen bond to the hydrosulphide *via* the C2 proton, and which have to be regarded as a pre-complex to the carbene formation, are on the DFT level predicted to be at least 16.9 kJ mol^{-1} higher in energy (Fig. 3). The complete dissociation to a free carbene and hydrogen sulphide is energetically disfavoured, but only to a small extent, thus allowing its occurrence (ΔH_0 = +48.1 kJ mol^{-1} for a singlet carbene). On the basis of these calculations, several SIP structures are viable for the selected system. Together with the results from EI MS experiments, the vaporisation of H_2S and the corresponding carbene appears likely. This is, however, strongly contradicted, by the quantitative sublimation in a dynamic vacuum. That the carbene is the major component detected in the EI mass spectra, leads us to agree with Hollóczki *et al.* that the very low pressure of the mass spectrometric experiments may lead to the dissociated molecules being favoured due to entropic reasons.[16] During the actual sublimation, the π-complex and H-bonded structures have to dominate.

A further non-negligible observation is the presence of 1,3-dialkyl-imidazole-2-chalcogenones among the decomposition products and in the EI mass spectra. The preferred decomposition pathway for imidazolium cations in the presence of highly nucleophilic reaction partners is demethylation.[19] This is in accordance with the alkylimidazoles being the major component of the decomposition mixture, as investigated by NMR spectroscopy and also certified by DFT calculations (see the ESI‡ for details). The stability of imidazolium cations towards related but solvated HO^- ions is strongly dependent on the substitution pattern.[20] In several literature reports, the formation of imidazole-2-chalcogenones results from the reaction of the respective NHC with elemental chalcogen or polychalco-genides.[21] While the presence of carbenes is absolutely feasible in view of the previous results, elemental chalcogen or poly-chalcogenides can be excluded in the sublimed and colourless samples. To the best of our knowledge, and in contrast to the heavier homologues, neither homolytic cleavage to elemental sulphur and hydrogen nor equilibria including polysulphide anions are known for pure hydrosulphide salts. While the latter reaction pathway cannot be fully excluded due to the so far unknown influence of the organic cation, we have investigated an alternative formation pathway by computational methods.

As already noted by Hollóczki *et al.*, a neutral thiol species **A**, resulting from a nucleophilic attack of the hydrosulphide at the C2 position cannot be stabilised.[16] This reaction becomes energetically favoured though, if a concerted deprotonation of the respective hydrosulphide is considered (Scheme 2). The resulting thiolate **B** has to be regarded as a strong hydride donor that will react with the strongest acid present, which is again the hydrosulphide anion. This leads to the formation of imidazole-2-thione, molecular hydrogen and formally a sulphide dianion, which will immediately react with the next imidazolium cation initiating an autocatalytic cycle. The reaction sequence is,

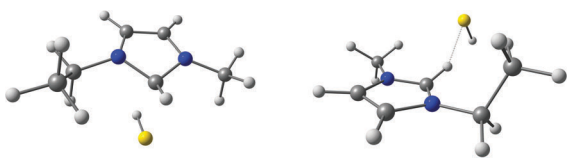

Fig. 3 Most stable SIP of [EMIm][HS] with a π-interaction (left, E_{rel} = 0.0 kJ mol^{-1}) and the H-bonded SIP with lowest energy (right, E_{rel} = 16.9 kJ mol^{-1}).

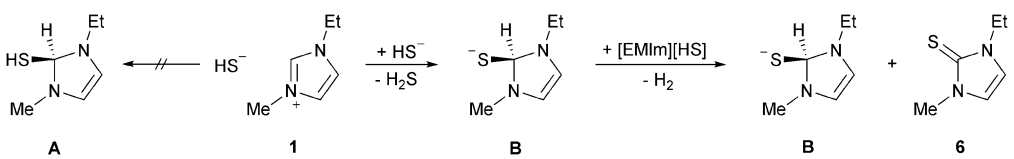

Scheme 2 Formation of 1-ethyl-3-methylimidazole-2-thione (**6**) from the hydrosulphide IL [EMIm][HS] (**1**).

according to DFT calculations for the gas phase, exothermic by -6.3 kJ mol^{-1} in the first and -51.0 kJ mol^{-1} in the second step. Owing to the complexity of the multimolecular reactions, no transition states could be calculated. Nevertheless, this pathway appears to be a viable alternative for the formation of imidazole-2-chalcogenones in the absence of polychalcogenides.

In conclusion, we presented a new and exceedingly convenient access to pure hydrosulphide and hydroselenide organic salts by reaction of methylcarbonate ILs with H_2E (E = S; Se). The title compounds are promising reagents, *e.g.* for the low temperature synthesis of metal chalcogenide clusters and semiconductor materials under ionothermal flux conditions, or as weakly solvated super nucleophiles in organic and inorganic syntheses. In contrast to earlier experiments on dissolving sulphur in ILs,[4a,c,7] these salts may allow the preparation of pure polysulphides, used *e.g.* as redox mediators in quantum dot sensitised solar cells. Imidazolium hydrochalcogenides exhibit remarkably high volatility, which allows their sublimation under moderate vacuum and at temperatures below 100 °C. DFT calculations were employed to calculate the most stable gas phase structures and the sublimation enthalpies of the respective salts. At elevated temperatures, decomposition occurs, the pathways of which have been backed by quantum chemical calculations.

EIG and RB gratefully acknowledge support from the DFG (SPP 1191). LHF and JS thank the VCI (FCI grant for LHF) and the DFG (GRK 1782) for financial support.

Notes and references

1 (*a*) J. D. Cotton and T. C. Waddington, *J. Chem. Soc. A*, 1966, 785; (*b*) D. H. McDaniel and W. G. Evans, *Inorg. Chem.*, 1966, **5**, 2180.
2 (*a*) J. S. Anderson and J. C. Peters, *Angew. Chem., Int. Ed.*, 2014, **53**, 5978; (*b*) H. Sugimoto, K. Hatakeda, K. Toyota, S. Tatemoto, M. Kubo, T. Ogura and S. Itoh, *Dalton Trans.*, 2013, **42**, 3059; (*c*) H. Sugimoto, S. Tatemoto, K. Toyota, K. Ashikari, M. Kubo, T. Ogura and S. Itoh, *Chem. Commun.*, 2013, **49**, 4358; (*d*) E. Galardon, T. Roger, P. Deschamps, P. Roussel, A. Tomas and I. Artaud, *Inorg. Chem.*, 2012, **51**, 10068.
3 (*a*) X.-D. Chen, W. Zhang, J. S. Duncan and S. C. Lee, *Inorg. Chem.*, 2012, **51**, 12891; (*b*) X.-D. Chen, J. S. Duncan, A. K. Verma and S. C. Lee, *J. Am. Chem. Soc.*, 2010, **132**, 15884; (*c*) C. P. Berlinguette and R. H. Holm, *J. Am. Chem. Soc.*, 2006, **128**, 11993.
4 (*a*) V. Jovanovski, V. Gonzalez-Pedro, S. Gimenez, E. Azaceta, G. Cabanero, H. Grande, R. Tena-Zaera, I. Mora-Sero and J. Bisquert, *J. Am. Chem. Soc.*, 2011, **133**, 20156; (*b*) J. Bisquert Mascarell, I. Mora Sero', V. Jovanovski, R. Marcilla Garcia, R. Tena-Zaera, D. Mecerreyes Molero and G. Cabanero Sevillano, EP 2 388 853, 2011; (*c*) J. Liu, X. Yang, J. Cong, L. Kloo and L. Sun, *Phys. Chem. Chem. Phys.*, 2012, **14**, 11592; (*d*) J. Cong, X. Yang, Y. Hao, L. Kloo and L. Sun, *RSC Adv.*, 2012, **2**, 3625.
5 (*a*) I. Bauer, M. Kohl, H. Althues and S. Kaskel, *Chem. Commun.*, 2014, **50**, 3208; (*b*) D. Bresser, S. Passerini and B. Scrosati, *Chem. Commun.*, 2013, **49**, 10545; (*c*) R. Chen, T. Zhao and F. Wu, *Chem. Commun.*, 2015, **51**, 18; (*d*) Y. Diao, K. Xie, S. Xiong and X. Hong, *J. Power Sources*, 2013, **235**, 181; (*e*) C. J. Hart, M. Cuisinier, X. Liang, D. Kundu, A. Garsuch and L. F. Nazar, *Chem. Commun.*, 2015, **51**, 2308; (*f*) E. S. Shin, K. Kim, S. H. Oh and W. I. Cho, *Chem. Commun.*, 2013, **49**, 2004.
6 (*a*) Z. Deng, D. Cao, J. He, S. Lin, S. M. Lindsay and Y. Liu, *ACS Nano*, 2012, **6**, 6197; (*b*) A. Nag, M. V. Kovalenko, J.-S. Lee, W. Liu, B. Spokoyny and D. V. Talapin, *J. Am. Chem. Soc.*, 2011, **133**, 10612.
7 (*a*) È. Boros, M. J. Earle, M. A. Gilea, A. Metlen, A.-V. Mudring, F. Rieger, A. J. Robertson, K. R. Seddon, A. A. Tomaszowska, L. Trusov and J. S. Vyle, *Chem. Commun.*, 2010, **46**, 716; (*b*) N. S. A. Manan, L. Aldous, Y. Alias, P. Murray, L. J. Yellowlees, M. C. Lagunas and C. Hardacre, *J. Phys. Chem. B*, 2011, **115**, 13873.
8 (*a*) R. Kalb (PROIONIC), WO 2008 052 861, 2008; (*b*) G. Degen and C. Stock (BASF), WO 2009 040 242, 2009.
9 Crystal data for **5**: $C_9H_{21}N_1S_1$, M = 175.33, tetragonal, a = 15.6635(6) Å, b = 15.6635 Å, c = 8.9408(5) Å, $\alpha = 90^\circ$, $\beta = 90^\circ$, $\gamma = 90^\circ$, V = 2193.6(2) Å^3, T = 100(2) K, $P42/mbc$, Z = 8, R_1 = 0.0601, wR_2 = 0.1680. GOOF = 1.056, CCDC 1414154.
10 Crystal data for **1**: $C_6H_{12}N_2S_1$, M = 144.24, monoclinic, a = 8.6023(3) Å, b = 7.6710(2) Å, c = 12.7600(4) Å, $\alpha = 90^\circ$, $\beta = 107.8620(10)^\circ$, $\gamma = 90^\circ$, V = 801.42(4) Å^3, T = 100(2) K, $P21/n$, Z = 4, R_1 = 0.0318, wR_2 = 0.0876. GOOF = 1.066, CCDC 1414150.
11 (*a*) L. P. N. Rebelo, J. N. C. Lopes, J. M. S. S. Esperanca and E. Filipe, *J. Phys. Chem. B*, 2005, **109**, 6040; (*b*) M. J. Earle, J. M. S. S. Esperanca, M. A. Gilea, J. N. Canongia Lopes, L. P. N. Rebelo, J. W. Magee, K. R. Seddon and J. A. Widegren, *Nature*, 2006, **439**, 831; (*c*) Y. U. Paulechka, D. H. Zaitsau, G. J. Kabo and A. A. Strechan, *Thermochim. Acta*, 2005, **439**, 158; (*d*) D. H. Zaitsau, G. J. Kabo, A. A. Strechan, Y. U. Paulechka, A. Tschersich, S. P. Verevkin and A. Heintz, *J. Phys. Chem. A*, 2006, **110**, 7303; (*e*) P. Wasserscheid, *Nature*, 2006, **439**, 797.
12 A. W. Taylor, K. R. J. Lovelock, A. Deyko, P. Licence and R. G. Jones, *Phys. Chem. Chem. Phys.*, 2010, **12**, 1772.
13 (*a*) J. P. Leal, J. M. S. S. Esperança, M. E. Minas da Piedade, J. N. Canongia Lopes, L. P. N. Rebelo and K. R. Seddon, *J. Phys. Chem. A*, 2007, **111**, 6176; (*b*) J. P. Armstrong, C. Hurst, R. G. Jones, P. Licence, K. R. J. Lovelock, C. J. Satterley and I. J. Villar-Garcia, *Phys. Chem. Chem. Phys.*, 2007, **9**, 982; (*c*) B. A. D. Neto, E. C. Meurer, R. Galaverna, B. J. Bythell, J. Dupont, R. G. Cooks and M. N. Eberlin, *J. Phys. Chem. Lett.*, 2012, **3**, 3435; (*d*) J. M. S. S. Esperanca, J. N. Canongia Lopes, M. Tariq, L. M. N. B. F. Santos, J. W. Magee and L. P. N. Rebelo, *J. Chem. Eng. Data*, 2010, **55**, 3.
14 (*a*) R. W. Berg, J. N. Canongia Lopes, R. Ferreira, L. P. N. Rebelo, K. R. Seddon and A. A. Tomaszowska, *J. Phys. Chem. A*, 2010, **114**, 10834; (*b*) M. Yoshizawa, W. Xu and C. A. Angell, *J. Am. Chem. Soc.*, 2003, **125**, 15411; (*c*) J. Vitorino, J. P. Leal, M. E. Minas da Piedade, J. N. Canongia Lopes, J. M. S. S. Esperanca and L. P. N. Rebelo, *J. Phys. Chem. B*, 2010, **114**, 8905; (*d*) J. Vitorino, C. E. S. Bernardes and M. E. Minas da Piedade, *Phys. Chem. Chem. Phys.*, 2012, **14**, 4440.
15 M. Horikawa, N. Akai, A. Kawai and K. Shibuya, *J. Phys. Chem. A*, 2014, **118**, 3280.
16 O. Hollóczki, D. Gerhard, K. Massone, L. Szarvas, B. Nemeth, T. Veszpremi and L. Nyulaszi, *New J. Chem.*, 2010, **34**, 3004.
17 (*a*) S. P. Verevkin, R. V. Ralys, D. H. Zaitsau, V. N. Emel'yanenko and C. Schick, *Thermochim. Acta*, 2012, **538**, 55; (*b*) S. P. Verevkin, D. H. Zaitsau, V. N. Emelyanenko, A. V. Yermalayeu, C. Schick, H. Liu, E. J. Maginn, S. Bulut, I. Krossing and R. Kalb, *J. Phys. Chem. B*, 2013, **117**, 6473.
18 (*a*) R. P. Matthews, T. Welton and P. A. Hunt, *Phys. Chem. Chem. Phys.*, 2014, **16**, 3238; (*b*) P. M. Richard, A. Claire, W. Tom and A. H. Patricia, *J. Phys.: Condens. Matter*, 2014, **26**, 284112.
19 M. T. Clough, K. Geyer, P. A. Hunt, J. Mertes and T. Welton, *Phys. Chem. Chem. Phys.*, 2013, **15**, 20480.
20 K. M. Hugar, H. A. Kostalik and G. W. Coates, *J. Am. Chem. Soc.*, 2015, **137**, 8730.
21 (*a*) H. Rodriguez, G. Gurau, J. D. Holbrey and R. D. Rogers, *Chem. Commun.*, 2011, **47**, 3222; (*b*) S. T. Manjare, S. Sharma, H. B. Singh and R. J. Butcher, *J. Organomet. Chem.*, 2012, **717**, 61; (*c*) S. Sauerbrey, P. K. Majhi, G. Schnakenburg, A. J. Arduengo III and R. Streubel, *Dalton Trans.*, 2012, **41**, 5368; (*d*) Y.-F. Han, L. Zhang, L.-H. Weng and G.-X. Jin, *J. Am. Chem. Soc.*, 2014, **136**, 14608.

Supporting Information

to

Access to Pure and Highly Volatile Hydrochalcogenide Ionic Liquids

*L. H. Finger,[a] F. Wohde,[a] E. I. Grigoryev,[a] A.-K. Hansmann,[a] R. Berger,[a] B. Roling[a] and J. Sundermeyer[a]**

a) Fachbereich Chemie,
Philipps-Universität Marburg,
Hans-Meerwein-Str. 4,
35043 Marburg,
Germany.
*E-Mail: JSU@staff.uni-marburg.de

Content

1. Devices and methods

Elemental analyses (C, N, H, S) were carried out by the service department for routine analysis and mass spectrometry with a vario MICRO cube (ELEMENTAR). The samples were weighed into tin capsules inside a nitrogen filled glove box (Labmaster 130, MBRAUN).

Melting points were determined with a BÜCHI Melting Point B540.

Combined TGA/ DSC measurements were performed with a NETZSCH STA 409 CD in aluminium oxide crucibles, with an argon flow rate of 40 mL/min and a heating rate of 10 K/min; TGA decomposition points are given as onset temperature, DSC data is given as peak value.

^{1}H and ^{13}C-NMR spectra were recorded in automation with a BRUKER Avance 300 spectrometer, ^{77}Se NMR-spectra were recorded by the service department for NMR-analyses with a BRUKER DRX 400 spectrometer. All spectra were recorded at ambient temperature. ^{1}H and ^{13}C-NMR spectra were calibrated using residual protons and solvent signals, respectively (DMSO-d_6: δ_H 2.50 ppm, δ_C 39.52 ppm).[1] NMR spectra of ^{77}Se were referenced externally against dimethyl selenide.

IR spectra were recorded on a BRUKER APLPHA FT-IR spectrometer with Platinum ATR-sampling.

2. Starting materials

All solvents were dried according to common procedures[2] and passed through columns of aluminium oxide, 3 Å molecular sieve and R3-11G-catalyst (BASF) or stored over molecular sieve (3 or 4 Å) until use. Reagents were used as received unless stated otherwise. 1-Ethyl-3-methylimidazolium methylcarbonate in methanol solution (30%) was donated by BASF. 1-Butyl-3-methylimidazolium methylcarbonate in methanol solution (50%) was purchased from IOLITEC, *N*-butylpyrrolidine from ACROS. 1-Ethyl-2-methylimidazole was synthesised in analogy to a published procedure.[3] Methylcarbonate ionic liquids were synthesised following the general procedure of R. Kalb.[4] Bis(trimethylsilyl) selenide was synthesised in analogy to the corresponding sulphide.[5]

3. Synthetic Procedures

3.1 Synthesis of 1-ethyl-3-methylimidazolium hydrosulphide ([EMIm][HS], 1).

Hydrogen sulphide was fed into a 30% solution of 1-ethyl-3-methylimidazolium methylcarbonate (26.9 g, 43.4 mmol) in methanol for 40 minutes. All volatiles were removed *in vacuo* and the residue recrystallised from a mixture of acetonitrile and diethyl ether at −30 °C. The solution was decanted and the crystals dried in fine vacuum. [EMIm][HS] (4.62 g, 32.0 mmol, 74%) was obtained as colourless solid. **Mp** 91-93 °C (from acetonitrile/ diethyl ether, 2 K/min). **DSC** (10 K/min): 92.8 °C (endoth.). **TGA** (10 K/min): 162.1 °C (decomp.). **Elem. anal.** found C, 49.9; H, 8.6; N, 19.6; S, 22.0; $C_6H_{12}N_2S_1$ requires C, 50.0; H, 8.4; N, 19.4; S, 22.2. **IR:** ν_{max}/cm^{-1}: 3022m, 2859m, 2565w (SH), 1570s, 1464m, 1420m, 1339m, 1178s, 1030w, 874m, 800s, 704w, 622vs. **^{1}H-NMR** (300.1 MHz, DMSO-d_6) $\delta_H = -3.85$ (s, 1H, *H*S), 1.39 (t, $^3J_{HH}$ = 7.3 Hz, 3H, CH_2CH_3), 3.88 (s, 3H, N*Me*), 4.24 (q, $^3J_{HH}$ = 7.3 Hz, 2H, CH_2CH_3), 7.87 (s, 1H, *H*4/5), 7.99 (s, 1H, *H*4/5), 9.97 (s, 1H, *H*2) ppm. **^{13}C-NMR** (75.5 MHz, DMSO-d_6): $\delta_C = 15.2$ (1C, CH_2CH_3), 35.6 (1C, N*Me*), 43.9 (1C, CH_2CH_3), 121.9 (1C, *C4/5*), 123.3 (1C, *C4/5*), 136.7 (1C, *C2*) ppm.

For sublimation [EMIm][HS] (535 mg, 3.71 mmol) was placed in a long Schlenk tube and heated to 70 °C at $1 \cdot 10^{-3}$ mbar. A colourless substance sublimed to the cooler parts of the flask. After 18 hours 465 mg (3.22 mmol, 87%) of purified, colourless [EMIm][HS] could be isolated. The light brown remainder (30 mg) consisted primarily of unchanged starting material. **Mp:** 92-93 °C**. Elem. anal.** found C, 50.0; H, 8.4; N, 19.7; S, 22.1; $C_6H_{12}N_2S_1$ requires C, 50.0; H, 8.4; N, 19.4; S, 22.2. The IR and NMR spectra stayed unchanged.

3.2 Synthesis of 1-ethyl-2,3-dimethylimidazolium hydrosulphide ([EMMIm][HS], 2).

1-Ethyl-2,3-dimethylimidazolium methylcarbonate (12.7 g, 63.4 mmol) was dissolved in methanol (20 mL) and hydrogen sulphide was fed into the solution for 75 minutes. All volatile components were removed in vacuum, and the residue recrystallised from a mixture of acetonitrile and diethyl ether. [EMMIm][HS] was isolated as light orange crystals in a yield of 4.60 g (29.1 mmol, 46%). **Mp** 125-126 °C (from acetonitrile/ diethyl ether, 2 K/min). **DSC** (10 K/min): 127.6 °C (endoth.). **TGA** (10 K/min): 179.5 °C (decomp.). **Elem. anal.** found C, 53.1; H, 9.1; N, 18.0; S, 19.0; $C_7H_{14}N_2S_1$ requires C, 53.1; H, 8.9; N, 17.7; S, 20.3. **IR:**

ν_{max}/cm^{-1}: 2971s, 2563m (HS), 1721w, 1580m, 1533m, 1327w, 1299m, 1253s, 1197m, 1128m, 954w, 818vs, 661m, 500w. **^{1}H-NMR** (300.1 MHz, DMSO-d_6) δ_H = −4.07 (s, 1H, *H*S), 1.33 (t, $^{3}J_{HH}$ = 7.3 Hz, 3H, CH_2CH_3), 2.60 (s, 3H, C-*Me*), 3.76 (s, 3H, N*Me*), 4.16 (q, $^{3}J_{HH}$ = 7.3 Hz, 2H, CH_2CH_3), 7.69 (s, 1H, *H*4/5), 7.73 (s, 1H, *H*4/5). **^{13}C-NMR** (75.5 MHz, DMSO-d_6): δ_C = 9.0 (1C, C-*Me*), 14.8 (1C, CH_2CH_3), 34.6 (1C, N*Me*), 42.7 (1C, CH_2CH_3), 120.3 (1C, *C4/5*), 122.3 (1C, *C4/5*), 144.0 (1C, *C2*) ppm.

For sublimation [EMMIm][HS] (349 mg, 2.21 mmol) was placed in a long Schlenk tube and heated to 85 °C at $1\cdot10^{-3}$ mbar. A colourless substance sublimed to the cooler parts of the flask. After 60 hours 284 mg (1.79 mmol, 81%) of purified, colourless [EMMIm][HS] could be isolated. The red remainder consisted partly of [EMMIm][HS] but mostly unidentifiable side and decomposition products. **Mp** 127-128 °C. **Elem. anal.** found C, 53.1; H, 9.1; N, 18.1; S, 20.4; $C_7H_{14}N_2S_1$ requires C, 53.1; H, 8.9; N, 17.7; S, 20.3. The IR and NMR spectra stayed unchanged.

3.3 Synthesis of 1-butyl-3-methylimidazolium hydrosulphide ([BMIm][HS], 3).

A 50% solution of 1-butyl-3-methylimidazolium methylcarbonate (8.39 g, 39.1 mmol) in methanol was mixed with additional methanol (10 mL) and hydrogen sulphide was fed into the solution for 45 minutes. All volatiles were removed *in vacuo* and the residue recrystallised from a mixture of acetonitrile and diethyl ether at −30 °C. The solution was decanted and the crystals dried in fine vacuum. [BMIm][HS] (3.54 g, 53%) was obtained as colourless solid. **Mp** 54-55 °C (from acetonitrile/ diethyl ether, 2 K/min). **DSC** (10 K/min): 56.0 °C (endoth.). **TGA** (10 K/min): 157.4 °C (decomp.). **Elem. anal.** found C, 55.8; H, 9.6; N, 16.7; S, 18.55; $C_8H_{16}N_2S_1$ requires C, 55.8; H, 9.4; N, 16.3; S, 18.6. **IR:** ν_{max}/cm^{-1}: 2928m, 2806m, 2559w (HS), 1665w, 1556s, 1453m, 1418w, 1362w, 1165vs, 1011m, 908m, 801s, 753m, 655s, 630s. **^{1}H-NMR** (300.1 MHz, DMSO-d_6) δ_H = −3.92 (s, 1H, *H*S), 0.88 (t, $^{3}J_{HH}$ = 7.3 Hz, 3H, CH_2CH_3), 1.18-1.30 (m, 2H, CH_2CH_3), 1.71-1.81 (m, 2H, NCH_2CH_2), 3.88 (s, 3H, N*Me*), 4.20 (t, $^{3}J_{HH}$ = 7.2 Hz, 2H, NCH_2CH_2), 7.81 (s, 1H, *H*4/5), 7.90 (s, 1H, *H*4/5), 9.76 (s, 1H, *H*2) ppm. **^{13}C-NMR** (75.5 MHz, DMSO-d_6) δ_C = 13.2 (1C, CH_2CH_3), 18.7 (1C, CH_2CH_3), 31.3 (1C, NCH_2CH_2), 35.6 (1C, N*Me*), 48.3 (1C, NCH_2CH_2), 121.1 (1C, *C4/5*), 123.4 (1C, *C4/5*), 136.7 (1C, *C2*) ppm.

For sublimation [BMIm][HS] (549 mg, 3.19 mmol) was placed in a long Schlenk tube and heated to 50 °C at $1\cdot10^{-3}$ mbar. A colourless substance sublimed to the cooler parts of the flask. After 48 hours 420 mg (1.79 mmol, 77%) of purified, colourless [BMIm][HS] could be

isolated. The light green remainder consisted of unchanged starting material. **Mp** 54-55 °C. **Elem. anal.** found C, 55.8; H, 9.5; N, 16.7; S, 18.3; $C_8H_{16}N_2S_1$ requires C, 55.8; H, 9.4; N, 16.3; S, 18.6. The IR and NMR spectra stayed unchanged.

3.4 Synthesis of 1-ethyl-3-methylimidazolium hydroselenide ([EMIm][HSe], 4).

A 30% solution of 1-ethyl-3-methylimidazolium methylcarbonate (3.68 g, 5.93 mmol) was cooled in an ice bath and degassed thoroughly. Bis(trimethylsilyl)selenide (1.63 g, 7.23 mmol) was added in small portions within 15 minutes and the resulting mixture was stirred at 0 °C for 30 minutes and further 30 minutes at ambient temperature. After removal of volatile contents the residue was recrystallised from an acetonitrile/ diethylether mixture at −30 °C. [EMIm][HSe] (796 mg, 70%) was obtained as a colourless solid. **Mp** 101-102 °C (from acetonitrile/ diethyl ether, 2 K/min). **Elem. anal.** found C, 37.7; H, 6.4; N, 15.0; $C_6H_{12}N_2Se_1$ requires C, 37.7; H, 6.3; N, 14.7. **IR:** ν_{max}/cm^{-1}: 3049m, 2962m, 2274w (HSe), 1569m, 1418w, 1362w, 1339w, 1259m, 1173s, 1091m, 1027m, 863m, 789vs, 704m, 645m, 620vs. **^{1}H-NMR** (300.1 MHz, DMSO-d_6) $\delta_H = -6.56$ (s, 1H, *H*Se), 1.40 (t, $^3J_{HH} = 7.3$ Hz, 3H, CH_2CH_3), 3.87 (s, 3H, N*Me*), 4.22 (q, $^3J_{HH} = 7.3$ Hz , 2H, CH_2CH_3), 7.77 (t, $^{3/4}J_{HH} = 1.7$ Hz, 1H, *H4/5*), 7.87 (t, $^{3/4}J_{HH} = 1.7$ Hz, 1H, *H4/5*), 9.46 (s, 1H, *H2*) ppm. **^{13}C-NMR** (75.5 MHz, DMSO-d_6): $\delta_C = 15.1$ (1C, CH_2CH_3), 35.7 (1C, N*Me*), 44.0 (1C, CH_2CH_3), 121.9 (1C, *C4/5*), 123.4 (1C, *C4/5*), 136.2 (1C, *C2*) ppm. **^{77}Se-NMR** (76.3 MHz, DMSO-d_6): $\delta_{Se} = -312.3$ ppm.

For sublimation [EMIm][HSe] (418 mg, 2.19 mmol) was placed in a long Schlenk tube and heated to 95 °C at $1 \cdot 10^{-3}$ mbar. A colourless substance sublimed to the cooler parts of the flask. After 80 hours 330 mg (1.73 mmol, 79%) of purified, colourless [EMIm][HSe] could be isolated. The light green remainder consisted of unchanged starting material. **Mp** 101-103 °C. **Elem. anal.** found C, 37.6; H, 6.3; N, 15.2.; $C_6H_{12}N_2Se_1$ requires C, 37.7; H, 6.3; N, 14.7. The IR and NMR spectra stayed unchanged.

3.5 Synthesis of N-butyl-N-methylpyrrolidinium hydrosulphide ([BMPyr][HS], 5).

N-Butyl-*N*-methylpyrrolidinium methylcarbonate (15.1 g 69.5 mmol) was dissolved in methanol (40 mL) and hydrogen sulphide fed into the solution for one hour. All volatiles were removed *in vacuo* and the residue recrystallised from a mixture of acetonitrile and diethyl ether at −30 °C. The solution was decanted and the crystals dried in fine

vacuum. [BMPyr][HS] (5.65 g, 46%) was obtained as colourless solid. **Mp** 153-155 °C (decomp., from acetonitrile/ diethyl ether, 2 K/min). **DSC** (10 K/min): 166.5 °C (endoth.). **TGA** (10 K/min): 153.4 °C (decomp.). **Elem. anal.** found C, 61.8; H, 12.3; N, 8.1; S, 17.7; $C_9H_{21}N_1S_1$ requires C, 61.65; H, 12.1; N, 8.0; S, 18.3. **UV-Vis**: λ_{max} (DMSO)/nm 264. **IR:** ν_{max}/cm^{-1}: 2959vs, 2934s, 2873m, 2560w (HS), 1459vs, 1379w, 1260w, 1060m, 1004s, 910s, 743m, 587w. **^{1}H-NMR** (300.1 MHz, DMSO-d_6) $\delta_H = -4.03$ (s, 1H, *H*S), 0.92 (t, $^3J_{HH} = 7.4$ Hz, 3H, CH_2CH_3), 1.24-1.38 (m, 2H, CH_2CH_3), 1.60-1.74 (m, 2H, NCH_2CH_2), 2.00-2.14 (m, 4H, *CH_2(3,4)*), 3.02 (s, 3H, N*Me*), 3.30-3.60 (m, 6H, NCH_2CH_2, *CH_2(2,5)*) ppm. **^{13}C-NMR** (75.5 MHz, DMSO-d_6) $\delta_C = 13.4$ (1C, CH_2CH_3), 19.2 (1C), 21.0 (1C), 24.8 (1C), 47.4 (t, $^3J_{CN} = 3.9$ Hz, 2C, *C3/4*), 62.6 (t, $^2J_{CN} = 2.8$ Hz, 2C, *C2/5*), 63.2 (t, $^2J_{CN} = 3.1$ Hz, 1C) ppm.

Upon attempting to sublime the substance analogously to the prior imidazolium salts the condensation of colourless droplets at cooler parts of the Schlenk flask was observed. These were identified as a mixture of decomposition products. No traces of the former salt could be detected.

4. Crystal Structures

Single crystals of [EMIm][HS] (**1**), where grown by sublimation, the resulting structure was analogous but of higher quality when compared to crystals grown from a saturated methanol solution. Crystals of **2** were obtained by layering a solution of the compound in acetonitrile with diethyl ether. [BMPyr][HS] (**5**) crystallised from an oversaturated acetonitrile solution at room temperature. The data collection for the single crystal structure determinations was performed in rotation method on a Bruker D8 QUEST diffractometer by the X-ray service department of the Fachbereich Chemie, University of Marburg. The spectrometer is equipped with a Mo-K_α X-ray micro source (0.71073 Å, Incotec), a fixed chi goniometer and a PHOTON 100 CMOS detector. Bruker software (Bruker Instrument Service, APEX2, SAINT) was used for data collection, cell refinement and data reduction.[6] The structures were solved with SIR-97[7] or SIR2011[8] refined with SHELXL-2014[9] and finally validated using PLATON[10] software, all within the WinGX[11] software bundle. EnCIFer aided in the editing and validation of the CIF files.[12] Absorption corrections where applied beforehand within the APEX2 software (multi-scan).[13] Graphic representations were created using Diamond 4.[14] C-bound H-atoms were constrained to parent site; The sulphur bound H-atom in [EMIm][HS] was located in the Fourier map and refined independently. Analogous treatment of the sulphur bound H-atom in [BMPyr][HS], did not lead to a stable position for the H-atom and convergence of the structure, possibly attributable to the strong disorder of the cation along a mirror plane (figure S1 and S2). In this case the H-atom was located in the Fourier map and coordinates and displacement were fixed before the next refinement cycles. In all graphics the ellipsoids are shown for the 50% probability level. Hydrogen atoms are shown with arbitrary radius, only those bound to hetero atoms or involved in hydrogen bonds are shown in the graphic representations. Selected crystal data and experimental parameters are listed in table S1. Crystallographic data for the structures presented in this paper have been deposited with the Cambridge Crystallographic Data Centre. CCDC-141450 and 141454 contain the supplementary crystallographic data for this paper. These data can be obtained free of charge from The Cambridge Crystallographic Data Centre via www.ccdc.cam.ac.uk/data%5Frequest/cif.

Table S1. Crystal data for the structures of compounds 1 and 5.

	[EMIm][HS] (**1**)	[BMPyr][HS] (**5**)
Formula	C6 H12 N2 S	C9 H21 N S
FW / g mol^{-1}	144.24	175.33
Crystal system	monoclinic	tetragonal
Space group	P 21/n	P 42/m b c
Colour, habit	colourless block	colourless needle
Crystal size / mm^3	0.21 x 0.20 x 0.10	0.38 x 0.14 x 0.12
a / Å	8.6023(3)	15.6635(6)
b / Å	7.6710(2)	15.6635
c / Å	12.7600(4)	8.9408(5)
α /°	90	90
β /°	107.8620(10)	90
γ /°	90	90
V / Å^3	801.42(4)	2193.6(2)
Z	4	8
D_{calc}/g cm^{-3}	1.195	1.062
Min./max. Transm.	0.6361/ 0.7457	0.6668/ 0.7456
μ / cm^{-1}	0.323	0.244
F(000)	312	784
T / K	100(2)	100(2)
θ range /°	2.54 : 26.33	2.60 : 25.99
range h,k,l	−11:11; −10:10; −17:17	−16:19; −18:19; −11:11
Refl. Coll.	18404	16725
Refl. Indep.	1993	1154
Refl. I > 2σ(I)	1777	871
Data / restr. / param.	1993/ 0/ 88	1154/ 2/ 90
R_{int}	0.0447	0.0514
R_1 (obs)	0.0318	0.0601
wR_2 (all)	0.0876	0.1680
GooF (F^2)	1.066	1.056
Res. e$^-$ dens. (min./ max.)	−0.238/ 0.338	−0.368/ 0.248
CCDC	1414150	1414154

Table S2. Hydrogen bonds in the solid state structure of [EMIm][HS] (1).

D-H···A	d(H···A) /Å	d(D···A) /Å	<(DHA)/°
[EMIm][HS], (**1**)			
C2-H2…S1’	2.68	3.520(1)	148.2
C4-H4…S1’’	2.79	3.731(1)	172.7
C6-H6B…S1	2.88	3.786(1)	152.7
I: x+1/2, −y+3/2, z−1/2; II: −x+1, −y+1, −z+1.			

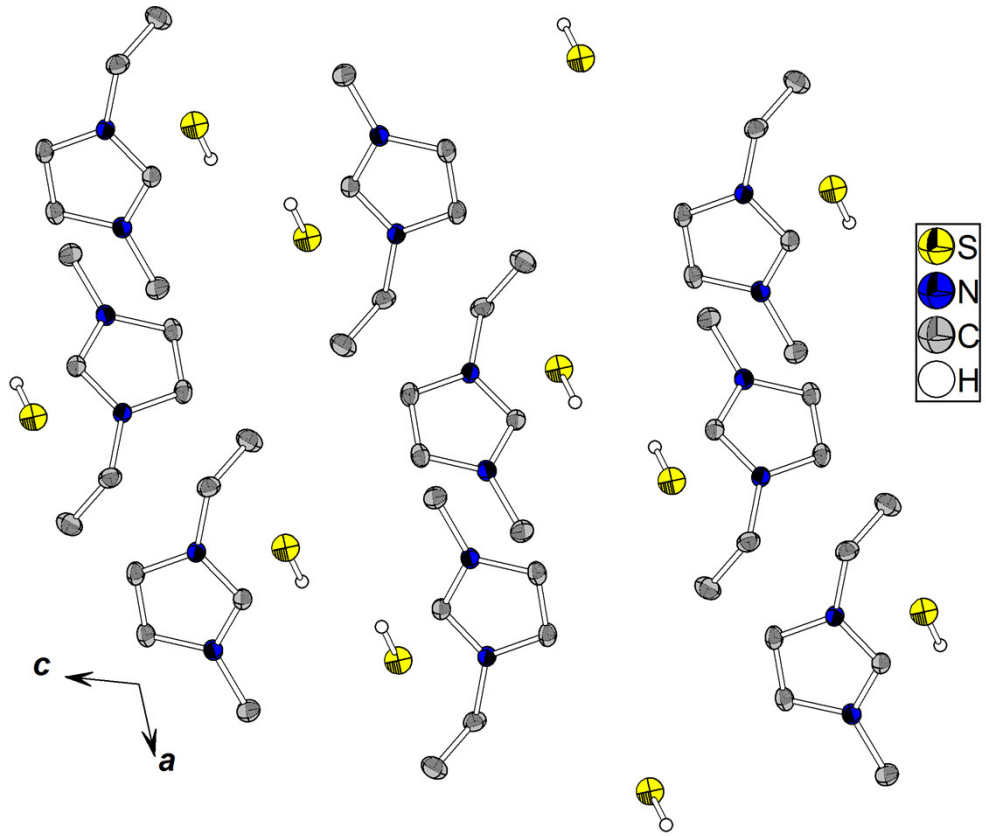

Figure S1. Crystal structure of [EMIm][HS] (1) viewing along the b-axis.

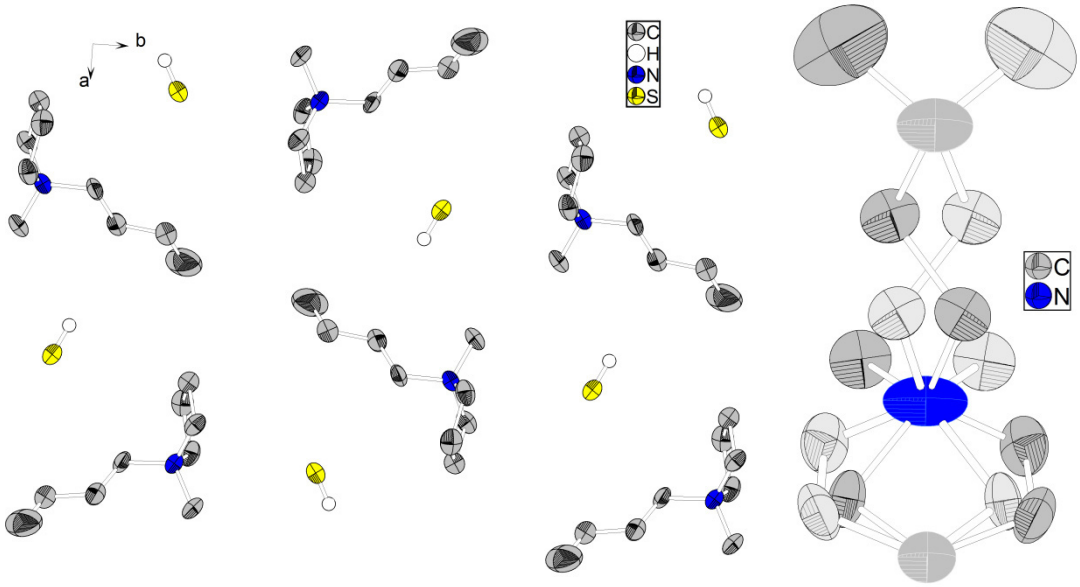

Figure S2. Crystal structure of [BMPyr][HS] (5) viewing along the c-axis and disorder of the pyrrolidinium cation along a mirror plane.

5. Details concerning the sublimation process

All sublimed imidazolium salts could unambiguously be identified as the original hydrochalcogenide salt. The NMR and IR spectra fully coincide; the elemental composition was proven by elemental analysis (CHNS). The melting points were increased by ca. 1 K after sublimation demonstrating the already high purity of the originally isolated hydrochalcogenide salts. The residue after a first sublimation consists mainly of unsublimed starting material, only in case of [EMMIm][HS] (**2**) a larger amount of unidentified side products was observed. Typically the isolated sublimate accounted for more than 80% of the employed amount. After a second sublimation no visible residue remained, 95% of the deployed substance could be re-isolated.

Figure S3. Crystals of [EMIm][HS] (1) after sublimation.

Figure S4. [EMMIm][HS] (2) before and after sublimation.

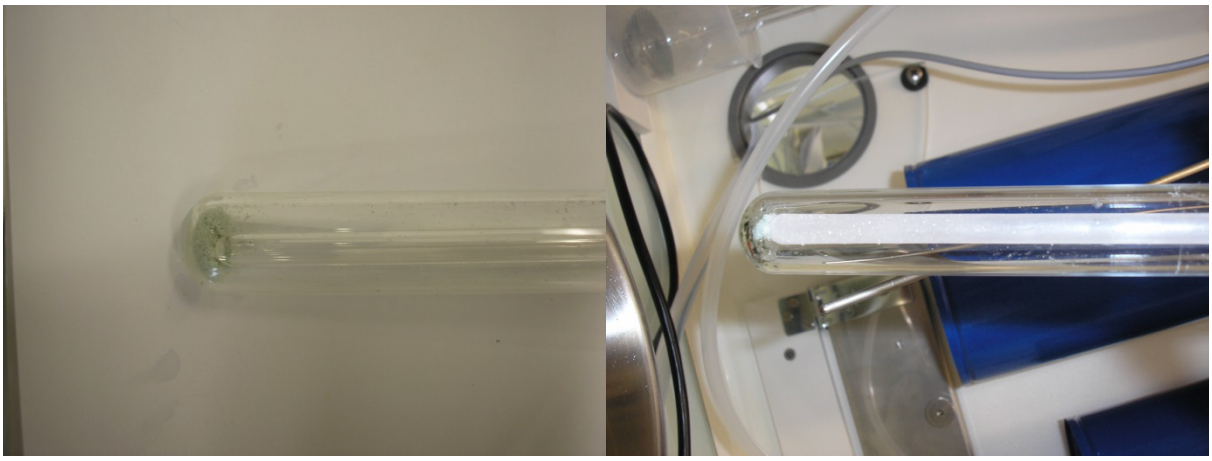

Figure S5. [BMIm][HS] (2) before and after sublimation.

Figure S6. Crystalline [BMIm][HS] (3) after sublimation.

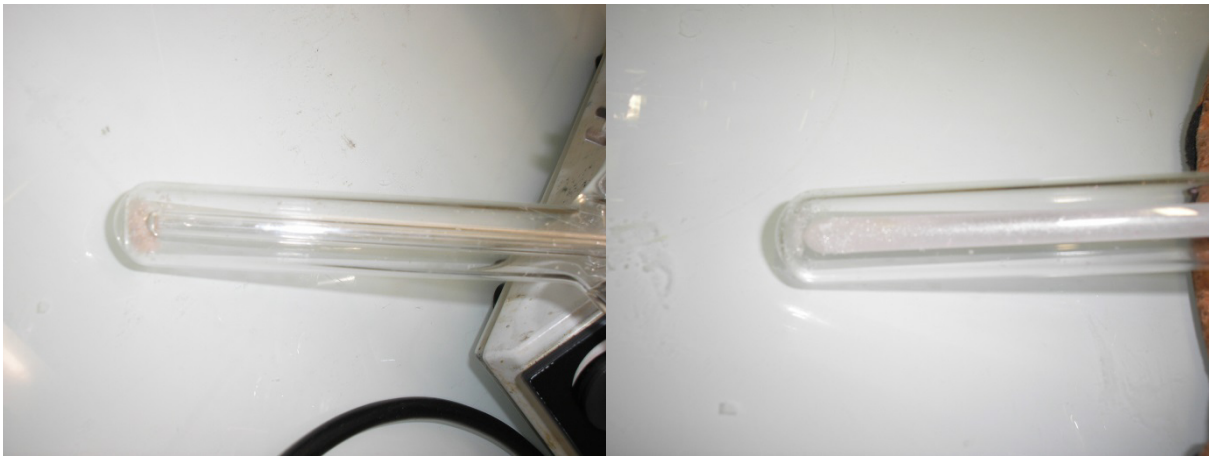

Figure S7. [EMIm][HSe] (4) before and after sublimation.

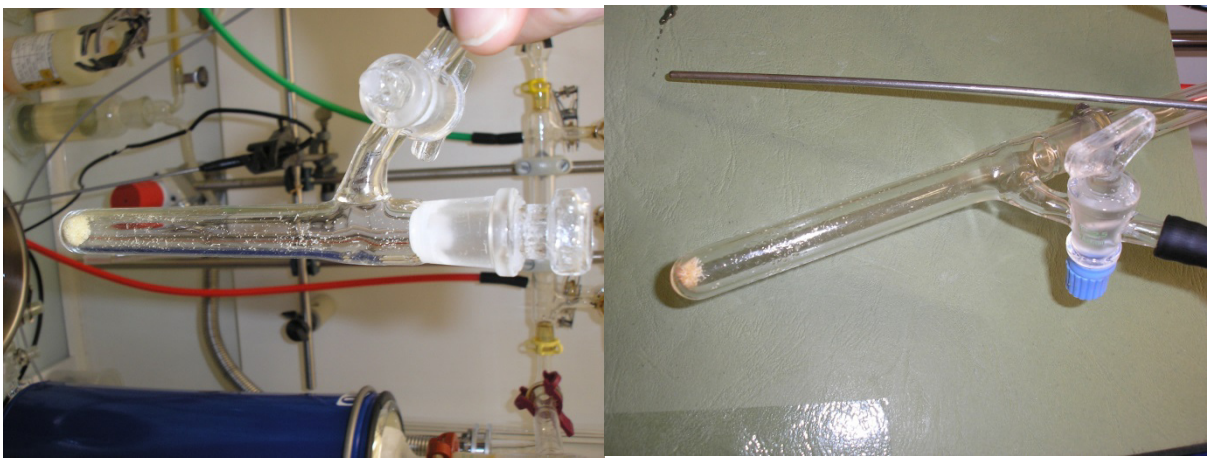

Figure S8. [BMPyr][HS] (5) before and after the attempted sublimation, the right picture shows the oily decomposition products.

In case of [BMPyr][HS] the condensated substance consists primarily of the acyclic aminothiole S**7**, which results from a ring opening S_N2 attack at one of the pyrrolidinium C atoms next to the nitrogen atom. This reaction behaviour is well documented for pyrrolidinium cations. It can be traced back to an increased ring strain in comparison with related 6-ring piperidinium, where primarily a demethylation occurs.[15]

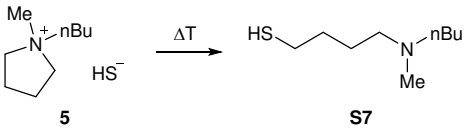

5 **S7**

Scheme S1. Thermal decomposition of [BMPyr][HS] (5), only the main product is shown.

We also investigated the vaporisation behaviour of the hydrosulphide salts **1** and **5** under ambient pressure, in order to mimic the conditions in the TGA measurements for ΔH_{vap} determination (*vide infra*). Larger samples were placed in a Schlenk tube with a coldfinger at −30 °C reaching as far as 1 cm above the substance. The tube was then heated to 100 °C and after reaching the final temperature the pressure was adjusted to atmospheric conditions. After several hours, when a sufficient amount of material was visible on the cold finger, the experiment was stopped and the complete condensate analysed by NMR spectroscopy. Figures S9 compares the ^{1}H-NMR spectra of pure [EMIm][HS] and the collected substance, figure S10 correspondingly compares the spectra of [BMPyr][HS] and its decomposition products.

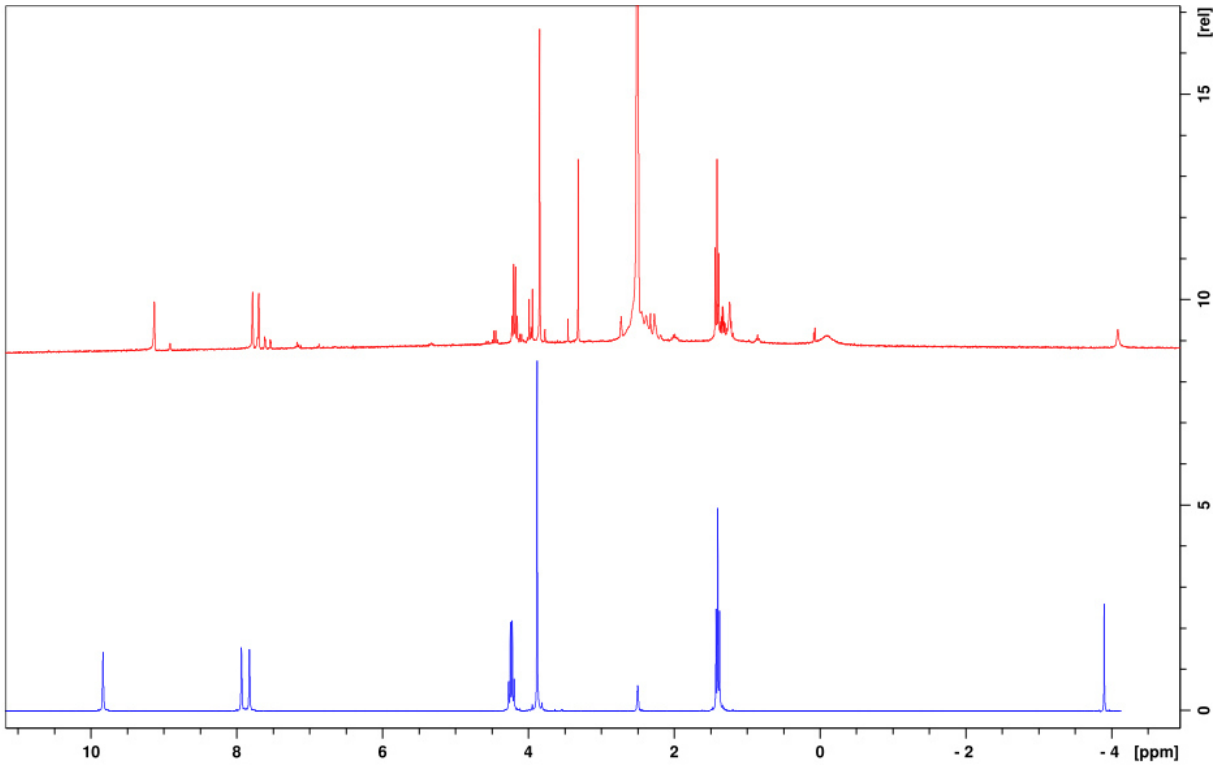

Figure S9. ^{1}H-NMR spectra of pure [EMIm][HS] (blue) and the substance collected after the attempted sublimation at ambient pressure (red). The variation of the chemical shift of the aromatic imidazolium protons is due to the difference in concentration of the two samples.

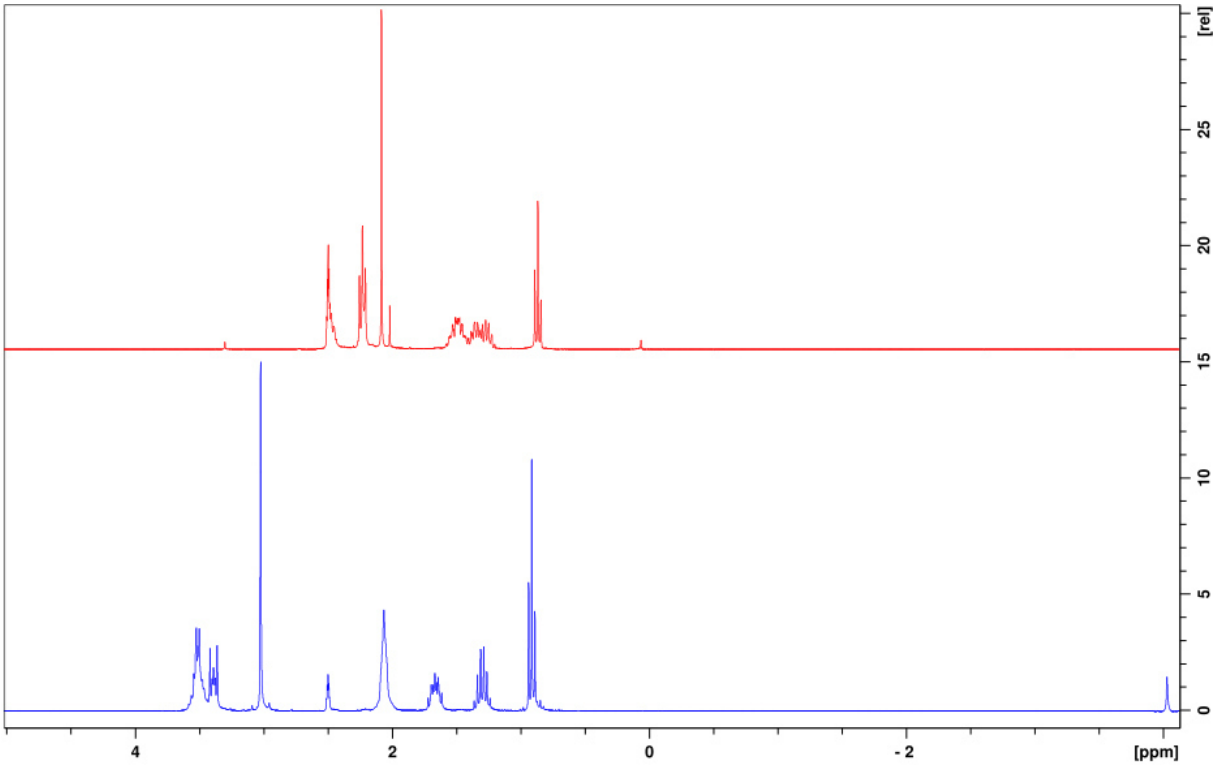

Figure S10. 1H-NMR spectra of pure [BMPyr][HS] (blue) and the decomposition products collected after the attempted sublimation at ambient pressure (red).

6. Isothermal TGA measurements for ΔH_{vap} determination

Isothermal TGA experiments for determination of vaporisation enthalpies were conducted using a TGA/SDTA 851 equipped with a LF/1100 °C oven from METTLER TOLEDO. The measurements were carried out in encapsulated 40 µL Al crucibles, which have been perforated with a 0.64 mm opening for a defined effusion at isothermal steps. Dry nitrogen was used as carrier gas with a flow rate of 50 mL/min. The calibration of the experimental setup was undertaken with ferrocene as calibration substance with known vapour pressure, following the NIST recommendation.[16] Ferrocene was purchased from ACROS ORGANICS (98%)

For all experiments the purest available samples were chosen; in case of the imidazolium salts, the salts were sublimed once before further use. In case of [BMPyr][HS] a double recrystallisation of the sample was carried out. As further test substance for the TGA experiments, [BMIm][TFSI] was purchased from IOLITEC (99.5%) and dried 24 h in fine vacuum at 90 °C prior to the TGA experiment. All measurements were conducted with a stepwise temperature programme of isothermal plateaus (10 min) and a heating rate of 10 K/min. The mass loss rate per unit area $\frac{1}{A} \cdot \left|\frac{dm}{dt}\right|_T$ is related to the apparent vapour pressure P_T via equation (1):[16a]

$$log\left(\frac{1}{A} \cdot \left|\frac{dm}{dt}\right|\right)_T + C \propto log\ P_T \qquad (1)$$

Here, C is a device specific constant.

From Arrhenius plots of the mass loss rates per unit area, the vaporisation enthalpy ΔH_{vap} could be extracted according to the Clausius-Clapeyron equation (2), where C' is a sample specific constant.

$$\log\left(\frac{1}{A} \cdot \left|\frac{dm}{dt}\right|\right) = \frac{\Delta H_{vap}}{R} \cdot \frac{1000}{T} + C' \qquad (2)$$

The determined ΔH_{vap} values were corrected to 298 K via equation (3).

$$\Delta H_{vap}(298\ K) = \Delta H_{vap}\,(T_{av}) + \Delta C_m(298\ K - T_{av}) \qquad (3)$$

The value of the molar heat capacity difference ΔC_m was set to -0.1 kJ•mol^{-1}, which has evolved as a rough standard approximation in this field of research, although not undisputed.[17]

To allow for a comparison of the apparent vapour pressures between different substances, the molar weight of the gas-phase molecules has to be considered. Here, we assumed contact ion pairs to constitute the gas phase. Therefore, the IL-specific molar masses were employed to the Arrhenius plots of the molar loss rates per unit area $log\left(\frac{1}{A}\cdot\left|\frac{dn}{dt}\right|\right) = log\left(\frac{1}{A}\cdot\left|\frac{dm}{dt}\right|\cdot\frac{1}{M}\right)$, presented in figure S11-right, compared with the mass loss rate (figure S11-left). Comparing substances **1**, **2**, **5**, ferrocene and [BMIm][TFSI] shows the striking difference between the classical IL test substance [BMIm][TFSI] and the hydrochalcogenides investigated in this work (figure S12).

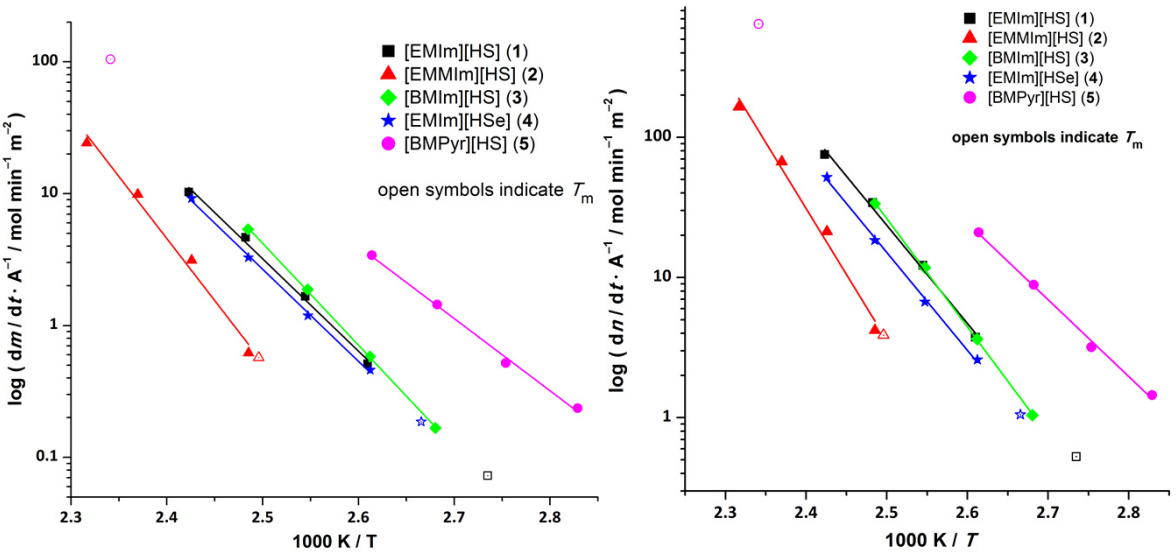

Figure S11. Arrhenius plots of the mass loss rate (left) and the molar loss rates (right) per unit area of compounds 1 to 5, the melting temperature of [BMIm][HS] lies outside of the current graph borders at 3.05.

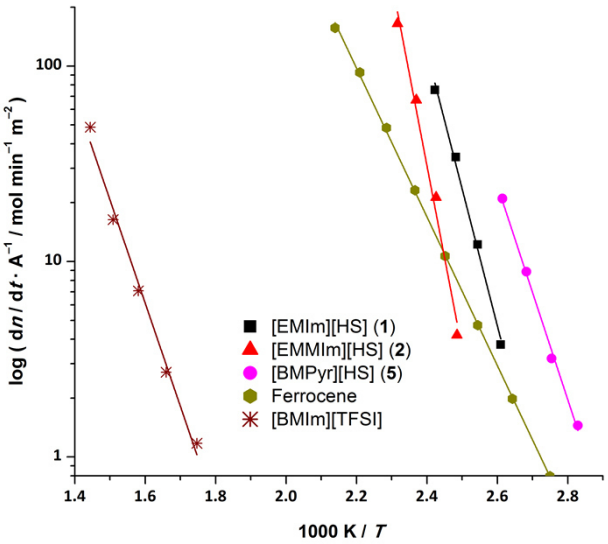

Figure S12. Arrhenius plots of the molar loss rates per unit area, comparing the hydrosulphides 1, 2, 5, ferrocene and [BMIm][TFSI].

7. Computational methods

Structure optimisation for the most stable conformations of [EMIm][HS] single ion pairs (SIPs) in the gas phase (figure S13) as well as reaction path search for the decomposition processes occurring during the vaporisation were studied with the quantum chemistry programme Gaussian 09.[18] These calculations for gas phase structures were performed within density functional theory on a BP86/def2-TZVP level.[19] Molecular structures for stationary points on the Born-Oppenheimer hypersurface were obtained such that the root mean square (RMS) of all force components with respect to internal coordinates dropped below $10^{-5}\,E_h \cdot a_0^{-1}$ and $10^{-5}\,E_h \cdot rad^{-1}$. Convergence criteria in the self-consistent field (SCF) procedure were that RMS changes in the density matrix between two successive SCF cycles remained below 10^{-8}. The integration scheme is "UltraFine", i.e. a pruned (99, 590) grid for the numerical integration step involved in the construction of the exchange correlation potential. All stationary points were characterised by harmonic vibrational frequency calculations and minimum energy reaction paths were obtained *via* the steepest gradient descent approach. To identify the type of bonding interaction present in the SIP b) (figure S13), the program AIMALL[20] was employed to perform the QTAIM (Quantum Theory of Atoms in Molecules) analysis according to R. F. W. Bader.[21] Additionally to that, a natural bond orbital analysis[22] in NBO 3.1[23] and an energy decomposition analysis (EDA)[24] in ADF[25] were performed.

Calculations concerning cohesive energies were performed with the Vienna Ab initio Simulation Package (VASP). The experimental crystal structures of compounds **1** and **3,** which were determined in the course of this work, were used as input. The structure of **1** is submitted with this publication (*vide supra*). The CIF files of all structures have been deposited with the CCDC and can be obtained under CCDC 1414150 to 1414153. Structure optimisations were performed for monoclinic [EMIm][HS] (**1**) and [EMIm][[HSe] (**4**) and orthorhombic [EMMIm][HS] (**2**) and [BMIm][HS] (**3**) crystal structures, as well as for single ion pairs in the gas phase. These calculations were performed within the non-spin polarised density functional theory and the Generalised Gradient Approximation PBE (GGA-PBE)[26] together with the projector-augmented-wave (PAW) method[27] as implemented in the Vienna Ab initio Simulation Package (VASP.5.3.5).[28] A kinetic energy cut-off of 480 eV is used for convergence of the total energy within 1 meV. Gamma k-point meshes of 4 x 4 x 6 for [EMMIm][HS], 4 x 6 x 4 for [EMIm][HSe] and $4 \times 4 \times 4$ for the two other crystal unit cells are used for Brillouin zone integration to calculate the electronic ground states. Long-range

van-der-Waals interactions were accounted for by employing the zero damping DFT-D3 scheme of Grimme.[29]

Cohesive energies (E_{coh}) are assumed to be approximately equal to the sublimation enthalpies (ΔH_{sub}) and were calculated using the relation

$$\Delta H_{sub} \approx E_{coh} = E_{unit} - E_{bulk}/N_{unit},$$

where E_{unit} is the energy of a single ion pair in the most stable conformation in vacuum and E_{bulk} is the energy per unit cell of the respective salt. N_{unit} is the number of formula units in the simulation cell of the given crystalline structure ($N_{Unit} = 8$ for [EMMIm][HS], and $N_{Unit} = 4$ for the others). E_{unit} was calculated in a simulation cell, which is sufficiently large to avoid artificial interactions between a SIP and its periodic images. For the same purpose, the cut-off radius of the force field within the context of the PBE-D3 scheme was reduced. Equilibrium structures were obtained using the conjugate gradient optimisation. All atoms were fully relaxed until the change in forces on the ionic displacements was below 0.01 eV/Å. No other constraints were imposed for structure optimisation calculations in the bulk systems. The optimized lattice parameters (a, b, c, β) for the crystal structures (table S3) show a slight deviation from the experimental values.

Table S3. Strucutral parameters of the unit cells of compounds 1 to 4 after structure optimisation (exprimental values in parenthesis).

Compound	a/ Å	b/ Å	c/ Å	β/°
[EMIm][HS] (**1**)	8.58 (8.60)	7.54 (7.67)	12.67 (12.76)	107.7 (107.9)
[EMMIm][HS] (**2**)	7.84 (8.02)	13.32 (13.43)	16.46 (16.64)	- -
[BMIm][HS] (**3**)	9.84 (9.91)	12.04 (12.14)	8.16 (8.23)	- -
[EMIm][HSe] (**4**)	8.57 (8.60)	7.60 (7.78)	13.20 (13.30)	108.4 (108.2)

7.1 Gas phase structure optimisation of [EMIm][HS] single ion pairs

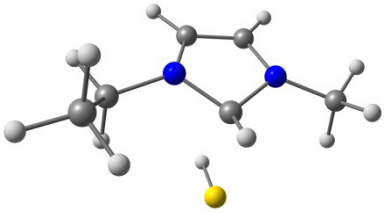

a) E_{rel} = 0.0 kJ·mol^{-1}

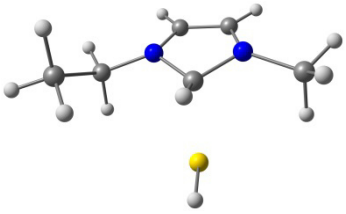

b) E_{rel} = 1.9 kJ·mol^{-1}

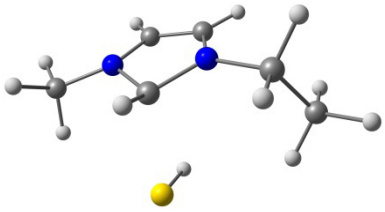

c) E_{rel} = 4.0 kJ·mol^{-1}

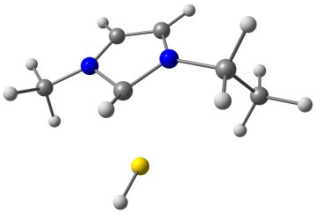

d) E_{rel} = 5.7 kJ·mol^{-1}

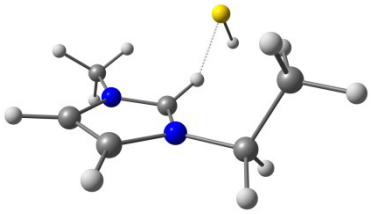

e) E_{rel} = 16.9 kJ·mol^{-1}
D(C−H···S): 3.07 Å
<(C−H···S): 149.9°

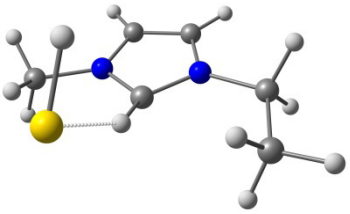

f) E_{rel} = 18.3 kJ·mol^{-1}
D(C−H···S): 3.08 Å
<(C−H···S): 152.7°

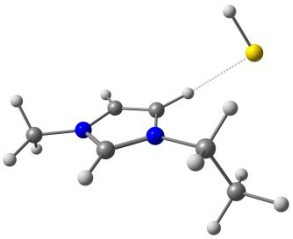

g) E_{rel} = 53.5 kJ·mol^{-1}
D(C−H···S): 3.21 Å
<(C−H···S): 146.8°

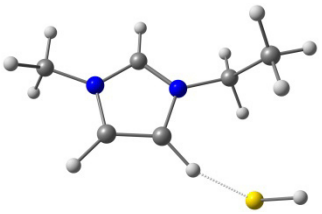

h) E_{rel} = 54.6 kJ·mol^{-1}
D(C−H···S): 3.21 Å
<(C−H···S): 144.8°

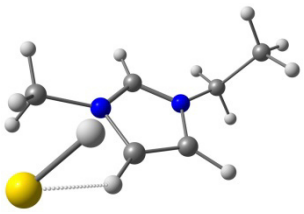

i) E_{rel} = 54.6 kJ·mol^{-1}
D(C−H···S): 3.19 Å
<(C−H···S): 145.8°

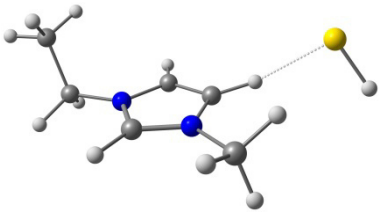

j) E_{rel} = 55.4 kJ·mol^{-1}
D(C−H···S): 3.20 Å
<(C−H···S): 143.9°

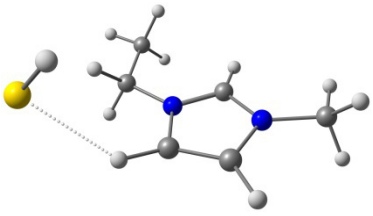

k) E_{rel} = 58.5 kJ·mol^{-1}
D(C−H···S): 3.19 Å
<(C−H···S): 136.2°

Figure S13. Most stable ion pairs of [EMIm][HS] (without ZPE correction).

Table S4. Total electronic energies of the [EMIm][HS] SIPs (without ZPE correction).

	E/ E_h	E_{rel}/ kJ·mol^{-1}
(a)	−743.703593	0.0
(b)	−743.702876	1.9
(c)	−743.702057	4.0
(d)	−743.701422	5.7
(e)	−743.697161	16.9
(f)	−743.696625	18.3
(g)	−743.683208	53.5
(h)	−743.682816	54.6
(i)	−743.682783	54.6
(j)	−743.682511	55.4
(k)	−743.681308	58.5

7.2 S_N2 reactions and carbene formation as decomposition pathways

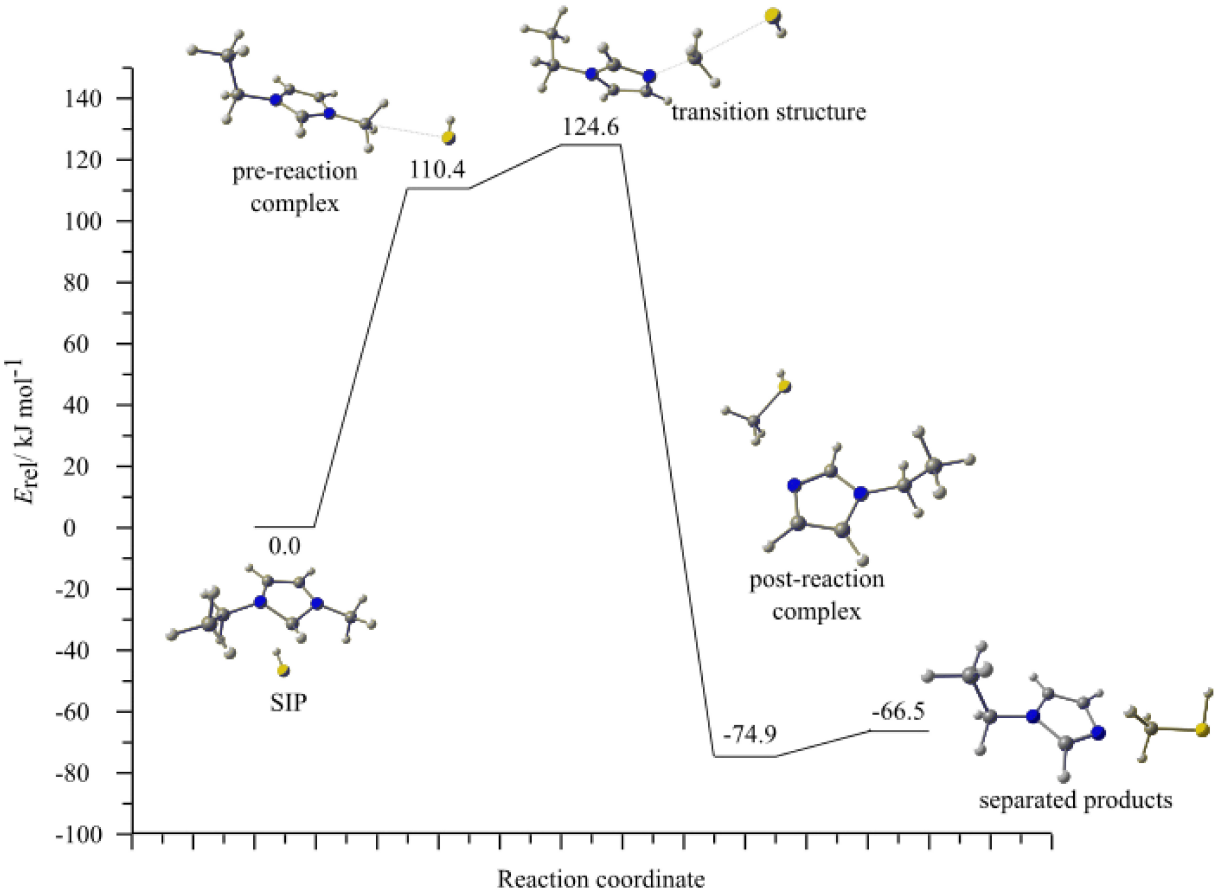

Figure S14. Decomposition of [EMIm][HS] by nucleophilic attack at the methyl group.

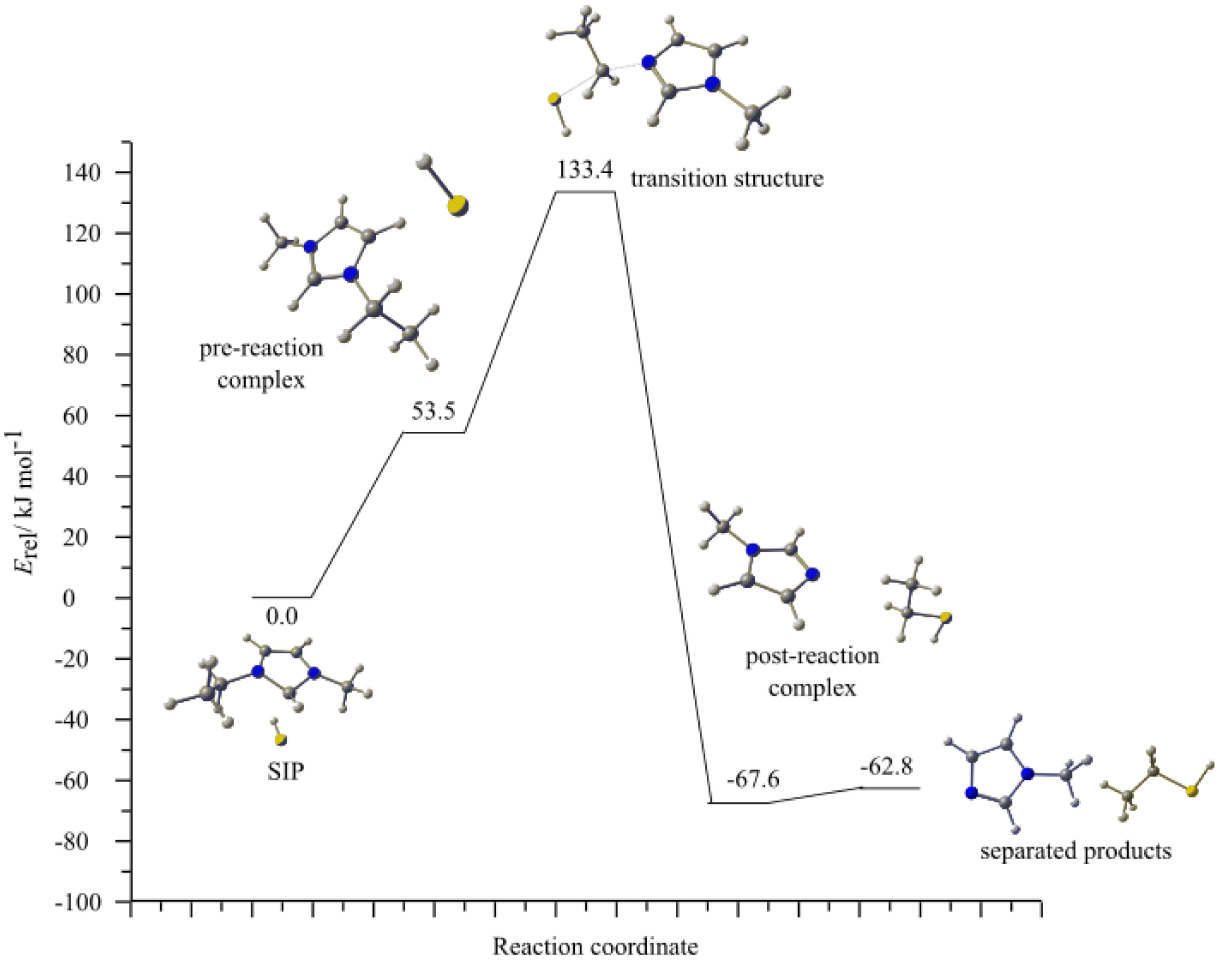

Figure S15. Decomposition of [EMIm][HS] by nucleophilic attack at the ethyl group.

Table S5. Total electronic energies of the S_N2-type reactions (without ZPE correction).

Attack at the methyl group	E/ E_h	E_{rel}/ kJ·mol^{-1}
Ion pair (most stable one)	−743.703593	0.0
Pre-reaction complex	−743.661534	110.4
Transition structure	−743.656123	124.6
Post-reaction complex	−743.732113	−74.9
Products (separated)	−743.728935	−66.5
Attack at the ethyl group		
Ion pair (most stable one)	−743.703593	0.0
Pre-reaction complex	−743.683208	53.5
Transition structure	−743.652775	133.4
Post-reaction complex	−743.729330	−67.6
Products (separated)	−743.727514	−62.8

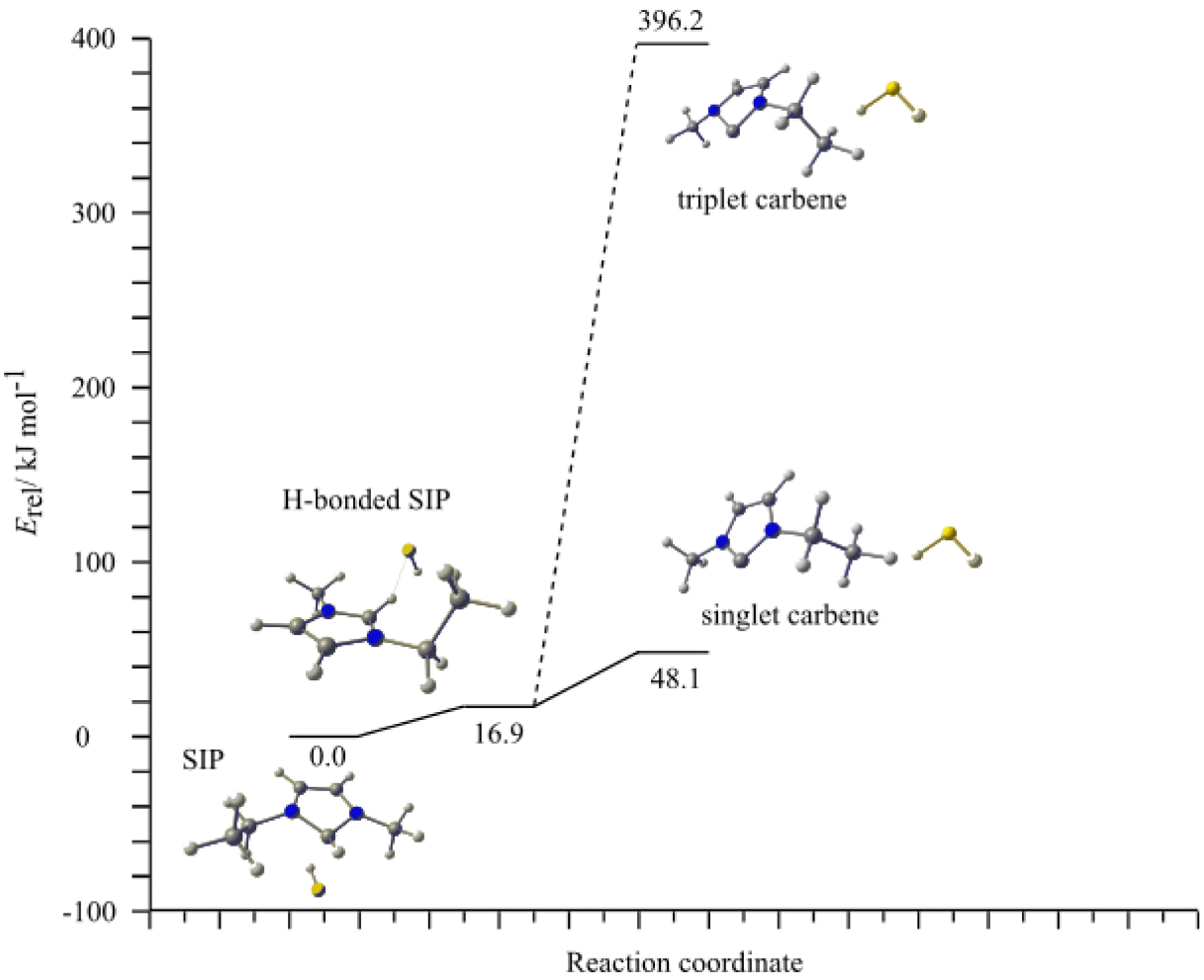

Figure S16. Energy profile of the carbene formation.

Table S6. Total electronic energies of the carbene formation (without ZPE correction).

Attack at the methyl group	E/ E_h	E_{rel}/ kJ·mol^{-1}
Ion pair (most stable one)	−743.703593	0.0
H−bonded SIP	−743.697161	16.9
Singlet carbene	−743.685269	48.1
Triplet carbene	−743.552676	396.2

7.3 Formation of 1-ethyl-3-methylimidazole-2-thione

As already noted by Hollóczki *et al.* a neutral thiol species **A**, resulting from nucleophilic attack of the hydrosulphide at the C2 position (scheme S2) cannot be stabilised.[30] This forced reaction is accompanied by slight increase in energy by about 28.2 kJ·mol^{-1}, with the corresponding structure not being a stationary point on the potential energy hypersurface.

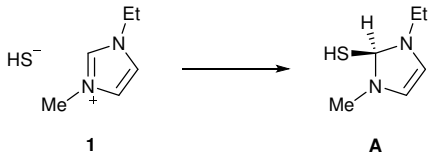

Scheme S2. Formation of an imidazole-2-thiole by nucleophilic attack of HS^- at the C2-carbon.

The reaction becomes thinkable if another hydrosulphide anion is included, which will act as Brønstedt base and concertedly deprotonates the thiole to anion **B** (scheme S3). According to DFT calculations, in the gas phase this reaction would be accompanied by an overall energy loss of −6.3 kJ·mol^{-1}.

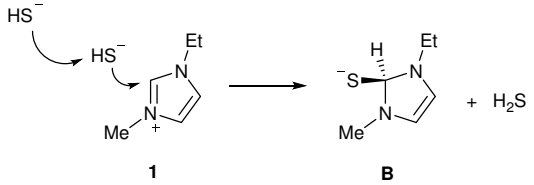

Scheme S3. Formation of an imidazole-2-thiolate by nucleophilic attack of HS^- at the C2-carbon and concerted deprotonation by anonther hydrosulphide anion.

Thiolate **B** will act as a strong hydride donor and reacts with the strongest acid present in the system, which is again the hydrosulphide anion (pK_a (HS^-) ≈ 14, pKa ($[EMIm]^+$) = 23).[31] Thiole **A** will certainly show a lower pK_a value, but its questionable existence and, if at all, very low abundance renders it an improbable reaction partner. The forming sulphide dianion will immediately attack the next [EMIm] cation initiating an autocatalytic cycle (scheme S4). The overall energy balance of the reaction is computed to be exothermic by −51.01 kJ/mol.

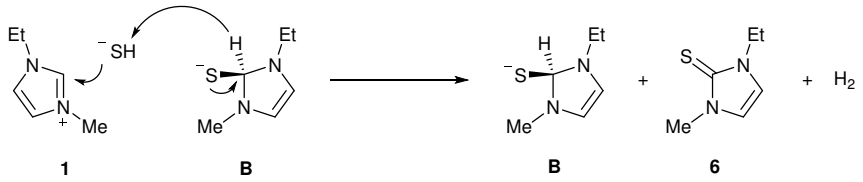

Scheme S4. Generation of the thione 6 and initiation of an autocatalytic decomposition cycle.

Table S7 summarises the computed energies of the single components and table S8 reports the total energies of the reactions depicted in schemes S2 to S4.

Table S7. Total electronic energies of the single components (without ZPE correction).

	E/ E_h
Most stable SIP [EMIm][HS]	−743.703593
Thiole **A**	−743.692868
Hydrosulphide anion (HS^-)	−398.871600
Thiolate **B**	−743.128954
Hydrogen sulphide (H_2S)	−399.448640
Thione **6**	−742.545439
Hydrogen (H_2)	−1.177586

Table S8. Total energies of the reactions depicted in schemes S2 to S4.

Reaction of scheme S2	E/ E_h	ΔE_{rel}/ kJ·mol^{-1}
[EMIm][HS] SIP	−743.703593	0.0
Thiole **A**	−743.692868	28.2
Reaaction of scheme S3		
Separated reactants	−1142.575196	0.0
Separated products	−1142.577594	−6.3
Reaction of scheme S4		
Separated reactants	−1486.832550	0.0
Separated products	−1486.851979	−51.0

7.4 Analysis of the bonding interaction in the single ion pair b) and thiol A

The formation of a 1-ethyl-3-methylimidazol-2-thiole was anticipated as a possible intermediate during the generation of the respective thione. However, the structure with separated ion and a C−S distance of 2.26 Å (equivalent to ion pair b) of figure S13) is more stable than the covalently bound molecule, where the bond length was fixed to 1.82 Å, which was assumed a typical C−S single bond length. Figure S17 visualises the relative energy change with varying C−S distance.

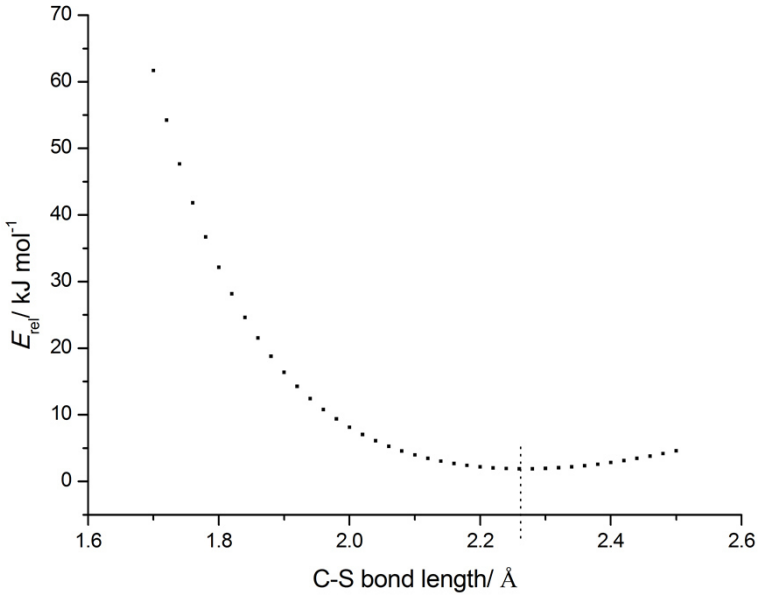

Figure S17. Relative energy of the [EMIm][HS] SIP b) in dependency of the C−S distance (E_{rel} = 0 corresponds to the most stable SIP a) of figure S13).

Comparing the bond length with other ionic pairs, where the anion is not located above the ring-system of the imidazolium, the abnormality gets fortified. There, the C−S bond length is always larger than 3 Å, which indicates that ion pair b) has a more covalent character than other ionic pairs like the H-bonded ion pair e). To identify the type of bonding interaction present in the structure b) a Bader analysis,[21] a natural bond orbital analysis[22] and an energy

decomposition analysis[24] were performed, comparing structure b), methanethiol and sodium hydrosulphide. A bond critical point was found between sulphur and the carbon of interest, with an electron (charge) density $\rho = 7.64 \cdot 10^{-2}\ (-e) \cdot a_0^{-3}$ and a Laplacian of the electron density of $\nabla^2\rho = 3.63 \cdot 10^{-2}\ (-e) \cdot a_0^{-5}$. The criterion for a covalent bonding interaction is that $\rho/(-e) \cdot a_0^{-3}$ should be higher than 0.2 and $\nabla^2\rho/(-e) \cdot a_0^{-5}$ should be negative.[32] This indicates the carbon-sulphur interaction to be mostly of ionic character (figure S18). For methanethiol the values $\rho = 1.73 \cdot 10^{-1}\ (-e) \cdot a_0^{-3}$ and $\nabla^2\rho = -2.57 \cdot 10^{-1}\ (-e) \cdot a_0^{-5}$ and for sodium hydrosulphide the values $\rho = 3.07 \cdot 10^{-2}\ (-e) \cdot a_0^{-3}$ and $\nabla^2\rho = 1.38 \cdot 10^{-1}\ (-e) \cdot a_0^{-5}$ were calculated. These fit to the expectations of mainly covalent and ionic interactions, respectively.

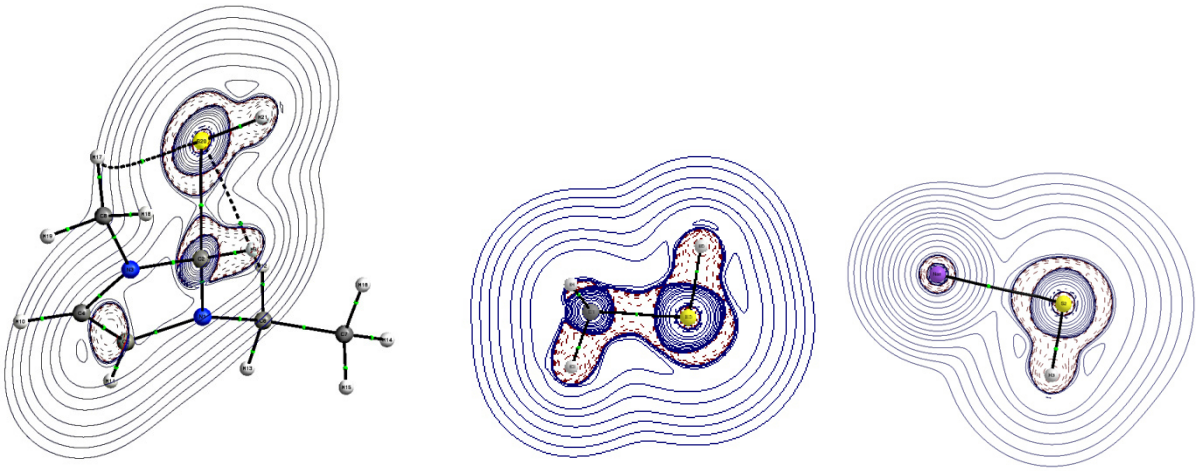

Figure S18. Bader analysis of the ion pair b), methanethiol and sodium hydrosulphide (from left to right).

The NBO analysis (figure S19), in contrast reveals a σ-like bond orbital, indicating a covalent bond. It is overt, that the orbital is highly deformed; the electron density is located more on the sulphur atom due to its higher electronegativity.

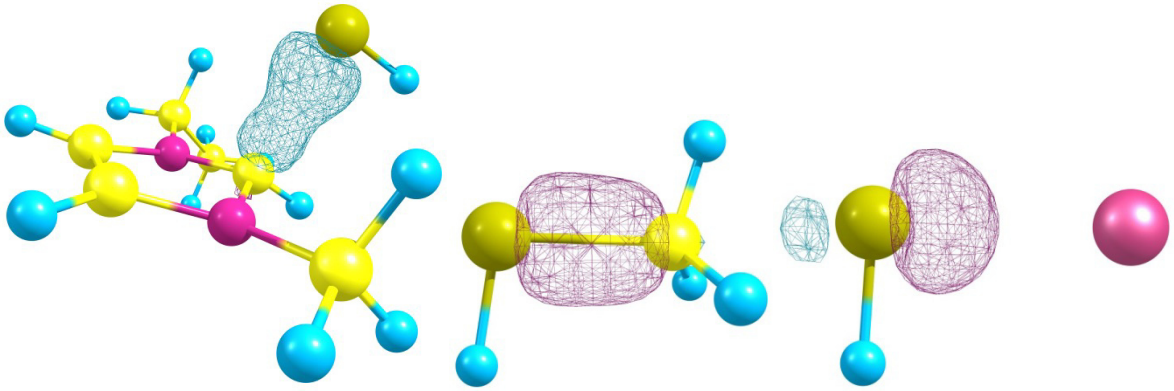

Figure S19. Natural bonding orbitals of the ion pair b), methanethiol and sodium hydrosulphide (from left to right) .

The energy decomposition analysis (EDA) of the three compounds finally confirms an intermediate state between a covalent bond and an ionic character of the interaction. The H−bonded ion pair e) in comparison shows a significantly higher electrostatic contribution (Tabel S9).

Table S9. Energy decomposition analysis of Ion pairs b), e), methanethiol and sodium hydrosulphide.

	Ion pair b)	Ion pair e)	Methanethiol	Sodium hydrosulphide
E_{total}/ kJ•mol^{-1}	−116.0	−102.8	−285.1	−133.7
E_{pauli}/ kJ•mol^{-1}	127.2	48.9	187.9	30.4
$E_{el.static}$/ kJ•mol^{-1}	−160.5	−110.3	−223.8	−146.5
	(66.0%)	(72.7%)	(47.3%)	(89.3%)
$E_{orbital}$/ kJ•mol^{-1}	−82.8	−41.4	−249.2	−17.6
	(34.0%)	(27.3%)	(52.7%)	(10.7%)
E_{diss}/ kJ•mol^{-1}	99.2	95.8		

Also the bond indices of the carbon-sulphur bond according to Wiberg[22a] produce an intermediate value for the ion pair b) (BI = 0.5681). The values for methyl-thiol (BI = 1.0486) and sodium hydrosulphide (BI = 0.3576) clearly indicate covalent and ionic interactions, respectively.

11. References

1 G. R. Fulmer, A. J. M. Miller, H. E. Gottlieb, N. H. Sherden, A. Nudelman, B. M. Stoltz, K. I. Goldberg and J. E. Bercaw, *Organometallics*, 2010, **29**, 2176.

2 W. L. Amarego and D. D. Perrin, *Purification of Laboratory Chemicals*, Elsevier, Burlington, 1996.

3 J. E. Bara, *Ind. Eng. Chem. Res.*, 2011, **50**, 13614.

4(a) R. Kalb (PROIONIC), WO 2008 052 861, **2008**; (b) (PROIONIC), WO 2008 052 860, **2008**.

5(a) J.-H. So and P. Boudjouk, *Synthesis*, 1989, 306; (b) M. W. DeGroot, N. J. Taylor and J. F. Corrigan, *J. Mater. Chem.*, 2004, **14**, 654.

6 Bruker Instrument Service v3.0.26, APEX2 v2012.10-0, SAINT v8.27B, Bruker, Bruker AXS Inc., Madison, Wisconsin, USA, 2012.

7 A. Altomare, M. C. Burla, M. Camalli, G. Cascarano, C. Giacovazzo, A. Guagliardi, A. G. G. Moliterni, G. Polidori and R. Spagna, *J. Appl. Crystallogr.*, 1999, **32**, 115.

8 M. C. Burla, R. Caliandro, M. Camalli, B. Carrozzini, G. L. Cascarano, C. Giacovazzo, M. Mallamo, A. Mazzone, G. Polidori and R. Spagna, *J. Appl. Cryst.*, 2012, **45**, 357.

9 G. Sheldrick, *Acta Cryst. A*, 2008, **64**, 112.

10 A. L. Spek, *Acta Cryst. D*, 2009, **65**, 148.

11 L. Farrugia, *J. Appl. Cryst.*, 2012, **45**, 849.

12 F. H. Allen, O. Johnson, G. P. Shields, B. R. Smith and M. Towler, *J. Appl. Crystallogr.*, 2004, **37**, 335.

13 SADABS v2012/1, Bruker, Bruker AXS Inc., Madison, Wisconsin, USA, 2012.

14 Diamond - Crystal and Molecular Structure Visualization v3.2i, K. Brandenburg and H. Putz, Crystal Impact GbR, Bonn, Germany, 2012.

15 G. Illuminati and C. Lillocci, *J. Org. Chem.*, 1977, **42**, 2201.

16(a) D. M. Price, *Thermochim. Acta*, 2001, **367–368**, 253; (b) W. E. Acree, Jr. and J. S. Chickos, in *NIST Chemistry WebBook, NIST Standard Reference Database Number 69*, eds. P. J. Linstrom and W. G. Mallard, National Institute of Standards and Technology, Gaithersburg MD, 20899, http://webbook.nist.gov, (retrieved June 26, 2015).

17 S. P. Verevkin, D. H. Zaitsau, V. N. Emelyanenko, A. V. Yermalayeu, C. Schick, H. Liu, E. J. Maginn, S. Bulut, I. Krossing and R. Kalb, *J. Phys. Chem. B*, 2013, **117**, 6473.

18 Gaussian 09, Revision C.01, M. J. Frisch, G. W. Trucks, H. B. Schlegel, G. E. Scuseria, M. A. Robb, J. R. Cheeseman, G. Scalmani, V. Barone, B. Mennucci, G. A. Petersson, H. Nakatsuji, M. Caricato, X. Li, H. P. Hratchian, A. F. Izmaylov, J. Bloino, G. Zheng, J. L. Sonnenberg, M. Hada, M. Ehara, K. Toyota, R. Fukuda, J. Hasegawa, M. Ishida, T. Nakajima, Y. Honda, O. Kitao, H. Nakai, T. Vreven, J. A. Montgomery Jr., J. E. Peralta, F. Ogliaro, M. J. Bearpark, J. Heyd, E. N. Brothers, K. N. Kudin, V. N. Staroverov, R. Kobayashi, J. Normand, K. Raghavachari, A. P. Rendell, J. C. Burant, S. S. Iyengar, J. Tomasi, M. Cossi, N. Rega, N. J. Millam, M. Klene, J. E. Knox, J. B. Cross, V. Bakken, C. Adamo, J. Jaramillo, R. Gomperts, R. E. Stratmann, O. Yazyev, A. J. Austin, R. Cammi, C. Pomelli, J. W. Ochterski, R. L. Martin, K. Morokuma, V. G. Zakrzewski, G. A. Voth, P. Salvador, J. J. Dannenberg, S. Dapprich, A. D. Daniels, Ö. Farkas, J. B. Foresman, J. V. Ortiz, J. Cioslowski and D. J. Fox, Gaussian, Inc., Wallingford, CT, USA, 2010.

19(a) J. P. Perdew, *Phys. Rev. B*, 1986, **33**, 8822; (b) A. D. Becke, *Phys. Rev. A*, 1988, **38**, 3098; (c) F. Weigend and R. Ahlrichs, *Phys. Chem. Chem. Phys.*, 2005, **7**, 3297; (d) F. Weigend, *Phys. Chem. Chem. Phys.*, 2006, **8**, 1057.

20 AIMAll (Version 14.11.23), T. A. Keith, TK Gristmill Software, Overland Park KS, USA, 2014.
21 R. F. W. Bader, *J. Phys. Chem. A*, 2009, **113**, 10391.
22(a) F. Jensen, *Introduction to Computational Chemistry*, John Wiley & Sons Ltd, Chichester, 2007; (b) A. E. Reed, L. A. Curtiss and F. Weinhold, *Chem. Rev.*, 1988, **88**, 899.
23 NBO Version 3.1, E. D. Glendening, A. E. Reed, J. E. Carpenter and F. Weinhold, Theoretical Chemistry Institute, University of Wisconsin, Madison.
24 M. v. Hopffgarten and G. Frenking, *Wiley Interdiscip. Rev.: Comput. Mol. Sci.*, 2012, **2**, 43.
25(a) C. Fonseca Guerra, J. G. Snijders, G. te Velde and E. J. Baerends, *Theor. Chem. Acc.*, 1998, **99**, 391; (b) G. te Velde, F. M. Bickelhaupt, E. J. Baerends, C. Fonseca Guerra, S. J. A. van Gisbergen, J. G. Snijders and T. Ziegler, *J. Comput. Chem.*, 2001, **22**, 931; (c) ADF2014, SCM, E. J. Baerends, T. Ziegler, J. Autschbach, D. Bashford, A. Bérces, F. M. Bickelhaupt, C. Bo, P. M. Boerrigter, L. Cavallo, D. P. Chong, L. Deng, R. M. Dickson, D. E. Ellis, M. v. Faassen, L. Fan, T. H. Fischer, C. F. Guerra, M. Franchini, A. Ghysels, A. Giammona, S. J. A. v. Gisbergen, A. W. Götz, J. A. Groeneveld, O. V. Gritsenko, M. Grüning, S. Gusarov, F. E. Harris, P. v. d. Hoek, C. R. Jacob, H. Jacobsen, L. Jensen, J. W. Kaminski, G. v. Kessel, F. Kootstra, A. Kovalenko, M. V. Krykunov, E. v. Lenthe, D. A. McCormack, A. Michalak, M. Mitoraj, S. M. Morton, J. Neugebauer, V. P. Nicu, L. Noodleman, V. P. Osinga, S. Patchkovskii, M. Pavanello, P. H. T. Philipsen, D. Post, C. C. Pye, W. Ravenek, J. I. Rodríguez, P. Ros, P. R. T. Schipper, H. v. Schoot, G. Schreckenbach, J. S. Seldenthuis, M. Seth, J. G. Snijders, M. Solà, M. Swart, D. Swerhone, G. t. Velde, P. Vernooijs, L. Versluis, L. Visscher, O. Visser, F. Wang, T. A. Wesolowski, E. M. v. Wezenbeek, G. Wiesenekker, S. K. Wolff, T. K. Woo and A. L. Yakovlev, Theoretical Chemistry, Vrije Universiteit, Amsterdam, The Netherlands, http://www.scm.com.
26 J. P. Perdew, K. Burke and M. Ernzerhof, *Phys. Rev. Lett.*, 1996, **77**, 3865.
27 G. Kresse and D. Joubert, *Phys. Rev. B*, 1999, **59**, 1758.
28 G. Kresse and J. Furthmüller, *Phys. Rev. B*, 1996, **54**, 11169.
29 S. Grimme, J. Antony, S. Ehrlich and H. Krieg, *J. Chem. Phys.*, 2010, **132**, 154104.
30 O. Holloczki, D. Gerhard, K. Massone, L. Szarvas, B. Nemeth, T. Veszpremi and L. Nyulaszi, *New J. Chem.*, 2010, **34**, 3004.
31(a) A. J. Ellis and R. M. Golding, *J. Chem. Soc.*, 1959, 127; (b) E. M. Higgins, J. A. Sherwood, A. G. Lindsay, J. Armstrong, R. S. Massey, R. W. Alder and A. C. O'Donoghue, *Chem. Commun.*, 2011, **47**, 1559.
32 C. F. Matta and R. J. Boyd, in *The Quantum Theory of Atoms in Molecules*, eds. C. F. Matta and R. J. Boyd, Wiley-VCH, Weinheim, 2007, pp. 1-34.

6.2 Halogenidfreie Synthese von Hydrogenchalkogenid Ionischen Flüssigkeiten des Typs [Kation][HE] (E = S, Se, Te)

Chem. Eur. J. **2016**, DOI: 10.1002/chem.201504577, *in press*

Halide Free Synthesis of Hydrochalcogenide Ionic Liquids of the Type [Cation][HE] (E = S, Se, Te)

Lars H. Finger, Jörg Sundermeyer

Halide Free Synthesis of Hydrochalcogenide Ionic Liquids of the Type [Cation][HE] (E = S, Se, Te)

Lars H. Finger,[a] and Jörg Sundermeyer*[a]

Abstract: *We present the synthesis and thorough characterization of ionic liquids and organic salts based on hydrochalcogenide HE^- (E: S, Se, Te) anions. Our approach is based on the halide, metal and water free decarboxylation of methylcarbonate precursors under acidic conditions resulting from the easily dissociating reagents H_2E. The compounds were characterized by elemental analysis, multinuclear NMR spectroscopy, thermal and single crystal XRD analyses. The hydrosulfide salts were investigated with respect to their ability to dissolve elemental sulfur in varying stoichiometry. Thus prepared polysulfide ILs were analyzed by UV-Vis spectroscopy and cyclic voltammetry.*

Introduction

Lithium sulfur batteries are among the most promising energy storage systems currently under development.[1] The application of ionic liquids as electrolyte solution is intensely investigated.[2] Reports concerning the general characteristics of sulfur in ionic liquids, which are of uttermost importance for the understanding and optimization of lithium sulfur batteries are scarce, though. The electrochemistry of sulfur was investigated in *N-n*butyl-pyridinium tetrachloroaluminate several decades ago[3] and Manan *et al.* more recently reported detailed electrochemical studies of sulfur and sodium polysulfides in 1-butyl-3-methylimidazolium dicyanamide.[4] The solubility of chalcogens and phosphorus in a variety of ionic liquids comprising tosylate, bistriflimide, dithiocarbamate and di- and trithiocarbonate anions was investigated by Seddon and coworkers.[5] The sulfur solubility in 1-ethyl-3-methylimidazolium bistriflimide was also studied with the aim to electrodeposit metal sulfide films.[6] In contrast, the respective behavior in organic solvents was addressed repeatedly.[7]

The sulfur atom is a prominent building block in ionic liquids but sulfur based anions are mainly restricted to oxoanions of sulfur, including triflate, methylsulfate and various forms of triflimide anions. Anions comprising electron rich nucleophilic sulfur atoms are scarce and for a long time thiocyanate was the only notable representative.[8] An exception to this are tetraalkylammonium hydrosulfides (especially alkyl = methyl, ethyl, butyl), which have been known since the 1960s, but were never characterized in detail.[9] They are primarily employed as reagents in the synthesis of transition metal complexes[10] and clusters,[11] the application in organic thiolation reactions was described several decades ago.[12]

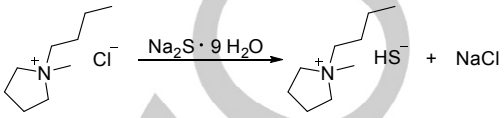

Scheme 1. Synthesis of *N*-butyl-*N*-methylpyrrolidinium hydrosulfide according to Jovanovski et al.[13]

Jovanovski *et al*. reported the synthesis of oily pyrrolidinium and imidazolium hydrosulfides obtained via salt metathesis in the presence of water (Scheme 1).[13] Additionally they described the dissolution of sulfur in the new systems and demonstrated the application of the resulting polysulfides as redox mediators in quantum dot sensitized solar cells.[14] The possibility to react organic hydrosulfides with sulfur to form polysulfide species was first demonstrated by Chivers *et al*.[15] Sun and Kloo claimed the synthesis of tetramethylammonium sulfide $(NMe_4)_2S$ and 1-propyl-2,3-dimethyl-imidazolium sulfide $(DMPI)_2S$.[16] Due to the very high basicity and nucleophilicity of the sulfide dianion towards mentioned organic cations and the fact that the reactions were carried out under aqueous conditions, this claim seems questionable (*vide infra*).[17] They equally described the dissolution of sulfur in these salts and tested the resulting substances as redox mediators in dye sensitized solar cells.[16, 18]

The homologous hydroxide ion is typically not found in water free ionic liquids. Because of its very high basicity and nucleophilicity very few organic cations are suitable for the preparation of pure hydroxide salts. Hugar *et al.* recently presented a detailed study, which showed that even solvated hydroxide ions demand a sophisticated aromatic substitution pattern on the imidazolium cations to avoid their decomposition.[19]

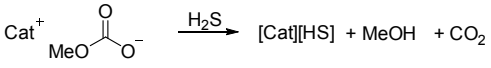

Scheme 2. Water, halide and metal free synthesis of hydrosulfide salts from the respective methylcarbonate precursors.

The previous synthetic procedures to access hydrosulfide ionic liquids start from water containing reagents, and mostly use the traditional salt metathesis approach. This automatically leads to water, halide and alkali metal impurities, which are undesirable for electrochemical applications and very difficult to remove. In contrast, the proton induced decarboxylation of methyl carbonate ionic liquids by hydrogen sulfide, offers a water, metal and halide free route to pure hydrosulfide ILs (Scheme 2), which we presented with focus on the astonishing volatility of imidazolium hydrochalcogenides recently.[20] We were able to extend this procedure to hydrotelluride salts, which we present herein next to a broader set of hydrosulfides and -selenides and their detailed characterization. Hydroselenide and hydrotelluride based salts

[a] Lars H. Finger, Prof. Dr. Jörg Sundermeyer
Fachbereich Chemie and Materials Science Center
Philipps-Universität Marburg
Hans-Meerwein-Str. 4
35032 Marburg, Deutschland
E-mail: jsu@chemie.uni-marburg.de

Supporting information for this article is given via a link at the end of the document.

with organic cations were described for the first time more than two decades ago.[21] Dehnen and coworkers recently published a review article highlighting organic cation and complex cation stabilized selenides and polyselenides.[22] Tetralkylammonium hydroselenides have been employed as reagents occasionally.[10b, 11c, 23]

The hydrosulfides offer the possibility to access polysulfide ionic liquids without water and salt impurities, which may on the one hand serve as model systems for the intermediates occurring during charge and discharge cycles of lithium sulfur batteries and on the other hand find application as redox shuttles in organic solar cells. In this context we investigated the dissolution behavior of sulfur in the respective hydrosulfides and the corresponding effect on the UV-Vis absorption spectra and redox behavior of the mixture.

Next to the class of trimethylsilylchalcogenolate organic salts[24] presented recently the now readily available class of hydrochalcogenide salts comprising highly nucleophilic and reactive anions may also find application in the preparation of chalcogenido metal clusters and metallate complexes as well as metal chalcogenide semiconductor materials. The latter class of compounds is applicable in a variety of systems.[25] However, the actual value for a specific application is usually heavily dependent on the purity, the morphology of the respective chalcogenide material and thereby also on the chemical synthesis. E.g., while crystalline bulk MoS_2 is an indirect bandgap semiconductor,[26] monolayers act as a direct bandgap semiconductor[27] and amorphous or nano sized MoS_2 is an especially active catalyst for the hydrogen evolution reaction.[28] Variation of the synthetic procedure, e.g. by applying ionothermal flux conditions, are a starting point to improve and fine tune the properties of these materials.

Results and Discussion

Synthesis of hydrochalcogenide salts

Synthesis of the title compounds was accomplished by the proton induced decarboxylation of methylcarbonate anions employing H_2E (E = S, Se, Te) as the acidic reagent (Scheme 3). The reaction is characterized by yielding only volatile, easily separated by-products and comprising no equilibria due to the irreversible decay of the methylcarbonate anion. The corresponding methylcarbonate salts are readily prepared in methanol solution via methylation of organic cation precursors with dimethyl carbonate under solvothermal conditions.[29] In some cases a solvent free isolation[24] or even a solvent free synthesis are possible.[30] The hydrosulfide salts (**1** to **5**) were prepared by introducing hydrogen sulfide gas into solutions of the respective methylcarbonate based ionic liquid in methanol at ambient temperature. After removing all volatile components and recrystallization of the residue the compounds [Cat][HS] could be isolated in moderate to good yields. If H_2S is not available the pyrrolidinium and phosphonium salts may also be prepared by employing the corresponding bis(trimethylsilyl)sulfide. However, even if an excess of $(TMS)_2S$ is added directly to the methanol solution of the methylcarbonate salt, the protolysis was usually not complete and a significant amount of the methylcarbonate anion remained. Pure products can be obtained if the corresponding trimethylsilylthiolate[24] is prepared in advance and protonated in a second step. However, feeding readily available H_2S gas into the solution is the simplest procedure. In contrast, the corresponding H_2Se is not readily available but hydroselenide salts are accessible by adding only a minor excess of bis(trimethylsilyl)selenide directly to the methanol solution of the appropriate methylcarbonate precursor. Methanolysis leads to quantitative in situ formation of H_2Se, which rapidly reacts with the $MeOCO_2$ anions. Care has to be taken that the solvents are not only water free but also thoroughly degassed as the hydroselenide anion is very liable to oxidation. The synthesis of selected hydrotelluride salts was also successful but several challenges have to be mastered. Hydrogen telluride gas decomposes already at 0 °C to elemental tellurium and hydrogen. In order to ensure a selective reaction with the methyl carbonate anion the temperature had to be kept at about −30 °C, even during the subsequent evaporation of the volatiles. Otherwise intensely colored polytelluride ions are formed to a significant extent. Furthermore it proved helpful to employ silicon free vacuum grease and to keep the products in the dark. The stability of the prepared hydrotelluride salts strongly depends on the cation. *N*-Butyl-*N*-methylpyrrolidinium hydrotelluride (**10**) changes color even inside the −30 °C freezer of a nitrogen filled glovebox within three days due to the formation of polytelluride traces. It decomposes completely within two weeks if stored at ambient temperature.

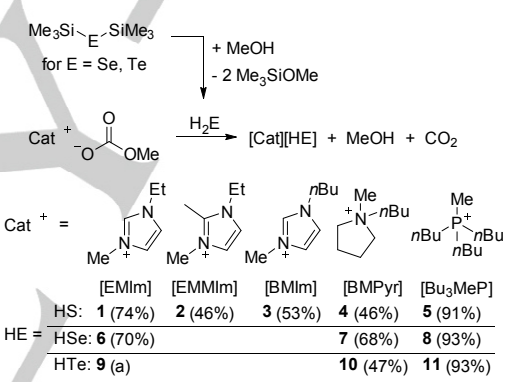

HE =	[EMIm]	[EMMIm]	[BMIm]	[BMPyr]	[Bu_3MeP]
HS:	**1** (74%)	**2** (46%)	**3** (53%)	**4** (46%)	**5** (91%)
HSe:	**6** (70%)			**7** (68%)	**8** (93%)
HTe:	**9** (a)			**10** (47%)	**11** (93%)

Scheme 3. Synthesis of a series of organic hydrochalcogenide salts, yields in parentheses, **a**: yield was not determined as the substance is not sufficiently stable (vide infra). The synthesis of substances **1** to **4** and **6** was communicated recently.[20]

The tri-*n*butyl-methylphosphonium salt **11** is significantly more stable under the same conditions; even after 6 weeks, the color had only slightly darkened. [EMIm][HTe] (**9**) partly decomposed already during isolation from the reaction mixture and could not be isolated in a pure form so far. NMR and IR spectra confirm that hydrotelluride is present as the predominant anion, though. Within hours the substance decomposes even under inert conditions and at low temperatures. In contrast, all hydrosulfide and hydroselenide salts form room temperature and long-time stable substances. After purification and storage at ambient temperature under inert conditions imidazolium, pyrrolidinium and phosphonium hydrosulfides and selenides stayed unchanged over a period of several months. With exception of [$n$$Bu_3$MeP][HS] (**5**) which is a highly viscous oil, all compounds were isolated as almost colorless solids. In most cases elemental analysis yielded good to satisfactory results after recrystallization. We were however not able to high-end-purify the honey and wax-like phosphonium hydrosulfide **5** and hydroselenide **8**, respectively. All

attempts to recrystallize the substances also at temperatures as low as −80 °C failed. Also after repeated extractions with diethyl ether NMR detectable impurities remained and only a ≥ 95% technical grade purity is reached.

Thermal stability

All solid compounds were investigated with respect to their melting and decomposition temperatures. This was accomplished in the first instance with a Büchi B540 melting point device in sealed melting capillaries. The hydrosulfide salts were additionally investigated by combined TGA and DSC measurements. Due to their very high sensitivity towards oxygen this was not possible for the hydroselenide and hydrotelluride systems. The observed melting and decomposition temperatures are summarized in Table 1.

Table 1. Melting and decomposition temperatures of organic hydrochalcogenide salts.

Substance	T_m/ °C	T_{dec}/ °C
[EMIm][HS] (**1**)	93[a]	162[b]
[EMMIm][HS] (**2**)	126[a]	180[b]
[BMIM][HS] (**3**)	55[a]	157[b]
[BMPyr][HS] (**4**)	-[c]	154[a]
[Bu_3PMe][HS] (**5**)	<RT	262[b]
[EMIm][HSe] (**6**)	102[a]	-[d]
[BMPyr][HSe] (**7**)	-[c]	149[a]
[Bu_3PMe][HSe] (**8**)	57[a]	-[d]
[BMPyr][HTe] (**10**)	-[c]	116[a]
[Bu_3PMe][HTe] (**11**)	-[c]	163[a]

a: determined with a Büchi B540, heating rate 2 K·min^{-1}; **b**: determined with a Netzsch STA 409 CD, heating rate 10 K·min^{-1}; **c**: substance decomposes immediately upon melting; **d**: not to be determined reliably.

Melting points range from 55 °C in case of the 1-butyl-3-methylimidazolium-hydrosulfide [BMIm][HS] (**3**) to 126 °C for [EMMIm][HS] (**2**). They are clearly identifiably by endothermic peaks in the respective DSC curves (view SI) and could be verified by visual melting point determination at lower heating rates. Decomposition of the imidazolium salts occurs at temperatures exceeding 150 °C according to the TGA measurements. Detailed investigations of these compounds showed that a partial decomposition occurs already at lower temperatures, though, if the substance is kept at e.g. 110 °C for several hours. Our results concerning the thermal decay paths have been published elsewhere.[20] While the phosphonium hydrosulfide **5** appears to be a RTIL the phosphonium hydroselenide **8** shows a melting point of 57 °C. For the corresponding hydrotelluride no melting point could be observed; the substance decomposed at 163 °C. Similarly, the pyrrolidinium salts **4**, **7** and **10** decompose immediately upon melting, which occurs at around 150 °C for the hydrosulfide and selenide salts. Figure 1 shows three representative TGA curves of compounds **2**, **4**, and **5**. As it was also observed for e.g. imidazolium halides the decomposition is accompanied by a total mass loss of 100% in each case, only trace amounts of residue remained in the TGA crucibles.[31] The decay curves of the imidazolium and the phosphonium salt indicate the decomposition to be a single step S_N2 type dealkylation process.[20] The phosphonium salt shows a slightly stronger gradual decay before reaching the actual decomposition temperature. The pyrrolidinium salt **4** appears to decompose in a stepwise process. After an initial rapid mass loss the process slows and forms a minor plateau at 225 °C and a second at 275 °C before reaching 100% mass loss near 325 °C

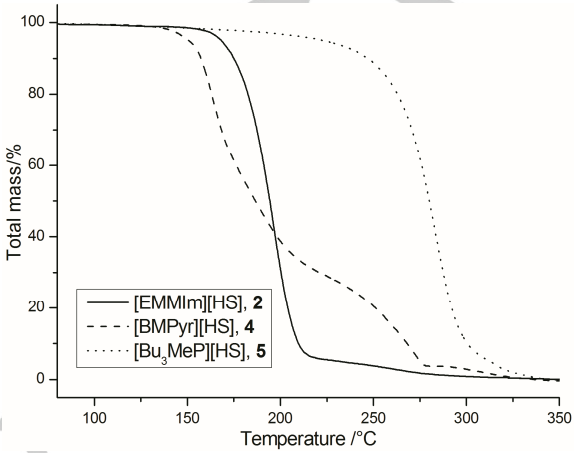

Figure 1. TGA curves of [EMMIm][HS] (**2**), [BMPyr][HS] (**4**) and [Bu_3PMe][HS] (**5**), heating rate 10 K·min^{-1}.

During the melting process of [BMPyr][HS] a gas evolution can be observed and a slightly yellow oil is formed. To analyze the decomposition products a larger sample of **4** was slowly heated to 160 °C. NMR spectroscopic analysis confirmed a complete decomposition of the substance, no traces of the former salt could be observed. *N*-butylpyrrolidine (**13**) could be identified among the decomposition products by comparison of the ^{13}C NMR spectroscopic data. The ESI(+) mass spectrum revealed 4-(butylmethylamino)-1-butanethiol (**14**) to be present along with *N*-butylpyrrolidine and the secondary decomposition products **14a** and **14b** (Scheme 4). Those can be formed if the thiol **14** itself attacks a remaining pyrrolidinium cation. Judging from the NMR spectra reaction **C** is the predominant decomposition pathway, allowing for the observed secondary steps. This can be attributed to the ring strain in the pyrrolidinium cation, which leads to the ring opening reaction, being favored over a demethylation.[32] In contrast, for imidazolium cations the side chain dealkylation is the dominant decomposition reaction.[33] Neither *N*-methylpyrrolidine, nor the alkylmercaptanes could be detected. While the absence of methylmercaptane can be explained by its high volatility, the absence of butylmercaptane and *N*-methylpyrrolidine (**12**) has to be ascribed to S_N2 type reaction **A** being the least favored, and the products being formed to only negligible amounts.

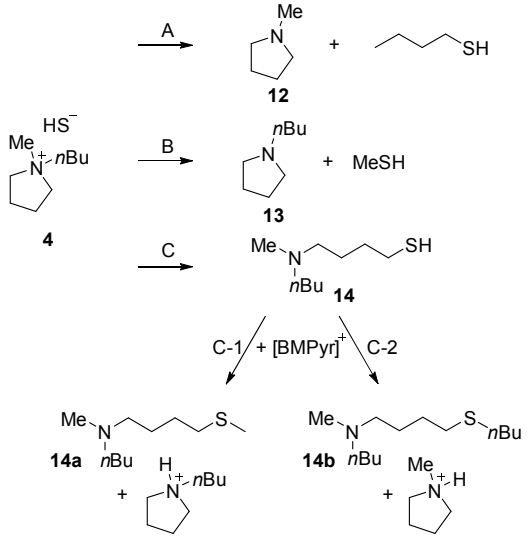

Scheme 4. Thermal decomposition pathways of [BMPyr][HS] (**4**).

Single crystal X-ray structures

For the imidazolium salts **1** to **3** and **6** and the pyrrolidinium hydrosulfide **4** single crystals could be obtained and were investigated by X-ray diffraction. The structures of **1** and **4** were presented recently but not discussed in detail.[20] For comparison with the present structures this will be accomplished here.

[EMMIm][HS] (**2**) crystallized by layering a saturated acetonitrile solution with the equivalent volume of diethyl ether. [BMIm][HS] (**3**) crystallized by cooling a saturated acetonitrile solution to −30 °C, [EMIm][HSe] (**6**) by cooling a saturated solution in an acetonitrile diethyl ether mixture to −30 °C. Table S1 of the supporting information summarizes the crystal data for compounds **2**, **3** and **6**. Complete crystallographic information files for all structures discussed in this paper have been deposited with the Cambridge Crystallographic Data Centre.[34] Figures 2 to 6 show the molecular structures of the three hydrochalcogenide salts. Representations of the lattice structures are included in the supplementary information as figures S8 to S10.

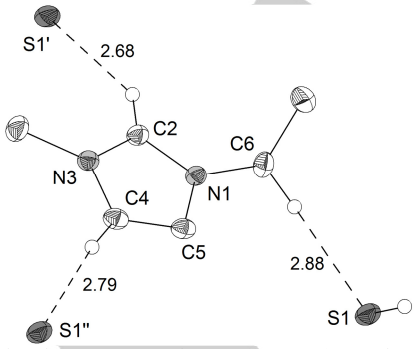

Figure 2. Molecular structure of [EMIm][HS] (**1**), H-bond distances in Å, only H-atoms on sulfur and those participating in H-bonds are shown, symmetry operations:I: x+1/2, −y+3/2, z−1/2; II: −x+1, −y+1, −z+1.

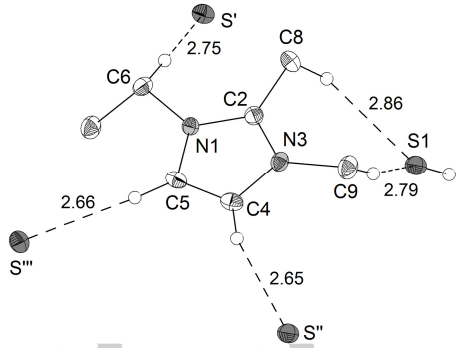

Figure 3. Molecular structure of [EMMIm][HS] (**2**), H-bond distances in Å, only H-atoms on sulfur and those participating in H-bonds are shown, symm. op.: I: x−1/2, y, −z+1/2; II: −x+1, −y, −z+1; III: −x+1/2, y−1/2, z.

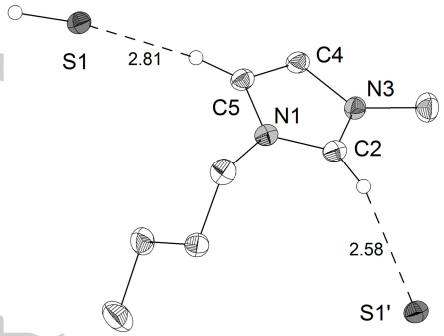

Figure 4. Molecular structure of [BMIm][HS] (**3**), H-bond distances in Å, only H-atoms on sulfur and those participating in H-bonds are shown, symm. op.: I: −x+1/2, y−1/2, z−1/2.

[EMMIm][HS] (Figure 2) crystallized in the orthorhombic space group *Pbca,* [BMIm][HS] (Figure 3) exhibits also orthorhombic symmetry ($Pna2_1$), while [EMIm][HSe] crystallized in the monoclinic space group $P2_1/n$. In all structures the ions are distinctively separated, no covalent bonding between anion and cation can be observed. Within all salts hydrogen bonding interactions between C-H donors and the hydrosulfide or hydroselenide anion as acceptor are evident. The hydrogen bonding distances and angles are summarized in Table 2.

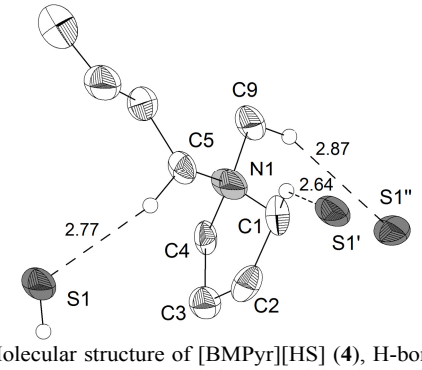

Figure 5. Molecular structure of [BMPyr][HS] (**4**), H-bond distances in Å, only H-atoms on sulfur and those participating in H-bonds are shown, symm. op.: I: −y+1/2,−x+1/2,z−1/2; II −x+1/2,y−1/2,−z.

Within the imidazolium salts the strongest H-bonds typically occur between the C2-H as the most acidic position and the respective anion

(d(C2···E) in [EMIm][HS]: 3.520(1) Å, [BMIm][HS]: 3.488(2) Å, [EMIm][HSe]: 3.659(2) Å). The contacts of C4-H or C5-H are significantly longer. The results of a computational study concerning the anion-cation interaction in [EMIm][HS] have been published elsewhere.[20] In case of the C2 methylated salt **2**, the strongest contacts are accordingly formed by the remaining aromatic protons (d(C4···S1) = 3.567(2) Å, d(C5···S1) = 3.603(2) Å). The apical methyl group shows only weak H-bonding interactions (d(C8···S1) = 3.807(2) Å), which are even weaker than those of several CH groups of the aliphatic side chains. Also selected CH moieties in the pyrrolidinium cation show C-H···S distances well in range of H-bonding interactions (e.g. d(C1···S1) = 3.470(5) Å, d(C5···S1) = 3.780(5) Å). In the structures presented here, no instance was observed, where the SH group worked as a hydrogen bond donor. During crystallization potential H-bond acceptors like acetonitrile and diethyl ether were present, though. Comparable hydrogen bonds from CH donors to S acceptors are e.g. found in tetrathiomolybdate salts with organic cations[35] and imidazolium salts of thiocyanatometallate[36] nickelthiophosphate[37] and aluminumsulfide complexes.[38] Uncoordinated hydrosulfide anions are so far rarely found in crystal structures. The few examples include a triphenylethylphosphonium-hydrosulfide, which exhibits CH···S distances between 3.619 Å and 3.845 Å.[39] In all other cases NH donor moieties are present, which form significantly stronger H-bonds. E.g. NH···S = 2.971 Å in 4-methylpyridnium-hydrosulfide,[40] NH···S = 2.059 Å in Piperidinium-hydrosulfide[41] and NH···S = 3.367Å in cyclam complexes of cobalt(II)-hydrosulfide.[42]

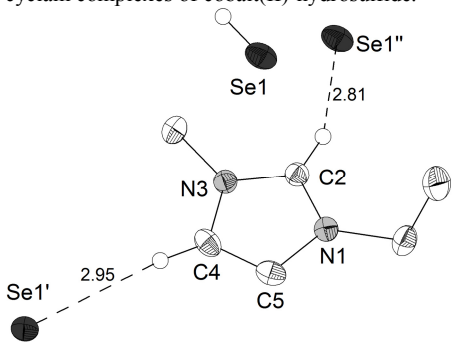

Figure 6. Molecular structure of [EMIm][HSe] (**6**), H-bond distances in Å, only H-atoms on selenium and those participating in H-bonds are shown, symm. op.: I: x−1/2,−y+1/2,z−1/2; II: −x+1,−y+1,−z+2.

While the imidazolium salts form layered structures, cations and anions are strictly alternating in the structure of [BMPyr][HS] (Figures S8-S10, supplementary information).

Table 2. Hydrogen bonds in the molecular structures of **1** to **4** and **6**. For an explanation of the symmetry operations please view the corresponding graphics.

Substance	D-H···A	d(H···A)/ Å	d(D···A)/ Å	<(DHA)/°
[EMIm][HS] (**1**)	C2-H2···S1^{I}	2.68	3.520(1)	148.2
	C4-H4···S1^{II}	2.79	3.731(1)	172.7
	C6-H6B···S1	2.88	3.786(1)	152.7
[EMMIm][HS] (**2**)	C4-H4···S1^{II}	2.65	3.567(2)	162.8
	C5-H5···S1^{III}	2.66	3.603(2)	172.7
	C6-H6A···S1^{I}	2.75	3.704(2)	162.0
	C9-H9A···S1	2.79	3.735(2)	161.9
	C8-H8C···S1	2.86	3.807(2)	162.5
[BMIm][HS] (**3**)	C2-H2···S1^{I}	2.58	3.488(2)	160.8
	C5-H5···S1	2.81	3.610(2)	143.0
[BMPyr][HS] (**4**)	C1-H1A···S1^{I}	2.64	3.470(5)	141.7
	C5-H5A···S1	2.77	3.732(4)	163.3
	C9-H9C···S1^{II}	2.87	3.780(5)	154.0
[EMIm][HSe] (**6**)	C2-H2···Se1^{II}	2.81	3.659(2)	149.1
	C4-H4···Se1^{I}	2.95	3.887(2)	169.6

IR spectroscopy

In the IR spectra of the hydrochalcogenide salts the chalcogen hydrogen stretching vibration results in a distinctive band. It can easily be observed as each of them appears in the weakly populated range between the lattice vibrations and the C-H vibrations of the cation. The respective cation slightly influences the precise wavenumber of the stretching vibration ν(H-E). In case of the pyrrolidinium cation, as shown in Figure 7, the HS^- anion leads to a band at 2561 cm^{-1}, HSe^- and HTe^- exhibit bands at 2286 cm^{-1} and 1988 cm^{-1}, respectively. With the tri-*n*butyl-methylphosphonium cation the respective wavenumbers are lower by 4 cm^{-1} to 7 cm^{-1}.

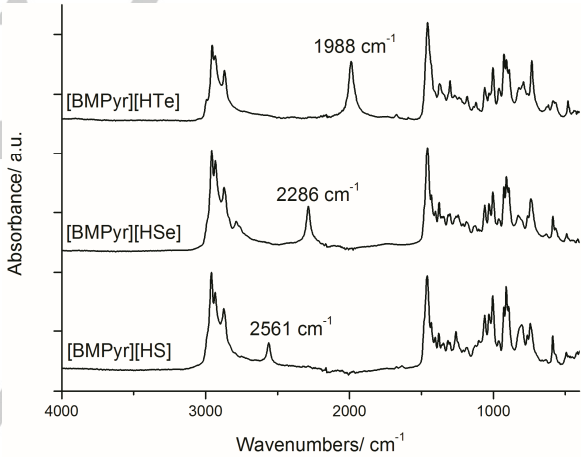

Figure 7. IR spectra of the pyrrolidinium hydrochalcogenides **4**, **7** and **10** (ATR-IR spectra of the pure substance, recorded in a nitrogen filled glove box on a Bruker ALPHA FT-IR).

In the ATR-IR spectra of the imidazolium salts **1**, **3**, **6** and **9** the respective hydrogen chalcogenide stretching vibration is distinctively broadened and is also shifted to lower wavenumbers. In the case of [EMIm][HS] the band is even split with maxima at 2545 cm^{-1} and 2565 cm^{-1} (see supplement). The immediate cause of the phenomenon is so far unknown. It cannot be explained purely by the relatively stronger hydrogen bonding interactions, which will influence the bond strength of the HS^- moiety due to a partial reduction of the negative charge. The EMMIm salt **2** shows a single very sharp band at 2563 cm^{-1}, despite showing almost as strong H-bonds as the other structures. A further reason may lie in the orientation of the HE^- anion. In the isotypic structures of **1** and **6** neighboring hydrochalcogenide anions are oriented in such a way that the protons face each other and may influence each other's stretching vibration. In case of **1** the interatomic distance of the hydrogen atoms is 2.21 Å and thereby very close to the sum of the van der Waals radii of hydrogen atoms (1.1 Å –

1.2 Å).[43] In the hydroselenide **6** the interatomic distance between the hydrogen atoms amounts to 2.55 Å, the splitting is significantly less pronounced. In all other structurally characterized salts the hydrosulfide ions are oriented differently and no close contacts of the hydrogen atoms are observed.

NMR spectroscopy

The synthesized compounds were investigated by NMR spectroscopy with respect to proton, carbon and common hetero nuclei resonances. ^{13}C and ^{31}P NMR spectra only show the respective cation and will not be discussed; full details can be found in the experimental part of the supporting information. In contrast, the ^{1}H NMR spectra also show the anion part of the compounds, which regardless of the cation appears at almost identical shifts in the high field. The HS^- resonance can be found at about −3.9 ppm, HSe^- leads to a signal at −6.6 ppm and HTe^- resonances at −13.0 ppm (all in DMSO). The signal for HS^- was not described by Jovanovski *et al.* but our findings agree well with other NMR spectroscopic studies concerning hydrochalcogenide anions.[21b, 44] Figure 8 directly compares the ^{1}H NMR spectra of the 1-ethyl-3-methylimidazolium hydrochalcogenides. Hydrogen bonding between the respective C2-H and hydrochalcogenide anion appears to prevail also in solution, as the resonance signal of the C2-H is slightly shifted to higher field going from [EMIm][HS] to [EMIm][HTe].

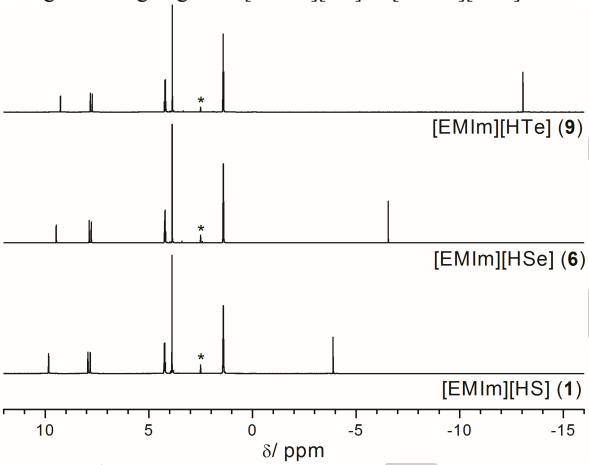

Figure 8. ^{1}H NMR-Spectra of [EMIm][HS] (**1**), [EMIm][HSe] (**6**) and [EMIm][HTe] (**9**), *DMSO-d_6, 300.1 MHz.

The hydroselenide salts were also characterized by ^{77}Se NMR spectroscopy, yielding resonance signals in the range of −312 to −316 ppm (standard: Me_2Se) and the coupling constant $^{1}J(^{1}H\text{-}^{77}Se)$ = 7.5 Hz. The slight differences may be traced back to a strong solvent dependence of selenium resonance.[45] In the present cases the solvent is always the same, but especially at the high concentration, which is necessary for well resolved signals, the respective cation may have a noticeable influence. ^{125}Te NMR spectroscopy of the hydrotelluride salts showed resonance signals in the range of −921 to −925 ppm (standard: Me_2Te) for the HTe^- anion and a $^{1}J(^{1}H\text{-}^{125}Te)$ coupling constant of 147.5 Hz was observed. Both results are in agreement with previously published values.[21b] The hydrotelluride NMR samples rapidly decompose forming deep violet solutions, as it was also observed for the corresponding trimethylsilytellurolates.[24] This rarely affects the NMR spectra as presumably diamagnetic polytelluride species with a low concentration and low sensitivity are formed. Only after deliberate decomposition of a hydrotelluride substance and with concentrated samples and a high number of scans additional ^{125}Te resonance signals become visible. In further analogy to the trimethylsilytellurolates the salt $[BMPyr]_4Te_{12}$ could be crystallized from a decomposed hydrotelluride sample. Details of the decomposition experiments and the crystal structure are presented as supporting information.

Preparation and characterization of polysulfide ionic liquids

In previous experiments to generate polysulfide ionic liquids from organic cation hydrosulfides unspecified amounts of sulfur were employed, not allowing any directed reproduction.[13, 16a] In another case equimolar amounts of hydrosulfide and sulfur initially formed a green solution, which turned colorless overnight and allowed the isolation of colorless crystals. Elemental analysis indicated this substance to be tetramethylammonium pentasulfide.[16b] This is hardly imaginable, firstly because of the reaction stoichiometry and secondly as so far all ionic polysulfides are intensely colored compounds.[17] These ambiguous results intrigued us to investigate the reaction behavior of one of our pure hydrosulfides with elemental sulfur in more detail.

To obtain polysulfide salts with the formal constitution $[BMPyr]_2[S_{n+1}]$ (n = 1, 3, 5, 7) two equivalents of **4** were reacted with 1, 3, 5 and 7 molar equivalents of sulfur according to Scheme 5.

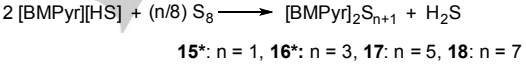

15*: n = 1, **16***: n = 3, **17**: n = 5, **18**: n = 7

Scheme 5. Synthesis of pyrrolidinium polysulfides, *: in the synthesis of **15** and **16** 40% and 10%, respectively, of hydrosulfide anions remain (*vide infra*).

The reaction takes place at room temperature under neat conditions but is greatly accelerated in solvents such as methanol, acetonitrile and THF. As most of the products are highly viscous oils the experiments were conducted in solution to ensure homogeneous products. The highest sulfur content, which could be dissolved in these experiments, corresponds to a ratio of approximately 2 : 9. This was observed regardless of the cation. For the formal products $[BMPyr]_2S_2$ (**15**) and $[BMPyr]_2S_4$ (**16**) the reactions do not lead to the pure polysulfides. In both cases the HS^- resonance signal is still evident in the ^{1}H NMR spectrum. Although the mixtures were heated under reflux conditions in protic (methanol) as well as aprotic (MeCN, THF) solvents from several hours up to several days, about 40% of the original hydrosulfide anion remained in substance **15** and about 10% in compound **16**. Equilibrium between longer chain polysulfides, hydrosulfide and hydrogen sulfide potentially bound in hydrogen bonding networks seems to prevail. As none of the mentioned attempts led to a significantly different result we are confident that under the chosen conditions an equilibrium is reached. If the RTIL [nBu$_3$MeP][HS] (**5**) is reacted with the appropriate amounts of sulfur the same phenomenon is observed. After stirring the mixture 24 hours at 80 °C the same hydrosulfide residues are observed. The amount of hydrosulfide is slightly reduced if the reaction is continued for 72 hours but the phosphonium cation starts to decompose as well. These

results coincide with calculations that the disulfide dianion S_2^{2-} is in principle unstable[46] and is only stabilized in inorganic salts with a sufficiently high lattice energy. The only structurally proven instance, where an isolated S_2^{2-} ion was observed alongside organic molecules is the co-crystallization of a potassium 1,1-dithiolate with one third of dipotassium disulfide.[47] Without any doubt Scheme 5 and similar published equations[13] of such sulfur redox chemistry with HS^- are an ideal picture of the scenario, which is never reached for organic cations and smaller polysulfide chains. This is in agreement with inorganic polysulfide salts, where e.g. the synthesis of alkali metal tetra-, penta- and hexasulfides is possible starting from corresponding hydrosulfides. However, the respective disulfides, are accessible only from the elements or sulfur and the dimetal sulfide.[17] Starting from the trimethylsilylthiolate salts hexasulfides can be prepared in a highly selective manner.[24] Although substances **15** and **16** cannot be regarded as pure and the actual anion is questionable we chose to denote them as di- and tetrasulfide for identification purposes and to emphasize the average polysulfide chain length. Furthermore these two substances are not long time stable. Upon storage at 25 °C in an inert atmosphere the salts form colorless oils which prove to be analogous decomposition products as obtained by thermal decomposition of [BMPyr][HS] (*vide supra*). All polysulfide products are intensely colored, while the actual color depends on the average chain length and the state of solvation. Unsolvated *N*-butyl-*N*-methyl-pyrrolidinium polysulfides show colors ranging from yellow (S_2) to deep red (S_8). Concentrated solutions in DMSO show colors ranging from bluish-green (S_2) via green and brown (S_4, S_6) to red (S_8). Upon dilution all solutions turn blue which is attributable to the tendency of polysulfides to form primarily the blue $S_3^{\bullet-}$ radical anion under these conditions.[48] We investigated the polysulfides **15** to **18** and the pyrrolidinium hydrosulfide **6** with respect to their absorption features in the UV-Vis spectral range. In all polysulfide salts a mixture of polysulfide species is present but a distinctive shift to higher chain length polysulfides with increasing sulfur content can be observed. Figure 9 compares UV-Vis spectra of the polysulfides **15** to **18** and [BMPyr][HS]. While for lower chain lengths the absorption maxima at 265 nm (S_2^-, HS^-) 338 nm and 437 nm (both S_4^{2-} and S_6^{2-}) dominate, substances **17** and **18** exhibit absorption maxima at 270 nm (S_3^{2-}, S_2^{2-}), 350 nm to 358 nm and 482 nm to 490 nm (all S_8^{2-}).[4] An absorption band at 620 nm, which is attributable to the aforementioned $S_3^{\bullet-}$ can be observed in each substance, it is especially distinctive for the hexasulfide.

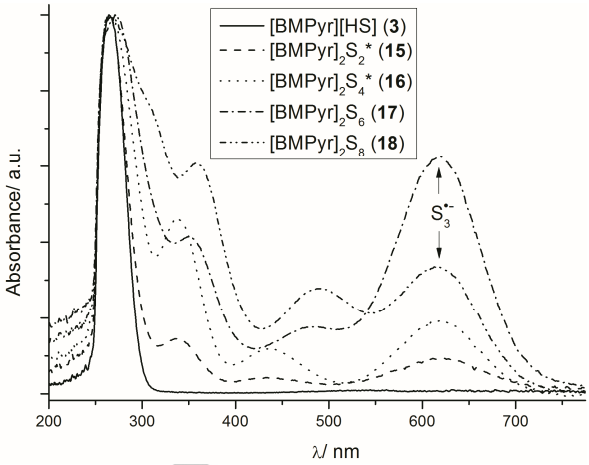

Figure 9. Comparison of UV-Vis spectra of polysulfides **15** to **18** and [BMPyr][HS] (**4**) in DMSO, *: for compounds **15** and **16**, 40% and 10%, respectively, of hydrosulfide anions remain.

The redox behavior of the polysulfide salts and the hydrosulfide **6** was investigated utilizing cyclic voltammetry (CV). The CV experiments were conducted in DMSO containing 50 mmol·L^{-1} of tetrabutylammonium hexafluorophosphate as supporting electrolyte at a scan rate of 100 mV·s^{-1} and a temperature of 25 °C. A glassy carbon (GC) working electrode, platinum counter electrode and an Ag/Ag_2S reference electrode were employed. All spectra have been referenced against the ferrocene/ ferrocenium (Fc/Fc^+) redox couple added internally at the end of each CV experiment.

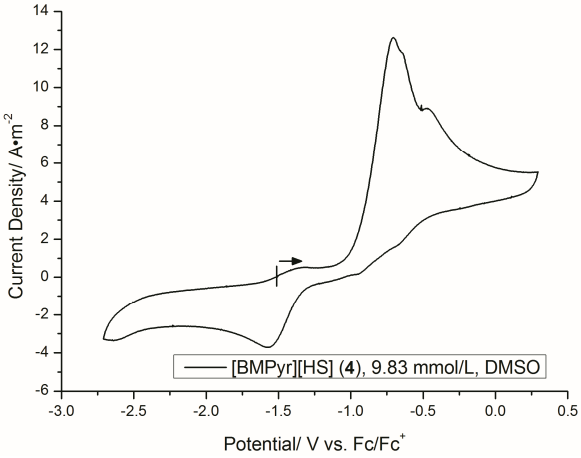

Figure 10. Cyclic voltammogram of [BMPyr][HS] (**4**), GC electrode, scan rate 100 mV·s^{-1}, the arrow indicates scanning direction and starting potential.

The cyclic voltammogram of [BMPyr][HS] (Figure 10) shows irreversible redox processes, most notably an oxidation at −0.78 V with smaller maxima following at −0.73 V and −0.55 V and a reduction at −1.64 V. The electrochemical oxidation of aqueous hydrosulfide solutions on gold electrodes was shown to proceed in a two electron process according to equation **I**.[49]

This reaction can be assumed for our system as well. Due to the inertness of the glassy carbon electrode and the reactivity of

hydrosulfide ions towards elemental sulfur follow-up reactions according to **II** have to be anticipated.

$$HS^- \xrightarrow{-2\,e^-} H^+ + S \qquad \textbf{(I)}$$

$$S + 2\,HS^- \rightarrow H_2S + S_2^{2-} \qquad \textbf{(II)}$$

This is in agreement with the fact that no reduction of elemental sulfur can be observed, but that the occurring reduction lies in the range of reduction potentials of polysulfide anions as it is observed for the compounds **15** and **16**. Furthermore the samples turned from colorless to light blue green during the CV experiments indicating the presence of polysulfides and their radical anion fragments. The electrochemical characteristics of the polysulfide salts strongly depend on the actual sulfur content. The formal $[BMPyr]_2S_2$ shows still a strong resemblance to the pyrrolidinium hydrosulfide. This has to be expected as according to the ^{1}H NMR spectrum the substance still contains 40% of the hydrosulfide ions of the starting material. The reduction peak at −1.68 V gets considerably stronger, though.

The cyclic voltammograms of the formal hexa- and octasulfides are almost identical and show two distinct oxidation and reduction peaks. This was equally observed in CVs of sulfur in DMSO.[7a, 7e] The CV of the formal tetrasulfide **16** combines features of the analogues with lower and higher sulfur content. Figure 11 shows a comparison of the formal di-, tetra- and hexasulfide with increasing sulfur content a slight shift to lower potentials can be observed. This trend continues for the octasulfide (not displayed in Figure 11 for clarity, please refer to the SI for a colored version including all substances). Separate cyclic voltammograms of all substances are displayed in the supplementary information.

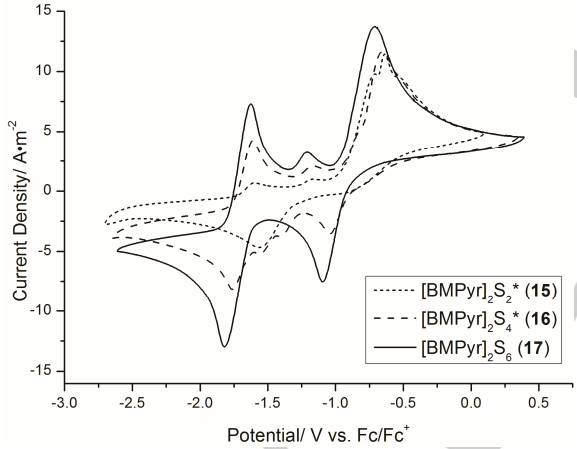

Figure 11. Comparison of cyclic voltammograms of $[BMPyr]_2S_2$, $[BMPyr]_2S_4$ and $[BMPyr]_2S_6$, GC electrode, scan rate 100 mV·s^{-1}, analyte concentrations of the respective samples are noted in the SI.

Earlier experiments typically found the most reversible appearance of polysulfide CVs on Au electrodes.[4, 50] This partly agrees with our experiments, where for compound **17** the peak separation of associated oxidation and reduction processes is also lowest on the Au electrode (Table 3, for graphic representations of CVs on different working electrode materials and at different scan rates please refer to the SI). However the curve integral for the process R_A is significantly decreased, that is why glassy carbon electrodes were chosen for the main investigation.

Table 3. Peak potentials and peak separation of $[BMPyr]_2S_6$ (**17**) on different working electrode materials at a scan rate of 100 mV·s^{-1}.

	Au	GC	Pt
O_A	−0.60 V	−0.61 V	−0.42 V
R_A	−1.02 V	−1.09 V	−1.13 V
Δφ	0.42 V	0.48 V	0.71 V
O_B	−1.61 V	−1.60 V	−1.60 V
R_B	−1.69 V	−1.78 V	−1.73 V
Δφ	0.08 V	0.18 V	0.13 V
O_C	−1.15 V	−1.14 V	−1.00 V

Figure 12 shows the voltammogram for $[BMPyr]_2S_8$ (**18**), which will serve as a basis for the discussion. The first process (O_A, R_A) shows an oxidation potential of −0.75 V and a reduction at −1.13 V ($\varphi_{0,A}$ = −0.94 V, Δφ = 0.38 V), in the second process (O_B, R_B) oxidation occurs at −1.67 V and the corresponding reduction at −1.88 V ($\varphi_{0,B}$ = −1.78 V, Δφ = 0.21 V). Additionally an oxidation peak (O_C) is observed at −1.27 V.

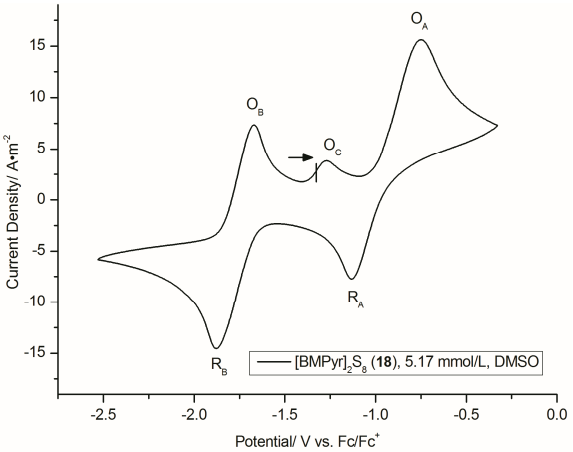

Figure 12. Cyclic voltammogram of $[BMPyr]_2S_8$ (**18**), 5.17 mmol·L^{-1} in DMSO , GC electrode, scan rate 100 mV·s^{-1}, the arrow indicates scanning direction and starting potential.

The CVs show an overall good agreement with reported CV experiments of sulfur and different polysulfides in ionic liquids[4] and organic solvents.[7a-c, 7e] Comparison with earlier investigations suggests the assignment of process O_A to the reaction **III**. The corresponding reduction can be described as the two electron reduction of elemental sulfur to S_8^{2-} (eq. **IV**).

$$S_n^{2-} \xrightarrow{-2e^-} \left(\frac{n}{8}\right) S_8 \qquad (O_A) \qquad \textbf{(III)}$$

$$S_8 \xrightarrow{+2e^-} S_8^{2-} \rightarrow S_6^{2-} + \left(\frac{2}{8}\right) S_8 \qquad (R_A) \qquad \textbf{(IV)}$$

Hardacre and co-workers suggested a rapid disproportionation of S_8^{2-} to S_6^{2-} and S_8 to follow the reduction of elemental sulfur (eq. **IV**), as they were able to assign the second reduction wave R_B to the two electron reduction of S_6^{2-} to S_3^{2-} (eq. **V**) by thorough spectroelectrochemical experiments.[4]

$$S_6^{2-} \xrightarrow{+2e^-} 2\,S_3^{2-} \qquad (R_B) \qquad \textbf{(V)}$$

Under the assumption that no dis- or comproportionation reactions occur, the corresponding oxidation wave can be assigned to the back reaction of eq. **V**. The oxidation process O_C at −1.26 V has been observed before[7d] but could not be assigned to a specific reaction so far. Our experiments clearly show that it is directly associated with the preceding process O_B and is only observed, if this potential zone was crossed before.

The preceding assumptions are mostly confirmed by our own spectroelectrochemical investigations. Those were equally conducted in DMSO containing 50 mmol·L^{-1} of tetrabutylammonium hexafluorophosphate as supporting electrolyte at a temperature of 25 °C, the analyte concentration was 0.95 mmol·L^{-1}. A gold mesh working electrode, platinum counter electrode and an Ag wire as pseudo reference electrode were employed. The gold mesh working electrode was positioned in the center between two quartz windows with a 2 mm path length, which are set into the PEEK casing of the measurement cell (PEEK = polyether ether ketone). Absorption in the UV-Vis range was monitored with an Avantes UV-Vis spectrometer. During a cyclic voltammetry experiment even at very low scan rates the absorbance of the bulk substance was too strong to observe distinctive changes. We therefore chose to conduct the spectroelectrochemical experiments in a chronoamperometric fashion, staying at every peak potential for 10 minutes.

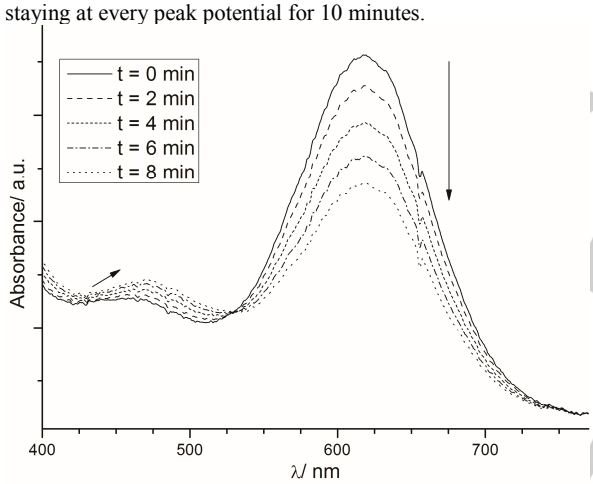

Figure 13. Change in the UV-Vis absorption during chronoamperometry of $[BMPyr]_2S_6$ (**17**) at the potential of O_A.

At the potential of O_A a strong decrease of the absorption band at 620 nm together with the slight shift of a band at 455 nm toward 470 nm is observed. At 530 nm an isosbestic point prevails (Figure 13).

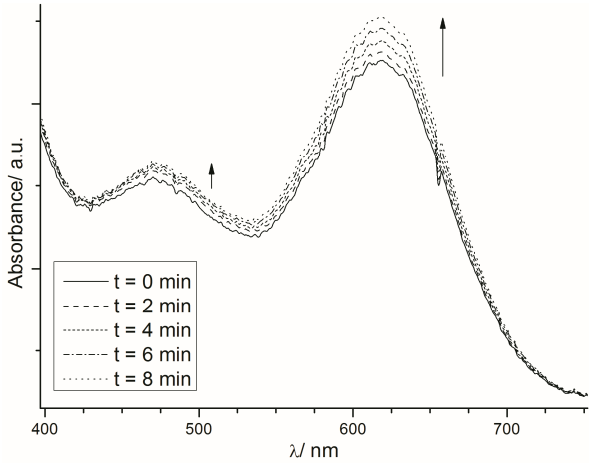

Figure 14. Change in the UV-Vis absorption during chronoamperometry of $[BMPyr]_2S_6$ (**17**) at the potential of R_A.

This is in agreement with especially hexasulfide ions being oxidized to longer chains, which finally disproportionate to elemental sulfur. The reduction wave R_A at –1.12 V is associated with a small increase of the $S_3^{\bullet-}$ concentration and a further increase of the band at 470 nm indicative of a formation of octasulfide dianions and there consecutive equilibration also to hexasulfide dianions (Figure 14).

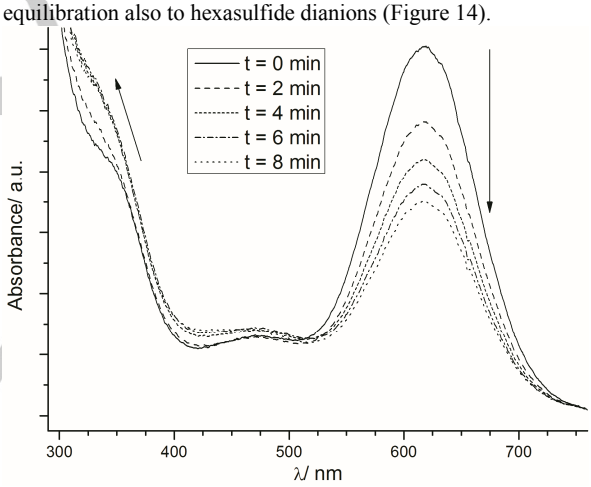

Figure 15. Change in the UV-Vis absorption during chronoamperometry of $[BMPyr]_2S_6$ (**17**) at the potential of R_B.

The second reduction wave at R_B (Figure 15) leads to opposing phenomena; a significant decrease of the $S_3^{\bullet-}$ concentration is accompanied by a band shift and increase from 350 nm to 330 nm, which indicates a further reduction of the hexasulfide to shorter polysulfides. The absorption band at 470 nm shows only slight variation. These results strongly support the findings of Manan *et al.*, who concluded equation **V** from the slight shift of the band at 470 nm without being able to observe the trisulfur radical anion in the chosen IL.[4] For so far unknown reasons the associated oxidation O_B does not lead to an increase of the hexasulfide and thereby trisulfide radical anion concentration. In two independent experiments only an overall, rather homogeneous intensity decrease could be observed. This phenomenon is under further investigation. During chronoamperometry at O_C we did not observe any significant change in

the UV-Vis absorption spectra, affirming the assumption that this potential wave rather corresponds to an electrode centered process than an actual oxidation of the analyte.

Conclusions

We herein presented the broad application and scope of a new synthetic approach to hydrochalcogenide salts with organic cations Cat[HE] (E = S, Se, Te), which is completely water, halide and metal free. Thus prepared ionic liquids and organic salts exhibit a high purity and are - in contrast to ILs prepared by traditional salt metathesis reactions - preferential for their electrochemical and synthetic applications. We have presented the detailed characterization of the substances in terms of NMR and IR spectroscopy, selected crystal structures and thermal behavior, including decomposition routes. Pyrrolidinium hydrosulfides were used to synthesize corresponding polysulfides by reaction with elemental sulfur. Variation of the employed sulfur amount allows the synthesis of a series of compounds with different intermediate polysulfide chain length. The imminent effect of the chain length on the UV-Vis absorption and electrochemical redox behavior was investigated. Only for longer polysulfide chain lengths a reversible redox behavior could be observed. Contradictory to preceding publications, none of the polysulfide salts appeared to be colorless. Their decomposition products are colorless.

The naked hydrochalcogenide anions exhibit a very high nucleophilicity which qualifies these as key substances for reactions where the traditionally used hydrogen, silyl or alkali metal chalcogenides are insufficient. We are confident that the now readily available title compounds [Cat][HE] (E = S, Se, Te) will expand the starting material basis for many chemists working in the topical areas of metal chalcogenido clusters, chalcogenidometallates, metal chalcogenide semiconductor materials and polychalcogenide redox mediators.

Experimental Section

X-ray analysis

The data collection for the single crystal structure determinations was performed in rotation method on a Bruker D8 QUEST diffractometer by the X-ray service department of the Fachbereich Chemie, University of Marburg. The spectrometer is equipped with a Mo-K_α X-ray micro source (0.71073 Å, Incotec), a fixed chi goniometer and a PHOTON 100 CMOS detector. Bruker software (Bruker Instrument Service, APEX2, SAINT) was used for data collection, cell refinement and data reduction.[51] The structures were solved with SIR-97,[52] SIR2011[53] or SUPERFLIP,[54] refined with SHELXL-2014[55] and finally validated using PLATON[56] software, all within the WinGX[57] software bundle. Absorption corrections where applied beforehand within the APEX2 software (multi-scan).[58] Graphic representations were created using Diamond 4.[59] C-bound H-atoms were constrained to parent site; H-atoms on heteroatoms were located in the Fourier map and refined independently. In all graphics the ellipsoids are shown for the 50% probability level. Hydrogen atoms are shown with arbitrary radius, only those bound to hetero atoms or involved in hydrogen bonds are shown in the graphic representations.

Devices and methods

Elemental analyses (C, N, H, S) were carried out by the service department for routine analysis and mass spectrometry with a vario MICRO cube (Elementar). The samples were weighed into tin capsules inside a nitrogen filled glove box. Melting points were determined with a Büchi Melting Point B540. TGA/ DSC measurements were performed with a Netzsch STA 409 CD in aluminium oxide crucibles, with an argon flow rate of 40 mL/min and a heating rate of 10 K/min; TGA decomposition points are given as onset temperature, DSC data is given as peak value. ^{1}H and ^{13}C NMR spectra were recorded in automation with a Bruker Avance 300 spectrometer, ^{31}P NMR-spectra were recorded on a Bruker DPX 250 spectrometer, ^{77}Se and ^{125}Te NMR-spectra were recorded by the service department for NMR analyses with a Bruker DRX 400 or Avance 500 spectrometer. All spectra were recorded at ambient temperature. ^{1}H and ^{13}C-NMR spectra were calibrated using residual protons and solvent signals, respectively (DMSO-d_6; δ_H 2.50 ppm, δ_C 39.52 ppm).[60] NMR spectra of hetero nuclei were referenced externally as follows: ^{31}P: 85% H_3PO_4; ^{77}Se: Dimethyl selenide; ^{125}Te: Dimethyl telluride. IR spectra were recorded on a Bruker APLPHA FT-IR spectrometer with Platinum ATR-sampling. UV-Vis spectra were recorded with an Avantes AvaLight-DHc and AvaSpec-2048 combination. Cyclic voltammetry and spectroelectrochemical chronoamperometry experiments were accomplished with an RHD Instruments Microcell HC device[61] (WE: glassy carbon, gold, platinum or gold mesh, CE: platinum crucible, RE: Ag/Ag_2S or Ag wire (pseudo RE)), Microcell HC temperature controller and a Metrohm Autolab PGStat 204 as potentiostat. For IR, UV-Vis and CV all steps were carried out in a nitrogen filled glovebox (type Labmaster 130, mBraun).

Starting materials

All solvents were dried according to common procedures[62] and passed through columns of aluminium oxide, 3 Å molecular sieve and R3-11G-catalyst (BASF) or stored over molecular sieve (3 or 4 Å) until use. Reagents were used as received unless stated otherwise. 1-Ethyl-3-methylimidazolium methylcarbonate in methanol solution (30%) was donated by BASF. 1-butyl-3-methylimidazolium methylcarbonate in methanol solution (50%) was purchased from Iolitec, *N*-butylpyrrolidine from Acros. Methylcarbonate ionic liquids were synthesized following published procedures.[29a, 29b] The higher bis(trimethylsilyl)chalcogenides were synthesized in analogy to the sulfide.[63] For a recent exemplary procedure of the bis(trimethylsilyl)telluride please view the SI to ref.[24] The compounds **1** to **4** and **6** were synthesized as presented recently.[20]

Representative synthetic procedures

Synthetic procedures for compounds **1** to **6** and **8** to **10** and the polysulfides **15** to **18** are submitted as supplementary information.

Synthesis of N-butyl-N-methylpyrrolidinium hydroselenide ([BMPyr][HSe], 7). *N*-butyl-*N*-methylpyrrolidinium methylcarbonate (2.86 g, 13.2 mmol) was dissolved in methanol (18 mL) the mixture cooled in an ice bath and degassed in three cycles. Bis(trimethylsilyl)selenide (3.21 g, 14.2 mmol) was added in small portions within 30 minutes and the solution stirred for further 30 minutes at 0 °C. The mixture was then warmed to ambient temperature and the solvent removed *in vacuo*. The slightly yellow residue was recrystallized from an acetonitrile/ diethyl ether mixture at −30 °C. Colorless needles were collected by filtration washed with diethyl ether and dried in fine vacuum. Additional material was obtained analogously from the filtrate and washings. [BMPyr][HSe] (1.99 g, 68%) was obtained as slightly greenish needles. **Mp** 149 °C (decomp., from acetonitrile/ diethyl ether, 2 K/min). **Elem. anal.** found C, 48.4; H, 9.6; N, 6.7; $C_9H_{21}N_1Se_1$ requires **C**, 48.6; H, 9.5; N, 6.3. **IR:** ν_{max}/cm^{-1}: 2957vs, 2932s, 2872m, 2286m (H-Se), 1458vs, 1377w, 1345w, 1301w, 1245w, 1060m, 1030m, 1004m, 909m, 740m, 586m. **^{1}H-NMR** (300.1 MHz, DMSO-d_6) δ_H = −6.64 (s, 1H, *H*Se), 0.92 (t, $^{3}J_{HH}$ = 7.3 Hz, 3H, CH_2CH_3), 1.24-1.37 (m, 2H, CH_2CH_3), 1.62-1.73 (m, 2H, NCH_2CH_2), 2.02-2.13 (m, 4H, CH_2*(3,4)*), 3.01 (s, 3H, N*Me*), 3.33-3.39 (m, 2H, NCH_2CH_2), 3.44-3.54 (m, 4H, CH_2*(2,5)*) ppm. **^{13}C-NMR**

(75.5 MHz, DMSO-d_6): δ_C = 13.5 (1C, CH_2CH_3), 19.2 (1C, br), 21.0 (1C), 24.9 (1C), 47.5 (t, $^3J_{CN}$ = 3.7 Hz, 2C, *C3/4*), 62.7 (br s, 2C, *C2/5*), 63.3 (t, $^2J_{CN}$ = 2.8 Hz, 1C) ppm. **^{77}Se-NMR** (76.3 MHz, DMSO-d_6): δ_{Se} = −316.2 ppm.

Synthesis of tri-nbutyl-methylphosphonium hydrotelluride ([(nBu)$_3$MeP][HTe], 11). Tri-*n*butyl-methylphosphonium methylcarbonate (1.11 g, 3.80 mmol) was dissolved in methanol (6 mL), the solution cooled to −20 °C and degassed by repeated cycles of evacuation and purging with inert gas. Bis(trimethylsilyl) telluride (1.14 g, 4.18 mmol) was added dropwise within 10 minutes and the colorless solution stirred at 0 °C for half hour. Small amounts of a black precipitate were removed by a syringe filter, the solution again cooled to −20 °C and all volatiles removed in fine vacuum. The red residue was dried at 0 °C and shortly at ambient temperature, then triturated with THF (5 mL) and the mixture stored at −30 °C. The mixture was filtered and the residue washed with diethyl ether (2 mL). After drying in fine vacuum [(*n*Bu)$_3$MeP][HTe] (2.96 g, 93%) was isolated as a slightly red solid. **Mp** 163 °C (decomp., from diethyl ether, 2 K/min). **Elem. anal.** found C, 45.1; H, 9.2; $C_{13}H_{31}P_1Te_1$ requires **C,** 45.1; H, 9.0. **IR:** ν_{max}/cm^{-1}: 2956s, 2931s, 2870s, 1981m (H-Te), 1459m, 1383m, 1305m, 1230w, 1200w, 1097m, 971s, 941vs, 816s, 766m, 716m, 455m. **^{1}H-NMR** (300.1 MHz, DMSO-d_6) δ_H = −13.0 (s, 1H, *H*Te), 0.90 (t, $^3J_{HH}$ = 7.1 Hz, 9H, CH_2CH_3), 1.32-1.53 (m, 12H, CH_2CH_2), 1.82 (d, $^2J_{HP}$ = 14.0 Hz, 3H, PCH_3), 2.13-2.27 (m, 6H, PCH_2) ppm. **^{13}C-NMR** (75.5 MHz, DMSO-d_6) δ_C = 3.4 (d, $^1J_{CP}$ = 51.4 Hz, 1C, PCH_3), 13.2 (3C, CH_2CH_3), 19.0 (d, $^1J_{CP}$ = 49.2 Hz, 3C, PCH_2), 22.6 (d, J_{CP} = 4.3 Hz, 3C, CH_2), 23.2 (d, J_{CP} = 15.9 Hz, 3C, CH_2) ppm. **^{31}P-NMR** (101.3 MHz, DMSO-d_6): δ_P = 35.6 ppm. **^{125}Te-NMR** (126.2 MHz, DMSO-d_6): δ_{Te} = −920.9 ppm.

Acknowledgements

We thank the "Fond der Chemischen Industrie" (doctoral fellowship for L.H.F.) and the "Deutsche Forschungsgemeinschaft" (GRK 1782, Functionalization of Semiconductors) for financial support. For his advice with crystal structure refinement we thank Dr. K. Harms. We thank Prof. S. Dehnen for the possibility to perform TGA/DSC analyses and are very grateful to Dr. B. Huber and Dr. M. Drüschler of RHD Instruments for their advice with cyclic voltammetry, the development of the spectroelectrochemical cell and their comprehensive support. Dr. G. Thiele is thanked for fruitful discussion and the recording of selected ^{125}Te-NMR spectra.

[1] a) J. Scheers, S. Fantini, P. Johansson, *J. Power Sources* **2014**, *255*, 204-218; b) M. Barghamadi, A. S. Best, A. I. Bhatt, A. F. Hollenkamp, M. Musameh, R. J. Rees, T. Ruther, *Energy Environ. Sci.* **2014**, *7*, 3902-3920.

[2] a) K. Dokko, N. Tachikawa, K. Yamauchi, M. Tsuchiya, A. Yamazaki, E. Takashima, J.-W. Park, K. Ueno, S. Seki, N. Serizawa, M. Watanabe, *J. Electrochem. Soc.* **2013**, *160*, A1304-A1310; b) J.-W. Park, K. Ueno, N. Tachikawa, K. Dokko, M. Watanabe, *J. Phys. Chem. C* **2013**, *117*, 20531-20541; c) J.-W. Park, K. Yamauchi, E. Takashima, N. Tachikawa, K. Ueno, K. Dokko, M. Watanabe, *J. Phys. Chem. C* **2013**, *117*, 4431-4440; d) K. Ueno, J.-W. Park, A. Yamazaki, T. Mandai, N. Tachikawa, K. Dokko, M. Watanabe, *J. Phys. Chem. C* **2013**, *117*, 20509-20516; e) J. Zheng, M. Gu, H. Chen, P. Meduri, M. H. Engelhard, J.-G. Zhang, J. Liu, J. Xiao, *J. Mater. Chem. A* **2013**, *1*, 8464-8470; f) L. Wang, H. R. Byon, *J. Power Sources* **2013**, *236*, 207-214; g) A. Unemoto, H. Ogawa, Y. Gambe, I. Honma, *Electrochim. Acta* **2014**, *125*, 386-394; h) A. Rosenman, E. Markevich, G. Salitra, D. Aurbach, A. Garsuch, F. F. Chesneau, *Adv. Energy Mater.* **2015**, *5*, n/a; i) C. Liao, B. Guo, X.-G. Sun, S. Dai, *ChemSusChem* **2015**, *8*, 353-360; j) Y. Zhao, T. Bostrom, *Curr. Org. Chem.* **2015**, *19*, 556-566; k) M. Barghamadi, A. S. Best, A. I. Bhatt, A. F. Hollenkamp, P. J. Mahon, M. Musameh, T. Ruther, *J. Power Sources* **2015**, *295*, 212-220; l) F. Wu, Q. Zhu, R. Chen, N. Chen, Y. Chen, Y. Ye, J. Qian, L. Li, *J. Power Sources* **2015**, *296*, 10-17; m) S. Xiong, J. Scheers, L. Aguilera, D.-H. Lim, K. Xie, P. Jacobsson, A. Matic, *RSC Adv.* **2015**, *5*, 2122-2128.

[3] R. Marassi, T. M. Laher, D. S. Trimble, G. Mamantov, *J. Electrochem. Soc.* **1985**, *132*, 1639-1643.

[4] N. S. A. Manan, L. Aldous, Y. Alias, P. Murray, L. J. Yellowlees, M. C. Lagunas, C. Hardacre, *J. Phys. Chem. B* **2011**, *115*, 13873-13879.

[5] È. Boros, M. J. Earle, M. A. Gîlea, A. Metlen, A.-V. Mudring, F. Rieger, A. J. Robertson, K. R. Seddon, A. A. Tomaszowska, L. Trusov, J. S. Vyle, *Chem. Commun.* **2010**, *46*, 716-718.

[6] Y. Chen, J.-M. Tarascon, C. Guéry, *Electrochim. Acta* **2013**, *99*, 46-53.

[7] a) R. P. Martin, W. H. Doub, Jr., J. L. Roberts, Jr., D. T. Sawyer, *Inorg. Chem.* **1973**, *12*, 1921-1925; b) B. S. Kim, S. M. Park, *J. Electrochem. Soc.* **1993**, *140*, 115-122; c) F. Gaillard, E. Levillain, *J. Electroanal. Chem.* **1995**, *398*, 77–87; d) D.-H. Han, B.-S. Kim, S.-J. Choi, Y. Jung, J. Kwak, S.-M. Park, *J. Electrochem. Soc.* **2004**, *151*, E283-E290; e) S. K. Yongju Jung, Bum-Soo Kim, Dong-Hun Han, Su-Moon Park, Juhyoun Kwak, *Int. J. Electrochem. Sci.* **2008**, *3*, 566-577; f) Y. Ren, H. Shui, C. Peng, H. Liu, Y. Hu, *Fluid Phase Equilib.* **2011**, *312*, 31-36; g) D. H. Webber, J. J. Buckley, P. D. Antunez, R. L. Brutchey, *Chem. Sci.* **2014**, *5*, 2498-2502; h) M. Vijayakumar, N. Govind, E. Walter, S. D. Burton, A. Shukla, A. Devaraj, J. Xiao, J. Liu, C. Wang, A. Karim, S. Thevuthasan, *Phys. Chem. Chem. Phys.* **2014**, *16*, 10923-10932; i) Y.-C. Lu, Q. He, H. A. Gasteiger, *J. Phys. Chem. C* **2014**, *118*, 5733-5741.

[8] P. Wasserscheid, T. Welton, (Eds.), *Ionic Liquids in Synthesis, Vol. 1 & 2*, 2nd ed., Wiley VCH, Weinheim, **2007**.

[9] a) D. H. McDaniel, W. G. Evans, *Inorg. Chem.* **1966**, *5*, 2180-2181; b) J. D. Cotton, T. C. Waddington, *J. Chem. Soc. A* **1966**, 785-789.

[10] a) J. S. Anderson, J. C. Peters, *Angew. Chem. Int. Ed.* **2014**, *53*, 5978-5981; b) H. Sugimoto, K. Hatakeda, K. Toyota, S. Tatemoto, M. Kubo, T. Ogura, S. Itoh, *Dalton Trans.* **2013**, *42*, 3059-3070; c) H. Sugimoto, S. Tatemoto, K. Toyota, K. Ashikari, M. Kubo, T. Ogura, S. Itoh, *Chem. Commun.* **2013**, *49*, 4358-4360; d) E. Galardon, T. Roger, P. Deschamps, P. Roussel, A. Tomas, I. Artaud, *Inorg. Chem.* **2012**, *51*, 10068-10070.

[11] a) X.-D. Chen, W. Zhang, J. S. Duncan, S. C. Lee, *Inorg. Chem.* **2012**, *51*, 12891-12904; b) X.-D. Chen, J. S. Duncan, A. K. Verma, S. C. Lee, *J. Am. Chem. Soc.* **2010**, *132*, 15884-15886; c) C. P. Berlinguette, R. H. Holm, *J. Am. Chem. Soc.* **2006**, *128*, 11993-12000.

[12] E. Schaumann, U. Wriede, J. Ehlers, *Synthesis* **1980**, *1980*, 907-908.

[13] V. Jovanovski, V. Gonzalez-Pedro, S. Gimenez, E. Azaceta, G. Cabanero, H. Grande, R. Tena-Zaera, I. Mora-Sero, J. Bisquert, *J. Am. Chem. Soc.* **2011**, *133*, 20156-20159.

[14] a) V. González-Pedro, Q. Shen, V. Jovanovski, S. Giménez, R. Tena-Zaera, T. Toyoda, I. Mora-Seró, *Electrochim. Acta* **2013**, *100*, 35-43; b) J. Bisquert Mascarell, I. Mora Sero', V. Jovanovski, R. Marcilla Garcia, R. Tena-Zaera, D. Mecerreyes Molero, G. Cabanero Sevillano EP 2 388 853, **2011**.

[15] T. Chivers, F. Edelmann, J. F. Richardson, K. J. Schmidt, *Can. J. Chem.* **1986**, *64*, 1509-1513.

[16] a) J. Liu, X. Yang, J. Cong, L. Kloo, L. Sun, *Phys. Chem. Chem. Phys.* **2012**, *14*, 11592-11595; b) J. Cong, X. Yang, Y. Hao, L. Kloo, L. Sun, *RSC Adv.* **2012**, *2*, 3625-3629.

[17] R. Steudel, in *Elemental Sulfur und Sulfur-Rich Compounds II, Vol. 231* (Ed.: R. Steudel), Springer Berlin Heidelberg, **2003**, pp. 127-152.

[18] L. Li, X. Yang, J. Gao, H. Tian, J. Zhao, A. Hagfeldt, L. Sun, *J. Am. Chem. Soc.* **2011**, *133*, 8458-8460.

[19] K. M. Hugar, H. A. Kostalik, G. W. Coates, *J. Am. Chem. Soc.* **2015**, *137*, 8730-8737.

[20] L. H. Finger, F. Wohde, E. I. Grigoryev, A. K. Hansmann, R. Berger, B. Roling, J. Sundermeyer, *Chem. Commun.* **2015**, *51*, 16169-16172.

[21] a) J. C. Huffman, R. C. Haushalter, **1989**, *8*, 531–532; b) R. J. Batchelor, F. W. B. Einstein, I. D. Gay, C. H. W. Jones, R. D. Sharma, *Inorg. Chem.* **1993**, *32*, 4378-4383; c) J. Amarasekera, E. J. Houser, T. B. Rauchfuss, C. L. Stern, *Inorg. Chem.* **1992**, *31*, 1614-1620.

[22] G. Thiele, L. Vondung, C. Donsbach, S. Pulz, S. Dehnen, *Z. Anorg. Allg. Chem.* **2014**, *640*, 2684-2700.

[23] a) E. J. Houser, S. Dev, A. E. Ogilvy, T. B. Rauchfuss, S. R. Wilson, *Organometallics* **1993**, *12*, 4678-4681; b) Y. Zhang, R. H. Holm, *J. Am. Chem. Soc.* **2003**, *125*, 3910-3920; c) W. B. B. Krebs, H.-J. Wellmer, K. Wiesmann, *Z. Anorg. Allg. Chem.* **1994**, *620*, 1234-1246.

[24] L. H. Finger, B. Scheibe, J. Sundermeyer, *Inorg. Chem.* **2015**, *54*, 9568-9575.

[25] a) T. Heine, *Acc. Chem. Res.* **2015**, *48*, 65-72; b) M.-R. Gao, Y.-F. Xu, J. Jiang, S.-H. Yu, *Chem. Soc. Rev.* **2013**, *42*, 2986-3017; c) S. V. Kershaw, A. S. Susha, A. L. Rogach, *Chem. Soc. Rev.* **2013**, *42*, 3033-3087; d) I. Chung, M. G. Kanatzidis, *Chem. Mater.* **2014**, *26*, 849-869; e) M. Pumera, Z. Sofer, A. Ambrosi, *J. Mater. Chem. A* **2014**, *2*, 8981-8987.

[26] K. K. Kam, B. A. Parkinson, *J. Phys. Chem.* **1982**, *86*, 463-467.

[27] a) T. Li, G. Galli, *J. Phys. Chem. C* **2007**, *111*, 16192-16196; b) K. F. Mak, C. Lee, J. Hone, J. Shan, T. F. Heinz, *Phys. Rev. Lett.* **2010**, *105*, 136805.

[28] a) X. Zhang, Y. Zhang, B.-B. Yu, X.-L. Yin, W.-J. Jiang, Y. Jiang, J.-S. Hu, L.-J. Wan, *J. Mater. Chem. A* **2015**, *3*, 19277-19281; b) Y. Li, H. Wang, L. Xie, Y. Liang, G. Hong, H. Dai, *J. Am. Chem. Soc.* **2011**, *133*, 7296-7299; c) F. Niefind, J. Djamil, W. Bensch, B. R. Srinivasan, I. Sinev, W. Grunert, M. Deng, L. Kienle, A. Lotnyk, M. B. Mesch, J. Senker, L. Dura, T. Beweries, *RSC Adv.* **2015**, *5*, 67742-67751.

[29] a) R. Kalb (PROIONIC), WO 2008 052 861, **2008**; b) R. Kalb (PROIONIC), WO 2008 052 860, **2008**; c) J. D. Holbrey, R. D. Rogers, S. S. Shukla, C. D. Wilfred, *Green Chem.* **2010**, *12*, 407-413.

[30] B. Oelkers, J. Sundermeyer, *Green Chem.* **2011**, *13*, 608-618.

[31] A. Efimova, G. Hubrig, P. Schmidt, *Thermochim. Acta* **2013**, *573*, 162-169.

[32] G. Illuminati, C. Lillocci, *J. Org. Chem.* **1977**, *42*, 2201-2203.

[33] M. T. Clough, K. Geyer, P. A. Hunt, J. Mertes, T. Welton, *Phys. Chem. Chem. Phys.* **2013**, *15*, 20480-20495.

[34] CCDC-1414150 to 1414154 and 1429785 contain the supplementary crystallographic data for the structures discussed in this paper. These data can be obtained free of charge from The Cambridge Crystallographic Data Centre via www.ccdc.cam.ac.uk/data%5Frequest/cif.

[35] a) B. R. Srinivasan, S. N. Dhuri, A. R. Naik, C. Näther, W. Bensch, *Polyhedron* **2008**, *27*, 25-34; b) B. R. Srinivasan, A. R. Naik, C. Näther, W. Bensch, *Z. Anorg. Allg. Chem.* **2007**, *633*, 582-588.

[36] a) P. Nockemann, B. Thijs, N. Postelmans, K. Van Hecke, L. Van Meervelt, K. Binnemans, *J. Am. Chem. Soc.* **2006**, *128*, 13658-13659; b) T. Peppel, M. Köckerling, M. Geppert-Rybczyńska, R. V. Ralys, J. K. Lehmann, S. P. Verevkin, A. Heintz, *Angew. Chem., Int. Ed.* **2010**, *49*, 7116-7119; c) T. Peppel, P. Thiele, M.-B. Tang, J.-T. Zhao, M. Köckerling, *Inorg. Chem.* **2015**, *54*, 982-988.

[37] J. A. Cody, K. B. Finch, G. J. Reynders, G. C. B. Alexander, H. G. Lim, C. Näther, W. Bensch, *Inorg. Chem.* **2012**, *51*, 13357-13362.

[38] V. Jancik, H. W. Roesky, *Inorg. Chem.* **2005**, *44*, 5556-5558.

[39] I. V. Borisova, N. N. Zemlyanskii, A. K. Shestakova, V. N. Khrustalev, Y. A. Ustynyuk, E. A. Chernyshev, *Russ. Chem. Bull.* **2000**, *49*, 933-941.

[40] M. T. Andras, A. F. Hepp, P. E. Fanwick, R. A. Martuch, S. A. Duraj, E. M. Gordon, *Acta Crystallogr. C* **1996**, *52*, 1701-1702.

[41] E. J. Smail, G. M. Sheldrick, *Acta Crystallogr. B* **1973**, *29*, 2027-2028.

[42] R. J. Pleus, H. Waden, W. Saak, D. Haase, S. Pohl, *J. Chem. Soc., Dalton Trans.* **1999**, 2601-2610.

[43] a) R. S. Rowland, R. Taylor, *J. Phys. Chem.* **1996**, *100*, 7384-7391; b) A. Bondi, *J. Phys. Chem.* **1964**, *68*, 441-451.

[44] a) G. M. Sheldrick, *Trans. Faraday Soc.* **1967**, *63*, 1065-1070; b) M. Bjoergvinsson, G. J. Schrobilgen, *Inorg. Chem.* **1991**, *30*, 2540-2547.

[45] J. Cusick, I. Dance, **1991**, *10*, 2629–2640.

[46] M. Trsic, W. G. Laidlaw, *Int. J. Quantum Chem.* **1980**, *17*, 969-974.

[47] N. Kuhn, G. Weyers, G. Henkel, *Chem. Commun.* **1997**, 627-628.

[48] T. Chivers, P. J. W. Elder, *Chem. Soc. Rev.* **2013**, *42*, 5996-6005.

[49] a) S. C. A. Briceno, *J. Appl. Electrochem.* **1990**, *20*, 506-511; b) S. C. A. Briceno, *J. Appl. Electrochem.* **1990**, *20*, 512-517.

[50] M. V. Merritt, D. T. Sawyer, *Inorg. Chem.* **1970**, *9*, 211-215.

[51] Bruker, Bruker AXS Inc., Madison, Wisconsin, USA, **2012**.

[52] A. Altomare, M. C. Burla, M. Camalli, G. Cascarano, C. Giacovazzo, A. Guagliardi, A. G. G. Moliterni, G. Polidori, R. Spagna, *J. Appl. Crystallogr.* **1999**, *32*, 115-119.

[53] M. C. Burla, R. Caliandro, M. Camalli, B. Carrozzini, G. L. Cascarano, C. Giacovazzo, M. Mallamo, A. Mazzone, G. Polidori, R. Spagna, *J. Appl. Crystallogr.* **2012**, *45*, 357-361.

[54] L. Palatinus, G. Chapuis, *J. Appl. Crystallogr.* **2007**, *40*, 786-790.

[55] G. Sheldrick, *Acta Crystallogr. C* **2015**, *71*, 3-8.

[56] A. L. Spek, *Acta Crystallogr. D* **2009**, *65*, 148-155.

[57] L. Farrugia, *J. Appl. Crystallogr.* **2012**, *45*, 849-854.

[58] Bruker, Bruker AXS Inc., Madison, Wisconsin, USA, **2012**.

[59] K. Brandenburg, H. Putz, Crystal Impact GbR, Bonn, Germany, **2012**.

[60] G. R. Fulmer, A. J. M. Miller, H. E. Gottlieb, N. H. Sherden, A. Nudelman, B. M. Stoltz, K. I. Goldberg, J. E. Bercaw, *Organometallics* **2010**, *29*, 2176-2179.

[61] RHD Instruments GmbH & Co. KG, c/o FB Chemie, Hans-Meerwein-Straße 6, 35043 Marburg, Germany.

[62] W. L. Amarego, D. D. Perrin, *Purification of Laboratory Chemicals*, 4th ed., Elsevier, Burlington, **1996**.

[63] J.-H. So, P. Boudjouk, *Synthesis* **1989**, 306-307.

Supplementary Information to "Halide Free Synthesis of Hydrochalcogenide Ionic Liquids"

Lars H. Finger[a], J. Sundermeyer[a,*]

a) Fachbereich Chemie and Materials Science Center,
Philipps-Universität Marburg,
Hans-Meerwein-Str. 4,
35043 Marburg,
Germany.
*E-Mail: JSU@staff.uni-marburg.de

Content:

Devices and methods

Elemental analyses (C, N, H, S) were carried out by the service department for routine analysis and mass spectrometry with a vario MICRO cube (ELEMENTAR). The samples were weighed into tin capsules inside a nitrogen filled glove box. Melting points were determined with a BÜCHI Melting Point B540. TGA/ DSC measurements were performed with a NETZSCH STA 409 CD in aluminium oxide crucibles, with an argon flow rate of 40 mL/min and a heating rate of 10 K/min; TGA decomposition points are given as onset temperature, DSC data is given as peak value. ^{1}H and ^{13}C-NMR spectra were recorded in automation with a BRUKER Avance 300 spectrometer, ^{31}P-NMR-spectra were recorded on a BRUKER DPX 250 spectrometer, ^{77}Se and ^{125}Te-NMR-spectra were recorded by the service department for NMR-analyses with a BRUKER DRX 400 or Avance 500 spectrometer. All spectra were recorded at ambient temperature. ^{1}H and ^{13}C-NMR spectra were calibrated using residual protons and solvent signals, respectively (DMSO-d_6: δ_H 2.50 ppm, δ_C 39.52 ppm).[1] NMR spectra of hetero nuclei were referenced externally as follows: ^{31}P: 85% H_3PO_4; ^{77}Se: Dimethyl selenide; ^{125}Te: Dimethyl telluride. IR spectra were recorded on a BRUKER APLPHA FT-IR spectrometer with Platinum ATR-sampling. UV-Vis spectra were recorded with an AVANTES AvaLight-DHc and AvaSpec-2048 combination. Cyclic voltammetry and spectroelectrochemical chronoamperometric experiments were accomplished with an RHD Instruments microcell device (WE: glassy carbon, gold, platinum or gold mesh, CE: platinum crucible, RE: Ag/Ag_2S or Ag wire (pseudo RE)), microcell HC temperature controller and a Metrohm Autolab PGStat 204 as Potentiostat. For IR, UV-Vis and CV all steps were carried out in a nitrogen filled glovebox (type Labmaster 130, MBRAUN).

Starting materials

All solvents were dried according to common procedures[2] and passed through columns of aluminium oxide, 3 Å molecular sieve and R3-11G-catalyst (BASF) or stored over molecular sieve (3 or 4 Å) until use. Reagents were used as received unless stated otherwise. 1-Ethyl-3-methylimidazolium methylcarbonate in methanol solution (30%) was donated by BASF. 1-butyl-3-methylimidazolium methylcarbonate in methanol solution (50%) was purchased from IOLITEC, *N*-butylpyrrolidine from ACROS. Methylcarbonate ionic liquids were synthesised following published procedures.[3] The bis(trimethylsilyl)chalcogenides were synthesized in analogy to the sulfide.[4] For a recent exemplary procedure of the bis(trimethylsilyl)telluride

please view the SI to ref.[5] The compounds **1** to **4** and **6** were synthesized as presented recently.[6]

Synthetic procedures

Synthesis of 1-ethyl-3-methylimidazolium hydrosulfide ([EMIm][HS], 1). Hydrogen sulfide was fed into a 30% solution of 1-ethyl-3-methylimidazolium methylcarbonate (26.9 g, 43.4 mmol) in methanol for 40 minutes. All volatiles were removed *in vacuo* and the residue recrystallized from a mixture of acetonitrile and diethyl ether at −30 °C. The solution was decanted and the solid residue dried in fine vacuum. [EMIm][HS] (4.62 g, 32.0 mmol 74%) was obtained as colourless solid. **Mp** 91-93 °C (from acetonitrile/ diethyl ether, 2 K/min). **DSC** (10 K/min): 92.8 °C (endoth.). **TGA** (10 K/min): 162.1 °C (decomp.). **Elem. anal.** found C, 49.9; H, 8.6; N, 19.6; S, 22.0; $C_6H_{12}N_2S_1$ requires C, 50.0; H, 8.4; N, 19.4; S, 22.2. **IR:** ν_{max}/cm^{-1}: 3022m, 2859m, 2565w (SH), 1570s, 1464m, 1420m, 1339m, 1178s, 1030w, 874m, 800s, 704w, 622vs. **^{1}H-NMR** (300.1 MHz, DMSO-d_6) δ_H = −3.85 (s, 1H, *H*S), 1.39 (t, $^3J_{HH}$ = 7.3 Hz, 3H, CH_2CH_3), 3.88 (s, 3H, N*Me*), 4.24 (q, $^3J_{HH}$ = 7.3 Hz, 2H, CH_2CH_3), 7.87 (s, 1H, *H*4/5), 7.99 (s, 1H, *H*4/5), 9.97 (s, 1H, *H*2) ppm. **^{13}C-NMR** (75.5 MHz, DMSO-d_6): δ_C = 15.2 (1C, CH_2CH_3), 35.6 (1C, N*Me*), 43.9 (1C, CH_2CH_3), 121.9 (1C, *C4/5*), 123.3 (1C, *C4/5*), 136.7 (1C, *C2*) ppm.

Synthesis of 1-ethyl-2,3-dimethylimidazolium hydrosulfide ([EMMIm][HS], 2). 1-Ethyl-2,3-dimethylimidazolium methylcarbonate (12.7 g, 63.4 mmol) was dissolved in methanol (20 mL) and hydrogen sulfide was fed into the solution for 75 minutes. All volatile components were removed in vacuum, and the residue recrystallised from a mixture of acetonitrile and diethyl ether. [EMMIm][HS] was isolated as light orange crystals in a yield of 4.60 g (29.1 mmol, 46%). Mp 125-126 °C (from acetonitrile/ diethyl ether, 2 K/min). DSC (10 K/min): 127.6 °C (endoth.). TGA (10 K/min): 179.5 °C (decomp.). Elem. anal. found C, 53.1; H, 9.1; N, 18.0; S, 19.0; $C_7H_{14}N_2S_1$ requires C, 53.1; H, 8.9; N, 17.7; S, 20.3. IR: ν_{max}/cm^{-1}: 2971s, 2563m (HS), 1721w, 1580m, 1533m, 1327w, 1299m, 1253s, 1197m, 1128m, 954w, 818vs, 661m, 500w. ^{1}H-NMR (300.1 MHz, DMSO-d_6) δ_H = −4.07 (s, 1H, HS), 1.33 (t, $^3J_{HH}$ = 7.3 Hz, 3H, CH_2CH_3), 2.60 (s, 3H, C-Me), 3.76 (s, 3H, NMe), 4.16 (q, $^3J_{HH}$ = 7.3 Hz, 2H, CH_2CH_3), 7.69 (s, 1H, H4/5), 7.73 (s, 1H, H4/5). ^{13}C-NMR (75.5 MHz, DMSO-d_6): δ_C = 9.0 (1C, C-Me), 14.8 (1C, CH_2CH_3), 34.6 (1C, NMe), 42.7 (1C, CH_2CH_3), 120.3 (1C, C4/5), 122.3 (1C, C4/5), 144.0 (1C, C2) ppm.

Synthesis of 1-butyl-3-methylimidazolium hydrosulfide ([BMIm][HS], 3). A 50% solution of 1-butyl-3-methylimidazolium methylcarbonate (8.39 g, 39.1 mmol) in methanol was mixed with additional methanol (10 mL) and hydrogen sulfide was fed into the solution for 45 minutes. All volatiles were removed *in vacuo* and the residue recrystallized from a mixture of acetonitrile and diethyl ether at −30 °C. The solution was decanted and the crystals dried in fine vacuum. [BMIm][HS] (3.54 g, 53%) was obtained as colourless solid. **Mp** 54-55 °C (from acetonitrile/ diethyl ether, 2 K/min). **DSC** (10 K/min): 56.0 °C (endoth.). **TGA** (10 K/min): 157.4 °C (decomp.). **Elem. anal.** found C, 55.8; H, 9.6; N, 16.7; S, 18.55; $C_8H_{16}N_2S_1$ requires C, 55.8; H, 9.4; N, 16.3; S, 18.6. **IR:** ν_{max}/cm^{-1}: 2928m, 2806m, 2559w (HS), 1665w, 1556s, 1453m, 1418w, 1362w, 1165vs, 1011m, 908m, 801s, 753m, 655s, 630s. **^{1}H-NMR** (300.1 MHz, DMSO-d_6) δ_H = −3.92 (s, 1H, *H*S), 0. 88 (t, $^3J_{HH}$ = 7.3 Hz, 3H, CH_2CH_3), 1.18-1.30 (m, 2H, CH_2CH_3), 1.71-1.81 (m, 2H, NCH_2CH_2), 3.88 (s, 3H, N*Me*), 4.20 (t, $^3J_{HH}$ = 7.2 Hz, 2H, NCH_2CH_2), 7.81 (s, 1H, *H*4/5), 7.90 (s, 1H, *H*4/5), 9.76 (s, 1H, *H*2) ppm. **^{13}C-NMR** (75.5 MHz, DMSO-d_6) δ_C = 13.2 (1C, CH_2CH_3), 18.7 (1C, CH_2CH_3), 31.3 (1C, NCH_2CH_2), 35.6 (1C, N*Me*), 48.3 (1C, NCH_2CH_2), 121.1 (1C, *C4/5*), 123.4 (1C, *C4/5*), 136.7 (1C, *C2*) ppm.

Synthesis of N-butyl-N-methylpyrrolidinium hydrosulfide ([BMPyr][HS], 4). *N*-Butyl-*N*-methylpyrrolidinium methylcarbonate (15.1 g 69.5 mmol) was dissolved in methanol (40 mL) and hydrogen sulfide fed into the solution for one hour. All volatiles were removed *in vacuo* and the residue recrystallized from a mixture of acetonitrile and diethyl ether at −30 °C. The solution was decanted and the crystals dried in fine vacuum. [BMPyr][HS] (5.65 g, 46%) was obtained as colourless solid. **Mp** 153-155 °C (decomp., from acetonitrile/ diethyl ether, 2 K/min). **DSC** (10 K/min): 166.5 °C (endoth.). **TGA** (10 K/min): 153.4 °C (decomp.). **Elem. anal.** found C, 61.8; H, 12.3; N, 8.1; S, 17.7; $C_9H_{21}N_1S_1$ requires C, 61.65; H, 12.1; N, 8.0; S, 18.3. **UV-Vis**: λ_{max} (DMSO)/nm 264. **IR:** ν_{max}/cm^{-1}: 2959vs, 2934s, 2873m, 2560w (HS), 1459vs, 1379w, 1260w, 1060m, 1004s, 910s, 743m, 587w. **^{1}H-NMR** (300.1 MHz, DMSO-d_6) δ_H = −4.03 (s, 1H, *H*S), 0.92 (t, $^3J_{HH}$ = 7.4 Hz, 3H, CH_2CH_3), 1.24-1.38 (m, 2H, CH_2CH_3), 1.60-1.74 (m, 2H, NCH_2CH_2), 2.00-2.14 (m, 4H, CH_2*(3,4)*), 3.02 (s, 3H, N*Me*), 3.30-3.60 (m, 6H, NCH_2CH_2, CH_2*(2,5)*) ppm. **^{13}C-NMR** (75.5 MHz, DMSO-d_6) δ_C = 13.4 (1C, CH_2CH_3), 19.2 (1C), 21.0 (1C), 24.8 (1C), 47.4 (t, $^3J_{CN}$ = 3.9 Hz, 2C, *C3/4*), 62.6 (t, $^2J_{CN}$ = 2.8 Hz, 2C, *C2/5*), 63.2 (t, $^2J_{CN}$ = 3.1 Hz, 1C) ppm.

Synthesis of N-butyl-N-methylpyrrolidinium hydrosulfide ([BMPyr][HS], 4) from bis(trimethylsilyl)sulfide.

N-Butyl-*N*-methylpyrrolidinium methylcarbonate (245 mg 1.13 mmol) was dissolved in acetonitrile (5 mL) and the solution cooled to 0 °C. Bis(trimethylsilyl)sulfide (255 mg, 1.43 mmol) was added and the mixture stirred at 0 °C for 30 minutes, and at ambient temperature for two hours. Volatile components were removed in vacuo until a viscous oil remained. The residue was dissolved in acetonitrile (5 mL) and methanol (2 mL) added to the solution. The solution was stirred at ambient temperature for 14 hours. Removal of all volatiles yielded [BMPyr][HS] (182 mg, 1.04 mmol, 92%). Analytical data fully agrees with the preceding values.

Synthesis of tri-nbutyl-methylphosphonium hydrosulfide ([(nBu)$_3$MeP][HS], 5). Tri-*n*butyl-methylphosphonium methylcarbonate (23.4 g, 80.0 mmol) was dissolved in methanol (40 mL) and hydrogen sulfide fed into the solution for 1.5 hours. All volatiles were removed *in vacuo* and the residue cocrystallized with acetonitrile from a mixture of acetonitrile and diethyl ether at −80 °C. The supernatant was decanted and the residue dried in fine vacuum. [(*n*Bu)$_3$MeP][HS] (18.3 g, 91%) was isolated as slightly yellow, highly viscous oil. **TGA** (10 K/min): 262.4 °C (decomp.). **Elem. anal.** found C, 62.3; H, 12.75; S, 10.4; $C_{13}H_{31}P_1S_1$ requires C, 62.35; H, 12.5; S, 12.8. **IR:** ν_{max}/cm^{-1}: 2956s, 2931s, 2870s, 2557w (HS), 1673w, 1463m, 1380w, 1230w, 1068m, 942vs, 817m, 719m, 570w. **^{1}H-NMR** (300.1 MHz, DMSO-d_6) δ_H = −4.04 (s, 1H, *H*S), 0.90 (t, $^3J_{HH}$ = 7.1 Hz, 9H, CH_2CH_3), 1.33-1.53 (m, 12H, CH_2CH_2), 1.85 (d, $^2J_{HP}$ = 14.1 Hz, 3H, PCH_3), 2.19-2.29 (m, 6H, PCH_2) ppm. **^{13}C-NMR** (75.5 MHz, DMSO-d_6) δ_C = 3.3 (d, $^1J_{CP}$ = 51.3 Hz, 1C, PCH_3), 13.2 (3C, CH_2CH_3), 18.9 (d, $^1J_{CP}$ = 49.2 Hz, 3C, PCH_2), 22.6 (d, J_{CP} = 4.4 Hz, 3C, CH_2), 23.2 (d, J_{CP} = 15.8 Hz, 3C, CH_2) ppm. **^{31}P-NMR** (101.3 MHz, DMSO-d_6): δ_P = 34.0 ppm.

Synthesis of 1-ethyl-3-methylimidazolium hydroselenide ([EMIm][HSe], 6). A 30% solution of 1-ethyl-3-methylimidazolium methylcarbonate (3.68 g, 5.93 mmol) was cooled in an ice bath and degassed thoroughly. Bis(trimethylsilyl)selenide (1.63 g, 7.23 mmol) was added in small portions within 15 minutes and the resulting mixture was stirred at 0 °C for 30 minutes and further 30 minutes at ambient temperature. After removal of volatile contents the residue was recrystallized from an acetonitrile/ diethylether mixture at −30 °C. [EMIm][HSe] (796 mg, 70%) was obtained as a colourless solid. **Mp** 101-102 °C (from acetonitrile/ diethyl ether, 2 K/min). **Elem. anal.** found C, 37.7; H, 6.4; N, 15.0; $C_6H_{12}N_2Se_1$ requires

C, 37.7; H, 6.3; N, 14.7. **IR:** ν_{max}/cm^{-1}: 3049m, 2962m, 2274w (HSe), 1569m, 1418w, 1362w, 1339w, 1259m, 1173s, 1091m, 1027m, 863m, 789vs, 704m, 645m, 620vs. **^{1}H-NMR** (300.1 MHz, DMSO-*d*$_6$) $\delta_H = -6.56$ (s, 1H, *H*Se), 1.40 (t, $^{3}J_{HH} = 7.3$ Hz, 3H, CH_2CH_3), 3.87 (s, 3H, N*Me*), 4.22 (q, $^{3}J_{HH} = 7.3$ Hz , 2H, CH_2CH_3), 7.77 (t, $^{3/4}J_{HH} = 1.7$ Hz, 1H, *H4/5*), 7.87 (t, $^{3/4}J_{HH} = 1.7$ Hz, 1H, *H4/5*), 9.46 (s, 1H, *H2*) ppm. **^{13}C-NMR** (75.5 MHz, DMSO-*d*$_6$): $\delta_C = 15.1$ (1C, CH_2CH_3), 35.7 (1C, N*Me*), 44.0 (1C, CH_2CH_3), 121.9 (1C, *C4/5*), 123.4 (1C, *C4/5*), 136.2 (1C, *C2*) ppm. **^{77}Se-NMR** (76.3 MHz, DMSO-*d*$_6$): $\delta_{Se} = -312.3$ ppm.

Synthesis of N-butyl-N-methylpyrrolidinium hydroselenide ([BMPyr][HSe], 7). *N*-butyl-*N*-methylpyrrolidinium methylcarbonate (2.86 g, 13.2 mmol) was dissolved in methanol (18 mL) the mixture cooled in an ice bath and degassed in three cycles. Bis(trimethylsilyl)selenide (3.21 g, 14.2 mmol) was added in small portions within 30 minutes and the solution stirred for further 30 minutes at 0 °C. The mixture was then warmed to ambient temperature and the solvent removed *in vacuo*. The slightly yellow residue was recrystallized from an acetonitrile/ diethyl ether mixture at −30 °C. Colorless needles were collected by filtration washed with diethyl ether and dried in fine vacuum. Additional material was obtained analogously from the filtrate and washings. [BMPyr][HSe] (1.99 g, 68%) was obtained as slightly greenish needles. **Mp** 148-149 °C (decomp., from acetonitrile/ diethyl ether, 2 K/min). **Elem. anal.** found C, 48.4; H, 9.6; N, 6.7; $C_9H_{21}N_1Se_1$ requires C, 48.6; H, 9.5; N, 6.3. **IR:** ν_{max}/cm^{-1}: 2957vs, 2932s, 2872m, 2286m (H-Se), 1458vs, 1377w, 1345w, 1301w, 1245w, 1060m, 1030m, 1004m, 909m, 740m, 586m. **^{1}H-NMR** (300.1 MHz, DMSO-*d*$_6$) $\delta_H = -6.64$ (s, 1H, *H*Se), 0.92 (t, $^{3}J_{HH} = 7.3$ Hz, 3H, CH_2CH_3), 1.24-1.37 (m, 2H, CH_2CH_3), 1.62-1.73 (m, 2H, NCH_2CH_2), 2.02-2.13 (m, 4H, CH_2*(3,4)*), 3.01 (s, 3H, N*Me*), 3.33-3.39 (m, 2H, NCH_2CH_2), 3.44-3.54 (m, 4H, CH_2*(2,5)*) ppm. **^{13}C-NMR** (75.5 MHz, DMSO-*d*$_6$): $\delta_C = 13.5$ (1C, CH_2CH_3), 19.2 (1C, br), 21.0 (1C), 24.9 (1C), 47.5 (t, $^{3}J_{CN} = 3.7$ Hz, 2C, *C3/4*), 62.7 (br s, 2C, *C2/5*), 63.3 (t, $^{2}J_{CN} = 2.8$ Hz, 1C) ppm. **^{77}Se-NMR** (76.3 MHz, DMSO-*d*$_6$): $\delta_{Se} = -316.2$ ppm.

Synthesis of tri-nbutyl-methylphosphonium hydroselenide ([(nBu)$_3$MeP][HSe], 8). Tri-*n*butyl-methylphosphonium methylcarbonate (3.13 g, 10.7 mmol) was dissolved in methanol (20 mL), the solution cooled to 0 °C and degassed by repeated cycles of evacuation and purging with inert gas. Bis(trimethylsilyl)selenide (2.67 g, 11.8 mmol) was added in small portions within 30 minutes and the colourless solution stirred at 0 °C for another half hour. The mixture was then allowed to stir at ambient temperature for 30 minutes before all

volatiles were removed *in vacuo*. The colourless oil was dissolved in acetonitrile (6 mL) and stored at −30 °C for 14 hours. The solvent was again removed *in vacuo* and the residing solid triturated with diethyl ether (5 mL). After decantation of the liquid phase and extensive drying in fine vacuum [(*n*Bu)$_3$MeP][HSe] (2.96 g, 93%) was isolated as a colourless solid. **Mp** 55-57 °C (from diethyl ether, 2 K/min). **Elem. anal.** found C, 53.40; H, 10.97; $C_{13}H_{31}P_1Se_1$ requires C, 52.52; H, 10.51. **IR:** ν_{max}/cm^{-1}: 2958s, 2930s, 2863s, 2279w (H-Se), 1627w, 1462m, 1381w, 1310w, 1260w, 1080s, 1010m, 943s, 801vs, 716m. **^{1}H-NMR** (300.1 MHz, DMSO-d_6) δ_H = −6.63 (s, 1H, *H*Se), 0.90 (t, $^3J_{HH}$ = 7.1 Hz, 9H, CH_2CH_3), 1.32-1.53 (m, 12H, CH_2CH_2), 1.85 (d, $^2J_{HP}$ = 14.0 Hz, 3H, PC*H*$_3$), 2.19-2.29 (m, 6H, PC*H*$_2$) ppm. **^{13}C-NMR** (75.5 MHz, DMSO-d_6) δ_C = 3.4 (d, $^1J_{CP}$ = 51.4 Hz, 1C, P*C*H$_3$), 13.2 (3C, CH_2CH_3), 19.0 (d, $^1J_{CP}$ = 49.1 Hz, 3C, P*C*H$_2$), 22.6 (d, J_{CP} = 4.2 Hz, 3C, *C*H$_2$), 23.2 (d, J_{CP} = 15.9 Hz, 3C, *C*H$_2$) ppm. **^{31}P-NMR** (101.3 MHz, DMSO-d_6): δ_P = 33.4 ppm. **^{77}Se-NMR** (76.3 MHz, DMSO-d_6): δ_{Se} = −312.3 ppm.

Synthesis of 1-ethyl-3-methylimidazolium hydrotelluride ([EMIm][HTe], 9).

A 30% solution of 1-ethyl-3-methylimidazolium methylcarbonate (0.274 g, 1.47 mmol) was combined with methanol (5 mL), the solution cooled to −30 °C and degassed thoroughly. Bis(trimethylsilyl) telluride (0.434 g, 1.58 mmol) was added in one portion and the mixture was stirred for 30 minutes. The mixture was slowly warmed to −15 °C stirred for 30 minutes and then stored over night at −30 °C. All volatile contents were removed at 0 °C and the residue was dried at ambient temperature in fine vacuum for one hour before the already purple substance was transferred to a glove box and analysed by IR and NMR spectroscopy. Due to the instability of the substance elemental analysis and determination of the melting/ decomposition temperature were not possible. **IR:** ν_{max}/cm^{-1}: 3065m, 3008m, 2966m, 1950w (H-Te), 1631w, 1566m, 144w, 1336w, 1167s, 1091m, 1026w, 847m, 772s, 640m, 617vs. **^{1}H-NMR** (300.1 MHz, DMSO-d_6) δ_H = −13.05 (s, 1H, *H*Te), 1.41 (t, $^3J_{HH}$ = 7.3 Hz, 3H, CH_2CH_3), 3.86 (s, 3H, N*Me*), 4.21 (q, $^3J_{HH}$ = 7.3 Hz , 2H, CH_2CH_3), 7.73 (t, $^{3/4}J_{HH}$ = 1.6 Hz, 1H, *H4/5*), 7.82 (t, $^{3/4}J_{HH}$ = 1.7 Hz, 1H, *H4/5*), 9.26 (s, 1H, *H2*) ppm. **^{13}C-NMR** (75.5 MHz, DMSO-d_6): δ_C = 15.0 (1C, CH_2CH_3), 35.8 (1C, N*Me*), 44.0 (1C, CH_2CH_3), 121.8 (1C, *C4/5*), 123.3 (1C, *C4/5*), 136.2 (1C, *C2*) ppm. **^{125}Te-NMR** (157.8 MHz, DMSO-d_6): δ_{Te} = −923.0 ppm.

Synthesis of N-butyl-N-methylpyrrolidinium hydrotelluride ([BMPyr][HTe], 10). The reaction was carried out in the dark. *N*-butyl-*N*-methylpyrrolidinium methylcarbonate (933 mg, 4.29 mmol) was dissolved in methanol (10 mL) the mixture cooled to −30 °C and degassed in three cycles. Bis(trimethylsilyl) telluride (1.18 g, 4.31 mmol) was added quickly and the solution slowly warmed to −15 °C. The solvent was removed *in vacuo* while keeping the temperature between −5 °C and −15 °C. The purple residue was recrystallised from an acetonitrile/ diethyl ether mixture at −30 °C. The blue solution was decanted from a colourless precipitate and the residue dried in fine vacuum. [BMPyr][HTe] (543 mg, 47%) was obtained as a greyish solid. **Mp** 114-116 °C (decomp., from acetonitrile/ diethyl ether, 2 K/min). **Elem. anal.** found C, 40.0; H, 8.05; N, 5.5; $C_9H_{21}N_1Te_1$ requires C, 39.9; H, 7.8; N, 5.2. **IR:** ν_{max}/cm^{-1}: 2955s, 2934m, 2869m, 1988m (H-Te), 1457vs, 1374w, 1301w, 1182w, 1060m, 1003m, 733m, 481w. **^{1}H-NMR** (300.1 MHz, DMSO-d_6) $\delta_H = -13.1$ (s, 1H, *H*Te), 0.92 (t, $^3J_{HH} = 7.3$ Hz, 3H, CH_2CH_3), 1.25-1.37 (m, 2H, CH_2CH_3), 1.62-1.73 (m, 2H, NCH_2CH_2), 2.02-2.13 (m, 4H, *CH$_2$(3,4)*), 2.99 (s, 3H, N*Me*), 3.30-3.36 (m, 2H, NCH_2CH_2), 3.42-3.52 (m, 4H, *CH$_2$(2,5)*) ppm. **^{13}C-NMR** (75.5 MHz, DMSO-d_6): $\delta_C = 13.5$ (1C), 19.3 (1C), 21.1 (1C), 24.9 (1C), 47.6 (t, $^3J_{CN} = 3.7$ Hz, 2C), 62.8 (br s, 2C), 63.4 (t, $^2J_{CN} = 2.8$ Hz, 1C) ppm. **^{125}Te-NMR** (157.8 MHz, DMSO-d_6): $\delta_{Te} = -924.9$ ppm.

Synthesis of tri-nbutyl-methylphosphonium hydrotelluride ([(nBu)$_3$MeP][HTe], 11). Tri-*n*butyl-methylphosphonium methylcarbonate (1.11 g, 3.80 mmol) was dissolved in methanol (6 mL), the solution cooled to −20 °C and degassed by repeated cycles of evacuation and purging with inert gas. Bis(trimethylsilyl) telluride (1.14 g, 4.18 mmol) was added dropwise within 10 minutes and the colourless solution stirred at 0 °C for half hour. Small amounts of a black precipitate were removed by a syringe filter, the solution again cooled to −20 °C and all volatiles removed in fine vacuum. The solid residue was dried at 0 °C and shortly at ambient temperature. The red solid was triturated with THF (5 mL) and the mixture stored at −30 °C. The mixture was filtered and the residue washed with diethyl ether (2 mL). After drying in fine vacuum [(*n*Bu)$_3$MeP][HTe] (2.96 g, 93%) was isolated as a slightly red solid. **Mp** 160-163 °C (decomp., from diethyl ether, 2 K/min). **Elem. anal.** found C, 45.1; H, 9.2; $C_{13}H_{31}P_1Te_1$ requires C, 45.1; H, 9.0. **IR:** ν_{max}/cm^{-1}: 2956s, 2931s, 2870s, 1981m (H-Te), 1459m, 1383m, 1305m, 1230w, 1200w, 1097m, 971s, 941vs, 816s, 766m, 716m, 455m. **^{1}H-NMR** (300.1 MHz, DMSO-d_6) $\delta_H = -13.0$ (s, 1H, *H*Te), 0.90 (t, $^3J_{HH} = 7.1$ Hz, 9H, CH_2CH_3), 1.32-1.53 (m, 12H, CH_2CH_2), 1.82 (d, $^2J_{HP} = 14.0$ Hz, 3H, PCH_3), 2.13-2.27 (m, 6H, PCH_2)

ppm. **^{13}C-NMR** (75.5 MHz, DMSO-d_6) δ_C = 3.4 (d, $^1J_{CP}$ = 51.4 Hz, 1C, P*C*H$_3$), 13.2 (3C, CH$_2$*C*H$_3$), 19.0 (d, $^1J_{CP}$ = 49.2 Hz, 3C, P*C*H$_2$), 22.6 (d, J_{CP} = 4.3 Hz, 3C, *C*H$_2$), 23.2 (d, J_{CP} = 15.9 Hz, 3C, *C*H$_2$) ppm. **^{31}P-NMR** (101.3 MHz, DMSO-d_6): δ_P = 35.6 ppm. **^{125}Te-NMR** (126.2 MHz, DMSO-d_6): δ_{Te} = −920.9 ppm.

Preparation of N-butyl-N-methylpyrrolidinium polysulfides 15, 16, 17 and 18.

The following amounts of [BMPyr][HS] and sulfur were reacted in methanol (5 mL) by heating the reaction mixture to 50 °C for 5 hours and afterwards removing all volatiles and extensive drying of the residue in fine vacuum.

For [BMPyr]$_2$S$_2$ (**15**): 289 mg (1.65 mmol, 2.0 eq) of [BMPyr][HS] and 27 mg (0.84 mmol, 1.0 eq) of sulfur. An orange honey like substance is formed, according to the ^{1}H-NMR spectrum ca. 40% of the hydrosulfide anion remains. **UV-Vis**: λ_{max} (DMSO)/nm 265, 338, 434, 620.

For [BMPyr]$_2$S$_4$ (**16**): 233 mg (1.33 mmol, 2.0 eq) of [BMPyr][HS] and 64 mg (2.0 mmol, 3.0 eq) of sulfur. A light red honey like substance is formed, according to the ^{1}H-NMR spectrum ca. 10% of the hydrosulfide anion remains. **UV-Vis**: λ_{max} (DMSO)/nm 265, 338, 435, 620.

Note: The remaining hydrosulfide salt could neither be removed from the mixture, nor the reaction be brought to completion by prolonged reactions times (24 h), alternative solvents (acetonitrile, THF, dimethyl carbonate) or increase of the reaction temperature (80 °C). With the thermally more stable tri-*n*butyl-methyl-phosphonium cation we attempted the analogous synthesis under neat conditions heating the mixture of hydrosulfide ionic liquid and sulfur to 80 °C for 24 to 96 hours in dynamic fine vacuum. After 24 hours analogous results were obtained where 40% and 10% of the hydrosulfide anion remained in the product of the di- and tetrasulfide, respectively. After 96 hours the amount of hydrosulfide was slightly reduced and the substance showed partial decomposition. As none of the mentioned attempts led to a significantly different result we are confident that under the chosen conditions equilibrium is reached. Although the substances **15** and **16** cannot be regarded as pure and the actual anion is questionable we chose to denote them as di- and tetrasulfide, respectively, for identification purposes and to emphasise the average polysulfide chain length.

For [BMPyr]$_2$S$_6$ (**17**): 251 mg (1.43 mmol, 2.00 eq) of [BMPyr][HS] and 119 mg (3.71 mmol, 5.18 eq) of sulfur. A red solid is formed. **Elem. anal.** found C, 44.68; H, 8.18; N, 6.44; S,

42.29; $C_{18}H_{40}N_2S_6$ requires C, 45.33; H, 8.45; N, 5.87;S, 40.34. (The very high sulfur content leads to increased uncertainty of the results (especially concerning sulfur) as the calibration regime of the instrument is exceeded.) **UV-Vis**: λ_{max} (DMSO)/nm 271, 349, 482, 619.

For $[BMPyr]_2S_8$ (**18**): 282 mg (1.61 mmol, 2.00 eq) of [BMPyr][HS] and 181 mg (5.64 mmol, 7.02 eq) of sulfur. A deep red honey like substance is formed. Before removal of volatiles in fine vacuum the solution was filtered in order to remove minor amounts of unreacted sulfur. **UV-Vis**: λ_{max} (DMSO)/nm 268, 307sh, 358, 489, 618.

Temperature induced decomposition of [BMPyr][HS] (4).

A sample of the substance (159 mg, 0.91 mmol) was placed in a Schlenk tube and the tube was evacuated to a pressure of $1 \cdot 10^{-3}$ mbar. The substance was slowly heated to 160 °C in an oil bath whereupon the substance melted and left at this temperature for 45 minutes. Upon cooling the substance did not solidify again but stayed a slightly yellow oil. ESI-MS revealed 4-(butylmethylamino)-1-butanethiol (**14**) and secondary decomposition products 14a and 14b to be present. (Figures S2 to S6). Figure S1 shows the C-NMR spectrum of the substance mixture wherein *N*-butylpyrrolidine and *N*-methylpyrrolidine can be identified as well.

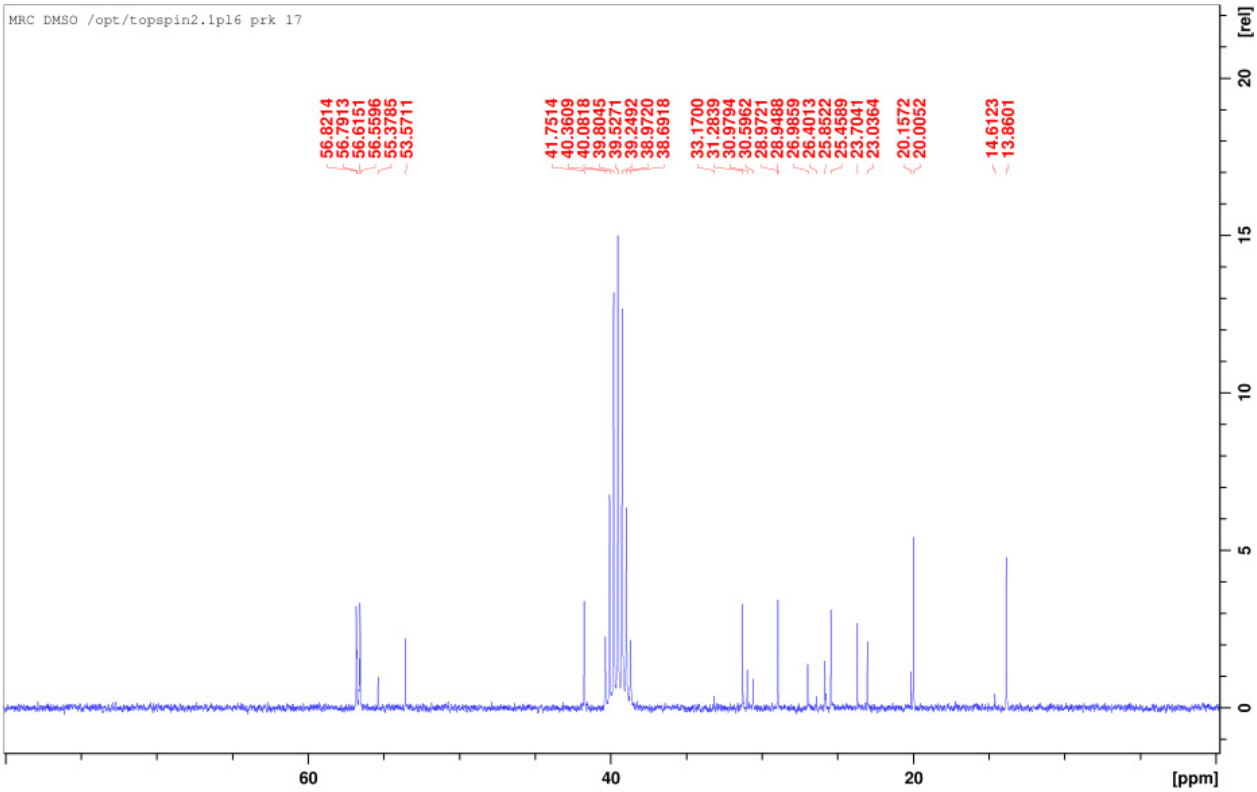

Figure S1. ^{13}C NMR spectrum of the thermal decomposition products of [BMPyr][HS].

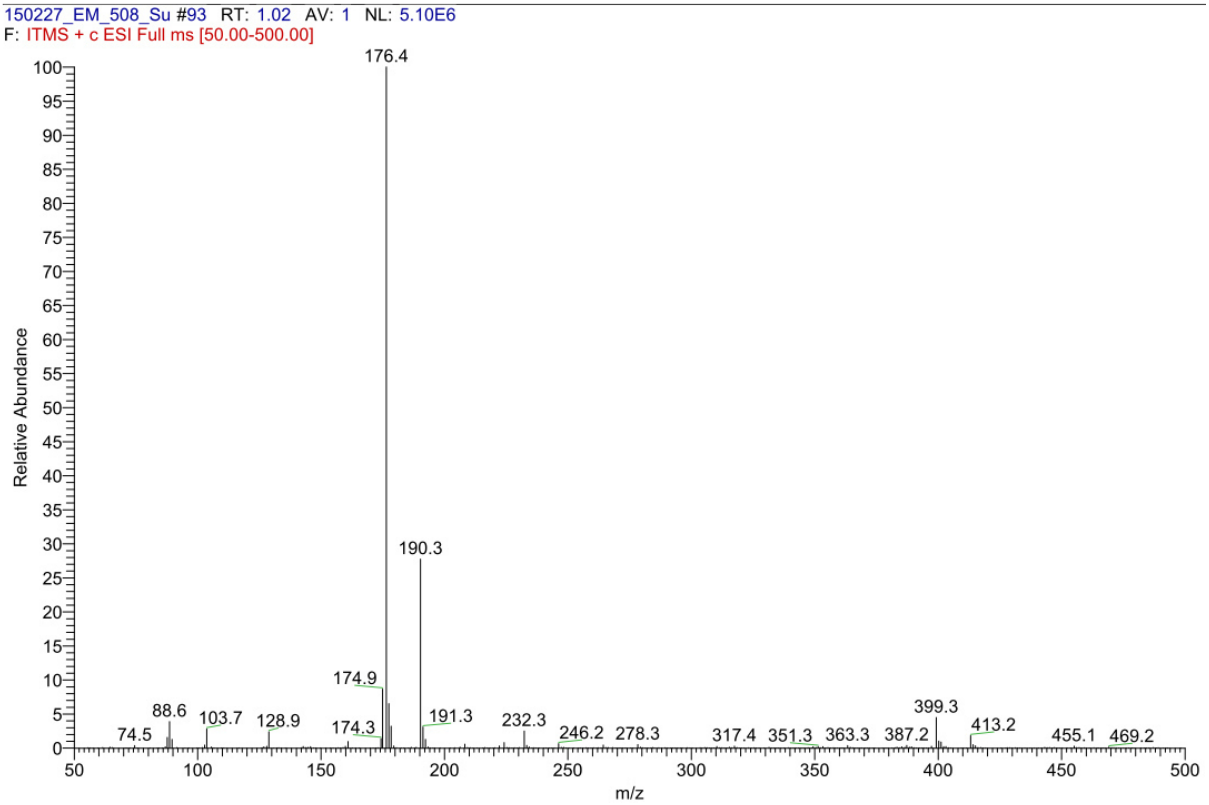

Figure S2. ESI mass spectrum of the decomposition mixture of [BMPyr][HS] (**4**).

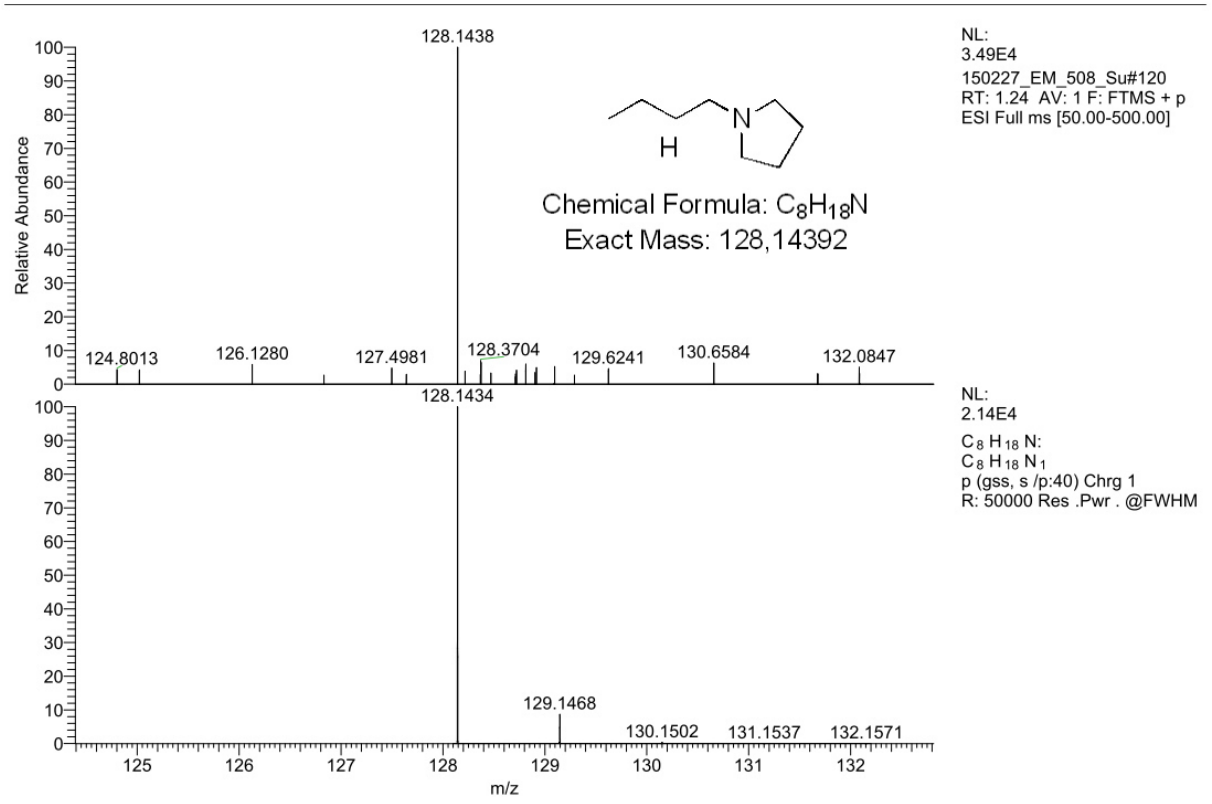

Figure S3. ESI mass spectrum of the decomposition mixture of [BMPyr][HS] (**4**), HRMS of m/z: 128.

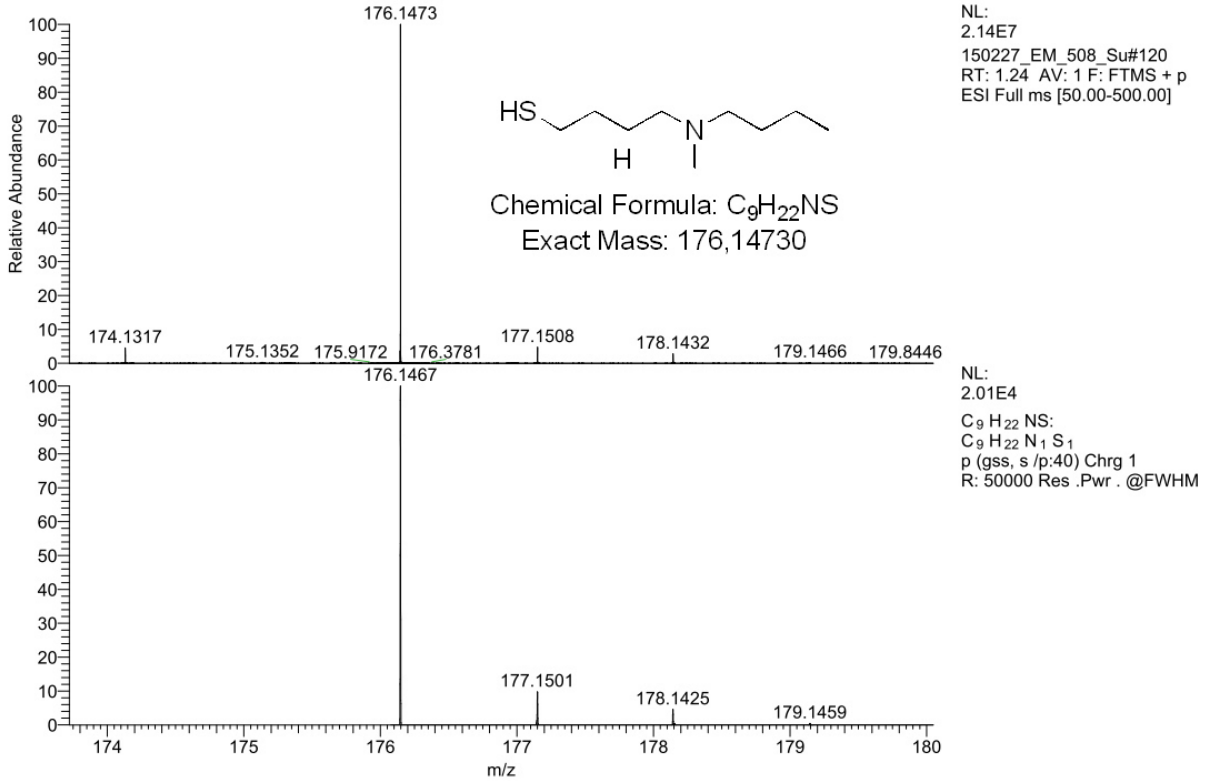

Figure S4. ESI mass spectrum of the decomposition mixture of [BMPyr][HS] (**4**), HRMS of m/z: 176 (**14**).

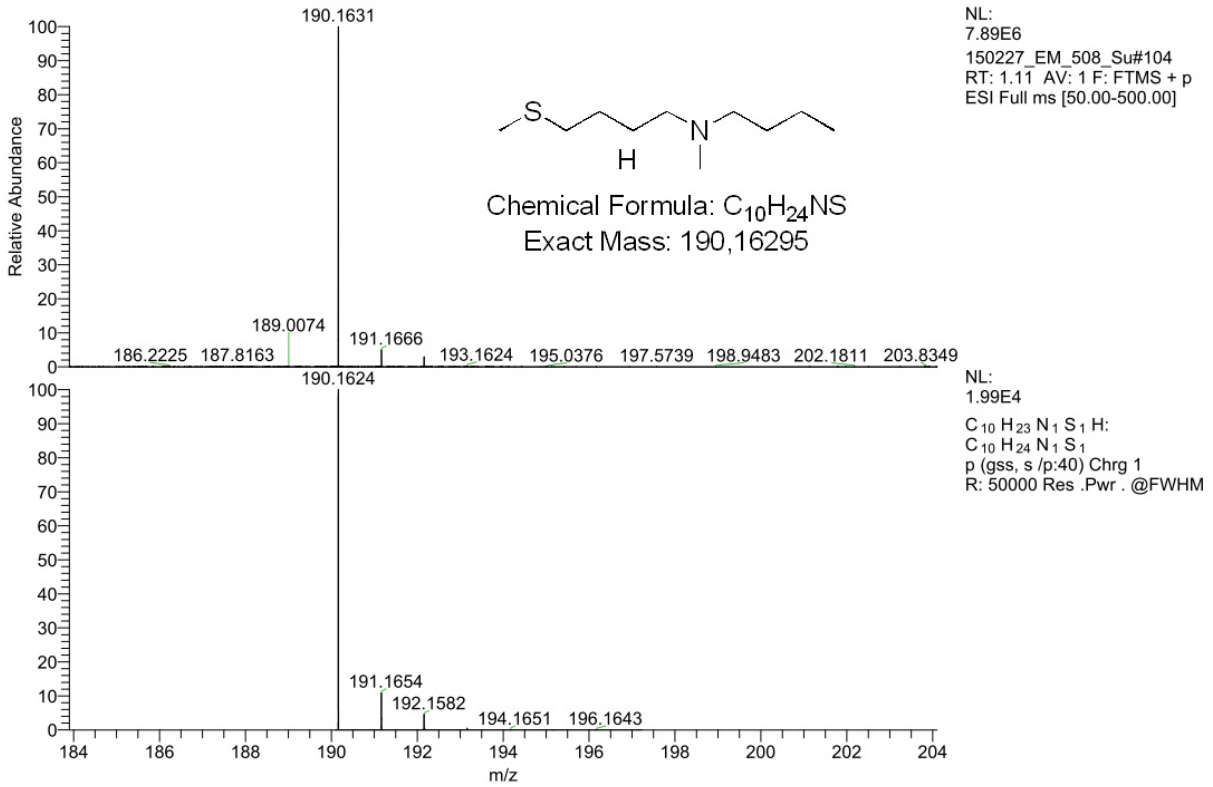

Figure S5. ESI mass spectrum of the decomposition mixture of [BMPyr][HS] (**4**), HRMS of m/z: 190 (**14a**).

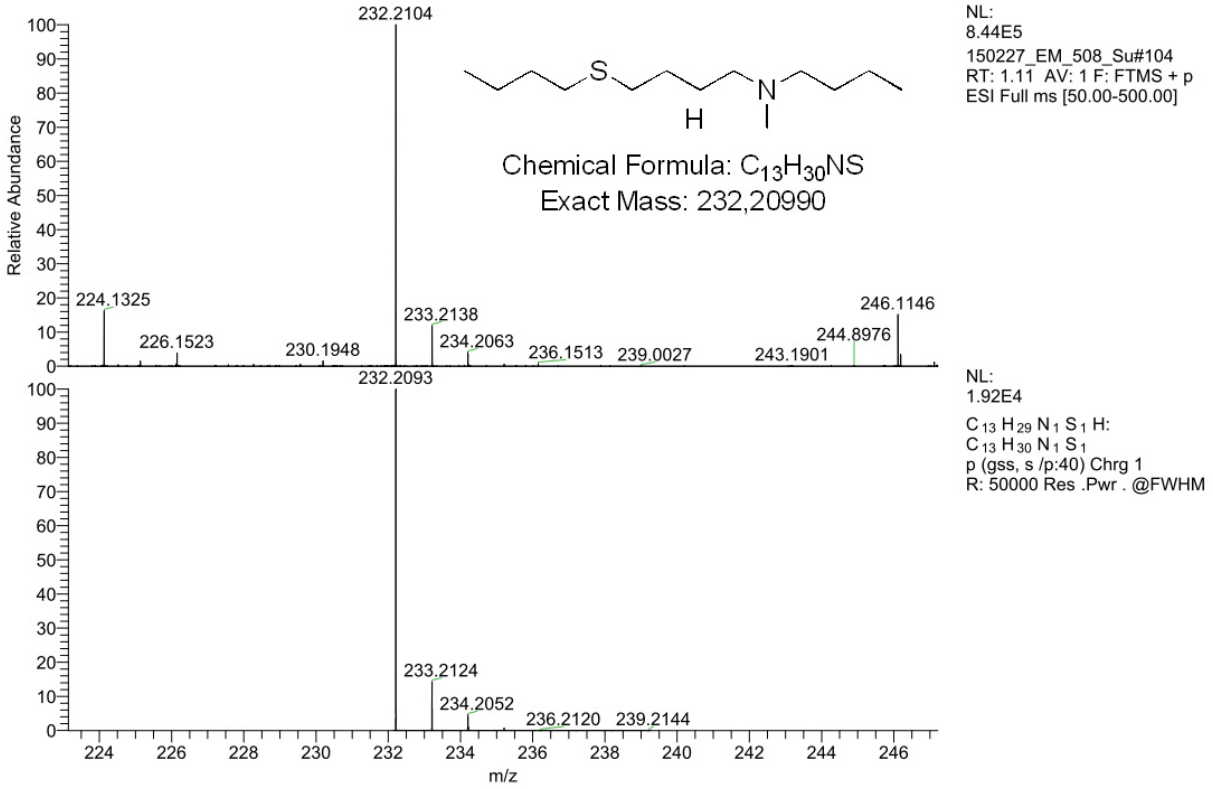

Figure S6. ESI mass spectrum of the decomposition mixture of [BMPyr][HS] (**4**), HRMS of m/z: 232 (**14b**).

Decomposition behavior of hydrotelluride salts

The phosphonium salt **11** was decomposed in THF solution by exposure to bright light over several hours. The formerly colorless sample turned dark violet, a reference sample in the dark stayed unchanged.[7] In the ^{125}Te NMR spectrum several new signals appeared. Intense signals appeared at −51.3 and +259.7 ppm rather weak ones at −1233.9, −545.7, −333.9 and −248.0 ppm. The signal at +259.7 ppm appeared as a doublet with a coupling constant of 146.8 Hz which is typical of a $^{1}J(^{1}\text{H-}^{125}\text{Te})$ coupling.[8] The signal at −51.3 ppm displayed a splitting of 33.0 Hz which is typical of a $^{3}J(^{1}\text{H-}^{125}\text{Te})$ coupling.[9] In this case the decomposition was not yet complete; the resonance signal of the hydrotelluride anion was still prominent in the spectrum. A sample of [BMPyr][HTe] (**10**) was decomposed in the dark under inert conditions in a nitrogen filled glovebox over three months. In this case a weak and broad signal at −269.5 ppm and further ones at −30.3 (weak), +94.0, +220.1 and +247.7 ppm (weak) where observed. No more traces of the hydrotelluride could be witnessed in the ^{125}Te-NMR spectrum. It is interesting to note that the decomposition products of the organic cation are analogous to those formed by temperature induced decomposition of [BMPyr][HS] and

the lower chain length polysulfides **17** and **18** (*vide infra*). As sodium hydrotelluride has been employed as a dealkylation reagent for ammonium cations, a dealkylation is plausible at any rate.[10] As the deeply colored polytellurides leave no doubt about their presence the decomposition pathways proposed for the hydrosulfides salts cannot be the only reactions occurring during decomposition of the hydrotellurides. It is assumed that the initial attack is in fact a dealkylation producing in part highly labile methanetellurol. Sink and Harvey describe the compound to decompose to dimethylditelluride,[11] Hamada and Morishita[12] observed the formation of elemental tellurium even under inert conditions. The latter would allow the formation of polytellurides from tellurium and hydrotelluride anions. An unambiguous identification of all the tellurium containing decomposition products in solution was not possible on the basis of ^{125}Te NMR spectra as no comparable values were found for DMSO. However we did obtain single crystals from a decomposed sample of [BMPyr][HTe] in acetonitrile after several weeks in a −30 °C freezer. The structure proved to be tetra(*N*-butyl-*N*-methylpyrrolidinium) dodecatelluride (Figure S7). The salt crystallized in the triclinic space group $P-1P\bar{1}$, the asymmetric unit consists of two cations and a hexatelluride chain. The structure was interpreted as a non-merohedral two component twin.

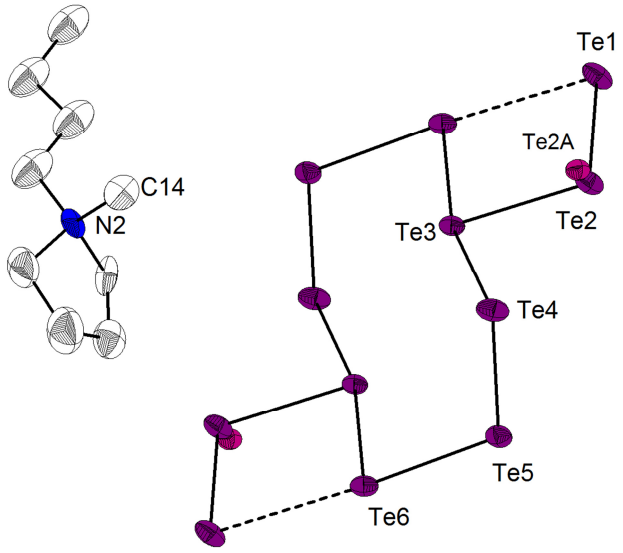

Figure S7. Molecular structure of $[BMPyr]_4Te_{12}$, three cations, respective disordered positions and hydrogen atoms omitted for clarity, symm. operation: I: –x, −y+1, −z+1.

While the pyrrolidinium cations are strongly disordered, each showing two overlying positions, within the tellurium chain only the atom at position Te2 is disordered to position Te2A, the site occupancy was freely refined to a ratio of 0.67:0.33. The analogous tetra(di-*N*-methylpyrrolidinium) dodecatelluride was formed upon decomposition of di-N-

methylpyrrolidinium trimethylsilyltellurolate,[13] and the dodecatelluride anion was previously observed in a 12-crown-4 solvated lithium salt.[14] The structure of the anion is in good agreement with these previous examples. Unfortunately the amount of crystals was not sufficient for further ^{125}Te-NMR spectroscopic studies. Therefore we are not able to unambiguously assign the three strong resonance signals of the previous spectrum at −269.5, +94.0 and +246.7 ppm to the dodecatelluride. The fact that no ^{125}Te-^{1}H coupling could be observed on any signal suggests the presence of a pure polytelluride, though.

Crystal structures

Crystal data

Table S1. Crystal data of Compounds **2**, **3**, **6** and $[BMPyr]_4Te_{12}$.

	[EMMIm][HS] (**2**)	[BMIm][HS] (**3**)	[EMIm][HSe] (**6**)	$[BMPyr]_4Te_{12}$
Formula	C7 H14 N2 S	C8 H16 N2 S	C6 H12 N2 Se	C18 H40 N2 Te6
FW / g mol^{-1}	158.26	172.29	191.14	1050.12
Crystal system	orthorhombic	orthorhombic	monoclinic	triclinic
Space group	*P b c a*	*P n a* 2_1	*P* $2_1/n$	*P* −1
Colour, habit	yellow block	colourless block	colourless block	dark red needle
Crystal size / mm^3	0.37 x 0.27 x 0.08	0.24 x 0.175 x 0.14	0.14 x 0.13 x 0.095	0.365 x 0.13 x 0.06
a / Å	8.0154(9)	9.9131(4)	8.6014(7)	9.5233(6)
b / Å	13.4251(14)	12.1432(5)	7.7800(6)	11.4728(7)
c / Å	16.6433(18)	8.2285(3)	13.2988(9)	15.0443(9)
α /°	90	90	90	109.476(2)
β /°	90	90	108.249(3)	108.300(2)
γ /°	90	90	90	92.404(2)
V / Å^3	1790.9(3)	990.52(7)	845.18(11)	1451.42(16)
Z	8	4	4	2
D_{calc}/g cm^{-3}	1.174	1.155	1.502	2.403
Abs. corr.	multi-scan	multi-scan	multi-scan	multi-scan
Min./max. transm.	0.6538/ 0.7452	0.7051/ 0.7457	0.5800/ 0.7457	0.4030/ 0.7461
μ / cm^{-1}	2.95	2.72	43.66	59.57
F(000)	688	376	384	948
T / K	100(2)	100(2)	105(2)	110(2)
θ Range /°	3.04 : 25.27	2.65 : 28.50	2.51 : 28.36	2.73 : 30.53
Range h,k,l	−9:9; −16:16; −16:19	−13:13; −16:15; −10:10	−11:11; −10:10; −16:17	−13:12; −16:15; 0:21
Refl. coll.	7823	12552	15559	8156
Refl. indep.	1603	2462	2109	8156
Refl. I > 2σ(I)	1240	2320	1772	6869
Data / restr. / param.	1603/ 0/ 98	2462/ 1/ 106	2109/ 0/ 88	8156 / 0 / 292
R_{int}	0.0599	0.0278	0.0354	- (hklf5)
R_1 (obs)	0.0360	0.0255	0.0230	0.0423
wR_2 (all)	0.0845	0.0641	0.0520	0.0780
GooF (F^2)	1.024	1.055	1.032	1.103
Res. e$^-$ dens. (min./ max.)	−0.197/ 0.269	−0.161/ 0.190	−0.419/ 0.460	−1.604/ 1.606
CCDC	1414151	1414152	1414153	1429785

Lattice structures

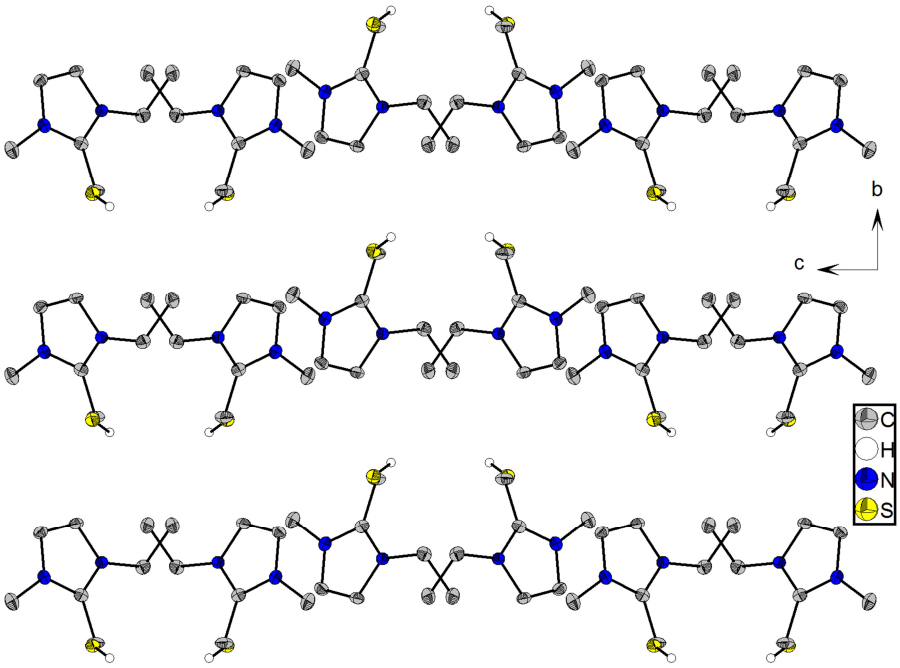

Figure S8. Lattice structure of [EMMIm][HS] (**2**), view along the a axis.

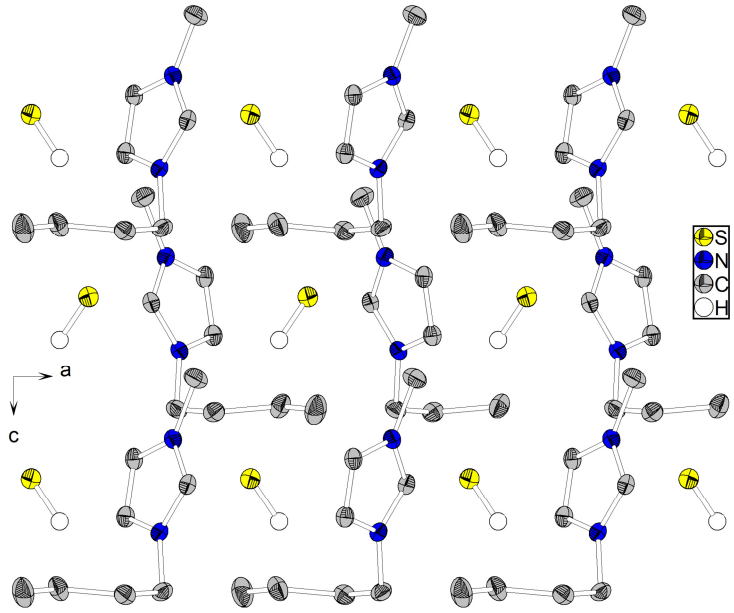

Figure S9. Lattice structure of [BMIm][HS] (**3**), view along the b axis.

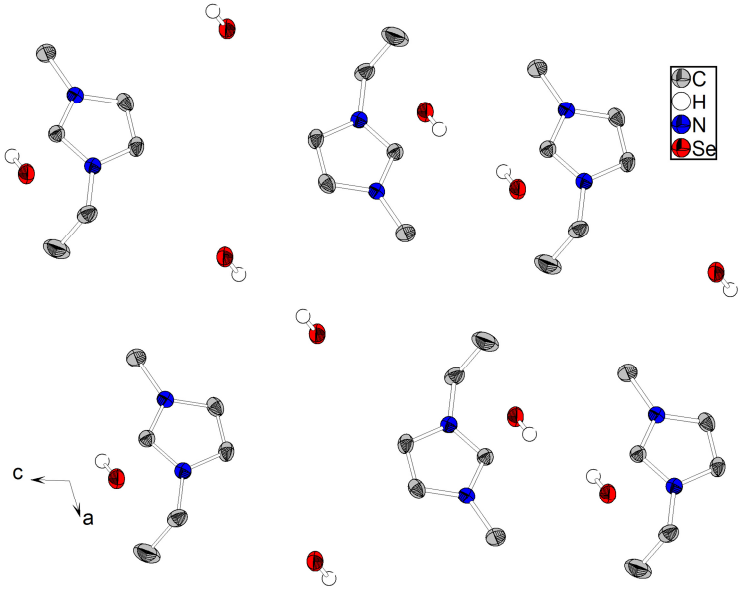

Figure S10. Crystal structure of [EMIM][HSe] (**6**), view along the b axis.

Cyclic voltammetry

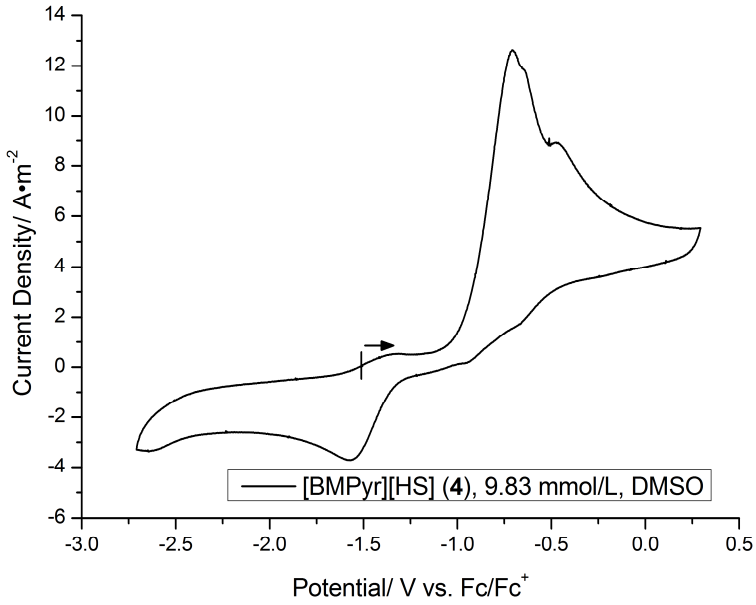

Figure S11. Cyclic voltammogram of [BMPyr][HS] (**4**), GC electrode, scan rate 100 mV/s, the arrow indicates scanning direction and starting potential.

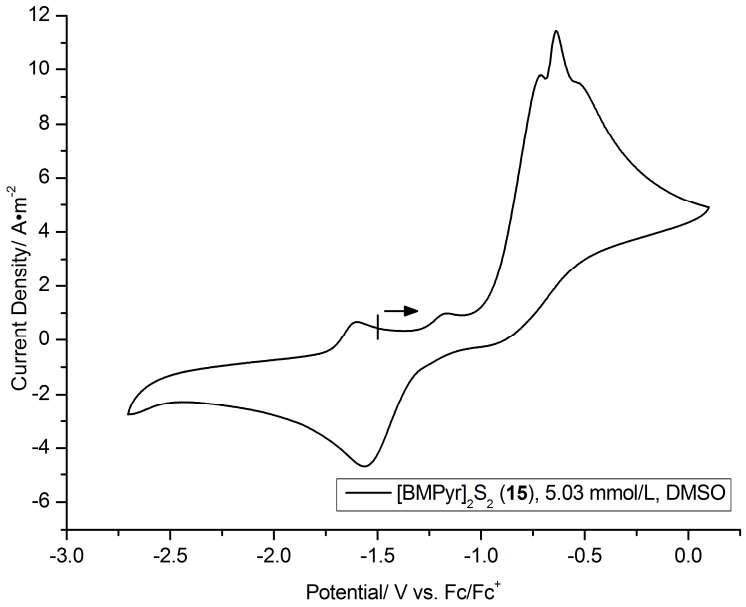

Figure S12. Cyclic voltammogram of $[BMPyr]_2S_2$ (**15**), GC electrode, scan rate 100 mV/s, the arrow indicates scanning direction and starting potential.

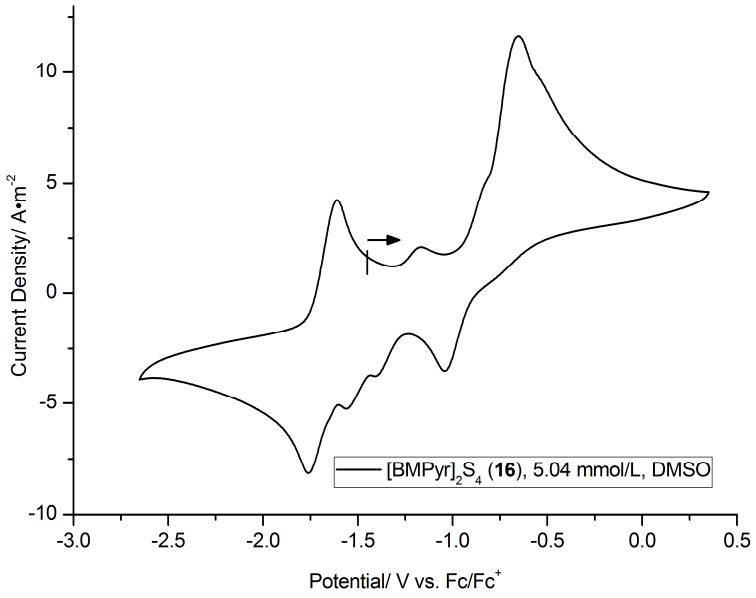

Figure S13. Cyclic voltammogram of $[BMPyr]_2S_4$ (**16**), GC electrode, scan rate 100 mV/s, the arrow indicates scanning direction and starting potential.

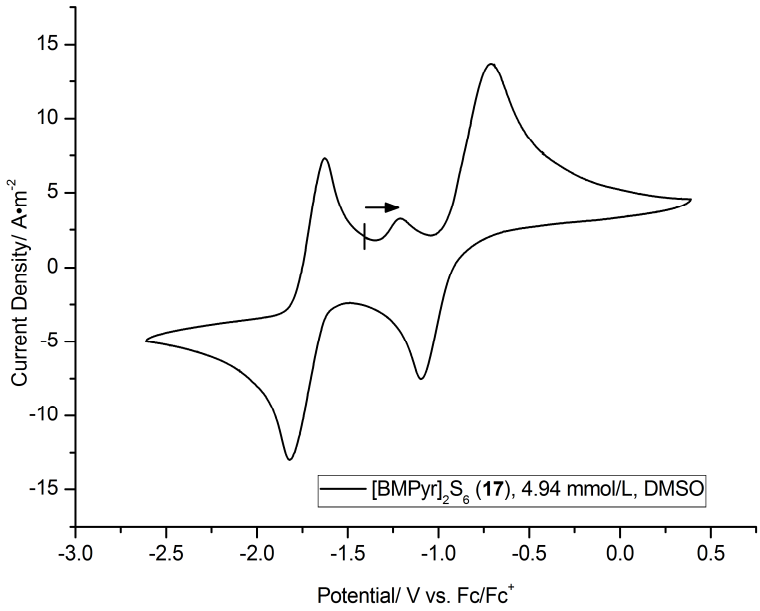

Figure S14. Cyclic voltammogram of $[BMPyr]_2S_6$ (**17**), GC electrode, scan rate 100 mV/s, the arrow indicates scanning direction and starting potential.

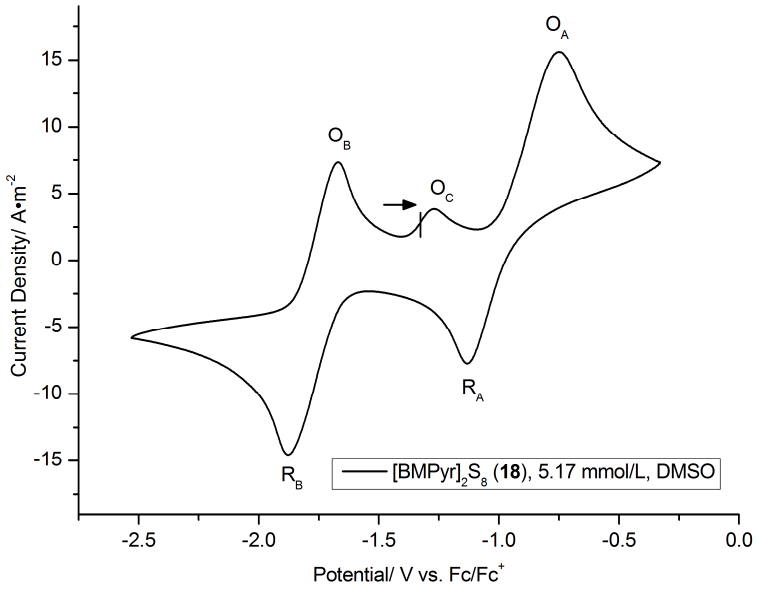

Figure S15. Cyclic voltammogram of $[BMPyr]_2S_8$ (**18**), GC electrode, scan rate 100 mV/s, the arrow indicates scanning direction and starting potential.

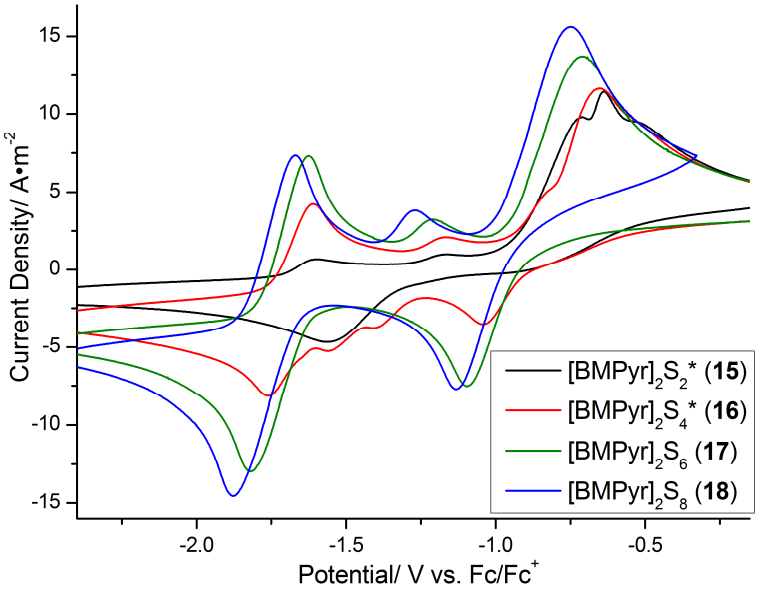

Figure 16. Comparison of cyclic voltammograms of $[BMPyr]_2S_2$, $[BMPyr]_2S_4$, $[BMPyr]_2S_6$ and $[BMPyr]_2S_8$, GC electrode, scan rate 100 mV/s.

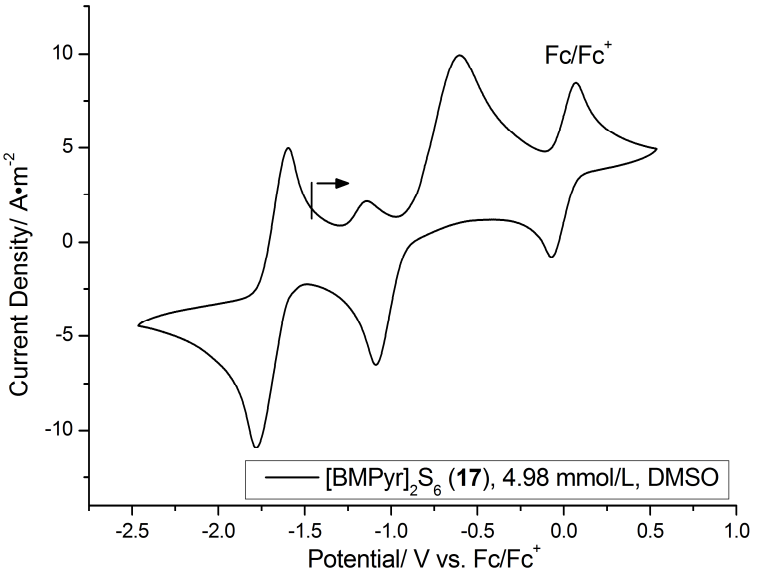

Figure S17. Cyclic voltammogram of $[BMPyr]_2S_6$ (**17**) with ferrocene as internal standard, **glassy carbon (GC)** electrode, scan rate 100 mV/s, the arrow indicates scanning direction and starting potential.

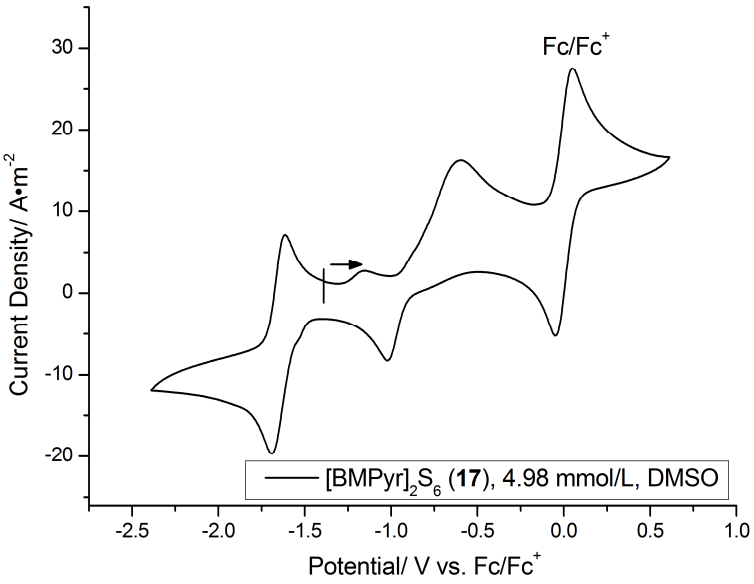

Figure S18. Cyclic voltammogram of $[BMPyr]_2S_6$ (**17**) with ferrocene as internal standard, **gold** electrode, scan rate 100 mV/s, the arrow indicates scanning direction and starting potential.

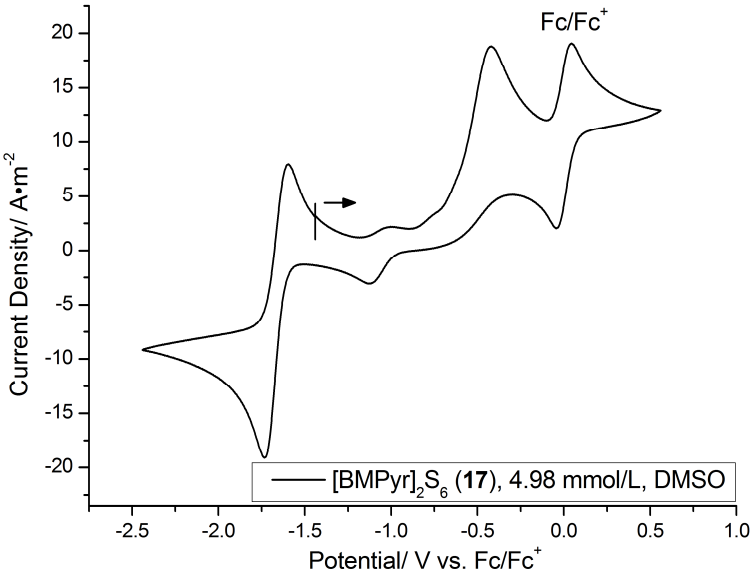

Figure S19. Cyclic voltammogram of $[BMPyr]_2S_6$ (**17**) with ferrocene as internal standard, **platinum** electrode, scan rate 100 mV/s, the arrow indicates scanning direction and starting potential.

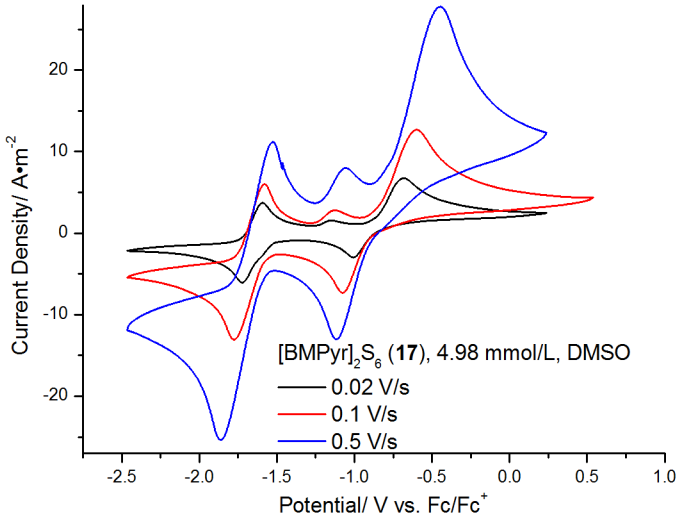

Figure S20. Cyclic voltammogram of $[BMPyr]_2S_6$ (**17**) at different scan rates on a glassy carbon electrode.

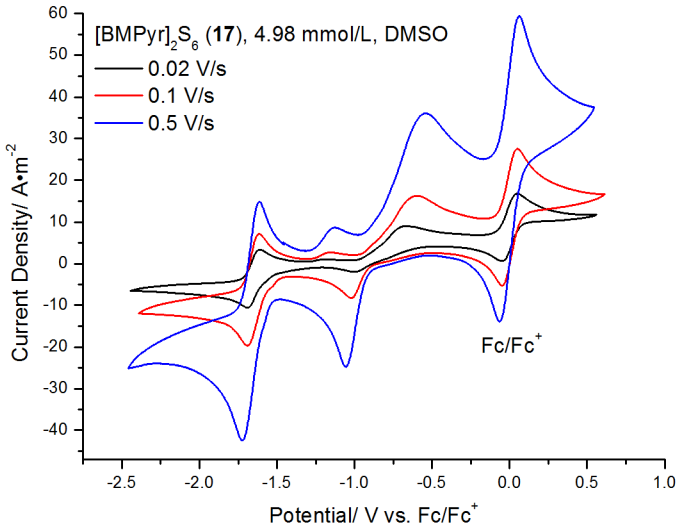

Figure S21. Cyclic voltammogram of $[BMPyr]_2S_6$ (**17**) at different scan rates on a gold electrode.

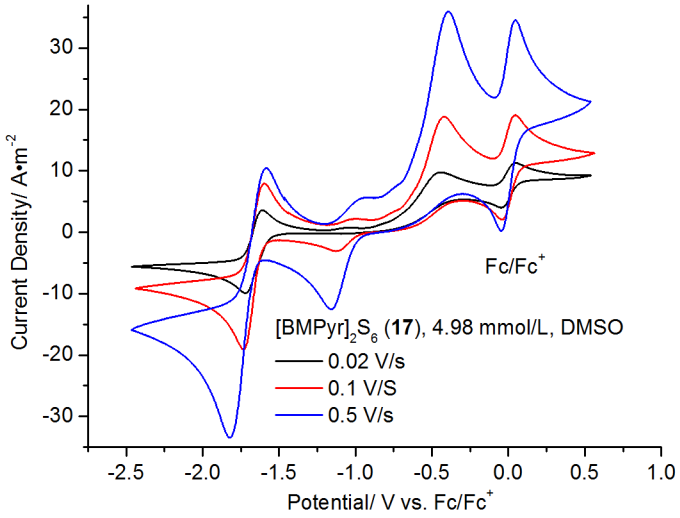

Figure S22. Cyclic voltammogram of $[BMPyr]_2S_6$ (**17**) at different scan rates on a platinum electrode.

References

[1] G. R. Fulmer, A. J. M. Miller, H. E. Gottlieb, N. H. Sherden, A. Nudelman, B. M. Stoltz, K. I. Goldberg, J. E. Bercaw, *Organometallics* **2010**, *29*, 2176-2179.

[2] W. L. Amarego, D. D. Perrin, *Purification of Laboratory Chemicals*, 4th ed., Elsevier, Burlington, **1996**.

[3] a) R. Kalb (PROIONIC), WO 2008 052 861, **2008**; b) R. Kalb (PROIONIC), WO 2008 052 860, **2008**.

[4] J.-H. So, P. Boudjouk, *Synthesis* **1989**, 306-307.

[5] L. H. Finger, B. Scheibe, J. Sundermeyer, *Inorg. Chem.* **2015**, 10.1021/acs.inorgchem.5b01665.

[6] L. H. Finger, F. Wohde, E. I. Grigoryev, A. K. Hansmann, R. Berger, B. Roling, J. Sundermeyer, *Chem. Commun.* **2015**, 10.1039/C5CC06224A.

[7] Osram Ultra Vitalux 300W was used as light source from a distance of 40 cm, the sample thereby warmed to 35 °C, the reference sample was therefore heated to 35 °C in an oil bath while in the dark.

[8] R. J. Batchelor, F. W. B. Einstein, I. D. Gay, C. H. W. Jones, R. D. Sharma, *Inorg. Chem.* **1993**, *32*, 4378-4383.

[9] H. C. E. McFarlane, W. McFarlane, *J. Chem. Soc., Dalton Trans.* **1973**, 2416-2418.

[10] D. H. R. Barton, A. Fekih, X. Lusinchi, *Tetrahedron Lett.* **1985**, *26*, 6197-6200.

[11] C. W. Sink, A. B. Harvey, *J. Chem. Phys.* **1972**, *57*, 4434-4442.

[12] K. Hamada, H. Morishita, *Synth. React. Inorg. Met.-Org. Chem.* **1977**, *7*, 355-366.

[13] L. H. Finger, B. Scheibe, J. Sundermeyer, *Inorg. Chem.* **2015**, *54*, 9568-9575.

[14] C. Feldmann, A. Okrut, *Z. Anorg. Allg. Chem.* **2009**, *635*, 1807-1811.

6.3 Synthese organischer Trimethylsilylchalkogenolatsalze Cat[TMS−E] (E = S, Se, Te): Das Methylcarbonatanion als Desilylierungsreagenz

Inorg. Chem. **2015**, *54*, 9568−9575

Synthesis of Organic (Trimethylsilyl)chalcogenolate Salts Cat[TMS-E] (E = S, Se, Te): the Methylcarbonate Anion as a Desilylating Agent

Lars H. Finger, Benjamin Scheibe, Jörg Sundermeyer

Inorganic Chemistry

Article

pubs.acs.org/IC

Synthesis of Organic (Trimethylsilyl)chalcogenolate Salts Cat[TMS-E] (E = S, Se, Te): the Methylcarbonate Anion as a Desilylating Agent†

Lars H. Finger, Benjamin Scheibe, and Jörg Sundermeyer*

Fachbereich Chemie and Materials Science Center, Philipps-Universität Marburg, Hans-Meerwein-Strasse 4, 35032 Marburg, Germany

Supporting Information

ABSTRACT: A high-yield synthesis of the class of (trimethylsilyl)-chalcogenolate organic salts [Cat][TMS-E] (E = S, Se, Te; Cat = BMPyr, DMPyr, NMe_4, nBu_3MeP) is presented. The title compounds have been prepared by the strictly aprotic reaction between the respective bis-(trimethylsilyl)chalcogenide (TMS_2E) and methylcarbonate ionic liquids (ILs). This constitutes a novel reaction behavior of methylcarbonate ILs, acting as a nucleophilic desilylating agent and a Lewis base instead of as a Brønsted base. Thus prepared silylchalcogenolate salts represent an activated form of the multifunctional TMS_2E reactant series. Pyrrolidinium TMS-S salts have proven to be excellent precursors for the synthesis of pyrrolidinium hexasulfides. The scope of the desilylation reaction can be extended to other silyl-bearing synthons such as (trimethylsilyl)azide and (trimethylsilyl)cyanide.

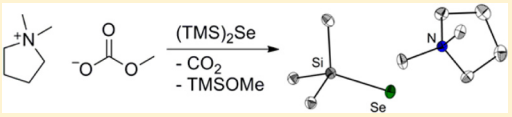

INTRODUCTION

Organic methylcarbonate salts[1] offer by far the most attractive route for a strictly water- and halide-free production of ionic liquids (ILs). While other halide-free procedures often include toxic reagents, involve highly reactive and unstable intermediates, or demand laborious workup,[2] the *green* reagent dimethylcarbonate is easily available and nontoxic.[3] The preparation of methylcarbonate salts can start from a wide range of nucleophiles and is high yielding and reliable. This particular atom-efficient variant is, however, limited to at least one methyl substituent at the cation, resulting from methylation of the nucleophilic cation precursor with dimethylcarbonate. Subsequently, the methylcarbonate salts can easily be transformed into a variety of further ILs by reaction with Brønsted acidic reagents. Methanol and carbon dioxide (CO_2) are the volatile and only side products of this transformation. So far, this method was limited to Brønsted acidic reaction partners. A comparatively low acidity (e.g., NH_4^+ ions) is sufficient though. That means that even a pK_a value higher than the one of methylcarbonic acid (5.61[4]) will allow the equilibrium to shift to the product side because of irreversible decay to methanol and CO_2.[1d,5]

It turned out that methylcarbonate ILs can also act as mild and selective desilylating agents (Scheme 1). On the one hand, this significantly extends the applicability of methylcarbonate ILs; on the other hand, an easy to prepare, strictly aprotic, and long-term stable desilylating agent becomes available. Comparable aprotic desilylating agents are, e.g., alkali alkoxides or tetraalkylammonium fluorides like TMAF[6] and TBAF.[7] While TBAF is not storable in a pure form because of E2-type elimination and decomposition reactions and has to be freshly prepared, TMAF and most alkali alkoxides suffer from a decreased solubility. Because of the extreme nucleophilicity and basicity of the weakly solvated fluoride ion, side reactions are likely and the toxicity of the fluoride ion may not be neglected. Furthermore, fluoride anions only tolerate very few organic cations in a solvate-free form, thereby limiting the variability of the reagent. In contrast, for methylcarbonate salts, a huge variety of cations are possible, which allows adjustment of the solubility.

Our present investigations primarily focused on the synthesis of silylchalcogenolate salts, which present more stable and completely aprotic alternatives to the corresponding hydrochalcogenide salts[8] and may serve as an activated form of the charge-neutral bis(trimethylsilyl)chalcogenides (TMS_2E). These are versatile reagents that are employed most notably as starting materials for transition-metal chalcogenide clusters,[9] chalcogenide semiconductors, and quantum dots[10] and in a range of organic syntheses.[11] The only published example of an uncoordinated (trimethylsilyl)thiolate anion was prepared by reacting TMS_2S with TMAF.[12] Alkali-metal salts of (trimethylsilyl)chalcogenolate anions have been accessed, e.g., by reductive cleavage of the TMS_2E precursors with sodium in liquid ammonia[13] or *n*BuLi in tetrahydrofuran (THF).[14] However, the application of methylcarbonate salts as desilylating agents can also be transferred to other silylated compounds, which will be exemplified in the last paragraph.

Scheme 1. Reaction of Methylcarbonate ILs with Brønsted Acids ($pK_a \leq 5.61$)

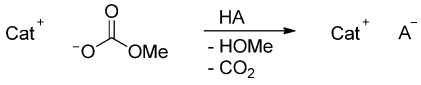

Received: July 23, 2015
Published: September 15, 2015

DOI: 10.1021/acs.inorgchem.5b01665
Inorg. Chem. 2015, 54, 9568−9575

RESULTS

The preparation of organic methylcarbonate salts is usually performed in a methanol solution. For imidazolium salts, the presence of methanol has proven vital in order to prevent side and follow-up reactions,[1a,c] which lead to a series of imidazolium carboxylate zwitterions.[15] We noticed that also the synthesis of ammonium and phosphonium methylcarbonate ILs appears to proceed more smoothly in the presence of methanol and conducted all syntheses of methylcarbonate ILs in methanol under solvothermal conditions at 130 °C. In order to employ the substances under strictly aprotic conditions in the following reactions, all methylcarbonate salts were thoroughly dried in fine vacuum and recrystallized from a mixture of acetonitrile and diethyl ether. The products form hygroscopic colorless solids, which can be stored indefinitely if they are kept under an inert atmosphere. Only tributylmethylphosphonium methylcarbonate was isolated as a slightly yellow, very viscous oil.

This work-up is, however, not transferable to imidazolium cations because the methanol-free methylcarbonates are not accessible. The reaction, which leads to the imidazolium 2-carboxylates, does not solely occur at elevated temperatures, but equilibrium between imidazolium methylcarbonate and imidazolium-2-carboxylate plus methanol is already observed at ambient temperature (Scheme 2).

Scheme 2. Equilibrium between [EMIm]-methylcarbonate and 1-Ethyl-2-methylimidazolium 2-Carboxylate at Ambient Temperature

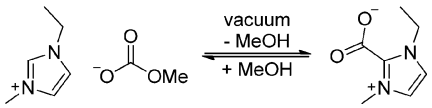

Removing methanol from an imidazolium methylcarbonate solution in vacuum results in formation of the corresponding carboxylate; upon the addition of methanol, the methylcarbonate salt is regenerated. When attempting to employ a C2-methylated imidazolium ion in order to prevent this reaction, we found that the equivalent phenomenon can also be observed for these systems, although to a lesser extent. Apparently the methyl group is deprotonated, leading to a ketene-*N*,*N*-diacetal or N-heterocyclic olefin (NHO) intermediate,[2g,16] which attacks the forming CO_2, resulting in a CH_2-spaced zwitterion (Scheme 3). This is formed as a nonremovable impurity

Scheme 3. Formation of an NHO−CO_2 Adduct upon Drying of 1-Ethyl-2,3-dimethylimidazolium Methylcarbonate

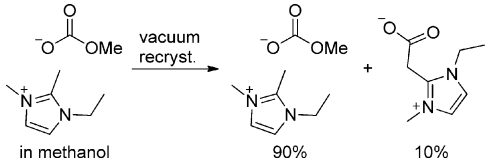

between 5 and 10% (according to ^{1}H NMR spectroscopy). Details concerning the synthesis, characterization, and reactivity of the respective imidazolium carboxylates will be published in due course.

However, the methanol-free ammonium and phosphonium methylcarbonates were used in subsequent reactions with a series of bis(trimethylsilyl)chalcogenides (TMS_2E; E = S, Se, Te), yielding the almost unstudied class of organic TMS-E salts (Scheme 4). So far, the only known example, [NMe_4][TMS-S], was prepared and characterized by Nieboer et al.[12]

Scheme 4. Synthesis of (Trimethylsilyl)chalcogenolate Organic Salts 1−9[a]

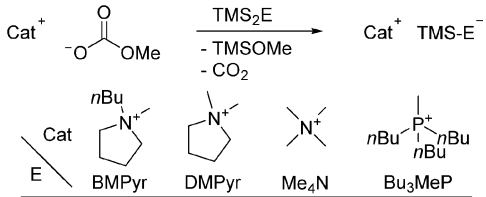

E	BMPyr	DMPyr	Me_4N	Bu_3MeP
S	**1** (73%)	**4** (78%)	**6** (80%)	**9** (98%)
Se	**2** (81%)	**5** (53%)	**7** (77%)	
Te	**3** (91%)		**8** (78%)	

[a]Yields in parentheses (mol %) refer to the methylcarbonate precursor as the limiting reagent.

Slowly adding the TMS_2E reagent to a cooled solution of the methylcarbonate precursor in acetonitrile and warming the mixture to ambient temperature to complete the reaction yields the respective (trimethylsilyl)chalcogenolate salts in a very simple procedure. The initially formed methyl(trimethylsilyl) carbonate is unstable at ambient temperature and decomposes to CO_2 and methyl(trimethylsilyl) ether. The substances are isolated in overall good yield by either removal of all volatile components and recrystallization or direct precipitation of the product from the reaction mixture by the addition of diethyl ether and cooling to −25 °C. All substances are highly sensitive toward moisture, which decomposes the salts in a matter of seconds. The silylselenolate and silyltellurolate compounds are, furthermore, very liable to oxidation, forming intense green (selenium) or violet (tellurium) polychalcogenides.

All ammonium salts were isolated as colorless solids and investigated with respect to their melting points. None of them showed a true melting point; instead, all substances slowly decomposed during melting. As anticipated, the respective decomposition temperatures generally increase in the series BMPyr < DMPyr < NMe_4. However, no distinctive trend could be observed concerning the series of TMS-E anions. For example, $TMS\text{-}S^-$ and $TMS\text{-}Se^-$ show almost identical decomposition temperatures in combination with the DMPyr cation (T_{dec} = 167 and 168 °C, respectively); with the BMPyr cation, the $TMS\text{-}Se^-$ salt is apparently more stable ($TMS\text{-}S^-$, T_{dec} = 121 °C; $TMS\text{-}Se^-$, T_{dec} = 128 °C). In combination with the tetramethylammonium cation, all salts show a remarkable stability, decomposing at 184 °C. Decomposition of the NMe_4 salts is accompanied by an instantaneous vaporization. Trimethylamine and methyl(trimethylsilyl)sulfide were found as the major components after condensation of the volatile decomposition products. The phosphonium salt **9**, which was isolated as a slightly yellow oil, substantiates that, with careful choice of the cation, also room temperature ILs are accessible.

Thus prepared (trimethylsilyl)chalcogenolate salts were investigated in detail utilizing ^{1}H, ^{13}C, and heteronuclear NMR spectroscopy. Table 1 summarizes the NMR data for the bis(trimethylsilyl)chalcogenides and (trimethylsilyl)-chalcogenolate anions (Cat = [BMPyr]).[17] As anticipated, the ^{77}Se and ^{125}Te NMR spectra of the (trimethylsilyl)-chalcogenolate anions show strongly high-field-shifted resonance signals compared to the neutral TMS_2E starting

DOI: 10.1021/acs.inorgchem.5b01665
Inorg. Chem. 2015, 54, 9568−9575

Table 1. NMR Data for the [TMS-E] Anions (Cat = [BMPyr]) and the Neutral TMS_2E Precursors

substance	δ_H	δ_C	δ_{Si}	$\delta_{Se/Te}$	$^1J_{Si-E}$
TMS_2S[a]	0.29	4.3	15.0		
TMS-S^- [b]	−0.07	8.9	−0.7		
TMS_2Se[a]	0.37	4.7	10.8	−330.8	108
TMS-Se^- [b]	0.09	9.2	−4.7	−417.5	175
TMS_2Te[a]	0.50	5.7	−5.7	−858.5	277
TMS-Te^- [b]	0.32	10.1	−27.0	−1142.0	468

[a]In C_6D_6. [b]In DMSO-d_6. δ values are in ppm and J values in Hz.

materials. An analogous trend can be observed in the respective ^{29}Si NMR spectra. Furthermore, the signals in the silicon NMR spectra are shifted to high field upon going from sulfur to tellurium for the neutral as well as anionic molecules. The local effects resulting from a decrease in the electronegativity of the chalcogenide substituent apparently dominate the shielding. The $^1J_{Si-E}$ coupling constants increase significantly upon going from the neutral precursor to the silylchalcogenolate anion. All values are in good agreement with literature values of the bis(trimethylsilyl)chalcogenides and alkali-metal salts of oligosilanylchalcogenolates.[18] The ^1H and ^{13}C NMR shifts of the TMS moieties show an opposing trend, being shifted to lower field with increasing atomic number of the chalcogen. This is also observed for the respective lithium salts,[14] the copper and zinc TMS-E complexes,[19] and the isoelectronic series of (trimethylsilyl)halides.[20] So far, no definite explanation for this antipodal trend has been provided. While Harris and Kimber[20] and Drake et al.[21] conclude that anisotropic and more intricate factors than plain inductive substituent effects may be responsible, Tran and Corrigan,[19a] in contrast, trace the phenomenon back to inductive effects. We strongly agree with the former approach because the trend concerning the chemical shift of the ^{13}C resonance is reversed in the series of bis(dihydromethylsilyl)chalcogenides $(H_2MeSi)_2E$.[21]

The IR spectra of all (trimethylsilyl)chalcogenolate salts are dominated by several distinct bands in the range from 400 to 1500 cm^{-1}, with the band at ≈820 cm^{-1} in all cases being the most intense. The Si−S stretching vibration of the TMS-S anion is the only silicon chalcogen vibration within the range of the recorded mid-IR spectra, leading to a band at 500−507 cm^{-1}. By comparison with the spectra of (trimethylsilyl)halides, the bands at ca. 630, 670, 740, and 820 cm^{-1} can be assigned to Si−C stretching vibrations.[22] According to the intensive theoretical studies, the latter three are overlapped with CH_3 rocking vibrations. In contrast to the (trimethylsilyl)halide spectra, where no distinctive alteration in these vibration frequencies is observed, they are shifted to higher wavenumbers with increasing atomic number of the chalcogen substituent. The band at ≈630 cm^{-1} shows the opposite trend, appearing at 633−637 cm^{-1} for TMS-S^- salts, at 621−632 cm^{-1} for TMS-Se^-, and at 616−625 cm^{-1} for the TMS-Te^- anions. Whether these trends are to be explained by a substituent effect on the reduced mass or can be traced back to an alteration in the Si−C bond strength, which might correlate with the ^{13}C and ^1H NMR shifts of the methyl groups, is not yet elucidated.

In addition, the (trimethylsilyl)chalcogenolate salts [DMPyr][TMS-Se] (**5**) and [NMe_4][TMS-S] (**6**) could be structurally characterized by single-crystal X-ray diffraction (XRD), proving the ionic structure in the solid state. **5** (Figure 1) crystallized in the monoclinic space group $P2_1/c$ and features two ion pairs in the asymmetric unit. The Si−Se bond lengths

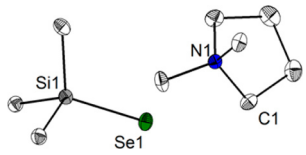

Figure 1. Molecular structure of **5**. Hydrogen atoms were omitted for clarity; only one of two independent ion pairs in the unit cell is displayed. d(Se1−Si1) = 2.220(1) Å and d(Se2−Si2) = 2.216(1) Å.

are 2.220(1) and 2.216(1) Å and thereby well in the range of Si−Se distances found in copper phosphine TMS-Se complexes[19a] but significantly shorter than those in zinc complexes bearing a TMS-Se ligand.[19b]

6 (Figure 2) crystallized in the monoclinic space group $P2_1/m$ with one molecule of acetonitrile as the crystal solvate. The

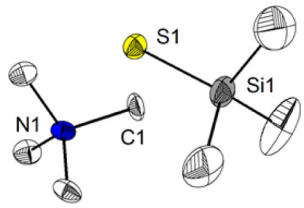

Figure 2. Molecular structure of **6**. Hydrogen atoms and one molecule of acetonitrile solvate were omitted for clarity. d(S1−Si1) = 2.052(1) Å.

asymmetric unit contains half an ion pair and half a molecule of acetonitrile. The structure was treated as a nonmerohedral twin, whose components were freely refined to a ratio of 49% to 51%. The S−Si bond length [2.052(1) Å] is significantly shorter than that in the neutral parent molecule TMS_2S [2.152(2) Å][23] and also shorter than those in copper and zinc TMS-S complexes [2.078(1)−2.119(2) Å].[19]

The corresponding organic salts of chalcogenide dianions $(Cat)_2E$ proved to be inaccessible by a 2-fold desilylation of 1 equiv of TMS_2E with 2 jointly or consecutively applied equiv of the methylcarbonate precursor. While no reaction occurred at lower temperatures, elevated temperatures (>60 °C) led to decomposition of the chalcogenide anion to unknown side products. In each case, the methylcarbonate anion was detected in the product mixture by NMR spectroscopy.

Nevertheless, the (trimethylsilyl)thiolates have proven to be excellent starting materials for the preparation of organic hexasulfides (Scheme 5). The reaction proceeds most conveniently in THF, in which the TMS-S^- salt and sulfur are partly soluble. The product is almost insoluble and precipitates as a fine bright-red solid, which can be isolated by filtration or centrifugation and is usually obtained in an analytically pure form after washing with THF and drying in fine vacuum. Bis(trimethylsilyl)sulfide is formed as the only side product. The hexasulfide apparently represents the thermodynamically most stable member of this series of pyrrolidinium polysulfides. The attempted synthesis of di- or tetrasulfides by variation of the reaction stoichiometry only led to decreased yields of the hexasulfides. The hexasulfide **11** was structurally characterized by single-crystal XRD (Figure 3; monoclinic $P2_1/c$; two cations and one dianion per asymmetric unit). The sulfur chain adopts a helical structure and is disordered over two positions (ratio 93:7), which exhibit opposing rotating directions. The S−S bond lengths differ significantly along the chain. The longest bond is situated at the

DOI: 10.1021/acs.inorgchem.5b01665
Inorg. Chem. 2015, 54, 9568−9575

Table 2. Crystal Data for 5, 6·CH_3CN, 11, $[BMPyr]_2Se_3$, and $[DMPyr]_4Te_{12}$

	[DMPyr][TMS-Se] (**5**)	$[NMe_4][TMS\text{-}S]\cdot CH_3CN$ (**6**)	$[DMPyr]_2S_6$ (**11**)	$[BMPyr]_2Se_3$	$[DMPyr]_4Te_{12}$
formula	$C_{18}H_{46}N_2Se_2Si_2$	$C_9H_{24}N_2SSi$	$C_{12}H_{28}N_2S_6$	$C_{36}H_{80}N_4Se_6$	$C_{24}H_{56}N_4Te_{12}$
fw/g·mol^{-1}	504.67	220.45	392.72	1042.80	1931.92
cryst syst	monoclinic	monoclinic	monoclinic	monoclinic	monoclinic
space group	$P2_1/c$	$P2_1/m$	$P2_1/c$	Cc	$P2_1/n$
color, habit	colorless block	colorless plate	red block	dark-green block	dark-violet plate
cryst size/mm^3	0.25 × 0.1 × 0.05	0.24 × 0.175 × 0.14	0.14 × 0.10 × 0.10	0.23 × 0.11 × 0.06	0.28 × 0.13 × 0.03
a/Å	12.2500(8)	7.6236(11)	13.9975(10)	14.0988(8)	9.5497(7)
b/Å	10.8215(7)	7.6281(11)	12.2771(9)	24.8538(12)	18.7183(14)
c/Å	19.3331(12)	13.2227(18)	12.6705(8)	14.4105(8)	13.2276(10)
α/deg	90	90	90	90	90
β/deg	90.166(3)	104.094(4)	115.568(2)	116.435(2)	107.817(2)
γ/deg	90	90	90	90	90
V/Å^3	2562.9(3)	745.80(18)	1964.2(2)	4521.6(4)	2251.1(3)
Z	4	2	4	4	2
D_{calc}/g·cm^{-3}	1.308	0.982	1.328	1.532	2.850
abs corrn	multiscan	multiscan	multiscan	multiscan	multiscan
min/max transmn	0.7452/0.6204	0.7460/0.5002	0.7455/0.5398	0.7455/0.5006	0.7452/0.5263
μ/cm^{-1}	29.83	2.68	6.90	48.83	76.68
F(000)	784	244	840	2112	1704
T/K	100(2)	100(2)	100(2)	100(2)	100(2)
θ range/deg	2.16−25.37	2.76−30.31	2.31−27.17	2.84−27.78	2.18−25.34
h, k, l indices	−14:14, −13:13, −23:23	−10:10, 0:10, 0:18	−16:17, −15:15, −16:15	−18:16, 0:31, 0:18	−11:11, −22:22, −15:14
reflns coll	38995	2198	18591	5047	35122
reflns indep	4683	2198	4304	5047	4100
reflns [$I > 2\sigma(I)$]	4335	1545	3075	4199	3923
data/restraint/param	4683/0/228	2198/0/77	4304/36/240	5047/23/437	4100/0/185
R_{int}	0.0730	−(*hklf*5)	0.0862	−(*hklf*5)	0.0385
R1 (obs)	0.0306	0.0784	0.0551	0.0616	0.0280
wR2 (all)	0.0692	0.1505	0.1275	0.1114	0.0630
GOF (F_2)	1.117	1.100	1.035	1.145	1.291
residual electron density (min/max)	−0.550/0.521	−0.439/0.508	−0.411/0.569	−1.001/1.014	−0.867/1.495
CCDC	1413729	1413730	1413731	1413732	1413733

Scheme 5. Synthesis of Pyrrolidinium Hexasulfides 10 and 11

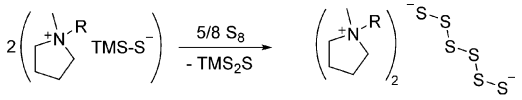

R = Bu (**1**), Me (**2**) R = Bu (**10**), Me (**11**)

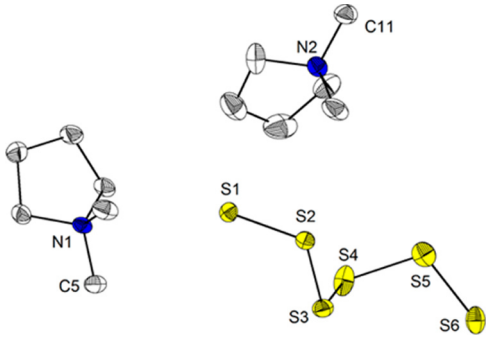

Figure 3. Molecular structure of **11**. Hydrogen atoms were omitted for clarity; only the sulfur chain with the higher site occupancy is shown.

central position [d(S3−S4) = 2.085(1) Å]; toward the final atoms, the bond lengths decrease stepwise [e.g., d(S4−S5) = 2.040(2) Å and d(S5−S6) = 2.031(2) Å]. The helical S_6 structure is the predominant conformation among comparable crystal structures. Also, the S−S bond lengths lie in a similar range, with the central bond always being the weakest.[24] The torsion within the S_6 chain varies over a large range, resulting in differences in the total chain length of almost 1 Å (e.g., 7.60 Å in $[NBu_4]_2S_6$[24a] vs 6.63 Å in $[enH_2]S_6$).[24b] The present dimethylpyrrolidinium hexasulfide shows an intermediate distance of 7.04 Å between S1 and S6.

While pure (trimethylsilyl)selenolate and -tellurolate salts are colorless and storable without decomposition at 25 °C in the dark under an inert atmosphere, solutions of them, especially in the presence of silicon grease or traces of air, show some decomposition, resulting in intensely green and violet solutions. The colors clearly indicate the presence of polyselenides and polytellurides, respectively. For the silylselenolates and -tellurolates, a lability similar to those of H_2Se and H_2Te and the hydroselenide and hydrotelluride anions, which are prone to homolytic dissociation to hydrogen and the elemental chalcogen, has to be expected. During crystallization, previously colorless solutions of [BMPyr][TMS-Se] and [DMPyr][TMS-Te] yielded green and violet-black single crystals suitable for X-

DOI: 10.1021/acs.inorgchem.5b01665
Inorg. Chem. 2015, 54, 9568−9575

ray structure determination; the substances could be identified as $[BMPyr]_2Se_3$ and $[DMPyr]_4Te_{12}$. Preliminary experiments indicate that polyselenides and polytellurides can be synthesized analogously to the polysulfides from TMS-E^- and E_n. A more detailed investigation is still underway though and will be published in due course.

The triselenide (Figure 4) crystallized in the monoclinic space group *Cc* comprising four cations and two dianions in the asymmetric unit. The structure was treated as a nonmerohedral twin, whose components were freely refined to a ratio of 51% to 49%; additionally, one of the triselenide anions is disordered over two positions with a freely refined ratio of 91% to 9%. Considering only the nondisordered anion, the Se−Se bond lengths are 2.352(2) and 2.356(2) Å, while the triatomic structure is bent at an angle of 113.4(1)°. Similar bond lengths are found in other triselenides; the best agreement persists with Cs_2Se_3 [2.358(1) Å].[25] The Se−Se distances in the closer-related structure with distinctively separated ions ($[Mn(en)_3]Se_3$; en = ethylenediamine) are considerably shorter [2.3394(4) Å].[26] The angles in the known triselenide structures are smaller by approximately 10°.[26] The structural diversity of polyselenides was recently reviewed and classified.[27]

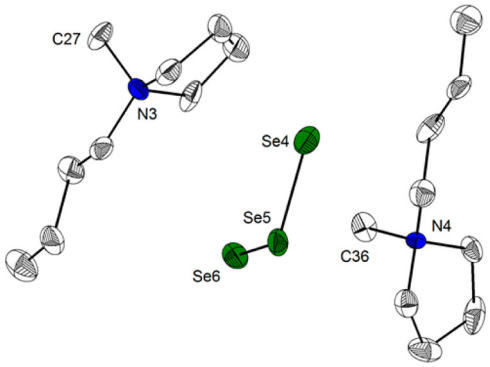

Figure 4. Molecular structure of $[BMPyr]_2Se_3$. Hydrogen atoms were omitted for clarity; only one of two ion pairs in the asymmetric unit is displayed.

The polytelluride (Figure 5) crystallized in the monoclinic space group $P2_1/n$; the asymmetric unit comprises two cations and a Te_6 chain. Two neighboring Te_6 chains form a tetraanionic tricyclic structure. A related tetraanion was observed by Feldmann and Okrut, who synthesized the corresponding Li(12-crown-4)$_2$ salt from elemental tellurium and lithium antimonide.[28] The present structure is not disordered though, allowing a higher precision in comparison with the previous structure report. As pointed out by Feldmann and Okrut, two different Te−Te bonding modes can be observed in the anion structure. Te_2 units with a pseudotetrahedral coordination geometry show short Te−Te distances typical of polytelluride chains [d(Te4−Te5) = 2.737(1) Å and d(Te1−Te2) = 2.759(1) Å]. T-shaped Te_4 units with a pseudotrigonal-bipyrimidal coordination of the central, hypervalent atom show distinctively longer distances, e.g., d(Te2−Te3) = 2.819(1) Å, d(Te3−Te4) = 2.981(1) Å, and d(Te3−Te6′) = 2.972(1) Å. The particularly elongated Te−Te bond between Te1 and Te6′ [3.208(1) Å] in the second T-shaped fragment points to a secondary interaction. Nevertheless, Te6 can be regarded as hypervalent, judging from the bonding geometry and the anisotropic displacement parameters of the neighboring atoms: The four three-coordinate tellurium atoms are formally Te^-, which can be regarded as pseudo-I. The largest polytelluride with organic cations known so far is the dodecatelluride dianion found in $(NEt_4)_2Te_{12}$;[29] other structurally characterized polytellurides with organic cations include Te_2^{2-},[8a] Te_3^{2-},[29] Te_4^{2-},[30] and Te_5^{2-}.[24a,31] For an extensive overview, the attentive reader is referred to the excellent reviews by Smith and Ibers[32] and Sheldrick.[27a]

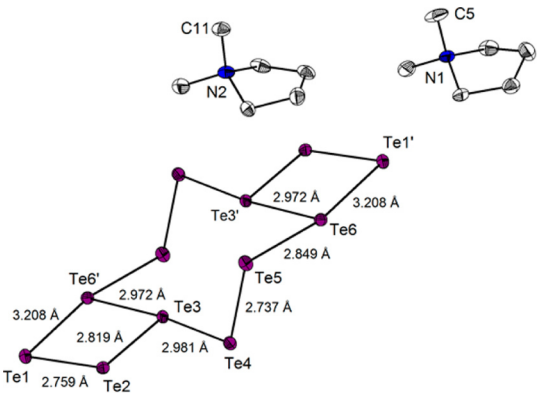

Figure 5. Molecular structure of $[DMPyr]_4Te_{12}$. Hydrogen atoms and two symmetry-equivalent cations were omitted for clarity. Symmetry operation: ′, 2 − x, −y, −z.

After successfully implementing methylcarbonate ILs as desilylating agents for bis(trimethylsilyl)sulfide, -selenide, and -telluride, we were curious whether this procedure is transferable to other TMS-substituted reagents. As may be expected, no reaction occurs with the lightest homologue of the series, TMS_2O. Apparently, the formation of a Si−O bond is needed as the driving force for the reaction. Accordingly, (trimethylsilyl)azide and (trimethylsilyl)cyanide react selectively with hexamethylguanidinium methylcarbonate to form hexamethylguanidinium azide and cyanide (Scheme 6).

Scheme 6. Synthesis of Hexamethylguanidinium Azide (12) and Cyanide (13) by Methylcarbonate-Induced Desilylation

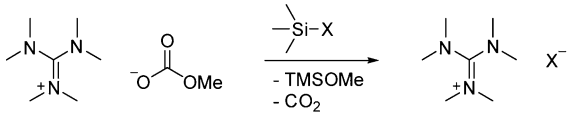

X = N_3 (**12**, 62%), CN (**13**, 92%)

This provides an elegant access to these organic salts, whose synthesis is usually challenging because of unfavorable solubility equilibria for alkali halide salt metathesis reactions and the very high toxicity of the corresponding free acids. The completely aprotic procedure allows total exclusion of highly hazardous and volatile HCN and HN_3. The preparation of organic silylchalcogenolate salts and the additional examples demonstrate the attractive desilylation potential of organic methylcarbonate salts. These readily available reagents supplement the typically weakly coordinated fluoride salts, e.g., cesium, TBAF, and TMAF, whose desilylation behavior has been well-known for decades.[33]

CONCLUSION AND OUTLOOK

A series of nine quaternary ammonium and phosphonium (trimethylsilyl)thiolates, -selenolates, and -tellurolates Cat-[TMS-E] were synthesized by a new method of mild

DOI: 10.1021/acs.inorgchem.5b01665
Inorg. Chem. 2015, 54, 9568−9575

desilylation of the respective bis(trimethylsilyl)chalcogenides TMS_2E (E = S, Se, Te) with known methylcarbonate ILs. Our synthesis is based on the observed desilylating capability of the highly nucleophilic methylcarbonate anion, followed by irreversible decarboxylation. This method offers a high yield and, in terms of cation and anion variability, broad access to well-soluble and pure silylchalcogenolates with purely organic cations. Upon exploration of the scope of this method, desilylation could be extended to representative *C*- and *N*-silyl derivatives, allowing a safe access to organic azide and cyanide salts, difficult to obtain in pure form by other methods. The new ionic chalcogenides were investigated regarding their decomposition temperatures and spectroscopic properties (NMR and IR). The crystal structures of **6** and **5** constitute the first structurally characterized examples of uncoordinated (trimethylsilyl)chalcogenolate anions. These are highly valuable precursors for the synthesis of polychalcogenides with purely organic cations, as demonstrated by the selective synthesis of pyrrolidinium hexasulfides via a redox reaction with elemental sulfur. The XRD structural characterization of the side products $[BMPyr]_2Se_3$ and $[DMPyr]_4Te_{12}$ demonstrates that this strategy can be extended to the higher homologues. We are confident that the now readily available title compounds Cat[TMS-E] (E = S, Se, Te) will expand the starting material basis for many chemists working in the topical areas of metal chalcogenido clusters, (silyl)chalcogenidometallates, metal chalcogenide semiconductor materials, and polychalcogenide redox mediators.

EXPERIMENTAL SECTION

Details of solvothermal syntheses and isolation of methylcarbonate salts and other starting materials, e.g., TMS_2Te, as well as synthetic procedures for compounds **4**−**10** are submitted as Supporting Information. Representative procedures:

Synthesis of *N*-Butyl-*N*-methylpyrrolidinium (Trimethylsilyl)thiolate ([BMPyr][TMS-S], 1). *N*-Butyl-*N*-methylpyrrolidinium methylcarbonate (617 mg, 2.84 mmol, 1.00 equiv) was dissolved in acetonitrile (5 mL), and the solution was cooled to 0 °C. TMS_2S (688 mg, 3.86 mmol, 1.36 equiv) was added dropwise, and the mixture was stirred for 1 h at 0 °C and a further 30 min at ambient temperature. The solution was concentrated in fine vacuum to two-thirds of its original volume, and diethyl ether (2 mL) was added. Storage at −25 °C yielded colorless crystals. The precipitate was filtered over a precooled frit, washed with diethyl ether (10 mL), and dried in fine vacuum. [BMPyr][TMS-S] was isolated as a colorless solid. Yield: 514 mg (2.08 mmol, 73%). Mp: 120.9−121.9 °C (5 K/min, dec, MeCN/Et_2O). Elem anal. Calcd for $C_{12}H_{29}N_1S_1Si_1$: C, 58.2; H, 11.8; N, 5.7; S, 12.95. Found: C, 58.3; H, 12.2; N, 5.8; S, 12.5. IR (ν_{max}/cm^{-1}): 2938 (m), 1478 (w), 1384 (w), 1231 (m), 1030 (w), 1007 (w), 937 (w), 814 (vs), 735 (m), 663 (m), 633 (s), 499 (s). ^1H NMR (300.1 MHz, DMSO-d_6): δ −0.07 (s, 9H, *TMS*-S), 0.93 (t, $^3J_{HH}$ = 7.5 Hz, 3H, CH_2CH_3), 1.25−1.38 (m, 2H, CH_2CH_3), 1.62−1.73 (m, 4H), 2.08 (br s, 4H), 3.01 (s, 3H, N*Me*), 3.33−3.39 (m, 2H), 3.44−3.56 (m, 4H). ^{13}C NMR (75.5 MHz, DMSO-d_6): δ 8.9 (3C, *TMS*-S), 13.4 (1C), 19.2 (1C), 21.0 (1C), 24.9 (1C), 47.4 (br s, 2C), 62.7 (br s, 2C), 63.3 (br s, 1C). ^{29}Si NMR (99.4 MHz, DMSO-d_6): δ −0.7 (s).

Synthesis of *N*-Butyl-*N*-methylpyrrolidinium (Trimethylsilyl)selenolate ([BMPyr][TMS-Se], 2). *N*-Butyl-*N*-methylpyrrolidinium methylcarbonate (997 mg, 4.59 mmol, 1.00 equiv) was dissolved in acetonitrile (10 mL), and the solution was cooled to 0 °C and degassed three times. TMS_2Se (1.24 g, 5.50 mmol, 1.20 equiv) was added dropwise, and the mixture was stirred for 1 h at 0 °C and a further 30 min at ambient temperature. The solution was concentrated in fine vacuum to half of the original volume and stored at −20 °C. The resulting suspension was filtered over a precooled frit, and the precipitate was washed with diethyl ether (10 mL) and dried in fine vacuum. A second crop of material was obtained analogously by cooling the combined mother liquor and washings to −20 °C. [BMPyr][TMS-Se] was isolated as a colorless solid. Yield: 1.10 g (3.74 mmol, 81%). Mp: 127.8−128.4 °C (5 K/min, dec, MeCN/Et_2O). Elem anal. Calcd for $C_{12}H_{29}N_1Se_1Si_1$: C, 49.0; H, 9.9; N, 4.8. Found: C, 48.5; H, 9.8; N, 5.3. IR (ν_{max}/cm^{-1}): 2941 (m), 2889 (w), 1465 (w), 1383 (w), 1231 (m), 1004 (w), 931 (w), 818 (vs), 735 (m), 667 (m), 621 (m). ^1H NMR (300.1 MHz, DMSO-d_6): δ 0.09 (s, 9H, *TMS*-Se), 0.93 (t, $^3J_{HH}$ = 7.5 Hz, 3H, CH_2CH_3), 1.25−1.38 (m, 2H, CH_2CH_3), 1.62−1.73 (m, 4H), 2.08 (br s, 4H), 2.99 (s, 3H, N*Me*), 3.29−3.35 (m, 2H), 3.39−3.54 (m, 4H). ^{13}C NMR (75.5 MHz, DMSO-d_6): δ 9.2 (3C, *TMS*-Se), 13.4 (1C), 19.2 (1C), 21.0 (1C), 24.9 (1C), 47.5 (br s, 2C), 62.8 (br s, 2C), 63.3 (br s, 1C). ^{29}Si NMR (59.7 MHz, DMSO-d_6): δ −4.7 (s). ^{77}Se NMR (57.3 MHz, DMSO-d_6): δ −417.5 (s).

Synthesis of *N*-Butyl-*N*-methylpyrrolidinium (Trimethylsilyl)tellurolate ([BMPyr][TMS-Te], 3). *N*-Butyl-*N*-methylpyrrolidinium methylcarbonate (1.00 g, 4.60 mmol, 1.00 equiv) was dissolved in acetonitrile (8 mL), and the solution was cooled to 0 °C and degassed three times. TMS_2Te (1.28 g, 4.66 mmol, 1.01 equiv) was added dropwise, whereupon the solution turned slightly red. The mixture was stirred for 30 min at 0 °C and a further 60 min at ambient temperature. All volatile components were removed in vacuo, and a reddish-gray solid remained, which proved to be pure according to elemental analysis. [BMPyr][TMS-Te] was isolated in a yield of 1.44 g (4.19 mmol, 91%). Mp: 120.4−121.2 °C (5 K/min, dec, MeCN). Elem anal. Calcd for $C_{12}H_{29}N_1Si_1Te_1$: C, 42.0; H, 8.5; N, 4.1. Found: C, 42.4; H, 8.7; N, 4.5. IR (ν_{max}/cm^{-1}): 2939 (m), 2880 (w), 1461 (w), 1230 (m), 1060 (w), 933 (w), 822 (vs), 738 (m), 672 (m), 616 (s). ^1H NMR (300.1 MHz, DMSO-d_6): δ 0.32 (s, 9H, *TMS*-Te), 0.92 (t, $^3J_{HH}$ = 7.4 Hz, 3H, CH_2CH_3), 1.25−1.38 (m, 2H, CH_2CH_3), 1.61−1.75 (m, 4H), 2.08 (br s, 4H), 3.01 (s, 3H, N*Me*), 3.32−3.41 (m, 2H), 3.44−3.56 (m, 4H). ^{13}C NMR (75.5 MHz, DMSO-d_6): δ 10.1 (3C, *TMS*-Te), 13.4 (1C), 19.2 (1C), 21.0 (1C), 24.9 (1C), 47.5 (br s, 2C), 62.7 (br s, 2C), 63.3 (br s, 1C). ^{29}Si NMR (79.5 MHz, DMSO-d_6): δ −27.0 (s). ^{125}Te NMR (126.2 MHz, DMSO-d_6): δ −1142.0 (s).

Synthesis of Bis(*N*,*N*-dimethylpyrrolidinium)hexasulfide ($[DMPyr]_2S_6$, 11). A suspension of sulfur (201 mg, 6.27 mmol, 4.95 equiv) in THF (20 mL) was added to [DMPyr][TMS-S] (520 mg, 2.53 mmol, 2.00 equiv). The mixture immediately turned bright red and was stirred for 3 days, after which a fine red precipitate had formed. The solid was filtered, washed with THF (10 mL), and dried in fine vacuum. **11** was isolated in a yield of 485 mg (1.23 mmol, 98%). Mp: 128.2−128.8 °C (5 K/min, dec, THF). Elem anal. Calcd for $C_{12}H_{28}N_2S_6$: C, 36.7; H, 7.2; N, 7.1; S, 50.0.[34] Found: C, 36.9; H, 7.3; N, 8.4; S, 52.51. IR (ν_{max}/cm^{-1}): 2982 (w), 1459 (w), 1000 (w), 975 (w), 935 (w), 818 (w), 503 (vs), 439 (w). ^1H NMR (300.1 MHz, DMSO-d_6): δ 2.12 (br s, 4H, CH_2), 3.14 (s, 6H, NMe_2), 3.51 (br s, 4H, NCH_2). ^{13}C NMR (75.5 MHz, DMSO-d_6): δ 22.1 (2C, CH_2), 52.3 (br s, 2C, NMe_2), 65.8 (br s, 2C, NCH_2).

Synthesis of Hexamethylguanidinium Azide ($[Me_6Gua]N_3$, 12). Hexamethylguanidinium methylcarbonate (288 mg, 1.31 mmol, 1.00 equiv) was dissolved in acetonitrile (8 mL) and the mixture cooled to 0 °C. (Trimethylsilyl)azide (189 mg, 1.64 mmol, 1.25 equiv) was added dropwise, whereupon gas evolution could be witnessed. The mixture was stirred at 0 °C for 20 min and at ambient temperature for 30 min. Trace amounts of solid residue were removed by syringe filtration, and all volatile components were removed in fine vacuum. The solid residue was recrystallized from a mixture of acetonitrile and diethyl ether at −25 °C. $[Me_6Gua][N_3]$ was isolated in a yield of 152 mg (0.816 mmol, 62%) as colorless crystals. Mp: 299.9−300.7 °C (5 K/min, dec, MeCN/Et_2O). Elem anal. Calcd for $C_7H_{18}N_6$: C, 45.1; H, 9.7; N, 45.1. Found: C, 45.1; H, 9.5; N, 45.5. IR (ν_{max}/cm^{-1}): 3288 (w), 3000 (w), 2898 (w), 2803 (w), 1994 (vs), 1596 (vs), 1477 (m), 1402 (vs), 1254 (m), 1147 (m), 1069 (m), 895 (m), 630 (w), 536 (w). ^1H NMR (300.1 MHz, DMSO-d_6): δ 2.87 (s, 18H, *Me*). ^{13}C NMR (75.5 MHz, DMSO-d_6): δ 39.4 (6C, *Me*), 162.3 (1C, C_{quart}).

Synthesis of Hexamethylguanidinium Cyanide ($[Me_6Gua]$-[CN], 13). Hexamethylguanidinium methylcarbonate (210 mg, 0.958 mmol, 1.00 equiv) was dissolved in acetonitrile (8 mL) and the

DOI: 10.1021/acs.inorgchem.5b01665
Inorg. Chem. 2015, 54, 9568−9575

mixture cooled to 0 °C. (Trimethylsilyl)cyanide (120 mg, 1.21 mmol, 1.26 equiv) was added dropwise. The mixture was stirred at 0 °C for 15 min and at ambient temperature for 60 min. Trace amounts of solid residue were removed by syringe filtration, all volatile components were removed, and the residue was thoroughly dried in vacuo. [Me_6Gua][CN] was isolated in a yield of 149 mg (0.875 mmol, 92%) as a colorless powder. Mp: 258.5−259.9 °C (5 K/min, dec, MeCN). Elem anal. Calcd for $C_6H_{18}N_4$: C, 56.4; H, 10.7; N, 32.9. Found: C, 56.3; H, 10.7; N, 33.4. IR (ν_{max}/cm^{-1}): 3003 (w), 2898 (w), 2809 (w), 1600 (vs), 1480 (m), 1407 (vs), 1257 (m), 1152 (m), 1073 (m), 898 (m), 537 (w). ^{1}H NMR (300.1 MHz, DMSO-d_6): δ 2.87 (s, 18H, *Me*). ^{13}C NMR (75.5 MHz, DMSO-d_6): δ 39.4 (6C, *Me*), 162.3 (1C, C_{quart}), 166.8 (1C, CN^-).

■ ASSOCIATED CONTENT

Supporting Information

The Supporting Information is available free of charge on the ACS Publications website at DOI: 10.1021/acs.inorgchem.5b01665.

X-ray crystallographic data in CIF format (CIF)

Details concerning devices, methods, and starting materials, further synthetic procedures and analytical data of new compounds, details concerning crystal structure determination, notes concerning elemental analysis, and representations of NMR and IR spectra (PDF)

■ AUTHOR INFORMATION

Corresponding Author

*E-mail: jsu@staff.uni-marburg.de.

Notes

The authors declare no competing financial interest.

■ ACKNOWLEDGMENTS

We thank the "Fonds der Chemischen Industrie" (doctoral fellowship for L.H.F.) and the DFG, GRK 1782 "Functionalization of Semiconductors", for financial support. For his advice with crystal structure refinement, we are very grateful to Dr. K. Harms and thank J. Guschlbauer for his synthetic contribution. The analytical service department is thanked for their continued efforts.

■ DEDICATION

†Dedicated to Professor Herbert W. Roesky on the occasion of his 80th birthday.

■ REFERENCES

(1) (a) Kalb, R. Method for Producing 1,3-Heteroaromatic Carbonates Devoid of 4-Carboxylate. WO 2008 052 861, 2008. (b) Kalb, R. Method for Producing Quaternary Carbonates. WO 2008 052 860, 2008. (c) Degen, G.; Stock, C. Method for Producing Imidazolium Salts. WO 2009 040 242, 2009. (d) Holbrey, J. D.; Rogers, R. D.; Shukla, S. S.; Wilfred, C. D. *Green Chem.* **2010**, *12*, 407−413. (e) Oelkers, B.; Sundermeyer, J. *Green Chem.* **2011**, *13*, 608−618.

(2) (a) Holbrey, J. D.; Reichert, W. M.; Swatloski, R. P.; Broker, G. A.; Pitner, W. R.; Seddon, K. R.; Rogers, R. D. *Green Chem.* **2002**, *4*, 407−413. (b) Hechenbleikner, I.; Molt, K. R. Quaternary Phosphonium Dialkyl Phosphates U.S. Patent 3,652,735, 1972. (c) Bradaric, C. J.; Downard, A.; Kennedy, C.; Robertson, A. J.; Zhou, Y. *Green Chem.* **2003**, *5*, 143−152. (d) Arduengo, A. J., III Preparation of 1,3-Disubstituted Imidazolium Salts WO9114678, 1991. (e) Maase, M.; Massonne, K. Method for the Production of Purified 1,3-Disubstituted Imidazolium Salts DE10333239, 2005. (f) Earle, J. M.; Seddon, R. K. Imidazole Carbenes. U.S. Patent 6,939,974, 2005. (g) Linder, T.; Sundermeyer, J. *Chem. Commun.* **2009**, 2914−2916. (h) Ferguson, J. L.; Holbrey, J. D.; Ng, S.; Plechkova, N. V.; Seddon, K. R.; Tomaszowska, A. A.; Wassell, D. F. *Pure Appl. Chem.* **2011**, *84*, 723−744.

(3) Tundo, P.; Selva, M. *Acc. Chem. Res.* **2002**, *35*, 706−716.

(4) Gattow, G.; Behrendt, W. *Angew. Chem., Int. Ed. Engl.* **1972**, *11*, 534−535.

(5) (a) Clare, B.; Sirwardana, A.; MacFarlane, D. Synthesis, Purification and Characterization of Ionic Liquids. In *Ionic Liquids*; Kirchner, B., Ed.; Springer: Berlin, 2010; Vol. *290*, pp 1−40. (b) Wasserscheid, P.; Welton, T., Eds.; *Ionic Liquids in Synthesis*, 2nd ed.; Wiley-VCH: Weinheim, Germany, 2007; Vols. *1* and *2*. (c) Smiglak, M.; Hines, C. C.; Rogers, R. D. *Green Chem.* **2010**, *12*, 491.

(6) Christe, K. O.; Wilson, W. W.; Wilson, R. D.; Bau, R.; Feng, J. A. *J. Am. Chem. Soc.* **1990**, *112*, 7619−7625.

(7) Sun, H.; DiMagno, S. G. *J. Am. Chem. Soc.* **2005**, *127*, 2050−2051.

(8) (a) Batchelor, R. J.; Einstein, F. W. B.; Gay, I. D.; Jones, C. H. W.; Sharma, R. D. *Inorg. Chem.* **1993**, *32*, 4378−4383. (b) Jovanovski, V.; Gonzalez-Pedro, V.; Gimenez, S.; Azaceta, E.; Cabanero, G.; Grande, H.; Tena-Zaera, R.; Mora-Sero, I.; Bisquert, J. *J. Am. Chem. Soc.* **2011**, *133*, 20156−9.

(9) (a) Anson, C.; Eichhoefer, A.; Issac, I.; Fenske, D.; Fuhr, O.; Sevillano, P.; Persau, C.; Stalke, D.; Zhang, J. *Angew. Chem., Int. Ed.* **2008**, *47*, 1326−1331. (b) Deng, L.; Holm, R. H. *J. Am. Chem. Soc.* **2008**, *130*, 9878−9886. (c) Deng, L.; Majumdar, A.; Lo, W.; Holm, R. H. *Inorg. Chem.* **2010**, *49*, 11118−11126. (d) Fu, M.-L.; Issac, I.; Fenske, D.; Fuhr, O. *Angew. Chem., Int. Ed.* **2010**, *49*, 6899−6903. (e) Khadka, C. B.; Najafabadi, B. K.; Hesari, M.; Workentin, M. S.; Corrigan, J. F. *Inorg. Chem.* **2013**, *52*, 6798−6805. (f) MacDonald, D. G.; Eichhoefer, A.; Campana, C. F.; Corrigan, J. F. *Chem. - Eur. J.* **2011**, *17*, 5890−5902. (g) Yang, X.-X.; Issac, I.; Lebedkin, S.; Kuhn, M.; Weigend, F.; Fenske, D.; Fuhr, O.; Eichhofer, A. *Chem. Commun.* **2014**, *50*, 11043−11045.

(10) (a) Anikeeva, P. O.; Halpert, J. E.; Bawendi, M. G.; Bulovic, V. *Nano Lett.* **2009**, *9*, 2532−2536. (b) Ning, Z.; Voznyy, O.; Pan, J.; Hoogland, S.; Adinolfi, V.; Xu, J.; Li, M.; Kirmani, A. R.; Sun, J.-P.; Minor, J.; Kemp, K. W.; Dong, H.; Rollny, L.; Labelle, A.; Carey, G.; Sutherland, B.; Hill, I.; Amassian, A.; Liu, H.; Tang, J.; Bakr, O. M.; Sargent, E. H. *Nat. Mater.* **2014**, *13*, 822−828. (c) Pan, J.; El-Ballouli, A. a. O.; Rollny, L.; Voznyy, O.; Burlakov, V. M.; Goriely, A.; Sargent, E. H.; Bakr, O. M. *ACS Nano* **2013**, *7*, 10158−10166. (d) Steckel, J. S.; Snee, P.; Coe-Sullivan, S.; Zimmer, J. P.; Halpert, J. E.; Anikeeva, P.; Kim, L.-A.; Bulovic, V.; Bawendi, M. G. *Angew. Chem., Int. Ed.* **2006**, *45*, 5796−5799. (e) Turner, E. A.; Rosner, H.; Huang, Y.; Corrigan, J. F. *J. Phys. Chem. C* **2007**, *111*, 7319−7329.

(11) (a) Lebedev, E. P.; Mizhiritskii, M. D.; Baburina, V. A.; Zaripov, S. I. *Zh. Obshch. Khim.* **1979**, *49*, 1084−1087. (b) Mizhiritskii, M. D.; Lebedev, E. P.; Fufaeva, A. N. *Zh. Obshch. Khim.* **1982**, *52*, 2092−2094. (c) Degl'Innocenti, A.; Capperucci, A.; Castagnoli, G.; Malesci, I. *Synlett* **2005**, *2005*, 1965−1983.

(12) Nieboer, J.; Haiges, R.; Hillary, W.; Yu, X.; Richardet, T.; Mercier, H. P. A.; Gerken, M. *Inorg. Chem.* **2012**, *51*, 6350−6359.

(13) Schmidt, M.; Kiewert, E.; Lux, H.; Sametschek, C. *Phosphorus Sulfur Relat. Elem.* **1986**, *26*, 163−167.

(14) Taher, D.; Wallbank, A. I.; Turner, E. A.; Cuthbert, H. L.; Corrigan, J. F. *Eur. J. Inorg. Chem.* **2006**, *2006*, 4616−4620.

(15) (a) Fischer, J.; Siegel, W.; Bomm, V.; Fischer, M.; Mundinger, K. Process for preparation of 1,3-dimethyl-imidazolium-4-carboxylate. EP 0985668, 2001. (b) Aresta, M.; Tkatchenko, I.; Tommasi, I. Unprecedented Synthesis of 1,3-dialkylimidazolium-2-carboxylate. In *Ionic Liquids as Green Solvents*; Rogers, R. D., Seddon, K. R., Eds.; American Chemical Society: Washington, DC, 2003; Vol. *856*, pp 93−99. (c) Holbrey, J. D.; Reichert, W. M.; Tkatchenko, I.; Bouajila, E.; Walter, O.; Tommasi, I.; Rogers, R. D. *Chem. Commun.* **2003**, 28−29.

(16) Wang, Y.-B.; Wang, Y.-M.; Zhang, W.-Z.; Lu, X.-B. *J. Am. Chem. Soc.* **2013**, *135*, 11996−12003.

DOI: 10.1021/acs.inorgchem.5b01665
Inorg. Chem. 2015, 54, 9568−9575

(17) The cation has no effect on the ^{1}H, ^{13}C, and ^{29}Si chemical shifts of the anion. The ^{77}Se and ^{125}Te NMR spectra show a negligible deviation of ±1.5 ppm in dependence of the cation.
(18) Lange, H.; Herzog, U. *J. Organomet. Chem.* **2002**, *660*, 36−42.
(19) (a) Tran, D. T. T.; Corrigan, J. F. *Organometallics* **2000**, *19*, 5202−5208. (b) DeGroot, M. W.; Corrigan, J. F. *Organometallics* **2005**, *24*, 3378−3385.
(20) Harris, R. K.; Kimber, B. J. *J. Magn. Reson. (1969-1992)* **1975**, *17*, 174−188.
(21) Drake, J. E.; Glavinćevski, B. M.; Humphries, R.; Majid, A. *Can. J. Chem.* **1979**, *57*, 3253−3256.
(22) (a) Montejo, M.; Hinchley, S. L.; Altabef, A. B.; Robertson, H. E.; Urena, F. P.; Rankin, D. W. H.; Lopez Gonzalez, J. J. *Phys. Chem. Chem. Phys.* **2006**, *8*, 477−485. (b) Montejo, M.; Partal Ureña, F.; Márquez, F.; Ignatyev, I. S.; González, J. J. L. *Spectrochim. Acta, Part A* **2005**, *62*, 293−301. (c) Montejo, M.; Ureña, F. P.; Márquez, F.; González, J. J. L. *Spectrochim. Acta, Part A* **2005**, *62*, 1058−1069.
(23) Eußner, J. P.; Dehnen, S. *Chem. Commun.* **2014**, *50*, 11385−11388.
(24) (a) Teller, R. G.; Krause, L. J.; Haushalter, R. C. *Inorg. Chem.* **1983**, *22*, 1809−1812. (b) Böttcher, P.; Buchkremer-Hermanns, H.; Baron, J. *Z. Naturforsch., B: J. Chem. Sci.* **1984**, *39*, 416−420. (c) Chen, Y.; Liu, Q.; Deng, Y.; Zhu, H.; Chen, C.; Fan, H.; Liao, D.; Gao, E. *Inorg. Chem.* **2001**, *40*, 3725−3733.
(25) Böttcher, P. *Z. Anorg. Allg. Chem.* **1980**, *461*, 13−21.
(26) Wendland, F.; Näther, C.; Bensch, W. *Z. Naturforsch., B: J. Chem. Sci.* **2000**, *55*, 871−876.
(27) (a) Sheldrick, W. S. *Z. Anorg. Allg. Chem.* **2012**, *638*, 2401−2424. (b) Thiele, G.; Vondung, L.; Donsbach, C.; Pulz, S.; Dehnen, S. *Z. Anorg. Allg. Chem.* **2014**, *640*, 2684−2700.
(28) Feldmann, C.; Okrut, A. *Z. Anorg. Allg. Chem.* **2009**, *635*, 1807−1811.
(29) Warren, C. J.; Haushalter, R. C.; Bocarsly, A. B. *J. Alloys Compd.* **1996**, *233*, 23−29.
(30) (a) Huffman, J. C.; Haushalter, R. C. *Z. Anorg. Allg. Chem.* **1984**, *518*, 203−209. (b) Wolkers, H.; Schreiner, B.; Staffel, R.; Müller, U.; Dehnicke, K. *Z. Naturforsch., B: J. Chem. Sci.* **1991**, *46*, 1015−1019. (c) Klinkhammer, K. W.; Böttcher, P. *Z. Naturforsch., B: J. Chem. Sci.* **1990**, *45*, 141−147.
(31) Fenske, D.; Baum, G.; Wolkers, H.; Schreiner, B.; Weller, F.; Dehnicke, K. *Z. Anorg. Allg. Chem.* **1993**, *619*, 489−499.
(32) Smith, D. M.; Ibers, J. A. *Coord. Chem. Rev.* **2000**, *200−202*, 187−205.
(33) (a) Corey, E. J.; Venkateswarlu, A. *J. Am. Chem. Soc.* **1972**, *94*, 6190−6191. (b) Padwa, A.; Haffmanns, G.; Tomas, M. *Tetrahedron Lett.* **1983**, *24*, 4303−4306. (c) Gerken, M.; Schneider, S.; Schroer, T.; Haiges, R.; Christe, K. O. *Z. Anorg. Allg. Chem.* **2002**, *628*, 909−910.
(34) For a discussion of the deviation in *N* and *S* values, refer to the Supporting Information.

DOI: 10.1021/acs.inorgchem.5b01665
Inorg. Chem. 2015, 54, 9568−9575

Supporting Information

to

Synthesis of organic trimethylsilylchalcogenolate salts Cat[TMS−E] (E = S, Se, Te) – the methylcarbonate anion as desilylating agent.

Lars H. Finger[a], Benjamin Scheibe[a], Jörg Sundermeyer[a]

a) Fachbereich Chemie,
Philipps-Universität Marburg,
Hans-Meerwein-Str. 4,
35043 Marburg,
Germany.
*E-Mail: JSU@staff.uni-marburg.de

Content:

Devices and methods

All synthetic steps were conducted using standard Schlenk techniques. Elemental analyses (C, N, H, S) were carried out by the service department for routine analysis and mass spectrometry with a vario MICRO cube (ELEMENTAR). The samples were weighed into tin capsules inside a nitrogen filled glove box. Melting points were determined with a BÜCHI Melting Point B540. ^{1}H and proton decoupled ^{13}C NMR spectra were recorded in automation with a BRUKER Avance II 300 spectrometer, ^{31}P NMR spectra were recorded on a BRUKER DPX 250 spectrometer, ^{29}Si, ^{77}Se and ^{125}Te NMR spectra were recorded by the service department for NMR analyses with a BRUKER Avance III HD 300, DRX 400 or Avance III 500 spectrometer. All spectra were recorded at ambient temperature. ^{1}H and ^{13}C NMR spectra were calibrated using residual proton and solvent signals, respectively ($CDCl_3$: δ_H 7.26 ppm, δ_C 77.16 ppm; C_6D_6: δ_H 7.16 ppm, δ_C 128.06 ppm; DMSO-d_6: δ_H 2.50 ppm, δ_C 39.52 ppm).[1] NMR spectra of hetero nuclei were referenced externally as follows: ^{29}Si: Tetramethylsilane; ^{31}P: 85% H_3PO_4; ^{77}Se: Dimethyl selenide; ^{125}Te: Dimethyl telluride. IR spectra were recorded on a BRUKER APLPHA FT-IR spectrometer with Platinum ATR-sampling (diamond single crystal).

Starting materials

All solvents were dried according to common procedures[2] and passed through columns of aluminum oxide, 3 Å molecular sieve and R3-11G-catalyst (BASF) or stored over molecular sieve (3 or 4 Å) until use. Thoroughly degassing all solvents is mandatory for the handling of telluride and selenide substances. Reagents were used as received unless stated otherwise. Dry trimethylamine was generated by slowly feeding a commercial aqueous NMe_3 solution (45%) into a concentrated potassium hydroxide solution. The evolving gas was passed through a water cooled reflux condenser and a Claisen bridge cooled to −25 °C, before being condensed onto dry potassium hydroxide at −78 °C. NMe_3 was further dried over 3 Å molecular sieves before usage. Methylcarbonate ionic liquids were synthesized following published procedures.[3] For all the methylcarbonate salts employed herein more or less general procedures can be found in the literature.[4] As the methanol free isolation is mandatory for the following reactions the syntheses are given in detail. The bis(trimethylsilyl)chalcogenides were synthesized in analogy to the published procedure for bis(trimethylsilyl)sulfide.[5] The procedure for bis(trimethylsilyl)telluride is presented in detail to allow for an easy reproduction.

Solvothermal syntheses in MeOH at 130°C:

These reactions were performed in NORMAG glass autoclaves with 9 mm wall thickness and SCHOTT DN15 plane flanges (volume: 60 or 400 mL, outer diameter: 50 or 70 mm) surrounded by a protective mesh (figure S1 and S2). The custom made cover plate is equipped with two to three Swagelok fittings, a manometer and an adjustable brass safety valve for the 10 to 18 bar range. The DN15 flange is sealed by a PTFE collar gasket. As additional safety measure a safety shield was employed as long as the autoclave was pressurized. Typically pressures of 7 to 9 bar were reached during the solvothermal step. Parr-type glass tubes equipped with a high pressure Teflon valve (BO 6 mm, NORMAG, figure S3) are also suitable for pressures up to 10 bar.

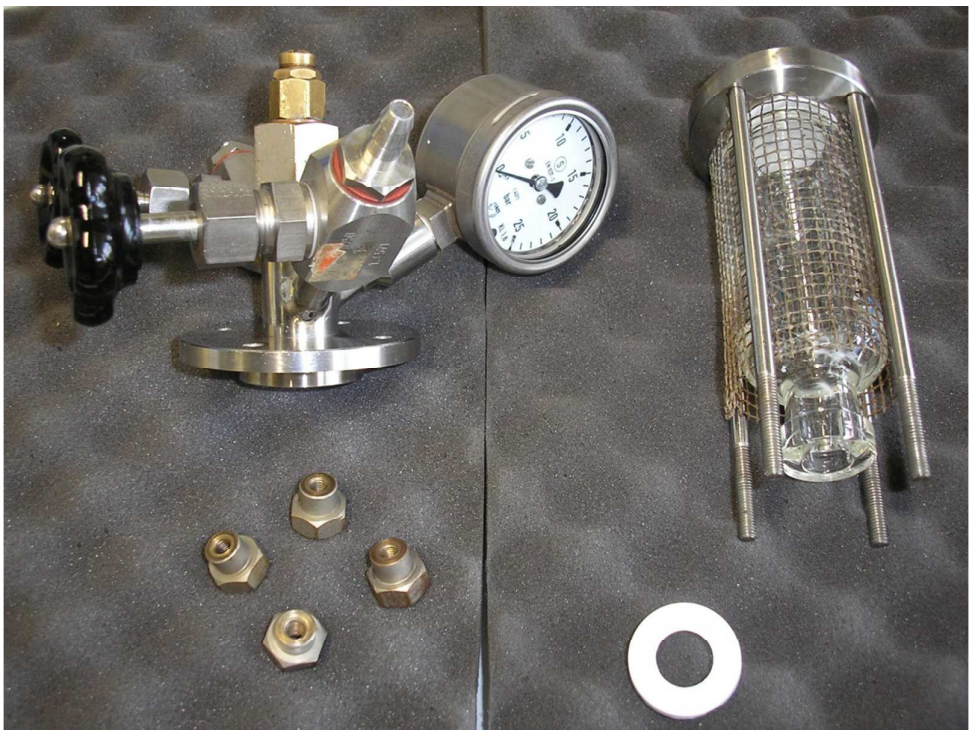

Figure S1. Normag glass autoclave (60 mL) with custom made cover plate.

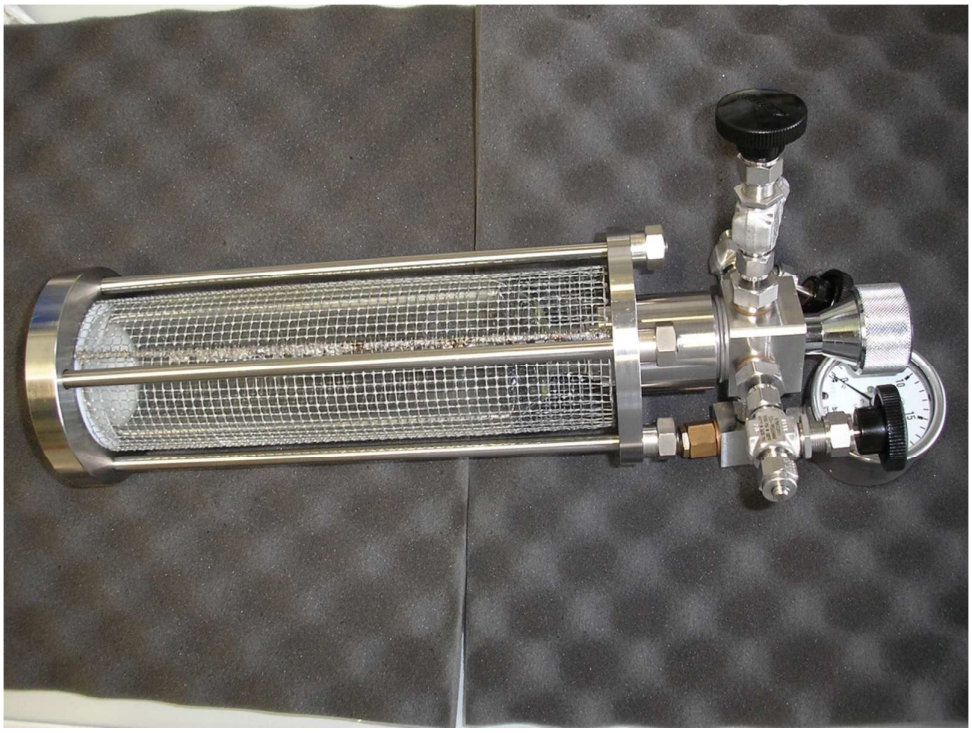

Figure S2. Normag glass autoclave (400 mL) with custom made cover plate.

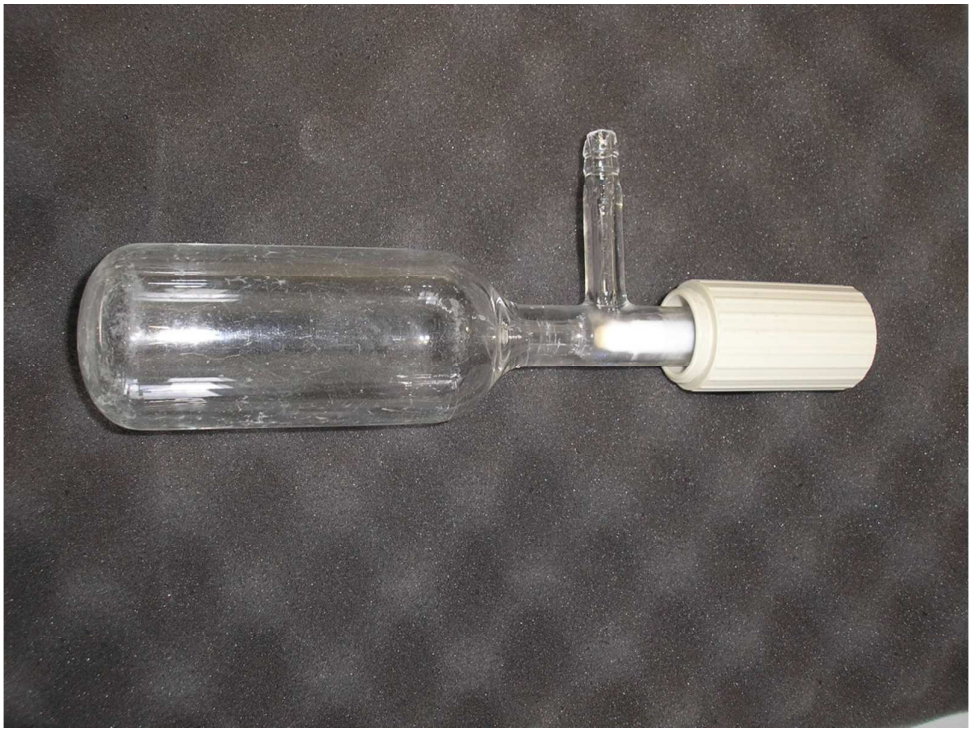

Figure S3. Parr-type glass tubes equipped with a high pressure Teflon valve (BO 6 mm, Normag).

Synthesis of N-butyl-N-methylpyrrolidinium-methylcarbonate ([BMPyr][OCO$_2$Me])

Butylpyrrolidine (61.1 mL. 49.9 g, 392 mmol, 1.00 eq), dimethyl carbonate (132 mL, 141 g, 1.57 mol, 4.00 eq) and methanol (25 mL) were combined in a glass autoclave and the mixture was heated to 130°C for 15 hours. After cooling to ambient temperature the orange solution was transferred to a Schlenk flask and all volatile components were removed *in vacuo*. The orange viscous residue was dissolved in acetonitrile (50 mL) and the solvent removed again, facilitating the removal of residing methanol. The solid residue was dissolved in acetonitrile (50 mL) and diethyl ether (50 mL) was added to the mixture. The product precipitated upon storage at –20 °C and was filtered over a precooled frit. Additional material was obtained by adding further 100 mL of diethyl ether and subsequent filtration. The precipitate was washed with diethyl ether (100 mL) and dried thoroughly in fine vacuum. [BMPyr][OCO$_2$Me] was isolated in a yield of 60.0 g (276 mmol, 70%) as a colorless solid. **^{1}H-NMR** (300.1 MHz, DMSO-d_6): δ = 0.91 (t, $^3J_{HH}$ = 7.3 Hz, 3H, CH$_2$C*H$_3$*), 1.23-1.36 (m, 2H, C*H$_2$*CH$_3$), 1.61-1.72 (m, 4H), 2.06 (br s, 4H), 3.00 (s, 3H, N*Me*), 3.17 (s, 3H, O*Me*), 3.31-3.38 (m, 2H), 3.40-3.57 (m, 4H) ppm. **^{13}C-NMR** (75.5 MHz, DMSO-d_6): δ = 13.5 (1C), 19.3 (1C), 21.0 (1C), 24.9 (1C), 47.2 (br s, 2C), 50.8 (s, 1C, O*Me*), 62.6 (br s, 2C), 63.2 (br s, 1C), 155.6 (1C, O*C*O$_2$). ppm.

Synthesis of N,N-dimethylpyrrolidinium-methylcarbonate ([DMPyr][OCO$_2$Me])

Methylpyrrolidine (40.8 mL, 33.4 g, 329 mmol, 1.00 eq) and dimethyl carbonate (132 mL, 141 g, 1.57 mol, 4.00 eq) were combined in an autoclave. Methanol (25 mL) was added to the mixture, which was heated to 130 °C for 18 hours. After cooling to ambient temperature the orange solution was transferred to a Schlenk flask and all volatile components were removed *in vacuo*. Warming the mixture to 40 °C helps evaporating the mayor part of the solvent and repeated freezing in liquid nitrogen when the substance becomes more viscous facilitates the remove of residual volatiles. The solid residue was recrystallized from a mixture of acetonitrile and diethyl ether. The precipitate was filtered and washed with 60 mL of diethyl ether in four portions. After drying in fine vacuum [DMPyr][OCO$_2$Me] was isolated in a yield of 40.0 g (228 mmol, 58%) as a colorless solid. **^{1}H-NMR** (300.1 MHz, DMSO-d_6): δ = 2.09 (br s, 4H, C*H$_2$*), 3.09 (s, 6H, N*Me$_2$*), 3.16 (s, 3H, O*Me*), 3.46 (br s, 4H, NC*H$_2$*) ppm. **^{13}C-NMR** (75.5 MHz, DMSO-d_6): δ = 21.3 (2C, *C*H$_2$), 50.8 (1C, O*Me*), 50.9 (t, $^1J_{CN}$ = 4.0 Hz, 2C, N*Me$_2$*), 64.7 (t, $^1J_{CN}$ = 3.1 Hz, 2C, N*C*H$_2$), 155.4 (1C, O*C*O$_2$).

Synthesis of tetramethylammonium-methylcarbonate ([NMe$_4$][OCO$_2$Me]).

Trimethylamine (22.4 g, 378 mmol, 1.00 eq) was condensed into a Schlenk tube at −196 °C and combined with dimethyl carbonate (85.6 g, 950 mmol, 2.51 eq) and methanol (30 mL). The mixture was slowly warmed to −60 °C and transferred into a glass autoclave. The mixture was warmed to room temperature and afterwards heated to 130 °C for 14 hours. The colorless solution was transferred to a Schlenk flask and all volatile components were removed *in vacuo.* Tetramethylammonium methylcarbonate was isolated in a yield of 43.7 g (293 mmol, 77%) as a colorless solid. **^{1}H-NMR** (300.1 MHz, DMSO-d_6): δ = 3.12 (s, 12H, N*Me*$_4$), 3.17 (s, 3H, O*Me*) ppm. **^{13}C-NMR** (75.5 MHz, DMSO-d_6): δ = 50.8 (1C, O*Me*), 54.1 (t, $^1J_{CN}$ = 3.9 Hz, 4C, N*Me*$_4$), 155.7 (1C, O*C*O$_2$) ppm.

Synthesis of tributyl-methylphosphonium-methylcarbonate ([Bu$_3$MeP][OCO$_2$Me])

Freshly distilled tri-*n*butylphosphine (82.0 g, 405 mmol, 1.00 eq), dimethyl carbonate (120 mL, 128 g, 1.43 mol, 3.52 eq) and methanol (40 mL) were combined in a glass autoclave and heated to 130 °C for seven hours. The colorless solution was transferred to a Schlenk flask and all volatiles removed *in vacuo*. The very viscous residue was mixed with acetonitrile (20 mL) and dried in fine vacuum until now further evaporation could be witnessed. This procedure is repeated two more times, whereupon methanol free [Bu$_3$MeP][OCO$_2$Me] is obtained in a yield of 110 g (376 mmol, 93%) as a light yellow viscous oil. **^{1}H-NMR** (300.1 MHz, DMSO-d_6) δ_H = 0.90 (t, $^3J_{HH}$ = 7.1 Hz, 9H, CH$_2$C*H$_3$*), 1.32-1.52 (m, 12H, C*H$_2$*C*H$_2$*), 1.83 (d, $^2J_{HP}$ = 14.2 Hz, 3H, PC*H$_3$*), 2.17-2.27 (m, 6H, PC*H$_2$*), 3.17 (s, 3H, O*Me*), ppm. **^{13}C-NMR** (75.5 MHz, DMSO-d_6) δ_C = 2.9 (d, $^1J_{CP}$ = 51.3 Hz, 1C, P*C*H$_3$), 13.2 (3C, CH$_2$*C*H$_3$), 18.8 (d, $^1J_{CP}$ = 49.2 Hz, 3C, P*C*H$_2$), 22.6 (d, J_{CP} = 4.4 Hz, 3C, *C*H$_2$), 23.3 (d, J_{CP} = 16.0 Hz, 3C, *C*H$_2$), 50.7 (1C, O*Me*), 155.5 (1C, O*C*O$_2$) ppm. **^{31}P-NMR** (101.3 MHz, DMSO-d_6): δ_P = 34.1 ppm.

Synthesis of bis(trimethylsiyl)telluride (TMS$_2$Te).

Freshly cut small pieces of sodium (4.11 g, 179 mmol) were suspended in dry THF (35 mL). Anthracene (928 mg, 5.21 mmol) was added resulting in a deep blue solution. After addition of tellurium powder (200 mesh, 11.5 g, 89.7 mmol) the suspension was vigorously stirred 21 hours at room temperature, refluxed for 9 hours and stirred at ambient temperature for further 15 hours. By then the mixture had turned to a thick turquoise suspension, which was cooled in

an ice bath. Trimethylchlorosilane (24.0 mL, 20.5 g, 189 mmol) was added drop wise within 25 minutes, whereupon the suspension turned at first colorless and then became dark brown. The mixture was stirred at 0 °C for further 15 minutes and then stirred at ambient temperature for half an hour. From this point onward silicon free Triboflon III (Merkel Freudenberg Fluidtechnic GmbH) grease was used for all glass joints. All volatile components were removed in fine vacuum and collected in a liquid nitrogen cooled trap. From the thawed condensate solvent and excess trimethylchlorosilane were removed in fine vacuum; the residue was fractionally distilled. Bis(trimethylsiyl)telluride (19.4 g, 70.9 mmol, 79%) was collected at 46 - 48 °C (1.3 mbar). The product is best stored in a Triboflon III greased Schlenk tube in the dark at −20 °C. **^{1}H-NMR** (300.1 MHz, $CDCl_3$) δ_H = 0.59 (s, 18H) ppm. **^{13}C-NMR** (75.5 MHz, $CDCl_3$): δ_C = 5.8 (s, 6C) ppm. **^{1}H-NMR** (300.1 MHz, C_6D_6) δ_H = 0.50 (s, 18H) ppm. **^{13}C-NMR** (75.5 MHz, C_6D_6): δ_C = 5.7 (s, 6C) ppm. **^{29}Si-NMR** (99.4 MHz, C_6D_6): δ_{Si} = −5.7 ppm. **^{125}Te-NMR** (157.8 MHz, C_6D_6): δ_{Te} = −858.5 ppm.

Desilylation reactions

Synthesis of N-butyl-N-methylpyrrolidinium-trimethylsilylthiolate ([BMPyr][TMS-S], 1). *N*-Butyl-*N*-methylpyrrolidinium-methylcarbonate (617 mg, 2.84 mmol, 1.00 eq) was dissolved in acetonitrile (5 mL) and the solution was cooled to 0 °C. TMS_2S (688 mg, 3.86 mmol, 1.36 eq) was added drop wise and the mixture was stirred one hour at 0 °C and further 30 minutes at ambient temperature. The solution was concentrated in fine vacuum to two thirds of its original volume and diethyl ether (2 mL) was added. Storage at −25 °C yielded colorless crystals. The precipitate was filtered over a precooled frit, washed with diethyl ether (10 mL) and dried in fine vacuum. [BMPyr][TMS-S] was isolated as a colorless solid. Yield: 514 mg (2.08 mmol, 73%). **Mp**: 120.9-121.9 °C (5 K/min, decomp., MeCN/Et_2O,). **Elem. anal.** found C, 58.3; H, 12.2; N, 5.8; S, 12.5; $C_{12}H_{29}N_1S_1Si_1$ requires C, 58.2; H, 11.8; N, 5.7; S, 12.95. **IR** ν_{max}/cm^{-1}: 2938 (m), 1478 (w), 1384 (w), 1231 (m), 1030 (w), 1007 (w), 937 (w), 814 (vs), 735 (m), 663 (m), 633 (s), 499(s). **^{1}H-NMR** (300.1 MHz, DMSO-d_6): δ = −0.07 (s, 9H, *TMS*-S), 0.93 (t, $^3J_{HH}$ = 7.5 Hz, 3H, CH_2CH_3), 1.25-1.38 (m, 2H, CH_2CH_3), 1.62-1.73 (m, 4H), 2.08 (br s, 4H), 3.01 (s, 3H, N*Me*), 3.33-3.39 (m, 2H), 3.44-3.56 (m, 4H) ppm. **^{13}C-NMR** (75.5 MHz, DMSO-d_6): δ = 8.9 (3C, *TMS*-S), 13.4 (1C), 19.2 (1C), 21.0 (1C), 24.9 (1C), 47.4 (br s, 2C), 62.7 (br s, 2C), 63.3 (br s, 1C) ppm. **^{29}Si-NMR** (99.4 MHz, DMSO-d_6): δ = −0.7 (s) ppm.

Synthesis of N-butyl-N-methylpyrrolidinium-trimethylsilylselenolate ([BMPyr][TMS-Se], 2). *N*-Butyl-*N*-methylpyrrolidinium-methylcarbonate (997 mg, 4.59 mmol, 1.00 eq) was dissolved in acetonitrile (10 mL), the solution was cooled to 0 °C and degassed three times. TMS_2Se (1.24 g, 5.50 mmol, 1.20 eq) was added drop wise and the mixture was stirred one hour at 0 °C and further 30 minutes at ambient temperature. The solution was concentrated in fine vacuum to half of the original volume and stored at −20 °C. The resulting suspension was filtered over a precooled frit and the precipitate was washed with diethyl ether (10 mL) and dried in fine vacuum. A second crop of material was obtained analogously by cooling the combined mother liquor and washings to −20 °C. [BMPyr][TMS-Se] was isolated as a colorless solid. Yield: 1.10 g (3.74 mmol, 81%). **Mp**: 127.8-128.4 °C (5 K/min, decomp., MeCN/Et_2O). **Elem. anal.** found C, 48.5; H, 9.8; N, 5.3; $C_{12}H_{29}N_1Se_1Si_1$ requires C, 49.0; H, 9.9; N, 4.8. **IR** ν_{max}/cm^{-1}: 2941 (m), 2889 (w), 1465 (w), 1383 (w), 1231 (m), 1004 (w), 931 (w), 818 (vs), 735 (m), 667(m), 621 (m). **^{1}H-NMR** (300.1 MHz, DMSO-d_6): δ = 0.09 (s, 9H, *TMS*-Se), 0.93 (t, $^3J_{HH}$ = 7.5 Hz, 3H, CH_2CH_3), 1.25-1.38 (m, 2H, CH_2CH_3), 1.62-1.73 (m,

4H), 2.08 (br s, 4H), 2.99 (s, 3H, N*Me*), 3.29-3.35 (m, 2H), 3.39-3.54 (m, 4H) ppm. **^{13}C-NMR** (75.5 MHz, DMSO-d_6): δ = 9.2 (3C, *TMS*-Se), 13.4 (1C), 19.2 (1C), 21.0 (1C), 24.9 (1C), 47.5 (br s, 2C), 62.8 (br s, 2C), 63.3 (br s, 1C) ppm. **^{29}Si-NMR** (59.7 MHz, DMSO-d_6): δ = −4.7 (s) ppm. **^{77}Se-NMR** (57.3 MHz, DMSO-d_6): δ_{Se} = −417.5 (s) ppm.

Synthesis of N-butyl-N-methylpyrrolidinium-trimethylsilyltellurolate ([BMPyr][TMS-Te], 3). *N*-Butyl-*N*-methylpyrrolidinium-methylcarbonate (1.00 g, 4.60 mmol, 1.00 eq) was dissolved in acetonitrile (8 mL), the solution was cooled to 0 °C and degassed three times. TMS_2Te (1.28 g, 4.66 mmol, 1.01 eq) was added drop wise whereupon the solution turned slightly red. The mixture was stirred 30 minutes at 0 °C and further 60 minutes at ambient temperature. All volatile components were removed *in vacuo* and a reddish-grey solid resided, which proved to be pure according to elemental analysis. [BMPyr][TMS-Te] was isolated in a yield of 1.44 g (4.19 mmol, 91%). **Mp**: 120.4-121.2 °C (5 K/min, decomp., MeCN). **Elem. anal.** found C, 42.4; H, 8.7; N, 4.5; $C_{12}H_{29}N_1Si_1Te_1$ requires C, 42.0; H, 8.5; N, 4.1 **IR** ν_{max}/cm^{-1}: 2939 (m), 2880 (w), 1461 (w), 1230 (m), 1060 (w), 933 (w), 822 (vs), 738 (m), 672 (m), 616 (s). **^{1}H-NMR** (300.1 MHz, DMSO-d_6): δ = 0.32 (s, 9H, *TMS*-Te), 0.92 (t, $^3J_{HH}$ = 7.4 Hz, 3H, CH_2CH_3), 1.25-1.38 (m, 2H, CH_2CH_3), 1.61-1.75 (m, 4H), 2.08 (br s, 4H), 3.01 (s, 3H, N*Me*), 3.32-3.41 (m, 2H), 3.44-3.56 (m, 4H) ppm. **^{13}C-NMR** (75.5 MHz, DMSO-d_6): δ = 10.1 (3C, *TMS*-Te), 13.4 (1C), 19.2 (1C), 21.0 (1C), 24.9 (1C), 47.5 (br s, 2C), 62.7 (br s, 2C), 63.3 (br s, 1C) ppm. **^{29}Si-NMR** (79.5 MHz, DMSO-d_6): δ = −27.0 (s) ppm. **^{125}Te-NMR** (126.2 MHz, DMSO-d_6): δ = −1142.0 (s) ppm.

Synthesis of N,N-dimethylpyrrolidinium-trimethylsilylthiolate ([DMPyr][TMS-S], 4). *N,N*-dimethylpyrrolidinium-methylcarbonate (921 mg, 5.26 mmol, 1.00 eq) was dissolved in acetonitrile (5 mL), the solution was cooled to 0 °C. TMS_2S (1.25 g, 7.00 mmol, 1.33 eq) was added drop wise and the mixture was stirred 30 minutes at 0 °C and further 1.5 hours at ambient temperature. Diethyl ether (4 mL) was added to the solution and the mixture stored at −25 °C. The colorless precipitate was filtered over a precooled frit, washed with diethyl ether (5 mL) and dried in fine vacuum. A second crop of material was obtained analogously by cooling the combined mother liquor and washings to −25 °C. [DMPyr][TMS-S] was isolated as a colorless solid. Yield: 846 mg (4.12 mmol, 78%). **Mp**: 166.7-167.7 °C (5 K/min, decomp., MeCN/Et_2O). **Elem. anal.** found C, 52.1; H, 12.0; N, 7.0; S, 14.9; $C_9H_{23}N_1S_1Si_1$

requires C, 52.6; H, 11.3; N, 6.8; S, 15.6. **IR** ν_{max}/cm^{-1}: 2991 (w), 2942 (w), 2889 (w), 1480 (w), 1230 (m), 1011 (w), 944 (w), 816 (vs), 736 (m), 664 (m), 635 (m), 500 (m). **^{1}H-NMR** (300.1 MHz, DMSO-d_6): δ = 0.07 (s, 9H, *TMS*-S), 2.08 (br s, 4H, CH_2), 3.14 (s, 6H, NMe_2), 3.51 (br s, 4H, NCH_2) ppm. **^{13}C-NMR** (75.5 MHz, DMSO-d_6): δ = 8.8 (3C, *TMS*-S), 21.2 (2C, CH_2), 50.8 (t, $^{1}J_{CN}$ = 3.9 Hz, 2C, NMe_2), 64.5 (t, $^{1}J_{CN}$ = 3.1 Hz, 2C, NCH_2). **^{29}Si-NMR** (59.7 MHz, DMSO-d_6): δ = −0.7 (s) ppm.

Synthesis of N,N-dimethyl-pyrrolidinium trimethylsilylselenolate ([DMPyr][TMS-Se], 5). *N,N*-dimethylpyrrolidinium-methylcarbonate (4.00 g, 22.8 mmol, 1.00 eq) was dissolved in acetonitrile (20 mL), the solution was cooled to 0 °C and degassed three times. TMS_2Se (5.63 g, 25.0 mmol, 1.10 eq) was added drop wise and the mixture was stirred one hour at 0 °C and further 30 minutes at ambient temperature. Diethyl ether (10 mL) was added to the solution and the mixture stored at −25 °C. The colorless crystals were filtered over a precooled frit and the precipitate was washed with diethyl ether (10 mL, three times) and dried in fine vacuum. [DMPyr][TMS-Se] was isolated as a colorless solid. Yield: 3.03 g (12.0 mmol, 53%). **Mp**: 168.0-168.6 °C (5 K/min, decomp., MeCN/Et_2O). **Elem. anal.** found C, 42.8; H, 9.3; N, 5.8; $C_9H_{23}N_1Se_1Si_1$ requires C, 42.8; H, 9.2; N, 5.6. **IR** ν_{max}/cm^{-1}: 2989 (w), 2942 (m), 2885 (w), 1478 (w), 1230 (m), 942 (w), 819 (vs), 738 (m), 669 (m), 625 (s). **^{1}H-NMR** (300.1 MHz, DMSO-d_6): δ = 0.09 (s, 9H, *TMS*-Se), 2.09 (br s, 4H, CH_2), 3.10 (s, 6H, NMe_2), 3.47 (br s, 4H, NCH_2) ppm. **^{13}C-NMR** (75.5 MHz, DMSO-d_6): δ = 9.1 (3C, *TMS*-Se), 21.2 (2C, CH_2), 50.9 (t, $^{1}J_{CN}$ = 3.9 Hz, 2C, NMe_2), 64.7 (t, $^{1}J_{CN}$ = 3.1 Hz, 2C, NCH_2). **^{29}Si-NMR** (99.4 MHz, DMSO-d_6): δ = −4.66 (s) ppm. **^{77}Se-NMR** (95.4 MHz, DMSO-d_6): δ = −416.4 (s) ppm.

Synthesis of tetramethylammonium-trimethylsilylthiolate ([Me_4N][TMS-S], 6). Tetramethylammonium-methylcarbonate (403 mg, 2.70 mmol, 1.00 eq) was dissolved in acetonitrile (10 mL) and the solution was cooled to 0 °C and degassed. TMS_2S (575 mg, 3.22 mmol, 1.19 eq) was added drop wise, whereupon a voluminous precipitate formed. The mixture was stirred 30 minutes at 0 °C and further 60 minutes at ambient temperature. The mixture was shortly warmed to 40 °C until all residual solid had dissolved. Diethyl ether (5 mL) was added and the suspension was cooled to −25 °C. The precipitate was filtered over a precooled frit, washed with diethyl ether (10 mL) and dried in fine vacuum. [Me_4N][TMS-

S] was isolated in a yield of 390 mg (2.17 mmol, 80%) as colorless powder. **Mp**: 184.0-184.8 °C (5 K/min, decomp., MeCN/Et_2O), Lit: 191 °C.[6] **Elem. anal.** found C, 46.7; H, 11.7; N, 8.8; S, 17.7; $C_7H_{21}N_2S_1Si_1$ requires C, 46.9; H, 11.8; N, 7.8; S, 17.9. **IR** ν_{max}/cm^{-1}: 2995 (w), 2939 (m), 2883 (w), 1489 (m), 1435 (w), 1416 (w), 1290 (w), 1229 (m), 952 (m), 817 (vs), 738 (m), 663 (m), 637 (s), 504 (s), 455 (w). **^{1}H-NMR** (300.1 MHz, DMSO-d_6): δ = 0.06 (s, 9H, *TMS*-S), 3.14 (s, 12H, N*Me*$_4$) ppm. **^{13}C-NMR** (75.5 MHz, DMSO-d_6): δ = 8.9 (3C, *TMS*-S), 54.3 (br s, 4C, N*Me*$_4$) ppm. **^{29}Si-NMR** (59.7 MHz, DMSO-d_6): δ = −0.5 (s) ppm.

Synthesis of tetramethylammonium-trimethylsilylselenolate ([Me$_4$N][TMS-Se], 7). Tetramethylammonium-methylcarbonate (352 mg, 2.36 mmol, 1.00 eq) was suspended in acetonitrile (10 mL), the solution was cooled to 0 °C and degassed three times. TMS_2Se (590 mg, 2.62 mmol, 1.11 eq) was added drop wise, a colorless precipitate formed. The mixture was stirred 30 minutes at 0 °C and further 60 minutes at ambient temperature. The mixture was shortly warmed to 40 °C until all residual solid had dissolved, diethyl ether (5 mL) was added and the suspension was cooled to −25 °C. The precipitate was filtered over a precooled frit, washed with diethyl ether (10 mL) and dried in fine vacuum. [Me_4N][TMS-Se] was isolated in a yield of 410 mg (1.81 mmol, 77%) as colorless powder. **Mp**: 183.8-184.2 °C (5 K/min, decomp., MeCN/Et_2O). **Elem. anal.** found C, 37.0; H, 9.3; N, 6.7; $C_7H_{21}N_1Se_1Si_1$ requires C, 37.15; H, 9.35; N, 37.15. **IR** ν_{max}/cm^{-1}: 2945 (w), 2886 (w), 1489 (m), 1293 (w), 1229 (m), 954 (m), 839 (s, sh), 819 (vs), 785 (m), 743 (m), 672 (m), 632 (s), 458(w). **^{1}H-NMR** (300.1 MHz, DMSO-d_6): δ = 0.09 (s, 9H, *TMS*-Se), 3.15 (s, 12H, N*Me*$_4$) ppm. **^{13}C-NMR** (75.5 MHz, DMSO-d_6): δ = 9.1 (3C, *TMS*-Se), 54.3 (br s, 4C, N*Me*$_4$) ppm. **^{29}Si-NMR** (59.7 MHz, DMSO-d_6): δ = −4.5 (s) ppm. **^{77}Se-NMR** (57.3 MHz, DMSO-d_6): δ = −413.7 (s) ppm.

Synthesis of tetramethylammonium-trimethylsilyltellurolate ([Me$_4$N][TMS-Te], 8). Tetramethylammonium-methylcarbonate (793 mg, 5.32 mmol, 1.00 eq) was suspended in acetonitrile (10 mL), the solution was cooled to 0 °C and thoroughly degassed. TMS_2Te (1.65 g, 6.00 mmol, 1.13 eq) was added drop wise, whereupon a colorless suspension formed. The mixture was stirred 30 minutes at 0 °C and further 60 minutes at ambient temperature, whereby the mixture turned slightly brown. All volatile components were removed in fine vacuum and the brown residue suspended in a mixture of acetonitrile (5 mL) and THF (5 mL).

The light colored solid was separated by centrifugation, the brown liquid decanted and the residue dried in fine vacuum. [Me_4N][TMS-Te] was isolated in a yield of 1.14 g (4.15 mmol, 78%) yield as slightly yellow powder. **Mp**: 183.5-184.6 (5 K/min, decomp., MeCN/THF). **Elem. anal.** found C, 30.5; H, 7.8; N, 5.55; $C_7H_{21}N_1Si_1Te_1$ requires C, 30.6; H, 7.7; N, 5.1. **IR** ν_{max}/cm^{-1}: 2991 (w), 2940 (w), 2878 (w), 1488 (w), 1293 (w), 1229 (m), 952 (m), 824 (vs), 746 (w), 680 (m), 625 (m), 455 (w). **^{1}H-NMR** (300.1 MHz, DMSO-d_6): δ = 0.32 (s, 9H, *TMS*-Te), 3.14 (s, 12H, N*Me*$_4$) ppm. **^{13}C-NMR** (75.5 MHz, DMSO-d_6): δ = 10.1 (3C, *TMS*-Te), 54.3 (br s, 4C, N*Me*$_4$) ppm. **^{29}Si-NMR** (99.4 MHz, DMSO-d_6): δ = −27.3 (s) ppm. **^{125}Te-NMR** (157.8 MHz, DMSO-d_6): δ = −1136.7 (s) ppm.

Synthesis of tributyl-methylphosphonium-trimethylsilylthiolate ([Bu$_3$MeP][TMS-S], 9).

Tributyl-methylphosphonium-methylcarbonate (630 mg, 2.15 mmol, 1.00 eq) was dissolved in acetonitrile (15 mL) and the solution cooled to 0 °C. $(TMS)_2S$ (535 mg, 3.00 mmol, 1.39 eq) was added slowly and the mixture stirred for 30 minutes in the ice bath. After stirring the solution for 60 minutes at ambient temperature all volatile components were removed in vacuum and the residing substance thoroughly dried. [Bu_3MeP][TMS-S] was isolated in a yield of 679 mg (2.10 mmol, 98%) as colorless oil. **Elem. anal.** Due to the very viscous nature of the substance no preparation of CHNS samples was possible. **IR** ν_{max}/cm^{-1}: 2934 (m), 2872 (m), 1464 (w), 1225 (m), 1097 (w), 940 (w), 837 (s, sh), 815 (vs), 736 (m), 659 (m), 637 (vs), 507(m). **^{1}H-NMR** (300.1 MHz, DMSO-d_6) δ_H = −0.06 (s, 9H, TMS-S), 0.91 (t, $^3J_{HH}$ = 7.1 Hz, 9H, CH_2CH_3), 1.34-1.53 (m, 12H, CH_2CH_2), 1.85 (d, $^2J_{HP}$ = 14.1 Hz, 3H, PCH_3), 2.18-2.28 (m, 6H, PCH_2) ppm. **^{13}C-NMR** (75.5 MHz, DMSO-d_6) δ_C = 3.3 (d, $^1J_{CP}$ = 51.4 Hz, 1C, PCH_3), 8.8 (3C, TMS-S), 13.2 (3C, CH_2CH_3), 19.0 (d, $^1J_{CP}$ = 49.1 Hz, 3C, PCH_2), 22.5 (d, J_{CP} = 4.3 Hz, 3C, CH_2), 23.2 (d, J_{CP} = 15.4 Hz, 3C, CH_2) ppm. **^{29}Si-NMR** (59.7 MHz, DMSO-d_6): δ = −0.7 (s) ppm. **^{31}P-NMR** (101.3 MHz, DMSO-d_6): δ_P = 35.1 ppm.

Synthesis of hexamethylguanidinium-azide ([Me$_6$Gua]N$_3$, 12).

Hexamethylguanidinium methylcarbonate (288 mg, 1.31 mmol, 1.00 eq) was dissolved in acetonitrile (8 mL) and the mixture cooled to 0 °C. Trimethylsilylazide (189 mg, 1.64 mmol, 1.25 eq) was added drop wise, whereupon a gas evolution could be witnessed. The mixture was stirred at 0 °C for 20 minutes and at ambient temperature for 30 minutes. Trace amounts of solid residue were removed by syringe filtration and all volatile components were removed

in fine vacuum. The solid residue was recrystallized from a mixture of acetonitrile and diethyl ether at −25 °C. [Me_6Gua][N_3] was isolated in a yield of 152 mg (0.816 mmol, 62%) as colorless crystals. **Mp**: 299.9-300.7 °C (5 K/min, decomp., MeCN/Et_2O). **Elem. anal.** found C, 45.1; H, 9.5; N, 45.5; $C_7H_{18}N_6$ requires C, 45.1; H, 9.7; N, 45.1. **IR** ν_{max}/cm^{-1}: 3288 (w), 3000 (w), 2898 (w), 2803 (w), 1994 (vs), 1596 (vs), 1477 (m), 1402 (vs), 1254 (m), 1147 (m), 1069 (m), 895 (m), 630 (w), 536 (w). **^{1}H-NMR** (300.1 MHz, DMSO-d_6): δ = 2.87 (s, 18H, *Me*) ppm. **^{13}C-NMR** (75.5 MHz, DMSO-d_6): δ = 39.4 (6C, *Me*), 162.3 (1C, C_{quart}) ppm.

Synthesis of hexamethylguanidinium-cyanide ([Me$_6$Gua][CN], 13).

Hexamethylguanidinium methylcarbonate (210 mg, 0.958 mmol, 1.00 eq) was dissolved in acetonitrile (8 mL) and the mixture cooled to 0 °C. Trimethylsilylcyanide (120 mg, 1.21 mmol, 1.26 eq) was added drop wise. The mixture was stirred at 0 °C for 15 minutes and at ambient temperature for 60 minutes. Trace amounts of solid residue were removed by syringe filtration, all volatile components were removed and the residue thoroughly dried *in vacuo*. [Me_6Gua][CN] was isolated in a yield of 149 mg (0.875 mmol, 92%) as colorless powder. **Mp**: 258.5-259.9 °C (5 K/min, decomp., MeCN). **Elem. anal.** found C, 56.3; H, 10.7; N, 33.4; $C_6H_{18}N_4$ requires C, 56.4; H, 10.7; N, 32.9. **IR** ν_{max}/cm^{-1}: 3003 (w), 2898 (w), 2809 (w), 1600 (vs), 1480 (m), 1407 (vs), 1257 (m), 1152 (m), 1073 (m), 898 (m), 537 (w). **^{1}H-NMR** (300.1 MHz, DMSO-d_6): δ = 2.87 (s, 18H, *Me*) ppm. **^{13}C-NMR** (75.5 MHz, DMSO-d_6): δ = 39.4 (6C, *Me*), 162.3 (1C, C_{quart}), 166.8 (1C, *C*N$^-$) ppm.

Reaction of trimethylsilylthiolate salts with sulfur

Synthesis of bis(N-butyl-N-methylpyrrolidinium)-hexasulfide ([BMPyr]$_2$S$_6$, 10).

[BMPyr][TMS-S] (300 mg, 1.21 mmol, 2.00 eq) was dissolved in THF (15 mL) and added to elemental sulfur (100 mg, 3.12 mmol, 5.15 eq). The mixture immediately turned bright red, later a red oily substance formed. After three days a fine red powder remained in a slightly blue-green solution. The suspension was filtered, the precipitate washed with THF (6 mL) and dried in fine vacuum. [BMPyr]$_2$[S_6] was isolated in a yield of 260 mg (0.545 mmol, 90%). The solvent was removed from the combined mother liquor and washings. Yellow oil remained, which could be identified as TMS_2S on the basis of its NMR-spectra. Analytical data for [BMPyr]$_2$[S_6]: **Mp**: 96.8-98.9 °C (5 K/min, decomp., THF) **Elem. anal.** found C,

45.0; H, 8.5; N, 6.4; S, 41.7; $C_{18}H_{40}N_2S_6$ requires C, 45.3; H, 8.45; N, 5.9; S, 40.3. **IR** ν_{max}/cm^{-1}: 2955 (w), 2933 (w), 2868 (w), 1457 (w), 1005 (w), 925 (w), 738 (w), 500 (vs), 443 (w). **^{1}H-NMR** (300.1 MHz, DMSO-d_6): $\delta = 0.95$ (t, $^3J_{HH} = 7.1$ Hz, 3H, CH_2CH_3), 1.28-1.40 (m, 2H, CH_2CH_3), 1.71 (br s, 4H), 2.11 (br s, 4H), 3.00 (s, 3H, N*Me*), 3.28-3.36 (m, 2H), 3.41-3.54 (m, 4H) ppm. **^{13}C-NMR** (75.5 MHz, DMSO-d_6): $\delta = 13.5$ (1C), 19.4 (1C), 21.4 (1C), 25.1 (1C), 48.5 (br s, 2C), 63. (br4 s, 2C), 64.0 (br s, 1C) ppm.

Attempt to synthesise bis(N-butyl-N-methylpyrrolidinium)-tetrasulfide ([BMPyr]$_2$S$_4$). [BMPyr][TMS-S] (296 mg, 1.20 mmol, 2.0 eq) was dissolved in THF (15 mL) and added to elemental sulfur (58 mg, 1.8 mmol, 3.0 eq). The mixture immediately turned red, later a red oily substance formed. After three days only a fine red powder remained in a slightly blue-green solution. The suspension was filtered, the precipitate washed with THF (6 mL) and dried in fine vacuum. The precipitate could be identified as $[BMPyr]_2[S_6]$, which was isolated in a yield of 170 mg (0.356mmol, 60%). **Elem. anal.** found C, 45.4; H, 8.8; N, 6.2; S, 41.55; $C_{18}H_{40}N_2S_6$ requires C, 45.3; H, 8.45; N, 5.9; S, 40.3; ($C_{18}H_{40}N_2$**S$_4$** requires C, 52.4; H, 9.8; N, 6.8; S, 31.1).

Synthesis of bis(N,N-dimethylpyrrolidinium)-hexasulfide ([DMPyr]$_2$S$_6$, 11). A suspension of sulfur (201 mg, 6.27 mmol, 4.95 eq) in THF (20 mL) was added to [DMPyr][TMS-S] (520 mg, 2.53 mmol, 2.00 eq).The mixture immediately turned bright red and was stirred for 3 days, after which a fine red precipitate had formed. The solid was filtered, washed with THF (10 mL) and dried in vacuum. $[DMPyr]_2S_6$ was isolated in 485 mg a yield of (1.23 mmol, 98%). **Mp**: 128.2-128.8 °C (5 K/min, decomp., THF). **Elem. anal.** found C, 36.9; H, 7.3; N, 8.4; S, 52.51; $C_{12}H_{28}N_2S_6$ requires C, 36.7; H, 7.2; N, 7.1; S, 50.0. **IR** ν_{max}/cm^{-1}: 2982 (w), 1459 (w), 1000 (w), 975 (w), 935 (w), 818 (w), 503 (vs), 439 (w). **^{1}H-NMR** (300.1 MHz, DMSO-d_6): $\delta = 2.12$ (br s, 4H, CH_2), 3.14 (s, 6H, NMe_2), 3.51 (br s, 4H, NCH_2) ppm. **^{13}C-NMR** (75.5 MHz, DMSO-d_6): $\delta = 22.1$ (2C, CH_2), 52.3 (br s, 2C, NMe_2), 65.8 (br s, 2C, NCH_2).

Crystal Structure Determination

Single crystals of [DMPyr][TMS-Se] (**5**) and [NMe_4][TMS-S] [**6**] were grown by layering a solution in acetonitrile with the equivalent volume of diethyl ether. Crystals of $[DMPyr]_2S_6$ (**11**) were grown by dissolving the substance in a mixture of THF and a small amount of acetonitrile and layering the green solution with pentane. $[BMPyr]_2Se_3$ crystals precipitated from a solution of previously colorless [BMPyr][TMS-Se] in acetonitrile after storage at −25 °C for several weeks. Crystals of $[DMPyr]_4Te_{12}$ grew from a solution of [DMPyr][TMS-Te] in acetonitrile, into which diethyl ether was allowed to diffuse via the gas phase from an attached Schlenk flask. The solution was not kept in the dark.

The data collection for the single crystal structure determinations was performed in rotation method on a Bruker D8 QUEST diffractometer by the X-ray service department of the Fachbereich Chemie, University of Marburg. The spectrometer is equipped with a Mo-K_α X-ray micro source (0.71073 Å, Incotec), a fixed chi goniometer and a PHOTON 100 CMOS detector. Bruker software (Bruker Instrument Service, APEX2, SAINT) was used for data collection, cell refinement and data reduction.[7] The structures were solved with SIR2011[8] or SHELXS,[9] refined with SHELXL-2014[9] and finally validated using PLATON[10] software, all within the WinGX[11] software bundle. Absorption corrections were applied beforehand within the APEX2 software (multi-scan).[12] Graphic representations were created using Diamond.[13] C-bound H-atoms were constrained to parent site; in all graphics the ellipsoids are shown for the 50% probability level. Selected crystal data and experimental parameters are listed in table 2 of the main article. Crystallographic data for the structures reported in this paper are supplied as supporting information and have been deposited with the Cambridge Crystallographic Data Centre. CCDC 1413729-1413733 contain the supplementary crystallographic data for this paper. These data can be obtained free of charge from The Cambridge Crystallographic Data Centre via www.ccdc.cam.ac.uk/data%5Frequest/cif.

Note concerning elemental analysis (CHNS)

Elemental analyses (C, N, H, S) were carried out by the service department for routine analysis and mass spectrometry with a vario MICRO cube (ELEMENTAR). Analysis of hygroscopic or water sensitive and in general air sensitive compounds presents the researcher and the analyst with several difficulties. First of all, under an inert atmosphere minute amounts of substance have to be weighed accurately into tiny tin capsules, which then have to

be firmly closed. This procedure is by now fairly well developed and manageable, thanks to our precision mechanical department and the skilled engineers. However, the capsules usually cannot be closed so tightly, that the enclosed substances endure more than one hour under natural atmosphere. The samples therefore have to be measured manually as soon as they are removed from their protective double enclosure – a standard MS-vial and a slightly larger screw top jar. Also this is well accomplishable thanks to a considerable extra effort of our analytical department. Unfortunately, weighing and closing the samples in a nitrogen filled glove box inevitably leads to nitrogen being trapped inside the capsules. However minute the capsules and the amount of gaseous nitrogen inside, the effect on the analytical results is more than noticeable. In our cases the measured nitrogen content is artificially increased by 0.2 to 1% as can be witnessed in tables S2 and S3. The exact amount is dependent on the actual sample mass, density of the substance and residual volume of the tin capsule, which depends on the actual position where the capsule is sealed. The variability of these parameters excludes a standard correction of the measurement files in the way of a systematic error. Table S2 compares measurements of sulfanilamide (recrystallized five times until analytical results stayed unchanged upon further purification). Samples for the first series of measurements were prepared in a glove box (GB). The samples for the second series were prepared by the service department under natural atmosphere (NA) and contained no residual atmosphere.

Table S1. Comparative elemental analysis of sulfanilamide (GB: glove box, NA: natural atmosphere).

Sulfanilamide		N	C	H	S
calculated		16.27	41.85	4.68	18.62
Preparation type	Sample mass				
GB	1.819	16.87	41.66	4.58	18.87
GB	2.089	16.71	41.59	4.56	18.84
GB	2.417	16.88	41.93	4.43	17.96
GB	2.971	16.79	41.95	4.73	18.06
GB	3.302	16.60	41.77	4.67	18.44
GB	3.328	16.52	41.76	4.65	18.79
GB	3.699	16.49	41.82	4.66	18.67
GB	5.135	16.26	41.83	4.80	18.40
GB	5.490	16.38	41.87	4.58	18.67
	Average	16.61	41.80	4.63	18.52
	Deviation	0.34	−0.05	−0.05	−0.10
Service	2.635	16.26	41.87	4.68	18.60

Service	2.643	16.23	41.88	4.68	18.60
Service	2.674	16.24	41.81	4.68	18.57
Service	2.839	16.33	41.89	4.51	18.35
Service	3.172	16.30	41.88	4.69	18.52
	Average	16.27	41.87	4.65	18.53
	Deviation	0.00	0.02	−0.03	−0.09

A further difficulty presents the analysis of compounds with very high sulfur contents. If a sulfur content of ca. 38% is exceeded, the calibration suddenly fails. As a consequence artificially high sulfur contents are detected, ultimately yielding CHNS percentage sums considerably exceeding 100%. This effect is worsened if large amounts of sulfur rich samples are analyzed, but cannot be avoided if especially small amounts are employed. If less than 2 mg of the sample are employed the accuracy of the CHN values decreases notably. This effect is regardless of the way in which the samples are prepared (glove box or natural atmosphere). To illustrate this phenomenon samples of thiourea (p.a., Grüssing) and Tetramethylthiuramdisulfid (95%, Sigma-Aldrich) have been analyzed (table S3). We ask the attentive reader to keep these results in mind when critically assessing the results of the presented elemental analyses.

Table S2. Comparative elemental analysis of tetramethylthiuramdisulfid and thiourea (GB: glove box, NA: natural atmosphere).

Tetramethylthiuramdisulfid		N	C	H	S	Sum
		11.65	29.97	5.03	53.35	100.00
Type of Preparation	Sample Mass					
GB	1.928	12.29	29.90	4.61	55.37	102.17
GB	2.061	12.00	29.78	4.87	55.96	102.61
GB	2.504	12.07	29.98	4.96	58.09	105.10
GB	3.582	11.93	30.03	5.07	65.05	112.08
	Average:	12.07	29.92	4.88	58.62	
	Deviation:	0.42	−0.05	−0.15	5.27	
NA	2.026	11.67	29.91	4.73	56.01	102.32
NA	2.086	11.65	30.07	4.95	56.66	103.33
NA	2.142	11.62	29.92	4.94	56.71	103.19
NA	2.244	11.66	30.00	4.94	57.25	103.85
	Average:	11.65	29.98	4.89	56.66	
	Deviation:	0.00	0.01	−0.14	3.31	
Thiourea		N	C	H	S	Sum
		36.80	15.78	5.30	42.12	100.00
Type of	Sample Mass					

Preparation						
GB	1.412	37.62	15.55	5.07	42.95	101.19
GB	1.726	37.69	15.66	4.80	41.88	100.03
GB	1.883	37.12	15.49	4.93	42.64	100.18
GB	2.039	37.18	15.47	5.14	42.97	100.76
GB	2.039	37.93	15.79	5.17	43.38	102.27
GB	2.059	37.41	15.63	5.19	43.63	101.86
GB	2.224	37.26	15.56	5.19	43.43	101.44
GB	2.684	37.24	15.65	5.23	44.29	102.41
	Average:	37.43	15.60	5.09	43.15	
	Deviation:	0.63	−0.18	−0.21	1.03	
NA	1.901	36.98	15.64	4.84	42.74	100.20
NA	2.017	36.82	15.58	5.11	42.83	100.34
NA	3.296	36.51	15.72	5.39	46.67	104.29
NA	3.418	36.55	15.71	5.21	46.56	104.03
	Average:	36.72	15.66	5.14	44.70	
	Deviation:	−0.08	−0.12	−0.16	2.58	

References

1. Fulmer, G. R.; Miller, A. J. M.; Gottlieb, H. E.; Sherden, N. H.; Nudelman, A.; Stoltz, B. M.; Goldberg, K. I.; Bercaw, J. E., *Organometallics* **2010,** *29*, 2176-2179.
2. Amarego, W. L.; Perrin, D. D., *Purification of Laboratory Chemicals*. 4th ed.; Elsevier: Burlington, 1996.
3. (a) Kalb, R. Method for Producing 1,3-Heteroaromatic Carbonates Devoid of 4-Carboxylate. WO 2008 052 861, 2008; (b) Kalb, R. Method for Producing Quaternary Carbonates. WO 2008 052 860, 2008.
4. (a) Holbrey, J. D.; Rogers, R. D.; Shukla, S. S.; Wilfred, C. D., *Green Chem.* **2010,** *12*, 407-413; (b) Chiappe, C.; Rajamani, S., *Pure Appl. Chem.* **2011,** *84*, 755; (c) Chiappe, C.; Sanzone, A.; Dyson, P. J., *Green Chem.* **2011,** *13*, 1437-1441; (d) Earl, G.; Weisshaar, D.; Paulson, D.; Hanson, M.; Uilk, J.; Wineinger, D.; Moeckly, S., *J. Surfactants Deterg.* **2005,** *8*, 325-329; (e) Albert, B.; Jansen, M., *Z. Anorg. Allg. Chem.* **1995,** *621*, 1735-1740; (f) Weisshaar, D.; Earl, G.; Amolins, M.; Mickalowski, K.; Norberg, J.; Rekken, B.; Burgess, A.; Kaemingk, B.; Behrens, K., *J. Surfactants Deterg.* **2012,** *15*, 199-205; (g) Selva, M.; Fabris, M.; Lucchini, V.; Perosa, A.; Noe, M., *Org. Biomol. Chem.* **2010,** *8*, 5187-5198.
5. (a) So, J.-H.; Boudjouk, P., *Synthesis* **1989**, 306-307; (b) DeGroot, M. W.; Taylor, N. J.; Corrigan, J. F., *J. Mater. Chem.* **2004,** *14*, 654-660.
6. Nieboer, J.; Haiges, R.; Hillary, W.; Yu, X.; Richardet, T.; Mercier, H. P. A.; Gerken, M., *Inorg. Chem.* **2012,** *51*, 6350−6359.
7. Bruker *Bruker Instrument Service v3.0.26, APEX2 v2012.10-0, SAINT v8.27B*, Bruker AXS Inc.: Madison, Wisconsin, USA, 2012.
8. Burla, M. C.; Caliandro, R.; Camalli, M.; Carrozzini, B.; Cascarano, G. L.; Giacovazzo, C.; Mallamo, M.; Mazzone, A.; Polidori, G.; Spagna, R., *J. Appl. Cryst.* **2012,** *45*, 357-361.
9. Sheldrick, G., *Acta Crystallogr. A* **2008,** *64*, 112-122.
10. Spek, A. L., *Acta Crystallogr. D* **2009,** *65*, 148-155.
11. Farrugia, L., *J. Appl. Cryst.* **2012,** *45*, 849-854.
12. Bruker *SADABS v2012/1*, Bruker AXS Inc.: Madison, Wisconsin, USA, 2012.
13. Brandenburg, K.; Putz, H. *Diamond - Crystal and Molecular Structure Visualization v3.2i*, Crystal Impact GbR: Bonn, Germany, 2012.

6.4 Kohlenstoffdioxid- und Schwefeldioxid-Addukte von N-heterozyklischen Olefinen: Strukturen und interessante Reaktivitätsmuster

in preparation

N-Heterocyclic Olefin – Carbon Dioxide and Sulfur Dioxide Adducts: Structures and Interesting Reactivity Patterns

Lars H. Finger, Jannick Guschlbauer, Klaus Harms, Jörg Sundermeyer

N-Heterocyclic Olefin – Carbon Dioxide and Sulfur Dioxide Adducts: Structures and Interesting Reactivity Patterns

Lars H. Finger,[a] Jannick Guschlbauer,[a] Klaus Harms,[a] Jörg Sundermeyer[a,*]

a) Fachbereich Chemie and Materials Science Centre,
Philipps-Universität Marburg,
Hans-Meerwein-Str. 4,
35043 Marburg,
Germany.
*E-Mail: JSU@staff.uni-marburg.de

TOC Graphic

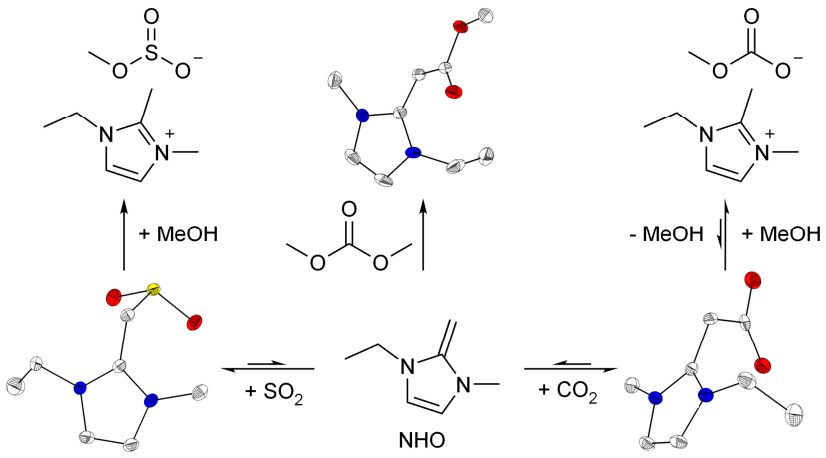

Abstract

Depending on the amount of methanol present in solution, CO_2 adducts of N-heterocyclic carbenes (NHC) and N-heterocyclic olefins (NHO) were found to be in fully reversible equilibrium with the corresponding methylcarbonate salts [EMIm][OCO_2Me] and [EMMIm][OCO_2Me]. The reactivity pattern of representative 1-ethyl-3-methyl NHO-CO_2 adduct **4** is investigated and compared with the corresponding NHC-CO_2 zwitterion: protonation of **4** with HX leads to imidazolium salts [NHO-CO_2H][X] which decarboxylate to [EMMIm][X] in the presence of nucleophilic catalysts. NHO-CO_2 zwitterion **4** can act as an efficient carboxylating agent towards CH-acids such as acetonitrile. The formed [EMMIm] cyanoacetate and [EMMIm]$_2$ cyanomalonate salts exemplify the first C-C bond forming carboxylations with NHO-activated CO_2. Reaction of the free NHO with dimethyl carbonate selectively leads to methoxycarbonylated NHO which is a perfect precursor in the synthesis of functionalized ILs [NHO-CO_2Me][X]. The first NHO-SO_2 adduct is structurally characterized and shows a similar reactivity pattern allowing the synthesis of imidazolium methylsulfites upon reaction with methanol.

Introduction

Employing dimethyl carbonate as mild and non-poisonous methylation agent for nucleophilic cation precursors is by far the most widely applicable way to synthesize ionic liquids (ILs) in a sustainable metal and halide free fashion.[1] This procedure towards methyl-onium methylcarbonates tolerates a vast number of starting nucleophiles, the only requirements being the thermal stability of the reagent towards elevated temperatures of ca. 130 °C and stability of the resulting IL cations towards the basic and nucleophilic, potentially weakly solvated methylcarbonate anion and towards unselective cation carboxylations. In this respect, pentamethylguanidine is one of the few nucleophiles not suitable: A hexamethylguanidinium cation is attacked, while sterically more protected methyl-pentaalkylguanidinium cations are inert towards nucleophilic attack of methylcarbonate at 130°C.[1g] 1-Alkylimidazoles as nucleophiles are just at the borderline of usability, as the ring protons of the resulting N-heterocyclic cations are sufficiently acidic to be engaged in follow-up reactions. This requires careful elucidation of the procedure to find reaction conditions yielding only the desired 1-alkyl-3-methylimidazolium methylcarbonate salts.[1a] If their methylcarbonate anion is not stabilized by solvating hydrogen bridges e.g. of a methanol solution, these salts tend to decompose to form imidazolium carboxylate zwitterions.[1f, 1j] The latter are formed *via*

deprotonation of the imidazolium cation and attack of the *in situ* generated NHC at CO_2. They proved to be highly versatile reagents themselves. Specifically, the imidazolium-2-carboxylates can be employed as proto-carbenes in the formation of transition metal complexes,[2] act as CO_2 transfer reagents and organocatalysts[3] and can still be used as masked carbenes for the synthesis of ILs by reaction with sufficiently acidic reagents.[1f, 4] The specific conditions which allow the removal of the CO_2 moiety generating a reactive carbene or the original imidazolium cation have been thoroughly investigated.[2b, 3a, 3b, 5] Due to their fascinating properties, the access to these NHC inner salts has been studied extensively. Considering the sometimes ambiguous results, it has to be noted that the exact dependence of the product on the reaction conditions is still not fully understood. According to literature reports imidazolium-2-carboxylates can be prepared selectively by feeding gaseous CO_2 into a solution of the corresponding carbene,[6] directly from 1-methyl-imidazole and dimethyl carbonate,[1f, 4c] in continuous flow at 200 °C on an Al_2O_3 catalyst[7] and even at ambient temperature by introducing CO_2 into imidazolium acetate ILs.[8] Specifically the latter and the first approach allow the extension to imidazolium-2-thio- and dithiocarboxylates.[9] The usually undesired 4- and 5- carboxylates are typically formed at elevated temperatures[10] but have also been witnessed at temperatures as low as 120 °C.[11] Recent investigations have shown that their formation is also dependent on the CO_2 partial pressure and the basicity of the reaction mixture.[12]

The introduction of a methyl group at the C2 position of the imidazolium ring, which is also accompanied by a distinct elevation of the respective melting points, is typically regarded as a protection against undesired side reactions due to the acidic proton. Recent investigations have shown that a much more sophisticated substitution pattern is necessary to create imidazolium cations, which are long time stable towards strong nucleophiles and bases like the hydroxide ion, even if they are solvated.[13] However, starting from methylcarbonate salts, so far no carboxylate formation was observed on the apical methyl group.[1e] It was already noted, though, that the C2-methyl group showed decreased or diffuse signals in the presence of hydrogen- or methylcarbonate anions, which can be attributed to an H/D exchange and implies the intermediate formation of a *N,N*-ketenediacetal or N-heterocyclic olefin (NHO).[14] The selective synthesis of such imidazolium-2-methylencarboxylates was achieved conveniently from the *in situ* generated NHOs and CO_2. These compounds have proven as efficient organocatalysts for the carboxylative cyclization of CO_2 and propargylic alcohols, yielding α−alkylidene cyclic carbonates.[15] The procedure can be extended to COS and CS_2

adducts,[16] the effect of the imidazolium substitution pattern on the reactivity was investigated in detailed computational studies.[17] The N-heterocyclic olefins, which are generated *in situ* and most likely the active species in these catalytic cycles have also been employed as polymerization catalysts for propylene oxide[18] and methyl methacrylate.[19] Furthermore they are interesting ligands in main group and transition metal complexes.[20]

During our investigations, which were primarily concerned with the preparation of organic salts with hydrochalcogenide and trimethylsilylchalcogenolate anions[1i, 1j] we noticed a selective and easy access to imidazolium-2-carboxylates and discovered that 1,3-dialkyl-2-methyl-imidazolium methylcarbonate salts form carboxylate zwitterions as well. As a consequence we investigated, if these zwitterionic imidazolium-2-methylencarboxylates, formally NHO-CO_2 adducts, show to some extent comparable reactivity to the well-known imidazolium-2-carboxylates, formally NHC-CO_2 adducts, with regard to the preparation of ionic liquids and in C-C coupling reactions.

Results

Formation of Imidazolium-2-carboxylate and Imidazolium-2-methylencarboxylate

It has proven advantageous to prepare 1-alkyl-3-methylimidazolium methylcarbonate salts from the corresponding alkyl imidazole and dimethyl carbonate in the presence of methanol, which not only accelerates the methylation but also prevents the formation of the undesired 4-carboxylates.[1a] As the resulting solutions typically contain some excess dimethyl carbonate and small amounts of colored impurities,[1d] we chose to isolate the respective salts by evaporation of solvent methanol and recrystallization of the solid residue from acetonitrile. During these preparations we noticed that in case of 1-ethyl-3-methylimidazolium (EMIm) methylcarbonate (**1**) even at ambient temperature only the respective 2-carboxlate (**2**) is obtained (Scheme 1). In view of the high basicity of the methylcarbonate anion and the instability of the forming methyl carbonic acid this has to be expected.

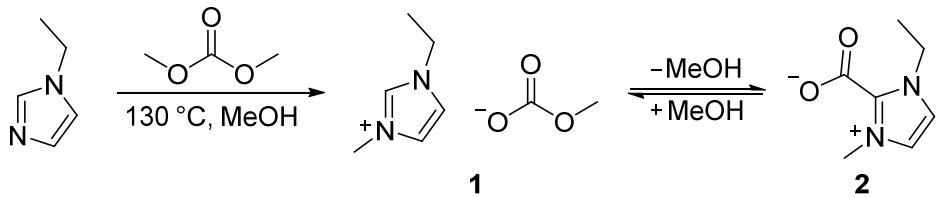

Scheme 1. Known synthesis of EMIm methylcarbonate (**1**) and up to quantitative shift between **1** and NHC-CO_2 adduct **2** at room temperature.

The driving force of this reaction is the removal of methanol in vacuum, which slowly shifts the methylcarbonate–carboxylate equilibrium towards **2**. The reaction proved to be perfectly reversible in NMR experiments. The process can be compared with the removal of acetic acid in the gas stream of CO_2 introduced into imidazolium acetate ILs.[8a]

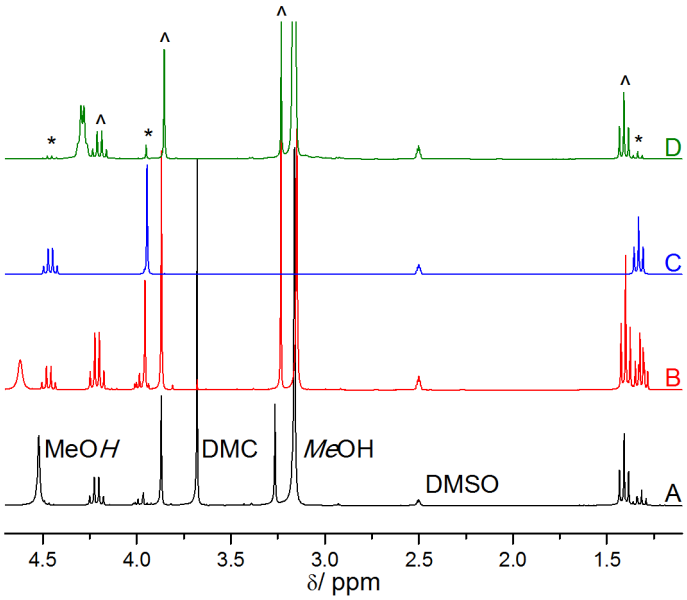

Figure 1. ^{1}H NMR spectra (300.1 MHz, DMSO-d_6) of A) the reaction mixture of Scheme 1 directly after the solvothermal synthesis, B) the residue of the reaction mixture after removing most of the solvent, C) the isolated EMIm-CO_2 (**2**) after recrystallization and D) the sample of C with an excess of methanol (**1**).

The NMR spectra in Figure 1 clearly show that the imidazolium carboxylate (**2**, marked by *) is not primarily formed during the solvothermal synthesis, but that only minimum amounts prevail in the reaction mixture next to the main product imidazolium methylcarbonate (**1**, marked by ^). Spectrum A also shows large amounts of methanol and dimethyl carbonate and minor amounts of ethyl imidazole which did not react. Only if the solvent is removed the carboxylate forms to a larger extent (B) until after thorough drying and recrystallization the pure carboxylate is obtained (C). If an excess of methanol (eight equivalents in this instance) is added to the NMR sample of C) the carboxylate is very quickly transformed back to the methylcarbonate. Despite the large excess of eight equivalents of methanol ca. 10% of the carboxylate zwitterion remain in the NMR sample even after several hours, which lets us conclude that equilibrium conditions are reached and only a larger excess will allow the full regeneration of the methylcarbonate. With respect to green IL synthesis protocols, this additional information is important as zwitterion **2** does not show an equally high activity in proton induced decarboxylation reactions as the methylcarbonate salt **1.**[1f, 4a] In our investigation of hydrochalcogenide ILs[1k] we also noticed, that higher concentrated methanol solutions of the carboxylate **2** react significantly slower than dilute solutions containing only

the methylcarbonate salt. A mixture of non-separable products can be the undesirable consequence in these IL syntheses.

The C2-methylated 1-ethyl-2,3-dimethylimidazolium (EMMIm) cation is engaged in an analogous highly selective reaction pattern, although not as much shifted to the zwitterion **4** as in case of imidazolium cations bearing a proton at C2 position (Scheme 2).

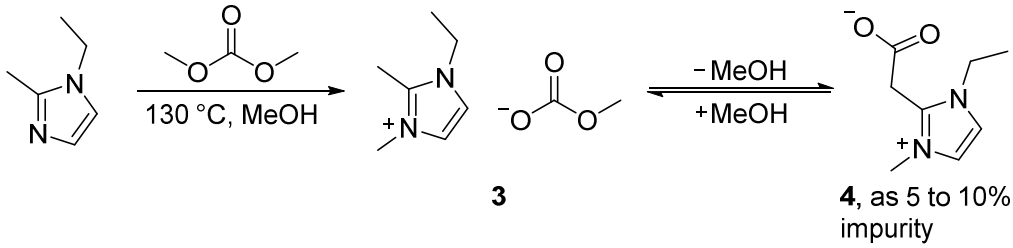

Scheme 2. Preparation of EMMIm methylcarbonate (**3**) and partial equilibrium shift between **3** and NHO-CO_2 adduct **4** at room temperature.

During the preparation of **3** we noticed the occurrence of slightly varying 5-10% amounts of a side product after the work-up, which we could later on identify as the corresponding NHO-CO_2 adduct 1-ethyl-3-methylimidazolium-2-methylencarboxylate (**4**).

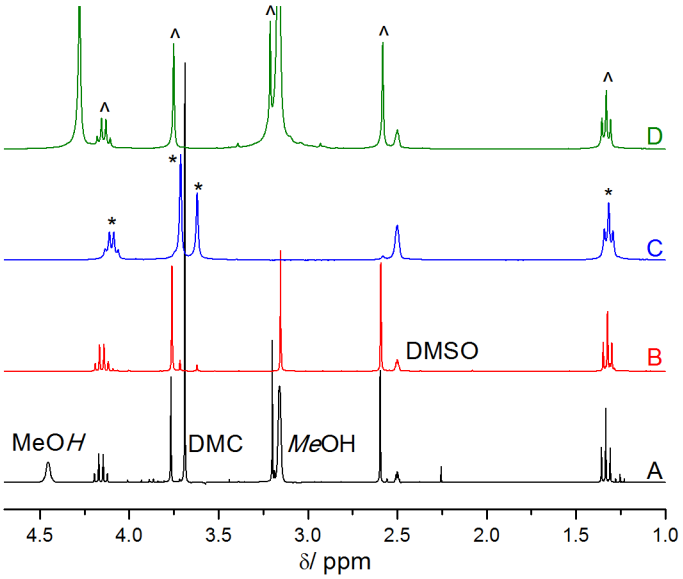

Figure 2. ^{1}H NMR spectra (300.1 MHz, DMSO-d_6) of A) the reaction mixture of Scheme 2 directly after the solvothermal synthesis in MeOH (130°C), B) the residue of the reaction mixture after removing most of the solvent, C) the isolated EMMIm-CO_2 (**4**) synthesized according to ref.[15] and D) the sample of C with an excess of methanol (**3**).

Analogously to the preceding synthesis, this side product is not present in the crude reaction mixture (Figure 2, A) but is formed at ambient temperature upon evaporating all volatile components and recrystallization from a acetonitrile diethyl ether solvent mixture, indicated by the small additional signals at 3.62 and 3.72 ppm (Figure 2, B). If the recrystallized

compound mixture is heated to 80 °C under a CO_2 atmosphere (1 bar) or in vacuum a significant increase of the 2-methylencarboxylate species compared with the original methylcarbonate salt is observed. This did not allow convenient synthesis of pure product, though. To gain access to a pure reference sample of the carboxylate **4** (Figure 2, C), the procedure of Wang et al.[15] starting from NHO and CO_2 was employed. Even with this pure standard **4** dissolved in DMSO, an immediate back-formation of the methylcarbonate salt is observed upon addition of excess methanol (Figure 2, D).

These observations lead to a partial reinterpretation previous results, where the formation of carboxylate impurities was solely traced back to the elevated reaction temperatures.[1e] The authors avoided the formation of carboxylate impurities by decreasing the reaction temperature to 70 °C while extending the reaction time to 10 days. This might shift the reaction path from thermodynamic into kinetic control. While attempting to reproduce this low temperature methylation by DMC in a sealed glass ampoule we observed only low conversion to a variety of unidentified products. None of these was the anticipated methylcarbonate salt. It is known, that at temperatures around 90 °C a methoxycarbonylation by DMC is preferred. Only if a reaction mixture is heated to above 120 °C under solvothermal conditions, DMC acts as a methylation agent.[21] With the findings presented here, we are convinced that the progressive removal of methanol induces two effects working hand-in-hand: Less solvated methylcarbonate anions act as a stronger base and the elimination of the reaction product methanol shifts the equilibria of these thermodynamically controlled (reversible) carboxylations quantitatively towards NHC-CO_2 or partly towards NHO-CO_2 adduct formation, even at room temperature.

It is anticipated, that increased anion basicity allows the formation of higher amounts of the NHO-CO_2 adduct **4**. This is exemplified by our attempted synthesis of 1-ethyl-2,3-dimethylimidazolium *tert*-butylthiolate (**5**) from the corresponding methylcarbonate precursor In contrast to H_2S,[1i, 1k] the weaker acid tBuSH is not deprotonated by 1-ethyl-2,3-dimethylimidazolium methylcarbonate in MeOH to any amount detectable by ^{1}H NMR. Apparently the solvated anion tBu-S^-(MeOH) is more basic than $MeOCO_2^-$(MeOH). In order to gain some extra driving force by Si-O bond formation, we now employed our method to use methylcarbonate as nucleophilic desilylating agent[1j] towards *t*BuS-TMS **6** under aprotic conditions. As expected TMS-OMe is formed in acetonitrile, however, the basic alkylthiolate anion formed initially, apparently leads to deprotonation of the 2-methyl-imidazolium cation,

forming the NHO **7,** which rapidly reacts with CO_2 released from the previous reaction step to form zwitterionic carboxylate **4** (Scheme 3).

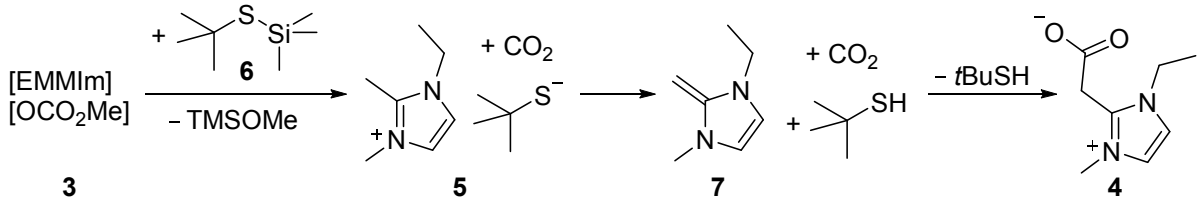

Scheme 3. Attempted synthesis of 1-ethyl-2,3-dimethylimidazolium tert-butylthiolate (**5**) in acetonitrile.

As a result, instead of the anticipated thiolate salt, the 2-methylencarboxylate **4** was isolated in 36% yield as crystallized, pure compound. The synthesis of **5** is also accomplished, by reacting the *in situ* prepared NHO with *tert*-butyl mercaptane. The 2-methylimidazolium cation is stable towards an unsolvated tert-butylthiolate anion (see XRD analysis below), but only in the absence of CO_2 as NHO trapping agent. In contrast the reaction of the imidazolium methylcarbonate **3** with bis(trimethylsilyl)sulfide leads to the imidazolium trimethylsilylthiolate **8** in good yield and acceptable purity. The only impurities are ca. 5% unreacted zwitterion **4,** which had been present as now expected side product in the EMMIm methylcarbonate starting material.

With this method of generating thiolates at hand, we could establish a competition experiment (Scheme 4): Salt **5** containing the stronger *tert*-butyl thiolate base is carboxylated in acetonitrile at 20 °C whereas **8** containing the weaker TMS-thiolate base is not carboxylated to NHO-CO_2 adduct **4**: After 30 minutes passing CO_2 over a solution of **5**, 32% conversion to **4** could be observed by ^{1}H NMR monitoring.

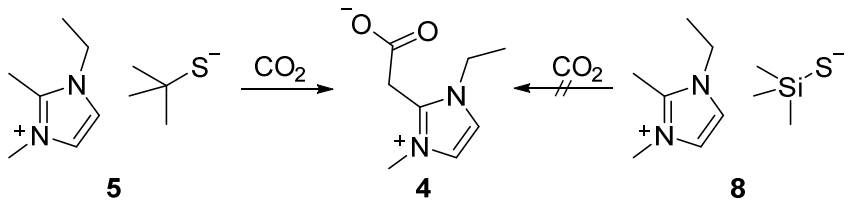

Scheme 4. Differing reactivity of **5** and **8** towards CO_2.

Anion Cation Interactions in the Crystalline State

The structures of all three imidazolium compounds in Scheme 4 could be elucidated by single crystal X-ray structure determination. Single crystals of the zwitterion **4** were obtained by slowly cooling a warm concentrated solution in DMSO to ambient temperatures. The molecular structure of **4** is analogous to known examples and will not be discussed in

detail.[15] Crystals of silylthiolate **8** and *tert*-butylthiolate **5** were grown by layering a concentrated solution in acetonitrile with diethyl ether or with THF/Et_2O, respectively. Crystallographic details of these and following structures can be found in the SI. The structures of **5** and **8** both exhibit a hydrogen bonding network between the imidazolium cation and the respective anion. However, the increased basicity of the *tert*-butylthiolate does not lead to a shortening of the hydrogen bonds. In both compounds stronger contacts are formed to the aromatic C4H and C5H groups. If only the shortest hydrogen bonds are considered the structure can be interpreted as dimers where two anion stabilizing imidazolium cations are connected via two thiolate anions (Figure 3).

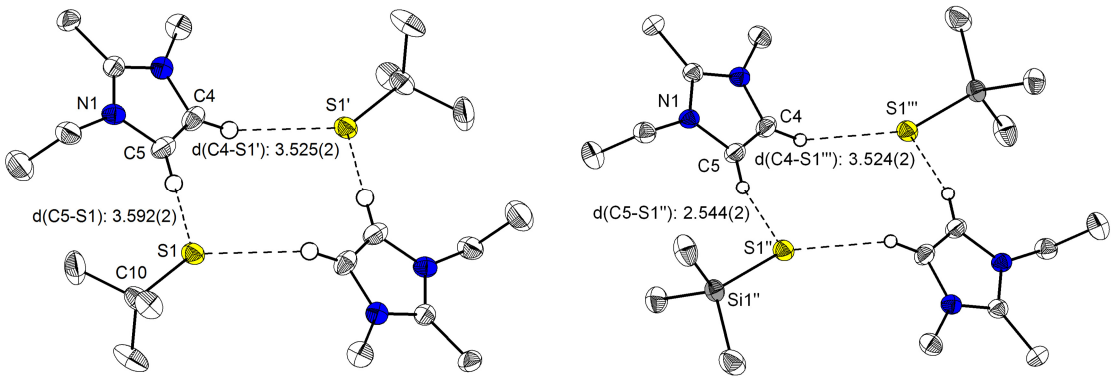

Figure 3. Molecular structure of the H-bonded dimers in [EMMIm][tBu-S] (**5**, left) and [EMMIm][TMS-S] (**8**, right); H-Bond (donor acceptor) distances in Å; disordered position of the tBu-S anion and THF solvate molecule of **5** not shown for clarity; symmetry operations: **I:** −x+1, −y+2, −z+2, **II:** x, −y+1/2, z+1/2, **III:** −x+1, y+1/2, −z+1/2.

This motif is found in both structures, while the overall structure of **5** is complicated by a rotary disorder of the anion and an additional THF solvate molecule. The latter may account for the increased H-bonding distance between C5-H···S1 of 3.592(2) Å in compound of **5**, compared to 3.544(2) Å in compound **8**. The aliphatic CH moieties show distinctively longer contacts, which is in agreement with the respective hydrosulfide salt.[1i]

Decarboxylation Behavior of NHO-CO_2 Adduct 4

Imidazolium-2-carboxylates have already proven as valuable starting materials for the synthesis of ionic liquids under protic conditions.[4a, 4c] The strong solvent dependence of the decarboxylation was investigated by Denning and Falvey.[5b] For us the question arose, whether the 2-methylencarboxylate **4** analogously allows the synthesis of corresponding organic EMMIm salts upon reaction with Brønsted acids. The observation that formation of **4** is reversible upon addition of methanol in DMSO strongly points to this possibility. Consequently we reacted **4** with HTFSI, HTFA and NH_4PF_6 in methanol and acetonitrile.

From the reaction with NH_4PF_6 the expected decarboxylation product [EMMIm][PF_6] (**9**) was isolated in quantitative yield (Scheme 5).

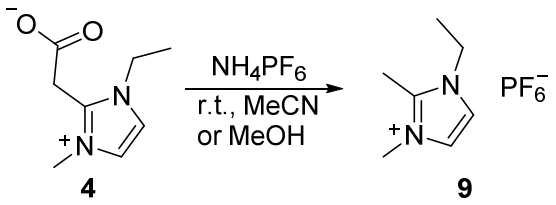

4 **9**

Scheme 5. Synthesis of [EMMIm][PF_6] (**9**) from NHO-CO_2 adduct **4** and NH_4PF_6.

However, when reacting **4** and bis(trifluoromethylsulfonyl)imide (HTFSI) at ambient temperature, regardless of the reaction time and the solvent (methanol or acetonitrile) only a marginal amount of the anticipated product forms (Figure 4, Spectrum B).

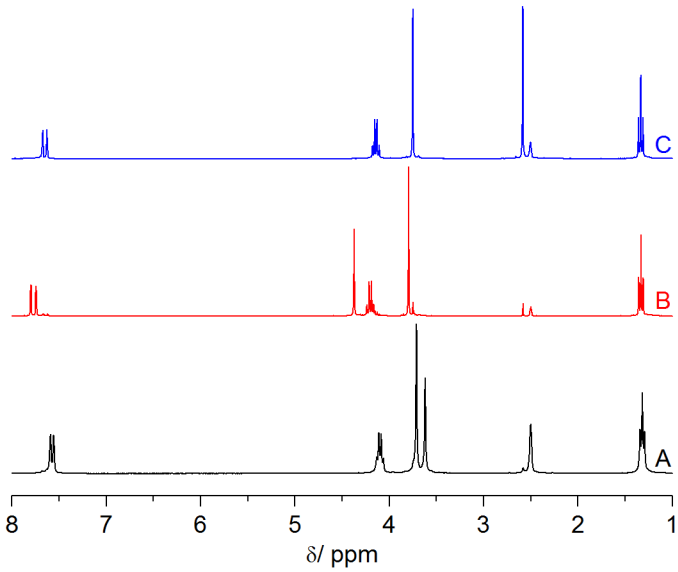

Figure 4. ^{1}H NMR spectra (300.1 MHz, DMSO-d_6) of the reaction between NHO-CO_2 (**4**, A) and HTFSI after 4 days at ambient temperature (**10**, B) and after further 3 hours at 80 °C (**11**, C).

Ca. 90% of the sample consisted of a so far unknown cationic species, which showed all signals of the preceding zwitterion, but at different chemical shift. In the ^{1}H NMR spectra especially the resonance signal of the CH_2 group adjacent to the carboxylate moiety is shifted strongly down field. Furthermore an additional signal appeared which had to be assigned to a proton with a certain degree of dynamics due to its broadened appearance and chemical shift of ca. 15 ppm. All findings indicate the formation of a stable carbonic acid intermediate [NHO-CO_2H][TFSI] (**10**). The small amount of final product is attributed to the isomeric C4 and C5 carboxylates which were observed as minor side products in the formation of **4** and apparently reacted with the strong acid under immediate decarboxylation. The ESI(+) mass spectrometric detection of the intermediate cation of **10** was not possible − only the

decarboxylated cation is observed − but IR spectra confirm the presence of C=O and O-H bonds. Analogous results were obtained from the reaction of **4** with trifluoroacetic acid. Apparently, under specific circumstances the CO_2 elimination apparently is kinetically hindered for the NHO-CO_2 adduct. The decarboxylation occurs quickly, though, upon heating of the reaction mixture to 60 °C to 80 °C (Figure 4, Spectrum C). Overall a temperature dependent reaction behavior of **4** with strong acids has to be considered (Scheme 6).

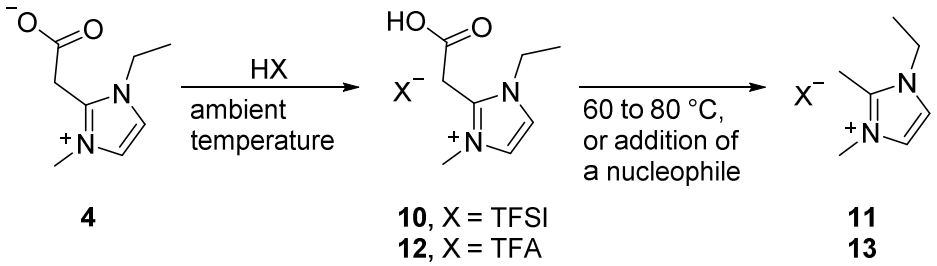

Scheme 6. Reactions of NHO-CO_2 adduct **4** with trifluoroacetic acid and bis(trifluoromethylsulfonyl)imide in methanol or acetonitrile.

This result is surprising in view of our previous observation that **4** can be converted to EMMIm methylcarbonate (**3**) by methanol in DMSO at ambient temperature. Weak acids seem to promote a decarboxylation path, which is hampered by a higher activation barrier for strong acids. It is presumed that this reactivity difference can be correlated to the nucleophilicity of the particular conjugate base and that CO_2 elimination does not occur in a spontaneous unimolecular fashion but demands the attack of a nucleophile at the carboxylate C-atom, similar to the Krapcho decarboxylation.[22] Accordingly, better nucleophiles such as DMSO or NH_3 present in equilibrium with NH_4^+ will allow a faster reaction, while weak nucleophiles like TFA and TFSI anions under acidic conditions lead to a significant increase of the activation barrier. This theory is substantiated by the observation that addition of sub-stoichiometric amounts (30 mol%) of nucleophilic catalysts such as 4-dimethylaminopyridine leads to the formation of the anticipated imidazolium salts **11** and **13** already at ambient temperature. A related observation was made by Rogers and coworkers, who noticed that 1,3-dimethyl-2-carboxylate reacted with almost all acids under decarboxylation to form the corresponding 1,3-dimethylimidazolium salts, but that upon reaction with nitric acid a carbonic acid intermediate occurred as very stable intermediate. This could be transformed to the desired IL by either heating to 140 °C or by dissolving the substance in DMSO, which allowed the transformation at ambient temperature.[4a]

These observations let us conclude, that under most circumstances the possible formation of the carboxylate will not influence the preparation of ILs with Brønsted acidic reagents.

However, care has to be taken if the methylcarbonate salt is isolated prior to follow up reactions and if the anion, which is to be introduced, shows a low nucleophilicity. With these prerequisites it is mandatory to carry out the reaction at elevated temperatures to avoid contamination of the final product with carboxylate impurities.

NHO-CO_2 Adduct 4 as Carboxylation Agent for Acetonitrile

During a preliminary exploration of the reaction of the CO_2 masked NHO **4** with CH acidic reaction partners, we noticed an interesting C-C coupling of CO_2 and MeCN to occur. Heating the weakly soluble zwitterion **4** in acetonitrile yields a well soluble orange oil which slowly solidifies upon thorough drying in fine vacuum. The substance could be identified as 1-ethyl-2,3-dimethylimidazolium cyanoacetate (**14**) from its NMR and MS spectra. Furthermore, a small amount of the cyanomalonate salt **14a**, which results from a second deprotonation and attack at CO_2, is present (Scheme 7). The cyanomalonate salt **14a** appears to be formed in equilibrium with the main product cyanoacetate **14** and NHO-CO_2 adduct **4** as it is found in almost identical percentages (ca. 10%) regardless of the reaction temperature, reaction time and initial NHO-CO_2 concentration in acetonitrile. If **14a** would be the final product and not in equilibrium with **14** the formed amount should significantly vary when different reactant dilutions are employed (the concentration of **4** in acetonitrile was varied from 0.034 mol·L^{-1} to 1.68 mol·L^{-1}). Such equilibrium is also formed in DMSO solution. If pure **14a** is dissolved in DMSO-d_6 the compound immediately starts to disproportionate to **14** and the NHO-CO_2 adduct **4**. If equimolar amounts of pure NHO-CO_2 adduct **4** and isolated cyanoacetate **14** are combined in DMSO-d_6 an analogous product mixture is formed consisting of **4**, **14** and **14a** in the approximate percentages 35%, 48% and 17%, respectively (see SI for details).

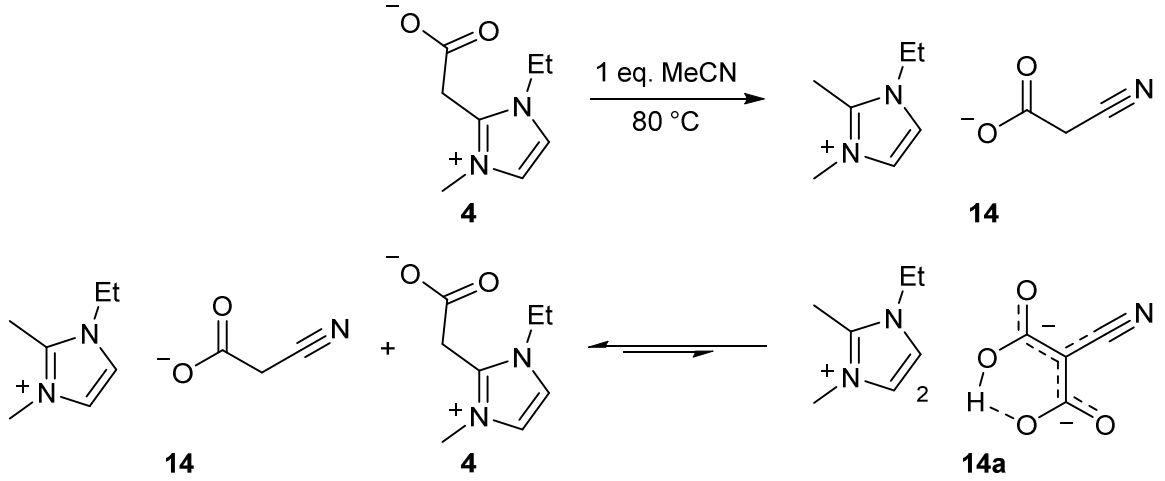

Scheme 7. Formation of the imidazolium cyanoacetate **14** and cyanomalonate **14a** from **4** and acetonitrile.

To conveniently separate the two salts the raw product is triturated with dichloromethane, which selectively dissolves **14** but not the dianion based salt **14a**. The isolated yields are 64% for **14** and 10% for **14a**. **14a** could be structurally characterized from single crystals, which formed from a saturated acetonitrile solution of the raw product layered with diethyl ether. These reactions serve as first examples where an N-heterocyclic olefin NHO acts as an organic mediator for C-C bond coupling carboxylations of CH acidic positions by NHO activated CO_2. A related C-O bond formation was already described by Wang et al. who employed NHO-CO_2 adducts as catalysts for the carboxylation of propargylic alcohols and propylene oxides yielding cyclic α-alkylidene and propylene carbonates, respectively.[15-16] Figure 5 depicts the molecular structure of the cyanomalonate **14a**.

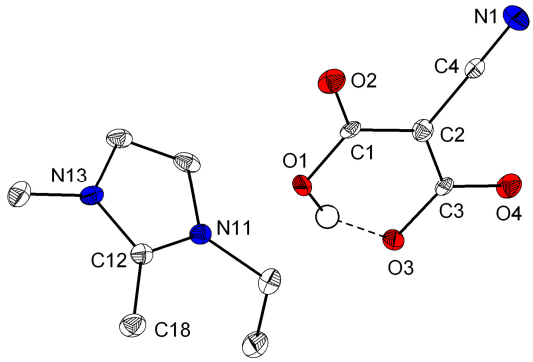

Figure 5. Molecular structure of $[EMMIm]_2[NC\text{-}C(CO_2)_2H]$ (**14a**), the second cation molecule, cation hydrogen atoms and a disordered position of the anion were omitted for clarity; relevant bond distances/ Å and angles/ °: C1-O1: 1.327(3), C1-O2: 1.247(3), C1-C2: 1.427(3), C2-C3: 1.443(3), C2-C4: 1.433(3), C4-N1: 1.154(4), C3-O3: 1.309(3), C3-O4: 1.253(3), O1-H1···O3: 2.432(2), O1-C1-O2: 119.9(2), C1-C2-C3: 124.1(2), O3-C3-O4: 122.0(2), C2-C4-N1: 179.2(2).

The cyanomalonate dianion is fully planar; the remaining hydrogen atom is not located at the central C2 atom but at O1 and is involved in an intramolecular hydrogen bond to O3 (O1-H1···O3: 2.432(2) Å). Two negative charges are delocalized, indicated by elongated C=O bonds (C1-O1: 1.247(3) Å, C3-O4: 1.253(3) Å) and shortened C-C bonds (C1-C2: 1.427(3) Å, C2-C3: 1.443(3) Å, C2-C4: 1.433(3) Å). Also the nitrile group shows a minor elongation attributable to the delocalization (C4-N1: 1.154(4) Å). The precipitation of a cyanomalonate salt was also observed by Van Ausdall *et al.* who combined 1,3-di-*tert*-butylimidazolium-2-carboxylate and acetonitrile.[23] The C-O bond lengths of this reference dianion agree very well with the present structure. The C-C bonds show a slightly different distribution indicative of somewhat less equally delocalized negative charges. In contrast to NHO-CO_2 adduct **4** the NHC-CO_2 adduct **2** did not lead to such selective carboxylation of acetonitrile, even under solvothermal conditions at 120°C. These observations are in accord

with the interpretation, that the *tert*-butyl substituted carbene (van Ausdall)[23] and NHO (this work) are sufficiently basic to assist the deprotonation of the CH acid while NHC **16** is not basic enough. The preliminary results presented here require a more detailed investigation of NHO mediated – in the presence of strong inorganic bases maybe even catalytic − carboxylations of CH acidic compounds.

Further C-C Coupling Reactions of NHO-CO_2 Adduct 4

We also reacted NHO-CO_2 adduct **4** with dimethyl carbonate hoping for either a selective O-methylation or, after decarboxylation, a C-methoxycarbonylation or C-methylation of the NHO. The latter reaction would be related to known NHC chemistry, precisely the methylation-deprotonation-methylation sequence at the C2 position of an NHC-CO_2 adduct, which was observed by Annese *et al*. and in sum led to a C2-ethylation by dimethyl carbonate at high temperatures.[24] However, at temperatures of 190 °C or 150 °C, reaction of **4** with dimethyl carbonate, led to a rather unselective decomposition of the reactants. Neither by NMR spectroscopy nor by ESI mass spectrometry, have we found evidence for a C-methylation leading to a 2-ethylimidazolium derivative. Upon further decreasing the reaction temperature a partly selective reaction could be achieved. The reaction of **4** with dimethyl carbonate at 90 °C resulted in a mixture of only three compounds. One of the major components of the mixture could be identified as methoxycarbonylated NHO **15** (Scheme 8).

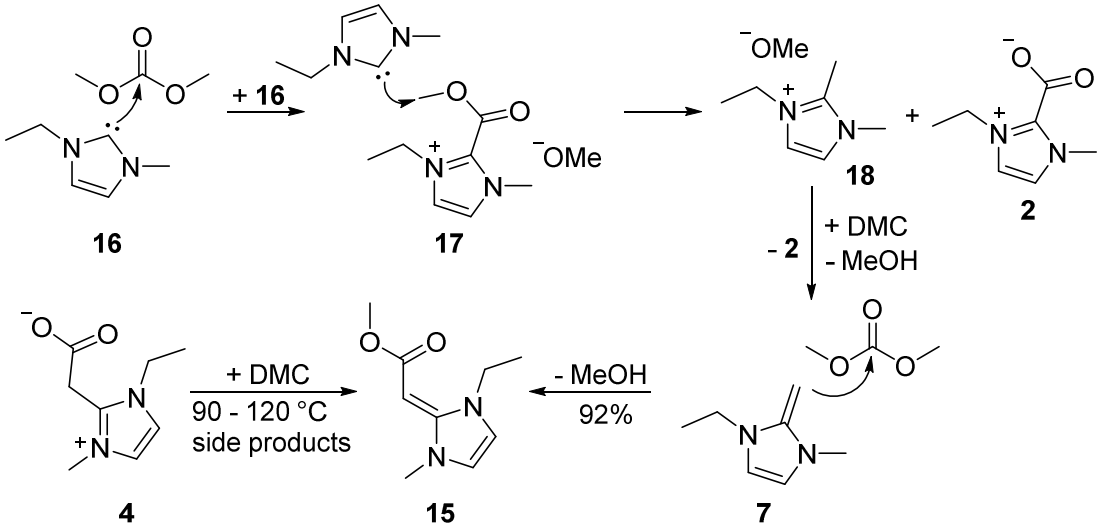

Scheme 8. Reactivity of NHC **16** and NHO **7** and its CO_2 adduct **4** towards dimethyl carbonate (DMC) and a proposed mechanism for the formation of **15** from NHC **16** and dimethyl carbonate.

The relative amount of this component **15** but also the number of side reactions was increased if the reaction temperature was set to 120 °C. The formation of **15** may occur in two ways, e. g. in a methylation of the carboxylate moiety and consequent deprotonation of the cation by

the formed methylcarbonate anion. However, as pointed out before, dimethyl carbonate does not typically act as a methylation agent below 120 °C. The alternative is a temperature induced decarboxylation of the NHO-CO_2 zwitterion, *in situ* formation of the NHO and consequent attack of this nucleophile at the central C atom of DMC: During a nucleophilic substitution reaction at the carbonyl group and in the presence of available protons, methanolate may act as leaving group deprotonating the imidazolium moiety and forming **15**. This scenario is supported by the observation that the corresponding unsubstituted NHO **7**, generated *in situ* from [EMMIm]Br and KH, very selectively reacts with dimethyl carbonate at ambient temperature to form the methoxycarbonylated NHO **15**.

Surprisingly, NHC **16**, generated in situ from [EMIm]Br and KH, is transformed into C-C coupling product **15** as well upon reaction with dimethyl carbonate. **15** is found in a mixture with the NHC-CO_2 adduct **2** in a 4 to 6 ratio (Scheme 8). To explain the joint formation of these species, it is assumed, that the carbene attacks dimethyl carbonate preferably at the carbonyl carbon atom leading to a cationic 2-methoxycarbonyl species **17** and a solvated methoxide anion. Cationic species such as **17**, which is an O-methylated NHC-CO_2 adduct, were synthesized previously by reacting a lithiated alkylimidazole with methyl chloroformate and subsequent methylation of the imidazole ring with methyl triflate.[25] Type **17** cations were also obtained via methanolysis of a 2-chlorocarbonyl substituted imidazolium cation.[6a] Such a cationic methylester **17** would certainly be a better methylating agent than neutral DMC. A S_N2 type demethylation would form **2** as the major product, precipitating from the reaction mixture (Scheme 8). The more nucleophilic NHC **16** is methylated at C-2 position via a first C-C coupling and the more basic methoxide anion is available to act as a sufficiently strong base to deprotonate the generated 2-methylimidazolium cation **18** yielding NHO **7**. The methoxycarbonylation of **7** to **15** by DMC has independently been proven with isolated **7** to be a highly selective second C-C coupling reaction. If an alternative mechanism involving methylation of NHC **16** by DMC would occur, a different product ratio than 4 to 6 (of **15** : **2**) would have to be expected. Nevertheless, it should be pointed out that in principle NHCs can also be methylated, e.g. by MeI (instead of DMC).[15] With an excess of strong base a second methylation or benzylation at the intermediate NHO with formation of 2-ethyl- or 2-ethylphenyl-imidazoles was observed as well.[26] The NHO methoxycarbonylation product **15** described here is thermally stable. It sublimes at 120 °C / $5 \cdot 10^{-3}$ mbar yielding colorless single crystals suitable for a molecular X-ray structure determination (Figure 6).

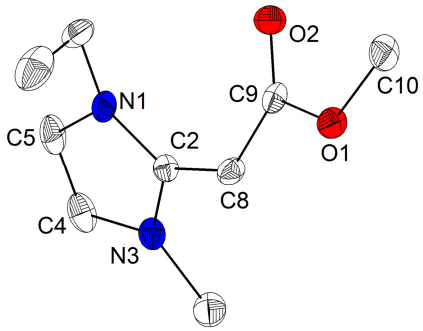

Figure 6. Molecular structure of methoxycarbonyl stabilized NHO **15**. Hydrogen atoms and a second crystallographically independent molecule were omitted for clarity.

The asymmetric unit consists of two crystallographically independent molecules, which show almost identical bond lengths and angles. For simplicity the structure discussion will detail only one of the molecules. In contrast to the carboxylate **4** and its literature known congeners, the CO_2 moiety is not roughly perpendicular to the imidazolium ring but is rotated with an interplanar angle of merely 32°. This indicates a partial but not perfect π-conjugation of the sp^2 carbanion at C8-H with both electron withdrawing substituents, the 2-imidazolium cation and the methoxycarbonyl group. The two C-C bonds competing about carbanion electron density d(C2-C8) = 1.407(2) Å and d(C8-C9) = 1.411(2) Å are within 2σ of the same length and of a bond order between a single and double bond. As expected, this is significantly shorter than the corresponding distances in the carboxylate **4** (d(C2-C8) = 1.474(2) Å, d(C8-C9) = 1.547(2) Å). The conjugate electron delocalization into the imidazolium cation of **15** leads to a shortening of both apical C-N bonds (d(N1-C2) = 1.363(2) Å, d(C2-N3) = 1.364(2) Å, an elongation of the other two and shortening of the C4-C5 distance compared to non-disturbed aromatic imidazolium cations such as in **4**. Due to the methyl substituent the charge delocalization by the carboxylate moiety is asymmetric with d(C9-O1) = 1.384(2) Å and d(C9-O2) = 1.232(2) Å as compared to the very symmetric zwitterion **4** (see SI for further bond lengths of **4**). The bond distances and angles of **15** are in very good agreement with the only closely related structure.[27] 2D-H,H-NOESY NMR spectra of **15** in DMSO-d_6 at 25 °C indicate that the double bond geometry is not fixed in solution but isomerizes. A strong cross peak is found between the olefinic H atom and the *N*-methyl group as well as between the olefinic H atom and the *N*-methylene group on the opposite side of the imidazolium moiety.

In following experiments we investigated the behavior of **15** towards acids. The latter is protonated by trifluoroacetic acid and even by the weak acid NH_4PF_6 at the carbanionic C8 atom with highly selective formation of functionalized ILs (Scheme 9).

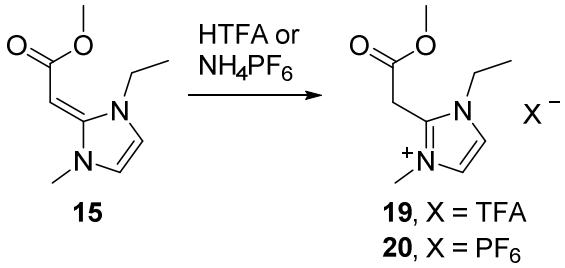

Scheme 9. Reaction of **15** with the acids HTFA and NH_4PF_6 to [NHO-CO_2Me][X].

This reaction behavior demonstrates that despite of one stabilizing methoxycarbonyl group, **15** still has the typical basicity of an NHO, which can be used in highly efficient IL syntheses.[28] In the light of the same reactivity pattern of NHO **7** and its -COOR stabilized derivative **15** towards electrophiles, protons in particular, it is interesting to note, that introduction of a –COOR substituent at a classical olefin leads to contrasting reactivity patterns, e.g. of ethylene and methylacrylate, towards electrophiles and nucleophiles.

NHO-SO_2 Adduct: A Zwitterionic Sulfinate

We have learned, that NHO-CO_2 adducts are stable storage forms of N-heterocyclic olefins. They can be used for the synthesis of a wide range of 2-alkylimidazolium ionic liquids as well as for interesting C-C coupling reactions involving two of the most prominent electrophiles of green chemistry, CO_2 and dimethyl carbonate. The question arises, whether NHO **7** forms a similar adduct with the Lewis acid SO_2 and whether a NHO-SO_2 adduct will show similar reaction patterns as its CO_2 counterpart, e.g. if reacted with methanol.

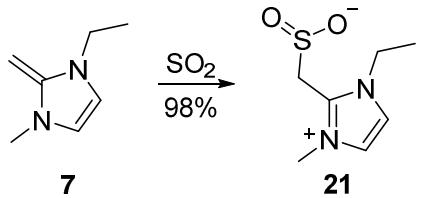

Scheme 10. Synthesis of 1-ethyl-3-methyl-imidazolium-2-methylensulfinate (NHO-SO_2, **21**).

According to literature reports aromatic NHCs such as **15** are unreactive towards SO_2.[29] Contrastingly, NHO-SO_2 adduct **21** precipitates as light yellow solid and is isolated in 98% yield when SO_2 gas is passed into a solution of NHO **7** in THF (Scheme 10).The molecular structure could be validated from single crystals grown in an acetonitrile solution layered with diethyl ether (Figure 7).

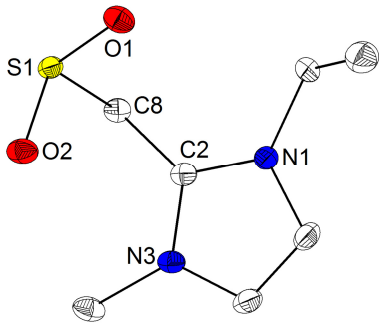

Figure 7. Molecular structure of NHO-SO_2 adduct **21**; hydrogen atoms were omitted for clarity.

As anticipated, the sulfur(IV) atom is coordinated in a pyramidal fashion due to the remaining electron lone pair. The C8-S1 bond has a length of 1.874(2) Å. This is significantly longer than the sp^3(C)-SO_2 bond in N-((1-phenylethyl)ammonio)propanesulfinate (1.807 Å)[30] and also metal complexes of e.g. O-ethyl- or methylsulfinato ligands (1.757-1.824 Å).[31] Only in a propynesulfinate ligand coordinated to tin via one of the oxygen atoms, a similar bond length (1.862 Å) is observed.[32] To the best of our knowledge no SO_2 adduct of a neutral C-base such as a NHC or P-ylid has been structurally characterized so far. The SO bonds in **21** (1.499(1) Å and 1.494(1) Å) are indicating negative charge delocalization in the SO_2 moiety. The comparatively long C-S distance suggests a weakened bond, which may be cleaved by appropriate nucleophiles. In a comparative experiment we elucidated the relative stability of NHO-CO_2 adduct **4** versus NHO-SO_2 **21** adduct. While **21** appears to be stable towards CO_2 at 50 °C, the NHO-CO_2 adduct immediately reacts with SO_2 at ambient temperature forming **21** (see SI for details). However, the latter is readily cleaved by methanol at ambient temperature forming the EMMIm methylsulfite salt **22** in quantitative yield (Scheme 11).

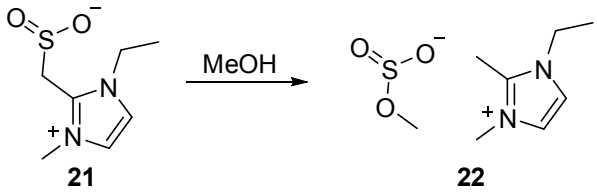

Scheme 11. Cleavage of **21** with methanol to yield [EMMIm][$MeOSO_2$] (**22**).

So far imidazolium alkylsulfites have been obtained in patented processes by methylation of N-alkylimidazoles with dimethyl sulfite[33] or by reaction of imidazolium halide or carboxylate salts with a symmetrically substituted dialkyl sulfite.[34] The potential of the zwitterionic sulfinate **21** to act as a precursor for other sulfite salts and sulfonylations related to corresponding carboxylations is under continued investigation.

Conclusion

We carefully investigated the conditions of the highly selective and fully reversible formation of NHC-CO_2 and NHO-CO_2 adducts in methanol from their imidazolium methylcarbonate precursors. In highly concentrated MeOH solution, in particular in the absence of methanol during isolation of [EMIm][OCO_2Me] or [EMMIm][OCO_2Me], the anion becomes less efficiently solvated, thus a stronger base, so that the fully reversible equilibria of these thermodynamically controlled carboxylations are shifted nearly quantitatively towards NHC-CO_2 adduct **2** or partly towards NHO-CO_2 adduct **4**, even at room temperature. Following this synthetic entry, the reaction patterns of NHO-CO_2 adduct **4** were investigated and compared to the nowadays well established chemistry of NHC-CO_2 adduct **2**.

Upon protonation, NHO-CO_2 adduct **4** can serve as masked NHO precursor for the preparation of ionic liquids [EMMIm][X] based on 2-methylimidazolium cations. However, decarboxylation in methanol or acetonitrile is much more dependent on the reaction conditions and partners than in case of NHC-CO_2 adducts: Its reaction with strong acids with weakly nucleophilic anions (X = TFA, TFSI) primarily leads to imidazolium salts [NHO-CO_2H][X] with 2-CH_2-COOH substituents at ambient temperature. Their decarboxylation to the corresponding 2-methylimidazolium salts [EMMIm][TFA] and [EMMIm][TFSI] occurs at elevated temperatures or is catalyzed by nucleophiles such as DMAP. In contrast, reaction of the NHO-CO_2 zwitterion **4** with the weak acid ammonium hexafluorophosphate, which provides a sufficiently nucleophilic conjugate base NH_3 as catalyst, leads to decarboxylation and quantitative formation of [EMMIm][PF_6] at ambient temperature.

Furthermore, we demonstrated that the NHO-CO_2 zwitterion **4** can act as an efficient carboxylating agent towards CH-acids such as acetonitrile: The decarboxylation of **4** at elevated temperatures generates an N-heterocyclic olefin *in situ*. This base assists the deprotonation of CH acidic positions of acetonitrile to form EMMIm cyanoacetate and $EMMIm_2$ cyanomalonate salts exemplifying the first C-C bond forming carboxylations with NHO-activated CO_2. Reaction of the NHO-CO_2 zwitterion with dimethyl carbonate under kinetic control leads to methoxycarbonylation and formation of the methoxycarbonyl stabilized NHO **15**. With highest selectivity **15** is accessible from the corresponding NHO and dimethyl carbonate. As an outlook we presented the synthesis of the novel NHO-SO_2 adduct **21**, which *via* methanolysis can be selectively transformed into the corresponding EMMIm methylsulfite IL **22**, demonstrating its potential to access a variety of organic salts. We

showed that CO_2 and SO_2 adducts of NHC and NHO are convenient storage forms of these carbon nucleophiles. The small deviations of their reactivity patterns compared to the NHC and NHO parent compounds can lead to undesired IL impurities, which are difficult to separate in otherwise highly efficient IL syntheses with these synthons. The insight presented here allows avoiding these difficulties and opens up opportunities for interesting new CO_2 and SO_2 reactions mediated by NHCs and NHOs.

Experimental Section

Methods and Devices

Unless stated otherwise all synthetic steps were conducted using standard Schlenk techniques and freshly dried solvents. Elemental analyses (C, H, N, S) were carried out by the service department for routine analysis and mass spectrometry with a vario MICRO cube (ELEMENTAR). Samples of air or moisture sensitive compounds were weighed into tin capsules inside a nitrogen filled glove box. Melting points were determined with a BÜCHI Melting Point B540. ^{1}H, proton decoupled ^{13}C and ^{19}F NMR spectra were recorded at 300 K in automation with a BRUKER Avance II 300 spectrometer. ^{1}H and ^{13}C NMR spectra were calibrated using residual proton and solvent signals, respectively (DMSO-d_6: δ_H 2.50 ppm, δ_C 39.52 ppm).[35] ^{19}F NMR spectra were referenced externally against $CFCl_3$. ^{1}H, ^{13}C-HMBC, ^{29}Si and ^{31}P NMR spectra were recorded with a BRUKER Avance III 500 or Avance III HD 300. The latter spectra were calibrated externally against Me_4Si and 85% H_3PO_4. IR spectra were recorded on a BRUKER APLPHA FT-IR spectrometer with Platinum ATR-sampling (diamond single crystal). HR-ESI mass spectra were acquired with a LTQ-FT Ultra mass spectrometer (THERMO FISCHER SCIENTIFIC). The resolution was set to 100.000. HR-EI mass spectra were acquired with a AccuTOF-GCv TOF mass spectrometer (JEOL). The data collection for the single crystal structure determinations was performed on a Bruker D8 QUEST diffractometer by the X-ray service department of the Fachbereich Chemie, University of Marburg. Bruker software (APEX2, SAINT) was used for data collection, cell refinement and data reduction.[36] The structures were solved with SIR97,[37] SIR2011[38] or SHELXS,[39] refined with SHELXL-2014[40] and finally validated using PLATON[41] software, all within the WinGX[42] or ShelXle[43] software bundle. Absorption corrections were applied beforehand within the APEX2 software (multi-scan).[44] Graphic representations were created using Diamond 4.[45] H-atoms were constrained to parent site and are not shown except when participating in hydrogen bonds. In all graphics the ellipsoids are shown for the

50% probability level. Crystallographic data for the structures reported in this paper are supplied as supporting information and have been deposited with the Cambridge Crystallographic Data Centre (CCDC to be inserted-to be inserted).

Starting Materials

All solvents were dried according to common procedures[46] and passed through columns of aluminum oxide, 3 Å molecular sieve and R3-11G-catalyst (BASF) or stored over molecular sieve (3 or 4 Å) until use. 1-Ethyl-2-methylimidazole was prepared according to published general procedures for the alkylation of imidazoles.[47] As the sodium salt of 2-methylimidazole turned out to react violently with ethyl bromide if following the original prescription, the sodium imidazolate was suspended in twice the recommended volume of THF and ethyl bromide was added dropwise at 0 °C before warming to room temperature.

Synthetic procedures

Synthesis of 1-ethyl-3-methylimidazolium-2-carboxylate inner salt ([NHO-CO_2], **2**). Ethyl imidazole (15.1 g, 157 mmol, 1.00 eq), dimethyl carbonate (25.1 g, 279 mmol, 1.77 eq) and methanol (25 mL) were combined in a glass autoclave and heated to 130 °C for 14.5 hours. All volatile components were removed *in vacuo* at 25 °C. Samples of the solution and the remainder were investigated by ^{1}H NMR spectroscopy during the removal of solvent methanol indicating >85% conversion into the zwitterion 2 in the solid raw product. This residue was recrystallized twice from acetonitrile yielding NHC-CO_2 as colorless crystals in a yield of 17.4 g (93.4 mmol, 59%). **Mp**: 123.3 °C (2 K/min, acetonitrile). **Elem. anal.** found C, 54.2; H, 6.5; N, 18.2; $C_7H_{10}N_2O_2$ requires C, 54.5; H, 6.5; N, 18.2. **IR** ν_{max}/cm^{-1}: 3086 (w), 1664 (vs), 1506 (m), 1426 (m), 1376 (m), 1314 (vs), 1286 (s), 1238 (m), 1110, (w), 1093 (w), 1037 (w), 837 (m), 818 (m), 786 (vs), 660 (m), 633 (m), 604 (w). **^{1}H NMR** (300.1 MHz, DMSO-d_6) δ_H = 1.33 (t, $^3J_{HH}$ = 7.2 Hz, 3H, CH_2CH_3), 3.95 (s, 3H, NCH_3), 4.46 (q, $^3J_{HH}$ = 7.2 Hz, 2H, CH_2CH_3), 7.56 (s, 1H, *H*4/5), 7.64 (s, 1H, *H*4/5) ppm. **^{13}C NMR** (75.5 MHz, DMSO-d_6): δ_C = 15.9 (1C, CH_2CH_3), 36.4 (1C, NCH_3), 44.0 (1C, CH_2CH_3), 120.4 (1C, *C4/5*), 122.3 (1C, *C4/5*), 141.9 (1C, *C2*), 154.0 (1C, CH_2CO_2) ppm.

Upon addition of an excess of methanol to the NMR sample [EMIm][OCO_2Me] (**1**) is generated *in situ*: **^{1}H NMR** (300.1 MHz, DMSO-d_6, MeOH) δ_H = 1.41 (t, $^3J_{HH}$ = 7.3 Hz, 3H, CH_2CH_3), 3.17 (s, $CH_{3,MeOH}$), 3.26 (s, 3H, OCH_3), 3.85 (s, 3H, NCH_3), 4.20 (q, $^3J_{HH}$ = 7.3 Hz, 2H, CH_2CH_3), 4.30 (s, OH_{MeOH}) 7.70 (s, 1H, *H*4/5), 7.79 (s, 1H, *H*4/5), 9.31 (br s, 1H,

H2) ppm. **^{13}C NMR** (75.5 MHz, DMSO-d_6, MeOH): δ_C = 15.1 (1C, CH_2CH_3), 35.6 (1C, NCH_3), 44.2 (1C, CH_2CH_3), 48.6 (MeOH), 51.3 (1C, OCH_3), 122.1 (1C, *C4/5*), 123.7 (1C, *C4/5*), 136.7 (1C, *C2*), 157.1 (1C, OCO_2Me) ppm.

Synthesis of 1-ethyl-2,3-dimethylimidazolium methylcarbonate ([EMMIm][OCO_2Me], **3**). 1-ethyl-2-methylimidazole (15.1 g, 136 mmol, 1.00 eq) was combined with dimethyl carbonate (25.5g, 283 mmol, 2.08 eq) and methanol (20 mL) in a glass autoclave. The mixture was heated to 130 °C for 14 hours, whereupon the solution turned red. All volatile components were removed in fine vacuum. The primary oily residue was dissolved in acetonitrile (10 mL), the solution was again concentrated *in vacuo*. The residual solid was recrystallized from a mixture of acetonitrile and diethyl ether, finally yielding 8.39 g (41.9 mmol, 31%) of [EMMIm][OCO_2Me]. Despite all effort impurities of NHO-CO_2 (**4**) ranging between 5% and 10% remained. Analytical data for [EMMIm][OCO_2Me], **3**: **Elem. anal.** found C, 53.3; H, 8.0; N, 14.6; $C_9H_{16}N_2O_3$ requires C, 54.0; H, 8.1; N, 14.0. **IR** ν_{max}/cm^{-1}: 3066 (w), 2937 (w), 1658 (s), 1540 (w), 1433 (w), 1277 (vs), 1208 (w), 1179 (w), 1135 (w), 1067 (s), 870 (s), 824 (m), 725 (w), 675 (w), 581 (m), 585(w). **^{1}H NMR** (300.1 MHz, DMSO-d_6) δ_H = 1.33 (t, $^3J_{HH}$ = 7.3 Hz, 3H, CH_2CH_3), 2.59 (s, 3H, CCH_3), 3.15 (s, 3H, OCH_3), 3.76 (s, 3H, NCH_3), 4.15 (q, $^3J_{HH}$ = 7.3 Hz, 2H, CH_2CH_3), 7.68 (d, $^3J_{HH}$ = 2.0 Hz, 1H, *H*4/5), 7.72 (d, $^3J_{HH}$ = 2.0 Hz, 1H, *H*4/5) ppm. **^{13}C NMR** (75.5 MHz, DMSO-d_6): δ_C = 9.0 (1C, CCH_3), 14.9 (1C, CH_2CH_3), 34.6 (1C, NCH_3), 42.7 (1C, CH_2CH_3), 50.8 (1C, OCH_3), 120.4 (1C, *C4/5*), 122.4 (1C, *C4/5*), 144.0 (1C, *C2*), 155.5 (1C, OCO_2Me) ppm.

Synthesis of 1-ethyl-3-methylimidazolium-2-methylencarboxylate inner salt (NHO-CO_2, **4**). The compound can be synthesized by slowly heating the parent methylcarbonate **3** in the presence of excess CO_2. This significantly enriches the percentage of the carboxylate in the mixture but separation of the zwitterion from the methylcarbonate salt by repeated extraction with acetonitrile is laborious and very low yielding. An elegant access to these compounds and also the COS and CS_2 analogues was recently published by Lu and coworkers.[15-16] Our version of the synthetic procedure is presented for completeness: 1-Ethyl-2,3-dimethylimidazolium bromide (1.99 g, 9.72 mmol, 1.00 eq), potassium hydride (492 mg, 11.7 mmol, 1.26 eq) and potassium *tert*-butanolate (62 mg, 0.55 mmol, 6mol%) were combined with THF (50 mL). The suspension was stirred for three days and then filtered over celite to remove all solid components and the filter cake extracted with THF (20 mL). Carbon dioxide, which was dried over a column of phosphorous pentoxide, was introduced into the clear solution at 0 °C for 10 minutes. A colorless precipitate occurred immediately. The

mixture was stirred at ambient temperature for 30 minutes before the precipitate was filtered, washed with diethyl ether (10 mL) and dried in fine vacuum. NHO-CO_2 (**4**) was isolated as a colorless powder in a yield of 1.53 g (9.04 mmol, 93%). **Elem. anal.** found C, 57.0; H, 7.4; N, 16.9; $C_8H_{12}N_2O_2$ requires C, 57.1; H, 7.2; N, 16.7. **IR** ν_{max}/cm^{-1}: 3061 (w), 1607 (vs), 1581 (sh, m), 1530 (m), 1339 (s), 1299 (w, sh), 1262 (w), 1244 (w), 1194 (m), 1112 (w), 962 (w), 883 (m), 812 (m), 799 (m), 730 (w), 714 (w), 653 (m), 630 (w), 437 (w). **^{1}H NMR** (300.1 MHz, DMSO-d_6) δ_H = 1.32 (t, $^3J_{HH}$ = 7.2 Hz, 3H, CH_2CH_3), 3.62 (s, 2H, CH_2CO_2), 3.72 (s, 3H, NCH_3), 4.10 (q, $^3J_{HH}$ = 7.2 Hz, 2H, CH_2CH_3), 7.56 (d, $^3J_{HH}$ = 1.9 Hz, 1H, *H*4/5), 7.59 (d, $^3J_{HH}$ = 1.9 Hz, 1H, *H*4/5) ppm. **^{13}C NMR** (75.5 MHz, DMSO-d_6): δ_C = 14.9 (1C, CH_2CH_3), 34.0 (1C, CH_2CO_2), 34.3 (1C, NCH_3), 42.5 (1C, CH_2CH_3), 119.5 (1C, *C4/5*), 121.7 (1C, *C4/5*), 145.8 (1C, *C2*), 163.6 (1C, CH_2CO_2) ppm. **HRMS** (ESI+): m/z found 169.0975; $[M+H]^+$ ($C_8H_{13}N_2O_2$) requires 169.0972.

Attempt to synthesize 1-ethyl-2,3-dimethylimidazolium *tert*-butylsulfide ([EMMIm][*t*Bu-S], **5**) via decarboxylation. 1-ethyl-2,3-dimethylimidazolium methylcarbonate (1.48 g, 7.39 mmol, 1.00 eq) was dissolved in acetonitrile (10 mL), the solution was degassed and cooled to 0 °C. *Tert*-butyl-trimethylsilylsulfide (1.35 g, 8.31 mmol, 1.12 eq) was added drop wise and the mixture was stirred 30 minutes at 0 °C. All volatile components were removed under reduced pressure and the residue recrystallized from a mixture of acetonitrile (13 mL) and diethyl ether (6 mL). A colorless solid remained undissolved, which was filtered, washed with diethyl ether (5 mL) and dried in fine vacuum. The compound could be identified as EMMIm-CO_2, which was isolated in yield of 450 mg (2.68 mmol, 36%).

Synthesis of 1-ethyl-2,3-dimethylimidazolium *tert*-butylsulfide ([EMMIm][*t*Bu-S], **5**). 1-Ethyl-2,3-dimethylimidazolium iodide (940 mg, 3.73 mmol, 1.00 eq), potassium hydride (168 mg, 4.19 mmol, 1.12 eq) and potassium *tert*-butanolate (22 mg, 0.20 mmol, 5mol%) were combined with THF (20 mL). The suspension was stirred for 48 hours and then filtered over celite to remove all solid components. The filter cake was washed with THF (10 mL). The clear solution was cooled to −78 °C and a solution of *tert*-butanethiol (0.51 mL, 0.41 g, 4.5 mmol, 1.2 eq) in THF (30 mL) was slowly added. A colorless precipitate occurred immediately; the mixture was warmed to 0 °C, stirred for 30 minutes and again cooled to −25 °C, before the precipitate was filtered, washed with diethyl ether (10 mL) and dried in fine vacuum. [EMMIm][*t*Bu-S] (**5**) was isolated as a colorless powder in a yield of 790 mg (3.69 mmol, 99%). **Elem. anal.** found C, 59.9; H, 9.9; N, 13.0; S, 14.6; $C_{11}H_{22}N_2S_1$ requires C, 61.6; H, 10.3; N, 13.1; S, 15.0. **IR** ν_{max}/cm^{-1}: 3098 (w), 2956 (vs), 2900 (s), 2874 (s), 2836

(s), 1586 (m), 1540 (m), 1509 (w), 1445 (m), 1422 (s), 1392 (m), 1346 (s), 1334 (m), 1310 (m), 1254 (s), 1208 (w), 1151 (vs), 1135 (s), 1089 (m), 1059 (w), 891 (w), 795 (vs),752 (w), 713 (w), 671 (s), 633 (m), 594 (m), 484 (w). **^{1}H NMR** (300.1 MHz, DMSO-d_6) δ_H = 1.23 (s, 9H, *tBu*), 1.33 (t, $^{3}J_{HH}$ = 7.3 Hz, 3H, CH_2CH_3), 2.63 (s, 3H, CCH_3), 3.80 (s, 3H, NCH_3), 4.19 (q, $^{3}J_{HH}$ = 7.3 Hz, 2H, CH_2CH_3), 7.83 (s br, 1H, *H*4/5), 7.85 (s br, 1H, *H*4/5) ppm. **^{13}C NMR** (75.5 MHz, DMSO-d_6): δ_C = 9.1 (1C, C CH_3), 14.8 (1C, CH_2CH_3), 34.6 (1C, NCH_3), 38.1 (1C, $C(CH_3)_3$), 40.6 (3C, $C(CH_3)_3$), 42.6 (1C, CH_2CH_3), 120.3 (1C, *C4/5*), 122.3 (1C, *C4/5*), 143.9 (1C, *C2*) ppm.

Synthesis of 1-ethyl-2,3-dimethylimidazolium trimethylsilylsulfide ([EMMIm][TMS-S], **8**). 1-ethyl-2,3-dimethylimidazolium methylcarbonate (2.08 g, 10.4 mmol, 1.00 eq) was dissolved in acetonitrile (10 mL), the solution was degassed and cooled to 0 °C. Bis(trimethylsilyl)sulfide (2.08 g, 11.7 mmol, 1.12 eq) was added drop wise within 25 minutes. The mixture was stirred further 30 minutes at 0 °C and 30 minutes at ambient temperature. The solution was concentrated in fine vacuum to half of its original volume before diethyl ether (4 mL) was added and the product was crystallized at −25 °C. The colorless crystals were filtered over a precooled frit, washed with diethyl ether (12 mL) and dried in fine vacuum. [EMMIm][S-TMS] was isolated in a yield of 1.26 g (5.47 mmol, 53%). **Elem. anal.** found C, 51.9; H, 9.6; N, 12.7; S, 13.55; $C_{10}H_{22}N_2S_1Si_1$ requires C, 52.1; H, 9.6; N, 12.2; S, 13.9. **IR** ν_{max}/cm^{-1}: 3098 (w), 3027 (w), 2942 (m), 1628 (w), 1584 (w), 1537 (w), 1422 (w), 1389 (w), 1309 (w), 1230 (m), 1133 (w), 1092 (w), 814 (vs), 793 (s, sh), 738 (m), 664 (m), 634 (s), 503 (s). **^{1}H NMR** (300.1 MHz, DMSO-d_6) δ_H = −0.07 (s, 9H, $SiMe_3$), 1.33 (t, $^{3}J_{HH}$ = 7.2 Hz, 3H, CH_2CH_3), 2.61 (s, 3H, CCH_3), 3.78 (s, 3H, NCH_3), 4.17 (q, $^{3}J_{HH}$ = 7.3 Hz, 2H, CH_2CH_3), 7.72 (d, $^{3}J_{HH}$ = 2.0 Hz, 1H, *H*4/5), 7.76 (d, $^{3}J_{HH}$ = 2.0 Hz, 1H, *H*4/5) ppm. **^{13}C NMR** (75.5 MHz, DMSO-d_6): δ_C = 8.8 (s, 9H, $SiMe_3$), 9.1 (1C, C CH_3), 14.8 (1C, CH_2CH_3), 34.6 (1C, NCH_3), 42.7 (1C, CH_2CH_3), 120.3 (1C, *C4/5*), 122.3 (1C, *C4/5*), 143.9 (1C, *C2*) ppm. **^{29}Si NMR** (99.4 MHz, DMSO-d_6): δ = −0.7 (s) ppm.

Reaction of NHO-CO_2 **4** with ammonium hexafluorophosphate. **4** (142 mg, 839 µmol, 1.00 eq) was dissolved in methanol (5 mL) and NH_4PF_6 (139 mg, 853 µmol, 1.02 eq) was added to the solution. The mixture was stirred at ambient temperature for 24 hours and then evaporated to dryness *in vacuo*. [EMMIm][PF_6] was isolated as a colorless solid with a yield of 201 mg (744 µmol, 89%). **^{1}H NMR** (300.1 MHz, DMSO-d_6) δ_H = 1.34 (t, $^{3}J_{HH}$ = 7.3 Hz, 3H, CH_2CH_3), 2.57 (s, 3H, CCH_3), 3.74 (s, 3H, NCH_3), 4.13 (q, $^{3}J_{HH}$ = 7.3 Hz, 2H, CH_2CH_3),

7.59 (d, $^3J_{HH}$ = 2.1 Hz, 1H, *H*4/5), 7.64 (d, $^3J_{HH}$ = 2.1 Hz, 1H, *H*4/5) ppm. **^{13}C NMR** (75.5 MHz, DMSO-d_6): δ_C = 8.9 (1C, C *C*H$_3$), 14.7 (1C, CH$_2$*C*H$_3$), 34.5 (1C, N*C*H$_3$), 42.7 (1C, *C*H$_2$CH$_3$), 120.2 (1C, *C4/5*), 122.3 (1C, *C4/5*), 144.0 (1C, *C2*) ppm. **^{19}F NMR** (282.4 MHz, DMSO-d_6): δ_F = -71.1 (d, $^1J_{FP}$ = 711 Hz, 6F, PF_6) ppm.

Synthesis of [NHO-CO$_2$H][TFSI] (**10**). Bis(trifluoromethyl-sulfonyl)imide (HTFSI, 175 mg, 0.62 mmol, 1.1 eq) was dissolved in acetonitrile (5 mL) and was added to NHO-CO$_2$ **4** (92 mg, 0.54 mmol, 1.0 eq). The mixture was stirred at ambient temperature for 18 hours and then evaporated to dryness *in vacuo*, leaving a colorless oil. The substance consists primarily (<80%) of the protonated carboxylate salt [NHO-CO$_2$H][TFSI] (**10**). Analogous results were obtained when varying the reaction time between two hours and two days and if exchanging the solvent for methanol. **IR** ν_{max}/cm^{-1}: 3450-3000 (br, w), 3149 (w), 1728 (w), 1540 (w), 1345 (m), 1327 (sh, m), 1180 (vs), 1132 (s), 1050 (s), 825 (w), 792 (w), 762 (w), 740 (w), 608 (s), 569 (s), 510 (m). **^{1}H NMR** (300.1 MHz, DMSO-d_6) δ_H =1.33 (t, $^3J_{HH}$ = 7.3 Hz, 3H, CH$_2$C*H*$_3$), 3.79 (s, 3H, NC*H*$_3$), 4.19 (q, $^3J_{HH}$ = 7.3 Hz, 2H, C*H*$_2$CH$_3$), 4.37 (s, 2H, C*H*$_2$CO$_2$H),7.73 (d, $^3J_{HH}$ = 1.7 Hz, 1H, *H*4/5), 7.79 (d, $^3J_{HH}$ = 1.7 Hz, 1H, *H*4/5), 13.20 (br s, 1H, CO$_2$*H*) ppm. **^{13}C NMR** (75.5 MHz, DMSO-d_6): δ_C = 15.0 (1C, CH$_2$*C*H$_3$), 29.3 (1C, C*C*H$_2$CO$_2$H), 34.8 (1C, N*C*H$_3$), 43.1 (1C, *C*H$_2$CH$_3$), 119.4 (q, $^1J_{CF}$ = 322 Hz, 1C, *C*F$_3$), 121.1 (1C, *C4/5*), 123.3 (1C, *C4/5*), 140.7 (1C, *C2*), 167.5 (1C, *C*O$_2$H) ppm. **^{19}F NMR** (282.4 MHz, DMSO-d_6): δ_F = -79.5 (3F, C*F*$_3$) ppm.

If the isolated substance is redissolved in acetonitrile or methanol and heated to 60−80 °C (30 min), or if the NMR sample in DMSO-d_6 is heated to 80 °C the substance is quantitatively transformed to [EMMIm][TFSI] (**11**). **IR** ν_{max}/cm^{-1}: 3152 (w), 1591 (w), 1541 (w), 1346 (m), 1330 (sh, m), 1174 (vs), 1132 (s), 1051 (s), 789 (w), 739 (w), 612 (m), 600 (m), 569 (m), 509 (m). **^{1}H NMR** (300.1 MHz, DMSO-d_6) δ_H = 1.33 (t, $^3J_{HH}$ = 7.3 Hz, 3H, CH$_2$C*H*$_3$), 2.58 (s, 3H, CC*H*$_3$), 3.74 (s, 3H, NC*H*$_3$), 4.13 (q, $^3J_{HH}$ = 7.3 Hz, 2H, C*H*$_2$CH$_3$), 7.61 (d, $^3J_{HH}$ = 1.9 Hz, 1H, *H*4/5), 7.65 (d, $^3J_{HH}$ = 1.9 Hz, 1H, *H*4/5) ppm. **^{13}C NMR** (75.5 MHz, DMSO-d_6): δ_C = 8.9 (1C, C *C*H$_3$), 14.7 (1C, CH$_2$*C*H$_3$), 34.5 (1C, N*C*H$_3$), 42.7 (1C, *C*H$_2$CH$_3$), 119.4 (q, $^1J_{CF}$ = 322 Hz, 1C, *C*F$_3$), 120.2 (1C, *C4/5*), 122.3 (1C, *C4/5*), 144.0 (1C, *C2*) ppm. **^{19}F NMR** (282.4 MHz, DMSO-d_6): δ_F = -78.9 (3F, C*F*$_3$) ppm.

Synthesis of [NHO-CO$_2$H][TFA] (**12**). NHO-CO$_2$ **4** (172 mg, 1.02 mmol, 1.00 eq) was dissolved in methanol (5 mL) and trifluoroacetic acid (137 mg, 1.20 mmol, 1.18 eq) was added to the solution. The mixture was stirred at ambient temperature for 24 hours and then

evaporated to dryness *in vacuo*, leaving a colorless oil. The substance consists primarily (<90%) of the protonated carboxylate salt [NHO-CO_2H][TFA]. Analogous results were obtained when increasing the reaction time to four days and if exchanging the solvent for acetonitrile. The addition of 0.2 mL of DMSO-d_6 and variation of the sequence of addition does not show any effect as well. **IR** ν_{max}/cm^{-1}: 3142 (w), 1716 (m), 1630 (w), 1539 (w), 1410 (w), 1324 (w), 1231 (w), 1171 (vs), 1117 (vs), 895 (w), 818 (m), 797 (m), 768 (m), 714 (s), 648 (w), 598 (w), 518 (w), 455 (m). **^{1}H NMR** (300.1 MHz, DMSO-d_6) δ_H = 1.33 (t, $^3J_{HH}$ = 7.2 Hz, 3H, CH_2CH_3), 3.79 (s, 3H, NCH_3), 4.20 (q, $^3J_{HH}$ = 7.2 Hz, 2H, CH_2CH_3), 4.37 (s, 2H, CH_2CO_2H),7.74 (d, $^3J_{HH}$ = 1.9 Hz, 1H, *H*4/5), 7.80 (d, $^3J_{HH}$ = 1.9 Hz, 1H, *H*4/5), 14.96 (br s, 1H, CO_2H) ppm. **^{13}C NMR** (75.5 MHz, DMSO-d_6): δ_C = 15.0 (1C, CH_2CH_3), 29.5 (1C, CCH_2CO_2H), 34.8 (1C, NCH_3), 43.1 (1C, CH_2CH_3), 116.6 (q, $^1J_{CF}$ = 296 Hz, 1C, CF_3), 121.1 (1C, *C4/5*), 123.3 (1C, *C4/5*), 140.9 (1C, *C2*), 158.2 (q, $^2J_{CF}$ = 34 Hz, 1C, CCF_3), 167.4 (1C, CO_2H) ppm. **^{19}F NMR** (282.4 MHz, DMSO-d_6): δ_F = -75.1 (3F, CF_3) ppm.

If [NHO-CO_2H][TFA] is dissolved in acetonitrile or methanol and heated to 60−80 °C (30 min), or if the NMR sample in DMSO-d_6 is heated to 80 °C the substance is quantitatively transformed to [EMMIm][TFA] (**13**). The final product is also generated if sub-stoichiometric amounts of 4-dimethylaminopryridine (0.31 eq) are added to the reaction mixture and stirring at ambient temperature is continued for two hours. **IR** ν_{max}/cm^{-1}: 3082 (w), 1684 (vs), 1589 (w), 1538 (w), 1456 (w), 1395 (w), 1337 (w), 1194 (s), 1161 (s), 1110 (vs), 817 (m), 798 (m), 715 (s), 669 (w), 517 (w). **^{1}H NMR** (300.1 MHz, DMSO-d_6) δ_H = 1.33 (t, $^3J_{HH}$ = 7.2 Hz, 3H, CH_2CH_3), 2.58 (s, 3H, CCH_3), 3.75 (s, 3H, NCH_3), 4.14 (q, $^3J_{HH}$ = 7.2 Hz, 2H, CH_2CH_3), 7.63 (d, $^3J_{HH}$ = 2.0 Hz, 1H, *H*4/5), 7.67 (d, $^3J_{HH}$ = 2.0 Hz, 1H, *H*4/5) ppm. **^{13}C NMR** (75.5 MHz, DMSO-d_6): δ_C = 8.9 (1C, C CH_3), 14.7 (1C, CH_2CH_3), 34.5 (1C, NCH_3), 42.7 (1C, CH_2CH_3), 117.4 (q, $^1J_{CF}$ = 300 Hz, 1C, CF_3), 120.2 (1C, *C4/5*), 122.3 (1C, *C4/5*), 144.0 (1C, *C2*), 157.8 (q, $^2J_{CF}$ = 30 Hz, 1C, CCF_3) ppm.

Synthesis of 1-ethyl-2,3-dimethylimidazolium cyanoacetate ([EMMIm][NC-CH_2-CO_2], **14**). NHO-CO_2 adduct **4** (264 mg, 1.56 mmol) was suspended in acetonitrile (5 mL) and the mixture was heated to 80 °C for 30 minutes, whereupon the solid dissolved and the solution turned light orange. After cooling to ambient temperature all volatile components were removed *in vacuo* and a light orange oil remained. The substance was triturated with dichloromethane forming an orange solution and a colorless solid. The suspension was filtered. Evaporation of the DCM extract yielded [EMMIm][NC-CH_2-CO_2] (**14**) in a yield of

208 mg (0.99 mmol, 64%) as an orange oil, which slowly solidified. The DCM unsoluble dried precipitate was identified as bis(1-ethyl-2,3-dimethylimidazolium) cyanomalonate (**14a**) and isolated in a yield of 28 mg (74 µmol, 10%) as a colorless powder. The compounds could be identified from their NMR and MS spectra.

Analytical data of **14**: **IR** ν_{max}/cm^{-1}: 3067 (w), 2242 (w), 1624 (vs), 1537 (w), 1315 (s), 1246 (w), 1135 (w), 869 (w), 669 (w), 582 (w), 482 (w). **^{1}H NMR** (300.1 MHz, DMSO-d_6) δ_H = 1.33 (t, $^{3}J_{HH}$ = 7.3 Hz, 3H, CH_2CH_3), 2.59 (s, 3H, CCH_3), 2.93 (s, 1–2H, CH_2CN), 3.76 (s, 3H, NCH_3), 4.15 (q, $^{3}J_{HH}$ = 7.3 Hz, 2H, CH_2CH_3), 7.66 (d, $^{3}J_{HH}$ = 2.0 Hz, 1H, *H*4/5), 7.70 (d, $^{3}J_{HH}$ = 2.0 Hz, 1H, *H*4/5) ppm. **^{13}C NMR** (75.5 MHz, DMSO-d_6): δ_C = 9.0 (1C, C CH_3), 14.8 (1C, CH_2CH_3), 27.4 (1C, CH_2CN), 34.5 (1C, NCH_3), 42.7 (1C, CH_2CH_3), 119.4 (1C, *C*N), 120.3 (1C, *C4/5*), 122.4 (1C, *C4/5*), 144.0 (1C, *C2*), 162.2 (1C, CO_2) ppm. **HRMS** (ESI−) m/z: [cyanoacetate] Calcd for $C_3H_2N_1O_2$: 84.0091; Found: 84.0091;

Analytical Data of **14a**: **IR** ν_{max}/cm^{-1}: 3067 (w), 2161 (m), 1631 (w), 1586 (w), 1515 (m), 1400 (vs, br), 1248 (w), 1181 (w), 1131 (m), 881 (w), 803 (s), 670 (w), 554 (w), 457 (m). **^{1}H NMR** (300.1 MHz, DMSO-d_6) δ_H = 1.33 (t, $^{3}J_{HH}$ = 7.3 Hz, 3H, CH_2CH_3), 2.59 (s, 3H, CCH_3), 3.76 (s, 3H, NCH_3), 4.15 (q, $^{3}J_{HH}$ = 7.3 Hz, 2H, CH_2CH_3), 7.66 (d, $^{3}J_{HH}$ = 1.6 Hz, 1H, *H*4/5), 7.70 (d, $^{3}J_{HH}$ = 1.6 Hz, 1H, *H*4/5), 17.95 (s, 1H, CO_2H) ppm. **^{13}C NMR** (75.5 MHz, DMSO-d_6): δ_C = 9.0 (1C, C CH_3), 14.8 (1C, CH_2CH_3), 34.5 (1C, NCH_3), 42.7 (1C, CH_2CH_3), 57.3 (1C, $C(CO_2)_2$), 120.3 (1C, *C4/5*), 122.4 (1C, *C4/5*), 144.0 (1C, *C2*), 175.5 (2C, CO_2) ppm. The nitrile C atom could not be found due to the low solubility and stability of **14a**. **HRMS** (ESI−) m/z: [cyanomalonate + EMMIm] Calcd for $C_{11}H_{14}N_3O_4$: 252.0990; Found: 252.0990.

Synthesis of *Z*-methyl 2-(1-ethyl-3-methyl-1,3dihydro-2*H*-imidazol-2-ylidene)acetate (**15**). 1-Ethyl-2,3-dimethylimidazolium bromide (935 mg, 4.56 mmol, 1.00 eq), potassium hydride (219 mg, 5.46 mmol, 1.20 eq) and potassium *tert*-butanolate (9 mg, 0.08 mmol, 2mol%) were combined with THF (25 mL). The suspension was stirred for 24 hours and then filtered over celite to remove all solid components and the filter cake washed with THF (10 mL). Dimethyl carbonate (0.42 mL, 0.45 g, 5.0 mmol, 1.1 eq), was added to the solution at −20 °C, whereupon the mixture became light yellow. The solution was stirred at –20 °C for 20 minutes and at ambient temperature for one hour before all volatile components were removed *in vacuo*. **15** remained as an off-white powder with a yield of 763 mg (4.19 mmol, 92%). The assignment of NMR resonance signals is based on HMQC and HMBC 2D spectra.

Elem. anal. found C, 59.35; H, 7.8; N, 15.6; $C_9H_{14}N_2O_2$ requires C, 59.3; H, 7.7; N, 15.4. **IR** ν_{max}/cm^{-1}: 3163 (w), 3122 (w), 2970 (w), 1629 (s), 1547 (vs), 1487 (m), 1434 (s), 1382 (m), 1326 (w), 1232 (m), 1147 (vs), 1056 (s), 1039 (s), 913 (s), 827 (m), 796 (w), 741 (s), 712 (m), 677 (m), 623 (s), 585 (s), 491 (w), 424 (w). **^{1}H NMR** (300.1 MHz, DMSO-d_6) δ_H = 1.18 (t, $^3J_{HH}$ = 7.2 Hz, 3H, CH_2CH_3), 3.36 (s, 3H, OCH_3), 3.37 (s, 3H, NCH_3), 3.72 (s, 1H, $CHCO_2Me$), 3.88 (q, $^3J_{HH}$ = 7.2 Hz, 2H, CH_2CH_3), 6.91 (m, 2H, *H*4/5) ppm. **^{13}C NMR** (75.5 MHz, DMSO-d_6): δ_C = 13.9 (1C, CH_2CH_3), 34.9 (1C, NCH_3), 41.8 (1C, CH_2CH_3), 48.4 (1C, OCH_3), 52.6 (1C, $CHCO_2Me$), 115.9 (1C, *C5*), 118.1 (1C, *C4*), 150.3 (1C, *C2*), 165.8 (1C, CO_2Me) ppm. **HRMS** (EI-TOF) m/z: [M] Calcd for $C_9H_{14}N_2O_2$: 182.10553; Found: 182.10550;

The substance sublimes at 120 °C and $5\cdot10^{-3}$ mbar yielding colorless crystals suitable for XRD analysis.

Synthesis of 1-ethyl-2-(2-methoxy-2-oxoethyl)-3-methyl-imidazolium trifluoroacetate ([NHO-CO_2Me][TFA], **19**). **15** (106 mg, 582 µmol, 1.0 eq) was dissolved in acetonitrile (5 mL) and trifluoroacetic acid (85 mg, 0.75 mmol, 1.3 eq) was added. The mixture turned from light yellow to colorless, was stirred at ambient temperature for one hour and then evaporated to dryness *in vacuo*, leaving a colorless oil. The substance was identified as [NHO-CO_2Me][TFA] (**19**) by NMR spectroscopy and mass spectrometry. **IR** ν_{max}/cm^{-1}: 3099 (w), 2961 (w), 1740 (m), 1684 (vs), 1540 (w), 1439 (w), 1339 (w), 1194 (s), 1160 (s), 1113 (vs), 995 (w), 818 (m), 798 (s), 715 (s), 662 (w), 591 (w), 517 (w), 427 (w). **^{1}H NMR** (300.1 MHz, DMSO-d_6) δ_H = 1.33 (t, $^3J_{HH}$ = 7.3 Hz, 3H, CH_2CH_3), 3.71 (s, 3H, OCH_3), 3.80 (s, 3H, NCH_3), 4.20 (q, $^3J_{HH}$ = 7.3 Hz, 2H, CH_2CH_3), 4.50 (s, 2H, CH_2CO_2Me),7.77 (d, $^3J_{HH}$ = 2.1 Hz, 1H, *H*4/5), 7.83 (d, $^3J_{HH}$ = 2.1 Hz, 1H, *H*4/5) ppm. **^{13}C NMR** (75.5 MHz, DMSO-d_6): δ_C = 15.0 (1C, CH_2CH_3), 28.8 (1C, CH_2CO_2H), 34.9 (1C, NCH_3), 43.1 (1C, CH_2CH_3), 52.9 (1C, OCH_3), 121.3 (1C, *C4/5*), 123.6 (1C, *C4/5*), 139.9 (1C, *C2*), 166.5 (1C, CO_2H) ppm. The quaternary C-Atoms of the TFA anion could not be observed due to their low intensity. **^{19}F NMR** (282.4 MHz, DMSO-d_6): δ_F = -73.4 (3F, CF_3) ppm. **HRMS** (ESI−) m/z: [TFA] Calcd for $C_2F_3O_2$: 112.9856; Found: 112.9856. **HRMS** (ESI+) m/z: [NHO-CO_2Me] Calcd for $C_9H_{15}N_2O_2$: 183.1128; Found: 183.1127.

Synthesis of 1-ethyl-2-(2-methoxy-2-oxoethyl)-3-methyl-imidazolium hexafluorophosphate ([NHO-CO_2Me][PF_6], **20**). **15** (61 mg, 0.33 mmol, 1.0 eq) was dissolved in acetonitrile (3 mL) and NH_4PF_6 (63 mg, 0.39 mmol, 1.2 eq) was added. The mixture was stirred at

ambient temperature for 15 hours. The colorless solution was filtered to remove residues of unreacted starting material and then evaporated to dryness *in vacuo*, leaving a colorless solid. The substance was identified as [NHO-CO_2Me][PF_6] (**20**) by NMR spectroscopy and mass spectrometry. **^{1}H NMR** (300.1 MHz, DMSO-d_6) δ_H = 1.33 (t, $^3J_{HH}$ = 7.3 Hz, 3H, CH_2CH_3), 3.72 (s, 3H, OCH_3), 3.79 (s, 3H, NCH_3), 4.19 (q, $^3J_{HH}$ = 7.3 Hz, 2H, CH_2CH_3), 4.48 (s, 2H, CH_2CO_2Me),7.75 (d, $^3J_{HH}$ = 1.8 Hz, 1H, *H*4/5), 7.81 (d, $^3J_{HH}$ = 1.8 Hz, 1H, *H*4/5) ppm. **^{13}C NMR** (75.5 MHz, DMSO-d_6): δ_C = 15.0 (1C, CH_2CH_3), 28.8 (1C, CH_2CO_2H), 34.9 (1C, NCH_3), 43.1 (1C, CH_2CH_3), 52.9 (1C, OCH_3), 121.3 (1C, *C4/5*), 123.5 (1C, *C4/5*), 139.9 (1C, *C2*), 166.5 (1C, CO_2H) ppm. **HRMS** (ESI−) m/z: [PF_6] Calcd for P_1F_6: 144.9647; Found: 144.9647. **HRMS** (ESI+) m/z: [NHO-CO_2Me] Calcd for $C_9H_{15}N_2O_2$: 183.1128; Found: 183.1127.

Synthesis of 1-ethyl-3-methylimidazolium-2-methylensulfinate inner salt (NHO-SO_2, **21**). 1-ethyl-3-methyl-2-methylenimidazoline (2.30 g, 18.5 mmol, prepared and isolated in analogy to a literature procedure)[28] was dissolved in THF (50 mL) and the solution cooled to 0 °C. SO_2 was introduced into the solution whereupon a light yellow solid precipitated immediately. The gas stream was stopped after 1 minute and the suspension was filtered. The filter cake was washed with diethyl ether (20 mL) and dried in fine vacuum. NHO-SO_2 (**21**) was isolated as a light yellow powder in 3.40 g (18.1 mmol, 98%) yield. **Elem. anal.** found C, 44.8; H, 6.5.; N, 15.3; S, 16.7 $C_7H_{12}N_2O_2S_1$ requires C, 44.7; H, 6.4; N, 14.9; S, 17.0. **IR** ν_{max}/cm^{-1}: 3072 (w), 1578 (w), 1526 (m), 1452 (w), 1298 (w), 1256 (w), 1166 (m), 1068 (vs), 1019 (m), 990(vs), 855 (w), 794 (m), 714 (m), 594 (w), 549 (w), 504 (s), 449 (s). **^{1}H-NMR** (300.1 MHz, DMSO-d_6) δ_H = 1.34 (t, $^3J_{HH}$ = 7.3 Hz, 3H, CH_2CH_3), 3.71 (s, 2H, CH_2SO_2), 3.79 (s, 3H, NCH_3), 4.15 (q, $^3J_{HH}$ = 7.3 Hz, 2H, CH_2CH_3), 7.56 (d, $^3J_{HH}$ = 2.1 Hz, 1H, *H*4/5), 7.62 (d, $^3J_{HH}$ = 2.1 Hz, 1H, *H*4/5) ppm. **^{13}C-NMR** (75.5 MHz, DMSO-d_6): δ_C = 15.2 (1C, CH_2CH_3), 35.1 (1C, NCH_3), 42.8 (1C, CH_2CH_3), 54.9 (1C, CH_2SO_2), 119.7 (1C, *C4/5*), 122.1 (1C, *C4/5*), 142.6 (1C, *C2*) ppm.

Synthesis of 1-ethyl-2,3-dimethylimidazolium methylsulfite ([EMMIm][OSO_2Me], **22**). NHO-SO_2 **21** (98 mg, 0.52 mmol, 1.0 eq) was dissolved in acetonitrile (5 mL). Upon addition of methanol (0.21 mL, 0.17 g, 5.2 mmol, 10 eq) the solution turned from light yellow to almost colorless. The mixture was stirred at ambient temperature for 15 hours. After removal of all volatile components [EMMIm][OSO_2Me] was isolated as a colorless oil. Yield: 112 mg (0.51 mmol, 98%). **IR** ν_{max}/cm^{-1}: 3078 (w),2975 (w), 1588 (w), 1541 (w), 1452 (w), 1338 (w), 1294 (w), 1249 (w), 1128 (vs), 1055 (s), 1010 (vs), 979 (m), 964 (m), 790 (br, w), 623

(s), 573 (w), 534 (m), 430 (w). **^{1}H NMR** (300.1 MHz, DMSO-d_6) δ_H = 1.33 (t, $^3J_{HH}$ = 7.3 Hz, 3H, CH_2CH_3), 2.59 (s, 3H, CCH_3), 3.02 (s, 3H. $SOCH_3$), 3.76 (s, 3H, NCH_3), 4.14 (q, $^3J_{HH}$ = 7.3 Hz, 2H, CH_2CH_3), 7.65 (d, $^3J_{HH}$ = 2.1 Hz, 1H, *H*4/5), 7.69 (d, $^3J_{HH}$ = 2.1 Hz, 1H, *H*4/5) ppm. **^{13}C NMR** (75.5 MHz, DMSO-d_6): δ_C = 9.0 (1C, C CH_3), 14.7 (1C, CH_2CH_3), 34.5 (1C, NCH_3), 42.7 (1C, CH_2CH_3), 44.3 ($SOCH_3$), 120.3 (1C, *C4/5*), 122.3 (1C, *C4/5*), 144.0 (1C, *C2*) ppm. **HRMS** (ESI−) m/z: [OSO_2Me] Calcd for $C_1H_3O_3S_1$: 94.9808; Found: 94.9809; [$(OSO_2Me)_2$ + Na] Calcd for $C_2H_6O_6S_2Na_1$: 212.9509; Found: 212.9509. **HRMS** (ESI+) m/z: [EMMIm] Calcd for $C_7H_{13}N_2$: 125.1073; Found: 125.1071.

Acknowledgement

We thank the "Fond der Chemischen Industrie" (doctoral fellowship for L.H.F.) and the "Deutsche Forschungsgemeinschaft" (GRK 1782, Functionalization of Semiconductors) for financial support.

Supporting Information

^{1}H NMR, ^{13}C NMR and IR spectra of the new and isolable substances **2** to **5**, **8**, **10**, **12**, **14**, **15** and **19** to **22** and relevant reaction mixtures. Crystallographic data and lattice structure images for compounds **4**, **5**, **8**, **14**, **15** and **21**.

References

[1] a) R. Kalb (PROIONIC), WO 2008052861, **2008**; b) R. Kalb (PROIONIC), WO 2008 052 860, **2008**; c) N. J. Bridges, C. C. Hines, M. Smiglak, R. D. Rogers, *Chem. - Eur. J.* **2007**, *13*, 5207-5212; d) J. D. Holbrey, R. D. Rogers, S. S. Shukla, C. D. Wilfred, *Green Chem.* **2010**, *12*, 407-413; e) M. Smiglak, C. C. Hines, R. D. Rogers, *Green Chem.* **2010**, *12*, 491; f) M. Aresta, I. Tkatchenko, I. Tommasi, in *Ionic Liquids as Green Solvents, Vol. 856* (Eds.: R. D. Rogers, K. R. Seddon), American Chemical Society, **2003**, pp. 93-99; g) B. Oelkers, J. Sundermeyer, *Green Chem.* **2011**, *13*, 608-618; h) L. H. Finger, F. G. Schröder, J. Sundermeyer, *Z. Anorg. Allg. Chem.* **2013**, *639*, 1140-1152; i) L. H. Finger, F. Wohde, E. I. Grigoryev, A. K. Hansmann, R. Berger, B. Roling, J. Sundermeyer, *Chem. Commun.* **2015**, *51*, 16169-16172; j) L. H. Finger, B. Scheibe, J. Sundermeyer, *Inorg. Chem.* **2015**, *54*, 9568-9575; k) L. H. Finger, J. Sundermeyer, *Chem. Eur. J.* **2016**, accepted manuscript.

[2] a) A. M. Voutchkova, L. N. Appelhans, A. R. Chianese, R. H. Crabtree, *J. Am. Chem. Soc.* **2005**, *127*, 17624-17625; b) A. M. Voutchkova, M. Feliz, E. Clot, O. Eisenstein, R. H. Crabtree, *J. Am. Chem. Soc.* **2007**, *129*, 12834-12846; c) A. M. Voutchkova, R. H. Crabtree, R. D. Putman, K. H. Kelley, T. B. Rachfuss, *Inorg. Synth.* **2010**, *35*, 88-91.

[3] a) I. Tommasi, F. Sorrentino, *Tetrahedron Lett.* **2005**, *46*, 2141-2145; b) H. Zhou, W.-Z. Zhang, C.-H. Liu, J.-P. Qu, X.-B. Lu, *J. Org. Chem.* **2008**, *73*, 8039-8044; c) B. Bantu, G. Manohar Pawar, K. Wurst, U. Decker, A. M. Schmidt, M. R. Buchmeiser, *Eur. J. Inorg. Chem.* **2009**, *2009*, 1970-1976; d) I. Tommasi, F. Sorrentino, *Tetrahedron Lett.* **2009**, *50*, 104-107; e) L.-Q. Gu, Y.-G. Zhang, *J. Am. Chem. Soc.* **2010**, *132*, 914-915; f) J. Sun, X. Yao, W. Cheng, S. Zhang, *Green Chem.* **2014**, *16*, 3297-3304.

[4] a) M. Smiglak, J. D. Holbrey, S. T. Griffin, W. M. Reichert, R. P. Swatloski, A. R. Katritzky, H. Yang, D. Zhang, K. Kirichenko, R. D. Rogers, *Green Chem.* **2007**, *9*, 90-98; b) C. Rijksen, R. D. Rogers, *J.*

Org. Chem **2008**, *73*, 5582-5584; c) J. D. Holbrey, W. M. Reichert, I. Tkatchenko, E. Bouajila, O. Walter, I. Tommasi, R. D. Rogers, *Chem. Commun.* **2003**, 28-29.

[5] a) S. Seo, M. A. DeSilva, J. F. Brennecke, *J. Phys. Chem. B* **2014**, *118*, 14870-14879; b) D. M. Denning, D. E. Falvey, *J. Org. Chem.* **2014**, *79*, 4293-4299; c) B. R. Van Ausdall, J. L. Glass, K. M. Wiggins, A. M. Aarif, J. Louie, *J. Org. Chem.* **2009**, *74*, 7935-7942; d) H. A. Duong, T. N. Tekavec, A. M. Arif, J. Louie, *Chem. Commun.* **2004**, 112-113.

[6] a) N. Kuhn, M. Steimann, G. Weyers, **1999**, *54*, 427-433; b) G. de Robillard, C. H. Devillers, D. Kunz, H. Cattey, E. Digard, J. Andrieu, *Org. Lett.* **2013**, *15*, 4410-4413.

[7] D. Breuch, H. Löwe, *Green Process. Synth.* **2012**, *1*, 261-267.

[8] a) G. Gurau, H. Rodríguez, S. P. Kelley, P. Janiczek, R. S. Kalb, R. D. Rogers, *Angew. Chem., Int. Ed.* **2011**, *50*, 12024-12026; b) M. Besnard, M. I. Cabaco, F. V. Chavez, N. Pinaud, P. J. Sebastiao, J. A. P. Coutinho, Y. Danten, *Chem. Commun.* **2012**, *48*, 1245-1247; c) M. Besnard, M. I. Cabaco, F. Vaca Chavez, N. Pinaud, P. J. Sebastiao, J. A. P. Coutinho, J. Mascetti, Y. Danten, *J. Phys. Chem. A* **2012**, *116*, 4890-4901; d) M. I. Cabaco, M. Besnard, Y. Danten, J. A. P. Coutinho, *J. Phys. Chem. A* **2012**, *116*, 1605-1620.

[9] a) M. Isabel Cabaco, M. Besnard, F. V. Chavez, N. Pinaud, P. J. Sebastiao, J. A. P. Coutinho, J. Mascetti, Y. Danten, *Chem. Commun.* **2013**, *49*, 11083-11085; b) M. I. Cabaco, M. Besnard, F. V. Chavez, N. Pinaud, P. J. Sebastiao, J. A. P. Coutinho, Y. Danten, *J. Chem. Phys.* **2014**, *140*, 244307/244301-244307/244308; c) L. Delaude, *Eur. J. Inorg. Chem.* **2009**, *2009*, 1681-1699.

[10] J. Fischer, W. Siegel, V. Bomm, M. Fischer, K. Mundinger (BASF), EP 0985668, **2001**.

[11] A. Schmidt, A. Beutler, M. Albrecht, B. Snovydovych, F. J. Ramirez, *Org. Biomol. Chem.* **2008**, *6*, 287-295.

[12] a) Z. Kelemen, B. Peter-Szabo, E. Szekely, O. Holloczki, D. S. Firaha, B. Kirchner, J. Nagy, L. Nyulaszi, *Chem. - Eur. J.* **2014**, *20*, 13002-13008; b) I. Tommasi, F. Sorrentino, *Tetrahedron Lett.* **2006**, *47*, 6453-6456.

[13] K. M. Hugar, H. A. Kostalik, G. W. Coates, *J. Am. Chem. Soc.* **2015**, *137*, 8730-8737.

[14] C. Maton, K. Van Hecke, C. V. Stevens, *New J. Chem.* **2015**, *39*, 461-468.

[15] Y.-B. Wang, Y.-M. Wang, W.-Z. Zhang, X.-B. Lu, *J. Am. Chem. Soc.* **2013**, *135*, 11996-12003.

[16] Y.-B. Wang, D.-S. Sun, H. Zhou, W.-Z. Zhang, X.-B. Lu, *Green Chem.* **2015**, *17*, 4009-4015.

[17] L. Dong, J. Wen, W. Li, *Org. Biomol. Chem.* **2015**, *13*, 8533-8544.

[18] S. Naumann, A. W. Thomas, A. P. Dove, *Angew. Chem., Int. Ed.* **2015**, *54*, 9550-9554.

[19] Y.-B. Jia, Y.-B. Wang, W.-M. Ren, T. Xu, J. Wang, X.-B. Lu, *Macromolecules* **2014**, *47*, 1966-1972.

[20] a) A. Fürstner, M. Alcarazo, R. Goddard, C. W. Lehmann, *Angew. Chem., Int. Ed.* **2008**, *47*, 3210-3214; b) A. El-Hellani, J. Monot, R. Guillot, C. Bour, V. Gandon, *Inorg. Chem.* **2013**, *52*, 506-514; c) K. Powers, C. Hering-Junghans, R. McDonald, M. J. Ferguson, E. Rivard, *Polyhedron* **2015**.

[21] P. Tundo, M. Selva, *Acc. Chem. Res.* **2002**, *35*, 706-716.

[22] a) A. P. Krapcho, G. A. Glynn, B. J. Grenon, *Tetrahedron Lett.* **1967**, *8*, 215-217; b) A. P. Krapcho, *Synthesis* **1982**, *1982*, 805-822; c) A. P. Krapcho, *Synthesis* **1982**, *1982*, 893-914; d) A. Paul Krapcho, E. Ciganek, in *Organic Reactions, Vol. 81*, John Wiley & Sons, Inc., **2013**, pp. 1-536.

[23] B. R. Van Ausdall, N. F. Poth, V. A. Kincaid, A. M. Arif, J. Louie, *J. Org. Chem.* **2011**, *76*, 8413-8420.

[24] C. Annese, L. D'Accolti, C. Fusco, I. Tommasi, *Catal. Commun.* **2014**, *46*, 94-97.

[25] C. Bakhtiar, E. H. Smith, *J. Chem. Soc., Perkin Trans. 1* **1994**, 239-243.

[26] a) S. T. Handy, M. Okello, *J. Org. Chem.* **2005**, *70*, 1915-1918; b) B. Huber, L. Rossrucker, J. Sundermeyer, B. Roling, *Solid State Ionics* **2013**, *247–248*, 15-21.

[27] R. C. F. Jones, J. N. Iley, M. Sanchis-Amat, X. Zhang, M. R. J. Elsegood, *Tetrahedron Lett.* **2009**, *50*, 3577-3579.

[28] T. Linder, J. Sundermeyer, *Chem. Commun.* **2009**, 2914-2916.

[29] Michael K. Denk, K. Hatano, Alan J. Lough, *Eur. J. Inorg. Chem.* **2003**, *2003*, 224-231.

[30] B. J. Wagner, J. T. Doi, W. K. Musker, *J. Org. Chem.* **1990**, *55*, 5940-5945.

[31] a) R. Eberhardt, M. Allmendinger, G. A. Luinstra, B. Rieger, *Organometallics* **2003**, *22*, 211-214; b) M. F. Pilz, C. Limberg, B. B. Lazarov, K. C. Hultzsch, B. Ziemer, *Organometallics* **2007**, *26*, 3668-3676; c) M. M. Ibrahim, H. Vahrenkamp, *Z. Anorg. Allg. Chem.* **2006**, *632*, 1083-1085; d) D. F. J. Piesik, S. Range, S. Harder, *Organometallics* **2008**, *27*, 6178-6187; e) C. Mealli, M. Peruzzini, P. Stoppioni, *J. Organomet. Chem.* **1980**, *192*, 437-446.

[32] D. Ginderow, M. Huber, *Acta Crystallogr. B* **1973**, *29*, 560-563.

[33] a) L. Szarvas, K. Massonne (BASF AG), WO 2006021303, **2006**; b) L. Szarvas, T. Rohde, L. Wittenbecher, K. Massonne (BASF AG), WO 2006021304, **2006**.

[34] N. M. Ignatyev, U. Welz-Biermann, A. Kucheryna, H. Willner (Merck Patent GMBH), EP 1902035, **2006**.

[35] G. R. Fulmer, A. J. M. Miller, H. E. Gottlieb, N. H. Sherden, A. Nudelman, B. M. Stoltz, K. I. Goldberg, J. E. Bercaw, *Organometallics* **2010**, *29*, 2176-2179.

[36] Bruker, Bruker AXS Inc., Madison, Wisconsin, USA, **2012**.

[37] A. Altomare, M. C. Burla, M. Camalli, G. Cascarano, C. Giacovazzo, A. Guagliardi, A. G. G. Moliterni, G. Polidori, R. Spagna, *J. Appl. Crystallogr.* **1999**, *32*, 115-119.

[38] M. C. Burla, R. Caliandro, M. Camalli, B. Carrozzini, G. L. Cascarano, C. Giacovazzo, M. Mallamo, A. Mazzone, G. Polidori, R. Spagna, *J. Appl. Crystallogr.* **2012**, *45*, 357-361.

[39] G. Sheldrick, *Acta Crystallogr. A* **2008**, *64*, 112-122.

[40] G. Sheldrick, *Acta Crystallogr. A* **2015**, *71*, 3-8.

[41] A. L. Spek, *Acta Crystallogr. D* **2009**, *65*, 148-155.

[42] L. Farrugia, *J. Appl. Crystallogr.* **2012**, *45*, 849-854.

[43] C. B. Hübschle, G. M. Sheldrick, B. Dittrich, *J. Appl. Crystallogr.* **2011**, *44*, 1281-1284.

[44] Bruker, Bruker AXS Inc., Madison, Wisconsin, USA, **2012**.

[45] Crystal Impact - H. Putz & K. Brandenburg GbR, Kreuzherrenstr. 102, 53227 Bonn, Germany.

[46] W. L. Amarego, D. D. Perrin, *Purification of Laboratory Chemicals*, 4th ed., Elsevier, Burlington, **1996**.

[47] J. E. Bara, *Ind. Eng. Chem. Res.* **2011**, *50*, 13614-13619.

6.5 Synthese von 1,3-Dialkylimidazol-2-chalkogenonen aus NHC-CO_2 Addukten

in preparation

Synthesis of 1,3-Dialkylimidazole-2-chalcogenones from NHC-CO_2 Adducts

Lars H. Finger, Philipp E. Hofmann, Jörg Sundermeyer

Synthesis of 1,3-Dialkylimidazole-2-chalcogenones from NHC-CO_2 Adducts

Lars H. Finger,[a] Philipp E. Hofmann[a], Jörg Sundermeyer[a]

a) Fachbereich Chemie and Materials Science Centre,
Philipps-Universität Marburg,
Hans-Meerwein-Str. 4,
35043 Marburg,
Germany.
*E-Mail: JSU@staff.uni-marburg.de

TOC Graphic

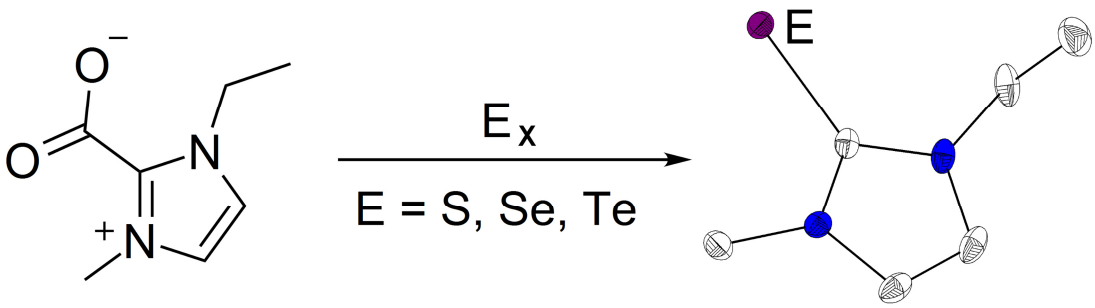

Abstract

We present the facile synthesis of imidazole-2-chalcogenones from the readily available imidazolium-2-carboxylate zwitterions. In contrast to other procedures the synthesis requires shorter reaction times, has only CO_2 as byproduct and is applicable to all heavier chalcogens S, Se and Te.

Introduction

Imidazole-2-chalcogenones – formally a N-heterocyclic carbene (NHC) chalcogen adducts NHC=E (E = S, Se, Te) – are a highly versatile and interesting class of compounds. First of all carbimazole and methimazole are important thyrostatic drugs for the treatment of hyperthyroidism.[1] The coordination chemistry of closely related compounds towards coinage metals and copper in particular was investigated in special detail.[2] These serve as mimics for naturally occurring selone and thione antioxidants, which prevent copper mediated oxidative DNA damage.[3] Furthermore, imidazole-2-thione copper(I) complexes have proven as highly regioselective catalysts for the hydroboration of internal alkynes[4] and complexes with bismuth trihalides were investigated as catalysts for the acylative cleavage of cyclic ethers.[5] Furthermore, complexes with Rh, Cr, Mo, W and Mn have been studied.[6] Especially imidazole-2-selones with divers ring substitution patterns were employed as model compounds to evaluate the π-acceptor characteristics of the corresponding NHCs.[7] The synthesis of free NHCs by reduction of an imidazole-2-thione with elemental potassium is possibly their most widely applied utilization.[8] The reaction of the chalcogenones with halogens and interhalogens yields NHC stabilized chalcogen dihalides.[9] A subsequent halide – pseudohalide exchange allows the preparation of highly active cyanation reagents.[10] Dialkylimidazole-2-thiones furthermore serve as starting material for the synthesis of cyclic thiouronium ionic liquids (ILs).[11]

The most common way to access NHC=E adducts is the reaction of free NHCs with elemental chalcogens[11-12] or sodium dichalcogenides.[13] The source of the NHC is quite variable; while isolable and sufficiently stabilized NHCs can be used as singular compounds from storage, most of the smaller and more instable NHCs have to be prepared *in situ*. For this, typically an imidazolium halide salt is reacted with a sufficiently strong base. In all cases the precipitating halide salt has to be removed from the solution, a task, which is not always trivial in polar solvents like THF. Rogers and coworkers showed, that imidazolium acetate ILs react with sulfur at 25 °C and with selenium at 75 °C to form the corresponding imidazole-2-

chalcogenones. The reaction times were in the range of several days, though.[14] Recently, the synthesis of dialkylimidazole-2-selones in high yields was reported in water, employing sodium carbonate as a base.[15] Especially for tetramethylimidazole-2-thione the synthesis from *N*,*N*'-dimethylthiourea and 3-hydroxybutan-2-one is widely applied.[8, 10, 16] In one instance imidazole-2-thiones were synthesized from imidazolium-2-carboxylates and the corresponding free carbenes, which were generated by electrolysis of imidazolium tetrafluoroborate ILs.[17] Imidazolium-2-carboxylates have been further employed as proto-carbenes in the formation of transition metal complexes[18] and as organocatalysts.[19] The specific conditions which allow the removal of the CO_2 moiety to generate a reactive carbene or the original imidazolium cation have been thoroughly investigated.[18b, 19a, 19b, 20]

1-Alkyl-3-methylimidazolium methylcarbonates are conveniently prepared in either a solvothermal reaction or a microwave assisted synthesis.[21] They can be employed as starting materials for a variety of organic salts as the methylcarbonate anion will deliberately react with Brønsted acids under irreversible decay to methanol and CO_2 and can also act as a desilylating agent.[22] We recently demonstrated that the formation of carboxylates does not require exceedingly high temperatures as sometimes described, but that they form at ambient temperature upon removal of methanol from the reaction mixture.[23]

We have found that the series of 1-ethyl-3-methylimidazole-2-chalcogenones NHC=E (NHC = 1-ethyl-3-methylimidazol-2-ylidene, E = S, Se, Te) can most conveniently be prepared from the corresponding imidazolium-2-carboxylate zwitterions. Furthermore, we came to notice that these imidazole-2-chalcogenones can be sublimed in fine vacuum allowing access to highly pure samples.

Results

1-Ethyl-3-methylimidazolium-2-carboxylate, respectively NHC-CO_2 (**1**), is a known colorless solid, which is well soluble in polar aprotic solvents like DMSO and acetonitrile. It is most selectively formed from EMIm methylcarbonate upon evaporation of methanol, the solvent used in its convenient synthesis.[24] With methanol and water **1** is cleaved resulting in the corresponding methyl- or bicarbonate, although this reaction is inhibited in the absence of nucleophiles. Under dry conditions at ambient temperature it is to the best of our knowledge indefinitely stable. This allows convenient storage and precise weighing of this proto-carbene.

When combining the carboxylate **1** and sulfur or selenium in acetonitrile no reaction is evident at ambient temperature. Upon heating to reflux the chalcogen slowly dissolves. After three (S) to twelve (grey Se) hours no further progress can be observed. After cooling to ambient temperature, separating the solution from potential solid residues and evaporation to dryness the chalcogenones NHC=S (**2**) and NHC=Se (**3**) were obtained as light yellow solids with no NMR-detectable impurities. Both compounds could be sublimed at $1 \cdot 10^{-3}$ mbar and temperatures between 80 °C and 90 °C affording highly pure colorless powders with yields still exceeding 80% (Scheme 1).

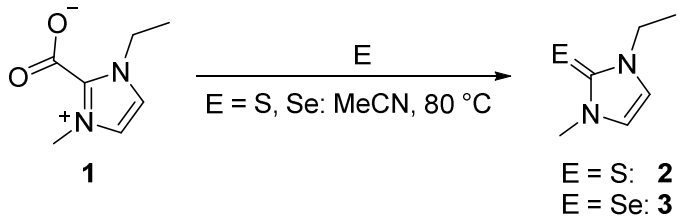

Scheme 1. Synthesis of NHC=S, **2** and NHC=Se, **3** from EMIm-CO_2.

For the synthesis of the corresponding tellone acetonitrile proved to be not suitable. After several hours to several days the starting material **1** could still be observed next to several unidentified species and minor amounts of the anticipated product. After four days at 100 °C the product percentage is significantly increased but several side products remain. However, if the reaction is conducted in refluxing toluene, **1** and the tellurium powder dissolve completely within 30 minutes. Upon syringe filtration and removal of all volatiles a light green solid remains, which shows only minimum impurities (Scheme 2). Taking into account, that 1,3-dialkylimidazole-2-ylidenes typically show the highest decarboxylation temperatures,[20c] it is assumed that this procedure will be transferable to a range of other NHC-CO_2 adducts.

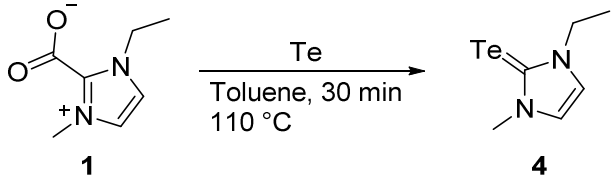

Scheme 2. Synthesis of 1-ethyl-3-methyl-imidazole-2-tellone (**4**).

The tellone **4** could be sublimed under equivalent conditions as the lighter homologues, reaching yields of more than 75%. Interestingly the freshly sublimed substance appeared colorless at first but returned to being light green after a couple of hours, although kept under inert conditions. The sublimation of NHC=Te also afforded single crystals suitable for an X-ray structure determination (Figure 1).

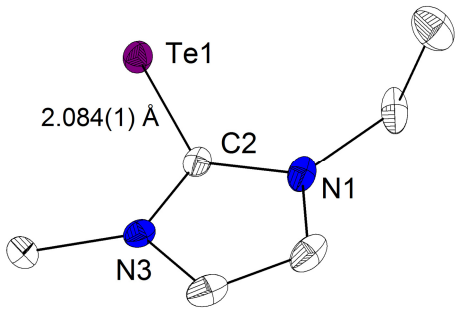

Figure 1. Molecular structure of 1-ethyl-3-methylimidazole-2-tellone (**4**), hydrogen atoms were omitted for clarity. Relevant bond distances/ Å and angles/ °: C2-Te1: 2.084(1), C2-N1: 1.360(2), C2-N3: 1.351(2), N1-C2-N3: 105.5(1), N1-C2-Te1: 127.6(1), N3-C2-Te1: 126.9(1).

Compound **4** crystallized in the monoclinic space group $P2_1/n$ with four molecules per unit cell. The carbon tellurium bond length is in perfect agreement with the structure of the closely related 1,3-di-isopropyl-4,5-dimethylimidazole-2-tellone. Furthermore, the ^{125}Te and ^{13}C NMR spectroscopic data are in good agreement (**4**, δ_{Te} = 189.1 ppm, $\delta_{C\text{-}2}$ = 127.5 ppm, Lit.: δ_{Te} = 167.8 ppm, $\delta_{C\text{-}2}$ = 132.1 ppm).[12d] If all compounds are considered, for which both values have been reported so far (Figure 2), the chemical shifts of the Te atom and the imidazole C-2 atom appear to be interdependent (Table1 and Figure 3).

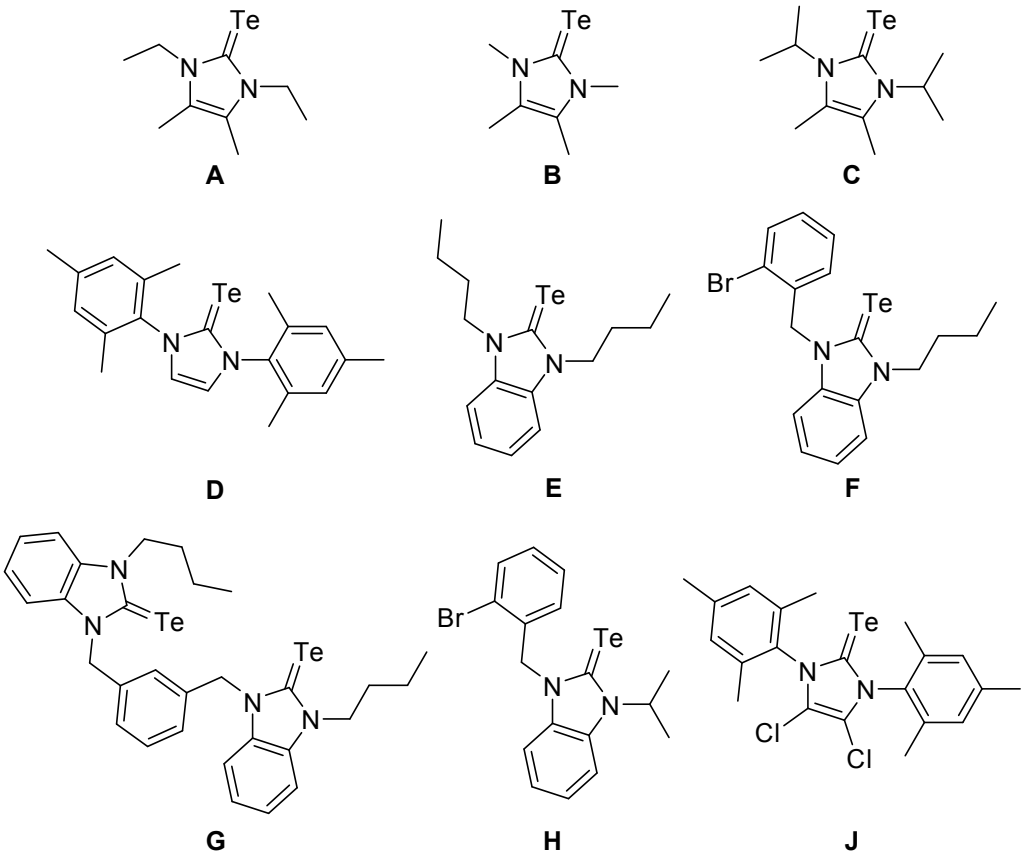

Figure 2. Valence formulae of literature known imidazole-2-tellones, for which are compared with respect to ^{125}Te NMR and ^{13}C NMR shifts have been reported. References: A, B, C,[12d] D, J,[25] E,[26] F, H,[13] G.[27]

Table 1. ^{125}Te and ^{13}C NMR shifts of reference imidazole-2-tellones.

NHC-type	δ_{Te}/ ppm	$\delta_{C\text{-}2}$/ppm	Ref. (solvent)
Dialkyl-Im, **A**	−200	126.8	[12d] (C_6D_6)
Dialkyl-Im, **4**	−189.1	127.5	this work (DMSO-d_6)
Dialkyl-Im, **B**	−168.1	131.0	[12d] (C_6D_6)
Dialkyl-Im, **C**	−167.8	132.1	[12d](C_6D_6)
Diaryl-Im, **D**	−149.8	133.1	[25] (THF-d_8)
Dialkyl-Benz, **E**	−143	143.7	[26] ($CDCl_3$)
Alkyl-Aryl-Benz, **F**	−130	147.5	[13] ($CDCl_3$)
Alkyl-Aryl-Benz, **G**	−129.1	146.2	[27] ($CDCl_3$)
Alkyl-Aryl-Benz, **H**	−126	147.5	[13] ($CDCl_3$)
Diaryl-Im, **J**	−4	134.3	[25] (THF-d_8)

Table 1 summarizes the known chemical shift values and in Figure 3 the $\delta_{C\text{-}2}$ chemical shift values are correlated with the δ_{Te} values. With **J** as a single exception the reference compounds show an almost linear dependence. A shift of the respective resonance signals to lower field indicates an increasing π-accepting capability of the NHC. An analogous correlation was observed for carbene phenylphosphinidene adducts,[28] but not for carbene selenium adducts.[7b] However, the limited range of tellurium adducts, which is available so far, and the inconsistent NMR solvents do not allow a fully reliable analysis.

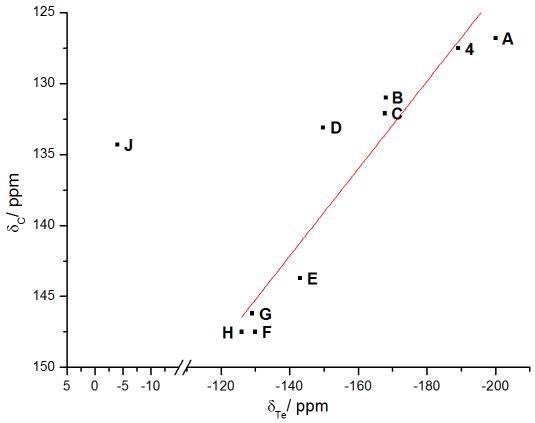

Figure 3. Correlation of the ^{125}Te and ^{13}C NMR chemical shift values in reference imidazole-2-tellones.

Solvate free methylcarbonate salts are not accessible with C-2 protonated imidazolium cations, because an equilibrium between the former and the carboxylate zwitterion plus methanol prevails. This prevented the synthesis of trimethylsilylchalcogenolate salts from the corresponding methylcarbonates.[22b] It was anticipated **1** might react with bis(trimethylsilyl)sulfide, potentially by forming a silyl substituted carboxylate and a trimethylsilylthiolate anion. Our results indicate that this is indeed the first step, but that the reaction proceeds rapidly with a nucleophilic attack of the thiolate anion at the carbonyl group and selective formation of 1-ethyl-3-methylimidazolium-2-thiocarboxylate NHC-COS **5** and TMS_2O (Scheme 3).

Scheme 3. Synthesis of 1-ethyl-3-methyl-imidazolium-2-thiocarboxylate (**5**).

This NHC-COS adduct is otherwise accessible by reacting a free carbene with a large excess of COS gas.[29] Our alternative synthesis is easily scaled up and of particular advantage, as convenient NHC-CO_2 adducts are the starting materials: It offers an elegant way to access the corresponding thiocarboxylates without repeated preparation of the free carbene and handling of COS. The molecular structure of **5** could be elucidated by single crystal X-ray diffraction on a crystal obtained from layering a concentrated solution in acetonitrile with diethyl ether. **5** crystallized in the triclinic space group *P*−1 with two molecules per unit cell (Figure 4). The structure was interpreted as a non-meroedral twin.

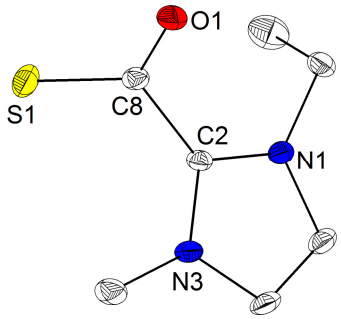

Figure 4. Molecular structure of 1-ethyl-3-methyl-imidazolium-2-thiocarboxylate (**5**), hydrogen atoms were omitted for clarity. Relevant bond distances/ Å and angles/ °: C2-C8: 1.511(3), C8-O1: 1.232(3), C8-S1: 1.692(2), C2-N1: 1.335(3), C2-N3: 1.339(3), N1-C2-N3: 107.9(2), O1-C8-S1: 129.2(2), N3-C2-C8-S1: 67.4(3).

The C-O and C-S bond lengths are 1.232(3) Å and 1.692(2) Å, respectively. In the only other crystalline example of a uncoordinated NHC-COS adduct derived from 1,3-dimesitylimidazol-2-ylidene these bonds are significantly shorter (d(C-O) = 1.217(2) Å, d(C-S) = 1.676(1) Å), while the C2-C8 bond is slightly elongated (1.524(2) Å vs. 1.511(3) Å in **5**).[29] The C-N bonds of **5** again show longer distances than the mesityl substituted counterpart (**5**: d(C2-N1) = 1.335(3) Å and d(C2-N3 = 1.339(3) Å; Lit.[29]: 1.320(2) Å and 1.324(2) Å, respectively). The torsion of the COS moiety from the imidazole ring is significantly smaller in **5** (67.4(3)° vs. 85.0(1)°).This is in accordance with the observations made for the series of NHC-CO_2 adducts.[20c] NHCs with bulkier substituents and a better stabilization of the free carbene show weaker interactions with the attached electrophile and a

lower influence on its structure. So far, the analogous reactions with TMS_2Se and TMS_2Te were not successful and led to unselective transformations.

Conclusion

We have presented a highly convenient access to 1-ethyl-3-imidazole-2-chalcogenones starting from the corresponding imidazolium-2-carboxylate zwitterions. The target compounds **2** to **4** are generated upon heating the carboxylate in presence of the elemental chalcogen in suitable solvents like acetonitrile or toluene. In contrast to earlier procedures the reaction times are significantly reduced and as CO_2 is the only and highly volatile side product the purification is greatly facilitated. For the generation of high-end purified samples the sublimation of the respective substances was employed. From imidazolium-2-carboxylate and (bistrimethylsilyl)sulfide the corresponding thiocarboxylate is accessible in a simple procedure rendering the preparation and handling of gaseous COS unnecessary for the synthesis of these NHC-COS adducts.

Experimental Section

Methods and Devices

Unless stated otherwise all synthetic steps were conducted using standard Schlenk techniques. Elemental analyses (C, H, N, S) were carried out by the service department for routine analysis and mass spectrometry with a vario MICRO cube (ELEMENTAR). The samples were weighed into tin capsules inside a nitrogen filled glove box. ^{1}H and proton decoupled ^{13}C NMR spectra were recorded at 300 K in automation with a BRUKER Avance II 300 spectrometer and were calibrated using residual proton and solvent signals (DMSO-d_6: δ_H 2.50 ppm, δ_C 39.52 ppm).[30] The ^{77}Se and ^{125}Te NMR spectra were recorded by the service department for NMR analyses with a BRUKER Avance III HD 300 or Avance III 500 spectrometer. These spectra were calibrated externally against dimethyl selenide and dimethyl telluride. IR spectra were recorded on a BRUKER APLPHA FT-IR spectrometer with Platinum ATR-sampling (diamond single crystal). HR-ESI mass spectra were acquired with a LTQ-FT Ultra mass spectrometer (THERMO FISCHER SCIENTIFIC). The resolution was set to 100.000. The data collection for the single crystal structure determinations was performed on a Bruker D8 QUEST diffractometer by the X-ray service department. Bruker software (APEX2, SAINT) was used for data collection, cell refinement and data reduction.[31] The structures were solved with SIR97[32] or SIR2011,[33] refined with SHELXL-2014[34] and finally

validated using PLATON[35] software, all within the WinGX[36] software bundle. Absorption corrections were applied beforehand within the APEX2 software (multi-scan).[37] Graphic representations were created using Diamond 4.[38] H atoms were constrained to parent site. In all graphics the ellipsoids are shown for the 50% probability level. Crystallographic data for the structures reported in this paper are supplied as supporting information and have been deposited with the Cambridge Crystallographic Data Centre (CCDC XXX-XXX).

Starting Materials

All solvents were dried according to common procedures[39] and passed through columns of aluminum oxide, 3 Å molecular sieve and R3-11G-catalyst (BASF) or stored over molecular sieve (3 or 4 Å) until use.

Synthetic procedures

Synthesis of 1-ethyl-3-methylimidazolium-2-carboxylate ([NHC-CO_2], **1**). Ethyl imidazole (15.1 g, 157 mmol, 1.00 eq), dimethyl carbonate (25.1 g, 279 mmol, 1.77 eq) and methanol (25 mL) were combined in a glass autoclave and heated to 130 °C for 14.5 hours. All volatile components were removed *in vacuo*. Samples of the solution and the remainder were investigated by ^{1}H NMR spectroscopy during the removal of the solvent. The residue was recrystallized from acetonitrile yielding NHC-CO_2 as colorless crystals in a yield of 17.4 g (93.4 mmol, 59%). **Mp**: 123.3 °C (2 K/min, acetonitrile). **Elem. anal.** found C, 54.2; H, 6.5; N, 18.2; $C_7H_{10}N_2O_2$ requires C, 54.5; H, 6.5; N, 18.2. **IR** ν_{max}/cm^{-1}: 3086 (w), 1664 (vs), 1506 (m), 1426 (m), 1376 (m), 1314 (vs), 1286 (s), 1238 (m), 1110, (w), 1093 (w), 1037 (w), 837 (m), 818 (m), 786 (vs), 660 (m), 633 (m), 604 (w). **^{1}H NMR** (300.1 MHz, DMSO-d_6) δ_H = 1.33 (t, $^3J_{HH}$ = 7.2 Hz, 3H, CH_2CH_3), 3.95 (s, 3H, NCH_3), 4.46 (q, $^3J_{HH}$ = 7.2 Hz, 2H, CH_2CH_3), 7.56 (s, 1H, *H*4/5), 7.64 (s, 1H, *H*4/5) ppm. **^{13}C NMR** (75.5 MHz, DMSO-d_6): δ_C = 15.9 (1C, CH_2CH_3), 36.4 (1C, NCH_3), 44.0 (1C, CH_2CH_3), 120.4 (1C, *C4/5*), 122.3 (1C, *C4/5*), 141.9 (1C, *C2*), 154.0 (1C, CH_2CO_2) ppm.

Synthesis of 1-ethyl-3-methylimidazole-2-thione (NHC=S, **2**). NHC-CO_2 (496 mg, 3.22 mmol, 1.00 eq) and sulfur (103 mg, 3.21 mmol, 1.00 eq) were suspended in acetonitrile (12 mL). The mixture was heated to 80°C for 14 hours, whereupon it became a clear light yellow solution. Volatile components were removed *in vacuo* and the residue was sublimed at 80 °C and $1 \cdot 10^{-3}$ mbar, while the cold finger was cooled with dry ice. NHC=S (**2**) was isolated as a colorless powder in 350 mg (2.73 mmol, 85%) yield. **Elem. anal.** found C, 50.4;

H, 7.3; N, 19.5; S, 22.3; $C_6H_{10}N_2S_1$ requires C, 50.7; H, 7.1; N, 19.7; S, 22.55. **^{1}H NMR** (300.1 MHz, DMSO-d_6) δ_H = 1.21 (t, $^3J_{HH}$ = 7.2 Hz, 3H, CH_2CH_3), 3.46 (s, 3H, NCH_3), 3.95 (q, $^3J_{HH}$ = 7.2 Hz, 2H, CH_2CH_3), 7.11 (d, $^3J_{HH}$ = 2.4 Hz, 1H, *H*4/5), 7.14 (d, $^3J_{HH}$ = 2.4 Hz, 1H, *H*4/5) ppm. **^{13}C NMR** (75.5 MHz, DMSO-d_6): δ_C = 14.0 (1C, CH_2CH_3), 34.2 (1C, NCH_3), 41.9 (1C, CH_2CH_3), 116.4 (1C, *C4/5*), 118.3 (1C, *C4/5*), 161.0 (1C, *C2*) ppm. (^{1}H and ^{13}C NMR data agree well with literature values[14]) **HRMS** (ESI+): m/z found 143.0640; $[M+H]^+$ ($C_6H_{11}N_2S_1$) requires 143.0637.

Synthesis of 1-ethyl-3-methylimidazole-2-selone (NHC=Se, **3**). NHC=Se (**3**) was synthesized in complete analogy to the sulfur compounds from NHC-CO_2 (400 mg, 2.60 mmol, 1.00 eq) and grey selenium (206 mg, 2.61 mmol, 1.00 eq) in acetonitrile (10 mL). After sublimation 402 mg (2.13 mmol, 82%) of NHC=Se (**3**) were isolated as a colorless powder. **Elem. anal.** found C, 38.1; H, 5.2.; N, 15.2; $C_6H_{10}N_2Se_1$ requires C, 38.1; H, 5.3; N, 14.8. **^{1}H NMR** (300.1 MHz, DMSO-d_6) δ_H = 1.22 (t, $^3J_{HH}$ = 7.3 Hz, 3H, CH_2CH_3), 3.55 (s, 3H, NCH_3), 4.05 (q, $^3J_{HH}$ = 7.3 Hz, 2H, CH_2CH_3), 7.33 (d, $^3J_{HH}$ = 2.2 Hz, 1H, *H*4/5), 7.35 (d, $^3J_{HH}$ = 2.2 Hz, 1H, *H*4/5) ppm. **^{13}C NMR** (75.5 MHz, DMSO-d_6): δ_C = 14.2 (1C, CH_2CH_3), 36.1 (1C, NCH_3), 43.8 (1C, CH_2CH_3), 118.7 (1C, *C4/5*), 120.5 (1C, *C4/5*), 154.0 (1C, *C2*) ppm. (^{1}H and ^{13}C NMR data agree well with literature values[14]) **^{77}Se NMR** (57.3 MHz, DMSO-d_6): δ_{Se} = 22.8 ppm. **HRMS** (ESI+): m/z found 190.0007; $[M]^+$ ($C_6H_{10}N_2Se_1$) requires 190.0004.

Synthesis of 1-ethyl-3-methylimidazole-2-tellone (NHC=Te, **4**). NHC-CO_2 (220 mg, 1.43 mmol, 1.00 eq) and tellurium powder (220 mg, 1.71 mmol, 1.21 eq) were suspended in toluene (18 mL). The mixture was heated to 110°C for 30 minutes, whereupon it became a clear light green solution. Volatile components were removed *in vacuo* yielding 263 mg (1.11 mmol, 77%) of NHC=Te as a light green powder. After sublimation a colorless powder was isolated with a yield of 63% (214 mg, 0.90 mmol). **Elem. anal.** found C, 30.4; H, 4.2.; N, 12.1; $C_6H_{10}N_2Te_1$ requires C, 30.3; H, 4.2; N, 11.8. **IR** ν_{max}/cm^{-1}: 3972 (w), 2960 (w), 1562 (w), 1460 (m), 1408 (m), 1377 (m), 1260 (s), 1219 (s), 1086 (s br), 1016 (s br), 795 (s), 724 (vs), 660 (s), 619 (m)m 465 (m). **^{1}H NMR** (300.1 MHz, DMSO-d_6) δ_H = 1.26 (t, $^3J_{HH}$ = 7.2 Hz, 3H, CH_2CH_3), 3.64 (s, 3H, NCH_3), 4.10 (q, $^3J_{HH}$ = 7.2 Hz, 2H, CH_2CH_3), 7.56 (d, $^3J_{HH}$ = 2.0 Hz, 1H, *H*4/5), 7.59 (d, $^3J_{HH}$ = 2.0 Hz, 1H, *H*4/5) ppm. **^{13}C NMR** (75.5 MHz, DMSO-d_6): δ_C = 14.2 (1C, CH_2CH_3), 39.5 (1C, NCH_3), 47.0 (1C, CH_2CH_3), 121.1 (1C, *C4/5*), 122.9 (1C, *C4/5*), 127.5 (1C, *C2*) ppm. **^{125}Te NMR** (157.8 MHz, DMSO-d_6): δ_{te} = −189.1 ppm.

Synthesis of 1-ethyl-3-methylimidazolium-2-thiocarboxylate ([NHC-COS], **5**). NHC-CO_2 (1.00 g, 6.49 mmol, 1.00 eq) was dissolved in acetonitrile (7 mL). TMS_2S (1.16 g, 6.50 mmol, 1.00 eq) was added to the solution, which was then refluxed for 2 hours. After cooling to ambient temperature all volatiles were removed under reduced pressure and the residue dried in fine vacuum. NHC-COS (**5**) was isolated as a yellow solid. **Mp:** 128.8 °C (2 K/min, acetonitrile) **Elem. anal.** found C, 49.8; H, 6.1; N, 17.0; S, 19.0; $C_7H_{10}N_2OS$ requires C, 49.4; H, 5.9; N, 16.5; S, 18.8. **IR** ν_{max}/cm^{-1}: 3116 (m), 2970 (w), 1506 (vs), 1464 (s), 1446 (s), 1389 (m), 1331 (w), 1291 (w), 1230 (m), 1201 (m), 1116 (m), 1055 (m), 968 (m), 937 (vs), 807 (m), 765 (m), 716 (vs), 628 (m), 611 (m), 565 (w). **^{1}H NMR** (300.1 MHz, DMSO-d_6) δ_H = 1.34 (t, $^3J_{HH}$ = 7.2 Hz, 3H, CH_2CH_3), 3.76 (s, 3H, NCH_3), 4.19 (q, $^3J_{HH}$ = 7.3 Hz, 2H, CH_2CH_3), 7.48 (d, $^3J_{HH}$ = 1.6 Hz, 1H, *H*4/5), 7.55 (d, $^3J_{HH}$ = 1.6 Hz, 1H, *H*4/5) ppm. **^{13}C NMR** (75.5 MHz, DMSO-d_6): δ_C = 15.1 (1C, CH_2CH_3), 35.0 (1C, NCH_3), 43.3 (1C, CH_2CH_3), 118.8 (1C, *C4/5*), 120.8 (1C, *C4/5*), 144.5 (1C, *C2*), 190.0 (1C, *C*SO) ppm. **HRMS** (ESI+): m/z found 193.0403; $[M+Na]^+$ ($C_7H_{10}N_2O_1S_1Na_1$) requires 193.0406; found 171.0586; $[M+H]^+$ ($C_7H_{11}N_2O_1S_1$) requires 171.0587.

TMS_2O was found as volatile side product.

Acknowledgement

We thank the "Fond der Chemischen Industrie" (doctoral fellowship for L.H.F.) and the "Deutsche Forschungsgemeinschaft" (GRK 1782, Functionalization of Semiconductors) for financial support.

Supporting Information

^{1}H NMR, ^{13}C NMR and heteronuclei NMR spectra of the substances **1** to **5** and crystallographic data for compounds **4** and **5**.

References

[1] D. Manna, G. Roy, G. Mugesh, *Acc. Chem. Res.* **2013**, *46*, 2706-2715.

[2] a) M. T. Aroz, M. C. Gimeno, M. Kulcsar, A. Laguna, V. Lippolis, *Eur. J. Inorg. Chem.* **2011**, *2011*, 2884-2894; b) M. M. Kimani, C. A. Bayse, J. L. Brumaghim, *Dalton Trans.* **2011**, *40*, 3711-3723; c) M. M. Kimani, D. Watts, L. A. Graham, D. Rabinovich, G. P. A. Yap, J. L. Brumaghim, *Dalton Trans.* **2015**, *44*, 16313-16324.

[3] a) M. M. Kimani, H. C. Wang, J. L. Brumaghim, *Dalton Trans.* **2012**, *41*, 5248-5259; b) M. M. Kimani, C. A. Bayse, B. S. Stadelman, J. L. Brumaghim, *Inorg. Chem.* **2013**, *52*, 11685-11687; c) M. M. Kimani, J. L. Brumaghim, D. VanDerveer, *Inorg. Chem.* **2010**, *49*, 9200-9211.

[4] H. R. Kim, I. G. Jung, K. Yoo, K. Jang, E. S. Lee, J. Yun, S. U. Son, *Chem. Commun.* **2010**, *46*, 758-760.

[5] K. Srinivas, P. Suresh, C. N. Babu, A. Sathyanarayana, G. Prabusankar, *RSC Adv.* **2015**, *5*, 15579-15590.

[6] a) B. Choi, D. W. Paley, T. Siegrist, M. L. Steigerwald, X. Roy, *Inorg. Chem.* **2015**, *54*, 8348-8355; b) N. Kuhn, R. Fawzi, T. Kratz, M. Steimann, G. Henkel, *Phosphorus, Sulfur Silicon Relat. Elem.* **1996**, *108*, 107-119; c) A. Neveling, G. R. Julius, S. Cronje, C. Esterhuysen, H. G. Raubenheimer, *Dalton Trans.* **2005**, 181-192.

[7] a) A. Liske, K. Verlinden, H. Buhl, K. Schaper, C. Ganter, *Organometallics* **2013**, *32*, 5269-5272; b) S. V. C. Vummaleti, D. J. Nelson, A. Poater, A. Gomez-Suarez, D. B. Cordes, A. M. Z. Slawin, S. P. Nolan, L. Cavallo, *Chem. Sci.* **2015**, *6*, 1895-1904.

[8] N. Kuhn, T. Kratz, *Synthesis* **1993**, *1993*, 561-562.

[9] a) A. J. Arduengo, E. M. Burgess, *J. Am. Chem. Soc.* **1977**, *99*, 2376-2378; b) F. Bigoli, P. Deplano, F. A. Devillanova, V. Lippolis, M. L. Mercuri, M. A. Pellinghelli, E. F. Trogu, *Eur. J. Inorg. Chem.* **1998**, *1998*, 137-141; c) D. J. Williams, D. Vanderveer, B. R. Crouse, R. R. Raye, T. Carter, K. S. Hagen, M. Brewer, *Main Group Chem.* **1997**, *2*, 61-66; d) E. J. Juárez-Pérez, M. C. Aragoni, M. Arca, A. J. Blake, F. A. Devillanova, A. Garau, F. Isaia, V. Lippolis, R. Núñez, A. Pintus, C. Wilson, *Chem. Eur. J.* **2011**, *17*, 11497-11514; e) N. Kuhn, T. Kratz, G. Henkel, *Z. Naturforsch. B* **1996**, *51*, 295-197.

[10] G. Talavera, J. Peña, M. Alcarazo, *J. Am. Chem. Soc.* **2015**, *137*, 8704-8707.

[11] N. Taccardi, I. Niedermaier, F. Maier, H.-P. Steinrück, P. Wasserscheid, *Chem. Eur. J.* **2012**, *18*, 8288-8291.

[12] a) M. Banerjee, R. Karri, K. S. Rawat, K. Muthuvel, B. Pathak, G. Roy, *Angew. Chem., Int. Ed.* **2015**, *54*, 9323-9327; b) G. Roy, P. N. Jayaram, G. Mugesh, *Chem. Asian J.* **2013**, *8*, 1910-1921; c) S. Sauerbrey, P. K. Majhi, G. Schnakenburg, A. J. Arduengo III, R. Streubel, *Dalton Trans.* **2012**, *41*, 5368-5376; d) N. Kuhn, G. Henkel, T. Kratz, *Chem. Ber.* **1993**, *126*, 2047-2049.

[13] S. T. Manjare, S. Sharma, H. B. Singh, R. J. Butcher, *J. Organomet. Chem.* **2012**, *717*, 61-74.

[14] H. Rodriguez, G. Gurau, J. D. Holbrey, R. D. Rogers, *Chem. Commun.* **2011**, *47*, 3222-3224.

[15] F. Tian, Y. Chen, P. Li, S. Lu, *Phosphorus, Sulfur Silicon Relat. Elem.* **2014**, *189*, 1391-1395.

[16] M. B. Ansell, D. E. Roberts, F. G. N. Cloke, O. Navarro, J. Spencer, *Angew. Chem., Int. Ed.* **2015**, *54*, 5578-5582.

[17] a) M. Feroci, M. Orsini, A. Inesi, *Adv. Synth. Catal.* **2009**, *351*, 2067-2070; b) M. Feroci, I. Chiarotto, S. V. Ciprioti, A. Inesi, *Electrochim. Acta* **2013**, *109*, 95-101.

[18] a) A. M. Voutchkova, L. N. Appelhans, A. R. Chianese, R. H. Crabtree, *J. Am. Chem. Soc.* **2005**, *127*, 17624-17625; b) A. M. Voutchkova, M. Feliz, E. Clot, O. Eisenstein, R. H. Crabtree, *J. Am. Chem. Soc.* **2007**, *129*, 12834-12846; c) A. M. Voutchkova, R. H. Crabtree, R. D. Putman, K. H. Kelley, T. B. Rachfuss, *Inorg. Synth.* **2010**, *35*, 88-91; d) J. Olguin, H. Mueller-Bunz, M. Albrecht, *Chem. Commun.* **2014**, *50*, 3488-3490; e) A. Tudose, L. Delaude, B. Andre, A. Demonceau, *Tetrahedron Lett.* **2006**, *47*, 8529-8533.

[19] a) I. Tommasi, F. Sorrentino, *Tetrahedron Lett.* **2005**, *46*, 2141-2145; b) H. Zhou, W.-Z. Zhang, C.-H. Liu, J.-P. Qu, X.-B. Lu, *J. Org. Chem.* **2008**, *73*, 8039-8044; c) B. Bantu, G. Manohar Pawar, K. Wurst, U. Decker, A. M. Schmidt, M. R. Buchmeiser, *Eur. J. Inorg. Chem.* **2009**, *2009*, 1970-1976; d) I. Tommasi, F. Sorrentino, *Tetrahedron Lett.* **2009**, *50*, 104-107; e) L.-Q. Gu, Y.-G. Zhang, *J. Am. Chem. Soc.* **2010**, *132*, 914-915; f) J. Sun, X. Yao, W. Cheng, S. Zhang, *Green Chem.* **2014**, *16*, 3297-3304; g) M. Fèvre, J. Pinaud, A. Leteneur, Y. Gnanou, J. Vignolle, D. Taton, K. Miqueu, J.-M. Sotiropoulos, *J. Am. Chem. Soc.* **2012**, *134*, 6776-6784.

[20] a) S. Seo, M. A. DeSilva, J. F. Brennecke, *J. Phys. Chem. B* **2014**, *118*, 14870-14879; b) D. M. Denning, D. E. Falvey, *J. Org. Chem.* **2014**, *79*, 4293-4299; c) B. R. Van Ausdall, J. L. Glass, K. M. Wiggins, A. M. Aarif, J. Louie, *J. Org. Chem.* **2009**, *74*, 7935-7942; d) H. A. Duong, T. N. Tekavec, A. M. Arif, J. Louie, *Chem. Commun.* **2004**, 112-113.

[21] a) R. Kalb (PROIONIC), WO 2008052861, **2008**; b) J. D. Holbrey, R. D. Rogers, S. S. Shukla, C. D. Wilfred, *Green Chem.* **2010**, *12*, 407-413.

[22] a) M. Smiglak, C. C. Hines, R. D. Rogers, *Green Chem.* **2010**, *12*, 491; b) L. H. Finger, B. Scheibe, J. Sundermeyer, *Inorg. Chem.* **2015**, *54*, 9568-9575; c) L. H. Finger, F. G. Schröder, J. Sundermeyer, *Z. Anorg. Allg. Chem.* **2013**, *639*, 1140-1152; d) L. H. Finger, F. Wohde, E. I. Grigoryev, A. K. Hansmann, R. Berger, B. Roling, J. Sundermeyer, *Chem. Commun.* **2015**, *51*, 16169-16172.

[23] L. H. Finger, J. Sundermeyer.

[24] L. H. Finger, J. Sundermeyer, *Chem. Eur. J.* **2016**, accepted manuscript.

[25] A. J. Arduengo, F. Davidson, H. V. R. Dias, J. R. Goerlich, D. Khasnis, W. J. Marshall, T. K. Prakasha, *J. Am. Chem. Soc.* **1997**, *119*, 12742-12749.

[26] S. T. Manjare, S. Yadav, H. B. Singh, R. J. Butcher, *Eur. J. Inorg. Chem.* **2013**, *2013*, 5344-5357.

[27] N. Ghavale, S. T. Manjare, H. B. Singh, R. J. Butcher, *Dalton Trans.* **2015**, *44*, 11893-11900.

[28] O. Back, M. Henry-Ellinger, C. D. Martin, D. Martin, G. Bertrand, *Angew. Chem., Int. Ed.* **2013**, *52*, 2939-2943.

[29] M. Hans, J. Wouters, A. Demonceau, L. Delaude, *Eur. J. Org. Chem.* **2011**, *2011*, 7083-7091.

[30] G. R. Fulmer, A. J. M. Miller, H. E. Gottlieb, N. H. Sherden, A. Nudelman, B. M. Stoltz, K. I. Goldberg, J. E. Bercaw, *Organometallics* **2010**, *29*, 2176-2179.

[31] Bruker, Bruker AXS Inc., Madison, Wisconsin, USA, **2012**.

[32] A. Altomare, M. C. Burla, M. Camalli, G. Cascarano, C. Giacovazzo, A. Guagliardi, A. G. G. Moliterni, G. Polidori, R. Spagna, *J. Appl. Crystallogr.* **1999**, *32*, 115-119.

[33] M. C. Burla, R. Caliandro, M. Camalli, B. Carrozzini, G. L. Cascarano, C. Giacovazzo, M. Mallamo, A. Mazzone, G. Polidori, R. Spagna, *J. Appl. Crystallogr.* **2012**, *45*, 357-361.

[34] G. Sheldrick, *Acta Crystallogr. C* **2015**, *71*, 3-8.

[35] A. L. Spek, *Acta Crystallogr. D* **2009**, *65*, 148-155.

[36] L. Farrugia, *J. Appl. Crystallogr.* **2012**, *45*, 849-854.

[37] Bruker, Bruker AXS Inc., Madison, Wisconsin, USA, **2012**.

[38] Crystal Impact - H. Putz & K. Brandenburg GbR, Kreuzherrenstr. 102, 53227 Bonn, Germany.

[39] W. L. Amarego, D. D. Perrin, *Purification of Laboratory Chemicals*, 4th ed., Elsevier, Burlington, **1996**.

6.6 Synthese und Charakterisierung von 5,5'-Bistetrazolatsalzen mit Alkalimetall-, Ammonium- und Imidazolium-Kationen

Z. Anorg. Allg. Chem. **2013**, *639*, 1140–1152

Synthesis and Characterisation of 5,5'-Bistetrazolate Salts with Alkali Metal, Ammonium and Imidazolium Cations

Lars H. Finger, Fabian G. Schröder, Jörg Sundermeyer

DOI: 10.1002/zaac.201300150

Synthesis and Characterisation of 5,5'-Bistetrazolate Salts with Alkali Metal, Ammonium and Imidazolium Cations

Lars H. Finger,[a] Fabian G. Schröder,[a] and Jörg Sundermeyer*[a]

Dedicated to Professor Heinrich Nöth on the Occasion of His 85th Birthday

Keywords: Alkali metals; 5,5'-Bistetrazolate salts; Crystal structures; Coordination chemistry; Ionic liquids

Abstract. We report on the synthesis and characterisation of the alkali metal 5,5'-bistetrazolate (BT^{2-}) salts Li_2BT (**1**), Na_2BT (**2**), K_2BT (**3**), Rb_2BT (**4**) and Cs_2BT (**5**) as well as the mono ammonium (**9**) and the mono (**10**) and bis(1-ethyl-3-methylimidazolium) (**11**) salts of 5,5'-bistetrazole. The crystal structures of the hydrates of the alkali metal salts (**1h**–**4h**) and hydrate free (**9**) to (**11**) are presented. Additionally we present structures of the monocaesium 5,5'-bistetrazolate (**6**) and alternative modifications of the known salts barium (**7h**) and diammonium (**8**) 5,5'-bistetrazolate. Among the presented compounds are the first reversibly melting 5,5'-bistetrazolate salts (**10**, **11**) and also the first ionic liquid on the basis of 5,5'-bistetrazole (**11**). All substances were investigated by NMR and IR spectroscopy, elemental analysis and combined TGA/DSC measurements. Corresponding to our main motive, the evaluation of the coordination behaviour of 5,5'-bistetrazole, we give a short summary of the metal 5,5'-bistetrazole salts structurally characterised so far.

Introduction

The first synthesis of 5,5'-bistetrazole (H_2BT) was already reported at the beginning of the 20th century.[1] The potential of this nitrogen-rich compound as an explosive was noticed soon.[2] *Friederich* developed a novel synthesis for the title compound which no longer utilised handling of the highly hazardous reactants cyanogen and hydrazoic acid in aqueous solutions.[3] This procedure was improved and simplified by *Nelson* et al.[4] Whereas 5,5'-bistetrazole and its derivatives have been intensively studied regarding their energetic properties and numerous patents claim their use in explosive compositions,[5] very little is known about the coordination behaviour of this intriguing ligand. *Steel* et al. were the first to publish three transition metal complexes in 1995 and presented also the crystal structure of the free acid.[6] The group of *Klein* prepared and characterised several rare earth metal salts,[7] *Klapötke* et al. presented a series of alkaline earth metal salts[8] and the first structurally characterised transition metal salt.[9] Combinations of 5,5'-bistetrazole with nitrogen-rich cations such as ammonium, hydrazinium, guanidinium and related have been investigated most recently by *Klapötke* et al. and also *Shreeve* et al.[10]

Intrigued by the first detailed description of the rare earth metal salts, we wanted to further investigate the coordination behaviour of 5,5'-bistetrazole. We chose the alkali metal salts as a first model system. Our special interest concerned the question if a chelating coordination mode is dependent on the cation size. In addition we specifically wanted to analyse the sodium and the barium salt of 5,5'-bistetrazole which have been utilised in the synthesis of the free acid and the rare earth metal salts, respectively. During our literature research we were surprised to find that the monoammonium salt of 5,5'-bistetrazole is regarded a promising gas generating compound used in airbag systems.[5b] We wished to prepare and investigate this compound to evaluate in which way it deviates from similar substances. Finally we were interested if the 5,5'-bistetrazolate anion can be employed in organic salts with weakly coordinating cations. The specific aim was to prepare unusual ionic compounds in which an isolated 5,5'-bistetrazolate dianion is present.

We wish to report herein on the synthesis and characterisation including single crystal XRD structure determination of a series of alkali metal salts, the monoammonium salt and two 1-ethyl-3-methylimidazolium salts of 5,5'-bistetrazole. Additionally we want to present alternative crystal structure modifications of the previously described barium and diammonium 5,5'-bistetrazolate.

Results and Discussion

Synthesis

The high acidity of 5,5'-bistetrazole[11] allows the preparation of alkali metal salts starting from the respective metal

* Prof. Dr. J. Sundermeyer
Fax: +49-64-21-2825711
E-Mail: jsu@chemie.uni-marburg.de
[a] Fachbereich Chemie
Philipps-Universität Marburg
Hans-Meerwein-Str. 4
35032 Marburg, Germany

Supporting information for this article is available on the WWW under http://dx.doi.org/10.1002/zaac.201300150 or from the author.

Zeitschrift für anorganische und allgemeine Chemie ZAAC Journal of Inorganic and General Chemistry

hydroxide or carbonate. This route was also employed for the barium salt. The dilithium (**1h**) and dirubidium (**4h**) salts crystallised from hot water with two, the disodium (**2h**) and barium (**7h**) salts with five water molecules per molecular unit (Scheme 1) and were characterised by XRD. The dipotassium (**3**) and dicaesium (**5**) salts usually crystallised without hydrating water molecules in the structure. Both compounds have not afforded publishable structure solutions so far, though. Instead the single crystal structures of dipotassium 5,5'-bistetrazolate dihydrate (**3h**) and monocaesium 5,5'-bistetrazolate (CsHBT, **6**) are presented. In each case also the water-free phase was prepared and investigated. Water-free Li_2BT is highly hygroscopic.

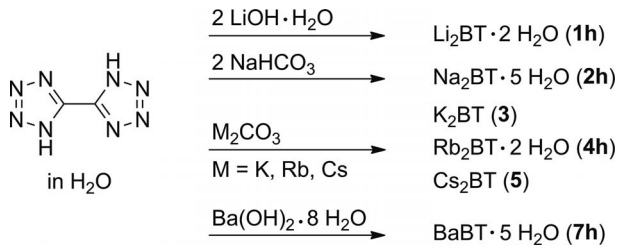

Scheme 1. Synthesis of alkali metal 5,5′-bistetrazolates (**3**) and (**5**), the hydrates (**1h**), (**2h**) and (**4h**) and barium 5,5′-bistetrazolate pentahydrate (**7h**).

Monoammonium 5,5'-bistetrazolate ((NH_4)HBT, **9**) was prepared by reacting equimolar amounts of 5,5'-bistetrazole and diammonium 5,5'-bistetrazolate ($(NH_4)_2$BT, **8**). To our surprise the crystallisation of this mixture by cooling a boiling aqueous solution to room temperature yielded again $(NH_4)_2$BT (**8**) as evidenced by ^{13}C-NMR spectroscopy, elemental analysis and XRD unit cell determination. Only if the remaining solution is decanted and cooled further to 4 °C, the monoammonium 5,5'-bistetrazolate crystallises.

Mono(1-ethyl-3-methylimidazolium) 5,5'-bistetrazolate ((EMIM)HBT, **10**) was prepared by combining barium 5,5'-bistetrazolate and 1-ethyl-3-methylimidazolium bisulfate in water. Bis(1-ethyl-3-methylimidazolium) 5,5'-bistetrazolate ($EMIM_2$BT, **11**) was synthesised by reacting 5,5'-bistetrazole with EMIM carbonate in dry methanol (Scheme 2). The product $EMIM_2$BT is again highly hygroscopic.

Molecular Structures

The data collection for the single crystal structure determinations was performed with a Stoe IPDS-II or a Bruker D8 QUEST diffractometer by the X-ray service department of the Fachbereich Chemie, University of Marburg. The Stoe IPDS-II device is equipped with a Mo-K_α X-ray source (λ = 0.71073 Å), graphite mono-chromator and active imaging plate. Stoe IPDS software (X-AREA) was used for data collection, cell refinement and data reduction, respectively.[12] The D8-QUEST is equipped with a Mo-K_α X-ray micro source (Incotec), a fixed chi goniometer and a PHOTON 100 CMOS detector. Bruker software (Bruker Instrument Service, APEX2, SAINT) was used for data collection, cell refinement and data reduction.[13] The structures were solved with SIR-97,[14]

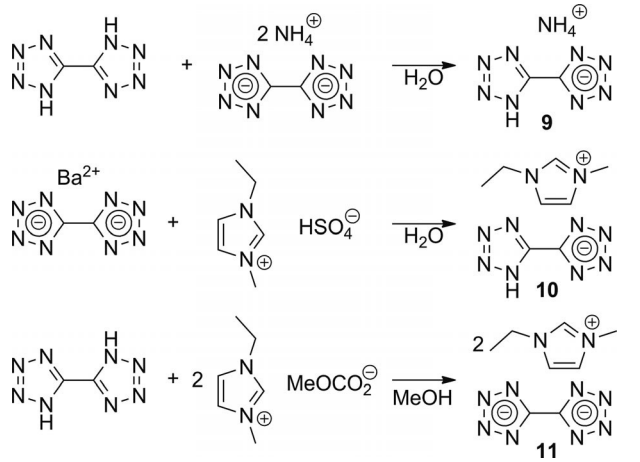

Scheme 2. Synthesis of monoammonium (**9**) and mono (**10**) and di (**11**) (1-ethyl-3-methyl-imidazolium) 5,5′-bistetrazolate.

SIR2004[15] or SUPERFLIP,[16] refined with SHELXL-97[17] and finally validated using PLATON[18] software, all within the WinGX[19] software bundle. Absorption corrections where either applied within WinGX (multi-scan[20] or gaussian[21]) or beforehand within the APEX2 software (multi-scan).[22] Graphic representations were created using Diamond 3.[23] C-bound hydrogen atoms were constrained to parent site; hydrogen atoms on heteroatoms were located in the *Fourier* map and refined independently. In all graphics the displacement ellipsoids are shown for the 50 % probability level, hydrogen atoms are shown with arbitrary radius. Selected crystal data and experiment parameters are listed in Table 1 and Table 2. Crystallographic data (excluding structure factors) for the structures reported in this paper have been deposited with the Cambridge Crystallographic Data Centre as supplementary publication no. CCDC-927399, -927400, -927401, -927402, -927403, -927404, -927405, -927406, -927407, -927408. Copies of the data can be obtained free of charge on application to CCDC, 12 Union Road, Cambridge CB2 1EZ, UK [Fax: +44-1223-336-033; E-Mail: deposit@ccdc.cam.ac.uk; http://www.ccdc.cam.ac.uk/cgi-bin/catreq.cgi].

Dilithium 5,5'-bistetrazolate dihydrate ($Li_2BT{\cdot}2H_2O$, **1h**) crystallised in the triclinic space group $P\bar{1}$ with a single molecule in the unit cell and half a molecule in the asymmetric unit. The bond lengths in the tetrazole moiety are in the same range as values which have been found in the free 5,5'-bistetrazole acid[6b] and published 5,5'-bistetrazolate salts.[7–10]

The N2–N3 distance is generally the shortest whereas N1–N2 and N3–N4 are the longest bonds. The observed bond lengths lie between typical values for N–N single (1.366 Å) and N=N double (1.300 Å) bonds in heterocyclic aromatic systems. The observed C–N distances show evenly good agreement with bond lengths in common aromatic heterocycles (1.331 Å (pyrazole), 1.338 Å (pyridine)).[24] A tabular comparison of bond lengths and angles in the bistetrazole moiety of all presented structures is given in the Supporting Information.

The bistetrazole moiety in structure **1h** is perfectly planar and builds almost planar chains in which bistetrazolate and lithium ions are alternating (Figure 1). The lithium atoms are

Table 1. Selected crystallographic data for compounds **1h** to **4h** and **6**.

	$Li_2BT{\cdot}2H_2O$ (**1h**)	$Na_2BT{\cdot}5H_2O$ (**2h**)	$K_2BT{\cdot}2H_2O$ (**3h**)	$Rb_2BT{\cdot}2H_2O$ (**4h**)	CsHBT (**6**)
Formula	$C_2H_4Li_2N_8O_2$	$C_2H_{10}N_8Na_2O_5$	$C_2H_4K_2N_8O_2$	$C_2H_4N_8O_2Rb_2$	$C_2H_1Cs_1N_8$
FW /g·mol^{-1}	186.01	272.16	250.33	343.08	270.02
Crystal system	Triclinic	Triclinic	Monoclinic	Monoclinic	Monoclinic
Space group	$P\bar{1}$	$P\bar{1}$	$P2_1/c$	$P2_1/c$	Pc
Colour, habit	colourless block	colourless block	colourless block	colourless block	colourless block
Crystal size /mm	0.13 × 0.08 × 0.07	0.83 × 0.61 × 0.41	0.21 × 0.09 × 0.09	0.33 × 0.13 × 0.09	0.32 × 0.12 × 0.05
a /Å	3.3677(8)	7.2089(6)	3.8505(4)	4.0884(2)	4.6222(4)
b /Å	7.3623(2)	7.4623(6)	11.3156(12)	11.3281(7)	8.6949(6)
c /Å	7.5007(2)	10.7752(8)	9.7354(10)	9.9483(6)	16.2896(17)
α /°	82.897(18)	81.333(3)	90	90	90
β /°	87.120(19)	76.478(3)	93.006(9)	93.510(5)	94.123(8)
γ /°	80.761(18)	67.604(3)	90	90	90
V /Å^3	182.06(4)	519.85(7)	423.59(8)	459.88(5)	652.98(10)
Z	1	2	2	2	4
D_{calc} /g·cm^{-3}	1.679	1.739	1.963	2.478	2.747
μ /cm^{-1}	1.38	2.23	11.08	106.32	56.11
F(000)	94	280	252	324	496
T / K	100(2)	100(2)	100(2)	100(2)	100(2)
θ range /°	2.74 : 26.69	2.96 : 27.17	2.76 : 26.72	2.73 : 26.72	2.34 : 26.67
h, *k*, *l* range	–4:4, –9:9, –9:9	–9:8, –9:9, –13:13	–4:4, –12:14, –12:12	–5:5, –14:14, –12:12	–5:5, –10:10, –18:20
Refl. Coll.	1476	6166	2267	5725	3188
Refl. Indep.	762	2310	893	973	2313
Refl. $I > 2\sigma(I)$	602	1952	778	888	2152
Data/ rest./ param.	762 / 2 / 72	2310 / 1 / 194	893 / 0 / 72	973 / 0 / 72	2313 / 4 / 209
R_{int}	0.0287	0.0616	0.0244	0.0575	0.0473
R_1 (obs)	0.0349	0.0532	0.0224	0.0210	0.0266
wR_2 (all)	0.0872	0.1386	0.0546	0.0492	0.0629
GooF (F^2)	0.968	1.047	0.987	1.047	0.999
CCDC	927399	927400	927401	927402	927403

Table 2. Selected crystallographic data for compounds **7h** and **8** to **11**.

	$BaBT{\cdot}5H_2O$ (**7h**)	$(NH_4)_2BT$ (**8**)	$(NH_4)HBT$ (**9**)	(EMIM)HBT (**10**)	$(EMIM)_2BT$ (**11**)
Formula	$C_2H_{10}BaN_8O_5$	$C_2H_8N_{10}$	$C_2H_5N_9$	$C_8H_{12}N_{10}$	$C_{14}H_{22}N_{12}$
FW /g·mol^{-1}	363.52	172.18	155.15	248.28	358.44
Crystal system	Triclinic	Orthorhombic	Monoclinic	Monoclinic	Monoclinic
Space group	$P\bar{1}$	Pban	$P2_1/c$	$P2_1/n$	$P2_1/n$
Colour, habit	colourless block	colourless block	colourless needle	colourless block	colourless block
Crystal size /mm	0.21 × 0.13 × 0.08	0.18 × 0.16 × 0.14	0.66 × 0.10 × 0.07	0.17 × 0.15 × 0.12	0.27 × 0.23 × 0.16
a /Å	7.4404(7)	9.1301(10)	4.5136(6)	4.5978(3)	9.8020(6)
b /Å	8.1615(7)	10.7631(13)	8.4692(12)	18.9191(11)	7.9782(6)
c /Å	9.2594(9)	3.6660(6)	15.522(2)	13.0052(7)	12.0450(8)
α /°	88.638(8)	90	90	90	90
β /°	73.671(7)	90	94.320(6)	94.586(4)	108.716(5)
γ /°	88.933(7)	90	90	90	90
V /Å^3	539.40(9)	360.25(8)	591.67(14)	1127.65(12)	892.13(10)
Z	2	2	4	4	2
D_{calc} /g·cm^{-3}	2.238	1.587	1.742	1.462	1,334
μ /cm^{-1}	37.07	1.24	1.37	1.05	0.92
F(000)	348	180	320	520	380
T / K	100(2)	100(2)	100(2)	100(2)	100(2)
θ range /°	2.29 : 26.68	2.93 : 26.70	2.63 : 27.08	1.90 : 26.71	2.34 : 26.72
h, *k*, *l* range	–9:9, –10:10, –11:11	–10:11, –13:13, –4:4	–5:4, –10:10, –19:19	–5:5, –23:20, –16:14	–10:12, –12:10, –15:15
Refl. Coll.	6259	2935	3538	7731	7475
Refl. Indep.	2289	392	1302	2383	1882
Refl. $I > 2\sigma(I)$	2073	319	1025	1470	1355
Data/ rest./ param.	2289 / 12 / 185	392 / 0 / 37	1302 / 0 / 124	2383 / 0 / 169	1882 / 0 / 120
R_{int}	0.0471	0.0382	0.0448	0.0528	0.0429
R_1 (obs)	0.0226	0.0273	0.0517	0.0337	0.0339
wR_2 (all)	0.0547	0.0661	0.0970	0.0696	0.0843
GooF (F^2)	0.989	0.939	1.211	0.781	0.893
CCDC	927404	927405	927406	927407	927408

Zeitschrift für anorganische und allgemeine Chemie ZAAC Journal of Inorganic and General Chemistry

coordinated in a tetrahedral fashion by two oxygen and two nitrogen atoms with bond angles ranging from 104.1(1)° to 115.5(1)°. In the crystal structure the chains are stacked and connected over lithium oxygen bonds, the stacks (Figure 2) are held together by strong hydrogen bonds ($O1^{IV}$···N3: 2.785(2) Å).

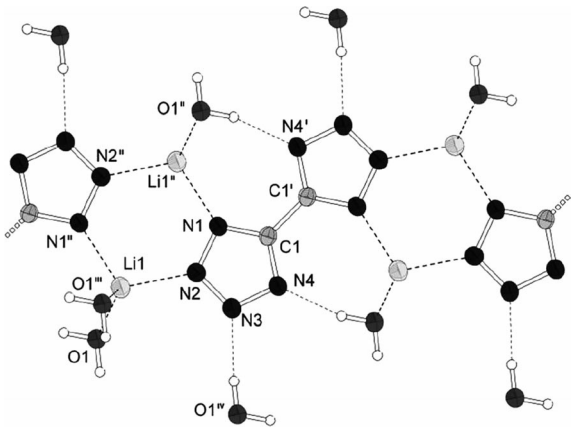

Figure 1. Chain structure in dilithium 5,5′-bistetrazolate dihydrate (**1h**); selected bond lengths /Å and angles /°: C1–$C1^{I}$: 1.468(3), C1–N1: 1.335(2), N1–N2: 1.347(2), N2–N3: 1.316(2), N3–N4: 1.345(2), C1–N4: 1.335(2), N1–$Li1^{II}$: 2.060(3), N2–Li1: 2.034(3), O1–Li1: 1.991(3), $O1^{III}$–Li1: 2.012(3), $O1^{II}$···$N4^{I}$: 2.786(2), $O1^{IV}$···N3: 2.785(2), O1–Li1–N2: 115.5(1), N2–Li1–$N1^{II}$: 111.0(1), O1–Li1–$O1^{III}$: 114.6(2), $N1^{II}$–Li1–$O1^{IV}$: 104.1(1); symmetry operations: ^{I} = 1 – *x*, –y, 2 –*z*, ^{II} = 1 –*x*, 1 –*y*, 2 –*z*, ^{III} = –1+x, *y*, *z*, ^{IV} = 2 –*x*, 1 –*y*, 1 –*z*.

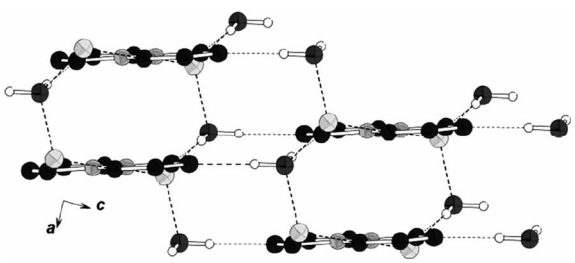

Figure 2. Chain stacking in the crystal structure of dilithium 5,5′-bistetrazolate dihydrate (**1h**); view along the *b* axis.

$Na_2BT{\cdot}5H_2O$ (**2h**) crystallised in the space group $P\bar{1}$ with two molecular units per elementary cell and one molecule per asymmetric unit. The sodium atoms are six fold coordinated in an octahedral fashion. Na1 is surrounded by two nitrogen and four oxygen atoms, Na2 by one nitrogen atom and five oxygen atoms, the coordination polyhedron around Na2 is considerably distorted. Sodium nitrogen distances range from 2.408(2) Å (N1–Na1) to 2.556(2) Å (N7–Na2), sodium oxygen bond lengths lie between 2.345(2) Å (O1–Na2) and 2.473(2) Å (O4–Na1). Dimeric entities prevail in which two bistetrazolate moieties are linked by two sodium atoms (Figure 3). When viewing along the line which is connecting the dimers (direction [$\bar{1}$20]) a stacked structure appears (Figure 4).

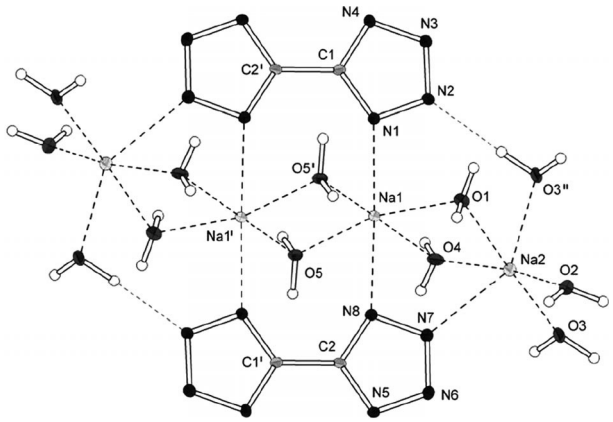

Figure 3. Dimeric units in disodium 5,5′-bistetrazolate pentahydrate (**2h**); selected bond lengths /Å and angles /°: C1–$C2^{I}$: 1.463(2), C1–N1: 1.341(2), N1–N2: 1.349(2), N2–N3: 1.320(2), N3–N4: 1.354(2), C1–N4: 1.338(2), C2–N5: 1.342(2), N5–N6: 1.351(2), N6–N7: 1.315(2), N7–N8: 1.346(2), C2–N8: 1.338(2), N1–Na1: 2.408(2), N8–Na1: 2.450(2), N7–Na2: 2.556(2), O1–Na1: 2.377(2), O4–Na1: 2.473(2), O5–Na1: 2.351(2), $O5^{I}$–Na1: 2.380(2), O1–Na2: 2.345(2), O2–Na2: 2.355(2), O3–Na2: 2.357(2), $O3^{II}$–Na2: 2.524(2), O4–Na2: 2.407(2), $O3^{II}$···N2: 2.968(2), N1–Na1–N8: 178.0(1), N7–Na2–$O3^{II}$: 147.0(1); symmetry operations: ^{I} = 1–*x*, –*y*, 1–*z*, ^{II} = –*x*, –*y*, 2–*z*.

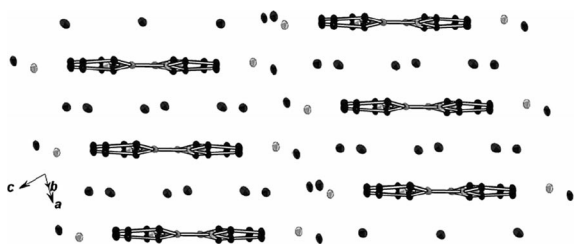

Figure 4. Stacked structure of dimeric units in $Na_2BT{\cdot}5H_2O$ (**2h**), hydrogen atoms are omitted for clarity; viewing direction [$\bar{1}$20].

The potassium salt exhibits a special behaviour concerning crystallisation. In multiple attempts the water-free substance could be crystallised. This could be proven by IR spectroscopy, elemental analysis and XRD single crystal analysis. The resulting structure solution clearly evidences the water-free phase but does not allow any discussion of bond lengths due to bad crystal quality. In one instance the chosen crystal turned out to be a dihydrate of the respective salt whose solution is presented here. Dipotassium 5,5'-bistetrazolate dihydrate (**3h**) crystallised in the space group $P2_1/c$ with four asymmetric units consisting of half a molecule per unit cell. The potassium atom is coordinated by five nitrogen and three oxygen atoms forming a doubly capped trigonal prism (Figure 5).

In one case the potassium atom is coordinated in a distorted chelating fashion (between $N4^{III}$ and $N1^{V}$) with an angle of 57.24(3)° at the central atom. The potassium atom is not in plane with the chelating NCCN fragment, though. Potassium nitrogen distances range from 2.916(1) Å ($N2^{II}$) to 2.977(1) Å (N2) and are in good agreement with distances found in the potassium tetrazolate.[25] The K1–$N1^{V}$ distance (3.211(1) Å) is considerably longer than typical K–N bonds but can still be regarded as a coordinating bond. Similar distances have been

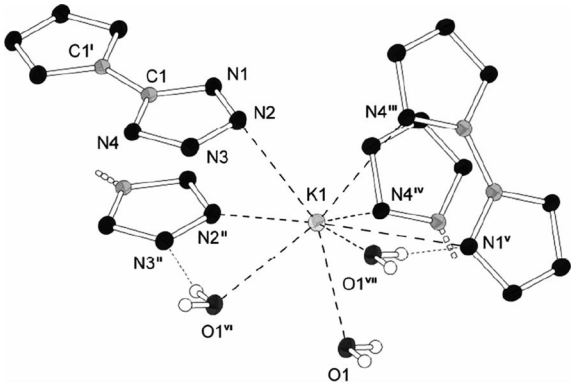

Figure 5. Coordination of the potassium atoms in dipotassium 5,5′-bistetrazolate dihydrate (**3h**); selected bond lengths /Å and angles /°: C1–C1^{I}: 1.457(3), C1–N1: 1.335(2), N1–N2: 1.351(2), N2–N3: 1.315(2), N3–N4: 1.348(2), C1–N4: 1.341(2), K1–N2: 2.977(1), K1–N2^{II}: 2.916(1), K1–N4^{III}: 2.922(1), K1–N4^{IV}: 2.949(1), K1–N1^{V}: 3.211(1), K1–O1: 2.760(1), K1–O1^{VI}: 2.892(1), K1–O1^{VII}: 2.860(1), O1^{VI}···N3^{II}: 2.823(2), O1^{VII}···N1^{V}: 2.844(2), N4^{III}–K1–N1^{V}: 57.24(3); symmetry operations: ^{I} = 1–*x*, 1–*y*, –*z*, ^{II} = 1+*x*, *y*, *z*, ^{III} = *x*, 0.5–*y*, 0.5+*z*, ^{IV} = 1–*x*, 0.5–*y*, 0.5+*z*, ^{V} = 1–*x*, –0.5+*y*, 0.5–*z*, ^{VI} = 2–*x*, –*y*, –*z*, ^{VII} = –1+*x*, *y*, *z*.

observed in potassium phenanthroline complexes.[26] The packing in the crystal structure is dominated by a wave like topology (viewing along the *c* axis) in which layers of 5,5'-bistetrazolate dianions alternate with layers consisting of potassium atoms and water molecules (Figure 6).

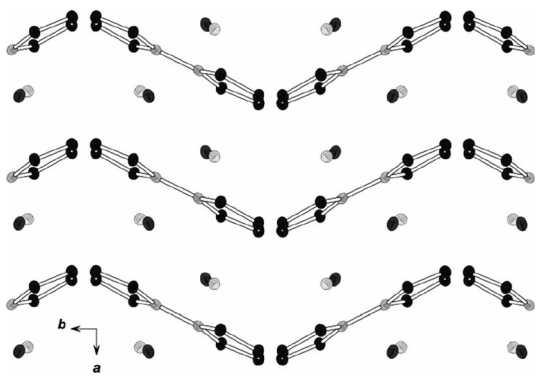

Figure 6. Wave-like topology in dipotassium 5,5′-bistetrazolate dihydrate (**3h**); view along the *c* axis; hydrogen atoms are omitted for clarity.

Dirubidium 5,5'-bistetrazolate dihydrate (**4h**, Figure 7) crystallised in the monoclinic space group $P2_1/c$ with four asymmetric units consisting of half a molecule per unit cell. It is isostructural, although according to the XRD results enantiomeric, to the potassium salt.

The Rb–N distances range from 3.035(2) Å (Rb1–N4^{III}) to 3.238(2) Å (Rb1–N1^{V}) in the longest case. Rubidium oxygen distances deviate between 2.941(2) Å (Rb1–O1) and 3.016(2) Å (Rb–O1^{VI}). As in the potassium salt (**3h**) a wave-like structure is visible, when viewing along the *c* axis (Figure 8). The tilting angle between the 5,5'-bistetrazolate moieties is higher, though (59.1° in (**4h**) compared to 52.3° in (**3h**)). The presented structures show an overall good agreement with

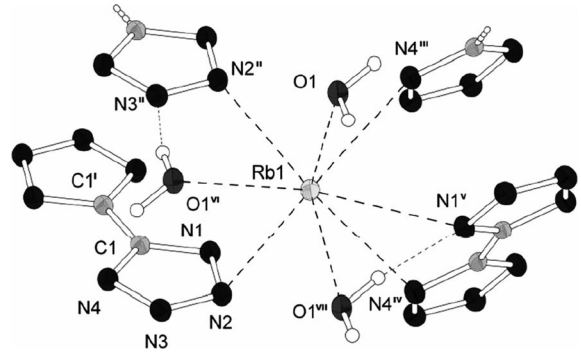

Figure 7. Coordination of the rubidium atoms in dirubidium 5,5′-bistetrazolate dihydrate (**4h**); selected bond lengths /Å and angles /°: C1–C1^{I}: 1.457(4), C1–N1: 1.340(3), N1–N2: 1.347(3), N2–N3: 1.317(3), N3–N4: 1.346(2), C1–N4: 1.340(3), Rb1–N2: 3.101(2), Rb1–N2^{II}: 3.046(2), Rb1–N4^{III}: 3.035(2), Rb1–N4^{IV}: 3.087(2), Rb1–N1^{V}: 3.238(2), Rb1–O1: 2.941(2), Rb1–O1^{VI}: 3.016(2), Rb1–O1^{VII}: 2.997(2), O1^{VI}···N3^{II}: 2.844(3), O1^{VII}···N1^{V}: 2.872(3), N4^{III}–Rb1–N1^{V}: 55.63(5); symmetry operations: ^{I} = –*x*, –*y*, –*z*, ^{II} = 1+*x*, *y*, *z*, ^{III} = 1+*x*, 0.5–*y*, 0.5+*z*, ^{IV} = *x*, 0.5–*y*, 0.5+*z*, ^{V} = –*x*, 0.5+*y*, 0.5–*z*, ^{VI} = 1 –*x*, 1–*y*, –*z*, ^{VII} = –1+*x*, *y*, *z*.

the related salts of 1H-tetrazole[25] and 5-aminotetrazole[27] with respect to alkali metal nitrogen and alkali metal oxygen bond lengths.

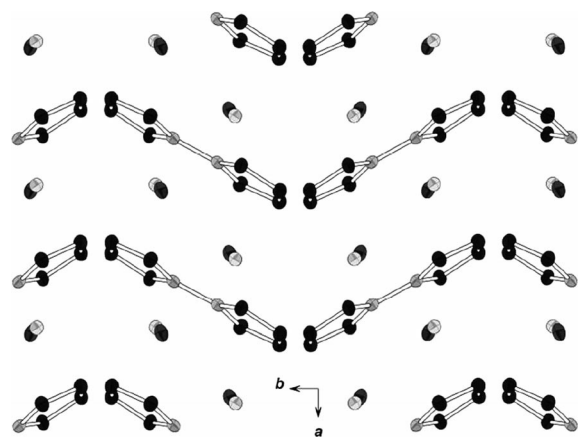

Figure 8. Wave-like structure in dirubidium 5,5′-bistetrazolate dihydrate (**4h**); hydrogen atoms are omitted for clarity.

Dicaesium 5,5'-bistetrazolate could be crystallised from aqueous solution in the form of colourless blocks. However, XRD experiments led to several analogous data sets for which no reasonable solution could be generated so far. In one case instead of the dicaesium salt a crystal of monocaesium 5,5'-bistetrazolate (**6**) was investigated. Compound **6** crystallised in the monoclinic space group *Pc* with two asymmetric entities per unit cell (Figure 9). The asymmetric unit consists of two molecular units. PLATON suggests the space group $P2_1/c$ on the basis of an additional inversion centre. However, neither in $P2_1/c$ nor in *P*2/*c*, a reasonable refinement is possible, and the expected extinction of reflexes for the 2_1 axis is not present. The suggestion by PLATON has therefore to be attributed to a pseudo inversion centre. Additionally a partial mix of enantiomers is present in the structure; a TWIN refinement has been applied resulting in a freely refined BASF value of

Zeitschrift für anorganische und allgemeine Chemie ZAAC Journal of Inorganic and General Chemistry

0.3935. The asymmetric unit consists of two caesium atoms and two 5,5'-bistetrazole moieties with a single proton remaining in each case.

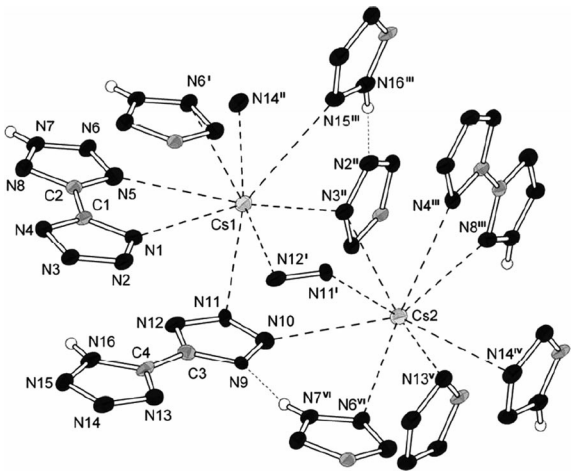

Figure 9. Molecular structure of caesium 5,5′-bistetrazolate (**6**), the isolated atoms $N11^{I}$, $N12^{I}$ and $N14^{II}$ belong to respective tetrazole rings which are not displayed to avoid an overcrowding of the picture; selected bond lengths /Å and angles /°: N1–Cs1: 3.183(9), N5–Cs1: 3.318(9), $N6^{I}$–Cs1: 3.337(7), $N14^{II}$–Cs1: 3.388(8), $N15^{III}$–Cs1: 3.400(10), $N3^{II}$–Cs1: 3.268(9), $N12^{I}$–Cs1: 3.221(8), N11–Cs1: 3.333(8), N10–Cs2: 3.308(10), $N11^{I}$–Cs2: 3.257 (8), $N3^{II}$–Cs2: 3.251(6), $N4^{III}$–Cs2: 3.295(9), $N8^{III}$–Cs2: 3.205(9), $N14^{IV}$–Cs2: 3.341(8), $N13^{V}$–Cs2: 3.293(8), $N6^{VI}$–Cs2: 3.322(9), $N7^{VI}$···N9: 2.728(11), $N16^{III}$···$N2^{II}$: 2.709(11), N1–Cs1–N5: 53.6(2), $N4^{III}$–Cs2–$N8^{III}$: 53.9(2); symmetry operations: ^{I}:1+*x*, *y*, *z*, ^{II}: *x*, 1–*y*, 0.5+*z*, ^{III}: 1+*x*, 1–*y*, 0.5+*z*, ^{IV}: 1+*x*, 2–*y*, 0.5+*z*, ^{V}: *x*, 2–*y*, 0.5+*z*, ^{VI}: 1+*y*, 1+*y*, *z*.

The coordination polyhedra around the caesium atoms approximate doubly capped trigonal prisms. Cs–N distances range from 3.183(9) Å to 3.400(10) Å and compare well to related substances.[25,28] In two cases the 5,5'-bistetrazolate ligand coordinates in a chelating fashion (N1–Cs1: 3.183(9) Å, N5–Cs1: 3.318(9) Å, $N4^{III}$–Cs2: 3.295(9) Å, $N8^{III}$–Cs2: 3.205(9) Å). In these cases the pentacycle from two carbon, two nitrogen and one caesium atom is almost planar. In comparison to the potassium (**3h**) and rubidium salts (**4h**) the chelating angles are further decreased (N1–Cs1–N5: 53.6(2)°, $N4^{III}$–Cs2–$N8^{III}$: 53.9(2)°]. It is noteworthy that in multiple cases not only a single atom of a respective tetrazole ring lies in bonding distance to the caesium atom, but two neighbouring atoms show very similar distances (most prominent: $N12^{I}$–Cs1: 3.221(8) Å and $N11^{I}$–Cs1: 3.225(8) Å). A η^2-bonding situation might be considered, but the unchanged bond lengths in the tetrazole rings contradict a participation of the π-orbitals in the coordination. The same phenomenon was observed with the caesium tetrazolate[25] and the caesium cyanotetrazolate.[28]

In the crystal structure hydrogen bonded chains of 5,5'-bistetrazolate ($N7^{VI}$···N9: 2.728(11) Å, $N16^{III}$···$N2^{II}$: 2.709(11) Å) prevail, between which the caesium atoms are located (Figure 10). The chains are tilted by 90° with respect to neighbouring chains and arranged in stacks (viewing direction [210]). Within the stacks the chains are shifted with respect to each other so that every fifth chain is analogous (Figure 11).

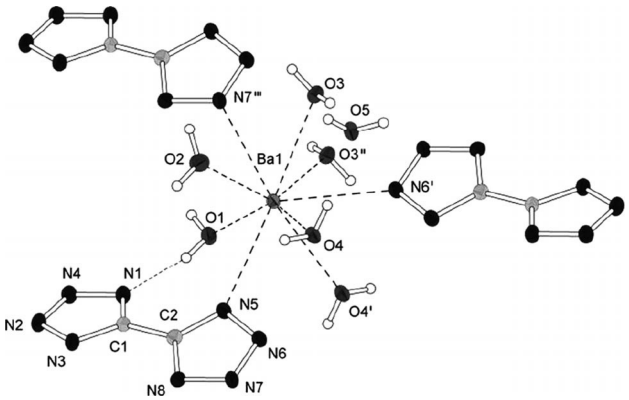

Figure 12. Molecular unit of barium 5,5′-bistetrazolate pentahydrate (**7h**); selected bond lengths /Å and angles /°: C1–C2: 1.459(4), C1–N1: 1.342(4), N1–N2: 1.341(4), N2–N3: 1.322(4), N3–N4: 1.352(4), C1–N4: 1.334(4), C2–N5: 1.341(4), N5–N6: 1.348(4), N6–N7: 1.319(4), N7–N8: 1.343(4), C2–N8: 1.335(4), N5–Ba1: 2.971(3), $N6^{I}$–Ba1: 2.961(3), $N7^{II}$–Ba1: 2.946(3), O1–Ba1: 2.782(2), O2–Ba1: 2.700(3), O3–Ba1: 2.871(2), $O3^{II}$–Ba1: 2.805(2), O4–Ba1: 2.860(2), $O4^{I}$–Ba1: 2.816(3), O1···N1: 2.782(4), N5–Ba1–$N6^{I}$: 116.2(1), $N6^{I}$–Ba1–$N7^{II}$: 113.8(1); symmetry operations: ^{I}: 2–*x*, 2–*y*, 1–*z*, ^{II}: 1–*x*, 2–*y*, 1–*z*, ^{III}: –1+*x*, *y*, *z*.

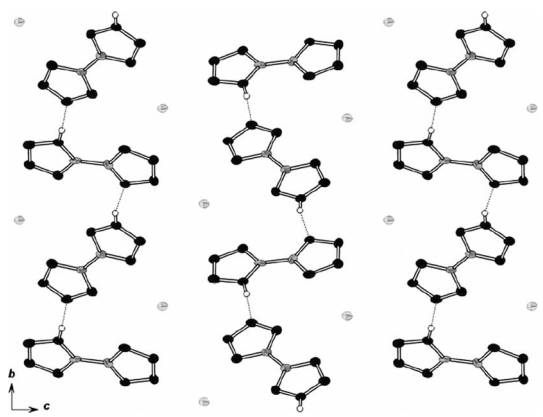

Figure 10. Hydrogen-bonded chains of 5,5′-bistetrazolate in the crystal structure of caesium 5,5′-bistetrazolate (**6**); view along the *a* axis.

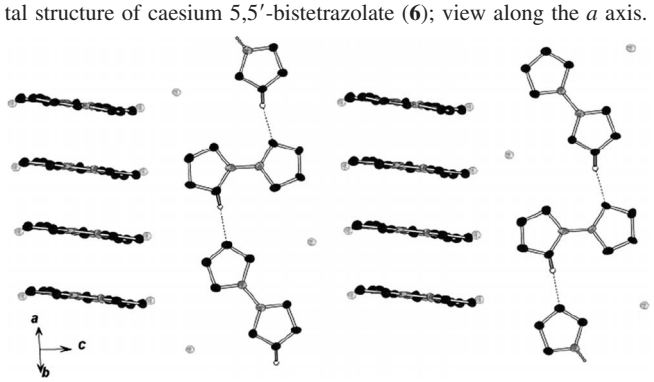

Figure 11. Crystal structure of caesium 5,5′-bistetrazolate; view along [210]; stacked chains are tilted against each other by 90°.

Barium 5,5'-bistetrazolate has been described previously as a tetrahydrate.[8,29] We found it to crystallise as a pentahydrate (**7h**) in the space group $P\bar{1}$ with two molecular entities per unit cell. The structure is very similar to the already known modification. The barium atom is coordinated ninefold in a triply capped trigonal prism by six oxygen and three nitrogen atoms (Figure 12). O–Ba distances range from 2.700(3) Å

(O2–Ba1) to 2.871(2) Å (O3–Ba1), nitrogen barium bond lengths are 2.971(3) Å (N5–Ba1), 2.961(3) Å ($N6^{II}$–Ba1) and 2.946(3) Å ($N7^{III}$–Ba1).

Zigzag chains of barium atoms which are connected over two water molecules (the trigonal prisms share edges) and the bistetrazole moieties filling the cavities between the chains are a main motive in both crystal structures (Figure 13a). The additional water molecule in the present structure does not coordinate to the barium atom. Its position in the crystal becomes evident when the structure is viewed along the *a* axis (Figure 13b). Situated between chains of barium atoms and the adjacent bistetrazole moieties it connects the chains over strong hydrogen bonds (O5···N2: 2.815(4) Å, O5···O1: 2.775(3) Å). These are not the only hydrogen bonds, almost every OH-bond is participating in a strong network of H-bonds constraining the crystal structure.

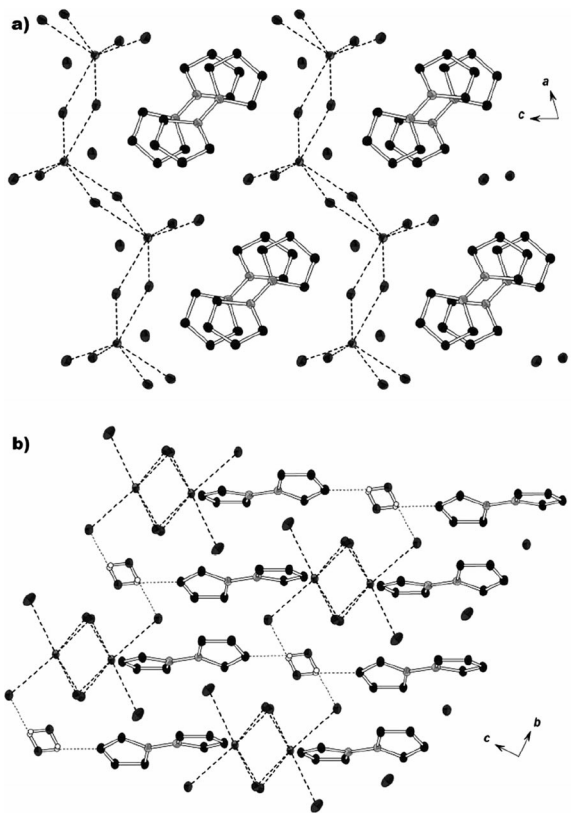

Figure 13. Crystal structure of **7h**; a) Zigzag chains of barium atoms; view in *b* direction; b) barium chains and adjacent bistetrazolate anions connected over the fifth water molecule; view in *a* direction; hydrogen atoms other than those on O5 are omitted for clarity.

When comparing the ionic radii of the metal atoms in 5,5'-bistetrazole salts structurally characterised so far and correlating those to the coordination mode and potential chelating angle an almost fully consecutive picture forms. Within the rare earth metal salts a chelating coordination is observed for La, Ce, Nd, Sm and Eu.[7a] The ionic radii for the respective coordination number range from 1.26 Å (Eu^{3+}, CN9) to 1.36 Å (La^{3+}, CN9).[30] Among the alkaline earth metal salts only with strontium (ionic radius 1.32 Å, CN6) a chelating coordination is observed. Whereas the small cations Li^+ (0.73 Å, CN4) and Na^+ (1.16 Å, CN6) are not coordinated in a chelating fashion, the larger alkali metal ions are chelated by the 5,5'-bistetrazolate moiety. In the case of the potassium and the rubidium salt, the chelation is less pronounced, as the metal atoms are not in plane with the 5,5'-bistetrazolate moiety. So far all atoms except Ba^{2+} which have an ionic radius above 1.26 Å are chelated; the ones with smaller radii are not. We are convinced that this effect is of course on the one hand affected by the increasing *Lewis* acidity of the cations with decreasing radius and therefore preferred coordination by water, but on the other hand can also be attributed to the rigid nature of the bicyclic ligand. Very small cations considerably increase the chelating angle and thereby decrease the C–N–M angle in the metallapentacycle. Open chelating ligands like oxalic acid can easily balance this by decreasing the distance between the coordinating atoms which is less easily possible for the bicyclic 5,5'-bistetrazolate. A considerable decrease of the C–N–M angle will lead to less orbital overlap between the anionic lone pairs of the nitrogen atoms and the metal orbitals, which we believe to be the reason why small atoms are chelated less likely. The only exception to this trend is the copper(II) salt.[9] Despite having a very small ionic radius of 0.87 Å (CN6) it is chelated by 5,5'-bistetrazole. The differences in bond lengths indicate, though, that only one of the chelating atoms forms a strong ionic bond (2.027(4) Å) whereas the other one only forms a weak coordinative bond (2.760(5) Å). The chelating angles N–M–N follow a distinct and natural trend by increasing with the cation becoming smaller. In Table 3 the ionic radii of the respective metal ions are opposed to the coordination mode and if applicable the chelating angle.

The structure of the diammonium 5,5'-bistetrazolate (**8**) was described previously with a monoclinic cell.[10a] During our own independent research we were able to confirm this structure, but also observed a second orthorhombic modification. In this case $(NH_4)_2$BT (**8**) crystallised in the space group *Pban* with two molecules in the unit cell but only a quarter molecule in the asymmetric unit (Figure 14). In contrast to the known structure in which the bistetrazolate moiety is perfectly planar, here the tetrazole rings are strongly tilted against each other ($N1–C1–C1^{I}–N^{IV}$: 35.6(1)°).

In both crystal structures a layered topology is prominent. Viewing along the *c* axis a picture almost indistinguishable from the previously reported structure appears (Figure 15a). Bistetrazolate moieties are connected over the ammonium ions via a hydrogen-bonding network. Only when viewing the structure along the *b* axis a considerable difference becomes visible. Whereas in the structure described by *Klapötke* et al. the bistetrazolate anions are ordered in a stair like fashion here they are completely coplanar in each layer (Figure 15b).

The monoammonium salt of 5,5'-bistetrazole crystallised in the monoclinic space group $P2_1/c$ with four molecules per unit cell. The asymmetric unit consists of one ammonium cation and two symmetrically non-equivalent tetrazole rings. The remaining proton is disordered over the positions H1 and H2 with site occupation factors of roughly 50 % (Figure 16). The bond lengths in the tetrazole moieties are consistent with the previous structures.

Zeitschrift für anorganische und allgemeine Chemie ZAAC Journal of Inorganic and General Chemistry

Table 3. Comparison of ionic radii and coordination modes in known 5,5′-bistetrazole salts, ions ordered according to ionic radius.

Ion (CN)[a]	Be^{2+} (4)	Li^{+} (4)	Mg^{2+} (6)	Cu^{2+} (6)	Ca^{2+} (6)	Er^{3+} (8)	Na^{+} (6)	Tb^{3+} (8)	Th^{4+} (9)	Eu^{3+} (9)
Ionic radius /Å[30]	0.41	0.73	0.86	0.87	1.14	1.14	1.16	1.18	1.23	1.26
Coord. mode	none	single	none	chelate	single	none	single	none	none	chelate
Chelating angle /° N–M–N				72.7						62.9
Ion (CN)	Sm^{3+} (9)	Nd^{3+} (9)	Sr^{2+} (6)	Ce^{3+} (9)	La^{3+} (9)	Ba^{2+} (9)	K^{+} (8)	Rb^{+} (8)	Cs^{+} (8)	
Ionic radius /Å	1.27	1.30	1.32	1.34	1.36	1.61	1.65	1.75	1.88	
Coord. mode	chelate	chelate	chelate	chelate	chelate	single	chelate	chelate	chelate	
Chelating angle /° N–M–N	62.7	62.2	64.1, 62.8	61.2	60.8		57.2	55.6	53.6, 53.9	

[a] Original literature: For Be, Mg, Ca, Sr and Ba see Ref. [8], for Cu see Ref. [9], for Er, Tb, Eu, Sm, Nd, Ce and La see Ref. [7a], for Th see Ref. [7b], Li, Na, K, Rb and Cs are part of this work.

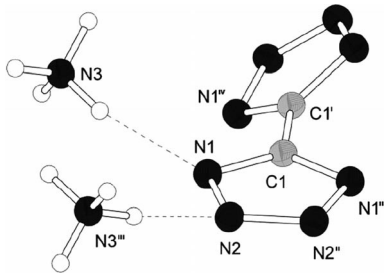

Figure 14. Molecular unit of diammonium 5,5′-bistetrazolate (**8**); selected bond lengths /Å and angles /°: C1–$C1^{I}$: 1.461(3), C1–N1: 1.337(1), N1–N2: 1.345(1), N2–$N2^{II}$: 1.318(2), N3···N1: 2.949(1), $N3^{III}$···N2: 2.938(1), N1–C1–$C1^{I}$–$N1^{IV}$: 35.55(5), symmetry operations: ^{I}: 1.5–*x*, 0.5–*x*, *z*; ^{II}: *x*, 0.5–*y*, –*z*; ^{III}: 1–*x*, 1–*y*, 1–*z*; ^{IV}: 1,5–*x*, *y*, –*z*.

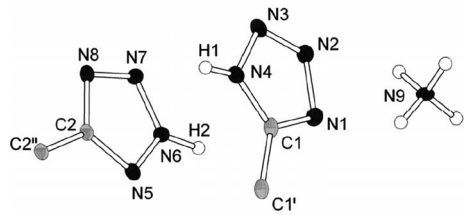

Figure 16. Molecular structure of ammonium 5,5′-bistetrazolate (**9**); selected bond lengths /Å: C1–$C1^{I}$: 1.463(4), C1–N1: 1.329(3), N1–N2: 1.358(3), N2–N3: 1.310(3), N3–N4: 1.347(3), C1–N4: 1.327(3), C2–$C2^{II}$: 1.453(4), C2–N5: 1.337(3), N5–N6: 1.337(3), N6–N7: 1.318(3), N7–N8: 1.334(3), C2–N8: 1.345(3); symmetry operations: ^{I}:–*x*, 1–*y*, 1–*z*, ^{II}: –*x*, –*y*, 1–*z*.

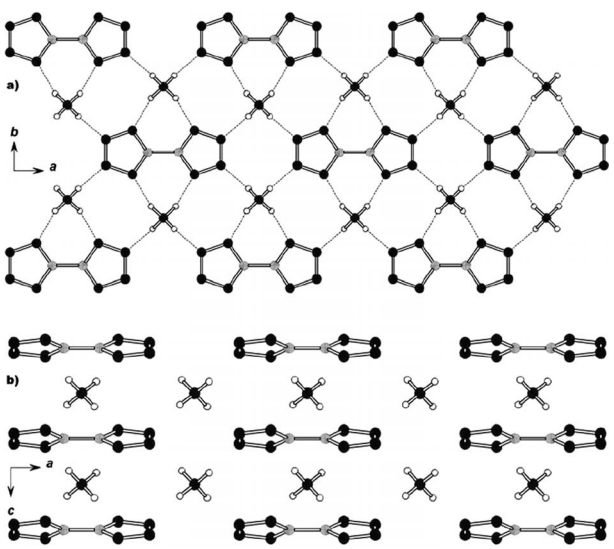

Figure 15. Crystal structure of diammonium 5,5′-bistetrazolate; a) hydrogen bonding; view in *c* direction; b) layered structure; view along the *b* axis.

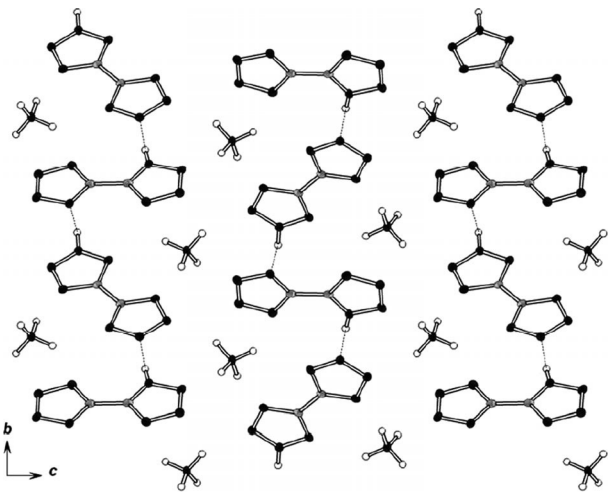

Figure 17. Crystal structure of monoammonium 5,5′-bistetrazolate (**9**); view along the *a* axis; chains of BT monoanions connected over H-bonds; only one position of the disordered hydrogen atom is displayed.

The structure is analogous to the structure of the caesium 5,5'-bitetrazolate (**6**). The positions of the caesium atoms are occupied by ammonium ions. The bistetrazole moieties build hydrogen bonded chains (N4···N6: 2.679(3) Å), between which the ammonium ions form a comparatively weaker hydrogen bonding network (donor acceptor distances between 3.037(3) Å (N9···N8) and 3.065(3) Å (N9···N7), Figure 17).

As in the structure of CsHBT (**6**) the chains of bistetrazolate anions are stacked and shifted with respect to each other so that every fifth layer is analogous. The stacks are tilted in a perpendicular fashion with respect to each other which becomes evident when the structure is viewed along the [210] direction (Figure 18).

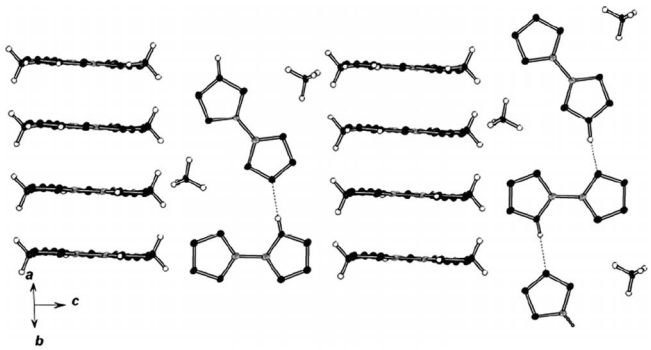

Figure 18. Stacked layer structure of ammonium 5,5′-bistetrazolate, neighboured stacks are tilted against each other by 90°; viewing direction [210]; only one position of the disordered hydrogen atom is displayed.

(EMIM)HBT (**10**) crystallised in the space group $P2_1/n$ with four molecules per unit cell (Figure 19). The bond lengths in the bistetrazolate anion correspond well to the previous structures the imidazolium cation shows almost identical values, when compared to common compounds.[31]

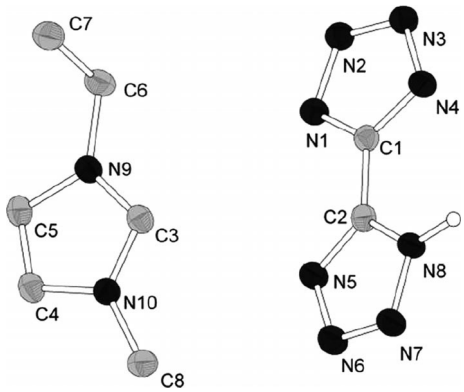

Figure 19. Molecular structure of (EMIM)HBT (**10**); carbon bound hydrogen atoms are omitted for clarity; selected bond lengths /Å: C1–C2:1.454(2), C1–N1: 1.334(2), N1–N2: 1.354(2), N2–N3: 1.315(2), N3–N4: 1.353(2), C1–N4: 1.335(2), C2–N5:1.324(2), N5–N6: 1.366(2), N6–N7: 1.299(2), N7–N8: 1.349(2), C2–N8: 1.334(2), C3–N9: 1.329(2), C3–N10: 1.329(2), C4–N10: 1.373(2), C4–C5: 1.350(2), C5–N9: 1.386(2).

In this case the monoanion of the 5,5'-bistetrazolate does not form hydrogen-bonded chains as in compounds (**6**) and (**9**) but hydrogen-bonded dimers (N8···N4: 2769(2) Å]. The dimers are stacked in *a* direction and separated from neighbouring stacks by imidazolium cations (Figure 20).

Bis(1-ethyl-3-methylimidazolium) 5,5'-bistetrazolate ($(EMIM)_2BT$, **11**) crystallised in the monoclinic space group $P2_1/n$ with two molecules in the unit cell; the asymmetric unit consists of half a molecule (Figure 21). All bond lengths correspond well to previous structures. The bistetrazolate dianion being isolated from any further bonding contacts does not alter its conformation. In the crystal structure stacks of molecular units prevail when viewing along the *a* axis (Figure 22).

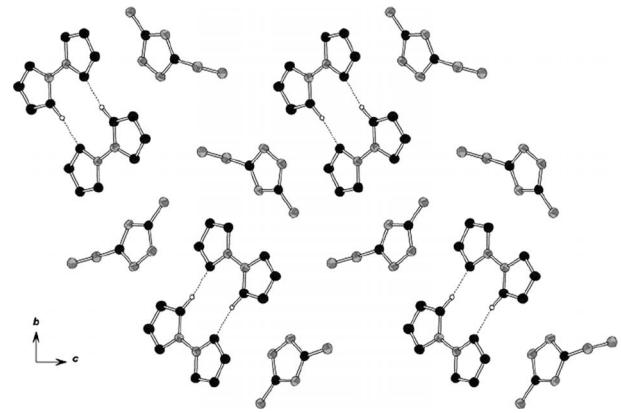

Figure 20. Crystal structure of (EMIM)HBT (**10**); view along the *a* axis.

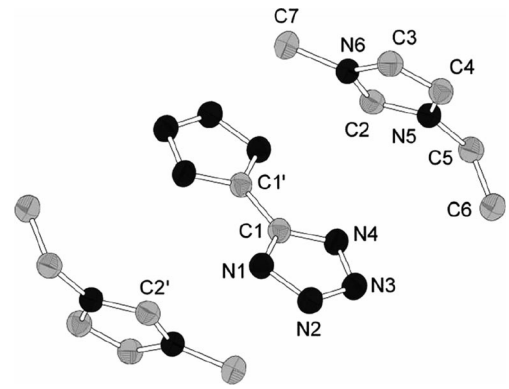

Figure 21. Molecular structure of Bis(1-ethyl-3-methylimidazolium) 5,5′-bistetrazolate; hydrogen atoms are omitted for clarity; selected bond lengths /Å: C1–C1^{I}: 1.460(2), C1–N1: 1.345(2), N1–N2: 1.354(2), N2–N3: 1.320(2), N3–N4: 1.355(2), C1–N4: 1.336(2), C2–N5: 1.330(2), C2–N6: 1.327(2), C3–N6: 1.378(2), C3–C4: 1.350(2), C4–N5: 1.385(2); symmetry operation: ^{I}: –*x*, –*y*, –*z*.

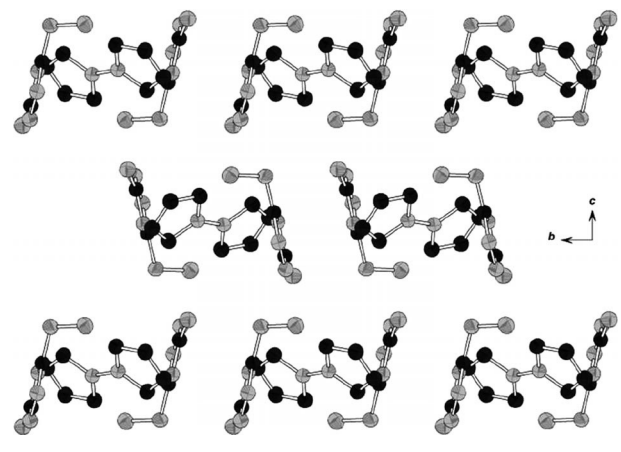

Figure 22. Crystal structure of bis(1-ethyl-3-methylimidazolium) 5,5′-bistetrazolate; view along the *a* axis; hydrogen atoms are omitted for clarity.

Thermal Analysis

Combined TGA and DSC measurements were conducted with a Netzsch STA 409 CD under inert gas conditions (Ar,

Zeitschrift für anorganische und allgemeine Chemie ZAAC Journal of Inorganic and General Chemistry

40 mL·min^{-1}) in aluminium oxide crucibles with a hole in the lid. The applied heating rate was 10 K·min^{-1}. Probe masses were in the range of 5.5 to 6.8 mg. The lithium salt (**1h**) loses two equivalents of crystal water at 165 °C, the sodium salt (**2h**) is dehydrated at 63 °C but the amount differs distinctively from the values observed in the crystal structure and the elemental analysis. Instead of a weight loss of 33.1 % corresponding to the pentahydrate, only a loss of 13.5 % was observed. This indicates a crystal water content of one to two equivalents. It is assumed, that water was lost during storage and while evacuating the oven in order to ensure an inert gas atmosphere. Among the alkali metal salts only the caesium salt (**5**) decomposes below 400 °C (392 °C). The other salts show decomposition at onset temperatures of 416 (Rb_2BT), 424 (K_2BT), 453 (Na_2BT) and 478 °C (Li_2BT). These values coincide with the observations of *Klapötke* et al. who found no decomposition of the alkaline earth metal salts below 400 °C.[8] In all cases the decomposition is not complete at the stated temperatures but only a fraction of the total mass is lost. Upon continued heating the residues decompose in a stepwise manner but rather gradually so that no further definite decomposition temperatures can be determined. Thermal decomposition is complete at close to 1000 °C. The monoammonium salt (**9**) shows decomposition at an onset temperature of 282 °C, the diammonium salt (**8**) measured for direct comparison showed decomposition at 290 °C. This value corresponds well to the temperature observed by *Chavez* et al. (280 °C, the difference may be due to a higher heating rate in our case).[29] The monoammonium and the diammonium salt show no large difference concerning thermal behaviour. If there is a specific and considerable advantage of the monoammonium 5,5'-bistetrazolate over the diammonium salt it has to affect different properties. The DSC curve of (EMIM)HBT (**10**) shows an endothermic peak at 147 °C, which is not accompanied by a weight loss in the TGA curve and can therefore be attributed to the substance melting. Decomposition takes place at 266 °C. $(EMIM)_2BT$ even melts at just 95 °C and can therefore be classified as an ionic liquid. The decomposition of the substance follows at 250 °C. The melting points were redetermined with a slower heating rate (2 K·min^{-1}) rate with a Büchi Melting Point B540. The melting point of **10** was determined as 145.5 °C, $(EMIM)_2BT$ (**11**) melted at 92.5 °C. The melting points stayed unchanged over three temperature cycles between room temperature and 10 °C above the melting point. To the best of our knowledge these are the first bistetrazolate salts exhibiting a distinct melting point. Compound **11** is a rare example of an ionic liquid containing a dianion, nevertheless having low lattice energy. The TGA of **11** reveals an abrupt loss of 80 % weight at an onset of 249.6 °C in connection with an exothermic peak in the DSC (see electronic supplement). Only small amounts of substance remain after the first decomposition.

IR Spectroscopy

IR spectra were recorded with a Bruker ALPHA FT IR spectrometer with platinum ATR sampling as the pure substance. There is a strong difference between the spectra of the hydrated and dehydrated salts. The hydrated salts show strong and broad stretching modes of the OH bonds involved in hydrogen bonds roughly between 2500 and 3700 cm^{-1} and below 900 cm^{-1} the corresponding bending modes. The latter are often partly obscuring the vibrations of the BT fragment. The water-free substances show a very concise spectrum built up of seven major bands all lying within the fingerprint region at about 700 to 1400 cm^{-1}. All bands slowly shift to lower wavenumbers when proceeding from lithium to caesium as counterion. A distinct effect of the atomic weight of the counterion onto the lattice vibrations of the BT-fragment can be observed. A comparison of the region from 680 to 1400 cm^{-1} of the water-free alkali metal salts of 5,5'-bistetrazole are presented in Figure 23. The barium salt roughly fits into this trend taking into account that the atomic weight of the barium atom has to be considered with 50 % as only one barium atom is present per BT moiety.

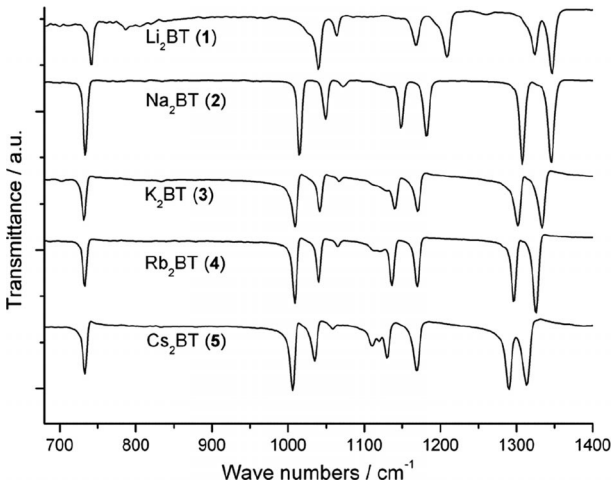

Figure 23. Comparison of the IR spectra of the water-free alkali metal 5,5′-bistetrazolates in the region from 680 to 1400 cm^{-1}.

Conclusions

The alkali metal salts **1** to **5** of the nitrogen-rich diacid 5,5'-bistetrazole were synthesised and characterised by elemental analysis, carbon NMR and IR spectroscopy and TGA and DSC measurements. The corresponding hydrates **1h** to **4h** and the mono caesium 5,5'-bistetrazolate (**6**) were structurally characterised by means of XRD single crystal analyses. Additionally, a second crystal modification of the known barium 5,5'-bistetrazolate (**7h**) was presented. The compounds have been analysed with respect to the coordination behaviour of the bicyclic ligand and the results compared with all metal 5,5'-bistetrazolates structurally characterised so far. A consecutive trend between chelation and the cation size was found and attributed to the *Lewis* acidity of the cation and the geometric limitations of the rather rigid ligand. Furthermore the monoammonium 5,5'-bistetrazolate (**9**), and mono- (**10**) and bis(1-ethyl-3-methylimidazolium) 5,5'-bistetrazolate (**11**) were synthesised and fully characterised including single crystal structure determination. The diammonium 5,5'-bistetrazolate (**8**) is additionally

presented in a different crystal modification as it was known so far. No special properties could be attributed to the monoammonium salt **9**, to be used in airbag technology, setting it apart from the diammonium salt (**8**), so far. The imidazolium salts are the first reversibly melting 5,5'-bistetrazolate compounds, the bis(1-ethyl-3-methylimidazolium) 5,5'-bistetrazolate (**11**) being the first ionic liquid on the basis of 5,5'-bistetrazolate dianions.

Experimental Section

All chemicals and solvents were used as received unless stated otherwise. Methanol, acetonitrile and diethyl ether were dried and purified according to common procedures[32] and stored over 3 Å molecular sieves until use. Elemental analyses were carried out by the service department for routine analysis and mass spectrometry with a vario MICRO cube (Elementar). NMR spectra were recorded in automation with a Bruker Avance 300 spectrometer at room temperature. IR spectra were recorded with a Bruker APLPHA FT-IR spectrometer with Platinum ATR-sampling. Hygroscopic substances were investigated on an identical device inside a glove box (type MB 150 B-G, mBraun). TGA/DSC measurements were performed with a Netzsch STA 409 CD in aluminium oxide crucibles, with an argon flow rate of 40 mL·min^{-1} and a heating rate of 10 K· min^{-1}; TGA decomposition points are given as onset temperature, DSC data is given as peak value. Melting points were determined with a Büchi Melting Point B540.

Caution! 5,5'-Bistetrazole and its derivatives are potential explosives and sensitive to heat, shock, friction and electrical spark. Although no unintended decomposition was observed during our experiments cautious handling of all substances and protective gear like safety shields, gloves, earthed equipment and earplugs are strongly recommended. Furthermore the handling and storage of larger quantities should be avoided.

5,5'-Bistetrazole was prepared following the procedure invented by *Friederich*[3] and optimised by *Nelson* et al.[4] Diammonium 5,5'-bistetrazolate (**8**) was synthesised according to *Hyoda* et al.[33] and later on in a way also described by *Klapötke* et al.[10a] Analysis for compound **8**: **TGA** (10 K·min^{-1}): 290 °C (decomp.); **DSC** (10 K·min^{-1}): 305 °C (exoth.)

Dilithium 5,5'-bistetrazolate dihydrate (1h): Lithium hydroxide monohydrate (301 mg, 7.18 mmol) and 5,5'-bistetrazole (496 mg, 3.59 mmol) were suspended in water (5 mL) and the mixture heated to reflux. The clear hot solution was filtered and the solvents evaporated to dryness. The raw product (654 mg, 3.52 mmol, 98 %) was recrystallised from a minimum amount of water yielding 48 % (319 mg) of **1h** and crystals suitable for XRD.

$C_2H_4Li_2N_8O_2$ (185.99 g·mol^{-1}) C 12.80 (calcd. 12.92), H 2.05 (2.17), N 59.80 (60.25)%; **^{13}C NMR** (75.5 MHz, [D$_6$]DMSO): δ = 155.4 (s, CN_4) ppm; **^{13}C NMR** (75.5 MHz, D_2O): δ = 154.5 (s, CN_4) ppm. **IR** (1034 (m), 1066 (w), 1169 (w), 1212 (m), 1317 (w), 1345 (m), 2600–3400 (m, br) cm^{-1}; **TGA** (10 K·min^{-1}): 165 (dehydr.), 478 (decomp.) °C; **DSC** (10 K·min^{-1}): 182 (endoth.), 479 (exoth.) °C.

Drying the product at 180 °C in fine vacuum yielded the water-free salt (**1**). The substance is highly hygroscopic and upon air contact absorbs two equivalents of water within minutes.

$C_2Li_2N_8$ (149.96 g·mol^{-1}) C 15.72 (calcd. 16.02), N 74.63 (74.72)%; **^{13}C NMR** (75.5 MHz, [D$_6$]DMSO): δ = 155.6 (s, CN_4) ppm. **IR** (ATR): 417 (s), 742 (w), 1040 (w), 1064 (w), 1168 (w), 1209 (w), 1324 (w), 1346 (w) cm^{-1}.

Disodium 5,5'-bistetrazolate pentahydrate (2h): Sodium hydrogen carbonate (1.38 g, 16.5 mmol) and 5,5'-bistetrazole (1.14 g, 8.24 mmol) were suspended in water (5 mL). The solids dissolved slowly accompanied by gas evolution. After the gas evolution had stopped, the mixture was heated to obtain a clear solution. The solvent was evaporated to dryness and the residue recrystallised from a minimum amount of hot water (ca. 3 mL) obtaining single crystals suitable for XRD. The sodium salt crystallised as a pentahydrate in 60 % yield (1.35 g, 4.96 mmol).

$C_2H_{10}N_8Na_2O_5$ (272.13 g·mol^{-1}) C 8.73 (calcd. 8.83), H 3.38 (3.70), N 41.11 (41.18)%; **^{13}C NMR** (75.5 MHz, D_2O): δ = 154.5 (s, CN_4) ppm. **IR** (ATR): 499 (m, sh), 579 (s, br), 730 (m), 1022 (m), 1047 (w), 1148 (m), 1186 (m), 1307 (s), 1326 (s), 1628 (s), 2600–3600 (s, br) cm^{-1}; **TGA** (10 K·min^{-1}): 63 (dehydr.), 453 (decomp.) °C; **DSC** (10 K·min^{-1}): 85 (endoth.), 464 (exoth.) °C.

Drying in fine vacuum at 90 °C yielded the water-free disodium salt (**2**).

$C_2N_8Na_2$ (182.06) C 12.99 (calcd. 13.19), N 60.52 (61.55)%. **IR** (ATR): 734 (s), 1015 (s), 1049 (m), 1148 (m), 1182 (m), 1308 (s), 1345 (s) cm^{-1}.

Dipotassium 5,5'-bistetrazolate (3): Potassium carbonate (1.65 g, 12.0 mmol) and 5,5'-bistetrazole (1.50 g, 10.9 mmol) were suspended in water (15 mL) and after the gas evolution had ceased the mixture was heated to reflux. The solvent was evaporated at room temperature and the residue recrystallised from boiling water (4.5 mL). Single crystals suitable for XRD were obtained but did not lead to publishable solutions. In one case the investigated crystal turned out to be the corresponding dihydrate **3h**. The product was dried in air at room temperature yielding 1.42 g (6.63 mmol, 61 %).

$C_2K_2N_8$ (214.27 g·mol^{-1}) C 11.14 (calcd. 11.21), N 52.42 (52.30)%; **^{13}C NMR** (75.5 MHz, D_2O): δ = 154.7 (s, CN_4) ppm. **IR** (ATR): 732 (s), 1009 (s), 1042 (m), 1140 (m), 1170 (m), 1302 (s), 1334 (s) cm^{-1}; **TGA** (10 K·min^{-1}): 424 (decomp.) °C; **DSC** (10 K·min^{-1}): 429 (exoth.) °C.

Dirubidium 5,5'-bistetrazolate dihydrate (4h): Rubidium carbonate (1.32 g, 5.72 mmol) was suspended in water (15 mL) and 5,5'-bistetrazole (790 mg, 5.72 mmol) was added. After the gas evolution had ceased the water was evaporated on a hot plate and the slightly yellow residue recrystallised from a minimum amount of water (3 mL). Single crystals suitable for XRD could be obtained. The X-ray structure includes two water molecules per molecular unit which are lost while drying in air at room temperature**.** During the drying process the crystals transform from colourless translucent needles to a colourless powder. Water-free rubidium 5,5'-bistetrazolate (**4**) was obtained in 62 % yield (1.10 g).

$C_2Rb_2N_8$ (307.02 g·mol^{-1}) C 7.75 (calcd. 7.82), N 36.36 (36.50)%; **^{13}C NMR** (75.5 MHz, D_2O): δ = 154.7 (s, CN_4) ppm. **IR** (ATR): 733 (m), 1009 (s), 1040 (m), 1136 (m), 1169 (m), 1296 (s), 1325 (s) cm^{-1}; **TGA** (10 K·min^{-1}): 416 (decomp.) °C; **DSC** (10 K·min^{-1}): 424 (exoth.) °C.

Dicaesium 5,5'-bistetrazolate (5): Caesium carbonate (2.16 g, 8.96 mmol) and 5,5'-bistetrazole (760 mg, 5.50 mmol) were dissolved in water (15 mL) and the solution was evaporated to dryness after stirring for 30 minutes. The residue was recrystallised from a small amount of hot water and the product was isolated in 70 % yield (1.55 g,

Zeitschrift für anorganische und allgemeine Chemie ZAAC Journal of Inorganic and General Chemistry

3.86 mmol). Single crystals could be obtained but did not lead to a publishable solution so far.

$C_2Cs_2N_8$ (401.90 g·mol^{-1}) C 6.09 (calcd. 5.89), N 27.92 (27.88); **^{13}C NMR** (75.5 MHz, D_2O): δ = 154.6 (s, CN_4) ppm. **IR** (ATR): 733 (m), 1006 (s), 1035 (m), 1111 (w), 1120 (w), 1130 (m), 1169 (m), 1290 (s), 1314 (s) cm^{-1}; **TGA** (10 K·min^{-1}): 392 (decomp.) °C; **DSC** (10 K·min^{-1}): 402 (exoth.) °C.

Barium 5,5'-bistetrazolate pentahydrate (7h): Barium hydroxide octahydrate (3.88 g, 12.3 mmol) and 5,5′-bistetrazole (1.70 g, 12.3 mmol) were dissolved in boiling water (100 mL). The solution was filtered hot and slowly cooled to room temperature. The product crystallised in 79 % yield (3.55 g, 9.77 mmol), single crystals suitable for XRD analysis could be obtained.

Pentahydrate: $C_2H_{10}BaN_8O_5$ (363.49 g·mol^{-1}) C 6.61 (calcd. 6.61), H 2.20 (2.77); N 31.00 (30.83)%; **^{13}C NMR** (75.5 MHz, D_2O): δ = 155.4 (s, CN_4) ppm. **IR** (ATR): 400–850 (s, br), 1021 (s), 1048 (m), 1121 (w), 1151 (m), 1181 (s), 1308 (s), 1327 (s), 1650 (m), 2700–3600 (s, br) cm^{-1}. The comparatively high deviation of the hydrogen value may indicate a partial mixture of e.g. the penta- and tetrahydrate. This is not confirmed by the nitrogen value, though. Drying the Substance in air at room temperature yielded the dihydrate after four days.

Dihydrate: $C_2H_4BaN_8O_2$ (309.45 g·mol^{-1}) C 7.70 (calcd. 7.76), H 1.26 (1.30), N 35.94 (36.21)%. **IR** (ATR): 542 (s, br), 571 (s, sh), 675 (m, br), 725 (m), 819 (w, br), 1019 (m), 1047 (w), 1085 (w), 1143 (w), 1186 (w), 1218 (w), 1310 (m), 1339 (m), 3057 (w, br) 3523 (w, br) cm^{-1}.

Drying the product at 120 °C in fine vacuum for four hours yielded the water-free salt.

C_2BaN_8 (273.42 g·mol^{-1}) C 8.79 (calcd. 8.79), N 41.54 (40.98)%. **IR** (ATR): 728 (m), 1021 (s), 1057 (m), 1085 (w), 1143 (s), 1191 (m), 1312 (m), 1340 (s) cm^{-1}.

Ammonium 5,5'-bistetrazolate (9): Diammonium 5,5'-bistetrazolate (554 mg, 3.22 mmol) and 5,5'-bistetrazole (445 mg, 3.22 mmol) were dissolved in water (25 mL), the solution heated to reflux and then evaporated to dryness. The residue was recrystallised from a minimum amount of hot water (ca. 5 mL) so that an aqueous solution at 115 °C in a closed flask was saturated. The solution was then slowly cooled to room temperature yielding needles of diammonium 5,5'-bistetrazolate (201 mg, 1.17 mmol, 36 % of the starting material. $C_2H_8N_{10}$ (172.15 g·mol^{-1}) C 13.86 (calcd. 13.95), H 4.55 (4.68), N 80.98 (81.36)%). The supernatant solution was transferred to a second flask and slowly cooled to 4 °C whereupon the desired product crystallised in 60 % yield (302 mg, 1.95 mmol). Single crystals suitable for XRD were obtained.

$C_2H_5N_9$ (155.12 g·mol^{-1}) C 15.65 (calcd. 15.49); H 2.92 (3.25), N 80.64 (81.27)%; **^{13}C NMR** (75.5 MHz, D_2O): 149.4 (s, CN_4) ppm. **IR** (ATR): 426 (m), 476 (s), 687 (m), 851 (s, br), 1009 (s), 1070 (m), 1105 (m), 1224 (w), 1282 (m), 1335 (w), 1377(s), 1409 (m), 1528 (w), 2100–3300 (m, br); **TGA** (10 K·min^{-1}): 282 (decomp.) °C; **DSC** (10 K·min^{-1}): 289 (exoth.) °C. The deviation of the nitrogen value in the elemental analysis may be attributed to the product not being completely pure. The tendency of equimolecular solutions of diammonium 5,5'-bistetrazole and the free acid to yield the diammonium salt upon crystallisation makes it not possible to purify the product by recrystallisation.

1-Ethyl-3-methylimidazolium 5,5'-bistetrazolate (10): Barium 5,5'-bistetrazolate (467 mg, 1.71 mmol) was added to a solution of 1-ethyl-3-methylimidazolium bisulfate (356 mg, 1.71 mmol) in water (20 mL). The suspension was stirred for three days and then filtered. The solution was evaporated to dryness and the residue recrystallised from a hot mixture of acetone and water. Single crystals suitable for XRD were obtained by layering a concentrated solution in acetonitrile with diethyl ether. Yield: 220 mg (0.87 mmol, 52 %).

$C_8H_{12}N_{10}$ (248.25 g·mol^{-1}) C 38.48 (calcd. 38.71), H 4.80 (4.87), N 55.60 (56.42)%; **^{1}H NMR** (300.1 MHz, [D$_6$]DMSO): δ = 1.40 (t, 3 H, ^3J(H,H) = 7.2 Hz, CH_2CH_3), 3.85 (s, 3 H, *Me*), 4.19 (q, $^3J_{H,H}$ = 7.2 Hz, 2 H, CH_2CH_3), 7.70 (s, 1 H, H_{Im}), 7.78 (s, 1 H, H_{Im}), 9.15 (s, 1 H, H_{Im}), 16.19 (br. s, 1 H, H_{BT}) ppm; **^{13}C NMR** (75.5 MHz, [D$_6$]DMSO): δ = 15.0 (s, CH_2CH_3), 35.7 (s, CH_3), 44.1 (s, CH_2CH_3), 121.9 (s, C_{Im}), 123.5 (s, C_{Im}), 136.3 (s, C_{Im}), 149.4 (s, CN_4) ppm. **IR** (ATR): 412 (w), 483 (s), 627 (s), 650 (s), 703 (m), 758 (s), 866 (m), 890 (m), 999 (m), 1017 (m), 1029 (m), 1092 (m), 1161 (s), 1281 (m), 1341 (s), 1465 (w), 1560 (w), 1574 (w), 1617 (w), 2300–2700 (w, br), 3112 (w), 3141 (w) cm^{-1}; **TGA** (10 K·min^{-1}): 266 (decomp.) °C; **DSC** (10 K·min^{-1}): 147 (endoth.), 282 (exoth.) °C; **M. P.** (2 K·min^{-1}): 145.5 °C.

Bis(1-ethyl-3-methylimidazolium) 5,5'-bistetrazolate (11): A solution of 5,5'-bistetrazole (349 mg, 2.53 mmol) in dry methanol (10 mL) was slowly added to a solution of 1-Ethyl-3-methylimidazolium methyl carbonate (938 mg, 5.04 mmol) in dry methanol (5 mL). Slow gas evolution was observed and the mixture was heated to 50 °C for sixteen hours before the solvent was removed in vacuo. The residue was recrystallised by layering a concentrated solution in dry acetonitrile with dry diethyl ether. Large crystals suitable for XRD formed within hours, crystallisation was complete after a few days. After a second recrystallisation from dry acetonitrile at –30 °C 560 mg (1.56 mmol, 62 %) of the pure product were obtained.

$C_{14}H_{22}N_{12}$ (358.41 g·mol^{-1}) C 47.10 (calcd. 46.92), H 6.21 (6.19), N 46.91 (46.90)%; **^{1}H NMR** (300.1 MHz, [D$_6$]DMSO): δ = 1.37 (t, 3 H, $^3J_{H,H}$ = 7.1 Hz, CH_2CH_3), 3.89 (s, 3 H, Me), 4.25 (q, $^3J_{H,H}$ = 7.1 Hz, 2 H, CH_2CH_3), 7.76 (s, 1 H, H_{Im}), 7.85 (s, 1 H, H_{Im}), 9.67 (s, 1 H, H_{Im}) ppm; **^{13}C NMR** (75.5 MHz, [D$_6$]DMSO): δ = 15.2 (s, CH_2CH_3), 35.5 (s, CH_3), 44.0 (s, CH_2CH_3), 121.9 (s, C_{Im}), 123.5 (s, C_{Im}), 136.8 (s, C_{Im}), 156.0 (s, CN_4) ppm. **IR** (ATR): 621 (m), 651 (s), 732 (s), 739 (s), 800 (m), 850 (w), 894 (m), 1006 (w), 1027 (m), 1094 (w), 1156 (s), 1293 (m), 1315 (m), 1428 (w), 1453 (w), 1561 (m), 1659 (w), 2978 (w), 3053 (m), 3136 (w) cm^{-1} **TGA** (10 K·min^{-1}): 250 (decomp.) °C; **DSC** (10 K·min^{-1}): 94.5 (endoth.), 298 (exoth.) °C; **M. P.** (2 K·min^{-1}): 92.5 °C.

Supporting Information (see footnote on the first page of this article): Table with bond lengths, bond angles and torsion angles in the bistetrazolate anions of compounds, **1h** to **4h**, **6**, **7h** and **8** to **11**; TGA and DSC Curve of $(EMIM)_2BT$ (**11**).

Acknowledgments

Financial support by the Studienstiftung des deutschen Volkes and the Fond der Chemischen Industrie is gratefully acknowledged. We thank Jens Eußner (M. Sc.) for his introduction into and continued help with TGA/ DSC measurements. We are very thankful to Dr. Klaus Harms for fruitful discussions and valuable advice regarding XRD single crystal structure determination.

References

[1] E. Oliveri-Mandalà, T. Passalacqua, *Gazz. Chim. Ital.* **1913**, *43(2)*, 465–475.

[2] a) H. Rathsburg, *GB* 185555, **1922**; b) H. Rathsburg, *DE* 401344, **1924**.
[3] W. Friederich, *DE* 952811, **1956**.
[4] J. H. Nelson, N. E. Takach, A. H. Ronald, D. W. Moore, W. M. Tolles, G. A. Gray, *Magn. Reson. Chem.* **1986**, *24*, 984–994.
[5] a) T. Hiroaki, O. Akihisa, *JP* 06157484, **1994**; b) D. L. Hordos, S. P. Burns, *US* 7714143, **2010**; c) S. Hyoda, M. Kita, H. Sawada, S. Nemugaki, S. Otsuka, Y. Miyawaki, T. Ogawa, Y. Kubo, *US* 6040453, **2000**; d) I. V. Mendenhall, *US* 6689237, **2004**; e) I. V. Mendenhall, M. W. Barnes, *US Appl.* 2003/106624, **2003**.
[6] a) A. J. Downard, P. J. Steel, J. Steenwijk, *Aust. J. Chem.* **1995**, *48*, 1625–1642; b) P. J. Steel, *J. Chem. Crystallogr.* **1996**, *26*, 399–402.
[7] a) P. J. Eulgem, A. Klein, N. Maggiarosa, R. W. H. Pohl, D. Naumann, *Chem. Eur. J.* **2008**, *14*, 3727–3736; b) R. W. H. Pohl, J. Wiebke, A. Klein, N. Maggiarosa, M. Dolg, *Eur. J. Inorg. Chem.* **2009**, 2472–2476.
[8] N. Fischer, T. M. Klapötke, K. Peters, M. Rusan, J. Stierstorfer, *Z. Anorg. Allg. Chem.* **2011**, *637*, 1693–1701.
[9] M. Joas, T. M. Klapötke, J. Stierstorfer, *Crystals* **2012**, *2*, 958–966.
[10] a) N. Fischer, D. Izsák, T. M. Klapötke, S. Rappenglück, J. Stierstorfer, *Chem. Eur. J.* **2012**, *18*, 4051–4062; b) Y. Guo, G.-H. Tao, Z. Zeng, H. Gao, J. M. Shreeve, D. A. Parrish, *Chem. Eur. J.* **2010**, *16*, 3753–3762; c) R. Wang, Y. Guo, R. Sa, J. M. Shreeve, *Chem. Eur. J.* **2010**, *16*, 8522–8529.
[11] V. A. Ostrovskii, N. P. Shirokova, G. I. Koldobskii, V. S. Poplavskii, *Chem. Hetercycl. Compd.* **1981**, *17*, 1148–1151.
[12] Stoe & Cie: *X-AREA v1.56*, Stoe & Cie GmbH, Darmstadt, Germany, **2011**.
[13] Bruker: Bruker Instrument Service v3.0.26, *APEX2 v2012.10–0, SAINT v8.27B*, Bruker AXS Inc., Madison, Wisconsin, USA, **2012**.
[14] A. Altomare, M. C. Burla, M. Camalli, G. Cascarano, C. Giacovazzo, A. Guagliardi, A. G. G. Moliterni, G. Polidori, R. Spagna, *J. Appl. Crystallogr.* **1999**, *32*, 115–119.
[15] M. C. Burla, R. Caliandro, M. Camalli, B. Carrozzini, G. L. Cascarano, L. D. Caro, C. Giacovazzo, G. Polidori, R. Spagna, *J. Appl. Crystallogr.* **2005**, *38*, 381–388.
[16] L. Palatinus, G. Chapuis, *J. Appl. Crystallogr.* **2007**, *40*, 786–790.
[17] G. Sheldrick, *Acta Crystallogr., Sect. A* **2008**, *64*, 112–122.
[18] A. L. Spek, *Acta Crystallogr., Sect. D* **2009**, *65*, 148–155.
[19] L. Farrugia, *J. Appl. Crystallogr.* **1999**, *32*, 837–838.
[20] R. H. Blessing, *Acta Crystallogr., Sect. A* **1995**, *51*, 33–38.
[21] P. Coppens, in *Crystallographic Computing* (Eds.: F. R. Ahmed, S. R. Hall, C. P. Huber), Munksgaard, Copenhagen, **1970**, pp. 255–270.
[22] Bruker: *SADABS v2012/1*, Bruker AXS Inc., Madison, Wisconsin, USA, **2012**.
[23] K. Brandenburg, H. Putz: *Diamond - Crystal and Molecular Structure Visualization v3.2i*, Crystal Impact GbR, Bonn, Germany, **2012**.
[24] in *CRC Handbook of Chemistry and Physics*, 91 ed. (Eds.: W. M. Haynes, D. R. Linde), CRC Press, London, **2011**.
[25] T. M. Klapötke, M. Stein, J. Stierstorfer, *Z. Anorg. Allg. Chem.* **2008**, *634*, 1711–1723.
[26] J. H. N. Buttery, Effendy, S. Mutrofin, N. C. Plackett, B. W. Skelton, N. Somers, C. R. Whitaker, A. H. White, *Z. Anorg. Allg. Chem.* **2006**, *632*, 1839–1850.
[27] V. Ernst, T. M. Klapötke, J. Stierstorfer, *Z. Anorg. Allg. Chem.* **2007**, *633*, 879–887.
[28] H. P. H. Arp, A. Decken, J. Passmore, D. J. Wood, *Inorg. Chem.* **2000**, *39*, 1840–1848.
[29] D. E. Chavez, M. A. Hiskey, D. L. Naud, *J. Pyrotech.* **1999**, *10*, 17–36.
[30] N. Wiberg, *Lehrbuch der Anorganischen Chemie*, 102nd ed., de Gruyter, New York, **2007**.
[31] A. R. Choudhury, N. Winterton, A. Steiner, A. I. Cooper, K. A. Johnson, *J. Am. Chem. Soc.* **2005**, *127*, 16792–16793.
[32] W. L. Amarego, D. D. Perrin, *Purification of Laboratory Chemicals*, 4th ed., Elsevier, Burlington, **1996**.
[33] S. Hyoda, M. Kita, H. Sawada, S. Nemugaki, S. Otsuka, Y. Miyawaki, T. Ogawa, Y. Kubo, *EP* 1035118, **1999**.

Received: March 12, 2013
Published Online: May 22, 2013

6.7 Neue Boratanionen mit Bistetrazolato^{2-} und Pyrazindiolato^{2-} Liganden

in preparation

New Borate Anions with Bistetrazolato^{2-} and Pyrazinediolato^{2-} Ligands

Lars H. Finger, Fabian G. Schröder, Jörg Sundermeyer

New Borate Anions with Bistetrazolato^{2-} and Pyrazinediolato^{2-} Ligands

Lars H. Finger,[a] Fabian G. Schröder,[a] Jörg Sundermeyer*[a]

a) Fachbereich Chemie and Materials Science Centre,
Philipps-Universität Marburg,
Hans-Meerwein-Str. 4,
35043 Marburg,
Germany.
*E-Mail: JSU@staff.uni-marburg.de

TOC Graphic

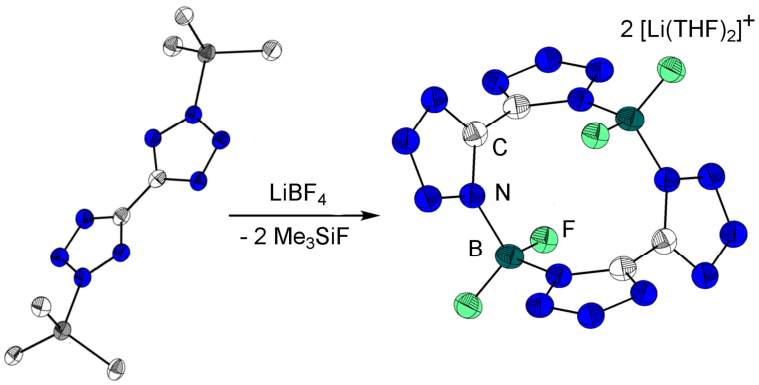

Abstract

We herein present the synthesis of the first silylated bistetrazole via a catalyzed twin [2+3] cycloaddition of TMS-azide at cyanogen and its application to access the first bistetrazolatoborates. New borate anions with pyrazine-2,3-diolato ligands were synthesized from tetrafluoroborate salts with organic cations. These borates might be interesting as additives for lithium ion battery electrolytes.

Introduction

Lithium ion batteries are among the most prominent and most important energy storage systems available today. They are the basis for the modern market of portable electronic devices and by now increasingly employed in large scale applications as electric vehicles and stationary energy storage units. The most common form of lithium ion batteries consists of a graphite anode, an organic solvent electrolyte and a metal oxide cathode.[1] The solid electrolyte interface (SEI), which is formed on the anode during the first charge-discharge cycles, is an indispensable part ensuring safe operation of the battery cell. Without initial formation of the SEI the organic solvent would be decomposed upon every recharge process, leading to very fast capacity loss and severe safety hazards.[2] Lithium bis(oxalato)borate (LiBOB) is an important electrolyte additive, which aids the formation of a stable SEI.[3]

Carboxylate (CO_2^-) and tetrazolate (CN_4^-) are bioisosteric groups.[4] Their relation is most evident when comparing the respective acidity of the corresponding acids, the electron delocalization within the flat anionic functionality and the capability to form hydrogen donor and acceptor bonds. Their exchange is a commonly employed principle to obtain related drugs of similar mechanism of action.[5] This analogy intrigued us to analyze if the concept of bioisosterism can be extended to the coordination behavior of oxalate and bistetrazolate. Specifically, we desired the synthesis of bistetrazolato borates corresponding to known oxalato borates, which would have to be investigated concerning their electrochemical stability and ability to form SEI layers. The coordination behavior of 5,5'-bistetrazole was so far investigated with respect to rare earth metals,[6] alkaline[7] and alkaline earth metals[8] and copper.[9] The derivatization of 5,5'-bistetrazole with further functionalities was most notably advanced by Klapötke and coworkers.[10] Due to several synthetic difficulties we later on modified our objectives towards the synthesis of new borates with pyrazine-2,3-diolato ligands, which possess an electron-poor diolate moiety compared to known phenylene-1,2-

diolato borates. These are versatile compounds employed not only in lithium ion batteries but also as anti-fungal wood preservatives and as catalysts in organic syntheses.[11]

Results

Catalytic Synthesis and Characterization of Bis(trimethylsilyl)bistetrazole

A silylation of the free acid (**1**) with trimethylsilyl chloride in presence of triethyl amine leads to the silyl substituted bistetrazole (**2**). This procedure was reported for the silylation of 1H-tetrazole.[12] However, for bistetrazole the yields were low and residues of triethyl ammonium chloride remained in the product, which is hydrolytically too sensitive for column chromatography. We developed a superior and in principle atom economic alternative in an $AlCl_3$ catalyzed reaction between cyanogen and two equivalents of trimethylsilyl azide (Scheme 1).

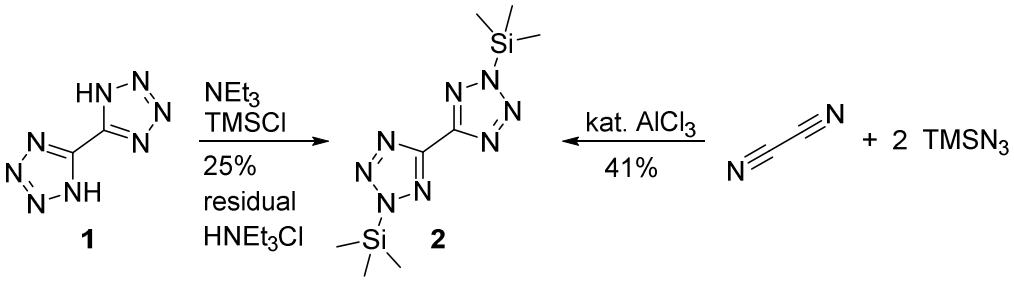

Scheme 1. Synthesis of 2,2'-bis(trimethylsilyl)-5,5'-bistetrazolate (**2**).

Via this twin [2+3]-cycloaddition approach, **2** is obtained in adequate yields after purification by sublimation at $1 \cdot 10^{-2}$ mbar and 120 °C. To the best of our knowledge this compound is the first bistetrazole derivative, which can be vaporized and condensed without decomposition. During sublimation single crystals of **2** suitable for XRD analysis could be obtained, which confirmed the 2,5-substitution pattern (*vide infra*). No evidence for isomeric structures was observed by means of ^{1}H, ^{13}C and ^{29}Si NMR spectroscopy. The [2+3] cycloaddition of nitriles and azides to form tetrazoles, also known as the Finnegan tetrazole synthesis,[13] typically leads to the 1,5-substituted isomer.[14] Whether the reaction occurs in a concerted or stepwise mechanism is still under dispute. Currently, for alkyl and aryl substituted azides a concerted mechanism is presumed, while for azide salts and very electron poor nitriles a stepwise mechanism is favored based on experimental and computational results.[15] The fact that in the current example the 2,5-substituted isomer is obtained may be explained by the high steric demand of the TMS group.[16] It can be assumed, that the isolated 2,5-isomer is either the result of a thermodynamically controlled reaction path or the result of reversible silyl

migration following a conceivable kinetically controlled reaction path via the 1,5-substituted isomer as intermediate product. The employment of catalytic amounts of $AlCl_3$ is mandatory as evidenced by two comparative experiments. Without addition of the Lewis acid and upon addition of stoichiometric amounts of $AlCl_3$ (1:1, relative to cyanogen), no product formation could be observed. As commonly assumed, the catalyst $AlCl_3$ may enhance the nucleophilicity of the azide moiety, e. g. by promoting an intermediate N-Si bond cleavage within a [TMS-N_3-$AlCl_3$] complex and formation of the anion $[Cl_3AlN_3]^-$, or may enhance the electrophilicity of cyanogen by coordinating one nitrile group.[15a] In any case, the catalyst induces a stepwise reaction mechanism for the present transformation.

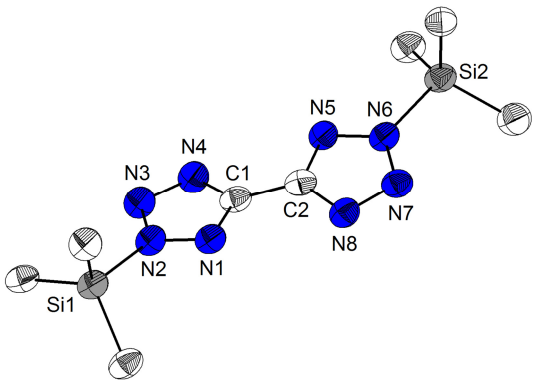

Figure 1. Molecular structure of TMS_2BT (**2**), hydrogen atoms omitted for clarity. Relevant bond distances/ Å and angles/ °: C1-N1: 1.331(4), N1-N2: 1.341(4), N2-N3: 1.347(4), N3-N4: 1.326(4), N4-C1: 1.350(4), C1-C2: 1.456(5), C2-N5: 1.325(4), N5-N6: 1.351(4), N6-N7: 1.357(4), N7-N8: 1.322(4), N8-C2:1.356(4), N2-Si1: 1.826(3), N6-Si2: 1.827(3), N1-C1-C2-N5: 167.2(4).

The molecular structure of **2** is depicted in Figure 1. The compound crystallized in the monoclinic space group $P2_1/c$ with 4 molecules per unit cell. The 2,5 substitution pattern has a significant effect on the bond lengths in the tetrazole moieties, if compared to free H_2BT.[17] The latter structure shows the shortest bond lengths between the carbon and the non-proton bearing nitrogen atom (C1-N4) and at N2-N3. In TMS_2BT the shortest bonds are found at C1-N1 and N3-N4. The outermost N2-N3 bond of the present silylated BT derivative is drastically elongated in comparison to other literature known 2,5-substituted tetrazole moieties.[18] This observation corresponds directly to the resonance structures presented in Scheme 1. The two tetrazole moieties show a N1-C1-C2-N5 torsion angle of 167°.

Attempts to Synthesize Bistetrazolato Borates

Our first attempts to access bistetrazolato borates typically started from the free acid H_2BT (**1**) or its alkali metal salts,[7] which were reacted with a vast series of boron compounds BX_3. These included boric acid in the presence of water trapping agents, the series of boron

trihalides (X = F, Cl, Br) and their etherates, borane adducts L-BH_3 and alkali metal hydrido borates, and amino boranes such as $B(NMe_2)_3$. With none of the former a selective transformation could be achieved. In the product mixtures, which were obtained from alkali metal hydrido borates and boron trihalides, traces of anionic fragments with a sum formula corresponding to bistetrazolato-dihydroborates or bistetrazolato-dihaloborates (Figure 2) were occasionally observed by ESI mass spectrometry. All attempts to purify these salts failed.

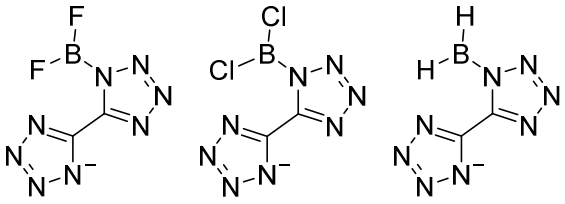

Figure 2. Anionic bistetrazolato borate species or fragments repeatedly observed by ESI-MS.

Finally, slightly more selective reactions could be achieved by the reaction of 2,2'-bis(trimethylsilyl)bistetrazolate (**2**) with lithium tetrafluoroborate (Scheme 2). The ESI(−) mass spectra of the product mixture again revealed an anionic [(BT)BF_2] fragment next to unidentified species. However, ^{13}C, ^{11}B, and ^{19}F NMR spectra show a number of signals, that cannot be solely attributed to a single substance such as the anticipated LiBOB analogues Li[$(BT)_2B$] or Li[(BT)BF_2]. Neither excess of **2** nor excess of $LiBF_4$ leads to a more selective reaction, which would have allowed to isolate larger amounts of a pure lithium BT-borate from this mixture of ionic compounds.

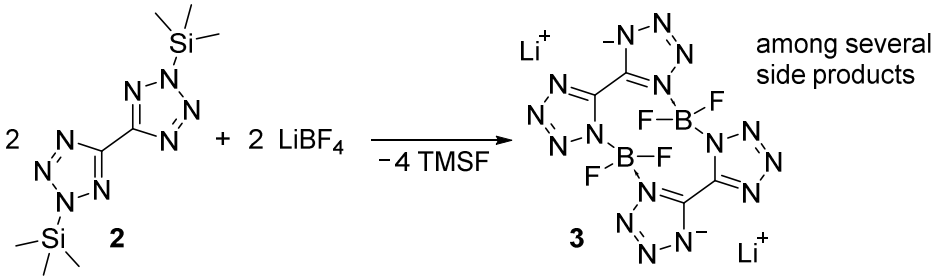

Scheme 2. Preparation of the lithium bistetrazolato difluoroborate dimer **3** obtained in a mixture with unidentified side products.

Nevertheless, in one recrystallization attempt from THF few single crystals were obtained next to significant amounts of amorphous residue. The X-ray diffraction analysis of one of these crystals confirmed the borate fragments, which were observed in mass spectra. In contrast to the molecular oxalato-difluoroborate anion with two chelating oxalate ligands a dimeric structure prevails in which two bridging bistetrazolate moieties are connected by two BF_2 fragments (Figure 3).

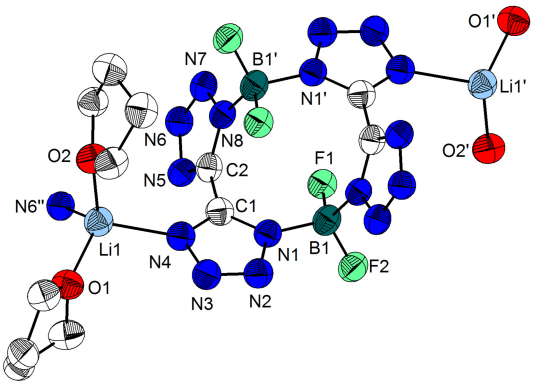

Figure 3. Molecular structure of compound **3**·2 THF, hydrogen atoms omitted for clarity, the symmetry equivalent THF molecules are reduced to the coordination oxygen atoms. Relevant bond distances/ Å and angles/ °: C1-N1: 1.340(3), N1-N2: 1.358(2), N2-N3: 1.303(2), N3-N4: 1.361(2), N4-C1: 1.326(3), C1-C2: 1.465(3), C2-N5: 1.322(2), N5-N6: 1.353(2), N6-N7: 1.307(2), N7-N8: 1.346(2), N8-C2: 1.352(3), N1-B1: 1.574(3). N8-B1^{I}: 1.581(3), B1-F1: 1.367(3), B1-F2: 1.360(3), Li1-N4: 2.068(4), Li1-N6^{II}: 2.063(4), Li1-O1: 1.906(4), Li1-O2: 1.918(4), N1-B1-N8^{I}: 108.2(2), F1-B1-F2:114.9(2), N1-C1-C2-N8: 70.2(3). Symm. op. I: −x, 2−y, 1−z; II: −x, 1−y, 1−z.

The compound crystallized in the triclinic space group *P*−1 with two THF molecules per asymmetric unit, which are coordinated to the lithium atoms. The asymmetric unit further consists of one BT-BF_2 moiety, which is completed to a dimeric unit via a crystallographic inversion center. A $C_4N_4B_2$ decacycle is formed; this motive was observed only once so far in a dimeric benzil-diimino-borane.[19] The lithium atoms are coordinated in a tetrahedral fashion by two N and two O atoms. They connect the BT-BF_2 dimers forming a 1D chain structure. Similar to the crystal structure of LiBT hydrate,[7] where lithium ions do not occur chelated by BT, the boron atom seems to be too small to allow a monomeric structure as it occurs in the bisoxalato borate or bisoxalato difluoroborate anions. This structure suggests that a molecular di(bistetrazolato) borate will probably not be accessible. If a further reaction of **2** with the BF_2 fragments of **3** took place, polymeric structures would likely be formed; this may account for the repeatedly observed insoluble residues of the reaction mixtures. In the molecular structure of **3** the bistetrazole moiety strongly deviates from planarity with a N1-C1-C2-N8 torsion angle of 70°. Although the substance was never isolated in a pure form, allowing the unambiguous and full characterization, we are confident that it can be associated with a quartet resonance at −150 ppm ($^{1}J_{BF}$ = 17.5 Hz) in the ^{19}F NMR spectrum and a triplet resonance at 2.1 ppm ($^{1}J_{BF}$ = 17.6 Hz) in the ^{11}B NMR spectrum. These values are comparable to oxalato difluoroborates and related substances.[20]

In a further attempt of crystallization from MeCN a partially hydrolyzed derivative of **3** was obtained in a single crystalline form and investigated by X-ray diffraction. Figure 4 displays

the structure of **4**·5 MeCN. An oxido ligand bridging two boron atoms has formally replaced two fluorine atoms of **3**.

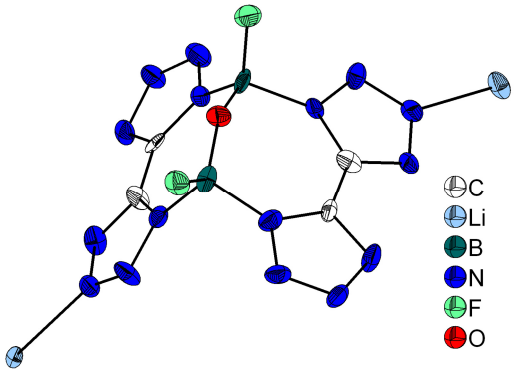

Figure 4. Molecular structure of a partially hydrolyzed bistetrazolato fluoro-oxoborate. Five acetonitrile molecules were omitted for clarity. Bond distances and angles are not discussed due to low crystal quality.

Compound **4** crystallized with five molecules of acetonitrile per asymmetric unit in the monoclinic space group $P2_1/n$. Two MeCN molecules are bound to bridging lithium atoms, three are non-coordinating. As the selected crystal was very weakly scattering only a very low percentage of reflections meets the $I > 2\sigma(I)$ criterion. This resulted in a very low S-value and poor bond precision, which does not allow a more detailed discussion. A similar structure was observed with bis-2,2'-imidazole replacing the bistetrazole moiety and ethyl groups replacing the remaining fluorine atoms of structure **4**.[21]

Synthesis of pyrazine-2,3-diolato borates

In contrast to the previous experiments, the formation of borates with catechol like ligands is significantly more preferred.[11] We opted for the 2,3-dioxo-5,6-pyrazinedicarbonitrile (H_2OPN), the privileged catechol chelate functionality with an electron-poor dicyanopyrazine moiety, which might act as electron acceptor in battery materials. Next to potential electrolyte applications, the OPN moiety might allow the development of well-engineered H-bonding networks[22] or might act as bridging ligands in coordination chemistry.[23] Most interesting in view of the potential borates and their application in lithium ion batteries is the recent observation that the addition of minor amounts of H_2OPN to the electrolyte significantly enhances the long-term discharge capacity of respective cells.[24]

The synthesis of borates with the OPN moiety as a ligand was accomplished by combining the free ligand with a tetrafluoroborate salt and $SiCl_4$ as promoter for the condensation reaction similar to related systems (Scheme 4).[20b, 25]

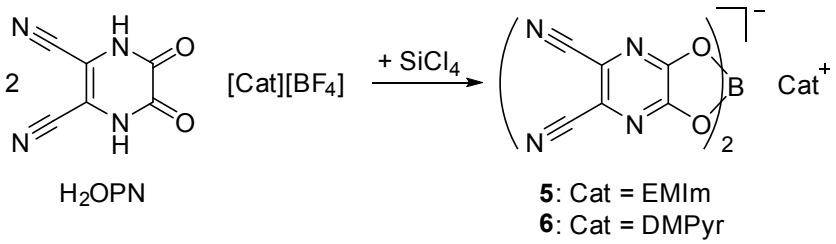

Scheme 3. Synthesis of the new borate salts **5** and **6**.

During the reaction the mixture typically turned orange to brown, which can be attributed to a partial decomposition of a very small fraction of H_2OPN. In comparative experiments with benzene catechol derivatives no coloration was observed. Compounds **5** and **6** could be isolated as light brown solids after recrystallization. Salt **6** was additionally treated with decolorizing carbon. The ^{11}B NMR spectra of the salts **5** and **6** show a resonance at 13 ppm, which is in the typical range for bis(oxalato)borates and related anions.[26] Both borates could be obtained in single crystalline form and elucidated by X-ray diffraction (Figure 5 and 6).

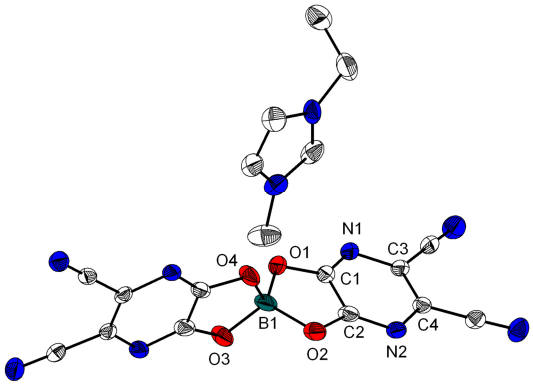

Figure 5. Molecular structure of compound **5**, hydrogen atoms omitted for clarity. Relevant bond distances/ Å and angles/ °: C1-O1: 1.322(3), C1-C2: 1.426(4), C1-N1: 1.302(3), N1-C3: 1.376(3), C3-C4: 1.368(3), C4-N2: 1.370(3), N2-C2: 1.300(3), C2-O2: 1.322(3), O1-B1: 1.502(4), O2-B1: 1.481(4), B1-O3: 1.468(4), B1-O4: 1.468(4), O1-B1-O2: 104.3(2), O1-B1-O4: 112.5(2).

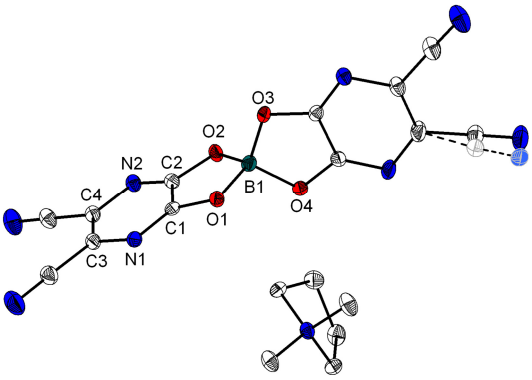

Figure 6. Molecular structure of compound **6**, hydrogen atoms omitted for clarity. Relevant bond distances/ Å and angles/ °: C1-O1: 1.326(2), C1-C2: 1.423(2), C1-N1: 1.298(2), N1-C3: 1.372(2), C3-C4: 1.380(3), C4-N2: 1.369(2), N2-C2: 1.299(2), C2-O2: 1.323(2), O1-B1: 1.488(2), O2-B1: 1.475(2), B1-O3: 1.482(2), B1-O4: 1.487(2), O1-B1-O2: 105.2(2), O1-B1-O4: 110.5(2).

5 crystallized in the monoclinic crystal system *C*2/*c* with 1.5 molecular units and one equivalent of acetonitrile per asymmetric unit. The half occupied cation is disordered over an inversion center and had to be strongly restrained to allow a stable refinement. Compound **6** crystallized in the triclinic space group *P*−1 with two molecular units per asymmetric unit. This structure equally shows a high degree of disorder in the cation as well as the anion part. The borate anions of the two structures are with 1 σ equivalent to each other. Therefore only the structure of **6**, which exhibits the higher precision, will be discussed in detail. The boron atom is coordinated in a tetrahedral fashion with B-O bond distances between 1.47 Å and 1.50 Å. These and the coordination angles around the boron atoms agree very well with the values found in oxalato and catecholato borates.[27] The structural details of the OPN moiety differ strongly from the mono deprotonated uncoordinated ligand, which shows bond lengths suiting the tautomeric form of the free ligand H_2OPN depicted in Scheme 3.[28] In the presented structures the tautomeric form dominates where the negative charge is primarily located at the oxygen atoms. The C-O bonds are elongated to 2.323(2) Å and 1.326(2) Å, while the adjacent C-N bonds measure 1.298(2) Å and 1.299(2) Å. The respective distances for the NH tautomer are d(C-O) = 1.223 Å and d(C-N) = 1.359 Å.[28] Most notably the C-C bond between the CO groups appears significantly shortened in the borates **5** and **6** (d(C-C) = 1.423(2) Å) indicative of an increased double bonding character. This bond distance is elongated to 1.513 Å in the NH tautomer of the free ligand H_2OPN.[28] In transition metal complexes of H_2OPN an intermediate distance is found.[22, 29]

Conclusion

2,2'-Bis(trimethylsilyl)-5,5'-bistetrazolate is conveniently prepared by reacting cyanogen and trimethylsilyl azide in the presence of catalytic amounts of aluminum trichloride. This substance is to the best of our knowledge the first bistetrazole derivative, which can be vaporized and recondensed without decomposition. Sublimation under vacuum yielded single crystals and allowed highly effective purification. This BT-silane derivative served as starting material for the synthesis of the first lithium bistetrazolatoborates. They contain bridging instead of B-chelating BT ligands and cannot be structurally compared to corresponding bioisosteric lithium oxalatoborates. Furthermore two salts with the new bis(pyrazine-2,3-dicarbonitrile-5,6-diolato)borate anion were synthesized and structurally characterized. This anion is an interesting candidate as an electrolyte additive for lithium ion batteries.

Experimental Section

Methods and Devices

Unless stated otherwise all synthetic steps were conducted using standard Schlenk techniques. Elemental analyses (C, N, H, S) were carried out by the service department for routine analysis and mass spectrometry with a vario MICRO cube (ELEMENTAR). The samples were weighed into tin capsules inside a nitrogen filled glove box. Melting points were determined with a Büchi Melting Point B540. ^{1}H, proton decoupled ^{13}C and ^{19}F NMR spectra were recorded at 300 K in automation with a BRUKER Avance II 300 spectrometer and were calibrated using residual proton and solvent signals (DMSO-d_6: δ_H 2.50 ppm, δ_C 39.52 ppm; CD_3CN: δ_H 1.94 ppm, δ_C 1.32 ppm, C_6D_6: δ_H 7.16 ppm, δ_C 128.06 ppm; $CDCl_3$: δ_H 7.26 ppm, δ_C 77.16 ppm)[30] or externally against $CFCl_3$. The ^{11}B NMR spectra were recorded by the service department for NMR analyses with a BRUKER Avance III HD 300 or Avance III 500 spectrometer. These spectra were calibrated externally against $BF_3{\cdot}OEt_2$. IR spectra were recorded on a BRUKER APLPHA FT-IR spectrometer with Platinum ATR-sampling (diamond single crystal). HR-ESI mass spectra were acquired with a LTQ-FT Ultra mass spectrometer (THERMO FISCHER SCIENTIFIC). The resolution was set to 100.000. The data collection for the single crystal structure determinations was performed on a BRUKER D8 QUEST or a STOE IPDS-II diffractometer. BRUKER software (APEX2, SAINT)[31] or STOE IPDS software (X-AREA)[32] was used for data collection, cell refinement and data reduction. The structures were solved with SIR97,[33] SIR2004[34] or SIR2011,[35] refined with SHELXL-2014[36] and finally validated using PLATON[37] software, all within the WinGX[38] software bundle. Absorption corrections were applied beforehand within the APEX2 software (multi-scan)[39] or applied within WinGX (multi-scan).[40] Graphic representations were created using Diamond 4.[41] H-atoms were constrained to parent site. In all graphics the ellipsoids are shown for the 50% probability level. Crystallographic data for the structures reported in this paper are supplied as supporting information and have been deposited with the Cambridge Crystallographic Data Centre (CCDC to be inserted-to be inserted).

Starting Materials

All solvents were dried according to common procedures[42] and passed through columns of aluminum oxide, 3 Å molecular sieve and R3-11G-catalyst (BASF) or stored over molecular sieve (3 or 4 Å) until use. 2,3-Dioxo-5,6-pyrazinedicarbonitrile (H_2OPN)[43] and 1-ethyl-3-methylimidazolium tetrafluoroborate[44] were synthesized according to literature procedures.

N,N-Dimethylpyrrolidinium tetrafluoroborate was synthesized in resemblance of a literature procedure from the corresponding methylcarbonate salt.[45] 5,5'-Bistetrazole (H_2BT) was prepared following the procedure invented by Friederich[46] and optimised by Nelson *et al*.[16a]

Caution! 5,5'-Bistetrazole and its derivatives are potential explosives and sensitive to heat, shock, friction and electrical spark. Although no unintended decomposition was observed during our experiments cautious handling of all substances and protective gear like safety shields, gloves, earthed equipment and earplugs are strongly recommended. Furthermore the handling and storage of larger quantities should be avoided.

Synthetic procedures

Synthesis of 2,2'-bis-(trimethylsilyl)-5,5'-bistetrazol (TMS_2BT, **2**). Cyanogen (2.26 g, 43.4 mmol, 1.00 eq) was condensed into a liquid nitrogen cooled Schlenk tube with a Teflon plug valve containing toluene (50 mL). The Schlenk tube was then slowly warmed to 0 °C and trimethylsilyl azide (13.0 g, 112 mmol, 2.58 eq) and sublimed $AlCl_3$ (0.589 g, 4.42 mmol, 9.8mol%) were added to the reaction mixture. The suspension was further warmed to ambient temperature and then refluxed for 48 hours. After cooling to ambient temperature, the solid was removed by filtration and the resulting light yellow solution was evaporated to dryness. The initial light yellow residue was sublimed in vacuum ($1 \cdot 10^{-2}$ mbar) at an oil bath temperature of 120 °C. TMS_2BT (**2**, 5.02 g, 17.8 mmol, 41%) was isolated as a colorless powder. **Mp:** 118-120 °C (2 K/min). **Elem. anal.** found C, 34.1; H, 6.4; N, 39.4; $C_8H_{18}N_8Si_2$ requires C, 34.0; H, 6.4; N, 39.7. **IR:** ν_{max}/cm^{-1}: 632 (m), 718 (m), 729 (m), 765 (s), 832 (s, br), 855 (s, sh), 1000 (w), 1045 (m), 1103 (w), 1188 (m), 1231 (m), 1259 (m), 1367 (w), 2906 (w), 2963 (w). **^{1}H NMR** (300.1 MHz, C_6D_6) $\delta_H = 0.24$ (s, 18H, Si*Me*$_3$). **^{13}C NMR** (75.5 MHz, C_6D_6): $\delta_C = -1.4$ (s, 6C, Si*Me*$_3$), 158.2 (s, 2C, *BT*) ppm. **^{1}H NMR** (300.1 MHz, $CDCl_3$) $\delta_H = 0.71$ (s, 18H, Si*Me*$_3$). **^{29}Si NMR** (59.7 MHz, $CDCl_3$) $\delta_{Si} = 28.5$ (s, 2Si, *Si*Me$_3$) ppm.

The substance could also be synthesized in resemblance to a literature procedure for the silylation of 1H-Tetrazole.[12] In this case 5,5'-bistetrazole (499 mg, 3.61 mmol, 1.00 eq) was suspended in a mixture of benzene (10 mL) and diethyl ether (5 mL). During vigorous stirring at 0 °C triethyl amine (818 mg, 8.08 mmol, 2.24 eq) and trimethylsilyl chloride (862 mg, 7.93 mmol, 2.20 eq) were added successively. During the addition the solid agglomerated and had to be triturated repeatedly. The mixture was warmed to ambient temperature and stirred for 15 hours. The solid residue was filtered off and extracted with diethyl ether (10 mL). The

combined liquid phases were evaporated to dryness and the residue was sublimed as stated before. TMS_2BT (250 mg, 0.89 mmol, 25%) was isolated as a colorless powder still containing traces of triethylammonium chloride (ca. 3% according to the ^1H NMR spectrum).

Attempts to synthesize lithium bistetrazolatoborates (**3** and **4**). In a typical experiment TMS_2BT (800 mg, 2.83 mmol, 1.98 eq) and $LiBF_4$ (134 mg, 1.43 mmol, 1.00 eq) were combined in acetonitrile (10 mL). A light gas evolution could be witnessed. The mixture was stirred at 50 °C for 5 days and then evaporated to dryness. The ^{11}B and especially the ^{19}F NMR spectra show numerous signals of which two can be associated with a $BTBF_2$ fragment. This is also observed in ESI(−) mass spectra. **^{11}B NMR** (128.3 MHz, CD_3CN) δ_B = 2.1 (t, $^1J_{BF}$ = 17.6 Hz) and further signals at −0.8 (s), 0.7 (br s), 1.4 (br s), 1.7 (s) ppm. **^{19}F NMR** (282.4 MHz, CD_3CN) δ_F = −150.4 (q, $^1J_{BF}$ = 17.6 Hz) and further signals at −142.6 (dq, *J* = 92.0, 19.5 Hz), −144.3 (dq, *J* = 88.4, 20.6 Hz), −147.2 (q, *J* = 19.4 Hz), −148.3 (br), −151.1 (q, *J* = 18.7 Hz), −156.7 (dq, *J* = 92.2, 25.6 Hz) ppm. **HRMS** (ESI−): m/z found 185.0315; $[BTBF_2$ (anion fragment)$]^-$ ($C_2B_1F_2N_8$) requires 185.0313.

Upon addition of traces of water to a freshly prepared NMR sample BF_4^- and $B(OH)_3$ could be observed. **^{11}B NMR** (160.5 MHz, CD_3CN) δ_B = −0.7 (br s, BF_4^-), 20.4 (br s, $B(OH)_3$) ppm.

Repeated reprecipitation did not lead to a significant purification. Altering the reagent ratio or the reaction time did not lead to an improved selectivity. During these experiments in two cases a few single crystals were obtained, which allowed the determination of the X-ray structures **3** and **4**.

Synthesis of 1-ethyl-3-methylimidazolium bis(pyrazine-5,6-dicarbonitrile-2,3-diolato)borate ([EMIm][OPN_2B], **5**). 1-ethyl-3-methylimidazolium tetrafluoroborate (98 mg, 0.50 mmol, 1.0 eq) and 2,3-dioxo-5,6-pyrazinedicarbonitrile (176 mg, 1.09 mmol, 2.2 eq) were dissolved in acetonitrile (6 mL). $SiCl_4$ (102 mg, 0.60 mmol, 1.2 eq) was slowly added to the mixture within 30 minutes. A slight gas evolution could be witnessed and after complete addition stirring was continued for one hour. The brown solution was then concentrated to half the original volume and stored at −20 °C whereupon a light brown solid precipitated. The solution was decanted and the residue dried in fine vacuum. [EMIm][OPN_2B] (**5**) was isolated as a light brown solid in a yield of 110 mg (0.27 mmol, 54%). **Elem. anal.** found C, 48.6; H, 2.4; N, 31.8; $C_{18}H_{11}B_1N_{10}O_4$ requires C, 48.9; H, 2.5; N, 31.7. **IR:** ν_{max}/cm^{-1}: 3153 (w), 3104 (w), 2234 (m), 1595 (m), 1579 (m), 1502 (s), 1358 (s), 1273 (vs), 1236 (m), 1168 (m), 1115 (s, br), 906 (m), 837 (m), 727 (m), 706 (m), 620 (m), 560 (m), 546 (m), 439 (vs). **^{1}H NMR**

(300.1 MHz, DMSO-d_6) δ_H = 1.41 (t, $^3J_{HH}$ = 7.3 Hz, 3H, CH_2CH_3), 3.84 (s, 3H, N*Me*), 4.19 (q, $^3J_{HH}$ = 7.3 Hz, 2H, CH_2CH_3), 7.69 (s, 1H, *H*4/5), 7.77 (s, 1H, *H*4/5), 9.10 (s, 1H, *H*2) ppm. **^{13}C-NMR** (75.5 MHz, DMSO-d_6): δ_C = 15.1 (1C, CH_2CH_3), 35.7 (1C, N*Me*), 44.1 (1C, CH_2CH_3), 114.9 (4C, *C*N), 122.0 (1C, *C4/5*), 123.2 (4C, *C*CN), 123.6 (1C, *C4/5*), 136.2 (1C, *C2*), 156.3 (4C, *C*O-B) ppm. **^{11}B NMR** (128.3 MHz, DMSO-d_6) δ_B = 12.6 (br s) ppm. **^{11}B NMR** (128.3 MHz, CD_3CN) δ_B = 12.9 (s) ppm. **HRMS** (ESI−): m/z found 331.0140; [OPN_2B (anion)]$^-$ ($C_{12}B_1N_8O_4$) requires 331.0143. **HRMS** (ESI+): m/z found 111.0917; [EMIm (cation)]$^+$ ($C_6H_{11}N_2$) requires 111.0917. Single crystals were grown by layering a solution in acetonitrile with diethyl ether.

Synthesis of N,N-dimethylpyrrolidinium bis(pyrazine-5,6-dicarbonitrile-2,3-diolato)borate ([DMPyr][OPN_2B], **6**). *N,N*-Dimethylpyrrolidinium tetrafluoroborate (400 mg, 2.14 mmol, 1.00 eq) and 2,3-dioxo-5,6-pyrazinedicarbonitrile (697 mg, 4.30 mmol, 2.01 eq) were dissolved in acetonitrile (10 mL). A solution of $SiCl_4$ in MeCN (20.09%, 458 mg, 2.70 mmol, 1.26 eq) was slowly added to the mixture within 5 minutes. The mixture was stirred at ambient temperature for 15 hours and the brown solution was separated from traces of solid residue. After removing all volatiles under vacuum a dark brown solid remained. To remove colored impurities the substances was dissolved in acetonitrile (15 mL), and decolorizing charcoal was added. After stirring for 10 minutes the suspension was filtered over Celite® and the volume of the red solution was reduced until a solid started to precipitate. After storing at −25 °C [DMPyr][OPN_2B] (**6**) was isolated with a yield of 230 mg (533 µmol, 25%). **Elem. anal.** found C, 49.3; H, 3.4; N, 28.3; $C_{18}H_{14}B_1N_9O_4$ requires C, 50.1; H, 3.3; N, 29.2. **IR:** ν_{max}/cm^{-1}: 2234 (w), 1586 (m), 1481 (s), 1351 (s), 1276 (s), 1236 (w), 1049 (vs), 918 (m, sh), 728 (s), 561 (m), 546 (w), 441 (s). **^{1}H NMR** (300.1 MHz, DMSO-d_6) δ_H = 2.05-2.14 (m, 4H, NCH_2CH_2), 3.09 (s, 6H, N*Me*), 3.42-3.49 (m, NCH_2CH_2) ppm. **^{13}C-NMR** (75.5 MHz, DMSO-d_6): δ_C = 21.3 (2C, NCH_2CH_2), 51.0 (t, $^1J_{CN}$ = 4.0 Hz, 2C, N*Me*), 64.8 (t, $^1J_{CN}$ = 3.2 Hz, 2C, NCH_2CH_2), 114.8 (4C, *C*N), 123.2 (4C, *C*CN), 156.2 (4C, *C*O-B) ppm. **^{11}B NMR** (128.3 MHz, DMSO-d_6) δ_B = 13.1 (br s) ppm. **HRMS** (ESI−): m/z found 331.0140; [OPN_2B (anion)]$^-$ ($C_{12}B_1N_8O_4$) requires 331.0143. Single crystals were grown by layering a solution in acetonitrile with diethyl ether.

Acknowledgement

We thank the "Fond der Chemischen Industrie" (doctoral fellowship for L.H.F.), "Deutsche Forschungsgemeinschaft" (GRK 1782, Functionalization of Semiconductors) and Rockwood Lithium GmbH, Frankfurt/Höchst for financial support.

Supporting Information

^{1}H NMR, ^{13}C NMR and ^{11}B NMR spectra of the isolated new substances; crystallographic data for compounds **1** to **5**.

References

[1] a) B. Scrosati, J. Hassoun, in *Electrochemically Enabled Sustainability*, CRC Press, **2014**, pp. 121-162; b) B. Scrosati, J. Garche, *J. Power Sources* **2010**, *195*, 2419-2430.

[2] a) J. Kalhoff, G. G. Eshetu, D. Bresser, S. Passerini, *ChemSusChem* **2015**, *8*, 2154-2175; b) Z. Liu, J. Chai, G. Xu, Q. Wang, G. Cui, *Coord. Chem. Rev.* **2015**, *292*, 56-73.

[3] a) U. Lischka, U. Wietelmann, M. Wegner (CHEMETAL GmbH), DE 19829030, **1999**; b) K. Xu, S. S. Zhang, T. R. Jow, W. Xu, C. A. Angell, *Electrochem. Solid-State Lett.* **2002**, *5*, A26-A29; c) K. Xu, S. S. Zhang, B. A. Poese, T. R. Jow, *Electrochem. Solid-State Lett.* **2002**, *5*, A259-A262; d) S. S. Zhang, *J. Power Sources* **2006**, *162*, 1379-1394.

[4] R. M. Herbst, in *Essays Biochem.* (Ed.: S. Graff), John Wiley and Sons, New York, **1956**, pp. 141-155.

[5] a) C. Biot, H. Bauer, R. H. Schirmer, E. Davioud-Charvet, *J. Med. Chem.* **2004**, *47*, 5972-5983; b) C. F. Matta, A. A. Arabi, D. F. Weaver, *Eur. J. Med. Chem.* **2010**, *45*, 1868-1872; c) R. J. Herr, *Bioorg. Med. Chem.* **2002**, *10*, 3379-3393; d) L. V. Myznikov, A. Hrabalek, G. I. Koldobskii, *Chem. Heterocycl. Compd.* **2007**, *43*, 1-9.

[6] P. J. Eulgem, A. Klein, N. Maggiarosa, R. W. H. Pohl, D. Naumann, *Chem. Eur. J.* **2008**, *14*, 3727-3736.

[7] L. H. Finger, F. G. Schröder, J. Sundermeyer, *Z. Anorg. Allg. Chem.* **2013**, *639*, 1140-1152.

[8] N. Fischer, T. M. Klapötke, K. Peters, M. Rusan, J. Stierstorfer, *Z. Anorg. Allg. Chem.* **2011**, *637*, 1693-1701.

[9] M. Joas, T. M. Klapötke, J. Stierstorfer, *Crystals* **2012**, *2*, 958-966.

[10] a) N. Fischer, D. Fischer, T. M. Klapötke, D. G. Piercey, J. Stierstorfer, *J. Mater. Chem.* **2012**, *22*, 20418-20422; b) D. Fischer, T. M. Klapötke, J. Stierstorfer, *Angew. Chem., Int. Ed.* **2015**, *54*, 10299-10302; c) D. Fischer, T. M. Klapötke, J. Stierstorfer, *Angew. Chem., Int. Ed.* **2014**, *53*, 8172-8175.

[11] C. M. Vogels, S. A. Westcott, *Chem. Soc. Rev.* **2011**, *40*, 1446-1458.

[12] L. Birkhofer, A. Ritter, P. Richter, *Chem. Ber.* **1963**, *96*, 2750-2757.

[13] W. G. Finnegan, R. A. Henry, R. Lofquist, *J. Am. Chem. Soc.* **1958**, *80*, 3908-3911.

[14] a) Z. P. Demko, K. B. Sharpless, *Angew. Chem.* **2002**, *114*, 2214-2217; b) Z. P. Demko, K. B. Sharpless, *Angew. Chem.* **2002**, *114*, 2217-2220.

[15] a) T. T. Curran, in *Name Reactions in Heterocyclic Chemistry II* (Ed.: J. J. Li), John Wiley & Sons, Inc., Hoboken, **2011**, pp. 278-298; b) F. Himo, Z. P. Demko, L. Noodleman, K. B. Sharpless, *J. Am. Chem. Soc.* **2002**, *124*, 12210-12216.

[16] a) J. H. Nelson, N. E. Takach, A. H. Ronald, D. W. Moore, W. M. Tolles, G. A. Gray, *Magn. Res. Chem.* **1986**, *24*, 984-994; b) N. E. Takach, E. M. Holt, N. W. A. andRonald A. Henry, J. H. Nelson, *J. Am. Chem. Soc.* **1980**, *102*, 2968-2979.

[17] P. J. Steel, *J. Chem. Crystallogr.* **1996**, *26*, 399-402.

[18] a) A. Alvanipour, N. H. Buttrus, C. Eaborn, P. B. Hitchcock, A. I. Mansour, A. K. Saxena, *J. Organomet. Chem* **1988**, *349*, 29-36; b) B. Nagaraj, R. S. Narasegowda, H. S. Yathirajan, S. L. Gaonkara, M. Bolte, *Acta Cryst. E* **2005**, *61*, o767-o768; c) G.-X. Wang, H.-Y. Ye, *Acta Cryst. E* **2007**, *63*, o4410-o4410; d) P. Wang, Z. Yue, J. Zhang, S.-Y. Feng, *Acta Cryst. E* **2011**, *67*, o368-o368.

[19] N. Weis, H. Pritzkow, W. Siebert, *Eur. J. Inorg. Chem.* **1999**, *1999*, 7-9.

[20] a) M. Broering, R. Krüger, S. Link, C. Kleeberg, Xiulian Xie, S. Köhler, B. Ventura, L. Flamigni, *Chem. Eur. J.* **2008**, *14*, 2976-2983; b) C. Schreiner, M. Amereller, H. J. Gores, *Chem. Eur. J.* **2009**, *15*, 2270-2272.

[21] K. Niedenzu, H. Deng, D. Knoeppel, J. Krause, S. G. Shore, *Inorg. Chem.* **1992**, *31*, 3162-3164.

[22] K. Adachi, Y. Sugiyama, K. Yoneda, K. Yamada, K. Nozaki, A. Fuyuhiro, S. Kawata, *Chemistry - A European Journal* **2005**, *11*, 6616-6628.

[23] F. A. Cotton, J. P. Donahue, C. A. Murillo, L. M. Pérez, R. Yu, *J. Am. Chem. Soc.* **2003**, *125*, 8900-8910.

[24] F. F. Chesneau, Z. Baan, B. Gaspar, M. Schmidt, A. Garsuch, H. Wolf, K. Leitner, C. Saffert, W. Klaus, M. Kuhl (BASF SE, Germany), WO 2015007554, **2015**.

[25] a) Y. Isono, S. Tsujioka (Central Glass Company, Limited, Japan .), US7557233, **2006**; b) S. Tsujioka, H. Takase, M. Takahashi, Y. Isono (Central Glass Co., Ltd., Japan .), EP1308449A2, **2003**.

[26] W. Xu, L.-M. Wang, R. A. Nieman, C. A. Angell, *J. Phys. Chem. B* **2003**, *107*, 11749-11756.

[27] a) W. Clegg, A. J. Scott, F. J. Lawlor, N. C. Norman, T. B. Marder, C. Dai, P. Nguyen, *Acta Crystallographica Section C* **1998**, *54*, 1875-1880; b) P. Y. Zavalij, S. Yang, M. S. Whittingham, *Acta Crystallographica Section B* **2003**, *59*, 753-759.

[28] S. Kawata, K. Adachi, Y. Sugiyama, M. K. Kabir, S. Kaizaki, *CrystEngComm* **2002**, *4*, 496-498.

[29] a) K. Adachi, Y. Sugiyama, H. Kumagai, K. Inoue, S. Kitagawa, S. Kawata, *Polyhedron* **2001**, *20*, 1411-1415; b) Y. Sugiyama, K. Adachi, S. Kawata, H. Kumagai, K. Inoue, M. Katada, S. Kitagawa, *CrystEngComm* **2000**, *2*, 174-176; c) Y. Yamamura, H. Shimoi, M. Sumita, S. Yasuzuka, K. Adachi, A. Fuyuhiro, S. Kawata, K. Saito, *J. Phys. Chem. A* **2008**, *112*, 4465-4469.

[30] G. R. Fulmer, A. J. M. Miller, H. E. Gottlieb, N. H. Sherden, A. Nudelman, B. M. Stoltz, K. I. Goldberg, J. E. Bercaw, *Organometallics* **2010**, *29*, 2176-2179.

[31] Bruker, Bruker AXS Inc., Madison, Wisconsin, USA, **2012**.

[32] Stoe, Cie, Stoe & Cie GmbH, Darmstadt, Germany, **2011**.

[33] A. Altomare, M. C. Burla, M. Camalli, G. Cascarano, C. Giacovazzo, A. Guagliardi, A. G. G. Moliterni, G. Polidori, R. Spagna, *J. Appl. Crystallogr.* **1999**, *32*, 115-119.

[34] M. C. Burla, R. Caliandro, M. Camalli, B. Carrozzini, G. L. Cascarano, L. D. Caro, C. Giacovazzo, G. Polidori, R. Spagna, *J. Appl. Crystallogr.* **2005**, *38*, 381-388.

[35] M. C. Burla, R. Caliandro, M. Camalli, B. Carrozzini, G. L. Cascarano, C. Giacovazzo, M. Mallamo, A. Mazzone, G. Polidori, R. Spagna, *J. Appl. Crystallogr.* **2012**, *45*, 357-361.

[36] G. Sheldrick, *Acta Crystallogr. C* **2015**, *71*, 3-8.

[37] A. L. Spek, *Acta Crystallogr. D* **2009**, *65*, 148-155.

[38] L. Farrugia, *J. Appl. Crystallogr.* **2012**, *45*, 849-854.

[39] Bruker, Bruker AXS Inc., Madison, Wisconsin, USA, **2012**.

[40] R. H. Blessing, *Acta Cryst. A* **1995**, *51*, 33-38.

[41] Crystal Impact - H. Putz & K. Brandenburg GbR, Kreuzherrenstr. 102, 53227 Bonn, Germany.

[42] W. L. Amarego, D. D. Perrin, *Purification of Laboratory Chemicals*, 4th ed., Elsevier, Burlington, **1996**.

[43] E. H. Mørkved, L. T. Holmaas, H. Kjøsen, G. Hvistendahl, *Acta Chem. Scand.* **1996**, *50*, 1153-1156.

[44] Y. Lingscheid, S. Arenz, R. Giernoth, *ChemPhysChem* **2012**, *13*, 261-266.

[45] B. Oelkers, J. Sundermeyer, *Green Chem.* **2011**, *13*, 608-618.

[46] W. Friederich, De 952811, **1956**.

6.8 μ-Rhodizonato-1κO,1:2κO',2κO''-tetra(triphenylphosphin)-disilber(I): Ein molekularer Komplex mit $[C_6O_6]^{2-}$ Ligandmotiv

Z. Anorg. Allg. Chem. **2015**, *641*, 2565–2569

μ-Rhodizonato-1κO,1:2κO',2κO''-tetra(triphenylphosphine)disilver(I): A Molecular Complex with the $[C_6O_6]^{2-}$ Ligand Template

Lars H. Finger, Jörg Sundermeyer

Journal of Inorganic and General Chemistry
ZAAC
Zeitschrift für anorganische und allgemeine Chemie
www.zaac.wiley-vch.de
ARTICLE

DOI: 10.1002/zaac.201500589

μ-Rhodizonato-1κO,1:2κO′,2κO′′-tetra(triphenylphosphine)disilver(I): A Molecular Complex with the $[C_6O_6]^{2-}$ Ligand Template

Lars H. Finger*[a] and Jörg Sundermeyer*[a]

Keywords: Coordination modes; Silver; Bridging ligands; Quinoid ligand

Abstract. The first silver rhodizonate and overall fourth transition metal rhodizonate complex is presented. The title compound shows a so far unobserved coordination mode of the rhodizonate ligand, which is atypically distorted from planarity. The structure discussion is accompanied by a thorough literature review of the hitherto structurally characterized rhodizonate salts and complexes.

Introduction

Recently we have presented a series of alkali ammonium and imidazolium salts of the 5,5′-bistetrazolate anion.[1] Apart from its energetic potential[2] the formally inorganic $C_2N_8^{2-}$ ligand is especially fascinating due to its versatile coordination behavior and compelling carbon/nitrogen ratio. During our investigation of similarly intriguing ligands we also considered rhodizonate ($C_6O_6^{2-}$), the largest, stable representative in the series of cyclic oxocarbonic acids ($C_nH_2O_n$, Figure 1). This group, furthermore including deltic (n = 3), squaric (n = 4), and croconic (n = 5) acid, equally displays a versatile and fascinating coordination chemistry.

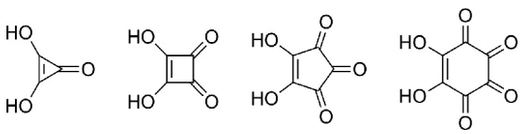

Figure 1. The series of cyclic oxocarbonic acids.

After several detailed studies consensus has been reached, that the tri- and tetracycle can indeed be regarded as aromatics, while croconate and rhodizonate do not exhibit aromaticity.[3] In every respect, squaric acid has been the center of attention within this family of compounds. Apart from its aromaticity increased stability, the squarate dianion allows for a rational design of coordination compounds due to its rigid structure. As important for its success is the fact that it can actually be prepared on a small industrial scale and is thereby sufficiently abundant and inexpensive.[4] In comparison, the synthesis of rhodizonic acid is low yielding and laborious.[5] This causes the coordination chemistry of squaric acid to have been investigated to a tremendously higher extent, although squaric acid[6] was discovered 125 years after rhodizonic acid.[7]

While CCDC currently lists more than 360 structures, in which squarate acts as a ligand, only three structures are known, where rhodizonate ligates transition metal cations.[8] Apart from this first class of actual coordination compounds, which will be considered in more detail with direct reference to the crystal structure of the title compound (vide infra), the literature known and structurally characterized rhodizonate compounds have to be divided into two further classes. The second group consist of solvate free rhodizonate salts of sodium, potassium, and rubidium.[9] They are characterized by a high number of metal oxygen contacts. For rubidium and potassium, all C–C and C–O distances are almost equal within the respective structure. In case of the sodium salt, all C–O bonds are equal, but two opposite C–C bonds are significantly shorter than the other four. While the C6 ring is planar in the rubidium salt, it is slightly twisted in case of sodium and potassium. The third class comprises rhodizonate salts with organic[10] or metal organic cations.[11] The structures are dominated by an extensive hydrogen bonding network between NH groups of the cation and the rhodizonate anion; no metal rhodizonate interactions prevail. The rhodizonate anion is typically planar with only a minimum degree of twisting. The only exception with a significant distortion is the structure of $[Pt(mimt)_4][C_6O_6]\cdot 4(H_2O)$ (mimt = 1-methyl-imidazol-2-thione).[11a] The C–C and C–O distances typically vary considerably within the respective anion. Only one structure shows equal bond lengths over the whole anion, implying an increased degree of charge delocalization.[10b] Lastly, the formal dihydrate was structurally characterized while the water-free rhodizonic acid has withstood all attempts to grow single crystals.[9c]

The gallium and indium coordination compounds, which were generated by reacting water-free rhodizonic acid with digallan and diindane precursors deserve a separate note (Fig-

* L. H. Finger
E-Mail: Lars.Finger@chemie.uni-marburg.de
* Prof. Dr. J. Sundermeyer
E-Mail: jsu@staff.uni-marburg.de
[a] Fachbereich Chemie
Philipps-Universität Marburg
Hans-Meerwein-Strasse 4
35032 Marburg, Germany
Supporting information for this article is available on the WWW under **http://dx.doi.org/10.1002/zaac.201500589** or from the author.

ure 2).[12] Although the dinuclear complexes were generated from rhodizonic acid, they cannot be viewed as complexes thereof. Rhodizonic acid inserts into the Ga–Ga and In–In bonds whereby the metal atoms are oxidized from +II to +III. Vice versa the rhodizonic acid is reduced by two electrons resulting formally in tetrahydroxyquinone. The observed coordination mode, where the metal atoms are coordinated at opposite sides of the six-membered ring, is typical for this compound.

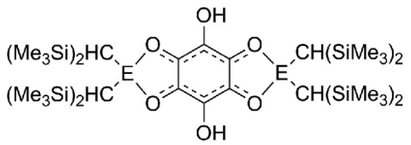

Figure 2. Gallium (E = Ga) and indium (E = In) compounds of tetrahydroxyquinone, synthesized from rhodizonic acid and the corresponding digallane and diindane, respectively.[12]

Results and Discussion

The title compound, μ-rhodizonato-1κO,1:2κO′,2κO′′-tetra(triphenylphosphine)disilver(I), was prepared from a two phasic mixture of barium rhodizonate in water and a bis(triphenylphosphine)silver(I) sulfate complex in dichloromethane (Scheme 1).

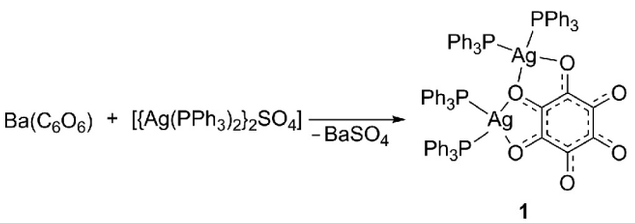

Scheme 1. Synthesis of the first silver rhodizonate complex.

The bright red product is obtained from the organic phase, while barium sulfate and excess barium rhodizonate are filtered of or remain in the aqueous phase, respectively. Single crystals were grown by layering a dichloromethane solution with diethyl ether. The product crystallized in space group $P\bar{1}$ with one complex molecule per asymmetric unit. The structure was treated as a non-merohedral two-component twin. The fractional volumes of the components were freely refined to a ratio of 0.34 to 0.66. Due to twinning and comparatively weak scattering, only a low bond precision between lighter atoms is reached. With this limitation in mind, just the general trends in bond lengths and angles are discussed. The molecular structure is presented in Figure 3. Relevant bond lengths, angles, and torsion angles are listed in Table 1, and crystallographic data and structure refinement results are summarized in Table 2.

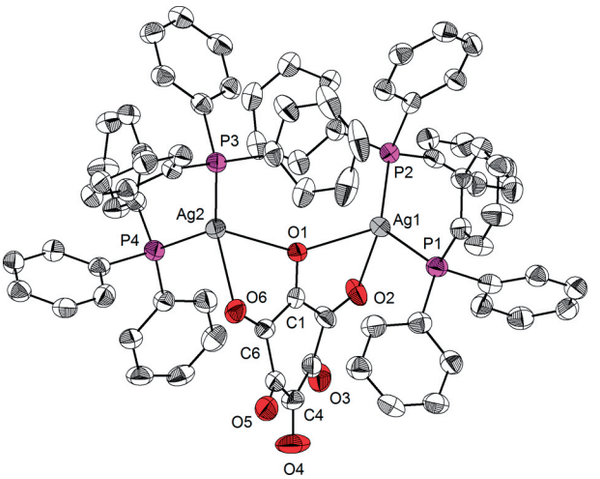

Figure 3. Molecular structure of μ-rhodizonato-1κO,1:2κO′,2κO′′-tetra(triphenylphosphine)disilver(I). Hydrogen atoms are omitted for clarity, all ellipsoids shown for the 50% probability level.

Table 1. Bond lengths /Å, bond and torsion angles /° of [{Ag(PPh$_3$)$_2$}$_2$C$_6$O$_6$] (**1**).

C1–C2	1.441(10)	O1–Ag2	2.416(5)
C2–C3	1.486(9)	O1–Ag1	2.425(5)
C3–C4	1.473(11)	O2–Ag1	2.459(5)
C4–C5	1.481(11)	O6–Ag2	2.491(5)
C5–C6	1.480(9)	P1–Ag1	2.440(2)
C6–C1	1.454(9)	P2–Ag1	2.401(2)
C1–O1	1.290(7)	O1–Ag1–O2	68.15(15)
C2–O2	1.243(8)	P2–Ag1–P1	129.17(6)
C3–O3	1.231(8)	O1–Ag2–O6	67.55(15)
C4–O4	1.242(8)	P3–Ag2–P4	129.37(6)
C5–O5	1.243(8)	C1–C2–C3–C4	–35.9(9)
C6–O6	1.247(8)		

The rhodizonate ligand coordinates each silver cation with two oxygen atoms in a chelating fashion. In the row of oxygen atoms (O6, O1, O2), which are coordinated to Ag1 and Ag2, the central O1 binds to both silver atoms. This constitutes a so far unknown coordination behavior of the rhodizonate anion. Ag–O distances of O1 differ slightly [Ag1–O1: 2.425(5) Å, Ag2–O1: 2.416(5) Å]; they are equal within 2 σ. The distances Ag1–O2 and Ag2–O6 are distinctively longer [2.459(5) Å and 2.491(5) Å, respectively]. Each silver atom is furthermore coordinated by two triphenylphosphine ligands, leading overall to a distorted tetrahedral coordination arrangement around the silver atoms. The Ag–P distances are distinctively longer for those PPh$_3$ ligands, which are oriented towards the rhodizonate moiety [e.g. Ag1–P1: 2.440(2) Å vs. Ag1–P2: 2.401(2) Å]. The phenomenon can be traced back to increased steric hindrance between the phenyl rings and the rhodizonate ligand.

The C–C distances within the six-membered ring deviate slightly, being shorter between the coordinating oxygen atoms [e.g. C1–C2: 1.441(10) Å vs. C4–C5: 1.481(11) Å], which is in agreement with an increased π delocalization between these atoms, according to Figure 1. This observation is substantiated by the variation in C–O distances. The longest bond lengths are found for C1–O1 [1.290(7) Å] and C6–O6 [1.247(8) Å],

Table 2. Crystal data for $[\{Ag(PPh_3)_2\}_2C_6O_6]$ (**1**).

	$[\{Ag(PPh_3)_2\}_2C_6O_6]$ (**1**)
Formula	$C_{78}H_{60}Ag_2O_6P_4$
Fw /g·mol^{-1}	1432.88
Crystal system	triclinic
Space group	$P\bar{1}$
Color, habit	red plate
Crystal size /mm^3	$0.23 \times 0.11 \times 0.06$
a /Å	12.2219(7)
b /Å	13.1375(11)
c /Å	22.9002(17)
α /°	85.444(6)
β /°	79.380(5)
γ /°	63.821(5)
V /Å^3	3243.3(4)
Z	2
D_{calc} /g·cm^{-3}	1.467
Abs. corr.	none
μ /cm^{-1}	7.58
$F(000)$	1460
T /K	100(2)
θ range /°	1.73 : 27.17
Range h,k,l	–15:15; –16:16; –29:29
Refl. coll.	20644
Refl. indep.	20644
Refl. $I > 2\sigma(I)$	11262
Data / restr. / param.	20644 / 0 / 812
R_1 (obs)	0.0542
wR_2 (all)	0.1285
GooF (F^2)	0.788
Res. dens. (min./ max.) /e·Å^{-3}	–1.728/ 1.178

the shortest C–O distances are found on the opposite ring side [e.g.: C3–O3: 1.231(8) Å]. The rhodizonate moiety in itself is distinctively distorted leading to a twist-boat conformation of the ring when viewing along the C1–C4 axis. The largest torsion is found along C1–C2–C3–C4 [–35.9(9)°].

The ^{13}C NMR spectrum shows only one resonance signal for the C_6O_6 moiety at δ = 176.9 ppm. The literature known zinc complex shows a single ^{13}C NMR resonance signal as well. Its chemical shift is in very good agreement with the value reported herein.[8b] The signal is sharp and shows no signs of line broadening due to dynamics at ambient temperature indicating a perfect charge delocalization within the rhodizonate ligand in solutions of the title compound. This is in agreement with the intermediate bond lengths observed in the single crystal structure. A complete dissociation of the complex into the rhodizonate dianion and silver phosphine cations is considered unlikely. Instead, rather a migration of the silver phosphine fragments around the C_6O_6 fragment – rapid on the NMR time scale - is assumed. It was attempted to resolve this phenomenon by investigating the ^{13}C and ^{31}P NMR spectra at decreased temperatures. While the ^{13}C NMR spectrum (125.8 MHz) upon cooling to –60 °C showed no alteration in the chemical shift region of the rhodizonate anion, in the ^{31}P NMR spectrum a splitting of the broad signal into two doublets could be observed. This can be attributed to the ^1J coupling of the phosphorus nucleus to the spin ½ nuclei of ^{107}Ag ($^1J_{107Ag–P}$ = 436.5 Hz) and ^{109}Ag ($^1J_{109Ag–P}$ = 499.9 Hz). This phenomenon is well known for silver phosphine complexes.[13] Additionally we recorded a ^{109}Ag NMR spectrum yielding a chemical shift of 1296.3 ppm, which also lies in the range of comparable literature known compounds.[14] Cooling the solution to –60 °C apparently allows the fixation of the Ag–P bonds on the ^{31}P NMR timescale resulting in the observed splitting. However, in solution the charge and silver ion delocalization at the rhodizonate moiety is not affected or resolved by this temperature reduction.

Until now only three other examples of rhodizonate transition metal complexes have been published. In 2004 *Wang* et al. presented the first rhodizonate complexes with manganese and cadmium central atoms.[8a] The rhodizonate anion acts as bridging ligand in a $1\kappa^2O,O',2\kappa^2O'',O'''$ fashion leading to a 2D metal organic framework (under inclusion of bipyrimidine as additional bridging ligand). In both cases, the metal oxygen distances adopt intermediate values for O and O′; O′′ exhibits the shortest metal oxygen bond, while the metal-O′′′ contact is significantly elongated (Figure 4).

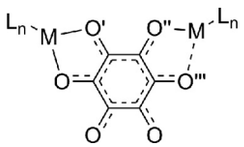

Figure 4. Coordination mode of literature known rhodizonato complexes [*M* = Mn, Cd, L = bipyrimidine, water;[8a] *M* = Zn, L = tris(2-pyridylmethyl)amine].[8b]

In case of the manganese structure, this is in coherence with the observed C–C and C–O distances. O′ and O′′ show the longest C–O distances, O and O′′′ exhibit shorter bond lengths and the oxygen atoms not participating in the coordination display the shortest C–O bonds. The C–C bonds substantiate the picture of a partial charge localization on O′ and O′′. In the cadmium salt a charge delocalization over all four coordinating C–O moieties appears. In both structures the C_6O_6 moiety is slightly distorted towards a twist-boat shape. The third example of an rhodizonate complex was published in 2009 by *Asato* et al.[8b] The dinuclear zinc complex contains tris(2-pyridylmethyl)amine as additional ligand preventing the metal atoms from forming extended coordination networks. The coordination mode is very similar to the manganese and cadmium complexes. The distance of O′′′ to the zinc atom is elongated to such an extent, that no actual bonding interaction can be assumed, though. The C–C and C–O distances agree well with the manganese structure and a partial charge localization on O′ and O′′. The distortion of the rhodizonate ring is less pronounced than in the previously reported complexes. Overall, a delocalized structure has to be anticipated for the rhodizonate moiety in these coordination compounds. Although distinctive differences in C–O and C–C bond lengths are evident, they still show intermediate values between the respective single and double bonds in each case.

Comparing the presented silver complex with the literature known coordination compounds, the differing coordination mode and the strong distortion of the rhodizonate stand out. None of the known complexes comprises a bridging oxygen atom. The increased distortion with a torsion angle C1–C2–C3–C4 of –35.9(9)° may be a result of this constrained ar-

rangement and the consequent steric clash of the bulky PPh_3 ligands. The highest torsion angles so far prevail in the structure of the cadmium complex[8a] (15.0°) and interestingly in the structure of $[Pt(mimt)_4][C_6O_6]\cdot 4(H_2O)$[11a] (14.1°), where the rhodizonate anion interacts only in form of hydrogen bonds with the imidazolethione ligands of Pt. However, this has no apparent effect upon the bond lengths in the rhodizonate anion, which are in a well comparable range with the values of the literature known complexes.

A very similar oxygen silver complex fragment is found in a silver croconate coordination polymer.[15] In this compound the oxygen silver distances are overall longer than in the present rhodizonate complex, which can be attributed to the fact, that in the croconate complex the anion interacts with overall four Ag atoms. In turn this will lead to an increased charge delocalization within the anion and vice versa to a decreased bonding interaction of the individual contacts.

Conclusions

The first silver rhodizonate complex and its molecular structure were presented. The compound shows a so far unknown coordination mode of the rhodizonate moiety, in which it acts as a bridging ligand with three coordinating oxygen atoms. The central oxygen atom binds to both silver cations. Additionally the usually planar rhodizonate moiety shows an unprecedented strong distortion. NMR spectra indicate, that in solution Ag–P and Ag–O bonds are dissociating on the NMR time scale. Currently we are investigating the coordination behavior of rhodizonate towards divalent metal cations to investigate the coordination modes adopted in mononuclear complexes.

Experimental Section

Devices and Methods: Elemental analyses (C, N, H, S) were carried out by the service department for routine analysis and mass spectrometry with a vario MICRO cube (Elementar). Melting points were determined with a Büchi Melting Point B540. ^{1}H and ^{13}C NMR spectra were recorded in automation with a Bruker Avance II 300 spectrometer. ^{31}P NMR spectra were recorded with a Bruker Avance III HD 300 or HD 500 spectrometer and ^{109}Ag NMR spectra with a Bruker Avance III HD 500 spectrometer. Unless stated otherwise, all spectra were recorded at ambient temperature. ^{1}H and ^{13}C NMR spectra were calibrated using residual protons and solvent signals, respectively (CD_2Cl_2: δ_H 5.32 ppm, δ_C 53.84 ppm).[16] ^{31}P NMR spectra were referenced externally with 85 % H_3PO_4, ^{109}Ag NMR Spectra where referenced against 4 m $AgNO_3$ in D_2O. IR spectra were recorded with a Bruker APLPHA FT-IR spectrometer with Platinum ATR sampling. The data collection for the single crystal structure determination was performed in rotation method with a STOE IPDS-II diffractometer by the X-ray service department of the Fachbereich Chemie, University of Marburg. The device is equipped with a Mo-K_α X-ray source (λ = 0.71073 Å), graphite monochromator and active imaging plate. STOE IPDS software (X-AREA) was used for data collection, cell refinement and data reduction, respectively.[17] The structure was solved with SIR-97,[18] refined with SHELXL-2014[19] and finally validated using PLATON[20] software, all within the WinGX[21] software bundle. Instead of a HKLF5 absorption correction, which yielded only minor improvement compared to the uncorrected data, the advanced integration options of X-Area (merging of Friedel pairs and equivalent reflections) were chosen. Graphic representations were created using Diamond-4.[22] Hydrogen atoms were constrained to parent site; the ellipsoids are shown for the 50 % probability level.

Crystallographic data (excluding structure factors) for the structure in this paper have been deposited with the Cambridge Crystallographic Data Centre, CCDC, 12 Union Road, Cambridge CB21EZ, UK. Copies of the data can be obtained free of charge on quoting the depository number CCDC-1410933 (Fax: +44-1223-336-033; E-Mail: deposit@ccdc.cam.ac.uk, http://www.ccdc.cam.ac.uk)

Synthesis of $[\{Ag(PPh_3)_2\}_2C_6O_6]$ (1): The title compound was synthesized by reacting a silver sulfate triphenylphosphine adduct with barium rhodizonate: $[\{Ag(PPh_3)_2\}_2SO_4]$ (799 mg, 587 µmol, 1.00 equiv.) was dissolved in dichloromethane (20 mL). Water (18 mL) was added to the solution and barium rhodizonate (197 mg, 645 µmol, 1.10 equiv.) and tetrabutylammonium bromide (16 mg, 50 µmol, 5 mol-%) were added as solids. The mixture turned red immediately, the dark barium rhodizonate gradually dissolved, while a colorless precipitate formed. The mixture was stirred for 16 h and filtered to remove barium sulfate and unreacted barium rhodizonate. The two phases were separated and the organic phase extracted with water (three times 15 mL). The bright red organic phase was evaporated to dryness and the title compound was isolated in 623 mg (435 µmol, 74 %) yield as a fine red powder. Single crystals suitable for X-ray structure determination were grown by layering a solution of the compound in dichloromethane with the equivalent volume of diethyl ether. Mp: 213.2–215.5 °C (5 K·min^{-1}, decomp., DCM/ Et_2O). $C_{78}H_{60}Ag_1O_6P_4$: calcd. C 65.38; H 4.22 %; found (average of four measurements) C 65.32; H 4.55 %. **IR**: $\tilde{\nu}_{max}$ = 3055 (w), 1603 (w) 1468 (br., s), 1431 (s), 1155 (m), 1092 (m), 1025 (m), 996 (m), 742 (s), 691 (vs), 512 (sh, m), 502 (sh, s), 490 (s) cm^{-1}. **^{1}H NMR** (300.1 MHz, CD_2Cl_2): δ = 7.21–7.30 (m, 24 H, *o-Ph*), 7.30–7.43 (m, 36 H, *m,p-Ph*) ppm. **^{13}C NMR** (75.5 MHz, CD_2Cl_2): δ = 129.3 (d, $^3J_{CP}$ = 9.6 Hz, 24C, *m-Ph*), 130.7 (s, 12C, *p-Ph*), 132.7 (d, $^2J_{CP}$ = 27.1 Hz, 24C, *o-Ph*), 134.3 (d, $^1J_{CP}$ = 16.8 Hz, 12C, *ipso-Ph*), 176.9 (s, 6C, C_6O_6) ppm. **^{31}P NMR** (121.5 MHz, CD_2Cl_2): δ = 9.9 (s) ppm. **^{31}P NMR** (202.5 MHz, CD_2Cl_2, 213 K): δ = 10.3 (2·d, $^1J_{107Ag-P}$ = 436.5, $^1J_{109Ag-P}$ = 499.9 Hz) ppm **^{109}Ag NMR** (23.3 MHz, CD_2Cl_2): δ = 1296 ppm.

Synthesis of $[\{Ag(PPh_3)_2\}_2SO_4]$: The precursor was prepared similarly to a published procedure.[13a] Silver sulfate (498 mg, 1.60 mmol, 1.00 equiv.) was suspended in a solution of triphenyl phosphine (1.69 g, 6.43 mmol, 4.03 equiv.) in ethanol (30 mL). The mixture was heated to 80 °C for 2.5 h in the dark. The clear solution was filtered hot and cooled to –24 °C. The compound precipitated as a colorless solid, which was collected by filtration and dried in vacuo. The substance contains two equivalents of ethanol per molecular unit. Yield: 2.10 g, (1.45 mmol, 90 %) The compound could be freed from ethanol by recrystallization from a dichloromethane solution layered with pentane. Analytical data of the ethanol adduct: Mp: 243.8–245.8 °C (10 K·min^{-1}, decomp., EtOH). **IR**: $\tilde{\nu}_{max}$ = 3302 (br., w), 3050 (w), 1478 (w), 1433 (m), 1309 (w), 1046 (m), 741 (m), 692 (vs), 599 (m), 496 (s), 421 (w) cm^{-1}. **^{1}H NMR** (300.1 MHz, CD_2Cl_2): δ = 1.15 (t, $^3J_{HH}$ = 7.0 Hz, 6 H, C*H*$_3$), 2.15 (br. s, 2 H, O*H*), 3.62 (q, $^3J_{HH}$ = 7.0 Hz, 4 H, C*H*$_2$), 7.19–7.29 (m, 24 H), 7.30–7.47 (m, 36 H) ppm. **^{13}C NMR** (75.5 MHz, CD_2Cl_2): δ = 18.7 (s, C*H*$_3$), 58.5 (s, C*H*$_2$), 129.2 (d, $^3J_{CP}$ = 9.5 Hz, 24C, *m*-Ph), 130.4 (s, 12C, *p*-Ph), 133.2 (d, $^2J_{CP}$ = 23.8 Hz, 24C, *o*-Ph), 134.5 (d, $^1J_{CP}$ = 16.8 Hz, 12C, *ipso*-Ph) ppm. **^{31}P NMR** (121.5 MHz, CD_2Cl_2): δ = 8.0 (s) ppm. Analytical data after recrystallization: **IR**: $\tilde{\nu}_{max}$ = 3050 (w), 1477 (w), 1432 (m), 1308 (w), 1093 (m), 742 (m), 692 (vs), 616 (m), 594(m), 513 (m, sh), 493 (s), 437 (w) cm^{-1}. **^{1}H NMR** (300.1 MHz, CD_2Cl_2): δ = 7.21–7.30 (m, 24

H), 7.31–7.39 (m, 12 H), 7.40–7.50 (m, 24 H) ppm. **^{13}C NMR** (75.5 MHz, CD_2Cl_2): δ = 129.2 (d, $^3J_{CP}$ = 9.6 Hz, 24C, *m*-Ph), 130.5 (s, 12C, *p*-Ph), 133.2 (d, $^2J_{CP}$ = 24.5 Hz, 24C, *o*-Ph), 134.5 (d, $^1J_{CP}$ = 16.9 Hz, 12C, *ipso*-Ph) ppm. **^{31}P NMR** (121.5 MHz, CD_2Cl_2): δ = 7.5 (s) ppm.

Synthesis of Barium Rhodizonate: The rhodizonate salt was synthesized by combining rhodizonic acid dihydrate (230 mg, 1.12 mmol, 1.01 equiv.) and barium hydroxide octahydrate (350 mg, 1.11 mmol, 1.00 equiv.) in water (25 mL). A dark violet suspension was formed immediately, which was agitated by ultra-sonication for 30 min and stirred at ambient temperature for 1 h. The dark violet precipitate was collected by centrifugation, the supernatant solution was decanted. The residue was washed with water (15 mL) and dried in fine vacuum at 80 °C. Barium rhodizonate was isolated as a dark powder in 326 mg (1.07 mmol, 96 %) yield. Mp: >380 °C. **IR** $\tilde{\nu}_{max}$ = 1458 (br., vs), 1064 (w), 997 (w), 811 (w), 719 (w), 637 (w) cm^{-1}. Under atmospheric condition the substances quickly absorbed two equivalents of water. $C_6H_4Ba_1O_8$: calcd. C 21.11; H 1.18 %; found C 21.14; H 1.02 %.

Supporting Information (see footnote on the first page of this article): ^{1}H, ^{13}C, ^{31}P and ^{109}Ag NMR spectra, and the IR spectrum of the title compound.

Acknowledgements

The authors are indebted to the X-ray department of Philipps-Universität Marburg, *Dr. Klaus Harms*, *Michael Marsch* and *Radostan Riedel* for the collection of crystal data. We thank *Dr. Klaus Harms* for the detailed assessment of the crystal structure and valuable discussion, and *Dr. Xiulan Xie* for the in depth discussion of NMR spectra. Financial support by Fond der Chemischen Industrie (doctoral fellowship for *LHF*) and Deutsche Forschungsgemeinschaft (GRK 1782, "Functionalization of semiconductors") is gratefully acknowledged.

References

[1] L. H. Finger, F. G. Schröder, J. Sundermeyer, *Z. Anorg. Allg. Chem.* **2013**, *639*, 1140–1152.
[2] a) N. Fischer, T. M. Klapötke, K. Peters, M. Rusan, J. Stierstorfer, *Z. Anorg. Allg. Chem.* **2011**, *637*, 1693–1701; b) N. Fischer, D. Izsák, T. M. Klapötke, S. Rappenglück, J. Stierstorfer, *Chem. Eur. J.* **2012**, *18*, 4051–4062; c) Y. Guo, G.-H. Tao, Z. Zeng, H. Gao, J. M. Shreeve, D. A. Parrish, *Chem. Eur. J.* **2010**, *16*, 3753–3762; d) R. Wang, Y. Guo, R. Sa, J. M. Shreeve, *Chem. Eur. J.* **2010**, *16*, 8522–8529.
[3] a) J. Aihara, *J. Am. Chem. Soc.* **1981**, *103*, 1633–1635; b) P. v. R. Schleyer, K. Najafian, B. Kiran, H. Jiao, *J. Org. Chem.* **2000**, *65*, 426–431; c) D. Quiñonero, C. Garau, A. Frontera, P. Ballester, A. Costa, P. M. Deyà, *Chem. Eur. J.* **2002**, *8*, 433–438.
[4] G. Seitz, P. Imming, *Chem. Rev.* **1992**, *92*, 1227–1260.
[5] This adequately reproduces in the per gram prices of these substances. The roughly show a ratio of 1:13:25 in the series C~4~:C~6~:C~5~, whereas squaric acid starts at three to four Euros per gram; abcr GmbH: http://www.abcr.de/ (accessed 4 July 2015).
[6] J. D. Park, S. Cohen, J. R. Lacher, *J. Am. Chem. Soc.* **1962**, *84*, 2919–2922.
[7] J. F. Heller, *Annalen der Pharmacie* **1837**, *24*, 1–17.
[8] a) C.-C. Wang, C.-T. Kuo, P.-T. Chou, G.-H. Lee, *Angew. Chem. Int. Ed.* **2004**, *43*, 4507–4510; b) E. Asato, S. Miyazato, H. Tohma, S. Takara, M. Tadokoro, Y. Miyazato, D. Yoshioka, M. Mikuriya, *Chem. Lett.* **2009**, *38*, 1170–1171.
[9] a) R. E. Dinnebier, H. Nuss, M. Jansen, *Acta Crystallogr., Sect. E* **2005**, *61*, m2148-m2150; b) J. A. Cowan, J. A. K. Howard, *Acta Crystallogr., Sect. E* **2004**, *60*, m511-m513; c) D. Braga, G. Cojazzi, L. Maini, F. Grepioni, *New J. Chem.* **2001**, *25*, 1221–1223.
[10] a) B. F. Abrahams, M. G. Haywood, R. Robson, *CrystEngComm* **2005**, *7*, 629–632; b) C.-K. Lam, T. C. W. Mak, *Angew. Chem. Int. Ed.* **2001**, *40*, 3453–3455; c) C.-K. Lam, T. C. W. Mak, *Chem. Commun.* **2001**, 1568–1569.
[11] a) M. G. Fisher, P. A. Gale, M. E. Light, R. Quesada, *CrystEngComm* **2008**, *10*, 1180–1190; b) P. A. Gale, M. E. Light, R. Quesada, *CrystEngComm* **2006**, *8*, 178–188.
[12] W. Uhl, M. Prött, *Z. Anorg. Allg. Chem.* **2002**, *628*, 2259–2263.
[13] a) G. A. Bowmaker, J. V. Hanna, C. E. F. Rickard, A. S. Lipton, *J. Chem. Soc., Dalton Trans.* **2001**, 20–28; b) D. E. Bergbreiter, Y.-C. Yang, *J. Org. Chem.* **2010**, *75*, 873–878.
[14] a) S. J. Berners-Price, P. J. Sadler, C. Brevard, *Magn. Reson. Chem.* **1990**, *28*, 145–148; b) S. J. B. Price, C. Brevard, A. Pagelot, P. J. Sadler, *Inorg. Chem.* **1985**, *24*, 4278–4281.
[15] S. Feng, H. Yang, X. Jiang, Y. Wang, M. Zhu, *J. Mol. Struct.* **2015**, *1081*, 1–5.
[16] G. R. Fulmer, A. J. M. Miller, H. E. Gottlieb, N. H. Sherden, A. Nudelman, B. M. Stoltz, K. I. Goldberg, J. E. Bercaw, *Organometallics* **2010**, *29*, 2176–2179.
[17] *X-AREA*, Stoe & Cie GmbH, Darmstadt, Germany, **2011**.
[18] A. Altomare, M. C. Burla, M. Camalli, G. Cascarano, C. Giacovazzo, A. Guagliardi, A. G. G. Moliterni, G. Polidori, R. Spagna, *J. Appl. Crystallogr.* **1999**, *32*, 115–119.
[19] G. Sheldrick, *Acta Crystallogr., Sect. A* **2008**, *64*, 112–122.
[20] A. L. Spek, *Acta Crystallogr., Sect. D* **2009**, *65*, 148–155.
[21] L. Farrugia, *J. Appl. Crystallogr.* **2012**, *45*, 849–854.
[22] K. Brandenburg, H. Putz, *Diamond*, Crystal Impact GbR, Bonn, Germany, **2012**.

Received: July 13, 2015
Published Online: September 23, 2015

7 Kristallographischer Teil

7.1 Allgemeine Informationen

Im Rahmen der Promotion wurden neben den eigenen Kristallstrukturen auch die mehrerer Arbeitskreismitglieder gelöst und verfeinert. Im folgenden Teil werden diese Strukturen mit einer Strukturabbildung den wichtigsten kristallographischen Kenngrößen und den fraktionellen Atomkoordinaten der nicht-H-Atome zusammengefasst.

7.1.1 Datensammlung

Die Probenpräparation und die Datensammlung wurden von den Mitarbeitern der Serviceabteilung für Kristallstrukturanalyse des Fachbereichs Chemie der Philipps-Universität Marburg (Dr. Klaus Harms, Michael Marsch und Radostan Riedel) durchgeführt. Dazu wurden Diffraktometer des Typs Stoe IPDS II, Stoe IPDS 2T und Bruker D8 Quest verwendet. Zellbestimmung, Datenintegration und Datenreduktion erfolgten mit dem Programm des jeweiligen Herstellers (X-Area und X-Red[95] bzw. APEX2 und SAINT[96]).

7.1.2 Strukturlösung und Verfeinerung

Die Lösung der Strukturen erfolgte mit den Programmen SIR-92,[97] SIR-97,[98] SIR-2004,[99] SIR-2008,[100] SIR-2011,[101] SHELXS,[102] SHELXT[103] oder SUPERFLIP[104] und die Verfeinerung mit SHELXL.[103] Dazu wurde innerhalb des Programmbündels WinGX[105] gearbeitet, während Ortep-3[106] und Mercury[107] zur unterstützenden Visualisierung genutzt wurden. Gelegentlich wurde auf die Software shelXle[108] zurückgegriffen. Zur abschließenden Validierung der Strukturlösung wurde PLATON[109] verwendet.

7.1.3 Strukturabbildung und Aufbau der Datenblätter

Die Strukturabbildungen in den Datenblättern wurden mit Diamond 4[110] erstellt und zeigen die formale Molekülstruktur der jeweiligen Verbindung im ORTEP-Stil. Die Ellipsoide spiegeln eine Aufenthaltswahrscheinlichkeit von 50% wieder. Wasserstoffatome sind nur an Heteroatomen abgebildet, nicht koordinierte Lösungsmittelmoleküle sind der Übersichtlichkeit wegen nicht abgebildet. Falls mehrere identische nicht koordinierte Gegenionen vorliegen ist nur eines davon exemplarisch abgebildet. Die farbliche Kennzeichnung der Elemente erfolgte nach dem unten abgebildeten Schema in Anlehnung an die Farbzuordnung von Dr. Benjamin Oelkers.[111]

H							**He**
Li	**Be**	**B**	**C**	**N**	**O**	**F**	**Ne**
Na	**Mg**	**Al**	**Si**	**P**	**S**	**Cl**	**Ar**
K	**Ca**	**Ga**	**Ge**	**As**	**Se**	**Br**	**Kr**
Rb	**Sr**	**In**	**Sn**	**Sb**	**Te**	**I**	**Xe**
Cs	**Ba**	**Tl**	**Pb**	**Bi**	**Po**	**At**	**Rn**

Sc	**Ti**	**V**	**Cr**	**Mn**	**Co**	**Fe**	**Ni**	**Cu**	**Zn**
Y	**Zr**	**Nb**	**Mo**	**Tc**	**Rh**	**Ru**	**Pd**	**Ag**	**Cd**
La	**Hf**	**Ta**	**W**	**Re**	**Ir**	**Os**	**Pt**	**Au**	**Hg**

Ce	**Pr**	**Nd**	**Pm**	**Sm**	**Eu**	**Gd**	**Tb**	**Dy**	**Ho**	**Er**	**Tm**	**Yb**	**Lu**

Nach dem Strukturbild findet sich eine tabellarische Auflistung wesentlicher kristallographischer Kenngrößen gemäß dem folgenden Schema:

Kristalldaten

Summenformel	*M*, molare Masse	Kristallsystem, Raumgruppe
	Kantenlängen der Elementarzelle: *a, b, c*	
	Winkel der Elementarzelle: α, β, γ	
V, Zellvolumen	*Z*, Anzahl der Formeleinheiten pro Elementarzelle	*F*(000), (effektive) Zahl der Elektronen pro Elementarzelle
D_{calc}, berechnete Dichte	μ, Absorptionskoeffizient	
Kristallfarbe und -form	Kristallgröße	

Datensammlung

Diffraktometer	*T*, Messtemperatur	λ; Wellenlänge der Strahlung
	Minimale und maximale Millerindizes (h, k, l) der gemessenen Reflexe	
Zahl gemessener Reflexe	Zahl unabhängiger Reflexe	Zahl der Reflexe mit signifikanter Intensität (grösser als die zweifache Standardabweichung, $I > 2\sigma(I)$)
θ, Winkelbereich der gemessenen Reflexe	R_{int}, Zuverlässigkeitsfaktor bzgl. Der Mittelung symmetrieabhängiger Reflexe	*C* (25.00°), Vollständigkeit der Reflexe bis θ = 25°
Art der Absorptionskorrektur	Minimale Transmission gemäß Absorptionskorrektur	Maximale Transmission gemäß Absorptionskorrektur

Verfeinerung

Zahl der für die Verfeinerung verwendeten Reflexe	Zahl der verwendeten Restraints	Zahl der verfeinerten Parameter
SHELXL Programmversion	Finales Maximalverhältnis der Änderung im letzten Verfeinerungszyklus zur Standardabweichung	
R_1 ($I > 2\sigma(I)$), konventioneller Zuverlässigkeitsfaktor für Reflexe mit signifikanter Intensität	wR_2 ($I > 2\sigma(I)$), gewichteter Zuverlässigkeitsfaktor für Reflexe mit signifikanter Intensität	
R_1 (all), konventioneller Zuverlässigkeitsfaktor für alle Reflexe	wR_2 (all), gewichteter Zuverlässigkeitsfaktor für alle Reflexe	GoF (S), Gütefaktor S für alle Reflexe
$\Delta\varphi_{min}$, finale, minimale Differenzelektronendichte	$\Delta\varphi_{max}$, finale, maximale Differenzelektronendichte	

In einem optionalen Kommentar werden Besonderheiten der Struktur oder der Verfeinerung vermerkt, bevor die fraktionellen Atomkoordinaten und isotropen Auslenkungsfaktoren der nicht-Wasserstoffatome aufgelistet werden.

7.2 Eigene Strukturen

7.2.1 Dirubidium-bistetrazolat-dihydrat (fin025)

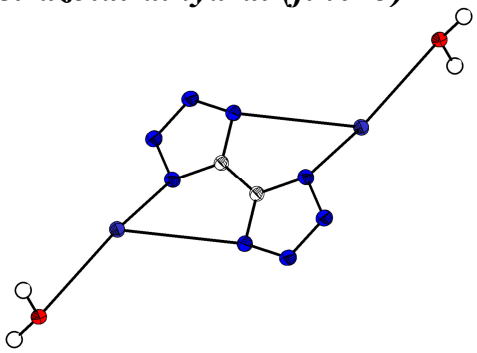

Kristalldaten

C2 H4 N8 O2 Rb2	M = 343.04 g/mol	Monoclinic, $P2_1/c$
a = 4.0884(2) Å	b = 11.3281(7) Å	c = 9.9483(6) Å
α = 90°	β = 93.510(5)°	γ = 90°
V = 459.88(5) Å^3	Z = 2	F(000) = 324
D_{calc} = 2.478 g/cm^3	μ = 10.632 mm^{-1}	
colourless block	0.33 · 0.13 · 0.09 mm^3	

Datensammlung

Diffraktometer: STOE IPDS 2	T = 100(2) K	λ = 0.71069 Å
h = -5 bis 5	k = -14 bis 14	l = -12 bis 12
5725 gemessene Reflexe	973 unabhängige Reflexe	888 Reflexe mit $I > 2\sigma(I)$
θ = 2.73 bis 26.72°	R_{int} = 0.0575	C (25.00°) = 1.000
Absorptionskorrektur: Multi-scan	T_{min} = 0.1087	T_{max} = 0.284

Verfeinerung

973 Reflexe	0 Restraints	72 Parameter
Verfeinerung mit SHELXL-97	bis χ = 0.001	
R_1 ($I > 2\sigma(I)$) = 0.0210	wR_2 ($I > 2\sigma(I)$) = 0.0482	
R_1 (all) = 0.0242	wR_2 (all) = 0.0492	GoF (S) = 1.047
$\Delta\varphi_{min}$ = -1.041 e·Å^{-3}	$\Delta\varphi_{max}$ = 0.450 e·Å^{-3}	

Kommentar

Die Struktur wurde bereits veröffentlicht: L. H. Finger, F. G. Schröder, J. Sundermeyer, *Z. Anorg. Allg. Chem.* **2013**, *639*, 1140-1152.

Fraktionelle Atomkoordinaten (*x, y, z*) und äquivalente isotrope Auslenkungsfaktoren *U*(eq)

	x	*y*	*z*	*U*(eq)/Å^2
Rb(1)	0.2394(1)	0.4002(1)	0.1729(1)	0.0155(1)
N(3)	-0.3578(5)	0.2108(2)	-0.0425(2)	0.0182(4)
N(1)	-0.1071(5)	0.1146(2)	0.1221(2)	0.0171(4)
C(1)	-0.0849(5)	0.0561(2)	0.0059(2)	0.0138(4)
N(2)	-0.2833(5)	0.2117(2)	0.0882(2)	0.0180(4)
O(1)	0.7228(5)	0.5862(2)	0.1285(2)	0.0186(4)
N(4)	-0.2360(5)	0.1132(2)	-0.0982(2)	0.0177(4)

7.2.2 *Diammonium-bistetrazolat (fin062)*

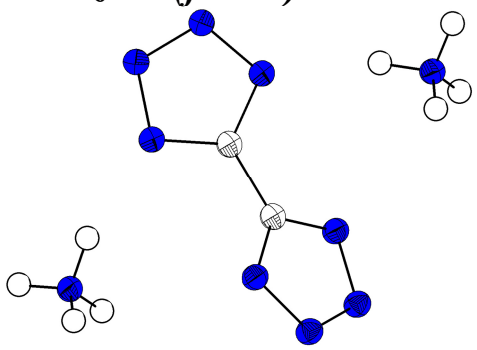

Kristalldaten

C2 H8 N10	M = 172.18 g/mol	Orthorhombic, *Pban*
a = 9.1301(10) Å	b = 10.7631(13) Å	c = 3.6660(6) Å
α = 90°	β = 90°	γ = 90°
V = 360.25(8) Å^3	Z = 2	F(000) = 180
D_{calc} = 1.587 g/cm^3	μ = 0.124 mm^{-1}	
colourless block	0.18 · 0.16 · 0.14 mm^3	

Datensammlung

Diffraktometer: STOE IPDS 2	T = 100(2) K	λ = 0.71069 Å
h = -10 bis 11	k = -13 bis 13	l = -4 bis 4
2935 gemessene Reflexe	392 unabhängige Reflexe	319 Reflexe mit $I > 2\sigma(I)$
θ = 2.93 bis 26.70°	R_{int} = 0.0382	C (25.00°) = 1.000
Absorptionskorrektur: Multi-scan	T_{min} = 0.9065	T_{max} = 1.0761

Verfeinerung

392 Reflexe	0 Restraints	37 Parameter
Verfeinerung mit SHELXL-97	bis χ = 0.000	
R_1 ($I > 2\sigma(I)$) = 0.0273	wR_2 ($I > 2\sigma(I)$) = 0.0649	
R_1 (all) = 0.0340	wR_2 (all) = 0.0661	GoF (S) = 0.939
$\Delta\varphi_{min}$ = -0.191 e·Å^{-3}	$\Delta\varphi_{max}$ = 0.242 e·Å^{-3}	

Kommentar

Die Struktur wurde bereits veröffentlicht: L. H. Finger, F. G. Schröder, J. Sundermeyer, *Z. Anorg. Allg. Chem.* **2013**, *639*, 1140-1152.

Fraktionelle Atomkoordinaten (*x, y, z*) und äquivalente isotrope Auslenkungsfaktoren *U*(eq)

	x	*y*	*z*	*U*(eq)/Å^2
N(1)	0.5883(1)	0.3482(1)	0.0924(2)	0.0216(3)
N(2)	0.4494(1)	0.3083(1)	0.0547(2)	0.0220(3)
C(1)	0.6700(2)	0.2500	0.0000	0.0195(3)
N(3)	0.7500	0.5405(1)	0.5000	0.0207(3)

7.2.3 Ammonium-hydrogenbistetrazolat (fin062b_0m)

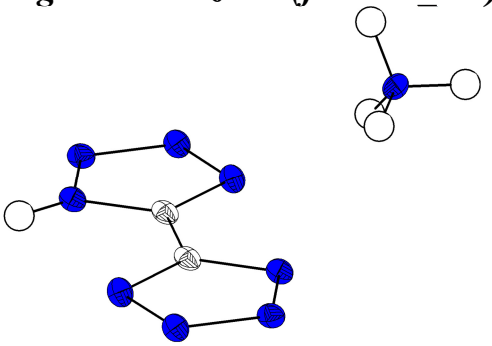

Kristalldaten

C2 H5 N9	M = 155.15 g/mol	Monoclinic, $P2_1/c$
a = 4.5136(6) Å	b = 8.4692(12) Å	c = 15.522(2) Å
α = 90°	β = 94.320(6)°	γ = 90°
V = 591.67(14) Å^3	Z = 4	F(000) = 320
D_{calc} = 1.742 g/cm^3	μ = 0.137 mm^{-1}	
colourless needle	0.66 · 0.10 · 0.07 mm^3	

Datensammlung

Diffraktometer: D8 Quest (Bruker)	T = 100(2) K	λ = 0.71069 Å
h = -5 bis 4	k = -10 bis 10	l = -19 bis 19
3538 gemessene Reflexe	1302 unabhängige Reflexe	1025 Reflexe mit $I > 2\sigma(I)$
θ = 2.63 bis 27.08°	R_{int} = 0.0448	C (25.00°) = 0.998
Absorptionskorrektur: Multi-scan	T_{min} = 0.6500	T_{max} = 0.7455

Verfeinerung

1302 Reflexe	0 Restraints	124 Parameter
Verfeinerung mit SHELXL-97	bis χ = 0.000	
R_1 ($I > 2\sigma(I)$) = 0.0517	wR_2 ($I > 2\sigma(I)$) = 0.0910	
R_1 (all) = 0.0749	wR_2 (all) = 0.0970	GoF (S) = 1.211
$\Delta\varphi_{min}$ = -0.283 e·Å^{-3}	$\Delta\varphi_{max}$ = 0.299 e·Å^{-3}	

Kommentar

Die Struktur wurde bereits veröffentlicht: L. H. Finger, F. G. Schröder, J. Sundermeyer, *Z. Anorg. Allg. Chem.* **2013**, *639*, 1140-1152.

Fraktionelle Atomkoordinaten (*x, y, z*) und äquivalente isotrope Auslenkungsfaktoren *U*(eq)

	x	*y*	*z*	*U*(eq)/Å^2
C(1)	0.0043(5)	0.4987(3)	0.4530(2)	0.0117(5)
C(2)	0.0904(5)	0.0427(3)	0.4710(1)	0.0102(5)
N(1)	0.1867(4)	0.5828(2)	0.4077(1)	0.0135(4)
N(2)	0.1135(4)	0.5418(2)	0.3242(1)	0.0132(4)
N(3)	-0.1030(4)	0.4384(2)	0.3201(1)	0.0127(4)
N(4)	-0.1737(5)	0.4097(3)	0.4013(1)	0.0119(4)
N(5)	0.2906(4)	0.1518(2)	0.4978(1)	0.0113(4)
N(6)	0.4016(4)	0.1959(3)	0.4241(1)	0.0108(4)
N(7)	0.2772(4)	0.1204(2)	0.3565(1)	0.0117(4)
N(8)	0.0768(4)	0.0211(2)	0.3849(1)	0.0115(4)
N(9)	0.5924(5)	0.8048(3)	0.3063(1)	0.0123(4)

7.2.4 *Dinatrium-bistetrazolat-pentahydrat (fin065_0m)*

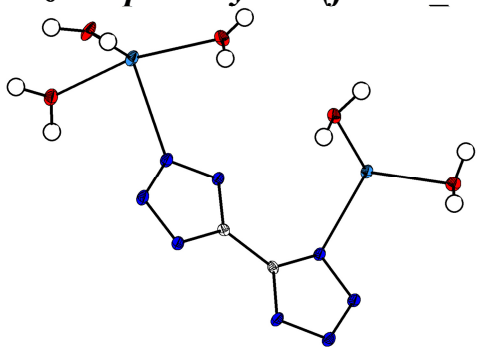

Kristalldaten

C2 H10 N8 Na2 O5	M = 272.16 g/mol	Triclinic, $P\bar{1}$
a = 7.2089(6) Å	b = 7.4623(6) Å	c = 10.7752(8) Å
α = 81.333(3)°	β = 76.478(3)°	γ = 67.604(3)°
V = 519.85(7) Å^3	Z = 2	F(000) = 280
D_{calc} = 1.739 g/cm^3	μ = 0.223 mm^{-1}	
colourless block	0.83 · 0.61 · 0.41 mm^3	

Datensammlung

Diffraktometer: D8 Quest (Bruker)	T = 100(2) K	λ = 0.71069 Å
h = -9 bis 8	k = -9 bis 9	l = -13 bis 13
6166 gemessene Reflexe	2310 unabhängige Reflexe	1952 Reflexe mit $I > 2\sigma(I)$
θ = 2.96 bis 27.17°	R_{int} = 0.0616	C (25.00°) = 0.998
Absorptionskorrektur: Multi-scan	T_{min} = 0.4396	T_{max} = 0.7455

Verfeinerung

2310 Reflexe	1 Restraints	194 Parameter
Verfeinerung mit SHELXL-97	bis χ = 0.000	
R_1 ($I > 2\sigma(I)$) = 0.0532	wR_2 ($I > 2\sigma(I)$) = 0.1320	
R_1 (all) = 0.0621	wR_2 (all) = 0.1386	GoF (S) = 1.047
$\Delta\varphi_{min}$ = -0.745 e·Å^{-3}	$\Delta\varphi_{max}$ = 0.481 e·Å^{-3}	

Kommentar

Die Struktur wurde bereits veröffentlicht: L. H. Finger, F. G. Schröder, J. Sundermeyer, *Z. Anorg. Allg. Chem.* **2013**, *639*, 1140-1152.

Fraktionelle Atomkoordinaten (*x, y, z*) und äquivalente isotrope Auslenkungsfaktoren *U*(eq)

	x	*y*	*z*	*U*(eq)/Å^2
Na(2)	0.1353(1)	0.1277(1)	0.9210(1)	0.0112(2)
Na(1)	0.4071(1)	-0.0213(1)	0.6417(1)	0.0101(2)
N(7)	0.1470(3)	0.3820(2)	0.7347(1)	0.0112(4)
O(1)	0.4873(2)	0.0117(2)	0.8368(1)	0.0122(3)
N(5)	0.0677(2)	0.6452(2)	0.6076(2)	0.0096(4)
O(5)	0.2650(2)	0.0138(2)	0.4600(1)	0.0113(3)
O(3)	-0.2174(2)	0.2277(2)	1.0083(1)	0.0142(3)
O(4)	0.0634(2)	-0.0092(2)	0.7574(1)	0.0130(3)
N(1)	0.5436(2)	-0.3711(2)	0.6554(1)	0.0096(3)
O(2)	0.2258(2)	0.3020(2)	1.0468(1)	0.0142(3)
N(4)	0.7398(2)	-0.6836(2)	0.6636(1)	0.0101(4)
N(8)	0.2682(2)	0.3344(2)	0.6199(2)	0.0099(4)
N(2)	0.5015(2)	-0.4517(2)	0.7742(1)	0.0105(4)
N(6)	0.0280(3)	0.5662(2)	0.7275(2)	0.0113(4)
C(1)	0.6898(3)	-0.5172(3)	0.5904(2)	0.0079(4)
N(3)	0.6172(3)	-0.6378(2)	0.7792(2)	0.0113(4)
C(2)	0.2164(3)	0.4983(2)	0.5445(2)	0.0077(4)

7.2.5 1-Ethyl-3-methylimidazolium-hydrogenbistetrazolat (lhf160)

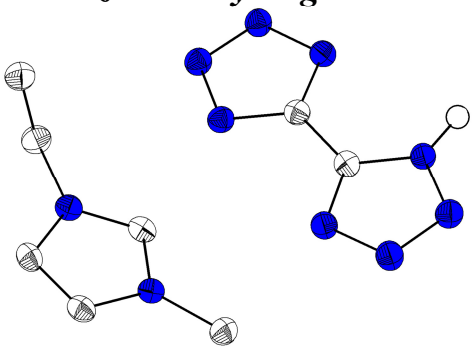

Kristalldaten

C8 H12 N10	M = 248.28 g/mol	Monoclinic, $P2_1/n$
a = 4.5978(3) Å	b = 18.9191(11) Å	c = 13.0052(7) Å
α = 90°	β = 94.586(4)°	γ = 90°
V = 1127.65(12) Å^3	Z = 4	F(000) = 520
D_{calc} = 1.462 g/cm^3	μ = 0.105 mm^{-1}	
colourless block	0.17 · 0.15 · 0.12 mm^3	

Datensammlung

Diffraktometer: STOE IPDS 2	T = 100(2) K	λ = 0.71069 Å
h = -5 bis 5	k = -23 bis 20	l = -16 bis 14
7731 gemessene Reflexe	2383 unabhängige Reflexe	1470 Reflexe mit $I > 2\sigma(I)$
θ = 1.90 bis 26.71°	R_{int} = 0.0528	C (25.00°) = 1.000
Absorptionskorrektur: Multi-scan	T_{min} = 0.9824	T_{max} = 0.9875

Verfeinerung

2383 Reflexe	0 Restraints	169 Parameter
Verfeinerung mit SHELXL-97	bis χ = 0.000	
R_1 ($I > 2\sigma(I)$) = 0.0337	wR_2 ($I > 2\sigma(I)$) = 0.0643	
R_1 (all) = 0.0706	wR_2 (all) = 0.0696	GoF (S) = 0.781
$\Delta\varphi_{min}$ = -0.163 e·Å^{-3}	$\Delta\varphi_{max}$ = 0.182 e·Å^{-3}	

Kommentar

Die Struktur wurde bereits veröffentlicht: L. H. Finger, F. G. Schröder, J. Sundermeyer, *Z. Anorg. Allg. Chem.* **2013**, *639*, 1140-1152.

Fraktionelle Atomkoordinaten (*x, y, z*) und äquivalente isotrope Auslenkungsfaktoren *U*(eq)

	x	*y*	*z*	*U*(eq)/Å^2		*x*	*y*	*z*	*U*(eq)/Å^2
N(3)	-0.3006(3)	0.3526(1)	0.5499(1)	0.0234(3)	N(2)	-0.2362(3)	0.2919(1)	0.5079(1)	0.0234(3)
N(9)	0.4405(3)	0.1400(1)	0.3558(1)	0.0217(3)	C(2)	0.1998(3)	0.4080(1)	0.3735(1)	0.0204(4)
N(5)	0.3351(3)	0.3780(1)	0.2987(1)	0.0235(3)	C(4)	0.7374(3)	0.1347(1)	0.2320(1)	0.0236(4)
N(8)	0.2670(3)	0.4766(1)	0.3779(1)	0.0217(3)	C(5)	0.6080(3)	0.0946(1)	0.3013(1)	0.0234(4)
N(10)	0.6481(3)	0.2032(1)	0.2444(1)	0.0209(3)	C(6)	0.2795(3)	0.1203(1)	0.4446(1)	0.0260(4)
N(6)	0.4896(3)	0.4312(1)	0.2573(1)	0.0263(3)	C(3)	0.4691(3)	0.2051(1)	0.3196(1)	0.0220(4)
N(1)	-0.0406(3)	0.3024(1)	0.4369(1)	0.0224(3)	C(8)	0.7464(3)	0.2641(1)	0.1864(1)	0.0256(4)
N(7)	0.4503(3)	0.4905(1)	0.3045(1)	0.0255(3)	C(1)	0.0061(3)	0.3720(1)	0.4395(1)	0.0196(4)
N(4)	-0.1485(3)	0.4049(1)	0.5078(1)	0.0214(3)	C(7)	0.4845(3)	0.1033(1)	0.5387(1)	0.0285(4)

7.2.6 Di(1-ethyl-3-methylimidazolium)-bistetrazolat (lhf159)

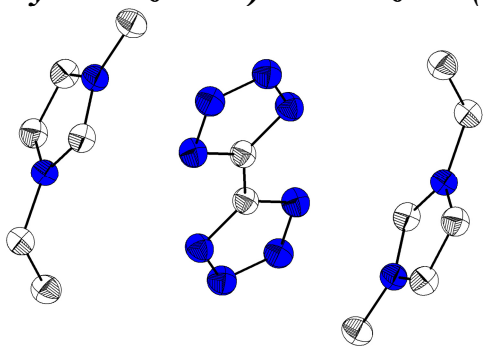

Kristalldaten

C14 H22 N12	M = 358.40 g/mol	Monoclinic, $P2_1/n$
a = 9.8020(6) Å	b = 7.9780(6) Å	c = 12.0450(8) Å
α = 90°	β = 108.716(5)°	γ = 90°
V = 892.11(10) Å^3	Z = 2	F(000) = 380
D_{calc} = 1.334 g/cm^3	μ = 0.092 mm^{-1}	
colourless block	0.27 · 0.23 · 0.16 mm^3	

Datensammlung

Diffraktometer: STOE IPDS 2	T = 100(2) K	λ = 0.71069 Å
h = -10 bis 12	k = -10 bis 10	l = -15 bis 15
7475 gemessene Reflexe	1882 unabhängige Reflexe	1355 Reflexe mit $I > 2\sigma(I)$
θ = 2.34 bis 26.72°	R_{int} = 0.0429	C (25.00°) = 1.000
Absorptionskorrektur: Multi-scan	T_{min} = 0.8321	T_{max} = 1.1598

Verfeinerung

1882 Reflexe	0 Restraints	120 Parameter
Verfeinerung mit SHELXL-97	bis χ = 0.000	
R_1 ($I > 2\sigma(I)$) = 0.0339	wR_2 ($I > 2\sigma(I)$) = 0.0802	
R_1 (all) = 0.0518	wR_2 (all) = 0.0843	GoF (S) = 0.893
$\Delta\varphi_{min}$ = -0.203 e·Å^{-3}	$\Delta\varphi_{max}$ = 0.135 e·Å^{-3}	

Kommentar

Die Struktur wurde bereits veröffentlicht: L. H. Finger, F. G. Schröder, J. Sundermeyer, *Z. Anorg. Allg. Chem.* **2013**, *639*, 1140-1152.

Fraktionelle Atomkoordinaten (*x, y, z*) und äquivalente isotrope Auslenkungsfaktoren *U*(eq)

	x	y	z	U(eq)/Å^2
C(1)	0.0515(1)	-0.0615(2)	-0.0074(1)	0.0288(3)
C(2)	0.2325(2)	0.3193(1)	-0.0030(1)	0.0319(3)
C(3)	0.4199(1)	0.3568(2)	0.1546(1)	0.0333(3)
C(4)	0.4693(2)	0.3230(2)	0.0646(1)	0.0334(3)
C(5)	0.3501(2)	0.2598(2)	-0.1534(1)	0.0356(3)
C(6)	0.4263(2)	0.0962(2)	-0.1577(1)	0.0388(3)
C(7)	0.1724(2)	0.3925(2)	0.1760(1)	0.0368(3)
N(1)	0.0908(1)	-0.1988(1)	0.0601(1)	0.0330(3)
N(2)	0.1862(1)	-0.2770(1)	0.0175(1)	0.0349(3)
N(3)	0.2016(1)	-0.1898(1)	-0.0708(1)	0.0351(3)
N(4)	0.1172(1)	-0.0514(1)	-0.0888(1)	0.0336(3)
N(5)	0.3501(1)	0.2998(1)	-0.0340(1)	0.0313(3)
N(6)	0.2717(1)	0.3529(1)	0.1108(1)	0.0309(3)

7.2.7 μ-Rhodizonato-1κO,1:2κO',2κO''-tetra(triphenylphosphin)-disilber(I) (lhf176f5)

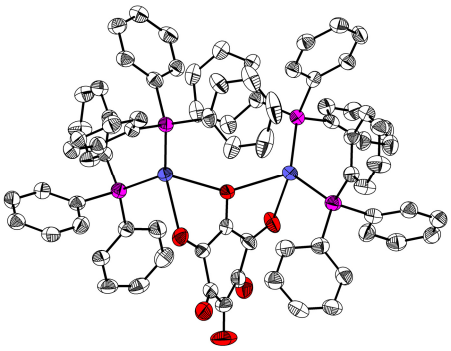

Kristalldaten

C78 H60 Ag2 O6 P4	M = 1432.88 g/mol	Triclinic, $P\bar{1}$
a = 12.2240(5) Å	b = 13.1383(8) Å	c = 22.8958(12) Å
α = 85.418(5)°	β = 79.380(4)°	γ = 63.796(4)°
V = 3242.7(3) Å^3	Z = 2	F(000) = 1460
D_{calc} = 1.468 g/cm^3	μ = 0.758 mm^{-1}	
red plate	0.330 · 0.150 · 0.070 mm^3	

Datensammlung

Diffraktometer: STOE IPDS 2	T = 100(2) K	λ = 0.71069 Å
h = -15 bis 15	k = -16 bis 16	l = -29 bis 29
37648 gemessene Reflexe	37648 unabhängige Reflexe	20804 Reflexe mit $I > 2\sigma(I)$
θ = 1.727 bis 27.170°	R_{int} = -(hklf5)	C (25.00°) = 0.999
Absorptionskorrektur: Keine		

Verfeinerung

37648 Reflexe	0 Restraints	812 Parameter
Verfeinerung mit SHELXL-2014/7	bis χ = 0.001	
R_1 ($I > 2\sigma(I)$) = 0.0683	wR_2 ($I > 2\sigma(I)$) = 0.1530	
R_1 (all) = 0.1054	wR_2 (all) = 0.1640	GoF (S) = 0.829
$\Delta\varphi_{min}$ = -1.925 e·Å^{-3}	$\Delta\varphi_{max}$ = 1.325 e·Å^{-3}	

Kommentar

Die Struktur wurde als nicht-meroedrischer Zwilling integriert und verfeinert. Anstelle einer HKLF5 Absorptionskorrektur, die im Vergleich mit den unkorrigierten Daten nur eine geringe Verbesserung zeigte, wurden die erweiterten Integrationsoptionen von X-Area (merging von Friedel-Paaren und equivalenten Reflexen) gewählt. Diese Struktur wurde bereits veröffentlicht: L. H. Finger, J. Sundermeyer, *Z. Anorg. Allg. Chem*. **2015**, *Z. Anorg. Allg. Chem.* **2015**, *641*, 2565–2569.

Fraktionelle Atomkoordinaten (*x, y, z*) und äquivalente isotrope Auslenkungsfaktoren *U*(eq)

	x	*y*	*z*	*U*(eq)/Å^2		*x*	*y*	*z*	*U*(eq)/Å^2
C(1)	1.0059(7)	0.0080(6)	0.7498(4)	0.0335(15)	C(15)	0.6370(8)	0.0609(7)	1.0686(4)	0.045(2)
C(2)	1.0623(7)	-0.0417(7)	0.8017(4)	0.0394(18)	C(16)	0.7557(8)	0.0021(7)	1.0798(4)	0.0426(19)
C(3)	1.1606(7)	-0.1600(7)	0.7951(4)	0.0427(19)	C(17)	0.8538(8)	-0.0271(8)	1.0333(5)	0.048(2)
C(4)	1.1416(7)	-0.2344(6)	0.7569(5)	0.048(2)	C(18)	0.8339(8)	0.0034(7)	0.9757(4)	0.043(2)
C(5)	1.0534(8)	-0.1836(7)	0.7150(4)	0.045(2)	C(19)	0.7034(7)	-0.0209(7)	0.8536(4)	0.0400(19)
C(6)	1.0152(7)	-0.0622(6)	0.7014(4)	0.0359(17)	C(20)	0.6905(7)	-0.1089(7)	0.8881(4)	0.046(2)
C(7)	0.5334(7)	0.2072(7)	0.8916(4)	0.0374(17)	C(21)	0.6961(7)	-0.2013(7)	0.8594(5)	0.050(2)
C(8)	0.5038(7)	0.3227(7)	0.8961(4)	0.0360(17)	C(22)	0.7158(7)	-0.2077(8)	0.7996(5)	0.050(2)
C(9)	0.3818(7)	0.4037(7)	0.9015(4)	0.0411(19)	C(23)	0.7325(8)	-0.1239(8)	0.7646(4)	0.049(2)
C(10)	0.2882(8)	0.3719(7)	0.9015(4)	0.046(2)	C(24)	0.7271(8)	-0.0300(7)	0.7922(4)	0.046(2)
C(11)	0.3161(8)	0.2587(8)	0.8965(5)	0.056(3)	C(25)	0.9618(7)	0.3893(7)	0.8292(4)	0.0365(17)
C(12)	0.4378(7)	0.1776(7)	0.8922(5)	0.048(2)	C(26)	0.9501(8)	0.4999(7)	0.8281(4)	0.0422(19)
C(13)	0.7127(7)	0.0644(6)	0.9640(4)	0.0394(18)	C(27)	1.0339(7)	0.5301(8)	0.7916(4)	0.045(2)
C(14)	0.6156(7)	0.0912(7)	1.0106(4)	0.0412(19)	C(28)	1.1318(8)	0.4493(8)	0.7546(4)	0.047(2)

	x	*y*	*z*	*U*(eq)/Å^2
C(29)	1.1460(8)	0.3386(9)	0.7554(4)	0.049(2)
C(30)	1.0611(7)	0.3072(8)	0.7925(4)	0.043(2)
C(31)	0.8983(6)	0.3294(6)	0.9506(4)	0.0342(17)
C(32)	0.8456(7)	0.2763(7)	0.9947(4)	0.0425(19)
C(33)	0.8760(8)	0.2599(8)	1.0512(4)	0.049(2)
C(34)	0.9596(8)	0.2957(8)	1.0647(4)	0.050(2)
C(35)	1.0132(8)	0.3478(8)	1.0211(4)	0.047(2)
C(36)	0.9821(7)	0.3650(7)	0.9646(4)	0.0415(19)
C(37)	0.7064(6)	0.4738(6)	0.8846(4)	0.0329(16)
C(38)	0.6459(7)	0.5310(7)	0.9383(4)	0.0385(18)
C(39)	0.5289(7)	0.6210(7)	0.9422(4)	0.0429(19)
C(40)	0.4725(7)	0.6557(7)	0.8928(4)	0.043(2)
C(41)	0.5308(7)	0.6007(7)	0.8390(4)	0.0414(19)
C(42)	0.6474(7)	0.5094(7)	0.8351(4)	0.0397(18)
C(43)	0.8384(6)	0.4625(7)	0.6138(4)	0.0361(17)
C(44)	0.8651(7)	0.4952(7)	0.6641(4)	0.0393(18)
C(45)	0.8871(7)	0.5909(7)	0.6621(4)	0.044(2)
C(46)	0.8833(7)	0.6534(7)	0.6109(4)	0.045(2)
C(47)	0.8571(8)	0.6214(7)	0.5610(4)	0.045(2)
C(48)	0.8342(7)	0.5266(7)	0.5626(4)	0.0404(18)
C(49)	0.7834(7)	0.3221(6)	0.5456(4)	0.0345(17)
C(50)	0.8818(8)	0.2669(7)	0.5000(4)	0.0418(19)
C(51)	0.8623(8)	0.2561(8)	0.4441(4)	0.047(2)
C(52)	0.7426(8)	0.2988(7)	0.4323(4)	0.044(2)
C(53)	0.6435(8)	0.3512(8)	0.4767(5)	0.048(2)
C(54)	0.6627(7)	0.3648(7)	0.5332(4)	0.0416(19)
C(55)	0.6734(7)	0.3652(8)	0.6688(4)	0.0417(19)
C(56)	0.6565(8)	0.2795(9)	0.7015(4)	0.053(2)
C(57)	0.5439(10)	0.3030(12)	0.7386(5)	0.074(3)
C(58)	0.4505(9)	0.4154(13)	0.7432(5)	0.073(4)
C(59)	0.4677(9)	0.5003(11)	0.7113(5)	0.066(3)
C(60)	0.5775(7)	0.4763(8)	0.6746(5)	0.052(2)
C(61)	1.2292(6)	0.0596(6)	0.5248(4)	0.0342(16)
C(62)	1.3006(7)	0.0899(7)	0.4785(4)	0.0389(18)
C(63)	1.3054(7)	0.0639(7)	0.4202(4)	0.0418(19)
C(64)	1.2407(7)	0.0060(7)	0.4082(4)	0.0429(19)
C(65)	1.1716(8)	-0.0262(7)	0.4543(4)	0.0418(19)
C(66)	1.1652(7)	0.0007(7)	0.5119(4)	0.0417(19)
C(67)	1.2690(7)	0.2029(6)	0.5993(4)	0.0356(17)
C(68)	1.3935(7)	0.1764(7)	0.5985(4)	0.046(2)
C(69)	1.4325(8)	0.2601(7)	0.5959(5)	0.053(2)
C(70)	1.3496(8)	0.3724(7)	0.5944(4)	0.046(2)
C(71)	1.2256(7)	0.4018(7)	0.5954(4)	0.0414(19)
C(72)	1.1849(7)	0.3177(7)	0.5984(4)	0.0372(18)
C(73)	1.3267(7)	-0.0277(7)	0.6334(4)	0.0371(18)
C(74)	1.3299(8)	-0.0293(8)	0.6933(4)	0.047(2)
C(75)	1.4189(8)	-0.1215(8)	0.7191(5)	0.051(2)
C(76)	1.5044(7)	-0.2129(7)	0.6837(5)	0.047(2)
C(77)	1.5004(8)	-0.2123(7)	0.6240(5)	0.048(2)
C(78)	1.4130(7)	-0.1206(7)	0.5985(4)	0.0398(18)
O(1)	0.9454(5)	0.1166(4)	0.7467(3)	0.0372(11)
O(2)	1.0424(5)	0.0157(5)	0.8463(3)	0.0472(15)
O(3)	1.2460(5)	-0.1958(6)	0.8237(3)	0.0563(16)
O(4)	1.1986(6)	-0.3388(5)	0.7613(4)	0.076(2)
O(5)	1.0185(7)	-0.2409(6)	0.6892(3)	0.0603(18)
O(6)	0.9778(5)	-0.0180(5)	0.6540(3)	0.0435(13)
P(1)	0.6945(2)	0.1055(2)	0.8869(1)	0.0361(4)
P(2)	0.8537(2)	0.3472(2)	0.8774(1)	0.0334(4)
P(3)	0.8169(2)	0.3328(2)	0.6183(1)	0.0338(4)
P(4)	1.2102(2)	0.0970(2)	0.6025(1)	0.0347(4)
Ag(1)	0.8419(1)	0.1822(1)	0.8468(1)	0.0356(2)
Ag(2)	0.9907(1)	0.1669(1)	0.6443(1)	0.0347(2)

7.2.8 N,N-Dimethylpyrrolidinium-trimethylsilylselenolate (finjg11)

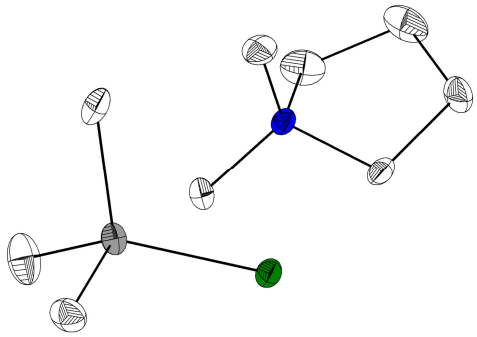

Kristalldaten

C18 H46 N2 Se2 Si2	M = 504.67 g/mol	Monoclinic, $P2_1/c$
a = 12.2500(8) Å	b = 10.8215(7) Å	c = 19.3331(12) Å
α = 90°	β = 90.166(3)°	γ = 90°
V = 2562.9(3) Å^3	Z = 4	F(000) = 1056
D_{calc} = 1.308 g/cm^3	μ = 2.983 mm^{-1}	
colourless block	0.25 · 0.1 · 0.05 mm^3	

Datensammlung

Diffraktometer: D8 Quest (Bruker)	T = 100(2) K	λ = 0.71073 Å
h = -14 bis 14	k = -13 bis 13	l = -23 bis 23
38995 gemessene Reflexe	4683 unabhängige Reflexe	4335 Reflexe mit $I > 2\sigma(I)$
θ = 2.157 bis 25.374°	R_{int} = 0.0730	C (25.00°) = 1.000
Absorptionskorrektur: Multi-scan	T_{min} = 0.6204	T_{max} = 0.7452

Verfeinerung

4683 Reflexe	0 Restraints	228 Parameter
Verfeinerung mit SHELXL-2014/7	bis χ = 0.001	
R_1 ($I > 2\sigma(I)$) = 0.0306	wR_2 ($I > 2\sigma(I)$) = 0.0674	
R_1 (all) = 0.0360	wR_2 (all) = 0.0692	GoF (S) = 1.117
$\Delta\varphi_{min}$ = -0.550 e·Å^{-3}	$\Delta\varphi_{max}$ = 0.521 e·Å^{-3}	

Kommentar

Die Struktur wurde bereits veröffentlicht: L. H. Finger, B. Scheibe, J. Sundermeyer, *Inorg. Chem.* **2015**, *54*, 9568-9575.

Fraktionelle Atomkoordinaten (*x, y, z*) und äquivalente isotrope Auslenkungsfaktoren *U*(eq)

	x	*y*	*z*	*U*(eq)/Å^2
Se(1)	0.7840(1)	0.1835(1)	0.2308(1)	0.0169(1)
Se(2)	0.7353(1)	0.6335(1)	0.4682(1)	0.0152(1)
Si(2)	0.7141(1)	0.8064(1)	0.4083(1)	0.0153(2)
Si(1)	0.7959(1)	0.3120(1)	0.1417(1)	0.0136(2)
N(2)	0.5035(3)	0.4133(3)	0.3663(2)	0.0130(7)
C(18)	0.7674(3)	0.7937(3)	0.3175(2)	0.0218(9)
C(7)	0.7400(3)	0.2455(3)	0.0587(2)	0.0160(8)
C(14)	0.4434(3)	0.5227(4)	0.3935(2)	0.0195(9)
C(9)	0.9394(3)	0.3605(4)	0.1217(2)	0.0195(9)
C(10)	0.5557(3)	0.3397(4)	0.4237(2)	0.0174(9)
C(5)	0.9128(3)	0.4952(4)	0.3133(2)	0.0209(9)
C(8)	0.7167(3)	0.4587(3)	0.1550(2)	0.0174(8)
C(6)	1.0437(3)	0.5013(4)	0.4077(2)	0.0170(9)
C(13)	0.4280(4)	0.3208(4)	0.3340(2)	0.0268(10)
C(15)	0.5872(3)	0.4550(4)	0.3157(2)	0.0211(9)
C(3)	1.0833(4)	0.2316(4)	0.3752(2)	0.0249(10)
C(4)	1.0544(3)	0.3313(4)	0.3231(2)	0.0192(9)
C(2)	0.9901(4)	0.2335(4)	0.4288(2)	0.0240(9)
C(17)	0.7845(4)	0.9415(3)	0.4492(2)	0.0239(9)
C(12)	0.4955(4)	0.2023(4)	0.3315(2)	0.0287(11)
C(11)	0.5774(4)	0.2135(4)	0.3920(2)	0.0258(10)
N(1)	0.9791(3)	0.4181(3)	0.3613(2)	0.0128(7)
C(1)	0.9098(3)	0.3300(4)	0.4022(2)	0.0166(9)
C(16)	0.5677(4)	0.8533(4)	0.3969(3)	0.0317(11)

7.2.9 *Tetramethylammonium-trimethylsilylthiolat-acetonitrilsolvat (fin184f5)*

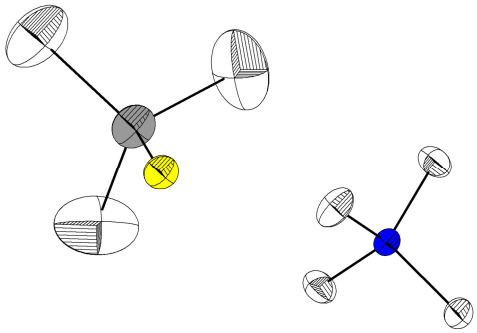

Kristalldaten

C9 H24 N2 S Si	M = 220.45 g/mol	Monoclinic, $P2_1/m$
a = 7.6236(11) Å	b = 7.6281(11) Å	c = 13.2227(18) Å
α = 90°	β = 104.094(4)°	γ = 90°
V = 745.80(18) Å^3	Z = 2	F(000) = 244
D_{calc} = 0.982 g/cm^3	μ = 0.268 mm^{-1}	
colourless plate	0.320 · 0.180 · 0.040 mm^3	

Datensammlung

Diffraktometer: D8 Quest (Bruker)	T = 110(2) K	λ = 0.71073 Å
h = -10 bis 10	k = 0 bis 10	l = 0 bis 18
2198 gemessene Reflexe	2198 unabhängige Reflexe	1545 Reflexe mit $I > 2\sigma(I)$
θ = 2.755 bis 30.314°	R_{int} = - (hklf5)	C (25.00°) = 0.999
Absorptionskorrektur: Multi-scan	T_{min} = 0.5002	T_{max} = 0.7460

Verfeinerung

2198 Reflexe	0 Restraints	77 Parameter
Verfeinerung mit SHELXL-2014/7	bis χ = 0.000	
R_1 ($I > 2\sigma(I)$) = 0.0784	wR_2 ($I > 2\sigma(I)$) = 0.1331	
R_1 (all) = 0.1308	wR_2 (all) = 0.1505	GoF (S) = 1.100
$\Delta\varphi_{min}$ = -0.439 e·Å^{-3}	$\Delta\varphi_{max}$ = 0.508 e·Å^{-3}	

Kommentar

Die Struktur wurde als nicht-meroedrischer Zwilling integriert und verfeinert. Die Struktur wurde bereits veröffentlicht: L. H. Finger, B. Scheibe, J. Sundermeyer, *Inorg. Chem*. **2015**, *54*, 9568-9575.

Fraktionelle Atomkoordinaten (*x, y, z*) und äquivalente isotrope Auslenkungsfaktoren *U*(eq)

	x	*y*	*z*	*U*(eq)/Å^2
C(1)	0.6171(7)	0.2500	0.0682(5)	0.0251(16)
C(2)	0.9356(7)	0.2500	0.0678(6)	0.0243(15)
C(3)	0.7221(6)	0.0914(3)	-0.0678(2)	0.0248(6)
C(4)	-0.1381(9)	0.2500	0.6451(5)	0.072(2)
C(5)	0.2010(9)	0.0515(8)	0.6425(4)	0.089(2)
C(6)	0.3697(10)	0.2500	0.3052(4)	0.0435(12)
C(7)	0.4140(15)	0.2500	0.4185(5)	0.087(3)
N(1)	0.7493(7)	0.2500	-0.0002(2)	0.0183(6)
N(2)	0.3343(9)	0.2500	0.2174(4)	0.0491(11)
Si(1)	0.1130(3)	0.2500	0.6981(1)	0.0335(3)
S(1)	0.1880(2)	0.2500	0.8580(1)	0.0240(2)

7.2.10 Bis(N,N-dimethylpyrrolidinium)-hexasulfid (fin227)

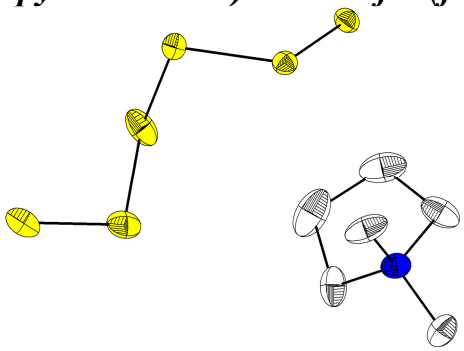

Kristalldaten

C12 H28 N2 S6	M = 392.72 g/mol	Monoclinic, $P2_1/c$
a = 13.9975(10) Å	b = 12.2771(9) Å	c = 12.6705(8) Å
α = 90°	β = 115.568(2)°	γ = 90°
V = 1964.2(2) Å^3	Z = 4	F(000) = 840
D_{calc} = 1.328 g/cm^3	μ = 0.690 mm^{-1}	
red block	0.140 · 0.100 · 0.100 mm^3	

Datensammlung

Diffraktometer: D8 Quest (Bruker)	T = 100(2) K	λ = 0.71073 Å
h = -16 bis 17	k = -15 bis 15	l = -16 bis 15
18591 gemessene Reflexe	4304 unabhängige Reflexe	3075 Reflexe mit $I > 2\sigma(I)$
θ = 2.314 bis 27.168°	R_{int} = 0.0862	C (25.00°) = 0.991
Absorptionskorrektur: Multi-scan	T_{min} = 0.5398	T_{max} = 0.7455

Verfeinerung

4304 Reflexe	36 Restraints	240 Parameter
Verfeinerung mit SHELXL-2014/7	bis χ = 0.001	
R_1 ($I > 2\sigma(I)$) = 0.0551	wR_2 ($I > 2\sigma(I)$) = 0.1147	
R_1 (all) = 0.0894	wR_2 (all) = 0.1275	GoF (S) = 1.035
$\Delta\varphi_{min}$ = -0.411 e·Å^{-3}	$\Delta\varphi_{max}$ = 0.569 e·Å^{-3}	

Kommentar

Die schwächer besetzten Positionen des fehlgeordneten S_6-Dianions wurden über DELU und RIGU restrained. Die Struktur wurde bereits veröffentlicht: L. H. Finger, B. Scheibe, J. Sundermeyer, *Inorg. Chem*. **2015**, *54*, 9568-9575.

Fraktionelle Atomkoordinaten (*x, y, z*) und äquivalente isotrope Auslenkungsfaktoren *U*(eq)

	x	*y*	*z*	*U*(eq)/Å^2		*x*	*y*	*z*	*U*(eq)/Å^2
C(1)	0.5122(3)	0.3950(3)	0.2074(3)	0.0248(8)	N(2)	0.0749(2)	0.1361(2)	0.8751(3)	0.0244(7)
C(2)	0.4675(3)	0.2800(3)	0.1763(3)	0.0288(8)	S(1)	0.1918(2)	0.4208(1)	0.7232(2)	0.0216(3)
C(3)	0.4679(3)	0.2347(3)	0.2906(3)	0.0294(8)	S(2)	0.3106(1)	0.4382(1)	0.8879(1)	0.0201(2)
C(4)	0.5145(3)	0.3248(3)	0.3807(3)	0.0253(8)	S(3)	0.2856(1)	0.5765(1)	0.9623(1)	0.0267(2)
C(5)	0.6027(3)	0.5028(2)	0.3891(3)	0.0263(8)	S(4)	0.1679(1)	0.5423(1)	1.0168(1)	0.0344(3)
C(6)	0.6840(3)	0.3343(3)	0.3636(4)	0.0323(9)	S(5)	0.2355(1)	0.4605(1)	1.1719(1)	0.0315(3)
C(7)	0.0009(3)	0.1893(3)	0.9176(4)	0.0365(9)	S(6)	0.3122(2)	0.5667(2)	1.3047(2)	0.0314(4)
C(8)	-0.0412(4)	0.2878(3)	0.8384(5)	0.0538(13)	S(1A)	0.199(5)	0.419(4)	0.713(5)	0.099(14)
C(9)	-0.0389(3)	0.2553(3)	0.7242(4)	0.0459(11)	S(2A)	0.2434(16)	0.545(2)	0.839(2)	0.070(6)
C(10)	0.0118(3)	0.1445(3)	0.7442(3)	0.0355(9)	S(3A)	0.3404(17)	0.488(2)	0.998(2)	0.079(7)
C(11)	0.0971(3)	0.0208(3)	0.9113(3)	0.0305(8)	S(4A)	0.245(2)	0.416(2)	1.070(2)	0.085(7)
C(12)	0.1770(3)	0.1967(3)	0.9173(4)	0.0392(10)	S(5A)	0.1990(18)	0.532(2)	1.138(2)	0.074(7)
N(1)	0.5808(2)	0.3914(2)	0.3371(2)	0.0209(6)	S(6A)	0.289(3)	0.599(3)	1.289(3)	0.081(12)

7.2.11 Bis(N-butyl-N-methylpyrrolidinium)-triselenid (bsvta15f5)

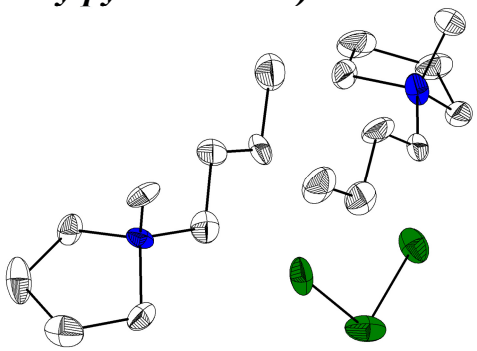

Kristalldaten

C36 H80 N4 Se6	M = 1042.80 g/mol	Monoclinic, *Cc*
a = 14.0988(8) Å	b = 24.8538(12) Å	c = 14.4105(8) Å
α = 90°	β = 116.435(2)°	γ = 90°
V = 4521.6(4) Å^3	Z = 4	F(000) = 2112
D_{calc} = 1.532 g/cm^3	μ = 4.883 mm^{-1}	
black block	0.230 · 0.110 · 0.060 mm^3	

Datensammlung

Diffraktometer: D8 Quest (Bruker)	T = 100(2) K	λ = 0.71073 Å
h = -18 bis 16	k = 0 bis 31	l = 0 bis 18
5047 gemessene Reflexe	5047 unabhängige Reflexe	4199 Reflexe mit $I > 2\sigma(I)$
θ = 2.835 bis 27.776°	R_{int} = -(hklf5)	C (25.00°) = 0.999
Absorptionskorrektur: Multi-scan	T_{min} = 0.5006	T_{max} = 0.7455

Verfeinerung

5047 Reflexe	23 Restraints	437 Parameter
Verfeinerung mit SHELXL-2014/7	bis χ = 0.000	
R_1 ($I > 2\sigma(I)$) = 0.0616	wR_2 ($I > 2\sigma(I)$) = 0.1009	
R_1 (all) = 0.0910	wR_2 (all) = 0.1114	GoF (S) = 1.145
$\Delta\varphi_{min}$ = -1.001 e·Å^{-3}	$\Delta\varphi_{max}$ = 1.014 e·Å^{-3}	

Kommentar

Die Struktur wurde als nicht-meroedrischer Zwilling integriert und verfeinert. Ein fehlgeordnetes Se_3-Dianion wurde über ISOR und SAME restrained. Die Struktur wurde bereits veröffentlicht: L. H. Finger, B. Scheibe, J. Sundermeyer, *Inorg. Chem*. **2015**, *54*, 9568-9575.

Fraktionelle Atomkoordinaten (*x, y, z*) und äquivalente isotrope Auslenkungsfaktoren *U*(eq)

	x	*y*	*z*	*U*(eq)/Å^2
C(1)	0.6706(12)	0.0063(7)	0.3825(13)	0.037(4)
C(2)	0.6607(14)	-0.0354(7)	0.3034(14)	0.047(5)
C(3)	0.5661(16)	-0.0184(6)	0.1964(14)	0.049(5)
C(4)	0.5330(12)	0.0359(6)	0.2192(12)	0.029(3)
C(5)	0.5874(13)	0.0950(6)	0.3786(11)	0.028(3)
C(6)	0.6142(10)	0.1024(5)	0.4924(11)	0.024(3)
C(7)	0.6452(15)	0.1599(7)	0.5237(14)	0.047(4)
C(8)	0.6810(13)	0.1721(7)	0.6402(12)	0.042(4)
C(9)	0.4935(12)	0.0086(7)	0.3656(12)	0.033(4)
C(10)	0.2238(10)	0.0461(6)	0.4352(12)	0.028(3)
C(11)	0.2963(12)	0.0807(6)	0.5256(13)	0.037(4)
C(12)	0.2372(13)	0.1349(6)	0.5073(13)	0.035(4)
C(13)	0.1377(12)	0.1300(5)	0.4004(11)	0.022(3)
C(14)	0.0488(11)	0.0538(5)	0.2817(10)	0.020(3)
C(15)	0.0139(11)	-0.0045(5)	0.2673(11)	0.021(3)
C(16)	-0.0418(11)	-0.0193(6)	0.1501(10)	0.027(3)
C(17)	-0.0759(12)	-0.0762(6)	0.1321(12)	0.036(4)
C(18)	0.0708(12)	0.0561(6)	0.4671(11)	0.027(3)

	x	*y*	*z*	*U*(eq)/Å^2
C(19)	0.5444(12)	0.2142(6)	0.2157(12)	0.033(4)
C(20)	0.6084(13)	0.2650(6)	0.2336(14)	0.039(4)
C(21)	0.5949(14)	0.2795(6)	0.1209(16)	0.047(5)
C(22)	0.5187(12)	0.2399(6)	0.0462(13)	0.034(4)
C(23)	0.4165(12)	0.1613(6)	0.0640(12)	0.029(3)
C(24)	0.3368(13)	0.1588(5)	-0.0450(13)	0.036(4)
C(25)	0.3217(13)	0.0995(6)	-0.0888(13)	0.038(4)
C(26)	0.2423(15)	0.0943(7)	-0.2003(13)	0.050(5)
C(27)	0.3794(12)	0.2558(6)	0.0980(13)	0.035(4)
C(28)	0.9716(12)	0.1996(6)	-0.0275(12)	0.029(3)
C(29)	0.9737(13)	0.1579(8)	-0.1026(13)	0.047(5)
C(30)	0.9237(14)	0.1073(7)	-0.0828(12)	0.042(4)
C(31)	0.9184(12)	0.1191(5)	0.0209(12)	0.031(3)
C(32)	0.9405(13)	0.1970(6)	0.1354(12)	0.034(4)
C(33)	0.9287(12)	0.2565(6)	0.1466(12)	0.035(4)
C(34)	1.0011(12)	0.2738(6)	0.2648(12)	0.033(4)
C(35)	0.9882(15)	0.3341(6)	0.2790(13)	0.046(4)
C(36)	0.7943(11)	0.1936(6)	-0.0487(12)	0.030(4)

	x	*y*	*z*	*U*(eq)/Å^2
N(1)	0.5708(8)	0.0366(4)	0.3387(9)	0.020(2)
N(2)	0.1180(8)	0.0697(4)	0.3947(8)	0.017(2)
N(3)	0.4608(10)	0.2172(5)	0.1022(9)	0.027(3)
N(4)	0.9043(9)	0.1800(4)	0.0193(9)	0.023(3)
Se(1)	0.3484(1)	0.1743(1)	0.3252(1)	0.0285(4)
Se(2)	0.2123(1)	0.1480(1)	0.1634(1)	0.0211(4)
Se(3)	0.2231(3)	0.0561(2)	0.1352(3)	0.0256(9)
Se(1B)	0.2516(12)	0.2031(5)	0.2421(12)	0.029(4)
Se(2B)	0.3167(12)	0.1165(5)	0.2708(11)	0.024(4)
Se(3B)	0.237(4)	0.0578(14)	0.132(3)	0.023(11)
Se(4)	0.8295(1)	0.1624(1)	0.3401(1)	0.0370(4)
Se(5)	0.7876(1)	0.0859(1)	0.2331(1)	0.0398(5)
Se(6)	0.6603(1)	0.1026(1)	0.0616(1)	0.0365(4)

7.2.12 Bis(N,N-dimethylpyrrolidinium)-dodecatellurid (jg32)

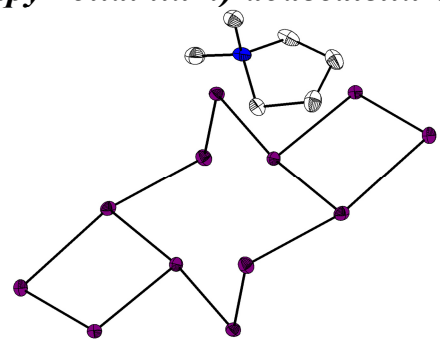

Kristalldaten

C24 H56 N4 Te12	M = 1931.92 g/mol	Monoclinic, $P2_1/n$
a = 9.5497(7) Å	b = 18.7183(14) Å	c = 13.2276(10) Å
α = 90°	β = 107.817(2)°	γ = 90°
V = 2251.1(3) Å^3	Z = 2	F(000) = 1704
D_{calc} = 2.850 g/cm^3	μ = 7.668 mm^{-1}	
dark violet plate	0.280 · 0.130 · 0.030 mm^3	

Datensammlung

Diffraktometer: D8 Quest (Bruker)	T = 100(2) K	λ = 0.71073 Å
h = -11 bis 11	k = -22 bis 22	l = -15 bis 14
35122 gemessene Reflexe	4100 unabhängige Reflexe	3923 Reflexe mit $I > 2\sigma(I)$
θ = 2.176 bis 25.340°	R_{int} = 0.0385	C (25.00°) = 0.998
Absorptionskorrektur: Multi-scan	T_{min} = 0.5263	T_{max} = 0.7452

Verfeinerung

4100 Reflexe	0 Restraints	185 Parameter
Verfeinerung mit SHELXL-2014/7	bis χ = 0.001	
R_1 ($I > 2\sigma(I)$) = 0.0280	wR_2 ($I > 2\sigma(I)$) = 0.0624	
R_1 (all) = 0.0300	wR_2 (all) = 0.0630	GoF (S) = 1.291
$\Delta\varphi_{min}$ = -0.867 e·Å^{-3}	$\Delta\varphi_{max}$ = 1.495 e·Å^{-3}	

Kommentar

Die Struktur wurde bereits veröffentlicht: L. H. Finger, B. Scheibe, J. Sundermeyer, *Inorg. Chem*. **2015**, *54*, 9568-9575.

Fraktionelle Atomkoordinaten (*x, y, z*) und äquivalente isotrope Auslenkungsfaktoren *U*(eq)

	x	*y*	*z*	*U*(eq)/Å^2		*x*	*y*	*z*	*U*(eq)/Å^2
N(2)	0.6190(6)	0.2115(3)	0.1527(4)	0.0194(11)	C(3)	0.6883(8)	0.0824(4)	0.8453(6)	0.0320(17)
N(1)	0.6138(6)	0.1074(3)	0.6608(4)	0.0226(12)	C(1)	0.5709(8)	0.0313(3)	0.6696(6)	0.0259(15)
C(7)	0.5906(7)	0.1362(3)	0.1803(5)	0.0203(13)	C(5)	0.4892(8)	0.1555(4)	0.6594(7)	0.0327(18)
C(8)	0.6351(8)	0.1352(4)	0.3003(5)	0.0263(15)	C(6)	0.6590(11)	0.1196(4)	0.5634(6)	0.043(2)
C(4)	0.7384(7)	0.1188(4)	0.7612(6)	0.0271(15)	Te(5)	1.2732(1)	0.0803(1)	-0.0885(1)	0.0186(1)
C(10)	0.7650(7)	0.2280(4)	0.2356(6)	0.0246(15)	Te(6)	1.0937(1)	0.0232(1)	-0.2851(1)	0.0159(1)
C(2)	0.5926(8)	0.0202(4)	0.7885(5)	0.0245(14)	Te(3)	0.9913(1)	0.0653(1)	0.1268(1)	0.0144(1)
C(11)	0.5023(7)	0.2609(4)	0.1648(6)	0.0237(14)	Te(2)	1.1824(1)	0.1454(1)	0.2928(1)	0.0154(1)
C(9)	0.7596(7)	0.1904(4)	0.3355(6)	0.0266(15)	Te(1)	1.1331(1)	0.0735(1)	0.4609(1)	0.0185(1)
C(12)	0.6278(8)	0.2172(4)	0.0426(6)	0.0287(16)	Te(4)	1.0986(1)	0.1652(1)	-0.0088(1)	0.0171(1)

7.2.13 1-Ethyl-3-methylimidazolium-hydrogensulfid (fin110sub)

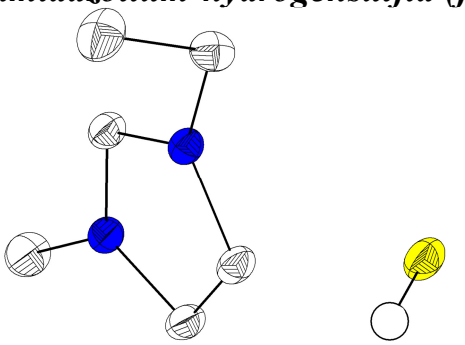

Kristalldaten

C6 H12 N2 S	M = 144.24 g/mol	Monoclinic, $P2_1/n$
a = 8.6023(3) Å	b = 7.6710(2) Å	c = 12.7600(4) Å
α = 90°	β = 107.8620(10)°	γ = 90°
V = 801.42(4) Å^3	Z = 4	F(000) = 312
D_{calc} = 1.195 g/cm^3	μ = 0.323 mm^{-1}	
colourless block	0.210 · 0.200 · 0.100 mm^3	

Datensammlung

Diffraktometer: D8 Quest (Bruker)	T = 100(2) K	λ = 0.71073 Å
h = -11 bis 11	k = -10 bis 10	l = -17 bis 17
18404 gemessene Reflexe	1993 unabhängige Reflexe	1777 Reflexe mit $I > 2\sigma(I)$
θ = 2.538 bis 28.331°	R_{int} = 0.0447	C (25.00°) = 1.000
Absorptionskorrektur: Multi-scan	T_{min} = 0.6361	T_{max} = 0.7457

Verfeinerung

1993 Reflexe	0 Restraints	88 Parameter
Verfeinerung mit SHELXL-2014/7	bis χ = 0.000	
R_1 ($I > 2\sigma(I)$) = 0.0318	wR_2 ($I > 2\sigma(I)$) = 0.0833	
R_1 (all) = 0.0373	wR_2 (all) = 0.0876	GoF (S) = 1.066
$\Delta\varphi_{min}$ = -0.238 e·Å^{-3}	$\Delta\varphi_{max}$ = 0.338 e·Å^{-3}	

Kommentar

Die Struktur wurde bereits veröffentlicht: L. H. Finger, F. Wohde, E. I. Grigoryev, A.-K. Hansmann, R. Berger, B. Roling, J. Sundermeyer, *Chem. Commun.* **2015**, *51*, 16169-16172.

Fraktionelle Atomkoordinaten (*x, y, z*) und äquivalente isotrope Auslenkungsfaktoren *U*(eq)

	x	*y*	*z*	*U*(eq)/Å^2		*x*	*y*	*z*	*U*(eq)/Å^2
C(2)	0.5120(1)	0.6493(2)	0.1572(1)	0.0168(2)	C(7)	0.1271(2)	0.6494(2)	0.0915(1)	0.0296(3)
C(4)	0.6219(2)	0.5399(2)	0.3236(1)	0.0186(2)	C(8)	0.7799(2)	0.5091(2)	0.1861(1)	0.0240(3)
C(5)	0.4759(1)	0.6112(2)	0.3193(1)	0.0181(2)	N(1)	0.4092(1)	0.6785(1)	0.2148(1)	0.0157(2)
C(6)	0.2488(1)	0.7642(2)	0.1726(1)	0.0203(3)	N(3)	0.6421(1)	0.5667(1)	0.2216(1)	0.0164(2)
					S(1)	0.1224(1)	0.7002(1)	0.4292(1)	0.0225(1)

7.2.14 N-Butyl-N-methylpyrrolidinium-Hydrogensulfid (fin1072)

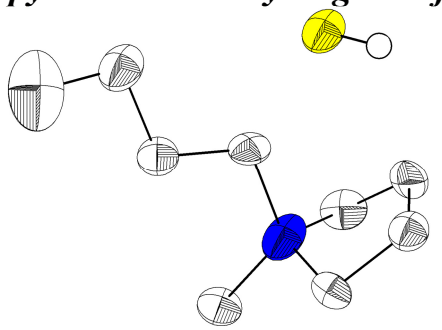

Kristalldaten

C9 H21 N S	M = 175.33 g/mol	Tetragonal, $P4_2/mbc$
a = 15.6635(6) Å	b = 15.6635(6) Å	c = 8.9408(5) Å
α = 90°	β = 90°	γ = 90°
V = 2193.6(2) Å^3	Z = 8	F(000) = 784
D_{calc} = 1.062 g/cm^3	μ = 0.244 mm^{-1}	
colourless needle	0.378 · 0.138 · 0.118 mm^3	

Datensammlung

Diffraktometer: D8 Quest (Bruker)	T = 100(2) K	λ = 0.71073 Å
h = -16 bis 19	k = -18 bis 19	l = -11 bis 11
16725 gemessene Reflexe	1154 unabhängige Reflexe	871 Reflexe mit $I > 2\sigma(I)$
θ = 2.601 bis 25.991°	R_{int} = 0.0514	C (25.00°) = 0.999
Absorptionskorrektur: Multi-scan	T_{min} = 0.6668	T_{max} = 0.7456

Verfeinerung

1154 Reflexe	2 Restraints	90 Parameter
Verfeinerung mit SHELXL-2014/6	bis χ = 0.000	
R_1 ($I > 2\sigma(I)$) = 0.0601	wR_2 ($I > 2\sigma(I)$) = 0.1535	
R_1 (all) = 0.0785	wR_2 (all) = 0.1680	GoF (S) = 1.056
$\Delta\varphi_{min}$ = -0.368 e·Å^{-3}	$\Delta\varphi_{max}$ = 0.248 e·Å^{-3}	

Kommentar

Das Pyrrolidiniumkation ist über eine Spiegelebene fehlgeordnet, einzelne Bindungslängen wurden über DFIX restrained. Die Struktur wurde bereits veröffentlicht: L. H. Finger, F. Wohde, E. I. Grigoryev, A.-K. Hansmann, R. Berger, B. Roling, J. Sundermeyer, *Chem. Commun.* **2015**, *51*, 16169-16172.

Fraktionelle Atomkoordinaten (*x, y, z*) und äquivalente isotrope Auslenkungsfaktoren *U*(eq)

	x	*y*	*z*	*U*(eq)/Å^2		*x*	*y*	*z*	*U*(eq)/Å^2
C(1)	0.1773(4)	0.0838(3)	-0.1366(5)	0.0428(12)	C(6)	0.0914(3)	0.2532(3)	0.0561(6)	0.0442(12)
C(2)	0.2694(4)	0.1037(4)	-0.1475(6)	0.0439(13)	C(7)	0.0797(3)	0.3453(2)	0.0000	0.0588(11)
C(3)	0.3081(2)	0.0952(2)	0.0000	0.0439(9)	C(8)	0.0295(5)	0.3815(6)	0.1299(12)	0.106(3)
C(4)	0.2311(4)	0.0781(3)	0.1072(5)	0.0340(11)	C(9)	0.0767(3)	0.0725(3)	0.0847(6)	0.0447(12)
C(5)	0.1534(3)	0.2085(3)	-0.0454(5)	0.0384(14)	N(1)	0.1570(2)	0.1119(2)	0.0000	0.0587(11)
					S(1)	0.3433(1)	0.3500(1)	0.0000	0.0522(4)

7.2.15 1-Ethyl-2,3-dimethylimidazolium-hydrogensulfid (finph13)

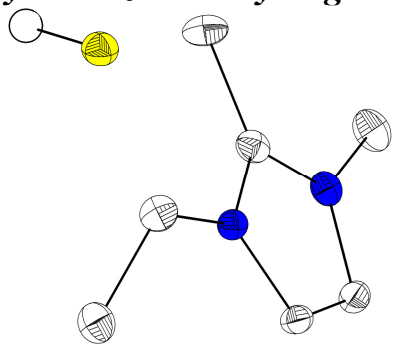

Kristalldaten

C7 H14 N2 S	*M* = 158.26 g/mol	Orthorhombic, *Pbca*
a = 8.0154(9) Å	*b* = 13.4251(14) Å	*c* = 16.6433(18) Å
α = 90°	β = 90°	γ = 90°
V = 1790.9(3) Å^3	*Z* = 8	*F*(000) = 688
D_{calc} = 1.174 g/cm^3	μ = 0.295 mm^{-1}	
yellow block	0.374 · 0.268 · 0.078 mm^3	

Datensammlung

Diffraktometer: D8 Quest (Bruker)	*T* = 100(2) K	λ = 0.71073 Å
h = -9 bis 9	*k* = -16 bis 16	*l* = -16 bis 19
7823 gemessene Reflexe	1603 unabhängige Reflexe	1240 Reflexe mit $I > 2\sigma(I)$
θ = 3.035 bis 25.271°	R_{int} = 0.0599	*C* (25.00°) = 0.991
Absorptionskorrektur: Multi-scan	T_{min} = 0.6538	T_{max} = 0.7452

Verfeinerung

1603 Reflexe	0 Restraints	98 Parameter
Verfeinerung mit SHELXL-2014/7	bis χ = 0.000	
R_1 ($I > 2\sigma(I)$) = 0.0360	wR_2 ($I > 2\sigma(I)$) = 0.0766	
R_1 (all) = 0.0589	wR_2 (all) = 0.0845	GoF (S) = 1.024
$\Delta\varphi_{min}$ = -0.197 e·Å^{-3}	$\Delta\varphi_{max}$ = 0.269 e·Å^{-3}	

Kommentar

Die Struktur wurde bereits veröffentlicht: L. H. Finger, J. Sundermeyer, *Chem. Eur. J.,* accepted manuscript.

Fraktionelle Atomkoordinaten (*x, y, z*) und äquivalente isotrope Auslenkungsfaktoren *U*(eq)

	x	*y*	*z*	*U*(eq)/Å^2		*x*	*y*	*z*	*U*(eq)/Å^2
C(2)	0.1532(2)	0.0759(1)	0.3902(1)	0.0158(4)	C(8)	0.1713(3)	0.1814(1)	0.3643(1)	0.0228(5)
C(4)	0.1757(2)	-0.0620(1)	0.4622(1)	0.0174(5)	C(9)	0.3280(3)	0.0900(1)	0.5135(1)	0.0224(5)
C(5)	0.0774(3)	-0.0822(1)	0.3990(1)	0.0161(4)	N(1)	0.0644(2)	0.0040(1)	0.3537(1)	0.0136(4)
C(6)	-0.0353(3)	0.0143(1)	0.2798(1)	0.0182(5)	N(3)	0.2225(2)	0.0366(1)	0.4559(1)	0.0156(4)
C(7)	-0.0243(3)	-0.0780(1)	0.2278(1)	0.0213(5)	S(1)	0.6460(1)	0.1877(1)	0.3696(1)	0.0195(2)

7.2.16 1-Butyl-3-metyhlimidazolium-hydrogensulfid (fin168)

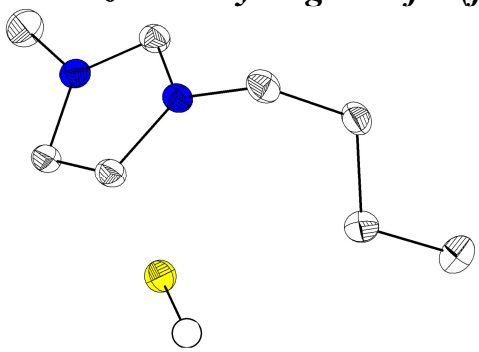

Kristalldaten

C8 H16 N2 S	M = 172.29 g/mol	Orthorhombic, $Pna2_1$
a = 9.9131(4) Å	b = 12.1432(5) Å	c = 8.2285(3) Å
α = 90°	β = 90°	γ = 90°
V = 990.52(7) Å^3	Z = 4	F(000) = 376
D_{calc} = 1.155 g/cm^3	μ = 0.272 mm^{-1}	
colourless block	0.243 · 0.175 · 0.144 mm^3	

Datensammlung

Diffraktometer: D8 Quest (Bruker)	T = 100(2) K	λ = 0.71069 Å
h = -13 bis 13	k = -16 bis 15	l = -10 bis 10
12552 gemessene Reflexe	2462 unabhängige Reflexe	2320 Reflexe mit $I > 2\sigma(I)$
θ = 2.652 bis 28.498°	R_{int} = 0.0278	C (25.00°) = 1.000
Absorptionskorrektur: Multi-scan	T_{min} = 0.7051	T_{max} = 0.7457

Verfeinerung

2462 Reflexe	1 Restraints	106 Parameter
Verfeinerung mit SHELXL-2014/7	bis χ = 0.000	
R_1 ($I > 2\sigma(I)$) = 0.0255	wR_2 ($I > 2\sigma(I)$) = 0.0633	
R_1 (all) = 0.0286	wR_2 (all) = 0.0647	GoF (S) = 1.061
$\Delta\varphi_{min}$ = -0.161 e·Å^{-3}	$\Delta\varphi_{max}$ = 0.191 e·Å^{-3}	

Kommentar

Die Struktur wurde bereits veröffentlicht: L. H. Finger, J. Sundermeyer, *Chem. Eur. J.,* accepted manuscript.

Fraktionelle Atomkoordinaten (*x, y, z*) und äquivalente isotrope Auslenkungsfaktoren *U*(eq)

	x	*y*	*z*	*U*(eq)/Å^2
C(2)	0.2913(2)	0.6934(1)	0.3848(2)	0.0177(3)
C(4)	0.1694(2)	0.8381(1)	0.3147(2)	0.0187(4)
C(5)	0.1501(2)	0.8204(2)	0.4749(2)	0.0189(4)
C(6)	0.2337(2)	0.6783(2)	0.6791(2)	0.0214(4)
C(7)	0.1484(2)	0.5747(1)	0.6870(2)	0.0215(4)
C(8)	-0.0030(2)	0.5946(2)	0.6705(3)	0.0265(4)
C(9)	-0.0834(2)	0.4879(2)	0.6805(3)	0.0362(5)
C(10)	0.3100(2)	0.7470(2)	0.0947(2)	0.0268(4)
N(1)	0.2273(2)	0.7300(1)	0.5168(2)	0.0168(3)
N(3)	0.2582(2)	0.7578(1)	0.2606(2)	0.0179(3)
S(1)	0.0655(1)	0.9312(1)	0.8690(1)	0.0199(1)

7.2.17 1-Ethyl-3-methylimidazolium-hydrogenselenid (fin109)

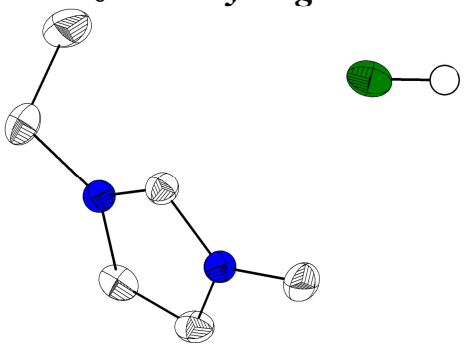

Kristalldaten

C6 H12 N2 Se	M = 191.14 g/mol	Monoclinic, $P2_1/n$
a = 8.6014(7) Å	b = 7.7800(6) Å	c = 13.2988(9) Å
α = 90°	β = 108.249(3)°	γ = 90°
V = 845.18(11) Å^3	Z = 4	F(000) = 384
D_{calc} = 1.502 g/cm^3	μ = 4.366 mm^{-1}	
colourless block	0.137 · 0.127 · 0.095 mm^3	

Datensammlung

Diffraktometer: D8 Quest (Bruker)	T = 105(2) K	λ = 0.71073 Å
h = -11 bis 11	k = -10 bis 10	l = -16 bis 17
15559 gemessene Reflexe	2109 unabhängige Reflexe	1772 Reflexe mit $I > 2\sigma(I)$
θ = 2.510 bis 28.362°	R_{int} = 0.0354	C (25.00°) = 1.000
Absorptionskorrektur: Multi-scan	T_{min} = 0.5800	T_{max} = 0.7457

Verfeinerung

2109 Reflexe	0 Restraints	88 Parameter
Verfeinerung mit SHELXL-2014/7	bis χ = 0.001	
R_1 ($I > 2\sigma(I)$) = 0.0230	wR_2 ($I > 2\sigma(I)$) = 0.0489	
R_1 (all) = 0.0334	wR_2 (all) = 0.0521	GoF (S) = 1.032
$\Delta\varphi_{min}$ = -0.419 e·Å^{-3}	$\Delta\varphi_{max}$ = 0.460 e·Å^{-3}	

Kommentar

Die Struktur wurde bereits veröffentlicht: L. H. Finger, J. Sundermeyer, *Chem. Eur. J.,* accepted manuscript.

Fraktionelle Atomkoordinaten (*x, y, z*) und äquivalente isotrope Auslenkungsfaktoren *U*(eq)

	x	*y*	*z*	*U*(eq)/Å^2
C(2)	0.4875(2)	0.6460(2)	0.8422(1)	0.0209(3)
C(4)	0.3763(2)	0.5394(2)	0.6827(1)	0.0244(4)
C(5)	0.5220(2)	0.6089(2)	0.6869(1)	0.0237(4)
C(6)	0.7497(2)	0.7612(2)	0.8280(2)	0.0274(4)
C(7)	0.8693(3)	0.6564(4)	0.9122(2)	0.0518(6)
C(8)	0.2208(2)	0.5044(3)	0.8147(2)	0.0301(4)
N(1)	0.5896(2)	0.6752(2)	0.7873(1)	0.0203(3)
N(3)	0.3567(2)	0.5648(2)	0.7804(1)	0.0206(3)
Se(1)	0.6224(1)	0.2024(1)	0.9285(1)	0.0294(1)

7.2.18 Tetra(N-butyl-N-methylpyrrolidinium)-dodecatellurid (fin163af5)

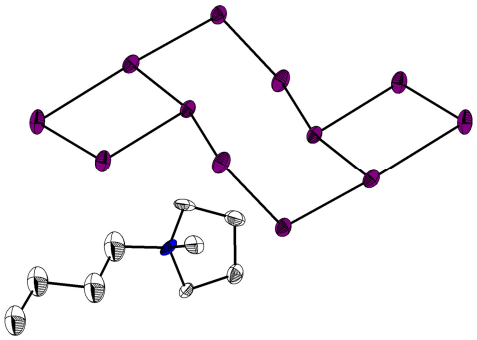

Kristalldaten

C36 H80 N4 Te12	M = 2100.24 g/mol	Triclinic, $P\bar{1}$
a = 9.5233(6) Å	b = 11.4728(7) Å	c = 15.0443(9) Å
α = 109.476(2)°	β = 108.300(2)°	γ = 92.404(2)°
V = 1451.42(16) Å^3	Z = 1	F(000) = 948
D_{calc} = 2.403 g/cm^3	μ = 5.957 mm^{-1}	
dark red needle	0.365 · 0.126 · 0.062 mm^3	

Datensammlung

Diffraktometer: D8 Quest (Bruker)	T = 110(2) K	λ = 0.71073 Å
h = -13 bis 12	k = -16 bis 15	l = 0 bis 21
8156 gemessene Reflexe	8156 unabhängige Reflexe	6869 Reflexe mit $I > 2\sigma(I)$
θ = 2.726 bis 30.530°	R_{int} = -(hklf5)	C (25.00°) = 0.999
Absorptionskorrektur: Multi-scan	T_{min} = 0.4030	T_{max} = 0.7461

Verfeinerung

8156 Reflexe	0 Restraints	292 Parameter
Verfeinerung mit SHELXL-2014/6	bis χ = 0.001	
R_1 ($I > 2\sigma(I)$) = 0.0423	wR_2 ($I > 2\sigma(I)$) = 0.0711	
R_1 (all) = 0.0623	wR_2 (all) = 0.0780	GoF (S) = 1.103
$\Delta\varphi_{min}$ = -1.604 e·Å^{-3}	$\Delta\varphi_{max}$ = 1.606 e·Å^{-3}	

Kommentar

Die Struktur wurde als nicht-meroedrischer Zwilling integriert und verfeinert. Die Struktur wurde bereits veröffentlicht: L. H. Finger, J. Sundermeyer, *Chem. Eur. J.,* accepted manuscript.

Fraktionelle Atomkoordinaten (*x, y, z*) und äquivalente isotrope Auslenkungsfaktoren *U*(eq)

	x	*y*	*z*	*U*(eq)/Å^2
Te(1)	0.0236(1)	0.7703(1)	0.2303(1)	0.0303(1)
Te(2)	-0.1745(8)	0.5846(6)	0.2202(3)	0.0263(7)
Te(2A)	-0.1508(8)	0.5588(11)	0.2065(7)	0.0209(10)
Te(3)	0.0024(1)	0.5093(1)	0.3758(1)	0.0207(1)
Te(4)	-0.2681(1)	0.3173(1)	0.2849(1)	0.0285(1)
Te(5)	-0.3933(1)	0.3798(1)	0.4309(1)	0.0241(1)
Te(6)	-0.2444(1)	0.2735(1)	0.5697(1)	0.0224(1)
N(1)	0.2367(13)	0.1506(12)	0.4926(8)	0.022(3)
C(1)	0.3149(13)	0.0788(10)	0.4246(9)	0.018(2)
C(2)	0.2399(12)	0.0969(10)	0.3230(8)	0.028(2)
C(3)	0.0882(14)	0.1360(11)	0.3238(9)	0.030(3)
C(4)	0.0763(12)	0.1289(10)	0.4213(10)	0.026(3)
C(5)	0.2987(19)	0.2884(13)	0.5340(10)	0.029(3)
C(6)	0.2403(18)	0.1017(13)	0.5738(11)	0.054(2)
C(7)	0.396(2)	0.1176(14)	0.6493(13)	0.054(2)
C(8)	0.374(2)	0.0530(15)	0.7228(12)	0.054(2)
C(9)	0.5249(19)	0.0698(13)	0.8031(11)	0.054(2)
N(1A)	0.270(3)	0.154(3)	0.520(2)	0.034(2)
C(1A)	0.292(3)	0.109(2)	0.418(2)	0.034(2)
C(2A)	0.160(2)	0.1393(19)	0.3505(17)	0.034(2)
C(3A)	0.035(3)	0.144(2)	0.3957(19)	0.034(2)
C(4A)	0.1077(19)	0.1150(17)	0.4924(16)	0.034(2)
C(5A)	0.313(4)	0.293(3)	0.567(2)	0.034(2)
C(6A)	0.369(2)	0.0977(18)	0.5917(17)	0.034(2)
C(7A)	0.338(2)	0.1167(17)	0.6844(16)	0.034(2)
C(8A)	0.436(2)	0.048(2)	0.7391(19)	0.034(2)
C(9A)	0.401(2)	0.0683(17)	0.8397(15)	0.034(2)
N(2)	0.784(2)	0.613(2)	0.8913(14)	0.029(4)
C(10)	0.773(2)	0.501(2)	0.9211(17)	0.069(6)
C(11)	0.6098(19)	0.4809(15)	0.9157(14)	0.075(5)
C(12)	0.5834(15)	0.6180(12)	0.9565(9)	0.051(3)
C(13)	0.700(2)	0.6955(16)	0.9504(12)	0.036(3)
C(14)	0.7057(14)	0.5724(12)	0.7804(7)	0.045(3)
C(15)	0.9483(15)	0.6623(14)	0.9216(11)	0.061(2)
C(16)	0.9820(15)	0.7764(15)	0.8990(12)	0.061(2)
C(17)	1.1460(16)	0.8370(15)	0.9517(12)	0.061(2)
C(18)	1.1834(15)	0.9463(14)	0.9259(11)	0.061(2)
N(2A)	0.759(8)	0.615(7)	0.884(5)	0.048(3)

	x	*y*	*z*	*U*(eq)/Å^2
C(10A)	0.630(3)	0.509(3)	0.785(2)	0.048(3)
C(11A)	0.602(3)	0.414(3)	0.8109(19)	0.048(3)
C(12A)	0.714(3)	0.428(3)	0.909(2)	0.048(3)
C(13A)	0.831(4)	0.526(5)	0.932(4)	0.048(3)

	x	*y*	*z*	*U*(eq)/Å^2
C(14A)	0.680(6)	0.710(5)	0.939(4)	0.048(3)
C(15A)	0.857(3)	0.698(3)	0.8618(19)	0.048(3)
C(16A)	0.990(3)	0.776(3)	0.953(2)	0.048(3)
C(17A)	1.085(3)	0.862(3)	0.931(2)	0.048(3)
C(18A)	1.232(3)	0.936(3)	1.012(2)	0.048(3)

7.2.19 Hexamethylguanidinium-hydrogenselenid (bsbsc34)

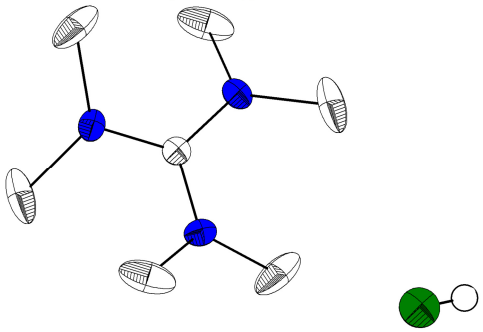

Kristalldaten

C7 H19 N3 Se	M = 224.21 g/mol	Hexagonal, $P6_3/mmc$
a = 7.8227(3) Å	b = 7.8227(3) Å	c = 10.5610(5) Å
α = 90°	β = 90°	γ = 120°
V = 559.69(5) Å^3	Z = 2	F(000) = 232
D_{calc} = 1.330 g/cm^3	μ = 3.309 mm^{-1}	
colourless block	0.252 · 0.082 · 0.078 mm^3	

Datensammlung

Diffraktometer: D8 Quest (Bruker)	T = 100(2) K	λ = 0.71073 Å
h = -10 bis 10	k = -10 bis 10	l = -13 bis 13
5066 gemessene Reflexe	268 unabhängige Reflexe	255 Reflexe mit $I > 2\sigma(I)$
θ = 3.007 bis 27.084°	R_{int} = 0.0313	C (25.00°) = 1.000
Absorptionskorrektur: Multi-scan	T_{min} = 0.6085	T_{max} = 0.7455

Verfeinerung

268 Reflexe	0 Restraints	17 Parameter
Verfeinerung mit SHELXL-2014/7	bis χ = 0.000	
R_1 ($I > 2\sigma(I)$) = 0.0175	wR_2 ($I > 2\sigma(I)$) = 0.0435	
R_1 (all) = 0.0182	wR_2 (all) = 0.0439	GoF (S) = 1.246
$\Delta\varphi_{min}$ = -0.129 e·Å^{-3}	$\Delta\varphi_{max}$ = 0.216 e·Å^{-3}	

Kommentar

Die Synthese der Substanz und die Kristallzucht erfolgten durch Benjamin Scheibe im Rahmen seiner von mir betreuten Bachelorarbeit.[93]

Fraktionelle Atomkoordinaten (*x, y, z*) und äquivalente isotrope Auslenkungsfaktoren *U*(eq)

	x	*y*	*z*	*U*(eq)/Å^2
N(1)	0.0000	0.1709(3)	0.0000	0.0207(5)
C(1)	0.0000	0.0000	0.0000	0.0171(6)
C(2)	0.1727(1)	0.3454(2)	-0.0664(2)	0.0418(5)
Se(1)	0.3333	0.6667	0.2500	0.0333(2)

7.2.20 Bis(N-butyl-N-methylpyrrolidinium)-hexasulfid (bsvta17)

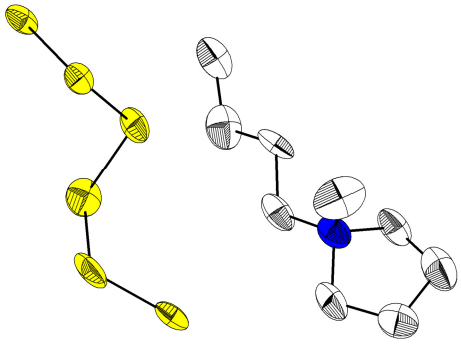

Kristalldaten

C18 H40 N2 S6	M = 476.88 g/mol	Monoclinic, $P2_1/c$
a = 13.129(5) Å	b = 16.000(6) Å	c = 12.004(4) Å
α = 90°	β = 92.262(9)°	γ = 90°
V = 2519.6(16) Å^3	Z = 4	F(000) = 1032
D_{calc} = 1.257 g/cm^3	μ = 0.550 mm^{-1}	
orange plate	0.087 · 0.072 · 0.041 mm^3	

Datensammlung

Diffraktometer: D8 Quest (Bruker)	T = 100(2) K	λ = 0.71073 Å
h = -15 bis 15	k = -19 bis 19	l = -14 bis 14
22638 gemessene Reflexe	4695 unabhängige Reflexe	1779 Reflexe mit $I > 2\sigma(I)$
θ = 2.546 bis 25.615°	R_{int} = 0.3522	C (25.00°) = 0.999
Absorptionskorrektur: Multi-scan	T_{min} = 0.3685	T_{max} = 0.7452

Verfeinerung

4695 Reflexe	12 Restraints	264 Parameter
Verfeinerung mit SHELXL-2014/7	bis χ = 0.001	
R_1 ($I > 2\sigma(I)$) = 0.1311	wR_2 ($I > 2\sigma(I)$) = 0.2734	
R_1 (all) = 0.2908	wR_2 (all) = 0.3451	GoF (S) = 1.017
$\Delta\varphi_{min}$ = -0.410 e·Å^{-3}	$\Delta\varphi_{max}$ = 0.819 e·Å^{-3}	

Kommentar

Durch eine geringe Kristallqualität und starke Fehlordnung ist keine zufriedenstellende Verfeinerung möglich.

Fraktionelle Atomkoordinaten (*x, y, z*) und äquivalente isotrope Auslenkungsfaktoren *U*(eq)

	x	*y*	*z*	*U*(eq)/Å^2
N(1)	-0.1025(7)	-0.7402(6)	-0.4914(7)	0.050(2)
C(1)	-0.1666(10)	-0.6709(8)	-0.5438(11)	0.078(4)
C(2)	-0.1055(11)	-0.5915(9)	-0.5248(12)	0.091(5)
C(3)	-0.0283(10)	-0.6119(9)	-0.4279(10)	0.076(4)
C(4)	-0.0562(9)	-0.6970(8)	-0.3910(9)	0.060(3)
C(5)	-0.1678(7)	-0.8139(7)	-0.4667(9)	0.053(3)
C(6)	-0.1082(7)	-0.8874(7)	-0.4186(8)	0.046(3)
C(7)	-0.1780(9)	-0.9554(8)	-0.3790(10)	0.070(4)
C(8)	-0.1242(9)	-1.0341(8)	-0.3434(9)	0.065(4)
C(9)	-0.0210(11)	-0.7626(8)	-0.5683(11)	0.087(5)
N(2)	0.4060(7)	-0.7488(6)	-1.0284(7)	0.057(3)
C(10)	0.3500(9)	-0.6674(8)	-1.0536(9)	0.065(4)
C(11)	0.4287(10)	-0.6008(9)	-1.0534(11)	0.079(4)
C(12)	0.5093(11)	-0.6326(9)	-0.9670(12)	0.092(5)
C(13)	0.4863(14)	-0.7207(11)	-0.9500(15)	0.135(7)
C(14)	0.3367(9)	-0.8102(8)	-0.9800(8)	0.056(3)
C(15)	0.3873(9)	-0.8946(9)	-0.9505(11)	0.076(4)
C(16)	0.3283(11)	-0.9498(10)	-0.8811(11)	0.088(5)
C(17)	0.3761(10)	-1.0315(9)	-0.8553(9)	0.070(4)
C(18)	0.4418(12)	-0.7845(10)	-1.1384(12)	0.109(6)
S(1)	-0.1766(4)	-1.2196(5)	-0.7358(7)	0.0426(14)
S(2)	-0.1419(2)	-1.1046(2)	-0.7950(3)	0.0388(10)
S(3)	-0.1703(3)	-1.0167(3)	-0.6786(3)	0.0492(11)
S(4)	-0.3249(3)	-0.9921(3)	-0.6874(4)	0.0602(13)
S(5)	-0.3507(3)	-0.9045(3)	-0.8090(4)	0.0660(15)
S(6)	-0.3189(6)	-0.7897(5)	-0.7471(7)	0.0417(13)
S(1B)	-0.196(3)	-1.224(3)	-0.732(4)	0.093(4)
S(2B)	-0.1711(11)	-1.1158(13)	-0.6551(13)	0.093(4)
S(3B)	-0.1536(11)	-1.0254(14)	-0.7635(15)	0.093(4)
S(4B)	-0.3058(11)	-0.9856(13)	-0.8263(13)	0.093(4)
S(5B)	-0.3599(11)	-0.9093(14)	-0.7201(15)	0.093(4)
S(6B)	-0.305(3)	-0.783(3)	-0.760(3)	0.093(4)

7.2.21 Dimethylpyrrolidinium-dimethylindiumselenolat (jg14)

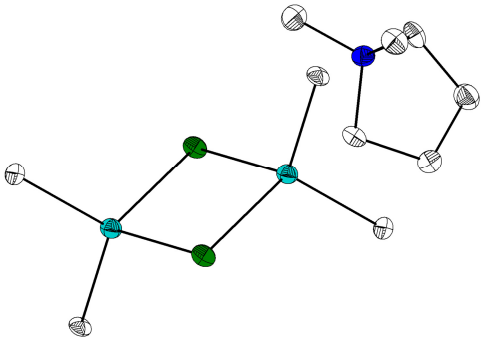

Kristalldaten

C16 H40 In2 N2 Se2	M = 648.06 g/mol	Monoclinic, $P2_1/n$
a = 9.9187(6) Å	b = 12.2925(9) Å	c = 9.9398(8) Å
α = 90°	β = 100.434(2)°	γ = 90°
V = 1191.88(15) Å^3	Z = 2	F(000) = 632
D_{calc} = 1.806 g/cm^3	μ = 4.988 mm^{-1}	
yellow block	0.250 · 0.106 · 0.083 mm^3	

Datensammlung

Diffraktometer: D8 Quest (Bruker)	T = 100(2) K	λ = 0.71073 Å
h = -11 bis 11	k = -14 bis 14	l = -11 bis 11
11756 gemessene Reflexe	2148 unabhängige Reflexe	1825 Reflexe mit $I > 2\sigma(I)$
θ = 2.662 bis 25.245°	R_{int} = 0.0464	C (25.00°) = 1.000
Absorptionskorrektur: Multi-scan	T_{min} = 0.6075	T_{max} = 0.7452

Verfeinerung

2148 Reflexe	0 Restraints	104 Parameter
Verfeinerung mit SHELXL-2014/7	bis χ = 0.001	
R_1 ($I > 2\sigma(I)$) = 0.0209	wR_2 ($I > 2\sigma(I)$) = 0.0407	
R_1 (all) = 0.0306	wR_2 (all) = 0.0431	GoF (S) = 1.068
$\Delta\varphi_{min}$ = -0.382 e·Å^{-3}	$\Delta\varphi_{max}$ = 0.508 e·Å^{-3}	

Fraktionelle Atomkoordinaten (*x, y, z*) und äquivalente isotrope Auslenkungsfaktoren *U*(eq)

	x	*y*	*z*	*U*(eq)/Å^2
In(1)	0.9540(1)	0.0853(1)	0.8595(1)	0.0159(1)
Se(1)	0.8260(1)	0.0318(1)	1.0585(1)	0.0174(1)
N(1)	0.4669(2)	0.1815(2)	0.8389(3)	0.0171(6)
C(8)	1.0017(3)	0.2612(2)	0.8619(3)	0.0160(7)
C(3)	0.3000(3)	0.1465(3)	0.6376(4)	0.0253(8)
C(4)	0.3225(3)	0.2082(3)	0.7713(3)	0.0201(7)
C(6)	0.4862(3)	0.1968(3)	0.9894(4)	0.0257(8)
C(7)	0.8354(3)	0.0380(3)	0.6580(3)	0.0236(8)
C(5)	0.5689(3)	0.2492(3)	0.7815(4)	0.0224(8)
C(1)	0.4806(3)	0.0624(2)	0.8023(3)	0.0180(7)
C(2)	0.4090(3)	0.0558(3)	0.6539(4)	0.0246(8)

7.2.22 1-Ethyl-2,3-dimethylimidazolium-tert-butylthiolat-tetrahydrofuransolvat (bsvta16)

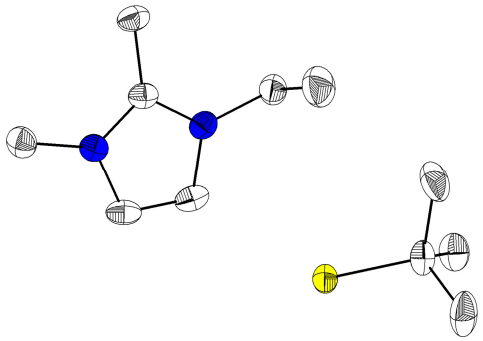

Kristalldaten

C13 H26 N2 O0.50 S	M = 250.42 g/mol	Monoclinic, $P2_1/c$
a = 13.0270(11) Å	b = 7.2335(5) Å	c = 16.9130(13) Å
α = 90°	β = 106.865(3)°	γ = 90°
V = 1525.2(2) Å^3	Z = 4	F(000) = 552
D_{calc} = 1.091 g/cm^3	μ = 0.198 mm^{-1}	
colourless needle	0.388 · 0.060 · 0.053 mm^3	

Datensammlung

Diffraktometer: D8 Quest (Bruker)	T = 100(2) K	λ = 0.71073 Å
h = -16 bis 16	k = -9 bis 9	l = -16 bis 21
29341 gemessene Reflexe	3388 unabhängige Reflexe	2612 Reflexe mit $I > 2\sigma(I)$
θ = 2.517 bis 27.226°	R_{int} = 0.0631	C (25.00°) = 0.999
Absorptionskorrektur: Multi-scan	T_{min} = 0.7080	T_{max} = 0.7455

Verfeinerung

3388 Reflexe	6 Restraints	209 Parameter
Verfeinerung mit SHELXL-2014/7	bis χ = 0.001	
R_1 ($I > 2\sigma(I)$) = 0.0505	wR_2 ($I > 2\sigma(I)$) = 0.1133	
R_1 (all) = 0.0724	wR_2 (all) = 0.1247	GoF (S) = 1.043
$\Delta\varphi_{min}$ = -0.271 e·Å^{-3}	$\Delta\varphi_{max}$ = 0.501 e·Å^{-3}	

Kommentar

Das THF-Molekül ist über ein Inversionszentrum, das *tert*-Butylthiolat-Anion über zwei symmetrieunabhängige Positionen fehlgeordnet. Einzelne Atome wurden über ISOR restrained.

Fraktionelle Atomkoordinaten (*x, y, z*) und äquivalente isotrope Auslenkungsfaktoren *U*(eq)

	x	*y*	*z*	*U*(eq)/Å^2
C(1)	0.4079(1)	0.4044(3)	1.0636(1)	0.0248(4)
C(2)	0.3919(2)	0.6933(3)	1.0177(1)	0.0306(4)
C(3)	0.4617(2)	0.6934(3)	1.0932(1)	0.0298(4)
C(4)	0.2786(2)	0.4558(3)	0.9229(1)	0.0333(4)
C(5)	0.1673(2)	0.4505(4)	0.9340(2)	0.0517(6)
C(6)	0.3945(2)	0.2024(3)	1.0690(1)	0.0309(4)
C(7)	0.5343(2)	0.4576(3)	1.2041(1)	0.0328(4)
C(8)	0.2043(2)	0.9700(3)	0.7528(1)	0.0313(4)
C(9)	0.1251(3)	1.1148(6)	0.7634(2)	0.0476(11)
C(10)	0.1490(3)	0.7755(5)	0.7536(2)	0.0497(11)
C(11)	0.2239(3)	0.9889(5)	0.6703(2)	0.0371(8)
C(9A)	0.1938(7)	1.1734(13)	0.7095(5)	0.073(3)
C(10A)	0.2137(6)	0.8330(16)	0.6908(5)	0.072(3)
C(11A)	0.1189(5)	0.9483(12)	0.7900(5)	0.052(2)
C(12)	0.1340(4)	0.5639(7)	0.5096(4)	0.0536(13)
C(13)	0.0208(9)	0.6324(18)	0.4833(9)	0.112(4)
C(14)	-0.0394(7)	0.4690(12)	0.4993(7)	0.086(3)
C(15)	0.0325(6)	0.3890(14)	0.5664(5)	0.089(2)
O(1)	0.1392(3)	0.4117(6)	0.5600(3)	0.0683(11)
N(1)	0.3590(1)	0.5105(2)	0.9996(1)	0.0262(3)
N(2)	0.4708(1)	0.5113(2)	1.1213(1)	0.0253(3)
S(1)	0.3306(1)	0.9806(1)	0.8367(1)	0.0289(2)

7.2.23 1-Ethyl-2,3-dimethylimidazolium-trimethylsilylthiolat (ph07b)

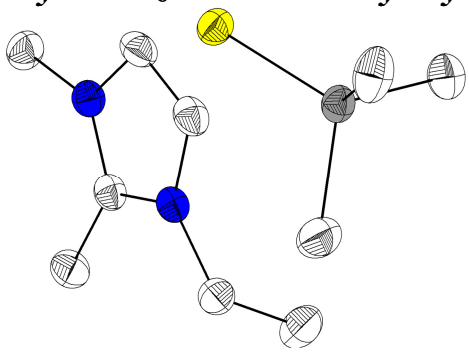

Kristalldaten

C10 H22 N2 S Si	M = 230.44 g/mol	Monoclinic, $P2_1/c$
a = 12.537(2) Å	b = 7.1760(13) Å	c = 15.886(3) Å
α = 90°	β = 90.007(6)°	γ = 90°
V = 1429.2(4) Å^3	Z = 4	F(000) = 504
D_{calc} = 1.071 g/cm^3	μ = 0.283 mm^{-1}	
colourless plate	0.606 · 0.210 · 0.209 mm^3	

Datensammlung

Diffraktometer: D8 Quest (Bruker)	T = 100(2) K	λ = 0.71069 Å
h = -16 bis 16	k = -9 bis 7	l = -20 bis 20
13715 gemessene Reflexe	3090 unabhängige Reflexe	2025 Reflexe mit $I > 2\sigma(I)$
θ = 2.564 bis 27.168°	R_{int} = 0.0961	C (25.00°) = 0.983
Absorptionskorrektur: Multi-scan	T_{min} = 0.5551	T_{max} = 0.7455

Verfeinerung

3090 Reflexe	0 Restraints	133 Parameter
Verfeinerung mit SHELXL-2014/7	bis χ = 0.000	
R_1 ($I > 2\sigma(I)$) = 0.0499	wR_2 ($I > 2\sigma(I)$) = 0.0927	
R_1 (all) = 0.0990	wR_2 (all) = 0.1087	GoF (S) = 1.017
$\Delta\varphi_{min}$ = -0.392 e·Å^{-3}	$\Delta\varphi_{max}$ = 0.464 e·Å^{-3}	

Fraktionelle Atomkoordinaten (*x, y, z*) und äquivalente isotrope Auslenkungsfaktoren *U*(eq)

	x	*y*	*z*	*U*(eq)/Å^2		*x*	*y*	*z*	*U*(eq)/Å^2
C(2)	0.6079(2)	-0.0975(3)	0.4191(2)	0.0237(6)	C(10)	0.8149(2)	0.2180(4)	0.2686(2)	0.0422(8)
C(4)	0.5531(2)	0.1949(3)	0.4098(2)	0.0279(6)	C(11)	0.8648(2)	-0.1876(4)	0.2373(2)	0.0422(8)
C(5)	0.6304(2)	0.1897(3)	0.4681(2)	0.0277(6)	C(12)	0.9148(2)	0.0937(4)	0.1042(2)	0.0356(7)
C(6)	0.7485(2)	-0.0577(4)	0.5300(2)	0.0281(6)	N(1)	0.6642(2)	0.0065(3)	0.4734(1)	0.0233(4)
C(7)	0.8543(2)	-0.0833(4)	0.4847(2)	0.0383(7)	N(2)	0.5399(2)	0.0150(3)	0.3800(1)	0.0237(5)
C(8)	0.6174(2)	-0.3007(3)	0.4062(2)	0.0302(6)	Si(1)	0.8138(1)	0.0298(1)	0.1867(1)	0.0252(2)
C(9)	0.4647(2)	-0.0367(4)	0.3133(2)	0.0295(6)	S(1)	0.6625(1)	-0.0074(1)	0.1370(1)	0.0272(2)

7.2.24 1-Ethyl-3-methyl-imidazolium-2-methylencarboxylat-dimethylsulfoxidsolvat (bsvta12b)

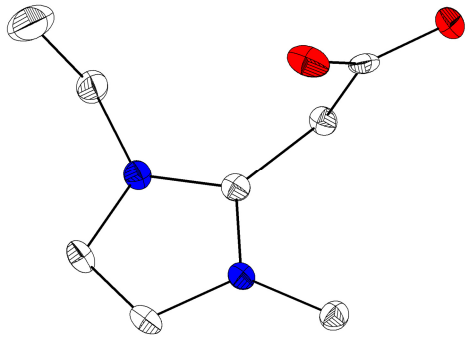

Kristalldaten

C10 H18 N2 O3 S	M = 246.32 g/mol	Monoclinic, $P2_1/c$
a = 11.8171(7) Å	b = 12.3884(7) Å	c = 8.8481(7) Å
α = 90°	β = 103.012(4)°	γ = 90°
V = 1262.06(15) Å^3	Z = 4	F(000) = 528
D_{calc} = 1.296 g/cm^3	μ = 0.252 mm^{-1}	
colourless needle	0.530 · 0.200 · 0.170 mm^3	

Datensammlung

Diffraktometer: D8 Quest (Bruker)	T = 100(2) K	λ = 0.71073 Å
h = -15 bis 14	k = -15 bis 15	l = -11 bis 11
12294 gemessene Reflexe	2796 unabhängige Reflexe	2145 Reflexe mit $I > 2\sigma(I)$
θ = 2.415 bis 27.190°	R_{int} = 0.0849	C (25.00°) = 0.999
Absorptionskorrektur: Multi-scan	T_{min} = 0.5493	T_{max} = 0.7455

Verfeinerung

2796 Reflexe	0 Restraints	149 Parameter
Verfeinerung mit SHELXL-2014/6	bis χ = 0.000	
R_1 ($I > 2\sigma(I)$) = 0.0417	wR_2 ($I > 2\sigma(I)$) = 0.0954	
R_1 (all) = 0.0627	wR_2 (all) = 0.1056	GoF (S) = 1.016
$\Delta\varphi_{min}$ = -0.326 e·Å^{-3}	$\Delta\varphi_{max}$ = 0.443 e·Å^{-3}	

Fraktionelle Atomkoordinaten (*x, y, z*) und äquivalente isotrope Auslenkungsfaktoren *U*(eq)

	x	*y*	*z*	*U*(eq)/Å^2		*x*	*y*	*z*	*U*(eq)/Å^2
O(1)	0.4555(1)	0.8608(1)	0.2365(1)	0.0222(3)	C(5)	0.4342(2)	0.8743(1)	0.3670(2)	0.0136(4)
O(2)	0.3494(1)	0.9232(1)	0.3979(2)	0.0204(3)	C(6)	0.7872(2)	0.8597(2)	0.5165(2)	0.0218(4)
N(1)	0.7174(1)	0.7612(1)	0.4749(2)	0.0151(3)	C(7)	0.8153(2)	0.9103(2)	0.3743(3)	0.0405(6)
N(2)	0.5743(1)	0.6492(1)	0.4140(2)	0.0131(3)	C(8)	0.4560(2)	0.6055(1)	0.3786(2)	0.0153(4)
C(1)	0.6032(2)	0.7492(1)	0.4676(2)	0.0130(4)	S(1)	0.1295(1)	0.6484(1)	0.5027(1)	0.0201(1)
C(2)	0.7603(2)	0.6671(2)	0.4240(2)	0.0174(4)	O(5)	0.0198(1)	0.6779(1)	0.3873(2)	0.0252(3)
C(3)	0.6707(2)	0.5975(2)	0.3859(2)	0.0160(4)	C(17)	0.1890(2)	0.7707(2)	0.5929(2)	0.0289(5)
C(4)	0.5218(2)	0.8281(1)	0.5091(2)	0.0133(4)	C(18)	0.0881(2)	0.5933(2)	0.6693(2)	0.0245(4)

7.2.25 1-Ethyl-3-methyl-imidazolium-2-thiocarboxylat (ph06f5)

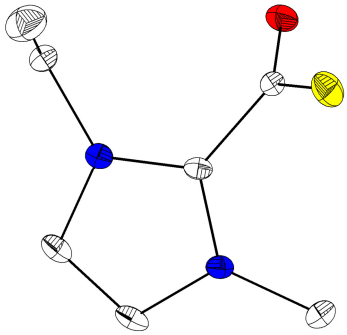

Kristalldaten

C7 H10 N2 O S	M = 170.23 g/mol	Triclinic, $P\bar{1}$
a = 6.9542(6) Å	b = 7.7894(7) Å	c = 8.4255(6) Å
α = 76.743(3)°	β = 78.993(3)°	γ = 70.487(3)°
V = 415.46(6) Å^3	Z = 2	F(000) = 180
D_{calc} = 1.361 g/cm^3	μ = 0.332 mm^{-1}	
colourless needle	0.490 · 0.120 · 0.060 mm^3	

Datensammlung

Diffraktometer: D8 Quest (Bruker)	T = 100(2) K	λ = 0.71069 Å
h = -8 bis 8	k = -9 bis 9	l = 0 bis 10
1697 gemessene Reflexe	1697 unabhängige Reflexe	1457 Reflexe mit $I > 2\sigma(I)$
θ = 2.820 bis 27.125°	R_{int} = -(hklf5)	C (25.00°) = 0.949
Absorptionskorrektur: Multi-scan	T_{min} = 0.6637	T_{max} = 0.7455

Verfeinerung

1697 Reflexe	0 Restraints	103 Parameter
Verfeinerung mit SHELXL-2014/7	bis χ = 0.000	
R_1 ($I > 2\sigma(I)$) = 0.0430	wR_2 ($I > 2\sigma(I)$) = 0.1145	
R_1 (all) = 0.0549	wR_2 (all) = 0.1228	GoF (S) = 1.085
$\Delta\varphi_{min}$ = -0.387 e·Å^{-3}	$\Delta\varphi_{max}$ = 0.354 e·Å^{-3}	

Kommentar

Die Struktur wurde als nicht-meroedrischer Zwilling integriert und verfeinert.

Fraktionelle Atomkoordinaten (*x, y, z*) und äquivalente isotrope Auslenkungsfaktoren *U*(eq)

	x	*y*	*z*	*U*(eq)/Å^2
C(2)	0.4557(4)	0.3808(3)	0.8048(3)	0.0127(5)
C(4)	0.7268(4)	0.4665(4)	0.8114(3)	0.0176(5)
C(5)	0.5688(4)	0.6205(3)	0.7779(3)	0.0163(5)
C(6)	0.1939(4)	0.6912(3)	0.7466(3)	0.0171(5)
C(7)	0.1472(4)	0.6978(4)	0.5771(3)	0.0271(6)
C(8)	0.3122(3)	0.2672(3)	0.8202(3)	0.0134(5)
C(9)	0.7762(4)	0.1233(3)	0.8687(3)	0.0190(5)
N(1)	0.4002(3)	0.5654(3)	0.7755(2)	0.0136(4)
N(3)	0.6546(3)	0.3176(3)	0.8271(2)	0.0137(4)
O(1)	0.1692(3)	0.2903(2)	0.9327(2)	0.0192(4)
S(1)	0.3657(1)	0.1322(1)	0.6765(1)	0.0202(2)

7.2.26 1-Ethyl-3-methyl-imidazolyliden-2-methylacetat (fin259)

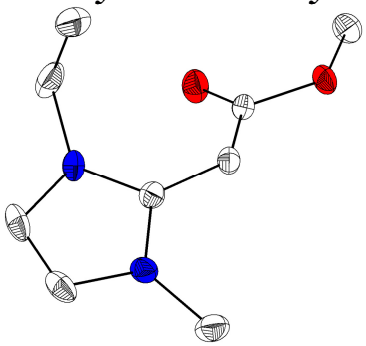

Kristalldaten

C9 H14 N2 O2	M = 182.22 g/mol	Triclinic, $P\bar{1}$
a = 7.7630(4) Å	b = 11.1839(6) Å	c = 11.5786(6) Å
α = 103.873(2)°	β = 103.774(2)°	γ = 90.465(2)°
V = 945.60(9) Å^3	Z = 4	F(000) = 392
D_{calc} = 1.280 g/cm^3	μ = 0.092 mm^{-1}	
colourless plate	0.260 · 0.130 · 0.050 mm^3	

Datensammlung

Diffraktometer: D8 Quest (Bruker)	T = 100(2) K	λ = 0.71073 Å
h = -9 bis 9	k = -14 bis 14	l = -14 bis 14
15884 gemessene Reflexe	4166 unabhängige Reflexe	3278 Reflexe mit $I > 2\sigma(I)$
θ = 2.298 bis 27.164°	R_{int} = 0.0333	C (25.00°) = 0.998
Absorptionskorrektur: Multi-scan	T_{min} = 0.7219	T_{max} = 0.7455

Verfeinerung

4166 Reflexe	0 Restraints	241 Parameter
Verfeinerung mit SHELXL-2014/7	bis χ = 0.000	
R_1 ($I > 2\sigma(I)$) = 0.0471	wR_2 ($I > 2\sigma(I)$) = 0.1041	
R_1 (all) = 0.0672	wR_2 (all) = 0.1127	GoF (S) = 1.059
$\Delta\varphi_{min}$ = -0.248 e·Å^{-3}	$\Delta\varphi_{max}$ = 0.441 e·Å^{-3}	

Fraktionelle Atomkoordinaten (*x, y, z*) und äquivalente isotrope Auslenkungsfaktoren *U*(eq)

	x	*y*	*z*	*U*(eq)/Å^2		*x*	*y*	*z*	*U*(eq)/Å^2
C(2)	0.7577(2)	0.0474(1)	0.8585(1)	0.0182(3)	C(17)	0.4210(3)	0.3126(2)	0.6292(2)	0.0319(4)
C(4)	0.9264(2)	0.2183(2)	0.9741(2)	0.0256(4)	C(18)	0.1761(2)	0.4853(1)	0.8400(1)	0.0184(3)
C(5)	0.8990(2)	0.2224(2)	0.8567(2)	0.0264(4)	C(19)	0.0374(2)	0.4795(1)	0.7352(1)	0.0183(3)
C(6)	0.7759(3)	0.0756(2)	0.6511(2)	0.0307(4)	C(20)	-0.1659(2)	0.6012(2)	0.6316(2)	0.0285(4)
C(7)	0.9037(3)	-0.0220(2)	0.6225(2)	0.0410(5)	C(21)	0.3186(2)	0.4764(2)	1.0971(2)	0.0249(4)
C(8)	0.6608(2)	-0.0672(1)	0.8293(2)	0.0197(3)	N(1)	0.7953(2)	0.1164(1)	0.7841(1)	0.0212(3)
C(9)	0.5153(2)	-0.1105(1)	0.7271(1)	0.0188(3)	N(3)	0.8386(2)	0.1106(1)	0.9756(1)	0.0207(3)
C(10)	0.2999(2)	-0.2794(2)	0.6242(2)	0.0272(4)	N(4)	0.3094(2)	0.2782(1)	0.8025(1)	0.0201(3)
C(11)	0.8158(2)	0.0767(2)	1.0857(2)	0.0281(4)	N(6)	0.3461(2)	0.3853(1)	0.9907(1)	0.0196(3)
C(12)	0.2697(2)	0.3863(1)	0.8721(1)	0.0171(3)	O(1)	0.4556(2)	-0.2292(1)	0.7212(1)	0.0228(3)
C(14)	0.4324(2)	0.2784(2)	0.9952(2)	0.0244(4)	O(2)	0.4376(2)	-0.0559(1)	0.6513(1)	0.0252(3)
C(15)	0.4085(2)	0.2117(2)	0.8794(2)	0.0248(4)	O(3)	-0.0240(2)	0.5955(1)	0.7348(1)	0.0221(3)
C(16)	0.2885(2)	0.2420(2)	0.6691(2)	0.0256(4)	O(4)	-0.0345(2)	0.3888(1)	0.6528(1)	0.0252(3)

7.2.27 1-Ethyl-3-methylimidazoltellon (fin214)

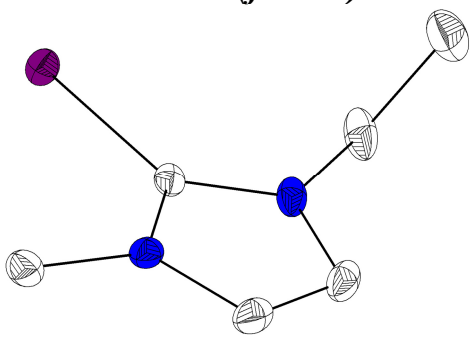

Kristalldaten

C6 H10 N2 Te	M = 237.76 g/mol	Monoclinic, $P2_1/n$
a = 6.9077(4) Å	b = 14.1382(8) Å	c = 8.4492(5) Å
α = 90°	β = 93.537(2)°	γ = 90°
V = 823.60(8) Å^3	Z = 4	F(000) = 448
D_{calc} = 1.917 g/cm^3	μ = 3.533 mm^{-1}	
light green block	0.158 · 0.076 · 0.063 mm^3	

Datensammlung

Diffraktometer: D8 Quest (Bruker)	T = 100(2) K	λ = 0.71073 Å
h = -8 bis 8	k = -18 bis 18	l = -10 bis 10
29299 gemessene Reflexe	1823 unabhängige Reflexe	1696 Reflexe mit $I > 2\sigma(I)$
θ = 2.812 bis 27.150°	R_{int} = 0.0262	C (25.00°) = 1.000
Absorptionskorrektur: Multi-scan	T_{min} = 0.6451	T_{max} = 0.7455

Verfeinerung

1823 Reflexe	0 Restraints	84 Parameter
Verfeinerung mit SHELXL-2014/7	bis χ = 0.001	
R_1 ($I > 2\sigma(I)$) = 0.0122	wR_2 ($I > 2\sigma(I)$) = 0.0293	
R_1 (all) = 0.0138	wR_2 (all) = 0.0298	GoF (S) = 1.157
$\Delta\varphi_{min}$ = -0.472 e·Å^{-3}	$\Delta\varphi_{max}$ = 0.276 e·Å^{-3}	

Fraktionelle Atomkoordinaten (*x, y, z*) und äquivalente isotrope Auslenkungsfaktoren *U*(eq)

	x	*y*	*z*	*U*(eq)/Å^2
C(2)	0.1184(2)	0.1045(1)	0.1938(2)	0.0130(3)
C(4)	-0.1797(2)	0.1321(1)	0.0822(2)	0.0193(3)
C(5)	-0.0738(3)	0.2111(1)	0.0651(2)	0.0204(3)
C(6)	0.2711(3)	0.2610(1)	0.1355(2)	0.0219(3)
C(7)	0.3494(3)	0.2720(1)	-0.0263(2)	0.0280(4)
C(8)	-0.1211(2)	-0.0271(1)	0.2100(2)	0.0181(3)
N(1)	0.1094(2)	0.1936(1)	0.1335(2)	0.0158(3)
N(3)	-0.0597(2)	0.0670(1)	0.1617(2)	0.0142(2)
Te(1)	0.3543(1)	0.0394(1)	0.3150(1)	0.0151(1)

7.2.28 1-Ethyl-3-methylimidazolium-2-methylensulfinat (jg25f5)

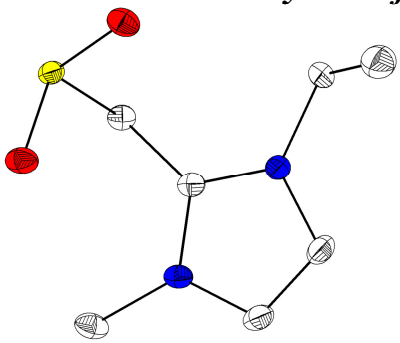

Kristalldaten

C7 H12 N2 O2 S	M = 188.25 g/mol	Monoclinic, $P2_1/c$
a = 7.4081(4) Å	b = 14.0607(7) Å	c = 8.6897(4) Å
α = 90°	β = 104.202(2)°	γ = 90°
V = 877.48(8) Å^3	Z = 4	F(000) = 400
D_{calc} = 1.425 g/cm^3	μ = 0.330 mm^{-1}	
yellow block	0.500 · 0.210 · 0.140 mm^3	

Datensammlung

Diffraktometer: D8 Quest (Bruker)	T = 100(2) K	λ = 0.71073 Å
h = -9 bis 9	k = 0 bis 18	l = 0 bis 11
1940 gemessene Reflexe	1940 unabhängige Reflexe	1703 Reflexe mit $I > 2\sigma(I)$
θ = 2.819 bis 27.111°	R_{int} = -(hklf5)	C (25.00°) = 1.000
Absorptionskorrektur: Multi-scan	T_{min} = 0.6881	T_{max} = 0.7455

Verfeinerung

1940 Reflexe	0 Restraints	112 Parameter
Verfeinerung mit SHELXL-2014/7	bis χ = 0.000	
R_1 ($I > 2\sigma(I)$) = 0.0365	wR_2 ($I > 2\sigma(I)$) = 0.0735	
R_1 (all) = 0.0476	wR_2 (all) = 0.0788	GoF (S) = 1.045
$\Delta\varphi_{min}$ = -0.357 e·Å^{-3}	$\Delta\varphi_{max}$ = 0.317 e·Å^{-3}	

Kommentar

Die Struktur wurde als nicht-meroedrischer Zwilling integriert und verfeinert.

Fraktionelle Atomkoordinaten (*x, y, z*) und äquivalente isotrope Auslenkungsfaktoren *U*(eq)

	x	*y*	*z*	*U*(eq)/Å^2		*x*	*y*	*z*	*U*(eq)/Å^2
C(2)	0.9186(3)	0.2748(1)	0.9213(2)	0.0138(4)	C(9)	1.0839(3)	0.1182(1)	0.9457(2)	0.0191(4)
C(4)	0.7641(3)	0.1574(1)	0.7765(3)	0.0188(4)	N(1)	0.7558(2)	0.3087(1)	0.8360(2)	0.0169(3)
C(5)	0.6575(3)	0.2356(2)	0.7472(3)	0.0216(4)	N(3)	0.9264(2)	0.1824(1)	0.8841(2)	0.0146(3)
C(6)	0.6898(3)	0.4071(1)	0.8419(3)	0.0198(4)	O(1)	1.1140(2)	0.4521(1)	0.8212(2)	0.0195(3)
C(7)	0.5969(3)	0.4439(2)	0.6792(3)	0.0276(5)	O(2)	1.2846(2)	0.3002(1)	0.8392(2)	0.0198(3)
C(8)	1.0657(3)	0.3277(1)	1.0326(2)	0.0143(4)	S(1)	1.2351(1)	0.3823(1)	0.9299(1)	0.0140(1)

7.2.29 Bis(1-ethyl-2,3-dimethylimidazolium)-cyanomalonat (fin251)

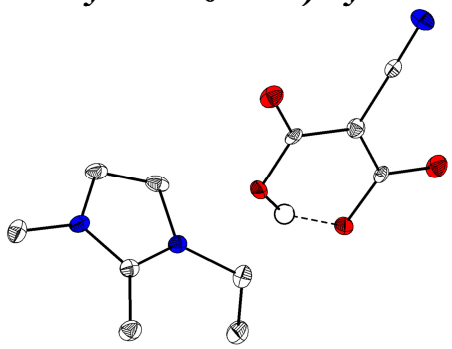

Kristalldaten

C18 H27 N5 O4	M = 377.44 g/mol	Triclinic, $P\bar{1}$
a = 6.9940(4) Å	b = 9.0238(5) Å	c = 15.6298(8) Å
α = 94.761(2)°	β = 92.476(2)°	γ = 102.408(2)°
V = 958.18(9) Å^3	Z = 2	F(000) = 404
D_{calc} = 1.308 g/cm^3	μ = 0.094 mm^{-1}	
colourless needle	0.460 · 0.070 · 0.060 mm^3	

Datensammlung

Diffraktometer: D8 Quest (Bruker)	T = 100(2) K	λ = 0.71073 Å
h = -8 bis 8	k = -10 bis 10	l = -18 bis 18
20590 gemessene Reflexe	3486 unabhängige Reflexe	2709 Reflexe mit $I > 2\sigma(I)$
θ = 2.321 bis 25.302°	R_{int} = 0.0476	C (25.00°) = 0.999
Absorptionskorrektur: Multi-scan	T_{min} = 0.6338	T_{max} = 0.7455

Verfeinerung

3486 Reflexe	3 Restraints	313 Parameter
Verfeinerung mit SHELXL-2014/7	bis χ = 0.000	
R_1 ($I > 2\sigma(I)$) = 0.0502	wR_2 ($I > 2\sigma(I)$) = 0.1228	
R_1 (all) = 0.0678	wR_2 (all) = 0.1332	GoF (S) = 1.048
$\Delta\varphi_{min}$ = -0.344 e·Å^{-3}	$\Delta\varphi_{max}$ = 0.205 e·Å^{-3}	

Kommentar

Diese Struktur wurde durch Dr. Klaus Harms gelöst und bis zum vollständigen Modell verfeinert. Nur die abschließende Verfeinerung und Vervollständigung der kristallographischen Daten habe ich selbst übernommen.

Fraktionelle Atomkoordinaten (*x, y, z*) und äquivalente isotrope Auslenkungsfaktoren *U*(eq)

	x	*y*	*z*	*U*(eq)/Å^2
N(23)	0.0572(2)	0.6443(2)	0.1180(1)	0.0152(4)
C(14)	0.1213(3)	0.8777(2)	0.3969(1)	0.0167(4)
C(15)	0.1315(3)	0.8386(2)	0.4776(1)	0.0168(4)
C(12)	-0.1838(3)	0.7994(2)	0.4350(1)	0.0138(4)
C(16)	-0.1158(3)	0.7393(2)	0.5852(1)	0.0182(4)
C(18)	-0.4001(3)	0.7639(2)	0.4315(1)	0.0197(5)
C(17)	-0.1750(3)	0.5674(2)	0.5837(1)	0.0237(5)
C(19)	-0.1564(3)	0.8807(2)	0.2871(1)	0.0195(4)
C(25)	-0.1367(3)	0.6748(2)	0.0098(1)	0.0176(4)
C(24)	-0.1362(3)	0.6326(2)	0.0904(1)	0.0178(4)
C(22)	0.1727(3)	0.6928(2)	0.0555(1)	0.0152(4)
C(26)	0.1233(3)	0.7677(2)	-0.0927(1)	0.0207(5)
C(28)	0.3886(3)	0.7169(2)	0.0602(1)	0.0215(5)
C(27)	0.1979(3)	0.9382(2)	-0.0842(1)	0.0262(5)
C(29)	0.1278(3)	0.6141(2)	0.2026(1)	0.0222(5)
O(1)	0.3246(2)	0.6540(2)	0.6216(1)	0.0169(4)

	x	*y*	*z*	*U*(eq)/Å^2
N(1)	0.7430(4)	0.9908(3)	0.8321(2)	0.0243(5)
C(1)	0.4352(3)	0.7776(2)	0.6650(1)	0.0113(5)
O(2)	0.4647(2)	0.9017(2)	0.6327(1)	0.0204(3)
N(13)	-0.0752(2)	0.8525(2)	0.3710(1)	0.0149(4)
N(11)	-0.0591(2)	0.7898(2)	0.5007(1)	0.0137(4)
C(2)	0.5115(3)	0.7567(2)	0.7483(1)	0.0148(4)
O(4)	0.5420(2)	0.5995(2)	0.8594(1)	0.0202(3)
N(21)	0.0560(2)	0.7117(2)	-0.0111(1)	0.0150(4)
C(3)	0.4753(3)	0.6129(2)	0.7854(1)	0.0109(5)
O(3)	0.3618(2)	0.4982(2)	0.7383(1)	0.0168(4)
C(4)	0.6399(3)	0.8858(3)	0.7951(1)	0.0121(5)
O(3A)	0.6770(16)	0.8485(14)	0.8756(7)	0.051(3)
C(4A)	0.357(2)	0.611(2)	0.7013(12)	0.037(4)
O(1A)	0.6362(15)	1.0051(12)	0.7586(7)	0.042(3)
C(3A)	0.573(2)	0.7287(17)	0.8339(9)	0.034(4)
N(1A)	0.257(3)	0.5048(18)	0.6678(12)	0.053(4)
C(1A)	0.526(2)	0.8939(17)	0.7105(9)	0.032(3)

7.2.30 Dilithium-rhodizonat-dimethylsulfoxidaddukt-solvat (fin017a)

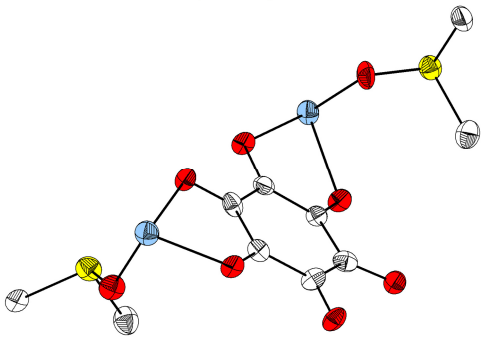

Kristalldaten

C12 H18 Li2 O9 S3	M = 416.32 g/mol	Monoclinic, $P2_1/c$
a = 14.6040(16) Å	b = 7.7088(7) Å	c = 16.182(3) Å
α = 90°	β = 94.810(12)°	γ = 90°
V = 1815.3(4) Å^3	Z = 4	F(000) = 864
D_{calc} = 1.523 g/cm^3	μ = 0.450 mm^{-1}	
red needle	0.310 · 0.040 · 0.030 mm^3	

Datensammlung

Diffraktometer: STOE IPDS 2	T = 100(2) K	λ = 0.71073 Å
h = -18 bis 16	k = -9 bis 8	l = -20 bis 20
12668 gemessene Reflexe	3849 unabhängige Reflexe	1679 Reflexe mit $I > 2\sigma(I)$
θ = 2.526 bis 26.798°	R_{int} = 0.1114	C (25.00°) = 0.999
Absorptionskorrektur: Multi-scan	T_{min} = 0.8739	T_{max} = 1.0660

Verfeinerung

3849 Reflexe	150 Restraints	277 Parameter
Verfeinerung mit SHELXL-2014/7	bis χ = 0.000	
R_1 ($I > 2\sigma(I)$) = 0.1002	wR_2 ($I > 2\sigma(I)$) = 0.2346	
R_1 (all) = 0.2039	wR_2 (all) = 0.2639	GoF (S) = 1.045
$\Delta\varphi_{min}$ = -0.546 e·Å^{-3}	$\Delta\varphi_{max}$ = 0.512 e·Å^{-3}	

Kommentar

Die geringe Kristallqualität und Fehlordnung lassen keine optimale Verfeinerung zu. Die Struktur wurde über, DELU, RIGU, SIMU und ISOR restrained, einzelne Atome wurden über EADP constrained.

Fraktionelle Atomkoordinaten (*x, y, z*) und äquivalente isotrope Auslenkungsfaktoren *U*(eq)

	x	*y*	*z*	*U*(eq)/Å^2
C(1)	0.6747(7)	0.4143(13)	0.8107(5)	0.024(2)
C(2)	0.6251(7)	0.2552(13)	0.7964(5)	0.025(2)
C(3)	0.6722(7)	0.0945(13)	0.8161(5)	0.024(2)
C(4)	0.7686(7)	0.0917(13)	0.8462(6)	0.024(2)
C(5)	0.8218(7)	0.2546(14)	0.8585(5)	0.026(2)
C(6)	0.7739(6)	0.4189(12)	0.8342(5)	0.021(2)
C(10)	0.8669(7)	0.6121(14)	1.0462(6)	0.035(3)
C(11)	0.7337(7)	0.7397(16)	1.1369(5)	0.034(2)
C(12)	1.0107(7)	0.0863(15)	0.2464(6)	0.036(3)
C(13)	0.9832(8)	0.1673(15)	0.0833(6)	0.038(3)
Li(2)	0.7102(11)	0.751(2)	0.8542(9)	0.027(3)
O(1)	0.6324(5)	0.5563(7)	0.7985(4)	0.0246(10)
O(2)	0.5408(4)	0.2565(8)	0.7720(3)	0.0237(14)
O(3)	0.6282(5)	-0.0480(7)	0.8067(4)	0.0246(10)
O(4)	0.8061(5)	-0.0543(8)	0.8633(4)	0.0286(17)

	x	*y*	*z*	*U*(eq)/Å^2
O(5)	0.9023(4)	0.2531(9)	0.8906(4)	0.0270(14)
O(6)	0.8153(5)	0.5605(8)	0.8397(4)	0.0257(16)
O(10)	0.7038(5)	0.7021(9)	0.9747(4)	0.0324(18)
O(11)	0.8531(5)	0.2231(10)	0.1839(4)	0.0369(18)
S(10)	0.7779(2)	0.7680(3)	1.0380(1)	0.0294(6)
S(11)	0.9196(2)	0.0828(3)	0.1645(2)	0.0295(6)
C(14)	0.5100(14)	0.151(2)	0.4718(12)	0.0246(10)
C(15)	0.679(2)	0.254(7)	0.544(3)	0.038(7)
Li(1)	0.509(3)	0.010(4)	0.733(3)	0.031(7)
O(12)	0.5586(10)	0.0419(17)	0.6231(8)	0.032(3)
S(12)	0.5541(5)	0.2065(12)	0.5740(4)	0.0320(17)
C(14A)	0.5059(15)	0.332(2)	0.4738(11)	0.021(4)
C(15A)	0.663(2)	0.263(8)	0.550(3)	0.037(6)
Li(1A)	0.508(3)	0.499(4)	0.727(2)	0.022(6)
O(12A)	0.5615(10)	0.4689(17)	0.6196(8)	0.028(3)
S(12A)	0.5618(5)	0.2974(11)	0.5762(4)	0.0263(17)

7.2.31 1-Ethyl-3-methylimidazolium-bis(5,6-dicyanopyrazin-2,3-diolato)borat (fin085)

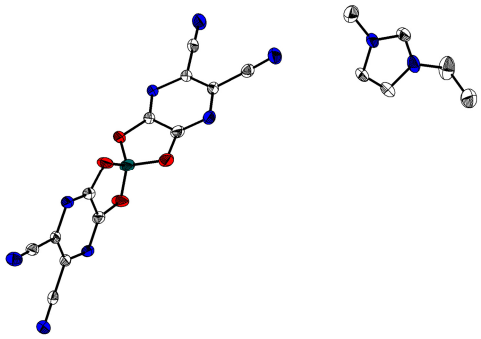

Kristalldaten

C58 H39 B3 N32 O12	M = 1408.64 g/mol	Monoclinic, $C2/c$
a = 15.460(5) Å	b = 9.897(5) Å	c = 41.241(5) Å
α = 90.000(5)°	β = 93.289(5)°	γ = 90.000(5)°
V = 6300(4) Å^3	Z = 4	F(000) = 2888
D_{calc} = 1.485 g/cm^3	μ = 0.110 mm^{-1}	
fluorescent colourless plate	0.520 · 0.170 · 0.120 mm^3	

Datensammlung

Diffraktometer: D8 Quest (Bruker)	T = 100(2) K	λ = 0.71069 Å
h = -19 bis 19	k = -12 bis 12	l = -52 bis 52
54995 gemessene Reflexe	6977 unabhängige Reflexe	4187 Reflexe mit $I > 2\sigma(I)$
θ = 2.445 bis 27.161°	R_{int} = 0.0961	C (25.00°) = 0.999
Absorptionskorrektur: Multi-scan	T_{min} = 0.5733	T_{max} = 0.7455

Verfeinerung

6977 Reflexe	98 Restraints	516 Parameter
Verfeinerung mit SHELXL-2014/7	bis χ = 0.001	
R_1 ($I > 2\sigma(I)$) = 0.0623	wR_2 ($I > 2\sigma(I)$) = 0.1282	
R_1 (all) = 0.1259	wR_2 (all) = 0.1526	GoF (S) = 1.014
$\Delta\varphi_{min}$ = -0.366 e·Å^{-3}	$\Delta\varphi_{max}$ = 0.603 e·Å^{-3}	

Kommentar

Ein Imidazoliumkation ist über eine zweizählige Drehachse fehlgeordnet (50:50). Dieses wurde über DFIX, DELU, RIGU, FLAT und SAME restrained.

Fraktionelle Atomkoordinaten (*x, y, z*) und äquivalente isotrope Auslenkungsfaktoren *U*(eq)

	x	*y*	*z*	*U*(eq)/Å^2		*x*	*y*	*z*	*U*(eq)/Å^2
C(1)	0.2414(2)	0.1812(3)	0.6744(1)	0.0291(7)	C(41)	0.8862(2)	0.9551(3)	0.5925(1)	0.0463(8)
C(2)	0.1568(2)	0.2313(3)	0.6794(1)	0.0268(6)	C(42)	0.8494(2)	0.9697(3)	0.5595(1)	0.0456(8)
C(3)	0.2087(2)	0.1822(3)	0.6212(1)	0.0232(6)	B(1)	0.2286(3)	0.2110(3)	0.7286(1)	0.0387(9)
C(4)	0.1270(2)	0.2271(3)	0.6263(1)	0.0219(6)	B(2)	0.5000	-0.0518(4)	0.7500	0.0237(9)
C(5)	0.2346(2)	0.1583(3)	0.5888(1)	0.0258(6)	N(1)	0.2704(1)	0.1575(2)	0.6459(1)	0.0287(5)
C(6)	0.0662(2)	0.2467(3)	0.5990(1)	0.0253(6)	N(2)	0.0978(1)	0.2540(2)	0.6563(1)	0.0251(5)
C(7)	0.2825(2)	0.2831(3)	0.7772(1)	0.0293(7)	N(3)	0.2536(2)	0.1418(3)	0.5627(1)	0.0373(6)
C(8)	0.2505(2)	0.1492(3)	0.7808(1)	0.0296(7)	N(4)	0.0187(2)	0.2605(3)	0.5768(1)	0.0376(6)
C(9)	0.3245(2)	0.2834(3)	0.8295(1)	0.0219(6)	N(5)	0.2549(1)	0.0810(2)	0.8077(1)	0.0262(5)
C(10)	0.2943(2)	0.1539(3)	0.8326(1)	0.0219(6)	N(6)	0.3195(1)	0.3536(2)	0.8008(1)	0.0268(5)
C(11)	0.3668(2)	0.3524(3)	0.8566(1)	0.0234(6)	N(7)	0.4013(2)	0.4076(2)	0.8781(1)	0.0323(6)
C(12)	0.3059(2)	0.0844(3)	0.8633(1)	0.0225(6)	N(8)	0.3158(1)	0.0289(2)	0.8875(1)	0.0291(5)
C(13)	0.4981(2)	0.0042(3)	0.6967(1)	0.0200(6)	N(9)	0.3889(1)	-0.1526(2)	0.6769(1)	0.0218(5)
C(14)	0.4370(2)	-0.1001(3)	0.7006(1)	0.0208(6)	N(10)	0.5110(1)	0.0631(2)	0.6693(1)	0.0205(5)
C(15)	0.4606(2)	0.0099(2)	0.6441(1)	0.0194(5)	N(11)	0.4735(2)	0.1211(2)	0.5877(1)	0.0316(6)
C(16)	0.4034(2)	-0.0945(2)	0.6477(1)	0.0195(5)	N(12)	0.3139(1)	-0.1883(2)	0.5979(1)	0.0323(6)
C(17)	0.4686(2)	0.0719(3)	0.6127(1)	0.0235(6)	N(41)	0.8209(2)	0.9803(3)	0.5337(1)	0.0626(9)
C(18)	0.3531(2)	-0.1464(3)	0.6200(1)	0.0223(6)	O(1)	0.2858(1)	0.1648(2)	0.7025(1)	0.0382(5)

	x	y	z	U(eq)/Å^2
O(2)	0.1464(1)	0.2499(2)	0.7107(1)	0.0352(5)
O(3)	0.2705(2)	0.3231(2)	0.7467(1)	0.0402(6)
O(4)	0.2148(2)	0.1051(2)	0.7527(1)	0.0413(6)
O(5)	0.4352(1)	-0.1360(2)	0.7316(1)	0.0262(4)
O(6)	0.5386(1)	0.0349(2)	0.7251(1)	0.0243(4)
C(27)	0.4318(2)	-0.4062(4)	0.4629(1)	0.0525(9)
C(22)	0.3747(2)	-0.0631(3)	0.4688(1)	0.0393(8)
C(24)	0.3738(2)	-0.0678(3)	0.5211(1)	0.0361(7)
C(25)	0.3685(2)	-0.1954(3)	0.5107(1)	0.0402(8)
C(26)	0.3636(2)	-0.3072(4)	0.4555(1)	0.0525(10)
C(28)	0.3825(2)	0.1644(3)	0.4956(1)	0.0505(9)
N(21)	0.3687(2)	-0.1908(3)	0.4775(1)	0.0352(6)
N(23)	0.3784(2)	0.0143(3)	0.4948(1)	0.0341(6)
C(37)	-0.0723(6)	-0.0960(10)	0.6787(2)	0.073(2)
C(32)	0.0140(7)	0.0454(8)	0.7612(2)	0.087(3)
C(34)	0.0142(7)	-0.1598(8)	0.7768(2)	0.075(3)
C(35)	-0.0131(9)	-0.1601(7)	0.7440(2)	0.083(3)
C(36)	-0.0233(5)	0.0197(11)	0.7040(2)	0.063(2)
C(38)	0.0520(7)	0.0044(9)	0.8183(2)	0.075(3)
N(31)	-0.0083(4)	-0.0385(6)	0.7386(1)	0.0529(15)
N(33)	0.0380(4)	-0.0560(7)	0.7882(2)	0.0547(16)

7.2.32 Dimethylpyrrolidinium-bis(5,6-dicyanopyrazin-2,3-diolato)borat (fin289)

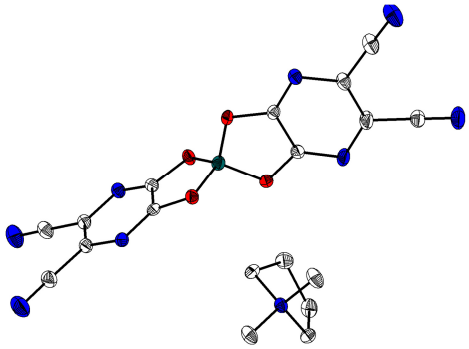

Kristalldaten

C18 H14 B N9 O4	M = 431.19 g/mol	Triclinic, P-1
a = 10.1140(6) Å	b = 11.7988(7) Å	c = 17.7771(10) Å
α = 87.703(2)°	β = 74.253(2)°	γ = 79.855(2)°
V = 2009.8(2) Å^3	Z = 4	F(000) = 888
D_{calc} = 1.425 g/cm^3	μ = 0.105 mm^{-1}	
colourless block	0.460 · 0.220 · 0.120 mm^3	

Datensammlung

Diffraktometer: D8 Quest (Bruker)	T = 100(2) K	λ = 0.71073 Å
h = -12 bis 12	k = -15 bis 15	l = -22 bis 22
22424 gemessene Reflexe	8855 unabhängige Reflexe	5996 Reflexe mit $I > 2\sigma(I)$
θ = 2.381 bis 27.151°	R_{int} = 0.0391	C (25.00°) = 0.997
Absorptionskorrektur: Multi-scan	T_{min} = 0.6730	T_{max} = 0.7455

Verfeinerung

8855 Reflexe	149 Restraints	730 Parameter
Verfeinerung mit SHELXL-2014/7	bis χ = 0.001	
R_1 ($I > 2\sigma(I)$) = 0.0531	wR_2 ($I > 2\sigma(I)$) = 0.0979	
R_1 (all) = 0.0944	wR_2 (all) = 0.1102	GoF (S) = 1.045
$\Delta\varphi_{min}$ = -0.286 e·Å^{-3}	$\Delta\varphi_{max}$ = 0.336 e·Å^{-3}	

Kommentar

Pro asymmetrische Einheit liegen zwei Kationen und Anionen vor. Jeweils ein Kation und Teile beider Anionen sind ca. im Verhältnis 50:50 fehlgeordnet. Die Fehlordnungen wurden über DELU, RIGU und SAME restrained

Fraktionelle Atomkoordinaten (*x, y, z*) und äquivalente isotrope Auslenkungsfaktoren *U*(eq)

	x	*y*	*z*	*U*(eq)/Å^2
C(1)	0.7278(2)	0.7911(2)	0.9487(1)	0.0146(4)
C(2)	0.8428(2)	0.8476(2)	0.9139(1)	0.0151(4)
C(3)	0.6423(2)	0.9325(2)	1.0360(1)	0.0172(4)
C(4)	0.7535(2)	0.9873(2)	1.0021(1)	0.0168(4)
C(5)	0.5338(2)	0.9832(2)	1.1023(1)	0.0230(4)
C(6)	0.7633(2)	1.0953(2)	1.0334(1)	0.0216(4)
C(7)	0.9810(2)	0.5171(2)	0.7833(1)	0.0150(4)
C(8)	0.9009(2)	0.5813(2)	0.7358(1)	0.0172(4)
C(9)	1.0495(2)	0.3769(2)	0.6947(1)	0.0197(4)
C(10)	0.9691(2)	0.4378(2)	0.6503(1)	0.0243(5)
C(11)	1.1286(2)	0.2648(2)	0.6694(1)	0.0249(5)
C(13)	0.1250(2)	0.9924(2)	0.7805(1)	0.0152(4)
C(14)	0.0022(2)	1.0097(2)	0.7541(1)	0.0179(4)
C(15)	0.0383(2)	1.1479(2)	0.8548(1)	0.0142(4)
C(16)	-0.0803(2)	1.1651(2)	0.8291(1)	0.0158(4)
C(17)	0.0551(2)	1.2267(2)	0.9103(1)	0.0146(4)
C(18)	-0.1883(2)	1.2631(2)	0.8558(1)	0.0212(4)
O(7)	0.1466(1)	0.7335(1)	0.6963(1)	0.0206(3)
O(8)	0.2358(2)	0.8718(1)	0.6066(1)	0.0347(4)
C(19)	0.2132(2)	0.6853(2)	0.6274(1)	0.0242(5)
C(20)	0.2661(3)	0.7693(2)	0.5732(1)	0.0371(6)
N(13)	0.2292(2)	0.5766(1)	0.6110(1)	0.0293(4)
C(31)	0.2885(2)	0.5964(2)	0.8199(1)	0.0180(4)
C(32)	0.4149(2)	0.6508(2)	0.7789(1)	0.0231(5)
C(34)	0.5296(2)	0.5995(2)	0.8175(1)	0.0258(5)
C(35)	0.4514(2)	0.5650(2)	0.8974(1)	0.0225(5)
C(36)	0.2119(2)	0.5265(2)	0.9561(1)	0.0235(5)
C(37)	0.3735(2)	0.3975(2)	0.8555(1)	0.0262(5)
B(1)	0.8696(2)	0.6847(2)	0.8457(1)	0.0168(5)
B(2)	0.1509(3)	0.8588(2)	0.6886(1)	0.0227(5)
N(1)	0.6264(2)	0.8298(1)	1.0089(1)	0.0165(3)
N(2)	0.8590(2)	0.9453(1)	0.9382(1)	0.0175(3)
N(3)	0.4471(2)	1.0265(2)	1.1536(1)	0.0364(5)
N(4)	0.7714(2)	1.1817(2)	1.0576(1)	0.0317(4)
N(5)	1.0564(2)	0.4165(1)	0.7648(1)	0.0172(3)
N(6)	0.8911(2)	0.5447(1)	0.6699(1)	0.0242(4)
N(7)	1.1895(2)	0.1752(2)	0.6484(1)	0.0356(5)
N(9)	0.1469(2)	1.0591(1)	0.8304(1)	0.0163(3)
N(10)	-0.1015(2)	1.0940(1)	0.7760(1)	0.0201(4)
N(11)	0.0692(2)	1.2881(1)	0.9545(1)	0.0208(4)
N(12)	-0.2719(2)	1.3428(2)	0.8766(1)	0.0337(5)
N(18)	0.3296(2)	0.5196(1)	0.8835(1)	0.0166(3)
O(1)	0.7399(1)	0.6935(1)	0.9110(1)	0.0175(3)
O(2)	0.9297(1)	0.7873(1)	0.8539(1)	0.0178(3)
O(3)	0.9656(1)	0.5749(1)	0.8482(1)	0.0171(3)
O(4)	0.8370(1)	0.6819(1)	0.7692(1)	0.0182(3)
O(5)	0.2138(1)	0.9014(1)	0.7449(1)	0.0201(3)
O(6)	0.0112(2)	0.9294(1)	0.7015(1)	0.0244(3)
N(17)	0.3042(12)	0.0881(7)	0.3837(8)	0.0155(18)
C(25)	0.3723(5)	0.0463(3)	0.4481(2)	0.0230(10)
C(26)	0.4887(4)	-0.0459(4)	0.4094(3)	0.0321(11)
C(27)	0.4505(5)	-0.0910(3)	0.3383(3)	0.0327(11)
C(28)	0.3041(9)	-0.0226(6)	0.3448(5)	0.0268(18)
C(29)	0.1612(4)	0.1529(4)	0.4144(3)	0.0289(11)
C(30)	0.3905(4)	0.1632(4)	0.3281(2)	0.0263(10)
N(17A)	0.3281(13)	0.0570(8)	0.3843(8)	0.0174(19)
C(25A)	0.2816(10)	-0.0504(7)	0.3655(5)	0.028(2)
C(26A)	0.1447(4)	-0.0542(3)	0.4239(2)	0.0264(10)
C(27A)	0.1185(4)	0.0457(4)	0.4818(3)	0.0358(12)
C(28A)	0.2615(5)	0.0762(4)	0.4704(2)	0.0265(10)
C(29A)	0.4823(4)	0.0481(5)	0.3644(3)	0.0430(13)
C(30A)	0.2746(5)	0.1578(3)	0.3393(2)	0.0250(10)
N(14)	0.3034(16)	0.7509(5)	0.4990(3)	0.0205(19)
N(15)	0.3149(14)	0.3450(7)	0.4875(6)	0.0303(18)
N(16)	0.437(2)	0.5806(9)	0.3371(4)	0.065(4)
C(21)	0.2744(13)	0.5550(6)	0.5353(5)	0.0161(16)
C(22)	0.3189(16)	0.6362(6)	0.4815(3)	0.0218(19)
C(23)	0.2946(13)	0.4377(7)	0.5092(6)	0.0202(16)
C(24)	0.3843(19)	0.6045(7)	0.4007(4)	0.038(3)
N(14A)	0.3618(12)	0.7449(4)	0.5020(3)	0.0172(14)
N(15A)	0.3706(16)	0.3381(8)	0.4863(6)	0.041(2)
N(16A)	0.5091(13)	0.5753(8)	0.3395(4)	0.046(2)
C(21A)	0.3255(13)	0.5492(6)	0.5338(4)	0.0151(16)
C(22A)	0.3776(13)	0.6312(5)	0.4827(3)	0.0166(15)
C(23A)	0.3479(15)	0.4312(7)	0.5089(6)	0.0244(18)
C(24A)	0.4507(13)	0.6020(6)	0.4024(3)	0.0265(18)
N(8A)	0.986(3)	0.3492(7)	0.5175(7)	0.035(4)
C(12A)	0.982(2)	0.3925(10)	0.5741(7)	0.021(2)
N(8)	0.925(2)	0.3424(8)	0.5292(6)	0.024(2)
C(12)	0.938(2)	0.3819(14)	0.5837(8)	0.019(2)

7.2.33 Dilithium-di(bistetrazolato)-difluoro-oxodiborat-acetonitriladdukt-solvat (fin145_2)

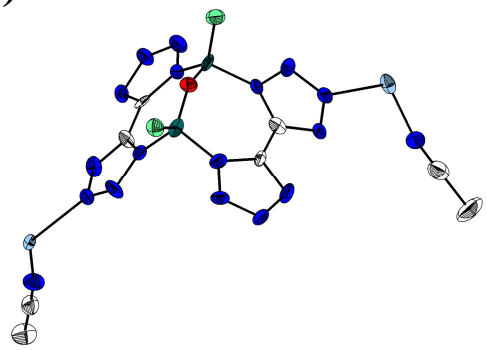

Kristalldaten

C14 H15 B2 F2 Li2 N21 O	*M* = 566.97 g/mol	Monoclinic, $P2_1/n$
a = 9.6535(14) Å	*b* = 18.036(2) Å	*c* = 15.8966(18) Å
α = 90°	β = 101.860(10)°	γ = 90°
V = 2708.6(6) Å^3	*Z* = 4	*F*(000) = 1152
D_{calc} = 1.390 g/cm^3	μ = 0.109 mm^{-1}	
colourless block	0.260 · 0.090 · 0.080 mm^3	

Datensammlung

Diffraktometer: STOE IPDS 2	T = 100(2) K	λ = 0.71073 Å
h = -11 bis 11	k = -21 bis 21	l = -19 bis 19
13720 gemessene Reflexe	13720 unabhängige Reflexe	2420 Reflexe mit $I > 2\sigma(I)$
θ = 1.729 bis 25.612°	R_{int} = -(hklf5)	C (25.00°) = 1.000
Absorptionskorrektur: Keine		

Verfeinerung

13720 Reflexe	7 Restraints	385 Parameter
Verfeinerung mit SHELXL-2014/7	bis χ = 0.031	
R_1 ($I > 2\sigma(I)$) = 0.0612	wR_2 ($I > 2\sigma(I)$) = 0.0895	
R_1 (all) = 0.2816	wR_2 (all) = 0.1400	GoF (S) = 0.589
$\Delta\varphi_{min}$ = -0.317 e·Å^{-3}	$\Delta\varphi_{max}$ = 0.387 e·Å^{-3}	

Kommentar

Die Struktur wurde als nicht-meroedrischer Zwilling integriert und verfeinert. Anstelle einer Absorptionskorrektur wurden die erweiterten Integrationsoptionen von X-Area (Merging von Friedel-Paaren und equivalenten Reflexen) gewählt. Aufgrund des Zwillingsanteils und der sehr schwachen Streuung ist keine optimale Verfeinerung möglich. Mehrere Atome wurden über DELU restrained.

Fraktionelle Atomkoordinaten (*x, y, z*) und äquivalente isotrope Auslenkungsfaktoren *U*(eq)

	x	*y*	*z*	*U*(eq)/Å^2		*x*	*y*	*z*	*U*(eq)/Å^2
C(1)	0.9522(11)	0.1988(6)	0.1973(7)	0.018(3)	N(4)	0.9990(8)	0.2291(5)	0.1319(6)	0.023(2)
C(2)	1.0357(10)	0.2035(6)	0.2827(7)	0.022(3)	N(5)	1.0154(8)	0.1755(5)	0.3570(6)	0.020(2)
C(3)	0.5853(11)	0.2014(6)	0.3125(7)	0.021(3)	N(6)	1.1258(9)	0.1967(5)	0.4198(6)	0.028(2)
C(4)	0.6702(10)	0.1974(6)	0.3968(7)	0.021(3)	N(7)	1.2076(8)	0.2358(5)	0.3822(6)	0.026(2)
C(5)	0.8053(14)	0.4424(8)	1.0412(9)	0.080(5)	N(8)	1.1542(9)	0.2428(5)	0.2962(6)	0.026(2)
C(6)	0.8774(11)	0.4315(8)	0.9677(9)	0.050(4)	N(9)	0.4648(8)	0.2407(5)	0.2980(6)	0.023(2)
C(7)	0.4676(13)	0.1289(6)	0.9667(8)	0.047(3)	N(10)	0.4123(9)	0.2351(5)	0.2134(6)	0.027(2)
C(8)	0.3607(13)	0.0849(7)	0.9962(8)	0.049(4)	N(11)	0.4954(9)	0.1912(5)	0.1765(6)	0.023(2)
C(9)	0.0835(13)	0.4915(7)	0.2737(9)	0.065(4)	N(12)	0.6083(8)	0.1703(5)	0.2383(5)	0.017(2)
C(10)	0.1390(12)	0.4320(7)	0.2264(8)	0.038(3)	N(13)	0.7983(9)	0.1642(5)	0.4253(6)	0.024(2)
C(11)	0.5642(11)	0.4058(6)	0.1839(8)	0.045(3)	N(14)	0.8312(9)	0.1753(5)	0.5115(6)	0.025(2)
C(12)	0.6871(12)	0.3617(6)	0.2253(7)	0.029(3)	N(15)	0.7290(9)	0.2136(5)	0.5333(6)	0.028(2)
C(13)	1.4966(12)	0.5232(5)	0.3775(8)	0.041(3)	N(16)	0.6266(9)	0.2287(5)	0.4639(6)	0.027(2)
C(14)	1.4586(12)	0.4466(7)	0.3943(8)	0.033(3)	N(17)	0.9333(11)	0.4225(5)	0.9119(8)	0.061(3)
Li(1)	0.2129(17)	0.2756(11)	0.1617(11)	0.026(5)	N(18)	0.2775(12)	0.0481(7)	1.0187(8)	0.077(4)
Li(2)	1.4158(16)	0.2752(10)	0.4307(10)	0.025(5)	N(19)	0.1790(12)	0.3850(5)	0.1920(7)	0.037(3)
B(1)	0.7322(12)	0.1169(7)	0.2181(9)	0.023(3)	N(20)	0.7871(9)	0.3296(5)	0.2587(6)	0.044(3)
B(2)	0.8912(13)	0.1198(7)	0.3720(9)	0.021(3)	N(21)	1.4315(10)	0.3862(5)	0.4062(6)	0.036(3)
N(1)	0.8238(9)	0.1690(5)	0.1682(6)	0.021(2)	F(1)	0.6682(6)	0.0648(3)	0.1637(4)	0.0302(16)
N(2)	0.7896(9)	0.1800(6)	0.0827(6)	0.032(3)	F(2)	0.9584(6)	0.0648(3)	0.4271(4)	0.0272(16)
N(3)	0.8942(9)	0.2156(5)	0.0612(6)	0.026(2)	O(1)	0.8133(8)	0.0926(3)	0.2962(5)	0.0225(14)

7.2.34 Dilithium-di(bistetrazolato)-tetrafluorodiborat-tetrahydrofuranaddukt (lhf172)

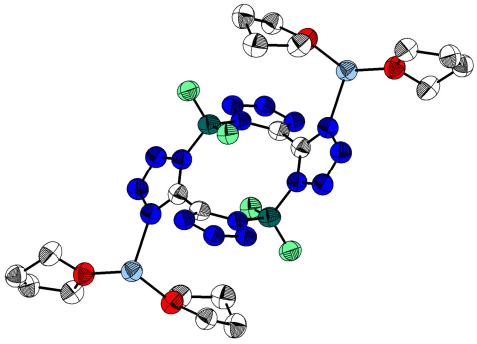

Kristalldaten

C10 H16 B F2 Li N8 O2	M = 336.06 g/mol	Triclinic, $P\bar{1}$
a = 8.1367(13) Å	b = 9.2057(16) Å	c = 11.0783(17) Å
α = 107.287(13)°	β = 101.500(13)°	γ = 97.456(13)°
V = 760.4(2) Å^3	Z = 2	F(000) = 348
D_{calc} = 1.468 g/cm^3	μ = 0.121 mm^{-1}	
colourless block	0.240 · 0.180 · 0.070 mm^3	

Datensammlung

Diffraktometer: STOE IPDS 2	T = 100(2) K	λ = 0.71073 Å
h = -10 bis 10	k = -11 bis 11	l = -14 bis 13
6652 gemessene Reflexe	3209 unabhängige Reflexe	1528 Reflexe mit $I > 2\sigma(I)$
θ = 1.989 bis 26.828°	R_{int} = 0.0599	C (25.00°) = 0.995

Verfeinerung

3209 Reflexe	0 Restraints	217 Parameter
Verfeinerung mit SHELXL-2014/7	bis χ = 0.000	
R_1 ($I > 2\sigma(I)$) = 0.0401	wR_2 ($I > 2\sigma(I)$) = 0.0803	
R_1 (all) = 0.0991	wR_2 (all) = 0.0915	GoF (S) = 0.762
$\Delta\varphi_{min}$ = -0.157 e·Å^{-3}	$\Delta\varphi_{max}$ = 0.157 e·Å^{-3}	

Fraktionelle Atomkoordinaten (*x, y, z*) und äquivalente isotrope Auslenkungsfaktoren *U*(eq)

	x	*y*	*z*	*U*(eq)/Å^2		*x*	*y*	*z*	*U*(eq)/Å^2
C(1)	0.1251(3)	0.8729(3)	0.6291(2)	0.0478(5)	N(1)	0.2072(2)	1.0177(2)	0.6508(2)	0.0481(5)
C(2)	0.0325(3)	0.7573(2)	0.5027(2)	0.0479(5)	N(2)	0.2714(2)	1.0827(2)	0.7820(2)	0.0547(5)
C(3)	0.1037(3)	0.7214(3)	1.0853(2)	0.0620(7)	N(3)	0.2286(2)	0.9793(2)	0.8350(2)	0.0546(5)
C(4)	0.2575(3)	0.7140(3)	1.1861(2)	0.0615(6)	N(4)	0.1367(2)	0.8452(2)	0.7410(2)	0.0511(5)
C(5)	0.3586(3)	0.6189(3)	1.1026(2)	0.0593(6)	N(5)	0.0815(2)	0.6270(2)	0.4487(2)	0.0504(5)
C(6)	0.3280(3)	0.6707(3)	0.9856(2)	0.0662(7)	N(6)	-0.0416(2)	0.5522(2)	0.3368(2)	0.0521(5)
C(7)	-0.3499(3)	0.6029(3)	0.6565(2)	0.0566(6)	N(7)	-0.1612(2)	0.6322(2)	0.3223(2)	0.0523(5)
C(8)	-0.4877(3)	0.6956(3)	0.6823(2)	0.0660(7)	N(8)	-0.1175(2)	0.7627(2)	0.4270(2)	0.0476(5)
C(9)	-0.3886(3)	0.8487(3)	0.7799(2)	0.0677(7)	F(1)	0.1739(2)	1.0095(1)	0.4307(1)	0.0530(3)
C(10)	-0.2470(3)	0.8011(3)	0.8622(2)	0.0642(7)	F(2)	0.3997(2)	1.1849(1)	0.5870(1)	0.0585(4)
Li(1)	0.0292(5)	0.6601(4)	0.7886(4)	0.0535(9)	O(1)	0.1497(2)	0.6855(2)	0.9621(2)	0.0603(4)
B(1)	0.2333(4)	1.1110(3)	0.5556(3)	0.0527(7)	O(2)	-0.2084(2)	0.6683(2)	0.7713(2)	0.0582(4)

7.2.35 Dikalium-bistetrazolat (fin069)

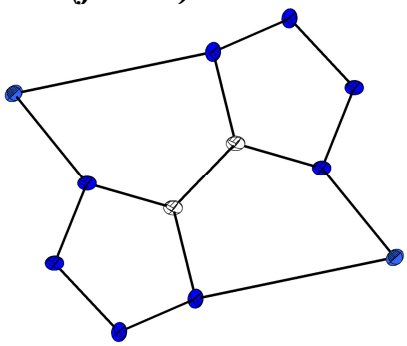

Kristalldaten

C2 K2 N8	M = 214.30 g/mol	Monoclinic, $C2/m$
a = 10.417(2) Å	b = 8.9251(18) Å	c = 3.5524(8) Å
α = 90°	β = 93.828(8)°	γ = 90°
V = 329.55(12) Å^3	Z = 2	F(000) = 212
D_{calc} = 2.160 g/cm^3	μ = 1.384 mm^{-1}	
colourless block	0.405 · 0.086 · 0.078 mm^3	

Datensammlung

Diffraktometer: D8 Quest (Bruker)	T = 100(2) K	λ = 0.71073 Å
h = -12 bis 12	k = -10 bis 10	l = -4 bis 3
855 gemessene Reflexe	333 unabhängige Reflexe	320 Reflexe mit $I > 2\sigma(I)$
θ = 3.008 bis 25.611°	R_{int} = 0.0540	C (25.00°) = 0.984
Absorptionskorrektur: Multi-scan	T_{min} = 0.3825	T_{max} = 0.7455

Verfeinerung

333 Reflexe	0 Restraints	21 Parameter
Verfeinerung mit SHELXL-2014/7	bis χ = 0.000	
R_1 ($I > 2\sigma(I)$) = 0.0818	wR_2 ($I > 2\sigma(I)$) = 0.1921	
R_1 (all) = 0.0828	wR_2 (all) = 0.1963	GoF (S) = 1.106
$\Delta\varphi_{min}$ = -1.090 e·Å^{-3}	$\Delta\varphi_{max}$ = 2.369 e·Å^{-3}	

Kommentar

Das Kaliumatom ist über mehrere Positionen fehlgeordnet, die sich jedoch nicht stabil verfeinern lassen. Nur durch die Verfeinerung eines Auslöschungsparameters (EXTI) verfeinern die C und N-Atome mit positiven Auslenkungsparametern.

Fraktionelle Atomkoordinaten (*x, y, z*) und äquivalente isotrope Auslenkungsfaktoren *U*(eq)

	x	*y*	*z*	*U*(eq)/Å^2
K(1)	0.7101(1)	0.5000	1.0019(2)	0.0084(8)
N(1)	0.6031(3)	0.1644(3)	0.4378(8)	0.0089(9)
N(2)	0.5614(3)	0.3062(3)	0.4632(9)	0.0089(9)
C(1)	0.5000	0.0817(5)	0.5000	0.0089(9)

7.2.36 *Bis(1-butyl-3-methylimidazolium)-bistetrazolat (fin073)*

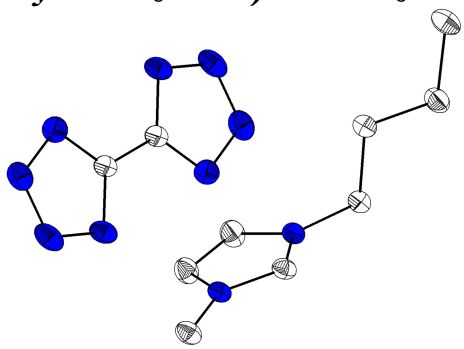

Kristalldaten

C18 H30 N12	M = 414.54 g/mol	Monoclinic, $P2_1/n$
a = 8.1366(19) Å	b = 11.642(2) Å	c = 11.236(3) Å
α = 90°	β = 96.809(19)°	γ = 90°
V = 1056.8(4) Å^3	Z = 2	F(000) = 444
D_{calc} = 1.303 g/cm^3	μ = 0.087 mm^{-1}	
colourless block	0.230 · 0.220 · 0.190 mm^3	

Datensammlung

Diffraktometer: STOE IPDS 2T	T = 100(2) K	λ = 0.71069 Å
h = -10 bis 10	k = -14 bis 14	l = -14 bis 11
5442 gemessene Reflexe	2171 unabhängige Reflexe	1767 Reflexe mit $I > 2\sigma(I)$
θ = 2.528 bis 26.715°	R_{int} = 0.0558	C (25.00°) = 0.975
Absorptionskorrektur: Multi-scan	T_{min} = 0.8827	T_{max} = 1.1291

Verfeinerung

2171 Reflexe	0 Restraints	138 Parameter
Verfeinerung mit SHELXL-2014/7	bis χ = 0.000	
R_1 ($I > 2\sigma(I)$) = 0.0553	wR_2 ($I > 2\sigma(I)$) = 0.1244	
R_1 (all) = 0.0651	wR_2 (all) = 0.1287	GoF (S) = 1.002
$\Delta\varphi_{min}$ = -0.495 e·Å^{-3}	$\Delta\varphi_{max}$ = 0.514 e·Å^{-3}	

Fraktionelle Atomkoordinaten (*x, y, z*) und äquivalente isotrope Auslenkungsfaktoren *U*(eq)

	x	*y*	*z*	*U*(eq)/Å^2
C(1)	0.9609(2)	0.5531(1)	0.5166(1)	0.0177(3)
C(12)	0.4546(2)	0.5582(1)	0.6712(1)	0.0200(3)
C(14)	0.6054(2)	0.4981(1)	0.8349(1)	0.0246(3)
C(15)	0.5511(2)	0.6051(1)	0.8561(1)	0.0257(4)
C(16)	0.3657(2)	0.7505(1)	0.7355(1)	0.0219(3)
C(17)	0.4716(2)	0.8493(1)	0.6996(1)	0.0201(3)
C(18)	0.3631(2)	0.9543(1)	0.6708(2)	0.0257(4)
C(19)	0.4582(2)	1.0630(1)	0.6491(2)	0.0273(4)
C(20)	0.5748(2)	0.3626(1)	0.6572(1)	0.0236(3)
N(1)	0.7998(2)	0.5627(1)	0.5294(1)	0.0242(3)
N(2)	0.7806(2)	0.6737(1)	0.5598(1)	0.0276(3)
N(3)	0.9246(2)	0.7269(1)	0.5646(1)	0.0282(3)
N(4)	1.0421(2)	0.6525(1)	0.5372(1)	0.0240(3)
N(11)	0.4564(1)	0.6411(1)	0.7527(1)	0.0199(3)
N(13)	0.5444(1)	0.4705(1)	0.7188(1)	0.0194(3)

7.2.37 Bis(tri(iso-propyl)-methylphosphonium)-bistetrazolat (fin084)

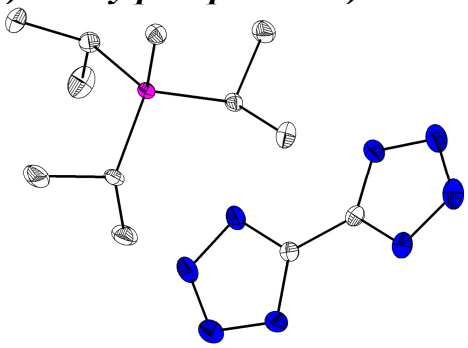

Kristalldaten

C22 H48 N8 P2	M = 486.62 g/mol	Orthorhombic, *Pbca*
a = 14.2198(8) Å	b = 14.0842(7) Å	c = 26.7567(15) Å
α = 90°	β = 90°	γ = 90°
V = 5358.7(5) Å^3	Z = 8	F(000) = 2128
D_{calc} = 1.206 g/cm^3	μ = 0.188 mm^{-1}	
colourless needle	0.300 · 0.090 · 0.080 mm^3	

Datensammlung

Diffraktometer: D8 Quest (Bruker)	T = 100(2) K	λ = 0.71069 Å
h = -17 bis 17	k = -17 bis 14	l = -33 bis 33
30776 gemessene Reflexe	5237 unabhängige Reflexe	4034 Reflexe mit $I > 2\sigma(I)$
θ = 2.090 bis 25.999°	R_{int} = 0.0631	C (25.00°) = 0.996
Absorptionskorrektur: Multi-scan	T_{min} = 0.6663	T_{max} = 0.7455

Verfeinerung

5237 Reflexe	0 Restraints	303 Parameter
Verfeinerung mit SHELXL-2014/7	bis χ = 0.001	
R_1 ($I > 2\sigma(I)$) = 0.0466	wR_2 ($I > 2\sigma(I)$) = 0.1002	
R_1 (all) = 0.0706	wR_2 (all) = 0.1155	GoF (S) = 1.162
$\Delta\varphi_{min}$ = -0.301 e·Å^{-3}	$\Delta\varphi_{max}$ = 0.426 e·Å^{-3}	

Fraktionelle Atomkoordinaten (*x, y, z*) und äquivalente isotrope Auslenkungsfaktoren *U*(eq)

	x	*y*	*z*	*U*(eq)/Å^2		*x*	*y*	*z*	*U*(eq)/Å^2
P(1)	0.2095(1)	0.8887(1)	1.0246(1)	0.0103(1)	C(19)	0.3558(2)	0.9592(1)	0.7908(1)	0.0143(5)
P(2)	0.4374(1)	0.8735(1)	0.7645(1)	0.0119(1)	C(3)	0.2346(2)	0.8211(2)	1.0814(1)	0.0159(5)
N(8)	0.1053(1)	0.6130(1)	0.8991(1)	0.0175(4)	C(9)	0.1528(2)	0.8100(1)	0.9803(1)	0.0126(4)
N(1)	0.3017(1)	0.6170(1)	0.9350(1)	0.0188(4)	C(22)	0.3730(2)	0.7761(2)	0.7382(1)	0.0189(5)
N(2)	0.3965(1)	0.6195(1)	0.9337(1)	0.0195(4)	C(10)	0.0701(2)	0.7562(2)	1.0033(1)	0.0207(5)
N(7)	0.0279(1)	0.6367(1)	0.8724(1)	0.0227(5)	C(20)	0.2913(2)	0.9108(2)	0.8290(1)	0.0229(5)
N(5)	0.1482(1)	0.6977(1)	0.8324(1)	0.0190(4)	C(4)	0.2723(2)	0.8808(2)	1.1250(1)	0.0212(5)
N(4)	0.3487(1)	0.6653(1)	0.8603(1)	0.0209(4)	C(12)	0.1278(2)	0.9804(1)	1.0411(1)	0.0148(5)
N(3)	0.4249(1)	0.6483(1)	0.8896(1)	0.0222(4)	C(14)	0.5484(2)	0.8960(2)	0.8518(1)	0.0255(6)
C(2)	0.1768(2)	0.6520(1)	0.8736(1)	0.0131(5)	C(15)	0.5878(2)	0.7619(2)	0.7932(1)	0.0259(6)
C(1)	0.2751(2)	0.6451(1)	0.8895(1)	0.0121(4)	C(8)	0.3699(2)	0.8716(2)	0.9653(1)	0.0215(5)
C(6)	0.3102(2)	0.9427(2)	0.9944(1)	0.0138(5)	C(16)	0.5113(2)	0.9274(2)	0.7166(1)	0.0176(5)
C(13)	0.5091(2)	0.8237(2)	0.8144(1)	0.0153(5)	C(7)	0.3713(2)	1.0010(2)	1.0300(1)	0.0261(6)
N(6)	0.0535(1)	0.6869(1)	0.8327(1)	0.0231(5)	C(5)	0.2985(2)	0.7352(2)	1.0718(1)	0.0268(6)
C(11)	0.1203(2)	0.8656(2)	0.9341(1)	0.0199(5)	C(18)	0.4639(2)	0.9308(2)	0.6651(1)	0.0270(6)
C(21)	0.2978(2)	1.0117(2)	0.7512(1)	0.0206(5)	C(17)	0.5460(2)	1.0255(2)	0.7335(1)	0.0239(5)

7.2.38 Bis(tri(n-butyl)-methylphosphonium)-bistetrazolat (jhl04)

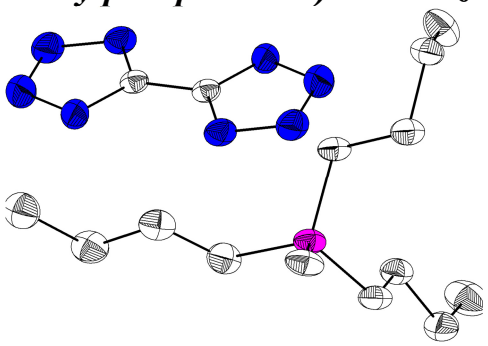

Kristalldaten

C28 H60 N8 P2	M = 570.78 g/mol	Tetragonal, $I4_1/a$
a = 18.7183(8) Å	b = 18.7183 Å	c = 19.3890(10) Å
α = 90°	β = 90°	γ = 90°
V = 6793.4(7) Å^3	Z = 8	F(000) = 2512
D_{calc} = 1.116 g/cm^3	μ = 0.157 mm^{-1}	
colourless block	0.240 · 0.240 · 0.140 mm^3	

Datensammlung

Diffraktometer: D8 Quest (Bruker)	T = 100(2) K	λ = 0.71069 Å
h = -24 bis 21	k = -21 bis 23	l = -24 bis 24
28651 gemessene Reflexe	3735 unabhängige Reflexe	2485 Reflexe mit $I > 2\sigma(I)$
θ = 2.604 bis 27.110°	R_{int} = 0.0979	C (25.00°) = 0.999
Absorptionskorrektur: Multi-scan	T_{min} = 0.6714	T_{max} = 0.7455

Verfeinerung

3735 Reflexe	21 Restraints	205 Parameter
Verfeinerung mit SHELXL-2014/7	bis χ = 0.001	
R_1 ($I > 2\sigma(I)$) = 0.0457	wR_2 ($I > 2\sigma(I)$) = 0.0941	
R_1 (all) = 0.0881	wR_2 (all) = 0.1115	GoF (S) = 1.009
$\Delta\varphi_{min}$ = -0.302 e·Å^{-3}	$\Delta\varphi_{max}$ = 0.344 e·Å^{-3}	

Kommentar

Eine fehlgeordnete Butylkette (65:35) wurde über SADI und ISOR restrained.

Fraktionelle Atomkoordinaten (*x, y, z*) und äquivalente isotrope Auslenkungsfaktoren *U*(eq)

	x	*y*	*z*	*U*(eq)/Å^2		*x*	*y*	*z*	*U*(eq)/Å^2
P(1)	0.0707(1)	0.0756(1)	0.7271(1)	0.0288(2)	C(7)	-0.0068(1)	-0.0422(1)	0.7731(1)	0.0328(5)
N(1)	0.1816(1)	0.2521(1)	0.8183(1)	0.0328(4)	C(8)	-0.0672(1)	-0.0944(1)	0.7604(1)	0.0405(5)
N(2)	0.1205(1)	0.2898(1)	0.8140(1)	0.0405(4)	C(5)	0.0627(1)	0.0841(1)	0.9721(1)	0.0476(6)
N(4)	0.1783(1)	0.3093(1)	0.7182(1)	0.0325(4)	C(9)	-0.0688(2)	-0.1542(1)	0.8127(1)	0.0572(7)
N(3)	0.1184(1)	0.3238(1)	0.7549(1)	0.0388(4)	C(10)	0.1409(1)	0.0267(1)	0.6848(1)	0.0379(5)
C(1)	0.2154(1)	0.2653(1)	0.7590(1)	0.0240(4)	C(11)	0.2116(3)	0.0586(3)	0.6738(3)	0.0357(14)
C(3)	0.0355(1)	0.1338(1)	0.8533(1)	0.0335(5)	C(12)	0.2636(2)	0.0071(2)	0.6367(3)	0.0414(11)
C(2)	0.0939(1)	0.0933(1)	0.8149(1)	0.0301(4)	C(13)	0.3369(2)	0.0390(2)	0.6277(2)	0.0452(12)
C(6)	-0.0080(1)	0.0217(1)	0.7233(1)	0.0320(5)	C(12A)	0.2819(6)	0.0337(8)	0.6648(7)	0.107(5)
C(14)	0.0561(1)	0.1582(1)	0.6842(1)	0.0364(5)	C(13A)	0.2736(8)	0.0191(8)	0.5977(8)	0.144(7)
C(4)	0.0565(1)	0.1500(1)	0.9276(1)	0.0356(5)	C(11A)	0.2081(8)	0.0813(8)	0.6770(9)	0.072(5)

7.2.39 Bis(4,4'-di-tert-butyl-2,2'-bipyridin)-bistetrazolato-cobalt(II)-methanolsolvat (yabt40)

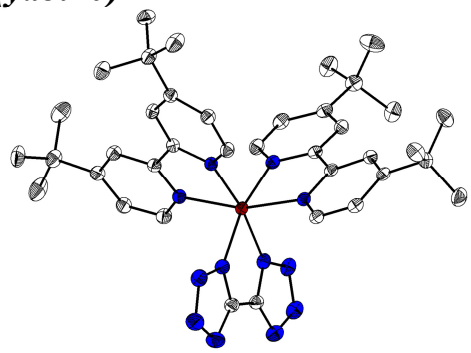

Kristalldaten

C41 H60 Co N12 O3	M = 827.94 g/mol	Triclinic, $P\bar{1}$
a = 11.3278(4) Å	b = 12.9807(5) Å	c = 16.6610(6) Å
α = 111.145(3)°	β = 102.237(3)°	γ = 97.906(3)°
V = 2170.59(15) Å^3	Z = 2	F(000) = 882
D_{calc} = 1.267 g/cm^3	μ = 0.447 mm^{-1}	
colourless prism	0.380 · 0.350 · 0.120 mm^3	

Datensammlung

Diffraktometer: STOE IPDS 2T	T = 100(2) K	λ = 0.71069 Å
h = -14 bis 13	k = -16 bis 16	l = -21 bis 20
18835 gemessene Reflexe	9152 unabhängige Reflexe	7209 Reflexe mit $I > 2\sigma(I)$
θ = 1.366 bis 26.772°	R_{int} = 0.0300	C (25.00°) = 0.996
Absorptionskorrektur: Multi-scan	T_{min} = 0.8306	T_{max} = 0.907

Verfeinerung

9152 Reflexe	5 Restraints	562 Parameter
Verfeinerung mit SHELXL-2014/7	bis χ = 0.002	
R_1 ($I > 2\sigma(I)$) = 0.0353	wR_2 ($I > 2\sigma(I)$) = 0.0908	
R_1 (all) = 0.0473	wR_2 (all) = 0.0937	GoF (S) = 1.002
$\Delta\varphi_{min}$ = -0.381 e·Å^{-3}	$\Delta\varphi_{max}$ = 1.418 e·Å^{-3}	

Kommentar

Ein Methanolmolekül ist über drei Positionen fehlgeordnet und wurde über DFIX restrained. Die Synthese der Substanz und die Kristallzucht erfolgten durch Yodita Asfaha im Rahmen ihrer von mir betreuten Bachelorarbeit.[94]

Fraktionelle Atomkoordinaten (*x, y, z*) und äquivalente isotrope Auslenkungsfaktoren *U*(eq)

	x	*y*	*z*	*U*(eq)/Å^2		*x*	*y*	*z*	*U*(eq)/Å^2
C(1)	-0.2291(2)	0.2269(1)	0.8158(1)	0.0193(3)	C(17)	0.4605(2)	0.2237(2)	0.6053(1)	0.0225(4)
C(2)	-0.2009(2)	0.1223(1)	0.7606(1)	0.0203(4)	C(18)	0.5581(2)	0.3362(2)	0.6612(1)	0.0283(4)
C(3)	0.1300(2)	0.3189(2)	0.9517(1)	0.0224(4)	C(19)	0.5096(2)	0.1245(2)	0.6187(1)	0.0273(4)
C(4)	0.2290(2)	0.3237(2)	1.0190(1)	0.0221(4)	C(20)	0.4339(2)	0.2022(2)	0.5057(1)	0.0337(5)
C(5)	0.3418(2)	0.3105(1)	1.0018(1)	0.0206(4)	C(21)	0.1204(2)	0.5553(2)	0.8924(1)	0.0221(4)
C(6)	0.3483(2)	0.2930(1)	0.9148(1)	0.0207(4)	C(22)	0.1393(2)	0.6721(2)	0.9225(1)	0.0224(4)
C(7)	0.2457(2)	0.2889(1)	0.8505(1)	0.0178(3)	C(23)	0.0830(2)	0.7200(1)	0.8668(1)	0.0204(4)
C(8)	0.2459(2)	0.2682(1)	0.7566(1)	0.0170(3)	C(24)	0.0082(2)	0.6445(1)	0.7814(1)	0.0194(3)
C(9)	0.3506(2)	0.2569(1)	0.7268(1)	0.0189(3)	C(25)	-0.0064(2)	0.5281(1)	0.7553(1)	0.0176(3)
C(10)	0.3439(2)	0.2317(1)	0.6367(1)	0.0189(3)	C(26)	-0.0845(2)	0.4436(1)	0.6655(1)	0.0170(3)
C(11)	0.2272(2)	0.2145(2)	0.5799(1)	0.0206(4)	C(27)	-0.1302(2)	0.4732(1)	0.5947(1)	0.0180(3)
C(12)	0.1270(2)	0.2298(1)	0.6145(1)	0.0206(4)	C(28)	-0.2007(2)	0.3901(1)	0.5113(1)	0.0176(3)
C(13)	0.4568(2)	0.3189(2)	1.0728(1)	0.0269(4)	C(29)	-0.2253(2)	0.2781(1)	0.5042(1)	0.0190(3)
C(14)	0.4244(2)	0.3173(2)	1.1572(1)	0.0419(6)	C(30)	-0.1756(2)	0.2544(1)	0.5769(1)	0.0186(3)
C(15)	0.5165(2)	0.2190(2)	1.0357(1)	0.0341(5)	C(31)	0.0979(2)	0.8480(1)	0.8954(1)	0.0238(4)
C(16)	0.5493(2)	0.4317(2)	1.0971(1)	0.0373(5)	C(32)	-0.0298(2)	0.8751(2)	0.8951(1)	0.0288(4)

	x	y	z	U(eq)/Å^2
C(33)	0.1458(2)	0.8836(2)	0.8274(2)	0.0392(5)
C(34)	0.1887(2)	0.9157(2)	0.9890(1)	0.0330(5)
C(35)	-0.2508(2)	0.4175(1)	0.4307(1)	0.0205(4)
C(36)	-0.2275(2)	0.3325(2)	0.3466(1)	0.0292(4)
C(37)	-0.3908(2)	0.4061(2)	0.4161(1)	0.0300(4)
C(38)	-0.1884(2)	0.5375(2)	0.4449(1)	0.0288(4)
C(39)	0.7147(2)	0.6880(2)	0.6705(1)	0.0304(4)
C(40)	0.4816(3)	0.9704(3)	0.8015(2)	0.0641(8)
N(1)	-0.1503(1)	0.3240(1)	0.8330(1)	0.0197(3)
N(2)	-0.1973(2)	0.4074(1)	0.8816(1)	0.0238(3)
N(3)	-0.3000(2)	0.3600(1)	0.8924(1)	0.0267(3)
N(4)	-0.3229(2)	0.2449(1)	0.8511(1)	0.0252(3)
N(5)	-0.1067(1)	0.1333(1)	0.7254(1)	0.0205(3)
N(6)	-0.0985(2)	0.0270(1)	0.6794(1)	0.0264(3)
N(7)	-0.1852(2)	-0.0438(1)	0.6880(1)	0.0304(4)
N(8)	-0.2525(2)	0.0139(1)	0.7388(1)	0.0290(4)
N(9)	0.1364(1)	0.3016(1)	0.8689(1)	0.0184(3)
N(10)	0.1348(1)	0.2583(1)	0.7013(1)	0.0175(3)
N(11)	0.0496(1)	0.4833(1)	0.8108(1)	0.0185(3)
N(12)	-0.1053(1)	0.3343(1)	0.6564(1)	0.0174(3)
Co(1)	-0.0072(1)	0.3036(1)	0.7654(1)	0.0165(1)
O(1)	0.8232(1)	0.7307(1)	0.6525(1)	0.0276(3)
O(2)	0.4911(2)	0.9044(2)	0.7129(1)	0.0597(5)
C(41)	0.1711(2)	0.9668(2)	0.6450(2)	0.0381(5)
O(3)	0.0735(5)	0.9487(6)	0.5707(3)	0.057(2)
O(3B)	0.2888(11)	0.9510(9)	0.6507(8)	0.050(5)
O(3A)	0.0573(5)	0.8932(8)	0.5945(5)	0.044(3)

7.2.40 Bis(4,4'-dimethyl-2,2'-bipyridin)-bistetrazolato-cobalt(II)-tetrahydrofuransolvat (yabt49l)

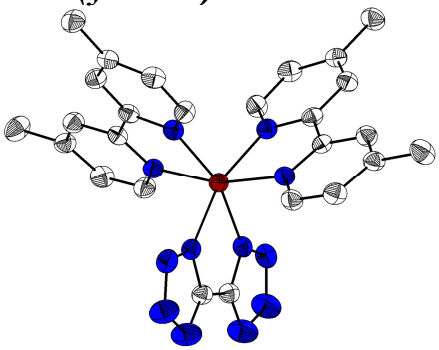

Kristalldaten

C34 H40 Co N12 O2	M = 707.71 g/mol	Monoclinic, $C2/c$
a = 19.0790(10) Å	b = 13.3180(8) Å	c = 15.7767(8) Å
α = 90°	β = 124.485(3)°	γ = 90°
V = 3304.3(3) Å^3	Z = 4	F(000) = 1484
D_{calc} = 1.423 g/cm^3	μ = 0.572 mm^{-1}	
yellow needle	0.300 · 0.090 · 0.080 mm^3	

Datensammlung

Diffraktometer: STOE IPDS 2	T = 100(2) K	λ = 0.71069 Å
h = -24 bis 24	k = -16 bis 16	l = -19 bis 19
20341 gemessene Reflexe	3496 unabhängige Reflexe	1927 Reflexe mit $I > 2\sigma(I)$
θ = 2.004 bis 26.735°	R_{int} = 0.0928	C (25.00°) = 0.999
Absorptionskorrektur: Multi-scan	T_{min} = 0.8068	T_{max} = 1.0844

Verfeinerung

3496 Reflexe	12 Restraints	224 Parameter
Verfeinerung mit SHELXL-2014/7	bis χ = 0.001	
R_1 ($I > 2\sigma(I)$) = 0.0506	wR_2 ($I > 2\sigma(I)$) = 0.1116	
R_1 (all) = 0.0931	wR_2 (all) = 0.1203	GoF (S) = 0.818
$\Delta\varphi_{min}$ = -0.515 e·Å^{-3}	$\Delta\varphi_{max}$ = 0.729 e·Å^{-3}	

Kommentar

Ein THF-Molekül wurde über DFIX und DELU restrained. Die Synthese der Substanz und die Kristallzucht erfolgten durch Yodita Asfaha im Rahmen ihrer von mir betreuten Bachelorarbeit.[94]

Fraktionelle Atomkoordinaten (*x, y, z*) und äquivalente isotrope Auslenkungsfaktoren *U*(eq)

	x	*y*	*z*	*U*(eq)/Å^2
C(1)	0.5339(2)	1.2609(2)	0.2422(2)	0.0277(7)
C(2)	0.6292(2)	0.9011(3)	0.2469(3)	0.0309(8)
C(3)	0.6571(2)	0.8341(2)	0.2053(3)	0.0322(8)
C(4)	0.6023(2)	0.8034(2)	0.1036(3)	0.0292(8)
C(5)	0.5214(2)	0.8450(2)	0.0479(3)	0.0296(8)
C(6)	0.4971(2)	0.9128(2)	0.0941(3)	0.0273(7)
C(7)	0.6290(2)	0.7291(3)	0.0555(3)	0.0384(9)
C(8)	0.6802(2)	1.0667(2)	0.4548(3)	0.0317(8)
C(9)	0.7447(2)	1.0496(3)	0.5556(2)	0.0344(8)
C(10)	0.7306(2)	0.9842(2)	0.6134(3)	0.0309(8)
C(11)	0.6511(2)	0.9399(2)	0.5644(2)	0.0312(8)
C(12)	0.5886(2)	0.9601(2)	0.4619(2)	0.0263(7)
C(13)	0.7975(2)	0.9612(3)	0.7242(3)	0.0434(9)
N(1)	0.5616(2)	1.1719(2)	0.2341(2)	0.0282(6)
N(2)	0.6252(2)	1.1923(2)	0.2226(2)	0.0347(7)
N(3)	0.6339(2)	1.2897(2)	0.2239(3)	0.0457(8)
N(4)	0.5766(2)	1.3363(2)	0.2367(3)	0.0461(8)
N(5)	0.5502(2)	0.9402(2)	0.1936(2)	0.0284(6)
N(6)	0.6031(2)	1.0240(2)	0.4069(2)	0.0280(6)
Co(1)	0.5000	1.0448(1)	0.2500	0.0270(2)
C(17)	0.6759(4)	0.6715(5)	0.5057(5)	0.0990(19)
C(14)	0.5847(6)	0.5763(6)	0.4914(7)	0.139(3)
C(15)	0.5421(5)	0.5969(8)	0.3850(7)	0.171(4)
C(16)	0.6076(5)	0.6897(7)	0.3972(6)	0.144(3)
O(1)	0.6677(4)	0.5811(5)	0.5498(4)	0.150(2)

7.2.41 Tris(4,4'-dimethyl-2,2'-bipyridin)-cobalt(II)-diperchlorat-diethylethersolvat (yabt38xa)

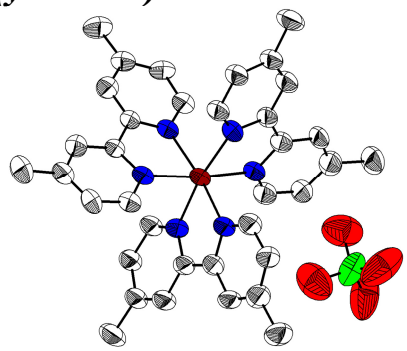

Kristalldaten

C38 H41 Cl2 Co N6 O8.50	*M* = 847.60 g/mol	Monoclinic, *C*2/*c*
a = 10.5519(11) Å	*b* = 27.373(3) Å	*c* = 14.7353(14) Å
α = 90°	β = 102.496(8)°	γ = 90°
V = 4155.3(8) Å^3	*Z* = 4	*F*(000) = 1760
D_{calc} = 1.355 g/cm^3	μ = 0.599 mm^{-1}	
colourless prism	0.200 · 0.060 · 0.060 mm^3	

Datensammlung

Diffraktometer: STOE IPDS 2	*T* = 100(2) K	λ = 0.71069 Å
h = -12 bis 13	*k* = -34 bis 34	*l* = -18 bis 18
22928 gemessene Reflexe	4433 unabhängige Reflexe	1338 Reflexe mit $I > 2\sigma(I)$
θ = 1.488 bis 26.775°	R_{int} = 0.2823	*C* (25.00°) = 1.000
Absorptionskorrektur: refdelf	T_{min} = 0.1727	T_{max} = 0.6447

Verfeinerung

4433 Reflexe	21 Restraints	280 Parameter
Verfeinerung mit SHELXL-2014/7	bis χ = 0.000	
R_1 ($I > 2\sigma(I)$) = 0.0848	wR_2 ($I > 2\sigma(I)$) = 0.1947	
R_1 (all) = 0.2112	wR_2 (all) = 0.2380	GoF (S) = 0.757
$\Delta\varphi_{min}$ = -0.576 e·Å^{-3}	$\Delta\varphi_{max}$ = 0.837 e·Å^{-3}	

Kommentar

Eine sehr schwache Streuung und Fehlordnung der Perchloratanionen erlauben keine optimale Verfeinerung der Struktur. Die Perchloratanionen wurden über RIGU, DELU und ISOR restrained, und schwachbesetzte Positionen über EADP constrained. Die Synthese der Substanz und die Kristallzucht erfolgten durch Yodita Asfaha im Rahmen ihrer von mir betreuten Bachelorarbeit.[94]

Fraktionelle Atomkoordinaten (*x, y, z*) und äquivalente isotrope Auslenkungsfaktoren *U*(eq)

	x	*y*	*z*	*U*(eq)/Å^2
Co(1)	0.5000	0.1540(1)	0.7500	0.0551(5)
N(4)	0.5716(6)	0.0929(2)	0.6877(3)	0.0560(15)
N(10)	0.6469(7)	0.1606(2)	0.8746(3)	0.0614(16)
N(12)	0.5765(7)	0.2078(2)	0.6747(4)	0.0611(17)
C(1)	0.7531(8)	0.1331(3)	0.8955(4)	0.0587(19)
C(2)	0.8317(8)	0.1317(3)	0.9847(4)	0.064(2)
C(3)	0.8005(8)	0.1593(3)	1.0552(4)	0.0635(19)
C(4)	0.6878(9)	0.1888(3)	1.0315(5)	0.066(2)
C(5)	0.6166(8)	0.1891(2)	0.9416(4)	0.0565(19)
C(6)	0.5046(8)	0.2188(3)	0.5882(4)	0.060(2)
C(7)	0.5419(9)	0.2557(3)	0.5359(5)	0.063(2)
C(8)	0.6576(9)	0.2831(3)	0.5709(5)	0.073(2)
C(9)	0.7311(9)	0.2702(3)	0.6579(5)	0.070(2)
C(10)	0.6861(9)	0.2328(3)	0.7051(5)	0.067(2)
C(11)	0.8761(9)	0.1561(3)	1.1525(4)	0.082(2)
C(12)	0.6960(9)	0.3257(3)	0.5167(6)	0.083(3)
C(13)	0.6359(7)	0.0945(3)	0.6162(4)	0.061(2)
C(14)	0.6691(8)	0.0540(3)	0.5739(5)	0.066(2)
C(15)	0.6383(8)	0.0080(3)	0.6005(5)	0.066(2)
C(16)	0.5689(8)	0.0061(3)	0.6726(5)	0.065(2)
C(17)	0.5365(7)	0.0480(2)	0.7120(4)	0.0528(18)
C(23)	0.6797(10)	-0.0377(3)	0.5606(5)	0.085(3)
Cl(2)	0.0000	0.3690(1)	0.7500	0.0991(11)
O(5)	-0.0273(8)	0.3371(3)	0.8170(5)	0.146(3)
O(7)	0.1103(8)	0.3981(3)	0.7845(8)	0.170(4)
O(9)	0.0000	-0.0162(5)	0.7500	0.067(4)
C(200)	0.1215(14)	-0.0238(5)	0.6361(9)	0.059(4)
C(201)	0.0585(16)	0.0122(6)	0.6906(10)	0.072(4)
Cl(1)	0.0000	0.1697(1)	0.7500	0.0686(14)
O(2)	0.1093(7)	0.1414(3)	0.7846(5)	0.071(2)
O(3)	0.0285(7)	0.2008(3)	0.6768(4)	0.079(2)
Cl(1A)	0.0000	0.1062(9)	0.7500	0.152(10)
O(2A)	0.127(2)	0.1162(19)	0.788(2)	0.152(10)
O(3A)	-0.007(3)	0.0855(13)	0.6574(16)	0.152(10)

7.2.42 Tris(2,2'-bipyridin)-cobalt(III)-tris(tetrafluoroborat)-acetonsolvat-methanolsolvat (yabt45f5c)

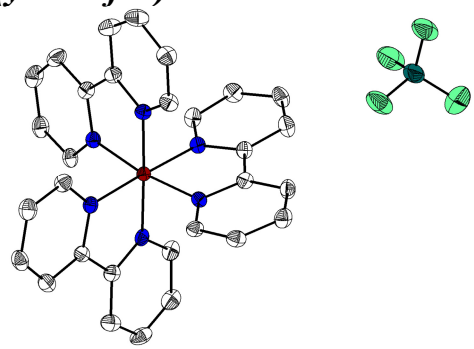

Kristalldaten

C34 H34 B3 Co F12 N6 O2	M = 878.03 g/mol	Monoclinic, $C2/c$
a = 39.5106(9) Å	b = 15.1657(4) Å	c = 13.0017(3) Å
α = 90°	β = 93.336(2)°	γ = 90°
V = 7777.5(3) Å^3	Z = 8	F(000) = 3568
D_{calc} = 1.500 g/cm^3	μ = 0.539 mm^{-1}	
colourless prism	0.430 · 0.290 · 0.240 mm^3	

Datensammlung

Diffraktometer: STOE IPDS 2T	T = 100(2) K	λ = 0.71069 Å
h = -50 bis 50	k = -19 bis 19	l = -16 bis 16
76697 gemessene Reflexe	76697 unabhängige Reflexe	55235 Reflexe mit I > 2σ(I)
θ = 1.438 bis 27.170°	R_{int} = 0.0000	C (25.00°) = 1.000
Absorptionskorrektur: Multi-scan	T_{min} = 0.7971	T_{max} = 0.9027

Verfeinerung

76697 Reflexe	0 Restraints	543 Parameter
Verfeinerung mit SHELXL-2014/7	bis χ = 0.004	
R_1 (I > 2σ(I)) = 0.0723	wR_2 (I > 2σ(I)) = 0.2105	
R_1 (all) = 0.0943	wR_2 (all) = 0.2402	GoF (S) = 1.022
$\Delta\varphi_{min}$ = -0.601 e·Å^{-3}	$\Delta\varphi_{max}$ = 2.015 e·Å^{-3}	

Kommentar

Die Struktur wurde als nicht-meroedrischer Zwilling integriert und verfeinert. Die Synthese der Substanz und die Kristallzucht erfolgten durch Yodita Asfaha im Rahmen ihrer von mir betreuten Bachelorarbeit.[94]

Fraktionelle Atomkoordinaten (*x, y, z*) und äquivalente isotrope Auslenkungsfaktoren *U*(eq)

	x	*y*	*z*	*U*(eq)/Å^2		*x*	*y*	*z*	*U*(eq)/Å^2
C(1)	0.9307(1)	0.4004(3)	0.4397(4)	0.0232(10)	B(1)	0.7487(2)	-0.0412(6)	0.3485(6)	0.0447(19)
C(2)	0.9578(2)	0.4465(4)	0.4048(4)	0.0274(11)	B(2)	0.9008(2)	0.1208(6)	0.9317(5)	0.0419(18)
C(3)	0.9897(1)	0.4094(4)	0.4132(4)	0.0259(11)	B(3)	1.0000	0.3751(6)	0.7500	0.0241(17)
C(4)	0.9938(1)	0.3276(3)	0.4594(4)	0.0233(10)	B(4)	1.0000	0.1886(6)	0.2500	0.0248(17)
C(5)	0.9656(1)	0.2844(3)	0.4933(3)	0.0178(9)	N(1)	0.9344(1)	0.3197(3)	0.4816(3)	0.0177(8)
C(6)	0.9666(1)	0.1983(3)	0.5447(3)	0.0186(9)	N(2)	0.9361(1)	0.1710(3)	0.5746(3)	0.0179(8)
C(7)	0.9956(1)	0.1478(4)	0.5633(4)	0.0240(11)	N(3)	0.8943(1)	0.1746(3)	0.4026(3)	0.0167(8)
C(8)	0.9932(2)	0.0679(4)	0.6121(4)	0.0274(12)	N(4)	0.8635(1)	0.1667(3)	0.5708(3)	0.0177(8)
C(9)	0.9623(2)	0.0402(4)	0.6436(4)	0.0278(12)	N(5)	0.8960(1)	0.3151(3)	0.6497(3)	0.0175(8)
C(10)	0.9341(2)	0.0929(3)	0.6240(4)	0.0233(10)	N(6)	0.8626(1)	0.3231(3)	0.4739(3)	0.0177(8)
C(11)	0.9123(1)	0.1851(3)	0.3184(3)	0.0197(10)	F(1)	0.7483(1)	-0.0278(3)	0.4537(3)	0.0511(10)
C(12)	0.9037(1)	0.1415(3)	0.2277(4)	0.0228(10)	F(2)	0.7196(1)	-0.0014(3)	0.3003(3)	0.0524(11)
C(13)	0.8761(1)	0.0849(4)	0.2231(4)	0.0250(11)	F(3)	0.7769(1)	0.0019(3)	0.3119(3)	0.0553(12)
C(14)	0.8582(1)	0.0721(3)	0.3103(4)	0.0239(11)	F(4)	0.7492(2)	-0.1282(4)	0.3223(5)	0.0904(19)
C(15)	0.8678(1)	0.1182(3)	0.3997(4)	0.0196(10)	F(7)	0.9205(1)	0.1842(3)	0.9824(3)	0.0497(11)
C(16)	0.8504(1)	0.1131(3)	0.4956(3)	0.0189(10)	F(6)	0.9117(2)	0.1062(4)	0.8394(3)	0.088(2)
C(17)	0.8225(1)	0.0598(4)	0.5107(4)	0.0262(11)	F(5)	0.8676(2)	0.1553(5)	0.9099(5)	0.0902(19)
C(18)	0.8080(1)	0.0618(4)	0.6046(4)	0.0259(11)	F(8)	0.8963(1)	0.0514(3)	0.9941(3)	0.0569(12)
C(19)	0.8220(1)	0.1155(4)	0.6824(4)	0.0242(11)	F(9)	0.9755(1)	0.4256(2)	0.6983(3)	0.0401(9)
C(20)	0.8497(1)	0.1661(3)	0.6636(4)	0.0213(10)	F(10A)	0.9809(3)	0.3431(14)	0.8346(10)	0.042(4)
C(21)	0.9146(1)	0.3034(3)	0.7383(4)	0.0211(10)	F(10)	0.9893(4)	0.3036(12)	0.7990(16)	0.033(5)
C(22)	0.9071(1)	0.3482(4)	0.8270(4)	0.0250(11)	F(11)	0.9887(1)	0.1356(2)	0.3280(2)	0.0384(9)
C(23)	0.8802(2)	0.4065(4)	0.8239(4)	0.0279(12)	F(12)	1.0264(1)	0.2422(3)	0.2861(3)	0.0444(10)
C(24)	0.8616(2)	0.4204(4)	0.7325(4)	0.0266(11)	Co(1)	0.8985(1)	0.2449(1)	0.5268(1)	0.0146(2)
C(25)	0.8700(1)	0.3733(3)	0.6456(4)	0.0198(10)	O(1)	0.8856(1)	0.4254(3)	0.0716(3)	0.0451(12)
C(26)	0.8517(1)	0.3804(3)	0.5447(4)	0.0202(10)	C(100)	0.9138(2)	0.4042(5)	0.1380(5)	0.0460(17)
C(27)	0.8255(2)	0.4387(4)	0.5208(4)	0.0289(11)	O(2)	0.8387(2)	0.2966(5)	0.1272(5)	0.0764(19)
C(28)	0.8105(2)	0.4393(4)	0.4218(4)	0.0313(12)	C(102)	0.8177(3)	0.2618(7)	0.0705(8)	0.069(3)
C(29)	0.8220(1)	0.3816(4)	0.3496(4)	0.0253(11)	C(101)	0.8092(3)	0.2982(9)	-0.0364(8)	0.088(3)
C(30)	0.8481(1)	0.3248(3)	0.3775(4)	0.0225(10)	C(103)	0.7960(4)	0.1896(9)	0.1092(12)	0.122(6)

7.2.43 Tris(2,2'-bipyridin)-cobalt(II)-bis(hexafluorophosphat) (sub63)

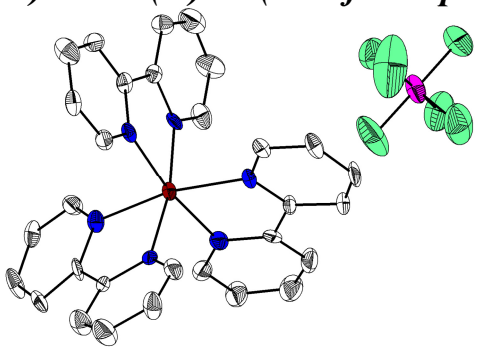

Kristalldaten

C30 H24 Co F12 N6 P2	*M* = 817.42 g/mol	Trigonal, $P3_1$
a = 10.2820(19) Å	*b* = 10.282 Å	*c* = 26.028(5) Å
α = 90°	β = 90°	γ = 120°
V = 2383.0(10) Å^3	*Z* = 3	*F*(000) = 1233
D_{calc} = 1.709 g/cm^3	μ = 0.746 mm^{-1}	
orange needle	0.354 · 0.052 · 0.050 mm^3	

Datensammlung

Diffraktometer: D8 Quest (Bruker)	T = 100(2) K	λ = 0.71069 Å
h = -12 bis 12	k = -12 bis 12	l = -32 bis 32
24290 gemessene Reflexe	6237 unabhängige Reflexe	4412 Reflexe mit $I > 2\sigma(I)$
θ = 2.287 bis 25.998°	R_{int} = 0.1378	C (25.00°) = 1.000
Absorptionskorrektur: Multi-scan	T_{min} = 0.4051	T_{max} = 0.7455

Verfeinerung

6237 Reflexe	85 Restraints	461 Parameter
Verfeinerung mit SHELXL-2014/7	bis χ = 0.000	
R_1 ($I > 2\sigma(I)$) = 0.0548	wR_2 ($I > 2\sigma(I)$) = 0.0946	
R_1 (all) = 0.1065	wR_2 (all) = 0.1104	GoF (S) = 1.011
$\Delta\varphi_{min}$ = -0.422 e·Å^{-3}	$\Delta\varphi_{max}$ = 0.477 e·Å^{-3}	

Kommentar

Die Struktur wurde als pseudo-meroedrischer Zwilling verfeinert. Ein PF_6-Anion wurde über DELU und RIGU restrained. Die Synthese der Substanz und die Kristallzucht erfolgten durch Sebastian Ullrich im Rahmen seiner von mir betreuten Bachelorarbeit.[112]

Fraktionelle Atomkoordinaten (*x, y, z*) und äquivalente isotrope Auslenkungsfaktoren *U*(eq)

	x	*y*	*z*	*U*(eq)/Å^2
C(1)	0.6721(12)	0.2175(12)	0.3086(4)	0.020(3)
C(2)	0.6141(16)	0.1506(14)	0.3557(4)	0.033(3)
C(3)	0.4796(15)	0.1332(15)	0.3711(5)	0.034(3)
C(4)	0.4065(14)	0.1843(15)	0.3410(4)	0.032(3)
C(5)	0.4712(13)	0.2521(15)	0.2945(4)	0.027(3)
C(6)	0.8161(15)	0.2407(14)	0.2880(4)	0.026(3)
C(7)	0.9184(15)	0.2204(15)	0.3171(5)	0.033(3)
C(8)	1.0493(15)	0.2452(15)	0.2962(5)	0.040(4)
C(9)	1.0751(15)	0.2836(15)	0.2462(5)	0.039(4)
C(10)	0.9736(13)	0.3019(13)	0.2193(5)	0.029(3)
C(11)	0.7331(12)	0.6464(13)	0.2238(4)	0.019(3)
C(12)	0.7819(14)	0.7806(13)	0.2463(4)	0.025(3)
C(13)	0.9078(16)	0.8422(15)	0.2766(5)	0.043(4)
C(14)	0.9852(16)	0.7712(15)	0.2827(5)	0.038(4)
C(15)	0.9333(14)	0.6332(15)	0.2598(4)	0.032(3)
C(16)	0.5967(12)	0.5664(12)	0.1918(4)	0.019(3)
C(17)	0.5217(13)	0.6360(13)	0.1737(4)	0.027(3)
C(18)	0.3962(15)	0.5610(16)	0.1442(4)	0.039(3)
C(19)	0.3418(16)	0.4082(15)	0.1344(4)	0.031(3)
C(20)	0.4212(13)	0.3487(14)	0.1539(4)	0.025(3)
C(21)	0.7649(13)	0.2683(13)	0.1026(3)	0.023(3)
C(22)	0.8476(15)	0.2687(14)	0.0615(4)	0.034(3)
C(23)	0.9793(14)	0.4025(15)	0.0480(4)	0.037(3)
C(24)	1.0189(13)	0.5266(15)	0.0776(4)	0.029(3)
C(25)	0.9325(13)	0.5149(14)	0.1195(4)	0.026(3)
C(26)	0.6230(13)	0.1351(12)	0.1182(4)	0.019(3)
C(27)	0.5450(15)	0.0175(14)	0.0858(5)	0.035(3)
C(28)	0.4073(16)	-0.1010(16)	0.1014(5)	0.043(4)
C(29)	0.3591(16)	-0.1004(15)	0.1505(5)	0.035(4)
C(30)	0.4476(14)	0.0196(14)	0.1812(5)	0.027(3)
N(1)	0.5989(9)	0.2639(10)	0.2779(3)	0.021(2)
N(2)	0.8473(11)	0.2854(11)	0.2395(3)	0.023(2)
N(3)	0.8085(11)	0.5682(11)	0.2312(3)	0.019(2)
N(4)	0.5493(11)	0.4229(11)	0.1812(3)	0.019(2)
N(5)	0.8092(10)	0.3909(11)	0.1330(3)	0.023(2)
N(6)	0.5745(11)	0.1357(10)	0.1661(3)	0.016(2)
F(1)	0.4120(9)	0.8078(8)	0.9881(2)	0.0406(19)
F(2)	0.1925(7)	0.6098(10)	0.9599(3)	0.053(2)
F(3)	0.3326(9)	0.5768(10)	1.0201(3)	0.052(2)
F(4)	0.5295(8)	0.6805(9)	0.9670(3)	0.047(2)
F(5)	0.3945(8)	0.7215(8)	0.9083(2)	0.0464(19)
F(6)	0.3159(9)	0.4881(9)	0.9392(3)	0.059(3)
F(7)	-0.0435(12)	-0.1245(10)	0.4658(3)	0.078(3)
F(8)	0.0539(11)	-0.0374(12)	0.3877(3)	0.082(3)
F(9)	-0.1122(12)	0.0131(18)	0.4187(4)	0.128(5)
F(10)	0.0277(13)	0.1058(11)	0.4898(3)	0.094(3)
F(11)	0.1937(9)	0.0552(10)	0.4576(3)	0.067(2)
F(12)	0.1294(10)	0.1943(10)	0.4118(3)	0.062(2)
P(1)	0.3635(4)	0.6474(5)	0.9640(1)	0.0345(10)
P(2)	0.0412(4)	0.0333(5)	0.4389(1)	0.0361(9)
Co(1)	0.6972(2)	0.3448(2)	0.2046(1)	0.0187(3)

7.2.44 Tris(2-(1-methylimidazol-2-yl)pyridin)-cobalt(II)-bis(hexafluorophosphat) (sub65)

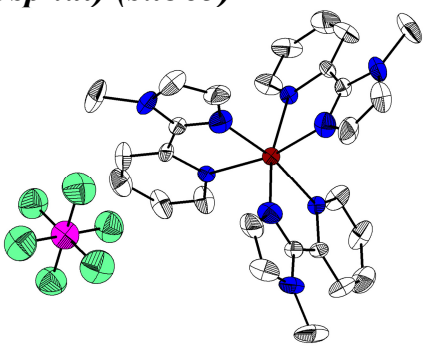

Kristalldaten

C27 H27 Co F12 N9 P2	M = 826.44 g/mol	Trigonal, $P\bar{3}c1$
a = 10.9579(17) Å	b = 10.9579 Å	c = 16.103(3) Å
α = 90°	β = 90°	γ = 120°
V = 1674.5(6) Å^3	Z = 2	F(000) = 834
D_{calc} = 1.639 g/cm^3	μ = 0.711 mm^{-1}	
orange needle	0.440 · 0.060 · 0.050 mm^3	

Datensammlung

Diffraktometer: D8 Quest (Bruker)	T = 100(2) K	λ = 0.71069 Å
h = -13 bis 13	k = -13 bis 13	l = -20 bis 20
19413 gemessene Reflexe	1223 unabhängige Reflexe	927 Reflexe mit $I > 2\sigma(I)$
θ = 2.146 bis 26.973°	R_{int} = 0.1382	C (25.00°) = 1.000
Absorptionskorrektur: Multi-scan	T_{min} = 0.3509	T_{max} = 0.7455

Verfeinerung

1223 Reflexe	27 Restraints	121 Parameter
Verfeinerung mit SHELXL-2014/7	bis χ = 0.000	
R_1 ($I > 2\sigma(I)$) = 0.0776	wR_2 ($I > 2\sigma(I)$) = 0.2140	
R_1 (all) = 0.0979	wR_2 (all) = 0.2326	GoF (S) = 1.115
$\Delta\varphi_{min}$ = -0.628 e·Å^{-3}	$\Delta\varphi_{max}$ = 1.253 e·Å^{-3}	

Kommentar

Die Pyridyl und Imidazolylringe sind in allen Fällen substitutionell fehlgeordnet (50:50) und wurden über ISOR, FLAT und DANG restrained. Die Synthese der Substanz und die Kristallzucht erfolgten durch Sebastian Ullrich im Rahmen seiner von mir betreuten Bachelorarbeit.[112]

Fraktionelle Atomkoordinaten (*x, y, z*) und äquivalente isotrope Auslenkungsfaktoren *U*(eq)

	x	*y*	*z*	*U*(eq)/Å^2		*x*	*y*	*z*	*U*(eq)/Å^2
N(1)	0.894(2)	0.821(2)	0.1735(13)	0.043(5)	N(3)	0.8779(13)	0.8050(13)	0.1871(10)	0.025(4)
C(1)	0.7729(17)	0.7271(15)	0.2035(9)	0.024(3)	C(5)	0.7442(14)	0.7167(13)	0.2190(7)	0.028(4)
C(2)	0.7996(19)	0.6416(19)	0.0873(11)	0.045(4)	C(6)	0.6494(10)	0.5969(10)	0.1754(6)	0.049(3)
C(3)	0.9098(19)	0.768(2)	0.1023(16)	0.051(8)	C(7)	0.6885(11)	0.5654(9)	0.0998(6)	0.055(3)
N(2)	0.7111(10)	0.6152(9)	0.1506(7)	0.041(2)	F(3)	0.4676(4)	0.7524(4)	0.1723(2)	0.0727(11)
C(4)	0.5772(13)	0.4818(10)	0.1551(8)	0.063(3)	F(4)	0.1975(5)	0.5800(4)	0.0582(2)	0.0832(13)
C(8)	0.8223(14)	0.6537(16)	0.0678(8)	0.048(5)	P(2)	0.3333	0.6667	0.1158(1)	0.0535(7)
C(9)	0.9170(12)	0.7735(16)	0.1115(10)	0.039(8)	Co(1)	1.0000	1.0000	0.2500	0.0253(5)

7.2.45 2-(Tetrazolyl)pyridin-zwitterion (fblf007)

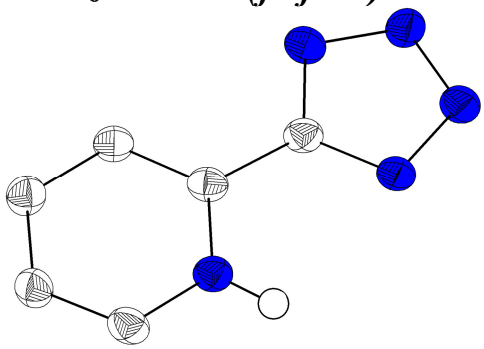

Kristalldaten

C6 H5 N5	M = 147.15 g/mol	Monoclinic, $P2_1/c$
a = 9.4348(7) Å	b = 13.1331(9) Å	c = 10.1072(7) Å
α = 90°	β = 97.424(6)°	γ = 90°
V = 1241.87(15) Å^3	Z = 8	F(000) = 608
D_{calc} = 1.574 g/cm^3	μ = 0.110 mm^{-1}	
colourless block (cut)	0.180 · 0.110 · 0.060 mm^3	

Datensammlung

Diffraktometer: STOE IPDS 2	T = 100(2) K	λ = 0.71073 Å
h = -11 bis 11	k = -16 bis 16	l = -12 bis 12
13368 gemessene Reflexe	2638 unabhängige Reflexe	1429 Reflexe mit $I > 2\sigma(I)$
θ = 2.177 bis 26.802°	R_{int} = 0.0749	C (25.00°) = 1.000
Absorptionskorrektur: Multi-scan	T_{min} = 0.9283	T_{max} = 1.0665

Verfeinerung

2638 Reflexe	0 Restraints	207 Parameter
Verfeinerung mit SHELXL-2014/7	bis χ = 0.000	
R_1 ($I > 2\sigma(I)$) = 0.0412	wR_2 ($I > 2\sigma(I)$) = 0.0833	
R_1 (all) = 0.0892	wR_2 (all) = 0.0920	GoF (S) = 0.803
$\Delta\varphi_{min}$ = -0.215 e·Å^{-3}	$\Delta\varphi_{max}$ = 0.243 e·Å^{-3}	

Fraktionelle Atomkoordinaten (*x, y, z*) und äquivalente isotrope Auslenkungsfaktoren *U*(eq)

	x	*y*	*z*	*U*(eq)/Å^2		*x*	*y*	*z*	*U*(eq)/Å^2
N(1)	0.2473(2)	0.9064(2)	-0.0153(2)	0.0261(5)	C(5)	0.2968(2)	0.8314(2)	-0.0886(2)	0.0286(5)
N(2)	0.1381(2)	1.0714(1)	0.1285(2)	0.0264(4)	C(1)	0.1575(2)	0.8872(2)	0.0756(2)	0.0254(5)
N(3)	0.0638(2)	1.1236(1)	0.2130(2)	0.0285(4)	C(6)	0.1076(2)	0.9740(2)	0.1483(2)	0.0251(5)
N(4)	-0.0063(2)	1.0578(1)	0.2795(2)	0.0295(4)	C(2)	0.1156(2)	0.7882(2)	0.0952(2)	0.0258(5)
N(5)	0.0190(2)	0.9617(2)	0.2408(2)	0.0298(5)	C(3)	0.1648(2)	0.7104(2)	0.0203(2)	0.0290(5)
N(6)	0.7422(2)	0.7581(1)	-0.0182(2)	0.0257(4)	C(10)	0.7732(2)	0.5827(2)	-0.0572(2)	0.0286(5)
N(7)	0.6199(2)	0.9241(1)	0.1125(2)	0.0265(4)	C(11)	0.8029(2)	0.6824(2)	-0.0821(2)	0.0289(5)
N(8)	0.5375(2)	0.9767(1)	0.1896(2)	0.0291(4)	C(7)	0.6502(2)	0.7393(2)	0.0709(2)	0.0262(5)
N(9)	0.4637(2)	0.9115(1)	0.2536(2)	0.0289(4)	C(12)	0.5893(2)	0.8263(2)	0.1338(2)	0.0261(5)
N(10)	0.4936(2)	0.8148(1)	0.2205(2)	0.0277(4)	C(9)	0.6790(2)	0.5609(2)	0.0340(2)	0.0288(5)
C(4)	0.2566(2)	0.7327(2)	-0.0729(2)	0.0284(5)	C(8)	0.6179(2)	0.6395(2)	0.0983(2)	0.0271(5)

7.3 Strukturen Für Timo Gneuß

7.3.1 Iodo-tri(pyrid-2-yl)phosphinoxid-kupfer(I)-acetonitrilsolvat (tgn343)

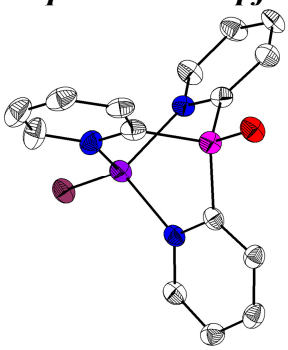

Kristalldaten

C16.50 H14.25 Cu I N3.75 O P	M = 502.48 g/mol	Monoclinic, $P2_1/n$
a = 8.6959(3) Å	b = 29.6332(11) Å	c = 14.5579(6) Å
α = 90°	β = 105.894(3)°	γ = 90°
V = 3608.0(2) Å^3	Z = 8	F(000) = 1956
D_{calc} = 1.850 g/cm^3	μ = 3.021 mm^{-1}	
red needle	0.210 · 0.040 · 0.040 mm^3	

Datensammlung

Diffraktometer: STOE IPDS 2	T = 100(2) K	λ = 0.71069 Å
h = -10 bis 10	k = -37 bis 33	l = -18 bis 18
33130 gemessene Reflexe	7632 unabhängige Reflexe	4265 Reflexe mit $I > 2\sigma(I)$
θ = 1.374 bis 26.730°	R_{int} = 0.0768	C (25.00°) = 1.000
Absorptionskorrektur: Multi-scan	T_{min} = 0.6549	T_{max} = 0.9041

Verfeinerung

7632 Reflexe	0 Restraints	453 Parameter
Verfeinerung mit SHELXL-2014/6	bis χ = 0.002	
R_1 ($I > 2\sigma(I)$) = 0.0300	wR_2 ($I > 2\sigma(I)$) = 0.0451	
R_1 (all) = 0.0707	wR_2 (all) = 0.0492	GoF (S) = 0.689
$\Delta\varphi_{min}$ = -0.768 e·Å^{-3}	$\Delta\varphi_{max}$ = 0.804 e·Å^{-3}	

Kommentar

Ein Acetonitrilmolekül ist über ein Inversionszentrum fehlgeordnet. Die Struktur wurde bereits veröffentlicht: T. Gneuß, M. J. Leitl, L. H. Finger, N. Rau, H. Yersin, J. Sundermeyer, *Dalton Trans.* **2015**, *44*, 8506–8520.

Fraktionelle Atomkoordinaten (*x, y, z*) und äquivalente isotrope Auslenkungsfaktoren *U*(eq)

	x	*y*	*z*	*U*(eq)/Å^2		*x*	*y*	*z*	*U*(eq)/Å^2
N(1)	-0.0800(4)	0.4903(1)	0.7543(2)	0.0237(8)	C(27)	0.5133(5)	0.6291(2)	0.5239(3)	0.0270(10)
C(5)	-0.1671(5)	0.4557(2)	0.7708(3)	0.0292(11)	C(28)	0.5651(6)	0.6345(2)	0.4417(3)	0.0347(12)
C(4)	-0.3272(6)	0.4597(2)	0.7681(3)	0.0333(12)	C(29)	0.6409(5)	0.6743(2)	0.4299(3)	0.0309(11)
C(3)	-0.4012(5)	0.5008(2)	0.7451(3)	0.0300(11)	C(30)	0.6618(5)	0.7076(2)	0.4990(3)	0.0302(11)
C(2)	-0.3142(5)	0.5371(2)	0.7275(3)	0.0284(11)	C(21)	0.6348(5)	0.6690(2)	0.7977(3)	0.0227(9)
N(2)	0.1431(4)	0.5224(1)	0.6316(2)	0.0243(9)	C(22)	0.6709(5)	0.6389(2)	0.8730(3)	0.0285(11)
C(10)	0.2116(5)	0.5106(2)	0.5629(3)	0.0267(10)	C(23)	0.7967(6)	0.6495(2)	0.9524(3)	0.0348(12)
C(9)	0.1957(5)	0.5359(2)	0.4810(3)	0.0284(11)	C(24)	0.8814(6)	0.6887(2)	0.9529(3)	0.0317(11)
C(8)	0.1003(5)	0.5737(2)	0.4666(3)	0.0293(11)	C(25)	0.8375(5)	0.7167(2)	0.8741(3)	0.0306(11)
C(7)	0.0282(5)	0.5863(2)	0.5365(3)	0.0257(10)	C(16)	0.3302(5)	0.7047(2)	0.6863(3)	0.0231(10)
N(3)	0.2287(4)	0.5414(1)	0.8432(3)	0.0305(9)	C(17)	0.1717(5)	0.6974(2)	0.6850(3)	0.0263(11)
C(15)	0.3524(6)	0.5431(2)	0.9213(3)	0.0378(12)	C(18)	0.0722(5)	0.7344(2)	0.6792(3)	0.0279(11)
C(14)	0.3913(7)	0.5806(2)	0.9784(3)	0.0432(14)	C(19)	0.1331(5)	0.7772(2)	0.6744(3)	0.0274(11)
C(13)	0.2979(6)	0.6189(2)	0.9555(3)	0.0375(13)	C(20)	0.2922(5)	0.7817(2)	0.6760(3)	0.0266(11)
C(12)	0.1687(6)	0.6181(2)	0.8749(3)	0.0292(11)	C(31)	0.5733(8)	0.8013(2)	0.9170(4)	0.0576(17)
C(26)	0.5394(5)	0.6639(1)	0.5893(3)	0.0226(10)	C(32)	0.4898(6)	0.7592(2)	0.9194(3)	0.0383(13)

	x	y	z	U(eq)/Å^2
C(1)	-0.1535(5)	0.5308(2)	0.7333(3)	0.0249(10)
C(6)	0.0540(5)	0.5599(2)	0.6175(3)	0.0232(10)
C(11)	0.1385(5)	0.5792(2)	0.8206(3)	0.0259(11)
N(6)	0.6120(4)	0.7031(1)	0.5786(2)	0.0240(9)
N(5)	0.7149(4)	0.7078(1)	0.7973(2)	0.0242(8)
N(4)	0.3911(4)	0.7463(1)	0.6826(2)	0.0234(8)
N(7)	0.4198(6)	0.7266(2)	0.9194(3)	0.0441(11)
O(1)	-0.1167(3)	0.6208(1)	0.6938(2)	0.0305(7)
O(2)	0.3916(3)	0.6132(1)	0.6984(2)	0.0270(7)

	x	y	z	U(eq)/Å^2
P(1)	-0.0300(1)	0.5775(1)	0.7140(1)	0.0248(3)
P(2)	0.4664(1)	0.6575(1)	0.6947(1)	0.0234(3)
Cu(1)	0.1574(1)	0.4868(1)	0.7553(1)	0.0254(1)
Cu(2)	0.6285(1)	0.7501(1)	0.6834(1)	0.0241(1)
I(1)	0.2620(1)	0.4079(1)	0.7718(1)	0.0274(1)
I(2)	0.7372(1)	0.8289(1)	0.6930(1)	0.0262(1)
C(34)	0.0629(19)	0.4939(5)	0.0189(9)	0.041(4)
N(8)	0.1491(17)	0.4643(5)	0.0306(8)	0.061(3)
C(33)	-0.0442(17)	0.5320(7)	0.0011(10)	0.044(3)

7.3.2 Chloro-tri(pyrid-2-yl)phosphinoxid-kupfer(I)-acetonitrilsolvat (tgn355)

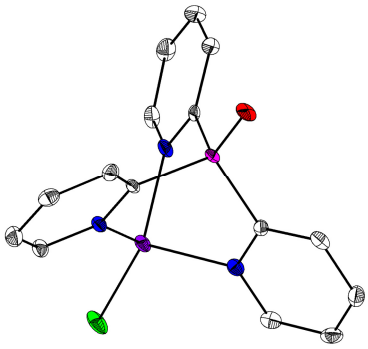

Kristalldaten

C16 H13.50 Cl Cu N3.50 O P	M = 400.76 g/mol	Orthorhombic, *Pbca*
a = 8.4558(6) Å	b = 27.6843(13) Å	c = 28.3435(16) Å
α = 90°	β = 90°	γ = 90°
V = 6635.0(7) Å^3	Z = 16	F(000) = 3248
D_{calc} = 1.605 g/cm^3	μ = 1.582 mm^{-1}	
red needle	0.660 · 0.260 · 0.190 mm^3	

Datensammlung

Diffraktometer: D8 Quest (Bruker)	T = 100(2) K	λ = 0.71069 Å
h = -10 bis 9	k = -33 bis 35	l = -32 bis 36
25305 gemessene Reflexe	7307 unabhängige Reflexe	5432 Reflexe mit $I > 2\sigma(I)$
θ = 2.610 bis 27.109°	R_{int} = 0.0891	C (25.00°) = 0.998
Absorptionskorrektur: Multi-scan	T_{min} = 0.414	T_{max} = 0.7455

Verfeinerung

7307 Reflexe	0 Restraints	425 Parameter
Verfeinerung mit SHELXL-2014/6	bis χ = 0.001	
R_1 ($I > 2\sigma(I)$) = 0.0658	wR_2 ($I > 2\sigma(I)$) = 0.1534	
R_1 (all) = 0.0911	wR_2 (all) = 0.1677	GoF (S) = 1.037
$\Delta\varphi_{min}$ = -1.633 e·Å^{-3}	$\Delta\varphi_{max}$ = 1.752 e·Å^{-3}	

Kommentar

Die Struktur wurde bereits veröffentlicht: T. Gneuß, M. J. Leitl, L. H. Finger, N. Rau, H. Yersin, J. Sundermeyer, *Dalton Trans.* **2015**, *44*, 8506–8520.

Fraktionelle Atomkoordinaten (*x, y, z*) und äquivalente isotrope Auslenkungsfaktoren *U*(eq)

	x	y	z	U(eq)/Å^2
Cu(2)	0.6896(1)	0.0261(1)	0.6115(1)	0.0127(2)
Cu(1)	0.5749(1)	0.2828(1)	0.6383(1)	0.0116(2)
Cl(1)	0.4700(1)	0.2846(1)	0.7098(1)	0.0206(3)
P(2)	0.5163(1)	0.0375(1)	0.7069(1)	0.0104(2)
Cl(2)	0.7745(1)	0.0164(1)	0.5380(1)	0.0186(2)

	x	y	z	U(eq)/Å^2
P(1)	0.7470(1)	0.2609(1)	0.5437(1)	0.0097(2)
O(1)	0.8278(3)	0.2510(1)	0.4981(1)	0.0155(7)
O(2)	0.4353(3)	0.0437(1)	0.7530(1)	0.0167(7)
N(6)	0.7252(4)	-0.0234(1)	0.6646(1)	0.0124(7)
N(1)	0.5370(4)	0.2186(1)	0.6028(1)	0.0118(7)

	x	y	z	U(eq)/Å^2
N(4)	0.4450(4)	0.0242(1)	0.6145(1)	0.0105(7)
C(5)	0.4400(5)	0.1836(2)	0.6172(2)	0.0150(9)
C(6)	0.8831(5)	0.2722(1)	0.5922(1)	0.0090(8)
N(2)	0.8166(4)	0.2826(1)	0.6344(1)	0.0107(7)
C(29)	0.8145(5)	-0.0983(2)	0.6972(2)	0.0202(10)
N(5)	0.7280(4)	0.0864(1)	0.6524(1)	0.0128(7)
C(26)	0.6390(5)	-0.0164(1)	0.7040(1)	0.0107(8)
C(19)	0.1821(5)	0.0198(1)	0.5828(2)	0.0140(9)
C(2)	0.6170(5)	0.1688(2)	0.5381(2)	0.0144(9)
C(3)	0.5176(5)	0.1319(2)	0.5536(2)	0.0168(9)
C(20)	0.3459(5)	0.0181(1)	0.5781(2)	0.0119(8)
C(17)	0.2173(5)	0.0347(1)	0.6652(2)	0.0139(9)
C(9)	1.0773(5)	0.2881(2)	0.6671(2)	0.0165(9)
N(3)	0.5391(4)	0.3261(1)	0.5808(1)	0.0125(7)
C(8)	1.1450(5)	0.2771(2)	0.6238(2)	0.0156(9)
C(1)	0.6207(5)	0.2112(1)	0.5633(1)	0.0099(8)
C(11)	0.6207(5)	0.3144(1)	0.5417(1)	0.0095(8)
C(12)	0.6135(5)	0.3412(2)	0.5004(2)	0.0154(9)
C(14)	0.4338(6)	0.3946(2)	0.5395(2)	0.0197(10)

	x	y	z	U(eq)/Å^2
C(30)	0.8126(5)	-0.0641(2)	0.6619(2)	0.0174(9)
C(4)	0.4246(5)	0.1402(2)	0.5933(2)	0.0171(9)
C(22)	0.6491(6)	0.1278(2)	0.7231(2)	0.0184(9)
C(27)	0.6376(5)	-0.0490(2)	0.7411(2)	0.0151(9)
C(21)	0.6433(5)	0.0890(1)	0.6926(1)	0.0115(8)
N(7)	0.3572(6)	-0.0888(2)	0.6460(2)	0.0311(10)
C(10)	0.9140(5)	0.2908(1)	0.6708(2)	0.0133(9)
C(7)	1.0451(5)	0.2685(1)	0.5852(2)	0.0134(9)
C(24)	0.8382(6)	0.1636(2)	0.6714(2)	0.0212(10)
C(16)	0.3805(5)	0.0319(1)	0.6577(1)	0.0092(8)
C(25)	0.8238(5)	0.1234(2)	0.6426(2)	0.0178(9)
C(15)	0.4481(5)	0.3652(2)	0.5793(2)	0.0159(9)
C(13)	0.5212(6)	0.3821(2)	0.4996(2)	0.0218(10)
C(28)	0.7246(6)	-0.0906(2)	0.7378(2)	0.0207(10)
C(23)	0.7464(6)	0.1663(2)	0.7119(2)	0.0236(11)
C(31)	0.5516(7)	-0.0977(2)	0.5757(2)	0.0422(15)
C(18)	0.1178(5)	0.0287(2)	0.6265(2)	0.0156(9)
C(32)	0.4421(6)	-0.0925(2)	0.6158(2)	0.0238(11)

7.3.3 Bromo-tri(pyrid-2-yl)phosphinoxid-kupfer(I)-acetonitrilsolvat (tgn356)

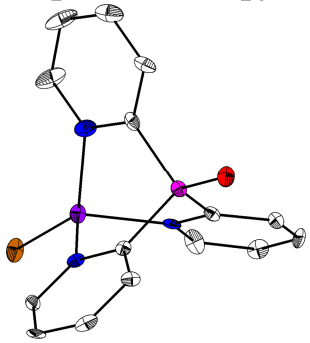

Kristalldaten

C16.50 H14.25 Br Cu N3.75 O P	M = 455.49 g/mol	Monoclinic, $P2_1/n$
a = 8.5684(10) Å	b = 28.964(3) Å	c = 14.501(2) Å
α = 90°	β = 106.175(5)°	γ = 90°
V = 3456.3(7) Å^3	Z = 8	F(000) = 1812
D_{calc} = 1.751 g/cm^3	μ = 3.679 mm^{-1}	
orange needle	0.450 · 0.190 · 0.130 mm^3	

Datensammlung

Diffraktometer: D8 Quest (Bruker)	T = 100(2) K	λ = 0.71069 Å
h = -10 bis 10	k = -37 bis 33	l = -18 bis 18
21656 gemessene Reflexe	7647 unabhängige Reflexe	4427 Reflexe mit $I > 2\sigma(I)$
θ = 2.029 bis 27.166°	R_{int} = 0.1277	C (25.00°) = 0.999
Absorptionskorrektur: Multi-scan	T_{min} = 0.5766	T_{max} = 0.7455

Verfeinerung

7647 Reflexe	0 Restraints	429 Parameter
Verfeinerung mit SHELXL-2014/6	bis χ = 0.005	
R_1 ($I > 2\sigma(I)$) = 0.0610	wR_2 ($I > 2\sigma(I)$) = 0.0912	
R_1 (all) = 0.1393	wR_2 (all) = 0.1068	GoF (S) = 1.031
$\Delta\varphi_{min}$ = -0.772 e·Å^{-3}	$\Delta\varphi_{max}$ = 0.820 e·Å^{-3}	

Kommentar

Ein Acetonitrilmolekül ist über ein Inversionszentrum fehlgeordnet. Dieses Molekül und einzelne Atome eines Komplexmoleküls wurde über EADP constrained. Die Struktur wurde bereits veröffentlicht: T. Gneuß, M. J. Leitl, L. H. Finger, N. Rau, H. Yersin, J. Sundermeyer, *Dalton Trans.* **2015**, *44*, 8506–8520.

Fraktionelle Atomkoordinaten (*x, y, z*) und äquivalente isotrope Auslenkungsfaktoren *U*(eq)

	x	*y*	*z*	*U*(eq)/Å^2
C(11)	0.3581(7)	0.5783(2)	0.6766(4)	0.0125(14)
C(12)	0.3305(7)	0.6182(2)	0.6221(4)	0.0164(14)
C(13)	0.2001(8)	0.6193(2)	0.5410(5)	0.0242(17)
C(14)	0.0998(8)	0.5819(2)	0.5182(5)	0.0287(18)
C(15)	0.1332(8)	0.5435(2)	0.5772(5)	0.0272(17)
C(1)	0.6508(7)	0.5269(2)	0.7640(4)	0.0112(13)
C(2)	0.8132(7)	0.5332(2)	0.7697(4)	0.0133(14)
C(3)	0.8987(7)	0.4954(2)	0.7516(4)	0.0173(15)
C(4)	0.8213(7)	0.4528(2)	0.7291(4)	0.0156(14)
C(5)	0.6582(7)	0.4501(2)	0.7261(4)	0.0186(15)
C(6)	0.4443(6)	0.5586(2)	0.8798(4)	0.0097(8)
C(7)	0.4773(7)	0.5849(2)	0.9634(4)	0.0120(13)
C(8)	0.4060(7)	0.5726(2)	1.0354(4)	0.0157(14)
C(9)	0.3037(7)	0.5349(2)	1.0200(4)	0.0134(14)
C(10)	0.2804(6)	0.5096(2)	0.9367(4)	0.0122(13)
C(21)	-0.1344(6)	0.6694(2)	0.7051(4)	0.0105(13)
C(22)	-0.1687(7)	0.6395(2)	0.6293(4)	0.0171(14)
C(23)	-0.2945(8)	0.6493(2)	0.5486(4)	0.0211(16)
C(24)	-0.3819(7)	0.6897(2)	0.5484(4)	0.0196(15)
C(25)	-0.3438(7)	0.7184(2)	0.6281(4)	0.0160(14)
C(16)	0.1751(7)	0.7065(2)	0.8175(4)	0.0088(13)
C(17)	0.3341(6)	0.6998(2)	0.8172(4)	0.0111(13)
C(18)	0.4339(7)	0.7373(2)	0.8234(4)	0.0160(15)
C(19)	0.3703(7)	0.7809(2)	0.8266(4)	0.0143(14)
C(20)	0.2085(6)	0.7852(2)	0.8255(4)	0.0097(8)
C(26)	-0.0385(6)	0.6636(2)	0.9154(4)	0.0097(8)
C(27)	-0.0120(6)	0.6282(2)	0.9814(4)	0.0137(14)
C(28)	-0.0662(7)	0.6332(2)	1.0625(4)	0.0175(15)
C(29)	-0.1430(7)	0.6729(2)	1.0748(4)	0.0195(15)
C(30)	-0.1648(6)	0.7074(2)	1.0051(4)	0.0152(14)
C(31)	-0.0815(9)	0.8057(2)	0.5925(5)	0.041(2)
C(32)	0.0002(8)	0.7628(2)	0.5874(5)	0.0221(16)
C(34)	0.558(2)	0.5063(6)	0.5149(13)	0.038(3)
N(8)	0.6568(16)	0.5333(5)	0.5296(10)	0.038(3)
C(33)	0.441(2)	0.4698(6)	0.4986(14)	0.038(3)
N(3)	0.2607(6)	0.5411(2)	0.6547(3)	0.0163(12)
N(1)	0.5737(5)	0.4870(2)	0.7429(3)	0.0100(11)
N(2)	0.3497(5)	0.5209(2)	0.8666(3)	0.0100(11)
N(5)	-0.2189(5)	0.7088(2)	0.7064(3)	0.0109(11)
N(4)	0.1115(5)	0.7493(2)	0.8216(3)	0.0093(11)
N(6)	-0.1129(5)	0.7034(2)	0.9261(3)	0.0095(11)
N(7)	0.0672(7)	0.7295(2)	0.5816(4)	0.0282(14)
O(1)	0.6207(4)	0.6198(1)	0.8037(3)	0.0165(10)
O(2)	0.1127(4)	0.6127(1)	0.8052(3)	0.0152(10)
P(1)	0.5293(2)	0.5759(1)	0.7839(1)	0.0107(3)
P(2)	0.0364(2)	0.6581(1)	0.8093(1)	0.0104(3)
Cu(1)	0.3314(1)	0.4846(1)	0.7416(1)	0.0131(2)
Cu(2)	-0.1303(1)	0.7517(1)	0.8211(1)	0.0117(2)
Br(1)	0.2321(1)	0.4088(1)	0.7293(1)	0.0186(2)
Br(2)	-0.2337(1)	0.8271(1)	0.8141(1)	0.0147(2)

7.3.4 Iodo-tri(pyrid-2-yl)methan-kupfer(I) (tgn430)

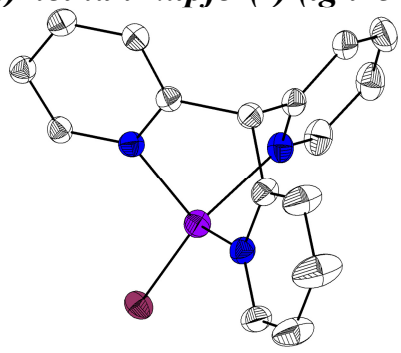

Kristalldaten

C16 H13 Cu I N3	M = 437.73 g/mol	Monoclinic, $P2_1/n$
a = 14.7528(4) Å	b = 13.4193(3) Å	c = 16.0010(4) Å
α = 90°	β = 90.266(2)°	γ = 90°
V = 3167.72(14) Å^3	Z = 8	F(000) = 1696
D_{calc} = 1.836 g/cm^3	μ = 3.324 mm^{-1}	
yellow plate	0.490 · 0.250 · 0.100 mm^3	

Datensammlung

Diffraktometer: STOE IPDS 2T	T = 100(2) K	λ = 0.71069 Å
h = -18 bis 18	k = -16 bis 16	l = -20 bis 20
47871 gemessene Reflexe	6720 unabhängige Reflexe	5801 Reflexe mit $I > 2\sigma(I)$
θ = 1.873 bis 26.746°	R_{int} = 0.1108	C (25.00°) = 1.000
Absorptionskorrektur: Multi-scan	T_{min} = 0.2865	T_{max} = 0.5605

Verfeinerung

6720 Reflexe	0 Restraints	379 Parameter
Verfeinerung mit SHELXL-2014/6	bis χ = 0.002	
R_1 ($I > 2\sigma(I)$) = 0.0274	wR_2 ($I > 2\sigma(I)$) = 0.0705	
R_1 (all) = 0.0369	wR_2 (all) = 0.0745	GoF (S) = 1.098
$\Delta\varphi_{min}$ = -0.906 e·Å^{-3}	$\Delta\varphi_{max}$ = 0.534 e·Å^{-3}	

Kommentar

CheckCif/Platon liefert einen B-Alert wegen zusätzlicher (Pseudo)symmetrie. Diese findet sich in einem partiellen F und C Superlattice wieder. In der Raumgruppe *C*2/*c* liefert die Struktur aber deutlich höhere R-Werte und weist zwei fehlgeordnete Pyridylringe auf. Die Struktur wurde bereits veröffentlicht: T. Gneuß, M. J. Leitl, L. H. Finger, N. Rau, H. Yersin, J. Sundermeyer, *Dalton Trans.* **2015**, *44*, 8506–8520.

Fraktionelle Atomkoordinaten (*x, y, z*) und äquivalente isotrope Auslenkungsfaktoren *U*(eq)

	x	*y*	*z*	*U*(eq)/Å^2		*x*	*y*	*z*	*U*(eq)/Å^2
I(1)	0.9113(1)	0.2404(1)	0.8972(1)	0.0260(1)	C(7)	0.8366(2)	-0.2145(2)	0.7907(2)	0.0293(5)
I(2)	0.0962(1)	0.2443(1)	0.5961(1)	0.0250(1)	C(6)	0.8252(2)	-0.1118(2)	0.7874(1)	0.0249(5)
Cu(1)	0.8455(1)	0.1002(1)	0.8181(1)	0.0249(1)	C(11)	0.7810(2)	0.0018(2)	0.6688(1)	0.0253(5)
Cu(2)	0.1546(1)	0.1128(1)	0.6901(1)	0.0245(1)	C(16)	0.7469(2)	-0.0664(2)	0.7380(1)	0.0223(4)
N(1)	0.7092(1)	0.0653(1)	0.8383(1)	0.0224(4)	C(20)	0.4275(2)	0.0691(2)	0.5846(1)	0.0252(5)
N(3)	0.8253(1)	0.0851(1)	0.6914(1)	0.0244(4)	C(27)	0.2321(2)	0.0240(2)	0.8379(1)	0.0248(5)
N(4)	0.2891(1)	0.0699(1)	0.6623(1)	0.0217(4)	C(4)	0.5667(2)	0.0738(2)	0.9092(1)	0.0250(5)
N(6)	0.1843(1)	0.1048(1)	0.8153(1)	0.0254(4)	C(26)	0.0404(2)	-0.0726(2)	0.6501(2)	0.0295(5)
N(5)	0.1133(1)	-0.0350(1)	0.6888(1)	0.0267(4)	C(15)	0.8574(2)	0.1447(2)	0.6313(2)	0.0303(5)
N(2)	0.8816(1)	-0.0488(2)	0.8273(1)	0.0268(4)	C(8)	0.9086(2)	-0.2527(2)	0.8367(2)	0.0368(6)
C(1)	0.6802(2)	-0.0164(2)	0.7971(1)	0.0211(4)	C(23)	0.1556(2)	-0.1995(2)	0.7309(2)	0.0297(5)
C(17)	0.3180(2)	-0.0105(2)	0.7050(1)	0.0211(4)	C(10)	0.9514(2)	-0.0869(2)	0.8711(2)	0.0329(5)
C(2)	0.5946(2)	-0.0568(2)	0.8104(1)	0.0242(5)	C(25)	0.0214(2)	-0.1739(2)	0.6487(2)	0.0340(5)
C(21)	0.3430(2)	0.1087(2)	0.6036(1)	0.0226(4)	C(31)	0.1665(2)	0.1741(2)	0.8737(2)	0.0314(5)
C(18)	0.4014(2)	-0.0549(2)	0.6892(1)	0.0238(5)	C(12)	0.7685(2)	-0.0240(2)	0.5861(2)	0.0398(6)
C(5)	0.6530(2)	0.1092(2)	0.8926(1)	0.0227(4)	C(30)	0.1974(2)	0.1667(2)	0.9550(2)	0.0413(6)
C(22)	0.1702(2)	-0.0971(2)	0.7290(1)	0.0252(5)	C(28)	0.2639(2)	0.0107(2)	0.9186(2)	0.0370(6)
C(19)	0.4565(2)	-0.0144(2)	0.6285(1)	0.0254(5)	C(14)	0.8474(2)	0.1241(2)	0.5475(2)	0.0439(7)
C(32)	0.2538(2)	-0.0530(2)	0.7705(1)	0.0226(4)	C(9)	0.9669(2)	-0.1884(2)	0.8770(2)	0.0367(6)
C(24)	0.0801(2)	-0.2379(2)	0.6898(2)	0.0353(6)	C(29)	0.2473(2)	0.0840(2)	0.9780(2)	0.0456(7)
C(3)	0.5376(2)	-0.0112(2)	0.8671(1)	0.0273(5)	C(13)	0.8030(2)	0.0374(3)	0.5244(2)	0.0543(9)

7.3.5 Iodo-tri(pyrid-2-yl)phosphinsulfid-kupfer(I)-acetonitrilsolvat (tgv40)

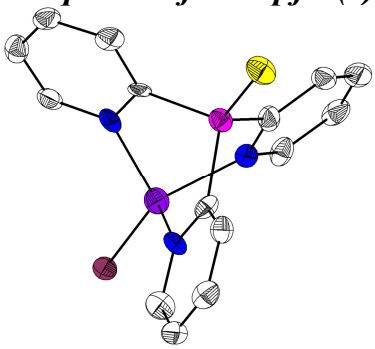

Kristalldaten

C47 H39 Cu3 I3 N10 P3 S3	*M* = 1504.35 g/mol	Orthorhombic, $Pc2_1b$
a = 13.2413(5) Å	*b* = 15.7217(6) Å	*c* = 25.7987(11) Å
α = 90°	β = 90°	γ = 90°
V = 5370.7(4) Å^3	*Z* = 4	*F*(000) = 2920
D_{calc} = 1.860 g/cm^3	μ = 3.152 mm^{-1}	
orange block	0.310 · 0.280 · 0.180 mm^3	

Datensammlung

Diffraktometer: STOE IPDS 2	T = 100(2) K	λ = 0.71069 Å
h = -14 bis 16	k = -19 bis 17	l = -32 bis 28
18930 gemessene Reflexe	10265 unabhängige Reflexe	6869 Reflexe mit $I > 2\sigma(I)$
θ = 1.729 bis 26.739°	R_{int} = 0.0583	C (25.00°) = 0.999
Absorptionskorrektur: Multi-scan	T_{min} = 0.4067	T_{max} = 0.4993

Verfeinerung

10265 Reflexe	1 Restraints	623 Parameter
Verfeinerung mit SHELXL-2014/6	bis χ = 0.001	
R_1 ($I > 2\sigma(I)$) = 0.0376	wR_2 ($I > 2\sigma(I)$) = 0.0796	
R_1 (all) = 0.0551	wR_2 (all) = 0.0822	GoF (S) = 0.747
$\Delta\varphi_{min}$ = -0.665 e·Å^{-3}	$\Delta\varphi_{max}$ = 1.097 e·Å^{-3}	

Kommentar

Die Struktur wurde bereits veröffentlicht: T. Gneuß, M. J. Leitl, L. H. Finger, N. Rau, H. Yersin, J. Sundermeyer, *Dalton Trans.* **2015**, *44*, 8506–8520.

Fraktionelle Atomkoordinaten (*x, y, z*) und äquivalente isotrope Auslenkungsfaktoren *U*(eq)

	x	*y*	*z*	*U*(eq)/Å^2
C(1)	0.2648(8)	0.6779(8)	0.8708(5)	0.023(3)
C(2)	0.2044(9)	0.7258(8)	0.9005(4)	0.027(3)
C(3)	0.2467(10)	0.7801(8)	0.9376(4)	0.030(3)
C(4)	0.3505(10)	0.7813(8)	0.9419(5)	0.031(3)
C(5)	0.4073(9)	0.7298(9)	0.9097(5)	0.031(3)
C(11)	0.2647(9)	0.6195(8)	0.7617(4)	0.026(3)
C(12)	0.2020(9)	0.6240(8)	0.7193(4)	0.026(3)
C(13)	0.2458(11)	0.6348(8)	0.6705(5)	0.035(3)
C(14)	0.3486(11)	0.6418(8)	0.6670(4)	0.035(3)
C(15)	0.4041(10)	0.6383(8)	0.7114(4)	0.028(3)
C(6)	0.2650(9)	0.4988(7)	0.8460(4)	0.020(3)
C(7)	0.2045(9)	0.4328(8)	0.8633(4)	0.028(3)
C(8)	0.2494(10)	0.3583(8)	0.8801(4)	0.029(3)
C(9)	0.3517(9)	0.3518(8)	0.8785(4)	0.029(3)
C(10)	0.4091(9)	0.4195(9)	0.8594(4)	0.026(3)
C(16)	0.2463(9)	0.4916(8)	0.0322(4)	0.024(3)
C(17)	0.1734(9)	0.4644(8)	-0.0025(4)	0.025(3)
C(18)	0.1001(9)	0.5211(9)	-0.0175(4)	0.029(3)
C(19)	0.1024(8)	0.6040(10)	0.0021(4)	0.029(3)
C(20)	0.1777(8)	0.6255(8)	0.0367(4)	0.026(3)
C(26)	0.4586(8)	0.4836(7)	0.0225(4)	0.019(2)
C(27)	0.5118(8)	0.4519(8)	-0.0194(4)	0.025(3)
C(28)	0.5797(9)	0.5044(8)	-0.0437(4)	0.025(3)
C(29)	0.5921(8)	0.5871(8)	-0.0268(4)	0.026(3)
C(30)	0.5383(8)	0.6128(9)	0.0161(4)	0.026(3)
C(21)	0.3616(8)	0.4225(7)	0.1195(4)	0.019(2)
C(22)	0.3585(9)	0.3454(8)	0.1464(4)	0.024(3)
C(23)	0.3622(9)	0.3488(8)	0.1998(4)	0.027(3)
C(24)	0.3708(9)	0.4263(8)	0.2251(4)	0.028(3)
C(25)	0.3745(8)	0.4995(8)	0.1952(4)	0.023(3)
C(36)	1.0498(9)	0.4970(8)	0.1902(4)	0.024(3)
C(37)	1.1223(9)	0.5359(9)	0.2218(4)	0.029(3)
C(38)	1.1526(8)	0.6170(9)	0.2103(4)	0.031(3)
C(39)	1.1105(8)	0.6580(8)	0.1678(4)	0.027(3)
C(40)	1.0387(8)	0.6170(8)	0.1397(4)	0.023(3)
C(31)	0.8728(10)	0.3855(8)	0.2017(4)	0.029(3)
C(32)	0.8218(11)	0.3458(9)	0.2421(5)	0.039(3)
C(33)	0.7168(11)	0.3448(9)	0.2399(4)	0.038(4)
C(34)	0.6671(11)	0.3816(9)	0.1993(5)	0.043(4)
C(35)	0.7236(9)	0.4194(8)	0.1602(5)	0.029(3)
C(41)	1.0449(9)	0.3310(8)	0.1408(4)	0.024(3)
C(42)	1.1080(9)	0.2625(9)	0.1410(4)	0.030(3)
C(43)	1.1304(9)	0.2226(9)	0.0954(5)	0.034(3)
C(44)	1.0888(8)	0.2528(9)	0.0505(5)	0.031(3)
C(45)	1.0254(8)	0.3242(8)	0.0529(4)	0.023(3)
C(46)	0.8526(10)	0.4345(9)	0.8857(5)	0.040(4)
C(47)	0.9256(11)	0.3718(9)	0.9049(5)	0.033(3)
N(1)	0.3663(7)	0.6777(6)	0.8749(3)	0.022(2)
N(3)	0.3658(7)	0.6264(6)	0.7594(3)	0.025(2)
N(2)	0.3668(7)	0.4932(6)	0.8444(3)	0.022(2)
N(4)	0.2494(7)	0.5708(6)	0.0512(4)	0.024(2)
N(6)	0.4705(7)	0.5625(6)	0.0405(3)	0.023(2)
N(5)	0.3708(7)	0.4997(6)	0.1433(3)	0.021(2)
N(8)	1.0084(7)	0.5379(7)	0.1493(3)	0.023(2)
N(7)	0.8247(7)	0.4217(7)	0.1615(3)	0.026(2)
N(9)	1.0049(7)	0.3636(7)	0.0970(3)	0.025(2)
N(10)	0.9823(10)	0.3241(9)	0.9200(5)	0.047(3)
P(1)	0.2094(2)	0.5991(3)	0.8260(1)	0.0236(6)
P(2)	0.3527(2)	0.4222(2)	0.0487(1)	0.0211(6)
P(3)	1.0112(3)	0.3870(2)	0.2011(1)	0.0272(8)
S(1)	0.0633(2)	0.5991(3)	0.8260(1)	0.0331(7)
S(2)	0.3429(2)	0.3087(2)	0.0195(1)	0.0255(7)
S(3)	1.0717(3)	0.3368(3)	0.2623(1)	0.0428(9)
Cu(1)	0.4481(1)	0.6009(1)	0.8251(1)	0.0273(3)
Cu(2)	0.3711(1)	0.6050(1)	0.0971(1)	0.0244(3)
Cu(3)	0.9147(1)	0.4681(1)	0.1026(1)	0.0245(3)
I(1)	0.6377(1)	0.6050(1)	0.8267(1)	0.0228(2)
I(2)	0.3756(1)	0.7559(1)	0.1283(1)	0.0329(2)
I(3)	0.8267(1)	0.5395(1)	0.0293(1)	0.0301(2)

7.3.6 Iodo-tri(pyrid-2-yl)phosphinselenid-kupfer(I)-acetonitrilsolvat (tgv41)

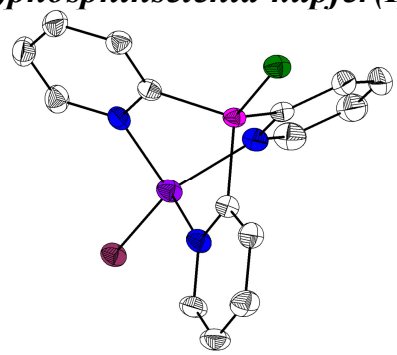

Kristalldaten

C20 H19.50 Cu I N5.50 P Se	M = 637.28 g/mol	Monoclinic, $P2_1/a$
a = 8.7685(3) Å	b = 15.6075(5) Å	c = 18.0144(8) Å
α = 90°	β = 104.011(3)°	γ = 90°
V = 2392.00(16) Å^3	Z = 4	F(000) = 1236
D_{calc} = 1.770 g/cm^3	μ = 3.809 mm^{-1}	
orange needle	0.440 · 0.110 · 0.040 mm^3	

Datensammlung

Diffraktometer: STOE IPDS 2	T = 100(2) K	λ = 0.71069 Å
h = -8 bis 11	k = -19 bis 18	l = -22 bis 22
13242 gemessene Reflexe	5056 unabhängige Reflexe	3816 Reflexe mit $I > 2\sigma(I)$
θ = 1.749 bis 26.724°	R_{int} = 0.0437	C (25.00°) = 0.999
Absorptionskorrektur: Multi-scan	T_{min} = 0.4536	T_{max} = 0.6916

Verfeinerung

5056 Reflexe	0 Restraints	284 Parameter
Verfeinerung mit SHELXL-2014/6	bis χ = 0.002	
R_1 ($I > 2\sigma(I)$) = 0.0298	wR_2 ($I > 2\sigma(I)$) = 0.0592	
R_1 (all) = 0.0440	wR_2 (all) = 0.0613	GoF (S) = 0.865
$\Delta\varphi_{min}$ = -0.836 e·Å^{-3}	$\Delta\varphi_{max}$ = 0.996 e·Å^{-3}	

Kommentar

Ein Acetonitrilmolekül ist über ein Inversionszentrum fehlgeordnet. Die Struktur wurde bereits veröffentlicht: T. Gneuß, M. J. Leitl, L. H. Finger, N. Rau, H. Yersin, J. Sundermeyer, *Dalton Trans.* **2015**, *44*, 8506–8520.

Fraktionelle Atomkoordinaten (*x, y, z*) und äquivalente isotrope Auslenkungsfaktoren *U*(eq)

	x	*y*	*z*	*U*(eq)/Å^2
I(1)	0.0811(1)	0.6736(1)	0.8431(1)	0.0252(1)
Se(1)	0.3816(1)	0.2439(1)	0.7229(1)	0.0268(1)
Cu(1)	0.1703(1)	0.5313(1)	0.8080(1)	0.0249(1)
P(1)	0.2979(1)	0.3596(1)	0.7582(1)	0.0194(2)
C(7)	0.0886(4)	0.3692(2)	0.6130(2)	0.0263(8)
C(12)	0.2512(5)	0.2761(2)	0.8880(2)	0.0306(9)
C(2)	0.6019(4)	0.4280(2)	0.7769(2)	0.0268(8)
C(1)	0.4492(4)	0.4437(2)	0.7807(2)	0.0236(7)
N(1)	0.4003(4)	0.5198(2)	0.8017(2)	0.0252(6)
C(10)	-0.0441(4)	0.5160(3)	0.6502(2)	0.0294(8)
N(2)	0.0728(3)	0.4799(2)	0.7029(2)	0.0239(6)
C(19)	0.3033(5)	0.7482(3)	0.5990(2)	0.0357(9)
C(6)	0.1369(4)	0.4070(2)	0.6845(2)	0.0219(7)
N(3)	0.1648(4)	0.4213(2)	0.8690(2)	0.0256(7)
C(11)	0.2292(4)	0.3510(2)	0.8466(2)	0.0234(7)

	x	*y*	*z*	*U*(eq)/Å^2
C(9)	-0.1000(5)	0.4808(3)	0.5786(2)	0.0333(9)
C(8)	-0.0319(5)	0.4073(3)	0.5597(2)	0.0326(9)
N(4)	0.4115(5)	0.5174(3)	0.5925(2)	0.0533(11)
C(17)	0.4613(5)	0.4526(3)	0.5808(2)	0.0378(10)
C(13)	0.2027(5)	0.2722(3)	0.9560(2)	0.0391(10)
C(4)	0.6625(5)	0.5726(3)	0.8163(2)	0.0341(9)
C(14)	0.1325(5)	0.3430(3)	0.9784(2)	0.0384(10)
C(18)	0.2600(6)	0.7042(3)	0.6616(2)	0.0454(11)
N(5)	0.3394(5)	0.7829(3)	0.5504(2)	0.0515(10)
C(5)	0.5073(5)	0.5829(2)	0.8194(2)	0.0293(8)
C(3)	0.7110(5)	0.4940(3)	0.7953(2)	0.0320(9)
C(16)	0.5221(5)	0.3695(3)	0.5642(2)	0.0418(10)
C(15)	0.1149(5)	0.4163(3)	0.9341(2)	0.0346(9)
C(21)	-0.0214(14)	-0.0118(7)	1.0157(6)	0.042(3)
C(20)	0.0569(19)	0.0643(12)	0.9964(7)	0.039(3)
N(6)	-0.084(2)	-0.0696(11)	1.0312(7)	0.067(5)

7.3.7 Chloro-tri(pyrid-2-yl)phosphinsulfid-kupfer(I)-acetonitrilsolvat (tgv54)

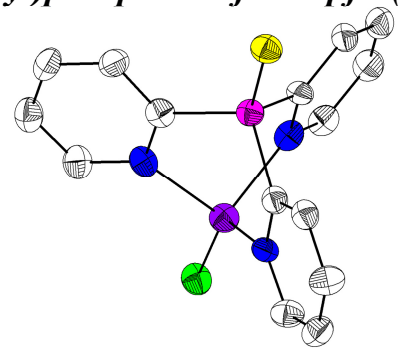

Kristalldaten

C18 H16.50 Cl Cu N4.50 P S	M = 457.88 g/mol	Orthorhombic, *Pccn*
a = 15.0776(12) Å	b = 30.280(2) Å	c = 8.6832(4) Å
α = 90°	β = 90°	γ = 90°
V = 3964.3(4) Å^3	Z = 8	F(000) = 1864
D_{calc} = 1.534 g/cm^3	μ = 1.434 mm^{-1}	
red needle	0.250 · 0.040 · 0.040 mm^3	

Datensammlung

Diffraktometer: STOE IPDS 2	T = 100(2) K	λ = 0.71069 Å
h = -16 bis 19	k = -32 bis 38	l = -9 bis 10
13790 gemessene Reflexe	4187 unabhängige Reflexe	1823 Reflexe mit $I > 2\sigma(I)$
θ = 1.509 bis 26.721°	R_{int} = 0.1005	C (25.00°) = 0.999
Absorptionskorrektur: Multi-scan	T_{min} = 0.8576	T_{max} = 0.8917

Verfeinerung

4187 Reflexe	0 Restraints	243 Parameter
Verfeinerung mit SHELXL-2014/6	bis χ = 0.001	
R_1 ($I > 2\sigma(I)$) = 0.0417	wR_2 ($I > 2\sigma(I)$) = 0.0583	
R_1 (all) = 0.1226	wR_2 (all) = 0.0703	GoF (S) = 0.715
$\Delta\varphi_{min}$ = -0.544 e·Å^{-3}	$\Delta\varphi_{max}$ = 0.467 e·Å^{-3}	

Kommentar

Ein Acetonitrilmolekül ist über ein Inversionszentrum fehlgeordnet. Dieses wurde über EADP constrained. Die Struktur wurde bereits veröffentlicht: T. Gneuß, M. J. Leitl, L. H. Finger, N. Rau, H. Yersin, J. Sundermeyer, *Dalton Trans.* **2015**, *44*, 8506–8520.

Fraktionelle Atomkoordinaten (*x, y, z*) und äquivalente isotrope Auslenkungsfaktoren *U*(eq)

	x	*y*	*z*	*U*(eq)/Å^2		*x*	*y*	*z*	*U*(eq)/Å^2
C(11)	0.3975(3)	0.1779(1)	0.6956(5)	0.0288(11)	C(5)	0.4221(3)	0.0376(2)	0.8756(6)	0.0368(12)
C(12)	0.3518(3)	0.2175(1)	0.6980(5)	0.0321(11)	C(16)	0.7656(3)	0.1772(2)	0.6424(7)	0.0549(15)
C(13)	0.3838(3)	0.2527(2)	0.7804(6)	0.0374(12)	C(17)	0.6944(3)	0.2037(2)	0.5801(7)	0.0494(15)
C(14)	0.4617(3)	0.2476(2)	0.8610(5)	0.0377(11)	N(3)	0.4751(2)	0.1724(1)	0.7751(4)	0.0308(9)
C(15)	0.5052(3)	0.2075(2)	0.8536(6)	0.0347(11)	N(2)	0.5280(2)	0.1110(1)	0.5134(4)	0.0323(8)
C(6)	0.4495(3)	0.1215(1)	0.4465(5)	0.0277(10)	N(1)	0.4241(2)	0.0743(1)	0.7872(4)	0.0321(10)
C(7)	0.4381(3)	0.1230(1)	0.2896(5)	0.0322(12)	N(4)	0.6390(3)	0.2244(2)	0.5292(7)	0.0809(18)
C(8)	0.5093(3)	0.1127(2)	0.1943(5)	0.0383(12)	P(1)	0.3576(1)	0.1324(1)	0.5784(1)	0.0290(3)
C(9)	0.5891(3)	0.1016(1)	0.2605(6)	0.0375(11)	S(1)	0.2464(1)	0.1459(1)	0.4760(2)	0.0354(3)
C(10)	0.5959(3)	0.1014(1)	0.4183(5)	0.0344(11)	Cl(1)	0.6598(1)	0.0879(1)	0.8594(1)	0.0360(3)
C(1)	0.3528(3)	0.0826(1)	0.6988(5)	0.0299(11)	Cu(1)	0.5359(1)	0.1131(1)	0.7504(1)	0.0328(1)
C(2)	0.2801(3)	0.0546(2)	0.6917(5)	0.0349(12)	C(19)	-0.0114(13)	-0.0066(8)	1.026(2)	0.078(4)
C(3)	0.2809(3)	0.0169(1)	0.7811(6)	0.0373(13)	N(5)	-0.061(2)	-0.0134(9)	1.099(4)	0.078(4)
C(4)	0.3522(3)	0.0086(2)	0.8748(6)	0.0391(12)	C(18)	0.066(2)	0.0010(11)	0.909(5)	0.078(4)

7.3.8 Bromo-tri(pyrid-2-yl)phosphinsulfid-kupfer(I)-acetonitrilsolvat (tgv55)

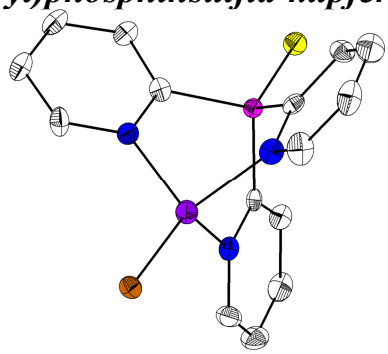

Kristalldaten

C20 H19.50 Br Cu N5.50 P S	M = 543.39 g/mol	Monoclinic, $P2_1/a$
a = 8.5838(3) Å	b = 15.2046(7) Å	c = 17.8716(6) Å
α = 90°	β = 103.386(3)°	γ = 90°
V = 2269.11(15) Å^3	Z = 4	F(000) = 1092
D_{calc} = 1.591 g/cm^3	μ = 2.904 mm^{-1}	
orange plate	0.200 · 0.130 · 0.050 mm^3	

Datensammlung

Diffraktometer: STOE IPDS 2T	T = 100(2) K	λ = 0.71069 Å
h = -10 bis 10	k = -19 bis 19	l = -22 bis 22
17036 gemessene Reflexe	4804 unabhängige Reflexe	3562 Reflexe mit $I > 2\sigma(I)$
θ = 1.779 bis 26.713°	R_{int} = 0.0599	C (25.00°) = 1.000
Absorptionskorrektur: Multi-scan	T_{min} = 0.6731	T_{max} = 0.7337

Verfeinerung

4804 Reflexe	0 Restraints	283 Parameter
Verfeinerung mit SHELXL-2014/6	bis χ = 0.001	
R_1 ($I > 2\sigma(I)$) = 0.0522	wR_2 ($I > 2\sigma(I)$) = 0.1145	
R_1 (all) = 0.0760	wR_2 (all) = 0.1196	GoF (S) = 1.085
$\Delta\varphi_{min}$ = -0.840 e·Å^{-3}	$\Delta\varphi_{max}$ = 0.763 e·Å^{-3}	

Kommentar

Ein Acetonitrilmolekül ist über ein Inversionszentrum fehlgeordnet. Die Struktur wurde bereits veröffentlicht: T. Gneuß, M. J. Leitl, L. H. Finger, N. Rau, H. Yersin, J. Sundermeyer, *Dalton Trans.* **2015**, *44*, 8506–8520.

Fraktionelle Atomkoordinaten (*x, y, z*) und äquivalente isotrope Auslenkungsfaktoren *U*(eq)

	x	y	z	U(eq)/Å^2
C(7)	0.7545(7)	0.7765(3)	0.3957(3)	0.0206(11)
N(3)	0.9010(5)	1.0242(3)	0.3039(2)	0.0180(9)
N(1)	0.5712(5)	0.9804(3)	0.2039(2)	0.0183(9)
C(9)	0.6257(7)	0.8477(4)	0.4848(3)	0.0287(13)
C(4)	0.4004(7)	0.9776(4)	0.0773(3)	0.0271(12)
C(5)	0.4542(7)	1.0160(4)	0.1494(3)	0.0250(12)
C(3)	0.4728(7)	0.9011(4)	0.0612(3)	0.0252(12)
C(14)	1.1680(7)	1.0796(4)	0.3172(3)	0.0270(12)
C(8)	0.7027(8)	0.7751(4)	0.4645(3)	0.0303(13)
C(19)	0.7910(7)	0.2531(4)	0.0998(3)	0.0277(13)
C(16)	0.0231(8)	0.8729(4)	0.0738(3)	0.0316(13)
C(6)	0.7283(6)	0.8520(3)	0.3511(3)	0.0164(10)
C(15)	1.0087(7)	1.0896(3)	0.3202(3)	0.0236(11)
C(13)	1.2174(7)	0.9984(4)	0.2967(3)	0.0243(11)
C(1)	0.6395(6)	0.9057(3)	0.1878(3)	0.0155(10)

	x	y	z	U(eq)/Å^2
N(5)	0.8224(8)	0.2796(4)	0.0460(3)	0.0431(14)
C(17)	-0.0355(8)	0.9601(4)	0.0850(3)	0.0336(14)
C(11)	0.9518(6)	0.9452(3)	0.2840(3)	0.0172(10)
N(4)	-0.0817(9)	1.0289(4)	0.0952(3)	0.0511(16)
C(18)	0.7523(9)	0.2182(5)	0.1690(3)	0.0437(17)
C(10)	0.6042(7)	0.9206(4)	0.4369(3)	0.0268(12)
C(2)	0.5933(6)	0.8639(3)	0.1169(3)	0.0198(11)
C(12)	1.1083(6)	0.9300(4)	0.2805(3)	0.0192(11)
N(2)	0.6567(5)	0.9240(3)	0.3716(2)	0.0203(9)
S(1)	0.8822(2)	0.7479(1)	0.2331(1)	0.0195(3)
P(1)	0.8008(2)	0.8587(1)	0.2628(1)	0.0136(3)
Cu(1)	0.6658(1)	1.0360(1)	0.3087(1)	0.0201(2)
Br(1)	0.5792(1)	1.1726(1)	0.3430(1)	0.0177(1)
N(6)	0.591(3)	0.5653(16)	0.4694(9)	0.053(5)
C(21)	0.5250(18)	0.5103(10)	0.4846(8)	0.033(3)
C(20)	0.430(3)	0.4324(18)	0.5000(11)	0.041(5)

7.3.9 Iodo-tri(pyrid-2-yl)arsinoxid-kupfer(I)-acetonitrilsolvat (tgv58)

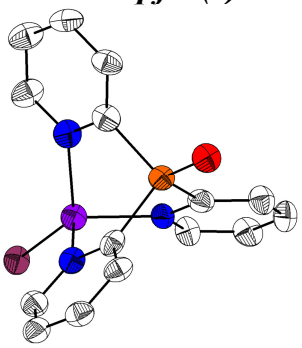

Kristalldaten

C16.50 H14.25 As Cu I N3.75 O	M = 546.43 g/mol	Monoclinic, $P2_1/n$
a = 8.7081(4) Å	b = 29.7666(14) Å	c = 14.5936(9) Å
α = 90°	β = 105.559(4)°	γ = 90°
V = 3644.2(3) Å^3	Z = 8	F(000) = 2100
D_{calc} = 1.992 g/cm^3	μ = 4.705 mm^{-1}	
yellow needle	0.280 · 0.050 · 0.040 mm^3	

Datensammlung

Diffraktometer: STOE IPDS 2	T = 100(2) K	λ = 0.71069 Å
h = -11 bis 11	k = -38 bis 38	l = -18 bis 18
35607 gemessene Reflexe	35607 unabhängige Reflexe	16911 Reflexe mit $I > 2\sigma(I)$
θ = 1.368 bis 27.167°	R_{int} = -(hklf5)	C (25.00°) = 1.000
Absorptionskorrektur: Multi-scan	T_{min} = 0.5068	T_{max} = 0.8350

Verfeinerung

35607 Reflexe	0 Restraints	454 Parameter
Verfeinerung mit SHELXL-2014/6	bis χ = 0.001	
R_1 ($I > 2\sigma(I)$) = 0.0580	wR_2 ($I > 2\sigma(I)$) = 0.1315	
R_1 (all) = 0.1118	wR_2 (all) = 0.1465	GoF (S) = 0.764
$\Delta\varphi_{min}$ = -1.379 e·Å^{-3}	$\Delta\varphi_{max}$ = 2.330 e·Å^{-3}	

Kommentar

Die Struktur wurde als nicht-meroedrischer Zwilling integriert und verfeinert. Ein Acetonitrilmolekül ist über ein Inversionszentrum fehlgeordnet. Die Struktur wurde bereits veröffentlicht: T. Gneuß, M. J. Leitl, L. H. Finger, N. Rau, H. Yersin, J. Sundermeyer, *Dalton Trans.* **2015**, *44*, 8506–8520.

Fraktionelle Atomkoordinaten (*x, y, z*) und äquivalente isotrope Auslenkungsfaktoren *U*(eq)

	x	*y*	*z*	*U*(eq)/Å^2		*x*	*y*	*z*	*U*(eq)/Å^2
C(1)	1.1671(15)	1.0297(4)	0.7653(9)	0.035(3)	C(29)	0.1455(15)	0.6766(4)	0.4288(9)	0.042(3)
C(2)	1.3261(15)	1.0346(4)	0.7687(9)	0.040(3)	C(30)	0.1641(15)	0.7088(4)	0.4990(9)	0.038(3)
C(3)	1.4084(15)	0.9980(4)	0.7521(10)	0.042(3)	C(16)	-0.1808(14)	0.7067(4)	0.6887(8)	0.032(3)
C(4)	1.3299(16)	0.9570(4)	0.7299(10)	0.040(3)	C(17)	-0.3395(16)	0.7008(4)	0.6871(9)	0.040(3)
C(5)	1.1704(15)	0.9545(4)	0.7271(9)	0.036(3)	C(18)	-0.4355(15)	0.7374(4)	0.6803(9)	0.037(3)
C(11)	0.8548(15)	1.0793(4)	0.6731(9)	0.037(3)	C(19)	-0.3662(15)	0.7805(4)	0.6758(9)	0.035(3)
C(12)	0.8164(16)	1.1174(4)	0.6176(9)	0.040(3)	C(20)	-0.2097(14)	0.7827(4)	0.6766(8)	0.033(3)
C(13)	0.6857(16)	1.1163(4)	0.5387(9)	0.045(3)	C(21)	0.1424(13)	0.6692(4)	0.8052(9)	0.033(3)
C(14)	0.5979(17)	1.0770(4)	0.5192(10)	0.047(3)	C(22)	0.1856(14)	0.6397(4)	0.8813(9)	0.037(3)
C(15)	0.6434(16)	1.0406(4)	0.5793(9)	0.045(3)	C(23)	0.3132(15)	0.6514(4)	0.9567(9)	0.041(3)
C(6)	0.9453(14)	1.0606(4)	0.8867(9)	0.034(3)	C(24)	0.3921(15)	0.6908(4)	0.9532(9)	0.042(3)
C(7)	0.9675(15)	1.0864(4)	0.9691(9)	0.038(3)	C(25)	0.3426(14)	0.7186(4)	0.8747(9)	0.037(3)
C(8)	0.8926(15)	1.0728(4)	1.0363(9)	0.039(3)	C(31)	0.425(2)	0.3001(5)	0.5802(12)	0.067(5)
C(9)	0.7984(15)	1.0346(4)	1.0196(9)	0.040(3)	C(32)	0.5086(18)	0.2582(5)	0.5797(10)	0.050(4)
C(10)	0.7858(15)	1.0098(4)	0.9380(9)	0.038(3)	N(1)	1.0854(11)	0.9899(4)	0.7444(7)	0.035(2)
C(26)	0.0404(14)	0.6633(4)	0.5857(9)	0.035(3)	N(3)	0.7716(12)	1.0406(3)	0.6545(7)	0.039(2)
C(27)	0.0181(13)	0.6298(4)	0.5178(9)	0.039(3)	N(2)	0.8585(11)	1.0219(3)	0.8710(7)	0.035(2)
C(28)	0.0697(16)	0.6365(4)	0.4380(9)	0.044(3)	N(6)	0.1115(11)	0.7032(3)	0.5768(7)	0.033(2)

	x	y	z	U(eq)/Å^2
N(4)	-0.1124(11)	0.7472(3)	0.6838(7)	0.031(2)
N(5)	0.2172(12)	0.7083(3)	0.8001(7)	0.034(2)
N(7)	0.5789(15)	0.2256(4)	0.5802(8)	0.051(3)
O(1)	1.1289(10)	1.1272(3)	0.8066(6)	0.039(2)
O(2)	-0.1172(9)	0.6071(2)	0.7018(6)	0.0360(19)
Cu(1)	0.8501(2)	0.9880(1)	0.7464(1)	0.0354(4)
Cu(2)	0.1243(2)	0.7489(1)	0.6846(1)	0.0332(3)

	x	y	z	U(eq)/Å^2
As(1)	1.0350(2)	1.0791(1)	0.7849(1)	0.0340(3)
As(2)	-0.0366(1)	0.6563(1)	0.6972(1)	0.0319(3)
I(1)	0.7451(1)	0.9090(1)	0.7283(1)	0.0382(2)
I(2)	0.2322(1)	0.8277(1)	0.6932(1)	0.0358(2)
N(8)	1.140(5)	1.0378(13)	0.532(3)	0.073(11)
C(33)	0.940(8)	0.9696(18)	0.496(4)	0.063(14)
C(34)	1.050(8)	1.0074(13)	0.513(4)	0.059(12)

7.3.10 Tri(pyrid-2-yl)arsin (tgv109)

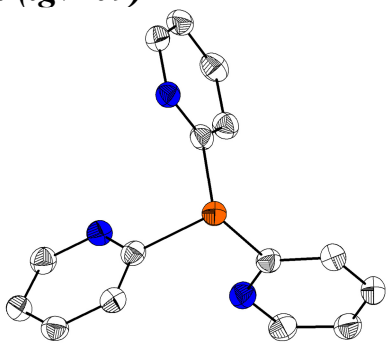

Kristalldaten

C15 H12 As N3	M = 309.20 g/mol	Monoclinic, $P2_1/c$
a = 9.1529(9) Å	b = 9.1102(6) Å	c = 16.0342(16) Å
α = 90°	β = 100.982(8)°	γ = 90°
V = 1312.5(2) Å^3	Z = 4	F(000) = 624
D_{calc} = 1.565 g/cm^3	μ = 2.578 mm^{-1}	
colourless block	0.230 · 0.230 · 0.220 mm^3	

Datensammlung

Diffraktometer: STOE IPDS 2	T = 100(2) K	λ = 0.71073 Å
h = -11 bis 11	k = -11 bis 11	l = -18 bis 20
8036 gemessene Reflexe	2763 unabhängige Reflexe	2318 Reflexe mit $I > 2\sigma(I)$
θ = 2.267 bis 26.699°	R_{int} = 0.0433	C (25.00°) = 0.999
Absorptionskorrektur: Multi-scan	T_{min} = 0.4643	T_{max} = 0.7453

Verfeinerung

2763 Reflexe	0 Restraints	172 Parameter
Verfeinerung mit SHELXL-2014/6	bis χ = 0.002	
R_1 ($I > 2\sigma(I)$) = 0.0254	wR_2 ($I > 2\sigma(I)$) = 0.0645	
R_1 (all) = 0.0338	wR_2 (all) = 0.0666	GoF (S) = 0.965
$\Delta\varphi_{min}$ = -0.304 e·Å^{-3}	$\Delta\varphi_{max}$ = 0.464 e·Å^{-3}	

Kommentar

Die Struktur wurde bereits veröffentlicht: T. Gneuß, M. J. Leitl, L. H. Finger, N. Rau, H. Yersin, J. Sundermeyer, *Dalton Trans.* **2015**, *44*, 8506–8520.

Fraktionelle Atomkoordinaten (*x, y, z*) und äquivalente isotrope Auslenkungsfaktoren *U*(eq)

	x	y	z	U(eq)/Å^2
As(1)	0.9005(1)	0.7905(1)	0.1290(1)	0.0285(1)
C(1)	0.7589(2)	0.7035(2)	0.1927(1)	0.0289(4)
N(1)	0.6212(2)	0.7584(2)	0.1840(1)	0.0315(4)
N(2)	0.8278(2)	1.0732(2)	0.1651(1)	0.0306(4)
C(5)	0.5319(2)	0.6975(2)	0.2321(2)	0.0338(5)
C(7)	0.7048(2)	1.0106(2)	0.0237(1)	0.0332(5)
C(11)	0.8399(2)	0.6852(2)	0.0205(1)	0.0296(4)
N(3)	0.7109(2)	0.6115(2)	0.0047(1)	0.0349(4)
C(6)	0.7959(2)	0.9773(2)	0.1003(1)	0.0291(4)

	x	y	z	U(eq)/Å^2
C(10)	0.7667(2)	1.2074(2)	0.1528(2)	0.0341(5)
C(12)	0.9393(3)	0.6891(2)	-0.0356(1)	0.0342(5)
C(9)	0.6750(3)	1.2509(2)	0.0780(2)	0.0363(5)
C(2)	0.8110(2)	0.5896(2)	0.2481(1)	0.0303(4)
C(15)	0.6783(3)	0.5403(2)	-0.0701(1)	0.0366(5)
C(14)	0.7693(3)	0.5387(2)	-0.1298(1)	0.0357(5)
C(4)	0.5729(2)	0.5826(2)	0.2884(1)	0.0335(5)
C(13)	0.9023(3)	0.6148(2)	-0.1120(1)	0.0375(5)
C(3)	0.7160(2)	0.5278(2)	0.2965(1)	0.0331(5)
C(8)	0.6422(3)	1.1500(2)	0.0121(2)	0.0375(5)

7.3.11 Tri(pyrid-2-yl)methan-triphenylphosphin-kupfer(I)-hexafluorophosphat-chloroformsolvat (tgn428)

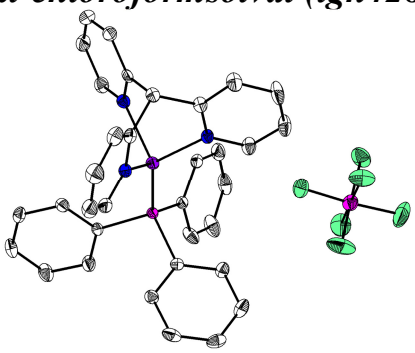

Kristalldaten

C35 H29 Cl3 Cu F6 N3 P2	M = 837.44 g/mol	Monoclinic, $P2_1$
a = 8.5970(3) Å	b = 18.9423(8) Å	c = 11.5950(5) Å
α = 90°	β = 107.2000(10)°	γ = 90°
V = 1803.77(13) Å^3	Z = 2	F(000) = 848
D_{calc} = 1.542 g/cm^3	μ = 0.978 mm^{-1}	
colourless plate	0.220 · 0.180 · 0.090 mm^3	

Datensammlung

Diffraktometer: D8 Quest (Bruker)	T = 100(2) K	λ = 0.71069 Å
h = -10 bis 10	k = -24 bis 24	l = -14 bis 14
26555 gemessene Reflexe	7884 unabhängige Reflexe	7265 Reflexe mit $I > 2\sigma(I)$
θ = 2.614 bis 27.134°	R_{int} = 0.0370	C (25.00°) = 0.999
Absorptionskorrektur: Multi-scan	T_{min} = 0.6938	T_{max} = 0.7455

Verfeinerung

7884 Reflexe	25 Restraints	506 Parameter
Verfeinerung mit SHELXL-2014/7	bis χ = 0.001	
R_1 ($I > 2\sigma(I)$) = 0.0290	wR_2 ($I > 2\sigma(I)$) = 0.0622	
R_1 (all) = 0.0349	wR_2 (all) = 0.0643	GoF (S) = 1.030
$\Delta\varphi_{min}$ = -0.476 e·Å^{-3}	$\Delta\varphi_{max}$ = 0.456 e·Å^{-3}	

Kommentar

Das PF_6-Anion ist über zwei Positionen fehlgeordnet. F11 bis F14 wurden über ISOR restrained. Diese Struktur wurde bereits veröffentlicht: T. Gneuß, M. J. Leitl, L. H. Finger, H. Yersin, J. Sundermeyer, *Dalton Trans.* **2015**, *44*, 20045−20055.

Fraktionelle Atomkoordinaten (*x, y, z*) und äquivalente isotrope Auslenkungsfaktoren *U*(eq)

	x	*y*	*z*	*U*(eq)/Å^2		*x*	*y*	*z*	*U*(eq)/Å^2
C(1)	0.8792(4)	0.6766(2)	0.9175(3)	0.0179(6)	C(17)	0.5865(3)	0.6977(2)	0.3582(3)	0.0141(6)
C(2)	0.9588(4)	0.6942(2)	1.0353(3)	0.0272(7)	C(18)	0.5063(4)	0.6375(2)	0.3781(3)	0.0179(6)
C(3)	1.0452(5)	0.7578(2)	1.0593(3)	0.0342(9)	C(19)	0.4018(4)	0.6006(2)	0.2822(3)	0.0205(7)
C(4)	1.0467(5)	0.8012(2)	0.9644(3)	0.0297(8)	C(20)	0.3751(4)	0.6250(2)	0.1660(3)	0.0242(7)
C(5)	0.9617(4)	0.7807(2)	0.8489(3)	0.0233(7)	C(21)	0.4547(4)	0.6848(2)	0.1443(3)	0.0281(7)
C(6)	0.8565(4)	0.5615(2)	0.8047(3)	0.0182(6)	C(22)	0.5617(4)	0.7208(2)	0.2400(3)	0.0242(7)
C(7)	0.9285(4)	0.4963(2)	0.8446(3)	0.0260(7)	C(23)	0.6427(4)	0.8331(2)	0.4796(3)	0.0154(6)
C(8)	0.9898(5)	0.4573(2)	0.7668(4)	0.0342(9)	C(24)	0.5760(4)	0.8581(2)	0.5680(3)	0.0218(7)
C(9)	0.9786(4)	0.4830(2)	0.6536(4)	0.0308(8)	C(25)	0.5115(4)	0.9262(2)	0.5591(4)	0.0290(9)
C(10)	0.9048(4)	0.5476(2)	0.6201(3)	0.0232(7)	C(26)	0.5126(4)	0.9691(2)	0.4632(4)	0.0304(9)
C(11)	0.6055(4)	0.6189(2)	0.8318(3)	0.0170(6)	C(27)	0.5840(5)	0.9458(2)	0.3776(3)	0.0314(8)
C(12)	0.4951(4)	0.5939(2)	0.8884(3)	0.0237(7)	C(28)	0.6492(4)	0.8784(2)	0.3861(3)	0.0242(7)
C(13)	0.3304(5)	0.6064(2)	0.8362(3)	0.0296(8)	C(29)	0.9095(3)	0.7534(2)	0.4549(3)	0.0142(6)
C(14)	0.2801(4)	0.6436(2)	0.7293(3)	0.0274(8)	C(30)	1.0110(4)	0.8104(2)	0.5034(3)	0.0202(7)
C(15)	0.3969(4)	0.6666(2)	0.6768(3)	0.0219(7)	C(31)	1.1576(4)	0.8183(2)	0.4788(3)	0.0273(8)
C(16)	0.7873(4)	0.6069(2)	0.8863(3)	0.0177(6)	C(32)	1.2070(4)	0.7698(2)	0.4082(3)	0.0258(8)

	x	y	z	U(eq)/Å^2
C(33)	1.1104(4)	0.7114(2)	0.3638(3)	0.0252(8)
C(34)	0.9606(4)	0.7033(2)	0.3856(3)	0.0189(7)
C(35)	0.5192(5)	0.8931(2)	0.9225(3)	0.0283(8)
N(1)	0.8798(3)	0.7196(1)	0.8246(2)	0.0169(5)
N(2)	0.8448(3)	0.5866(1)	0.6939(2)	0.0177(6)
N(3)	0.5565(3)	0.6547(1)	0.7265(2)	0.0176(5)
F(1)	0.9573(4)	0.9331(2)	0.7242(3)	0.0421(9)
F(2)	0.9957(4)	1.0349(2)	0.6404(3)	0.0416(9)
F(3)	1.2070(4)	1.0607(2)	0.8039(3)	0.0512(11)
F(4)	1.1718(4)	0.9581(2)	0.8897(3)	0.0401(9)
F(5)	1.2048(4)	0.9579(3)	0.7026(3)	0.0537(12)
F(6)	0.9637(4)	1.0331(2)	0.8281(3)	0.0372(9)

	x	y	z	U(eq)/Å^2
F(11)	0.957(2)	0.9769(11)	0.6366(16)	0.115(8)
F(12)	1.194(2)	1.0219(11)	0.6732(17)	0.110(7)
F(13)	0.997(2)	0.9589(10)	0.832(2)	0.114(7)
F(14)	1.2484(16)	1.0068(9)	0.8650(14)	0.083(6)
F(15)	1.1746(13)	0.9129(6)	0.7452(12)	0.046(3)
F(16)	1.0199(13)	1.0636(5)	0.7694(11)	0.042(3)
P(1)	0.7184(1)	0.7426(1)	0.4908(1)	0.0130(2)
P(2)	1.0860(1)	0.9945(1)	0.7616(1)	0.0237(2)
Cu(1)	0.7420(1)	0.6866(1)	0.6575(1)	0.0159(1)
Cl(1)	0.6974(1)	0.9301(1)	0.9032(1)	0.0449(3)
Cl(2)	0.5014(2)	0.8051(1)	0.8736(1)	0.0781(5)
Cl(3)	0.5192(2)	0.8972(1)	1.0739(1)	0.0431(3)

7.3.12 Tri(pyrid-2-yl)methan-triphenylphosphin-kupfer(I)-tetrafluoroborat-chloroformsolvat (tgn448)

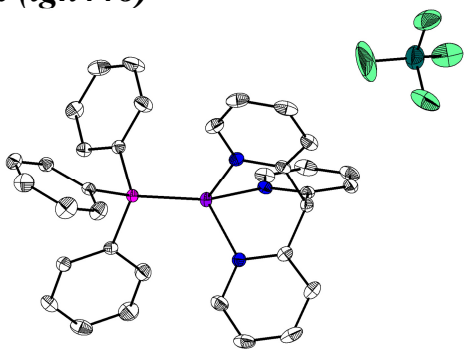

Kristalldaten

C34.50 H28.50 B Cl1.50 Cu F4 N3 P	M = 719.60 g/mol	Trigonal, $R\bar{3}c$
a = 12.8635(6) Å	b = 12.8635 Å	c = 67.361(3) Å
α = 90°	β = 90°	γ = 120°
V = 9652.9(10) Å^3	Z = 12	F(000) = 4404
D_{calc} = 1.485 g/cm^3	μ = 0.907 mm^{-1}	
clear light colourless needle	0.291 · 0.043 · 0.041 mm^3	

Datensammlung

Diffraktometer: D8 Quest (Bruker)	T = 100(2) K	λ = 0.71069 Å
h = -16 bis 16	k = -15 bis 16	l = -87 bis 86
28280 gemessene Reflexe	2458 unabhängige Reflexe	1742 Reflexe mit $I > 2\sigma(I)$
θ = 3.032 bis 27.481°	R_{int} = 0.1142	C (25.00°) = 0.991
Absorptionskorrektur: Multi-scan	T_{min} = 0.6837	T_{max} = 0.7456

Verfeinerung

2458 Reflexe	6 Restraints	150 Parameter
Verfeinerung mit SHELXL-2014/7	bis χ = 0.000	
R_1 ($I > 2\sigma(I)$) = 0.0383	wR_2 ($I > 2\sigma(I)$) = 0.0842	
R_1 (all) = 0.0699	wR_2 (all) = 0.0958	GoF (S) = 1.037
$\Delta\varphi_{min}$ = -0.389 e·Å^{-3}	$\Delta\varphi_{max}$ = 0.940 e·Å^{-3}	

Kommentar

Das BF_4-Anion und das Chloroformmolekül sind über drei bzw. zwei Positionen fehlgeordnet. F2 wurde über ISOR restrained. Diese Struktur wurde bereits veröffentlicht: T. Gneuß, M. J. Leitl, L. H. Finger, H. Yersin, J. Sundermeyer, *Dalton Trans.* **2015**, *44*, 20045−20055.

Fraktionelle Atomkoordinaten (*x, y, z*) und äquivalente isotrope Auslenkungsfaktoren *U*(eq)

	x	*y*	*z*	*U*(eq)/Å^2		*x*	*y*	*z*	*U*(eq)/Å^2
C(1)	0.3532(2)	0.7885(2)	0.0417(1)	0.0161(5)	C(11)	0.5223(2)	0.9544(2)	0.1486(1)	0.0232(5)
C(2)	0.3671(2)	0.8736(2)	0.0278(1)	0.0214(5)	C(12)	0.4311(2)	0.8488(2)	0.1406(1)	0.0175(5)
C(3)	0.3893(2)	0.9849(2)	0.0343(1)	0.0266(6)	C(13)	0.6667	0.3333	0.0833	0.080(3)
C(4)	0.3964(2)	1.0073(2)	0.0544(1)	0.0269(6)	B(1)	0.6667	0.3333	0.0197(1)	0.0406(14)
C(5)	0.3797(2)	0.9175(2)	0.0673(1)	0.0227(5)	N(1)	0.3583(2)	0.8090(2)	0.0613(1)	0.0161(4)
C(6)	0.3333	0.6667	0.0352(1)	0.0161(8)	F(1)	0.5666(2)	0.2328(2)	0.0117(1)	0.0509(5)
C(7)	0.4477(2)	0.8059(2)	0.1226(1)	0.0145(5)	F(2)	0.637(3)	0.346(3)	0.0387(1)	0.100(5)
C(8)	0.5572(2)	0.8707(2)	0.1129(1)	0.0249(6)	P(1)	0.3333	0.6667	0.1111(1)	0.0129(2)
C(9)	0.6485(2)	0.9756(2)	0.1211(1)	0.0321(7)	Cu(1)	0.3333	0.6667	0.0791(1)	0.0155(1)
C(10)	0.6305(2)	1.0177(2)	0.1390(1)	0.0293(6)	Cl(1)	0.5359(5)	0.3314(9)	0.0796(1)	0.0557(14)

7.3.13 Tri(pyrid-2-yl)methan-triphenylphosphin-kupfer(I)-tetraphenylborat-chloroformsolvat (tgn459)

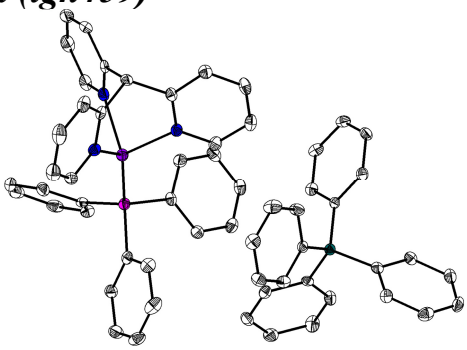

Kristalldaten

C60 H50 B Cl6 Cu N3 P	M = 1131.05 g/mol	Orthorhombic, *Pna*2$_1$
a = 19.4837(7) Å	b = 11.1499(4) Å	c = 24.6713(9) Å
α = 90°	β = 90°	γ = 90°
V = 5359.6(3) Å^3	Z = 4	F(000) = 2328
D_{calc} = 1.402 g/cm^3	μ = 0.780 mm^{-1}	
colourless plate	0.319 · 0.267 · 0.064 mm^3	

Datensammlung

Diffraktometer: D8 Quest (Bruker)	T = 100(2) K	λ = 0.71069 Å
h = -24 bis 24	k = -11 bis 14	l = -30 bis 31
54250 gemessene Reflexe	11572 unabhängige Reflexe	9836 Reflexe mit $I > 2\sigma(I)$
θ = 2.090 bis 27.921°	R_{int} = 0.0406	C (25.00°) = 0.999
Absorptionskorrektur: Multi-scan	T_{min} = 0.6812	T_{max} = 0.7456

Verfeinerung

11572 Reflexe	1 Restraints	649 Parameter
Verfeinerung mit SHELXL-2014/7	bis χ = 0.001	
R_1 ($I > 2\sigma(I)$) = 0.0294	wR_2 ($I > 2\sigma(I)$) = 0.0569	
R_1 (all) = 0.0454	wR_2 (all) = 0.0662	GoF (S) = 1.069
$\Delta\varphi_{min}$ = -0.260 e·Å^{-3}	$\Delta\varphi_{max}$ = 0.310 e·Å^{-3}	

Kommentar

Diese Struktur wurde bereits veröffentlicht: T. Gneuß, M. J. Leitl, L. H. Finger, H. Yersin, J. Sundermeyer, *Dalton Trans.* **2015**, *44*, 20045−20055.

Fraktionelle Atomkoordinaten (*x, y, z*) und äquivalente isotrope Auslenkungsfaktoren *U*(eq)

	x	*y*	*z*	*U*(eq)/Å^2		*x*	*y*	*z*	*U*(eq)/Å^2
C(1)	0.5378(2)	1.0433(3)	0.4446(1)	0.0153(7)	C(37)	0.8637(2)	0.9177(3)	0.6463(1)	0.0194(7)
C(2)	0.4830(2)	1.0906(3)	0.4737(1)	0.0195(7)	C(38)	0.9101(2)	0.9798(3)	0.6782(1)	0.0214(7)
C(3)	0.4926(2)	1.1251(3)	0.5269(1)	0.0227(7)	C(39)	0.8852(2)	1.0498(3)	0.7199(1)	0.0237(8)
C(4)	0.5567(2)	1.1134(3)	0.5505(1)	0.0215(7)	C(40)	0.8152(2)	1.0554(3)	0.7302(1)	0.0185(7)
C(5)	0.6091(2)	1.0657(3)	0.5193(1)	0.0185(7)	C(41)	0.6543(2)	1.1336(3)	0.6886(1)	0.0129(6)
C(6)	0.5486(2)	0.8729(3)	0.3777(1)	0.0152(6)	C(42)	0.6885(2)	1.2018(3)	0.6491(1)	0.0153(6)
C(7)	0.5006(2)	0.7919(3)	0.3585(1)	0.0218(7)	C(43)	0.6627(2)	1.3098(3)	0.6293(1)	0.0178(7)
C(8)	0.5200(2)	0.6743(3)	0.3499(1)	0.0287(8)	C(44)	0.6004(2)	1.3536(3)	0.6475(1)	0.0188(7)
C(9)	0.5865(2)	0.6401(3)	0.3613(1)	0.0265(8)	C(45)	0.5646(2)	1.2883(3)	0.6859(1)	0.0182(7)
C(10)	0.6316(2)	0.7251(3)	0.3801(1)	0.0204(7)	C(46)	0.5913(2)	1.1823(3)	0.7061(1)	0.0162(7)
C(11)	0.5704(2)	1.0832(3)	0.3470(1)	0.0154(7)	C(47)	0.6397(2)	0.8936(3)	0.6854(1)	0.0136(6)
C(12)	0.5386(2)	1.1370(3)	0.3029(1)	0.0216(7)	C(48)	0.5756(2)	0.9084(3)	0.6610(1)	0.0200(7)
C(13)	0.5771(2)	1.2104(3)	0.2693(1)	0.0288(8)	C(49)	0.5396(2)	0.8149(3)	0.6365(1)	0.0255(8)
C(14)	0.6454(2)	1.2288(3)	0.2809(1)	0.0263(8)	C(50)	0.5670(2)	0.7016(3)	0.6353(1)	0.0211(7)
C(15)	0.6741(2)	1.1690(3)	0.3242(1)	0.0206(7)	C(51)	0.6295(2)	0.6811(3)	0.6605(1)	0.0210(7)
C(16)	0.5301(2)	1.0046(3)	0.3859(1)	0.0153(7)	C(52)	0.6640(2)	0.7750(3)	0.6851(1)	0.0181(7)
C(17)	0.8415(2)	1.0121(3)	0.3838(1)	0.0154(7)	C(53)	0.6748(1)	1.0072(3)	0.7788(1)	0.0141(6)
C(18)	0.8258(2)	0.9657(3)	0.3327(1)	0.0211(7)	C(54)	0.6640(2)	0.9034(3)	0.8099(1)	0.0168(7)
C(19)	0.8655(2)	0.9956(3)	0.2882(1)	0.0276(8)	C(55)	0.6633(2)	0.9053(3)	0.8665(1)	0.0230(7)
C(20)	0.9209(2)	1.0710(3)	0.2939(1)	0.0267(8)	C(56)	0.6725(2)	1.0123(3)	0.8944(1)	0.0213(7)
C(21)	0.9378(2)	1.1157(3)	0.3444(1)	0.0232(7)	C(57)	0.6820(2)	1.1166(3)	0.8649(1)	0.0194(7)
C(22)	0.8984(2)	1.0862(3)	0.3891(1)	0.0189(7)	C(58)	0.6828(1)	1.1135(3)	0.8084(1)	0.0163(7)
C(23)	0.7971(2)	1.1043(3)	0.4857(1)	0.0152(6)	C(59)	0.6649(2)	0.8931(3)	0.1944(1)	0.0195(7)
C(24)	0.7686(2)	1.2145(3)	0.4720(1)	0.0198(7)	C(60)	0.5908(2)	0.4158(3)	0.5028(1)	0.0238(7)
C(25)	0.7788(2)	1.3142(3)	0.5044(1)	0.0216(7)	B(1)	0.6831(2)	1.0057(3)	0.7122(1)	0.0135(7)
C(26)	0.8164(2)	1.3034(3)	0.5520(1)	0.0198(7)	N(1)	0.6008(1)	1.0317(2)	0.4676(1)	0.0157(6)
C(27)	0.8436(2)	1.1937(3)	0.5667(1)	0.0192(7)	N(2)	0.6139(1)	0.8405(2)	0.3880(1)	0.0165(6)
C(28)	0.8343(1)	1.0938(3)	0.5337(1)	0.0167(7)	N(3)	0.6380(1)	1.0961(2)	0.3569(1)	0.0164(6)
C(29)	0.8183(2)	0.8514(3)	0.4754(1)	0.0155(6)	P(1)	0.7821(1)	0.9791(1)	0.4393(1)	0.0145(2)
C(30)	0.7747(2)	0.7859(3)	0.5093(1)	0.0206(7)	Cu(1)	0.6761(1)	0.9759(1)	0.4150(1)	0.0154(1)
C(31)	0.7999(2)	0.6919(3)	0.5402(1)	0.0263(8)	Cl(1)	0.6634(1)	0.8768(1)	0.2652(1)	0.0281(2)
C(32)	0.8683(2)	0.6609(3)	0.5365(1)	0.0253(8)	Cl(2)	0.5805(1)	0.8944(1)	0.1694(1)	0.0348(2)
C(33)	0.9118(2)	0.7230(3)	0.5030(1)	0.0238(7)	Cl(3)	0.7078(1)	1.0257(1)	0.1760(1)	0.0331(2)
C(34)	0.8871(2)	0.8190(3)	0.4724(1)	0.0183(7)	Cl(4)	0.5986(1)	0.3516(1)	0.4376(1)	0.0299(2)
C(35)	0.7662(2)	0.9936(3)	0.6991(1)	0.0132(6)	Cl(5)	0.6397(1)	0.5475(1)	0.5079(1)	0.0348(2)
C(36)	0.7935(2)	0.9262(3)	0.6563(1)	0.0167(7)	Cl(6)	0.5045(1)	0.4453(1)	0.5180(1)	0.0373(2)

7.3.14 Tri(pyrid-2-yl)phosphinoxid-triphenylphosphin-kupfer(I)-hexafluorophosphat-chloroformsolvat (tgn409)

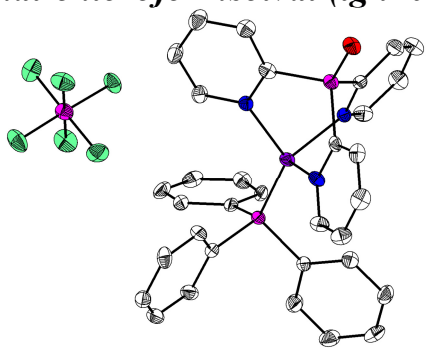

Kristalldaten

C35 H29 Cl6 Cu F6 N3 O P3	*M* = 990.76 g/mol	Monoclinic, $P2_1/n$
a = 23.4261(16) Å	*b* = 15.0644(10) Å	*c* = 23.4236(15) Å
α = 90°	β = 93.844(2)°	γ = 90°
V = 8247.6(9) Å^3	*Z* = 8	*F*(000) = 3984
D_{calc} = 1.596 g/cm^3	μ = 1.096 mm^{-1}	
colourless block	0.390 · 0.200 · 0.130 mm^3	

Datensammlung

Diffraktometer: D8 Quest (Bruker)	T = 100(2) K	λ = 0.71069 Å
h = -30 bis 29	k = -19 bis 19	l = -28 bis 30
75789 gemessene Reflexe	18260 unabhängige Reflexe	14688 Reflexe mit $I > 2\sigma(I)$
θ = 2.206 bis 27.180°	R_{int} = 0.0860	C (25.00°) = 0.999
Absorptionskorrektur: Multi-scan	T_{min} = 0.6367	T_{max} = 0.7455

Verfeinerung

18260 Reflexe	61 Restraints	1066 Parameter
Verfeinerung mit SHELXL-2014/7	bis χ = 0.002	
R_1 ($I > 2\sigma(I)$) = 0.0493	wR_2 ($I > 2\sigma(I)$) = 0.1015	
R_1 (all) = 0.0728	wR_2 (all) = 0.1102	GoF (S) = 1.024
$\Delta\varphi_{min}$ = -0.913 e·Å^{-3}	$\Delta\varphi_{max}$ = 0.965 e·Å^{-3}	

Kommentar

Die Struktur wurde als pseudo-meroedrischer Zwilling verfeinert. Jeweils ein PF_6-Anion und Chloroformmolekül sind über mehrere Positionen fehlgeordnet. Die fehlgeordneten Positionen wurden über SAME re- und über EADP constrained.

Fraktionelle Atomkoordinaten (*x, y, z*) und äquivalente isotrope Auslenkungsfaktoren *U*(eq)

	x	*y*	*z*	*U*(eq)/Å^2
C(11)	0.9697(2)	0.6038(3)	0.8698(2)	0.0169(9)
C(12)	1.0121(2)	0.5402(3)	0.8645(2)	0.0233(10)
C(13)	0.9993(2)	0.4679(3)	0.8294(2)	0.0276(10)
C(14)	0.9458(2)	0.4634(3)	0.8004(2)	0.0265(10)
C(15)	0.9065(2)	0.5308(3)	0.8080(2)	0.0224(9)
C(6)	0.9710(2)	0.7964(3)	0.8708(2)	0.0154(8)
C(7)	1.0111(2)	0.8621(3)	0.8673(2)	0.0210(9)
C(8)	0.9980(2)	0.9358(3)	0.8347(2)	0.0252(10)
C(9)	0.9440(2)	0.9422(3)	0.8070(2)	0.0253(10)
C(10)	0.9058(2)	0.8737(3)	0.8127(2)	0.0206(9)
C(1)	0.9322(2)	0.7022(3)	0.9662(2)	0.0154(8)
C(2)	0.9488(2)	0.7068(3)	1.0240(2)	0.0223(9)
C(3)	0.9060(2)	0.7168(3)	1.0625(2)	0.0241(10)
C(4)	0.8499(2)	0.7215(3)	1.0418(2)	0.0256(10)
C(5)	0.8365(2)	0.7146(3)	0.9838(2)	0.0214(9)
C(22)	0.7258(2)	0.6163(3)	0.8236(2)	0.0130(8)
C(23)	0.7487(2)	0.5369(3)	0.8450(2)	0.0205(9)
C(24)	0.7140(2)	0.4635(3)	0.8501(2)	0.0257(10)
C(25)	0.6561(2)	0.4696(3)	0.8350(2)	0.0248(10)
C(26)	0.6324(2)	0.5500(3)	0.8164(2)	0.0229(10)
C(27)	0.6671(2)	0.6225(3)	0.8105(2)	0.0169(8)
C(16)	0.7806(2)	0.7073(2)	0.7346(2)	0.0159(8)
C(17)	0.8344(2)	0.7109(3)	0.7128(2)	0.0179(9)
C(18)	0.8400(2)	0.7165(3)	0.6539(2)	0.0222(10)
C(19)	0.7911(2)	0.7153(3)	0.6168(2)	0.0229(10)
C(20)	0.7372(2)	0.7101(3)	0.6381(2)	0.0220(10)
C(21)	0.7320(2)	0.7065(3)	0.6963(2)	0.0185(9)
C(28)	0.7359(2)	0.8085(3)	0.8232(2)	0.0143(8)
C(29)	0.7021(2)	0.8165(3)	0.8697(2)	0.0192(9)
C(30)	0.6748(2)	0.8954(3)	0.8804(2)	0.0251(10)
C(31)	0.6819(2)	0.9685(3)	0.8460(2)	0.0268(10)
C(32)	0.7158(2)	0.9623(3)	0.8001(2)	0.0235(10)
C(33)	0.7417(2)	0.8820(3)	0.7884(2)	0.0199(9)
C(44)	0.3551(2)	0.8486(3)	0.9682(2)	0.0164(8)
C(45)	0.3434(2)	0.9166(3)	1.0052(2)	0.0219(10)
C(46)	0.3035(2)	0.9799(3)	0.9882(2)	0.0273(10)
C(47)	0.2768(2)	0.9747(3)	0.9342(2)	0.0265(10)
C(48)	0.2907(2)	0.9046(3)	0.8992(2)	0.0231(10)
C(34)	0.4581(2)	0.7569(3)	0.9351(2)	0.0201(9)
C(35)	0.5153(2)	0.7566(3)	0.9512(2)	0.0251(10)
C(36)	0.5537(2)	0.7474(3)	0.9083(2)	0.0316(11)
C(37)	0.5322(2)	0.7397(3)	0.8527(2)	0.0278(10)
C(38)	0.4741(2)	0.7388(3)	0.8402(2)	0.0232(10)
C(39)	0.3693(2)	0.6580(3)	0.9817(2)	0.0168(9)
C(40)	0.3718(2)	0.5981(3)	1.0264(2)	0.0234(10)
C(41)	0.3464(2)	0.5166(3)	1.0177(2)	0.0280(11)
C(42)	0.3181(2)	0.4975(3)	0.9655(2)	0.0256(10)
C(43)	0.3173(2)	0.5613(3)	0.9228(2)	0.0233(10)
C(55)	0.3183(2)	0.8257(3)	0.7409(2)	0.0185(9)
C(56)	0.3560(2)	0.8885(3)	0.7653(2)	0.0225(9)
C(57)	0.3665(2)	0.9675(3)	0.7370(2)	0.0266(10)
C(58)	0.3400(2)	0.9837(3)	0.6838(2)	0.0253(10)
C(59)	0.3034(2)	0.9213(3)	0.6592(2)	0.0262(10)
C(60)	0.2921(2)	0.8432(3)	0.6867(2)	0.0231(10)
C(61)	0.3192(2)	0.6336(3)	0.7340(2)	0.0170(9)
C(66)	0.3552(2)	0.6426(3)	0.6894(2)	0.0202(9)
C(65)	0.3672(2)	0.5697(3)	0.6563(2)	0.0251(10)
C(64)	0.3446(2)	0.4866(3)	0.6681(2)	0.0258(10)
C(63)	0.3101(2)	0.4778(3)	0.7133(2)	0.0252(10)
C(62)	0.2969(2)	0.5498(3)	0.7451(2)	0.0213(9)
C(49)	0.2266(2)	0.7215(3)	0.7836(2)	0.0180(9)
C(50)	0.2027(2)	0.7311(3)	0.8363(2)	0.0215(9)
C(51)	0.1440(2)	0.7317(3)	0.8402(2)	0.0261(10)
C(52)	0.1086(2)	0.7226(3)	0.7909(2)	0.0286(11)
C(53)	0.1308(2)	0.7112(3)	0.7386(2)	0.0297(11)
C(54)	0.1895(2)	0.7095(3)	0.7348(2)	0.0273(10)
C(67)	0.4537(2)	0.4309(4)	0.8699(2)	0.0437(14)
C(68)	0.6075(2)	0.5252(3)	0.5482(2)	0.0421(13)
N(3)	0.9177(1)	0.6000(2)	0.8423(1)	0.0159(7)
N(2)	0.9180(1)	0.8014(2)	0.8443(1)	0.0168(7)
N(1)	0.8766(2)	0.7050(2)	0.9459(1)	0.0181(7)
N(6)	0.3287(2)	0.8414(2)	0.9152(1)	0.0194(8)
N(4)	0.4363(1)	0.7470(2)	0.8805(1)	0.0176(7)
N(5)	0.3424(1)	0.6408(2)	0.9305(1)	0.0164(7)
O(1)	1.0454(1)	0.6994(2)	0.9411(1)	0.0220(7)
O(2)	0.4335(1)	0.7777(2)	1.0479(1)	0.0234(7)
F(7)	0.5484(1)	0.7706(2)	0.6290(1)	0.0359(7)
F(8)	0.4951(1)	0.6457(2)	0.6332(1)	0.0354(7)
F(9)	0.5226(1)	0.6328(2)	0.7270(1)	0.0283(6)
F(10)	0.5778(1)	0.7560(2)	0.7219(1)	0.0329(6)
F(11)	0.5894(1)	0.6418(2)	0.6615(1)	0.0349(6)
F(12)	0.4827(1)	0.7607(2)	0.6941(1)	0.0327(6)
P(1)	0.9861(1)	0.6995(1)	0.9153(1)	0.0158(2)
P(2)	0.7759(1)	0.7069(1)	0.8118(1)	0.0137(2)
P(3)	0.4069(1)	0.7631(1)	0.9897(1)	0.0173(2)
P(4)	0.3045(1)	0.7255(1)	0.7816(1)	0.0157(2)

	x	y	z	U(eq)/Å^2
P(6)	0.5362(1)	0.7012(1)	0.6774(1)	0.0231(2)
P(5)	0.6756(1)	0.7666(2)	1.0434(1)	0.0229(6)
F(1)	0.6744(2)	0.7031(2)	0.9889(2)	0.0395(12)
F(2)	0.6351(5)	0.8311(8)	1.0084(4)	0.0279(16)
F(3)	0.6798(2)	0.8318(3)	1.0979(2)	0.0299(11)
F(4)	0.7193(2)	0.6991(2)	1.0763(2)	0.0358(11)
F(5)	0.6227(2)	0.7127(3)	1.0665(2)	0.0486(15)
F(6)	0.7292(2)	0.8179(2)	1.0193(2)	0.0344(11)
P(5A)	0.6555(4)	0.7506(6)	1.0587(3)	0.0343(19)
F(1A)	0.6195(5)	0.6790(8)	1.0218(5)	0.0490(19)
F(2A)	0.6308(18)	0.834(3)	1.0171(14)	0.0490(19)
F(3A)	0.6989(7)	0.8175(11)	1.0882(7)	0.0490(19)
F(4A)	0.6764(5)	0.6784(7)	1.1029(5)	0.0490(19)
F(5A)	0.6054(5)	0.7750(8)	1.0920(5)	0.0490(19)
F(6A)	0.7082(5)	0.7190(8)	1.0194(5)	0.0490(19)
Cu(1)	0.8597(1)	0.7006(1)	0.8586(1)	0.0150(1)
Cu(2)	0.3489(1)	0.7319(1)	0.8660(1)	0.0170(1)
Cl(1)	0.4254(1)	0.4941(2)	0.8148(1)	0.1251(11)
Cl(2)	0.4841(1)	0.4986(1)	0.9236(1)	0.0725(5)
Cl(3)	0.5028(1)	0.3546(1)	0.8454(1)	0.0704(5)
Cl(4)	0.6165(1)	0.6194(1)	0.5072(1)	0.1034(9)
Cl(5)	0.5735(1)	0.4412(1)	0.5067(1)	0.0498(4)
Cl(6)	0.6727(1)	0.4882(1)	0.5799(1)	0.0707(5)
C(69)	0.6478(2)	0.8852(3)	0.5065(2)	0.0259(10)
Cl(7)	0.6374(1)	0.8956(1)	0.5795(1)	0.0473(3)
Cl(8)	0.7105(1)	0.8252(1)	0.4961(1)	0.0369(3)
Cl(9)	0.6507(1)	0.9910(1)	0.4752(1)	0.0492(4)
C(70)	0.5037(6)	0.0822(9)	0.8703(6)	0.0457(11)
Cl(10)	0.5113(2)	0.1290(4)	0.8008(2)	0.0457(11)
Cl(11)	0.5330(2)	-0.0254(3)	0.8717(2)	0.0457(11)
Cl(12)	0.4320(3)	0.0739(4)	0.8859(2)	0.0457(11)
C(71)	0.5058(9)	0.0758(17)	0.8799(10)	0.039(3)
Cl(20)	0.5166(5)	0.1035(8)	0.8079(6)	0.039(3)
Cl(21)	0.5346(3)	-0.0235(6)	0.9069(6)	0.039(3)
Cl(22)	0.4361(4)	0.0999(8)	0.8913(5)	0.039(3)
C(72)	0.4898(8)	0.0581(19)	0.8983(8)	0.053(2)
Cl(30)	0.5238(4)	0.0667(6)	0.8322(5)	0.053(2)
Cl(31)	0.5244(3)	-0.0120(6)	0.9497(5)	0.053(2)
Cl(32)	0.4200(7)	0.0217(17)	0.8831(10)	0.053(2)
C(73)	0.4858(6)	0.0569(14)	0.9088(5)	0.0428(14)
Cl(40)	0.5385(2)	0.0381(5)	0.8590(2)	0.0428(14)
Cl(41)	0.5061(2)	0.0080(4)	0.9755(2)	0.0428(14)
Cl(42)	0.4200(5)	0.0162(12)	0.8828(6)	0.0428(14)

7.3.15 Tri(pyrid-2-yl)phosphinoxid-triphenylarsin-kupfer(I)-hexafluorophosphat-chloroformsolvat (tgn411)

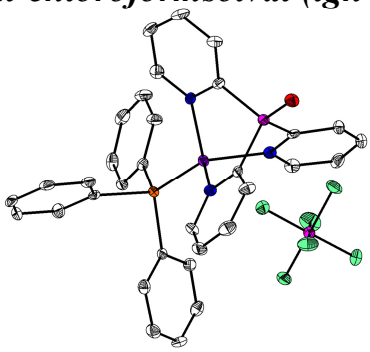

Kristalldaten

C35 H29 As Cl6 Cu F6 N3 O P2	M = 1034.71 g/mol	Monoclinic, $P2_1/n$
a = 23.5975(13) Å	b = 15.0545(7) Å	c = 23.6115(13) Å
α = 90°	β = 94.026(2)°	γ = 90°
V = 8367.3(8) Å^3	Z = 8	F(000) = 4128
D_{calc} = 1.643 g/cm^3	μ = 1.827 mm^{-1}	
colourless block	0.210 · 0.190 · 0.130 mm^3	

Datensammlung

Diffraktometer: D8 Quest (Bruker)	T = 100(2) K	λ = 0.71069 Å
h = -30 bis 30	k = -19 bis 18	l = -30 bis 30
150509 gemessene Reflexe	18536 unabhängige Reflexe	14642 Reflexe mit I >2σ(I)
θ = 2.196 bis 27.198°	R_{int} = 0.1198	C (25.00°) = 0.999
Absorptionskorrektur: Multi-scan	T_{min} = 0.6642	T_{max} = 0.7455

Verfeinerung

18536 Reflexe	127 Restraints	1076 Parameter
Verfeinerung mit SHELXL-2014/7	bis χ = 0.001	
R_1 (I > 2σ(I)) = 0.0401	wR_2 (I > 2σ(I)) = 0.0670	
R_1 (all) = 0.0694	wR_2 (all) = 0.0743	GoF (S) = 1.009
Δφ$_{min}$ = -0.495 e·Å^{-3}	Δφ$_{max}$ = 0.627 e·Å^{-3}	

Kommentar

Die Struktur wurde als pseudo-meroedrischer Zwilling verfeinert. Mehrere Chloroformmoleküle sind über mehrere Positionen fehlgeordnet. Die fehlgeordneten Positionen wurden über SAME re- und über EADP constrained.

Fraktionelle Atomkoordinaten (*x, y, z*) und äquivalente isotrope Auslenkungsfaktoren *U*(eq)

	x	*y*	*z*	*U*(eq)/Å^2
C(6)	0.5247(2)	0.2988(2)	0.1275(2)	0.0120(8)
C(7)	0.4846(2)	0.3644(2)	0.1329(2)	0.0185(9)
C(8)	0.4990(2)	0.4374(3)	0.1660(2)	0.0236(10)
C(9)	0.5529(2)	0.4430(2)	0.1922(2)	0.0234(9)
C(10)	0.5913(2)	0.3755(2)	0.1844(2)	0.0182(9)
C(1)	0.5604(2)	0.2053(2)	0.0308(2)	0.0122(7)
C(2)	0.5424(2)	0.2099(2)	-0.0260(2)	0.0170(8)
C(3)	0.5834(2)	0.2174(2)	-0.0650(2)	0.0189(9)
C(4)	0.6399(2)	0.2203(2)	-0.0457(2)	0.0201(9)
C(5)	0.6543(2)	0.2146(2)	0.0117(2)	0.0186(9)
C(11)	0.5250(2)	0.1068(2)	0.1273(2)	0.0128(8)
C(12)	0.4837(2)	0.0426(2)	0.1338(2)	0.0181(9)
C(13)	0.4972(2)	-0.0300(2)	0.1680(2)	0.0219(9)
C(14)	0.5503(2)	-0.0360(2)	0.1954(2)	0.0195(9)
C(15)	0.5893(2)	0.0312(2)	0.1864(2)	0.0182(8)
C(16)	0.7154(2)	0.2088(2)	0.2661(2)	0.0129(8)
C(17)	0.6620(2)	0.2127(2)	0.2870(2)	0.0166(8)
C(18)	0.6564(2)	0.2164(2)	0.3449(2)	0.0171(9)
C(19)	0.7046(2)	0.2144(2)	0.3815(2)	0.0209(9)
C(20)	0.7584(2)	0.2092(2)	0.3610(2)	0.0215(9)
C(21)	0.7637(2)	0.2066(2)	0.3031(2)	0.0186(8)
C(28)	0.7666(2)	0.3144(2)	0.1759(1)	0.0112(8)
C(29)	0.7606(2)	0.3861(2)	0.2114(2)	0.0166(8)
C(30)	0.7900(2)	0.4642(2)	0.2027(2)	0.0201(9)
C(31)	0.8267(2)	0.4689(2)	0.1593(2)	0.0212(9)
C(32)	0.8321(2)	0.3970(2)	0.1242(2)	0.0204(9)
C(33)	0.8016(2)	0.3204(2)	0.1312(2)	0.0154(8)
C(22)	0.7735(2)	0.1121(2)	0.1737(2)	0.0122(8)
C(23)	0.7504(2)	0.0326(2)	0.1522(2)	0.0180(8)
C(24)	0.7852(2)	-0.0424(2)	0.1488(2)	0.0219(9)
C(25)	0.8424(2)	-0.0355(3)	0.1649(2)	0.0223(9)
C(26)	0.8658(2)	0.0441(3)	0.1840(2)	0.0206(9)
C(27)	0.8311(2)	0.1179(2)	0.1890(2)	0.0142(8)
C(44)	0.8728(2)	0.8437(2)	0.9843(1)	0.0111(8)
C(45)	0.8741(2)	0.9045(2)	1.0279(2)	0.0154(8)
C(46)	0.8470(2)	0.9849(2)	1.0187(2)	0.0193(9)
C(47)	0.8198(2)	1.0019(2)	0.9663(2)	0.0216(9)
C(48)	0.8205(2)	0.9385(2)	0.9249(2)	0.0162(8)
C(34)	0.9632(2)	0.7474(2)	0.9398(2)	0.0130(7)
C(35)	1.0203(2)	0.7507(2)	0.9564(2)	0.0194(9)
C(36)	1.0589(2)	0.7608(3)	0.9151(2)	0.0221(9)
C(37)	1.0384(2)	0.7662(3)	0.8593(2)	0.0246(9)
C(38)	0.9804(2)	0.7636(2)	0.8462(2)	0.0179(9)
C(39)	0.8611(2)	0.6522(2)	0.9710(2)	0.0120(8)
C(40)	0.8491(2)	0.5860(2)	1.0086(2)	0.0167(8)
C(41)	0.8095(2)	0.5216(2)	0.9916(2)	0.0206(9)
C(42)	0.7843(2)	0.5256(2)	0.9375(2)	0.0200(9)
C(43)	0.7984(2)	0.5931(2)	0.9020(2)	0.0175(9)
C(61)	0.8232(2)	0.6671(2)	0.7406(2)	0.0114(8)
C(62)	0.8595(2)	0.6030(2)	0.7653(2)	0.0162(8)
C(63)	0.8681(2)	0.5235(2)	0.7382(2)	0.0232(9)
C(64)	0.8407(2)	0.5071(2)	0.6855(2)	0.0187(9)
C(65)	0.8055(2)	0.5710(2)	0.6602(2)	0.0181(8)
C(66)	0.7960(2)	0.6504(2)	0.6874(2)	0.0168(8)
C(55)	0.8220(2)	0.8691(2)	0.7296(2)	0.0142(8)
C(60)	0.8560(2)	0.8589(2)	0.6841(2)	0.0154(8)
C(59)	0.8650(2)	0.9296(3)	0.6484(2)	0.0219(9)
C(58)	0.8418(2)	1.0119(3)	0.6586(2)	0.0192(9)
C(57)	0.8091(2)	1.0230(2)	0.7046(2)	0.0184(9)
C(56)	0.7988(2)	0.9521(2)	0.7392(2)	0.0151(8)
C(49)	0.7279(2)	0.7772(2)	0.7850(2)	0.0114(7)
C(54)	0.6918(2)	0.7864(2)	0.7364(2)	0.0175(8)
C(53)	0.6334(2)	0.7816(2)	0.7398(2)	0.0213(9)
C(52)	0.6112(2)	0.7704(2)	0.7922(2)	0.0230(9)
C(51)	0.6465(2)	0.7632(2)	0.8408(2)	0.0208(9)
C(50)	0.7052(2)	0.7662(2)	0.8375(2)	0.0137(8)
C(67)	0.6104(2)	0.5283(3)	0.0538(2)	0.0416(13)
N(2)	0.5779(1)	0.3038(2)	0.1529(1)	0.0134(7)
N(1)	0.6156(1)	0.2068(2)	0.0501(1)	0.0133(7)
N(3)	0.5777(1)	0.1013(2)	0.1531(1)	0.0119(6)
N(6)	0.8466(1)	0.8592(2)	0.9326(1)	0.0129(6)
N(4)	0.9427(1)	0.7550(2)	0.8850(1)	0.0138(7)
N(5)	0.8357(1)	0.6574(2)	0.9182(1)	0.0130(7)
F(1)	1.0792(1)	0.7415(1)	0.7283(1)	0.0269(6)
F(2)	1.0259(1)	0.8658(1)	0.7339(1)	0.0254(5)
F(3)	0.9977(1)	0.8535(1)	0.6407(1)	0.0266(5)
F(4)	1.0501(1)	0.7283(1)	0.6356(1)	0.0263(5)
F(5)	0.9848(1)	0.7383(1)	0.7009(1)	0.0249(5)
F(6)	1.0915(1)	0.8562(1)	0.6686(1)	0.0280(5)
F(7)	0.8676(1)	0.2072(2)	-0.0635(1)	0.0320(6)
F(8)	0.8149(1)	0.3242(1)	-0.0976(1)	0.0270(5)
F(9)	0.7637(1)	0.3197(1)	-0.0209(1)	0.0262(5)
F(10)	0.8152(1)	0.2016(1)	0.0127(1)	0.0267(6)
F(11)	0.7719(1)	0.1964(1)	-0.0750(1)	0.0242(5)
F(12)	0.8597(1)	0.3295(1)	-0.0097(1)	0.0218(5)
P(1)	0.5082(1)	0.2028(1)	0.0833(1)	0.0119(2)
P(2)	0.9115(1)	0.7394(1)	0.9929(1)	0.0120(2)
P(3)	1.0384(1)	0.7974(1)	0.6844(1)	0.0164(2)
P(4)	0.8157(1)	0.2636(1)	-0.0425(1)	0.0158(2)
Cl(2)	0.5738(1)	0.4444(1)	0.0143(1)	0.0450(3)
C(68)	0.6521(2)	0.8827(2)	0.0058(2)	0.0245(10)
Cl(4)	0.6567(1)	0.9915(1)	-0.0206(1)	0.0476(3)
Cl(5)	0.6365(1)	0.8845(1)	0.0768(1)	0.0419(3)
Cl(6)	0.7157(1)	0.8243(1)	-0.0027(1)	0.0332(3)
Cu(1)	0.6331(1)	0.2021(1)	0.1358(1)	0.0123(1)
Cu(2)	0.8565(1)	0.7669(1)	0.8709(1)	0.0125(1)
As(1)	0.7204(1)	0.2086(1)	0.1841(1)	0.0104(1)
As(2)	0.8105(1)	0.7747(1)	0.7831(1)	0.0106(1)
O(1)	0.4487(1)	0.2029(2)	0.0588(1)	0.0171(6)
O(2)	0.9371(1)	0.7256(2)	1.0512(1)	0.0168(6)
C(69A)	0.9499(5)	0.0693(7)	0.8729(4)	0.0312(8)
Cl(7A)	0.9980(4)	0.1469(4)	0.8470(5)	0.057(2)
Cl(8A)	0.9089(3)	0.0283(10)	0.8168(3)	0.069(3)
Cl(9A)	0.9835(6)	-0.0022(6)	0.9210(5)	0.0484(17)
C(69B)	0.9539(6)	0.0847(9)	0.8650(5)	0.0312(8)
Cl(7B)	1.0063(5)	0.1434(6)	0.8338(4)	0.058(2)
Cl(8B)	0.9288(8)	-0.0018(5)	0.8161(4)	0.066(3)
Cl(9B)	0.9795(8)	0.0226(11)	0.9253(6)	0.054(3)
C(70)	0.9988(7)	0.4348(12)	0.8909(6)	0.0322(13)
Cl(10)	1.0177(2)	0.4435(6)	0.8201(3)	0.0322(13)
Cl(11)	0.9276(5)	0.4112(7)	0.8936(6)	0.0322(13)
Cl(12)	1.0215(2)	0.5267(3)	0.9325(4)	0.0322(13)
C(71)	0.9964(5)	0.4262(10)	0.8831(6)	0.0312(8)
Cl(20)	1.0132(2)	0.4079(6)	0.8112(2)	0.0312(8)
Cl(21)	0.9223(3)	0.4357(4)	0.8880(3)	0.0312(8)
Cl(22)	1.0248(2)	0.5290(3)	0.9075(4)	0.0312(8)
C(72)	0.9896(9)	0.449(2)	0.9027(8)	0.069(4)
Cl(30)	1.0232(6)	0.4864(13)	0.8420(7)	0.069(4)
Cl(31)	0.9167(7)	0.4620(13)	0.8874(9)	0.069(4)
Cl(32)	1.0097(6)	0.5062(10)	0.9663(7)	0.069(4)
C(73)	1.0020(7)	0.4162(10)	0.8700(7)	0.0357(14)
Cl(40)	1.0083(3)	0.3749(5)	0.8006(3)	0.0357(14)

	x	y	z	U(eq)/Å^2
Cl(41)	0.9310(5)	0.4012(8)	0.8877(7)	0.0357(14)
Cl(42)	1.0254(2)	0.5266(4)	0.8753(4)	0.0357(14)
Cl(1B)	0.6330(11)	0.6150(6)	0.0087(4)	0.069(4)
Cl(3B)	0.6777(5)	0.4756(12)	0.0814(6)	0.062(3)
Cl(3A)	0.6744(7)	0.5041(9)	0.0804(8)	0.056(2)
Cl(1A)	0.6026(8)	0.6268(3)	0.0127(2)	0.042(2)

7.3.16 Iodo-tri(pyrid-2-yl)amin-kupfer(I)-dimer (tgb33)

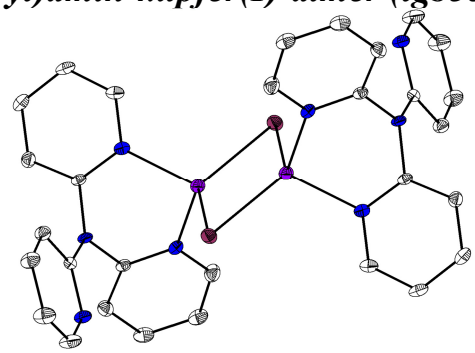

Kristalldaten

C15 H12 Cu I N4	M = 438.73 g/mol	Triclinic, $P\bar{1}$
a = 8.4951(6) Å	b = 9.4908(7) Å	c = 9.5082(7) Å
α = 93.619(3)°	β = 103.365(3)°	γ = 91.555(2)°
V = 743.66(9) Å^3	Z = 2	F(000) = 424
D_{calc} = 1.959 g/cm^3	μ = 3.541 mm^{-1}	
yellow block	0.310 · 0.170 · 0.140 mm^3	

Datensammlung

Diffraktometer: D8 Quest (Bruker)	T = 100(2) K	λ = 0.71069 Å
h = -10 bis 10	k = -12 bis 12	l = -12 bis 11
9157 gemessene Reflexe	3264 unabhängige Reflexe	3083 Reflexe mit $I > 2\sigma(I)$
θ = 2.466 bis 27.124°	R_{int} = 0.0360	C (25.00°) = 0.995
Absorptionskorrektur: Multi-scan	T_{min} = 0.5228	T_{max} = 0.7455

Verfeinerung

3264 Reflexe	0 Restraints	190 Parameter
Verfeinerung mit SHELXL-2014/7	bis χ = 0.000	
R_1 ($I > 2\sigma(I)$) = 0.0258	wR_2 ($I > 2\sigma(I)$) = 0.0702	
R_1 (all) = 0.0278	wR_2 (all) = 0.0713	GoF (S) = 1.074
$\Delta\varphi_{min}$ = -1.190 e·Å^{-3}	$\Delta\varphi_{max}$ = 1.060 e·Å^{-3}	

Fraktionelle Atomkoordinaten (*x, y, z*) und äquivalente isotrope Auslenkungsfaktoren *U*(eq)

	x	y	z	U(eq)/Å^2
C(1)	0.1343(3)	0.3904(3)	0.2112(3)	0.0109(5)
C(2)	0.2251(3)	0.5174(3)	0.2372(3)	0.0158(5)
C(3)	0.2966(3)	0.5625(3)	0.1300(3)	0.0177(5)
C(4)	0.2719(3)	0.4811(3)	0.0000(3)	0.0172(5)
C(5)	0.1755(3)	0.3595(3)	-0.0198(3)	0.0179(5)
C(6)	-0.1099(3)	0.3117(3)	0.2866(3)	0.0110(5)
C(7)	-0.2034(3)	0.3929(3)	0.3592(3)	0.0140(5)
C(8)	-0.3688(3)	0.3626(3)	0.3313(3)	0.0158(5)
C(9)	-0.4353(3)	0.2531(3)	0.2284(3)	0.0157(5)
C(10)	-0.3335(3)	0.1804(3)	0.1573(3)	0.0148(5)
C(11)	0.1580(3)	0.2703(3)	0.4359(3)	0.0109(5)
C(12)	0.0871(3)	0.1919(3)	0.5274(3)	0.0143(5)
C(13)	0.1889(3)	0.1258(3)	0.6358(3)	0.0183(5)
C(14)	0.3558(3)	0.1386(3)	0.6526(3)	0.0211(6)
C(15)	0.4124(3)	0.2201(3)	0.5584(3)	0.0202(6)
N(1)	0.0615(2)	0.3386(2)	0.3211(2)	0.0115(4)
N(2)	0.1085(2)	0.3119(2)	0.0848(2)	0.0125(4)
N(3)	-0.1720(2)	0.2066(2)	0.1865(2)	0.0123(4)
N(4)	0.3180(2)	0.2875(2)	0.4523(2)	0.0145(4)
Cu(1)	-0.0200(1)	0.1198(1)	0.0645(1)	0.0137(1)
I(1)	-0.1875(1)	0.0547(1)	-0.1971(1)	0.0157(1)

7.3.17 5,6-Dichloro-2-(3-methyl-imidazol-1-yliden)benzimidazolato-cyclooctadien-iridium(I) (tgn282-1)

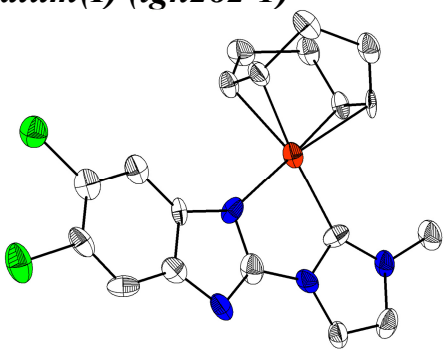

Kristalldaten

C19 H19 Cl2 Ir N4	M = 566.48 g/mol	Triclinic, $P\bar{1}$
a = 7.1427(7) Å	b = 9.8611(12) Å	c = 12.7756(12) Å
α = 73.876(8)°	β = 86.688(8)°	γ = 83.677(9)°
V = 858.84(16) Å^3	Z = 2	F(000) = 544
D_{calc} = 2.191 g/cm^3	μ = 8.096 mm^{-1}	
colourless prism	0.210 · 0.090 · 0.020 mm^3	

Datensammlung

Diffraktometer: STOE IPDS 2T	T = 100(2) K	λ = 0.71069 Å
h = -7 bis 9	k = -12 bis 12	l = -16 bis 16
6889 gemessene Reflexe	6889 unabhängige Reflexe	3319 Reflexe mit $I > 2\sigma(I)$
θ = 2.160 bis 27.038°	R_{int} = -(hklf5)	C (25.00°) = 0.998
Absorptionskorrektur: Keine		

Verfeinerung

6889 Reflexe	0 Restraints	237 Parameter
Verfeinerung mit SHELXL-2014/7	bis χ = 0.000	
R_1 ($I > 2\sigma(I)$) = 0.0840	wR_2 ($I > 2\sigma(I)$) = 0.1868	
R_1 (all) = 0.1574	wR_2 (all) = 0.2208	GoF (S) = 0.873
$\Delta\varphi_{min}$ = -6.304 e·Å^{-3}	$\Delta\varphi_{max}$ = 5.700 e·Å^{-3}	

Kommentar

Die Struktur wurde als nicht-meroedrischer Zwilling integriert und verfeinert. Wegen zusätzlich schwacher Streuung liegt nur eine geringe Datenqualitätvor. Anstelle einer hklf5-Absorptionskorrektur wurden die erweiterten Integrationsoptionen von X-Area (Merging of identical hkl and Friedel Pairs) gewählt

Fraktionelle Atomkoordinaten (*x, y, z*) und äquivalente isotrope Auslenkungsfaktoren *U*(eq)

	x	*y*	*z*	*U*(eq)/Å^2		*x*	*y*	*z*	*U*(eq)/Å^2
Ir(1)	0.6514(1)	0.3824(1)	0.2231(1)	0.0262(3)	N(4)	0.802(3)	0.636(2)	-0.0819(15)	0.033(4)
C(1)	0.652(3)	0.599(2)	0.196(2)	0.031(5)	C(3)	0.707(3)	0.809(2)	0.0791(18)	0.031(5)
N(1)	0.616(3)	0.705(2)	0.2444(14)	0.030(4)	C(6)	0.878(3)	0.497(2)	-0.220(2)	0.034(5)
C(14)	0.823(3)	0.092(3)	0.3609(18)	0.034(5)	C(10)	0.766(3)	0.396(2)	-0.0329(16)	0.025(4)
C(7)	0.883(3)	0.364(3)	-0.2344(18)	0.037(6)	C(18)	0.419(3)	0.193(2)	0.4032(17)	0.030(5)
N(2)	0.702(2)	0.6661(19)	0.0935(14)	0.029(4)	C(9)	0.774(3)	0.264(3)	-0.0504(18)	0.034(5)
C(12)	0.706(3)	0.333(2)	0.3894(16)	0.026(5)	C(8)	0.833(3)	0.248(3)	-0.152(2)	0.039(6)
C(4)	0.741(3)	0.587(3)	0.0171(19)	0.037(5)	C(5)	0.820(3)	0.513(2)	-0.1154(19)	0.032(5)
C(16)	0.564(3)	0.181(2)	0.2206(17)	0.027(5)	C(17)	0.404(3)	0.139(3)	0.3026(19)	0.037(5)
C(2)	0.653(3)	0.833(3)	0.175(2)	0.036(5)	C(15)	0.755(3)	0.164(2)	0.2454(17)	0.031(5)
N(3)	0.719(3)	0.4447(19)	0.0563(15)	0.028(4)	C(11)	0.551(4)	0.690(3)	0.3558(18)	0.039(6)
C(13)	0.834(3)	0.196(3)	0.4263(18)	0.037(5)	Cl(2)	0.8478(9)	0.0831(7)	-0.1754(6)	0.0450(16)
C(19)	0.508(3)	0.331(3)	0.3754(18)	0.026(5)	Cl(1)	0.9536(10)	0.3468(9)	-0.3644(6)	0.0553(19)

7.3.18 Tetrapyrazolylborato-triphenylphosphin-kupfer(I)-dimethylsulfoxidsolvat (tgn300)

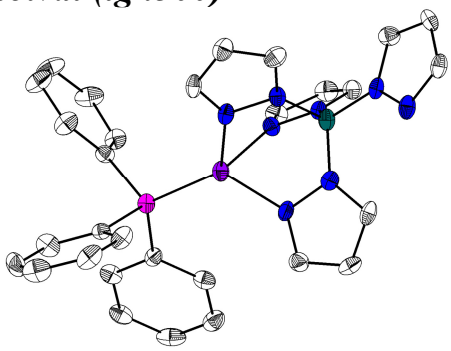

Kristalldaten

C32 H33 B Cu N8 O P S	M = 683.04 g/mol	Triclinic, $P\bar{1}$
a = 8.8697(5) Å	b = 16.5496(9) Å	c = 22.0966(13) Å
α = 87.444(5)°	β = 82.100(5)°	γ = 88.513(5)°
V = 3208.9(3) Å^3	Z = 4	F(000) = 1416
D_{calc} = 1.414 g/cm^3	μ = 0.836 mm^{-1}	
colourless block	0.370 · 0.100 · 0.070 mm^3	

Datensammlung

Diffraktometer: STOE IPDS 2	T = 100(2) K	λ = 0.71069 Å
h = -11 bis 9	k = -20 bis 20	l = -27 bis 27
45519 gemessene Reflexe	13541 unabhängige Reflexe	5196 Reflexe mit $I > 2\sigma(I)$
θ = 1.232 bis 26.753°	R_{int} = 0.1150	C (25.00°) = 0.999
Absorptionskorrektur: Multi-scan	T_{min} = 0.7992	T_{max} = 1.0104

Verfeinerung

13541 Reflexe	0 Restraints	815 Parameter
Verfeinerung mit SHELXL-2014/7	bis χ = 0.001	
R_1 ($I > 2\sigma(I)$) = 0.0412	wR_2 ($I > 2\sigma(I)$) = 0.0780	
R_1 (all) = 0.1319	wR_2 (all) = 0.0910	GoF (S) = 0.656
$\Delta\varphi_{min}$ = -0.519 e·Å^{-3}	$\Delta\varphi_{max}$ = 0.986 e·Å^{-3}	

Kommentar

Platon-CheckCif liefert B-Alerts wegen gefundener zusätzlicher (Pseudo)symmetrie und einer geringen Anzahl Reflexe mit $I > 2\sigma(I)$. Die Struktur kann tatsächlich durch die ausschließliche Berücksichtigung der Unterstrukturreflexe bei der Indizierung mit einer halbierten Elementarzelle gelöst und verfeinert werden (In diesem Fall reicht die Reflexzahl aus). In dieser ist jedoch das DMSO-Molekül fehlgeordnet. Da die Überstrukturreflexe deutlich erkennbar sind und in diesem Fall keine Fehlordnung vorliegt, ist die präsentierte Lösung nach Aussage von Dr. Harms zu bevorzugen.

Fraktionelle Atomkoordinaten (*x, y, z*) und äquivalente isotrope Auslenkungsfaktoren *U*(eq)

	x	*y*	*z*	*U*(eq)/Å^2		*x*	*y*	*z*	*U*(eq)/Å^2
Cu(1)	0.5938(1)	0.2282(1)	0.2989(1)	0.0222(2)	C(3)	0.5045(6)	0.1005(3)	0.4639(2)	0.0281(13)
P(1)	0.4821(2)	0.2664(1)	0.2218(1)	0.0195(3)	C(4)	0.9026(6)	0.1307(3)	0.2597(2)	0.0253(12)
N(1)	0.5845(5)	0.1454(2)	0.4174(2)	0.0195(10)	C(5)	1.0196(6)	0.0952(3)	0.2870(2)	0.0244(12)
N(2)	0.4957(5)	0.1578(2)	0.3717(2)	0.0229(10)	C(6)	0.9802(6)	0.1079(3)	0.3480(2)	0.0236(12)
N(3)	0.8460(5)	0.1487(2)	0.3562(2)	0.0205(10)	C(7)	0.6671(6)	0.3892(3)	0.3618(2)	0.0256(13)
N(4)	0.7971(5)	0.1639(2)	0.3003(2)	0.0231(10)	C(8)	0.7504(6)	0.4092(3)	0.4074(2)	0.0268(13)
N(5)	0.7327(5)	0.2760(2)	0.4043(2)	0.0178(10)	C(9)	0.7911(6)	0.3356(3)	0.4330(2)	0.0227(12)
N(6)	0.6566(5)	0.3083(2)	0.3588(2)	0.0201(10)	C(10)	0.8970(6)	0.0830(3)	0.5398(2)	0.0247(13)
N(7)	0.8052(5)	0.1608(2)	0.4734(2)	0.0204(10)	C(11)	0.8143(6)	0.1435(3)	0.5727(2)	0.0257(13)
N(8)	0.8919(5)	0.0910(2)	0.4801(2)	0.0249(11)	C(12)	0.7572(6)	0.1914(3)	0.5289(2)	0.0253(13)
C(1)	0.3659(6)	0.1202(3)	0.3899(2)	0.0259(13)	C(13)	0.3186(6)	0.3325(3)	0.2428(2)	0.0203(11)
C(2)	0.3665(6)	0.0838(3)	0.4478(2)	0.0281(13)	C(14)	0.3379(6)	0.4155(3)	0.2508(2)	0.0238(12)

	x	y	z	U(eq)/Å^2
C(15)	0.2188(7)	0.4646(3)	0.2737(2)	0.0331(14)
C(16)	0.0742(6)	0.4345(3)	0.2888(2)	0.0343(13)
C(17)	0.0499(6)	0.3520(3)	0.2813(2)	0.0360(13)
C(18)	0.1712(6)	0.3025(3)	0.2594(2)	0.0291(12)
C(19)	0.4034(6)	0.1851(3)	0.1831(2)	0.0178(11)
C(20)	0.3056(7)	0.1983(3)	0.1400(2)	0.0286(13)
C(21)	0.2466(6)	0.1326(3)	0.1143(2)	0.0337(14)
C(22)	0.2873(7)	0.0541(3)	0.1308(2)	0.0357(14)
C(23)	0.3850(6)	0.0406(3)	0.1730(2)	0.0332(13)
C(24)	0.4435(6)	0.1054(3)	0.1992(2)	0.0282(12)
C(25)	0.5993(6)	0.3255(3)	0.1617(2)	0.0204(11)
C(26)	0.5390(6)	0.3715(3)	0.1156(2)	0.0247(12)
C(27)	0.6373(7)	0.4152(3)	0.0729(2)	0.0277(13)
C(28)	0.7909(7)	0.4151(3)	0.0750(2)	0.0317(14)
C(29)	0.8538(7)	0.3695(3)	0.1201(2)	0.0295(13)
C(30)	0.7553(6)	0.3251(3)	0.1638(2)	0.0239(12)
B(1)	0.7456(7)	0.1816(3)	0.4130(3)	0.0207(14)
Cu(2)	0.3937(1)	0.7768(1)	0.2036(1)	0.0208(2)
P(2)	0.5071(2)	0.7347(1)	0.2790(1)	0.0185(3)
N(9)	0.1503(5)	0.8526(2)	0.1410(2)	0.0181(9)
N(10)	0.1948(5)	0.8427(2)	0.1976(2)	0.0221(10)
N(11)	0.4182(5)	0.8532(2)	0.0825(2)	0.0181(9)
N(12)	0.4997(5)	0.8407(2)	0.1299(2)	0.0212(10)
N(13)	0.2643(5)	0.7237(2)	0.0961(2)	0.0182(10)
N(14)	0.3271(5)	0.6931(2)	0.1462(2)	0.0198(9)
N(15)	0.2001(5)	0.8380(2)	0.0241(2)	0.0193(10)
N(16)	0.1074(5)	0.9050(2)	0.0159(2)	0.0215(10)
C(31)	0.0855(6)	0.8752(3)	0.2368(2)	0.0240(12)
C(32)	-0.0322(6)	0.9052(3)	0.2065(2)	0.0239(12)
C(33)	0.0124(6)	0.8899(3)	0.1463(2)	0.0223(12)
C(34)	0.6317(6)	0.8790(3)	0.1133(2)	0.0261(13)
C(35)	0.6361(6)	0.9153(3)	0.0551(2)	0.0272(13)
C(36)	0.4978(6)	0.8986(3)	0.0371(2)	0.0212(12)

	x	y	z	U(eq)/Å^2
C(37)	0.3159(6)	0.6123(3)	0.1449(2)	0.0233(12)
C(38)	0.2496(6)	0.5901(3)	0.0947(2)	0.0224(12)
C(39)	0.2165(6)	0.6627(3)	0.0659(2)	0.0214(12)
C(40)	0.1088(6)	0.9130(3)	-0.0445(2)	0.0242(13)
C(41)	0.2025(6)	0.8547(3)	-0.0756(2)	0.0272(13)
C(42)	0.2596(6)	0.8092(3)	-0.0311(2)	0.0231(12)
C(43)	0.5986(6)	0.8084(3)	0.3200(2)	0.0219(12)
C(44)	0.5566(6)	0.8906(3)	0.3126(2)	0.0263(12)
C(45)	0.6248(7)	0.9496(3)	0.3424(2)	0.0320(13)
C(46)	0.7341(6)	0.9286(3)	0.3785(2)	0.0298(12)
C(47)	0.7790(7)	0.8478(3)	0.3853(2)	0.0349(14)
C(48)	0.7117(6)	0.7885(3)	0.3564(2)	0.0254(12)
C(49)	0.3902(6)	0.6729(3)	0.3376(2)	0.0207(12)
C(50)	0.4521(6)	0.6240(3)	0.3825(2)	0.0277(13)
C(51)	0.3541(7)	0.5796(3)	0.4254(2)	0.0328(14)
C(52)	0.2007(7)	0.5826(3)	0.4249(2)	0.0311(14)
C(53)	0.1388(7)	0.6312(3)	0.3814(2)	0.0314(14)
C(54)	0.2335(6)	0.6756(3)	0.3377(2)	0.0250(12)
C(55)	0.6640(6)	0.6667(3)	0.2513(2)	0.0199(11)
C(56)	0.8063(6)	0.6976(3)	0.2270(2)	0.0287(12)
C(57)	0.9190(6)	0.6488(3)	0.1980(2)	0.0315(12)
C(58)	0.8923(6)	0.5660(3)	0.1922(2)	0.0333(13)
C(59)	0.7536(6)	0.5354(3)	0.2171(2)	0.0290(12)
C(60)	0.6411(6)	0.5841(3)	0.2460(2)	0.0239(12)
B(2)	0.2549(7)	0.8180(3)	0.0856(2)	0.0180(13)
S(2)	0.8249(1)	0.6291(1)	0.0175(1)	0.0250(3)
S(1)	0.2004(2)	0.3399(1)	0.4977(1)	0.0346(3)
O(2)	0.7762(5)	0.6074(2)	-0.0411(2)	0.0436(10)
O(1)	0.2047(5)	0.4123(2)	0.5341(2)	0.0422(10)
C(64)	0.6573(5)	0.6402(3)	0.0709(2)	0.0293(10)
C(63)	0.8663(5)	0.7350(2)	0.0099(2)	0.0300(10)
C(61)	0.3916(6)	0.2996(3)	0.4891(2)	0.0462(13)
C(62)	0.2031(7)	0.3687(3)	0.4219(2)	0.0537(15)

7.3.19 *Bis(tris(3,4,5-trimethylimidazol-2-yl)phosphin)-kupfer(II)-hexaiodo-tetracuprat(I) (tgn338)*

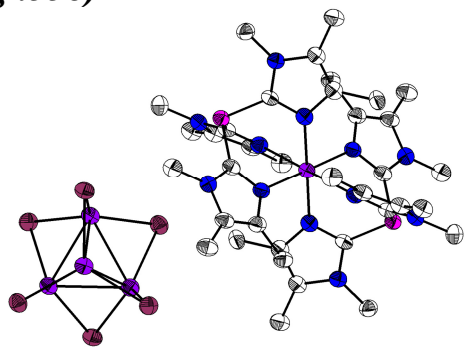

Kristalldaten

C36 H54 Cu5 I6 N12 P2	M = 1795.95 g/mol	Trigonal, $R\bar{3}$
a = 30.7930(9) Å	b = 30.7930(9) Å	c = 19.2340(8) Å
α = 90°	β = 90°	γ = 120°
V = 15794.4(11) Å^3	Z = 12	F(000) = 10164
D_{calc} = 2.266 g/cm^3	μ = 5.606 mm^{-1}	
colourless block	0.180 · 0.160 · 0.110 mm^3	

Datensammlung

Diffraktometer: STOE IPDS 2T	T = 100(2) K	λ = 0.71069 Å
h = -37 bis 38	k = -38 bis 38	l = -24 bis 24
40798 gemessene Reflexe	7444 unabhängige Reflexe	4188 Reflexe mit $I > 2\sigma(I)$
θ = 1.305 bis 26.755°	R_{int} = 0.1175	C (25.00°) = 1.000
Absorptionskorrektur: Multi-scan	T_{min} = 0.3651	T_{max} = 0.571

Verfeinerung

7444 Reflexe	0 Restraints	405 Parameter
Verfeinerung mit SHELXL-2014/7	bis χ = 0.001	
R_1 ($I > 2\sigma(I)$) = 0.0407	wR_2 ($I > 2\sigma(I)$) = 0.0893	
R_1 (all) = 0.0793	wR_2 (all) = 0.1021	GoF (S) = 0.849
$\Delta\varphi_{min}$ = -1.488 e·Å^{-3}	$\Delta\varphi_{max}$ = 0.710 e·Å^{-3}	

Kommentar

Die vier Kupferatome innerhalb des Komplexanions sind in der Form fehlgeordnet, dass das durch sie aufgespannte Tetraeder um 90° gedreht wird.

Fraktionelle Atomkoordinaten (*x, y, z*) und äquivalente isotrope Auslenkungsfaktoren *U*(eq)

	x	*y*	*z*	*U*(eq)/Å^2		*x*	*y*	*z*	*U*(eq)/Å^2
C(1)	0.0461(2)	0.0548(2)	0.1356(3)	0.0348(12)	C(24)	0.0744(2)	0.2298(2)	0.0942(3)	0.0407(13)
C(2)	0.0885(2)	0.1094(2)	0.0552(3)	0.0382(12)	Cu(1)	0.0000	0.0000	0.0000	0.0301(3)
C(3)	0.1116(2)	0.1307(2)	0.1166(3)	0.0388(12)	Cu(2)	0.1667	0.3333	0.3333	0.0306(2)
C(4)	0.1026(2)	0.1325(2)	-0.0161(3)	0.0453(14)	Cu(3)	0.0000	0.0000	0.4124(1)	0.0367(5)
C(5)	0.1564(2)	0.1800(2)	0.1327(3)	0.0444(14)	Cu(4)	0.0384(1)	0.0589(1)	0.4705(1)	0.0362(3)
C(6)	0.0949(2)	0.1027(2)	0.2418(3)	0.0424(13)	Cu(5)	0.2735(1)	0.1438(1)	0.1390(1)	0.0363(3)
C(7)	0.2248(2)	0.3438(2)	0.1931(2)	0.0315(11)	Cu(6)	0.3699(1)	0.2251(1)	0.1340(1)	0.0368(3)
C(8)	0.2819(2)	0.3580(2)	0.2700(3)	0.0368(12)	Cu(7)	0.3118(1)	0.2045(1)	0.1956(1)	0.0364(3)
C(9)	0.3014(2)	0.3551(2)	0.2076(3)	0.0369(12)	Cu(8)	0.3321(1)	0.1649(1)	0.0793(1)	0.0371(3)
C(10)	0.3052(2)	0.3677(2)	0.3413(3)	0.0434(13)	I(1)	0.0941(1)	0.0328(1)	0.4057(1)	0.0399(1)
C(11)	0.3502(2)	0.3597(2)	0.1900(3)	0.0410(13)	I(2)	0.2962(1)	0.2236(1)	0.0711(1)	0.0398(1)
C(12)	0.2697(2)	0.3415(2)	0.0851(2)	0.0386(12)	I(3)	0.2402(1)	0.1331(1)	0.2640(1)	0.0393(1)
C(13)	0.1587(2)	0.3791(2)	0.2002(2)	0.0315(11)	I(4)	0.3946(1)	0.2635(1)	0.2558(1)	0.0403(1)
C(14)	0.1442(2)	0.4189(2)	0.2829(3)	0.0363(12)	N(1)	0.0481(2)	0.0621(2)	0.0668(2)	0.0348(10)
C(15)	0.1466(2)	0.4430(2)	0.2219(3)	0.0343(11)	N(2)	0.0842(2)	0.0958(2)	0.1673(2)	0.0362(10)
C(16)	0.1339(2)	0.4315(2)	0.3540(2)	0.0399(13)	N(3)	0.2340(2)	0.3505(2)	0.2610(2)	0.0346(10)
C(17)	0.1422(2)	0.4882(2)	0.2078(3)	0.0410(13)	N(4)	0.2650(2)	0.3465(2)	0.1591(2)	0.0340(10)
C(18)	0.1597(2)	0.4289(2)	0.0960(2)	0.0383(12)	N(5)	0.1208(2)	0.2728(2)	0.2684(2)	0.0323(9)
C(19)	0.1228(2)	0.2792(2)	0.1995(2)	0.0330(11)	N(6)	0.0851(2)	0.2377(2)	0.1687(2)	0.0342(10)
C(20)	0.0806(2)	0.2256(2)	0.2818(3)	0.0361(12)	N(7)	0.1521(2)	0.3793(2)	0.2687(2)	0.0339(10)
C(21)	0.0581(2)	0.2035(2)	0.2204(3)	0.0353(12)	N(8)	0.1557(2)	0.4172(2)	0.1699(2)	0.0313(9)
C(22)	0.0667(2)	0.2026(2)	0.3523(2)	0.0379(12)	P(1)	0.0000	0.0000	0.1820(1)	0.0327(5)
C(23)	0.0130(2)	0.1542(2)	0.2050(3)	0.0428(13)	P(2)	0.1680(1)	0.3340(1)	0.1513(1)	0.0306(3)

7.3.20 Cyanido-tri(pyrid-2-yl)phosphinoxid-kupfer(I)-dimer-isocyanido-kupfer(I)-addukt (tgn362)

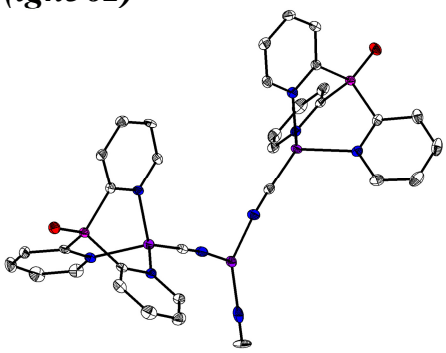

Kristalldaten

C37 H30 Cu3 N11 O2 P2	*M* = 913.28 g/mol	Orthorhombic, *Fdd*2
a = 27.1473(8) Å	*b* = 33.0974(12) Å	*c* = 8.5649(3) Å
α = 90°	β = 90°	γ = 90°
V = 7695.6(4) Å^3	*Z* = 8	*F*(000) = 3696
D_{calc} = 1.577 g/cm^3	μ = 1.776 mm^{-1}	
yellow block	0.450 · 0.270 · 0.190 mm^3	

Datensammlung

Diffraktometer: D8 Quest (Bruker)	T = 100(2) K	λ = 0.71073 Å
h = -34 bis 34	k = -42 bis 41	l = -9 bis 10
9517 gemessene Reflexe	3756 unabhängige Reflexe	3572 Reflexe mit $I > 2\sigma(I)$
θ = 2.461 bis 27.086°	R_{int} = 0.0255	C (25.00°) = 0.999
Absorptionskorrektur: Multi-scan	T_{min} = 0.6438	T_{max} = 0.7455

Verfeinerung

3756 Reflexe	1 Restraints	251 Parameter
Verfeinerung mit SHELXL-2014/7	bis χ = 0.001	
R_1 ($I > 2\sigma(I)$) = 0.0235	wR_2 ($I > 2\sigma(I)$) = 0.0557	
R_1 (all) = 0.0260	wR_2 (all) = 0.0570	GoF (S) = 1.079
$\Delta\varphi_{min}$ = -0.249 e·Å^{-3}	$\Delta\varphi_{max}$ = 0.350 e·Å^{-3}	

Fraktionelle Atomkoordinaten (*x, y, z*) und äquivalente isotrope Auslenkungsfaktoren *U*(eq)

	x	*y*	*z*	*U*(eq)/Å^2
C(1)	0.7014(1)	0.0476(1)	0.0689(4)	0.0129(6)
C(2)	0.6604(1)	0.0224(1)	0.0702(4)	0.0191(7)
C(3)	0.6208(1)	0.0328(1)	-0.0238(5)	0.0253(8)
C(4)	0.6239(1)	0.0667(1)	-0.1165(5)	0.0263(8)
C(5)	0.6661(1)	0.0899(1)	-0.1111(4)	0.0205(7)
C(6)	0.7593(1)	0.0787(1)	0.3245(4)	0.0126(6)
C(7)	0.7592(1)	0.0724(1)	0.4846(4)	0.0150(6)
C(8)	0.7632(1)	0.1055(1)	0.5820(4)	0.0178(7)
C(9)	0.7664(1)	0.1440(1)	0.5155(5)	0.0157(6)
C(10)	0.7666(1)	0.1477(1)	0.3541(4)	0.0154(7)
C(11)	0.8078(1)	0.0391(1)	0.0679(4)	0.0129(6)
C(12)	0.8391(1)	0.0063(1)	0.0566(4)	0.0183(7)
C(13)	0.8802(1)	0.0096(1)	-0.0384(5)	0.0238(8)
C(14)	0.8887(1)	0.0453(1)	-0.1167(4)	0.0221(8)
C(15)	0.8558(1)	0.0770(1)	-0.0989(4)	0.0182(7)
C(16)	0.7613(1)	0.1704(1)	-0.0836(4)	0.0138(7)
C(17)	0.7500	0.2500	-0.6292(6)	0.0221(11)
C(18)	0.6488(2)	0.1690(2)	0.1753(8)	0.078(2)
C(19)	0.6445(2)	0.1325(2)	0.2747(9)	0.0548(15)
N(1)	0.7043(1)	0.0811(1)	-0.0178(3)	0.0138(5)
N(2)	0.7631(1)	0.1156(1)	0.2580(4)	0.0129(6)
N(3)	0.8157(1)	0.0744(1)	-0.0078(3)	0.0138(5)
N(4)	0.7579(1)	0.2013(1)	-0.1461(4)	0.0167(6)
N(5)	0.7500	0.2500	-0.5010(6)	0.0209(10)
N(6)	0.6415(2)	0.1052(2)	0.3523(6)	0.0595(14)
O(1)	0.7495(1)	-0.0037(1)	0.2724(3)	0.0181(5)
P(1)	0.7538(1)	0.0358(1)	0.1927(1)	0.0120(2)
Cu(1)	0.7641(1)	0.1199(1)	0.0166(1)	0.0132(1)
Cu(2)	0.7500	0.2500	-0.2703(1)	0.0141(1)

7.3.21 Acetonitril-N^1,N^2-bis(2,6-diisopropylphenyl)ethane-1,2-diimin-iodo-kupfer(I)-dimer (tgn404)

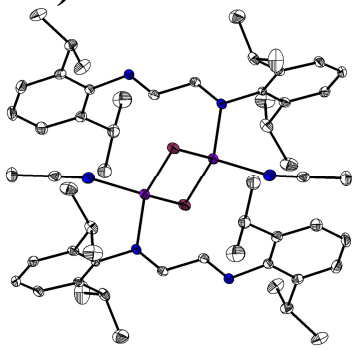

Kristalldaten

C28 H39 Cu I N3	M = 608.06 g/mol	Monoclinic, $P2_1/n$
a = 14.9069(6) Å	b = 12.8302(5) Å	c = 15.3820(6) Å
α = 90°	β = 101.1380(10)°	γ = 90°
V = 2886.5(2) Å^3	Z = 4	F(000) = 1240
D_{calc} = 1.399 g/cm^3	μ = 1.845 mm^{-1}	
orange block	0.240 · 0.230 · 0.170 mm^3	

Datensammlung

Diffraktometer: D8 Quest (Bruker)	T = 100(2) K	λ = 0.71069 Å
h = -19 bis 19	k = -16 bis 16	l = -19 bis 19
32040 gemessene Reflexe	6421 unabhängige Reflexe	5465 Reflexe mit $I > 2\sigma(I)$
θ = 2.083 bis 27.205°	R_{int} = 0.0318	C (25.00°) = 0.999
Absorptionskorrektur: Multi-scan	T_{min} = 0.6747	T_{max} = 0.7455

Verfeinerung

6421 Reflexe	0 Restraints	307 Parameter
Verfeinerung mit SHELXL-2014/7	bis χ = 0.001	
R_1 ($I > 2\sigma(I)$) = 0.0219	wR_2 ($I > 2\sigma(I)$) = 0.0560	
R_1 (all) = 0.0313	wR_2 (all) = 0.0671	GoF (S) = 1.149
$\Delta\varphi_{min}$ = -0.442 e·Å^{-3}	$\Delta\varphi_{max}$ = 0.616 e·Å^{-3}	

Fraktionelle Atomkoordinaten (*x, y, z*) und äquivalente isotrope Auslenkungsfaktoren *U*(eq)

	x	*y*	*z*	*U*(eq)/Å^2
C(1)	0.3065(1)	0.2413(1)	0.4850(1)	0.0106(4)
C(2)	0.2385(1)	0.2372(2)	0.4081(1)	0.0136(4)
C(3)	0.2076(1)	0.3316(2)	0.3678(1)	0.0158(4)
C(4)	0.2440(1)	0.4254(2)	0.4015(1)	0.0167(4)
C(5)	0.3126(1)	0.4272(2)	0.4768(1)	0.0150(4)
C(6)	0.3450(1)	0.3355(2)	0.5203(1)	0.0123(4)
C(7)	0.2002(1)	0.1347(2)	0.3677(1)	0.0183(4)
C(8)	0.2124(2)	0.1250(2)	0.2715(2)	0.0269(5)
C(9)	0.1006(2)	0.1228(2)	0.3757(2)	0.0319(6)
C(10)	0.4168(1)	0.3364(2)	0.6049(1)	0.0157(4)
C(11)	0.4881(2)	0.4213(2)	0.6059(2)	0.0352(6)
C(12)	0.3701(2)	0.3469(2)	0.6853(1)	0.0280(5)
C(13)	0.3134(1)	-0.1509(1)	0.6945(1)	0.0125(4)
C(14)	0.2813(1)	-0.2352(2)	0.6387(1)	0.0147(4)
C(15)	0.3019(1)	-0.3354(2)	0.6715(1)	0.0187(4)
C(16)	0.3519(2)	-0.3511(2)	0.7562(1)	0.0203(5)
C(17)	0.3829(1)	-0.2671(2)	0.8099(1)	0.0185(4)
C(18)	0.3642(1)	-0.1651(2)	0.7805(1)	0.0140(4)
C(19)	0.2229(1)	-0.2165(2)	0.5472(1)	0.0189(4)
C(20)	0.1242(2)	-0.1930(2)	0.5554(2)	0.0341(6)
C(21)	0.2265(2)	-0.3054(2)	0.4819(1)	0.0276(5)
C(22)	0.3976(1)	-0.0717(2)	0.8381(1)	0.0173(4)
C(23)	0.4913(2)	-0.0351(2)	0.8227(1)	0.0252(5)
C(24)	0.4017(2)	-0.0918(2)	0.9369(1)	0.0248(5)
C(25)	0.3033(1)	0.1006(1)	0.5799(1)	0.0118(4)
C(26)	0.3341(1)	-0.0010(2)	0.6172(1)	0.0129(4)
C(27)	0.4105(2)	0.3351(2)	0.2617(2)	0.0267(5)
C(28)	0.4423(1)	0.2554(2)	0.3282(1)	0.0178(4)
Cu(1)	0.4558(1)	0.0882(1)	0.4761(1)	0.0144(1)
I(1)	0.4010(1)	-0.0897(1)	0.3952(1)	0.0160(1)
N(1)	0.3441(1)	0.1449(1)	0.5245(1)	0.0111(3)
N(2)	0.2867(1)	-0.0480(1)	0.6655(1)	0.0135(3)
N(3)	0.4641(1)	0.1928(1)	0.3803(1)	0.0196(4)

7.3.22 Fluoro-tri(pyrid-2-yl)phosphinoxid-kupfer(II)-dimer-bis(hexafluorophosphat) (tgn413)

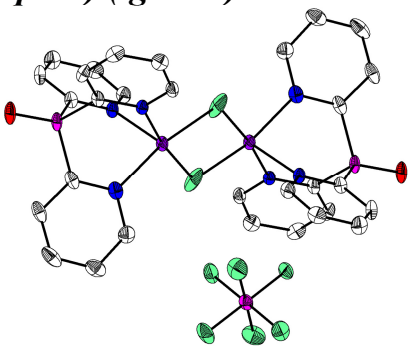

Kristalldaten

C30 H24 Cu2 F14 N6 O2 P4	M = 1017.51 g/mol	Monoclinic, $P2_1/n$
a = 10.4480(10) Å	b = 12.6833(11) Å	c = 13.7639(12) Å
α = 90°	β = 94.290(3)°	γ = 90°
V = 1818.8(3) Å^3	Z = 2	F(000) = 1012
D_{calc} = 1.858 g/cm^3	μ = 1.458 mm^{-1}	
yellow-blue plate	0.250 · 0.060 · 0.040 mm^3	

Datensammlung

Diffraktometer: D8 Quest (Bruker)	T = 100(2) K	λ = 0.71069 Å
h = -13 bis 13	k = -16 bis 14	l = -17 bis 17
14772 gemessene Reflexe	4001 unabhängige Reflexe	2890 Reflexe mit $I > 2\sigma(I)$
θ = 2.186 bis 27.123°	R_{int} = 0.0660	C (25.00°) = 0.999
Absorptionskorrektur: Multi-scan	T_{min} = 0.6320	T_{max} = 0.7455

Verfeinerung

4001 Reflexe	0 Restraints	262 Parameter
Verfeinerung mit SHELXL-2014/7	bis χ = 0.001	
R_1 ($I > 2\sigma(I)$) = 0.0422	wR_2 ($I > 2\sigma(I)$) = 0.1034	
R_1 (all) = 0.0754	wR_2 (all) = 0.1301	GoF (S) = 1.119
$\Delta\varphi_{min}$ = -0.954 e·Å^{-3}	$\Delta\varphi_{max}$ = 0.555 e·Å^{-3}	

Fraktionelle Atomkoordinaten (*x, y, z*) und äquivalente isotrope Auslenkungsfaktoren *U*(eq)

	x	*y*	*z*	*U*(eq)/Å^2
C(1)	0.7060(4)	0.2647(3)	0.1142(3)	0.0177(8)
C(2)	0.7239(4)	0.3725(3)	0.1056(3)	0.0231(9)
C(3)	0.6657(4)	0.4231(3)	0.0243(3)	0.0252(9)
C(4)	0.5934(4)	0.3642(3)	-0.0432(3)	0.0249(9)
C(5)	0.5802(4)	0.2564(3)	-0.0289(3)	0.0207(8)
C(6)	0.8617(4)	0.0816(3)	0.1636(3)	0.0211(9)
C(7)	0.9932(4)	0.0710(4)	0.1801(3)	0.0260(9)
C(8)	1.0515(4)	-0.0168(4)	0.1439(3)	0.0327(11)
C(9)	0.9786(4)	-0.0902(3)	0.0928(3)	0.0312(10)
C(10)	0.8481(4)	-0.0738(3)	0.0766(3)	0.0255(9)
C(11)	0.6532(4)	0.1304(3)	0.2764(3)	0.0165(8)
C(12)	0.6388(4)	0.1530(3)	0.3728(3)	0.0196(8)
C(13)	0.5357(4)	0.1086(3)	0.4167(3)	0.0238(9)
C(14)	0.4551(4)	0.0409(3)	0.3637(3)	0.0228(9)
C(15)	0.4778(4)	0.0186(3)	0.2682(3)	0.0200(8)
N(1)	0.6354(3)	0.2061(2)	0.0495(2)	0.0171(7)
N(2)	0.7886(3)	0.0104(3)	0.1113(2)	0.0217(7)
N(3)	0.5740(3)	0.0626(2)	0.2237(2)	0.0157(7)
O(1)	0.8665(3)	0.2578(2)	0.2839(2)	0.0275(7)
F(1)	0.5958(3)	-0.0203(2)	-0.0538(2)	0.0403(7)
F(2)	0.2664(2)	0.1611(2)	0.1807(2)	0.0371(7)
F(3)	0.3262(3)	0.2663(2)	0.0599(2)	0.0395(7)
F(4)	0.3025(2)	0.4101(2)	0.1543(2)	0.0331(6)
F(5)	0.2418(3)	0.3048(2)	0.2750(2)	0.0378(7)
F(6)	0.1382(2)	0.2949(2)	0.1251(2)	0.0361(6)
F(7)	0.4305(2)	0.2764(2)	0.2097(2)	0.0243(5)
P(1)	0.7820(1)	0.1932(1)	0.2168(1)	0.0189(2)
P(2)	0.2848(1)	0.2860(1)	0.1683(1)	0.0199(2)
Cu(1)	0.5968(1)	0.0336(1)	0.0819(1)	0.0168(2)

7.3.23 Iodo-tri(6-methylpyrid-2-yl)phosphinoxid-kupfer(I) (tgn429)

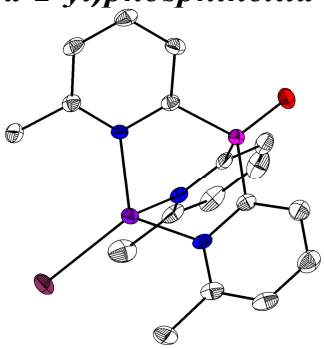

Kristalldaten

C18 H18 Cu I N3 O P	M = 513.76 g/mol	Monoclinic, $P2_1/c$
a = 13.7147(5) Å	b = 8.2314(4) Å	c = 17.4322(6) Å
α = 90°	β = 107.099(3)°	γ = 90°
V = 1880.95(13) Å^3	Z = 4	F(000) = 1008
D_{calc} = 1.814 g/cm^3	μ = 2.898 mm^{-1}	
yellow plate	0.200 · 0.120 · 0.060 mm^3	

Datensammlung

Diffraktometer: STOE IPDS 2T	T = 100(2) K	λ = 0.71069 Å
h = -17 bis 16	k = -10 bis 10	l = -22 bis 22
13832 gemessene Reflexe	3986 unabhängige Reflexe	3343 Reflexe mit $I > 2\sigma(I)$
θ = 1.553 bis 26.779°	R_{int} = 0.0581	C (25.00°) = 1.000
Absorptionskorrektur: Multi-scan	T_{min} = 0.6669	T_{max} = 0.7351

Verfeinerung

3986 Reflexe	0 Restraints	229 Parameter
Verfeinerung mit SHELXL-2014/7	bis χ = 0.001	
R_1 ($I > 2\sigma(I)$) = 0.0344	wR_2 ($I > 2\sigma(I)$) = 0.0790	
R_1 (all) = 0.0437	wR_2 (all) = 0.0805	GoF (S) = 1.306
$\Delta\varphi_{min}$ = -0.617 e·Å^{-3}	$\Delta\varphi_{max}$ = 0.907 e·Å^{-3}	

Fraktionelle Atomkoordinaten (*x, y, z*) und äquivalente isotrope Auslenkungsfaktoren *U*(eq)

	x	*y*	*z*	*U*(eq)/Å^2		*x*	*y*	*z*	*U*(eq)/Å^2
C(1)	0.7694(3)	0.7206(5)	0.0756(3)	0.0161(9)	C(13)	0.6649(3)	0.4173(5)	0.0156(3)	0.0170(9)
C(2)	0.7815(3)	0.8608(6)	0.0360(3)	0.0200(10)	C(14)	0.6146(4)	0.3612(6)	-0.0602(3)	0.0238(11)
C(3)	0.7698(3)	1.0086(6)	0.0694(3)	0.0228(10)	C(15)	0.5294(4)	0.2647(7)	-0.0688(3)	0.0330(13)
C(4)	0.7465(3)	1.0100(6)	0.1413(3)	0.0211(10)	C(16)	0.4973(4)	0.2335(6)	-0.0031(3)	0.0286(11)
C(5)	0.7336(3)	0.8644(6)	0.1779(3)	0.0181(9)	C(17)	0.5503(4)	0.2967(6)	0.0717(3)	0.0232(10)
C(6)	0.7046(4)	0.8680(6)	0.2542(3)	0.0261(11)	C(18)	0.5138(4)	0.2656(7)	0.1430(3)	0.0334(13)
C(7)	0.8794(3)	0.4097(5)	0.0952(3)	0.0166(9)	N(1)	0.7465(3)	0.7194(4)	0.1463(2)	0.0140(7)
C(8)	0.9555(4)	0.3485(6)	0.0662(3)	0.0237(10)	N(2)	0.8728(3)	0.3819(4)	0.1705(2)	0.0164(8)
C(9)	1.0299(4)	0.2514(6)	0.1165(3)	0.0289(12)	N(3)	0.6350(3)	0.3870(5)	0.0818(2)	0.0167(8)
C(10)	1.0243(4)	0.2219(6)	0.1923(3)	0.0259(11)	O(1)	0.8036(2)	0.5564(4)	-0.0499(2)	0.0237(7)
C(11)	0.9464(3)	0.2879(6)	0.2189(3)	0.0213(10)	P(1)	0.7814(1)	0.5305(1)	0.0267(1)	0.0161(2)
C(12)	0.9418(4)	0.2540(7)	0.3021(3)	0.0303(12)	Cu(1)	0.7353(1)	0.4815(1)	0.1886(1)	0.0178(1)
					I(1)	0.7077(1)	0.4392(1)	0.3248(1)	0.0301(1)

7.3.24 Triphenylarsin-tri(pyrid-2-yl)methan-kupfer(I)-hexafluorophosphat-chloroformsolvat (tgn439)

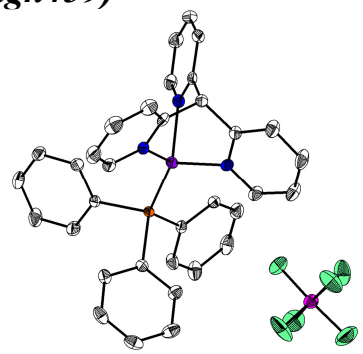

Kristalldaten

C35 H29 As Cl3 Cu F6 N3 P	M = 881.39 g/mol	Monoclinic, $P2_1$
a = 8.6252(4) Å	b = 18.9346(8) Å	c = 11.7180(5) Å
α = 90°	β = 108.000(2)°	γ = 90°
V = 1820.06(14) Å^3	Z = 2	F(000) = 884
D_{calc} = 1.608 g/cm^3	μ = 1.828 mm^{-1}	
colourless block	0.322 · 0.285 · 0.156 mm^3	

Datensammlung

Diffraktometer: D8 Quest (Bruker)	T = 100(2) K	λ = 0.71073 Å
h = -11 bis 11	k = -24 bis 24	l = -15 bis 15
55128 gemessene Reflexe	8710 unabhängige Reflexe	8222 Reflexe mit $I > 2\sigma(I)$
θ = 2.120 bis 27.967°	R_{int} = 0.0332	C (25.00°) = 1.000
Absorptionskorrektur: Multi-scan	T_{min} = 0.6630	T_{max} = 0.7456

Verfeinerung

8710 Reflexe	1 Restraints	476 Parameter
Verfeinerung mit SHELXL-2014/7	bis χ = 0.001	
R_1 ($I > 2\sigma(I)$) = 0.0232	wR_2 ($I > 2\sigma(I)$) = 0.0533	
R_1 (all) = 0.0264	wR_2 (all) = 0.0545	GoF (S) = 1.037
$\Delta\varphi_{min}$ = -0.460 e·Å^{-3}	$\Delta\varphi_{max}$ = 0.502 e·Å^{-3}	

Kommentar

Das PF_6-Anion ist über zwei Positionen fehlgeordnet. Die schwach besetzten alternativen Positionen der F-Atome wurden über EADP constrained.

Fraktionelle Atomkoordinaten (*x, y, z*) und äquivalente isotrope Auslenkungsfaktoren *U*(eq)

	x	*y*	*z*	*U*(eq)/Å^2		*x*	*y*	*z*	*U*(eq)/Å^2
C(1)	0.7124(3)	0.1645(1)	0.6087(2)	0.0169(6)	C(29)	0.8547(3)	0.3971(2)	1.0238(3)	0.0155(5)
C(2)	0.6202(3)	0.2340(2)	0.5780(2)	0.0170(5)	C(30)	0.8453(4)	0.4394(2)	1.1184(3)	0.0225(6)
C(3)	0.5405(4)	0.2525(2)	0.4606(3)	0.0275(7)	C(31)	0.9077(5)	0.5075(2)	1.1312(3)	0.0294(7)
C(4)	0.4553(5)	0.3159(2)	0.4377(3)	0.0341(8)	C(32)	0.9789(4)	0.5335(2)	1.0484(3)	0.0292(7)
C(5)	0.4517(4)	0.3587(2)	0.5320(3)	0.0296(7)	C(33)	0.9840(4)	0.4928(2)	0.9525(3)	0.0276(7)
C(6)	0.5359(4)	0.3372(2)	0.6464(3)	0.0232(6)	C(34)	0.9214(4)	0.4245(2)	0.9394(3)	0.0205(6)
C(7)	0.8959(4)	0.1760(1)	0.6654(2)	0.0164(5)	C(35)	-0.0246(4)	0.4502(2)	0.5829(3)	0.0269(7)
C(8)	1.0049(4)	0.1510(2)	0.6099(3)	0.0235(7)	N(1)	0.6197(3)	0.2765(1)	0.6700(2)	0.0171(5)
C(9)	1.1704(4)	0.1632(2)	0.6639(3)	0.0282(7)	N(2)	0.9445(3)	0.2112(1)	0.7702(2)	0.0180(5)
C(10)	1.2209(4)	0.1997(2)	0.7705(3)	0.0274(7)	N(3)	0.6553(3)	0.1423(1)	0.7982(2)	0.0178(5)
C(11)	1.1040(4)	0.2227(2)	0.8212(3)	0.0227(6)	F(1)	0.3209(3)	0.5166(2)	0.6122(2)	0.0453(8)
C(12)	0.6437(3)	0.1181(1)	0.6878(3)	0.0173(6)	F(2)	0.2870(4)	0.5142(2)	0.7964(3)	0.0570(10)
C(13)	0.5709(4)	0.0532(2)	0.6467(3)	0.0267(7)	F(3)	0.2885(4)	0.6179(2)	0.6977(3)	0.0582(9)
C(14)	0.5104(4)	0.0132(2)	0.7215(4)	0.0337(8)	F(4)	0.5321(3)	0.5896(2)	0.6789(3)	0.0464(8)
C(15)	0.5219(4)	0.0379(2)	0.8343(4)	0.0322(8)	F(5)	0.5349(4)	0.4891(1)	0.7783(3)	0.0489(8)
C(16)	0.5954(4)	0.1024(2)	0.8694(3)	0.0240(7)	F(6)	0.4975(4)	0.5898(2)	0.8637(2)	0.0491(8)
C(17)	0.9154(3)	0.2536(1)	1.1486(2)	0.0154(5)	F(11)	0.504(2)	0.5138(9)	0.6760(18)	0.056(3)
C(18)	0.9398(4)	0.2778(2)	1.2649(3)	0.0265(7)	F(12)	0.247(2)	0.5695(10)	0.6426(18)	0.056(3)
C(19)	1.0463(4)	0.2424(2)	1.3614(3)	0.0310(7)	F(13)	0.327(2)	0.4701(10)	0.7566(19)	0.056(3)
C(20)	1.1266(4)	0.1826(2)	1.3418(3)	0.0250(7)	F(14)	0.551(2)	0.5316(9)	0.8609(18)	0.056(3)
C(21)	1.1018(4)	0.1575(2)	1.2277(3)	0.0233(6)	F(15)	0.479(2)	0.6221(10)	0.7350(19)	0.056(3)
C(22)	0.9956(4)	0.1932(2)	1.1310(3)	0.0191(6)	F(16)	0.300(2)	0.5847(9)	0.8260(17)	0.056(3)
C(23)	0.5757(3)	0.3119(1)	1.0442(2)	0.0158(5)	P(1)	0.4091(1)	0.5517(1)	0.7407(1)	0.0225(2)
C(24)	0.5269(4)	0.2612(2)	1.1119(3)	0.0200(6)	Cu(1)	0.7584(1)	0.2416(1)	0.8346(1)	0.0165(1)
C(25)	0.3787(4)	0.2697(2)	1.1352(3)	0.0258(7)	As(1)	0.7771(1)	0.3002(1)	1.0062(1)	0.0132(1)
C(26)	0.2827(4)	0.3280(2)	1.0919(3)	0.0273(7)	Cl(1)	-0.0330(1)	0.4540(1)	0.4314(1)	0.0430(2)
C(27)	0.3296(4)	0.3773(2)	1.0219(3)	0.0279(7)	Cl(2)	-0.2013(1)	0.4866(1)	0.6046(1)	0.0416(2)
C(28)	0.4763(4)	0.3692(2)	0.9975(3)	0.0217(6)	Cl(3)	-0.0017(2)	0.3629(1)	0.6335(1)	0.0687(4)

7.3.25 Tri(pyrid-2-yl)methan-tris(6-methylpyrid-2-yl)phoshin-kupfer(I)-hexafluorophosphat-acetonitrilsolvat (tgn442)

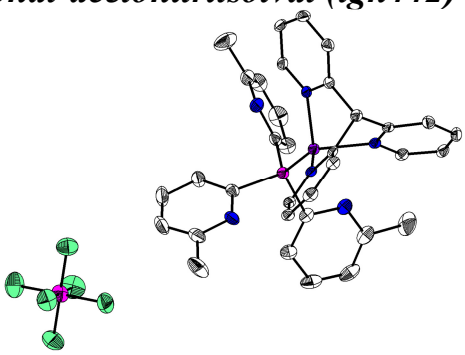

Kristalldaten

C35 H32.50 Cu F6 N6.50 P2	M = 783.65 g/mol	Trigonal, $R\bar{3}$
a = 11.9033(13) Å	b = 11.9033 Å	c = 42.764(5) Å
α = 90°	β = 90°	γ = 120°
V = 5247.4(13) Å^3	Z = 6	F(000) = 2406
D_{calc} = 1.488 g/cm^3	μ = 0.784 mm^{-1}	
colourless block	0.226 · 0.184 · 0.091 mm^3	

Datensammlung

Diffraktometer: D8 Quest (Bruker)	T = 100(2) K	λ = 0.71073 Å
h = -14 bis 13	k = -8 bis 14	l = -54 bis 30
4795 gemessene Reflexe	2483 unabhängige Reflexe	1934 Reflexe mit $I > 2\sigma(I)$
θ = 2.745 bis 27.085°	R_{int} = 0.0241	C (25.00°) = 0.972
Absorptionskorrektur: Multi-scan	T_{min} = 0.6783	T_{max} = 0.7455

Verfeinerung

2483 Reflexe	3 Restraints	154 Parameter
Verfeinerung mit SHELXL-2014/7	bis χ = 0.000	
R_1 ($I > 2\sigma(I)$) = 0.0394	wR_2 ($I > 2\sigma(I)$) = 0.0893	
R_1 (all) = 0.0590	wR_2 (all) = 0.0973	GoF (S) = 1.023
$\Delta\varphi_{min}$ = -0.651 e·Å^{-3}	$\Delta\varphi_{max}$ = 0.508 e·Å^{-3}	

Kommentar

Das Acetonitrilmolekül ist über ein Inversionszentrum auf einer dreizähligen Achse fehlgeordnet. Es wurde über DFIX und DANG re- sowie über EADP constrained.

Fraktionelle Atomkoordinaten (*x, y, z*) und äquivalente isotrope Auslenkungsfaktoren *U*(eq)

	x	*y*	*z*	*U*(eq)/Å^2		*x*	*y*	*z*	*U*(eq)/Å^2
C(1)	1.0000	1.0000	0.2016(1)	0.0171(8)	C(12)	0.5451(3)	0.6257(3)	0.0716(1)	0.0518(9)
C(2)	1.1229(2)	1.0009(2)	0.1910(1)	0.0158(5)	C(13)	0.3333	0.6667	0.1307(2)	0.100(3)
C(3)	1.2095(2)	1.0000(2)	0.2125(1)	0.0201(5)	C(14)	0.3333	0.6667	0.1667	0.100(3)
C(4)	1.3180(2)	0.9980(2)	0.2018(1)	0.0231(5)	N(1)	1.1424(2)	1.0022(2)	0.1599(1)	0.0155(4)
C(5)	1.3376(2)	0.9980(2)	0.1699(1)	0.0205(5)	N(2)	0.7555(2)	0.8203(2)	0.0732(1)	0.0250(5)
C(6)	1.2485(2)	1.0012(2)	0.1497(1)	0.0182(5)	N(3)	0.3333	0.6667	0.1938(2)	0.100(3)
C(7)	0.8421(2)	0.9405(2)	0.0630(1)	0.0204(5)	F(1)	0.2557(2)	0.7137(2)	-0.0560(1)	0.0555(5)
C(8)	0.8123(3)	1.0073(3)	0.0411(1)	0.0296(6)	F(2)	0.3823(2)	0.7926(2)	-0.0130(1)	0.0441(5)
C(9)	0.6867(3)	0.9457(3)	0.0290(1)	0.0387(7)	P(1)	1.0000	1.0000	0.0817(1)	0.0171(2)
C(10)	0.5996(3)	0.8217(3)	0.0386(1)	0.0363(7)	P(2)	0.3333	0.6667	-0.0344(1)	0.0309(3)
C(11)	0.6364(3)	0.7615(3)	0.0607(1)	0.0311(6)	Cu(1)	1.0000	1.0000	0.1320(1)	0.0154(2)

7.3.26 Tricarbonyl-tris(3,4,5-trimethylimidazol-2-yl)phosphin-wolfram(0)-acetonitrilsolvat (tgn456)

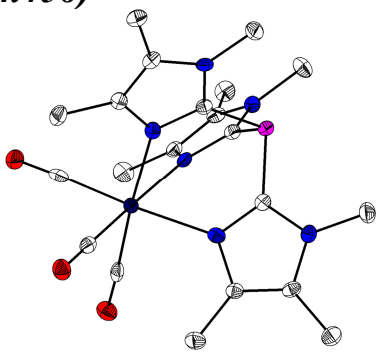

Kristalldaten

C22 H28.50 N6.50 O3 P W	M = 646.83 g/mol	Trigonal, $P\bar{3}$
a = 13.4712(7) Å	b = 13.4712(7) Å	c = 8.6622(5) Å
α = 90°	β = 90°	γ = 120°
V = 1361.35(16) Å^3	Z = 2	F(000) = 638
D_{calc} = 1.578 g/cm^3	μ = 4.335 mm^{-1}	
yellow needle	0.357 · 0.068 · 0.063 mm^3	

Datensammlung

Diffraktometer: STOE IPDS 2T	T = 100(2) K	λ = 0.71073 Å
h = -10 bis 17	k = -16 bis 17	l = -9 bis 10
3927 gemessene Reflexe	1918 unabhängige Reflexe	1700 Reflexe mit $I > 2\sigma(I)$
θ = 1.746 bis 26.719°	R_{int} = 0.0290	C (25.00°) = 1.000
Absorptionskorrektur: Multi-scan	T_{min} = 0.2991	T_{max} = 0.7038

Verfeinerung

1918 Reflexe	21 Restraints	113 Parameter
Verfeinerung mit SHELXL-2014/7	bis χ = 0.000	
R_1 ($I > 2\sigma(I)$) = 0.0234	wR_2 ($I > 2\sigma(I)$) = 0.0613	
R_1 (all) = 0.0290	wR_2 (all) = 0.0621	GoF (S) = 0.958
$\Delta\varphi_{min}$ = -1.668 e·Å^{-3}	$\Delta\varphi_{max}$ = 0.795 e·Å^{-3}	

Kommentar

Die Struktur wurde als meroedrischer Zwilling verfeinert. Das Acetonitrilmolekül ist entlang einer dreizähligen Achse über ein Inversionszentrum fehlgeordnet. Es wurde über DFIX, DANG und ISOR re- sowie mittels EADP constrained.

Fraktionelle Atomkoordinaten (*x, y, z*) und äquivalente isotrope Auslenkungsfaktoren *U*(eq)

	x	y	z	U(eq)/Å^2
W(1)	0.3333	0.6667	0.7512(1)	0.0132(1)
P(1)	0.3333	0.6667	0.3237(2)	0.0133(4)
O(1)	0.5226(3)	0.6807(4)	0.9718(4)	0.0223(8)
N(1)	0.4546(5)	0.7988(5)	0.5814(5)	0.0148(11)
N(2)	0.5368(4)	0.8766(3)	0.3578(5)	0.0147(8)
C(1)	0.4460(4)	0.7868(4)	0.4275(5)	0.0143(9)
C(2)	0.6065(4)	0.9504(4)	0.4701(6)	0.0156(10)
C(3)	0.5568(4)	0.9030(4)	0.6088(6)	0.0154(10)
C(4)	0.5592(5)	0.8905(5)	0.1907(5)	0.0216(10)
C(5)	0.7154(5)	1.0589(4)	0.4343(6)	0.0216(11)
C(6)	0.5977(5)	0.9463(5)	0.7677(6)	0.0225(11)
C(7)	0.4539(6)	0.6766(6)	0.8871(6)	0.0168(13)
C(8)	0.819(4)	0.869(4)	-0.013(4)	0.058(7)
C(9)	0.841(4)	0.900(4)	0.160(4)	0.058(7)
N(3)	0.867(3)	0.905(3)	0.288(4)	0.058(7)

7.3.27 Bis(tripyrid-2-yl)methan-kupfer(II)-bis(tetraphenylborat)-chloroformsolvat (tgn458)

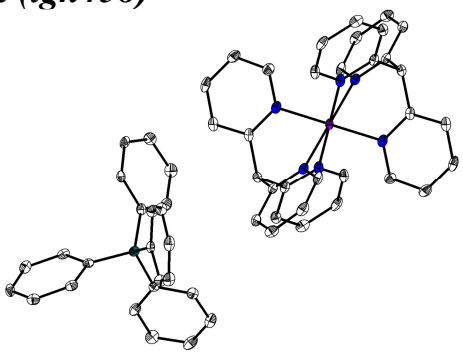

Kristalldaten

C82 H68 B2 Cl6 Cu N6	M = 1435.28 g/mol	Orthorhombic, *Pbca*
a = 16.8383(7) Å	b = 18.0912(6) Å	c = 22.0674(9) Å
α = 90°	β = 90°	γ = 90°
V = 6722.3(5) Å^3	Z = 4	F(000) = 2972
D_{calc} = 1.418 g/cm^3	μ = 0.617 mm^{-1}	
colourless block	0.098 · 0.093 · 0.058 mm^3	

Datensammlung

Diffraktometer: D8 Quest (Bruker)	T = 100(2) K	λ = 0.71069 Å
h = -19 bis 23	k = -21 bis 21	l = -28 bis 27
38435 gemessene Reflexe	7430 unabhängige Reflexe	5289 Reflexe mit $I > 2\sigma(I)$
θ = 2.433 bis 29.220°	R_{int} = 0.0931	C (25.00°) = 0.999
Absorptionskorrektur: Multi-scan	T_{min} = 0.6897	T_{max} = 0.7455

Verfeinerung

7430 Reflexe	0 Restraints	439 Parameter
Verfeinerung mit SHELXL-2014/7	bis χ = 0.001	
R_1 ($I > 2\sigma(I)$) = 0.0490	wR_2 ($I > 2\sigma(I)$) = 0.1115	
R_1 (all) = 0.0827	wR_2 (all) = 0.1257	GoF (S) = 1.013
$\Delta\varphi_{min}$ = -0.477 e·Å^{-3}	$\Delta\varphi_{max}$ = 0.588 e·Å^{-3}	

Fraktionelle Atomkoordinaten (*x, y, z*) und äquivalente isotrope Auslenkungsfaktoren *U*(eq)

	x	*y*	*z*	*U*(eq)/Å^2		*x*	*y*	*z*	*U*(eq)/Å^2
C(1)	0.5504(1)	0.6607(2)	-0.0566(1)	0.0122(5)	C(24)	0.4258(2)	-0.0168(2)	0.2492(1)	0.0159(6)
C(2)	0.5942(1)	0.6581(2)	0.0027(1)	0.0122(5)	C(25)	0.4139(2)	-0.0746(2)	0.2936(1)	0.0171(6)
C(3)	0.6371(1)	0.7217(2)	0.0214(1)	0.0154(6)	C(26)	0.3453(2)	-0.0825(2)	0.3205(1)	0.0176(6)
C(4)	0.6739(1)	0.7158(2)	0.0761(1)	0.0180(6)	C(27)	0.2887(2)	-0.0311(2)	0.3027(1)	0.0177(6)
C(5)	0.6679(1)	0.6471(2)	0.1096(1)	0.0170(6)	C(28)	0.3012(1)	0.0256(2)	0.2579(1)	0.0145(6)
C(6)	0.6231(2)	0.5871(2)	0.0884(1)	0.0169(6)	C(29)	0.3269(1)	0.1737(2)	0.1802(1)	0.0133(6)
C(7)	0.5696(1)	0.5928(2)	-0.0982(1)	0.0121(5)	C(30)	0.2786(2)	0.2011(2)	0.1356(1)	0.0175(6)
C(8)	0.6073(1)	0.6066(2)	-0.1520(1)	0.0159(6)	C(31)	0.2308(2)	0.2650(2)	0.1446(1)	0.0201(6)
C(9)	0.6228(2)	0.5437(2)	-0.1898(1)	0.0194(6)	C(32)	0.2286(2)	0.3034(2)	0.1998(1)	0.0191(6)
C(10)	0.5998(2)	0.4680(2)	-0.1741(1)	0.0203(6)	C(33)	0.2762(2)	0.2778(2)	0.2457(1)	0.0161(6)
C(11)	0.5633(2)	0.4587(2)	-0.1196(1)	0.0182(6)	C(34)	0.3237(1)	0.2151(2)	0.2355(1)	0.0143(6)
C(12)	0.4680(1)	0.6640(2)	-0.0424(1)	0.0112(5)	C(35)	0.4695(2)	0.1228(2)	0.1689(1)	0.0137(5)
C(13)	0.4284(2)	0.7331(2)	-0.0523(1)	0.0143(6)	C(36)	0.5232(2)	0.0743(2)	0.1410(1)	0.0171(6)
C(14)	0.3543(2)	0.7349(2)	-0.0365(1)	0.0186(6)	C(37)	0.5989(2)	0.0887(2)	0.1455(1)	0.0200(6)
C(15)	0.3216(2)	0.6669(2)	-0.0138(1)	0.0183(6)	C(38)	0.6246(2)	0.1535(2)	0.1777(1)	0.0194(6)
C(16)	0.3639(1)	0.6001(2)	-0.0056(1)	0.0161(6)	C(39)	0.5739(2)	0.2044(2)	0.2046(1)	0.0181(6)
C(17)	0.3564(1)	0.0497(2)	0.1087(1)	0.0132(5)	C(40)	0.4982(2)	0.1893(2)	0.1998(1)	0.0166(6)
C(18)	0.3822(2)	0.0721(2)	0.0513(1)	0.0162(6)	C(41)	0.4839(2)	0.8442(2)	0.1331(2)	0.0271(7)
C(19)	0.3565(2)	0.0382(2)	-0.0021(1)	0.0211(6)	N(1)	0.5487(1)	0.5190(1)	-0.0822(1)	0.0138(5)
C(20)	0.3033(2)	-0.0213(2)	-0.0002(1)	0.0217(6)	N(2)	0.5860(1)	0.5918(1)	0.0358(1)	0.0140(5)
C(21)	0.2764(2)	-0.0458(2)	0.0558(1)	0.0195(6)	N(3)	0.4369(1)	0.5985(1)	-0.0188(1)	0.0122(5)
C(22)	0.3028(2)	-0.0105(2)	0.1085(1)	0.0169(6)	Cu(1)	0.5000	0.5000	0.0000	0.0110(1)
C(23)	0.3701(1)	0.0346(2)	0.2288(1)	0.0124(5)	Cl(1)	0.5728(1)	0.8665(1)	0.1619(1)	0.0327(2)

	x	y	z	U(eq)/Å^2
Cl(2)	0.4739(1)	0.8763(1)	0.0583(1)	0.0318(2)

	x	y	z	U(eq)/Å^2
Cl(3)	0.4701(1)	0.7407(1)	0.1374(1)	0.0491(3)
B(1)	0.3817(2)	0.0962(2)	0.1711(1)	0.0128(6)

7.3.28 Triphenylphosphin-tri(pyrid-2-yl)arsin-kupfer(I)-hexafluorophosphat-chloroformsolvat (tgn475)

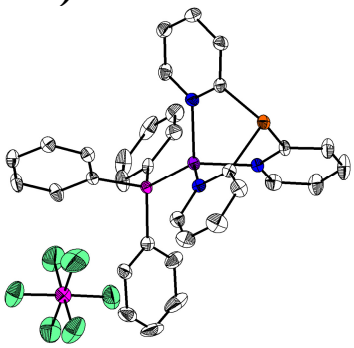

Kristalldaten

C34 H28 As Cl3 Cu F6 N3 P2	M = 899.34 g/mol	Monoclinic, $P2_1$
a = 8.5576(4) Å	b = 19.0028(10) Å	c = 11.3590(6) Å
α = 90°	β = 99.702(2)°	γ = 90°
V = 1820.76(16) Å^3	Z = 2	F(000) = 900
D_{calc} = 1.640 g/cm^3	μ = 1.871 mm^{-1}	
colourless plate	0.455 · 0.159 · 0.070 mm^3	

Datensammlung

Diffraktometer: D8 Quest (Bruker)	T = 115(2) K	λ = 0.71073 Å
h = -10 bis 10	k = -24 bis 24	l = -14 bis 14
26522 gemessene Reflexe	8034 unabhängige Reflexe	6924 Reflexe mit $I > 2\sigma(I)$
θ = 2.143 bis 27.134°	R_{int} = 0.0512	C (25.00°) = 0.998
Absorptionskorrektur: Multi-scan	T_{min} = 0.6471	T_{max} = 0.7455

Verfeinerung

8034 Reflexe	1 Restraints	471 Parameter
Verfeinerung mit SHELXL-2014/7	bis χ = 0.001	
R_1 ($I > 2\sigma(I)$) = 0.0350	wR_2 ($I > 2\sigma(I)$) = 0.0722	
R_1 (all) = 0.0480	wR_2 (all) = 0.0758	GoF (S) = 1.042
$\Delta\varphi_{min}$ = -0.387 e·Å^{-3}	$\Delta\varphi_{max}$ = 0.728 e·Å^{-3}	

Kommentar

Das PF_6-Anion ist über zwei Positionen fehlgeordnet. Einzelne Atome wurde über EADP constrained.

Fraktionelle Atomkoordinaten (*x, y, z*) und äquivalente isotrope Auslenkungsfaktoren *U*(eq)

	x	y	z	U(eq)/Å^2
C(1)	0.1821(6)	1.0391(3)	0.0764(4)	0.0195(10)
C(2)	0.1094(7)	1.0606(3)	-0.0356(5)	0.0309(14)
C(3)	0.0251(9)	1.1237(3)	-0.0467(6)	0.0397(17)
C(4)	0.0173(8)	1.1631(3)	0.0555(6)	0.0337(15)
C(5)	0.0940(7)	1.1373(3)	0.1632(5)	0.0274(13)
C(6)	0.4947(6)	0.9781(2)	0.1855(4)	0.0189(11)
C(7)	0.6335(6)	0.9602(3)	0.1442(5)	0.0238(12)
C(8)	0.7771(7)	0.9844(3)	0.2035(5)	0.0285(13)
C(9)	0.7819(7)	1.0263(3)	0.3060(5)	0.0273(12)
C(10)	0.6397(6)	1.0396(3)	0.3419(5)	0.0253(11)
C(11)	0.1841(6)	0.9072(2)	0.2113(5)	0.0186(11)
C(12)	0.0994(7)	0.8460(3)	0.1826(5)	0.0270(12)
C(13)	0.0157(8)	0.8169(3)	0.2644(6)	0.0357(15)

	x	y	z	U(eq)/Å^2
C(14)	0.0190(7)	0.8497(3)	0.3726(6)	0.0311(13)
C(15)	0.1057(6)	0.9112(3)	0.3956(5)	0.0239(12)
C(16)	0.3693(6)	1.1866(3)	0.5089(5)	0.0188(10)
C(17)	0.4409(6)	1.2085(3)	0.4141(6)	0.0274(13)
C(18)	0.5108(7)	1.2746(3)	0.4141(6)	0.0366(15)
C(19)	0.5103(8)	1.3185(3)	0.5112(7)	0.0412(17)
C(20)	0.4344(9)	1.2994(3)	0.6041(6)	0.0418(18)
C(21)	0.3657(8)	1.2334(3)	0.6044(5)	0.0316(14)
C(22)	0.4061(6)	1.0538(2)	0.6345(4)	0.0154(10)
C(23)	0.4888(6)	0.9936(3)	0.6115(5)	0.0204(11)
C(24)	0.5857(6)	0.9580(3)	0.7019(5)	0.0231(11)
C(25)	0.6013(7)	0.9833(3)	0.8182(5)	0.0270(12)
C(26)	0.5178(7)	1.0422(3)	0.8433(5)	0.0319(13)

	x	y	z	U(eq)/Å^2
C(27)	0.4201(7)	1.0770(3)	0.7522(5)	0.0257(12)
C(28)	0.0977(6)	1.1119(3)	0.5541(5)	0.0198(11)
C(29)	0.0038(7)	1.1695(3)	0.5104(6)	0.0303(14)
C(30)	-0.1423(7)	1.1794(4)	0.5423(7)	0.0456(19)
C(31)	-0.1979(7)	1.1318(4)	0.6177(7)	0.049(2)
C(32)	-0.1102(7)	1.0731(4)	0.6572(6)	0.0395(16)
C(33)	0.0376(7)	1.0628(3)	0.6263(5)	0.0265(12)
N(1)	0.1743(5)	1.0771(2)	0.1761(4)	0.0177(9)
N(2)	0.4983(5)	1.0173(2)	0.2849(4)	0.0201(9)
N(3)	0.1865(5)	0.9402(2)	0.3165(4)	0.0179(9)
F(1)	-0.0441(5)	0.8918(2)	0.6372(4)	0.0510(10)
F(2)	0.1298(10)	0.8028(5)	0.6822(6)	0.079(3)
F(3)	-0.1011(9)	0.7992(4)	0.7424(8)	0.061(2)
F(4)	-0.0496(10)	0.9052(4)	0.8346(5)	0.058(2)

	x	y	z	U(eq)/Å^2
F(5)	0.1841(8)	0.9069(5)	0.7684(6)	0.066(3)
F(4A)	0.012(5)	0.920(2)	0.812(5)	0.075(8)
F(5A)	0.213(4)	0.869(2)	0.737(4)	0.075(8)
F(3A)	-0.117(6)	0.822(3)	0.773(5)	0.075(8)
F(2A)	0.059(5)	0.780(2)	0.698(4)	0.075(8)
F(6)	0.1212(5)	0.8157(2)	0.8795(4)	0.0504(11)
P(1)	0.2876(2)	1.0979(1)	0.5065(1)	0.0153(3)
P(2)	0.0400(2)	0.8534(1)	0.7570(1)	0.0261(3)
Cu(1)	0.2846(1)	1.0403(1)	0.3392(1)	0.0173(1)
As(1)	0.2938(1)	0.9475(1)	0.0875(1)	0.0190(1)
C(34)	0.5397(8)	0.2573(3)	1.0573(6)	0.0399(16)
Cl(1)	0.5525(3)	0.2541(1)	0.9046(2)	0.0611(6)
Cl(2)	0.3530(2)	0.2894(1)	1.0786(2)	0.0621(6)
Cl(3)	0.5744(3)	0.1738(1)	1.1212(2)	0.0707(7)

7.3.29 Iodo-tri(pyrid-2-yl)arsin-kupfer(I)-dimer (tgv45f5)

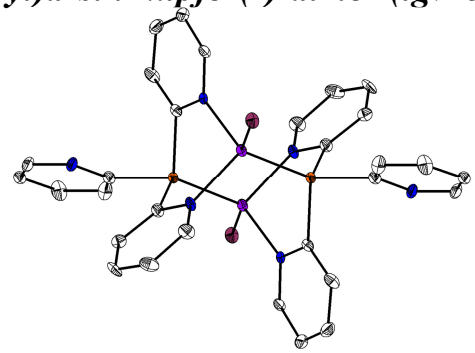

Kristalldaten

C32 H26 As2 Cl6 Cu2 I2 N6	M = 1238.01 g/mol	Triclinic, $P\bar{1}$
a = 8.6167(14) Å	b = 9.0560(16) Å	c = 13.394(2) Å
α = 88.437(7)°	β = 74.290(6)°	γ = 87.948(5)°
V = 1005.4(3) Å^3	Z = 1	F(000) = 592
D_{calc} = 2.045 g/cm^3	μ = 4.658 mm^{-1}	
colourless plate	0.193 · 0.138 · 0.064 mm^3	

Datensammlung

Diffraktometer: D8 Quest (Bruker)	T = 100(2) K	λ = 0.71069 Å
h = -10 bis 11	k = -11 bis 11	l = 0 bis 17
3947 gemessene Reflexe	3947 unabhängige Reflexe	3666 Reflexe mit $I > 2\sigma(I)$
θ = 2.726 bis 27.113°	R_{int} = -(hklf5)	C (25.00°) = 0.950
Absorptionskorrektur: Multi-scan	T_{min} = 0.5954	T_{max} = 0.7455

Verfeinerung

3947 Reflexe	0 Restraints	215 Parameter
Verfeinerung mit SHELXL-2014/7	bis χ = 0.001	
R_1 ($I > 2\sigma(I)$) = 0.0391	wR_2 ($I > 2\sigma(I)$) = 0.0916	
R_1 (all) = 0.0469	wR_2 (all) = 0.0962	GoF (S) = 1.141
$\Delta\varphi_{min}$ = -0.907 e·Å^{-3}	$\Delta\varphi_{max}$ = 0.869 e·Å^{-3}	

Kommentar

Die Struktur wurde als nicht-meroedrischer Zwilling integriert und verfeinert.

Fraktionelle Atomkoordinaten (*x, y, z*) und äquivalente isotrope Auslenkungsfaktoren *U*(eq)

	x	*y*	*z*	*U*(eq)/Å^2
C(2)	-0.0360(8)	0.7328(9)	0.5798(5)	0.0102(14)
C(3)	-0.1016(9)	0.6356(10)	0.6630(6)	0.0155(16)
C(4)	-0.2112(9)	0.5333(9)	0.6516(6)	0.0178(17)
C(5)	-0.2488(10)	0.5267(9)	0.5578(6)	0.0183(17)
C(6)	-0.1776(8)	0.6234(9)	0.4781(6)	0.0118(15)
C(7)	0.2879(9)	0.8632(9)	0.4667(6)	0.0141(9)
C(8)	0.4450(9)	0.8422(9)	0.4686(6)	0.0145(16)
C(9)	0.5658(9)	0.8527(10)	0.3751(6)	0.0175(17)
C(10)	0.5224(9)	0.8816(10)	0.2841(6)	0.0211(18)
C(11)	0.3617(10)	0.8977(10)	0.2879(6)	0.0184(17)
C(12)	0.2085(9)	0.7765(9)	0.6931(6)	0.0141(9)
C(13)	0.1966(10)	0.8391(10)	0.7882(6)	0.0194(17)
C(14)	0.2678(10)	0.7623(10)	0.8574(6)	0.0206(18)
C(15)	0.3458(9)	0.6290(9)	0.8281(6)	0.0141(9)
C(16)	0.3482(9)	0.5748(9)	0.7309(6)	0.0172(16)
C(17)	0.7313(10)	0.7271(10)	1.0134(7)	0.0223(19)
N(1)	-0.0782(7)	0.7296(7)	0.4899(5)	0.0105(13)
N(2)	0.2439(7)	0.8864(7)	0.3785(5)	0.0113(13)
N(3)	0.2810(8)	0.6471(7)	0.6638(5)	0.0157(14)
Cu(1)	-0.0076(1)	1.1181(1)	0.6265(1)	0.0109(2)
As(1)	0.1108(1)	0.8821(1)	0.5950(1)	0.0096(2)
I(1)	-0.0108(1)	1.2360(1)	0.8026(1)	0.0155(1)
Cl(1)	0.8235(3)	0.5764(3)	0.9387(2)	0.0286(5)
Cl(2)	0.7908(3)	0.8966(3)	0.9487(2)	0.0359(6)
Cl(3)	0.5184(3)	0.7153(3)	1.0475(2)	0.0275(5)

7.3.30 Iodo-tris(3,5-dimethylpyrazol-1-yl)phosphinsulfid-kupfer(I)-dimer (tgv79)

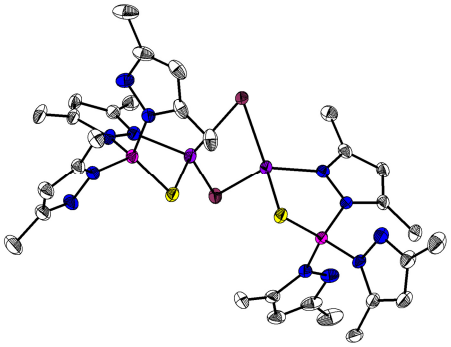

Kristalldaten

C15 H21 Cu I N6 P S	*M* = 538.85 g/mol	Orthorhombic, *Fdd*2
a = 21.0009(7) Å	*b* = 30.1898(11) Å	*c* = 13.3392(7) Å
α = 90°	β = 90°	γ = 90°
V = 8457.2(6) Å^3	*Z* = 16	*F*(000) = 4256
D_{calc} = 1.693 g/cm^3	μ = 2.678 mm^{-1}	
colourless block	0.260 · 0.210 · 0.150 mm^3	

Datensammlung

Diffraktometer: STOE IPDS 2	*T* = 100(2) K	λ = 0.71069 Å
h = -24 bis 26	*k* = -38 bis 37	*l* = -16 bis 16
17662 gemessene Reflexe	4477 unabhängige Reflexe	4248 Reflexe mit $I > 2\sigma(I)$
θ = 1.930 bis 26.681°	R_{int} = 0.0798	*C* (25.00°) = 1.000
Absorptionskorrektur: Multi-scan	T_{min} = 0.4945	T_{max} = 0.6587

Verfeinerung

4477 Reflexe	1 Restraints	232 Parameter
Verfeinerung mit SHELXL-2014/7	bis χ = 0.001	
R_1 ($I > 2\sigma(I)$) = 0.0223	wR_2 ($I > 2\sigma(I)$) = 0.0580	
R_1 (all) = 0.0240	wR_2 (all) = 0.0584	GoF (S) = 0.984
$\Delta\varphi_{min}$ = -0.341 e·Å^{-3}	$\Delta\varphi_{max}$ = 0.618 e·Å^{-3}	

Fraktionelle Atomkoordinaten (*x, y, z*) und äquivalente isotrope Auslenkungsfaktoren *U*(eq)

	x	*y*	*z*	*U*(eq)/Å^2
C(1)	0.9730(3)	0.1174(2)	0.3184(5)	0.0331(12)
C(2)	1.0170(3)	0.1492(2)	0.2824(5)	0.0337(13)
C(3)	1.0041(3)	0.1879(2)	0.3304(4)	0.0263(11)
C(4)	0.9656(4)	0.0701(2)	0.2864(6)	0.0493(18)
C(5)	1.0334(3)	0.2325(2)	0.3160(5)	0.0326(12)
C(6)	1.0272(3)	0.2950(2)	0.5501(4)	0.0343(13)

	x	*y*	*z*	*U*(eq)/Å^2
C(7)	0.9899(3)	0.3231(2)	0.4905(5)	0.0350(13)
C(8)	0.9408(3)	0.2985(2)	0.4534(4)	0.0289(12)
C(9)	1.0878(3)	0.3052(2)	0.6055(5)	0.0483(17)
C(10)	0.8890(3)	0.3114(2)	0.3844(5)	0.0376(13)
C(11)	0.8985(2)	0.1699(2)	0.7417(4)	0.0237(10)
C(12)	0.9596(2)	0.1515(2)	0.7246(4)	0.0256(10)
C(13)	0.9748(2)	0.1592(2)	0.6269(4)	0.0252(10)
C(14)	0.8598(3)	0.1709(2)	0.8346(4)	0.0287(11)
C(15)	1.0336(3)	0.1471(2)	0.5709(5)	0.0334(12)

	x	*y*	*z*	*U*(eq)/Å^2
N(1)	0.9545(2)	0.1788(1)	0.3955(3)	0.0233(9)
N(2)	0.9346(2)	0.1345(1)	0.3870(4)	0.0302(10)
N(3)	0.9497(2)	0.2561(1)	0.4918(3)	0.0224(8)
N(4)	1.0044(2)	0.2542(2)	0.5525(3)	0.0293(9)
N(5)	0.9225(2)	0.1808(1)	0.5862(3)	0.0219(8)
N(6)	0.8760(2)	0.1877(1)	0.6581(3)	0.0214(9)
P(1)	0.9102(1)	0.2082(1)	0.4766(1)	0.0199(2)
S(1)	0.8218(1)	0.2139(1)	0.4429(1)	0.0240(2)
Cu(1)	0.7979(1)	0.2233(1)	0.6212(1)	0.0224(1)
I(1)	0.6885(1)	0.1929(1)	0.6776(1)	0.0237(1)

7.3.31 Iodo-tris(3,5-dimethyl-pyrazol-1-yl)phosphinoxid-kupfer(I)-acetonitrilsolvat (tgv99)

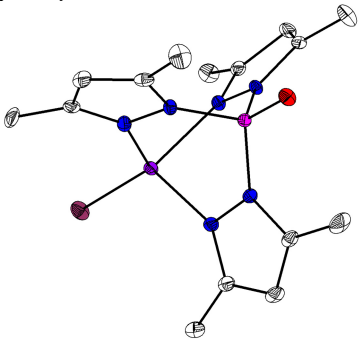

Kristalldaten

C17 H24 Cu I N7 O P	M = 563.84 g/mol	Monoclinic, $P2_1/n$
a = 7.749(2) Å	b = 21.684(5) Å	c = 13.125(3) Å
α = 90°	β = 90.192(9)°	γ = 90°
V = 2205.5(10) Å^3	Z = 4	F(000) = 1120
D_{calc} = 1.698 g/cm^3	μ = 2.485 mm^{-1}	
colourless block	0.430 · 0.190 · 0.170 mm^3	

Datensammlung

Diffraktometer: D8 Quest (Bruker)	T = 100(2) K	λ = 0.71069 Å
h = -8 bis 9	k = -25 bis 25	l = -15 bis 15
35711 gemessene Reflexe	3966 unabhängige Reflexe	3581 Reflexe mit $I > 2\sigma(I)$
θ = 2.436 bis 25.179°	R_{int} = 0.0682	C (25.00°) = 0.999
Absorptionskorrektur: Multi-scan	T_{min} = 0.5329	T_{max} = 0.7453

Verfeinerung

3966 Reflexe	0 Restraints	260 Parameter
Verfeinerung mit SHELXL-2014/7	bis χ = 0.002	
R_1 ($I > 2\sigma(I)$) = 0.0260	wR_2 ($I > 2\sigma(I)$) = 0.0631	
R_1 (all) = 0.0307	wR_2 (all) = 0.0653	GoF (S) = 1.047
$\Delta\varphi_{min}$ = -0.569 e·Å^{-3}	$\Delta\varphi_{max}$ = 0.995 e·Å^{-3}	

Fraktionelle Atomkoordinaten (*x, y, z*) und äquivalente isotrope Auslenkungsfaktoren *U*(eq)

	x	*y*	*z*	*U*(eq)/Å^2
I(1)	0.1725(1)	0.3989(1)	0.0789(1)	0.0160(1)
Cu(1)	0.2003(1)	0.2852(1)	0.0707(1)	0.0105(1)
P(1)	0.2171(1)	0.1363(1)	0.0626(1)	0.0090(2)
O(1)	0.2278(2)	0.0696(1)	0.0567(1)	0.0140(4)
N(5)	0.3127(3)	0.1711(1)	-0.0376(2)	0.0095(4)
N(2)	-0.0148(3)	0.2269(1)	0.0706(2)	0.0116(5)
C(11)	0.3970(3)	0.1445(1)	-0.1203(2)	0.0125(6)
N(3)	0.3126(3)	0.1661(1)	0.1669(2)	0.0102(5)
C(13)	0.4044(3)	0.2474(1)	-0.1289(2)	0.0118(5)

	x	*y*	*z*	*U*(eq)/Å^2
N(4)	0.3211(3)	0.2297(1)	0.1796(2)	0.0115(5)
C(7)	0.4521(3)	0.1816(1)	0.3106(2)	0.0153(6)
N(1)	0.0135(3)	0.1636(1)	0.0635(2)	0.0107(5)
C(17)	0.8976(5)	0.0042(2)	0.3440(3)	0.0339(8)
C(5)	-0.2650(4)	0.2961(1)	0.0739(2)	0.0174(6)
N(6)	0.3182(3)	0.2351(1)	-0.0443(2)	0.0100(5)
C(12)	0.4555(3)	0.1921(1)	-0.1773(2)	0.0133(6)
C(3)	-0.1841(3)	0.2335(1)	0.0691(2)	0.0125(6)
C(10)	0.4386(4)	0.3024(1)	0.3034(2)	0.0175(6)

	x	y	z	U(eq)/Å^2		x	y	z	U(eq)/Å^2
C(1)	-0.1411(3)	0.1321(1)	0.0565(2)	0.0132(6)	C(9)	0.4082(4)	0.0680(1)	0.2589(2)	0.0236(7)
C(8)	0.4058(3)	0.2386(1)	0.2657(2)	0.0126(6)	C(14)	0.4144(4)	0.0769(1)	-0.1389(2)	0.0197(6)
N(7)	0.9497(5)	0.0395(2)	0.2874(3)	0.0506(9)	C(2)	-0.2666(4)	0.1759(1)	0.0613(2)	0.0149(6)
C(6)	0.3936(3)	0.1362(1)	0.2481(2)	0.0132(6)	C(15)	0.4347(4)	0.3122(1)	-0.1611(2)	0.0164(6)
C(4)	-0.1561(4)	0.0641(1)	0.0428(2)	0.0222(7)	C(16)	0.8328(4)	-0.0405(2)	0.4170(3)	0.0356(9)

7.3.32 *Bromo-tris(3,5-dimethyl-pyrazol-1-yl)phosphinoxid-kupfer(I)-acetonitrilsolvat (tgv101)*

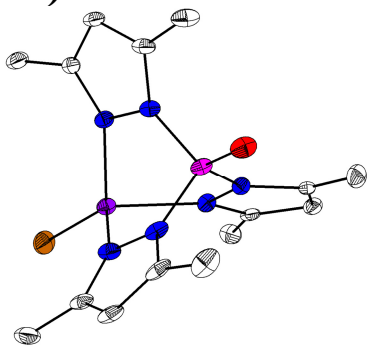

Kristalldaten

C18 H25.50 Br Cu N7.50 O P	M = 537.38 g/mol	Monoclinic, $C2/c$
a = 24.046(5) Å	b = 15.284(3) Å	c = 13.334(2) Å
α = 90°	β = 111.790(5)°	γ = 90°
V = 4550.2(15) Å^3	Z = 8	F(000) = 2184
D_{calc} = 1.569 g/cm^3	μ = 2.812 mm^{-1}	
colourless needle	0.410 · 0.070 · 0.030 mm^3	

Datensammlung

Diffraktometer: D8 Quest (Bruker)	T = 100(2) K	λ = 0.71069 Å
h = -29 bis 30	k = -19 bis 19	l = -16 bis 16
29280 gemessene Reflexe	4893 unabhängige Reflexe	3491 Reflexe mit $I > 2\sigma(I)$
θ = 2.049 bis 26.849°	R_{int} = 0.1183	C (25.00°) = 1.000
Absorptionskorrektur: Multi-scan	T_{min} = 0.5958	T_{max} = 0.7455

Verfeinerung

4893 Reflexe	3 Restraints	316 Parameter
Verfeinerung mit SHELXL-2014/7	bis χ = 0.002	
R_1 ($I > 2\sigma(I)$) = 0.0425	wR_2 ($I > 2\sigma(I)$) = 0.0665	
R_1 (all) = 0.0783	wR_2 (all) = 0.0763	GoF (S) = 1.026
$\Delta\varphi_{min}$ = -0.467 e·Å^{-3}	$\Delta\varphi_{max}$ = 0.515 e·Å^{-3}	

Kommentar

Pro asymmetrischer Einheit liegen 1.5 Äquivalente Acetonitril vor, die über drei Positionen fehlgeordnet sind. Zwei dieser Positionen sind außerdem über eine zweizählige Drehachse fehlgeordnet. Eines der Solvatmoleküle wurde über DFIX restrained.

Fraktionelle Atomkoordinaten (*x, y, z*) und äquivalente isotrope Auslenkungsfaktoren *U*(eq)

	x	y	z	U(eq)/Å^2		x	y	z	U(eq)/Å^2
C(1)	0.1305(2)	0.0943(2)	0.5013(2)	0.0162(7)	C(9)	0.0844(2)	-0.2005(2)	0.6429(3)	0.0262(9)
C(2)	0.1713(2)	0.1272(2)	0.4630(3)	0.0172(8)	C(10)	0.3138(2)	-0.2199(2)	0.7867(3)	0.0199(8)
C(3)	0.2293(2)	0.1063(2)	0.5381(2)	0.0138(7)	C(11)	0.1441(2)	0.0958(2)	0.8643(3)	0.0216(8)
C(4)	0.0640(2)	0.1004(2)	0.4578(3)	0.0245(8)	C(12)	0.1899(2)	0.1256(2)	0.9537(3)	0.0233(9)
C(5)	0.2891(2)	0.1270(2)	0.5336(3)	0.0184(8)	C(13)	0.2445(2)	0.1012(2)	0.9451(3)	0.0193(8)
C(6)	0.1500(2)	-0.1824(2)	0.6858(3)	0.0183(8)	C(14)	0.0784(2)	0.1076(2)	0.8298(3)	0.0311(9)
C(7)	0.1968(2)	-0.2396(2)	0.7142(2)	0.0167(8)	C(15)	0.3068(2)	0.1170(2)	1.0221(3)	0.0270(9)
C(8)	0.2501(2)	-0.1896(2)	0.7475(2)	0.0144(7)	N(1)	0.1642(1)	0.0540(2)	0.5987(2)	0.0141(6)

	x	y	z	U(eq)/Å^2
N(2)	0.2252(1)	0.0626(2)	0.6210(2)	0.0135(6)
N(3)	0.1755(1)	-0.0987(2)	0.7030(2)	0.0141(6)
N(4)	0.2379(1)	-0.1048(2)	0.7412(2)	0.0144(6)
N(5)	0.1723(1)	0.0531(2)	0.8033(2)	0.0173(6)
N(6)	0.2344(1)	0.0576(2)	0.8540(2)	0.0180(6)
O(1)	0.0764(1)	-0.0075(1)	0.6494(2)	0.0234(6)
P(1)	0.1411(1)	-0.0005(1)	0.6854(1)	0.0153(2)
Cu(1)	0.2851(1)	0.0108(1)	0.7673(1)	0.0150(1)
Br(1)	0.3876(1)	0.0311(1)	0.8200(1)	0.0239(1)

	x	y	z	U(eq)/Å^2
N(10)	0.0281(13)	0.2630(15)	0.620(3)	0.042(6)
C(100)	-0.0289(4)	0.3982(5)	0.6527(7)	0.040(2)
C(101)	0.0021(4)	0.3227(6)	0.6337(8)	0.033(2)
C(104)	0.0508(4)	0.4315(6)	0.4097(6)	0.041(2)
N(12)	0.0294(4)	0.2848(5)	0.3072(6)	0.064(3)
C(105)	0.0391(4)	0.3486(5)	0.3521(7)	0.0311(19)
N(11)	0.0248(15)	0.2741(16)	0.620(2)	0.057(8)
C(102)	0.0441(4)	0.3628(5)	0.4691(7)	0.038(2)
C(103)	0.0351(3)	0.3133(5)	0.5547(7)	0.0302(19)

7.3.33 Bromo-tris(3,5-dimethylpyrazol-1-yl)phosphinsulfid-kupfer(I)-dimer (tgv102)

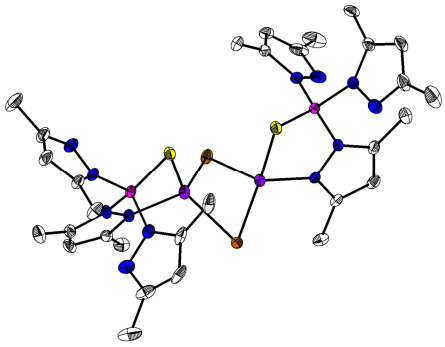

Kristalldaten

C15 H21 Br Cu N6 P S	M = 491.86 g/mol	Orthorhombic, *Fdd*2
a = 20.7400(8) Å	b = 29.6985(11) Å	c = 13.2401(5) Å
α = 90°	β = 90°	γ = 90°
V = 8155.2(5) Å^3	Z = 16	F(000) = 3968
D_{calc} = 1.602 g/cm^3	μ = 3.223 mm^{-1}	
colourless block	0.450 · 0.360 · 0.310 mm^3	

Datensammlung

Diffraktometer: STOE IPDS 2T	T = 298(2) K	λ = 0.71073 Å
h = -26 bis 26	k = -35 bis 37	l = -16 bis 16
20994 gemessene Reflexe	4333 unabhängige Reflexe	4262 Reflexe mit $I > 2\sigma(I)$
θ = 1.949 bis 26.726°	R_{int} = 0.0910	C (25.00°) = 1.000
Absorptionskorrektur: Multi-scan	T_{min} = 0.4350	T_{max} = 0.7122

Verfeinerung

4333 Reflexe	1 Restraints	232 Parameter
Verfeinerung mit SHELXL-2014/7	bis χ = 0.001	
R_1 ($I > 2\sigma(I)$) = 0.0312	wR_2 ($I > 2\sigma(I)$) = 0.0783	
R_1 (all) = 0.0319	wR_2 (all) = 0.0786	GoF (S) = 1.034
$\Delta\varphi_{min}$ = -0.849 e·Å^{-3}	$\Delta\varphi_{max}$ = 0.535 e·Å^{-3}	

Fraktionelle Atomkoordinaten (*x, y, z*) und äquivalente isotrope Auslenkungsfaktoren *U*(eq)

	x	y	z	U(eq)/Å^2
Br(1)	1.0567(1)	0.0543(1)	0.6241(1)	0.0197(1)
Cu(1)	0.9512(1)	0.0273(1)	0.6737(1)	0.0185(1)
S(1)	0.9239(1)	0.0342(1)	0.8518(1)	0.0184(2)
P(1)	0.8350(1)	0.0402(1)	0.8145(1)	0.0145(2)
N(2)	0.8724(2)	0.0629(1)	0.6340(3)	0.0157(6)
N(3)	0.7952(2)	-0.0084(1)	0.7960(3)	0.0188(7)
C(8)	0.7354(2)	0.0613(2)	0.9545(3)	0.0208(8)
N(1)	0.8241(2)	0.0687(1)	0.7053(3)	0.0168(7)
N(5)	0.7894(2)	0.0698(1)	0.8962(3)	0.0182(7)
C(1)	0.8519(2)	0.0832(1)	0.5515(3)	0.0172(8)

	x	y	z	U(eq)/Å^2
C(6)	0.7707(2)	0.1321(2)	0.9737(4)	0.0282(10)
C(3)	0.7728(2)	0.0920(1)	0.6640(3)	0.0196(8)
N(6)	0.8111(2)	0.1138(1)	0.9085(3)	0.0239(8)
C(7)	0.7224(2)	0.1009(2)	1.0036(4)	0.0266(10)
N(4)	0.7426(2)	-0.0068(1)	0.7302(3)	0.0235(8)
C(13)	0.8019(2)	-0.0511(2)	0.8392(4)	0.0231(9)
C(2)	0.7901(2)	0.1018(2)	0.5675(4)	0.0216(9)
C(11)	0.7187(3)	-0.0481(2)	0.7326(4)	0.0295(10)
C(5)	0.7120(2)	0.1028(2)	0.7185(4)	0.0294(10)
C(14)	0.6596(3)	-0.0590(2)	0.6716(4)	0.0400(14)

	x	y	z	U(eq)/Å^2
C(4)	0.8930(2)	0.0841(2)	0.4597(3)	0.0235(9)
C(10)	0.7015(2)	0.0172(2)	0.9624(4)	0.0267(10)
C(12)	0.7535(2)	-0.0760(2)	0.7986(4)	0.0272(10)
C(15)	0.8519(3)	-0.0632(2)	0.9143(4)	0.0310(10)
C(9)	0.7799(3)	0.1796(2)	1.0090(6)	0.0454(16)

7.3.34 2,2'-(Butylamino)-bis(chinolin-8-olato)-2,4,6-trimethylphenolato-aluminium(III) (tgn217)

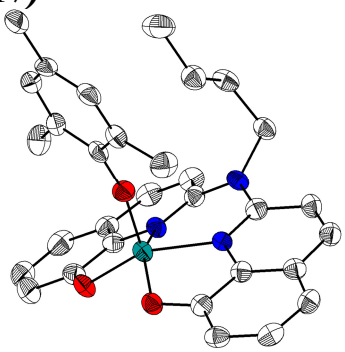

Kristalldaten

C31 H30 Al N3 O3	M = 519.56 g/mol	Orthorhombic, *Pbca*
a = 15.3287(7) Å	b = 16.4601(4) Å	c = 20.6068(13) Å
α = 90°	β = 90°	γ = 90°
V = 5199.3(4) Å^3	Z = 8	F(000) = 2192
D_{calc} = 1.327 g/cm^3	μ = 0.117 mm^{-1}	
colourless needle	0.282 · 0.066 · 0.032 mm^3	

Datensammlung

Diffraktometer: STOE IPDS 2	T = 100(2) K	λ = 0.71069 Å
h = -16 bis 18	k = -19 bis 19	l = -25 bis 25
35021 gemessene Reflexe	4860 unabhängige Reflexe	2307 Reflexe mit $I > 2\sigma(I)$
θ = 1.976 bis 25.557°	R_{int} = 0.2091	C (25.00°) = 1.000
Absorptionskorrektur: Multi-scan	T_{min} = 0.9677	T_{max} = 1.0062

Verfeinerung

4860 Reflexe	0 Restraints	347 Parameter
Verfeinerung mit SHELXL-2014/7	bis χ = 0.000	
R_1 ($I > 2\sigma(I)$) = 0.0675	wR_2 ($I > 2\sigma(I)$) = 0.0818	
R_1 (all) = 0.1674	wR_2 (all) = 0.1057	GoF (S) = 0.890
$\Delta\varphi_{min}$ = -0.252 e·Å^{-3}	$\Delta\varphi_{max}$ = 0.211 e·Å^{-3}	

Kommentar

Der Kristall wies eine schwache Streuung auf, worauf die B- und C-Alerts des Checkcif Reports beruhen.

Fraktionelle Atomkoordinaten (*x, y, z*) und äquivalente isotrope Auslenkungsfaktoren *U*(eq)

	x	y	z	U(eq)/Å^2
Al(1)	0.1913(1)	0.1072(1)	0.5070(1)	0.0269(3)
O(3)	0.2767(2)	0.1194(1)	0.4545(1)	0.0318(7)
O(1)	0.0973(2)	0.1644(2)	0.4791(1)	0.0318(7)
O(2)	0.2040(2)	0.1705(2)	0.5785(1)	0.0314(7)
N(3)	0.2442(2)	0.0204(2)	0.5620(2)	0.0232(8)
N(1)	0.2280(2)	-0.0931(2)	0.4936(2)	0.0276(8)
N(2)	0.1314(2)	0.0124(2)	0.4663(2)	0.0268(8)
C(9)	0.0587(3)	0.0393(2)	0.4326(2)	0.0281(10)
C(8)	0.0432(3)	0.1240(2)	0.4403(2)	0.0316(11)
C(2)	0.1053(3)	-0.1200(3)	0.4214(2)	0.0341(11)
C(17)	0.2507(3)	0.1370(2)	0.6268(2)	0.0297(10)
C(19)	0.2765(3)	-0.1633(2)	0.4652(2)	0.0323(10)
C(24)	0.3155(3)	0.1556(2)	0.3469(2)	0.0295(10)
C(10)	0.2595(3)	-0.0584(2)	0.5504(2)	0.0295(10)
C(28)	0.4204(3)	0.1640(2)	0.4347(2)	0.0317(10)
C(18)	0.2730(3)	0.0538(2)	0.6194(2)	0.0275(10)
C(16)	0.2775(3)	0.1755(3)	0.6827(2)	0.0339(11)
C(1)	0.1544(3)	-0.0654(2)	0.4609(2)	0.0289(10)
C(5)	-0.0617(3)	0.0251(3)	0.3588(2)	0.0403(12)
C(23)	0.3365(3)	0.1470(2)	0.4124(2)	0.0283(10)
C(11)	0.3057(3)	-0.1060(2)	0.5962(2)	0.0319(10)
C(12)	0.3377(3)	-0.0722(2)	0.6519(2)	0.0332(11)
C(13)	0.3217(3)	0.0111(2)	0.6656(2)	0.0298(10)
C(26)	0.4627(3)	0.2042(2)	0.3248(2)	0.0334(11)
C(14)	0.3490(3)	0.0531(3)	0.7219(2)	0.0340(11)
C(27)	0.4823(3)	0.1944(2)	0.3903(2)	0.0368(11)

	x	y	z	U(eq)/Å^2		x	y	z	U(eq)/Å^2
C(3)	0.0333(3)	-0.0928(3)	0.3889(2)	0.0348(11)	C(4)	0.0081(3)	-0.0101(3)	0.3923(2)	0.0311(10)
C(15)	0.3267(3)	0.1332(3)	0.7296(2)	0.0345(11)	C(7)	-0.0272(3)	0.1567(3)	0.4072(2)	0.0444(13)
C(30)	0.5293(3)	0.2367(3)	0.2770(2)	0.0486(14)	C(22)	0.3992(4)	-0.0547(3)	0.3233(3)	0.0582(15)
C(21)	0.3600(3)	-0.0670(2)	0.3912(2)	0.0392(12)	C(6)	-0.0783(3)	0.1064(3)	0.3667(2)	0.0420(12)
C(20)	0.3094(3)	-0.1463(2)	0.3966(2)	0.0369(11)	C(29)	0.2254(3)	0.1334(3)	0.3238(2)	0.0426(12)
C(25)	0.3792(3)	0.1835(2)	0.3047(2)	0.0350(11)	C(31)	0.4432(3)	0.1502(3)	0.5050(2)	0.0440(12)

7.3.35 Pyrazol (tgn305)

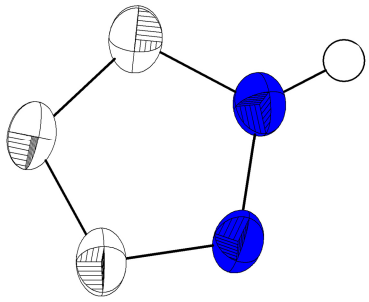

Kristalldaten

C3 H4 N2	M = 68.08 g/mol	Orthorhombic, *Pnca*
a = 6.8110(8) Å	b = 8.2490(10) Å	c = 12.581(2) Å
α = 90°	β = 90°	γ = 90°
V = 706.85(17) Å^3	Z = 8	F(000) = 288
D_{calc} = 1.280 g/cm^3	μ = 0.086 mm^{-1}	
colourless needle	0.410 · 0.110 · 0.080 mm^3	

Datensammlung

Diffraktometer: STOE IPDS 2	T = 100(2) K	λ = 0.71069 Å
h = -8 bis 7	k = -9 bis 10	l = -15 bis 13
2392 gemessene Reflexe	755 unabhängige Reflexe	485 Reflexe mit $I > 2\sigma(I)$
θ = 2.953 bis 26.685°	R_{int} = 0.0700	C (25.00°) = 1.000
Absorptionskorrektur: Multi-scan	T_{min} = 0.7804	T_{max} = 0.9508

Verfeinerung

755 Reflexe	0 Restraints	53 Parameter
Verfeinerung mit SHELXL-2014/7	bis χ = 0.000	
R_1 ($I > 2\sigma(I)$) = 0.0615	wR_2 ($I > 2\sigma(I)$) = 0.1529	
R_1 (all) = 0.0933	wR_2 (all) = 0.1619	GoF (S) = 1.102
$\Delta\varphi_{min}$ = -0.206 e·Å^{-3}	$\Delta\varphi_{max}$ = 0.174 e·Å^{-3}	

Kommentar

Mehrere andere Pyrazolmodifikationen sind bereits bekannt (vgl. CSD-Codes PYRZOL und PYRZOL01 bis PYRZOL05)

Fraktionelle Atomkoordinaten (*x, y, z*) und äquivalente isotrope Auslenkungsfaktoren *U*(eq)

	x	y	z	U(eq)/Å^2
C(3)	0.1261(4)	0.2064(3)	0.3056(2)	0.0361(7)
C(4)	-0.0039(4)	0.1109(3)	0.3633(2)	0.0350(7)
C(5)	-0.0745(4)	0.2119(3)	0.4422(2)	0.0353(7)
N(1)	0.0075(4)	0.3587(2)	0.4327(2)	0.0351(6)
N(2)	0.1318(3)	0.3551(2)	0.3481(2)	0.0350(6)

7.3.36 Tri(pyrid-2-yl)phosphinoxid (tgn365)

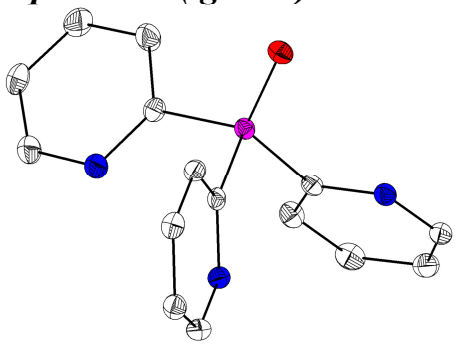

Kristalldaten

C15 H12 N3 O P	M = 281.25 g/mol	Monoclinic, $P2_1/c$
a = 9.0411(10) Å	b = 9.1140(8) Å	c = 16.0048(16) Å
α = 90°	β = 100.445(4)°	γ = 90°
V = 1297.0(2) Å^3	Z = 4	F(000) = 584
D_{calc} = 1.440 g/cm^3	μ = 0.210 mm^{-1}	
colourless block	0.230 · 0.200 · 0.180 mm^3	

Datensammlung

Diffraktometer: D8 Quest (Bruker)	T = 100(2) K	λ = 0.71073 Å
h = -9 bis 11	k = -11 bis 11	l = -20 bis 20
8650 gemessene Reflexe	2854 unabhängige Reflexe	2423 Reflexe mit $I > 2\sigma(I)$
θ = 2.582 bis 27.103°	R_{int} = 0.0266	C (25.00°) = 0.997
Absorptionskorrektur: Multi-scan	T_{min} = 0.6924	T_{max} = 0.7455

Verfeinerung

2854 Reflexe	0 Restraints	181 Parameter
Verfeinerung mit SHELXL-2014/7	bis χ = 0.000	
R_1 ($I > 2\sigma(I)$) = 0.0328	wR_2 ($I > 2\sigma(I)$) = 0.0810	
R_1 (all) = 0.0411	wR_2 (all) = 0.0857	GoF (S) = 1.054
$\Delta\varphi_{min}$ = -0.360 e·Å^{-3}	$\Delta\varphi_{max}$ = 0.381 e·Å^{-3}	

Kommentar

Diese Struktur wurde zuvor bereits von Bowen *et al.* beschrieben. (R. J. Bowen, M. A. Fernandes, P. W. Gitari, M. Layh, *Acta Cryst. C* **2004**, *60*, o258-o260)

Fraktionelle Atomkoordinaten (*x, y, z*) und äquivalente isotrope Auslenkungsfaktoren *U*(eq)

	x	y	z	U(eq)/Å^2		x	y	z	U(eq)/Å^2
C(1)	0.2508(2)	0.2912(2)	0.1875(1)	0.0128(3)	C(11)	0.3240(2)	0.3081(2)	0.0184(1)	0.0147(3)
C(2)	0.3113(2)	0.4014(2)	0.2433(1)	0.0148(3)	C(12)	0.4314(2)	0.3108(2)	-0.0334(1)	0.0226(3)
C(3)	0.2201(2)	0.4634(2)	0.2953(1)	0.0164(3)	C(13)	0.3999(2)	0.3891(2)	-0.1091(1)	0.0249(4)
C(4)	0.0746(2)	0.4118(2)	0.2897(1)	0.0172(3)	C(14)	0.2651(2)	0.4617(2)	-0.1289(1)	0.0208(3)
C(5)	0.0256(2)	0.2998(2)	0.2325(1)	0.0168(3)	C(15)	0.1644(2)	0.4530(2)	-0.0732(1)	0.0215(3)
C(6)	0.2888(2)	0.0257(2)	0.0982(1)	0.0136(3)	N(1)	0.1098(1)	0.2392(1)	0.1812(1)	0.0147(2)
C(7)	0.2006(2)	-0.0190(2)	0.0224(1)	0.0176(3)	N(2)	0.3286(1)	-0.0633(1)	0.1656(1)	0.0151(2)
C(8)	0.1508(2)	-0.1639(2)	0.0153(1)	0.0205(3)	N(3)	0.1908(1)	0.3776(1)	-0.0003(1)	0.0190(3)
C(9)	0.1932(2)	-0.2570(2)	0.0837(1)	0.0192(3)	O(1)	0.5300(1)	0.2102(1)	0.1540(1)	0.0175(2)
C(10)	0.2817(2)	-0.2023(2)	0.1573(1)	0.0163(3)	P(1)	0.3665(1)	0.2090(1)	0.1183(1)	0.0124(1)

7.3.37 2,2'-Bipyridyl (tgv44)

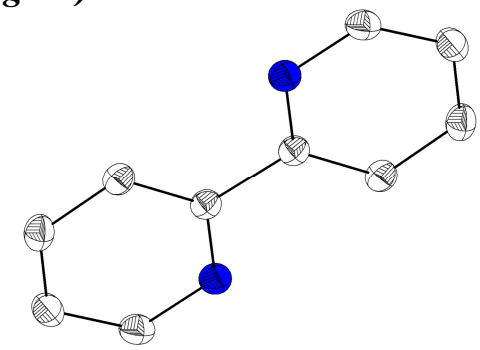

Kristalldaten

C10 H8 N2	M = 156.18 g/mol	Monoclinic, $P2_1/c$
a = 5.4799(5) Å	b = 6.1576(4) Å	c = 12.3562(12) Å
α = 90°	β = 110.786(7)°	γ = 90°
V = 389.80(6) Å^3	Z = 2	F(000) = 164
D_{calc} = 1.331 g/cm^3	μ = 0.082 mm^{-1}	
colourless block	0.290 · 0.260 · 0.140 mm^3	

Datensammlung

Diffraktometer: STOE IPDS 2T	T = 100(2) K	λ = 0.71069 Å
h = -6 bis 6	k = -7 bis 7	l = -15 bis 15
3262 gemessene Reflexe	825 unabhängige Reflexe	717 Reflexe mit $I > 2\sigma(I)$
θ = 3.527 bis 26.663°	R_{int} = 0.0398	C (25.00°) = 1.000
Absorptionskorrektur: Multi-scan	T_{min} = 0.8968	T_{max} = 1.1275

Verfeinerung

825 Reflexe	0 Restraints	55 Parameter
Verfeinerung mit SHELXL-2014/7	bis χ = 0.000	
R_1 ($I > 2\sigma(I)$) = 0.0323	wR_2 ($I > 2\sigma(I)$) = 0.0844	
R_1 (all) = 0.0375	wR_2 (all) = 0.0868	GoF (S) = 1.037
$\Delta\varphi_{min}$ = -0.212 e·Å^{-3}	$\Delta\varphi_{max}$ = 0.178 e·Å^{-3}	

Kommentar

Diese Sturktur wurde zuvor bereits von Chisholm *et al.* veröffentlicht. (M. H. Chisholm, J. C. Huffman, I. P. Rothwell, *J. Am. Chem. Soc.* **1981**, *103*, 4945-4941)

Fraktionelle Atomkoordinaten (*x, y, z*) und äquivalente isotrope Auslenkungsfaktoren *U*(eq)

	x	*y*	*z*	*U*(eq)/Å^2
C(1)	0.0153(2)	0.9046(2)	0.0389(1)	0.0181(3)
C(2)	-0.1962(2)	0.7707(2)	0.0304(1)	0.0207(3)
C(3)	-0.1563(2)	0.5939(2)	0.1038(1)	0.0236(3)
C(4)	0.0910(2)	0.5568(2)	0.1843(1)	0.0237(3)
C(5)	0.2889(2)	0.6999(2)	0.1878(1)	0.0232(3)
N(1)	0.2559(2)	0.8707(1)	0.1171(1)	0.0214(2)

7.3.38 Bis(bis(3,5-dimethyl-pyrazol-1-yl)phosphinato)-kupfer(II) (tgv88)

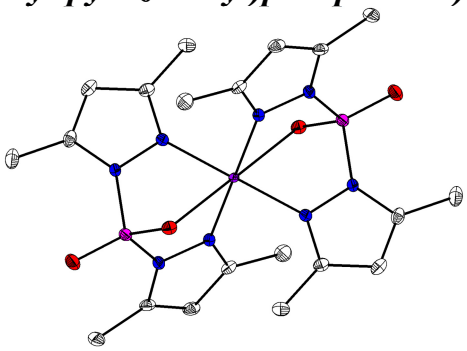

Kristalldaten

C20 H28 Cu N8 O4 P2	M = 569.98 g/mol	Monoclinic, $P2_1/n$
a = 7.7870(10) Å	b = 17.709(2) Å	c = 8.7459(13) Å
α = 90°	β = 95.694(5)°	γ = 90°
V = 1200.1(3) Å^3	Z = 2	F(000) = 590
D_{calc} = 1.577 g/cm^3	μ = 1.089 mm^{-1}	
light blue block	0.240 · 0.190 · 0.140 mm^3	

Datensammlung

Diffraktometer: D8 Quest (Bruker)	T = 100(2) K	λ = 0.71073 Å
h = -10 bis 9	k = -22 bis 21	l = -11 bis 11
13659 gemessene Reflexe	2657 unabhängige Reflexe	2299 Reflexe mit $I > 2\sigma(I)$
θ = 2.300 bis 27.164°	R_{int} = 0.0418	C (25.00°) = 1.000
Absorptionskorrektur: Multi-scan	T_{min} = 0.6685	T_{max} = 0.7455

Verfeinerung

2657 Reflexe	0 Restraints	164 Parameter
Verfeinerung mit SHELXL-2014/7	bis χ = 0.000	
R_1 ($I > 2\sigma(I)$) = 0.0308	wR_2 ($I > 2\sigma(I)$) = 0.0921	
R_1 (all) = 0.0393	wR_2 (all) = 0.0957	GoF (S) = 1.204
$\Delta\varphi_{min}$ = -0.406 e·Å^{-3}	$\Delta\varphi_{max}$ = 0.506 e·Å^{-3}	

Kommentar

Diese Verbindung wurde erstmals von Folkert *et al*. synthetisiert und strukturell charakterisiert. (S. Folkert, C. D. Bryan, A. W. Cordes, *Acta Cryst. C* **1995**. *51*, 863-865)

Fraktionelle Atomkoordinaten (*x, y, z*) und äquivalente isotrope Auslenkungsfaktoren *U*(eq)

	x	*y*	*z*	*U*(eq)/Å^2		*x*	*y*	*z*	*U*(eq)/Å^2
Cu(1)	0.0000	0.0000	0.5000	0.0085(1)	C(5)	0.3195(3)	-0.1424(1)	0.4615(3)	0.0169(5)
N(4)	0.0950(2)	0.0962(1)	0.5958(2)	0.0105(4)	N(3)	0.1535(2)	0.1494(1)	0.4974(2)	0.0112(4)
P(1)	0.1304(1)	0.1252(1)	0.3047(1)	0.0106(1)	N(2)	0.2167(2)	-0.0130(1)	0.3961(2)	0.0105(4)
O(2)	-0.0438(2)	0.0917(1)	0.2802(2)	0.0126(3)	C(4)	0.5083(3)	0.0845(1)	0.1542(3)	0.0195(5)
O(1)	0.1996(2)	0.1854(1)	0.2149(2)	0.0169(3)	C(10)	0.0705(3)	0.0826(1)	0.8731(2)	0.0174(5)
N(1)	0.2681(2)	0.0479(1)	0.3133(2)	0.0109(4)	C(8)	0.1186(3)	0.1254(1)	0.7366(2)	0.0122(4)
C(1)	0.4182(3)	0.0314(1)	0.2522(2)	0.0134(4)	C(7)	0.1923(3)	0.1976(1)	0.7296(2)	0.0145(4)
C(2)	0.4612(3)	-0.0412(1)	0.2968(2)	0.0154(4)	C(6)	0.2131(3)	0.2117(1)	0.5781(2)	0.0130(4)
C(3)	0.3333(3)	-0.0671(1)	0.3864(2)	0.0123(4)	C(9)	0.2803(3)	0.2797(1)	0.5028(3)	0.0177(5)

7.3.39 Di(pyrazolyl)phosphinsäure-zwitterion (tgv92a)

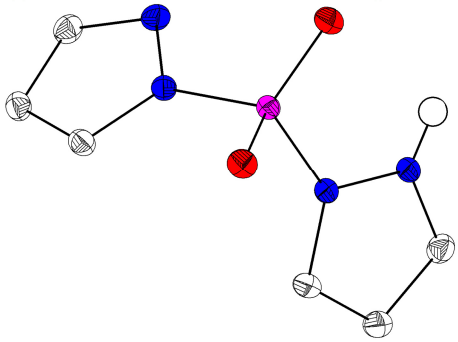

Kristalldaten

C6 H7 N4 O2 P	M = 198.13 g/mol	Monoclinic, $P2_1/c$
a = 9.8418(9) Å	b = 11.1183(8) Å	c = 7.3227(6) Å
α = 90°	β = 99.247(4)°	γ = 90°
V = 790.87(11) Å^3	Z = 4	F(000) = 408
D_{calc} = 1.664 g/cm^3	μ = 0.317 mm^{-1}	
colourless block	0.350 · 0.240 · 0.180 mm^3	

Datensammlung

Diffraktometer: D8 Quest (Bruker)	T = 100(2) K	λ = 0.71073 Å
h = -12 bis 12	k = -14 bis 14	l = -9 bis 9
10812 gemessene Reflexe	1765 unabhängige Reflexe	1602 Reflexe mit $I > 2\sigma(I)$
θ = 2.784 bis 27.280°	R_{int} = 0.0478	C (25.00°) = 0.998
Absorptionskorrektur: Multi-scan	T_{min} = 0.6406	T_{max} = 0.7455

Verfeinerung

1765 Reflexe	0 Restraints	122 Parameter
Verfeinerung mit SHELXL-2014/7	bis χ = 0.000	
R_1 ($I > 2\sigma(I)$) = 0.0362	wR_2 ($I > 2\sigma(I)$) = 0.0897	
R_1 (all) = 0.0403	wR_2 (all) = 0.0920	GoF (S) = 1.117
$\Delta\varphi_{min}$ = -0.416 e·Å^{-3}	$\Delta\varphi_{max}$ = 0.458 e·Å^{-3}	

Fraktionelle Atomkoordinaten (*x, y, z*) und äquivalente isotrope Auslenkungsfaktoren *U*(eq)

	x	*y*	*z*	*U*(eq)/Å^2		*x*	*y*	*z*	*U*(eq)/Å^2
P(1)	0.2620(1)	0.5429(1)	0.5710(1)	0.0120(1)	N(2)	0.3900(2)	0.3229(2)	0.6005(2)	0.0144(3)
C(1)	0.3643(2)	0.2059(2)	0.5802(3)	0.0172(4)	C(6)	0.1144(2)	0.5944(2)	0.2292(3)	0.0151(4)
N(1)	0.2727(2)	0.3853(1)	0.5448(2)	0.0132(3)	C(4)	0.2858(2)	0.6351(2)	0.0805(3)	0.0165(4)
O(1)	0.1307(1)	0.5615(1)	0.6371(2)	0.0171(3)	C(5)	0.1422(2)	0.6254(2)	0.0581(3)	0.0153(4)
O(2)	0.3998(1)	0.5778(1)	0.6605(2)	0.0177(3)	N(4)	0.3445(2)	0.6123(2)	0.2522(2)	0.0159(3)
C(2)	0.2259(2)	0.1909(2)	0.5079(3)	0.0180(4)	N(3)	0.2374(2)	0.5877(1)	0.3451(2)	0.0131(3)
					C(3)	0.1713(2)	0.3054(2)	0.4884(3)	0.0163(4)

7.3.40 1,4-Bis(4-(tert-butyl)phenyl)buta-1,3-diin (tgv98)

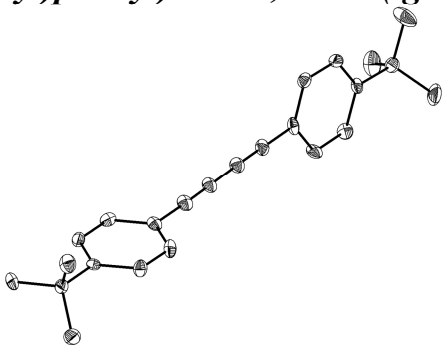

Kristalldaten

C24 H26	M = 314.45 g/mol	Monoclinic, $P2_1/c$
a = 12.2312(17) Å	b = 9.8141(13) Å	c = 15.810(2) Å
α = 90°	β = 94.654(6)°	γ = 90°
V = 1891.5(5) Å^3	Z = 4	F(000) = 680
D_{calc} = 1.104 g/cm^3	μ = 0.062 mm^{-1}	
colourless needle	0.360 · 0.080 · 0.050 mm^3	

Datensammlung

Diffraktometer: D8 Quest (Bruker)	T = 100(2) K	λ = 0.71073 Å
h = -15 bis 15	k = -11 bis 12	l = -19 bis 18
17474 gemessene Reflexe	3637 unabhängige Reflexe	2453 Reflexe mit $I > 2\sigma(I)$
θ = 2.445 bis 25.997°	R_{int} = 0.1147	C (25.00°) = 0.990
Absorptionskorrektur: Multi-scan	T_{min} = 0.4454	T_{max} = 1.00

Verfeinerung

3637 Reflexe	0 Restraints	223 Parameter
Verfeinerung mit SHELXL-2014/7	bis χ = 0.000	
R_1 ($I > 2\sigma(I)$) = 0.0931	wR_2 ($I > 2\sigma(I)$) = 0.1938	
R_1 (all) = 0.1344	wR_2 (all) = 0.2135	GoF (S) = 1.130
$\Delta\varphi_{min}$ = -0.321 e·Å^{-3}	$\Delta\varphi_{max}$ = 0.316 e·Å^{-3}	

Fraktionelle Atomkoordinaten (*x, y, z*) und äquivalente isotrope Auslenkungsfaktoren *U*(eq)

	x	*y*	*z*	*U*(eq)/Å^2		*x*	*y*	*z*	*U*(eq)/Å^2
C(5)	1.0856(2)	0.5133(3)	0.1117(2)	0.0192(6)	C(15)	0.8421(2)	0.4021(3)	0.5814(2)	0.0233(7)
C(7)	1.2702(2)	0.3904(3)	-0.0584(2)	0.0208(7)	C(14)	0.7820(2)	0.4036(3)	0.6511(2)	0.0214(7)
C(1)	1.1983(2)	0.3938(3)	0.0167(2)	0.0174(6)	C(12)	0.9547(2)	0.3942(3)	0.2907(2)	0.0209(7)
C(6)	1.1504(2)	0.5129(3)	0.0436(2)	0.0188(6)	C(17)	0.6756(2)	0.3960(3)	0.4908(2)	0.0199(6)
C(19)	0.6032(2)	0.4056(3)	0.7225(2)	0.0189(6)	C(24)	0.8996(2)	0.3950(3)	0.3630(2)	0.0203(7)
C(13)	0.6671(2)	0.4018(3)	0.6433(2)	0.0157(6)	C(11)	1.0050(2)	0.3936(3)	0.2288(2)	0.0209(7)
C(4)	1.0679(2)	0.3938(3)	0.1558(2)	0.0201(6)	C(21)	0.4795(2)	0.3911(3)	0.7006(2)	0.0255(7)
C(3)	1.1156(2)	0.2735(3)	0.1291(2)	0.0210(7)	C(22)	0.6243(2)	0.5412(3)	0.7676(2)	0.0273(7)
C(23)	0.8510(2)	0.3963(3)	0.4259(2)	0.0215(6)	C(20)	0.6410(2)	0.2894(3)	0.7824(2)	0.0283(7)
C(2)	1.1784(2)	0.2750(3)	0.0607(2)	0.0214(7)	C(10)	1.2943(3)	0.5323(4)	-0.0906(2)	0.0439(10)
C(16)	0.7901(2)	0.3984(3)	0.4995(2)	0.0179(6)	C(9)	1.3786(2)	0.3192(4)	-0.0319(2)	0.0374(9)
C(18)	0.6162(2)	0.3978(3)	0.5613(2)	0.0186(6)	C(8)	1.2103(3)	0.3096(4)	-0.1312(2)	0.0374(9)

7.4 Strukturen für David Grosse-Hagenbrock

7.4.1 Tetramethyloxalhydrazonamido-tetrakis(dimethyl-gallium(III)) (bpfdg12)

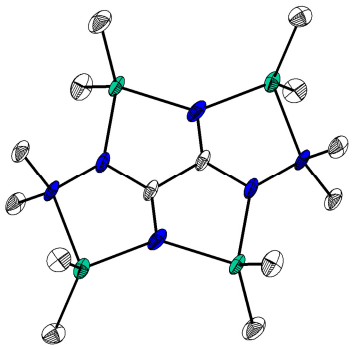

Kristalldaten

C14 H36 Ga4 N6	M = 567.37 g/mol	Triclinic, $P\bar{1}$
a = 6.9773(12) Å	b = 11.374(2) Å	c = 14.870(3) Å
α = 84.763(6)°	β = 89.671(6)°	γ = 89.339(6)°
V = 1175.1(4) Å^3	Z = 2	F(000) = 572
D_{calc} = 1.604 g/cm^3	μ = 4.545 mm^{-1}	
colourless block	0.380 · 0.220 · 0.130 mm^3	

Datensammlung

Diffraktometer: D8 Quest (Bruker)	T = 100(2) K	λ = 0.71073 Å
h = -8 bis 8	k = -13 bis 13	l = -16 bis 18
15169 gemessene Reflexe	4335 unabhängige Reflexe	4052 Reflexe mit $I > 2\sigma(I)$
θ = 2.361 bis 25.497°	R_{int} = 0.0393	C (25.00°) = 0.999
Absorptionskorrektur: Multi-scan	T_{min} = 0.5040	T_{max} = 0.7455

Verfeinerung

4335 Reflexe	0 Restraints	230 Parameter
Verfeinerung mit SHELXL-2014/7	bis χ = 0.000	
R_1 ($I > 2\sigma(I)$) = 0.0604	wR_2 ($I > 2\sigma(I)$) = 0.1624	
R_1 (all) = 0.0670	wR_2 (all) = 0.1738	GoF (S) = 1.098
$\Delta\varphi_{min}$ = -3.085 e·Å^{-3}	$\Delta\varphi_{max}$ = 1.498 e·Å^{-3}	

Kommentar

Die Struktur wurde als pseudomeroedrischer Zwilling verfeinert.

Fraktionelle Atomkoordinaten (*x, y, z*) und äquivalente isotrope Auslenkungsfaktoren *U*(eq)

	x	*y*	*z*	*U*(eq)/Å^2		*x*	*y*	*z*	*U*(eq)/Å^2
C(1)	0.0005(14)	0.4382(9)	0.4844(7)	0.016(2)	C(16)	0.0032(16)	0.9992(11)	0.1511(8)	0.029(3)
C(3)	0.311(2)	0.1989(12)	0.5053(9)	0.035(3)	C(17)	0.4273(19)	0.9396(12)	0.2665(8)	0.032(3)
C(2)	0.001(2)	0.1743(11)	0.5808(8)	0.034(3)	Ga(1)	-0.0329(2)	0.2598(1)	0.3824(1)	0.0201(3)
C(4)	-0.2352(17)	0.1436(10)	0.3899(8)	0.026(2)	Ga(2)	0.2302(2)	0.4402(1)	0.6400(1)	0.0188(3)
C(5)	0.1706(18)	0.2644(13)	0.2885(8)	0.033(3)	Ga(11)	0.5249(2)	0.7247(1)	-0.0738(1)	0.0184(3)
C(6)	0.0934(17)	0.3823(11)	0.7513(8)	0.027(3)	Ga(12)	0.2881(2)	0.9854(1)	0.1521(1)	0.0192(3)
C(7)	0.5138(16)	0.4399(11)	0.6321(8)	0.027(3)	N(1)	0.1169(13)	0.3655(8)	0.5356(6)	0.021(2)
C(11)	0.4918(14)	0.9354(9)	-0.0067(7)	0.017(2)	N(2)	0.1115(14)	0.2447(9)	0.5106(7)	0.024(2)
C(12)	0.1539(15)	0.7352(11)	0.0334(8)	0.025(3)	N(3)	-0.0999(13)	0.4168(8)	0.4157(6)	0.0199(19)
C(13)	0.4288(17)	0.6874(11)	0.1293(7)	0.026(3)	N(11)	0.3824(13)	0.8799(8)	0.0576(6)	0.0200(19)
C(14)	0.3442(17)	0.6835(11)	-0.1649(8)	0.026(3)	N(12)	0.3612(12)	0.7556(8)	0.0454(6)	0.0158(18)
C(15)	0.7307(17)	0.6122(10)	-0.0310(8)	0.026(2)	N(13)	0.5802(13)	0.8923(9)	-0.0752(6)	0.023(2)

7.4.2 *Bortrifluorid-triethylamin-addukt (dgh334f5)*

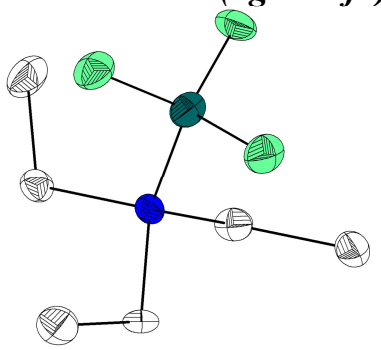

Kristalldaten

C6 H15 B F3 N	M = 169.00 g/mol	Monoclinic, $P2_1/c$
a = 13.5530(7) Å	b = 10.5940(6) Å	c = 11.9474(6) Å
α = 90°	β = 93.689(3)°	γ = 90°
V = 1711.86(16) Å^3	Z = 8	F(000) = 720
D_{calc} = 1.311 g/cm^3	μ = 0.121 mm^{-1}	
colourless block	0.490 · 0.300 · 0.180 mm^3	

Datensammlung

Diffraktometer: D8 Quest (Bruker)	T = 100(2) K	λ = 0.71073 Å
h = -17 bis 17	k = 0 bis 13	l = 0 bis 15
3895 gemessene Reflexe	3895 unabhängige Reflexe	3320 Reflexe mit $I > 2\sigma(I)$
θ = 2.442 bis 27.174°	R_{int} = -(hklf5)	C (25.00°) = 0.999
Absorptionskorrektur: Multi-scan	T_{min} = 0.4512	T_{max} = 0.7455

Verfeinerung

3895 Reflexe	2 Restraints	234 Parameter
Verfeinerung mit SHELXL-2014/7	bis χ = 0.000	
R_1 ($I > 2\sigma(I)$) = 0.0786	wR_2 ($I > 2\sigma(I)$) = 0.1591	
R_1 (all) = 0.1016	wR_2 (all) = 0.1731	GoF (S) = 1.198
$\Delta\varphi_{min}$ = -0.372 e·Å^{-3}	$\Delta\varphi_{max}$ = 0.408 e·Å^{-3}	

Kommentar

Die Struktur wurde als nicht-meroedrischer Zwilling integriert und verfeinert. Die schwächer besetzten Positionen fehlgeordneter Ethylgruppen (75:25) wurden über DFIX re- und über EADP constrained.

Fraktionelle Atomkoordinaten (*x, y, z*) und äquivalente isotrope Auslenkungsfaktoren *U*(eq)

	x	*y*	*z*	*U*(eq)/Å^2
C(1)	0.9699(4)	0.0814(6)	0.3164(5)	0.0227(13)
C(2)	1.0414(10)	0.1496(13)	0.3929(10)	0.030(3)
C(3)	0.8210(4)	0.1523(5)	0.4009(4)	0.0170(12)
C(4)	0.7193(17)	0.214(2)	0.3957(16)	0.022(3)
C(5)	0.8092(5)	0.0664(6)	0.2107(4)	0.0250(14)
C(6)	0.8497(14)	0.0440(14)	0.0975(10)	0.031(3)
C(7)	0.7407(3)	0.6157(4)	0.3019(3)	0.0181(8)
C(8)	0.7968(3)	0.7084(4)	0.3775(3)	0.0228(9)
C(9)	0.5840(3)	0.6280(4)	0.3901(3)	0.0167(8)
C(10)	0.4722(3)	0.6478(5)	0.3853(4)	0.0245(10)
C(11)	0.5887(3)	0.5395(4)	0.2017(3)	0.0174(8)
C(12)	0.6263(3)	0.5360(5)	0.0851(3)	0.0264(10)
B(1)	0.8867(3)	0.2893(5)	0.2406(4)	0.0165(9)
B(2)	0.6129(3)	0.7820(5)	0.2242(4)	0.0179(9)

	x	*y*	*z*	*U*(eq)/Å^2
F(1)	0.9656(2)	0.2844(2)	0.1729(2)	0.0248(6)
F(2)	0.9048(2)	0.3700(2)	0.3285(2)	0.0252(6)
F(3)	0.8015(2)	0.3223(2)	0.1778(2)	0.0283(6)
F(4)	0.6862(2)	0.8050(2)	0.1524(2)	0.0236(6)
F(5)	0.6166(2)	0.8692(2)	0.3107(2)	0.0239(6)
F(6)	0.5209(2)	0.7835(2)	0.1672(2)	0.0235(6)
N(1)	0.8719(2)	0.1467(3)	0.2912(3)	0.0138(7)
N(2)	0.6313(2)	0.6420(3)	0.2786(3)	0.0139(7)
C(1A)	0.9294(12)	0.1273(18)	0.4003(14)	0.023(2)
C(2A)	1.044(3)	0.132(4)	0.409(4)	0.023(2)
C(3A)	0.7648(12)	0.1195(17)	0.3032(14)	0.023(2)
C(4A)	0.716(6)	0.206(7)	0.382(6)	0.023(2)
C(5A)	0.9062(13)	0.0450(17)	0.2108(13)	0.023(2)
C(6A)	0.858(4)	0.028(5)	0.095(3)	0.023(2)

7.4.3 1,5-Di(tert-butyl)-3-methylformazano-bis(tetrahydrofuran)-kalium(I) (dgh350kris)

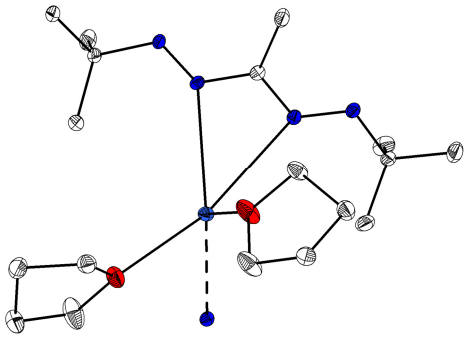

Kristalldaten

C18 H37 K N4 O2	M = 380.61 g/mol	Monoclinic, $P2_1/c$
a = 9.5707(4) Å	b = 19.8203(8) Å	c = 12.1953(5) Å
α = 90°	β = 111.3730(10)°	γ = 90°
V = 2154.28(15) Å^3	Z = 4	F(000) = 832
D_{calc} = 1.174 g/cm^3	μ = 0.264 mm^{-1}	
yellow block	0.181 · 0.135 · 0.078 mm^3	

Datensammlung

Diffraktometer: D8 Quest (Bruker)	T = 100(2) K	λ = 0.71073 Å
h = -12 bis 12	k = -25 bis 25	l = -15 bis 15
64291 gemessene Reflexe	4764 unabhängige Reflexe	3945 Reflexe mit $I > 2\sigma(I)$
θ = 2.285 bis 27.142°	R_{int} = 0.0821	C (25.00°) = 0.999
Absorptionskorrektur: Multi-scan	T_{min} = 0.6923	T_{max} = 0.7455

Verfeinerung

4764 Reflexe	0 Restraints	233 Parameter
Verfeinerung mit SHELXL-2014/7	bis χ = 0.001	
R_1 ($I > 2\sigma(I)$) = 0.0374	wR_2 ($I > 2\sigma(I)$) = 0.0757	
R_1 (all) = 0.0516	wR_2 (all) = 0.0814	GoF (S) = 1.079
$\Delta\varphi_{min}$ = -0.246 e·Å^{-3}	$\Delta\varphi_{max}$ = 0.301 e·Å^{-3}	

Fraktionelle Atomkoordinaten (*x, y, z*) und äquivalente isotrope Auslenkungsfaktoren *U*(eq)

	x	*y*	*z*	*U*(eq)/Å^2
K(1)	0.5099(1)	0.2998(1)	0.7131(1)	0.0114(1)
N(2)	0.2701(1)	0.3348(1)	0.7947(1)	0.0102(2)
N(4)	0.3889(1)	0.2376(1)	0.8720(1)	0.0100(2)
N(1)	0.2036(1)	0.3898(1)	0.8058(1)	0.0111(2)
O(2)	0.6798(1)	0.3887(1)	0.8784(1)	0.0263(3)
O(1)	0.7920(1)	0.2652(1)	0.7291(1)	0.0196(2)
C(3)	0.3239(2)	0.2944(1)	0.8915(1)	0.0102(3)
C(4)	0.1398(2)	0.4271(1)	0.6925(1)	0.0123(3)
C(18)	0.8033(2)	0.4948(1)	0.9313(1)	0.0170(3)
C(10)	0.5989(2)	0.1456(1)	0.8536(1)	0.0170(3)
C(6)	0.0926(2)	0.4958(1)	0.7236(1)	0.0220(4)
C(13)	0.9269(2)	0.2584(1)	0.8322(1)	0.0177(3)
C(7)	0.0026(2)	0.3886(1)	0.6114(1)	0.0198(3)
C(19)	0.6452(2)	0.4991(1)	0.9339(1)	0.0185(3)
C(5)	0.2526(2)	0.4364(1)	0.6315(1)	0.0182(3)
C(20)	0.6116(2)	0.4256(1)	0.9472(1)	0.0195(3)
C(14)	0.9930(2)	0.1909(1)	0.8185(2)	0.0216(3)
C(17)	0.8028(2)	0.4280(1)	0.8708(2)	0.0269(4)
C(15)	0.9579(2)	0.1892(1)	0.6865(2)	0.0249(4)
C(16)	0.8068(2)	0.2246(1)	0.6366(2)	0.0318(4)
N(5)	0.4404(1)	0.1953(1)	0.9597(1)	0.0100(2)
C(9)	0.4953(2)	0.1322(1)	0.9218(1)	0.0114(3)
C(8)	0.3079(2)	0.3103(1)	1.0061(1)	0.0154(3)
C(12)	0.5825(2)	0.0937(1)	1.0342(1)	0.0136(3)
C(11)	0.3594(2)	0.0909(1)	0.8453(1)	0.0168(3)

7.4.4 Chloro-1,5-di(tert-butyl)-3-methylformazano-zinn(II) (dgh363)

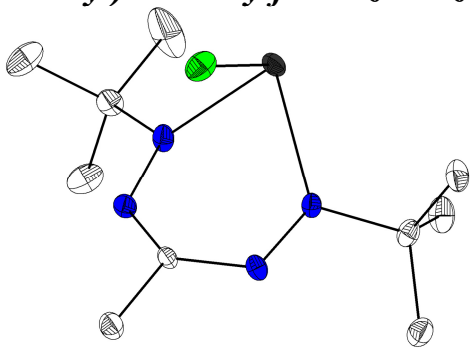

Kristalldaten

C10 H21 Cl N4 Sn	M = 351.45 g/mol	Monoclinic, $P2_1/c$
a = 10.9238(7) Å	b = 11.5431(7) Å	c = 11.9611(7) Å
α = 90°	β = 104.158(2)°	γ = 90°
V = 1462.42(16) Å^3	Z = 4	F(000) = 704
D_{calc} = 1.596 g/cm^3	μ = 1.913 mm^{-1}	
red plate	0.394 · 0.233 · 0.052 mm^3	

Datensammlung

Diffraktometer: D8 Quest (Bruker)	T = 100(2) K	λ = 0.71073 Å
h = -14 bis 14	k = -14 bis 14	l = -15 bis 15
13504 gemessene Reflexe	3160 unabhängige Reflexe	2573 Reflexe mit $I > 2\sigma(I)$
θ = 2.489 bis 27.135°	R_{int} = 0.0430	C (25.00°) = 0.983
Absorptionskorrektur: Multi-scan	T_{min} = 0.5942	T_{max} = 0.7455

Verfeinerung

3160 Reflexe	0 Restraints	152 Parameter
Verfeinerung mit SHELXL-2014/7	bis χ = 0.000	
R_1 ($I > 2\sigma(I)$) = 0.0349	wR_2 ($I > 2\sigma(I)$) = 0.0574	
R_1 (all) = 0.0516	wR_2 (all) = 0.0624	GoF (S) = 1.096
$\Delta\varphi_{min}$ = -0.963 e·Å^{-3}	$\Delta\varphi_{max}$ = 0.502 e·Å^{-3}	

Fraktionelle Atomkoordinaten (*x, y, z*) und äquivalente isotrope Auslenkungsfaktoren *U*(eq)

	x	*y*	*z*	*U*(eq)/Å^2		*x*	*y*	*z*	*U*(eq)/Å^2
C(3)	0.2750(3)	0.0644(3)	0.3758(3)	0.0107(7)	C(11)	0.5671(3)	0.2564(3)	0.2918(3)	0.0250(8)
C(4)	-0.0347(3)	0.1944(3)	0.2730(3)	0.0140(7)	C(12)	0.4968(4)	0.3365(3)	0.4592(3)	0.0224(9)
C(5)	-0.1130(3)	0.1657(3)	0.1525(3)	0.0193(8)	N(1)	0.0999(3)	0.1642(2)	0.2755(2)	0.0116(6)
C(6)	-0.0374(4)	0.3248(3)	0.2976(4)	0.0205(8)	N(2)	0.1494(3)	0.0862(2)	0.3492(2)	0.0117(6)
C(7)	-0.0828(3)	0.1266(3)	0.3631(3)	0.0185(8)	N(4)	0.3671(3)	0.1384(2)	0.3698(3)	0.0134(6)
C(8)	0.3147(3)	-0.0459(3)	0.4411(3)	0.0163(7)	N(5)	0.3471(3)	0.2296(2)	0.3035(3)	0.0142(6)
C(9)	0.4574(3)	0.3129(3)	0.3304(3)	0.0156(8)	Cl(1)	0.2331(1)	0.0452(1)	0.0901(1)	0.0213(2)
C(10)	0.4172(4)	0.4241(4)	0.2634(5)	0.0450(14)	Sn(1)	0.1931(1)	0.2426(1)	0.1494(1)	0.0151(1)

7.4.5 2-(tert-Butyl)-hydrazin-1-carbothio-N,N-dimethylamid (dgh376)

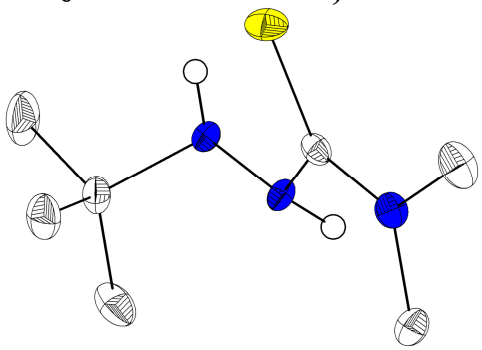

Kristalldaten

C7 H17 N3 S	M = 175.29 g/mol	Monoclinic, $P2_1/n$
a = 5.9735(2) Å	b = 16.9693(8) Å	c = 10.1186(4) Å
α = 90°	β = 95.6060(10)°	γ = 90°
V = 1020.78(7) Å^3	Z = 4	F(000) = 384
D_{calc} = 1.141 g/cm^3	μ = 0.267 mm^{-1}	
colourless plate	0.290 · 0.260 · 0.090 mm^3	

Datensammlung

Diffraktometer: D8 Quest (Bruker)	T = 100(2) K	λ = 0.71073 Å
h = -7 bis 7	k = -21 bis 21	l = -12 bis 12
19050 gemessene Reflexe	2262 unabhängige Reflexe	2079 Reflexe mit $I > 2\sigma(I)$
θ = 2.352 bis 27.124°	R_{int} = 0.0233	C (25.00°) = 1.000
Absorptionskorrektur: Multi-scan	T_{min} = 0.7244	T_{max} = 0.7455

Verfeinerung

2262 Reflexe	2 Restraints	113 Parameter
Verfeinerung mit SHELXL-2014/7	bis χ = 0.001	
R_1 ($I > 2\sigma(I)$) = 0.0295	wR_2 ($I > 2\sigma(I)$) = 0.0745	
R_1 (all) = 0.0334	wR_2 (all) = 0.0763	GoF (S) = 1.109
$\Delta\varphi_{min}$ = -0.198 e·Å^{-3}	$\Delta\varphi_{max}$ = 0.235 e·Å^{-3}	

Kommentar

Die N-H Bindungen wurden über DFIX restrained.

Fraktionelle Atomkoordinaten (*x, y, z*) und äquivalente isotrope Auslenkungsfaktoren *U*(eq)

	x	*y*	*z*	*U*(eq)/Å^2
C(3)	0.5959(2)	0.0161(1)	0.2636(1)	0.0139(2)
C(4)	0.3599(2)	0.1583(1)	0.0519(1)	0.0176(2)
C(5)	0.3132(2)	0.1906(1)	0.1876(1)	0.0249(3)
C(6)	0.1438(2)	0.1260(1)	-0.0214(1)	0.0267(3)
C(7)	0.4588(3)	0.2224(1)	-0.0305(2)	0.0351(3)
C(8)	0.3024(2)	-0.0810(1)	0.2948(1)	0.0195(2)
C(9)	0.6645(2)	-0.0839(1)	0.4382(1)	0.0249(3)
N(1)	0.5311(2)	0.0938(1)	0.0626(1)	0.0137(2)
N(2)	0.4685(2)	0.0318(1)	0.1470(1)	0.0133(2)
N(3)	0.5243(2)	-0.0463(1)	0.3298(1)	0.0168(2)
S(1)	0.8201(1)	0.0720(1)	0.3179(1)	0.0210(1)

7.4.6 Bis-(1,5-di(tert-butyl)-3-methylformazano)-zink(II) (dgh393)

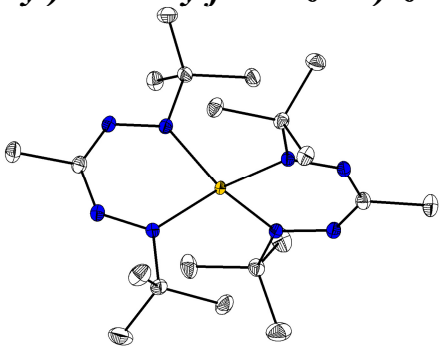

Kristalldaten

C20 H42 N8 Zn	M = 459.98 g/mol	Monoclinic, $C2/c$
a = 15.3906(6) Å	b = 9.5752(6) Å	c = 16.9980(7) Å
α = 90°	β = 90.019(2)°	γ = 90°
V = 2505.0(2) Å^3	Z = 4	F(000) = 992
D_{calc} = 1.220 g/cm^3	μ = 1.002 mm^{-1}	
orange plate	0.445 · 0.297 · 0.064 mm^3	

Datensammlung

Diffraktometer: D8 Quest (Bruker)	T = 100(2) K	λ = 0.71073 Å
h = -19 bis 19	k = -12 bis 12	l = -21 bis 21
27219 gemessene Reflexe	2777 unabhängige Reflexe	2600 Reflexe mit $I > 2\sigma(I)$
θ = 2.396 bis 27.154°	R_{int} = 0.0300	C (25.00°) = 1.000
Absorptionskorrektur: Multi-scan	T_{min} = 0.6780	T_{max} = 0.7455

Verfeinerung

2777 Reflexe	0 Restraints	139 Parameter
Verfeinerung mit SHELXL-2014/7	bis χ = 0.000	
R_1 ($I > 2\sigma(I)$) = 0.0232	wR_2 ($I > 2\sigma(I)$) = 0.0534	
R_1 (all) = 0.0263	wR_2 (all) = 0.0544	GoF (S) = 1.112
$\Delta\varphi_{min}$ = -0.236 e·Å^{-3}	$\Delta\varphi_{max}$ = 0.324 e·Å^{-3}	

Fraktionelle Atomkoordinaten (*x, y, z*) und äquivalente isotrope Auslenkungsfaktoren *U*(eq)

	x	*y*	*z*	*U*(eq)/Å^2
Zn(1)	0.5000	0.4225(1)	0.7500	0.0096(1)
N(1)	0.6097(1)	0.5328(1)	0.7382(1)	0.0113(2)
N(2)	0.6623(1)	0.5231(1)	0.6791(1)	0.0122(2)
N(3)	0.5868(1)	0.3412(1)	0.6029(1)	0.0127(2)
N(4)	0.5217(1)	0.3196(1)	0.6494(1)	0.0115(2)
C(5)	0.6527(1)	0.7805(1)	0.7550(1)	0.0190(3)
C(4)	0.6426(1)	0.6398(1)	0.7964(1)	0.0132(3)
C(3)	0.6495(1)	0.4357(1)	0.6180(1)	0.0133(3)
C(10)	0.5138(1)	0.0718(2)	0.6072(1)	0.0266(3)
C(12)	0.3891(1)	0.1882(2)	0.6747(1)	0.0221(3)
C(6)	0.7298(1)	0.5906(2)	0.8297(1)	0.0166(3)
C(9)	0.4630(1)	0.2079(1)	0.6165(1)	0.0151(3)
C(11)	0.4269(1)	0.2554(2)	0.5372(1)	0.0232(3)
C(8)	0.7188(1)	0.4450(2)	0.5553(1)	0.0182(3)
C(7)	0.5756(1)	0.6520(2)	0.8622(1)	0.0171(3)

7.4.7 2-Carbonitrile-4-(dimethylamin)-6-(2,2-dimethylhydrazinyl)-1,3,5-triazin (dghhb03)

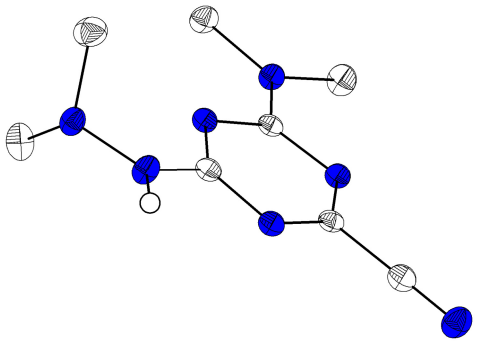

Kristalldaten

C8 H13 N7	M = 207.25 g/mol	Monoclinic, $C2/m$
a = 19.0856(9) Å	b = 6.5561(3) Å	c = 9.0885(4) Å
α = 90°	β = 111.665(2)°	γ = 90°
V = 1056.88(8) Å^3	Z = 4	F(000) = 440
D_{calc} = 1.303 g/cm^3	μ = 0.090 mm^{-1}	
colourless plate	0.310 · 0.260 · 0.060 mm^3	

Datensammlung

Diffraktometer: D8 Quest (Bruker)	T = 100(2) K	λ = 0.71073 Å
h = -24 bis 24	k = -8 bis 8	l = -11 bis 11
16616 gemessene Reflexe	1279 unabhängige Reflexe	1111 Reflexe mit $I > 2\sigma(I)$
θ = 2.296 bis 27.133°	R_{int} = 0.0323	C (25.00°) = 0.999
Absorptionskorrektur: Multi-scan	T_{min} = 0.7174	T_{max} = 0.7455

Verfeinerung

1279 Reflexe	4 Restraints	92 Parameter
Verfeinerung mit SHELXL-2014/7	bis χ = 0.000	
R_1 ($I > 2\sigma(I)$) = 0.0443	wR_2 ($I > 2\sigma(I)$) = 0.1144	
R_1 (all) = 0.0516	wR_2 (all) = 0.1184	GoF (S) = 1.069
$\Delta\varphi_{min}$ = -0.293 e·Å^{-3}	$\Delta\varphi_{max}$ = 0.254 e·Å^{-3}	

Kommentar

Zwei Methylgruppen liegen auf einer Spiegelebene, weswegen die Standardberechnung über AFIX 137 nicht möglich war. Die H-Atome wurden in der FT-Karte gefunden, isotrop verfeinert, mit DFIX restrained über AFIX 3 an den entsprechenden C-Atomen constrained.

Fraktionelle Atomkoordinaten (*x, y, z*) und äquivalente isotrope Auslenkungsfaktoren *U*(eq)

	x	*y*	*z*	*U*(eq)/Å^2		*x*	*y*	*z*	*U*(eq)/Å^2
C(1)	0.6478(1)	0.5000	0.4756(2)	0.0160(4)	N(1)	0.6639(1)	0.5000	0.3449(2)	0.0156(4)
C(2)	0.7383(1)	0.5000	0.3702(2)	0.0141(4)	N(2)	0.7947(1)	0.5000	0.5158(2)	0.0165(4)
C(3)	0.7687(1)	0.5000	0.6325(2)	0.0148(4)	N(3)	0.6987(1)	0.5000	0.6278(2)	0.0165(4)
C(4)	0.5050(1)	0.3141(3)	0.2307(2)	0.0281(4)	N(4)	0.5755(1)	0.5000	0.4644(2)	0.0205(4)
C(5)	0.7041(1)	0.5000	0.0833(2)	0.0199(4)	N(5)	0.5109(1)	0.5000	0.3233(2)	0.0193(4)
C(6)	0.8387(1)	0.5000	0.2661(2)	0.0225(4)	N(6)	0.7592(1)	0.5000	0.2448(2)	0.0165(4)
C(7)	0.8272(1)	0.5000	0.7922(2)	0.0187(4)	N(7)	0.8725(1)	0.5000	0.9167(2)	0.0252(4)

7.4.8 N'^1,N'^2-Di-tert-butyl-oxalhydrazonamid (dghhb04)

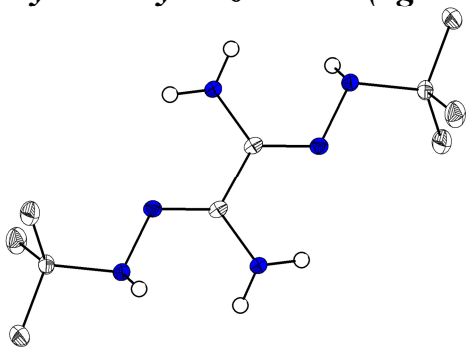

Kristalldaten

C10 H24 N6	M = 228.35 g/mol	Tetragonal, $I4_1/a$
a = 12.1374(5) Å	b = 12.1374(5) Å	c = 19.4319(12) Å
α = 90°	β = 90°	γ = 90°
V = 2862.6(3) Å^3	Z = 8	F(000) = 1008
D_{calc} = 1.060 g/cm^3	μ = 0.069 mm^{-1}	
colourless block	0.290 · 0.210 · 0.090 mm^3	

Datensammlung

Diffraktometer: D8 Quest (Bruker)	T = 100(2) K	λ = 0.71073 Å
h = -15 bis 15	k = -15 bis 14	l = -24 bis 24
15212 gemessene Reflexe	1586 unabhängige Reflexe	1334 Reflexe mit $I > 2\sigma(I)$
θ = 3.167 bis 27.139°	R_{int} = 0.0449	C (25.00°) = 0.999
Absorptionskorrektur: Multi-scan	T_{min} = 0.7047	T_{max} = 0.7455

Verfeinerung

1586 Reflexe	0 Restraints	88 Parameter
Verfeinerung mit SHELXL-2014/7	bis χ = 0.000	
R_1 ($I > 2\sigma(I)$) = 0.0409	wR_2 ($I > 2\sigma(I)$) = 0.0918	
R_1 (all) = 0.0534	wR_2 (all) = 0.0963	GoF (S) = 1.102
$\Delta\varphi_{min}$ = -0.214 e·Å^{-3}	$\Delta\varphi_{max}$ = 0.256 e·Å^{-3}	

Fraktionelle Atomkoordinaten (*x, y, z*) und äquivalente isotrope Auslenkungsfaktoren *U*(eq)

	x	*y*	*z*	*U*(eq)/Å^2		*x*	*y*	*z*	*U*(eq)/Å^2
N(1)	0.1580(1)	0.1830(1)	0.5088(1)	0.0133(2)	C(4)	0.2318(1)	0.2400(1)	0.4593(1)	0.0142(3)
N(2)	0.1042(1)	0.0933(1)	0.4780(1)	0.0126(2)	C(5)	0.1677(1)	0.2804(1)	0.3962(1)	0.0220(3)
N(3)	-0.0058(1)	0.0857(1)	0.5788(1)	0.0141(2)	C(6)	0.3213(1)	0.1590(1)	0.4381(1)	0.0232(3)
C(3)	0.0288(1)	0.0483(1)	0.5146(1)	0.0113(3)	C(7)	0.2819(1)	0.3368(1)	0.4983(1)	0.0210(3)

7.4.9 N'[1],N'[2]-Di-tert-butyl-oxalhydrazonamido-tetrakis(dimethyl-aluminium(III)) (dghhb07)

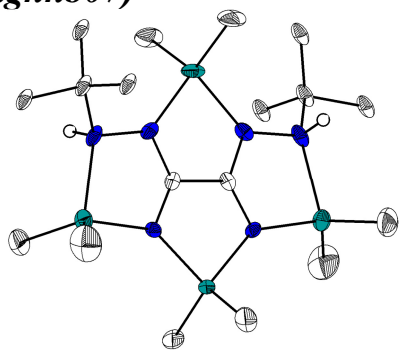

Kristalldaten

C18 H44 Al4 N6	M = 452.51 g/mol	Orthorhombic, *Pbcn*
a = 11.4550(8) Å	b = 18.1479(11) Å	c = 13.3424(8) Å
α = 90°	β = 90°	γ = 90°
V = 2773.7(3) Å^3	Z = 4	F(000) = 984
D_{calc} = 1.084 g/cm^3	μ = 0.183 mm^{-1}	
colourless block	0.250 · 0.200 · 0.200 mm^3	

Datensammlung

Diffraktometer: D8 Quest (Bruker)	T = 100(2) K	λ = 0.71073 Å
h = -13 bis 13	k = -21 bis 21	l = -15 bis 16
25569 gemessene Reflexe	2577 unabhängige Reflexe	2445 Reflexe mit $I > 2\sigma(I)$
θ = 2.598 bis 25.497°	R_{int} = 0.0503	C (25.00°) = 0.999
Absorptionskorrektur: Multi-scan	T_{min} = 0.6755	T_{max} = 0.7455

Verfeinerung

2577 Reflexe	15 Restraints	137 Parameter
Verfeinerung mit SHELXL-2014/7	bis χ = 0.000	
R_1 ($I > 2\sigma(I)$) = 0.1265	wR_2 ($I > 2\sigma(I)$) = 0.2944	
R_1 (all) = 0.1293	wR_2 (all) = 0.2954	GoF (S) = 1.341
$\Delta\varphi_{min}$ = -0.889 e·Å^{-3}	$\Delta\varphi_{max}$ = 0.610 e·Å^{-3}	

Kommentar

Die Tertbutylgruppe ist über zwei Positionen fehlgeordnet (48:52) und wurde über EADP constrained. Einzelne Atome des Komplexes wurden über DELU und SIMU restrained.

Fraktionelle Atomkoordinaten (*x, y, z*) und äquivalente isotrope Auslenkungsfaktoren *U*(eq)

	x	*y*	*z*	*U*(eq)/Å^2
C(3)	0.5536(6)	0.5336(4)	0.2832(5)	0.0133(13)
C(8)	0.8652(9)	0.4393(7)	0.3392(9)	0.059(3)
C(9)	0.6868(10)	0.4663(5)	0.5372(6)	0.046(2)
C(10)	0.4277(9)	0.7365(4)	0.3600(6)	0.037(2)
C(11)	0.5851(9)	0.3391(5)	0.1450(7)	0.040(2)
N(1)	0.6901(5)	0.5944(3)	0.3771(4)	0.0220(13)
N(2)	0.5943(5)	0.6004(3)	0.3057(4)	0.0167(12)
N(4)	0.5939(5)	0.4694(3)	0.3110(4)	0.0144(12)
Al(1)	0.7218(2)	0.4820(1)	0.3959(2)	0.0215(6)
Al(2)	0.5000	0.6799(2)	0.2500	0.0255(8)
Al(3)	0.5000	0.3946(2)	0.2500	0.0211(7)
C(4A)	0.781(2)	0.6540(12)	0.3567(17)	0.0220(13)
C(5A)	0.870(2)	0.6376(15)	0.4386(14)	0.0220(13)
C(6A)	0.735(3)	0.7313(11)	0.3724(14)	0.0220(13)
C(7A)	0.8284(17)	0.6451(17)	0.2516(14)	0.0220(13)
C(4B)	0.802(2)	0.6387(16)	0.358(2)	0.025(3)
C(5B)	0.895(2)	0.6167(17)	0.4338(18)	0.025(3)
C(6B)	0.771(3)	0.7221(13)	0.3708(18)	0.025(3)
C(7B)	0.844(2)	0.6204(19)	0.2512(17)	0.025(3)

7.4.10 N'[1],N'[2]-Di-tert-butyl-oxalhydrazonamido-bis(dimethyl-gallium(III)) (dghhb08)

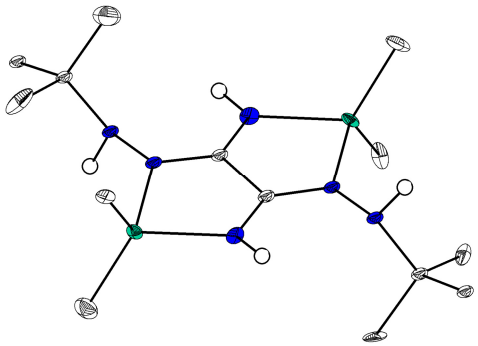

Kristalldaten

C14 H34 Ga2 N6	M = 425.91 g/mol	Orthorhombic, $P2_12_12_1$
a = 6.3749(8) Å	b = 16.4353(19) Å	c = 19.319(2) Å
α = 90°	β = 90°	γ = 90°
V = 2024.1(4) Å^3	Z = 4	F(000) = 888
D_{calc} = 1.398 g/cm^3	μ = 2.668 mm^{-1}	
colourless needle	0.650 · 0.080 · 0.040 mm^3	

Datensammlung

Diffraktometer: D8 Quest (Bruker)	T = 100(2) K	λ = 0.71073 Å
h = -8 bis 8	k = -18 bis 20	l = -24 bis 24
15109 gemessene Reflexe	4445 unabhängige Reflexe	3205 Reflexe mit $I > 2\sigma(I)$
θ = 2.108 bis 27.169°	R_{int} = 0.1034	C (25.00°) = 0.998
Absorptionskorrektur: Multi-scan	T_{min} = 0.5982	T_{max} = 0.7455

Verfeinerung

4445 Reflexe	28 Restraints	168 Parameter
Verfeinerung mit SHELXL-2014/7	bis χ = 0.000	
R_1 ($I > 2\sigma(I)$) = 0.0644	wR_2 ($I > 2\sigma(I)$) = 0.1058	
R_1 (all) = 0.1044	wR_2 (all) = 0.1155	GoF (S) = 1.062
$\Delta\varphi_{min}$ = -1.316 e·Å^{-3}	$\Delta\varphi_{max}$ = 1.097 e·Å^{-3}	

Kommentar

Die Struktur wurde als Inversionszwilling verfeinert. Die N-H Bindungen wurden über DFIX, einzelne Atome über ISOR re- und EADP constrained.

Fraktionelle Atomkoordinaten (*x, y, z*) und äquivalente isotrope Auslenkungsfaktoren *U*(eq)

	x	*y*	*z*	*U*(eq)/Å^2
C(3)	0.3560(15)	0.5957(5)	0.2442(4)	0.0095(5)
C(4)	0.1677(14)	0.6471(5)	0.2598(4)	0.0095(5)
C(5)	0.7048(13)	0.5332(6)	0.1242(4)	0.0095(5)
C(6)	0.6671(17)	0.5814(6)	0.0568(4)	0.016(2)
C(7)	0.9318(12)	0.5047(6)	0.1282(4)	0.0095(5)
C(8)	0.5608(15)	0.4583(6)	0.1264(5)	0.017(2)
C(9)	-0.1844(13)	0.7099(5)	0.3820(4)	0.0095(5)
C(10)	-0.4156(13)	0.7360(6)	0.3774(4)	0.0095(5)
C(11)	-0.1560(19)	0.6567(6)	0.4468(5)	0.027(3)
C(12)	-0.0397(16)	0.7825(7)	0.3825(6)	0.032(3)
C(13)	0.2266(15)	0.7154(7)	0.0570(5)	0.016(2)
C(14)	0.5748(15)	0.8085(6)	0.1668(5)	0.019(2)
C(15)	-0.0608(15)	0.4347(6)	0.3367(5)	0.021(2)
C(16)	0.2952(15)	0.5264(6)	0.4469(5)	0.013(2)
N(1)	0.6707(12)	0.5812(4)	0.1878(4)	0.0095(5)
N(2)	0.4723(11)	0.6221(5)	0.1923(4)	0.0095(5)
N(3)	0.3790(11)	0.5324(5)	0.2855(4)	0.0107(17)
N(4)	-0.1486(12)	0.6639(4)	0.3169(4)	0.0095(5)
N(5)	0.0513(11)	0.6222(4)	0.3126(4)	0.0095(5)
N(6)	0.1402(13)	0.7106(5)	0.2190(4)	0.0128(17)
Ga(1)	0.3620(2)	0.7249(1)	0.1481(1)	0.0105(2)
Ga(2)	0.1570(1)	0.5178(1)	0.3556(1)	0.0096(2)

7.4.11 N'[1],N'[2]-Di-(tert-butyl)-oxalhydrazonamido-bis(dimethyl-dimethylaminopyridin-indium(III)) (dghhb11)

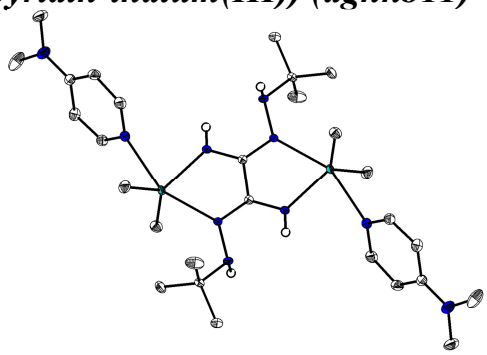

Kristalldaten

C28 H54 In2 N10	M = 760.45 g/mol	Monoclinic, $P2_1/n$
a = 8.1643(5) Å	b = 21.3853(11) Å	c = 10.2892(6) Å
α = 90°	β = 108.928(2)°	γ = 90°
V = 1699.31(17) Å^3	Z = 2	F(000) = 780
D_{calc} = 1.486 g/cm^3	μ = 1.390 mm^{-1}	
colourless block	0.440 · 0.220 · 0.130 mm^3	

Datensammlung

Diffraktometer: D8 Quest (Bruker)	T = 100(2) K	λ = 0.71073 Å
h = -10 bis 10	k = -27 bis 27	l = -12 bis 13
45687 gemessene Reflexe	3771 unabhängige Reflexe	3531 Reflexe mit $I > 2\sigma(I)$
θ = 2.299 bis 27.153°	R_{int} = 0.0365	C (25.00°) = 0.999
Absorptionskorrektur: Multi-scan	T_{min} = 0.6350	T_{max} = 0.7455

Verfeinerung

3771 Reflexe	0 Restraints	197 Parameter
Verfeinerung mit SHELXL-2014/7	bis χ = 0.001	
R_1 ($I > 2\sigma(I)$) = 0.0164	wR_2 ($I > 2\sigma(I)$) = 0.0389	
R_1 (all) = 0.0183	wR_2 (all) = 0.0395	GoF (S) = 1.138
$\Delta\varphi_{min}$ = -0.534 e·Å^{-3}	$\Delta\varphi_{max}$ = 0.385 e·Å^{-3}	

Fraktionelle Atomkoordinaten (*x, y, z*) und äquivalente isotrope Auslenkungsfaktoren *U*(eq)

	x	*y*	*z*	*U*(eq)/Å^2		*x*	*y*	*z*	*U*(eq)/Å^2
C(1)	0.4187(2)	0.0072(1)	0.9406(1)	0.0094(3)	C(9)	1.2956(2)	0.1019(1)	1.1925(2)	0.0173(3)
C(14)	1.5572(2)	0.2427(1)	1.3528(2)	0.0323(4)	C(10)	1.3454(2)	0.1622(1)	1.2470(1)	0.0144(3)
N(3)	0.2818(2)	-0.0280(1)	0.9294(1)	0.0124(2)	C(11)	1.2092(2)	0.2054(1)	1.2290(2)	0.0165(3)
C(2)	0.2726(2)	0.0900(1)	0.6257(2)	0.0127(3)	C(12)	1.0411(2)	0.1869(1)	1.1636(2)	0.0155(3)
C(3)	0.3661(2)	0.1526(1)	0.6363(2)	0.0196(3)	C(13)	1.6517(2)	0.1328(1)	1.3385(2)	0.0274(4)
C(4)	0.0835(2)	0.0992(1)	0.5375(2)	0.0214(3)	N(1)	0.4319(2)	0.0541(1)	0.8609(1)	0.0123(2)
C(5)	0.3567(2)	0.0411(1)	0.5613(2)	0.0272(4)	N(2)	0.2661(2)	0.0659(1)	0.7581(1)	0.0177(3)
C(6)	0.8174(2)	0.0941(1)	0.7848(2)	0.0191(3)	N(4)	0.9933(2)	0.1301(1)	1.1101(1)	0.0143(2)
C(7)	0.5844(2)	0.1936(1)	0.9957(2)	0.0172(3)	N(5)	1.5126(2)	0.1783(1)	1.3127(1)	0.0209(3)
C(8)	1.1239(2)	0.0891(1)	1.1264(2)	0.0174(3)	In(1)	0.6982(1)	0.1092(1)	0.9432(1)	0.0101(1)

7.4.12 N',2-Di-(tert-butyl)-hydrazin-1-carbothiohydrazid (dgh500)

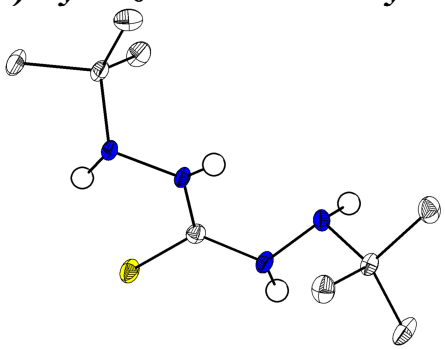

Kristalldaten

C9 H22 N4 S	M = 218.36 g/mol	Monoclinic, $P2_1/c$
a = 12.1326(5) Å	b = 11.7275(4) Å	c = 18.3136(6) Å
α = 90°	β = 94.323(2)°	γ = 90°
V = 2598.34(16) Å^3	Z = 8	F(000) = 960
D_{calc} = 1.116 g/cm^3	μ = 0.224 mm^{-1}	
colourless plate	0.260 · 0.180 · 0.060 mm^3	

Datensammlung

Diffraktometer: D8 Quest (Bruker)	T = 100(2) K	λ = 0.71073 Å
h = -15 bis 15	k = -15 bis 15	l = -23 bis 23
39629 gemessene Reflexe	5766 unabhängige Reflexe	4622 Reflexe mit $I > 2\sigma(I)$
θ = 2.230 bis 27.207°	R_{int} = 0.0538	C (25.00°) = 0.999
Absorptionskorrektur: Multi-scan	T_{min} = 0.6704	T_{max} = 0.7455

Verfeinerung

5766 Reflexe	0 Restraints	297 Parameter
Verfeinerung mit SHELXL-2014/7	bis χ = 0.000	
R_1 ($I > 2\sigma(I)$) = 0.0349	wR_2 ($I > 2\sigma(I)$) = 0.0740	
R_1 (all) = 0.0510	wR_2 (all) = 0.0795	GoF (S) = 1.024
$\Delta\varphi_{min}$ = -0.304 e·Å^{-3}	$\Delta\varphi_{max}$ = 0.253 e·Å^{-3}	

Fraktionelle Atomkoordinaten (*x, y, z*) und äquivalente isotrope Auslenkungsfaktoren *U*(eq)

	x	*y*	*z*	*U*(eq)/Å^2		*x*	*y*	*z*	*U*(eq)/Å^2
C(3)	0.6069(1)	0.2420(1)	0.2398(1)	0.0123(3)	C(18)	-0.0980(1)	0.1550(1)	0.1017(1)	0.0137(3)
C(4)	0.7668(1)	0.0549(1)	0.3564(1)	0.0152(3)	C(19)	0.0014(1)	0.1489(1)	0.0556(1)	0.0199(3)
C(5)	0.8544(1)	0.1304(1)	0.3963(1)	0.0236(3)	C(20)	-0.1273(1)	0.2784(1)	0.1173(1)	0.0221(3)
C(6)	0.8151(1)	-0.0630(1)	0.3442(1)	0.0273(3)	C(21)	-0.1966(1)	0.0931(1)	0.0629(1)	0.0236(3)
C(7)	0.6650(1)	0.0471(1)	0.3997(1)	0.0261(3)	N(1)	0.7330(1)	0.0971(1)	0.2817(1)	0.0137(2)
C(8)	0.4220(1)	0.1414(1)	0.1031(1)	0.0137(3)	N(2)	0.6999(1)	0.2128(1)	0.2803(1)	0.0141(2)
C(9)	0.4933(1)	0.2157(1)	0.0570(1)	0.0191(3)	N(4)	0.5423(1)	0.1565(1)	0.2144(1)	0.0132(2)
C(10)	0.4511(1)	0.0160(1)	0.0959(1)	0.0219(3)	N(5)	0.4336(1)	0.1743(1)	0.1823(1)	0.0129(2)
C(11)	0.3000(1)	0.1589(1)	0.0807(1)	0.0248(3)	N(11)	0.2223(1)	0.1619(1)	0.2758(1)	0.0135(2)
C(13)	0.0993(1)	0.0238(1)	0.2204(1)	0.0128(3)	N(12)	0.1926(1)	0.0464(1)	0.2628(1)	0.0142(2)
C(14)	0.2562(1)	0.1876(1)	0.3538(1)	0.0137(3)	N(14)	0.0289(1)	0.1102(1)	0.2076(1)	0.0134(2)
C(15)	0.2931(1)	0.3117(1)	0.3528(1)	0.0208(3)	N(15)	-0.0789(1)	0.0934(1)	0.1733(1)	0.0131(2)
C(16)	0.3513(1)	0.1119(1)	0.3845(1)	0.0219(3)	S(1)	0.5746(1)	0.3806(1)	0.2238(1)	0.0166(1)
C(17)	0.1564(1)	0.1738(1)	0.3983(1)	0.0210(3)	S(2)	0.0734(1)	-0.1094(1)	0.1874(1)	0.0180(1)

7.4.13 Dichloro-1,5-di(tert-butyl)-3-methylformazano-indium(III) (dgh434)

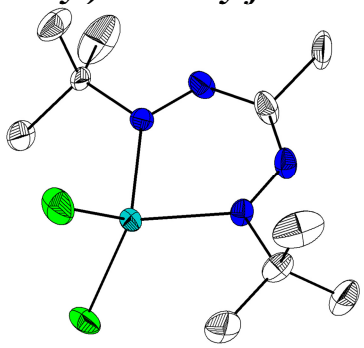

Kristalldaten

C10 H21 Cl2 In N4	M = 383.03 g/mol	Monoclinic, $P2_1/c$
a = 11.1065(6) Å	b = 9.1388(4) Å	c = 16.4206(7) Å
α = 90°	β = 101.907(2)°	γ = 90°
V = 1630.83(13) Å^3	Z = 4	F(000) = 768
D_{calc} = 1.560 g/cm^3	μ = 1.764 mm^{-1}	
yellow needle	0.204 · 0.089 · 0.047 mm^3	

Datensammlung

Diffraktometer: D8 Quest (Bruker)	T = 100(2) K	λ = 0.71073 Å
h = -14 bis 14	k = -11 bis 11	l = -21 bis 21
39868 gemessene Reflexe	3611 unabhängige Reflexe	2745 Reflexe mit $I > 2\sigma(I)$
θ = 2.535 bis 27.144°	R_{int} = 0.0677	C (25.00°) = 1.000
Absorptionskorrektur: Multi-scan	T_{min} = 0.6833	T_{max} = 0.7455

Verfeinerung

3611 Reflexe	52 Restraints	212 Parameter
Verfeinerung mit SHELXL-2014/7	bis χ = 0.004	
R_1 ($I > 2\sigma(I)$) = 0.0193	wR_2 ($I > 2\sigma(I)$) = 0.0385	
R_1 (all) = 0.0331	wR_2 (all) = 0.0411	GoF (S) = 0.999
$\Delta\varphi_{min}$ = -0.387 e·Å^{-3}	$\Delta\varphi_{max}$ = 0.316 e·Å^{-3}	

Kommentar

Eine *tert*-Butylgruppe (67:33) und die Methylgruppe (48:52) sind fehlgeordnet. Erstere wurde über DELU, RIGU, SAME und ISOR restrained.

Fraktionelle Atomkoordinaten (*x, y, z*) und äquivalente isotrope Auslenkungsfaktoren *U*(eq)

	x	*y*	*z*	*U*(eq)/Å^2
C(3)	0.1864(2)	0.2341(2)	0.9308(1)	0.0319(5)
C(4)	0.3741(2)	0.3272(2)	1.1328(1)	0.0294(5)
C(5)	0.4509(2)	0.4402(2)	1.0983(2)	0.0426(6)
C(6)	0.4560(2)	0.2312(3)	1.1965(1)	0.0434(6)
C(7)	0.2742(2)	0.4005(3)	1.1692(2)	0.0568(8)
C(9)	0.1519(8)	-0.1564(11)	0.9196(6)	0.0246(16)
C(10)	0.1328(9)	-0.1591(9)	0.8265(4)	0.067(2)
C(11)	0.0297(5)	-0.1821(8)	0.9476(5)	0.0418(15)
C(12)	0.2431(5)	-0.2742(6)	0.9598(6)	0.056(2)
C(8)	0.1455(19)	0.3501(19)	0.8616(9)	0.040(3)
C(8A)	0.1092(18)	0.3298(17)	0.8669(10)	0.044(3)

	x	*y*	*z*	*U*(eq)/Å^2
Cl(1)	0.5240(1)	-0.1172(1)	1.0885(1)	0.0309(1)
Cl(2)	0.2403(1)	-0.0930(1)	1.1811(1)	0.0469(2)
In(1)	0.3305(1)	-0.0034(1)	1.0732(1)	0.0220(1)
N(1)	0.3130(1)	0.2276(2)	1.0629(1)	0.0215(3)
N(2)	0.2514(2)	0.2975(2)	0.9995(1)	0.0262(4)
N(4)	0.1595(1)	0.0928(2)	0.9111(1)	0.0268(4)
N(5)	0.2027(1)	-0.0170(2)	0.9578(1)	0.0220(3)
C(9A)	0.1493(17)	-0.171(2)	0.9274(11)	0.024(3)
C(10A)	0.1893(14)	-0.1884(15)	0.8446(9)	0.047(3)
C(11A)	0.0116(10)	-0.1615(16)	0.9102(10)	0.043(3)
C(12A)	0.2005(15)	-0.2827(12)	0.9901(7)	0.048(3)

7.5 Strukturen für Nicholas Rau

7.5.1 Bromo-(1-(2-(diphenylphosphanyl)phenyl)-3,5-dimethyl-pyrazol)-kupfer(I)-dimer- acetonitrilsolvat (nrm049b)

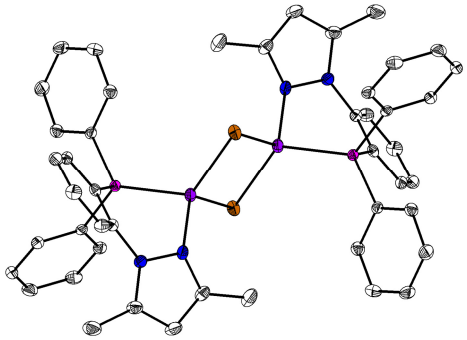

Kristalldaten

C50 H48 Br2 Cu2 N6 P2	M = 1081.78 g/mol	Triclinic, $P\bar{1}$
a = 9.2034(5) Å	b = 10.3705(6) Å	c = 13.4997(8) Å
α = 72.073(2)°	β = 72.563(2)°	γ = 79.322(2)°
V = 1163.41(12) Å^3	Z = 1	F(000) = 548
D_{calc} = 1.544 g/cm^3	μ = 2.742 mm^{-1}	
colourless block	0.270 · 0.160 · 0.120 mm^3	

Datensammlung

Diffraktometer: D8 Quest (Bruker)	T = 100(2) K	λ = 0.71069 Å
h = -12 bis 12	k = -13 bis 12	l = -17 bis 17
41297 gemessene Reflexe	5570 unabhängige Reflexe	4780 Reflexe mit $I > 2\sigma(I)$
θ = 2.332 bis 27.938°	R_{int} = 0.0415	C (25.00°) = 0.998
Absorptionskorrektur: Multi-scan	T_{min} = 0.6225	T_{max} = 0.7456

Verfeinerung

5570 Reflexe	0 Restraints	283 Parameter
Verfeinerung mit SHELXL-2014/7	bis χ = 0.001	
R_1 ($I > 2\sigma(I)$) = 0.0246	wR_2 ($I > 2\sigma(I)$) = 0.0509	
R_1 (all) = 0.0349	wR_2 (all) = 0.0542	GoF (S) = 1.036
$\Delta\varphi_{min}$ = -0.311 e·Å^{-3}	$\Delta\varphi_{max}$ = 0.381 e·Å^{-3}	

Fraktionelle Atomkoordinaten (*x, y, z*) und äquivalente isotrope Auslenkungsfaktoren *U*(eq)

	x	*y*	*z*	*U*(eq)/Å^2
C(1)	0.1840(2)	0.0548(2)	0.7624(1)	0.0123(3)
C(2)	0.2818(2)	0.1504(2)	0.6880(1)	0.0135(3)
C(3)	0.4321(2)	0.1423(2)	0.6919(2)	0.0172(4)
C(4)	0.4873(2)	0.0413(2)	0.7706(2)	0.0186(4)
C(5)	0.3916(2)	-0.0520(2)	0.8459(2)	0.0169(4)
C(6)	0.2416(2)	-0.0445(2)	0.8407(1)	0.0141(3)
C(7)	0.1649(2)	0.3544(2)	0.4577(2)	0.0185(4)
C(8)	0.2069(2)	0.4565(2)	0.4889(2)	0.0217(4)
C(9)	0.2486(2)	0.3940(2)	0.5828(2)	0.0195(4)
C(10)	0.1166(3)	0.3670(2)	0.3588(2)	0.0267(5)
C(11)	0.2977(3)	0.4542(2)	0.6535(2)	0.0286(5)
C(12)	-0.0803(2)	-0.0972(2)	0.8458(1)	0.0124(3)
C(13)	-0.0172(2)	-0.2233(2)	0.8266(2)	0.0168(4)
C(14)	-0.0742(2)	-0.3423(2)	0.8977(2)	0.0215(4)
C(15)	-0.1963(2)	-0.3366(2)	0.9865(2)	0.0220(4)
C(16)	-0.2611(2)	-0.2122(2)	1.0051(2)	0.0207(4)
C(17)	-0.2029(2)	-0.0923(2)	0.9352(1)	0.0162(4)
C(18)	-0.1188(2)	0.1939(2)	0.7983(1)	0.0117(3)
C(19)	-0.0891(2)	0.2331(2)	0.8798(1)	0.0146(3)
C(20)	-0.1897(2)	0.3298(2)	0.9252(2)	0.0174(4)
C(21)	-0.3193(2)	0.3881(2)	0.8896(2)	0.0199(4)
C(22)	-0.3482(2)	0.3513(2)	0.8075(2)	0.0187(4)
C(23)	-0.2474(2)	0.2556(2)	0.7611(1)	0.0152(4)
C(24)	0.4831(2)	0.8051(2)	0.6353(2)	0.0283(5)
C(25)	0.4270(2)	0.7012(2)	0.7346(2)	0.0245(4)
N(1)	0.2300(2)	0.2593(2)	0.6067(1)	0.0141(3)
N(2)	0.1780(2)	0.2339(2)	0.5289(1)	0.0148(3)
N(3)	0.3818(2)	0.6204(2)	0.8115(2)	0.0341(4)
P(1)	-0.0056(1)	0.0549(1)	0.7449(1)	0.0109(1)
Cu(1)	0.0405(1)	0.0738(1)	0.5710(1)	0.0146(1)
Br(1)	-0.1824(1)	0.1261(1)	0.4949(1)	0.0164(1)

7.5.2 Iodo-(1-(2-(diphenylphosphanyl)phenyl)-3,5-dimethyl-pyrazol)-kupfer(I)-dimer- acetonitrilsolvat (nrm049)

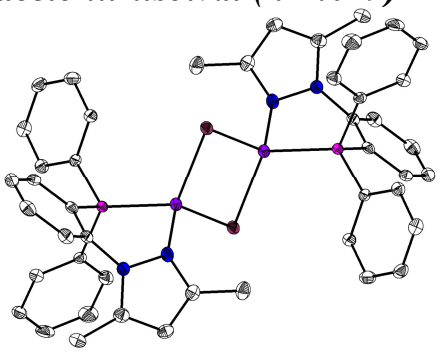

Kristalldaten

C27 H27 Cu I N4 P	M = 628.93 g/mol	Triclinic, $P\bar{1}$
a = 10.5021(3) Å	b = 11.1818(4) Å	c = 13.2788(5) Å
α = 106.287(2)°	β = 96.9770(10)°	γ = 115.1160(10)°
V = 1302.34(8) Å^3	Z = 2	F(000) = 628
D_{calc} = 1.604 g/cm^3	μ = 2.108 mm^{-1}	
colourless block	0.380 · 0.160 · 0.130 mm^3	

Datensammlung

Diffraktometer: D8 Quest (Bruker)	T = 100(2) K	λ = 0.71069 Å
h = -13 bis 13	k = -14 bis 14	l = -17 bis 17
26382 gemessene Reflexe	5763 unabhängige Reflexe	5148 Reflexe mit $I > 2\sigma(I)$
θ = 2.165 bis 27.180°	R_{int} = 0.0460	C (25.00°) = 0.999
Absorptionskorrektur: Multi-scan	T_{min} = 0.5776	T_{max} = 0.7455

Verfeinerung

5763 Reflexe	8 Restraints	340 Parameter
Verfeinerung mit SHELXL-2014/7	bis χ = 0.001	
R_1 ($I > 2\sigma(I)$) = 0.0232	wR_2 ($I > 2\sigma(I)$) = 0.0610	
R_1 (all) = 0.0300	wR_2 (all) = 0.0782	GoF (S) = 1.216
$\Delta\varphi_{min}$ = -0.802 e·Å^{-3}	$\Delta\varphi_{max}$ = 0.842 e·Å^{-3}	

Kommentar

Ein Acetonitrilmolekül ist über zwei Positionen fehlgeordnet und wurde mit DFIX und ISOR restrained.

Fraktionelle Atomkoordinaten (*x, y, z*) und äquivalente isotrope Auslenkungsfaktoren *U*(eq)

	x	*y*	*z*	*U*(eq)/Å^2
C(1)	0.4107(2)	0.4204(2)	0.2366(2)	0.0136(5)
C(2)	0.4866(3)	0.4289(3)	0.1569(2)	0.0152(5)
C(3)	0.5723(3)	0.5586(3)	0.1491(2)	0.0197(5)
C(4)	0.5897(3)	0.6834(3)	0.2239(2)	0.0206(5)
C(5)	0.5181(3)	0.6779(3)	0.3045(2)	0.0203(5)
C(6)	0.4279(3)	0.5471(3)	0.3097(2)	0.0163(5)
C(7)	0.3960(3)	0.1110(3)	-0.0561(2)	0.0182(5)
C(8)	0.5476(3)	0.1637(3)	-0.0211(2)	0.0201(5)
C(9)	0.6003(3)	0.2876(3)	0.0679(2)	0.0195(5)
C(10)	0.2862(3)	-0.0196(3)	-0.1513(2)	0.0233(6)
C(11)	0.7516(3)	0.3874(3)	0.1413(2)	0.0253(6)
C(12)	0.1998(3)	0.2886(2)	0.3421(2)	0.0135(5)
C(13)	0.2415(3)	0.2996(3)	0.4494(2)	0.0163(5)
C(14)	0.1640(3)	0.3263(3)	0.5221(2)	0.0192(5)
C(15)	0.0444(3)	0.3435(3)	0.4893(2)	0.0205(5)
C(16)	0.0024(3)	0.3337(3)	0.3826(2)	0.0215(5)
C(17)	0.0786(3)	0.3054(3)	0.3093(2)	0.0173(5)
C(18)	0.4191(3)	0.2051(3)	0.3075(2)	0.0135(5)
C(19)	0.5539(3)	0.3114(3)	0.3813(2)	0.0180(5)
C(20)	0.6438(3)	0.2756(3)	0.4381(2)	0.0209(5)
C(21)	0.5999(3)	0.1354(3)	0.4229(2)	0.0246(6)
C(22)	0.4673(3)	0.0296(3)	0.3495(3)	0.0276(6)
C(23)	0.3770(3)	0.0639(3)	0.2913(2)	0.0202(5)
C(26)	0.1894(3)	0.5905(3)	0.1177(2)	0.0274(6)
C(27)	0.1527(3)	0.6268(3)	0.2199(2)	0.0256(6)
N(1)	0.4820(2)	0.3045(2)	0.0836(2)	0.0159(4)
N(2)	0.3544(2)	0.1948(2)	0.0076(2)	0.0166(4)
N(4)	0.1237(3)	0.6549(3)	0.2998(3)	0.0463(7)
P(1)	0.2904(1)	0.2466(1)	0.2396(1)	0.0117(1)
Cu(1)	0.1646(1)	0.1123(1)	0.0651(1)	0.0154(1)
I(1)	-0.0347(1)	0.1661(1)	-0.0218(1)	0.0162(1)
C(24)	0.0093(12)	0.9145(10)	0.3283(9)	0.0306(18)
C(25)	0.1127(4)	0.9669(4)	0.4348(4)	0.0274(11)
N(3)	0.1941(4)	1.0118(4)	0.5180(5)	0.0332(10)
C(24A)	-0.015(5)	0.898(5)	0.325(4)	0.053(11)
N(3A)	-0.1806(14)	0.9776(14)	0.4230(17)	0.035(3)
C(25A)	-0.1020(15)	0.9516(13)	0.3800(11)	0.033(4)

7.5.3 Diphenylphosphinato-natrium(I)-tetrahydrofuranaddukt (nrm056)

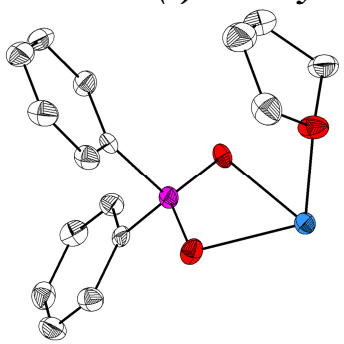

Kristalldaten

C16 H18 Na O3 P	M = 312.26 g/mol	Monoclinic, $P2_1/c$
a = 6.0831(11) Å	b = 16.898(3) Å	c = 15.678(3) Å
α = 90°	β = 100.071(5)°	γ = 90°
V = 1586.8(5) Å^3	Z = 4	F(000) = 656
D_{calc} = 1.307 g/cm^3	μ = 0.206 mm^{-1}	
colourless block	0.190 · 0.160 · 0.060 mm^3	

Datensammlung

Diffraktometer: D8 Quest (Bruker)	T = 100(2) K	λ = 0.71069 Å
h = -7 bis 7	k = -19 bis 21	l = -20 bis 20
11838 gemessene Reflexe	3530 unabhängige Reflexe	2119 Reflexe mit $I > 2\sigma(I)$
θ = 2.748 bis 27.726°	R_{int} = 0.1520	C (25.00°) = 0.999
Absorptionskorrektur: Multi-scan	T_{min} = 0.4044	T_{max} = 0.7455

Verfeinerung

3530 Reflexe	87 Restraints	237 Parameter
Verfeinerung mit SHELXL-2014/7	bis χ = 0.001	
R_1 ($I > 2\sigma(I)$) = 0.0755	wR_2 ($I > 2\sigma(I)$) = 0.1518	
R_1 (all) = 0.1413	wR_2 (all) = 0.1773	GoF (S) = 1.032
$\Delta\varphi_{min}$ = -0.436 e·Å^{-3}	$\Delta\varphi_{max}$ = 0.594 e·Å^{-3}	

Kommentar

Das THF-Molekül ist über zwei Positionen fehlgeordnet und wurde über DELU, RIGU DFIX und ISOR restrained.

Fraktionelle Atomkoordinaten (*x, y, z*) und äquivalente isotrope Auslenkungsfaktoren *U*(eq)

	x	y	z	U(eq)/Å^2
C(1)	0.5743(6)	0.9148(2)	0.7759(3)	0.0178(8)
C(2)	0.7221(6)	0.9436(2)	0.7261(3)	0.0242(9)
C(3)	0.6539(7)	0.9542(2)	0.6379(3)	0.0291(10)
C(4)	0.4360(7)	0.9363(2)	0.5964(3)	0.0273(9)
C(5)	0.2834(7)	0.9085(2)	0.6442(3)	0.0277(9)
C(6)	0.3537(6)	0.8979(2)	0.7327(3)	0.0229(9)
C(7)	0.7496(6)	0.7954(2)	0.9013(2)	0.0169(8)
C(8)	0.9741(6)	0.7741(2)	0.9285(3)	0.0239(9)
C(9)	1.0365(7)	0.6949(3)	0.9397(3)	0.0300(10)
C(10)	0.8737(7)	0.6367(2)	0.9232(3)	0.0310(10)
C(11)	0.6501(7)	0.6567(2)	0.8951(3)	0.0293(10)
C(12)	0.5887(6)	0.7357(2)	0.8849(3)	0.0235(9)
O(3)	0.803(2)	0.9096(7)	1.1547(16)	0.031(3)
C(13)	0.5913(13)	0.8755(6)	1.1617(6)	0.032(2)
C(14)	0.603(2)	0.7891(6)	1.1365(6)	0.043(2)
C(15)	0.846(2)	0.7671(5)	1.1708(8)	0.048(3)
C(16)	0.9678(19)	0.8448(7)	1.1681(10)	0.038(3)
O(3A)	0.793(6)	0.897(2)	1.148(4)	0.030(6)
C(13A)	0.601(3)	0.8451(15)	1.1457(14)	0.026(5)
C(14A)	0.705(5)	0.7660(13)	1.1395(13)	0.029(4)
C(15A)	0.946(4)	0.7785(12)	1.1917(15)	0.032(5)
C(16A)	0.997(5)	0.8636(16)	1.184(3)	0.042(8)
Na(1)	0.7878(2)	1.0026(1)	1.0504(1)	0.0198(4)
O(1)	0.8689(4)	0.9484(2)	0.9236(2)	0.0234(6)
O(2)	0.4697(4)	0.9102(2)	0.9334(2)	0.0234(6)
P(1)	0.6653(2)	0.8986(1)	0.8909(1)	0.0176(3)

7.5.4 1-(2-(diphenylphosphanyl)phenyl)-3,4,5-trimethyl-pyrazol (nrm071)

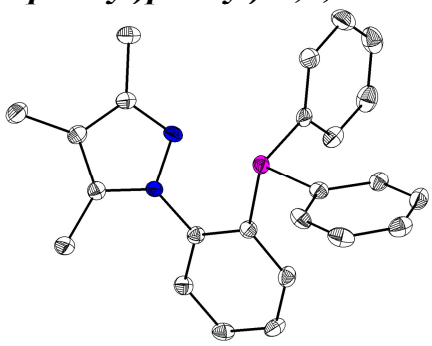

Kristalldaten

C24 H23 N2 P	M = 370.41 g/mol	Monoclinic, $P2_1/n$
a = 11.4870(5) Å	b = 19.0538(9) Å	c = 18.8926(9) Å
α = 90°	β = 106.940(2)°	γ = 90°
V = 3955.6(3) Å^3	Z = 8	F(000) = 1568
D_{calc} = 1.244 g/cm^3	μ = 0.150 mm^{-1}	
colourless block	0.380 · 0.150 · 0.100 mm^3	

Datensammlung

Diffraktometer: D8 Quest (Bruker)	T = 100(2) K	λ = 0.71069 Å
h = -14 bis 14	k = -24 bis 24	l = -24 bis 24
49762 gemessene Reflexe	8786 unabhängige Reflexe	6919 Reflexe mit $I > 2\sigma(I)$
θ = 2.138 bis 27.187°	R_{int} = 0.0706	C (25.00°) = 0.999
Absorptionskorrektur: Multi-scan	T_{min} = 0.5984	T_{max} = 0.7455

Verfeinerung

8786 Reflexe	0 Restraints	493 Parameter
Verfeinerung mit SHELXL-2014/7	bis χ = 0.000	
R_1 ($I > 2\sigma(I)$) = 0.0411	wR_2 ($I > 2\sigma(I)$) = 0.0985	
R_1 (all) = 0.0592	wR_2 (all) = 0.1092	GoF (S) = 1.022
$\Delta\varphi_{min}$ = -0.290 e·Å^{-3}	$\Delta\varphi_{max}$ = 0.944 e·Å^{-3}	

Fraktionelle Atomkoordinaten (*x, y, z*) und äquivalente isotrope Auslenkungsfaktoren *U*(eq)

	x	*y*	*z*	*U*(eq)/Å^2		*x*	*y*	*z*	*U*(eq)/Å^2
C(1)	-0.1254(1)	0.1330(1)	0.8591(1)	0.0170(3)	C(14)	-0.0693(2)	0.2664(1)	0.9603(1)	0.0236(4)
C(2)	-0.0732(1)	0.0714(1)	0.8960(1)	0.0167(3)	C(28)	0.6361(2)	0.5170(1)	0.8446(1)	0.0323(4)
C(3)	-0.1449(2)	0.0187(1)	0.9123(1)	0.0193(3)	C(20)	-0.1969(1)	0.3105(1)	0.7736(1)	0.0196(3)
C(4)	-0.2707(2)	0.0258(1)	0.8910(1)	0.0215(3)	C(18)	0.0940(2)	0.3105(1)	0.9178(1)	0.0225(3)
C(5)	-0.3243(2)	0.0856(1)	0.8543(1)	0.0226(3)	C(24)	-0.1661(2)	0.2230(1)	0.6898(1)	0.0226(3)
C(6)	-0.2520(2)	0.1385(1)	0.8388(1)	0.0208(3)	C(16)	0.0477(2)	0.3652(1)	1.0212(1)	0.0315(4)
C(7)	0.2403(1)	0.0945(1)	0.9595(1)	0.0177(3)	C(36)	0.2926(2)	0.5355(1)	0.9237(1)	0.0296(4)
C(19)	-0.1410(1)	0.2483(1)	0.7621(1)	0.0177(3)	C(45)	0.6841(2)	0.2058(1)	1.0326(1)	0.0294(4)
C(8)	0.2413(1)	0.0282(1)	0.9268(1)	0.0189(3)	C(27)	0.5099(2)	0.5187(1)	0.8247(1)	0.0311(4)
C(9)	0.1213(1)	0.0088(1)	0.8998(1)	0.0178(3)	C(17)	0.1177(2)	0.3615(1)	0.9729(1)	0.0299(4)
C(10)	0.3475(2)	0.1390(1)	0.9980(1)	0.0242(4)	C(15)	-0.0457(2)	0.3176(1)	1.0148(1)	0.0296(4)
C(11)	0.3503(2)	-0.0127(1)	0.9232(1)	0.0287(4)	C(41)	0.3314(2)	0.1558(1)	0.7657(1)	0.0278(4)
C(12)	0.0660(2)	-0.0561(1)	0.8599(1)	0.0255(4)	C(34)	0.0387(2)	0.3880(1)	0.7080(1)	0.0259(4)
C(42)	0.3345(2)	0.2082(1)	0.8175(1)	0.0231(4)	C(48)	0.5178(2)	0.3061(1)	1.0456(1)	0.0246(4)
C(31)	0.1382(1)	0.4266(1)	0.7626(1)	0.0189(3)	C(29)	0.6980(2)	0.4584(1)	0.8797(1)	0.0247(4)
C(21)	-0.2736(2)	0.3468(1)	0.7144(1)	0.0231(4)	C(23)	-0.2448(2)	0.2583(1)	0.6309(1)	0.0269(4)
C(30)	0.6339(2)	0.4013(1)	0.8950(1)	0.0203(3)	C(46)	0.6788(2)	0.2256(1)	1.1022(1)	0.0311(4)
C(37)	0.4099(1)	0.2669(1)	0.8221(1)	0.0184(3)	C(35)	0.0109(2)	0.4871(1)	0.8381(1)	0.0268(4)
C(25)	0.5073(1)	0.4017(1)	0.8755(1)	0.0178(3)	C(47)	0.5954(2)	0.2756(1)	1.1085(1)	0.0315(4)
C(39)	0.4729(2)	0.2208(1)	0.7197(1)	0.0243(4)	C(33)	0.2431(2)	0.4920(1)	0.8560(1)	0.0206(3)
C(13)	0.0001(1)	0.2625(1)	0.9110(1)	0.0178(3)	C(32)	0.1266(2)	0.4704(1)	0.8202(1)	0.0190(3)
C(26)	0.4463(1)	0.4615(1)	0.8401(1)	0.0201(3)	N(1)	0.0549(1)	0.0624(1)	0.9171(1)	0.0161(3)
C(44)	0.6072(2)	0.2366(1)	0.9694(1)	0.0242(4)	N(2)	0.1276(1)	0.1159(1)	0.9536(1)	0.0180(3)
C(38)	0.4777(1)	0.2727(1)	0.7721(1)	0.0207(3)	N(3)	0.3166(1)	0.4629(1)	0.8187(1)	0.0193(3)
C(40)	0.4006(2)	0.1622(1)	0.7169(1)	0.0265(4)	N(4)	0.2531(1)	0.4211(1)	0.7616(1)	0.0205(3)
C(43)	0.5235(1)	0.2875(1)	0.9752(1)	0.0197(3)	P(1)	-0.0275(1)	0.1996(1)	0.8345(1)	0.0170(1)
C(22)	-0.2979(2)	0.3209(1)	0.6430(1)	0.0257(4)	P(2)	0.4139(1)	0.3300(1)	0.8960(1)	0.0178(1)

7.5.5 Iodo-(1-(2-(diphenylphosphanyl)phenyl)-pyrazol)-kupfer(I)-dimer-dichlormethan- pentansolvat (nrm076)

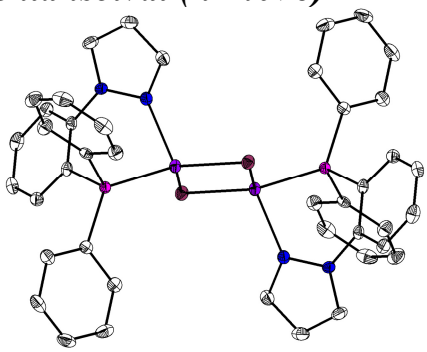

Kristalldaten

C45.08 H40.88 Cl2.56 Cu2 I2 N4 P2	M = 1172.26 g/mol	Triclinic, $P\bar{1}$
a = 9.5951(6) Å	b = 14.7708(7) Å	c = 16.2006(9) Å
α = 100.457(2)°	β = 91.403(2)°	γ = 93.417(2)°
V = 2252.5(2) Å^3	Z = 2	F(000) = 1154
D_{calc} = 1.728 g/cm^3	μ = 2.575 mm^{-1}	
colourless needle	0.400 · 0.060 · 0.030 mm^3	

Datensammlung

Diffraktometer: D8 Quest (Bruker)	T = 100(2) K	λ = 0.71069 Å
h = -12 bis 12	k = -16 bis 18	l = -20 bis 20
49227 gemessene Reflexe	9997 unabhängige Reflexe	8016 Reflexe mit $I > 2\sigma(I)$
θ = 2.128 bis 27.165°	R_{int} = 0.0591	C (25.00°) = 0.999
Absorptionskorrektur: Multi-scan	T_{min} = 0.6720	T_{max} = 0.7455

Verfeinerung

9997 Reflexe	6 Restraints	535 Parameter
Verfeinerung mit SHELXL-2014/7	bis χ = 0.003	
R_1 ($I > 2\sigma(I)$) = 0.0289	wR_2 ($I > 2\sigma(I)$) = 0.0627	
R_1 (all) = 0.0458	wR_2 (all) = 0.0700	GoF (S) = 1.057
$\Delta\varphi_{min}$ = -0.713 e·Å^{-3}	$\Delta\varphi_{max}$ = 0.963 e·Å^{-3}	

Kommentar

Ein Pentan und ein Dichlormethanmolekül sind substitutionell fehlgeordnet. Die Moleküle wurden über DFIX re- und über EADP constrained.

Fraktionelle Atomkoordinaten (*x, y, z*) und äquivalente isotrope Auslenkungsfaktoren *U*(eq)

	x	*y*	*z*	*U*(eq)/Å^2		*x*	*y*	*z*	*U*(eq)/Å^2
C(1)	0.6783(3)	0.3102(2)	0.0452(2)	0.0126(6)	C(19)	0.7671(4)	0.0773(2)	-0.2430(2)	0.0249(8)
C(2)	0.5842(3)	0.3577(2)	0.0033(2)	0.0134(6)	C(20)	0.6596(4)	0.0943(2)	-0.1885(2)	0.0240(8)
C(3)	0.4601(3)	0.3857(2)	0.0386(2)	0.0164(6)	C(21)	0.6821(3)	0.1550(2)	-0.1128(2)	0.0199(7)
C(4)	0.4276(3)	0.3682(2)	0.1172(2)	0.0201(7)	C(22)	0.7828(3)	0.3025(2)	0.5435(2)	0.0138(6)
C(5)	0.5188(3)	0.3226(2)	0.1602(2)	0.0176(7)	C(23)	0.8855(3)	0.3525(2)	0.5062(2)	0.0144(6)
C(6)	0.6419(3)	0.2938(2)	0.1243(2)	0.0156(6)	C(24)	1.0163(3)	0.3773(2)	0.5449(2)	0.0188(7)
C(7)	0.7239(3)	0.4237(2)	-0.1773(2)	0.0173(7)	C(25)	1.0469(4)	0.3550(2)	0.6224(2)	0.0215(7)
C(8)	0.5894(4)	0.3953(2)	-0.2096(2)	0.0214(7)	C(26)	0.9475(4)	0.3071(2)	0.6609(2)	0.0220(7)
C(9)	0.5204(4)	0.3663(2)	-0.1455(2)	0.0202(7)	C(27)	0.8170(3)	0.2809(2)	0.6217(2)	0.0179(7)
C(10)	0.9336(3)	0.2207(2)	0.0739(2)	0.0131(6)	C(28)	0.7569(3)	0.4333(2)	0.3298(2)	0.0162(7)
C(11)	1.0383(3)	0.2676(2)	0.1300(2)	0.0165(7)	C(29)	0.8860(4)	0.4079(2)	0.2993(2)	0.0209(7)
C(12)	1.1136(3)	0.2213(2)	0.1814(2)	0.0216(7)	C(30)	0.9495(4)	0.3731(2)	0.3625(2)	0.0204(7)
C(13)	1.0873(4)	0.1270(2)	0.1758(2)	0.0242(8)	C(31)	0.6169(3)	0.2036(2)	0.4000(2)	0.0145(6)
C(14)	0.9848(4)	0.0794(2)	0.1201(2)	0.0224(7)	C(32)	0.4986(4)	0.1888(2)	0.3458(2)	0.0197(7)
C(15)	0.9068(4)	0.1259(2)	0.0694(2)	0.0187(7)	C(33)	0.5042(4)	0.1351(2)	0.2664(2)	0.0239(8)
C(16)	0.8125(3)	0.2011(2)	-0.0921(2)	0.0127(6)	C(34)	0.6272(4)	0.0976(2)	0.2394(2)	0.0241(8)
C(17)	0.9200(4)	0.1843(2)	-0.1482(2)	0.0184(7)	C(35)	0.7444(4)	0.1115(2)	0.2927(2)	0.0227(7)
C(18)	0.8979(4)	0.1215(2)	-0.2228(2)	0.0236(8)	C(36)	0.7398(3)	0.1636(2)	0.3730(2)	0.0181(7)

	x	y	z	U(eq)/Å^2
C(37)	0.5090(3)	0.2145(2)	0.5655(2)	0.0156(6)
C(38)	0.5308(4)	0.1218(2)	0.5664(2)	0.0217(7)
C(39)	0.4514(4)	0.0740(2)	0.6165(2)	0.0238(8)
C(40)	0.3518(4)	0.1175(2)	0.6666(2)	0.0251(8)
C(41)	0.3295(4)	0.2097(2)	0.6672(2)	0.0249(8)
C(42)	0.4079(3)	0.2577(2)	0.6157(2)	0.0192(7)
C(43)	0.2721(4)	0.1530(2)	0.9899(2)	0.0286(8)
N(1)	0.6114(3)	0.3778(2)	-0.0782(2)	0.0131(5)
N(2)	0.7387(3)	0.4141(2)	-0.0972(2)	0.0142(5)
N(3)	0.8606(3)	0.3785(2)	0.4264(2)	0.0136(5)
N(4)	0.7405(3)	0.4161(2)	0.4069(2)	0.0135(5)
P(1)	0.8499(1)	0.2862(1)	0.0035(1)	0.0117(2)
P(2)	0.6035(1)	0.2831(1)	0.4994(1)	0.0124(2)

	x	y	z	U(eq)/Å^2
Cu(1)	0.9199(1)	0.4256(1)	-0.0210(1)	0.0146(1)
Cu(2)	0.5627(1)	0.4250(1)	0.4798(1)	0.0142(1)
I(1)	1.1289(1)	0.4477(1)	-0.1135(1)	0.0157(1)
I(2)	0.3551(1)	0.4505(1)	0.3843(1)	0.0159(1)
Cl(1)	0.3708(1)	0.0713(1)	1.0273(1)	0.0360(2)
Cl(2)	0.2948(1)	0.1498(1)	0.8815(1)	0.0309(2)
Cl(3)	0.1104(5)	0.1503(4)	0.3882(3)	0.0383(10)
C(44)	0.1548(18)	0.1112(9)	0.4813(10)	0.0383(10)
Cl(4)	0.1646(4)	-0.0091(3)	0.4633(2)	0.0383(10)
C(47)	0.0119(15)	0.0114(8)	0.4754(8)	0.047(3)
C(46)	0.0738(15)	0.1126(8)	0.4904(9)	0.047(3)
C(45)	0.1255(18)	0.1418(13)	0.4086(8)	0.047(3)
C(48)	-0.0467(15)	-0.0214(9)	0.5540(8)	0.047(3)
C(49)	-0.1204(14)	-0.1195(8)	0.5383(12)	0.047(3)

7.5.6 Iodo-(1-(2-(diphenylphosphanyl)phenyl)-3,4,5-trimethyl-pyrazol)-kupfer(I)-dimer (nrm078)

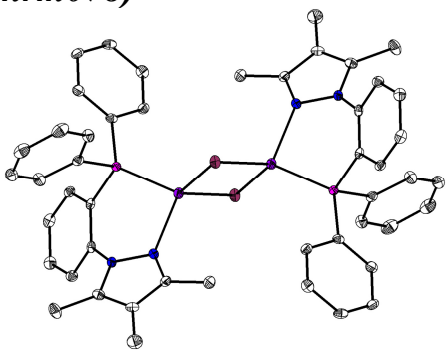

Kristalldaten

C48 H46 Cu2 I2 N4 P2	M = 1121.71 g/mol	Monoclinic, $P2_1/c$
a = 13.9419(6) Å	b = 14.9941(7) Å	c = 10.9344(4) Å
α = 90°	β = 107.633(2)°	γ = 90°
V = 2178.40(16) Å^3	Z = 2	F(000) = 1112
D_{calc} = 1.710 g/cm^3	μ = 2.506 mm^{-1}	
colourless block	0.100 · 0.070 · 0.040 mm^3	

Datensammlung

Diffraktometer: D8 Quest (Bruker)	T = 100(2) K	λ = 0.71073 Å
h = -17 bis 17	k = -19 bis 19	l = -13 bis 14
20732 gemessene Reflexe	4797 unabhängige Reflexe	4025 Reflexe mit $I > 2\sigma(I)$
θ = 2.380 bis 27.141°	R_{int} = 0.0390	C (25.00°) = 0.998
Absorptionskorrektur: Multi-scan	T_{min} = 0.7073	T_{max} = 0.7455

Verfeinerung

4797 Reflexe	0 Restraints	265 Parameter
Verfeinerung mit SHELXL-2014/7	bis χ = 0.002	
R_1 ($I > 2\sigma(I)$) = 0.0231	wR_2 ($I > 2\sigma(I)$) = 0.0471	
R_1 (all) = 0.0346	wR_2 (all) = 0.0504	GoF (S) = 1.037
$\Delta\varphi_{min}$ = -0.384 e·Å^{-3}	$\Delta\varphi_{max}$ = 0.489 e·Å^{-3}	

Fraktionelle Atomkoordinaten (*x, y, z*) und äquivalente isotrope Auslenkungsfaktoren *U*(eq)

	x	*y*	*z*	*U*(eq)/Å^2
C(1)	0.7036(2)	0.1063(2)	0.0686(2)	0.0110(5)
C(2)	0.7546(2)	0.1563(2)	0.1784(2)	0.0103(5)
C(3)	0.7161(2)	0.2374(2)	0.2032(2)	0.0137(5)
C(4)	0.6253(2)	0.2690(2)	0.1232(2)	0.0150(5)
C(5)	0.5742(2)	0.2214(2)	0.0137(2)	0.0151(5)
C(6)	0.6139(2)	0.1413(2)	-0.0130(2)	0.0126(5)
C(7)	1.0072(2)	0.1046(2)	0.3324(2)	0.0139(5)
C(8)	0.9776(2)	0.1216(2)	0.4428(2)	0.0143(5)
C(9)	0.8758(2)	0.1352(2)	0.3989(2)	0.0137(5)
C(10)	1.1106(2)	0.0868(2)	0.3264(3)	0.0200(6)
C(11)	1.0456(2)	0.1268(2)	0.5769(2)	0.0234(6)
C(12)	0.8048(2)	0.1548(2)	0.4734(2)	0.0201(6)
C(13)	0.7160(2)	-0.0762(2)	0.1436(2)	0.0122(5)
C(14)	0.7482(2)	-0.1648(2)	0.1528(2)	0.0172(5)
C(15)	0.7208(2)	-0.2238(2)	0.2337(3)	0.0240(6)
C(16)	0.6625(2)	-0.1943(2)	0.3091(3)	0.0229(6)
C(17)	0.6300(2)	-0.1077(2)	0.3003(3)	0.0211(6)
C(18)	0.6559(2)	-0.0487(2)	0.2180(2)	0.0168(5)
C(19)	0.6707(2)	-0.0301(2)	-0.1225(2)	0.0114(5)
C(20)	0.6970(2)	-0.0008(2)	-0.2289(2)	0.0135(5)
C(21)	0.6380(2)	-0.0221(2)	-0.3520(2)	0.0157(5)
C(22)	0.5521(2)	-0.0737(2)	-0.3695(2)	0.0149(5)
C(23)	0.5253(2)	-0.1042(2)	-0.2651(2)	0.0156(5)
C(24)	0.5843(2)	-0.0816(2)	-0.1417(2)	0.0148(5)
N(1)	0.8465(1)	0.1253(1)	0.2677(2)	0.0113(4)
N(2)	0.9288(2)	0.1066(1)	0.2258(2)	0.0132(4)
P(1)	0.7548(1)	-0.0006(1)	0.0358(1)	0.0099(1)
Cu(1)	0.9172(1)	0.0255(1)	0.0648(1)	0.0130(1)
I(1)	0.9713(1)	0.1218(1)	-0.1030(1)	0.0143(1)

7.5.7 Bromo-(1-(2-(diphenylphosphanyl)phenyl)-pyrazol)-kupfer(I)-dimer-acetonitrilsolvat (nrm080)

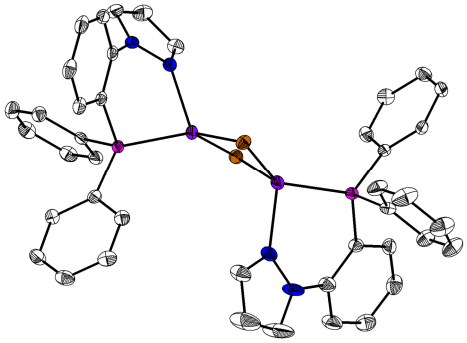

Kristalldaten

C94 H83 Br4 Cu4 N13 P4	M = 2092.41 g/mol	Monoclinic, *C*2/*c*
a = 36.6917(11) Å	b = 13.6388(4) Å	c = 21.0368(6) Å
α = 90°	β = 121.4370(10)°	γ = 90°
V = 8982.2(5) Å^3	Z = 4	F(000) = 4216
D_{calc} = 1.547 g/cm^3	μ = 2.839 mm^{-1}	
colourless block	0.170 · 0.150 · 0.150 mm^3	

Datensammlung

Diffraktometer: D8 Quest (Bruker)	T = 100(2) K	λ = 0.71069 Å
h = -48 bis 48	k = -17 bis 17	l = -27 bis 27
130930 gemessene Reflexe	10790 unabhängige Reflexe	8906 Reflexe mit $I > 2\sigma(I)$
θ = 1.940 bis 27.969°	R_{int} = 0.0569	C (25.00°) = 0.999
Absorptionskorrektur: Multi-scan	T_{min} = 0.6508	T_{max} = 0.7456

Verfeinerung

10790 Reflexe	15 Restraints	549 Parameter
Verfeinerung mit SHELXL-2014/7	bis χ = 0.001	
R_1 ($I > 2\sigma(I)$) = 0.0289	wR_2 ($I > 2\sigma(I)$) = 0.0668	
R_1 (all) = 0.0447	wR_2 (all) = 0.0768	GoF (S) = 1.124
$\Delta\varphi_{min}$ = -0.577 e·Å^{-3}	$\Delta\varphi_{max}$ = 1.132 e·Å^{-3}	

Kommentar
Ein Acetonitrilmolekül ist über ein Inversionszentrum fehlgeordnet und wurde über DFIX, DANG und ISOR restrained.

Fraktionelle Atomkoordinaten (*x, y, z*) und äquivalente isotrope Auslenkungsfaktoren *U*(eq)

	x	*y*	*z*	*U*(eq)/Å^2
C(1)	0.1776(1)	0.4407(2)	0.2138(1)	0.0159(4)
C(2)	0.2163(1)	0.4275(2)	0.2172(1)	0.0170(4)
C(3)	0.2538(1)	0.4693(2)	0.2733(1)	0.0220(5)
C(4)	0.2533(1)	0.5254(2)	0.3277(1)	0.0257(5)
C(5)	0.2156(1)	0.5407(2)	0.3252(1)	0.0237(5)
C(6)	0.1779(1)	0.4984(2)	0.2686(1)	0.0202(5)
C(7)	0.2078(1)	0.2627(2)	0.0823(1)	0.0220(5)
C(8)	0.2288(1)	0.3384(2)	0.0699(2)	0.0293(6)
C(9)	0.2350(1)	0.4096(2)	0.1203(1)	0.0263(5)
C(10)	0.1177(1)	0.4387(2)	0.0565(1)	0.0150(4)
C(11)	0.0931(1)	0.3879(2)	-0.0098(1)	0.0182(5)
C(12)	0.0819(1)	0.4311(2)	-0.0772(1)	0.0220(5)
C(13)	0.0959(1)	0.5249(2)	-0.0784(1)	0.0236(5)
C(14)	0.1208(1)	0.5760(2)	-0.0128(1)	0.0239(5)
C(15)	0.1317(1)	0.5334(2)	0.0547(1)	0.0193(5)
C(16)	0.0876(1)	0.4200(2)	0.1578(1)	0.0168(4)
C(17)	0.0822(1)	0.3685(2)	0.2096(1)	0.0192(5)
C(18)	0.0498(1)	0.3940(2)	0.2220(1)	0.0230(5)
C(19)	0.0227(1)	0.4711(2)	0.1827(1)	0.0261(5)
C(20)	0.0277(1)	0.5221(2)	0.1308(1)	0.0259(5)
C(21)	0.0599(1)	0.4968(2)	0.1183(1)	0.0210(5)
C(22)	0.0696(1)	-0.1670(2)	0.0882(1)	0.0175(4)
C(23)	0.0318(1)	-0.1182(2)	0.0711(1)	0.0227(5)
C(24)	-0.0074(1)	-0.1504(2)	0.0126(2)	0.0293(6)
C(25)	-0.0101(1)	-0.2321(2)	-0.0282(1)	0.0306(6)
C(26)	0.0263(1)	-0.2814(2)	-0.0129(1)	0.0271(5)
C(27)	0.0655(1)	-0.2483(2)	0.0444(1)	0.0215(5)
C(28)	0.0473(1)	0.0944(2)	0.1783(2)	0.0299(6)
C(29)	0.0067(1)	0.0700(3)	0.1614(2)	0.0571(10)
C(30)	-0.0036(1)	-0.0129(3)	0.1191(2)	0.0582(10)
C(31)	0.1596(1)	-0.1933(2)	0.1444(1)	0.0153(4)
C(32)	0.1600(1)	-0.1656(2)	0.0807(1)	0.0192(5)
C(33)	0.1907(1)	-0.2022(2)	0.0680(1)	0.0218(5)
C(34)	0.2218(1)	-0.2661(2)	0.1191(1)	0.0219(5)
C(35)	0.2220(1)	-0.2925(2)	0.1826(1)	0.0207(5)
C(36)	0.1908(1)	-0.2568(2)	0.1951(1)	0.0163(4)
C(37)	0.1284(1)	-0.1909(2)	0.2445(1)	0.0183(4)
C(38)	0.1083(1)	-0.2796(2)	0.2400(1)	0.0249(5)
C(39)	0.1146(1)	-0.3241(2)	0.3042(2)	0.0326(6)
C(40)	0.1410(1)	-0.2811(2)	0.3730(2)	0.0372(7)
C(41)	0.1611(1)	-0.1936(2)	0.3777(1)	0.0374(7)
C(42)	0.1547(1)	-0.1477(2)	0.3138(1)	0.0266(5)
C(43)	0.1942(1)	0.3436(3)	0.4145(2)	0.0605(10)
C(44)	0.2303(1)	0.3994(3)	0.4708(2)	0.0483(9)
C(45)	0.1249(1)	0.0494(2)	0.3864(2)	0.0427(7)
C(46)	0.1067(1)	0.1473(2)	0.3738(2)	0.0338(6)
N(1)	0.2183(1)	0.3753(1)	0.1601(1)	0.0180(4)
N(2)	0.2012(1)	0.2841(1)	0.1371(1)	0.0177(4)
N(3)	0.0302(1)	-0.0369(2)	0.1130(1)	0.0294(5)
N(4)	0.0617(1)	0.0312(1)	0.1484(1)	0.0210(4)
N(5)	0.2590(1)	0.4421(3)	0.5153(2)	0.0609(9)
N(6)	0.0926(1)	0.2235(2)	0.3634(2)	0.0495(7)
P(1)	0.1293(1)	0.3779(1)	0.1418(1)	0.0138(1)
P(2)	0.1228(1)	-0.1290(1)	0.1631(1)	0.0145(1)
Cu(1)	0.1512(1)	0.2247(1)	0.1497(1)	0.0170(1)
Cu(2)	0.1220(1)	0.0319(1)	0.1608(1)	0.0182(1)
Br(1)	0.1680(1)	0.1379(1)	0.2650(1)	0.0183(1)
Br(2)	0.1207(1)	0.1008(1)	0.0490(1)	0.0176(1)
N(7)	0.0000	0.6962(4)	0.2500	0.0869(18)
C(47)	0.0469(2)	0.8444(5)	0.3040(5)	0.058(2)
C(48)	0.0190(2)	0.7619(4)	0.2670(4)	0.0399(14)

7.5.8 1-(2-(Diphenylphosphanyl)phenyl)-3,5-diphenyl-pyrazol (nrm084)

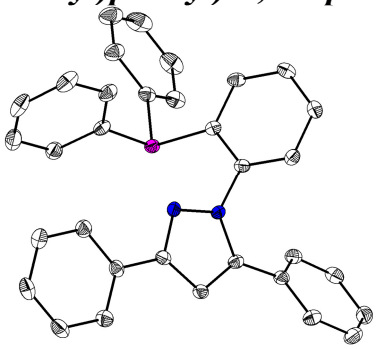

Kristalldaten

C33 H25 N2 P	*M* = 480.52 g/mol	Triclinic, *P*−1
a = 10.1620(6) Å	*b* = 10.2742(5) Å	*c* = 13.7499(7) Å
α = 94.715(2)°	β = 103.920(2)°	γ = 114.3860(10)°
V = 1242.06(12) Å^3	*Z* = 2	*F*(000) = 504
D_{calc} = 1.285 g/cm^3	μ = 0.136 mm^{-1}	
colourless needle	0.310 · 0.120 · 0.050 mm^3	

Datensammlung

Diffraktometer: D8 Quest (Bruker)	T = 100(2) K	λ = 0.71069 Å
h = -13 bis 13	k = -13 bis 13	l = -17 bis 17
35073 gemessene Reflexe	5500 unabhängige Reflexe	4398 Reflexe mit $I > 2\sigma(I)$
θ = 2.384 bis 27.188°	R_{int} = 0.0841	C (25.00°) = 0.999
Absorptionskorrektur: Multi-scan	T_{min} = 0.5715	T_{max} = 0.7455

Verfeinerung

5500 Reflexe	0 Restraints	325 Parameter
Verfeinerung mit SHELXL-2014/7	bis χ = 0.000	
R_1 ($I > 2\sigma(I)$) = 0.0436	wR_2 ($I > 2\sigma(I)$) = 0.0994	
R_1 (all) = 0.0612	wR_2 (all) = 0.1075	GoF (S) = 1.040
$\Delta\varphi_{min}$ = -0.415 e·Å^{-3}	$\Delta\varphi_{max}$ = 0.455 e·Å^{-3}	

Fraktionelle Atomkoordinaten (*x, y, z*) und äquivalente isotrope Auslenkungsfaktoren *U*(eq)

	x	*y*	*z*	*U*(eq)/Å^2		*x*	*y*	*z*	*U*(eq)/Å^2
C(1)	-0.1283(2)	0.2858(2)	0.2261(1)	0.0153(3)	C(19)	0.2333(2)	0.2181(2)	-0.0837(1)	0.0224(4)
C(2)	0.0147(2)	0.3574(2)	0.2118(1)	0.0151(3)	C(20)	0.0987(2)	0.1626(2)	-0.0593(1)	0.0214(4)
C(3)	0.0471(2)	0.4665(2)	0.1555(1)	0.0175(3)	C(21)	0.0977(2)	0.1917(2)	0.0406(1)	0.0188(3)
C(4)	-0.0635(2)	0.5091(2)	0.1130(1)	0.0189(3)	C(22)	-0.1445(2)	0.1777(2)	0.4157(1)	0.0181(3)
C(5)	-0.2031(2)	0.4457(2)	0.1302(1)	0.0198(3)	C(23)	-0.1377(2)	0.3079(2)	0.4597(1)	0.0223(4)
C(6)	-0.2355(2)	0.3351(2)	0.1853(1)	0.0180(3)	C(24)	-0.1137(2)	0.3420(2)	0.5640(2)	0.0276(4)
C(7)	0.2885(2)	0.3162(2)	0.3949(1)	0.0157(3)	C(25)	-0.0960(2)	0.2461(2)	0.6255(1)	0.0293(4)
C(8)	0.3399(2)	0.2953(2)	0.3113(1)	0.0170(3)	C(26)	-0.1050(2)	0.1150(2)	0.5823(1)	0.0277(4)
C(9)	0.2387(2)	0.3003(2)	0.2267(1)	0.0155(3)	C(27)	-0.1293(2)	0.0809(2)	0.4778(1)	0.0217(4)
C(10)	0.3528(2)	0.3210(2)	0.5038(1)	0.0177(3)	C(28)	-0.3825(2)	0.0346(2)	0.2304(1)	0.0183(3)
C(11)	0.4856(2)	0.3063(2)	0.5386(1)	0.0221(4)	C(29)	-0.4487(2)	-0.0407(2)	0.1292(1)	0.0233(4)
C(12)	0.5435(2)	0.3082(2)	0.6413(1)	0.0251(4)	C(30)	-0.6055(2)	-0.1152(2)	0.0874(2)	0.0315(4)
C(13)	0.4710(2)	0.3259(2)	0.7104(1)	0.0250(4)	C(31)	-0.6968(2)	-0.1141(2)	0.1464(2)	0.0351(5)
C(14)	0.3397(2)	0.3433(2)	0.6768(1)	0.0240(4)	C(32)	-0.6339(2)	-0.0389(2)	0.2466(2)	0.0336(5)
C(15)	0.2810(2)	0.3405(2)	0.5744(1)	0.0207(4)	C(33)	-0.4767(2)	0.0349(2)	0.2891(2)	0.0249(4)
C(16)	0.2329(2)	0.2766(2)	0.1185(1)	0.0163(3)	N(1)	0.1329(2)	0.3225(1)	0.2615(1)	0.0151(3)
C(17)	0.3685(2)	0.3329(2)	0.0930(1)	0.0205(4)	N(2)	0.1626(2)	0.3333(2)	0.3645(1)	0.0162(3)
C(18)	0.3679(2)	0.3043(2)	-0.0069(1)	0.0237(4)	P(1)	-0.1747(1)	0.1193(1)	0.2799(1)	0.0152(1)

7.5.9 Acetonitril-bromo-(1-(2-(diphenylphosphanyl)phenyl)-3,5-diphenyl-pyrazol)-kupfer(I)-acetonitrilsolvat (nrm088)

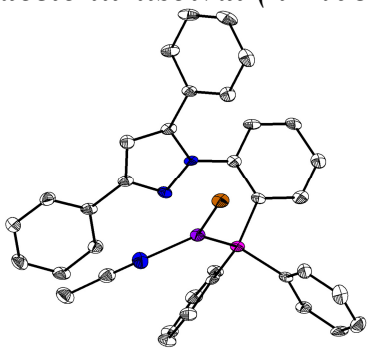

Kristalldaten

C39 H34 Br Cu N5 P	M = 747.13 g/mol	Triclinic, $P\bar{1}$
a = 10.3053(18) Å	b = 12.131(2) Å	c = 15.584(3) Å
α = 92.801(5)°	β = 105.495(5)°	γ = 107.613(5)°
V = 1771.4(5) Å^3	Z = 2	F(000) = 764
D_{calc} = 1.401 g/cm^3	μ = 1.824 mm^{-1}	
colourless block	0.300 · 0.130 · 0.070 mm^3	

Datensammlung

Diffraktometer: D8 Quest (Bruker)	T = 100(2) K	λ = 0.71073 Å
h = -12 bis 12	k = -14 bis 14	l = -19 bis 19
38321 gemessene Reflexe	7001 unabhängige Reflexe	5583 Reflexe mit $I > 2\sigma(I)$
θ = 2.087 bis 26.065°	R_{int} = 0.0990	C (25.00°) = 0.999
Absorptionskorrektur: Multi-scan	T_{min} = 0.5050	T_{max} = 0.7456

Verfeinerung

7001 Reflexe	40 Restraints	427 Parameter
Verfeinerung mit SHELXL-2014/7	bis χ = 0.000	
R_1 ($I > 2\sigma(I)$) = 0.0869	wR_2 ($I > 2\sigma(I)$) = 0.2029	
R_1 (all) = 0.1024	wR_2 (all) = 0.2177	GoF (S) = 1.063
$\Delta\varphi_{min}$ = -1.804 e·Å^{-3}	$\Delta\varphi_{max}$ = 2.525 e·Å^{-3}	

Fraktionelle Atomkoordinaten (*x, y, z*) und äquivalente isotrope Auslenkungsfaktoren *U*(eq)

	x	*y*	*z*	*U*(eq)/Å^2
C(1)	0.6646(5)	0.2528(4)	0.3588(3)	0.0158(9)
C(2)	0.5818(4)	0.2879(4)	0.4059(3)	0.0163(9)
C(3)	0.5614(5)	0.2390(4)	0.4819(3)	0.0193(10)
C(4)	0.6184(5)	0.1549(4)	0.5110(3)	0.0200(10)
C(5)	0.7006(5)	0.1178(4)	0.4655(3)	0.0207(10)
C(6)	0.7230(5)	0.1675(4)	0.3903(3)	0.0206(10)
C(7)	0.5291(5)	0.5466(4)	0.3453(3)	0.0184(9)
C(8)	0.3948(5)	0.4930(4)	0.3564(3)	0.0196(10)
C(9)	0.3906(5)	0.3845(4)	0.3770(3)	0.0178(9)
C(10)	0.5927(5)	0.6646(4)	0.3241(3)	0.0200(10)
C(11)	0.7316(5)	0.6994(4)	0.3183(3)	0.0214(10)
C(12)	0.7943(5)	0.8104(4)	0.3006(3)	0.0243(10)
C(13)	0.7187(6)	0.8897(4)	0.2893(3)	0.0263(11)
C(14)	0.5802(6)	0.8549(4)	0.2932(3)	0.0249(11)
C(15)	0.5172(5)	0.7427(4)	0.3099(3)	0.0230(10)
C(16)	0.2748(5)	0.2877(4)	0.3911(3)	0.0182(9)
C(17)	0.2428(5)	0.1734(4)	0.3525(3)	0.0222(10)
C(18)	0.1357(5)	0.0849(4)	0.3696(3)	0.0254(11)
C(19)	0.0574(5)	0.1102(5)	0.4230(3)	0.0298(12)
C(20)	0.0879(5)	0.2238(5)	0.4610(3)	0.0278(11)
C(21)	0.1960(5)	0.3119(4)	0.4458(3)	0.0227(10)
C(22)	0.7353(5)	0.1967(4)	0.1986(3)	0.0167(9)
C(23)	0.6280(5)	0.1043(4)	0.1385(3)	0.0213(10)
C(24)	0.6633(6)	0.0221(4)	0.0939(3)	0.0274(11)
C(25)	0.8033(6)	0.0291(5)	0.1063(3)	0.0271(11)
C(26)	0.9105(5)	0.1217(4)	0.1650(3)	0.0240(10)
C(27)	0.8770(5)	0.2052(4)	0.2115(3)	0.0218(10)
C(28)	0.8434(5)	0.4342(4)	0.2819(3)	0.0174(9)
C(29)	0.9407(5)	0.4693(4)	0.3664(3)	0.0205(10)
C(30)	1.0568(5)	0.5698(4)	0.3836(3)	0.0236(10)
C(31)	1.0787(5)	0.6372(4)	0.3155(3)	0.0234(10)
C(32)	0.9827(5)	0.6022(4)	0.2306(4)	0.0268(11)
C(33)	0.8649(5)	0.5012(4)	0.2137(3)	0.0231(10)
C(34)	0.5401(6)	0.6898(4)	0.0751(4)	0.0309(12)
C(35)	0.5165(5)	0.5737(4)	0.1002(3)	0.0242(10)
C(36)	0.1235(7)	0.4240(5)	0.1216(4)	0.0435(15)
C(37)	0.1597(6)	0.5214(6)	0.0748(5)	0.0437(15)
C(38)	0.1118(10)	0.8615(6)	0.0847(5)	0.066(2)
C(39)	0.1894(7)	0.8794(5)	0.1801(4)	0.0375(14)
N(1)	0.5217(4)	0.3756(3)	0.3778(2)	0.0153(8)
N(2)	0.6078(4)	0.4756(3)	0.3587(3)	0.0183(8)
N(3)	0.4992(4)	0.4823(4)	0.1190(3)	0.0255(9)
N(4)	0.1890(6)	0.6007(6)	0.0378(5)	0.0673(19)
N(5)	0.2467(6)	0.8936(5)	0.2545(4)	0.0452(13)
P(1)	0.6820(1)	0.3066(1)	0.2526(1)	0.0160(3)
Cu(1)	0.4907(1)	0.3324(1)	0.1643(1)	0.0191(2)
Br(1)	0.2699(1)	0.1851(1)	0.1005(1)	0.0246(2)

7.5.10 Iodo-(1-(2-(diphenylphosphanyl)phenyl)-3,5-diphenyl-pyrazol)-kupfer(I)-dimer (nrm090)

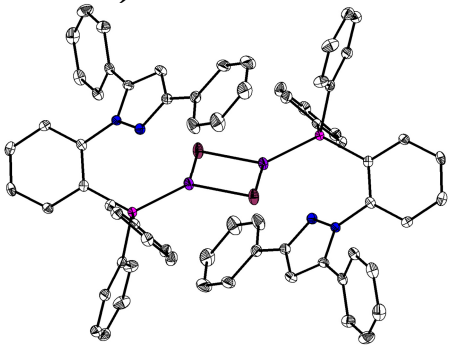

Kristalldaten

C66 H50 Cu2 I2 N4 P2	M = 1341.92 g/mol	Triclinic, $P\bar{1}$
a = 10.5086(5) Å	b = 11.4914(6) Å	c = 12.2816(6) Å
α = 104.915(2)°	β = 102.000(2)°	γ = 95.912(2)°
V = 1382.47(12) Å^3	Z = 1	F(000) = 668
D_{calc} = 1.612 g/cm^3	μ = 1.990 mm^{-1}	
colourless block	0.340 · 0.220 · 0.170 mm^3	

Datensammlung

Diffraktometer: D8 Quest (Bruker)	T = 100(2) K	λ = 0.71069 Å
h = -13 bis 13	k = -14 bis 14	l = -15 bis 15
31627 gemessene Reflexe	6119 unabhängige Reflexe	5523 Reflexe mit $I > 2\sigma(I)$
θ = 2.169 bis 27.155°	R_{int} = 0.0441	C (25.00°) = 0.999
Absorptionskorrektur: Multi-scan	T_{min} = 0.8609	T_{max} = 1.000

Verfeinerung

6119 Reflexe	0 Restraints	343 Parameter
Verfeinerung mit SHELXL-2014/7	bis χ = 0.000	
R_1 ($I > 2\sigma(I)$) = 0.0232	wR_2 ($I > 2\sigma(I)$) = 0.0627	
R_1 (all) = 0.0286	wR_2 (all) = 0.0730	GoF (S) = 1.191
$\Delta\varphi_{min}$ = -0.679 e·Å^{-3}	$\Delta\varphi_{max}$ = 0.643 e·Å^{-3}	

Fraktionelle Atomkoordinaten (*x, y, z*) und äquivalente isotrope Auslenkungsfaktoren *U*(eq)

	x	*y*	*z*	*U*(eq)/Å^2		*x*	*y*	*z*	*U*(eq)/Å^2
C(1)	0.2995(2)	0.2078(2)	0.3699(2)	0.0105(4)	C(20)	-0.1413(2)	0.3868(2)	0.4325(2)	0.0185(5)
C(2)	0.1946(2)	0.1851(2)	0.4200(2)	0.0109(4)	C(21)	-0.0788(2)	0.2928(2)	0.3864(2)	0.0156(4)
C(3)	0.1928(2)	0.2555(2)	0.5307(2)	0.0123(4)	C(22)	0.4044(2)	0.0096(2)	0.2323(2)	0.0116(4)
C(4)	0.2951(2)	0.3508(2)	0.5918(2)	0.0140(4)	C(23)	0.4390(2)	-0.0510(2)	0.1307(2)	0.0158(4)
C(5)	0.4013(2)	0.3742(2)	0.5452(2)	0.0144(4)	C(24)	0.5114(2)	-0.1458(2)	0.1299(2)	0.0188(5)
C(6)	0.4029(2)	0.3032(2)	0.4355(2)	0.0127(4)	C(25)	0.5472(2)	-0.1821(2)	0.2302(2)	0.0170(4)
C(7)	0.0117(2)	-0.1027(2)	0.2742(2)	0.0135(4)	C(26)	0.5147(2)	-0.1222(2)	0.3309(2)	0.0161(4)
C(8)	-0.0942(2)	-0.0458(2)	0.3026(2)	0.0147(4)	C(27)	0.4434(2)	-0.0266(2)	0.3325(2)	0.0140(4)
C(9)	-0.0420(2)	0.0753(2)	0.3575(2)	0.0128(4)	C(28)	0.3987(2)	0.2372(2)	0.1790(2)	0.0128(4)
C(10)	0.0148(2)	-0.2327(2)	0.2219(2)	0.0152(4)	C(29)	0.5361(2)	0.2506(2)	0.1986(2)	0.0157(4)
C(11)	0.1339(2)	-0.2721(2)	0.2135(2)	0.0236(5)	C(30)	0.6053(2)	0.3432(2)	0.1696(2)	0.0193(5)
C(12)	0.1393(3)	-0.3951(2)	0.1746(3)	0.0303(6)	C(31)	0.5382(3)	0.4230(2)	0.1215(2)	0.0204(5)
C(13)	0.0256(3)	-0.4813(2)	0.1416(2)	0.0290(6)	C(32)	0.4020(3)	0.4091(2)	0.0996(2)	0.0227(5)
C(14)	-0.0939(3)	-0.4427(2)	0.1461(2)	0.0296(6)	C(33)	0.3320(2)	0.3160(2)	0.1276(2)	0.0182(5)
C(15)	-0.0998(3)	-0.3198(2)	0.1862(2)	0.0228(5)	N(1)	0.0898(2)	0.0862(2)	0.3603(2)	0.0109(3)
C(16)	-0.1081(2)	0.1774(2)	0.4030(2)	0.0131(4)	N(2)	0.1240(2)	-0.0223(2)	0.3092(2)	0.0128(4)
C(17)	-0.2035(2)	0.1587(2)	0.4632(2)	0.0186(5)	P(1)	0.2984(1)	0.1235(1)	0.2202(1)	0.0100(1)
C(18)	-0.2661(2)	0.2538(2)	0.5087(2)	0.0235(5)	Cu(1)	0.1057(1)	0.0474(1)	0.0925(1)	0.0142(1)
C(19)	-0.2342(2)	0.3684(2)	0.4948(2)	0.0229(5)	I(1)	-0.0961(1)	0.1517(1)	0.0667(1)	0.0187(1)

7.6 Strukturen für Katrin Schlechter

7.6.1 1,2-Bis(dimethylamino)-3-dimethylguanidinium-chlorid (hsjbdmg)

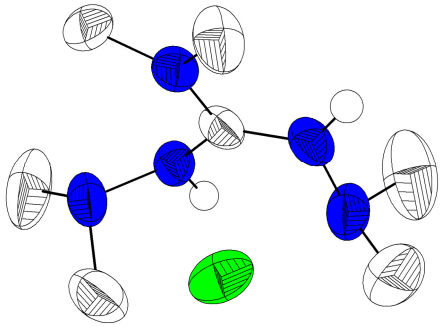

Kristalldaten

C7 H20 Cl N5	M = 209.73 g/mol	Orthorhombic, $P2_12_12_1$
a = 9.0842(8) Å	b = 10.1399(12) Å	c = 13.6286(15) Å
α = 90°	β = 90°	γ = 90°
V = 1255.4(2) Å^3	Z = 4	F(000) = 456
D_{calc} = 1.110 g/cm^3	μ = 0.277 mm^{-1}	
colourless block	0.210 · 0.180 · 0.170 mm^3	

Datensammlung

Diffraktometer: D8 Quest (Bruker)	T = 253(2) K	λ = 0.71069 Å
h = -10 bis 11	k = -12 bis 12	l = -17 bis 17
14059 gemessene Reflexe	2729 unabhängige Reflexe	2121 Reflexe mit $I > 2\sigma(I)$
θ = 2.503 bis 26.991°	R_{int} = 0.0387	C (25.00°) = 1.000
Absorptionskorrektur: Multi-scan	T_{min} = 0.7056	T_{max} = 0.7455

Verfeinerung

2729 Reflexe	1 Restraints	162 Parameter
Verfeinerung mit SHELXL-2014/7	bis χ = 0.000	
R_1 ($I > 2\sigma(I)$) = 0.0417	wR_2 ($I > 2\sigma(I)$) = 0.1014	
R_1 (all) = 0.0613	wR_2 (all) = 0.1116	GoF (S) = 1.079
$\Delta\varphi_{min}$ = -0.151 e·Å^{-3}	$\Delta\varphi_{max}$ = 0.223 e·Å^{-3}	

Kommentar

Die Dimethylaminogruppe ist über zwei Positionen fehlgeordnet.

Fraktionelle Atomkoordinaten (*x, y, z*) und äquivalente isotrope Auslenkungsfaktoren *U*(eq)

	x	*y*	*z*	*U*(eq)/Å^2		*x*	*y*	*z*	*U*(eq)/Å^2
C(1)	0.0528(3)	0.1178(3)	0.7264(2)	0.0458(6)	C(5)	-0.2169(4)	0.1099(6)	0.9110(3)	0.1008(15)
N(1)	-0.047(3)	0.132(3)	0.6533(18)	0.052(3)	C(6)	0.3918(5)	0.2192(5)	0.7855(4)	0.1143(17)
C(2)	-0.202(2)	0.099(2)	0.6583(17)	0.067(4)	C(7)	0.3639(5)	-0.0167(5)	0.8068(3)	0.1105(17)
C(3)	0.008(3)	0.178(3)	0.5574(14)	0.079(4)	N(2)	-0.0042(2)	0.0981(2)	0.8157(2)	0.0450(5)
N(1A)	-0.013(3)	0.160(3)	0.646(2)	0.056(4)	N(3)	-0.1201(3)	0.1828(2)	0.8463(2)	0.0552(6)
C(2A)	-0.170(3)	0.128(3)	0.633(2)	0.079(6)	N(4)	0.1981(3)	0.1062(3)	0.7145(2)	0.0542(6)
C(3A)	0.066(4)	0.208(3)	0.5587(16)	0.086(6)	N(5)	0.2887(3)	0.1090(3)	0.7969(2)	0.0630(7)
C(4)	-0.0549(5)	0.2964(4)	0.8955(3)	0.0836(12)	Cl(1)	0.1192(1)	-0.0074(1)	1.0348(1)	0.0740(3)

7.6.2 Bis(1,2-bis(dimethylamin)-3,3-dimethylguanidino)-eisen(II) (hsksfe)

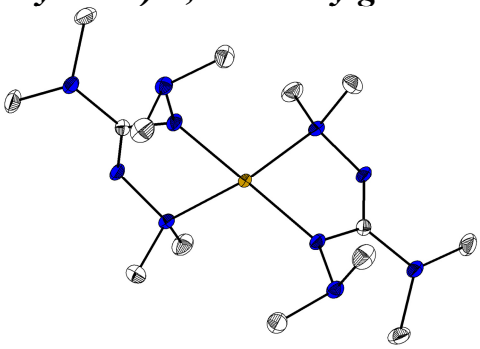

Kristalldaten

C14 H36 Fe N10	M = 400.38 g/mol	Monoclinic, $C2/c$
a = 15.7193(15) Å	b = 7.2818(6) Å	c = 18.3250(17) Å
α = 90°	β = 97.219(3)°	γ = 90°
V = 2080.9(3) Å^3	Z = 4	F(000) = 864
D_{calc} = 1.278 g/cm^3	μ = 0.744 mm^{-1}	
light yellow block	0.440 · 0.180 · 0.090 mm^3	

Datensammlung

Diffraktometer: D8 Quest (Bruker)	T = 100(2) K	λ = 0.71069 Å
h = -20 bis 20	k = -9 bis 9	l = -23 bis 23
15544 gemessene Reflexe	2321 unabhängige Reflexe	2194 Reflexe mit $I > 2\sigma(I)$
θ = 2.240 bis 27.190°	R_{int} = 0.0407	C (25.00°) = 1.000
Absorptionskorrektur: Multi-scan	T_{min} = 0.8336	T_{max} = 1.00

Verfeinerung

2321 Reflexe	0 Restraints	120 Parameter
Verfeinerung mit SHELXL-2014/7	bis χ = 0.000	
R_1 ($I > 2\sigma(I)$) = 0.0258	wR_2 ($I > 2\sigma(I)$) = 0.0765	
R_1 (all) = 0.0299	wR_2 (all) = 0.0915	GoF (S) = 1.283
$\Delta\varphi_{min}$ = -0.350 e·Å^{-3}	$\Delta\varphi_{max}$ = 0.394 e·Å^{-3}	

Fraktionelle Atomkoordinaten (*x, y, z*) und äquivalente isotrope Auslenkungsfaktoren *U*(eq)

	x	*y*	*z*	*U*(eq)/Å^2
C(1)	0.1319(1)	0.6184(2)	0.3626(1)	0.0124(3)
C(2)	0.2584(1)	0.5033(2)	0.4386(1)	0.0206(3)
C(3)	0.1320(1)	0.5841(2)	0.4945(1)	0.0197(3)
C(4)	0.1139(1)	1.0417(2)	0.3717(1)	0.0246(4)
C(5)	-0.0223(1)	0.9448(2)	0.4018(1)	0.0212(3)
C(6)	0.1773(1)	0.6661(2)	0.2052(1)	0.0211(3)
C(7)	0.1018(1)	0.3793(2)	0.1978(1)	0.0207(3)
Fe(1)	0.0000	0.6973(1)	0.2500	0.0117(1)
N(1)	0.1797(1)	0.6113(2)	0.4321(1)	0.0150(3)
N(2)	0.0656(1)	0.7392(2)	0.3483(1)	0.0132(3)
N(3)	0.0660(1)	0.8910(2)	0.3990(1)	0.0140(3)
N(4)	0.1559(1)	0.5057(2)	0.3130(1)	0.0144(3)
N(5)	0.1148(1)	0.5527(2)	0.2388(1)	0.0134(3)

7.6.3 Bis(1,2-bis(dimethylamin)-3,3-dimethylguanidino)-zink(II) (hsksZn)

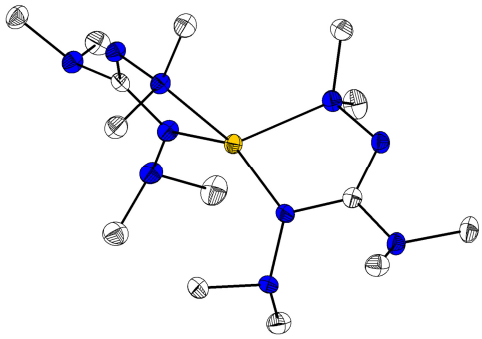

Kristalldaten

C14 H36 N10 Zn	M = 409.90 g/mol	Triclinic, P-1
a = 8.3045(5) Å	b = 8.6181(5) Å	c = 14.8574(9) Å
α = 81.740(3)°	β = 88.668(3)°	γ = 87.053(3)°
V = 1050.77(11) Å^3	Z = 2	F(000) = 440
D_{calc} = 1.296 g/cm^3	μ = 1.188 mm^{-1}	
colourless block	0.330 · 0.260 · 0.220 mm^3	

Datensammlung

Diffraktometer: D8 Quest (Bruker)	T = 100(2) K	λ = 0.71069 Å
h = -10 bis 10	k = -11 bis 11	l = -19 bis 19
23480 gemessene Reflexe	4903 unabhängige Reflexe	4408 Reflexe mit $I > 2\sigma(I)$
θ = 2.456 bis 27.962°	R_{int} = 0.0380	C (25.00°) = 0.998
Absorptionskorrektur: Multi-scan	T_{min} = 0.8688	T_{max} = 1.00

Verfeinerung

4903 Reflexe	0 Restraints	238 Parameter
Verfeinerung mit SHELXL-2014/7	bis χ = 0.001	
R_1 ($I > 2\sigma(I)$) = 0.0286	wR_2 ($I > 2\sigma(I)$) = 0.0632	
R_1 (all) = 0.0356	wR_2 (all) = 0.0665	GoF (S) = 1.090
$\Delta\varphi_{min}$ = -0.463 e·Å^{-3}	$\Delta\varphi_{max}$ = 0.342 e·Å^{-3}	

Fraktionelle Atomkoordinaten (*x, y, z*) und äquivalente isotrope Auslenkungsfaktoren *U*(eq)

	x	*y*	*z*	*U*(eq)/Å^2
C(1)	0.4813(2)	0.4421(2)	0.6705(1)	0.0145(3)
C(2)	0.6936(2)	0.4620(2)	0.5539(1)	0.0201(3)
C(3)	0.6203(2)	0.2073(2)	0.6295(1)	0.0252(4)
C(4)	0.0774(2)	0.4069(2)	0.6765(1)	0.0217(3)
C(5)	0.2055(2)	0.3352(2)	0.8201(1)	0.0251(4)
C(6)	0.6258(2)	0.8186(2)	0.6795(1)	0.0213(3)
C(7)	0.7031(2)	0.5966(2)	0.7892(1)	0.0214(3)
C(8)	0.0574(2)	0.8630(2)	0.8149(1)	0.0141(3)
C(9)	-0.1495(2)	1.0614(2)	0.8449(1)	0.0212(3)
C(10)	-0.0962(2)	0.8357(2)	0.9586(1)	0.0210(3)
C(11)	0.2294(2)	0.9736(2)	0.6270(1)	0.0204(3)
C(12)	0.0323(2)	0.7990(2)	0.5928(1)	0.0198(3)
C(13)	0.3759(2)	0.8771(2)	0.9209(1)	0.0246(4)
C(14)	0.2964(3)	0.6156(2)	0.9725(1)	0.0283(4)
N(1)	0.6207(2)	0.3745(2)	0.6352(1)	0.0179(3)
N(2)	0.3558(2)	0.3541(2)	0.6822(1)	0.0173(3)
N(3)	0.2211(2)	0.4284(2)	0.7290(1)	0.0163(3)
N(4)	0.4825(2)	0.5897(2)	0.6920(1)	0.0159(3)
N(5)	0.6406(2)	0.6485(2)	0.6986(1)	0.0161(3)
N(6)	-0.0331(2)	0.9356(2)	0.8786(1)	0.0171(3)
N(7)	0.0147(2)	0.9029(2)	0.7296(1)	0.0152(3)
N(8)	0.1314(2)	0.8411(2)	0.6657(1)	0.0153(3)
N(9)	0.1815(2)	0.7594(2)	0.8416(1)	0.0166(3)
N(10)	0.2434(2)	0.7713(2)	0.9301(1)	0.0190(3)
Zn(1)	0.2768(1)	0.6617(1)	0.7406(1)	0.0142(1)

7.6.4 Bis(1-dimethylamin-2,2,3-trimethylguanidino)-zink(II) (im2)

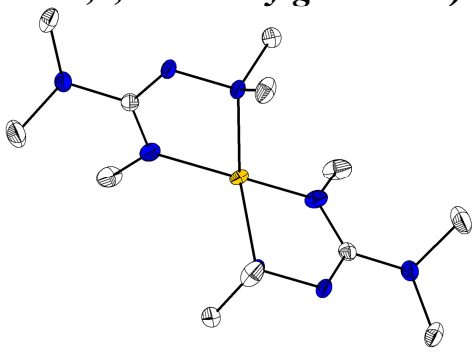

Kristalldaten

C12 H30 N8 Zn	M = 351.81 g/mol	Orthorhombic, *Pccn*
a = 8.2474(4) Å	b = 13.6855(5) Å	c = 15.9339(7) Å
α = 90°	β = 90°	γ = 90°
V = 1798.46(13) Å^3	Z = 4	F(000) = 752
D_{calc} = 1.299 g/cm^3	μ = 1.373 mm^{-1}	
colourless block	0.37 · 0.36 · 0.25 mm^3	

Datensammlung

Diffraktometer: D8 Quest (Bruker)	T = 100(2) K	λ = 0.71069 Å
h = -10 bis 10	k = -17 bis 17	l = -20 bis 20
20137 gemessene Reflexe	2002 unabhängige Reflexe	1779 Reflexe mit $I > 2\sigma(I)$
θ = 2.883 bis 27.150°	R_{int} = 0.0308	C (25.00°) = 0.999
Absorptionskorrektur: Multi-scan	T_{min} = 0.4044	T_{max} = 0.7455

Verfeinerung

2002 Reflexe	0 Restraints	101 Parameter
Verfeinerung mit SHELXL-2014/7	bis χ = 0.000	
R_1 ($I > 2\sigma(I)$) = 0.0219	wR_2 ($I > 2\sigma(I)$) = 0.0540	
R_1 (all) = 0.0264	wR_2 (all) = 0.0561	GoF (S) = 1.070
$\Delta\varphi_{min}$ = -0.294 e·Å^{-3}	$\Delta\varphi_{max}$ = 0.244 e·Å^{-3}	

Fraktionelle Atomkoordinaten (*x, y, z*) und äquivalente isotrope Auslenkungsfaktoren *U*(eq)

	x	*y*	*z*	*U*(eq)/Å^2
C(1)	0.8231(2)	0.0565(1)	0.3614(1)	0.0136(2)
C(2)	1.0824(2)	-0.0265(1)	0.3599(1)	0.0280(3)
C(3)	0.8382(2)	-0.1192(1)	0.3821(1)	0.0214(3)
C(4)	0.9638(2)	0.1367(1)	0.2448(1)	0.0243(3)
C(5)	0.4614(2)	0.1291(1)	0.3811(1)	0.0223(3)
C(6)	0.5843(2)	0.1567(1)	0.5156(1)	0.0225(3)
N(1)	0.9075(1)	-0.0314(1)	0.3446(1)	0.0163(2)
N(2)	0.8613(1)	0.1384(1)	0.3191(1)	0.0169(2)
N(3)	0.7085(1)	0.0505(1)	0.4190(1)	0.0138(2)
N(4)	0.6172(1)	0.1425(1)	0.4256(1)	0.0140(2)
Zn(1)	0.7500	0.2500	0.3648(1)	0.0131(1)

7.6.5 N,N,N',N',N'',N'',N''',N'''-2,2-Decamethylhydrazine-1,1-bis(carbohydrazonamide) (mj33)

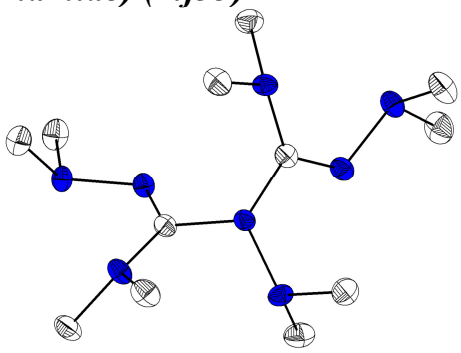

Kristalldaten

C12 H30 N8	M = 286.44 g/mol	Triclinic, $P\bar{1}$
a = 6.0646(8) Å	b = 8.8935(12) Å	c = 16.125(2) Å
α = 89.316(4)°	β = 83.164(4)°	γ = 75.769(4)°
V = 836.9(2) Å^3	Z = 2	F(000) = 316
D_{calc} = 1.137 g/cm^3	μ = 0.075 mm^{-1}	
colourless needle	0.552 · 0.092 · 0.055 mm^3	

Datensammlung

Diffraktometer: D8 Quest (Bruker)	T = 100(2) K	λ = 0.71073 Å
h = -8 bis 8	k = -11 bis 11	l = -21 bis 19
15242 gemessene Reflexe	4133 unabhängige Reflexe	2589 Reflexe mit $I > 2\sigma(I)$
θ = 2.363 bis 28.377°	R_{int} = 0.0804	C (25.00°) = 0.999
Absorptionskorrektur: Multi-scan	T_{min} = 0.5505	T_{max} = 0.7457

Verfeinerung

4133 Reflexe	0 Restraints	191 Parameter
Verfeinerung mit SHELXL-2014/7	bis χ = 0.000	
R_1 ($I > 2\sigma(I)$) = 0.0536	wR_2 ($I > 2\sigma(I)$) = 0.0975	
R_1 (all) = 0.1075	wR_2 (all) = 0.1147	GoF (S) = 1.017
$\Delta\varphi_{min}$ = -0.217 e·Å^{-3}	$\Delta\varphi_{max}$ = 0.203 e·Å^{-3}	

Fraktionelle Atomkoordinaten (*x, y, z*) und äquivalente isotrope Auslenkungsfaktoren *U*(eq)

	x	*y*	*z*	*U*(eq)/Å^2		*x*	*y*	*z*	*U*(eq)/Å^2
C(1)	0.5425(3)	0.7525(2)	0.5841(1)	0.0220(4)	C(11)	0.0492(3)	1.1098(2)	0.8345(1)	0.0225(4)
C(2)	0.2218(3)	0.6305(2)	0.6092(1)	0.0238(4)	C(12)	0.4533(3)	0.9751(2)	0.8198(1)	0.0222(4)
C(3)	0.3072(3)	0.6747(2)	0.7898(1)	0.0150(4)	N(1)	0.3379(2)	0.7672(2)	0.7199(1)	0.0148(3)
C(4)	-0.1491(3)	0.7148(2)	0.9518(1)	0.0225(4)	N(2)	0.4052(2)	0.6787(2)	0.6438(1)	0.0170(3)
C(5)	0.2457(3)	0.6670(2)	0.9721(1)	0.0212(4)	N(3)	0.1149(2)	0.7206(2)	0.8367(1)	0.0161(3)
C(6)	0.7180(3)	0.5413(2)	0.7603(1)	0.0223(4)	N(4)	0.0852(2)	0.6461(2)	0.9151(1)	0.0164(3)
C(7)	0.4368(3)	0.4010(2)	0.8179(1)	0.0225(4)	N(5)	0.4879(2)	0.5504(2)	0.8011(1)	0.0173(3)
C(8)	0.1974(3)	0.9211(2)	0.7220(1)	0.0153(4)	N(6)	0.0554(2)	0.9563(2)	0.6674(1)	0.0173(3)
C(9)	0.1124(3)	1.1998(2)	0.6203(1)	0.0263(4)	N(7)	-0.0522(2)	1.1191(2)	0.6607(1)	0.0182(3)
C(10)	-0.2370(3)	1.1271(2)	0.6097(1)	0.0273(4)	N(8)	0.2444(2)	1.0193(2)	0.7798(1)	0.0171(3)

7.6.6 *Tris(1,2-bis(dimethylamin)-3,3-dimethylguanidino)-ytterbium(III) (mj37)*

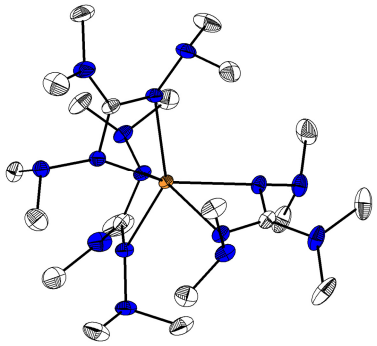

Kristalldaten

C21 H54 N15 Yb	M = 689.83 g/mol	Monoclinic, $C2/c$
a = 15.4625(7) Å	b = 14.9987(7) Å	c = 14.5068(7) Å
α = 90°	β = 95.290(2)°	γ = 90°
V = 3350.0(3) Å^3	Z = 4	F(000) = 1420
D_{calc} = 1.368 g/cm^3	μ = 2.826 mm^{-1}	
clear pale yellow block	0.260 · 0.147 · 0.138 mm^3	

Datensammlung

Diffraktometer: D8 Quest (Bruker)	T = 100(2) K	λ = 0.71069 Å
h = -20 bis 20	k = -20 bis 20	l = -19 bis 19
50066 gemessene Reflexe	4192 unabhängige Reflexe	4006 Reflexe mit $I > 2\sigma(I)$
θ = 2.288 bis 28.377°	R_{int} = 0.0288	C (25.00°) = 1.000
Absorptionskorrektur: Multi-scan	T_{min} = 0.5794	T_{max} = 0.7457

Verfeinerung

4192 Reflexe	0 Restraints	178 Parameter
Verfeinerung mit SHELXL-2014/7	bis χ = 0.002	
R_1 ($I > 2\sigma(I)$) = 0.0131	wR_2 ($I > 2\sigma(I)$) = 0.0317	
R_1 (all) = 0.0149	wR_2 (all) = 0.0324	GoF (S) = 1.118
$\Delta\varphi_{min}$ = -0.436 e·Å^{-3}	$\Delta\varphi_{max}$ = 1.001 e·Å^{-3}	

Fraktionelle Atomkoordinaten (*x, y, z*) und äquivalente isotrope Auslenkungsfaktoren *U*(eq)

	x	*y*	*z*	*U*(eq)/Å^2
C(1)	-0.0074(1)	0.1897(1)	0.4156(1)	0.0177(3)
C(2)	0.0627(1)	0.1406(1)	0.5659(1)	0.0382(4)
C(3)	-0.0888(1)	0.0981(1)	0.5188(1)	0.0376(4)
C(4)	0.1136(1)	0.0628(1)	0.3100(1)	0.0301(3)
C(5)	0.2134(1)	0.1651(1)	0.3882(1)	0.0361(4)
C(6)	-0.1302(1)	0.3507(1)	0.4575(1)	0.0285(3)
C(7)	-0.2260(1)	0.2483(1)	0.3723(1)	0.0284(3)
C(8)	0.0000	0.4739(1)	0.2500	0.0178(4)
C(9)	0.0786(1)	0.6158(1)	0.2435(2)	0.0378(4)
C(11)	-0.0997(1)	0.4353(1)	0.0554(1)	0.0284(3)
C(12)	-0.2135(1)	0.4361(1)	0.1559(1)	0.0373(4)
N(1)	-0.0104(1)	0.1429(1)	0.4958(1)	0.0279(3)
N(2)	0.0647(1)	0.1985(1)	0.3706(1)	0.0178(2)
N(3)	0.1270(1)	0.1266(1)	0.3863(1)	0.0231(3)
N(4)	-0.0752(1)	0.2329(1)	0.3714(1)	0.0169(2)
N(5)	-0.1433(1)	0.2582(1)	0.4282(1)	0.0196(2)
N(6)	0.0000	0.5643(1)	0.2500	0.0268(4)
N(7)	-0.0680(1)	0.4229(1)	0.2172(1)	0.0174(2)
N(8)	-0.1251(1)	0.4646(1)	0.1449(1)	0.0225(2)
Yb(1)	0.0000	0.2858(1)	0.2500	0.0125(1)

7.7 Strukturen für Jannick Guschlbauer

7.7.1 N,N-Dimethylpyrrolidinium-hydrogensulfid (majg06)

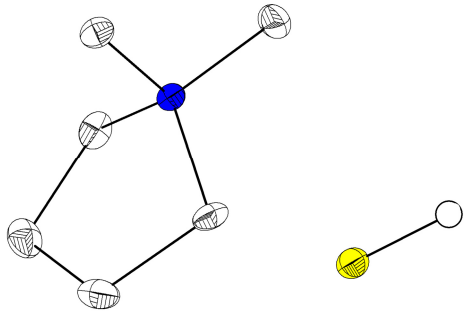

Kristalldaten

C6 H15 N S	M = 133.25 g/mol	Monoclinic, $P2_1/n$
a = 6.7084(4) Å	b = 11.7617(7) Å	c = 9.9595(5) Å
α = 90°	β = 94.632(2)°	γ = 90°
V = 783.26(8) Å^3	Z = 4	F(000) = 296
D_{calc} = 1.130 g/cm^3	μ = 0.322 mm^{-1}	
colourless block	0.250 · 0.190 · 0.130 mm^3	

Datensammlung

Diffraktometer: D8 Quest (Bruker)	T = 100(2) K	λ = 0.71073 Å
h = -8 bis 7	k = -14 bis 15	l = -12 bis 12
8889 gemessene Reflexe	1733 unabhängige Reflexe	1579 Reflexe mit $I > 2\sigma(I)$
θ = 2.685 bis 27.127°	R_{int} = 0.0254	C (25.00°) = 1.000
Absorptionskorrektur: Multi-scan	T_{min} = 0.7044	T_{max} = 0.7455

Verfeinerung

1733 Reflexe	0 Restraints	79 Parameter
Verfeinerung mit SHELXL-2014/7	bis χ = 0.000	
R_1 ($I > 2\sigma(I)$) = 0.0266	wR_2 ($I > 2\sigma(I)$) = 0.0655	
R_1 (all) = 0.0307	wR_2 (all) = 0.0674	GoF (S) = 1.081
$\Delta\varphi_{min}$ = -0.196 e·Å^{-3}	$\Delta\varphi_{max}$ = 0.252 e·Å^{-3}	

Fraktionelle Atomkoordinaten (*x, y, z*) und äquivalente isotrope Auslenkungsfaktoren *U*(eq)

	x	*y*	*z*	*U*(eq)/Å^2		*x*	*y*	*z*	*U*(eq)/Å^2
C(1)	0.3587(2)	0.1399(1)	0.4348(1)	0.0145(2)	C(5)	-0.0102(2)	0.1571(1)	0.4350(1)	0.0131(2)
C(2)	0.3467(2)	0.0553(1)	0.3184(1)	0.0188(3)	C(6)	0.2002(2)	0.3254(1)	0.4809(1)	0.0173(3)
C(3)	0.2352(2)	0.1195(1)	0.1989(1)	0.0181(3)	N(1)	0.1795(1)	0.2163(1)	0.4045(1)	0.0102(2)
C(4)	0.1821(2)	0.2356(1)	0.2546(1)	0.0139(2)	S(1)	0.6747(1)	0.3924(1)	0.2866(1)	0.0138(1)

7.7.2 Dimethylpyrrolidinium-dimethylindiumthiolat (majg12c1)

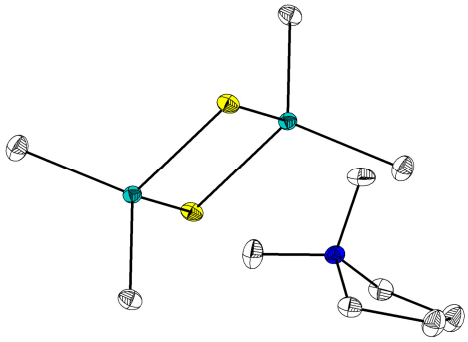

Kristalldaten

C16 H40 In2 N2 S2	M = 554.26 g/mol	Monoclinic, $P2_1/n$
a = 9.7075(4) Å	b = 12.1404(5) Å	c = 9.9277(5) Å
α = 90°	β = 100.208(2)°	γ = 90°
V = 1151.49(9) Å^3	Z = 2	F(000) = 560
D_{calc} = 1.599 g/cm^3	μ = 2.184 mm^{-1}	
colourless needle	0.530 · 0.070 · 0.060 mm^3	

Datensammlung

Diffraktometer: D8 Quest (Bruker)	T = 100(2) K	λ = 0.71073 Å
h = -12 bis 12	k = -15 bis 15	l = -12 bis 12
34138 gemessene Reflexe	2560 unabhängige Reflexe	2287 Reflexe mit $I > 2\sigma(I)$
θ = 2.676 bis 27.169°	R_{int} = 0.0527	C (25.00°) = 1.000
Absorptionskorrektur: Multi-scan	T_{min} = 0.6218	T_{max} = 0.7455

Verfeinerung

2560 Reflexe	0 Restraints	104 Parameter
Verfeinerung mit SHELXL-2014/7	bis χ = 0.000	
R_1 ($I > 2\sigma(I)$) = 0.0141	wR_2 ($I > 2\sigma(I)$) = 0.0296	
R_1 (all) = 0.0184	wR_2 (all) = 0.0303	GoF (S) = 1.071
$\Delta\varphi_{min}$ = -0.367 e·Å^{-3}	$\Delta\varphi_{max}$ = 0.277 e·Å^{-3}	

Fraktionelle Atomkoordinaten (*x, y, z*) und äquivalente isotrope Auslenkungsfaktoren *U*(eq)

	x	*y*	*z*	*U*(eq)/Å^2
C(1)	0.6813(2)	0.2092(1)	0.2284(2)	0.0155(3)
C(2)	0.7065(2)	0.1447(1)	0.3616(2)	0.0215(4)
C(3)	0.5953(2)	0.0529(1)	0.3450(2)	0.0204(4)
C(4)	0.5233(2)	0.0593(1)	0.1965(2)	0.0146(3)
C(5)	0.4297(2)	0.2470(1)	0.2193(2)	0.0194(3)
C(6)	0.5145(2)	0.1963(1)	0.0091(2)	0.0214(4)
C(7)	0.1620(2)	0.0366(1)	0.3391(2)	0.0187(3)
C(8)	0.0002(2)	0.2607(1)	0.1361(2)	0.0153(3)
S(1)	0.1696(1)	0.0307(1)	-0.0555(1)	0.0129(1)
In(1)	0.0452(1)	0.0826(1)	0.1357(1)	0.0105(1)
N(1)	0.5342(1)	0.1802(1)	0.1610(1)	0.0122(3)

7.7.3 Dimethylpyrrolidinium-dimethylgalliumthiolat (majg12c4)

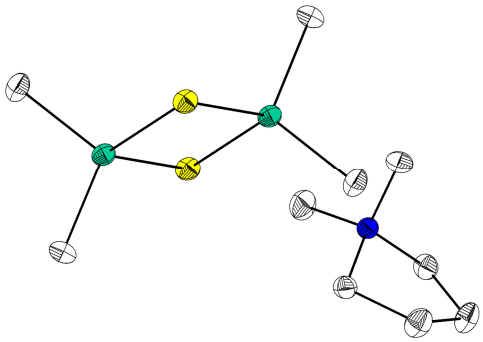

Kristalldaten

C16 H40 Ga2 N2 S2	M = 464.06 g/mol	Monoclinic, $P2_1/n$
a = 9.5961(4) Å	b = 12.0450(5) Å	c = 9.9485(4) Å
α = 90°	β = 102.3790(10)°	γ = 90°
V = 1123.16(8) Å^3	Z = 2	F(000) = 488
D_{calc} = 1.372 g/cm^3	μ = 2.584 mm^{-1}	
colourless block	0.450 · 0.230 · 0.180 mm^3	

Datensammlung

Diffraktometer: D8 Quest (Bruker)	T = 100(2) K	λ = 0.71073 Å
h = -12 bis 12	k = -15 bis 15	l = -12 bis 12
37739 gemessene Reflexe	2483 unabhängige Reflexe	2302 Reflexe mit $I > 2\sigma(I)$
θ = 2.676 bis 27.151°	R_{int} = 0.0382	C (25.00°) = 0.999
Absorptionskorrektur: Multi-scan	T_{min} = 0.5293	T_{max} = 0.7455

Verfeinerung

2483 Reflexe	85 Restraints	170 Parameter
Verfeinerung mit SHELXL-2014/7	bis χ = 0.001	
R_1 ($I > 2\sigma(I)$) = 0.0192	wR_2 ($I > 2\sigma(I)$) = 0.0505	
R_1 (all) = 0.0216	wR_2 (all) = 0.0513	GoF (S) = 1.055
$\Delta\varphi_{min}$ = -0.257 e·Å^{-3}	$\Delta\varphi_{max}$ = 0.591 e·Å^{-3}	

Kommentar

Das Dimethylpyrrolidiniumkation ist über zwei Positionen fehlgeordnet. Die schwächer besetzte Position wurde über DELU und RIGU restrained.

Fraktionelle Atomkoordinaten (*x, y, z*) und äquivalente isotrope Auslenkungsfaktoren *U*(eq)

	x	*y*	*z*	*U*(eq)/Å^2		*x*	*y*	*z*	*U*(eq)/Å^2
N(1)	-0.0427(2)	0.1758(2)	0.3352(2)	0.0159(4)	S(1)	0.3416(1)	0.0299(1)	0.5521(1)	0.0183(1)
C(1)	-0.0282(2)	0.0535(2)	0.3072(2)	0.0189(4)	Ga(1)	0.4542(1)	0.0776(1)	0.3757(1)	0.0166(1)
C(2)	-0.0973(3)	0.0415(2)	0.1557(3)	0.0262(6)	N(2)	-0.0576(18)	0.2087(11)	0.3041(16)	0.019(3)
C(3)	-0.2168(2)	0.1296(2)	0.1306(2)	0.0276(5)	C(11)	-0.0286(16)	0.1041(12)	0.3847(15)	0.021(3)
C(4)	-0.1923(2)	0.2018(2)	0.2584(2)	0.0205(4)	C(12)	-0.045(3)	0.0155(15)	0.275(2)	0.030(5)
C(5)	0.0651(3)	0.2427(3)	0.2811(3)	0.0230(7)	C(13)	-0.137(3)	0.0648(17)	0.145(2)	0.024(5)
C(6)	-0.0256(2)	0.1965(2)	0.4858(2)	0.0283(5)	C(14)	-0.1794(17)	0.1772(13)	0.1871(17)	0.021(3)
C(7)	0.4983(2)	0.2425(1)	0.3755(2)	0.0176(3)	C(15)	0.067(3)	0.239(3)	0.243(3)	0.022(5)
C(8)	0.3419(2)	0.0349(1)	0.1880(2)	0.0230(3)	C(16)	-0.1030(19)	0.3019(12)	0.3841(17)	0.026(4)

7.7.4 Bis(dimethylpyrrolidinium)-tricyclo-tetrakis(μ_3-thioxo)-hexakis(dimethylindat)-tetrahydrofuransolvat (majgl2inb)

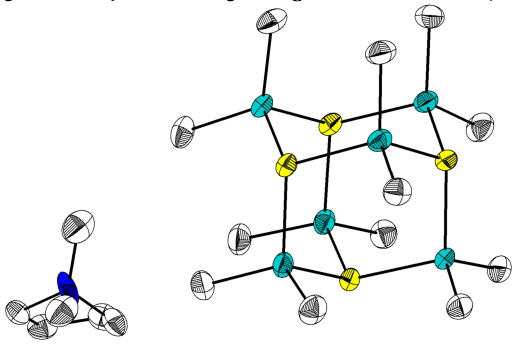

Kristalldaten

C14 H36 In3 N O0.50 S2	M = 635.02 g/mol	Tetragonal, $I4_1/acd$
a = 17.0977(11) Å	b = 17.0977 Å	c = 32.377(2) Å
α = 90°	β = 90°	γ = 90°
V = 9464.7(14) Å^3	Z = 16	F(000) = 4960
D_{calc} = 1.783 g/cm^3	μ = 3.072 mm^{-1}	
colourless block	0.435 · 0.403 · 0.195 mm^3	

Datensammlung

Diffraktometer: D8 Quest (Bruker)	T = 100(2) K	λ = 0.71073 Å
h = -21 bis 17	k = -19 bis 21	l = -41 bis 41
40556 gemessene Reflexe	2619 unabhängige Reflexe	1784 Reflexe mit $I > 2\sigma(I)$
θ = 2.382 bis 27.143°	R_{int} = 0.0961	C (25.00°) = 0.999
Absorptionskorrektur: Multi-scan	T_{min} = 0.4882	T_{max} = 0.7455

Verfeinerung

2619 Reflexe	132 Restraints	131 Parameter
Verfeinerung mit SHELXL-2014/7	bis χ = 0.000	
R_1 ($I > 2\sigma(I)$) = 0.0379	wR_2 ($I > 2\sigma(I)$) = 0.0612	
R_1 (all) = 0.0678	wR_2 (all) = 0.0684	GoF (S) = 1.046
$\Delta\varphi_{min}$ = -0.692 e·Å^{-3}	$\Delta\varphi_{max}$ = 0.894 e·Å^{-3}	

Kommentar

Das Pyrrolidiniumkation ist mittels eines Symmetriezentrums über zwei positionen fehlgeordnet (50:50) und wurde über DELU, RIGU, SIMU, DFIX und DANG restrained. Das THF-Molekül ist mittels mehrerer Symmetriezentren über vier Positionen fehlgeordnet (25:25.25:25) und wurde über DFIX, ISOR, SAME und EADP re- bzw. constrained.

Fraktionelle Atomkoordinaten (*x, y, z*) und äquivalente isotrope Auslenkungsfaktoren *U*(eq)

	x	*y*	*z*	*U*(eq)/Å^2
C(1)	0.5638(3)	0.3387(3)	-0.0001(2)	0.0483(15)
C(2)	0.5424(4)	0.4911(3)	0.0822(2)	0.0518(16)
C(3)	0.3851(3)	0.4772(3)	0.1619(2)	0.0461(15)
In(1)	0.5000	0.2500	0.0343(1)	0.0320(1)
In(2)	0.4729(1)	0.4192(1)	0.1238(1)	0.0360(1)
S(1)	0.4031(1)	0.3182(1)	0.0806(1)	0.0329(3)
N(1)	0.7534(7)	0.5680(4)	-0.0076(4)	0.051(3)
C(10)	0.7779(7)	0.5922(6)	-0.0498(3)	0.045(2)
C(11)	0.8201(7)	0.6647(6)	-0.0385(3)	0.049(3)
C(12)	0.7667(8)	0.7052(5)	-0.0079(4)	0.045(3)
C(13)	0.7164(6)	0.6420(6)	0.0114(3)	0.040(2)
C(14)	0.6858(4)	0.5193(4)	-0.0164(2)	0.0645(18)
O(100)	0.9330(16)	0.7233(17)	-0.1186(11)	0.081(4)
C(101)	0.936(2)	0.8037(18)	-0.1320(12)	0.081(4)
C(102)	1.019(2)	0.816(2)	-0.1446(17)	0.081(4)
C(103)	1.062(2)	0.767(2)	-0.113(2)	0.081(4)
C(104)	1.0109(13)	0.6976(16)	-0.1083(11)	0.081(4)

7.8 Strukturen für Dr. Julius Kögel

7.8.1 1,8-Bis(tris(dimethylamino)phosphazenido-bis(dimethylamino)-methylenphosphoran)naphthalin-dibromid (bisylidP2)

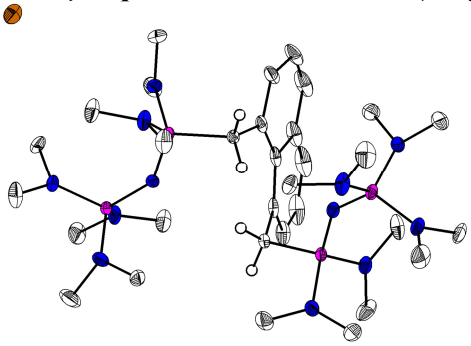

Kristalldaten

C32 H70 Br2 N12 P4	M = 906.70 g/mol	Orthorhombic, *Pnna*
a = 15.9852(6) Å	b = 34.8084(12) Å	c = 15.8419(6) Å
α = 90°	β = 90°	γ = 90°
V = 8814.7(6) Å^3	Z = 8	F(000) = 3808
D_{calc} = 1.366 g/cm^3	μ = 2.023 mm^{-1}	
colourless needle	0.200 · 0.050 · 0.050 mm^3	

Datensammlung

Diffraktometer: D8 Quest (Bruker)	T = 100(2) K	λ = 0.71073 Å
h = -21 bis 21	k = -46 bis 47	l = -21 bis 21
243361 gemessene Reflexe	11648 unabhängige Reflexe	8796 Reflexe mit $I > 2\sigma(I)$
θ = 2.155 bis 28.935°	R_{int} = 0.1131	C (25.00°) = 0.999
Absorptionskorrektur: Multi-scan	T_{min} = 0.6634	T_{max} = 0.7458

Verfeinerung

11648 Reflexe	150 Restraints	528 Parameter
Verfeinerung mit SHELXL-2014/7	bis χ = 0.001	
R_1 ($I > 2\sigma(I)$) = 0.0492	wR_2 ($I > 2\sigma(I)$) = 0.0985	
R_1 (all) = 0.0779	wR_2 (all) = 0.1094	GoF (S) = 1.067
$\Delta\varphi_{min}$ = -1.069 e·Å^{-3}	$\Delta\varphi_{max}$ = 2.174 e·Å^{-3}	

Kommentar

Mehrere stark fehlgeordnete Dimethylaminogruppen wurden über DFIX, ISOR, DELU, SIMU und RIGU restrained. Die Methylenprotonen der Phosphoraneinheiten wurden bezüglich ihrer isotropen Auslenkungsfaktoren an die jeweiligen Parent-C-Atome constrained aber in ihren Koordinaten frei verfeinert.

Fraktionelle Atomkoordinaten (*x, y, z*) und äquivalente isotrope Auslenkungsfaktoren *U*(eq)

	x	y	z	U(eq)/Å^2		x	y	z	U(eq)/Å^2
C(1)	0.7688(2)	0.0360(1)	0.3613(2)	0.0172(5)	C(13)	0.9266(2)	-0.0731(1)	0.3591(2)	0.0286(7)
C(2)	0.7752(2)	0.0689(1)	0.4097(2)	0.0255(7)	C(14)	1.1380(2)	-0.0102(1)	0.2680(2)	0.0268(7)
C(3)	0.7673(2)	0.0686(1)	0.4980(2)	0.0350(8)	C(15)	1.1204(2)	-0.0207(1)	0.1176(2)	0.0367(8)
C(4)	0.7572(2)	0.0348(1)	0.5381(2)	0.0380(9)	C(21)	0.0958(2)	0.2143(1)	0.2248(2)	0.0166(5)
C(4A)	0.7500	0.0000	0.4928(3)	0.0291(10)	C(22)	0.0474(2)	0.1830(1)	0.2033(2)	0.0195(6)
C(5)	0.7882(2)	0.0427(1)	0.2685(2)	0.0132(5)	C(23)	-0.0401(2)	0.1840(1)	0.2029(2)	0.0238(6)
C(6)	0.8575(2)	0.0675(1)	0.0986(2)	0.0291(7)	C(24)	-0.0798(2)	0.2170(1)	0.2257(2)	0.0223(6)
C(7)	1.0056(2)	0.0673(1)	0.1377(2)	0.0305(7)	C(24A)	-0.0339(2)	0.2500	0.2500	0.0179(8)
C(8)	0.9641(2)	0.0965(1)	0.3325(2)	0.0329(8)	C(25)	0.1888(2)	0.2070(1)	0.2176(2)	0.0195(6)
C(8A)	0.7500	0.0000	0.4010(2)	0.0181(8)	C(28)	0.1109(3)	0.1818(1)	0.0006(2)	0.0403(9)
C(9)	0.9836(2)	0.0333(1)	0.3972(2)	0.0292(7)	C(28A)	0.0561(2)	0.2500	0.2500	0.0145(7)
C(10)	1.0023(2)	-0.0985(1)	0.1166(2)	0.0388(9)	C(30)	0.3189(2)	0.3192(1)	0.0798(2)	0.0393(9)
C(11)	0.8785(2)	-0.0591(1)	0.0954(2)	0.0225(6)	C(34)	0.1140(3)	0.3562(1)	0.0177(3)	0.0510(11)
C(12)	1.0658(2)	-0.0929(1)	0.3161(2)	0.0312(7)	C(35)	0.0322(2)	0.3019(1)	0.0707(2)	0.0346(8)

	x	y	z	U(eq)/Å^2
N(1)	0.9191(2)	0.0633(1)	0.1663(2)	0.0218(5)
N(2)	0.9570(2)	0.0545(1)	0.3227(2)	0.0193(5)
N(3)	0.9154(1)	-0.0086(1)	0.2393(2)	0.0163(5)
N(4)	0.9606(2)	-0.0617(1)	0.1341(2)	0.0267(6)
N(5)	0.9980(2)	-0.0650(1)	0.3051(2)	0.0215(5)
N(6)	1.0826(2)	-0.0240(1)	0.2010(2)	0.0211(5)
N(8)	0.1894(2)	0.1797(1)	0.0460(2)	0.0338(7)
N(7)	0.3251(2)	0.2089(1)	0.1130(2)	0.0501(9)
N(9)	0.1907(2)	0.2537(1)	0.0787(2)	0.0299(6)
N(10)	0.1132(2)	0.3156(1)	0.0404(2)	0.0226(5)
N(11)	0.1588(2)	0.2710(1)	-0.0849(2)	0.0485(9)
N(12)	0.2740(2)	0.3090(1)	0.0029(2)	0.0325(7)
P(1)	0.8992(1)	0.0357(1)	0.2482(1)	0.0131(1)
P(2)	0.9875(1)	-0.0384(1)	0.2204(1)	0.0157(1)

	x	y	z	U(eq)/Å^2
P(3)	0.2235(1)	0.2138(1)	0.1095(1)	0.0227(2)
P(4)	0.1855(1)	0.2858(1)	0.0102(1)	0.0207(2)
Br(1)	0.2069(1)	0.1001(1)	0.2648(1)	0.0274(1)
Br(2)	0.2267(1)	0.1447(1)	0.7872(1)	0.0322(1)
C(33A)	0.0973(3)	0.2897(2)	-0.1381(3)	0.0653(13)
C(26A)	0.3706(6)	0.1890(3)	0.1845(5)	0.040(2)
C(27A)	0.3835(9)	0.2224(4)	0.0506(12)	0.074(5)
C(26B)	0.3801(6)	0.2096(7)	0.1792(7)	0.066(4)
C(27B)	0.3642(6)	0.2029(5)	0.0261(6)	0.052(3)
C(32A)	0.2252(13)	0.2466(4)	-0.1263(7)	0.077(4)
C(32B)	0.1883(12)	0.2398(3)	-0.1354(8)	0.035(3)
C(29A)	0.238(3)	0.1434(8)	0.0430(18)	0.061(6)
C(29B)	0.2149(15)	0.1395(4)	0.0528(15)	0.034(4)
C(31)	0.3098(2)	0.3219(2)	-0.0756(3)	0.0597(14)

7.8.2 1,8-Bis(tris(dimethylamino)methinphosphoran)naphthalin (jfk626f5)

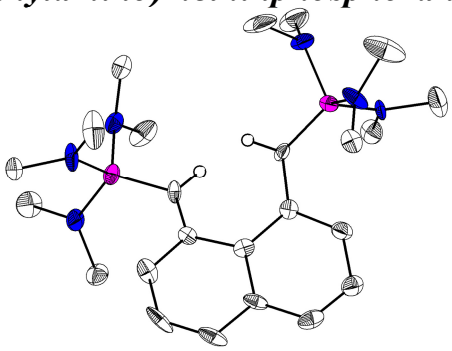

Kristalldaten

C24 H44 N6 P2	M = 478.59 g/mol	Triclinic, $P\bar{1}$
a = 11.8016(10) Å	b = 13.4856(10) Å	c = 18.3777(16) Å
α = 96.615(3)°	β = 94.631(3)°	γ = 110.904(3)°
V = 2690.6(4) Å^3	Z = 4	F(000) = 1040
D_{calc} = 1.181 g/cm^3	μ = 0.184 mm^{-1}	
colourless block	0.418 · 0.188 · 0.178 mm^3	

Datensammlung

Diffraktometer: D8 Quest (Bruker)	T = 100(2) K	λ = 0.71069 Å
h = -16 bis 16	k = -19 bis 19	l = 0 bis 26
12761 gemessene Reflexe	12761 unabhängige Reflexe	6486 Reflexe mit $I > 2\sigma(I)$
θ = 2.276 bis 30.539°	R_{int} = -(hklf5)	C (25.00°) = 0.971
Absorptionskorrektur: Multi-scan	T_{min} = 0.6430	T_{max} = 0.7461

Verfeinerung

12761 Reflexe	48 Restraints	625 Parameter
Verfeinerung mit SHELXL-2014/7	bis χ = 0.000	
R_1 ($I > 2\sigma(I)$) = 0.0805	wR_2 ($I > 2\sigma(I)$) = 0.1708	
R_1 (all) = 0.1971	wR_2 (all) = 0.2206	GoF (S) = 0.998
$\Delta\varphi_{min}$ = -0.492 e·Å^{-3}	$\Delta\varphi_{max}$ = 0.567 e·Å^{-3}	

Kommentar

Die Struktur wurde als nicht-meroedrischer Zwilling integriert und verfeinert. Mehrere stark fehlgeordnete Dimethylaminogruppen wurden über DELU und RIGU restrained. Die Methinprotonen der Phosphoraneinheiten wurden über DFIX restrained und bezüglich ihrer isotropen Auslenkungsfaktoren an die jeweiligen Parent-C-Atome constrained aber in ihren Koordinaten frei verfeinert. Die Verbindung ist mit der aus Probe jfk688f5 (Abschnitt 6.8.3) identisch.

Fraktionelle Atomkoordinaten (*x, y, z*) und äquivalente isotrope Auslenkungsfaktoren *U*(eq)

	x	*y*	*z*	*U*(eq)/Å^2
C(1)	0.8364(5)	0.2320(4)	0.9537(3)	0.0187(13)
C(2)	0.9187(5)	0.2001(4)	0.9154(3)	0.0248(14)
C(3)	0.9927(5)	0.1499(4)	0.9475(3)	0.0288(13)
C(4)	0.9898(5)	0.1343(4)	1.0183(3)	0.0294(15)
C(4A)	0.9055(5)	0.1612(4)	1.0605(2)	0.0235(14)
C(5)	0.9062(5)	0.1483(4)	1.1355(3)	0.0335(14)
C(6)	0.8248(6)	0.1731(4)	1.1760(3)	0.0365(17)
C(7)	0.7333(5)	0.2002(4)	1.1425(3)	0.0277(14)
C(8)	0.7197(5)	0.2071(4)	1.0669(3)	0.0163(13)
C(8A)	0.8191(5)	0.2005(4)	1.0262(3)	0.0191(12)
C(9)	0.7851(5)	0.3029(4)	0.9233(3)	0.0197(14)
C(10)	0.6200(6)	0.3936(5)	0.7971(3)	0.0474(19)
C(11)	0.7530(6)	0.5314(4)	0.8952(3)	0.055(2)
C(12)	0.7120(5)	0.1804(4)	0.7612(3)	0.0316(14)
C(13)	0.8935(5)	0.3039(4)	0.7205(3)	0.0412(15)
C(14)	1.0056(6)	0.5465(4)	0.8176(3)	0.063(2)
C(15)	1.0600(5)	0.4626(4)	0.9186(3)	0.0246(14)
C(16)	0.6104(5)	0.2126(4)	1.0302(3)	0.0182(13)
C(17)	0.6225(6)	0.4255(4)	1.1268(3)	0.0500(18)
C(18)	0.4783(5)	0.3295(4)	1.2033(2)	0.0348(13)
C(19)	0.4467(6)	0.0226(4)	1.1124(3)	0.0300(15)
C(20)	0.2854(5)	0.0950(4)	1.1260(3)	0.0394(14)
C(21)	0.3937(6)	0.3238(5)	0.9806(3)	0.0392(16)
C(22)	0.3251(5)	0.1270(4)	0.9498(3)	0.0386(17)
C(23)	0.1312(5)	0.2461(4)	0.5244(3)	0.0186(13)
C(24)	0.0454(4)	0.2833(4)	0.5544(3)	0.0220(12)
C(25)	-0.0206(5)	0.3309(4)	0.5133(3)	0.0306(15)
C(26)	-0.0056(5)	0.3397(4)	0.4413(3)	0.0285(13)
C(26A)	0.0840(5)	0.3084(4)	0.4085(3)	0.0193(12)
C(27)	0.0972(5)	0.3162(4)	0.3341(3)	0.0276(14)
C(28)	0.1863(5)	0.2911(4)	0.3025(3)	0.0263(13)
C(29)	0.2704(5)	0.2661(4)	0.3453(3)	0.0201(12)
C(30)	0.2689(5)	0.2621(4)	0.4212(3)	0.0162(13)
C(30A)	0.1623(5)	0.2706(3)	0.4525(3)	0.0153(11)
C(31)	0.1769(5)	0.1793(4)	0.5659(3)	0.0200(14)
C(32)	0.2688(6)	0.3474(4)	0.7081(3)	0.0490(17)
C(33A)	0.223(2)	0.2156(13)	0.7951(6)	0.048(6)
C(33B)	0.1554(14)	0.2423(9)	0.7880(5)	0.037(4)
C(34)	-0.0366(5)	0.0144(5)	0.7156(3)	0.066(2)
C(35)	-0.0915(5)	0.0405(4)	0.5916(3)	0.0296(15)
C(36)	0.1705(6)	-0.0500(4)	0.6250(3)	0.0457(17)
C(37)	0.3468(6)	0.0992(6)	0.6923(4)	0.062(2)
C(38)	0.3725(5)	0.2565(4)	0.4666(3)	0.0155(13)
C(39)	0.5959(6)	0.1553(4)	0.5248(3)	0.0325(15)
C(40)	0.6299(5)	0.3369(4)	0.5836(3)	0.0440(18)
C(41)	0.4206(5)	0.0867(4)	0.3529(3)	0.0327(15)
C(42)	0.6232(5)	0.2127(4)	0.3343(3)	0.0392(14)
C(43)	0.5350(5)	0.4732(4)	0.4097(3)	0.0238(14)
C(44)	0.7273(5)	0.4473(4)	0.4364(3)	0.0436(15)
N(1)	0.7415(4)	0.4424(3)	0.8371(2)	0.0281(13)
N(2)	0.8090(4)	0.2863(3)	0.7752(2)	0.0196(11)
N(3)	0.9634(4)	0.4583(3)	0.8628(2)	0.0303(12)
N(4)	0.5253(4)	0.3238(3)	1.1335(2)	0.0316(12)
N(5)	0.4092(4)	0.1141(3)	1.1100(2)	0.0272(11)
N(6)	0.3803(4)	0.2218(3)	1.0072(2)	0.0256(12)
N(7)	0.1979(5)	0.2424(3)	0.7162(2)	0.0333(12)
N(8)	0.0046(4)	0.0732(3)	0.6531(2)	0.0245(11)
N(9)	0.2169(4)	0.0574(4)	0.6679(3)	0.0277(12)
N(10)	0.6048(4)	0.2647(3)	0.5146(2)	0.0229(12)
N(11)	0.5147(4)	0.1958(3)	0.3720(2)	0.0208(11)
N(12)	0.5953(4)	0.4016(3)	0.4320(2)	0.0269(12)
P(1)	0.8264(1)	0.3695(1)	0.8528(1)	0.0183(4)
P(2)	0.4882(2)	0.2180(1)	1.0693(1)	0.0217(4)
P(3)	0.1474(1)	0.1397(1)	0.6471(1)	0.0161(4)
P(4)	0.5139(1)	0.2783(1)	0.4454(1)	0.0158(4)

7.8.3 1,8-Bis(tris(dimethylamino)methinphosphoran)naphthalin (jfk688f5)

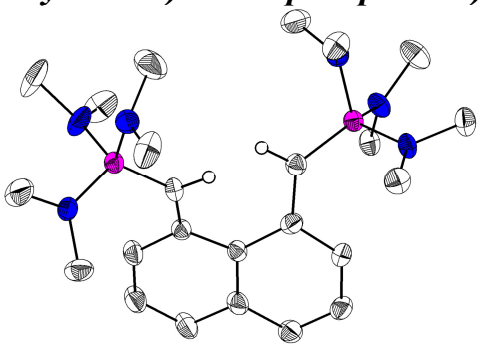

Kristalldaten

C24 H44 N6 P2	*M* = 478.59 g/mol	Triclinic, *P*−1
a = 11.7814(8) Å	*b* = 13.5189(9) Å	*c* = 18.4025(14) Å
α = 96.738(6)°	β = 94.636(6)°	γ = 110.872(5)°
V = 2695.9(3) Å^3	*Z* = 4	*F*(000) = 1040
D_{calc} = 1.179 g/cm^3	μ = 0.184 mm^{-1}	
colourless needle	0.390 · 0.060 · 0.060 mm^3	

Datensammlung

Diffraktometer: STOE IPDS 2T	*T* = 100(2) K	λ = 0.71069 Å
h = -14 bis 14	*k* = -17 bis 17	*l* = -23 bis 23
20216 gemessene Reflexe	20216 unabhängige Reflexe	8258 Reflexe mit $I > 2\sigma(I)$
θ = 1.632 bis 27.171°	R_{int} = -(hklf5)	*C* (25.00°) = 0.999
Absorptionskorrektur: Keine		

Verfeinerung

20216 Reflexe	4 Restraints	625 Parameter
Verfeinerung mit SHELXL-2014/7	bis $\chi = 0.001$	
R_1 ($I > 2\sigma(I)$) = 0.0606	wR_2 ($I > 2\sigma(I)$) = 0.0996	
R_1 (all) = 0.1545	wR_2 (all) = 0.1261	GoF (S) = 0.758
$\Delta\varphi_{min}$ = -0.463 e·Å^{-3}	$\Delta\varphi_{max}$ = 0.341 e·Å^{-3}	

Kommentar

Die Strukltur wurde als nicht meroedrischer Zwilling integriert und verfeinert. Anstelle einer hklf5-Absorptionskorrektur wurden die erweiterten Integrationsoptionen von X-Area (Merging of identical hkl and Friedel Pairs) gewählt. Die Methinprotonen der Phosphoraneinheiten wurden über DFIX restrained und bezüglich ihrer isotropen Auslenkungsfaktoren an die jeweiligen Parent-C-Atome constrained aber in ihren Koordinaten frei verfeinert. Die Verbindung ist mit der aus Probe jfk626f5 (Abschnitt 6.8.2) identisch.

Fraktionelle Atomkoordinaten (*x, y, z*) und äquivalente isotrope Auslenkungsfaktoren *U*(eq)

	x	*y*	*z*	*U*(eq)/Å^2
C(1)	0.8372(4)	0.2318(4)	0.9537(3)	0.0251(11)
C(2)	0.9184(4)	0.2002(4)	0.9141(3)	0.0309(12)
C(3)	0.9922(5)	0.1498(4)	0.9458(3)	0.0370(13)
C(4)	0.9891(5)	0.1348(5)	1.0174(4)	0.0368(14)
C(4A)	0.9057(4)	0.1610(4)	1.0593(3)	0.0283(12)
C(5)	0.9077(5)	0.1497(5)	1.1350(3)	0.0386(14)
C(6)	0.8251(5)	0.1720(5)	1.1751(3)	0.0429(16)
C(7)	0.7322(5)	0.2005(5)	1.1415(3)	0.0345(14)
C(8)	0.7204(4)	0.2067(4)	1.0658(3)	0.0267(12)
C(8A)	0.8189(4)	0.2002(4)	1.0259(3)	0.0265(12)
C(9)	0.7838(4)	0.3029(4)	0.9235(3)	0.0241(11)
C(10)	0.6181(6)	0.3930(6)	0.7964(4)	0.0480(16)
C(11)	0.7518(7)	0.5306(6)	0.8963(4)	0.0603(19)
C(12)	0.7097(5)	0.1801(5)	0.7603(3)	0.0395(14)
C(13)	0.8941(5)	0.3029(5)	0.7215(3)	0.0396(14)
C(14)	1.0033(6)	0.5455(5)	0.8167(4)	0.060(2)
C(15)	1.0594(5)	0.4626(5)	0.9178(3)	0.0380(14)
C(16)	0.6094(4)	0.2120(4)	1.0307(3)	0.0254(11)
C(17)	0.6213(6)	0.4258(5)	1.1253(4)	0.0524(19)
C(18)	0.4801(5)	0.3306(5)	1.2045(3)	0.0379(13)
C(19)	0.4461(5)	0.0222(5)	1.1129(4)	0.0361(14)
C(20)	0.2847(5)	0.0964(5)	1.1263(4)	0.0463(16)
C(21)	0.3920(6)	0.3219(5)	0.9806(4)	0.0462(16)
C(22)	0.3238(5)	0.1277(5)	0.9497(3)	0.0416(14)
C(23)	0.1298(4)	0.2459(4)	0.5247(3)	0.0227(10)
C(24)	0.0436(4)	0.2832(4)	0.5529(3)	0.0286(12)
C(25)	-0.0218(5)	0.3307(5)	0.5122(3)	0.0379(14)
C(26)	-0.0064(5)	0.3388(5)	0.4406(3)	0.0354(13)
C(26A)	0.0821(4)	0.3074(4)	0.4085(3)	0.0301(13)
C(27)	0.0955(5)	0.3155(4)	0.3331(3)	0.0316(12)
C(28)	0.1865(4)	0.2908(4)	0.3025(3)	0.0316(12)
C(29)	0.2711(5)	0.2650(4)	0.3459(3)	0.0276(11)
C(30)	0.2664(4)	0.2592(4)	0.4206(3)	0.0250(11)
C(30A)	0.1612(4)	0.2688(4)	0.4520(3)	0.0241(11)
C(31)	0.1758(4)	0.1801(4)	0.5651(3)	0.0259(11)
C(32)	0.2689(7)	0.3492(5)	0.7064(4)	0.0539(18)
C(33A)	0.223(3)	0.220(2)	0.7960(9)	0.050(8)
C(33B)	0.160(2)	0.2431(11)	0.7878(7)	0.052(5)
C(34)	-0.0357(6)	0.0132(7)	0.7154(4)	0.071(3)
C(35)	-0.0934(5)	0.0416(5)	0.5928(3)	0.0404(15)
C(36)	0.1675(7)	-0.0516(5)	0.6249(4)	0.0529(17)
C(37)	0.3458(6)	0.0987(8)	0.6926(5)	0.068(3)
C(38)	0.3713(5)	0.2550(4)	0.4656(3)	0.0260(11)
C(39)	0.5961(6)	0.1562(5)	0.5246(4)	0.0399(14)
C(40)	0.6281(6)	0.3363(6)	0.5843(3)	0.0472(15)
C(41)	0.4235(5)	0.0872(5)	0.3521(4)	0.0386(14)
C(42)	0.6253(5)	0.2134(5)	0.3352(3)	0.0392(13)
C(43)	0.5336(5)	0.4730(4)	0.4108(3)	0.0296(12)
C(44)	0.7286(5)	0.4487(5)	0.4390(4)	0.0431(15)
N(1)	0.7410(4)	0.4429(4)	0.8372(3)	0.0345(11)
N(2)	0.8076(4)	0.2864(4)	0.7749(3)	0.0285(10)
N(3)	0.9644(4)	0.4592(4)	0.8625(3)	0.0370(12)
N(4)	0.5271(4)	0.3245(4)	1.1343(3)	0.0377(12)
N(5)	0.4108(4)	0.1158(4)	1.1103(3)	0.0335(11)
N(6)	0.3794(4)	0.2213(4)	1.0068(3)	0.0309(10)
N(7)	0.1992(5)	0.2433(4)	0.7155(3)	0.0418(13)
N(8)	0.0028(4)	0.0730(4)	0.6539(2)	0.0308(10)
N(9)	0.2156(4)	0.0581(4)	0.6682(3)	0.0335(11)
N(10)	0.6040(4)	0.2642(4)	0.5149(3)	0.0275(10)
N(11)	0.5160(4)	0.1972(3)	0.3718(2)	0.0274(10)
N(12)	0.5940(3)	0.4016(3)	0.4327(3)	0.0277(10)
P(1)	0.8239(1)	0.3691(1)	0.8526(1)	0.0257(3)
P(2)	0.4871(1)	0.2172(1)	1.0699(1)	0.0260(3)
P(3)	0.1475(1)	0.1407(1)	0.6470(1)	0.0246(3)
P(4)	0.5139(1)	0.2783(1)	0.4454(1)	0.0231(3

7.8.4 1-(Tris(dimethylamino)methinphosphoran)-8-(tris(dimethylamino)-methylenphos-phoran)naphthalin-p-tolylsulfonat-tetrahydrofuran-solvat (jfk710)

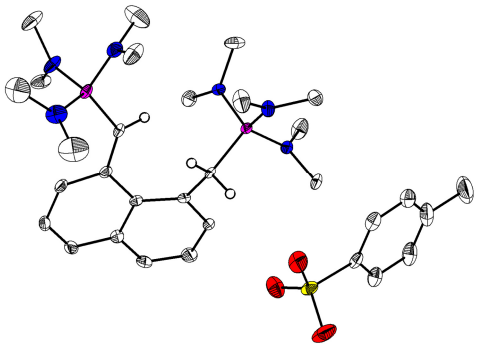

Kristalldaten

C33 H56 N6 O3.50 P2 S	M = 686.83 g/mol	Triclinic, $P\bar{1}$
a = 8.2853(6) Å	b = 16.1692(10) Å	c = 27.3787(18) Å
α = 84.578(2)°	β = 87.651(2)°	γ = 86.934(2)°
V = 3643.8(4) Å^3	Z = 4	F(000) = 1480
D_{calc} = 1.252 g/cm^3	μ = 0.219 mm^{-1}	
yellow plate	0.551 · 0.211 · 0.042 mm^3	

Datensammlung

Diffraktometer: D8 Quest (Bruker)	T = 100(2) K	λ = 0.71073 Å
h = -10 bis 10	k = -20 bis 20	l = -35 bis 35
47482 gemessene Reflexe	16107 unabhängige Reflexe	11036 Reflexe mit $I > 2\sigma(I)$
θ = 2.243 bis 27.163°	R_{int} = 0.0614	C (25.00°) = 0.998
Absorptionskorrektur: Multi-scan	T_{min} = 0.6212	T_{max} = 0.7455

Verfeinerung

16107 Reflexe	103 Restraints	949 Parameter
Verfeinerung mit SHELXL-2014/7	bis χ = 0.001	
R_1 ($I > 2\sigma(I)$) = 0.0638	wR_2 ($I > 2\sigma(I)$) = 0.1431	
R_1 (all) = 0.1023	wR_2 (all) = 0.1631	GoF (S) = 1.012
$\Delta\varphi_{min}$ = -0.826 e·Å^{-3}	$\Delta\varphi_{max}$ = 0.777 e·Å^{-3}	

Kommentar

Mehrere fehlgeordnete Dimethylaminogruppen wurden über DFIX; SIMU, DELU und RIGU restrained. Ein fehlgeordnetes THF-Molekül wurde über EADP constrained. Die Methylen- und Methinprotonen der Phosphoraneinheiten wurden bezüglich ihrer isotropen Auslenkungsfaktoren an die jeweiligen Parent-C-Atome constrained aber in ihren Koordinaten frei verfeinert.

Fraktionelle Atomkoordinaten (*x, y, z*) und äquivalente isotrope Auslenkungsfaktoren *U*(eq)

	x	*y*	*z*	*U*(eq)/Å^2		*x*	*y*	*z*	*U*(eq)/Å^2
C(1)	0.6521(3)	0.6750(2)	0.7016(1)	0.0160(5)	C(12)	0.4404(5)	0.4337(2)	0.7747(1)	0.0374(9)
C(2)	0.7388(3)	0.7289(2)	0.7250(1)	0.0198(6)	C(13)	0.1472(4)	0.6154(2)	0.7963(1)	0.0294(7)
C(3)	0.8058(4)	0.7997(2)	0.7001(1)	0.0263(7)	C(14)	0.2736(4)	0.7194(2)	0.7384(1)	0.0230(6)
C(4)	0.7953(3)	0.8115(2)	0.6503(1)	0.0232(6)	C(15)	0.4568(4)	0.7147(2)	0.8498(1)	0.0304(7)
C(4A)	0.7108(3)	0.7570(2)	0.6241(1)	0.0183(6)	C(16)	0.7020(3)	0.6231(2)	0.8462(1)	0.0221(6)
C(5)	0.7156(3)	0.7677(2)	0.5721(1)	0.0206(6)	C(17)	0.2449(6)	0.4558(3)	0.5367(2)	0.0573(12)
C(6)	0.6338(3)	0.7165(2)	0.5464(1)	0.0210(6)	C(18)	0.5000(5)	0.4435(3)	0.5796(2)	0.0586(12)
C(7)	0.5358(3)	0.6574(2)	0.5705(1)	0.0196(6)	C(19)	-0.0474(4)	0.5743(2)	0.5798(1)	0.0377(8)
C(8)	0.5186(3)	0.6444(2)	0.6220(1)	0.0170(5)	C(20)	0.1279(4)	0.6912(2)	0.5804(1)	0.0280(7)
C(8A)	0.6237(3)	0.6909(2)	0.6501(1)	0.0164(5)	C(21)	0.2175(4)	0.3920(2)	0.6673(1)	0.0393(9)
C(9)	0.6115(3)	0.5944(2)	0.7316(1)	0.0155(5)	C(22)	0.0355(5)	0.5090(2)	0.6903(1)	0.0519(11)
C(10)	0.3981(3)	0.5910(2)	0.6445(1)	0.0186(6)	C(23)	0.8936(3)	0.8929(2)	0.8864(1)	0.0206(6)
C(11)	0.4592(4)	0.4726(2)	0.8583(1)	0.0243(6)	C(24)	0.7882(4)	0.8394(2)	0.9118(1)	0.0278(7)

	x	*y*	*z*	*U*(eq)/Å^2
C(25)	0.7204(4)	0.8575(2)	0.9572(1)	0.0326(7)
C(26)	0.7600(4)	0.9283(2)	0.9781(1)	0.0354(8)
C(27)	0.8673(4)	0.9816(2)	0.9524(1)	0.0333(8)
C(28)	0.9350(4)	0.9638(2)	0.9071(1)	0.0269(7)
C(29)	0.6886(6)	0.9470(3)	1.0277(1)	0.0545(11)
C(31)	0.6715(3)	0.1734(2)	0.7002(1)	0.0192(6)
C(32)	0.7565(4)	0.2266(2)	0.7250(1)	0.0255(7)
C(33)	0.8204(4)	0.2987(2)	0.7013(1)	0.0319(7)
C(34)	0.8102(4)	0.3135(2)	0.6517(1)	0.0279(7)
C(34A)	0.7286(3)	0.2603(2)	0.6242(1)	0.0212(6)
C(35)	0.7341(3)	0.2745(2)	0.5725(1)	0.0236(6)
C(36)	0.6533(3)	0.2252(2)	0.5453(1)	0.0255(7)
C(37)	0.5555(3)	0.1643(2)	0.5681(1)	0.0242(6)
C(38)	0.5393(3)	0.1468(2)	0.6195(1)	0.0203(6)
C(38A)	0.6424(3)	0.1920(2)	0.6485(1)	0.0183(6)
C(39)	0.6335(4)	0.0909(2)	0.7288(1)	0.0187(6)
C(40)	0.4202(3)	0.0913(2)	0.6403(1)	0.0210(6)
C(41)	0.4502(4)	-0.0251(2)	0.8562(1)	0.0269(7)
C(42)	0.5037(4)	-0.0767(2)	0.7756(1)	0.0296(7)
C(43)	0.1657(4)	0.1016(2)	0.7896(1)	0.0301(7)
C(44)	0.2881(4)	0.2106(2)	0.7340(1)	0.0264(7)
C(45)	0.7078(4)	0.1212(2)	0.8460(1)	0.0251(6)
C(46)	0.4631(4)	0.2142(2)	0.8437(1)	0.0235(6)
C(53)	0.9702(3)	0.6117(2)	0.1197(1)	0.0180(6)
C(54)	0.9748(3)	0.5359(2)	0.1000(1)	0.0205(6)
C(55)	0.8941(4)	0.5280(2)	0.0571(1)	0.0281(7)
C(56)	0.8095(4)	0.5959(2)	0.0337(1)	0.0350(8)
C(57)	0.8064(4)	0.6713(2)	0.0537(1)	0.0357(8)
C(58)	0.8866(4)	0.6798(2)	0.0962(1)	0.0272(7)
C(59)	0.7225(5)	0.5875(3)	-0.0132(1)	0.0649(14)
P(1)	0.4708(1)	0.5972(1)	0.7839(1)	0.0135(2)
P(2)	0.2571(1)	0.5415(1)	0.6165(1)	0.0156(2)
P(3)	0.4899(1)	0.0920(1)	0.7803(1)	0.0145(2)
P(4)	0.2799(1)	0.0443(1)	0.6110(1)	0.0189(2)
S(1)	0.9716(1)	0.8737(1)	0.8267(1)	0.0227(2)
S(2)	1.0683(1)	0.6248(1)	0.1748(1)	0.0202(2)
N(1)	0.4555(3)	0.5016(1)	0.8061(1)	0.0207(5)
N(2)	0.2948(3)	0.6385(1)	0.7676(1)	0.0175(5)
N(3)	0.5441(3)	0.6480(1)	0.8259(1)	0.0169(5)
N(4)	0.3436(3)	0.4867(2)	0.5740(1)	0.0324(6)
N(5)	0.1120(3)	0.6022(1)	0.5914(1)	0.0248(6)
N(6)	0.1527(3)	0.4780(2)	0.6546(1)	0.0251(6)
N(7)	0.4834(3)	-0.0037(1)	0.8036(1)	0.0207(5)
N(8)	0.3127(3)	0.1294(1)	0.7627(1)	0.0181(5)
N(9)	0.5547(3)	0.1463(1)	0.8221(1)	0.0168(5)
O(1)	0.9030(3)	0.7975(1)	0.8162(1)	0.0353(6)
O(2)	1.1453(3)	0.8681(2)	0.8296(1)	0.0535(8)
O(3)	0.9146(3)	0.9455(1)	0.7951(1)	0.0353(5)
O(4)	1.1221(3)	0.5428(1)	0.1948(1)	0.0335(5)
O(5)	0.9451(3)	0.6612(2)	0.2057(1)	0.0600(9)
O(6)	1.2004(3)	0.6769(2)	0.1608(1)	0.0554(8)
N(10)	0.3621(8)	-0.0297(4)	0.5804(2)	0.0323(14)
C(47)	0.2758(10)	-0.0975(4)	0.5654(3)	0.072(3)
C(48)	0.5408(12)	-0.0349(5)	0.5674(4)	0.047(2)
N(11)	0.1814(6)	0.1119(3)	0.5721(2)	0.0237(11)
C(49)	0.0716(7)	0.0840(4)	0.5374(2)	0.0479(19)
C(50)	0.1527	0.1992	0.5833	0.038(4)
N(12)	0.1490(8)	-0.0010(4)	0.6489(3)	0.0289(14)
C(51)	-0.0003(7)	0.0413(4)	0.6637(2)	0.0409(16)
C(52)	0.2016(7)	-0.0729(4)	0.6820(2)	0.047(2)
N(10B)	0.3492(13)	-0.0031(8)	0.5620(5)	0.027(3)
C(47B)	0.2366(13)	-0.0336(8)	0.5278(4)	0.046(4)
C(48B)	0.497(2)	-0.0608(11)	0.5732(10)	0.063(6)
N(11B)	0.1221(11)	0.1039(5)	0.5936(3)	0.0197(19)
C(49B)	-0.0413(10)	0.0800(6)	0.5826(4)	0.034(3)
C(50B)	0.1453(13)	0.1925(7)	0.5781(5)	0.020(4)
N(12B)	0.1806(19)	-0.0297(8)	0.6461(6)	0.026(3)
C(51B)	0.083(2)	-0.0091(8)	0.6889(4)	0.054(4)
C(52B)	0.258(2)	-0.1157(7)	0.6526(5)	0.053(4)
O(60)	0.3613(7)	0.7967(4)	1.0048(2)	0.0694(14)
C(61)	0.2549(11)	0.8087(6)	0.9664(3)	0.0694(14)
C(62)	0.1621(15)	0.7340(6)	0.9660(4)	0.0694(14)
C(63)	0.2404(11)	0.6695(5)	1.0049(3)	0.0694(14)
C(64)	0.3201(12)	0.7262(6)	1.0370(3)	0.0694(14)
O(70)	0.3024(8)	0.6696(4)	0.9739(2)	0.0561(16)
C(71)	0.3040(14)	0.6761(6)	1.0250(3)	0.0561(16)
C(73)	0.1773(13)	0.7961(6)	0.9861(3)	0.0561(16)
C(72)	0.2648(13)	0.7662(6)	1.0337(3)	0.0561(16)
C(74)	0.1642(16)	0.7200(7)	0.9593(5)	0.0561(16)

7.9 Strukturen für weitere Personen

7.9.1 Tetrakis(1,1,4,4-tetramethyl-6,7-tetralino)phorphyrazinato-nickel(II)-chloroformsolvat (ai-nipc, Dr. Ahmed Bayoumi Ibrahim)

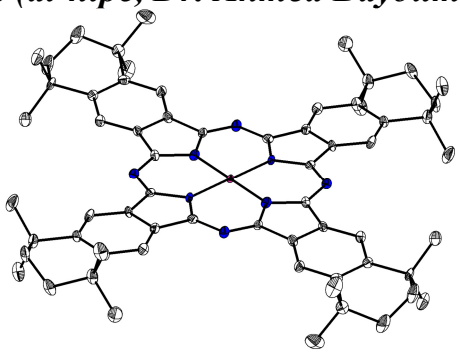

Kristalldaten

C68 H76 Cl12 N8 Ni	M = 1489.47 g/mol	Monoclinic, $P2_1/c$
a = 11.727(4) Å	b = 22.985(7) Å	c = 12.931(4) Å
α = 90°	β = 90.240(12)°	γ = 90°
V = 3485.5(19) Å^3	Z = 2	F(000) = 1544
D_{calc} = 1.419 g/cm^3	μ = 0.786 mm^{-1}	
green needle	0.370 · 0.070 · 0.040 mm^3	

Datensammlung

Diffraktometer: D8 Quest (Bruker)	T = 100(2) K	λ = 0.71069 Å
h = -14 bis 14	k = -25 bis 27	l = -15 bis 15
34047 gemessene Reflexe	6568 unabhängige Reflexe	3943 Reflexe mit $I > 2\sigma(I)$
θ = 2.481 bis 25.613°	R_{int} = 0.1712	C (25.00°) = 0.999
Absorptionskorrektur: Multi-scan	T_{min} = 0.4738	T_{max} = 0.7455

Verfeinerung

6568 Reflexe	0 Restraints	411 Parameter
Verfeinerung mit SHELXL-2014/7	bis χ = 0.000	
R_1 ($I > 2\sigma(I)$) = 0.0713	wR_2 ($I > 2\sigma(I)$) = 0.1591	
R_1 (all) = 0.1371	wR_2 (all) = 0.1877	GoF (S) = 1.017
$\Delta\varphi_{min}$ = -0.758 e·Å^{-3}	$\Delta\varphi_{max}$ = 1.047 e·Å^{-3}	

Fraktionelle Atomkoordinaten (*x, y, z*) und äquivalente isotrope Auslenkungsfaktoren *U*(eq)

	x	*y*	*z*	*U*(eq)/Å^2		*x*	*y*	*z*	*U*(eq)/Å^2
C(1)	0.0423(4)	0.1089(2)	0.1085(4)	0.0123(11)	C(21)	-0.6227(4)	0.0538(2)	-0.2213(4)	0.0152(11)
C(2)	-0.0126(4)	0.1631(2)	0.1370(4)	0.0140(11)	C(22)	-0.7089(5)	0.0121(2)	-0.2680(5)	0.0287(14)
C(3)	0.0258(4)	0.2105(2)	0.1912(4)	0.0148(11)	C(23)	-0.6601(5)	-0.0241(3)	-0.3519(5)	0.0318(14)
C(4)	-0.0481(4)	0.2570(2)	0.2080(4)	0.0143(11)	C(24)	-0.5655(4)	-0.0644(2)	-0.3142(4)	0.0185(12)
C(5)	-0.0015(4)	0.3094(2)	0.2670(4)	0.0210(12)	C(25)	-0.4846(4)	-0.0325(2)	-0.2404(4)	0.0149(11)
C(6)	-0.0985(4)	0.3495(2)	0.3015(4)	0.0233(13)	C(26)	-0.3829(4)	-0.0592(2)	-0.2153(4)	0.0158(11)
C(7)	-0.1840(4)	0.3593(2)	0.2174(4)	0.0227(13)	C(27)	-0.3067(4)	-0.0317(2)	-0.1504(4)	0.0137(11)
C(8)	-0.2458(4)	0.3039(2)	0.1856(4)	0.0180(11)	C(28)	-0.1943(4)	-0.0467(2)	-0.1151(4)	0.0113(10)
C(9)	-0.1597(4)	0.2551(2)	0.1675(4)	0.0143(11)	C(29)	-0.5986(5)	0.1035(2)	-0.2942(5)	0.0271(14)
C(10)	-0.1965(4)	0.2059(2)	0.1136(4)	0.0140(11)	C(30)	-0.6760(5)	0.0774(3)	-0.1224(4)	0.0342(15)
C(11)	-0.1220(4)	0.1601(2)	0.0993(4)	0.0101(10)	C(31)	-0.5003(5)	-0.0850(3)	-0.4094(5)	0.0382(16)
C(12)	-0.1330(4)	0.1048(2)	0.0476(4)	0.0113(10)	C(32)	-0.6164(5)	-0.1170(2)	-0.2592(5)	0.0345(15)
C(13)	0.0792(5)	0.3425(2)	0.1962(5)	0.0291(14)	C(33)	0.3439(6)	0.2100(3)	0.0822(5)	0.0394(16)
C(14)	0.0626(5)	0.2904(3)	0.3645(5)	0.0337(15)	C(34)	0.0742(6)	0.0752(3)	0.3764(5)	0.0484(19)
C(15)	-0.3133(5)	0.3173(2)	0.0877(5)	0.0306(14)	N(1)	0.1472(3)	0.0970(2)	0.1374(3)	0.0139(9)
C(16)	-0.3281(5)	0.2850(2)	0.2720(5)	0.0295(14)	N(2)	-0.0318(3)	0.0745(2)	0.0546(3)	0.0110(9)
C(17)	-0.2307(4)	0.0399(2)	-0.0511(4)	0.0122(11)	N(3)	-0.2260(3)	0.0892(2)	-0.0007(3)	0.0121(9)
C(18)	-0.3309(4)	0.0225(2)	-0.1109(4)	0.0119(10)	N(4)	-0.1483(3)	-0.0025(2)	-0.0572(3)	0.0125(8)
C(19)	-0.4331(4)	0.0496(2)	-0.1324(4)	0.0132(11)	Cl(1)	0.3579(1)	0.2294(1)	0.2133(1)	0.0388(4)
C(20)	-0.5114(4)	0.0224(2)	-0.1969(4)	0.0127(11)	Cl(2)	0.4798(2)	0.1858(1)	0.0364(2)	0.0575(6)

	x	*y*	*z*	*U*(eq)/Å^2
Cl(3)	0.3023(2)	0.2713(1)	0.0102(2)	0.0670(6)
Cl(4)	-0.0437(2)	0.1130(1)	0.4179(2)	0.0659(6)
Cl(5)	0.0338(2)	0.0061(1)	0.3301(2)	0.0753(7)
Cl(6)	0.1788(2)	0.0716(1)	0.4681(2)	0.0782(7)
Ni(1)	0.0000	0.0000	0.0000	0.0092(2)

7.9.2 Tetrakis(1,1,4,4-tetramethyl-6,7-tetralino)phorphyrazinato-oxo-hydroxo-vanadium(V)-dichlormethansolvat-hydrat (voa-tetra, Dr. Ahmed Bayoumi Ibrahim)

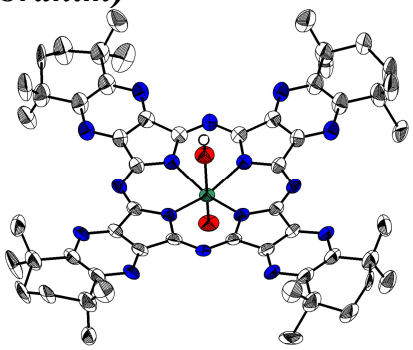

Kristalldaten

C128 H161 Cl32 N32 O12 V2	M = 3576.17 g/mol	Tetragonal, *P*4/*nmm*
a = 26.3873(17) Å	b = 26.3873 Å	c = 13.3566(11) Å
α = 90°	β = 90°	γ = 90°
V = 9300.1(14) Å^3	Z = 2	F(000) = 3678
D_{calc} = 1.277 g/cm^3	μ = 0.617 mm^{-1}	
blue plate	0.370 · 0.120 · 0.100 mm^3	

Datensammlung

Diffraktometer: D8 Quest (Bruker)	T = 100(2) K	λ = 0.71069 Å
h = -33 bis 33	k = -33 bis 33	l = -16 bis 17
109297 gemessene Reflexe	5551 unabhängige Reflexe	3874 Reflexe mit $I > 2\sigma(I)$
θ = 2.170 bis 27.166°	R_{int} = 0.1120	C (25.00°) = 0.999
Absorptionskorrektur: Multi-scan	T_{min} = 0.6408	T_{max} = 0.7455

Verfeinerung

5551 Reflexe	14 Restraints	323 Parameter
Verfeinerung mit SHELXL-2013	bis χ = 0.005	
R_1 ($I > 2\sigma(I)$) = 0.1146	wR_2 ($I > 2\sigma(I)$) = 0.3231	
R_1 (all) = 0.1503	wR_2 (all) = 0.3584	GoF (S) = 1.050
$\Delta\varphi_{min}$ = -1.108 e·Å^{-3}	$\Delta\varphi_{max}$ = 2.045 e·Å^{-3}	

Kommentar

Wegen nicht vollständig auflösbarer starker Fehlordnungen und einer geringen Kristallqualität eignet sich die Strukturlösung primär als grundsätzlicher Strukturnachweis.

Fraktionelle Atomkoordinaten (*x, y, z*) und äquivalente isotrope Auslenkungsfaktoren *U*(eq)

	x	*y*	*z*	*U*(eq)/Å^2
C(1)	0.2926(2)	0.1453(2)	0.8553(4)	0.0342(12)
C(2)	0.2763(2)	0.0926(2)	0.8449(4)	0.0376(13)
C(3)	0.2769(3)	0.0075(2)	0.8259(6)	0.0523(17)
C(4)	0.3083(3)	-0.0406(3)	0.8158(7)	0.065(2)
C(5)	0.2794(8)	-0.0889(5)	0.834(3)	0.083(8)
C(7)	0.3525(12)	-0.0404(8)	0.9024(18)	0.083(9)
C(5B)	0.2683(7)	-0.0831(6)	0.779(3)	0.059(7)
C(7B)	0.3251(9)	-0.0566(8)	0.910(2)	0.074(8)
C(6)	0.3421(3)	-0.0372(3)	0.7247(8)	0.077(3)
C(15)	0.3543(2)	0.2058(2)	0.3557(3)	0.0209(9)
C(16)	0.3799(2)	0.1573(2)	0.3448(3)	0.0228(9)
C(19)	0.4402(2)	0.0980(2)	0.3233(4)	0.0331(12)
C(20)	0.4966(2)	0.0859(2)	0.3110(5)	0.0445(15)
C(21)	0.5065(6)	0.0359(8)	0.266(2)	0.047(5)
C(23)	0.5215(6)	0.1294(9)	0.2310(15)	0.040(5)
C(21B)	0.5019(5)	0.0253(6)	0.324(2)	0.063(6)
C(23B)	0.5125(7)	0.1016(11)	0.2114(16)	0.071(7)
C(24)	0.5246(2)	0.1034(3)	0.4035(7)	0.066(2)
C(30)	0.4138(3)	0.0862(3)	0.9512(9)	0.081(4)
C(32)	0.2500	0.0146(4)	0.4492(11)	0.073(4)

	x	y	z	U(eq)/Å^2		x	y	z	U(eq)/Å^2
C(33)	0.3806(3)	0.1194(3)	0.6547(10)	0.096(5)	N(7)	0.4293(2)	0.1469(2)	0.3330(3)	0.0287(9)
Cl(1)	0.3926(1)	0.1074(1)	1.0679(3)	0.1142(18)	O(1)	0.2500	0.2500	1.0117(8)	0.050(3)
Cl(2)	0.4608(1)	0.0392(1)	0.9621(3)	0.151(3)	O(2)	0.2500	0.2500	0.7162(10)	0.051(3)
Cl(5)	0.2500	0.0464(2)	0.5662(3)	0.0993(13)	O(3)	0.2500	0.2500	0.5130(7)	0.034(2)
Cl(6)	0.2500	-0.0517(1)	0.4649(4)	0.0986(14)	V(1)	0.2500	0.2500	0.8924(2)	0.0317(6)
Cl(7)	0.3377(1)	0.1623(1)	0.6026(2)	0.0557(7)	V(2)	0.2500	0.2500	0.3943(2)	0.0195(5)
Cl(8)	0.4150(1)	0.0850(1)	0.5769(2)	0.0932(13)	Cl(4)	0.3722(1)	0.2500	0.1023(2)	0.0651(8)
N(1)	0.2500	0.1746(3)	0.8614(4)	0.0333(14)	Cl(3)	0.4823(2)	0.2500	0.0722(3)	0.1211(19)
N(2)	0.3403(2)	0.1597(2)	0.8534(5)	0.0346(15)	C(31)	0.4349(5)	0.2500	0.1515(10)	0.089(5)
N(3)	0.3039(2)	0.0504(2)	0.8344(4)	0.0440(12)	O(4)	0.2500	0.2500	0.2151(9)	0.045(3)
N(5)	0.3031(1)	0.1969(1)	0.3625(4)	0.0198(11)	O(6)	0.1985(5)	-0.1261(7)	0.1462(14)	0.130(7)
N(6)	0.3781(2)	0.2500	0.3547(4)	0.0226(11)	O(5)	0.3247(8)	0.8319(7)	0.5877(15)	0.142(7)

7.9.3 Cyclopentadienyl-fluorenyliden-diphenylphosphorano-trimethylsilyl-methylato-yttrium(III)-dimer-benzolsolvat (ma0213, Dr. Silas Böttger)

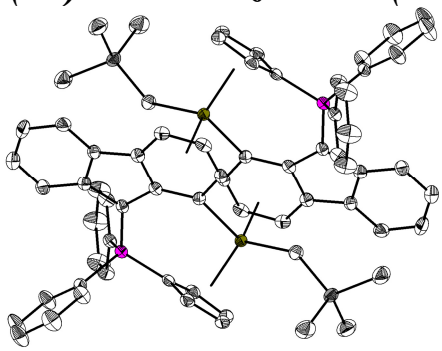

Kristalldaten

C74.44 H70.44 P2 Si2 Y2	M = 1261.45 g/mol	Triclinic, $P\bar{1}$
a = 9.7926(5) Å	b = 12.6839(7) Å	c = 13.7280(6) Å
α = 103.969(3)°	β = 101.937(3)°	γ = 90.297(3)°
V = 1616.19(14) Å^3	Z = 1	F(000) = 653
D_{calc} = 1.296 g/cm^3	μ = 1.914 mm^{-1}	
yellow plate	0.170 · 0.110 · 0.060 mm^3	

Datensammlung

Diffraktometer: D8 Quest (Bruker)	T = 100(2) K	λ = 0.71073 Å
h = -12 bis 12	k = -16 bis 16	l = -17 bis 17
34173 gemessene Reflexe	7181 unabhängige Reflexe	5295 Reflexe mit $I > 2\sigma(I)$
θ = 2.357 bis 27.201°	R_{int} = 0.1079	C (25.00°) = 0.999
Absorptionskorrektur: Multi-scan	T_{min} = 0.6413	T_{max} = 0.7455

Verfeinerung

7181 Reflexe	289 Restraints	466 Parameter
Verfeinerung mit SHELXL-2014/7	bis χ = 0.001	
R_1 ($I > 2\sigma(I)$) = 0.0496	wR_2 ($I > 2\sigma(I)$) = 0.1099	
R_1 (all) = 0.0832	wR_2 (all) = 0.1217	GoF (S) = 1.046
$\Delta\varphi_{min}$ = -0.854 e·Å^{-3}	$\Delta\varphi_{max}$ = 0.769 e·Å^{-3}	

Kommentar

Das über mehreren Positionen fehlgeordnete Benzolmolekül wurde über ISOR, DELU und RIGU restrained.

Fraktionelle Atomkoordinaten (*x, y, z*) und äquivalente isotrope Auslenkungsfaktoren *U*(eq)

	x	y	z	U(eq)/Å^2		x	y	z	U(eq)/Å^2
C(1)	0.6426(4)	0.2058(3)	0.2519(3)	0.0184(7)	C(5)	0.7093(4)	0.2793(3)	0.2098(3)	0.0218(8)
C(2)	0.5081(4)	0.2451(3)	0.2605(3)	0.0230(8)	C(6)	0.6313(3)	-0.0303(3)	0.2363(3)	0.0170(7)
C(3)	0.4924(4)	0.3374(3)	0.2229(3)	0.0294(9)	C(7)	0.5072(3)	-0.0579(3)	0.1560(2)	0.0165(7)
C(4)	0.6153(4)	0.3578(3)	0.1900(3)	0.0282(9)	C(8)	0.4307(3)	0.0037(3)	0.0904(3)	0.0165(7)

	x	y	z	U(eq)/Å^2
C(9)	0.3062(4)	-0.0513(3)	0.0258(3)	0.0203(8)
C(10)	0.2602(4)	-0.1581(3)	0.0205(3)	0.0216(8)
C(11)	0.3429(4)	-0.2194(3)	0.0787(3)	0.0204(8)
C(12)	0.4663(3)	-0.1704(3)	0.1461(3)	0.0187(7)
C(13)	0.5653(4)	-0.2118(3)	0.2192(3)	0.0194(7)
C(14)	0.5719(4)	-0.3137(3)	0.2407(3)	0.0256(8)
C(15)	0.6777(4)	-0.3303(3)	0.3178(3)	0.0340(10)
C(16)	0.7757(4)	-0.2464(3)	0.3737(3)	0.0324(9)
C(17)	0.7713(4)	-0.1451(3)	0.3543(3)	0.0233(8)
C(18)	0.6645(4)	-0.1257(3)	0.2755(3)	0.0190(7)
C(19)	0.8988(3)	0.0969(3)	0.2797(3)	0.0188(7)
C(20)	0.9904(4)	0.1879(3)	0.3247(3)	0.0255(8)
C(21)	1.1237(4)	0.1867(4)	0.3071(3)	0.0385(11)
C(22)	1.1651(4)	0.0954(4)	0.2443(4)	0.0420(11)
C(23)	1.0766(4)	0.0056(4)	0.2010(3)	0.0370(10)
C(24)	0.9425(4)	0.0058(3)	0.2184(3)	0.0246(8)
C(25)	0.7237(4)	0.1210(3)	0.4322(3)	0.0191(7)
C(26)	0.8449(4)	0.1418(4)	0.5078(3)	0.0316(10)
C(27)	0.8394(4)	0.1603(4)	0.6106(3)	0.0416(12)
C(28)	0.7123(5)	0.1588(4)	0.6379(3)	0.0415(11)
C(29)	0.5910(4)	0.1362(4)	0.5635(3)	0.0363(10)
C(30)	0.5959(4)	0.1168(3)	0.4609(3)	0.0277(9)
C(31)	0.2714(4)	0.2184(3)	-0.0083(3)	0.0228(8)
C(32)	0.0251(4)	0.3236(4)	-0.1190(4)	0.0393(11)
C(33)	0.2805(5)	0.4619(3)	0.0006(4)	0.0385(10)
C(34)	0.0909(5)	0.3680(4)	0.1134(3)	0.0389(11)
Si(1)	0.1708(1)	0.3396(1)	-0.0029(1)	0.0231(2)
P(1)	0.7198(1)	0.0951(1)	0.2960(1)	0.0161(2)
Y(1)	0.5011(1)	0.1733(1)	0.0579(1)	0.0165(1)
C(101)	0.8905(18)	0.4502(16)	0.5649(14)	0.042(6)
C(106)	0.8399(15)	0.4475(15)	0.4619(15)	0.030(6)
C(105)	0.9230(19)	0.4895(15)	0.4079(12)	0.032(6)
C(104)	1.0567(19)	0.5342(17)	0.4569(15)	0.034(6)
C(103)	1.1073(16)	0.5370(19)	0.5598(15)	0.045(7)
C(102)	1.024(2)	0.4950(19)	0.6139(12)	0.041(6)
C(205)	0.9774(15)	0.4766(13)	0.6453(10)	0.048(5)
C(204)	0.8448(17)	0.4369(13)	0.6450(9)	0.043(5)
C(203)	0.7401(14)	0.4196(12)	0.5564(11)	0.045(5)
C(202)	0.7681(16)	0.4421(13)	0.4680(9)	0.039(5)
C(201)	0.9008(18)	0.4818(16)	0.4683(11)	0.047(6)
C(206)	1.0054(14)	0.4991(15)	0.5569(14)	0.046(5)
C(301)	0.411(2)	0.3982(14)	0.4827(16)	0.050(6)
C(302)	0.5488(19)	0.4352(17)	0.5274(16)	0.052(6)
C(303)	0.5946(16)	0.5394(18)	0.5285(18)	0.064(7)
C(304)	0.502(2)	0.6068(14)	0.4849(19)	0.059(7)
C(305)	0.365(2)	0.5698(18)	0.4403(18)	0.062(7)
C(306)	0.3187(16)	0.466(2)	0.4392(17)	0.069(8)

7.9.4 Butyl-methyl-pyrrolidinium-methyloxalat (pm03, Dr. Axel Braam)

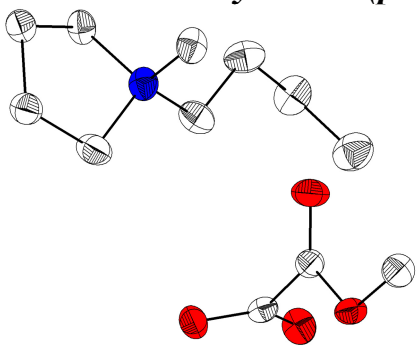

Kristalldaten

C12 H23 N O4	M = 245.31 g/mol	Orthorhombic, $Pna2_1$
a = 24.2200(9) Å	b = 8.0919(3) Å	c = 13.3522(7) Å
α = 90°	β = 90°	γ = 90°
V = 2616.84(19) Å^3	Z = 8	F(000) = 1072
D_{calc} = 1.245 g/cm^3	μ = 0.092 mm^{-1}	
colourless block	0.280 · 0.210 · 0.140 mm^3	

Datensammlung

Diffraktometer: STOE IPDS 2	T = 100(2) K	λ = 0.71073 Å
h = -30 bis 30	k = -10 bis 10	l = -16 bis 16
23397 gemessene Reflexe	5532 unabhängige Reflexe	3200 Reflexe mit $I > 2\sigma(I)$
θ = 1.682 bis 26.756°	R_{int} = 0.1000	C (25.00°) = 1.000
Absorptionskorrektur: Multi-scan	T_{min} = 0.8093	T_{max} = 1.1559

Verfeinerung

5532 Reflexe	6 Restraints	328 Parameter
Verfeinerung mit SHELXL-2014/7	bis χ = 0.000	
R_1 ($I > 2\sigma(I)$) = 0.0378	wR_2 ($I > 2\sigma(I)$) = 0.0769	
R_1 (all) = 0.0733	wR_2 (all) = 0.0833	GoF (S) = 0.775
$\Delta\varphi_{min}$ = -0.159 e·Å^{-3}	$\Delta\varphi_{max}$ = 0.205 e·Å^{-3}	

Kommentar
Die Struktur wurde als Inversionszwilling verfeinert. Die fehlgeordnete Butylgruppe (82:18) wurde über SAME re- und über EADP constrained.

Fraktionelle Atomkoordinaten (*x, y, z*) und äquivalente isotrope Auslenkungsfaktoren *U*(eq)

	x	*y*	*z*	*U*(eq)/Å^2		*x*	*y*	*z*	*U*(eq)/Å^2
C(1)	0.5896(2)	0.8812(6)	0.0726(4)	0.0359(12)	C(16)	0.2958(2)	0.8447(5)	0.4554(4)	0.0391(11)
C(2)	0.5965(2)	0.8479(6)	0.1855(4)	0.0323(12)	C(17)	0.3033(2)	0.8069(7)	0.5695(4)	0.0376(10)
C(3)	0.6023(2)	0.6582(6)	0.1932(4)	0.0308(11)	C(18)	0.2684(2)	0.6751(6)	0.6099(4)	0.0460(12)
C(4)	0.5990(2)	0.5925(6)	0.0866(4)	0.0337(12)	C(19)	0.4807(2)	0.7483(4)	0.4023(6)	0.0258(15)
C(5)	0.5060(2)	0.7074(6)	0.0579(4)	0.0315(11)	C(20)	0.5376(2)	0.8037(6)	0.4380(3)	0.0290(9)
C(6)	0.5755(2)	0.6952(6)	-0.0795(3)	0.0180(9)	C(21)	0.6299(2)	0.7259(4)	0.4680(5)	0.0335(12)
C(7)	0.5496(2)	0.8346(6)	-0.1448(3)	0.0207(10)	C(22)	0.2674(2)	0.2526(4)	0.4114(6)	0.0244(14)
C(8)	0.5603(2)	0.8070(6)	-0.2549(4)	0.0219(10)	C(23)	0.2093(2)	0.3045(6)	0.3777(3)	0.0253(9)
C(9)	0.5231(2)	0.6682(6)	-0.2994(4)	0.0303(12)	C(24)	0.1177(2)	0.2192(5)	0.3488(5)	0.0318(12)
C(6A)	0.5684(9)	0.800(3)	-0.0784(16)	0.0255(10)	N(1)	0.5658(2)	0.7231(4)	0.0319(4)	0.0255(10)
C(7A)	0.5466(7)	0.660(2)	-0.1457(14)	0.0255(10)	N(2)	0.3117(2)	0.7330(4)	0.2817(4)	0.0291(11)
C(8A)	0.5553(8)	0.697(3)	-0.2537(14)	0.0255(10)	O(1)	0.5749(1)	0.6812(3)	0.4354(2)	0.0306(6)
C(9A)	0.5169(7)	0.837(2)	-0.2955(16)	0.0255(10)	O(2)	0.5492(1)	0.9418(3)	0.4671(3)	0.0410(7)
C(10)	0.3493(2)	0.8678(5)	0.2442(4)	0.0290(11)	O(3)	0.4757(2)	0.7277(4)	0.3106(4)	0.0378(10)
C(11)	0.3549(2)	0.8336(7)	0.1323(4)	0.0308(12)	O(4)	0.4457(2)	0.7357(3)	0.4692(4)	0.0371(10)
C(12)	0.3483(2)	0.6446(6)	0.1225(4)	0.0321(13)	O(5)	0.1739(1)	0.1766(3)	0.3774(2)	0.0274(6)
C(13)	0.3342(2)	0.5840(6)	0.2273(4)	0.0359(11)	O(6)	0.1964(1)	0.4428(3)	0.3537(3)	0.0387(7)
C(14)	0.2537(2)	0.7677(5)	0.2501(5)	0.0310(12)	O(7)	0.2756(2)	0.2551(3)	0.5038(3)	0.0338(10)
C(15)	0.3143(2)	0.7026(6)	0.3949(4)	0.0334(10)	O(8)	0.3000(1)	0.2212(3)	0.3419(3)	0.0324(8)

7.9.5 Adamantylimino-methyliden-di(tert-butyl)phosphoran-tris(trimethylsilylmethyl)-zirkonium(IV) (dg134f5, Donathas Gesevicius)

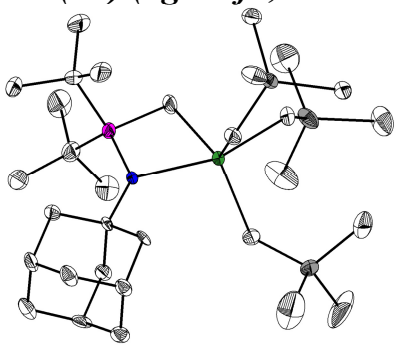

Kristalldaten

C31 H68 N P Si3 Zr	M = 661.32 g/mol	Monoclinic, $P2_1/n$
a = 10.5228(13) Å	b = 17.9348(15) Å	c = 20.3348(18) Å
α = 90°	β = 90.508(4)°	γ = 90°
V = 3837.5(7) Å^3	Z = 4	F(000) = 1432
D_{calc} = 1.145 g/cm^3	μ = 0.441 mm^{-1}	
colourless block	0.170 · 0.090 · 0.060 mm^3	

Datensammlung

Diffraktometer: D8 Quest (Bruker)	T = 100(2) K	λ = 0.71073 Å
h = -13 bis 13	k = 0 bis 22	l = 0 bis 26
8164 gemessene Reflexe	8164 unabhängige Reflexe	6232 Reflexe mit $I > 2\sigma(I)$
θ = 2.003 bis 27.118°	R_{int} = -(hklf5)	C (25.00°) = 0.981
Absorptionskorrektur: Multi-scan	T_{min} = 0.6075	T_{max} = 0.7455

Verfeinerung

8164 Reflexe	0 Restraints	380 Parameter
Verfeinerung mit SHELXL-2014/7	bis χ = 0.001	
R_1 ($I > 2\sigma(I)$) = 0.0651	wR_2 ($I > 2\sigma(I)$) = 0.1178	
R_1 (all) = 0.1057	wR_2 (all) = 0.1300	GoF (S) = 1.191
$\Delta\varphi_{min}$ = -0.743 e·Å^{-3}	$\Delta\varphi_{max}$ = 0.631 e·Å^{-3}	

Kommentar

Die Struktur wurde als nicht-meroedrischer Zwilling integriert und verfeinert.

Fraktionelle Atomkoordinaten (*x, y, z*) und äquivalente isotrope Auslenkungsfaktoren *U*(eq)

	x	*y*	*z*	*U*(eq)/Å^2
C(1)	0.8813(6)	0.2086(3)	0.1346(2)	0.0238(13)
C(2)	0.7618(8)	0.0647(4)	0.1838(3)	0.0511(19)
C(3)	0.5896(6)	0.1933(5)	0.1579(3)	0.053(2)
C(4)	0.7702(7)	0.1992(4)	0.2738(3)	0.0466(19)
C(5)	0.7286(5)	0.3427(3)	0.0617(2)	0.0197(12)
C(9)	1.0654(5)	0.2991(3)	0.0189(2)	0.0215(13)
C(10)	1.2226(6)	0.3136(3)	0.1466(2)	0.0265(13)
C(11)	1.3540(6)	0.3160(3)	0.0165(3)	0.0324(14)
C(12)	1.2408(6)	0.1725(3)	0.0646(3)	0.0236(13)
C(13)	0.8125(6)	0.1302(3)	0.0069(2)	0.0259(14)
C(14)	0.6248(7)	0.1093(3)	-0.1018(3)	0.0290(14)
C(15)	0.5805(6)	0.1261(3)	-0.1729(3)	0.0314(15)
C(16)	0.6206(7)	0.0241(3)	-0.0922(3)	0.0443(18)
C(17)	0.5281(6)	0.1440(3)	-0.0548(3)	0.0343(15)
C(18)	0.9153(6)	0.0995(3)	-0.1223(3)	0.0270(14)
C(19)	0.9402(8)	0.0201(3)	-0.0945(3)	0.0461(19)
C(20)	0.8933(7)	0.0904(3)	-0.1968(3)	0.0321(16)
C(21)	1.0363(6)	0.1451(3)	-0.1102(3)	0.0352(16)
C(22)	0.7739(5)	0.2995(2)	-0.1225(2)	0.0137(11)
C(23)	0.8102(6)	0.2802(3)	-0.1929(2)	0.0181(12)
C(24)	0.7877(6)	0.3478(3)	-0.2387(2)	0.0215(12)
C(25)	0.8713(6)	0.4135(3)	-0.2151(2)	0.0248(13)
C(26)	0.8358(5)	0.4340(3)	-0.1451(2)	0.0200(13)
C(27)	0.6964(5)	0.4570(3)	-0.1436(3)	0.0223(13)
C(28)	0.6129(6)	0.3922(3)	-0.1681(3)	0.0211(12)
C(29)	0.6355(6)	0.3252(3)	-0.1222(2)	0.0188(11)
C(30)	0.6491(6)	0.3702(3)	-0.2378(2)	0.0270(14)
C(31)	0.8572(5)	0.3655(2)	-0.1004(2)	0.0139(10)
N(1)	0.7980(4)	0.2385(2)	-0.0736(2)	0.0141(9)
Si(1)	0.7551(2)	0.1687(1)	0.1854(1)	0.0276(4)
Si(3)	1.2173(2)	0.2756(1)	0.0609(1)	0.0172(3)
P(1)	0.7851(2)	0.1469(1)	-0.0770(1)	0.0187(3)
Zr(1)	0.8671(1)	0.2549(1)	0.0305(1)	0.0143(1)
C(7)	0.8882(7)	0.4151(4)	0.1746(3)	0.0443(18)
Si(2A)	0.758(2)	0.4214(10)	0.1137(9)	0.027(3)
C(6A)	0.615(2)	0.443(2)	0.1622(16)	0.076(10)
C(8A)	0.799(5)	0.5025(14)	0.0615(12)	0.072(10)
Si(2B)	0.7769(17)	0.4358(9)	0.1011(9)	0.025(2)
C(6B)	0.637(2)	0.4858(14)	0.1288(13)	0.058(7)
C(8B)	0.865(2)	0.4987(8)	0.0432(10)	0.031(5)

7.9.6 Bis(1-ethyl-3-methylimidazolium)-disulfit (mhma4, Marius Hoffmann)

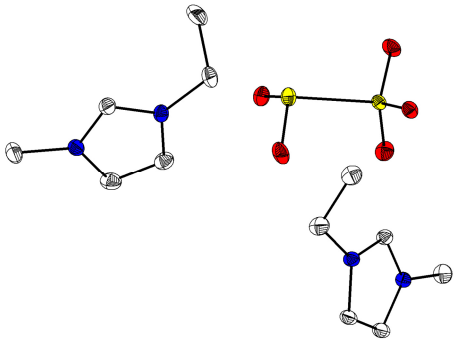

Kristalldaten

C6 H11 N2 O2.50 S	*M* = 183.23 g/mol	Triclinic, *P*–1
a = 7.5921(4) Å	*b* = 8.2049(4) Å	*c* = 14.4936(7) Å
α = 86.138(2)°	β = 77.835(2)°	γ = 73.942(2)°
V = 848.09(7) Å^3	*Z* = 4	*F*(000) = 388
D_{calc} = 1.435 g/cm^3	μ = 0.344 mm^{-1}	
colourless osterei	0.282 · 0.181 · 0.156 mm^3	

Datensammlung

Diffraktometer: D8 Quest (Bruker)	T = 100(2) K	λ = 0.71073 Å
h = -10 bis 10	k = -10 bis 10	l = -19 bis 19
17277 gemessene Reflexe	4203 unabhängige Reflexe	3368 Reflexe mit $I > 2\sigma(I)$
θ = 2.583 bis 28.350°	R_{int} = 0.0390	C (25.00°) = 0.999
Absorptionskorrektur: Multi-scan	T_{min} = 0.7042	T_{max} = 0.7457

Verfeinerung

4203 Reflexe	0 Restraints	212 Parameter
Verfeinerung mit SHELXL-2014/7	bis χ = 0.000	
R_1 ($I > 2\sigma(I)$) = 0.0374	wR_2 ($I > 2\sigma(I)$) = 0.0818	
R_1 (all) = 0.0548	wR_2 (all) = 0.0883	GoF (S) = 1.031
$\Delta\varphi_{min}$ = -0.419 e·Å^{-3}	$\Delta\varphi_{max}$ = 0.656 e·Å^{-3}	

Fraktionelle Atomkoordinaten (*x, y, z*) und äquivalente isotrope Auslenkungsfaktoren *U*(eq)

	x	*y*	*z*	*U*(eq)/Å^2
C(1)	0.2878(2)	0.8329(2)	-0.0116(1)	0.0167(3)
C(2)	0.0523(3)	0.7347(2)	-0.0245(1)	0.0217(4)
C(3)	0.1066(2)	0.6730(2)	0.0567(1)	0.0200(4)
C(4)	0.3559(3)	0.7014(2)	0.1422(1)	0.0193(4)
C(5)	0.5629(3)	0.6484(4)	0.1072(2)	0.0437(6)
C(6)	0.1654(3)	0.9164(3)	-0.1590(1)	0.0237(4)
C(7)	-0.1946(2)	0.3760(2)	0.3884(1)	0.0145(3)
C(8)	-0.4941(2)	0.4105(2)	0.3910(1)	0.0164(3)
C(9)	-0.4545(2)	0.5596(2)	0.3641(1)	0.0159(3)
C(10)	-0.1614(2)	0.6629(2)	0.3320(1)	0.0210(4)
C(11)	-0.0082(3)	0.6488(2)	0.3855(1)	0.0224(4)
C(12)	-0.3097(2)	0.1219(2)	0.4390(1)	0.0190(4)
N(1)	0.2542(2)	0.7354(2)	0.0635(1)	0.0152(3)
N(2)	0.1672(2)	0.8339(2)	-0.0661(1)	0.0159(3)
N(3)	-0.2670(2)	0.5357(2)	0.3633(1)	0.0144(3)
N(4)	-0.3302(2)	0.2977(2)	0.4058(1)	0.0133(3)
O(1)	0.4510(2)	-0.0494(2)	0.3079(1)	0.0195(3)
O(2)	0.2242(2)	0.1927(2)	0.3922(1)	0.0155(2)
O(3)	0.1187(2)	0.0027(2)	0.3083(1)	0.0201(3)
O(4)	0.3299(2)	0.1094(2)	0.1106(1)	0.0190(3)
O(5)	0.1180(2)	0.3591(2)	0.1983(1)	0.0227(3)
S(1)	0.2698(1)	0.0763(1)	0.3128(1)	0.0124(1)
S(2)	0.3060(1)	0.2350(1)	0.1852(1)	0.0159(1)

7.9.7 1,2-Bis(di-tert-butylphosphansulfid)disulfid (mhma30, Marius Hoffmann)

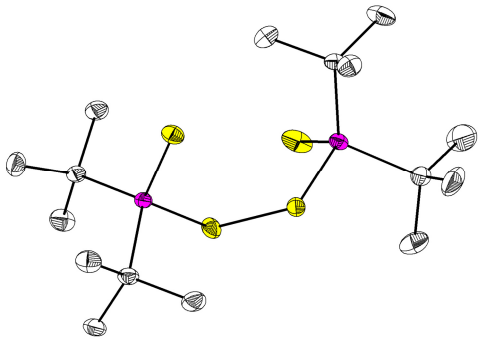

Kristalldaten

C16 H36 P2 S4	M = 418.63 g/mol	Monoclinic, $P2_1/n$
a = 7.9928(6) Å	b = 26.4138(17) Å	c = 11.0425(8) Å
α = 90°	β = 107.223(3)°	γ = 90°
V = 2226.8(3) Å^3	Z = 4	F(000) = 904
D_{calc} = 1.249 g/cm^3	μ = 0.567 mm^{-1}	
colourless block	0.546 · 0.404 · 0.256 mm^3	

Datensammlung

Diffraktometer: D8 Quest (Bruker)	T = 100(2) K	λ = 0.71073 Å
h = -10 bis 10	k = -33 bis 33	l = -13 bis 14
33120 gemessene Reflexe	4847 unabhängige Reflexe	4081 Reflexe mit $I > 2\sigma(I)$
θ = 2.471 bis 27.185°	R_{int} = 0.0561	C (25.00°) = 0.993
Absorptionskorrektur: Multi-scan	T_{min} = 0.560	T_{max} = 0.7455

Verfeinerung

4847 Reflexe	0 Restraints	211 Parameter
Verfeinerung mit SHELXL-2014/7	bis χ = 0.000	
R_1 ($I > 2\sigma(I)$) = 0.0372	wR_2 ($I > 2\sigma(I)$) = 0.0765	
R_1 (all) = 0.0495	wR_2 (all) = 0.0808	GoF (S) = 1.049
$\Delta\varphi_{min}$ = -0.451 e·Å^{-3}	$\Delta\varphi_{max}$ = 0.571 e·Å^{-3}	

Fraktionelle Atomkoordinaten (*x, y, z*) und äquivalente isotrope Auslenkungsfaktoren *U*(eq)

	x	*y*	*z*	*U*(eq)/Å^2		*x*	*y*	*z*	*U*(eq)/Å^2
C(1)	0.0145(2)	0.1928(1)	0.3388(2)	0.0172(4)	C(12)	0.0715(2)	0.0433(1)	0.6427(2)	0.0218(4)
C(2)	-0.0682(3)	0.1593(1)	0.4189(2)	0.0264(5)	C(13)	0.6306(2)	0.0853(1)	0.8019(2)	0.0179(4)
C(3)	0.1017(3)	0.2383(1)	0.4194(2)	0.0232(5)	C(14)	0.7121(3)	0.0329(1)	0.7996(2)	0.0217(4)
C(4)	-0.1281(3)	0.2112(1)	0.2211(2)	0.0285(5)	C(15)	0.6482(3)	0.1008(1)	0.9388(2)	0.0243(5)
C(5)	0.2726(3)	0.1833(1)	0.1718(2)	0.0249(5)	C(16)	0.7274(3)	0.1245(1)	0.7447(2)	0.0251(5)
C(6)	0.1319(4)	0.1887(1)	0.0422(3)	0.0595(9)	P(1)	0.1750(1)	0.1525(1)	0.2883(1)	0.0151(1)
C(7)	0.3589(4)	0.2339(1)	0.2190(3)	0.0427(7)	P(2)	0.3938(1)	0.0882(1)	0.7061(1)	0.0138(1)
C(8)	0.4122(3)	0.1471(1)	0.1517(2)	0.0320(5)	S(1)	0.0814(1)	0.0860(1)	0.2298(1)	0.0288(1)
C(9)	0.2602(2)	0.0316(1)	0.7214(2)	0.0169(4)	S(2)	0.4056(1)	0.1496(1)	0.4518(1)	0.0189(1)
C(10)	0.2673(3)	0.0251(1)	0.8609(2)	0.0257(5)	S(3)	0.4007(1)	0.0771(1)	0.5138(1)	0.0201(1)
C(11)	0.3187(3)	-0.0175(1)	0.6702(2)	0.0254(5)	S(4)	0.2893(1)	0.1518(1)	0.7355(1)	0.0202(1)

7.9.8 Bis(1-dimethylamino-8-diphenylphosphino)naphthalin-kupfer(I)-hexafluorophosphat (mk22, Marius Klein)

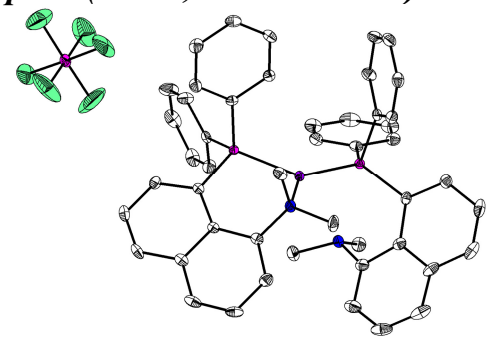

Kristalldaten

C48 H44 Cu F6 N2 P3	M = 919.30 g/mol	Monoclinic, $P2_1/n$
a = 13.8350(9) Å	b = 41.929(3) Å	c = 14.6101(10) Å
α = 90°	β = 100.269(2)°	γ = 90°
V = 8339.4(10) Å^3	Z = 8	F(000) = 3792
D_{calc} = 1.464 g/cm^3	μ = 0.704 mm^{-1}	
colourless block	0.360 · 0.340 · 0.310 mm^3	

Datensammlung

Diffraktometer: D8 Quest (Bruker)	T = 100(2) K	λ = 0.71073 Å
h = -17 bis 17	k = -53 bis 53	l = -18 bis 18
147121 gemessene Reflexe	18505 unabhängige Reflexe	16325 Reflexe mit $I > 2\sigma(I)$
θ = 2.288 bis 27.185°	R_{int} = 0.0341	C (25.00°) = 0.999
Absorptionskorrektur: Multi-scan	T_{min} = 0.7064	T_{max} = 0.7455

Verfeinerung

18505 Reflexe	210 Restraints	1217 Parameter
Verfeinerung mit SHELXL-2014/7	bis χ = 0.002	
R_1 ($I > 2\sigma(I)$) = 0.0339	wR_2 ($I > 2\sigma(I)$) = 0.0780	
R_1 (all) = 0.0417	wR_2 (all) = 0.0810	GoF (S) = 1.076
$\Delta\varphi_{min}$ = -0.411 e·Å^{-3}	$\Delta\varphi_{max}$ = 0.422 e·Å^{-3}	

Kommentar

Die fehlgeordneten Hexafluorphosphatanionen wurden über SAME, DELU und RIGU restrained.

Fraktionelle Atomkoordinaten (*x, y, z*) und äquivalente isotrope Auslenkungsfaktoren *U*(eq)

	x	*y*	*z*	*U*(eq)/Å^2
C(1)	0.2775(1)	0.2506(1)	0.5549(1)	0.0118(3)
C(2)	0.2487(1)	0.2401(1)	0.4647(1)	0.0147(3)
C(3)	0.2362(1)	0.2609(1)	0.3881(1)	0.0172(4)
C(4)	0.2468(1)	0.2927(1)	0.4036(1)	0.0162(4)
C(5)	0.2729(1)	0.3053(1)	0.4949(1)	0.0138(3)
C(6)	0.2730(1)	0.3389(1)	0.5063(1)	0.0175(4)
C(7)	0.2945(1)	0.3518(1)	0.5923(1)	0.0218(4)
C(8)	0.3240(1)	0.3321(1)	0.6699(1)	0.0184(4)
C(9)	0.3280(1)	0.2994(1)	0.6627(1)	0.0133(3)
C(10)	0.2943(1)	0.2843(1)	0.5737(1)	0.0118(3)
C(11)	0.3988(2)	0.3000(1)	0.8297(1)	0.0206(4)
C(12)	0.4672(1)	0.2670(1)	0.7243(1)	0.0168(4)
C(13)	0.1703(1)	0.1958(1)	0.6029(1)	0.0119(3)
C(14)	0.1740(1)	0.1631(1)	0.6193(1)	0.0167(4)
C(15)	0.0890(1)	0.1449(1)	0.6032(1)	0.0205(4)
C(16)	-0.0011(1)	0.1593(1)	0.5720(1)	0.0197(4)
C(17)	-0.0052(1)	0.1919(1)	0.5556(1)	0.0173(4)
C(18)	0.0796(1)	0.2101(1)	0.5703(1)	0.0137(3)
C(19)	0.3817(1)	0.1941(1)	0.6437(1)	0.0135(3)
C(20)	0.4299(1)	0.1817(1)	0.7279(1)	0.0213(4)
C(21)	0.5104(2)	0.1616(1)	0.7308(2)	0.0275(5)
C(22)	0.5430(1)	0.1537(1)	0.6497(2)	0.0265(5)
C(23)	0.4951(1)	0.1658(1)	0.5656(2)	0.0244(4)
C(24)	0.4150(1)	0.1859(1)	0.5621(1)	0.0174(4)
C(25)	0.2332(1)	0.2608(1)	1.0034(1)	0.0111(3)
C(26)	0.2794(1)	0.2574(1)	1.0948(1)	0.0140(3)
C(27)	0.2949(1)	0.2841(1)	1.1548(1)	0.0165(4)
C(28)	0.2737(1)	0.3141(1)	1.1209(1)	0.0159(4)
C(29)	0.2276(1)	0.3187(1)	1.0270(1)	0.0135(3)
C(30)	0.2096(1)	0.3496(1)	0.9876(1)	0.0171(4)
C(31)	0.1601(1)	0.3530(1)	0.8985(1)	0.0192(4)
C(32)	0.1193(1)	0.3263(1)	0.8470(1)	0.0169(4)
C(33)	0.1348(1)	0.2962(1)	0.8833(1)	0.0129(3)
C(34)	0.1978(1)	0.2915(1)	0.9707(1)	0.0114(3)
C(35)	-0.0017(1)	0.2614(1)	0.8828(1)	0.0171(4)
C(36)	0.0576(2)	0.2695(1)	0.7401(1)	0.0211(4)
C(37)	0.1384(1)	0.2021(1)	0.9163(1)	0.0112(3)
C(38)	0.0993(1)	0.1955(1)	0.9959(1)	0.0138(3)
C(39)	0.0221(1)	0.1741(1)	0.9921(1)	0.0170(4)
C(40)	-0.0168(1)	0.1591(1)	0.9087(1)	0.0180(4)
C(41)	0.0207(1)	0.1658(1)	0.8292(1)	0.0169(4)
C(42)	0.0982(1)	0.1873(1)	0.8326(1)	0.0137(3)
C(43)	0.3460(1)	0.2055(1)	0.9787(1)	0.0129(3)
C(44)	0.4392(1)	0.2145(1)	0.9639(1)	0.0191(4)
C(45)	0.5224(1)	0.1977(1)	1.0035(1)	0.0242(4)
C(46)	0.5138(1)	0.1713(1)	1.0585(1)	0.0238(4)
C(47)	0.4225(1)	0.1624(1)	1.0747(2)	0.0252(4)
C(48)	0.3386(1)	0.1792(1)	1.0349(1)	0.0196(4)
C(51)	0.2689(1)	0.5088(1)	0.5146(1)	0.0109(3)
C(52)	0.2415(1)	0.5017(1)	0.4211(1)	0.0146(3)
C(53)	0.2287(1)	0.5254(1)	0.3520(1)	0.0173(4)
C(54)	0.2386(1)	0.5565(1)	0.3777(1)	0.0170(4)
C(55)	0.2639(1)	0.5654(1)	0.4726(1)	0.0133(3)
C(56)	0.2647(1)	0.5983(1)	0.4945(1)	0.0184(4)
C(57)	0.2861(1)	0.6083(1)	0.5835(1)	0.0206(4)
C(58)	0.3141(1)	0.5857(1)	0.6549(1)	0.0186(4)
C(59)	0.3175(1)	0.5535(1)	0.6377(1)	0.0128(3)
C(60)	0.2848(1)	0.5416(1)	0.5441(1)	0.0107(3)
C(61)	0.3840(2)	0.5480(1)	0.8050(1)	0.0214(4)
C(62)	0.4536(1)	0.5186(1)	0.6929(1)	0.0171(4)
C(63)	0.1596(1)	0.4519(1)	0.5352(1)	0.0117(3)
C(64)	0.0660(1)	0.4632(1)	0.5396(1)	0.0179(4)
C(65)	-0.0168(1)	0.4456(1)	0.5045(1)	0.0230(4)
C(66)	-0.0071(1)	0.4162(1)	0.4644(2)	0.0251(4)
C(67)	0.0852(2)	0.4051(1)	0.4575(2)	0.0275(5)
C(68)	0.1687(1)	0.4228(1)	0.4926(1)	0.0197(4)
C(69)	0.3695(1)	0.4498(1)	0.5932(1)	0.0116(3)
C(70)	0.4063(1)	0.4336(1)	0.6757(1)	0.0156(4)
C(71)	0.4834(1)	0.4122(1)	0.6799(1)	0.0189(4)
C(72)	0.5242(1)	0.4067(1)	0.6014(1)	0.0187(4)
C(73)	0.4891(1)	0.4229(1)	0.5196(1)	0.0194(4)
C(74)	0.4121(1)	0.4444(1)	0.5152(1)	0.0167(4)
C(75)	0.2206(1)	0.5042(1)	0.9646(1)	0.0130(3)
C(76)	0.2690(1)	0.4961(1)	1.0520(1)	0.0168(4)
C(77)	0.2900(1)	0.5193(1)	1.1226(1)	0.0221(4)
C(78)	0.2713(1)	0.5508(1)	1.1030(1)	0.0225(4)
C(79)	0.2223(1)	0.5604(1)	1.0136(1)	0.0187(4)
C(80)	0.2070(1)	0.5928(1)	0.9879(2)	0.0248(4)
C(81)	0.1550(2)	0.6006(1)	0.9024(2)	0.0266(5)
C(82)	0.1085(2)	0.5771(1)	0.8416(2)	0.0224(4)
C(83)	0.1210(1)	0.5454(1)	0.8647(1)	0.0162(4)
C(84)	0.1873(1)	0.5364(1)	0.9470(1)	0.0149(3)
C(85)	-0.0170(1)	0.5109(1)	0.8589(1)	0.0199(4)
C(86)	0.0316(2)	0.5263(1)	0.7160(1)	0.0264(4)
C(87)	0.1199(1)	0.4498(1)	0.8602(1)	0.0138(3)
C(88)	0.0720(1)	0.4390(1)	0.7739(1)	0.0172(4)
C(89)	-0.0068(1)	0.4178(1)	0.7682(2)	0.0223(4)
C(90)	-0.0384(1)	0.4078(1)	0.8485(2)	0.0256(4)
C(91)	0.0109(1)	0.4184(1)	0.9349(2)	0.0229(4)
C(92)	0.0893(1)	0.4390(1)	0.9408(1)	0.0176(4)
C(93)	0.3286(1)	0.4516(1)	0.9072(1)	0.0125(3)
C(94)	0.4209(1)	0.4652(1)	0.9389(1)	0.0156(4)
C(95)	0.5044(1)	0.4465(1)	0.9549(1)	0.0182(4)
C(96)	0.4986(1)	0.4139(1)	0.9385(1)	0.0204(4)
C(97)	0.4077(2)	0.4001(1)	0.9081(1)	0.0214(4)
C(98)	0.3234(1)	0.4189(1)	0.8926(1)	0.0179(4)
N(1)	0.3729(1)	0.2807(1)	0.7436(1)	0.0139(3)
N(2)	0.0855(1)	0.2685(1)	0.8412(1)	0.0129(3)
N(3)	0.3593(1)	0.5321(1)	0.7131(1)	0.0139(3)
N(4)	0.0665(1)	0.5202(1)	0.8147(1)	0.0160(3)
P(5)	0.2075(3)	0.1609(1)	0.2799(2)	0.0254(8)
F(1)	0.2408(6)	0.1938(1)	0.2420(4)	0.0647(17)
F(2)	0.2633(4)	0.1415(1)	0.2131(4)	0.0641(13)
F(3)	0.1102(5)	0.1614(1)	0.2023(4)	0.0703(17)
F(4)	0.1487(2)	0.1802(1)	0.3475(3)	0.0479(11)
F(5)	0.3004(3)	0.1603(1)	0.3601(3)	0.0401(9)
F(6)	0.1807(5)	0.1266(1)	0.3121(4)	0.083(2)
P(6)	0.2952(1)	0.4127(1)	0.2352(1)	0.0220(3)
F(7)	0.3451(2)	0.4415(1)	0.1928(2)	0.0724(10)
F(8)	0.3512(1)	0.3879(1)	0.1813(2)	0.0611(7)
F(9)	0.2075(2)	0.4131(1)	0.1494(2)	0.0424(6)
F(10)	0.2382(2)	0.4363(1)	0.2898(2)	0.0966(11)
F(11)	0.3858(2)	0.4119(1)	0.3186(2)	0.0736(13)
F(12)	0.2472(2)	0.3829(1)	0.2783(2)	0.0692(8)
P(1)	0.2772(1)	0.2204(1)	0.6453(1)	0.0105(1)
P(2)	0.2415(1)	0.2291(1)	0.9186(1)	0.0099(1)
P(3)	0.2634(1)	0.4753(1)	0.5939(1)	0.0092(1)
P(4)	0.2219(1)	0.4774(1)	0.8662(1)	0.0109(1)
Cu(1)	0.2818(1)	0.2431(1)	0.7832(1)	0.0113(1)
Cu(2)	0.2619(1)	0.4947(1)	0.7348(1)	0.0108(1)
P(5A)	0.2022(5)	0.1599(2)	0.2798(5)	0.0136(17)
F(1A)	0.2108(9)	0.1963(2)	0.2541(11)	0.043(3)
F(2A)	0.2319(10)	0.1493(3)	0.1850(8)	0.055(3)
F(3A)	0.0934(6)	0.1593(3)	0.2299(10)	0.043(2)
F(4A)	0.1741(14)	0.1695(4)	0.3755(8)	0.071(3)
F(5A)	0.3135(8)	0.1613(4)	0.3290(12)	0.061(3)
F(6A)	0.1710(8)	0.1271(2)	0.3181(8)	0.029(2)
P(6A)	0.2937(10)	0.4151(3)	0.2354(9)	0.047(3)

	x	y	z	U(eq)/Å^2
F(7A)	0.2970(9)	0.4518(2)	0.2537(11)	0.054(3)
F(8A)	0.3362(11)	0.4147(4)	0.1433(9)	0.079(4)
F(9A)	0.1865(11)	0.4188(4)	0.1786(13)	0.060(4)
F(10A)	0.2563(11)	0.4133(5)	0.3301(9)	0.078(4)
F(11A)	0.3995(10)	0.4110(5)	0.2952(14)	0.049(4)
F(12A)	0.2817(11)	0.3782(3)	0.2345(13)	0.062(4)

7.9.9 1,1,2,2-Tetrabutyl-diphosphan-diiod (pk-bu2pi, Dr. Paul Kübler)

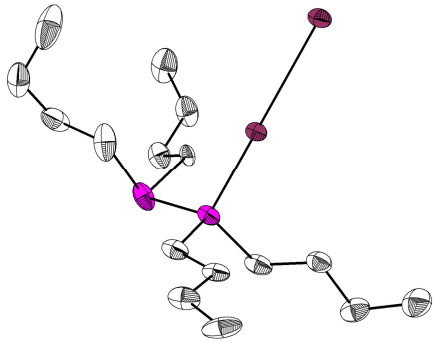

Kristalldaten

C16 H36 I2 P2	M = 544.19 g/mol	Triclinic, $P\bar{1}$
a = 9.9444(7) Å	b = 10.1246(7) Å	c = 12.3448(9) Å
α = 101.535(6)°	β = 109.233(6)°	γ = 94.055(5)°
V = 1137.24(15) Å^3	Z = 2	F(000) = 536
D_{calc} = 1.589 g/cm^3	μ = 2.899 mm^{-1}	
pale yellow needle	0.440 · 0.140 · 0.080 mm^3	

Datensammlung

Diffraktometer: STOE IPDS 2	T = 100(2) K	λ = 0.71073 Å
h = -12 bis 12	k = -12 bis 12	l = -15 bis 15
10553 gemessene Reflexe	4812 unabhängige Reflexe	3577 Reflexe mit $I > 2\sigma(I)$
θ = 1.798 bis 26.722°	R_{int} = 0.0531	C (25.00°) = 1.000
Absorptionskorrektur: Multi-scan	T_{min} = 0.5051	T_{max} = 0.6418

Verfeinerung

4812 Reflexe	40 Restraints	220 Parameter
Verfeinerung mit SHELXL-2014/7	bis χ = 0.001	
R_1 ($I > 2\sigma(I)$) = 0.0290	wR_2 ($I > 2\sigma(I)$) = 0.0680	
R_1 (all) = 0.0405	wR_2 (all) = 0.0695	GoF (S) = 0.857
$\Delta\varphi_{min}$ = -1.093 e·Å^{-3}	$\Delta\varphi_{max}$ = 1.145 e·Å^{-3}	

Kommentar

Eine fehlgeordnete Butylgruppe wurde über DELU und RIGU restrained.

Fraktionelle Atomkoordinaten (*x, y, z*) und äquivalente isotrope Auslenkungsfaktoren *U*(eq)

	x	y	z	U(eq)/Å^2
I(1)	0.4887(1)	0.7249(1)	0.4576(1)	0.0244(1)
I(2)	0.1333(1)	0.7233(1)	0.3715(1)	0.0276(1)
P(1)	0.7501(1)	0.7337(1)	0.5146(1)	0.0256(2)
P(2)	0.8618(1)	0.7849(1)	0.7050(1)	0.0326(3)
C(3)	0.8132(5)	0.9551(5)	0.2795(5)	0.0402(12)
C(1)	0.8138(5)	0.8662(5)	0.4556(4)	0.0315(10)
C(2)	0.7595(5)	0.8359(5)	0.3211(4)	0.0308(10)
C(9)	0.7780(6)	0.9396(5)	0.7412(4)	0.0445(13)
C(4)	0.7778(7)	0.9249(6)	0.1474(5)	0.0517(15)
C(5)	0.7987(4)	0.5729(4)	0.4536(4)	0.0315(10)
C(8)	0.6279(6)	0.2673(5)	0.1838(5)	0.0516(14)
C(10)	0.8343(5)	1.0036(6)	0.8707(4)	0.0413(12)
C(7)	0.7453(5)	0.3632(5)	0.2880(4)	0.0386(11)
C(6)	0.6864(5)	0.4851(5)	0.3399(4)	0.0326(10)
C(11)	0.7829(6)	1.1382(5)	0.9030(4)	0.0491(14)
C(12)	0.6234(7)	1.1260(7)	0.8719(6)	0.078(2)
C(14B)	0.7786(11)	0.6657(10)	0.8752(8)	0.025(2)
C(16B)	0.8476(12)	0.5077(10)	1.0199(9)	0.037(3)
C(15B)	0.728(3)	0.527(3)	0.896(2)	0.033(4)
C(13B)	0.7604(4)	0.6499(4)	0.7420(4)	0.021(4)
C(14A)	0.8503(11)	0.6275(9)	0.8596(8)	0.032(2)
C(16A)	0.7412(14)	0.5456(10)	1.0277(9)	0.050(3)
C(15A)	0.758(3)	0.541(3)	0.904(2)	0.039(5)
C(13A)	0.7604(4)	0.6499(4)	0.7420(4)	0.028(4)

7.9.10 1-Ethyl-3-methylimidazolium-hydrogensulfid (ds03, Dejan Premužić)

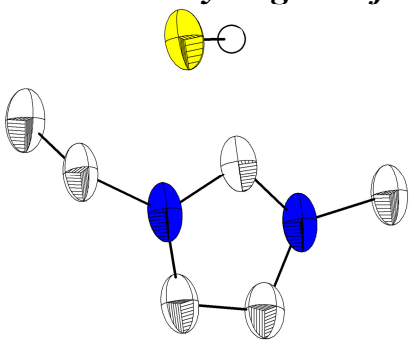

Kristalldaten

C6 H12 N2 S	M = 144.24 g/mol	Monoclinic, $P2_1/n$
a = 8.6101(12) Å	b = 7.6972(8) Å	c = 12.779(2) Å
α = 90°	β = 107.878(13)°	γ = 90°
V = 806.0(2) Å^3	Z = 4	F(000) = 312
D_{calc} = 1.189 g/cm^3	μ = 0.321 mm^{-1}	
colourless needle	0.300 · 0.100 · 0.100 mm^3	

Datensammlung

Diffraktometer: STOE IPDS 2	T = 100(2) K	λ = 0.71069 Å
h = -10 bis 10	k = -9 bis 9	l = -16 bis 16
6674 gemessene Reflexe	1707 unabhängige Reflexe	1173 Reflexe mit $I > 2\sigma(I)$
θ = 3.132 bis 26.757°	R_{int} = 0.1298	C (25.00°) = 0.996
Absorptionskorrektur: Multi-scan	T_{min} = 0.7002	T_{max} = 1.8653

Verfeinerung

1707 Reflexe	0 Restraints	88 Parameter
Verfeinerung mit SHELXL-2014/7	bis χ = 0.000	
R_1 ($I > 2\sigma(I)$) = 0.0625	wR_2 ($I > 2\sigma(I)$) = 0.1461	
R_1 (all) = 0.0817	wR_2 (all) = 0.1546	GoF (S) = 0.994
$\Delta\varphi_{min}$ = -0.365 e·Å^{-3}	$\Delta\varphi_{max}$ = 0.333 e·Å^{-3}	

Kommentar

Die Datensammlung erfolgte durch Dejan Premužić. Im Verlauf der eigenen Forschungsarbeiten konnte diese Substanz während einer Sublimation erneut kristallisiert werden.

Fraktionelle Atomkoordinaten (*x, y, z*) und äquivalente isotrope Auslenkungsfaktoren *U*(eq)

	x	*y*	*z*	*U*(eq)/Å^2
C(2)	0.4877(3)	0.1496(3)	0.8429(3)	0.0449(7)
C(4)	0.3787(3)	0.0397(3)	0.6766(3)	0.0473(7)
C(5)	0.5251(3)	0.1113(3)	0.6813(3)	0.0479(7)
C(6)	0.7512(3)	0.2639(3)	0.8280(3)	0.0481(7)
C(7)	0.8728(3)	0.1490(4)	0.9082(3)	0.0602(9)
C(8)	0.2204(3)	0.0088(4)	0.8139(3)	0.0541(8)
N(1)	0.5907(2)	0.1784(3)	0.7846(2)	0.0460(6)
N(3)	0.3584(2)	0.0664(3)	0.7781(2)	0.0458(6)
S(1)	0.6220(1)	0.7001(1)	0.9292(1)	0.0533(3)

7.9.11 Bis(1-ethyl-3-methylimidazolium)-tetrathiomolybdat (ds6, Dejan Premužić)

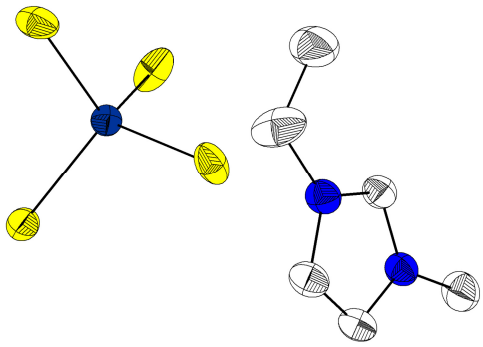

Kristalldaten

C12 H22 Mo N4 S4	M = 446.51 g/mol	Tetragonal, $I4_1/a$
a = 14.1958(5) Å	b = 14.1958(5) Å	c = 18.6254(8) Å
α = 90°	β = 90°	γ = 90°
V = 3753.4(3) Å^3	Z = 8	F(000) = 1824
D_{calc} = 1.580 g/cm^3	μ = 1.142 mm^{-1}	
red block	0.400 · 0.200 · 0.200 mm^3	

Datensammlung

Diffraktometer: STOE IPDS 2	T = 100(2) K	λ = 0.71073 Å
h = -17 bis 17	k = -17 bis 17	l = -23 bis 23
10566 gemessene Reflexe	1995 unabhängige Reflexe	1557 Reflexe mit $I > 2\sigma(I)$
θ = 1.804 bis 26.709°	R_{int} = 0.0522	C (25.00°) = 1.000
Absorptionskorrektur: Multi-scan	T_{min} = 0.6541	T_{max} = 0.8405

Verfeinerung

1995 Reflexe	50 Restraints	172 Parameter
Verfeinerung mit SHELXL-2014/7	bis χ = 0.001	
R_1 ($I > 2\sigma(I)$) = 0.0257	wR_2 ($I > 2\sigma(I)$) = 0.0643	
R_1 (all) = 0.0335	wR_2 (all) = 0.0659	GoF (S) = 0.915
$\Delta\varphi_{min}$ = -0.497 e·Å^{-3}	$\Delta\varphi_{max}$ = 0.509 e·Å^{-3}	

Kommentar

Die Datensammlung erfolgte durch Dejan Premužić. Das Imidazoliumkation ist über zwei Positionen fehlgeordnet und wurde über FLAT, RIGU, DELU, SAME und ISOR restrained.

Fraktionelle Atomkoordinaten (*x, y, z*) und äquivalente isotrope Auslenkungsfaktoren *U*(eq)

	x	*y*	*z*	*U*(eq)/Å^2		*x*	*y*	*z*	*U*(eq)/Å^2
Mo(1)	0.0000	0.2500	0.1250	0.0217(1)	C(7)	0.6545(3)	0.2788(3)	0.5947(3)	0.0662(12)
Mo(2)	0.5000	0.2500	0.8750	0.0262(1)	C(8)	0.8926(3)	0.4542(4)	0.7743(3)	0.0434(10)
S(1)	-0.0044(1)	0.3761(1)	0.0576(1)	0.0319(1)	N(1A)	0.7311(9)	0.4577(10)	0.6731(6)	0.045(5)
S(2)	0.6055(1)	0.3213(1)	0.8093(1)	0.0420(2)	N(3A)	0.6519(10)	0.3468(10)	0.6287(7)	0.040(4)
N(1)	0.6931(2)	0.4259(2)	0.6589(2)	0.0335(7)	C(2A)	0.7320(9)	0.3683(10)	0.6596(7)	0.037(4)
N(3)	0.8090(2)	0.4622(2)	0.7287(1)	0.0302(6)	C(4A)	0.5956(10)	0.4274(10)	0.6181(7)	0.038(4)
C(2)	0.7682(2)	0.3920(2)	0.6929(2)	0.0311(7)	C(5A)	0.6472(10)	0.4961(10)	0.6514(8)	0.038(4)
C(4)	0.7577(2)	0.5437(2)	0.7164(2)	0.0354(7)	C(6A)	0.8061(13)	0.5072(14)	0.7106(10)	0.040(4)
C(5)	0.6857(2)	0.5207(2)	0.6728(2)	0.0368(8)	C(7A)	0.8573(16)	0.4584(18)	0.7674(14)	0.040(5)
C(6)	0.6246(4)	0.3705(3)	0.6170(3)	0.0584(13)	C(8A)	0.6118(11)	0.2576(10)	0.6137(10)	0.039(4)

7.9.12 Adamantylimino-di(methyl)-tetramethylcyclopentadienyliden-phosphoran-diphenyl-yttrium(III)-toluolsolvat (pr12, Dr. Noa Pruß)

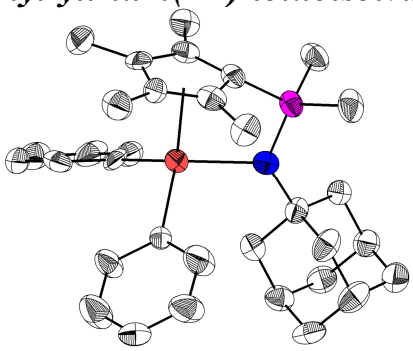

Kristalldaten

C43.50 H55 Lu N P	M = 797.82 g/mol	Monoclinic, $P2_1/n$
a = 14.7819(7) Å	b = 15.1613(5) Å	c = 17.1563(7) Å
α = 90°	β = 103.006(3)°	γ = 90°
V = 3746.3(3) Å^3	Z = 4	F(000) = 1636
D_{calc} = 1.415 g/cm^3	μ = 2.708 mm^{-1}	
colourless prism	0.370 · 0.220 · 0.140 mm^3	

Datensammlung

Diffraktometer: STOE IPDS 2	T = 100(2) K	λ = 0.71073 Å
h = -18 bis 18	k = -19 bis 16	l = -17 bis 21
20457 gemessene Reflexe	7881 unabhängige Reflexe	4167 Reflexe mit $I > 2\sigma(I)$
θ = 1.646 bis 26.742°	R_{int} = 0.1000	C (25.00°) = 0.995
Absorptionskorrektur: Multi-scan	T_{min} = 0.4340	T_{max} = 0.7030

Verfeinerung

7881 Reflexe	275 Restraints	519 Parameter
Verfeinerung mit SHELXL-2014/7	bis χ = 0.000	
R_1 ($I > 2\sigma(I)$) = 0.0399	wR_2 ($I > 2\sigma(I)$) = 0.0790	
R_1 (all) = 0.0832	wR_2 (all) = 0.0840	GoF (S) = 0.720
$\Delta\varphi_{min}$ = -1.929 e·Å^{-3}	$\Delta\varphi_{max}$ = 1.427 e·Å^{-3}	

Kommentar

Mehrere fehlgeordnete Toluolmoleküle und ein fehlgeordneter Phenylring des Komplexmoleküls wurden über DELU, RIGU, ISOR; DFIX, SADI, FLAT und SIMU restrained.

Fraktionelle Atomkoordinaten (*x, y, z*) und äquivalente isotrope Auslenkungsfaktoren *U*(eq)

	x	*y*	*z*	*U*(eq)/Å^2		*x*	*y*	*z*	*U*(eq)/Å^2
C(1)	0.4042(4)	0.4407(4)	0.4202(4)	0.0379(15)	C(21)	0.3614(4)	0.2485(5)	0.0581(4)	0.0504(18)
C(2)	0.4741(4)	0.3762(4)	0.4589(4)	0.0408(16)	C(28)	0.1813(4)	0.2560(5)	0.3555(4)	0.0479(18)
C(3)	0.4394(4)	0.3265(4)	0.5122(4)	0.0395(15)	C(29)	0.1575(5)	0.1918(4)	0.4060(4)	0.0535(19)
C(4)	0.3477(4)	0.3603(4)	0.5128(4)	0.0406(16)	C(33)	0.1041(4)	0.2949(5)	0.3052(4)	0.0494(16)
C(5)	0.3263(4)	0.4286(4)	0.4577(4)	0.0377(16)	C(30)	0.0657(6)	0.1652(5)	0.4042(5)	0.067(2)
C(6)	0.5669(4)	0.3608(5)	0.4370(4)	0.0501(18)	C(32)	0.0131(4)	0.2695(5)	0.3017(4)	0.061(2)
C(7)	0.4894(5)	0.2553(5)	0.5664(4)	0.0554(18)	C(31)	-0.0064(5)	0.2054(6)	0.3526(5)	0.066(2)
C(8)	0.2895(4)	0.3272(5)	0.5687(4)	0.0574(19)	N(1)	0.3609(3)	0.3903(3)	0.2751(3)	0.0355(12)
C(9)	0.2365(4)	0.4793(4)	0.4410(4)	0.0470(18)	P(1)	0.3962(1)	0.4788(1)	0.3232(1)	0.0374(4)
C(10)	0.5046(4)	0.5234(5)	0.3104(4)	0.054(2)	Lu(1)	0.3393(1)	0.2928(1)	0.3668(1)	0.0359(1)
C(11)	0.3220(4)	0.5744(4)	0.3049(4)	0.0503(18)	C(22)	0.4362(6)	0.1660(6)	0.3575(7)	0.028(3)
C(12)	0.3487(3)	0.3739(4)	0.1860(4)	0.0361(15)	C(23)	0.3963(6)	0.0856(7)	0.3697(9)	0.053(5)
C(13)	0.2828(3)	0.2955(5)	0.1652(3)	0.0404(14)	C(24)	0.4414(7)	0.0073(6)	0.3601(11)	0.080(6)
C(14)	0.3069(4)	0.4521(4)	0.1343(4)	0.0394(15)	C(25)	0.5265(6)	0.0093(6)	0.3384(8)	0.047(4)
C(16)	0.2679(4)	0.2723(4)	0.0773(4)	0.0448(17)	C(26)	0.5664(6)	0.0897(7)	0.3262(8)	0.066(5)
C(17)	0.2924(4)	0.4299(5)	0.0460(4)	0.0454(17)	C(27)	0.5212(8)	0.1680(6)	0.3358(9)	0.069(5)
C(19)	0.2269(4)	0.3511(4)	0.0268(4)	0.0476(17)	C(22A)	0.4131(8)	0.1532(6)	0.3618(7)	0.049(4)
C(20)	0.3851(4)	0.4058(5)	0.0278(4)	0.0553(19)	C(23A)	0.4094(6)	0.0914(8)	0.4209(8)	0.058(4)

	x	y	z	U(eq)/Å^2
C(24A)	0.4634(7)	0.0156(7)	0.4274(9)	0.069(4)
C(25A)	0.5211(8)	0.0015(7)	0.3749(9)	0.095(6)
C(26A)	0.5249(10)	0.0632(10)	0.3158(8)	0.116(7)
C(27A)	0.4709(11)	0.1391(9)	0.3093(7)	0.085(6)
C(106)	0.4443(11)	0.8998(10)	0.8758(10)	0.086(5)
C(102)	0.5214(11)	0.9878(8)	1.0866(10)	0.062(4)
C(103)	0.5369(11)	1.0761(8)	1.0724(11)	0.060(5)
C(104)	0.5228(12)	1.1071(6)	0.9943(12)	0.064(5)
C(105)	0.4933(12)	1.0497(7)	0.9305(11)	0.065(5)
C(100)	0.4778(11)	0.9613(7)	0.9448(10)	0.059(4)
C(101)	0.4919(11)	0.9304(6)	1.0228(11)	0.062(5)
C(15)	0.4421(4)	0.3498(5)	0.1666(4)	0.0504(19)
C(18)	0.4260(4)	0.3270(5)	0.0764(4)	0.056(2)

	x	y	z	U(eq)/Å^2
C(306)	0.2094(14)	0.2676(17)	0.7916(15)	0.102(9)
C(305)	0.2480(8)	0.1033(9)	0.8073(6)	0.060(5)
C(300)	0.2155(7)	0.1750(6)	0.7585(8)	0.046(5)
C(301)	0.1823(8)	0.1628(7)	0.6767(8)	0.055(6)
C(302)	0.1817(8)	0.0789(9)	0.6438(6)	0.070(5)
C(303)	0.2142(9)	0.0073(6)	0.6927(8)	0.077(6)
C(304)	0.2474(10)	0.0195(7)	0.7744(8)	0.079(6)
C(406)	0.1775(18)	0.0196(17)	0.6556(12)	0.104(9)
C(402)	0.2176(10)	0.2389(8)	0.7430(10)	0.074(6)
C(403)	0.2518(9)	0.2201(10)	0.8236(9)	0.078(7)
C(404)	0.2630(9)	0.1329(12)	0.8491(6)	0.073(6)
C(405)	0.2399(9)	0.0647(9)	0.7941(9)	0.083(8)
C(400)	0.2057(8)	0.0835(10)	0.7136(8)	0.066(6)
C(401)	0.1946(10)	0.1707(11)	0.6881(6)	0.087(10)

7.9.13 Di(tert-butyl)triazenido-lithium(I)-diethyletheraddukt-dimer (fgsp1f5, Dr. Fabian Schröder)

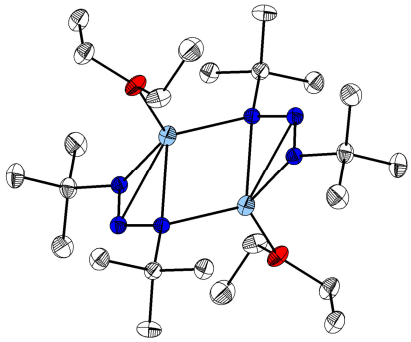

Kristalldaten

C24 H56 Li2 N6 O2	M = 474.62 g/mol	Triclinic, $P\bar{1}$
a = 9.4374(14) Å	b = 11.1191(18) Å	c = 15.233(2) Å
α = 85.065(5)°	β = 80.436(6)°	γ = 80.207(6)°
V = 1550.6(4) Å^3	Z = 2	F(000) = 528
D_{calc} = 1.017 g/cm^3	μ = 0.064 mm^{-1}	
colourless block	0.370 · 0.180 · 0.130 mm^3	

Datensammlung

Diffraktometer: D8 Quest (Bruker)	T = 100(2) K	λ = 0.71073 Å
h = -11 bis 12	k = -14 bis 14	l = 0 bis 19
6703 gemessene Reflexe	6703 unabhängige Reflexe	5506 Reflexe mit $I > 2\sigma(I)$
θ = 2.239 bis 27.104°	R_{int} = -(hklf5)	C (25.00°) = 0.997
Absorptionskorrektur: Multi-scan	T_{min} = 0.7264	T_{max} = 0.9090

Verfeinerung

6703 Reflexe	0 Restraints	324 Parameter
Verfeinerung mit SHELXL-2014/7	bis χ = 0.000	
R_1 ($I > 2\sigma(I)$) = 0.0585	wR_2 ($I > 2\sigma(I)$) = 0.1191	
R_1 (all) = 0.0802	wR_2 (all) = 0.1301	GoF (S) = 1.135
$\Delta\varphi_{min}$ = -0.324 e·Å^{-3}	$\Delta\varphi_{max}$ = 0.452 e·Å^{-3}	

Kommentar

Die Struktur wurde als nicht-meroedrischer Zwilling integriert und verfeinert. Für die symmetrieunabhängigen Lithiumatome Li1 und Li2 wird eine pseudo-Translationssymmetrie gefunden.

Fraktionelle Atomkoordinaten (*x, y, z*) und äquivalente isotrope Auslenkungsfaktoren *U*(eq)

	x	*y*	*z*	*U*(eq)/Å^2		*x*	*y*	*z*	*U*(eq)/Å^2
C(1)	-0.1947(2)	0.2395(2)	-0.0600(1)	0.0206(4)	C(18)	0.7472(2)	0.6706(2)	0.5065(2)	0.0247(5)
C(2)	-0.2587(3)	0.1707(2)	0.0246(2)	0.0320(6)	C(19)	0.7602(2)	0.8368(2)	0.6029(2)	0.0219(5)
C(3)	-0.3179(3)	0.3127(2)	-0.1044(2)	0.0292(5)	C(20)	0.5869(3)	0.6895(2)	0.6554(2)	0.0265(5)
C(4)	-0.1014(3)	0.1479(2)	-0.1241(2)	0.0380(6)	C(21)	0.6348(2)	0.9192(2)	0.2304(1)	0.0258(5)
C(5)	0.2001(2)	0.2769(2)	0.0672(1)	0.0169(4)	C(22)	0.4963(2)	0.9702(2)	0.1954(2)	0.0262(5)
C(6)	0.2954(2)	0.1905(2)	0.0002(1)	0.0218(4)	C(23)	0.7735(2)	0.9726(2)	0.3364(2)	0.0257(5)
C(7)	0.2897(2)	0.3667(2)	0.0919(2)	0.0228(5)	C(24)	0.8352(3)	1.0818(2)	0.2918(2)	0.0360(6)
C(8)	0.1419(2)	0.2034(2)	0.1514(1)	0.0248(5)	N(1)	-0.1078(2)	0.3292(2)	-0.0382(1)	0.0174(4)
C(9)	0.1191(3)	0.4273(3)	-0.2674(2)	0.0525(8)	N(2)	-0.0029(2)	0.2755(2)	0.0031(1)	0.0158(4)
C(10)	-0.0028(3)	0.4702(3)	-0.3140(2)	0.0447(7)	N(3)	0.0770(2)	0.3496(2)	0.0266(1)	0.0152(3)
C(11)	0.2235(3)	0.5713(2)	-0.1967(2)	0.0376(6)	N(4)	0.3593(2)	0.8489(2)	0.4631(1)	0.0165(4)
C(12)	0.3675(3)	0.5025(3)	-0.1798(2)	0.0385(6)	N(5)	0.4564(2)	0.7841(2)	0.5058(1)	0.0168(4)
C(13)	0.2647(2)	0.7695(2)	0.4353(1)	0.0204(4)	N(6)	0.5470(2)	0.8463(2)	0.5320(1)	0.0156(3)
C(14)	0.1947(3)	0.6953(2)	0.5152(2)	0.0282(5)	Li(1)	-0.0100(4)	0.4773(3)	-0.0770(2)	0.0194(7)
C(15)	0.1457(2)	0.8548(2)	0.3935(2)	0.0294(5)	Li(2)	0.4858(4)	0.9787(3)	0.4225(2)	0.0205(7)
C(16)	0.3546(3)	0.6826(2)	0.3665(2)	0.0285(5)	O(1)	0.1152(2)	0.4945(2)	-0.1904(1)	0.0268(4)
C(17)	0.6586(2)	0.7602(2)	0.5741(1)	0.0180(4)	O(2)	0.6315(2)	0.9680(1)	0.3151(1)	0.0230(3)

7.9.14 Chloro-tris(tripyrrolidin-phosphoranimin)phosphan-gold(I)-tetrahydrofuransolvat (sum0608, Sebastian Ullrich)

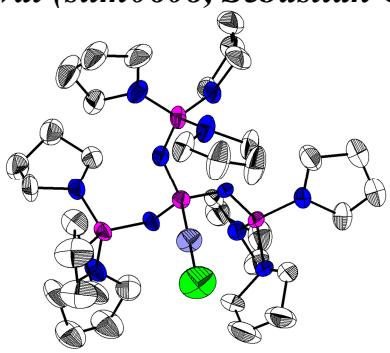

Kristalldaten

C40 H80 Au Cl N12 O P4	*M* = 1101.45 g/mol	Trigonal, *R*3*c*
a = 14.0210(5) Å	*b* = 14.0210(5) Å	*c* = 46.410(2) Å
α = 90°	β = 90°	γ = 120°
V = 7901.3(7) Å^3	*Z* = 6	*F*(000) = 3408
D_{calc} = 1.389 g/cm^3	μ = 3.007 mm^{-1}	
colourless block	0.410 · 0.340 · 0.240 mm^3	

Datensammlung

Diffraktometer: D8 Quest (Bruker)	*T* = 100(2) K	λ = 0.71073 Å
h = -17 bis 17	*k* = -17 bis 16	*l* = -59 bis 59
19064 gemessene Reflexe	3722 unabhängige Reflexe	3193 Reflexe mit $I > 2\sigma(I)$
θ = 2.906 bis 27.130°	R_{int} = 0.0419	*C* (25.00°) = 0.967
Absorptionskorrektur: Multi-scan	T_{min} = 0.5912	T_{max} = 0.7455

Verfeinerung

3722 Reflexe	366 Restraints	314 Parameter
Verfeinerung mit SHELXL-2014/7	bis χ = 0.000	
R_1 ($I > 2\sigma(I)$) = 0.0587	wR_2 ($I > 2\sigma(I)$) = 0.1486	
R_1 (all) = 0.0697	wR_2 (all) = 0.1588	GoF (S) = 1.163
$\Delta\varphi_{min}$ = -2.328 e·Å^{-3}	$\Delta\varphi_{max}$ = 1.219 e·Å^{-3}	

Kommentar

Die Struktur wurde als Inversionszwilling verfeinert. Das fehlgeordnete THF-Molekül und die fehlgeordneten Pyrrolidingruppen wurden über DELU, RIGU, DFIX, ISOR und SAME restrained.

Fraktionelle Atomkoordinaten (*x, y, z*) und äquivalente isotrope Auslenkungsfaktoren *U*(eq)

	x	*y*	*z*	*U*(eq)/Å^2
Au(1)	0.3333	0.6667	0.7715(1)	0.0575(3)
Cl(1)	0.3333	0.6667	0.7215(2)	0.111(5)
P(1)	0.3333	0.6667	0.8202(1)	0.0344(14)
N(1)	0.4240(8)	0.7845(7)	0.8328(2)	0.0359(18)
P(2)	0.4308(2)	0.8999(3)	0.8324(1)	0.0404(6)
N(2)	0.3433(15)	0.9002(15)	0.8547(5)	0.047(4)
C(1)	0.323(3)	0.842(3)	0.8819(7)	0.047(7)
C(2)	0.279(3)	0.901(2)	0.9025(8)	0.068(8)
C(3)	0.336(2)	1.0178(19)	0.8894(6)	0.080(7)
C(4)	0.321(2)	0.993(2)	0.8565(6)	0.071(6)
N(2A)	0.378(3)	0.922(3)	0.8647(8)	0.045(9)
C(1A)	0.333(6)	0.839(4)	0.8865(11)	0.038(10)
C(2A)	0.263(6)	0.872(5)	0.9059(11)	0.055(11)
C(3A)	0.250(4)	0.956(4)	0.8867(10)	0.074(12)
C(4A)	0.369(5)	1.019(3)	0.8722(13)	0.072(13)
N(3)	0.5610(8)	0.9922(8)	0.8358(3)	0.053(2)
C(5)	0.6093(19)	1.1126(14)	0.8332(8)	0.073(7)
C(6)	0.7291(19)	1.153(2)	0.8267(7)	0.087(8)
C(7)	0.7523(18)	1.077(2)	0.8403(8)	0.097(8)
C(8)	0.6481(14)	0.9664(17)	0.8411(7)	0.067(6)
N(4)	0.3941(12)	0.9368(17)	0.8011(4)	0.054(5)
C(9)	0.2769(15)	0.889(2)	0.7921(6)	0.067(7)
C(10)	0.285(2)	0.908(3)	0.7601(6)	0.103(10)
C(11)	0.396(2)	0.966(3)	0.7516(6)	0.101(10)
C(12)	0.4656(15)	0.961(2)	0.7757(5)	0.065(6)
C(5A)	0.587(3)	1.104(2)	0.8452(12)	0.049(10)
C(6A)	0.710(3)	1.169(3)	0.8407(14)	0.062(12)
C(7A)	0.737(4)	1.110(3)	0.8211(12)	0.059(12)
C(8A)	0.660(2)	0.989(3)	0.8289(9)	0.039(7)
N(4A)	0.391(3)	0.962(3)	0.8103(7)	0.032(10)
C(9A)	0.270(3)	0.918(3)	0.8085(9)	0.037(11)
C(10A)	0.249(4)	0.890(6)	0.7770(11)	0.065(17)
C(11A)	0.346(5)	0.970(7)	0.7624(10)	0.074(19)
C(12A)	0.440(4)	0.984(5)	0.7816(9)	0.045(13)
O(100)	0.6667	0.3333	0.7727(10)	0.153(14)
C(100)	0.711(4)	0.281(4)	0.7559(9)	0.140(14)
C(101)	0.686(8)	0.291(6)	0.7252(10)	0.17(2)

8 Literaturverzeichnis

[1] B. Scrosati, J. Garche, *J. Power Sources* **2010**, *195*, 2419-2430.

[2] M. D. Bhatt, C. O'Dwyer, *Phys. Chem. Chem. Phys.* **2015**, *17*, 4799-4844.

[3] N. Nitta, F. Wu, J. T. Lee, G. Yushin, *Mater. Today (Oxford, U. K.)* **2015**, *18*, 252-264.

[4] a) C. He, S. Wu, N. Zhao, C. Shi, E. Liu, J. Li, *ACS Nano* **2013**, *7*, 4459-4469; b) Y. Su, S. Li, D. Wu, F. Zhang, H. Liang, P. Gao, C. Cheng, X. Feng, *ACS Nano* **2012**, *6*, 8349-8356; c) J. Zhou, J. Qin, X. Zhang, C. Shi, E. Liu, J. Li, N. Zhao, C. He, *ACS Nano* **2015**, *9*, 3837-3848; d) X. Zhou, L.-J. Wan, Y.-G. Guo, *Adv. Mater. (Weinheim, Ger.)* **2013**, *25*, 2152-2157; e) S. Goriparti, E. Miele, F. De Angelis, E. Di Fabrizio, R. Proietti Zaccaria, C. Capiglia, *J. Power Sources* **2014**, *257*, 421-443.

[5] a) R. J. Gummow, Y. He, *J. Power Sources* **2014**, *253*, 315-331; b) C. Nan, J. Lu, L. Li, L. Li, Q. Peng, Y. Li, *Nano Res.* **2013**, *6*, 469-477.

[6] J. Kalhoff, G. G. Eshetu, D. Bresser, S. Passerini, *ChemSusChem* **2015**, *8*, 2154-2175.

[7] Y. Wang, W.-H. Zhong, *ChemElectroChem* **2015**, *2*, 22-36.

[8] L. H. Finger, Masterarbeit, Philipps-Universität Marburg (Marburg), **2011**.

[9] K. Xu, A. von Cresce, *J. Mater. Chem.* **2011**, *21*, 9849-9864.

[10] a) U. Lischka, U. Wietelmann, M. Wegner (CHEMETAL GmbH), DE 19829030, **1999**; b) W. Xu, C. A. Angell, *Electrochem. Solid-State Lett.* **2001**, *4*, E1-E4.

[11] a) S. S. Zhang, *J. Power Sources* **2006**, *162*, 1379-1394; b) S. S. Zhang, K. Xu, T. R. Jow, *J. Power Sources* **2006**, *156*, 629-633; c) K. Xu, U. Lee, S. S. Zhang, M. Wood, T. R. Jow, *Electrochem. Solid-State Lett.* **2003**, *6*, A144-A148.

[12] F. F. Chesneau, Z. Baan, B. Gaspar, M. Schmidt, A. Garsuch, H. Wolf, K. Leitner, C. Saffert, W. Klaus, M. Kuhl (BASF SE, Germany), WO 2015007554, **2015**.

[13] E. H. Mørkved, L. T. Holmaas, H. Kjøsen, G. Hvistendahl, *Acta Chem. Scand.* **1996**, *50*, 1153-1156.

[14] a) R. J. Herr, *Bioorg. Med. Chem.* **2002**, *10*, 3379-3393; b) L. V. Myznikov, A. Hrabalek, G. I. Koldobskii, *Chem. Heterocycl. Compd.* **2007**, *43*, 1-9.

[15] a) M. Barghamadi, A. S. Best, A. I. Bhatt, A. F. Hollenkamp, M. Musameh, R. J. Rees, T. Ruther, *Energy Environ. Sci.* **2014**, *7*, 3902-3920; b) P. G. Bruce, S. A. Freunberger, L. J. Hardwick, J.-M. Tarascon, *Nat. Mater.* **2012**, *11*, 19-29.

[16] D. Bresser, S. Passerini, B. Scrosati, *Chem. Commun.* **2013**, *49*, 10545-10562.

[17] M.-K. Song, Y. Zhang, E. J. Cairns, *Nano Lett.* **2013**, *13*, 5891-5899.

[18] S. S. Zhang, *J. Power Sources* **2013**, *231*, 153-162.

[19] S. Evers, L. F. Nazar, *Acc. Chem. Res.* **2013**, *46*, 1135-1143.

[20] R. Chen, T. Zhao, F. Wu, *Chem. Commun.* **2015**, *51*, 18-33.

[21] A. Manthiram, Y. Fu, S.-H. Chung, C. Zu, Y.-S. Su, *Chem. Rev.* **2014**, *114*, 11751-11787.

[22] a) J. Scheers, S. Fantini, P. Johansson, *J. Power Sources* **2014**, *255*, 204-218; b) Y. Diao, K. Xie, S. Xiong, X. Hong, *J. Power Sources* **2013**, *235*, 181-186.

[23] a) M. Barghamadi, A. S. Best, A. I. Bhatt, A. F. Hollenkamp, P. J. Mahon, M. Musameh, T. Ruther, *J. Power Sources* **2015**, *295*, 212-220; b) E. S. Shin, K. Kim, S. H. Oh, W. I. Cho, *Chem. Commun.* **2013**, *49*, 2004-2006.

[24] Arbeitsgruppe Erneuerbare Energien-Statistik (Bundesministerium für Wirtschaft und Energie), *Entwicklung der erneuerbaren Energien in Deutschland im Jahr 2014*, http://www.erneuerbare-energien.de/EE/Navigation/DE/Service/Erneuerbare_Energien_in_Zahlen/Entwicklung_der_erneuerbaren_Energien_in_Deutschland/entwicklung_der_erneuerbaren_energien_in_deutschland_im_jahr_2014.html, letzter Zugriff am 23.12.2015.

[25] a) A. Hagfeldt, G. Boschloo, L. Sun, L. Kloo, H. Pettersson, *Chem. Rev.* **2010**, *110*, 6595-6663; b) B. O'Regan, M. Grätzel, *Nature* **1991**, *353*, 737-740.

[26] A. Mishra, M. K. Fischer, P. Bäuerle, *Angew. Chem. Int. Ed.* **2009**, *48*, 2474-2499.

[27] M. Finze, *Cyanoborate – Synthesen, Eigenschaften und Anwendungen*, Anorganisch-chemisches Kolloquium, Philipps-Universität Marburg, **30.11.2015**.

[28] G. Schenke, *Photovoltaik und Solartechnik 3*, Vorlesungsskript der Hochschule Emden/Leer, **2014**, http://www.et-inf.fho-emden.de/~elmalab//PV_Solar/download/PV_Solar_3.pdf.

[29] M. A. Green, K. Emery, Y. Hishikawa, W. Warta, E. D. Dunlop, *Prog. Photovoltaics* **2016**, *24*, 3-11.

[30] *Solarzeit - Fotovoltaik am GSG*, http://www.gsg-physik.net/physik/fotovoltaik/d_kap6.html, letzter Zugriff am 25.12.2015.

[31] a) T. W. Hamann, *Dalton Trans.* **2012**, *41*, 3111-3115; b) L. Giribabu, R. Bolligarla, M. Panigrahi, *The Chemical Record* **2015**, *15*, 760-788.

[32] J. Wu, Z. Lan, J. Lin, M. Huang, Y. Huang, L. Fan, G. Luo, *Chem. Rev.* **2015**, *115*, 2136-2173.

[33] P. Wang, S. M. Zakeeruddin, J.-E. Moser, R. Humphry-Baker, M. Grätzel, *J. Am. Chem. Soc.* **2004**, *126*, 7164-7165.

[34] P. Kübler, J. Sundermeyer, *Dalton Trans.* **2014**, *43*, 3750-3766.

[35] J. Liu, X. Yang, J. Cong, L. Kloo, L. Sun, *Phys. Chem. Chem. Phys.* **2012**, *14*, 11592-11595.

[36] a) J. Cong, X. Yang, Y. Hao, L. Kloo, L. Sun, *RSC Adv.* **2012**, *2*, 3625-3629; b) V. González-Pedro, Q. Shen, V. Jovanovski, S. Giménez, R. Tena-Zaera, T. Toyoda, I. Mora-Seró, *Electrochim. Acta* **2013**, *100*, 35-43.

[37] L. Li, X. Yang, J. Gao, H. Tian, J. Zhao, A. Hagfeldt, L. Sun, *J. Am. Chem. Soc.* **2011**, *133*, 8458-8460.

[38] V. Jovanovski, V. Gonzalez-Pedro, S. Gimenez, E. Azaceta, G. Cabanero, H. Grande, R. Tena-Zaera, I. Mora-Seró, J. Bisquert, *J. Am. Chem. Soc.* **2011**, *133*, 20156-20159.

[39] P. Walden, *Bull. Acad. Imp. Sci. Saint-Pétersbourg* **1914**, 405-422.

[40] C. Schall, *Z. Elektrochem. Angew. Phys. Chem.* **1908**, *14*, 397-405.

[41] a) W. Sundermeyer, *Angew. Chem., Int. Ed. Engl.* **1965**, *4*, 222-238; b) W. Sundermeyer, W. Verbeek, *Angew. Chem., Int. Ed. Engl.* **1966**, *5*, 1-6.

[42] a) S. E. Fry, N. J. Pienta, *J. Am. Chem. Soc.* **1985**, *107*, 6399-6400; b) J. A. Boon, J. A. Levisky, J. L. Pflug, J. S. Wilkes, *J. Org. Chem.* **1986**, *51*, 480-483.

[43] a) J. S. Wilkes, M. J. Zaworotko, *J. Chem. Soc., Chem. Commun.* **1992**, 965-967; b) J. Fuller, R. T. Carlin, H. C. De Long, D. Haworth, *J. Chem. Soc., Chem. Commun.* **1994**, 299-300; c) T. Welton, *Chem. Rev.* **1999**, *99*, 2071-2084.

[44] a) M. T. Clough, C. R. Crick, J. Grasvik, P. A. Hunt, H. Niedermeyer, T. Welton, O. P. Whitaker, *Chem. Sci.* **2015**, *6*, 1101-1114; b) M. Y. Lui, L. Crowhurst, J. P. Hallett, P. A. Hunt, H. Niedermeyer, T. Welton, *Chem. Sci.* **2011**, *2*, 1491-1496; c) H. Niedermeyer, J. P. Hallett, I. J. Villar-Garcia, P. A. Hunt, T. Welton, *Chem. Soc. Rev.* **2012**, *41*, 7780-7802.

[45] a) A. Bordoloi, S. Sahoo, F. Lefebvre, S. B. Halligudi, *J. Catal.* **2008**, *259*, 232-239; b) B. Oelkers, J. Sundermeyer, *Dalton Trans.* **2011**, *40*, 12727-12741; c) A. Riisager, R. Fehrmann, S. Flicker, R. van Hal, M. Haumann, P. Wasserscheid, *Angew. Chem., Int. Ed.* **2005**, *44*, 815-819; d) A. Riisager, B. Jorgensen, P. Wasserscheid, R. Fehrmann, *Chem. Commun.* **2006**, 994-996; e) M. J. Schneider, M. Haumann, M. Stricker, J. Sundermeyer, P. Wasserscheid, *J. Catal.* **2014**, *309*, 71-78.

[46] a) F. Fabregat-Santiago, J. Bisquert, E. Palomares, L. Otero, D. Kuang, S. M. Zakeeruddin, M. Grätzel, *J. Phys. Chem. C* **2007**, *111*, 6550-6560; b) P. Wang, S. M. Zakeeruddin, J.-E. Moser, M. Grätzel, *J. Phys. Chem. B* **2003**, *107*, 13280-13285.

[47] a) M. Armand, F. Endres, D. R. MacFarlane, H. Ohno, B. Scrosati, *Nat. Mater.* **2009**, *8*, 621-629; b) M. Galinski, A. Lewandowski, I. Stepniak, *Electrochim. Acta* **2006**, *51*, 5567-5580.

[48] a) F. Karadas, M. Atilhan, S. Aparicio, *Energy Fuels* **2010**, *24*, 5817-5828; b) W. Wu, B. Han, H. Gao, Z. Liu, T. Jiang, J. Huang, *Angew. Chem., Int. Ed.* **2004**, *43*, 2415-2417.

[49] A. Pinkert, K. N. Marsh, S. Pang, M. P. Staiger, *Chem. Rev.* **2009**, *109*, 6712-6728.

[50] a) J. H. Davis, Jr., *Chem. Lett.* **2004**, *33*, 1072-1077; b) R. Giernoth, *Angew. Chem., Int. Ed.* **2010**, *49*, 2834-2839.

[51] a) Y. U. Paulechka, D. H. Zaitsau, G. J. Kabo, A. A. Strechan, *Thermochim. Acta* **2005**, *439*, 158-160; b) L. P. N. Rebelo, J. N. C. Lopes, J. M. S. S. Esperanca, E. Filipe, *J. Phys. Chem. B* **2005**, *109*, 6040-6043; c) M. J. Earle, J. M. S. S. Esperanca, M. A. Gilea, J. N. Canongia Lopes, L. P. N. Rebelo, J. W. Magee, K. R. Seddon, J. A. Widegren, *Nature* **2006**, *439*, 831-834.

[52] M. Yoshizawa, W. Xu, C. A. Angell, *J. Am. Chem. Soc.* **2003**, *125*, 15411-15419.

[53] J. P. Leal, J. M. S. S. Esperança, M. E. Minas da Piedade, J. N. Canongia Lopes, L. P. N. Rebelo, K. R. Seddon, *J. Phys. Chem. A* **2007**, *111*, 6176-6182.

[54] J. Vitorino, J. P. Leal, M. E. Minas da Piedade, J. N. Canongia Lopes, J. M. S. S. Esperanca, L. P. N. Rebelo, *J. Phys. Chem. B* **2010**, *114*, 8905-8909.

[55] a) O. Holloczki, D. Gerhard, K. Massone, L. Szarvas, B. Nemeth, T. Veszpremi, L. Nyulaszi, *New J. Chem.* **2010**, *34*, 3004-3009; b) J. A. Cowan, J. A. C. Clyburne, M. G. Davidson, R. L. W. Harris, J. A. K. Howard, P. Küpper, M. A. Leech, S. P. Richards, *Angew. Chem., Int. Ed.* **2002**, *41*, 1432-1434.

[56] M. Horikawa, N. Akai, A. Kawai, K. Shibuya, *J. Phys. Chem. A* **2014**, *118*, 3280-3287.

[57] P. Wasserscheid, T. Welton, (Eds.), *Ionic Liquids in Synthesis, Vol. 1 & 2*, 2nd ed., Wiley VCH, Weinheim, **2007**.

[58] J. H. Werntz (E. I. du Pont de Nemours & Co.), US 2635100, **1953**.

[59] a) S. Mori, K. Ida, M. Ue (Mitsubishi Petrochemical), EP 291074, **1988**; b) S. Mori, K. Ida, M. Ukei (Mitsubishi Petrochemical), JP 01197462, **1989**; c) O. Yagi, S. Shimizu, *Nippon Kagaku Kaishi* **1995**, 74-78; d) B. Albert, M. Jansen, *Z. Anorg. Allg. Chem.* **1995**, *621*, 1735-1740; e) M. Takeda, M. Takehara, M. Ue (Mitsubishi Chemical Corp.), JP 2003040869, **2003**; f) Z.-B. Zhou, M. Takeda, M. Ue, *J. Fluorine Chem.* **2004**, *125*, 471-476; g) R. Kalb (PROIONIC), WO 2008052861, **2008**; h) R. Kalb (PROIONIC), WO 2008052860, **2008**; i) G. Degen, C. Stock (BASF), WO 2009040242, **2009**; j) J. D. Holbrey, R. D. Rogers, S. S. Shukla, C. D. Wilfred, *Green Chem.* **2010**, *12*, 407-413; k) T. N. Glasnov, J. D. Holbrey, C. O. Kappe, K. R. Seddon, T. Yan, *Green Chem.* **2012**, *14*, 3071-3076.

[60] a) G. Gurau, H. Rodríguez, S. P. Kelley, P. Janiczek, R. S. Kalb, R. D. Rogers, *Angew. Chem., Int. Ed.* **2011**, *50*, 12024-12026; b) M. Besnard, M. I. Cabaco, F. V. Chavez, N. Pinaud, P. J. Sebastiao, J. A. P. Coutinho, Y. Danten, *Chem. Commun.* **2012**, *48*, 1245-1247; c) M. Besnard, M. I. Cabaco, F. Vaca Chavez, N. Pinaud, P. J. Sebastiao, J. A. P. Coutinho, J. Mascetti, Y. Danten, *J. Phys. Chem. A* **2012**, *116*, 4890-4901.

[61] A. M. Voutchkova, M. Feliz, E. Clot, O. Eisenstein, R. H. Crabtree, *J. Am. Chem. Soc.* **2007**, *129*, 12834-12846.

[62] D. M. Denning, D. E. Falvey, *J. Org. Chem.* **2014**, *79*, 4293-4299.

[63] A. Schmidt, A. Beutler, M. Albrecht, B. Snovydovych, F. J. Ramirez, *Org. Biomol. Chem.* **2008**, *6*, 287-295.

[64] J. D. Holbrey, W. M. Reichert, I. Tkatchenko, E. Bouajila, O. Walter, I. Tommasi, R. D. Rogers, *Chem. Commun.* **2003**, 28-29.

[65] J. Fischer, W. Siegel, V. Bomm, M. Fischer, K. Mundinger (BASF AG), DE 19836477, **2000**.

[66] G. de Robillard, C. H. Devillers, D. Kunz, H. Cattey, E. Digard, J. Andrieu, *Org. Lett.* **2013**, *15*, 4410-4413.

[67] D. Breuch, H. Löwe, *Green Process. Synth.* **2012**, *1*, 261-267.

[68] a) D. H. McDaniel, W. G. Evans, *Inorg. Chem.* **1966**, *5*, 2180-2181; b) J. D. Cotton, T. C. Waddington, *J. Chem. Soc. A* **1966**, 785-789.

[69] J. Bisquert Mascarell, I. Mora Seró, V. Jovanovski, R. Marcilla Garcia, R. Tena-Zaera, D. Mecerreyes Molero, G. Cabanero Sevillano (Fundacion Cidetec; Universitat Jaume I), EP 2388853, **2011**.

[70] R. Steudel, in *Elemental Sulfur und Sulfur-Rich Compounds II, Vol. 231* (Ed.: R. Steudel), Springer Berlin Heidelberg, **2003**, pp. 127-152.

[71] a) M. G. Kanatzidis, N. C. Baenziger, D. Coucouvanis, *Inorg. Chem.* **1983**, *22*, 290-292; b) W. K. Rybak, A. Cymbaluk, M. Siczek, J. Skonieczny, *Eur. J. Inorg. Chem.* **2012**, *2012*, 3675-3679.

[72] a) B. Czeska, K. Dehnicke, *Z. Naturforsch., B: Anorg. Chem., Org. Chem.* **1985**, *40B*, 120-121; b) E. Herdtweck, C. Schumacher, K. Dehnicke, *Z. Anorg. Allg. Chem.* **1985**, *526*, 93-102; c) A. Müller, E. Krickemeyer, M. Zimmermann, M. Römer, H. Bögge, M. Penk, K. Schmitz, *Inorg. Chim. Acta* **1984**, *90*, L69-L71.

[73] a) Q. Zhang, P. Wu, S. Chen, R. Ding, Y. Wang, D. Zhu, *Synth. Met.* **1999**, *105*, 155-159; b) R. G. Teller, L. J. Krause, R. C. Haushalter, *Inorg. Chem.* **1983**, *22*, 1809-1812.

[74] R. J. Batchelor, F. W. B. Einstein, I. D. Gay, C. H. W. Jones, R. D. Sharma, *Inorg. Chem.* **1993**, *32*, 4378-4383.

[75] a) G. Thiele, L. Vondung, C. Donsbach, S. Pulz, S. Dehnen, *Z. Anorg. Allg. Chem.* **2014**, *640*, 2684-2700; b) C. Feldmann, A. Okrut, *Z. Anorg. Allg. Chem.* **2009**, *635*, 1807-1811; c) J. C. Huffman, R. C. Haushalter, *Z. Anorg. Allg. Chem.* **1984**, *518*, 203-209; d) H. Wolkers, B. Schreiner, R. Staffel, U. Müller, K. Dehnicke, *Z. Naturforsch. B* **1991**, *46*, 1015-1019.

[76] W. Friederich, De 952811, **1956**.

[77] E. Oliveri-Mandalà, T. Passalacqua, *Gazz. Chim. Ital.* **1913**, *43(II)*, 465-475.

[78] a) H. Rathsburg, GB 185555, **1922**; b) H. Rathsburg, DE 401344, **1924**.

[79] J. H. Nelson, N. E. Takach, A. H. Ronald, D. W. Moore, W. M. Tolles, G. A. Gray, *Magn. Res. Chem.* **1986**, *24*, 984-994.

[80] V. A. Ostrovskii, G. I. Koldobskii, N. P. Shirokova, V. S. Poplavskii, *Chem. Hetercycl. Compd.* **1981**, *17*, 1148-1151.

[81] a) A. J. Downard, P. J. Steel, J. Steenwijk, *Aust. J. Chem.* **1995**, *48*, 1625-1642; b) P. J. Steel, *J. Chem. Crystallogr.* **1996**, *26*, 399-402.

[82] D. E. Chavez, M. A. Hiskey, D. L. Naud, *J. Pyrotech.* **1999**, *10*, 17-36.

[83] a) R. P. Singh, R. D. Verma, D. T. Meshri, J. n. M. Shreeve, *Angew. Chem., Int. Ed.* **2006**, *45*, 3584-3601; b) R. Wang, Y. Guo, R. Sa, J. M. Shreeve, *Chem. Eur. J.* **2010**, *16*, 8522-8529; c) C. Ye, J.-C. Xiao, B. Twamley, J. M. Shreeve, *Chem. Commun.* **2005**, 2750-2752.

[84] a) N. Fischer, T. M. Klapötke, K. Peters, M. Rusan, J. Stierstorfer, *Z. Anorg. Allg. Chem.* **2011**, *637*, 1693-1701; b) N. Fischer, D. Izsák, T. M. Klapötke, S. Rappenglück, J. Stierstorfer, *Chem. Eur. J.* **2012**, *18*, 4051-4062.

[85] a) N. Fischer, D. Fischer, T. M. Klapötke, D. G. Piercey, J. Stierstorfer, *J. Mater. Chem.* **2012**, *22*, 20418-20422; b) T. M. Klapötke, D. G. Piercey, J. Stierstorfer, *Dalton Trans.* **2012**, *41*, 9451-9459; c) D. Fischer, T. M. Klapötke, J. Stierstorfer, *Angew. Chem., Int. Ed.* **2014**, *53*, 8172-8175; d) D. Fischer, T. M. Klapötke, J. Stierstorfer, *Angew. Chem., Int. Ed.* **2015**, *54*, 10299-10302.

[86] a) B. Yuan, Z. Yu, E. R. Bernstein, *J. Chem. Phys.* **2015**, *142*, 124315; b) W. Zhu, C. Zhang, T. A. O. Wei, H. Xiao, *J. Comput. Chem.* **2011**, *32*, 2298-2312.

[87] a) P. J. Eulgem, A. Klein, N. Maggiarosa, R. W. H. Pohl, D. Naumann, *Chem. Eur. J.* **2008**, *14*, 3727-3736; b) R. W. H. Pohl, J. Wiebke, A. Klein, N. Maggiarosa, M. Dolg, *Eur. J. Inorg. Chem.* **2009**, 2472-2476.

[88] M. Joas, T. M. Klapötke, J. Stierstorfer, *Crystals* **2012**, *2*, 958-966.

[89] a) L. Moreira Lima, E. J. Barreiro, *Curr. Med. Chem.* **2005**, *12*, 23-49; b) C. W. Thornber, *Chem. Soc. Rev.* **1979**, *8*, 563-580.

[90] a) N. Brown, *Mol. Inf.* **2014**, *33*, 458-462; b) I. Ujváry, *Pestic. Sci.* **1997**, *51*, 92-95; c) C. Mayer, Y. L. Janin, *Chem. Rev.* **2014**, *114*, 2313-2342.

[91] a) C. Ballatore, D. M. Huryn, A. B. Smith, *ChemMedChem* **2013**, *8*, 385-395; b) C. F. Matta, A. A. Arabi, D. F. Weaver, *Eur. J. Med. Chem.* **2010**, *45*, 1868-1872.

[92] a) D. W. Esplin, D. M. Woodbury, *Pharmacol. Exp. Ther.* **1956**, *118*, 129-138; b) S. K. Figdor, M. Schach von Wittenau, *J. Med. Chem.* **1967**, *10*, 1158-1159.

[93] B. Scheibe, Bachelorarbeit, Philipps-Universität Marburg (Marburg), **2014**.

[94] Y. Asfaha, Bachelorarbeit, Philipps-Universität Marburg (Marburg), **2012**.

[95] Stoe, Cie, Stoe & Cie GmbH, Darmstadt, Germany, **2011**.

[96] Bruker, Bruker AXS Inc., Madison, Wisconsin, USA, **2012**.

[97] A. Altomare, G. Cascarano, C. Giacovazzo, A. Guagliardi, M. C. Burla, G. Polidori, M. Camalli, *J. Appl. Crystallogr.* **1994**, *27*, 435.

[98] A. Altomare, M. C. Burla, M. Camalli, G. Cascarano, C. Giacovazzo, A. Guagliardi, A. G. G. Moliterni, G. Polidori, R. Spagna, *J. Appl. Crystallogr.* **1999**, *32*, 115-119.

[99] M. C. Burla, R. Caliandro, M. Camalli, B. Carrozzini, G. L. Cascarano, L. D. Caro, C. Giacovazzo, G. Polidori, R. Spagna, *J. Appl. Crystallogr.* **2005**, *38*, 381-388.

[100] M. C. Burla, R. Caliandro, M. Camalli, B. Carrozzini, G. L. Cascarano, L. De Caro, C. Giacovazzo, G. Polidori, D. Siliqi, R. Spagna, *J. Appl. Crystallogr.* **2007**, *40*, 609-613.

[101] M. C. Burla, R. Caliandro, M. Camalli, B. Carrozzini, G. L. Cascarano, C. Giacovazzo, M. Mallamo, A. Mazzone, G. Polidori, R. Spagna, *J. Appl. Crystallogr.* **2012**, *45*, 357-361.

[102] G. Sheldrick, *Acta Crystallogr. A* **2008**, *64*, 112-122.

[103] G. Sheldrick, *Acta Crystallogr. A* **2015**, *71*, 3-8.

[104] L. Palatinus, G. Chapuis, *J. Appl. Crystallogr.* **2007**, *40*, 786-790.

[105] L. Farrugia, *J. Appl. Crystallogr.* **2012**, *45*, 849-854.

[106] L. J. Farrugia, *J. Appl. Crystallogr.* **2012**, *45*, 849-854.

[107] C. F. Macrae, P. R. Edgington, P. McCabe, E. Pidcock, G. P. Shields, R. Taylor, M. Towler, J. van de Streek, *J. Appl. Crystallogr.* **2006**, *39*, 453-457.

[108] C. B. Hübschle, G. M. Sheldrick, B. Dittrich, *J. Appl. Crystallogr.* **2011**, *44*, 1281-1284.

[109] A. L. Spek, *Acta Crystallogr. D* **2009**, *65*, 148-155.
[110] Crystal Impact - H. Putz & K. Brandenburg GbR, Kreuzherrenstr. 102, 53227 Bonn, Germany.
[111] B. Oelkers, Dissertation, Philipps-Universität Marburg (Marburg), **2011**.
[112] S. Ullrich, Bachelorarbeit, Philipps-Universität Marburg (Marburg), **2013**.